Institut de recherche pour le développement

ISAG

Georg August Universität Göttingen, Germany

Géodynamique Andine
Andean Geodynamics
Geodinámica Andina

Résumés étendus
Extended Abstracts
Resumenes expandidos

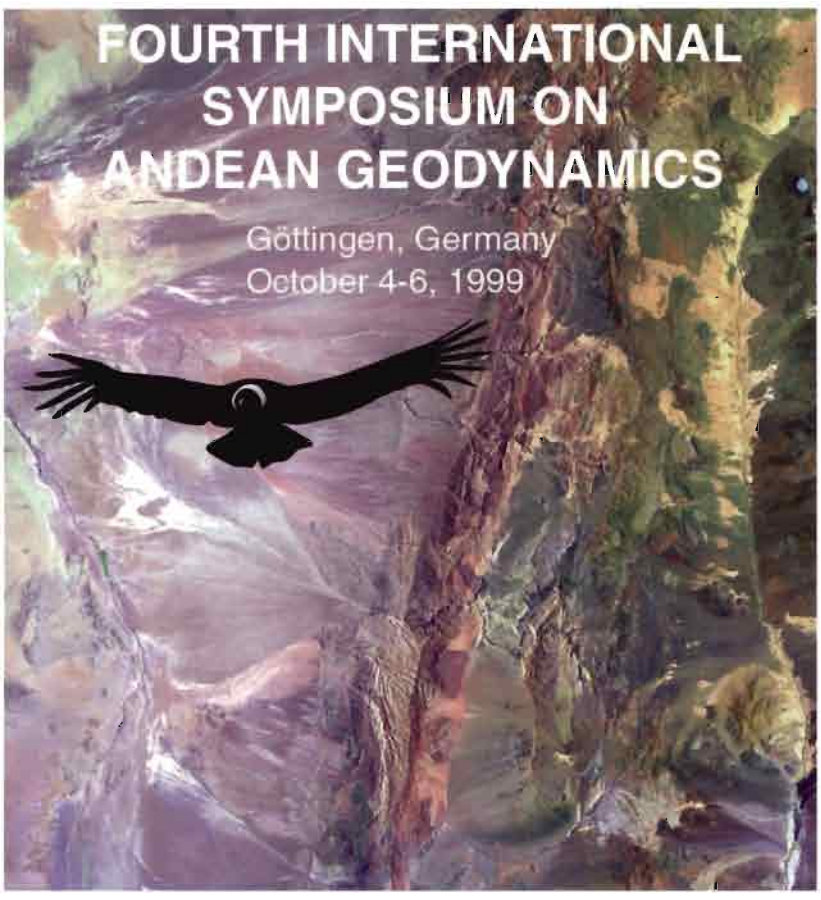

ORGANISATEURS ORGANIZERS ORGANIZADORES

I R D
Institut de Recherche pour le Développement, Paris, France

Georg August Universität
Geochemisches Institut
Göttingen, Germany

Institut de Recherche pour le Développement
PARIS 1999

4th International Symposium on Andean Geodynamics
4.-6. October 1999, Göttingen

Georg August Universität
Göttingen, Germany

Institut de recherche
pour le développement

October 4.-6. 1999

Résumés étendus - Extended Abstracts - Resumenes expandidos

ORGANISATEURS

I R D

Institut de Recherche pour le
Développement, Paris, France

ORGANIZERS

ORGANIZADORES

Georg August Universität

Geochemisches Institut
Göttingen, Germany

Institut de Recherche pour le Développement

PARIS 1999

4th International Symposium on Andean Geodynamics
Universität Göttingen, Germany, October 4 - 6, 1999

Georg August Universität
Göttingen

ISAG

ORSTOM
IRD Institut de Recherche pour le Développement

ISAG 99. Göttingen

COMITÉ D'ORGANISATION
ORGANIZING COMMITTEE
COMITÉ ORGANIZADOR

H.-J. Götze (F. Univ., Berlin)
G. Hérail (IRD, Paris)
E. Jaillard (IRD, Grenoble)
H. Miller (Univ. München)
T. Monfret (IRD, Villefranche)
C. Reichert (BGR, Hannover)
P. Roperch (IRD, Santiago)
L. Stroink (Univ. Bochum)
G. Wörner (Univ. Göttingen)

Le comité d'organisation tient à remercier particulièrement Mesdames Velder et Bell (Institut für Geochemie, Georg August Universität, Göttingen), Monsieur Sven Knollmann (Institut für Geochemie, Georg August Universität, Göttingen) et Monsieur Frédéric Christophoul (Laboratoire de Géodynamique des Bassins, Université Paul Sabatier, Toulouse) pour leur participation à l'édition de ce volume.

APPUIS FINANCIERS
FUNDINGS
APOYO FINANCIERO

L'organisation de l'ISAG 99 et les aides aux voyages pour un certain nombre de collègues latino-américains ont été rendues possibles grâce au soutien financier de l'IRD (Délégation à l'Information et à la Communication, Département Milieu et Environnement, Comission Scientifique de Géologie - Géophysique), de la Comission des Communantés Européennes (Coopération Scientifique Internationale), du Ministère des Affaires Étrangères (Ambassade de France au Chili), du Land de Basse Saxe (Allemagne), de l'Université de Göttingen, de l'International Lithosphere Programme et de la Deutsche Forschung Gesellschaft.

SOMMAIRE / SUMMARY / SUMARIO

ON THE SIGNIFICANCE OF TRANSVERSAL WRENCH-FAULT TECTONICS FOR THE STRUCTURING OF THE SOUTHERN CENTRAL ANDES

Andreas ABELS(1)

(1) Geologisches Institut, WWU Münster, 48149 Münster, Germany (abels@uni-muenster.de)

KEY WORDS: Southern Central Andes, transversal wrenching, strike-slip faults, block rotation

INTRODUCTION

The identification and characterization of basement-influenced wrench faulting obliquely to a subsequently established structural trend is probably one of the most difficult tasks in structural geology. Several primary factors influence the surficially appearing deformation (intitial state of stress, cover thickness, thermal regime, amount of displacement, width of wrench zone etc.), and disguising by coeval or subsequent magmatism and sedimentation as well as polyphase activity may complicate the setting in addition. It is, however, a common feature that superimposed structural pattern reveal changes of their along-strike character over a relatively short distance or they are limited by such pre-existing structures. For the southern Central Andes (SCA) only few studies explicitly address these phenomena so far (e.g., Grier et al. 1991), but the present Andean structural grain suggests, in combination with paleogeographic reconstructions, that such interaction may be of more widespread significance. In the following three potential examples are described for which however a comprehensive treatment is not possible here, but they should serve as a base for discussion. The large-scale spatial pattern and shear sense of such wrench zones in the SCA perhaps reflect indeed a fundamental large-scale deformation mechanism which accompanies oroclinal bending and shortening.

EXAMPLES

1) At the southern limit of the Chilean Precordillera (~27°15'S) ~NE-SW oriented 'Andean' structures are cut by significant morphostructural NW-SE trending features (Fig. 1). The most distinct fractures occur S of Puquios in one line with the Paleocene Cachiyuyo and Dulcinea volcanoes, although the whole structural anomaly appears to be over 25 km wide. A NW-SE striking basement structure is a plausible explanation for this setting, and it could represent the northern structural limit of marine basins through almost the whole Mesozoic (e.g., Prinz et al. 1994) which has been repeatedly reactivated up into the Tertiary. Such a setting can provide new clues to the origin of the peculiar Puquios 'chaos' and detachments (Mpodozis & Allmendinger 1992) of which the latter may be due to 'pull apart' movements then. Strike-slip reactivation is indicated, based on Landsat-TM image interpretation, by left-lateral offsets along NW-faults which is in accordance with long fractures of this direction to the W in the Coastal Cordillera (Randall et al. 1996). Large vertical displacements (SW-side down) occured at least on those faults SE of Qda. de Paipote (e.g., Sepulveda & Naranjo 1982).

2) The structural pattern in the Chilean Precordillera at around 25°30'S is not continuous, but bends from its overall ~NNE-SSW trend over a distance of ~45 km into a N-S direction. The hinges are pronounced by NW-SE trending faults and topographic features, and the whole map-scale pattern makes the impression of a sinistrally displacing horizontal flexure (Fig. 2, Naranjo & Puig 1982). A sinistral displacement was also suspected by Salfity (1985) who postulated a NW-extension of the 'Culambajá' lineament running from the Argentine Puna into the northern hinge of the flexure.

3) The Calama-Olacapato-El Toro lineament (COT) is probably the best documented example for a wrench fault cutting obliquely through the SCA, and its presence in NW-Argentina is in sections relatively well established (Marrett et al. 1994, and refs. therein). Salfity (1985) proposed an extension into Chile, based on a structural bending of the Precordillera at Calama. According to Reutter et al. (1996) the COT is in the Precordillera, if at all present, not exposed as a continuous fault, and only minor activity (< 1 km sinistrally) may have occured in the Neogene. Activity coeval with peak deformation and magmatism during the main orogeny in the Precordillera, the Eocene 'Incaic' phase has been, however, not discussed. To the SE a similar structural bending occurs within the range of the 'Cerros de Purilactis' pointing again, as already suggested by Dingman (1967), to left-lateral drag along a NW-SE trending fracture, but no clear continuations towards the NW (Llano de Quimal) or to the SE (Salar de Atacama basin) are exposed (Fig. 3). Breitkreuz (1995) mentioned a possible ~20 km left-lateral offset along ~NW-SE striking faults SE of the Salar de Atacama, a distance which is identical to a postulated offset at the COT in the Argentine Puna (e.g., Allmendinger et al. 1983). The COT shows evidently polyphase activity (e.g.,

Soriano et al. 1996), and it is unlikely that it was active over its whole length during the same time. This might contribute to the varying exposure. It is striking that eastward structural bending occurs only on the northern side of the COT, a phenomenon which points indirectly to the presence of the structure.

DISCUSSION

Significant transversal structures are as 'lineamentos' long known in the southern Central Andes (e.g., Mon 1979). Some segments of these structures are restricted to a single continuous fault, others are better described as distributed wrench zones that consist of a set of strike-slip faults and/or, due to rotation(s) of the principle stress directions, oblique thrusts/reverse faults, often paleogeographically controlled. The frequency of long ~NW-SE trending fractures in the S-Puna has been indicated, for instance, by Alonso et al. (1984), and extensions into Chile are likely (Salfity 1985; Abels & Bischoff 1998, and ref. therein). Observed and suggested strike-slip displacements are always left-lateral. This consistency indicates a mechanism which has affected large areas of the SCA, possibly of a non-coaxial, penetrative domino-type which involves overall clockwise rotations. The process may be already active since the initiation of Andean deformation in the Middle Cretaceous, interacting with oroclinal bending, crustal thickening, thrusting, and margin-parallel strike-slip faulting. At the eastern Andean deformation front, on the other hand, right-lateral wrenching within ~(E)NE-(W)SW oriented structural transition zones dominates, accommodating the northward increasing amount of horizontal shortening (e.g., 'Tucumán Transfer Zone'; De Urreiztieta et al. 1996). In both cases pre-Andean structures are probably the nuclei for the initiation of deformation.

REFERENCES

Abels A. & Bischoff L. 1998. A remote sensing study of the Chilean Precordillera (26°-27°30'S) with implications for its structural development. 3. Andean Geosci. Workshop, Plymouth, abstract vol., 1 p. **Allmendinger et al. 1983.** Paleogeography and Andean structural geometry, NW Argentina. Tectonics 2, 1-16. **Alonso et al. 1984.** Puna Austral – Bases para el subprovincialismo geológico de la Puna. 9. Cong. Geol. Argent., 43-63. **Breitkreuz C. 1995.** The Late Permian Peine and Cas Formations at the eastern margin of the Salar de Atacama, N Chile: stratigraphy, volcanic facies, and tectonics. Rev. Geol. Chile 22, 3-23. **Dingman R.J. 1967.** Geology and ground-water resources of the northern part of the Salar de Atacama Antofagasta province, Chile. U.S. Geol. Surv. Bull. 1219, 49 p. **Grier et al. 1991.** Andean reactivation of the Cretaceous Salta rift, NW Argentina. J. South Am. Earth Sci. 4, 351-372. **Marrett et al. 1994.** Late Cenozoic tectonic evolution of the Puna Plateau and adjacent foreland, NW Argentine

Andes. J. South Am. Earth Sci. 7, 179-207. **Mon R. 1979.** Esquema tectónico de los Andes del Norte Argentino. Asoc. Geol. Argent. 34, 53-60. **Mpodozis C. & Allmendinger R.W. 1992.** Tectónica extensional a gran escala en el Cretácico del norte de Chile (Puquios-Sierra Fraga, 27°S) ... Rev. Geol. Chile 19, 167-197. **Naranjo J.A. & Puig A. 1984.** Carta Geol. Chile, Hojas Taltal y Chañaral. Sernageomin 62-63. **Prinz et al. 1994.** Sediment accumulation and subsidence history in the Mesozoic marginal basin of N Chile. In: Tectonics of the Southern Central Andes, pp. 219-232; Springer. **Randall et al. 1996.** Major crustal rotations in the Andean margin: Paleomagnetic results from the Coastal Cordillera of N. Chile. J. Geophys. Res. 101, 15783-15798. **Reutter et al. 1996.** The Precordilleran fault system of Chuquicamata, N Chile: evidence for reversals along arc-parallel strike-slip faults. Tectonophysics, 259, 213-228. **Salfity J.A. 1985.** Lineamentos transversales al rumbo Andino en el Noroeste Argentino. 4. Cong. Geol. Chileno, 119-137. **Sepulveda P. & Naranjo J.A. 1982.** Carta Geol. Chile, Hoja Carrera Pinto. Sernageomin 53. **Soriano et al. 1996.** Influence of regional tectonics on Miocene volcanic caldera formation in the Puna Altiplano, NW of Argentina: The Aguas Calientes caldera complex. 3. ISAG, St. Malo, 493-496. **De Urreiztieta et al. 1996.** Tertiary kinematics and basin development at the southern edge of the Altiplano-Puna (NW Argentina). Tectonophysics 254, 17-39.

Fig.1. Landsat-TM image interpretation of the Puquios region (based on: 321 and 741 [rgb], 5/7-5/4-7/4 [ND, rgb], PC1). Outline of the 'Puquios Chaos' modified from Mpodozis & Allmendinger (1992); PD: Puquios detachments.

Fig. 2. Structural setting of the Precordillera around 25°30'S (based on Naranjo & Puig, 1982).

Fig. 3. a) Landsat-MSS image interpretation of the Salar de Atacama region (based on: 321 [rgb]); b) Major transversal structures along the COT lineament (refs. in the text).

Fig. 4. Simple, tentative sketch to a large-scale transpressional deformation pattern in the SCA.

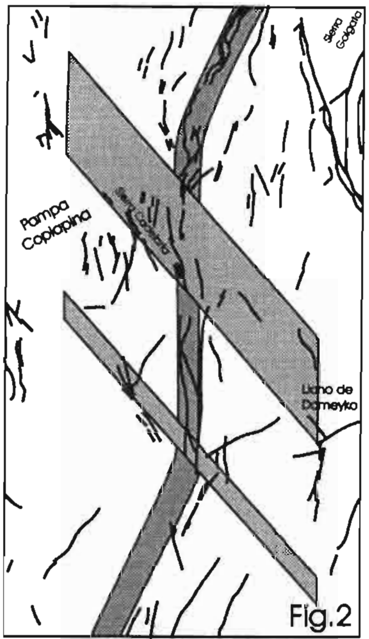

Fig.2

Fig.1

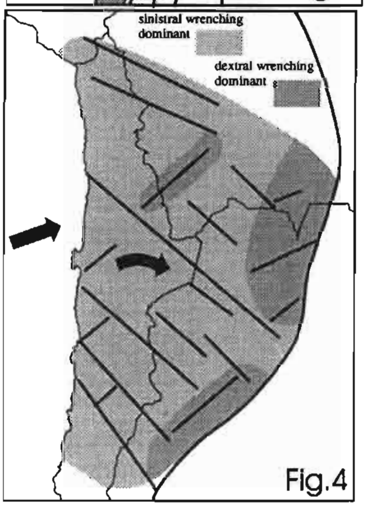

Fig.4

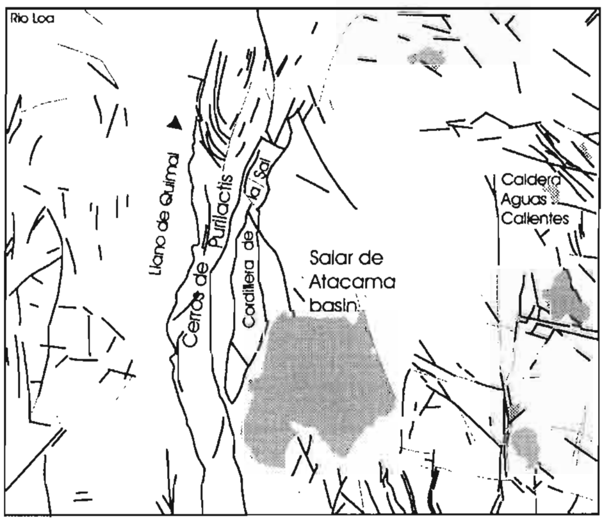

Fig.3a

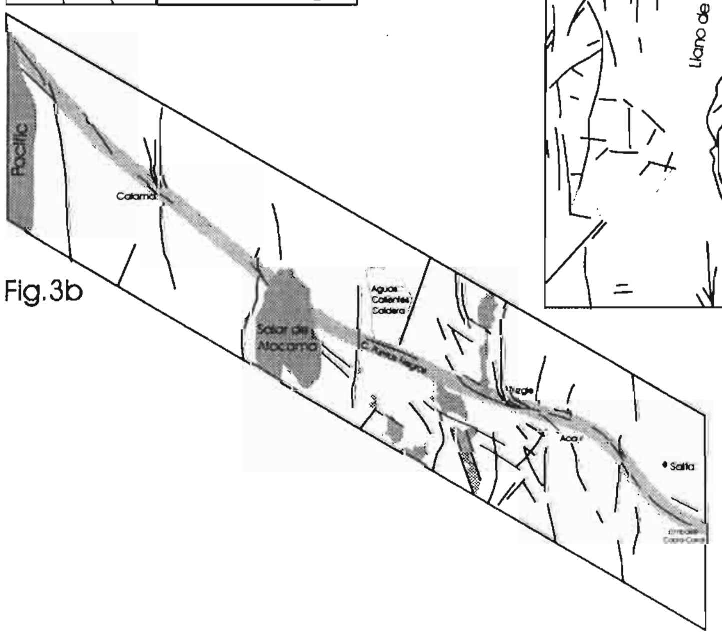

Fig.3b

PROTEROZOIC-LOWER PALEOZOIC TERRANE EVOLUTION IN WESTERN SOUTH AMERICA

Florencio Gilberto ACEÑOLAZA[1], Hubert MILLER[2] and Alejandro José TOSELLI[1]

[1]) Instituto Superior de Correlación Geológica, Universidad Nacional de Tucumán, Miguel Lillo 205, 4000 Tucumán, Argentina; e-mail: insugeo@unt.edu.ar
[2]) Institut für Allgemeine und Angewandte Geologie der LMU, Luisenstr. 37, 80333 München, Germany; e-mail: hubert.miller@iaag.geo.uni-muenchen.de

Applying the concept of exotic terranes in several places of Perú, Bolivia, Argentina and Chile has generated discussions about way and extent of accretional events that occurred in the southern portion of the Proto-Andes around the Proterozoic-Lower Paleozoic.

The initial discussion of a tectogenesis based on autochthonous mobile fold-belts, was followed by ideas emphasizing the fragmentation and collisional criteria of supercontinents at the Western Gondwana margin. These hypotheses interpret the beginning of the break-up of the Rodinia hypothetical supercontinent as a very important fact, when Laurentia moved on, impacting and breaking off terranes into the Gondwana occidental border. This concept of kinematic hypermobility of Laurentia does not agree with several arguments provided by the South-America/Antarctica regional geology. It is well known that the Mid Proterozoic levels (ca. 1.100/800 Ma) are represented by metasedimentary metamorphic and magmatic sequences developing perispherically to the arcaic nuclei, and formed an orogenic cycle (Sunsas/Uruçuan Orogenic Cycle). After this, a new orogenic cycle with different characteristics developed during the Upper Precambrian-Lower Paleozoic (Brazilian and Pampean Orogenic Cycle, ca. 800/520 Ma). The intercontinental relationships provide several data which contribute to the interpretation that the Precordillera-Patagonia terranes originated as parts of a hypothetical platform developed between **S**outh America, **Afr**ica and **An**tártica (SAFRAN platform) and shifted to their actual position just continent-parallel by transform faults, similar to the Liquiñe-Ofqui fault in southern Chile and the San Andreas fault in California (Fig. 1). The collisional events in the Pampean ranges resulted as a consequence of transpressional strike slip movements, being responsible for the S and I type magmatism along these Pampean and Famatinian terranes. The final result of this continent-parallel movement of slices is similar to that of a terrane spreading off from Laurentia, but the generally continuous plate convergence between a Proto-Pacific and a Gondwana plate seems not to be interrupted by a collision of Laurentia or part of it during the Ordovician. The similarity of Early Paleozoic faunas between the Argentinian Precordillera and Laurentia can easily be explained by their propagation through marine or aerial currents.

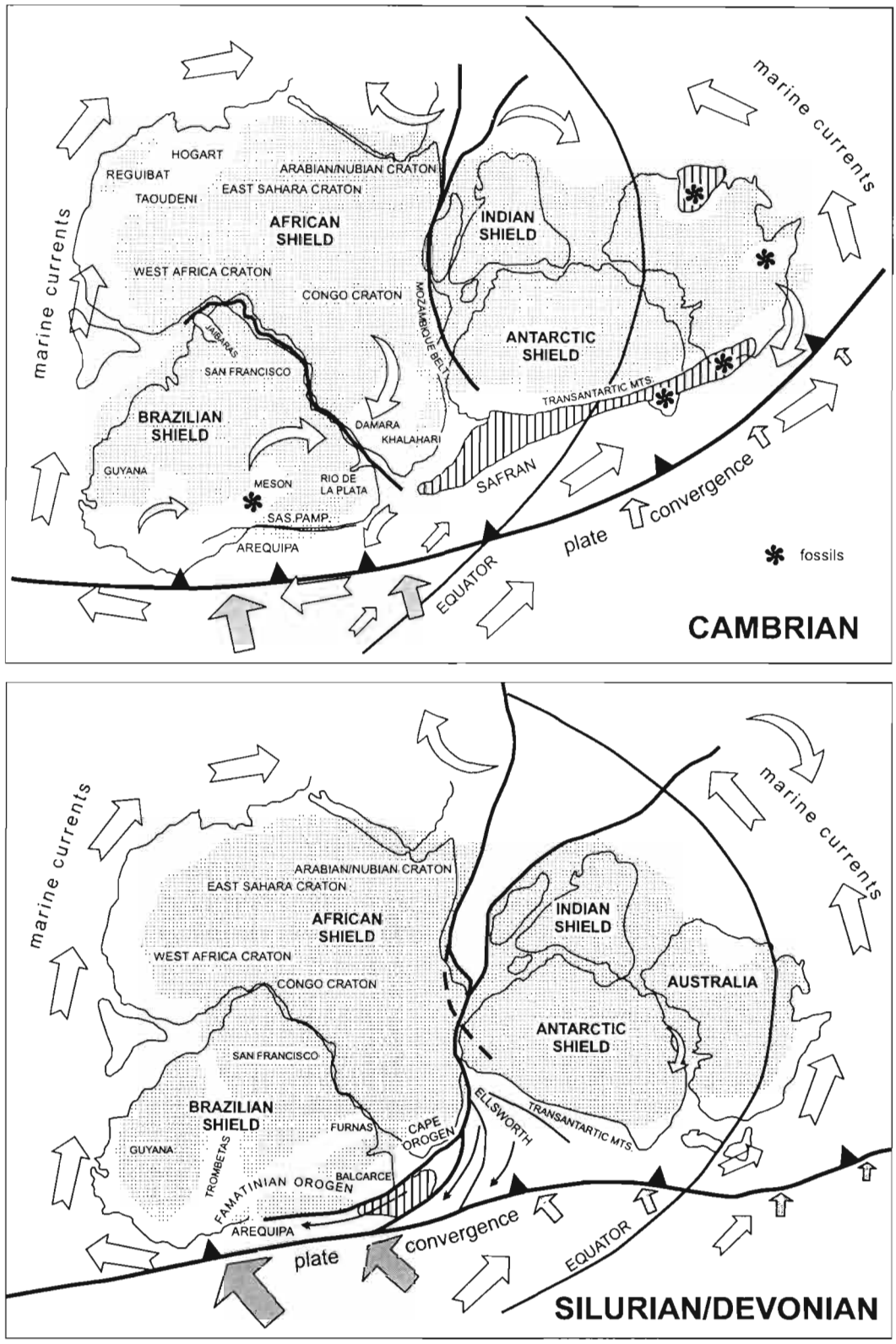

Fig. 1: The position of the SAFRAN terrane in the Cambrian and its way to compose the Precordillera terrane during Silurian/Devonian.

DISCRIMINATION BETWEEN THE VARIOUS AMS PLUNGES FOR THE LOCATION OF MAGMA CHAMBERS BENEATH THE DOLERITIC DYKES OF MAGDALENA ISLAND, SOUTHERN CHILE

Tahar AÏFA (1), Jean-Pierre LEFORT (2) and Francisco HERVÉ (3)

(1) Geophysics, Géosciences-Rennes, Université de Rennes1, CNRS UPR4661, Campus de Beaulieu, 35042 Rennes cedex (France), e-mail: aifa@univ-rennes1.fr
(2) Tectonophysics, Géosciences-Rennes, Université de Rennes1, CNRS UPR4661, Campus de Beaulieu, 35042 Rennes cedex (France), e-mail: lefort@univ-rennes1.fr
(3) Departamento de Geologia, Facultad de Ciencias Fisicas y Matematicas, Universidad de Chile, Dario Urzua 1625, Santiago de Chile (Chile), e-mail: fherve@tamarugo.cec.uchile.cl

KEY WORDS: AMS, magma flow, doleritic dyke, Magdalena island, triple junction, volcano.

INTRODUCTION

The Magdalena island, located Northeast of the Chonos Archipelago (southern Chile) is part of the active fore-arc associated with the subduction of the oceanic floor of the Pacific ocean beneath the South American Plate. It is characterized by many doleritic dykes cutting across the Paleozoic Chonos metamorphic complex, the Tertiary Traiguen volcano-sedimentary formation and the North Patagonian Batholith (Hervé, 1993). Some of these dykes have been dated, suggesting a main dykes emplacement during Miocene time. Most of the ages bracket between 17 and 14 Ma? (whole rock datation), but some others, located close to Pitipalena, are as young as 3.6 or 5.6 Ma (Pankhurst and Hervé, 1994). It is actually suggested that the opening of many of these dykes occurred when the triple junction, resulting from the intersection between the Chile oceanic ridge and the Chile subduction through, was close to the studied area (Lefort et al., companion paper).

The area is also characterized by four main volcanoes, the Monte Melimoyu, the Monte Maca and the Monte Montólat being the biggest of them. They are all Holocene in age and still active.

About 260 cores have been sampled in 14 sites, uniformly distributed on and around Magdalena island, for the AMS study (see e.g. Borradaile and Henry, 1997). Measurements were made using a Schonstedt DMS-1 spinner magnetometer with the Jelinek (1978) procedure. Kmax, Kint, Kmin components of the AMS tensor have been plotted on equal-area projections using the Kamb's contouring procedure (Kamb, 1959). It seems that the quality of the clustering of the results depends on the considered dykes. This is related with the petrography of the dykes which changes from dolerite to lamprophyre. This is supported by the distributions of susceptibilities (2.2×10^{-3}-75×10^{-3} SI) and remanences (15.7×10^{-3}-1 A/m).

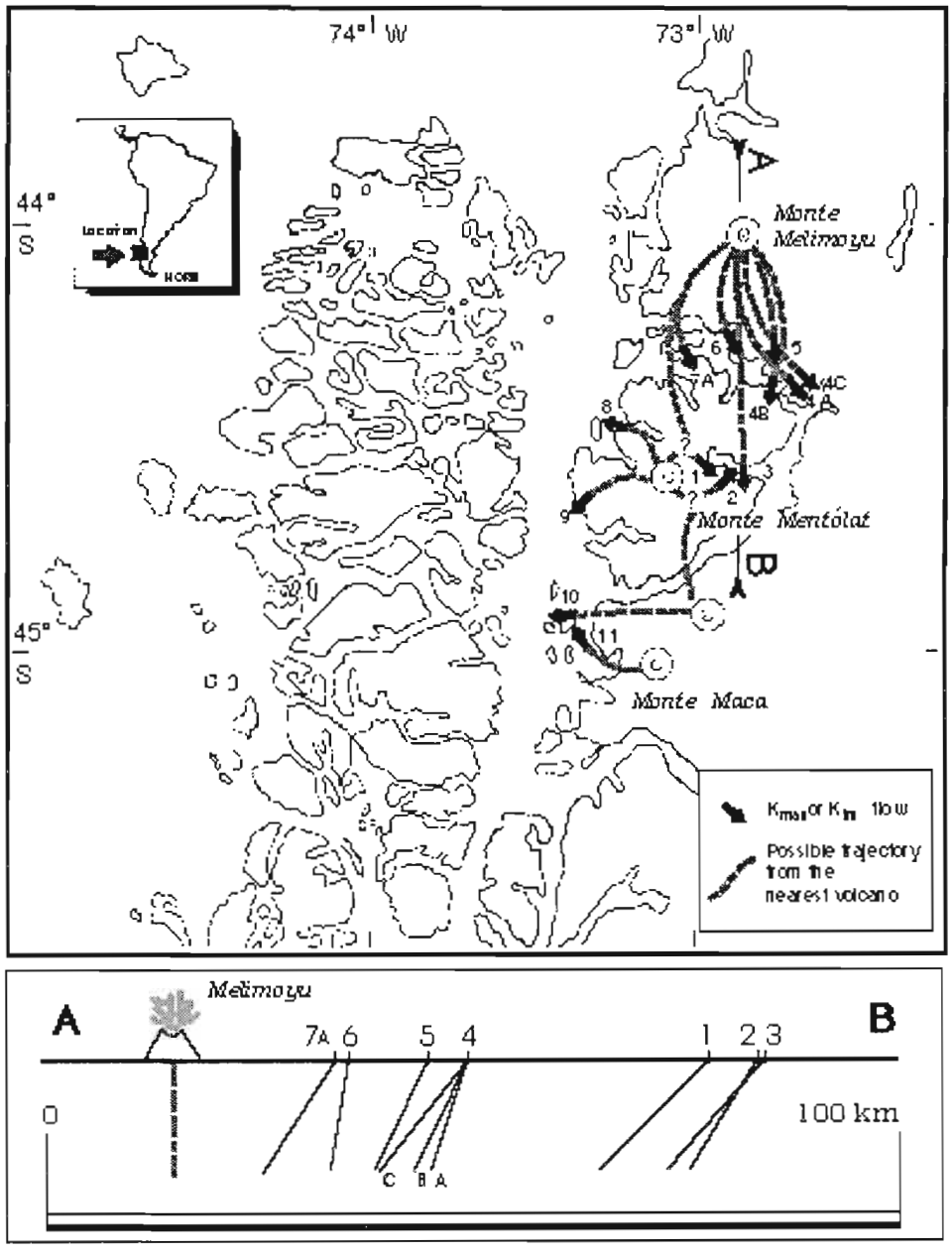

In mafic dykes already studied (less than 60 cm in width), the analysis of the magnetic fabric parameters (Tauxe et al., 1998) shows mainly a prolate shape when the magma flow is not disturbed. On the contrary, in Magdalena island, most of the dykes show an oblate distribution, which could be related with the existence of some disturbance either related with: 1- larger dykes (some are 8-12 m in width), 2- the regional stress associated with the subduction, 3- contemporaneous emplacement of other dykes associated with other magma chambers.

In previous AMS studies, it has been already observed that the Kmax is associated with the vertical or sub-vertical flow direction (Ernst and Baragar, 1992; Mushayandebvu et al., 1995). It has been also shown that the Kmax display, in section, a fanning distribution above the magma chambers (Lefort and Aïfa, 1996; Aïfa and Lefort, submitted). Just above or close to the magma chambers, the Kmax are always vertical or steeply dipping.

At Magdalena island, the Kmax are not necessarily the steepest components of the AMS tensors. In many places the steepest component is given by the Kint. In these places the Kmax is also often shallow dipping. Since, in a dyke, the steepest plunge corresponds necessarily with the flow, we must admit that the regional stress which disturb the flow can be, in certain conditions, associated with the Kmax. It is the reason why the steeppest plunges have been studied as a whole wheither they correspond with a Kmax or with a Kint. We assume that they both correspond with the magma flow.

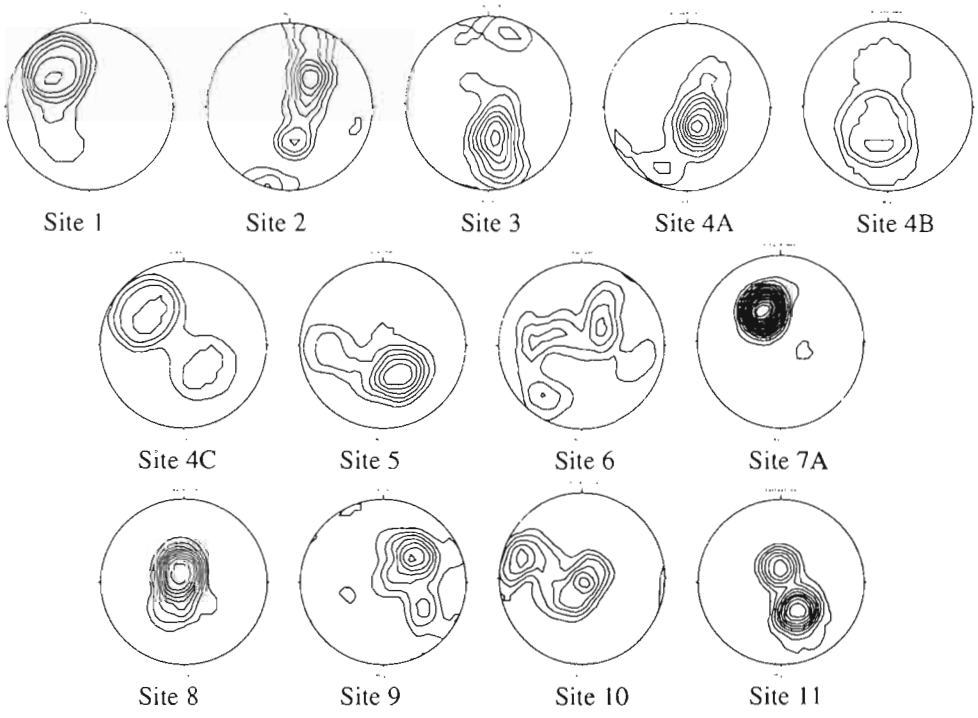

Flow directions computed using Pangea Scientific package (1992).

In these conditions, a clear pattern can be observed on and around Magdalena island; North of the island, 7 or 8 sites show a flow direction rouhgly deeping towards the Melimoyu volcano. If this flow directions are projected on a north south section passing through the Melimoyu volcano, it can be observed that the steepest plunges are closer to a magma chamber located beneath the volcano. East of the centre of the island, 3 or 4 sites show their flow directions pointing the Mentólat volcano. And onshore, south of Madgalena island, two sites show a flow which is towards the Maca or associated volcano. It is interesting to note that the flow directions of the so-called Lower Miocene dykes are dipping towards active Holocene volcanoes. This result suggests that either: 1- the magma chambers associated with the studied dykes have been active until the Upper Miocene or 2- the sampled dykes are Holocene in age.

CONCLUSION

In a classical dyke-volcano pattern (Smith, 1987), the dykes are radiating all around the volcano or its magma chamber. The magma flow itself radiates from this magma chamber. On Magdalena island the dykes are not radiating around the known volcanoes, since they are more or less directly controlled by the indentation of the triple junction along the South American Plate. However the measured flow trajectories seem to follow the control of the magma chambers associated with the Holocene volcanoes. In summary, the dykes orientation and their flow direction are two independant parameters.

All these data suggest that the studied dykes could be younger than the published Lower Miocene radiometric ages.

REFERENCES

AÏFA T., J.P. LEFORT (submitted). Relationship between dip and magma flow in the St Malo dolerite dyke swarm (Brittany, France). Tectonophysics, sp. publ.

BORRADAILE G.J., B. HENRY 1997. Tectonic applications of magnetic susceptibility and its anisotropy, Earth Sci. Rev., 42, 49-93.

ERNST, R.E., BARAGAR, W.R.A. 1992. Evidence from magnetic fabric for the flow pattern of magma in the Mackenzie giant radiating dyke swarm. Nature, 356, 512-513.

HERVE F. 1993. Paleozoic metamorphic complexes in the Andes of Aysen, Chile (West of Occidentalia). First Circum-Pacific and Circum Atlantic Terranes Conference, Guanajuaato, Mexico, Proceedings, 64-65,.

JELINEK, V. 1978. Statistical processing of anisotropy of magnetic susceptibility measured on groups of specimens. Studia Geoph. et Geod., 22, 50-62.

KAMB, W.B. 1959. Ice petrofabric observations from Blue Glacier, Washington, in relation to theory and experiments, J. Geophys. Res., 64, 1891-1909.

LEFORT J.P., T. AÏFA 1996. Origine et structuration de l'essaim nord-armoricain. C.R. Acad. Sci. Paris, 323, IIa, 981-986.

MUSHAYANDEBVU M.F., M.P. BATES, D.L. JONES, 1995. Anisotyropy of magnetic susceptibility results from the Mashonaland dolerite sills and dykes of northeast Zimbabwe, in G. Baer and A. Heimann (Eds.), Physics and Chemistry of Dykes, Balkema, Rotterdam, 151-161.

PANGEA SCIENTIFIC 1992. Spheristat 1 for Windows 3.1, Brockville, Ontario, Canada, 199p.

PANKHURST R.J. and HERVE F. 1994. Granitoids age distribution and emplacement control in the North Patagonian batholith in Aysen (44°-47° S). 7° Congreso Geologico Chileno, Concepcion, Actas, II, 1409-1413.

SMITH R.P. 1987. Dyke emplacement at Spanish Peaks, Colorado. Mafic dyke swarms, in H.C. Halls and W.F. Fahrig (Eds.), Geol. Ass. Can. Sp. Issue, 34, 47-54.

TAUXE L., J.S. GEE, H. STAUDIGEL 1998. Flow directions in dikes from anisotropy of magnetic susceptibility data: the bootstrap way., J. Geophys. Res., 103, B8, 17775-17790.

LATE CRETACEOUS FORE-ARC EXTENSION IN NORTHWEST PERU: GEODYNAMIC IMPLICATIONS

Antenor M. ALEMÁN(1)

(1) 2807 Stoney Wood Houston, TX 77082 antenor@swbell.net

KEY WORDS: Northwest Peru, Paita Basin, oblique convergence, Late Cretaceous NE-SW extension, and alluvial-fan sedimentation.

INTRODUCTION

Northwest Peru was the loci of four distinct Cretaceous basins each characterized by unique tectonic setting and facies controlled by the volcanic arc activity and the Paleozoic basement (Fig.1 and 2). The Lancones/Celica Basin recorded continuous sedimentation and the passage from onlapping Early Albian shallow-water to anoxic carbonate shelf deposition (Pananga and Muerto Fms.) to Late Albian/Early Campanian volcaniclastic deep-sea fan sedimentation (Copa Sombrero Gp.) coeval with volcanic arc extension (Morris and Alemán, 1975, Jaillard *et al.*, 1996). Volcaniclastic flysch deposition was coeval with basic volcanism and cessation of arc activity was marked by the Paleozoic-derived fluviatile facies abrupt facies change (Tablones Fm).

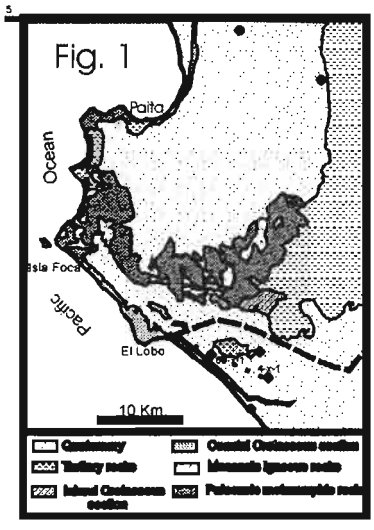

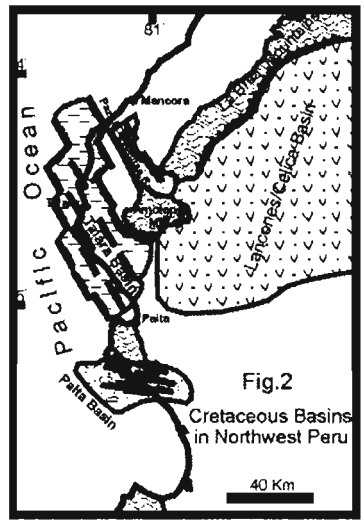

The Pazul-Coyonitas Basin was preserved in a NW-SE oriented graben, consisted of thick Campanian to Lower Maastrichtian rocks. Fluviatile sandstones and conglomerates (Sandino Fm.) locally onlap Paleozoic rocks which in turn is overlain by deepwater shales (Redondo Formation). A regressive fluvio-deltaic siliciclastic unit (Monte Grande Fm.) marked the top of the Cretaceous sequence.

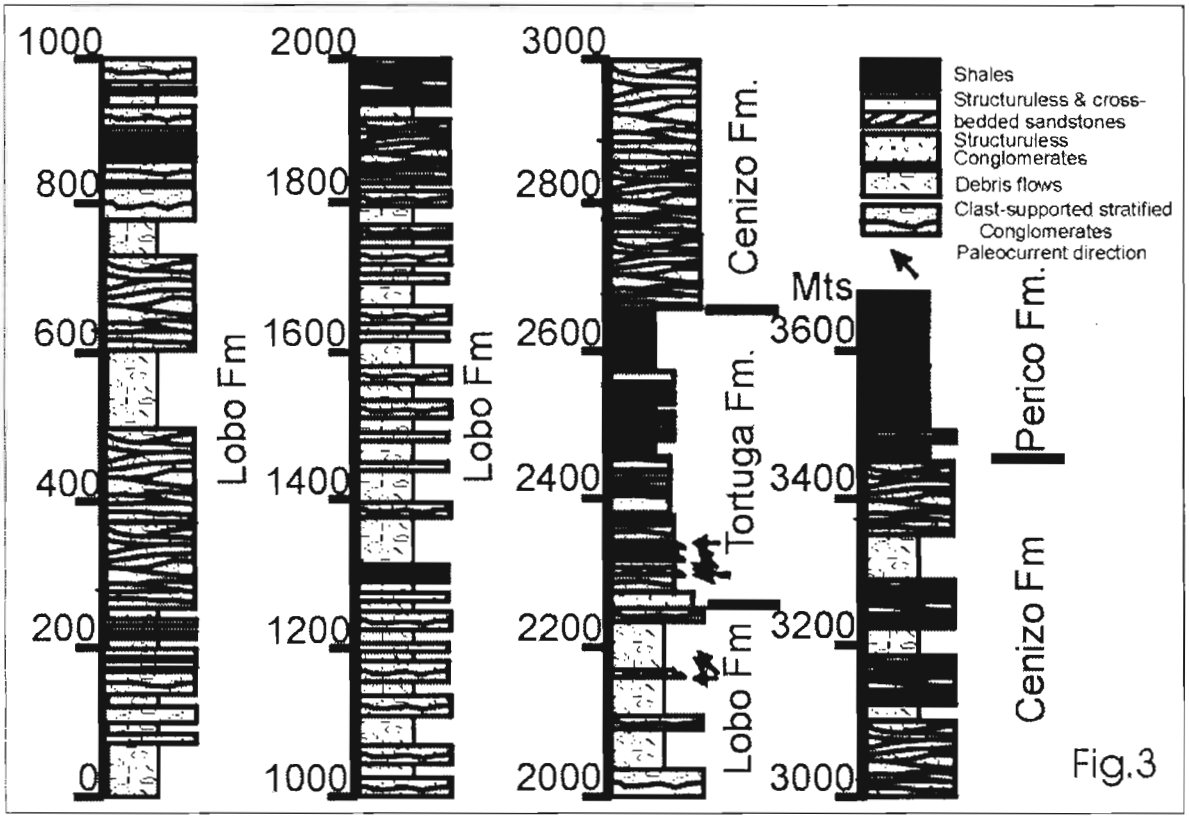

The Albian carbonate sequence (Gigantal, Pananga and Muerto Fms.) in the Talara Basin was also preserved in a series of isolated grabens prior to regional Albian to Santonian uplift. A new extension episode, with similar stratigraphy than the Pazul-Coyonitas Basin, was followed by a sagging phase with deposition of thick shallow muddy shelf facies (Petacas Fm.).

NE-SW Maastrichtian extension in the Paita Basin was accompanied by a thick siliciclastic deposition in rapidly subsiding grabens. The NW dipping sequence was cut by several NW verging normal faults. Uplifted Paleozoic low-grade metamorphic rocks were the main source and provenance of siliciclastics. Complex rapid facies and thickness change permit to distinguish three distinct sections. The Coastal section is more than 3600 m and crops out along the coast for a distance of 12 km. This section includes the Paita Group overlain by the Perico formation. The Paita Group consists of varicolored clast supported breccias, mud-supported breccias, and stratified conglomerates of the Lobo Formation. This unit is overlain by 425 m thick dark gray sandstones, pebbly mudstones and varicolored mudstones of the Tortuga Formation, which in turn is overlain by 775 m red mud supported breccias interbedded with red mudstones of the Cenizo Formation. Finally, the

uppermost Perico Formation is made up of more than 200 m of well-sorted sandstones with abundant marine fauna sometimes onlapping Paleozoic rocks.

The Inland section crops out 7 to 20 km east of the coast (Fig.3 and 4). The basal Petacas Formation consists of gray micaceous shales interbedded with sandstones and fossiliferous limestones. This formation is overlain by 51 meters of fossiliferous limestones of the Yuca Formation which in turn is transitionally overlain by sandstones and interbedded limestones of the Perico Formation. In subsurface,

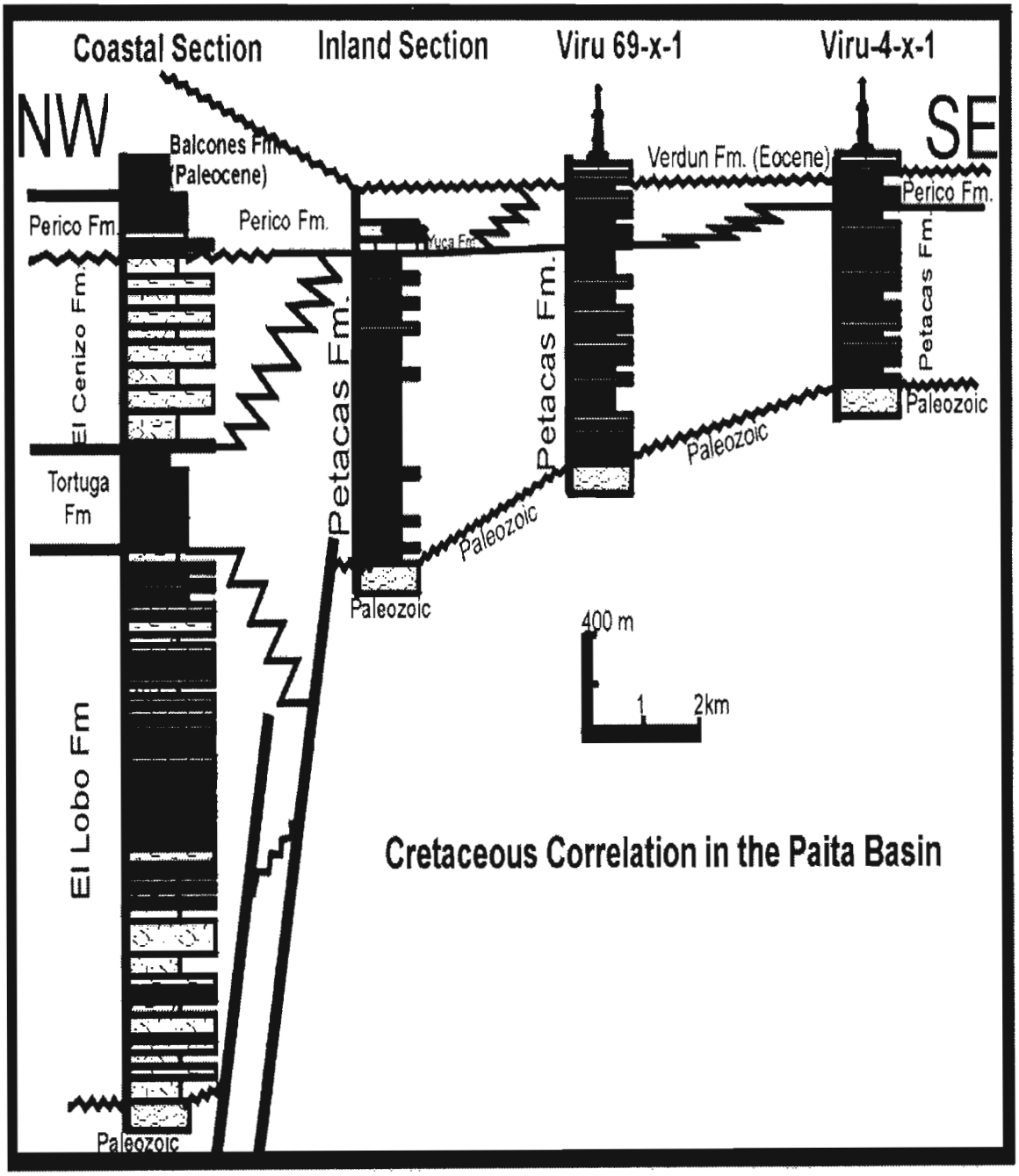

south of the inland section, two wells penetrated thick shales with subordinated sandstones of the Petacas Formation overlain by interbedded calcareous sandstones and shales of the Perico Formation (Fig. 3 and 4).

CONCLUSSIONS

A Middle Cretaceous back-arc extension postulated to explain the unique geochemistry of the thick volcaniclastics of the Casma Group (Atherton et al, xxx) has also been ascribed for the Copa Sombrero Group volcaniclastic flysch sequence (Morris and Alemán, 1975). The Lancones Basin extensional geometry was later modified by rotation of the Tahuin/Amotape Terrane with no evidence for the short-lived Mochica compressional deformation (Myers, 1974, Mourier, et al.,1988). However, the Late Cretaceous Peruvian compressional deformation in Northwest Peru was well documented.

This compressional deformation was marked by an abrupt change in facies and provenance of the Tablones Formation quartz-rich fluviatile sandstones and conglomerates. Contemporaneous with this event, a series of extensional basins were formed almost orthogonal to the Amotape/Tahuin, Paita and Illescas uplift. Formation of these basins are ascribed to strain partitioning during oblique convergence between the Farallon and South America plates, which caused extension in the fore-arc and compression in the back-arc and retro-arc.

REFERENCES

Atherton, M. P., and Webb, S., 1989, Volcanic facies, structure, and geochemistry of the marginal basin rocks of central Peru: Journal of South American Earth Sciences, 2, 241-261..

Jaillard, E., Ordoñez, M., Bengtson, P., Berrones, G., Bonhomme, M., Jimenez, N., and Zambrano, I., 1996, Sedimentary and tectonic evolution of the arc zone of southwestern Ecuador during Late Cretaceous and Early Tertiary times: Jour. South American Earth Sciences, 9, 131-140.

Morris, R. M., and Alemán, A. M., 1975, Sedimentation and tectonics of Middle Cretaceous Copa Sombrero formation in Northwest Peru:, Bol. Soc. Geol. Perú, v.48, 49-64.

Mourier, T., Laj, C., Megard, F., Roperch, P., Mitouard, P., and Farfan-Medrano, A., 1988, An accreted continental terrane in northwestern Peru: Earth and Planetary Science Letters, 88, 1-11.

Myers, J. S., 1974, Cretaceous stratigraphy and structure, Western Andes of Peru between latitudes 10°-10°30': American Association of Petroleum Geologists, 58, 474-487.

TRANSTENSIVE TECTONIC COMPLICATIONS IN THE WESTERN BORDER OF THE ECUADORIAN ANDES: THE EXAMPLE OF MINDO

A.ALVARADO [1], S. BES DE BERC [2], J.F. DUMONT [2], M. SEBRIER [3] y O. BELLIER [3]

(1) Instituto Geofísico – Escuela Politécnica Nacional Casilla 2759, Quito-Ecuador (geofísico@accessinter.net)
(2) IRD, Apartado 17-12-857, Quito-Ecuador
(3) Bat 509 Université de Paris-sud, 91405, Orsay-Francia

KEY WORDS: transtensive, Mindo, deformation.

INTRODUCTION

The Mindo Basin, in the western border of the Ecuadorian Andes, is located 35 km west of Quito, over the large Santo Domingo-Los Bancos alluvial fan (Figure 1). This fan, along with other similar structures, characterizes the western cordillera foothills.

GEOLOGY

The geology of this region is little known or even unknown. It is mainly determined from the alluvial fan deposits. This deposit is present for over 20 km in the direction parallel to the cordillera, and 500 km in the transversal direction. This alluvial fan consists of two sources that form juxtaposed cones. To the south the source are the Toachi River sediments that extend towards the Santo Domingo region, and to the north the source are the Blanco and Guayllabamba Rivers that extend to the San Miguel de los Bancos region.

The fan consists of blocks, gravel, sand, and clasts from a volcanic origin. The grade of alteration is variable, but in general, it is high due to the presence of hot and humid weather. The thickness of the sediments is unknown. Younger ash layers that are up to 7 m thick cover these materials.

The age of the fan is unknown, but it can be estimated assuming that the major and more recent Andean uplift occurred during Lower to Mid Miocene. This uplift was followed by a period of erosion in the Upper Miocene (Ego, 1995). This erosion could be a reason for the formation of these alluvial fans, dating them to the Upper Miocene. Subsequently, they received sediments from Plio-Quaternary volcanic deposits.

MORPHO-TECTONIC ANALYSIS

After an aerial photograph and terrain modeling analysis, we can see that the Mindo Basin is a depression limited with vertical walls that can reach 400 m. On these walls, sedimentary deposits that form the fan are exposed. Their approximate shape is rectangular with their maximum axis in NNE-SSW direction.

The main drainage in this area is the Mindo River that runs from East to West. On the western border of the basin, the Canchupi River and the Saguambi "estero" are captured by the Mindo River as these rivers descend towards the depression (Figure 1). In the same zone we can see a scarp with a NE-SE direction which makes up the eastern limit of the basin. This scarp has a very important erosion rate. It can be followed to the Hacienda El Carmelo (Figures 1 and 2).

A well-defined scarp with a NE-SW direction characterizes the western limit of the basin. On the road that descends to Mindo, it was possible to take microtectonic measurements that showed strike-slip dextral movement, although morphology also suggests a normal movement component (Figure 2). The western scarp is crossed by a NNW-SSE lineament that displaces it a little in a dextral sense. Its prolongation towards the east is not clear but we can see some anomalous drainage and a more eroded scarp.

Following the Mindo River, near Finca La Palma, a small plane is observed, limited to the east by a NNW-SSE scarp with triangular facets. These suggest a normal movement. There is also a sinestral drainage control. This lineament can be followed to the south by the southern limit of the basin. In this zone a sinestral movement component is suggesting (Figure 2).

The Northern border of the basin shows an eroded scarp with a WNW-ESE direction, parallel to the main drainage of the fan (Figure 2). Movement markers could not be found in this zone. It could be a erosion scarp or an older and inactive structure.

FAULT KINEMATICS AND STRESS STATE ANALYSIS

Measurements were taken over two periods. In the first phase, they were taken in three points, two of them in conglomerate deposits (Mindo 1,2, Figure 1), and the third one in basement (Mindo 3,

Figure 1). This set of data was regrouped according to the sedimentary environment, and afterwards cinematic analyses were done with the data from the basement and the conglomerates in order to obtain only one tensor.

The inversion results show a very complex stress state. For extension, three tensor directions were obtained: N293 (compatible with the three points), N171 (compatible with points 1 and 2), and N35 using the three point data. Chronology observed in the field shows that this last direction is older than the N171 direction.

For compression, only two tensor directions were obtained: a unreliable N215 (only three families of planes were used for the calculation), and N290 (using the three point data). During the second phase, measurements were taken in point Mindo 4 in the conglomerate. This point shows a compression tensor that was added to first phase data giving a compression tensor of N114.

DISCUSSION

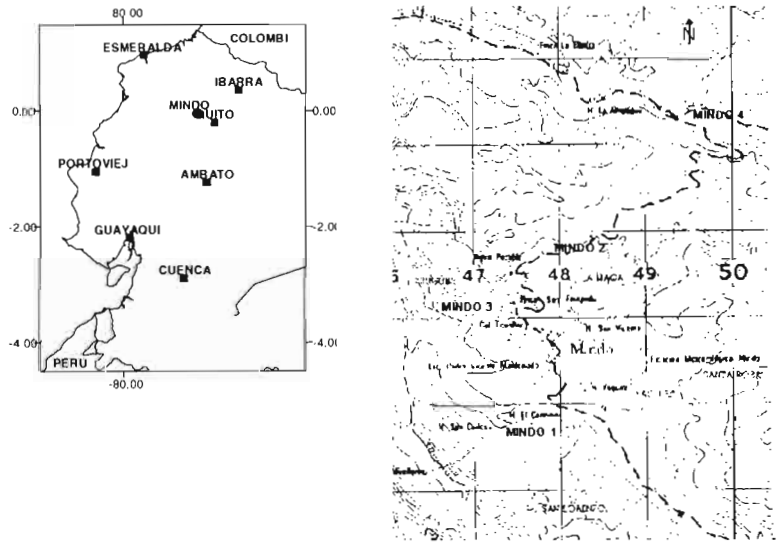

Figure 1. Mindo basin location. Microtectonic measure stations are named as Mindo 1,2,3 y 4.

In the interpretation of this data a few questions have been proposed: how the basin was formed, and how a pattern so complex fits into this scheme. This suggests the possibility of different periods of formation. Because of this, we offer an evolutionary model considering all data available.

In order to form the basin, we suppose that there was a system of transtension where would work the North and South borders of the basin. This transtensive system would permit the basin to open with perpendicular normal faults in which the evidence would be seen in western and eastern fault scarps (Figure 3a). On the other hand this opening would generate an extension in the direction NW-SE and NNW-SSE that could correspond to the extension

tensors determined later inversion. While the basin was opening, the fault located in the western border prolongated to the north. This would form a triangular block with a southern sinestral fault, reducing the activity of the East and North borders. This would lead us to obtain the scheme that we observe currently (Figure 2). This new system permits the ejection of the block to the north between the fault of direction NNE-SSW and NNW-SSE (Figure 3b). For this new state and later to calculate the tensor, we see that there exists a compression with a direction of N114 degrees.

The significance of the direction of this tensor can be explained, by a variation of the regional tensor direction or by a local tensor that mechanically adjusted the system of observed faults. By now we think that the second option is better because we have no evidence of recent variations in the field of regional forces (Ego,1995).

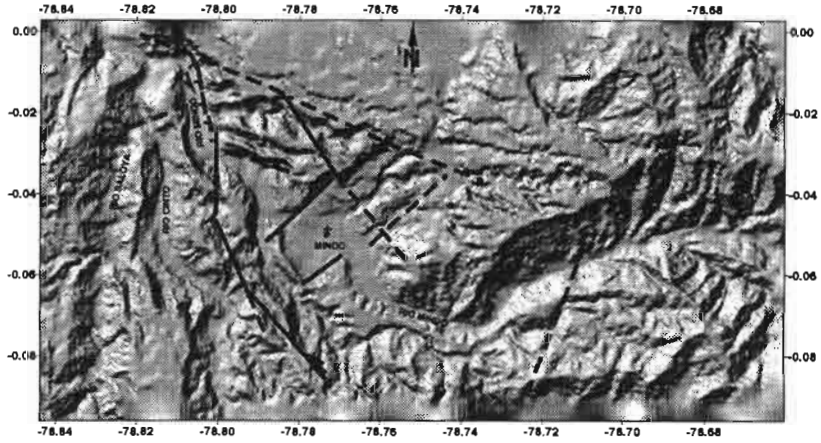

Figure 2. MNT with the main alignements including those observed in aereal photographs.

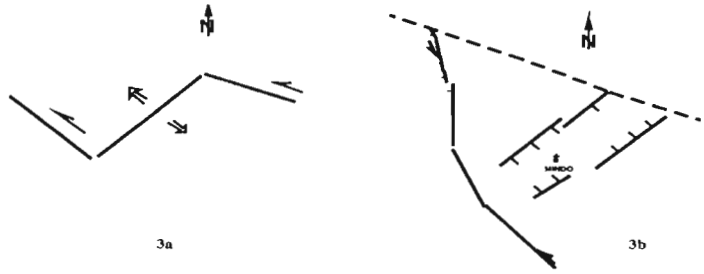

Figure 3.Schematic model proposed for the formation of the Mindo basin

REFERENCES

Ego F. 1995, Accommodation de la convergence oblique dans une chaîne de type cordilleraine: les Andes d'Equateur. Thèse, Université de Paris-Sud, centre Orsay. 167.

AFTERSHOCKS OF CARIACO-VENEZUELA EARTHQUAKE (MW=6.9), JULY 9, 1997: SEISMOLOGICAL ANALYSIS USING A LOCAL NETWORK

Patricia ALVARADO[1,2], Arturo BELMONTE[2,3], Michael SCHMITZ[4] and Enrique GAJARDO[5]

(1) Universidad Nacional de San Juan, Dpto. Geofísica y Astronomía, Facultad Ciencias Exactas, Físicas y Naturales. Meglioli 1160 S (5400) Rivadavia, San Juan, Argentina, palvarad@unsj.edu.ar
(2) Departamento Geofísica, Universidad de Chile. Blanco Encalada 2085, Casilla 2777 Santiago, Chile.
(3) Free University of Berlin, belmonte@geophysik.fu-berlin.de
(4) Fundación Venezolana de Investigaciones Sismológicas (FUNVISIS), PO-Box 76880, Caracas, 1070A, Venezuela, mschmitz@funvisis.internet.ve
(5) FUNVISIS. PO-Box 76880, Caracas, 1070A, Venezuela, gajardo@telcet.net.ve

KEY WORDS: Seismotectonics, Shallow earthquake, Cariaco, EL PILAR fault

INTRODUCTION

Northeastern Venezuela was struck by a M_w=6.9 earthquake on July 9, 1997 at GMT 19:24:10.5. The main shock was located at 10.543°N and 63.515°W with a focal depth of 9.4 km (FUNVISIS et al., 1997). This earthquake destroyed and severely damaged several schools and building in the towns of Cariaco and Casanay; a six-story building collapsed in Cumaná, 75 km west of the epicenter. The event reach an intensity of VIII on the Modified Mercalli Scale (FUNVISIS et al., 1997) arising 73 deaths and several hundreds of injured.

The Cariaco earthquake showed a surface rupture associated with the El Pilar fault which is part of the large continuous system of right lateral strike-slip faults located in the northeastern edge of the continent (Rod, 1956). Along this plate boundary the relative movement of the Caribbean and South America tectonic plates reaches some 2 cm/year (DeMets, 1993). Therefore, several destructive earthquakes shook this region in 1530, 1766, 1853 and 1929 (Grases, 1979; FUNVISIS et al., 1997). The 1997 Cariaco earthquake together with the 1929 Cumaná earthquake (Paige, 1930), are the largest events to strike the northeastern Venezuela during this century; both events have occurred along the El Pilar fault. Horizontal displacements of an average of 0.25 m associated with a dextral strike-slip movement of the El Pilar fault segment were observed at several points (fig. 1) after the 1997 Cariaco earthquake.

Fig. 1. Surface rupture observed in a road associated with a dextral strike-slip movement of the El Pilar fault segment. Other points located along this fault segment showed similar seismic displacements.

SEISMOLOGICAL OBSERVATIONS

In order to record the aftershocks, a deployment of six seismological stations belonging to the Geophysical Department - University of Chile was installed in the epicentral area. Beginning ten days after the mainshock, this local network monitored during two weeks the seismic activity of the region covered by the Buena Vista lagoon. The sites selected were Los Apamates, Chamariapa de Güiria, Caldera, Pica de La Maravilla, Campoma and Pantoño. The seismographs consisted of portable EDA instruments (PRS-4 Scintrex) equipped with 1 Hz vertical component sensors (Mark L4-C products) and one of them connected to a 1 Hz three component sensor (Lennartz); for operation a trigger mode was selected. The absolute time was downloaded to the seismographs using a portable clock (Nanometrics 502F) which synchronizes its internal time with a reference signal (broadcasted by different centers worldwide) using the Lithoseis software.

The array of University of Chile was part of a main temporary seismological network of 43 stations called RESICA ("Red Sismológica Cariaco"), with participation of FUNVISIS and University of Oriente - UDO (Venezuela), Northwestern University (Illinois, USA), German Task Force for Earthquakes, GFZ Potsdam and Bauhaus University Weimar (Germany) and University of Chile (Chile and CERESIS).

The University of Chile local network has recorded more than 300 aftershocks. The seismic activity was determined using Hypo71 (Lee y Valdés, 1985). A set of 187 events was selected with rms (root mean square) less than 0.25. Both, the hypocentral location of the earthquake (FUNVISIS et al., 1997) and the aftershocks recorded with this portable array, are associated with a fault plane solution related to the El Pilar fault segment. The epicentral distribution of the aftershocks showed a cluster localized to the northern end of a near east-west straight 60 km long segment and width of about 15 km. Their focal depths were less than 20 km with the main seismic activity concentrated in the uppermost 10 km. The seismic activity defines a plane with an approximately 60° dip to the north which coincides with

the location of the main shock (figs. 2, 3). The results obtained are in close agreement with other studies of the FUNVISIS and UDO (Romero et al., 1998).

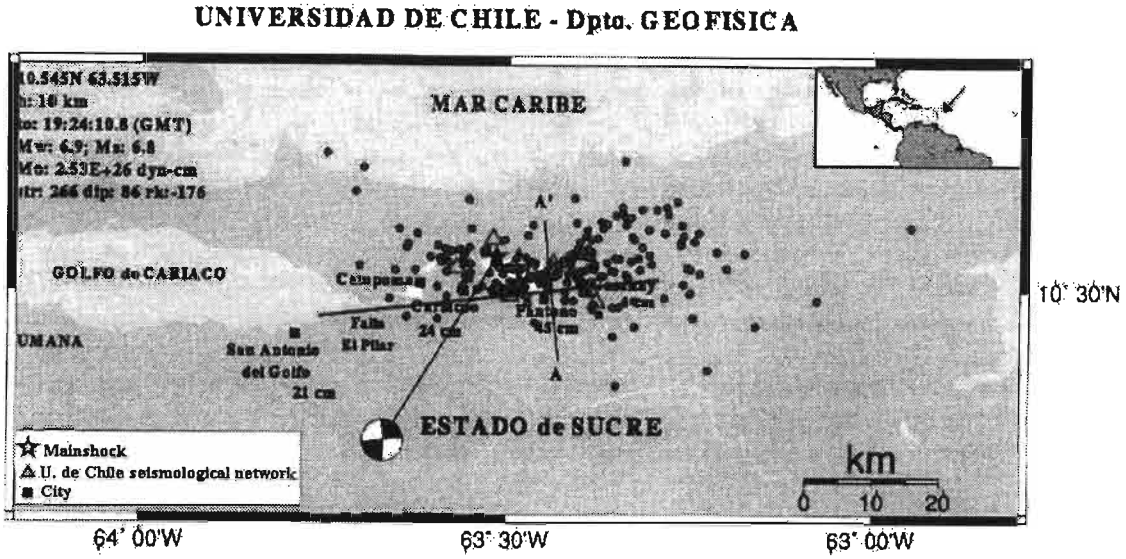

Fig. 2. Aftershocks recorded between July 18-31, 1997 by University of Chile seismological network. Six instruments installed around Buena Vista lagoon detected more than 300 events. A straight line connects the points where the surface rupture was observed. The epicenters are distributed mainly to the north of the surface rupture line, defining a region of 60 km lenth in east west direction and 15 km in width (see the profile A-A´ in *figure 3*).

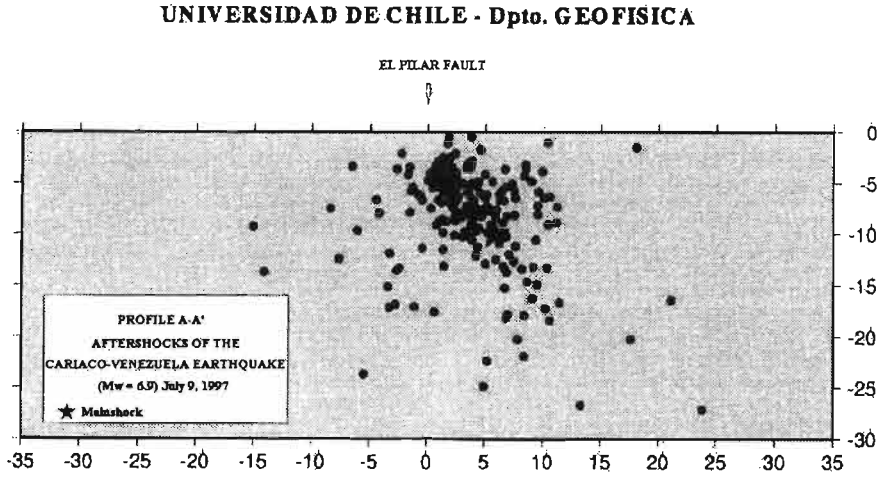

Fig. 3. The focal depths of the aftershocks are distributed down to 20 km but the main activity is located in the upper 10 km. The events define a plane associated with the El Pilar fault segment, which dips approximately 60° to the north.

CONCLUSIONS

The 1997 Cariaco earthquake, together with the 1929 Cumaná earthquake, is the most important shock occurred in this century in eastern Venezuela. Both events are associated to the El Pilar fault. The evidences for this earthquake indicate a dextral strike-slip movement associated to the El Pilar fault segment with a surface rupture of ~25 cm. Both, the hypocentral location of the main shock and the aftershocks determined using the data of the University of Chile local network, are located on a plane that dips some 60° to the north. The aftershock spatial distribution indicates a location along a 60 km long east

west line to the north of the El Pilar fault with about 15 km in width. The seismic activity is mainly concentrated within the upper 10 km, although there are aftershocks recorded down to 20 km in depth.

Evidences for this earthquake emphasizes the importance of the shallow seismicity in order to assess the seismic hazard to the northeastern of Venezuela. The next step to be realized will be the data integration with the other groups of RESICA.

Acknowledgments

This study was supported by grants of the Departamento Geofísica-Universidad de Chile, Centro Regional de Sismología para América del Sur (CERESIS) and FUNVISIS to the field work. We are grateful to Universidad de Oriente, FUNDAINCENDIOS and Defensa Civil de Venezuela for their logistical help. We specially thank Jaime Avendaño, Victor Díaz (UDO), Francisco Rodriguez (ULA), Sergio Barrientos and Mario Pardo (U de Chile) for their support.

REFERENCES

DeMets, C., 1993. Earthquake slip vectors and estimates of present-day plate motions, Journal of Geophysical Research, 98, 6703 - 6714.

FUNVISIS, IMME-UCV, UDO, ACV, CAV and CI-Sucre, 1997. The July 9, 1997, Cariaco, Eastern Venezuela Earthquake. EERI-Newsletter, Vol. 31 (10), EERI Special Earthquake Report, 1-8.

Grasses, J., 1979. Terremotos destructores en el Oriente de Venezuela, Delta del Orinoco y regiones adyacentes. Reporte técnico para el Instituto Tecnológico Venezolano del Petróleo -INTEVEP-, Caracas, Venezuela.

Lee, W. H. K. and M. Valdés, 1985. Hypo71PC: A personal computer version of the HYPO71 location program.

Paige, S., 1930. The earthquake at Cumaná, Venezuela, January 1929. Bulletin of the Seismological Society of America, 20, 1-10.

Rod, E., 1956. Strike-slip faults of northern Venezuela. AAPG Bulletin, 40, 457-476.

Romero, G., Audemard, F., Schmitz, M. and RESICA Working Group, 1998. Seismological aspects and fault characteristics of the July 9, 1997 Cariaco earthquake, eastern Venezuela. IX Venezuelan Geophysical Congress, II Conference on the Latin American Geophysical Union, Caracas, October 26 - 30, 1998, 5 pp.

EVOLUTION OF DOMEYKO RANGE, NORTHERN CHILE

Alejandro AMILIBIA (1), Francesc SÀBAT (2), Guillermo CHONG (3), Josep Anton MUÑOZ (4), Eduard ROCA (5) and Antonio RODRIGUEZ-PEREA (6)

(1) Universitat de Barcelona. Dpt. de Geodinàmica i Geofísica. Facultat de Geologia, 08028 - Barcelona (Spain). amilibia@geo.ub.es
(2) Universitat de Barcelona. Dpt. de Geodinàmica i Geofísica. Facultat de Geologia, 08028 - Barcelona (Spain). sabat@geo.ub.es
(3) Universidad Católica del Norte. Av. Angamos 06010. Antofagasta (Chile). gchong@socompa.cecun.ucn.cl
(4) Universitat de Barcelona. Dpt. de Geodinàmica i Geofísica. Facultat de Geologia, 08028 - Barcelona (Spain). josep@geo.ub.es
(5) Universitat de Barcelona. Dpt. de Geodinàmica i Geofísica. Facultat de Geologia, 08028 - Barcelona (Spain). eduard@geo.ub.es
(6) Universitat de les Illes Balears. Dpt. de Ciencies de la Terra. Carretera de Valldemossa km 6,5. 07071 - Palma de Mallorca (Spain). dctarp0@ps.uib.es

KEY WORDS: Inversion, strain partitioning, strike-slip, oblique convergence.

INTRODUCTION

Northern Chile is an ideal area to study structures resulting from oblique convergence in a subduction setting. In that way, strain can be partitioned in orogen-normal and orogen-parallel displacement structures. From one hand, plate kinematics studies have proposed a left-lateral oblique subduction from 153 to 70 Ma and a right lateral oblique subduction since 70 Ma (Scheuber et al., 1994). From the other hand, both strike slip faults and contractional structures have been described in this area. For instance Scheuber and Andriessen (1990) documented Jurassic and early Cretaceous sinistral displacement along Atacama fault zone and Chong (1977) and McElderry et al. (1996) documented Cenozoic folds and thrust faults in Domeyko Range.

Domeyko Range is part of Precordillera of Northern Chile (Fig. 1). During Jurassic this area was located in a back-arc setting which has evolved to a fore-arc setting in the present as the arc migrated eastward. The structure of Precordillera has been extensively described as an strike-slip system (Reutter et al. 1991; Reutter et al. 1996; Lindsay et al. 1996).

In the present paper we outline the evolution of the Domeyko Range underlying the following two aspects. 1) Domeyko Range results from (Cretaceous and) early Cenozoic inversion of Jurassic extensional basin. 2) Most structures in Domeyko Range are contractional.

STRUCTURE

A preliminary section across Domeyko Range (A-A', Fig. 2) show from east to west the following features. An extensional fault bounding uppermost Paleozoic rocks to the east and Mesozoic rocks to the west. Triassic to lower Cretaceous Mesozoic rocks of the eastern slope of the range shows open folds. Fold axes trend N-S and are sub-horizontal. The westernmost limb of these folds is vertical and east facing. The core of Domeyko Range is constituted by an asymmetric pop-up structure built-up by high angle thrust faults, where uppermost Paleozoic rocks outcrop. Domeyko Range is obliquely crossed by a late, extensional right-lateral fault affecting Miocene rock and uppermost Cenozoic sediments. Jurassic rocks outcropping at the western slope are deformed by tigh west facing folds showing both normal and overturned limbs. Fold axes trend N-S and are sub-horizontal. Jurassic rocks are thrust up to the west on lower Cenozoic rocks, which are slightly folded. Oligo-Miocene sediments overlap the thrust fault and folds. Western of the main range several outcrops (as B-B´ and C-C´ transverses) show folds on late Palaeozoic to Jurassic rocks which are overlapped by moderately to steeply west-dipping lower Cenozoic rocks.

Most of these structures are coherent with an early Cenozoic east-west, orogen-normal shortening. Moreover, extensional faults as the one at the eastern end of cross-section A-A´ and strike-slip faults as the one crossing the range are also present.

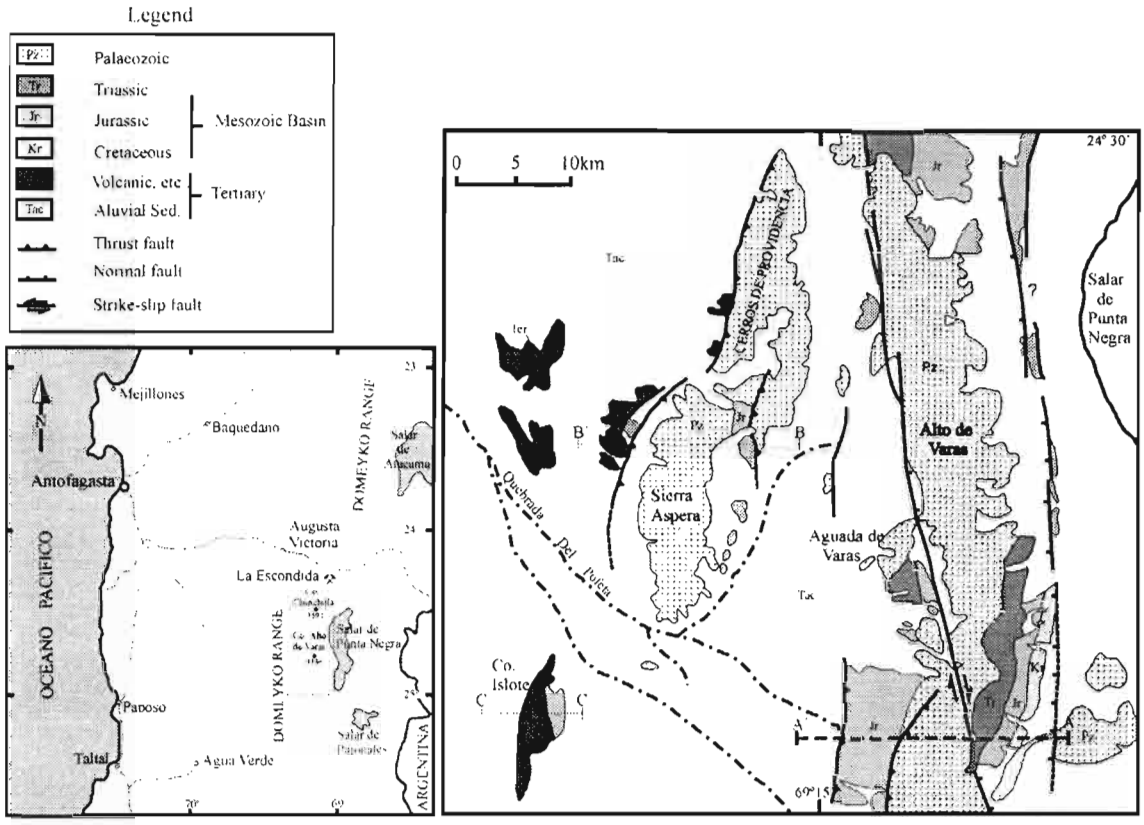

a) b)

Fig. 1 - a) Location map, **b)** Simplified geological map, showing location of A-A´cross section (Fig.2) and B-B´, C-C´transverses.

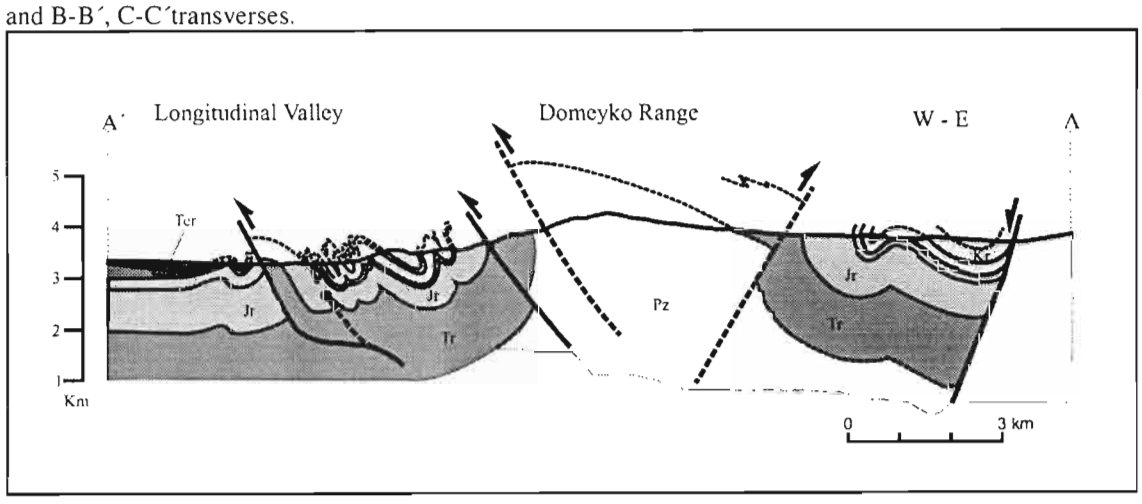

Fig. 2 – Geological section across Domeyko Range. Same legend as in Fig. 1.

EVOLUTION

Prinz et al. (1992) shows the geometry of the Northern Chile Triassic-Jurassic back-arc basin. Depocenters are N-S arranged and located at the eastern part of the basin, which is asymmetric. We suggest that the extensional fault at the eastern end of cross-section A-A´ correspond to the master extensional fault of this back-arc basin (Fig. 3). After comparing the relative sea-level changes in northern Chile with global, Ardill et al. (1998) concludes that late Jurassic sea level lowering corresponds to regional tectonics. We suggest that this sea level lowering (early Cretaceous continental sedimentation and late Cretaceous hiatus) be related to a first stage of contraction and basin inversion. Age of intrusives in Domeyko Range and relationships between rocks of different ages and contractional structures show that main inversion took place during latternost Cretaceous and Early Cenozoic. Purilactis sediments present

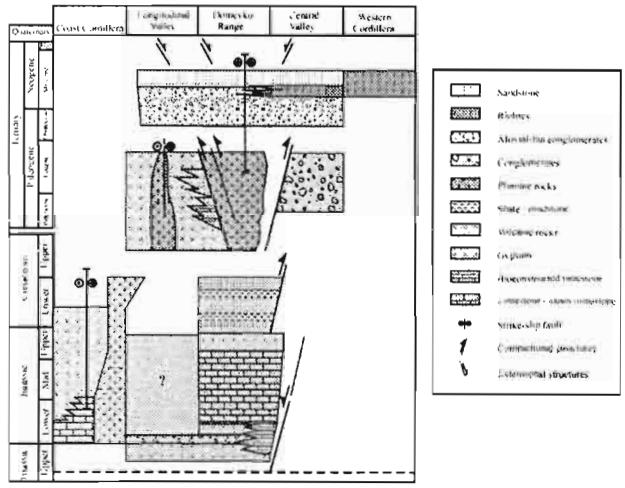

only to the east of Precordillera and Chile-Alemania volcanic rocks limited to the west are contemporaneous with Precordillera uplift related to the main stage of inversion. Later on post-Miocene right-lateral displacement of several kilometres took place along the strike-slip fault crossing the Range.

Fig. 3 – Chronostratigraphic diagram.

DISCUSSION AND CONCLUSION

The main conclusion is that most structures in Domeyko Range are contractional and correspond to the (Cretaceous and) early Cenozoic inversion of a Triassic-Jurassic extensional basin.

Because during inversion period convergence was oblique, two hypotheses can be considered. a) Oblique convergence is resolved as strain partitioning with Domeyko contractional structures resulting from normal component of convergence and parallel component producing strike slip along structures others

then Domeyko system. b) Convergence angle is high enough to preclude strike slip fault systems and associated structures. In fact, transpression analogue modelling shows that strike slip fault systems need small convergence angles or high convergence to be developed (Casas et al., 1998).

REFERENCES

Ardill J., Flint S., Chong G. and Wilke H. 1998. Sequence stratigraphy of the Mesozoic Domeyko Basin, northern Chile. Jour. Geol.Soc., 155, 71-88.

Casas A.M., Cortés A.L., Gapais D., Nalpas T. and Román-Berdiel T. 1998. Modelización analógica de estructuras asociadas a compresión oblicua y traspresión. Ejemplos del NE peninsular. Rev.Soc.Geol España, 11 (3/4), 331-344.

Chong G. 1977. Contribution to the knowledge of the Domeyko Range in the Andes of northern Chile. Geol. Rundschau, 66, 374-404.

Lindsay D.D., Zentilli M. and Ossandon G. 1996. Falla Oeste fault system: record of its regional significance as exposed in Chiquicamata open pit, northern Chile. Tird ISAG, St. Malo (France), 427-430.

McElderry S., Chong G., Prior D. and Flint S. 1996. Structural styles in the Domeyko Range, northern Chile. Tird ISAG, St. Malo (France), 439-442.

Prinz P., Wilke H. and Hillebrandt A.V. 1994. Sediment accumulation and subsidence history in the Mesozoic marginal basin of northern Chile. In: Tectonics of the Southern Central Andes, 219-232.

Reutter K-J., Scheuber E. and Helmcke D. 1991. Structural evidence of orogen-parallel strike-slip displacements in the Precordillera of northern Chile. Geol. Rundschau, 80 (1), 135-153.

Reutter K-J., Scheuber E. and Chong G. 1996. The Precordilleran fault system of Chuquicamata, Northern Chile: evidence for reversals along arc-parallel strike-slip faults. Tectonophysics, 259, 213-228.

Scheuber E. and Andriessen P.A.M. 1990. The kinematic and geodynamic significance of the Atacama fault zone, northern Chile. Jour.Struct.Geol., 12 (2), 243-257.

Scheuber E., Bogdanic T., Jensen A. and Reutter, K-J. 1994. Tectonic development of the north Chilean Andes in relation to plate convergence and magmatism since the Jurassic. In: Tectonics of the Southern Central Andes, 121-139.

THE EPITHERMAL AU-AG ORE DEPOSITS IN THE CORDILLERA SHILA, SOUTHERN PERU : FLUID INCLUSIONS AND MICROFISSURATION DATA.

Anne-Sylvie ANDRE (1), Jacques L. LEROY (1) and coworkers of the Peru 97-98 metallogeny GdR mission

(1) UMR 7566 G2R, Université Henri Poincaré, B.P. 239, 54 506 Vandœuvre Cedex
asandre@g2r.u-nancy.fr
jacques.leroy@g2r.u-nancy.fr

KEYWORDS : Peru, epithermal, fluid inclusions planes, boiling.

INTRODUCTION

The Shila low-sulfidation epithermal vein system cuts Early-Middle Miocene calc-alcaline volcanites of the Tacaza Group in the Western Cordillera, northwest of Arequipa (Figure 1).

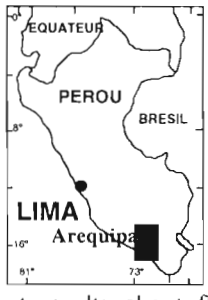

Figure 1 : Localization of the mining district of Shila.

This paper presents the first results about fluids and microfissuration on different deposits of this epithermal area. Six deposits have been studied more in details along a vertical profile : Desamparados, Ticlla, Puncuhuayco and the three deposits of the Shila district, Apacheta, Pillune and Sando Alcalde.

GEOMETRY OF THE FLUID MIGRATION

After healing, the microcraks form Fluid Inclusion Planes (FIP). These FIP are considered as mode I cracks and give thus valuable information about the local stress in rocks and can be assumed to be $(\sigma_1\text{-}\sigma_2)$ planes (Tuttle, 1949; Lespinasse and Cathelineau, 1995).

The geometry of the Fluid Inclusion Planes (FIP) network has been characterized in the Shila area with image analyzing on oriented thick double polished plates (Photo 1 and Figure2).

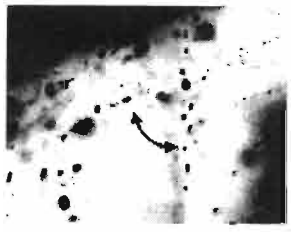

Photo 1 : The two major FIP observed in a Shila wafers, containing two different types of fluid

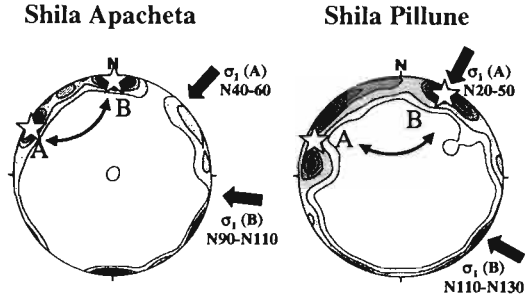

Figure 2 : Representation of the fluid inclusion plane poles for the Shila Apacheta and Shila Pillune deposits. The white stars symbolize the σ_3 positions

The poles of the FIP indicate two major σ_3 orientations (Figure 2). The tectonic events described in the area during the period of the epithermal activity are compressive events and we can therefore deduce that the two σ_1 corresponding to our two σ_3 orientations are horizontal (σ_1(A) and σ_1(B)) with N20-60 and N90-120 orientation (Figure 2). These orientations of compressive events, deduced from the FIP network, agree with the two orientations of the compressive events supposed to be at the origin of both fracturation and mineralization in this area (Cassard et al., 1998; Chauvet A., personal communication).

FLUIDS CHARACTERISTICS

In each deposits, the fluids have been characterized using standard techniques, e.g. microthermometry with a Chaixmeca heating-freezing stage and Raman microprobe (DILOR X-Y).
Two groups of deposits can be distinguished :

- Desamparados, Ticlla and Puncuhuayco deposits.

In these three deposits, the secondary fluid inclusions are little diversified showing low salinity (Tm_{ice} from 0 to –1.4°C; equivalent salinity from 0 to 2.4 wt% NaCl) for homogeneous Th (from 175 to 228°C) (Figure 3). Raman analyses on the volatile phase indicate the lack of gases.

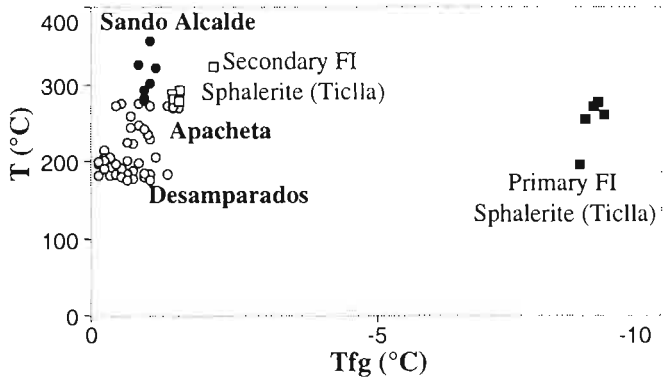

Figure 3 : Th vs Tm_{ice} diagram applied to aqueous fluids observed in Quartz (circles) and Sphalerite (squares) in the different deposits.

In Puncuhuayco, some fluid inclusions have been studied in light-coloured sphalerite. The fluids have been trapped as primary and secondary inclusions. Primary inclusions give Tm_{ice} from –8.5 to –9.0°C (equivalent salinity : 12.3 to 12.9 wt% NaCl) and Th from 196 to 274°C (in L phase) but most data are in the range of 255 to 274°C. Secondary fluid inclusions show low salinity (Tm_{ice} from –1.3 to –2.1°C, equivalent salinity: 2.2 to 3.6 wt% NaCl) with total homogeneization ranging from 271 to 323°C (in L phase). The Th-Tm_{ice} plot (Figure 3) shows a clear decrease of the salinity during these two percolation stages in sphalerite.

- Shila District with Apacheta, Pillune and Sando Alcalde deposits

Two major types of fluids are observed along the two major orientations of microcracks (Photo 1).

(i) Aqueous-carbonic fluids (Figure 4c) show Tm_{CO2} ranging from –57.3 to –59.3°C. The rare Th_{CO2} are observed at very low T between –1.3 and 6.5°C (in V phase) indicating a low fluid density. Aqueous-carbonic inclusions (with three phase H_2O, CO_2 (L) and CO_2 (V) at low temperature) are surprising in such deposits where CO_2 is generally only detected by the presence of clathrate.

(ii) Aqueous fluids with low salinity display Tm_{ice} from –0.4 to –1.5°C (0.7 to 2.6 wt% NaCl). The low eutectic T (<-30°C) indicate the presence of bivalent cations. Raman analyses show traces of CO_2 in the volatile phase. The Th are different according to the deposits, with higher Th for Sando Alcalde (Figure 3).

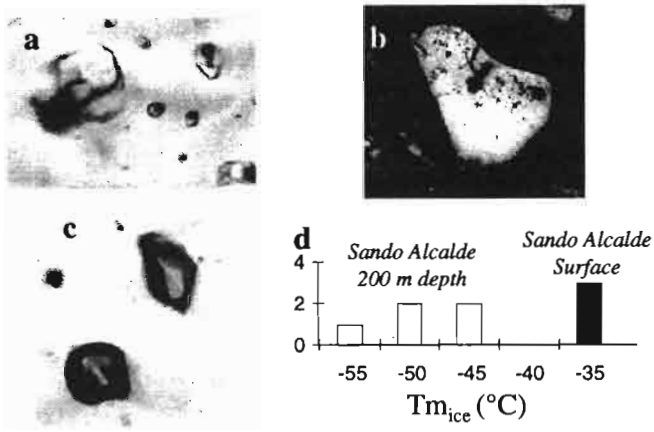

Figure 4 : Photos (a) high salinity aqueous fluid inclusions observed in (b) Rhyolitic quartz, (c) aqueous-carbonic inclusions. (d) high salinity aqueous inclusion Tm_{ice} histogram.

Some high salinity aqueous inclusions, with one or two daugther minerals (sylvite and halite), have been observed in rhyolitic quartz (Figure 4a and b) showing low Tm_{ice} (Figure 4d).

- Gas Analyses – Shila district

The volatile phase of the aqueous-carbonic fluids present in the Shila district is dominated by CO_2 (62.9 to 100 mol%) with less amount of N_2 (0 to 20.6 mol%) and H_2S (0.7 à 6.7 mol%) (Figure 5).

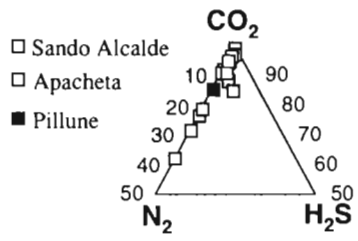

Figure 5 : Raman composition of the aqueous-carbonic volatile phase.

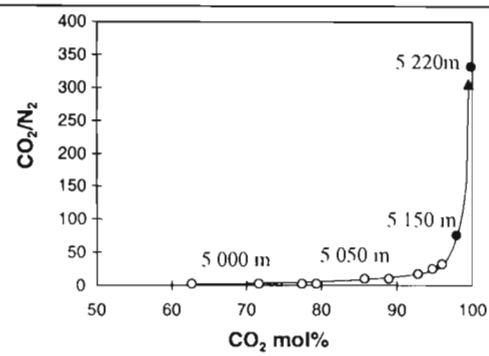

Figure 6 : CO_2/N_2 ratio versus CO_2 composition in mol.% according to the depth of the sample in the Shila Apacheta deposit.

In Sando Alcalde and Apacheta deposits, samples have been studied along a vertical profile. In both deposits, the analysis of the volatile phase shows a decrease of the nitrogene content towards the surface (Figure 6). Are this decrease due to the solubility difference between these two gases (Ellis and Mahon, 1977) ? For Hedenquist et al. (1992), a systematic variation in the ratios of any two gases with different solubilities is the result of a progressive boiling with gas loss in spatially-arrayed samples. This boiling should be at the origin of the mineralization which is often associated with bladed calcite (Simmons and Christenson, 1994) and Mn-carbonates (Roy, 1968).

This work has been carried out with the framework of the Metallogeny GdR program research. It was realized in collaboration with the BRGM (DR-LGM) and the University of Orléans.

REFERENCES

Cassard D., Marcoux E., Faure M., Llosa F., André A.S. and Leroy J. 1998. Formation and evolution of the epithermal Au-Ag veins in the Cordillera Shila, southern Peru. Tercer Simposium Internacional del Oro, 5-8 may 98, Lima (Peru).

Ellis A.J. and Mahon W.A.J. 1977. Chemistry and Geothermal Systems. New York, Academic Press, 392p.

Hedenquist J.W., Reyes A.G., Simmons S.F. and Taguchi S. 1992. The thermal and geochemical structure of geothermal and epithermal systems : a framework for interpreting fluid inclusion data. Eur. J. Mineral., 4, 989-1015.

Lespinasse M. and Cathelineau M. 1990. Fluid percolation in a fault zone : A study of fluid inclusions planes (FIP) in the St Sylvestre granite (NW French Massif Central). Tectonophysics, 184, 173-187.

Roy S. 1968. Mineralogy of the Different Genetic Types of Manganese Deposits. Economic Geology, 63, 760-786.

Simmons S.F. and Christenson B.W. 1994. Origins of calcite in a boiling geothermal system. American Journal of Science, vol. 294, p. 361-400.

Tuttle O.F. 1949. Structural petrology of planes of liquid inclusions. Journal of Petrology, 57,331p.

THE LIQUIÑE-OFQUI FAULT ZONE: A CASE OF DEFORMATION PARTITIONING AT OBLIQUELY CONVERGENT TRANSPRESSIONAL PLATE BOUNDARIES (SOUTHERN ANDES)

Gloria ARANCIBIA, Gloria LÓPEZ and José CEMBRANO

Departamento de Geología. Universidad de Chile. Casilla 13518. Correo 21. Santiago de Chile.
e-mail address: garancib@mail.cec.uchile.cl

Key words: Liquiñe-Ofqui Fault Zone, Southern Andes, transpression, deformation partitioning, stretching lineations.

INTRODUCTION

Oblique convergence along plate boundaries has been directly related to transpression within a deformation zone parallel to the margin. The simplest model of transpression (Sanderson and Marchini, 1984) exhibits a monoclinic geometry defined by two components of strain: horizontal shortening normal to the deformation zone and simple shear parallel to it. Later models considered partitioning of deformation, which accommodate transpression in different and separate domains across de deformation zone (*e.g.* Fossen et al., 1994, Tikoff and Teyssier, 1994; Jones and Tanner, 1995). The most general case for transpressional zones adds to the later a far field displacement vector oblique to the deformation zone bounding blocks *(e.g.* Jones and Holdsworth, 1998; Lin *et al.*, 1998), allowing the development of a triclinic symmetry with oblique stretching lineations.

The Liquiñe-Ofqui Fault Zone (LOFZ) (*e.g.* Hervé, 1976; Hervé and Thiele, 1987; Cembrano and Hervé, 1993) is an intra-arc fault zone parallel to the continental margin along the Southern Chilean Andes (Fig. 1). We studied the geometry and kinematics of five regions within the southern end of the LOFZ (44°-46°S) (Fig. 1) in order to better understand the geometry and kinematics of the fault zone in the framework of the available transpressional models.

DUCTILE DEFORMATION WITHIN THE LOFZ

Brittle-ductile shear zones of the LOFZ are Late Miocene-Pliocene in age (*e.g.* Cembrano, 1998) (Fig. 2) and affect rocks of the Meso-Cenozoic North Patagonian Batholith (NPB), Tertiary intra-arc

metavolcanic-sedimentary rocks and Paleozoic Basement. Ductile deformation is recorded in meter-wide mylonite zones. Subvertical foliations with horizontal, oblique and vertical stretching/mineral lineations, are documented in north-to-northeast-trending shear zones (Puyuguapi, Queulat, Fiordo Aysén and Canal Costa shear zones) and east-to-northeast trending shear zone (Pto. Cisnes shear zones). The Puyuguapi shear zone (Fig. 2A) lies within the NPB rocks and contains high strain rocks with north-south trending subvertical foliation, subvertical lineations, and reverse kinematics indicators with a small component of dextral shear. The Queulat shear zone (Fig. 2B) developed from mid-Tertiary rocks. Oblique-slip in rocks with northeast-trending foliations and oblique lineations, show dextral-reverse kinematics indicators. The Fiordo Aysén shear zone (Fig. 2D) contains high strain shear zones developed in basement Paleozoic rocks and contain north-south-trending subvertical to moderately-dipping foliations and strike-slip to

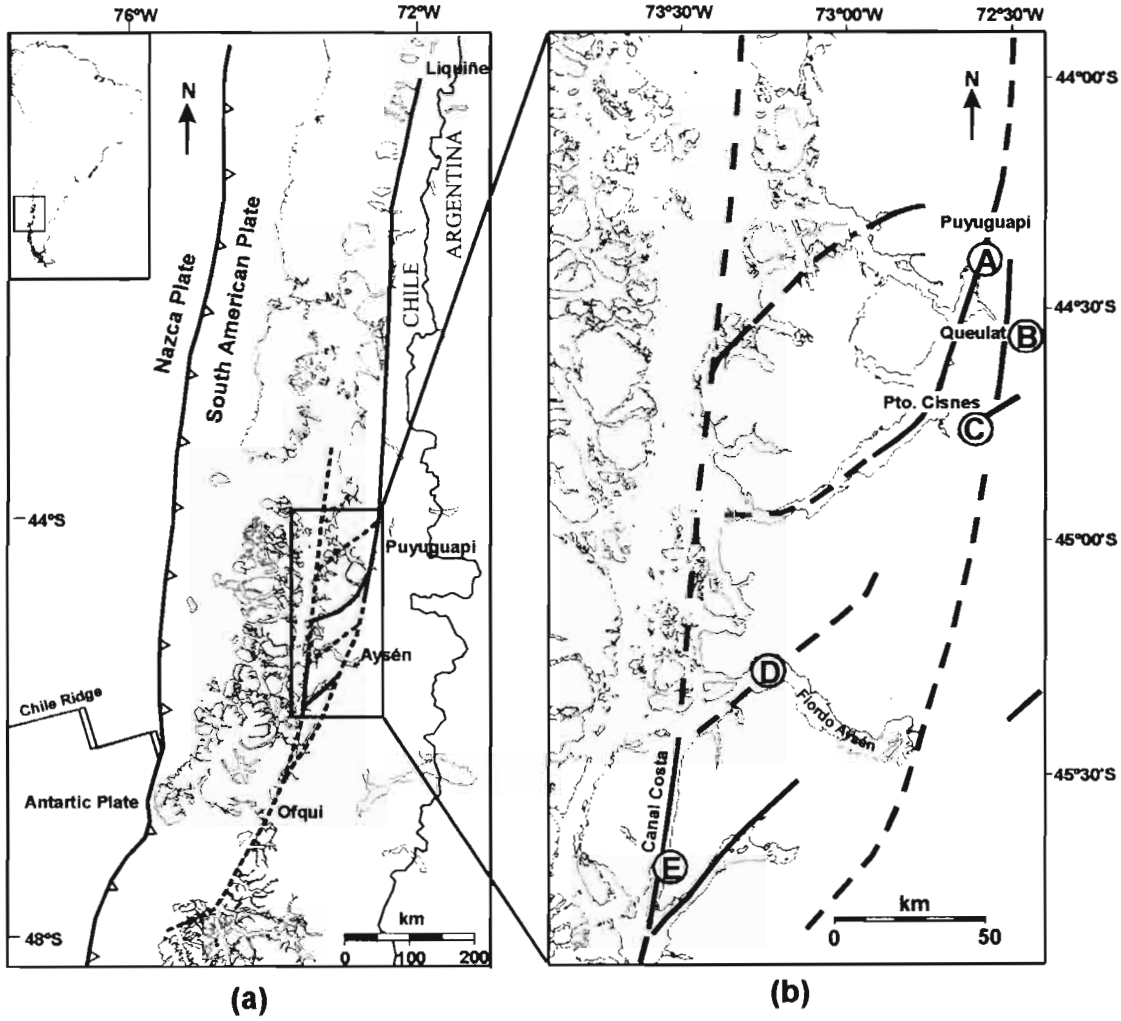

Figure 1. a) Regionale-scale geometry of the Liquiñe-Ofqui Fault Zone (Modified from Cembrano and Hervé, 1993) and location of study area. b) Location of structural analysis sites. Segmented line indicates inferred faults. Continuous line indicates observed fault zone.

Undeformed rocks in the Queulat and Canal Costa shear zones (*e.g.* Halpern and Fuenzalida, 1978; Bartholomew, 1984) suggest the deformation is Late Miocene to Pliocene, similar those from the Puyuguapi, Fiordo Aysén and Pto. Cisnes shear zones (Cembrano, 1998). Therefore, dip-slip, strike-slip and oblique-slip deformation along north-south and northeast-trending shear zones appears to be coeval. This suggests a high-degree of kinematic partitioning within the deformation zone. Oblique stretching lineations, on the other hand, indicate that the strain symmetry is triclinic rather than monoclinic, because the east-west shortening is not only accommodated by vertical extrusion but through dip-slip motion as well.

Acknowledgements. FONDECYT Project 1950497 funded this research. Dr. Hervé, Dr. Lavenu and Dr. Prior, are thanked for their participation in the fieldwork and discussions.

REFERENCES

Bartholomew D.S. and Tarney J. 1984. Crustal extension in the southern Andes (45°-46° S). *In* Volcanic processes in marginal basins. *B.P. Kokelaar M.F., Howells and R.A. Roach (eds)*. Special Publication, Geological Society of London, 195-205.

Cembrano J., Hervé F. 1993. The Liquiñe-Ofqui Fault Zone: a major Cenozoic strike slip duplex in the Southern Andes. *Second ISAG*, Oxford (UK), 175-178.

Cembrano J. 1998. Kinematics and timing of intra-arc deformation, southern Chilean Andes. *Ph.D. thesis (Unpublished)*, Dalhousie University, Canada, 231 p.

Halpern M., Fuenzalida R. 1978. Rubidium-strontium geochronology of a transect of the Chilean Andes between latitudes 45° and 46°S. *Earth and Planetary Science Letters*, 41, 60-66.

Hervé M. 1976. Estudio geológico de la Falla Liquiñe- Reloncaví en el área de Liquiñe; antecedentes de un movimiento transcurrente (provincia de Valdivia). *In I Congreso Geológico Chileno*, I, B-39-B56.

Hervé F., Thiele R. 1987. Estado de conocimiento de las megafallas en Chile y su significado tectónico, Megafaults in Chile: A review. *Comunicaciones*, 38, 67-91.

Fossen, H., Tikoff B., Teyssier, C. 1994. Strain modeling of transpressional and transtensional deformation. *Norsk Geologisk Tidsskrift*, 74, 134-145.

Jones R. and Tanner P.W. G. 1995. Strain partitioning in transpressional zones. *Journal of Structural Geology*, 17, N°6, 793-802.

Jones R. and Holdsworth R. 1998. Oblique simple shear in transpression zones. *In* Continental transpressional and transtensional tectonics, *Holdsworth, R., Strachan, R., and Dewey, J. (eds)*, Geological Society Special Publication,135, 35-40, London.

Lin S., Jiang D., Williams P. 1998. Transpression (or transtension) zones of triclinic symmetry: natural example and theoretical modeling. *In* Continental transpressional and transtensional tectonics, *Holdsworth, R., Strachan, R., and Dewey, J. (eds)*, Geological Society Special Publication, 135, 41-57, London.

Sanderson D. and Marchini W. 1984. Transpression. *Journal of Structural Geology*, 6, N° 5, 449-458.

Tikoff B. and Teyssier C. 1994. Strain modeling of displacement-field partitioning in transpressional orogens. *Journal of Structural Geology*, 16, N°11,1575-1588.

oblique-slip lineations. Dextral reverse kinematics indicators are observed. The Canal Costa shear zone (Fig. 2E) developed from NPB rocks. North-south-to-northeast-trending foliations and oblique-slip lineations are developed and reverse-dextral/sinistral kinematics indicators. The Pto. Cisnes (Fig. 2C) shear zone is a high strain shear zone developed from basement Paleozoic rocks. East-to-northeast-trending moderately-dipping to subvertical foliations, strike-slip lineations and dextral-normal kinematics indicators are observed.

CONCLUSIONS

A transpressional and transtensional dextral regime is developed within the LOFZ, resulting in east-west shortening on north-south and northeast-trending structures (Puyuguapi, Queulat, Fiordo Aysén and Canal Costa) and dextral transtension along north-east to east-west structures (Pto. Cisnes).

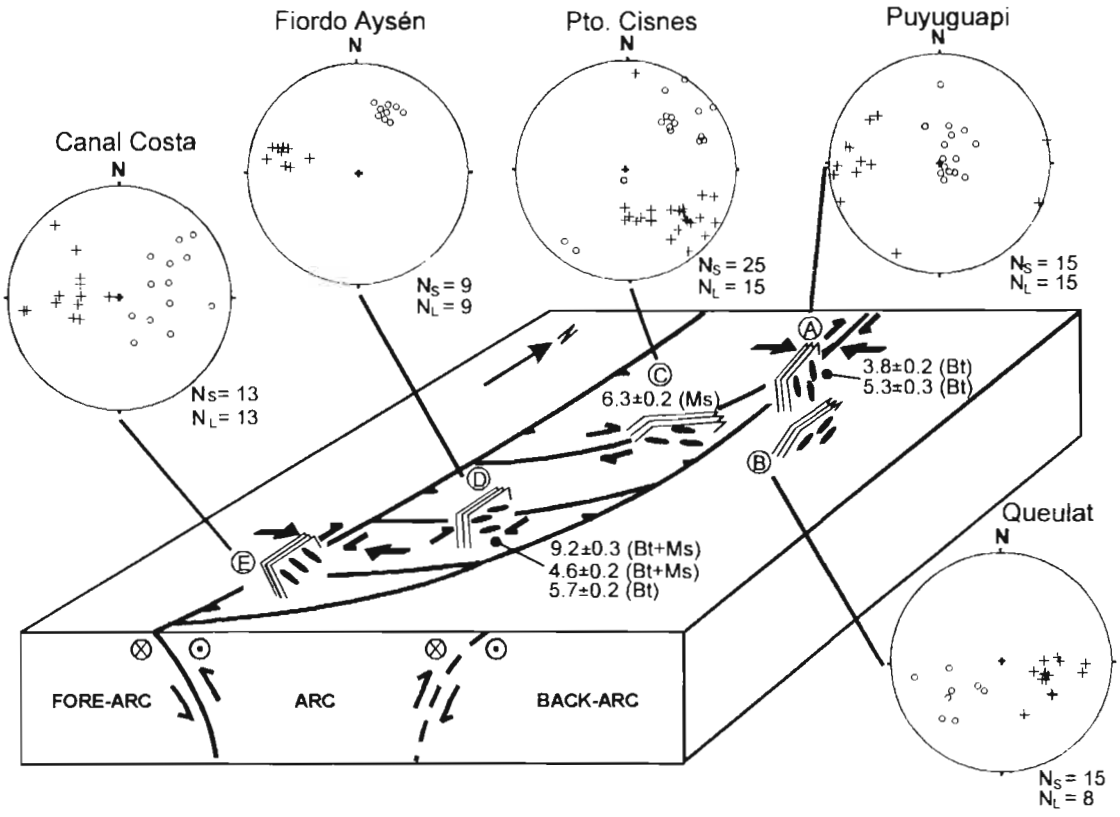

Figure 2. Three-dimensional schematic block showing foliations (planes) and mineral/stretching lineations (elipsoids on planes) from sites illustrated in figure 1b. Stereoplot diagrams contain poles to foliation (crosses) and lineations (circles), in Wulff diagram. Ns= number of measured foliations. NL= number of measured lineations. In A and D, the shortening component is very significant (dip-slip), whereas in C and D, the strike-slip component is more important. Notice that although A, B, D, and E have similar foliation trends, lineation are subvertical, subhorizontal or oblique. Ar/Ar deformation age is Pliocene (Cembrano, 1998) for sites A, C and D.

LITHOSPHERIC STRUCTURES IN THE SOUTHERN CENTRAL ANDES, PRELIMINARY RESULTS (38°-42°S)

Manuel ARANEDA(1), María Soledad AVENDAÑO(1), Hans Juergen GÖTZE(2), Sabine SCHMIDT(2), Jorge MUÑOZ(3) and Michael SCHMITZ(2)

(1) Depto. Geofísica U. de Chile, Chile (maraneda@dgf.uchile.cl)
(2) U. Libre de Berlín, Alemania (hajo@geophysik.fu-berlin.de)
(3) Servicio Nacional de Geología y Minería,Chile (sngmpd@entelchile.net)

Key words: Lithospheric Structures, 38-42°S, Gravity, Magnetism, Seismic Reflection.

INTRODUCTION

The Southern Central Andes has form part of the convergence system between the Nazca Plate (oceanic) and the Southamerican Plate (continental). The maximum width is approximately 200 km in this zone. The medium height,in the segment, is *ca.* 1,500 km These elevations reflect a cortical medium thickness of 45 km beneath the Andes axis. Part of the results, in this paper, corresponds to those obtained in the project 'Integrated Geophysical Study of the Seismic Risk Zone of the Southern Central Andes (38-42°S), financed by the Volkswagen Foundation of Germany. These investigations may be considered as the beginning of future studies contemplated in a special investigation program (SFB267) `Deformation Processes of the Andes` of Germany in the southerrn part of the Andes. The project objectives have a direct relationship with the orogenesis of the subduction of the Southern Central Andes and its comparison with the northern zone (27-28°S).Preliminary gravimetric investigation results are presented complemented with seismic magnetic studies existing in the Soutern Central Andes (38-42°S). The anomaly analysis is correlated with the most relevant geological structures of the segment. The Bouguer anomaly, the isostatic residual and isogam are presented in the form of maps. Of them, the following conclusions and correlations can be inferred: the negative medium gradient has its maximum expression in the Argentinian Andes (-100mGal) beginning at 73°W medium latitude..On the east of this divide, a positive gradient begins as far as the edge of the Pacific Ocean. Within these gradients, isolated anomalies of high frequencies can be seen. The most important feature, within the positive gradient, is its interruption by a a negative anomaly of –20 mGal in an approximately 100 km extension, located in nearby Valdivia. The isostatic residual is shown rather in an aleatory form, with positive and negative anomalies with a certain north-south lineament, and in some cases northwest-southeast. The magnetic anomalies have grouped in magnetic domains, which also, have preferred directions north-south and interrupted by north-west-.southeast lineaments. Most of the gravity and magnetic features can correlate with large and geological structures of the segment.

PRESENT GRAVIMETRIC DATA

The gravimetric investigations in the Southern Central Andes have been oriented to determine the isostatic status and the crust structures of the orogen associated to the densities. The gravimetric data,

gathered in 5 campaigns, between 1995 and 1998, 2 in Argentina and 3 in Chile. Later, they were homogenized with existing data, Araneda *et al.*, 1999. In total, the data presented in this paper add up to 13,050 gravity stations. All the gravimetric data are tied to ISGN 71, and they were corrected due to topography. The Bouguer anomaly (Fig. 1) was obtained by using the sea level as reference, with a 2.67 gr/cm^3 density. The Bouguer anomaly contains the topography according to Isacks (1988). South of parallel 40°S, the last Intermediate Depression commences in Chile. This phiysiographical change coincides with a remarkable change in the Bouguer anomaly, as the gravity anomalies do not have a direct correlation with the superficial geology; the east-west regional, that is normally seen in Chile, undergoes an abrupt change, being intercepted by a series of local anomalies that make it strongly vary in the Intermediate Depression, giving place to the major amplitude positive anomaly known in southern continental Chile..The medium negative 100 mGal gradient dips east, what indicates a thickening of the crust in that direction, reaching its maximum in the Argentinian Andes. In general, the Bouguer negative isoanomalies show a north-south trend, whose courses reflect a big number of local anomalies, as well as a deep structure of the Andes. The continental part is characterized by a series of positive and negative isostatic residuals, whose divide is found approximately in the center of the Chilean territory. In the western part of this divide, the major residuals of high frequencies are found, restricted to others of low freequencies, but of the same sign. The maximum values are found in the proximities of Purranque, Fresia and Maullín.

PRESENT MAGNETIC DATA

The magnetic information corresponds, exclusively, to the Chilean segment, as there is no available information from the Argentinian one. The magnetic data correspond, mainly, to those furnished by Corporación de Fomento de la Producción- Instituto de Investigaciones Geológicas, Chile (CORFO-IIG), 1969, Aeromagnetic Survey: Coastal Range, Nueva Imperial- Chile, ENAP, 1962, OEA/Chile Aerophotogrametric Project and the Magnetic Chart of Chile, Aeromagnetic flight in the Cordillara Principal between 39 and 44°S, Servicio Nacional de Geología y Minería (SERNAGEOMIN), 1997, Program of X Region, Northern area. All the aeromagnetic information was entered digitally, allowing a global analysis of the magnetic domains between 38 and 42°S, segment included in the study. Figure 2 shows the total field map, carried out by SERNAGEOMIN. The work permits to visualize the regional magnetic anomalies according to their nature, considering the amplitude, wave length, dimensions and orientation. These trends or magnetic domains, consider the amplitude, wave length, dimensions and orientation. These trends or magnetic domains, as defined by Ugalde *et al.* (1997), have been defined as of the total magnetic field map that corresponds with the morphological features of the region. The division proposed by Ugalde *et al.* (1997) corresponds to three magnetic domains associated to the Coastal Range, Central Valley and the Cordillera Principal, whose characteristics are: **a-** Coastal Range: this domains presents a small amplitude magnetic signal (20-30 nT), where there are relevant dipole anomalies that reach up to 70 nT. This belt coincides with schists belonging to the metamorphic basement. These rocks present very low magnetic susceptibilities (<0.1x103 emu); **b-** Central Valley: this domain is characterized by a set of medium to large wave length anomalies (20-40 km),and 200 nT intensities with well defined anomalies that allow to infer the presence of large bodies of high intensity in depth; **c-** Cordillera Principal: this domain is characterized by a set of large dipole assymetric anomalies of $\geq$ 200 nT high intensities. This assymetric polarity is expressed, in most of the cases, by strong positive anomalies that coincide with active eroded volcanos, Ugalde *et al.* (1997).

THE PRESENT SEISMIC REFLECTION DATA

The seismic data correspond to a reinterpreation carried out by McDonough *et al.* (1998) of seismic lines (300 km) carried out by Empresa Nacional del Petróleo (ENAP). These lines are located in the Central Valley, south of 40°S located in the Central Valley. This structure is composed by Quaternary age sediments, and reaches 2,000 to 4,000m and form the Osorno-Llanquihue Basin, composed of Oligocene

to Pliocene forearc basin flanked by the Andean arc. The cortical structure characteristics beneath the southern Chile forearc are inferred from 5,6, and 7 deismic lines. Line 6 is oriented roughly east-west and considered to be a dip-section. In the western part of the profile at 13s (two way time), the base of reflectivity is interpreted as the seismic reflection Moho. A reflection Moho at 13s is confirmed by line 5 and corresponds to a present-day crustal thickness of about 30 to 35 km depending on the velocity model utilized for the Tertiary in the shallow part of the profile. McDonough *et al.* (1998). This depth agrees with Barazagni and Isacks (1976) who estimated the crustal thickness, based on earthquake foci beneath a margin of normal subduction.

CONCLUSIONS

The Bouguer anomaly in the continental part has a maximum regional of 120 mGal in the 38-42°S segment. South of parallel 39°, the regional diminishes to 100 mGal. These effects are closely bound with the crust thickness due to the isostatic compensation. However there appear numerous unknown anomalies, *e.g.*, the positive anomaly in the 40-42°S and the 73-74°W segment that can be extended much farther south. This anomaly appears just in the Central Valley, beginning approximately in the proximities of La Unión as far as south of Maullín. The most symptomatic characteristic of this anomaly is that it is found practically all over Quaternary sediments. The mean value of this anomaly is +50 mGal. The gravimetric minimum of the Andes is found in Argentina with a value of –80 mGal, and in north-south direction. This minimum would be indicating that the maximum thickness of the Andes is approximately 45 km. This minimum is approximately in the Sierra of Catan-Lil, seen mainly in front of the cities of Aluminé and San Martin de los Andes. According to the magnitude of this anomaly, it extends far south and north of the region indicated above. The most interesting characteristics of the isostatic residual and other results are the following: **1-** the coast range basically composed of metamorphic rock of Paleozoic age shows, in general, negative anomalies.; **2-** the Central Valley in Chile, covered with 2,000 to 4,000 m of Quaternary sediments, shows positive anomalies; **3-** the major values of isostatic residuals are located approximately between latitudes 40.5°S and 42°S under Quaternary sediments of the Central Valley, and this is likely due to the existence of a minor abnormal thickness of the crust in the zone. This would infer that the high densities of the materials that make up the upper mantle are reflected in the residual anomalies; **4-**in general, the isostatic residual shows a general pattern of south-north orientation in which the major values are located in the Central Valley in a segmented way; **5-** in general there is no good correlation between the magnetic domains and the isostatic residuals, these are rather displaced to the west; **6-** the reinterpretation of the seismic data provide reliable facts, south of parallel 40°S; the depth of the basin of the Central Valley, 2,000 a 4,000 m of quaternary sediments, topography of the basement, irregular and 30 to 35 km Moho depth in the zone.

ACKNOWLEDGEMENTS

The authors thank the Volkswagen Foundation (Germany), Servicio Nacional de Geología y Minería (Chile) and Servicio Geológico Minero Argentino, for the sponsorship and collaboration given.

REFERENCES

Araneda M.,: Avendaño M.S.; Schmidt S.; Götze H.J.; Muñoz J.; Schmitz, M. 1999. 'South Central Andes Gravity, New Data Base'. Submitted to the 6th International Congress of the Brazilian. *Geophysical Society* ,p. 4.

Barazagni M.: Isacks, B.L. 1975. 'Spatial Distribution of Earthquakes and Subduction of the Nazca Plate beneath South America'. *Geology*, 4, p. 686-692.

Isacks, B.L. 1988. 'Uplift of the central Andean plateau and bending of the Bolivian orocline'. *Journal of Geophysical Research*, Vol. 93, p. 3211-3231.

McDonough M.; Duhart P., Herrero C.; Van der Velden A.; Cook, F.; Martin, M.; Ugalde H.; Villenueve, M.; Mpodozis, C. 1998. 'Accretionary Tectonics and Forearc Basin Evolution on the Southwestern Margin of Gondwana, Southern Chile: Implications of new crustal seismic and geochronological results'. Submitted to Tectonics, p.34.

Ugalde H.; Yáñez, G.; Muñoz, J. 1997. 'Dominios Magnéticos en la Región de los Lagos, 39°-42°S, Chile". *In Congreso Geológico Chileno, No. 7, Actas*, Vol. 1, p. 287-290. Concepción.

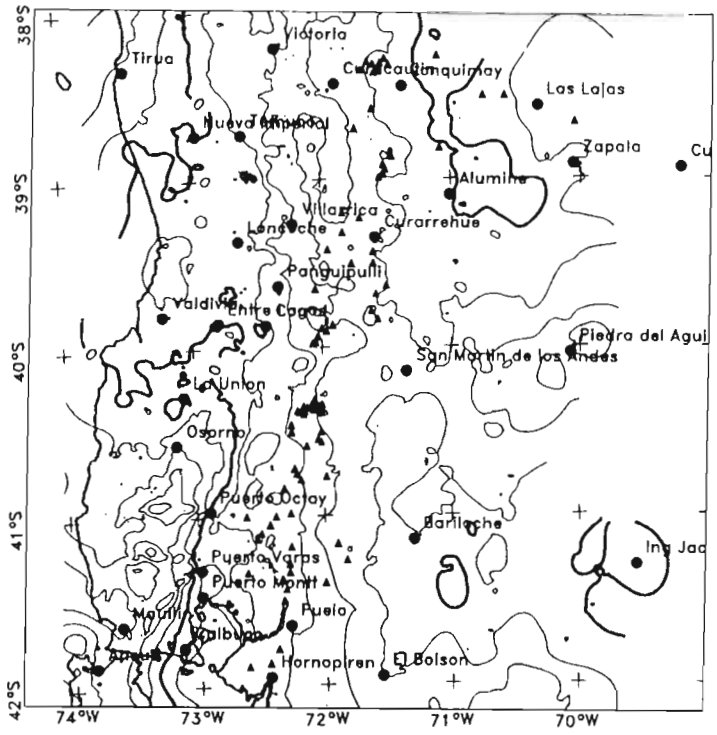

Figure 1: Bouguer anomaly, intervale 20 mGal.

TOTAL FIELD MAGNETIC MAP

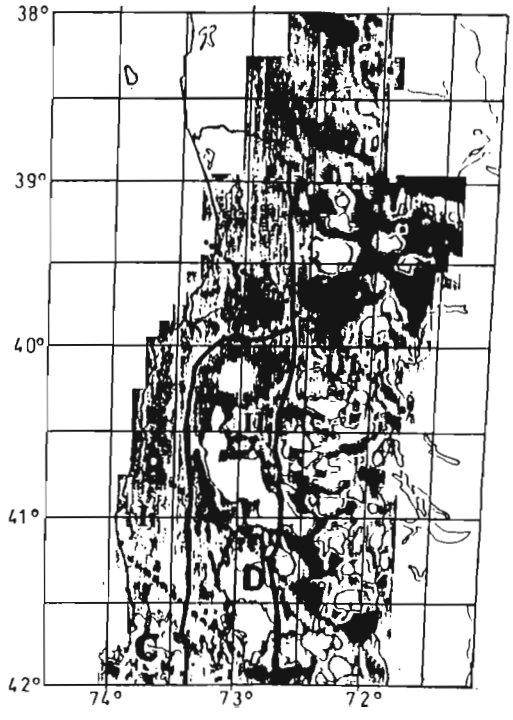

Figure 2: Digital compilation of aeromagnetic information between 38° and 42°S, indicating the Magnetic Domains, and highlighting some important anomalies and magnetic lineaments of north-west orientation, Ugalde et.al 1997.

SHALLOW SEISMICITY IN THE NORTH-WESTERN PART OF ARGENTINA AND ITS RELATION WITH TECTONICS

Mario A. ARAUJO(1,2), Graciela TELLO(2), Angel M. PEREZ(1,2), Irene PEREZ(1), Carlos A. PUIGDOMENECH(1)

(1) Instituto de Prevención Sísmica – INPRES – SEGEMAR. Roger Balet 47 Norte – 5400 San Juan – ARGENTINA. Maraujo@inpres.gov.ar
(2) Facultad de Ciencias Exactas, Físicas y Naturales. UNSJ. Av. Ignacio de la Roza y Meglioli. 5400 San Juan – Argentina

KEYWORDS: tectonic, shallow seismicity, extensional zones, compressional zones.

ABSTRACT

The region under study corresponds to the Puna and Subandean Ranges areas, in the north-western part of Argentina. For this region the shallow seismicity, the regional structures and the modern faulting have been related. It has been observed that east of the 3000 m contour line, which is the limit between both areas, there is an important seismicity and is related to compressive areas. Seismicity decreases remarkably to the west and vulcanism becomes relevant and extensional structures are observed.

INTRODUCTION

The shallow seismic activity of events with magnitude equal or greater than 4, corresponding to the northwest of Argentina, beetwen 22° and 28° south latitude, has been represented in the figure, in order to associate that seismicity to the main structures of the region (Puna Plateau and Subandean Ranges) and to modern faulting. Very important cities (Santa Victoria, San Ramón de la Nueva Orán, La Poma, Santa Clara, Güemes, Palomitas, Esteco y Metan en Salta; San Salvador de Jujuy en Jujuy; Tranca, Tafí del Valle y El Naranjo en Tucumán; Poman y Belen en Catamarca) have been affected by the main events ocurred in this region.

In the figure, some neogene structural features have been depicted, they have been identified by LandSat TM images and areal photographies. This has allowed to individualize extensional areas in Puna Plateau, compliant with extensional patterns propounded by others authors, and compressive areas at Subandean Ranges. Seismicity due to big events nearest to 65° west longitude is outstanding.
Compressive and transcurrent zones are observed in Puna Plateau, to which seismos depicted in the figure can be associated. From these seismos, the most important is the ocurred in La Poma in Salta province.

THE SEISMOTECTONIC SETTING

The region under study is located where the Nazca Plate subduces Southamerican Plate from 25° (21.5° – 23.5° south latitude) to 19° (23.5° – 27.5° south latitude). Two seismotectonic areas are individualized: Puna Plateau and Subandean Ranges. The 3000 m countour line is the boundary between both areas. A sparse shallow seismic activity, an important intermediate seismic activity and various actives volcanos, are the features of Puna Plateau area. An important shallow seismicity and a lack of vulcanism are the characteristics in the Subandean Ranges.

SEISMICITY-TECTONIC RELATION

In order to relate the shallow seismicity in the Puna Plateau and the Subandean Ranges areas, some regional structures (preexistent faults with Cenozoic reactivation and transversal megatraces) and neogene faulting has been depicted in the figure.

The 3000 m height contour line, beetwen 22° and 28° south latitude, is possibly related to reverse regional faulting of NNE-SSW and N-S trend which has been partially reactivated in Cenozoic. A correspondence between shallow seismicity and morfologic evidences of modern tectonic (reverse faults that trends NE-SW and NW-SE, and transcurrent sinistral faults), is observed to the east. A sparse seismicity and modern reverse faulting that trends NNE-SSW and N-S, generally asociated to mountain front, transcurrent faulting joined to modern volcanic edifices and normal faults associated to sinistral transcurrent megatraces, are observed to the west.

CONCLUTIONS

To the east of the contour line seismic activity is important, there is no evidence of vulcanism and the neogene faults are compressive and transcurrent which corresponds with the megatraces. As many authors have pointed out, this would indicate a cortical shortening region in accordance with the direction

and variations of the maximun horizontal stress which has been obtained from the geologic data and focal mechanism.

It is possible that the variation of the seismotectonic behavior is due to the dip change of the subducted plate, which varies from 25° (normal subduction) between the 21.5° and 23.5° S to an angle of 19° between the 23.5° S and 27.5° S, which would be the zone where the subducted plate suffers a N-S contorsion.

To the west of the contour line, the transversal megatraces from north to south with sinistral displacement are distinguished. These transversal megatraces affect the folded tertiary deposits and are related to the quaternary vulcanism.

Between the 22° and 24° south latitude, the seismic activity is very limited, the vulcanism is important and there is a noticeable evidence of modern faulting.

Between the 24° and 28° south latitude tha shallow seismicity increases, the vulcanism continues and extensional tectonic evidences are distinguished by N-S grabens and strike faults to which the basins created by the action of major transversal structures are related. This leads to a NW-SE extensional component for the neogene, which corresponds with the direction of the megatraces movement.

REFERENCES

- Allmendiger R. W., 1986. Tectonic Development, southeastern border of Puna Plateau, northwestern Argentine. Geol. Soc. Am. Bull., 97: 1070-1082.
- Allmendiger R. W., Strecker M., Eremchu K., J. E. and Francis P., 1989. Neotectonic Deformation of the southern Puna Plateau, NW Argentina. I.S. Earth Sci., 2: 111-130.
- Araujo M. and Suarez G., 1994. Geometry and State of Stress of the Subducted Nazca Plate beneath Central Chile and Argentine: Evidences from Teleseiemic Data. Geophysical Journal International, vol 116, pages 283-305.
- Araujo M. and Assumpçao M., 1992. Esfuerzos Tectónicos en una zona del noroeste argentino. XVII Reunión de la Asociación Argentina de Geofísicos y Geodestas. Resúmenes de la reunión, Ma MB3 CC.
- Araujo M., Castano J., 1997. Major Crustal Structures, Geometry of the Nazaca Plate, Intraplate Stress and Main Eathquakes in Argentina. Abstracts "The 29th General Assembly of the International Assiciation of Seismology and Physics of the Earths Interior", IASPEI 1997, Thessaloniki, Greece, 51 N° 2506.
- Assumpçao M., 1992. The regional intraplate stress field in South America. J. Geophys. Res., 98: 11.889-11.903.
- Assumpçao M. and Suarez G., 1988. Source Mechanism of Moderate-Size Earthquakes and Stress Orientation in Midplate South America. Geophys. J., 92: 253-267.

- Assumpçao M. and Araujo M., 1993. Effect of the Altiplano-Puna Plateau, South America on the Regional Intraplate Stresses. Technophysics, 221:475-496.
- Ayala R. and Wittlinger G., 1996. Seismicity and State of Stress in the Central Andes: Bolivian Orocline Region. Extended Abstract 3rd ISAG, St. Malo, France, 141-144.
- Baldis B., Uliarte E. and Vaca A., 1895. Los Sistemas de Megafracturación del Territorio Argentino. Sexto Congreso Latinoamericano de Geología, Bogotá, Colombia. 139-145.
- Cahil T., Isacks B. L., Whitman D., Chatelain J.L., Perez A., and Chin J.M., 1992. Sesimicity and Tectonics in Jujuy Province, NW Argentine, Tectonics, 11:944-959.
- Castano J.C. and Araujo M., 1993. Seimogenic Sources and Regional Tectonic Stresses in the Subandean Zone of major Seismic Hazard of Argentina. ISAG 92. Oxford England, pages 63-66.
- Froidevaux C. and Isacks B.L., 1984. The Mechanical State of the Litosphere in the Altiplano-Puna Segment of the Andes. Earth Planet. Sci. Lett., 71:305-314.Jordan T.E., Isacks B.L., Allmendiger R.W., Brewer J.A., Ramos V.A., and Ando C.F., 1983. Andean Tectonics Related to the Geometry of the Subducted Nazca Plate. Geol. Soc. Am. Bull. 94: 341-361.
- Kley J., Monaldi C., Salfiti J., 1996. Along Strike Segmentation of the Andean Foreland. 3rd ISAG, St. Malo, France, 403-406.
- Kley J., 1998. Variable Foreland Shortening Along the Southern-Central Andes (15°-42.5°): Correlation with Crustal Thickness, Lithospheric Structure and the Geometry of the Nazca Plate. Actas X Congreso Latinoamericano de Geología y VII Congreso Nacional de Geología Económica. Vol II, 88-93.
- Mercier J.L., 1981. Extensional – Compressional Tectonics Associated with the Aegean Arc: Comparison with the Andean Cordillera of South Peru and North Bolivia. Philos. Trans. – R. Soc. London sev. A., 300: 337-355.
- Ramos A., 1973. Estructura de los Primeros Contrafuertes de la Puna Salto-Jujeña y sus Manifestaciones Volcánicas Asociadas. V Congraso Geológico Argentino. Carlos Paz. Actas IV: 159-202.
- Wdowinski S. And O´Conell R.J., 1991. Deformation of the Central Andes (15°-27° S) derived froma Flow Model of Subduction Zones. J. Geophysical Res. 96: 12.245-12.255.
- Zoback M.L., 1992a. First and Second Order Pattern of Stress in the Litosphere: The World Step Map Project. J. Geophy. Res., 97:11.703-11.728.

Shallow Seismicity and Tectonic Features in the Northwest of Argentina

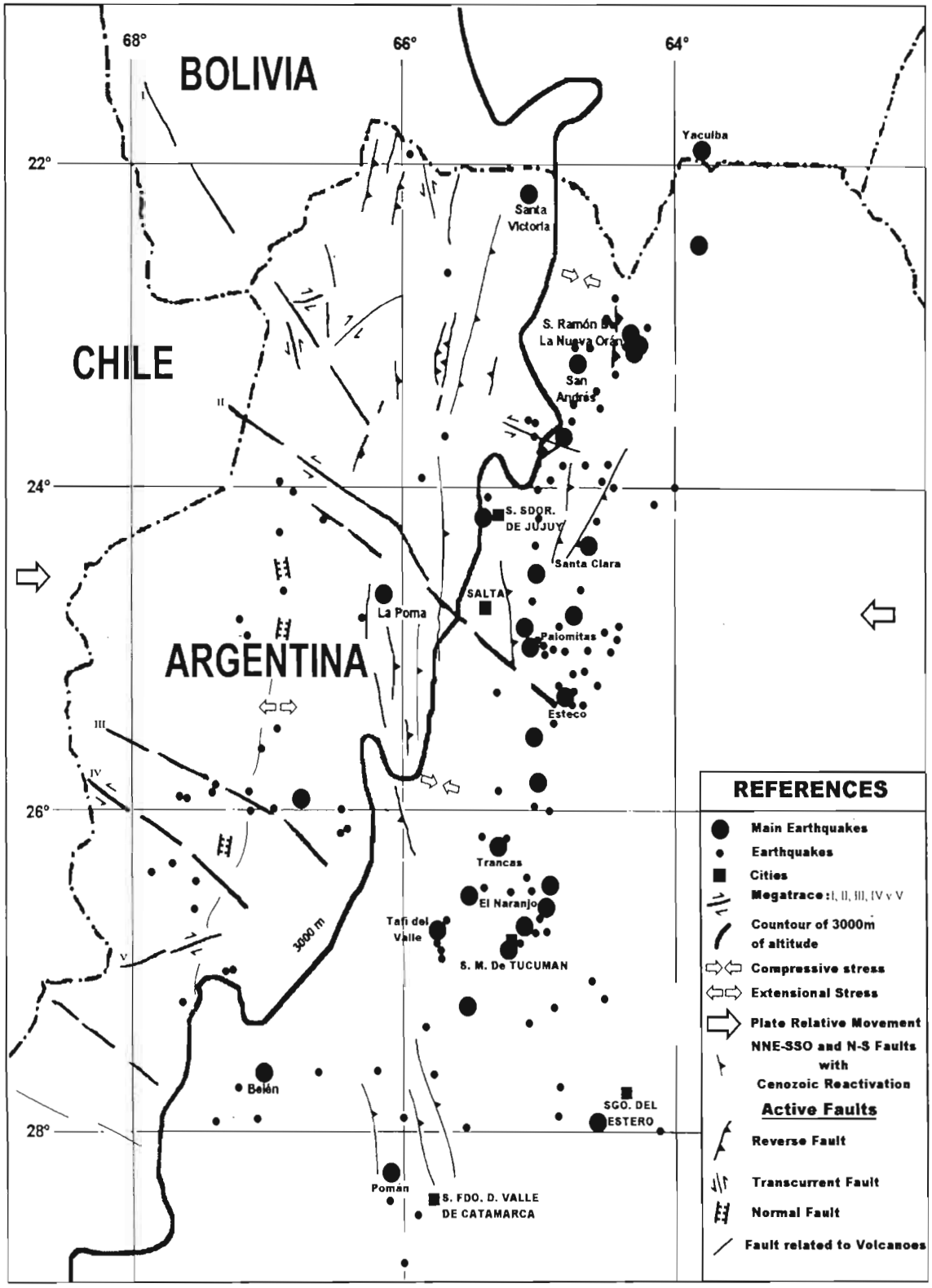

INDUCED SEISMIC ACTIVITY BY A GLACIER IN VOLCANIC AREAS: APPLICATION TO NORTH FLANK OF COTOPAXI VOLCANO, ECUADOR.

Sebastián ARAUJO (1,3), Jean-Philippe MÉTAXIAN (2,3)

(1) Observatorio Astronómico de Quito, EPN.e-mail: Fisica@mail.epn.edu.ec.
(2) IRD. Apartado 17-12-857, Quito, Ecuador. e-mail: jpmetaxi@uio.satnet.net
(3) Instituto Geofísico de la Escuela Politécnica Nacional, Quito, Ecuador.

KEYWORDS: volcano, Cotopaxi, glacier, earthquakes, LP

INTRODUCTION

Cotopaxi (5897m) is an active volcano covered by large glaciers and located on the eastern cordillera of the Ecuadorian Andes and which has a base diameter of 25 Km (Hall and Mothes; 1997). Due to its frequent eruptive activity during the last few centuries, future eruptions pose serious hazards for an important sector of Ecuadorian territory especially for East valleys of Quito and Latacunga.

The monitoring of seismic activity of Cotopaxi is carried out by four permanent telemetered one-component seismic stations of the Instituto Geofísico of the Escuela Politécnica Nacional (EPN) since 1989. Additional information about seismic activity related is based on an experiment made by ORSTOM-IG EPN in 1996-1997 using 12 additional seismic stations (Métaxian et al; this volume).

Worldwide, there are few monitored active glacier-clad volcanoes, thus only a few studies have produced in volcanic areas. Nevertheless investigations made on Mount St. Helens and Mount Rainier volcanoes (Washington State, USA) by Weaver and Malone (1976, 1979), serve to these authors to relate the discrete glacier movement with of icequakes. Experiments made on Mount St. Helens were carried out placing sensors over rock and in the icecap. They found that icequakes have similar characteristics to low frequency earthquakes when they are registered on rock and that most of the seismicity on Mount St. Helens was of glacier origin. The authors pointed out the risk of confusion between icequakes and low frequency events which have volcanic-related sources.

In this work, we analyzed the seismic activity produced by Cotopaxi glaciers and we present their principal characteristics, which allows differentiating the icequakes from the volcanic events.

EXPERIMENT DESCRIPTION AND DATA

The field experiment was made in July 1998 for three weeks. We installed two seismic stations equipped with Mark Products 3-component seismometers (L4-3D). The first one.(CORE) was located on a rock base near the Refuge "José Ribas" at 4800 meters. The second one (COHI), was placed on the glacier on the North side of the volcanic cone, 1100m distant from CORE. The seismometer of COHI station was buried inside the ice with an initial depth of 0.5 m below the surface. The seismometer was leveled once a week in accordance to glacier movement.

These stations registered a daily average of 350 events in CORE and 850 events in COHI. In order to process the data, we selected a packet of events respecting two conditions: to have been registered by both seismic stations and to have a signal to noise ratio greater than 7 at CORE station and greater than 10 at COHI. Considering these parameters we obtained a total of 171 events for signal processing.

Using the data of the permanent network of the Instituto Geofísico (EPN), we verified that the seismic activity of Cotopaxi was stable during the time frame of experiment

METODOLOGY AND RESULTS

In order to do this work, we look at the signal shape, the spectral content, the spectrogram and we measured the difference of amplitude between events registered at both stations. The signal shape and spectral analysis allowed us to identify tectonic earthquakes (local, regional and volcano-tectonic events) which represent 21% of the total activity. For the remaining events we analyzed the S-P arrival times for each station and also the arrival differences of the P waves in both sites. We also calculated the correlation function between each of the select events. Finally, the signal was filtered and graphics of particle motion were performed.

These analyses allow us to define two distintic types of events: 20% of total activity registered in both sites has a symmetric shape, similar amplitudes, emergent front and frequencies below 10 Hz. These events are similar to long-period- type events (LP) described by Chouet (1996).The 59% remaining events (Figure 1) show the following characteristics at COHI: asymmetric shape, impulsive front, short coda duration (~2s) and frequencies over 10Hz.In addition to this, the spectrogram shows concentrated energy in a short period of time (Figure 2 sup). Chouet (1996) associates this kind of spectrogram with shallow brittle failures. On the other hand, the same events registered at CORE have similar characteristics with LP events: symmetric envelopments, slight impulsive fronts, longer coda duration (~10 s), frequencies below 10 Hz and a broad spectrogram distribution of the event (Figure 2 inf).

Moreover, these events always arrive first at COHI which suggest that the source is closer to this station. This is confirmed by the value of ts-tp which is always smaller for the events registered at COHI

than those registered at CORE. Also the average amplitude of events registered at COHI station is ten times bigger than those registered at the CORE station. Finally, graphics of particle motion give a linear polarization in East-Vertical plane. The complete results strongly suggest that these events have shallow sources and are originated in the ice structure.

DISCUSSION ANDCONCLUSIONS

We observed two kinds of local events in Cotopaxi: 1) LP events which are related with volcanic process and 2) events normally associate with glacier movements. The characteristics of this second category of events coincides with the icequakes characterizied in the Cascade Volcanoes by Weaver-Malone (1976, 1979). In both cases we have: occurrence of almost one event per minute, initial detection and higher amplitude at the station placed on ice, shorter coda for an ice station's signals than those stations on bedrock and impulsive initial waves at the glacier station becomes emergent at the bed-rock station. We also observe, like for Mount St. Helens icequakes, a strong dispersion effect, which could be the result of an large velocity contrast across the ice-rock interface (Weaver-Malone; 1979). This observation is an additional argument to relate Cotopaxi events to a glacier origin.

The icequakes differ from LP events in all the analyzed parameters: signal shape, spectral content, spectrogram, wave front, duration, amplitude, S-P phases and particle motion. These differences are observable at the ice station but not at the bedrock station. No disperssion effects are observed for LP events. Icequakes and LP events are practically identical in the data registered on the bedrock, such was observed by Weaver and Malone (1976) at Mount St. Helens. This suggest that it is essential to install a seismometer on the glacier to differentiate both kinds of events.

Weaver and Malone (1979) suggest that icequakes are the result of a stick-slip type of motion taking place at the bed of the glacier. Other authors like Neave and Savage (1970) suggest that icequakes appear to originate fron extensional faulting near the surface of the glacier. Based on a particle motion diagram, we believe that icequakes are generated by cracks in crevasses produced by gravity force that moves the glacier downhill. Therefore, the registered seismic signal originates by elastic behavior of ice when it is submitted to the rupture process (Paterson; 1994, Feynman; 1972, Midelton-Wilcock; 1994)

We compared our set of LP events with the classification made by the IG EPN's data registered by the Cotopaxi permanent network (Convenio Inecel-EPN ; 1999). We found that 27% of the events classified as LP events are in reality icequakes (Fig 4). This confirms the similarity of LP events and icequakes when registered on bedrock. This could explain in part the great number of LP events registered in Cotopaxi by Ruiz et al. (1998).

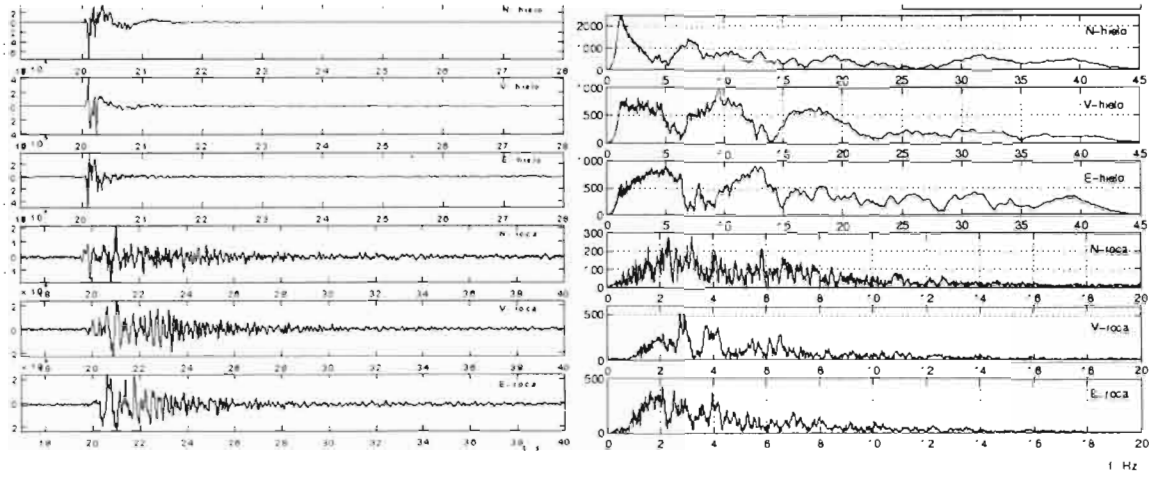

Fig.1: event 98.196.01.06.12. Example of an icequake registered by COHI (up) and CORE (down) stations with the corresponding spectra.

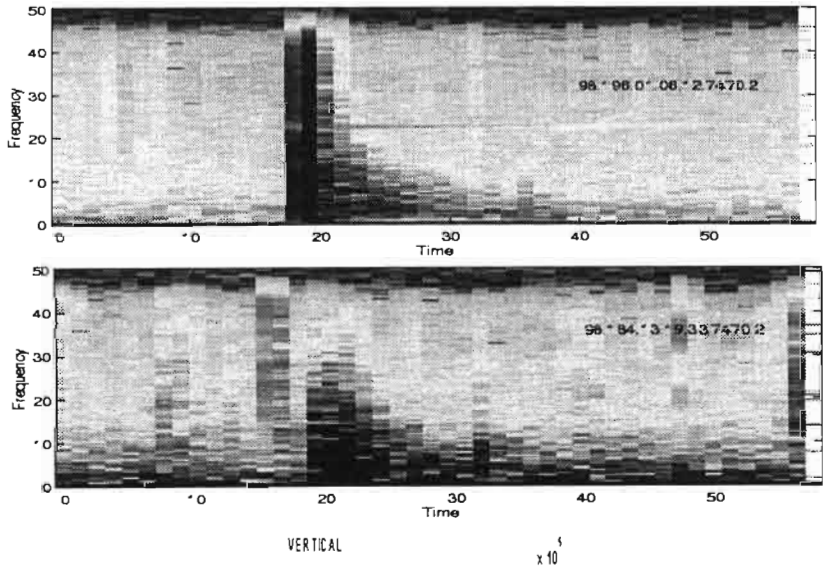

Fig.2 sup: Spectrogram calculated for the vertical component of an icequake registered in ice. The spectral density distribution is restrained to short period of time.

Fig 2 inf: Spectrogram calculated for the vertical component of a LP event registered in ice.

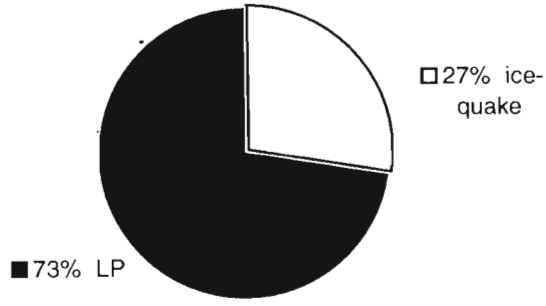

Fig 4: Comparison between the LP events detected by the network of Instituto Geofísico Escuela Politécnica Nacional and the classification established in our study. We found that 27% of events classified as LP events are in reality icequakes.

Geophysical Networks at Cotopaxi volcano (IRD/EPN)

(1) Sismological array

- EPN permanent seismic array
- IRD telemetered seismic array
- IRD seismic stations
- Temporary seismic stations
- 3 components station

(2) Ground deformation & Gravity repetition network

- GPS
- GPS/microgravity
- Levelling/microgravity
- EDM Base
- EDM reflector

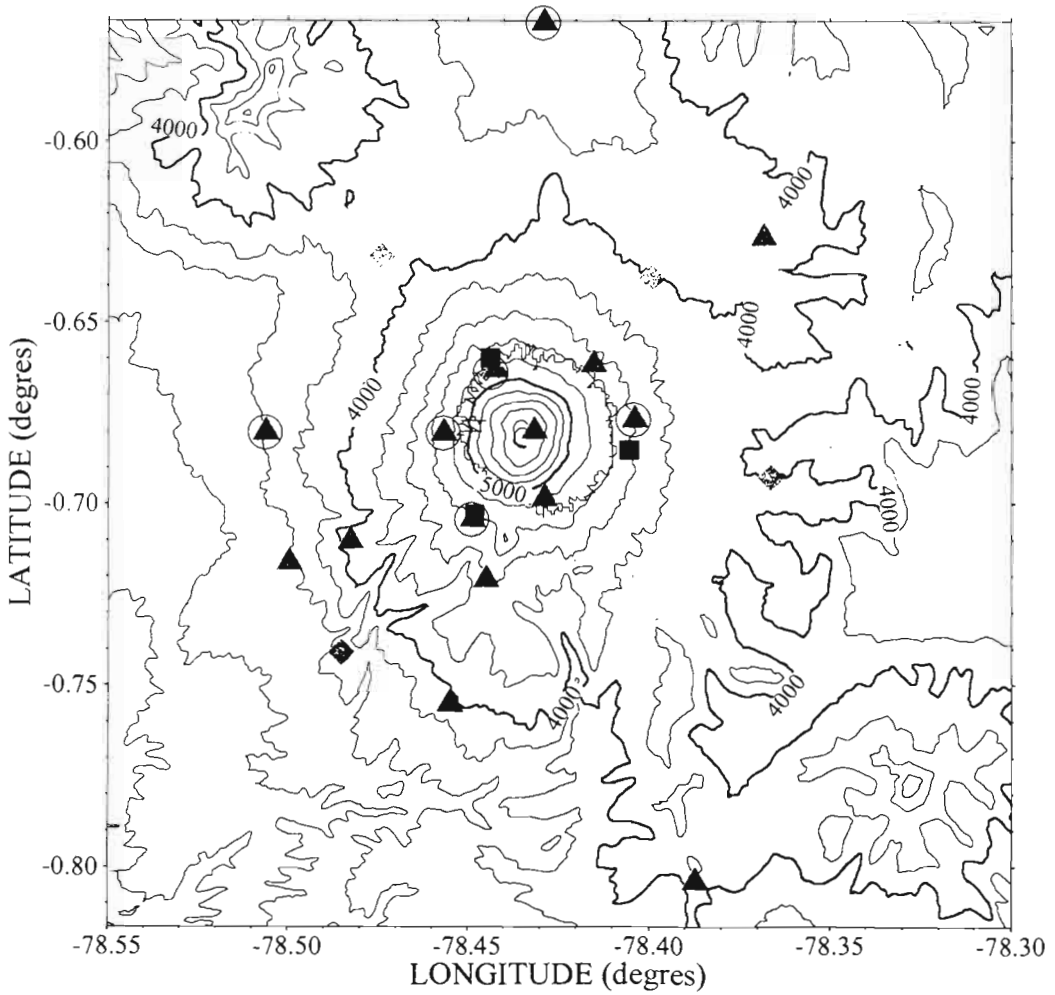

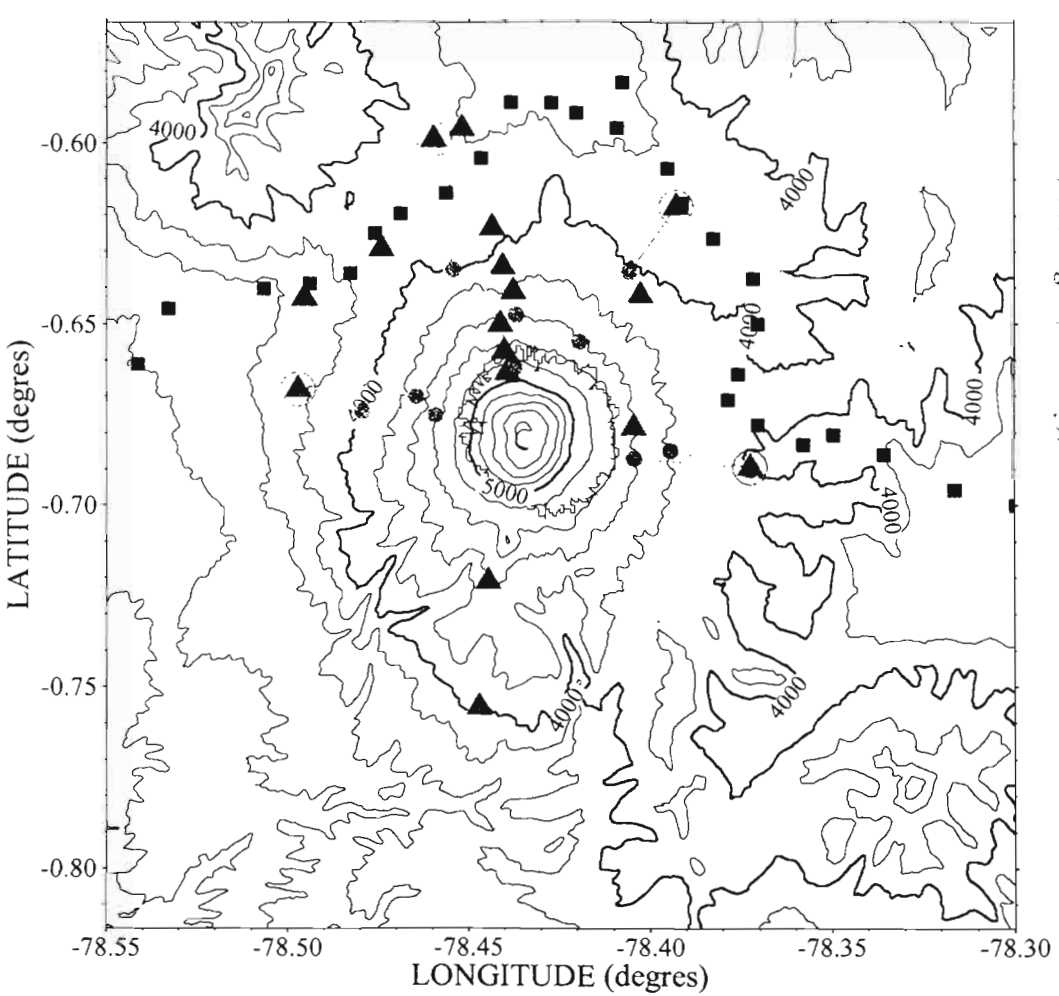

Fourth ISAG, Goettingen (Germany), 04 - 06/10/1996

REFERENCES

Convenio INECEL - EPN,Vigilancia de la actividad sísmica y volcánica de los volcanes Tungurahua y Cotopaxi. Informe Técnico No.23. Trimestre Julio - Septiembre 1998'. Quito, Enero 1999.

Chouet, Bernard, Long-period volcano seismicity: its source and use in eruption forecasting, Nature, Vol 380, 28 March1996.

Feynman,Richard, Lectures on Physics, vol 2; Fondo Educativo Interamericano; 1972.

Hall, M., and P.Mothes , Cotopaxi Volcano, Ecuador: Mitigation of Debris flow Impact-Daunting Task, IAVCEI News No.3; 1997.

Midleton-Wilcock, Mechanism in the Earth and Enviromental Sciences, Cambridge;1994.

Neave, K. G., and J.C. Savage, Icequakes on the Athabasca Glacier, J. of Geophys. Res., 75, 1351-1362.

Paterson,W.,The Physics of Glaciers, Redwood Books;Great Britain;1994.

Ruiz, M., B. Gullier, JL. Chatelain, H. Yépez, M. Hall, P. Ramón. Posisble causses for the seismic activity observed in Cotopaxi volcano, Ecuador. Geophysical Research Letters, Vol. 25, NO. 13, July 1, 1998.

Weaver, C., S. Malone, Mt. Saint Helens Seismic Events: Volcanic earthquakes or glacial noises?, Geophysical Research Letters; Vol. 3 , No. 3; March 1976.

Weaver, C., S. Malone, Seismic evidence for discrete glacier motion at the rock-ice interface, Journal of Glaciology; Vol. 23, No. 89; 1979.

SEDIMENTARY RECORD OF THE SALAR DE ATACAMA: PALAEOHYDROLOGICAL IMPLICATIONS

Virginia CARMONA ARRANZ(1), Juan Jose PUEYO (2), Conxita TABERNER (3), Carles AYORA (4), Ramon ARAVENA (5) and Guillermo CHONG D.(6)

(1) Institut Ciencies de la Terra, CSIC, Barcelona, Spain (vcarmona@ija.csic.es)
(2) Departament de Geoquimica, Universitat de Barcelona, Spain (juanj@natura.geo.ub.es)
(3) Institut Ciencies de la Terra, CSIC, Barcelona, Spain (ctaberner@ija.csic.es)
(4) Institut Ciencies de la Terra, CSIC, Barcelona, Spain (cayora@ija.csic.es)
(5) Department of Earth Sciences, University of Waterloo, Ontario, Canada (roaraven@sciborg.uwaterloo.ca)
(6) Departamento de Ciencias Geologicas, Universidad Catolica del Norte, Antofagasta, Chile (gchong@socompa.cecun.ucn.cl)

KEYWORDS: Salar de Atacama, geochemistry, fluid inclusions, halite cores, sulphate isotopic composition.

INTRODUCTION

The *Salar de Atacama* is the largest recent evaporitic basin in Chile, with a surface area of 2,900 km^2. It is located in the Atacama desert approximately 160km east of the city of Antofagasta, between the Cordillera de Domeyko to the west and the Andean Altiplano to the east.

Since Neogene times the Salar, as the whole Atacama desert, has been affected by an arid climate, due to the rain shadow effect caused by the Andean Range. Thus, the water inputs to the basin are mainly restricted to those supplied from the Andes, either by subterranean or surficial flows.

Three zones can be distinguished on the Salar surface (Bevacqua and Chong, 1995): a *saline nucleus* (with roughly 90% of halite, where interstitial evaporite precipitation is active); a marginal zone

surrounding the nucleus (composed mainly of sulphates, carbonates and detrital sediments); and the zone of the Rio San Pedro delta, at the northern part of the Salar.

Selected cores from seven of the boreholes drilled for lithium-rich brine prospection have been sampled. The central borehole (which is also the deepest one at 500 m deep) is manly composed of displacive halite. The four boreholes selected from the southern part of the *nucleus* are largely made of chevron halite facies. The two cores located in the delta zone are richer in terrigenous sediments, representing the record of the main sediment input into the salar.
The interpretation of the hydrological evolution of the salar is a major goal for understanding the mechanisms of distribution of K and Li-rich brines within the salar.

Methodology

In the seven cores studied the mineralogy of accessory minerals has been systematically determined by XRD and from the petrographic study of thin sections. Textures and relationships between the different mineral phases have provided information on the mineral paragenesis and the sedimentary / diagenetic environment where the evaporite minerals precipitated.

The concentration of major solutes (Cl^-, SO_4^{2-}, Na^+, K^+, Ca^{2+}, and Mg^{2+}), in primary brines trapped in halite as fluid inclusions, has been measured by means of Cryo-SEM-EDS (Scanning Electron Microscopy - Energy Dispersive System) following the methodology of Ayora and Fontarnau (1990) and improved in Ayora et al. (1994). Fluid inclusion analysis enables us to discover the brine composition from which halite precipitated.

The isotopic composition ($\delta^{18}O$ and $\delta^{34}S$) of accessory sulphates dispersed in halite has been determined. The information provided by these data gives insight on the source of brines as well as on the evaporation-concentration-precipitation mechanisms and their record through the different salar zones.

CONCLUSIONS

The evaporite deposits filling the basin are arranged cyclically. The cycles are dm-thick and are made of pure halite alternating with cm-thick terrigenous beds, which show lower erosional contacts. The mineral components of these beds are mainly plagioclase, quartz, and clay minerals, though gypsum is also present. In some of the studied cores, gypsum and anhydrite are found as cm-thick layers within the halite rock. Polyhalite is mainly present as vein infills, but also as coatings displaying botryoidal textures around halite crystals. Some samples show minor amounts of sylvite.

The isotopic compositions of sulphates from the studied boreholes are arranged along a positive trend, with the heavier $\delta^{18}O$ and $\delta^{34}S$ values mainly corresponding to polyhalite-rich layers. However, isotopic composition values also group according to the location of the samples within distinct salar zones: lighter values correspond to the south-western sector of the salar whilst the heavier values are those from the north-eastern areas. Two possible explanations for this distribution are:

1) Brine evolution during evaporation and fractionation during precipitation (i.e. heavier sulphates would precipitate in the initial stages and evolved waters migrating to the SW would then be impoverished in the heavier isotopes).

2) Existence of two water supplies (one from the eastern Cordillera de Domeyko and another from the Andean Ranges) feeding the *nucleus*. This agrees with the interpretation of Risacher and Alonso (1996).

The results obtained from fluid inclusion analysis give the composition of the synsedimentary brines present within the basin in the past, which are different from those of the recent interstitial brines. These results support the second hypothesis for the origin of brines feeding the salar through time. The SW part of the *nucleus* contains Ca-rich brines, while SO_4-rich brines are found at the NE. This distribution also changes with depth in the deepest central borehole, which also shows strong variations in K^+ and Mg^{2+} concentrations with depth.

The lateral and vertical variations of brine composition, as well as the isotopic composition of sulphates in the salar record, suggest that the salar was fed by two main water supplies. The proportion between the water supplies underwent significant relative changes in the past. This implies a variation in the dominance of each of these water sources through time and space in the different salar zones. Although, the central part of the *nucleus* was always submitted to both water inputs, one having higher concentrations of K^+ and Mg^{2+} than the other.

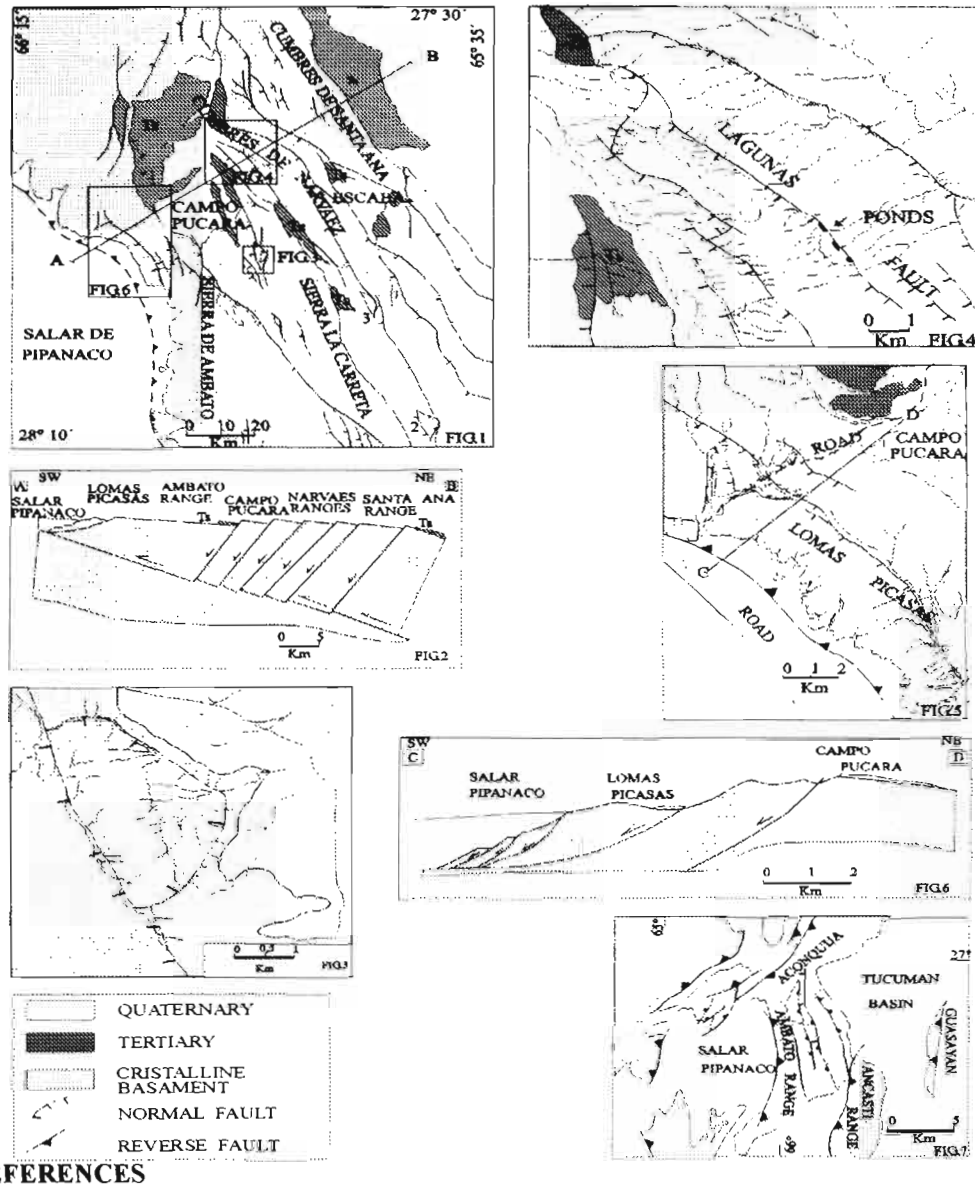

REFERENCES

Ayora C., Fontarnau R.1990. X-ray microanalysis of frozen fluid inclusions at - 140°C. Chem. Geol., 89, 135-148.

Ayora C., Garcia-Veigas J., Pueyo J.J. 1994. X-ray microanalysis of fluid inclusions and its application to the geochemical modeling of evaporite basins. Geochimica et Cosmochimca Acta, 58, 43-55.

Bevacqua P., Chong-D. G. 1995. The Salar de Atacama of Northern Chile: Evolution and Stratigraphy of its Nucleus. GLOPALS-IAS Meeting Abstracts. Chile. 21-22

Risacher F. Alonso H. 1996. Geoquimica del Salar de Atacama. Parte 2: Evolucion de las Aguas. Revista Geologica de Chile, 23, (2), 127-136.

CLOCKWISE BLOCK ROTATIONS ALONG THE EASTERN BORDER OF THE CORDILLERA de DOMEYKO, BETWEEN 22°45' and 23°30' (CHILE).

César ARRIAGADA [1], Pierrick ROPERCH. [2] and Constantino MPODOZIS [3]

[1] Departamento de Geología, Universidad de Chile, Santiago, Chile (carriaga@quad.dgl.uchile.cl)
[2] IRD/Dep. de Geología, Universidad de Chile, Santiago, Chile (properch@dgf.uchile.cl)
[3] Servicio Nacional de Geología y Minería, Santiago, Chile (cmpodozi@sernageomin.cl)

KEYWORDS: Tectonic Rotations, Cordillera de Domeyko, Paleomagnetism, Chile.

INTRODUCTION

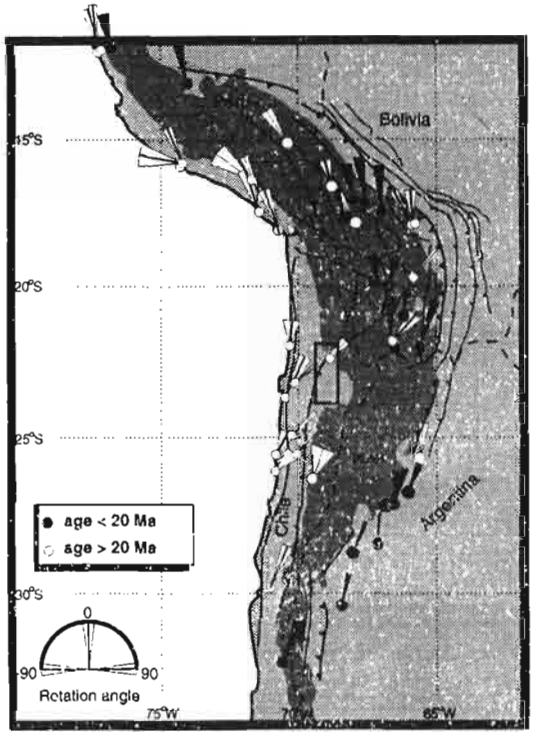

Figure 1: Summary of paleomagnetic rotations in the Central Andes. The box indicates our study area to the west of the Salar de Atacama.

Several paleomagnetic studies demonstrates that the occurrence of tectonic rotations is one of the major characteristic of the structural evolution of the Central Andes (Figure 1). These rotations are clockwise along the Chilean margin while counterclockwise rotations are found north of Arica.

The origin of these rotations is however still a matter of debate. In most of the published studies, the lack of a structural control and geographically restricted paleomagnetic sampling (few sites) impede a clear understanding of the age of the rotation and the size of the rotating blocks. Up to now, rotations within the Chilean forearc have been attributed either to early Cretaceous deformation along the Atacama Fault System (Forsythe and Chilsholm, 1994; Randall et al. 1996), oroclinal bending of the whole Andes or in situ block rotations in response to oblique convergence (Beck et al., 1986).

Preliminary results from the Northern Salar de Atacama (Hartley et al. 1992) indicate the presence of rotations, possibly associated to relative motions between thrust sheets. In this study, we report detailed results from 38 sites collected along the western border of the Salar de Atacama (El Bordo Escarpment, Figure 2). This area corresponds to a segment of the Cordillera de Domeyko where in situ clockwise block rotations have been suggested to interpret the complex structural pattern (Mpodozis et al., 1993). Although compressive deformation seems to play a role in shaping the oriental border of the Cordillera de Domeyko, multiple episodes of Tertiary strike-slip displacements, either in dextral or sinistral sense have been reported (Reutter et al., 1991; Tomlinson and Blanco, 1997).

GEOLOGY OF THE STUDY AREA

Thick continental red beds, conglomerates and intercalated volcanic rocks constitute most of the rocks outcropping along the El Bordo ("Purilactis Group", Ramírez and Gardeweg 1982; Hartley et al., 1992; Charrier and Reutter 1994, Figure 2) with ages ranging from Cretaceous at the bottom to Oligocene at the top. (See Mpodozis et al., this volume, for a new revision of the stratigraphy of the area).

MAGNETIC PROPERTIES

Relatively fine-grained sediments belonging to the base of the Purilactis Group, especially favourable to paleomagnetic studies, have lower magnetic susceptibility than intermediate and upper levels consisting of volcanodetrital material. Thirty-eight sites, with a total of 420 samples were drilled in the sedimentary sequences, interbedded volcanic rocks and associated intrusions (Fig. 2). Detailed progressive thermal demagnetization provided well-defined characteristic magnetizations for most sites.

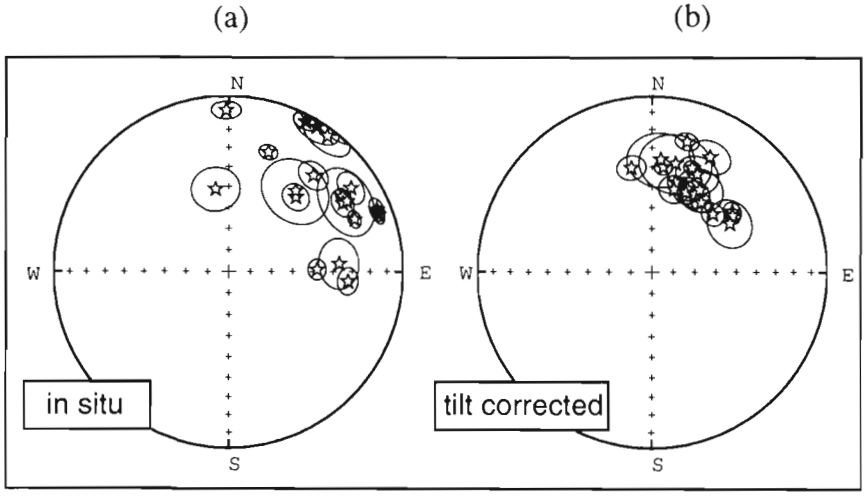

Figure 3: Equal -are projection of mean site paleomagnetic directions from the lower units of the Purilactis group.

In in situ coordinates, characteristic magnetizations are dispersed and away from the present day field direction, a feature that demonstrates that secondary overprint was well removed during demagnetization. (Fig. 3 a). All sites corresponding to the lower Purilactis Group, have normal polarity (Fig. 3 b). The fact that only the normal magnetic polarity is suggests deposition during the long normal

Cretaceous Chron (119-84 Ma). On the other hand, normal and reverse polarities are observed in the overlying volcanic rocks and cross cutting dikes. K-Ar ages (Mpodozis et al. this volume; Arriagada [in preparation]) indicate an emplacement for these volcanic rocks at the Cretaceous-Tertiary boundary (67-64 Ma).

The observed inclinations are in good agreement with the expected for stable South America during the Cretaceous. However, the magnetic declinations are very different from the expected directions, demonstrating the importance of clockwise rotations as a mechanism of the deformation. Upon grouping the samples according to their geographical location, distinct clusters are observed showing a well-defined gradient in the magnitude of the rotation increasing from north to south (Fig. 2). The largest rotation (~70°) is found South of Cerro Quimal, while to the north, the Barros Arana Syncline does not show evidence of rotations. The large rotation reported by Hartley et al. (1992) at one locality corresponds to a disrupted small block on the northern edge of the syncline. Dikes with ages of ~66 Ma, that intrude sediments from the lower Purilactis Group record the same amount of rotation, indicating that tectonic rotations are younger than Paleocene. Further work is needed to constrain the upper limit for the age of the rotation. However, rotations are likely related to a significant deformation phase that affected the Cordillera de Domeyko during the Eocene (Mpodozis et al., 1993).

CONCLUSIONS

The lack of the reverse polarity in the basal members of the Purilactis Group, suggests deposition during the long normal polarity period of the Cretaceous (119-84 Ma). Large clockwise rotations found in this study tend to support the tectonic model previously proposed by Mpodozis et al. (1993) for the Cordillera de Domeyko. However, paleomagnetic data are yet limited to the eastern border of this segment of the range where variations in the amount of shortening may enhance local tectonic rotations. Differences in the magnitude of Eocene (Oligocene?) rotations are strongly controlled by major heterogeneities of the Paleozoic basement and the presence of the partially inverted Purilactis basin. However, the reason why the sense of the rotations is systematically clockwise in most areas of the northern Chilean Andes is still poorly understood.

REFERENCES

Beck, M. E., Drake, R.E. and Butler, R. F. 1986. Geology, 14:132-136.

Charrier, R., Reutter, K. 1994. Tectonics of the Southern Central Andes, Springer Verlag, Berlin Heidelberg, New York.

Forsythe, R., and Chisholm, L. 1994. Journal of South American Earth Sciences 7(3/4), 279-295.

Hartley, A., Jolley, E., Turner, P. 1992 a. Tectonophysics, 205, 49-64.

Mpodozis, C., Marinovic, N., Smoje, I. 1993.. Second ISAG, Paris. ORSTOM. p. 225-228.

Ramírez, C. F., Gardeweg, M. 1982. Carta Geológica de Chile N°58 (1:250.000), p. 1-121, Santiago.

Randall D. E, Taylor G. K.and Grocott, J. 1996., J. Geophys. Res. 101 (B7), 15,783-15,798.

Reutter, K., Sheuber, E. 1991. Geologishe Rundschau 80/1, p. 135-153.

Tomlinson, Andrew J. and Blanco, Nicolás. 1997. VIII Congreso geológico chileno. Vol.III pp 1973-1882.

* Research funded by FONDECYT grant #197002

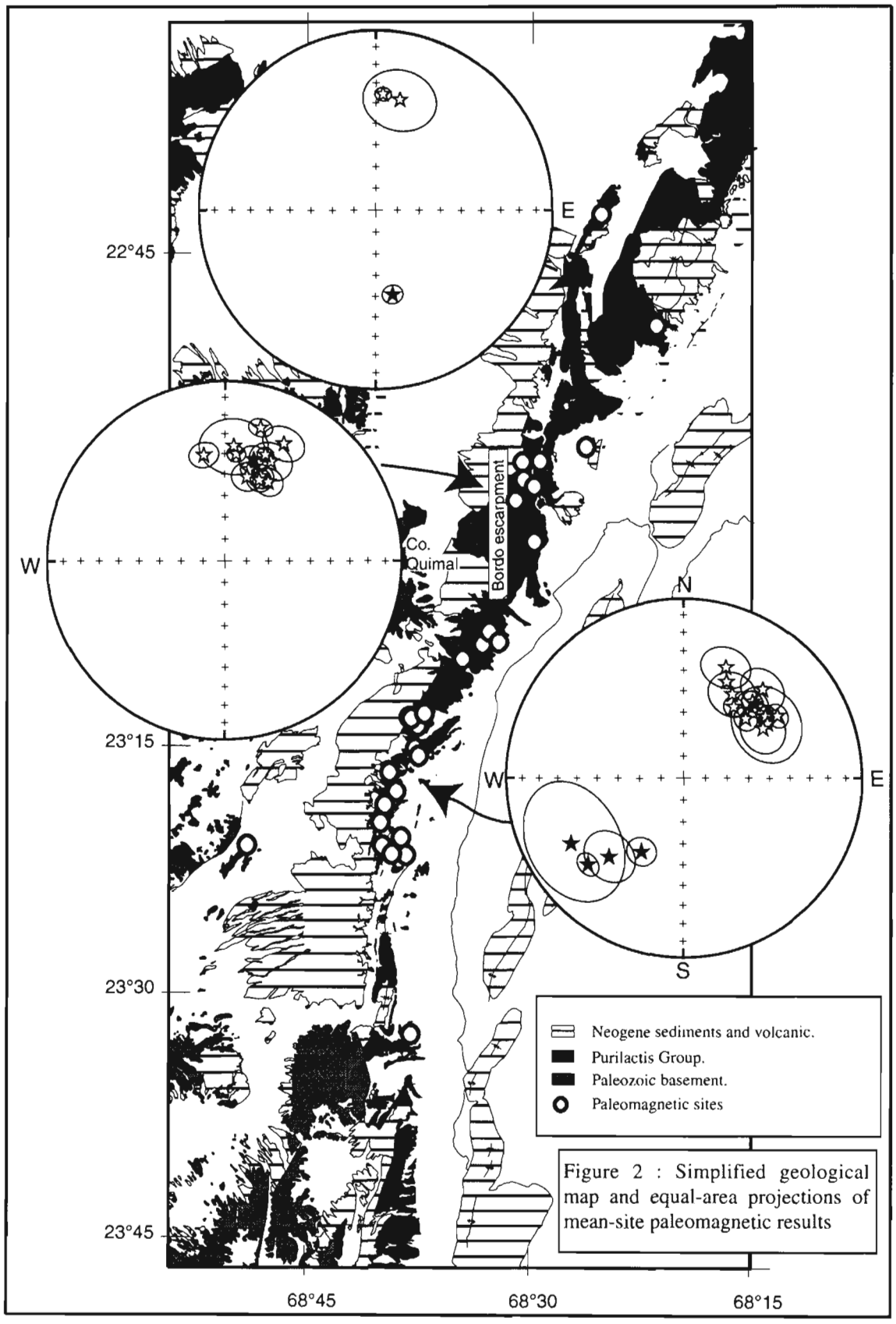

Figure 2 : Simplified geological map and equal-area projections of mean-site paleomagnetic results

SHAPE AND INTRUSION STYLE OF THE COASTAL BATHOLITH, PERU.

Michael P. ATHERTON (1) and Michael HAERDERLE (1)

(1) Department of Earth Sciences, University of Liverpool, Liverpool, L69 3BX, UK
(mikea@liverpool.ac.uk)

KEY WORDS: Batholith shape, aspect ratio, root, floor.

INTRODUCTION

Granite batholith emplacement in the upper crust is the final stage in a large scale exchange of energy and mass which started with generation and segregation of melt, then magma ascent and finally intrusion of magma to form the batholith pluton assemblage. In spite of much discussion there is still no consensus on how space is made for magmas in continental crust. A major problem involves the three dimensional shape/geometry and in particular evidence of the floors of plutons which are curiously rarely observed. Furthermore prejudices are common with regard to where melt originates and how it ascends to the high levels at which batholiths are commonly emplaced.

Here the shape of the Coastal Batholith in Peru determined from gravity modelling is described, together with some evidence for the form of the magma conduits. This is integrated with field, geophysical and geochemical modelling to help constrain possible emplacement mechanisms and limits to the energy/mass exchange.

THE SHAPE OF THE COASTAL BATHOLITH

The Coastal Batholith is the major plutonic phase of Mesozoic magmatism in Peru. This lineament-constrained multiple Batholith extends over 1600km parallel to the coast, with up to 1000 plutons cropping out mainly within the composite Huarmey/Cañete marginal basin (Atherton et al. 1983). Its extension to the north and south is markedly attenuated so that over 70% of the Batholith lies within the exposed Albian basinal rocks. The basin formed on major splitting/rifting of continental crust which typically produced an anomalous high heatflow shown by metamorphic thermal gradients in excess of $300°Ckm^{-1}$ (Atherton, 1990). The thermal structure within the rift induced shallow melting (5-10km) of the 'new crust' basic rocks at the bottom of the basin to form the magmas of the Coastal Batholith immediately after basin inversion. Atherton (1990) thought that the rapidly produced large amounts of magma was quickly intruded up axial fractures (parallel to the plutonic lineament) then horizontally to form thin tabular intrusions near the surface.

Recent gravity modelling of the Batholith and its envelope along three orthogonal traverses approximately 100km apart, north of Lima, confirms the geometry of the above model and shows the Batholith has a thin tabular shape, with the following characteristics:

- geometry is essentially *flat slab*;
- the three traverses show a width:thickness ratio across the whole Batholith (to sea level datum) in kilometres: 35:2, 60:3, 28:1.3 i.e. *aspect ratios* of 17.5, 20 and 21.5;
- individual superunits which may be considered to be individual/separate plutons have aspect ratios near 5, e.g. 3-7km thick, 18-25km wide. These values are similar to plutons from the European Hercynian, Maine, New Hampshire and Lake District, England; (see also McCaffrey & Petford, 1997)
- slabs anchored along the western margin by relatively *deep root* of granitic material;
- thick roots to the west are all 10km to the base, and are 6, 4 and 10km respectively at that base;
- western edge of the Batholith (-ve anomaly) is marked by the Santa Rosa tonalite which crops out in all three profiles ($2.66\ gcm^{-3}$);
- in the Pativilca-Conococha profile there is no granitic material below the datum line in the central part of the Batholith;
- on a crustal scale the Batholith forms a *thin veneer* on the top of the continental crust.

IMPLICATIONS

An important feature of the modelling is the existence of a thick "granitic" root to the west which extends to depths of more than 10km. This could well be a multiple dyke system which may have been the main conduit for magmas making up the western part of the Batholith. Thus the Santa Rosa superunit which is exposed over 250km along the lineament, forming 50% of the western outcrop of the Batholith (Atherton, 1983) could well have been fed by this system. The width of this root varies from 4 to 10km and may be compared to the dyke array feeding the Gangotri plutons in the Himalayas, i.e. 100 dykes of 10 to 20m width or 1000 to 2000m of dykes feeding a kilometric sized pluton (Scaillet et al. 1995) and the tabular root zone of the Bergell pluton, a 1km thick deformed dyke system feeding the 11km wide pluton. An important implication of the geometry seen in the Coastal Batholith model is that the bulk flow at the level of emplacement is horizontal cf. Cruden (1998). The root system of the Coastal Batholith intersected the melt zone, determined from the thermal structure in the basin (Atherton, 1990). This conduit transferred large amounts of granitic material from the source at about 10km to about 2km from the surface.

Tobisch et al (1995) estimate more than 4.5 x 10^5 km^3 of granitic material in the Central Sierra Nevada in a similar setting to Peru, was intruded in less than 30Ma. Myers (1975) considering the effect of intrusion of such large amounts of magma thought "the lack of distortion of the envelope particularly the lack of vertical compression of the roof rocks" was important in analysis of the space problem and consequently dilation and roof lifting were not important mechanisms. Most space in the Coastal Batholith was created by *downward displacement* of material (Myers, 1975).

Clearly the extraction of the huge amounts of magma from the shallow source beneath the site of the proto Batholith would induce floor depression. Field evidence suggests floor depression by cantilever and piston mechanisms (Cruden, 1998) are both important and can account for the geometry of the Batholith plutons (Myers, 1975). Together with the modelling of the source and melting conditions it forms a coherent dynamic model of Batholith formation. In Peru the shallow melting constrains the exchange process, that is *magma up and floor rock down*, to upper crustal domains. It is inherently more likely than the crustal scale exchange (over 50km) envisaged by Paterson & Miller (1998) and others.

REFERENCES

Atherton, M. P., Pitcher, W. S., & Warden, V., 1983. The Mesozoic marginal basin of Central Peru. Nature, 305, 303-306.

Atherton, M. P., 1990. The Coastal Batholith of Peru: the product of rapid recycling of new crust formed within rifted continental margin. Geol. Journ., 25, 335-349.

Cruden, A. R., 1998. On the emplacement of tabular granites. Journ. Geol. Soc. London, 155, 853-862.

McCaffrey, K. J. W., & Petford, N., 1997. Are granitic intrusions scale invariant? Journ. Geol. Soc. London, 154, 1-4.

Myers, J. S., 1975. Cauldron subsidence and fluidization: mechanisms of intrusion of the Coastal Batholith of Peru into its own volcanic ejecta. Geol. Soc. Amer. Bull., 86, 1209-1220.

Paterson, S. R., & Miller, R. B., 1998. Magma emplacement during arc-perpendicular shortening: an example from the Cascades crystalline core, Washington. Tectonics, 17, 571-586.

Scaillet, B., Pêcher, A., Rochett, P., & Champenois, M., 1995. The Gangotri Granite (Garhwal Himalaya): laccolithic emplacement in an extending collisional belt. Journ. Geophys. Res., 100, 585-687.

Tobisch, O., Saleeby, J. B., Renne, P. R., McNulty, B., & Tong, W., 1995. Variations in deformation fields during development of a large volume magmatic arc, Central Sierra Nevada. Geol. Soc. Amer. Bull., 107, 148-166.

STRUCTURE OF THE MÉRIDA ANDES, VENEZUELA: FACTS AND MODELS

Felipe E. AUDEMARD M. (1) & Franck A. AUDEMARD M. (2)

(1) PDVSA Exp. & Prod., Caracas, Venezuela. e-mail: audemardf@pdvsa.com
(2) FUNVISIS, Caracas, Venezuela. e-mail: faudem@funvisis.internet.ve

KEYWORDS: Triangular zones, Foothills, Type-A subduction, Models, Andes, Venezuela.

INTRODUCTION:

The Mérida Andes (MA) seem to be the northeastward topographic prolongation of the Eastern Cordillera of the Colombian Andes, but they do not keep any genetical relationship between them (Fig. 1), since the NE-SW trending Venezuelan Andes are not related to direct interactions between South American (SA) craton and either arc terrains or oceanic domains, as the rest of the SA Andes do. The chain growth results from Pliocene-Quaternary transpression due to oblique convergence between two independent continental lithospheric blocks. This tectonic setting is responsible for ongoing strain partitioning along MA where foothills are been shortened transversely whereas the Boconó fault –roughly located in the core and along the MA axis- accommodates dextral slip. This Plio-Quaternary compression has inverted Jurassic grabens, exposing Precambrian and Paleozoic rocks of the SA continental crust.

Several models have been proposed to explain the major structure of the MA. First, an essentially symmetric chain to a major axial strike slip fault, with both sides bounded by reverse faults, responsible for chain vertical growth, was suggested by González de Juana (1952) and Rod (1956). Consequently, the MA resembled a huge positive flower structure; a model that was also shared by Dallmus (1957; *in* Rod et al., 1958), at least for the upper crustal level. This idea soon became obsolete since models quickly started to consider the fact that MA are actually assymmetric, as proved by the gravimetric survey carried

out by Hospers & Van Wijnen (1959). This assymetry was first proposed by Bucher (1952). In the last 20 years, the majority of models have taken into account such fact, where other new modern concepts have been applied or introduced, such as: continental (type A) suduction with either NW polarity (Audemard, 1991, where major structuraction of the MA results of a NW-vergent crustal-scale wedging –Fig. 2-; "orogenic float" model by Jácome et al., 1995 –Fig.3-) or SE polarity (Kellogg & Bonini, 1982; De Toni & Kellogg, 1993 –Fig. 4-; Sánchez et al., 1994 –Fig. 5-; Coletta et al., 1996 –Fig.6-), crustal delamination, flexural basins, blind thrusting, intracutaneous wedging and triangular zones (Figs. 7 & 8); but without actually bringing new conclusive regional geological and geophysical data to support such crustal models. Definitely, improvement of geophysical data acquisition has led to a better understanding of the very few first kilometer-thick subsurface structure of both foothills, attesting the NW vergence of the MA, where a rather deep conventional foreland (flexural) basin develops on the north (the Maracaibo basin; Fig. 7). On the contrary, its southeastern counterpart is almost absent, although SE-thrusting has been identified (no general agreement exists on the thrust vergence along these southern foothills, probably due to masking introduced by triangular zones and intracutaneous wedges) which even deform the Plio-Quaternary molasses (Audemard, 1991; Funvisis, 1997; Audemard, 1999. Fig. 8). Nevertheless, some of these NW-dipping thrust faults seem to cut through the basement, acting as either crustal-scale (Fig. 5 & 6) or conjugated minor backthrusts of the type-A subduction (Fig. 3).

The conceptual application of such assymetric crustal models, relying on a type-A subduction anyhow, uneases comprehension of how present strain partitioning is taking place –originally proposed by Rod (1960) and solidly supported by numerous recent neotectonic studies-, unless the Maracaibo blocks is conceived as being totally delaminated and extruded northward between two opposite-dipping subductions (ENE-dipping type-B Pacific subduction and NW-dipping type-A (intercratonic) one; as proposed by Audemard, 1991). Besides, it is hard to conceive the Boconó fault as a plate boundary in these models, where the whole northwestern corner of South America is actually part of it.

In conclusion, only structural interpretations at upper levels on both foothills of MA are reliable, but its deep-crustal structuration is still unsolved, and the answer to model ambiguities actually relies on a pioneer acquisition of deep seismic data.

REFERENCES

Audemard, Fe. (1991) Tectonics of Western of Venezuela: Ph.D. Thesis, Rice University, Texas, 245 p.

Audemard, Fe. (1997) Los Andes Venezolanos, visión alterna. VIII Cong. Geol. Venezolano, Porlamar; 1:85-92.

Audemard, Fr. (1999) Morpho-structural expression of active thrust systems in humid tropical foothills of Colombia and Venezuela. Zeitschrift für Geomorphologie (in press).

Bucher, W. (1952) Structure and orogenic history of Venezuela. Memoir of the Geological Society of America, 49: 1-113

Colletta, B.; Roure, F.; De Toni, B.; Loureiro, D.; Passalacqua, H. & Gou, Y. (1996) Tectonic inheritance, crustal structure and contrasting structural styles in the Venezuelan Andes. Tectonics, 16(5): 777-794.

De Toni, B. & Kellogg, J. (1993) Seismic evidence for blind thrusting of the northwestern flank of the Venezuelan Andes. Tectonics, 12(6):1393-1409.

Duerto, L.; Audemard, Fe.; Lugo, J. & Ostos, M. (1998) Síntesis de las principales zonas triangulares en los frentes de montaña del occidente venezolano. IX Congreso Venezolano de Geofísica (CD-Rom; artículo N° 25).

Funvisis (1997) Estudio neotectónico y geología de fallas activas en el piedemonte surandino de los Andes venezolanos (Proyecto INTEVEP 95-061). Funvisis' unpubl. report for INTEVEP, S.A. 155 pp + appendices.

Gonzalez de Juana, C. (1952) Introducción al estudio de la geología de Venezuela. Boletín de Geología (Caracas), 2: 407-416.

Hospers, J. & Van Wijnen, J. (1959) The gravity field of the Venezuelan Andes and adjacent basins. Versl. Gewone Vergad. Afd. Natuurkd. K, Ned. Akad. Wet., 23(1): 1-95.

Jácome, M.; Audemard, Fe. & Graterol, V. (1995) A Seismic, Gravimetric and Geologic Interpretation of a Transandean Profile Across the Venezuelan Andes. I Latinoamerican Geophysical Congress, Rio de Janeiro, Brasil, 15-18.

Kellogg, J. & Bonini, W. (1982) Subduction of the Caribbean Plate and Basament Uplifts in the overriding South-American Plate: Tectonics, 1(3):251-276.

Rod, E. (1956) Strike-slip faults of northern Venezuela. American Association of Petroleum Geologists Bulletin, 40:457-476.

Rod, E. (1960) Comments on "The Gravity Field of the Venezuelan Andes and Adjacent Basins". Boletín Informativo Asociación Venezolana de Geología, Minería y Petróleo, 3:170-175.

Rod, E.; Jefferson, C.; Von Der Osten, E.; Mullen, R. & Graves, G. (1958) The determination of the Bocono fault. Boletín Informativo Asociación Venezolana de Geología, Minería y Petróleo; 1(1-6):69-100.

Sánchez, M.; Audemard, Fe.; Giraldo, C. & Ruiz, F. (1994) Interpretación sísmica y gravimétrica de un perfil a través de los Andes venezolanos. Memorias VII Congreso Venezolano de Geofísica, 251-258.

Figs. 1 to 8: (**1**)- Schematic tectonic location map of MA (after De Toni & Kellogg, 1993): section location is about valid for all models shown here. (**2**)- NW-vergent wedging model for MA, related to a NW-polarity type-A subduction (after Audemard, 1997). (**3**)- "Orogenic floating" model after Jácome et al. (1995). (**4**)- SE-dipping type-A subduction model after De Toni & Kellogg (1993). (**5**)- SE-dipping type-A subduction model after Sánchez et al. (1994), where MA are structured as a crustal-scale positive flower structure. (**6**)- SE-polarity continental subduction with well-developed backthrusting (after Colletta et al., 1996). (**7** and **8**)- Structures within K-Q sedimentary sequence at the northern (after De Toni & Kellogg, 1993) and southern (after Funvisis, 1997 and Audemard, 1999) foothills respectively.

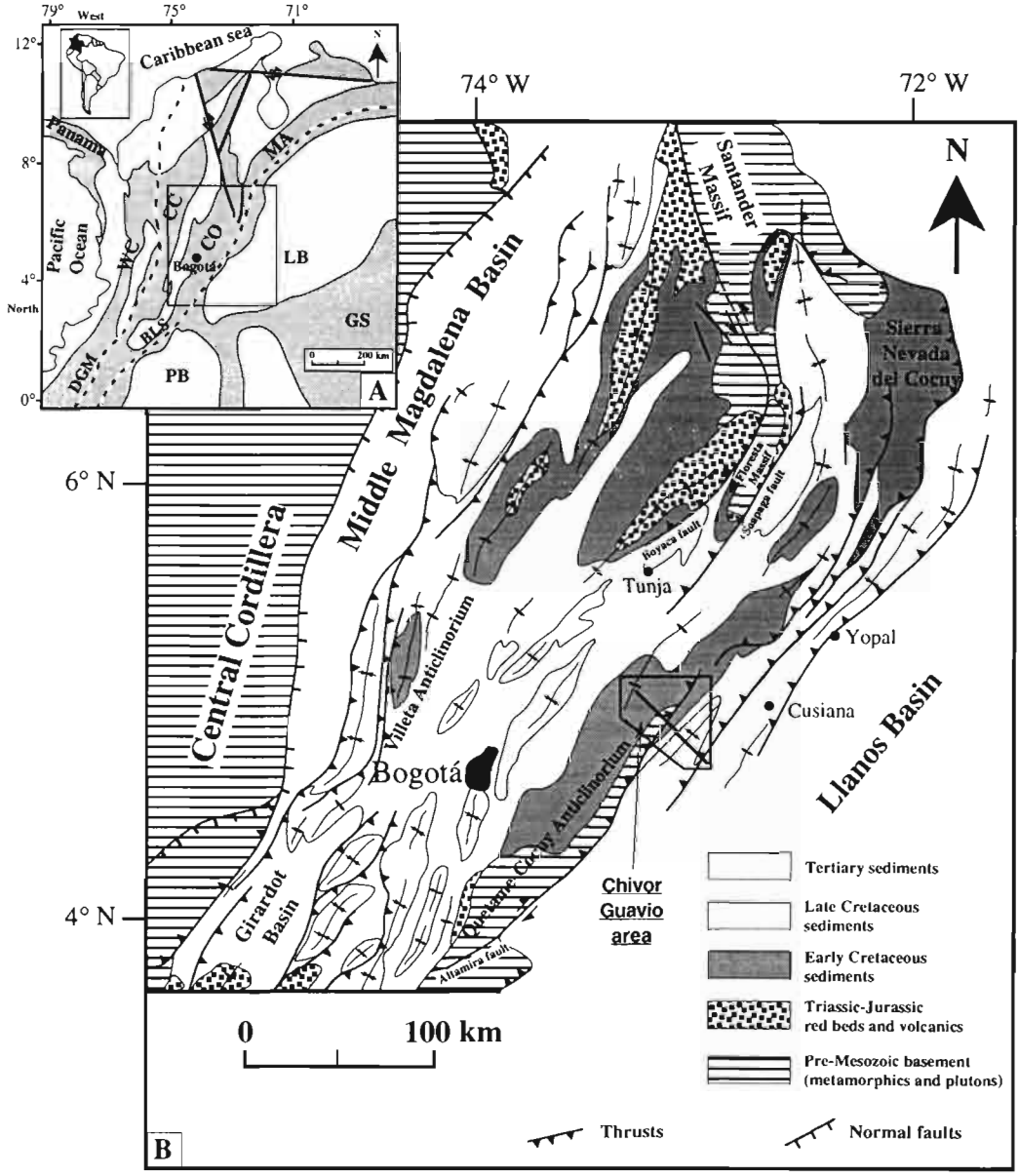

Figure 1: **A**: Major tectonic provinces (dark gray) of Colombia and western Venezuela (modified from Cooper et al, 1995). WC: Western Cordillera; CC: Central Cordillera; CO: Cordillera Oriental; MA: Merida Anes; GS: Guiana Shield. Present-day sedimentary basins shown in light gray. LB: Llanos basin; PB: Putumayo Basin. Two main suture zones are represented: The Dolores-Guayaquil Megashear (DGM, or Romeral fault) and the Borde Llanero Suture (BLS). Inset is Fig. 1B. **B**: Structural map of the Colombian Cordillera Oriental. Inset is the Chivor-Guavio area and line is the Las Juntas-Llanos cross-section.

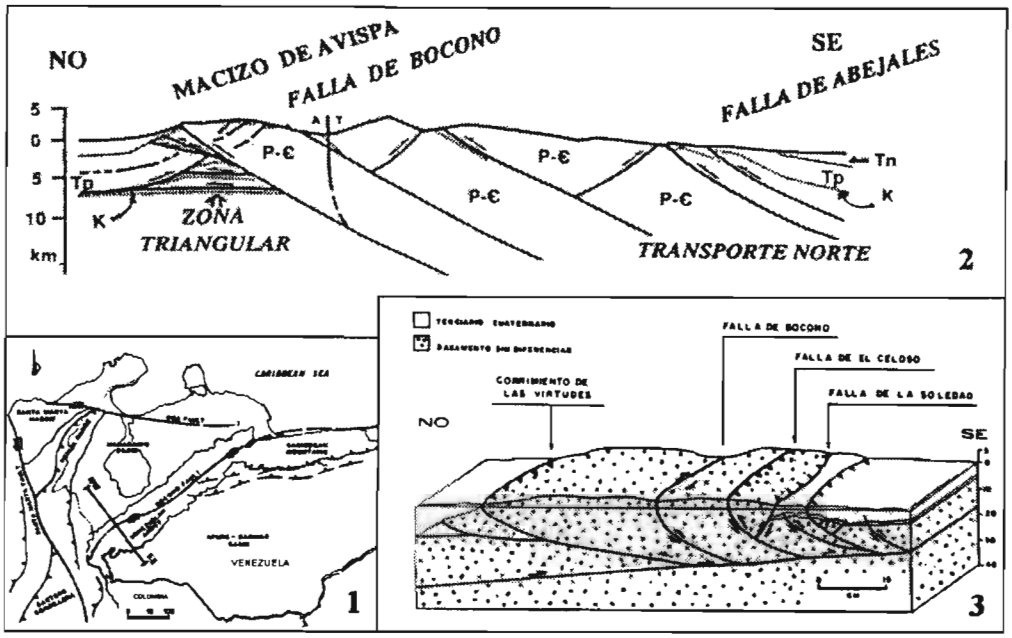
NO
MACIZO DE AVISPA
FALLA DE BOCONO
SE
FALLA DE ABEJALES
5
0
5
10
km
Td
K
P-Є
ZONA
TRIANGULAR
TRANSPORTE NORTE
Tn
Tp
2
CARIBBEAN SEA
VENEZUELA
1
FALLA DE BOCONO
FALLA DE EL CEDRO
FALLA DE LA SOLEDAD
CORRIMIENTO DE
LAS VIRTUDES
NO
SE
3

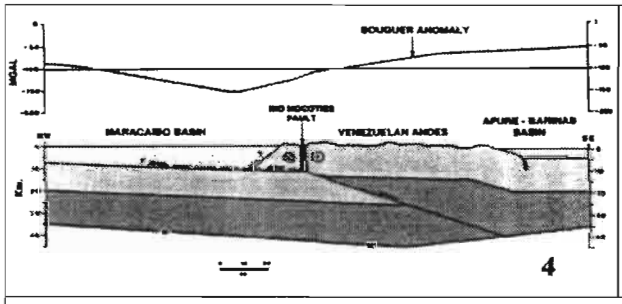
BOUGUER ANOMALY
MARACAIBO BASIN
RIO MOCOTIES
FAULT
VENEZUELAN ANDES
APURE - BARINAS
BASIN
4

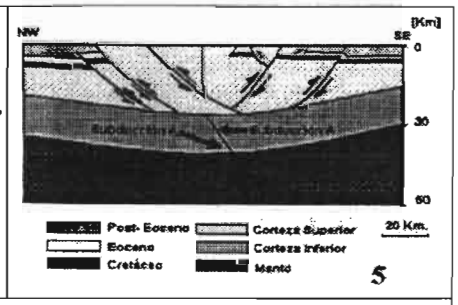
NW
SE
[Km]
0
30
60
Post- Eoceno
Eoceno
Cretácico
Corteza Superior
Corteza Inferior
Manto
20 Km.
5

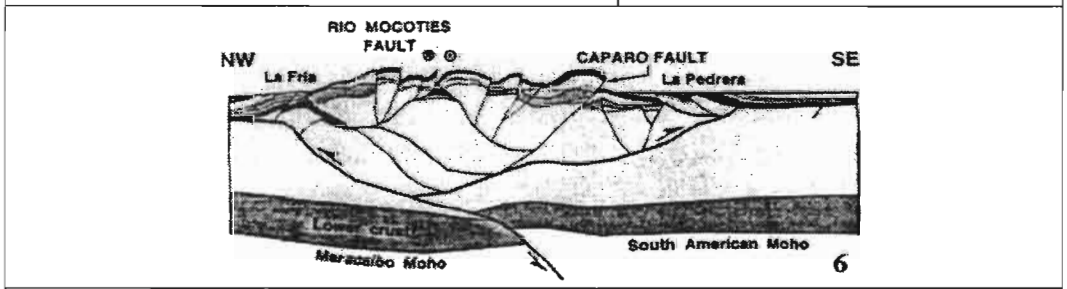
RIO MOCOTIES
FAULT
NW
CAPARO FAULT
SE
La Fria
La Pedrera
Lower crust
Maracaibo Moho
South American Moho
6

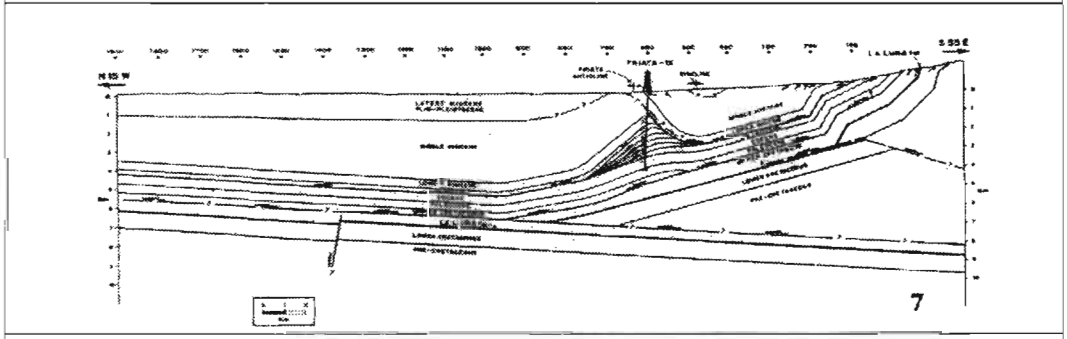
7

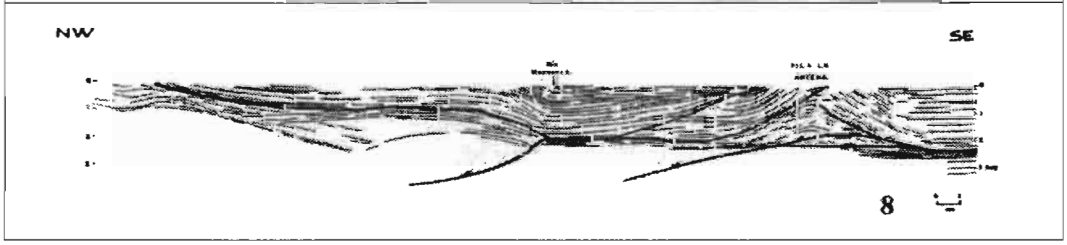
NW
SE
8

STYLE AND TIMING OF DEFORMATION IN THE ORIENTE BASIN OF ECUADOR

Patrice BABY(1), Marco RIVADENEIRA(1), Frédéric CHRISTOPHOUL(2), Roberto BARRAGAN(3)

(1) Convenio IRD- Petroproducción, Apartado 17 12 857, Quito, Ecuador; *pbaby@pi.pro.ec*
(2) Lab. de Dynamique des Bassins, 38 rue des 36 ponts, 31400 Toulouse, France, *geostruc@cict.fr*
(3) Kerr-McGee Corporation, 16666 Nothchase, Houston, TX 77060, USA; *rbarragan@kmg.com*

KEY WORDS: Ecuador, Oriente, inversion, tectonic history, petroleum basin

INTRODUCTION

The Oriente Basin of Ecuador (Dashwood and Abbotts, 1990) forms a Sub-Andean foothills and foreland basin comprised between the Putumayo Basin of Colombia and the Marañon Basin of Peru. Petroleum activities of the last 10 years provided new data which permit to clarify its structural features (Figs. 1 et 2) and tectonic evolution (Fig. 3). Stratigraphically, the Oriente Basin preserves a Phanerozoic sedimentary column ranging in age from Paleozoic to Recent (Tschopp, 1953; Canfield et al., 1982; Dashwood and Abbotts, 1990; Jaillard, 1997) which outcrops in the foothills (Napo and Cutucú uplifts). This sedimentary column can be subdivided into three mega-sequences: a pre-Cretaceous series, which is unconformably covered by a continental to shallow marine Cretaceous sedimentary preorogenic cycle and a Cenozoic continental foreland filling. In this paper, we resume the results of the IRD (Institut Français de Recherche pour le Développement) - PETROPRODUCCION tectonic teamwork. A revision and a new presentation of the sedimentary column involved in the deformation is proposed. A geometric and kinematic analysis and a new structural feature of the Oriente Basin are presented. On the base of the analysis of the tectonics-erosion-sedimentation relationships, principal tectonic events of the Oriente Basin development are defined. Geodynamic and Petroleum implications are then discussed.

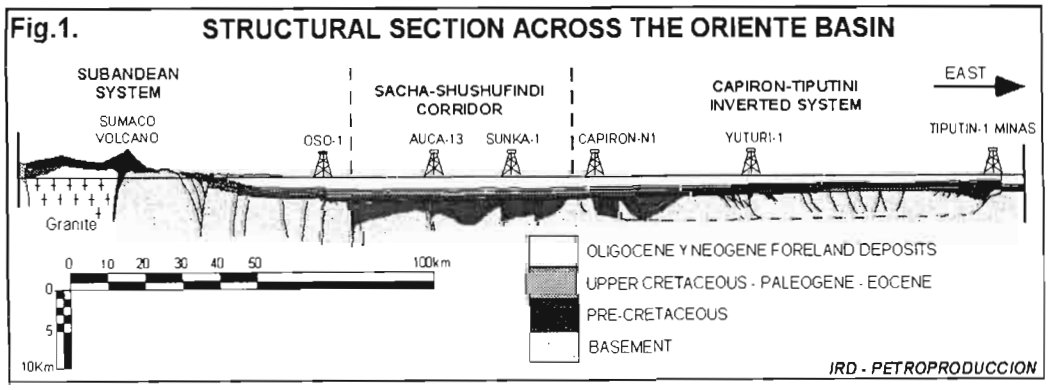

STRUCTURAL STYLE

The Oriente Basin is deformed by major compressive NNE-SSW wrench fault zones (Figs. 1 and 2), which correspond to inverted Mesozoic rift systems. Main structures correspond to positive flower structures developed along three NNE-SSW right-lateral convergent wrench-fault zones. (1) In the western part, the Subandean System (Napo Uplift and Cutucú Uplift) is still seismically and volcanically active. (2) In the centre of the basin, the Shushufindi-Sacha Corridor results from the inversion of a NNE-SSW trend of Upper Triassic to Lower Jurassic half-grabens which emerges actually in the Cutucú Uplift. (3) To the east, the Capirón-Tiputini play is an inverted system of half-grabens (Fig. 2) probably Permo-Triassic in age. In the Sacha-Shushufindi Corridor as in the Capirón-Tiputini Inverted System, half-grabens were eroded and sealed by Middle Jurassic to Basal Cretaceous volcano-clastic sediments (Chapiza-Yaupi Fm.), or by the Aptian-Lower Albian Hollín Formation. Locally, the Yaupi Fm. is affected by normal faults.

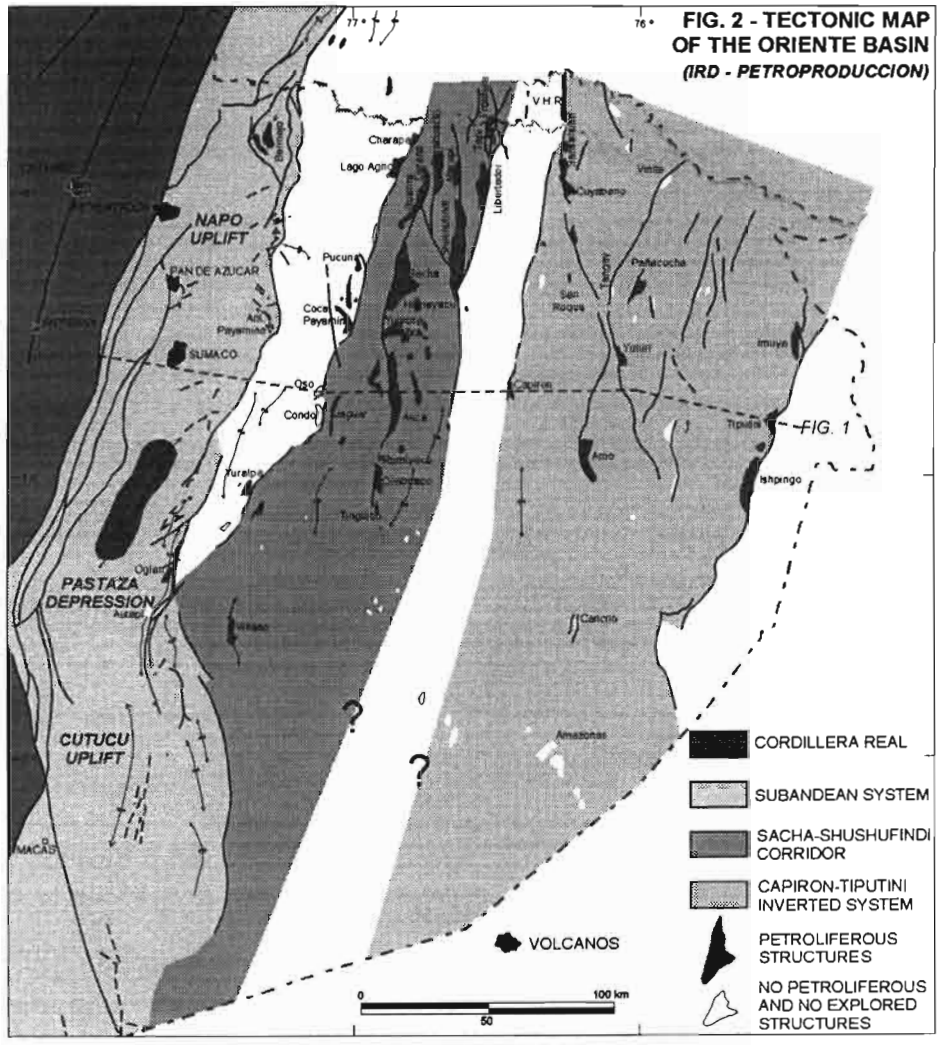

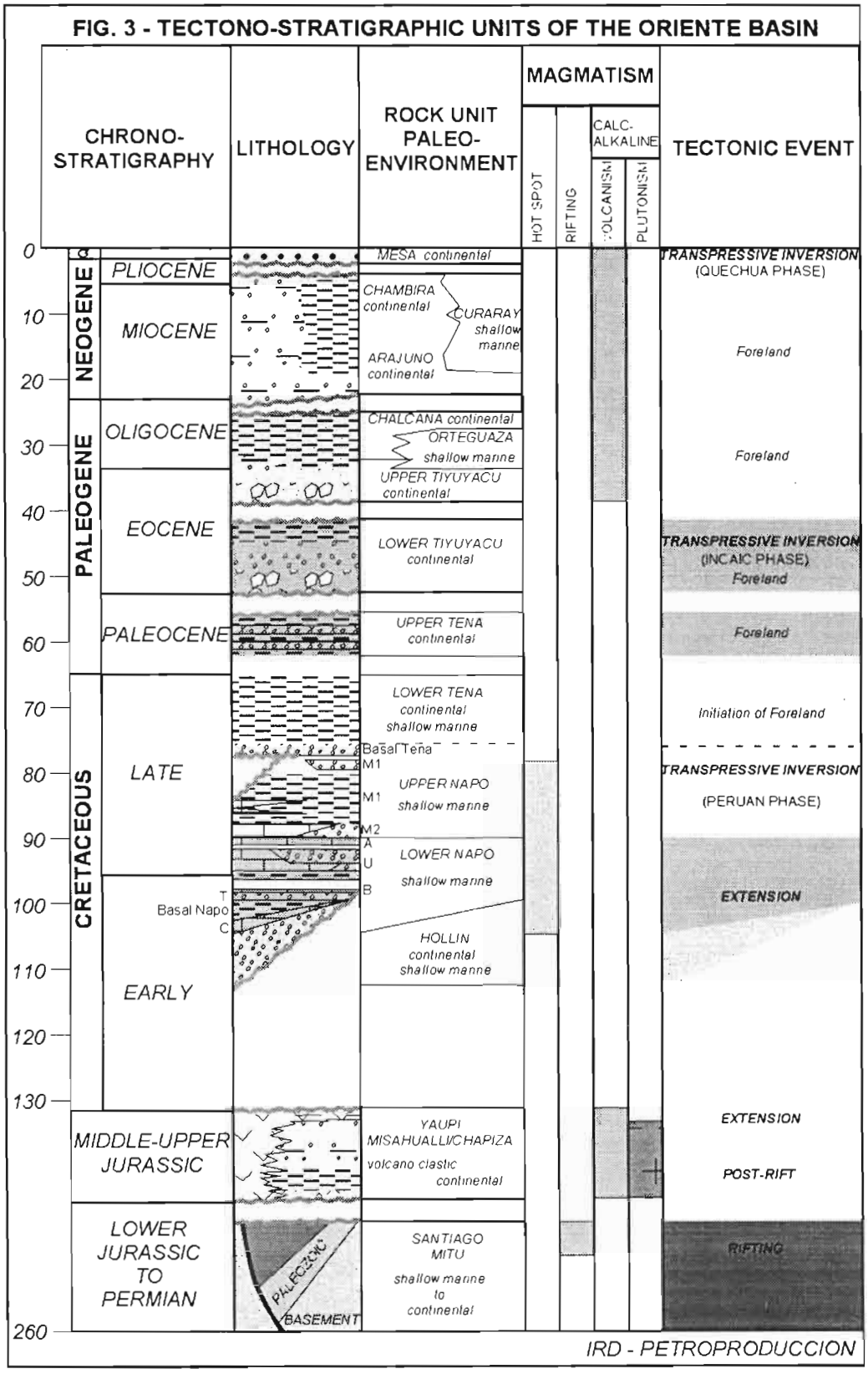
FIG. 3 - TECTONO-STRATIGRAPHIC UNITS OF THE ORIENTE BASIN
CHRONO-STRATIGRAPHY
LITHOLOGY
ROCK UNIT PALEO-ENVIRONMENT
MAGMATISM
HOT SPOT
RIFTING
CALC-ALKALINE
VOLCANISM
PLUTONISM
TECTONIC EVENT
0
10
20
30
40
50
60
70
80
90
100
110
120
130
260
Q
NEOGENE
PLIOCENE
MIOCENE
PALEOGENE
OLIGOCENE
EOCENE
PALEOCENE
CRETACEOUS
LATE
EARLY
MIDDLE-UPPER JURASSIC
LOWER JURASSIC TO PERMIAN
MESA continental
CHAMBIRA continental
CURARAY shallow marine
ARAJUNO continental
CHALCANA continental
ORTEGUAZA shallow marine
UPPER TIYUYACU continental
LOWER TIYUYACU continental
UPPER TENA continental
LOWER TENA continental shallow marine
Basal Tena
M1
UPPER NAPO shallow marine
M2
A
U
LOWER NAPO shallow marine
B
T
Basal Napo
C
HOLLIN continental shallow marine
YAUPI MISAHUALLI/CHAPIZA volcano clastic continental
SANTIAGO MITU shallow marine to continental
PALEOZOIC BASEMENT
TRANSPRESSIVE INVERSION (QUECHUA PHASE)
Foreland
Foreland
TRANSPRESSIVE INVERSION (INCAIC PHASE)
Foreland
Foreland
Initiation of Foreland
TRANSPRESSIVE INVERSION (PERUAN PHASE)
EXTENSION
EXTENSION
POST-RIFT
RIFTING
IRD - PETROPRODUCCION

TIMING OF CRETACEOUS AND CENOZOIC COMPRESSIVE DEFORMATIONS

Reflection seismic data show syn-tectonic sedimentation which recorded 3 stages of transpression: Turonian-Maastrichtian; Early Eocene; Pliocene-Quaternary. The Sacha-Shushufindi Corridor formed in large part between the Turonian and the Maastrichtian, while the Capirón-Tiputini Inverted System is principally Eocene in age. The Subandean uplift developed during the Pliocene and Quaternary, but includes some Maastrichtian structures as the Bermejo field.

The Turonian-Maastrichtian tectonic crisis is contemporaneous with an "intra-continental hot-spot" under the Oriente Basin, as show the extrusive magmatic bodies associated to the right-lateral wrench-fault zone of the Sacha-Shushufindi Corridor (Barragan et al., 1999). The maturity of Cretaceous source rocks in this zone is due to this thermal anomaly.

DISCUSION AND CONCLUSION

The Figure 3 resumes the tectonic and sedimentologic evolution of the Oriente Basin. Initialisation of the foreland basin starts during the Turonian-Maastrichtian tectonic crisis, and its Cenozoic evolution is controlled by interference of tectonic and eustatic events (Jaillard, 1997; Christophoul, 1999).

The more productive oil fields of the Oriente Basin correspond to Late Cretaceous and Eocene structural traps. Oil was accumulated in Aptian to Maastrichtian sandstones. Cretaceous source rocks maturity is due to subsidence of the Cenozoic foreland basin and the continental "intra-continental hot-spot" contemporaneous with the Turonian-Maastrichtian tectonic crisis. The Napo Uplift is probably the remnant part of a largest petroleum system which developed towards the west. Two peaks of oil generation and expulsion are evidenced. The first one occurred in the Lower and Middle Eocene, in a foreland basin which extended to the west of the present basin limits. Upper Eocene to Oligocene times correspond to a period of erosion and poor subsidence, where oil expulsion stopped. During the Neogene, the second peak of oil expulsion occurred with the return of the foreland basin subsidence, and the western part of the petroleum system was progressively deformed and destroyed by the Andes uplift.

REFERENCES

Barragan R. and Baby P. 1999. A Cretaceous hot spot in the Ecuadorian Oriente Basin: Geochimical, Geochronological and Tectonic indicators. ISAG 99, *this issue*.

Canfield R., Bonilla G., Robbins R. K. 1982. Sacha Oil Field of Ecuadorian Oriente. AAPG Bull. 61, 1076-1090.

Christophoul F., Baby P., Davila C. 1999. Descrimination of Eustatic and Tectonic influences in the Ecuadorian Oriente Basin from the aptian to the Oligocene. ISAG 99, *this issue*.

Dashwood M.F., Abbots J.L. 1990. Aspects of the Petroleum geology of the Oriente Basin, Ecuador, *in Brooks J. Ed.*, Classic Petroleum Provinces, Geological Society Special Publication, n° 50 , 89-117.

Jaillard E. 1997. Síntesis Estratigráfica y Sedimentológica del Cretáceo y Paleógeno de la Cuenca Oriental del Ecuador. Petroproducción-ORSTOM Edición, 163 p.

Tschopp H. J. 1953. Oil explorations in the Oriente of Ecuador. AAPG Bulletin. 37, 2303-2347.

MAGMA EVOLUTION PROCESSES AT THE TATARA-SAN PEDRO COMPLEX: 36° S, SOUTHERN VOLCANIC ZONE (SVZ), CHILEAN ANDES

Jenni BARCLAY (1), Andrea MARZOLI (1), Michael DUNGAN (1)

(1) Département de Minéralogie, Université de Genève, 13 rue des Maraîchers, 1211 Genève 4, Switzerland (barclay@terre.unige.ch, andrea.marzoli@terre.unge.ch, michael.dungan@terre.unige.ch)

KEY WORDS: Andean volcanism, Southern Volcanic Zone, open-system magma evolution

INTRODUCTION

Intermediate-composition continental arc magmas which have evolved in open systems (magma mixing, assimilation) are more common than those which have evolved via closed-system fractional crystallisation. As open-system magmas may reflect multiple processes, involvement of more than two components, and multiple (*i.e.*, polybaric) stages of evolution, unravelling the origin and evolution of a particular magma is difficult. Nonetheless, quantification of the factors that govern differentiation trends in arc volcanoes is crucial to assessments of elemental fluxes through subduction zones. Construction of models of growth of arc crust and the "open source" processes that operate in the sub-arc mantle requires identification of magmatic samples that record multiple mantle and/or crustal contributions. The question of open-system versus closed-system behavior with respect to Andean magmatic differentiation trends remains in the forefront of studies of the SVZ. Geochemical traverses along and across the ar , combined with studies of individual centers, provide a basis for discussion.

TATARA-SAN PEDRO VOLCANIC COMPLEX

Studies of the well characterized and long-lived Tatara-San Pedro complex (TSPC; Singer *et al.*, 1997) have the potential for contributing to the resolution of these issues (Dungan, 1999) under conditions where factors such as crustal thickness, age, and lithologic character are not variables, except insofar as modifications may have been induced by Quaternary magmatism. The TSPC comprises eight unconformity-bound volcanic sequences (~55 km^3 preserved) which range in age from ~930 ka to late Holocene, and which are short in duration compared to lacunae, probably reflecting a combination of episodic volcanism and glacial erosion. Older sequences have been substantially reduced in volume by erosion. Many sequences are dominated by basaltic andesitic lavas (~52.5-59 wt. % SiO_2), although one is entirely basaltic and others contain important volumes of silicic lavas (footnotes Table 1). None records a long-term progressive evolution trend. A range of differentiation trends from mildly tholeiitic to strongly calc-alkaline is present.

Comingled magmas comprising quenched mafic inclusions in silicic lavas were described previously (Singer *et al.*, 1995; Feeley and Dungan, 1996; Feeley *et al.*, 1997). This contribution focuses on the major and trace element chemistry of macroscopically homogeneous intermediate composition lavas with ~55.8±0.8 wt. % SiO_2 (Table 1), but otherwise different chemistry (*e.g.*, 5.4-2.3 wt. % MgO), that span most of the history of the TSPC, and which record a range of differentiation mechanisms from dominantly crystal fractionation to basalt-dacite mixing. Mineral chemistry data that will facilitate discussion of processes involved in the generation of these magmas will be presented in Göttingen. The selected lavas (Table 1, #1-#11, stratigraphic order) are representative of two end member types and an intermediate group (references to compositional parameters imply "with respect to TSPC lavas with 55-57 wt. % SiO_2"). A distinctive lava of the Muñoz sequence (#1) is an extreme composition by virtue of unusually low TiO_2, P_2O_5, and Fe_2O_3 in combination with high MgO and Cr, leading to high K/P, K/Ti, and Mg#. This magma cannot be derived from basalt by crystal fractionation, but may be the product of mixing (~4:1) of basaltic and dacitic magmas. Two lavas with equilibrated phenocryst assemblages and very low abundances of ferromagnesian minerals (#9-#10) have low MgO, V, and Mg#, very low Ni and Cr, and low K_2O, Rb, and Th (low K/Ti, K/P, Rb/Y and Rb/Zr; high Na_2O/K_2O, Ba/Rb, K/Rb, and Ba/V). These lavas evolved primarily by fractional crystallization from basaltic parent magmas. The remaining lavas are characterized by chemical signatures intermediate between these extremes, disequilibrium textures, and proportions of ferromagnesian phases that suggest the importance of immediately pre-eruptive basalt-andesite magma mixing.

Magma mixing, however, is not equivalent to crustal assimilation, as hybrid andesitic magmas may be generated by back-mixing of silicic liquids generated by closed-system fractionation with mafic magmas. The latter description applies to some evolved magmas at Volcán Puyehue (Gerlach *et al.*, 1988), wherein mildly contaminated basaltic mamas evolved at low pressure to generate tholeiitic (high FeO*/MgO, low Sr and Sr/Sc; see also Dungan, 1999), fractionation-dominated evolution trends, accompanied by occasional back-mixing. Proof that little assimilation of evolved crust accompanied fractionation-dominated basalt–rhyolite evolution at Puyehue comes from the near constancy of many incompatible trace element ratios (Fig. 1). By contrast, ratios readily modified by assimilation of silicic crustal components display variable but commonly large departures from basaltic values at the TSPC. Whereas Y-HREE enrichments at Puyehue reflect incompatible behavior during fractional crystallization, the TSPC trends range from weak enrichments to suppression of these elements due to variable incorporation of diverse crustal components carrying the signature of residual garnet. Isotopic variations support derivation of some silicic magmas by melting of the crust, as well as variable additions of crustal components to mafic and evolved magmas. In summary, a range of mainly open-system differentiation trends is recorded by evolved magmas at the TSPC. Variable degrees of crustal involvement are indicated, with perhaps a general decrease in assimilation with time as the crustal column below the volcano was modified by Quaternary magmatism. TSPC magmas record a spectrum of differentiation trends that primarily reflect a range of processes, although there is substantial parent magma variability as well. The large diversity observed at this single long-lived center suggests a need for caution in the interpretation of regional variations defined by reconnaissance sampling.

Table 1: Major and trace element analyses (XRF-INAA) of select andesitic lavas of the Tatara-San Pedro complex

#	1	2	3	4	5	6	7	8	9	10	11
Sequence	Muñoz	QTS	L-EMS	L-EMS	U-EMS	U-EMS	L-TAT	L-TAT	L-TAT	L-TAT	U-TAT
Age (ka)	~900	~775	~610	~610	~590	~590	~120	~120	~120	~120	~110
Section	QTW10	QTW11	QTW12	EML	EML	QCNE	ESPE1	ESPW3	QWT12	EMU3	UEP7
Sample	1	5	12	5	15	2	5	20	34	13	2
SiO_2	55.40	55.66	54.98	55.32	55.60	56.03	56.66	55.42	56.54	56.67	55.65
TiO_2	0.58	1.05	0.76	1.01	0.93	0.95	1.07	1.21	1.05	1.24	0.97
Al_2O_3	17.81	17.48	18.16	17.24	17.47	16.58	17.41	17.78	19.50	18.60	17.80
Fe_2O_3	6.75	8.20	7.55	8.31	7.97	7.75	7.91	8.54	6.76	7.49	7.95
MnO	0.13	0.14	0.14	0.15	0.12	0.13	0.13	0.14	0.13	0.16	0.13
MgO	5.35	4.22	5.07	4.38	5.29	5.08	4.00	3.96	2.30	2.56	4.50
CaO	8.77	7.17	8.54	7.13	7.30	7.35	6.61	7.09	7.11	6.72	7.11
Na_2O	2.95	3.87	3.60	3.83	3.73	3.73	4.10	4.07	4.85	4.98	4.07
K_2O	1.50	1.75	1.34	1.75	1.57	1.91	1.78	1.54	1.37	1.33	1.61
P_2O_5	0.11	0.26	0.13	0.27	0.27	0.27	0.29	0.42	0.33	0.39	0.25
Total	99.34	99.81	100.25	99.46	100.25	99.78	99.95	100.17	99.93	100.14	100.20
Mg#	61.1	50.5	57.1	51.1	56.8	56.5	50.1	47.9	40.2	40.4	52.9
Na_2O/K_2O	1.96	2.21	2.69	2.19	2.37	1.95	2.30	2.64	3.56	3.74	2.53
K/Ti	3.6	2.3	2.4	2.2	2.4	2.8	2.3	1.8	1.8	1.5	2.3
K/P	26.0	12.8	19.5	12.3	11.1	13.5	11.7	7.0	7.9	6.5	12.2
Nb	2.7	4.4	3.0	5.1	6.8	6.4	5.3	8.9	6.7	6.0	5.5
Zr	126	170	88	150	169	203	168	200	167	162	154
Sr	524	508	568	507	566	531	522	611	619	614	536
Rb	42.7	50.6	32.3	51.6	50.6	58.1	48.9	38.1	28.9	26.9	45.6
Ba	339	406	313	418	433	400	421	455	396	394	412
Y	14.1	21.2	16.6	22.7	15.2	21.4	18.1	23.1	25.9	27.0	18.7
Ni	32	34	32	37	66	43	35	33	7	12	36
Cr	108	29	67	32	124	137	64	12	3	0	48
V	136	162	205	161	157	159	155	161	112	105	156
Ce	26.3	39.4	20	42.7	48.5	47.6	43.0	58.3	42.8	44.1	38.6
Th	5.11	6.45	4	6.32	6.07	7.30	5.76	4.03	2.79	2.65	4.94
Sr/Y	37.2	24.0	34.2	22.4	37.2	24.8	28.8	26.5	23.9	22.8	28.7
Ba/Sr	0.65	0.80	0.55	0.82	0.76	0.75	0.81	0.74	0.64	0.64	0.77
Ba/Rb	8.0	8.0	9.7	8.1	8.6	6.9	8.6	11.9	13.7	14.6	9.0
Ba/V	2.5	2.5	1.5	2.6	2.8	2.5	2.7	2.8	3.5	3.8	2.6
Ba/Y	24.1	19.2	18.9	18.4	28.5	18.7	23.3	19.7	15.3	14.6	22.1
Sr/Rb	12.3	10.0	17.6	9.8	11.2	9.1	10.7	16.0	21.4	22.8	11.7
K/Rb	292	287	343	282	258	273	303	335	392	410	293
Nb/Y	0.19	0.21	0.18	0.22	0.45	0.30	0.29	0.39	0.26	0.22	0.29
Rb/Y	3.03	2.39	1.95	2.27	3.32	2.72	2.70	1.65	1.12	1.00	2.45
Zr/Y	9.0	8.0	5.3	6.6	11.1	9.5	9.3	8.7	6.4	6.0	8.3
Rb/Zr	0.34	0.30	0.37	0.34	0.30	0.29	0.29	0.19	0.17	0.17	0.30

Sequences (modified from Singer *et al.*, 1997) *Muñoz* (~52-76 % SiO_2): dominated by early Muñoz dacite and late Los Lunes rhyolite. Mafic to intermediate Sin Nombre lavas (~52.5-56.5 %SiO_2) are intermediate in age. *Quebrada Turbia* (~52.5-59 % SiO_2): dominated by an upper unit (~55-56 % SiO_2). *Lower Estero Molino* (~52.5-65.5 % SiO_2): dominated by mafic andesitic lavas (~54-59 % SiO_2). *Upper Estero Molino* (~51.5-56.5 % SiO_2): dominated by evolved basaltic andesitic lavas (~53-54.5 % SiO_2). *L-EMS* and *U-EMS* are represented by two lavas each, representing four magmatic suites (*Middle EMS* is not represented: ~49-54 % SiO_2). *Lower Tatara* (~51.5-68.5 % SiO_2): a bi-modal construct dominated by early, mafic to intermediate lavas (~51.5-59 % SiO_2) and late Tatara dacite. Four lavas from four magmatic suites were selected. *Upper Tatara* (~52-56.5 % SiO_2): entirely mafic to intermediate. *L-TAT* and *U-TAT* are separated by an erosional surface, but are unresolvable in age. New ages for *EMS* and *TAT* are based on unpublished $^{40}Ar/^{39}Ar$ dates.

Acknowledgements: We thank the many collaborators who have contributed generously to the Tatara-San Pedro project since 1984: L. Lopez-Escobar, G. Sanchez, J. Davidson, K. Ferguson, M. Colucci, R. Harmon, B. Singer, R. Thompson, L. Brown, J. Pickens, J.M. Rhodes, A. Wulff, F. Frey, T. Feeley, W. Hildreth, R. Drake, F. Costa, J. Lobato, and S. Nelson. Funding has been provided by the US NSF and the Swiss FNSRS.

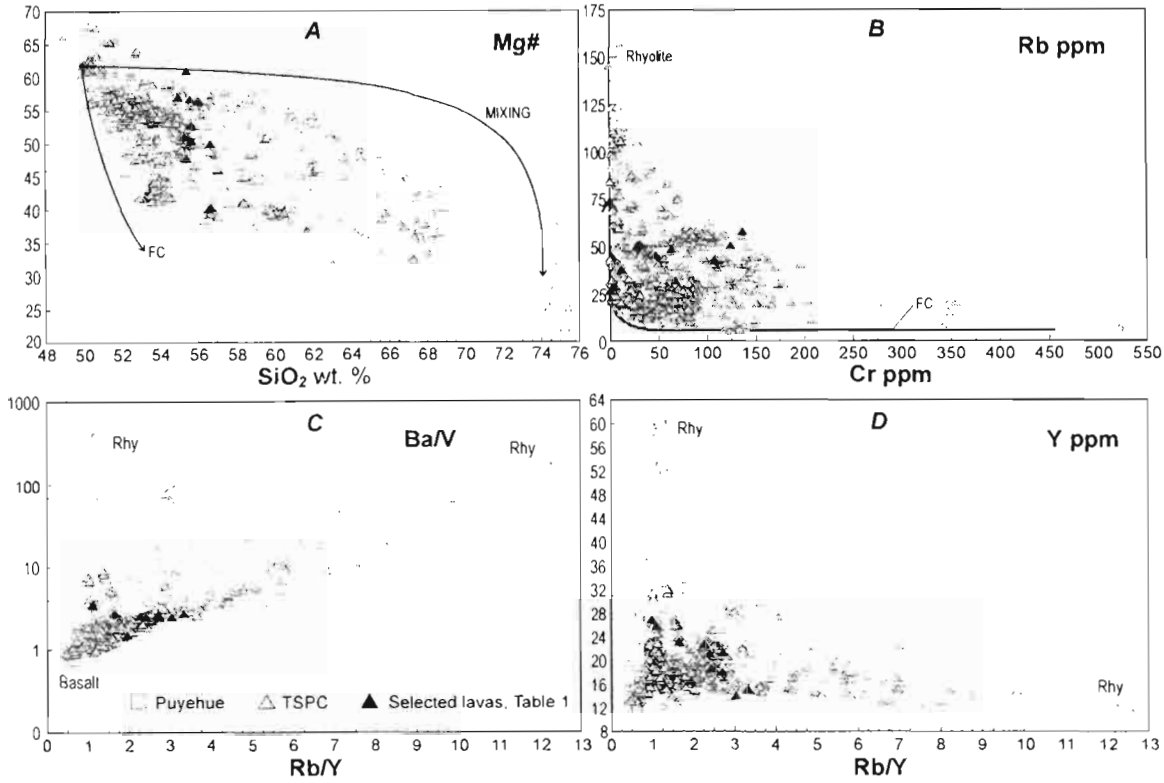

Figure 1: Some major and trace element variation diagrams illustrating evidence for a diversity of magma evolution paths at the TSPC, ranging from fractionation-dominated paths ("FC" in Fig. 1A, and similar to FC-dominated evolution paths defined by nearly constant Rb/Y in Puyehue trends), to those that approach basalt-dacite or basalt-rhyolite mixing (Table 1, #1). Note the distinctions between Puyehue and TSPC rhyolitic magmas for Rb/Y (high Rb/Y taken as evidence of large crustal inputs in silicic magmas).

Dungan, M. 1999. The Tatara-San Pedro volcanic complex (36° S): Implications for arc magma genesis and evolution in the Southern Volcanic Zone (SVZ) of the Chilean Andes. *this volume*

Feeley, T.C., & Dungan, M.A. 1996. Compositional and dynamic controls on mafic-silicic magma interactions at continental arc volcanoes: evidence from Cordón El Guadal, Tatara-San Pedro Complex, Chile. *J. Pet.*, 37, 1547-1577.

Feeley, T.C., Dungan, M.A., & Frey, F.A. 1998. Geochemical constraints on the origin of mafic and silicic magmas at Cordón El Guadal, Tatara-San Pedro Complex, central Chile. *Contr. Miner. Pet.*, 131, 393-411.

Gerlach, D.C., Frey, F.A., Moreno-Roa, H., & López-Escobar, L. 1988. Recent volcanism in the Puyehue-Cordon Caulle region, Southern Andes, Chile (40.5° S): Petrogenesis of evolved lavas. *J. Pet.*, 29, 333-382.

Singer, B.S., Dungan, M.A., & Layne, G.D. 1995. Textures and Sr, Ba, Mg, Fe, K, and Ti compositional profiles in volcanic plagioclase: clues to the dynamics of calc-alkaline magmas: *Amer. Miner.*, 80, 776-798.

Singer, B.S., Thompson, R.A., Dungan, M.A., Feeley, T.C., Nelson, S.T., Pickens, J.C., Brown, L.L., Davidson, J.P., & Metzger, J. 1997. Volcanism and erosion during the past 930 k.y. at the Tatara-San Pedro complex, Chilean Andes. *Geol. Soc. Amer. Bull.*, 109, 127-142.

A CRETACEOUS HOT SPOT IN THE ECUADORIAN ORIENTE BASIN: GEOCHEMICAL, GEOCHRONOLOGICAL, AND TECTONIC INDICATORS

R. BARRAGAN (1) and P. BABY (2)

(1) Kerr-McGee Corporation, 16666 Nothchase, Houston, TX 77060, USA; *rbarragan@kmg.com*
(2) Convenio IRD-Petroproduccion, P.O.Box, 17 11 6596, Quito, Ecuador; *pbaby@pi.pro.ec*

KEY WORDS: hot spot, Oriente Basin, HPT series, LIL/HFS ratios, Cretaceous

INTRODUCTION

A paleo intra-continental plume has been identified along the Ecuadorian "Oriente" Basin (Fig. 1) in the Cretaceous sediments of the Napo and Hollin Formations. Analysis of well log data, seismic sections, core and outcrop descriptions reveal two major facies of magmatism: i) Extrusive facies, mostly characterized by basaltic volcanoclastic deposits (altered tuffs and palagonitized hyaloclatites), reflecting shallow marine environment of emplacement and characteristic Surtseyan eruptive style, producing typically ring and tuff cones as is reflected in several seismic lines (Fig. 2). ii) Intrusive facies, characterized by major gabbroic sill complexes and diabasic dikes emplaced anywhere within the Cretaceous sedimentary series. Petrographic features suggest an alkaline type composition, fine-coarse grained phaneritic texture, and an intergrown phenocryst assemblage enriched in labradorite + olivine + clinopyroxene.

GEOCHEMISTRY AND GEOCHRONOLOGY

The geochemistry of representative Cretaceous igneous samples from different locations along the basin shows a restricted range of compositional variation). They lie within the alkaline basaltic field, show high contents in TiO2 (≥ 3 wt%), K2O (1-2 wt%), P2O5 (>0.6 wt %) (Fig. 3) and incompatible elements similar to the HPT series (high Ti and P) observed in several basaltic flood provinces (FBP) such as the northern portion of the Paraná-Etendenka and Karoo basalt provinces (Cox, 1988, Hawkesworth et al., 1988). Comparing the compositional range observed for other basalt tectonic settings, such as mid-ocean ridge basalts (MORB), intra-plate volcanism (OIB), and subduction-related basalts (Table 1; modified form Shinjo, 1998), the

Oriente Basin Basaltic magmas (OBB) are enriched in the whole spectrum of incompatible elements relative to normal MORB and subducted-related back arc basalts. On the other hand, they are characterized by LIL/HFS element ratios (i. e., K/Zr ≅ 36-68, Rb/Zr ≅ 0.06-0.15, Ba/Zr ≅1.8-2.8, Zr/Y ≅ 7.8-9.5, Ba/Nb ≅ 6.3-8.6, Ba/Ce ≅ 4.9-7.9, La/Nb ≅ 0.6, and Zr/Nb ≅ 3) and general trace element patterns (Fig. 4) similar to those compositional signatures observed in oceanic intraplate lavas (OIB). The Triangular Tb-Th-Ta discrimination diagram (after Cabanis and Thiéblemont, 1988) confirms the above conclusions and suggests that the OBB samples are associated with alkaline basaltic magmas of anorogenic series erupted within continental-plate (Fig 5).

Radiometric ages from several well locations ($^{40}Ar/^{39}K$ and $^{40}Ar/^{39}Ar$ data) and the distribution of igneous bodies suggest an Albian to Campanian age for the magmatism in the Ecuadorian Oriente Basin (OBB). Stratigraphic correlation supports the absolute age dating. The oldest evidences of igneous activity are contemporary to the Upper Hollin Formation (Albian) and identified along the north-central part of the Basin (106±5 My) (Fig. 1). Younger evidence of igneous activity are found contemporary to Lower Napo and Napo T in the Central part of the basin (92±3.9 Ma), and synsedimentary to the Campanian lower M1 Unit (Upper Napo Fm) in the west south-central part of the Oriente Basin (84±2 My; and 82±0.5 My). No evidence of basaltic volcanism has been found in younger sediments.

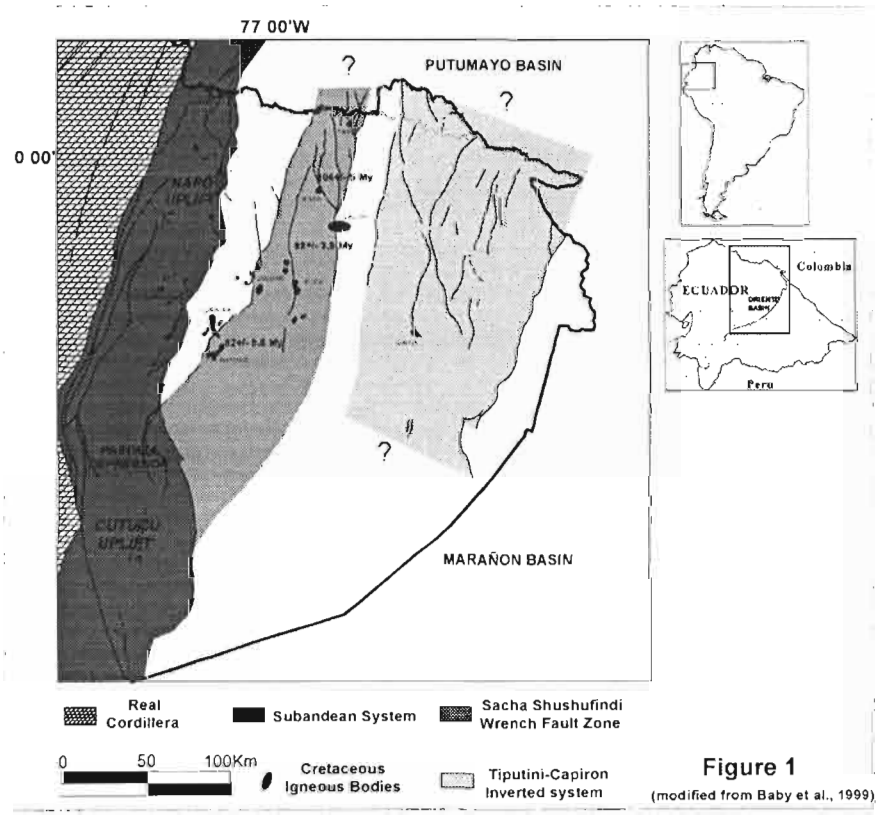

Figure 1
(modified from Baby et al., 1999)

TECTONIC CONTROL

It is also evident from reflection seismic data that the locations of major eruptive sites, are controlled by pre-existing basement structures in the Ecuadorian Oriente Basin reactived during the Cretaceous (Fig. 2). These represent major wrench-fault systems originated within Triassic and Jurassic basins that then acted as deep lithospheric shear zones and magma pathways to the surface during Cretaceous times. This is reflected in the regional geographic distribution of the Cretaceous magmatic bodies in the Ecuadorian Oriente Basin (Fig. 3). Either extrusive or intrusive facies, the igneous rock bodies are aligned in a very specific NNE-SSW trend vector along right-lateral convergent wrench-fault zones (Fig. 1), mainly in the center of the basin, where the Shushufindi-Sacha wrench-fault-zone results from the inversion of a NNE-SSW trend of Upper Triassic to Lower Jurassic half-grabens, in a transpressive stage during Coniacian-Maastrichtian times (Baby et al; 1999).

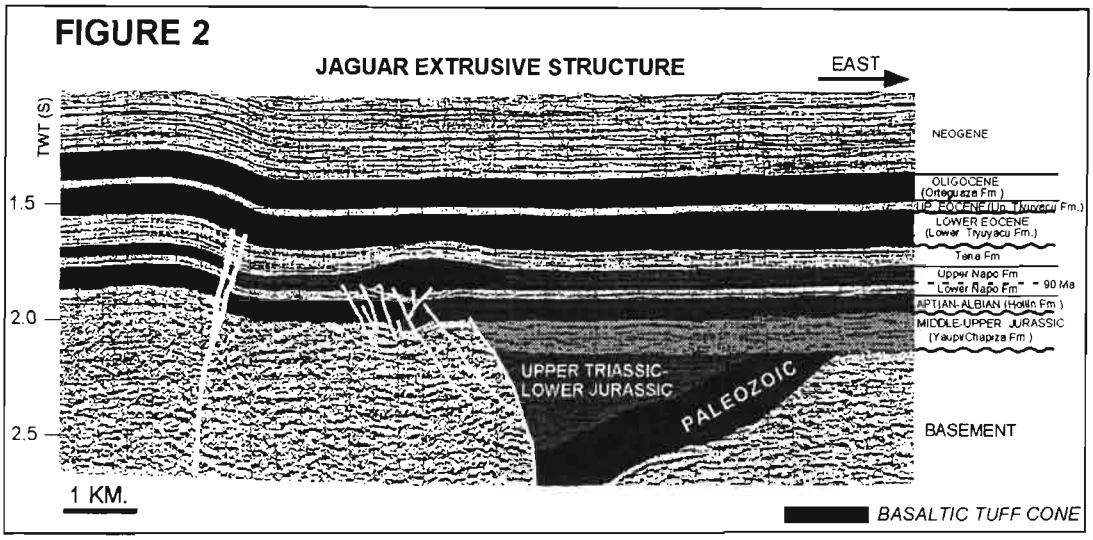

CONCLUSIONS

All the intrusive and extrusive facies recognized within the Cretaceous sedimentary series of the Ecuadorian Oriente Basin show similar geological and geochemical features, even though they were developed at different ages and at different geographic locations. Also, they are related to the main pre-Cretaceous extensional features, so their emplacements are associated to the regional field stresses that reactivate regional structures during Cretaceous times.

Geochemical signatures suggest that the different igneous facies recognized at the Oriente basin are genetically associated with magmas originated in an ancient "intra-continental plate hot spot" paleotectonic

setting. Geographic and chronological controls in the distribution of all the magmatic bodies in the Oriente Basin are evident. They are aligned in a very specific NNE-SSW trend direction, with the oldest facies placed since Lower Albian (≈105-110 My) and developed to the NNE and the youngest, Campanian (≈85 My) to the SSW. This observations suggest that magmatism has migrated to the SSW, and strongly support confirm the presence of an "intra-continental hot-spot" under the Oriente Basin.

REFERENCES

Baby P., Rivadenera M., Christophoul F., and Barragan R. 1999. Style and timing of deformation in the Ecuadorian Oriente Basin: ISAG 99, *this issue.*

Cabanis B., and Thieblemont D. 1988. La discrimination des tholéiites continentales et des basaltes arriére-arc: proposition d'un nouveau diagramme: le triangle Th-3xTb-2xTa. Bull: Soc. Géol. France, 8, 927-935.

Cox K. G. 1988. The Karoo Province, *in* MacDougall, J. D., ed., Continental Flood Basalts: Dordretcht , Kluger Academic Publishers, 239-271.

Hawkesworth C. J., Mantovani M., and Peate D. 1988. Lithosphere remobilization during Parana CFB magmatism: Journal of Petrology, Special Lithosphere Issue, 205-223.

Shinjo R. 1998. Petrochemistry and tectonic significance of the emerged late Cenozoic basalts behind the Okinawa Troughs Ryukyu arc system: Journal of Vulcanolgy and Geothermal Research, 80, 39-53.

Wilson M. 1993. Magmatism and the geodynamics of basin formation: Sedimetary Geology, 86, 5-29.

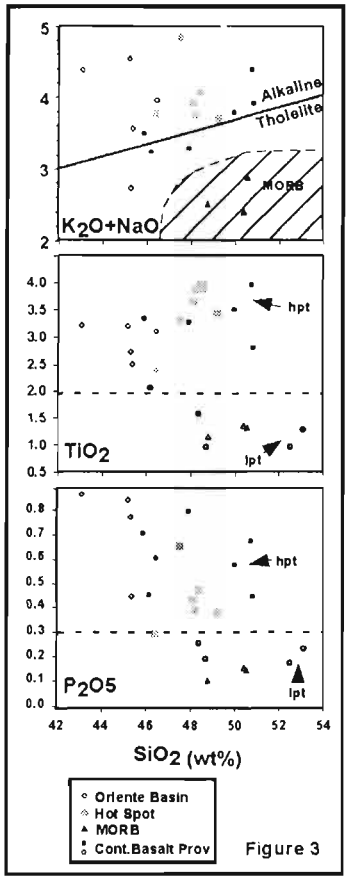

Figure 3

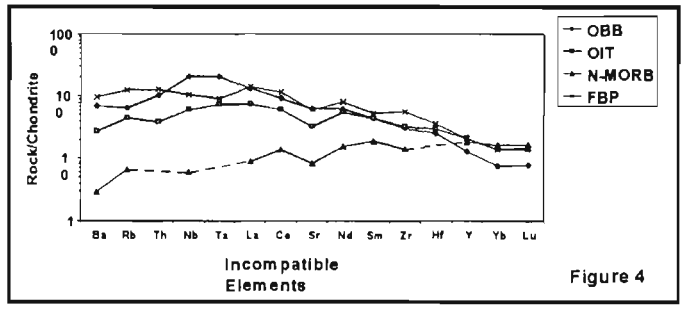

Figure 4

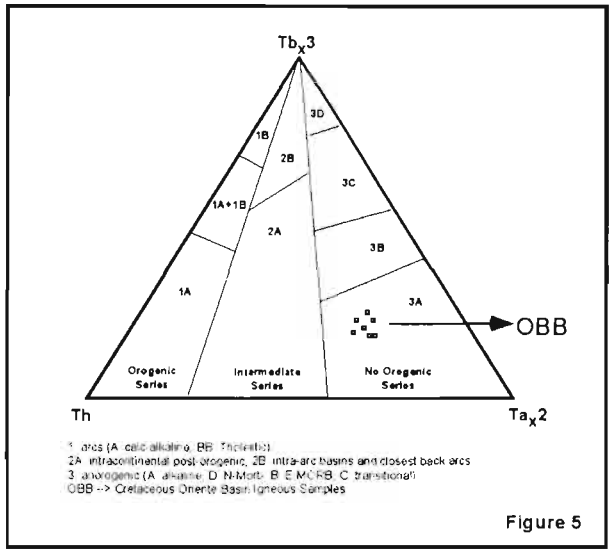

Figure 5

	OBB	Subduction-related basalts		MORB		OIB
		IAT	HAB and CA	N-MORB	E-MORB	
K/Zr	35.5-67.8	147	216	12	26	44
Rb/Zr	0.06-0.15	0.21	0.35	0.01	0.05	0.1
Ba/Zr	1.79-2.83	5	7.5	0.1	0.9	1.7
Ba/Nb	6.33-8.56	157	214	4	8	7
Ba/Ce	4.93-7.85	30	13	1	5	5
La/Nb	0.57-0.67	1.86	7.14	0.97	0.78	0.66
Zr/Nb	2.88-3.89	31	29	27	9	4
Zr/Y	7.79-9.46	1.8	2.7	2.9	3.4	7.3

TABLE 1 Selected incompatible ratios for the Cretaceous Oriente Basin Igneous Rocks and various tectonic settings. IAT = Island-arc tholeiitic; HAB = high-alumina basalt; CA = calc-alkaline basalt; OIB = ocean island basalt. Data source: (Sun, 1980; in Shinjo, 1998).

SHEAR WAVE VELOCITY IN THE LITHOSPHERE ACROSS THE CENTRAL ANDES.

David BAUMONT [1], Anne PAUL [2], Helle PEDERSEN [3], George Zandt [4] and Susan BECK [5]

(1) SASO and Dept. of Geosciences, University of Arizona, Tucson, AZ., U.S.A (dbaumont@lgit.obs.ujf-grenoble.fr)
(2) LGIT, BP 53, 38041 Grenoble Cedex 9, France (apaul@lgit.obs.ujf-grenoble.fr)
(3) LGIT, BP 53, 38041 Grenoble Cedex 9, France (pedersen@lgit.obs.ujf-grenoble.fr)
(4) SASO and Dept. of Geosciences, University of Arizona, Tucson, AZ., U.S.A (zandt@geo.Arizona.EDU)
(5) SASO and Dept. of Geosciences, University of Arizona, Tucson, AZ., U.S.A (beck@geo.Arizona.EDU)

KEYS WORDS: Altiplano, lithospheric structure, Central Andes, shear wave velocity, surface waves

INTRODUCTION

The most remarkable morphological feature of the Central Andes is the existence of the Altiplano-Puna (Fig. 1), the second widest high plateau in the world after Tibet. The question of its formation and the origin of its 65-70 km thick crust (James, 1971; Beck et al., 1996) are still debated partly due to the lack of knowledge on the large-scale structure of the lithosphere. In 1994 and 1995, two broadband three-component seismic networks were deployed in the Central Andes (Fig. 1) (Beck et al., 1994). These experiments consisted of an east-west profile running across the main structural features of the Andean chain, the BANJO (Broadband Andean JOint) experiment, and a north-south profile located . along the eastern boundary of the Altiplano, the SEDA (Seismic Exploration of the Deep Altiplano) experiment. The BANJO experiment was composed of 16 stations equipped with STS-2 sensors (To=100s) whereas the SEDA experiment was composed of 5 stations equipped with CMG3-ESP sensors (To=60s) and 2 stations equipped with CMG40 sensors (To=30s).

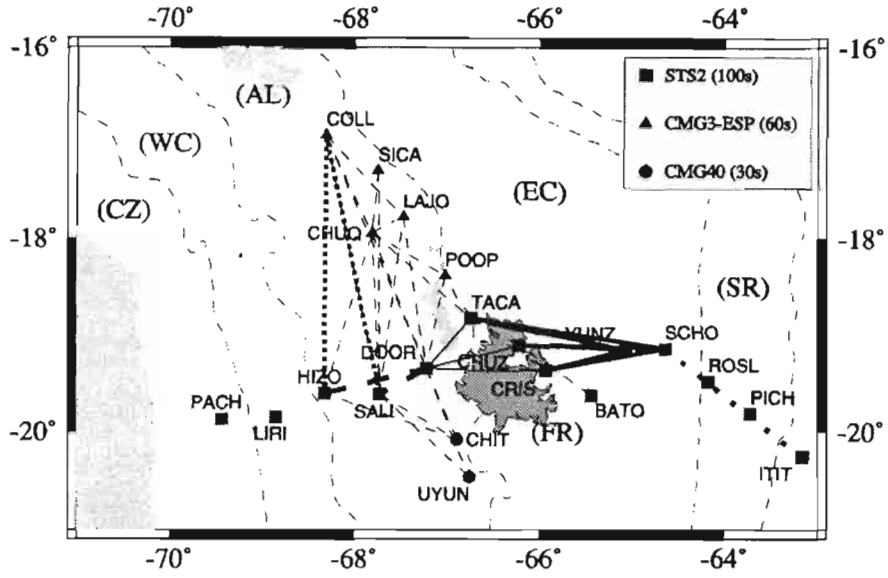

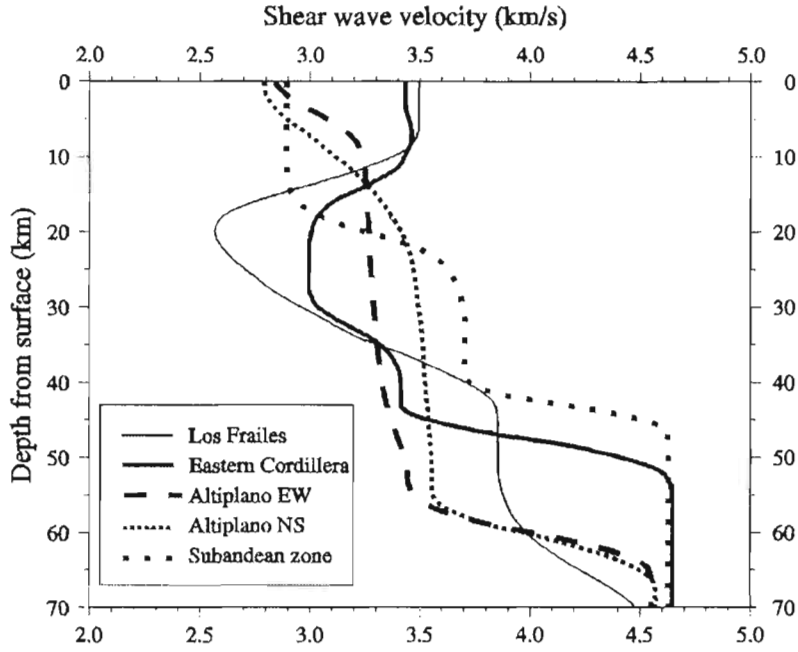

Figure 1 : Location map of the BANJO and SEDA stations. The paths along which we measured the phase velocity are shown (dashed and solid straight lines). The thin dashed lines separate the different morpho-tectonic units of the Andean chain. From west to east, there are : (CZ) Coastal Zone, (WC) Western Cordillera, (AL) Altiplano, (EC) Eastern Cordillera and (SR) Subandean Range. In the middle of the figure, the region of Los Frailes (FR) is indicated in grey.

Figure 2 : Summary of the shear-wave velocity average models for the crust in the Central Andes.

We present the determination of the shear-wave velocity in the lithosphere across the Central Andes inferred from the inversion of the phase velocity dispersion curves. The measurement of the phase velocity of the fundamental modes of the Rayleigh and Love waves was made in two steps. First, the signal corresponding to the fundamental modes of the Rayleigh and Love waves were extracted by appling a phase-matched filter. Secondly, the phase velocity dispersion curves were determined using both a two-stations Wiener filtering approach and a slant-stack approach. The phase velocity dispersion curves and their uncertainties were obtained for periods in the range of 10 and 100 s.

The preliminary results we obtained considering various stations pairs showed that there are strong lateral variations of the phase velocity across the Andean chain. Based on these observations, we conducted a regionalization of the phase velocity measurements in the Central Andes. The regions showing similar dispersion curves were gathered. Then, the dispersion curves were inverted in order to find as many S-wave velocity models as possible for which the corresponding theoretical phase velocity dispersion curves are totally included within our phase velocity determination and its uncertainty.

CONCLUSIONS

The lateral variations of the phase velocity are spatially correlated with the different morphotectonic units as revealed by the regionalization. These changes reflect strong lateral variations of shear wave velocity models, especially in the crust (Fig. 2). In the Altiplano, the S-wave velocity in the upper mantle (>110 km) is in favor of the presence of a lithospheric mantle. We do not see any major LVZ in the crust in the Altiplano. In figure 2, one can note that the S-wave velocity gradient in the crust in the Altiplano is weak. In the region of the ignimbrites surface outcrops of "Los Frailes", our results show that there is a marked LVZ in the upper crust (~20 km). This LVZ could be related to the presence of an active crustal magmatism. In the Eastern Cordillera, we also found a LVZ at a similar depth with recpect to the one found in "Los Frailes". However the velocity reduction associated to that LVZ is smaller in the Eastern Cordillera. In the upper mantle beneath the Eastern Cordillera, we found a negative anomaly of S-wave velocities with respect to the mean velocity at such depth. Consequently, in that region and contrary to the Altiplano, the upper mantle appears to be asthenopheric and not lithospheric. In the Subandean Range, the lithospheric S-wave velocities are higher than in the other regions reflecting the presence of the Brazilian craton and its cold and thick lithosphere.

REFERENCES

Beck, S., et al., 1994. Across the Andes and along the Altiplano: A passive seismic experiment. IRIS Newsletter, 13(3), 1-3.

Beck, S. L., G. Zandt, S. C. Myers, T. C. Wallace, P. G. Silver, and L. Drake, 1996. Crustal-thickness variations in the Central Andes. Geology, 24, 407-410.

James D. E., 1971. Andean crustal and upper mantle structure. J. Geophys. Res., 76, 3246-3271.

THE CAUSE OF THICK, SLOW CRUST IN THE ALTIPLANO, CENTRAL ANDES; MELT OR COMPOSITION?

Susan BECK(1), Jennifer SWENSON(1), and George ZANDT(1)

(1) Southern Arizona Seismic Observatory and Department of Geosciences
University of Arizona, Tucson AZ 85721 USA

KEY WORDS: Altiplano crustal structure, partial melt, receiver functions

INTRODUCTION

The Altiplano of the central Andes (20°S) is a high, relatively flat plateau with an average elevation of 3.6 km. It is part of an active continental margin mountain belt bounded to the west by the Western Cordillera active volcanic arc and to the east by the Eastern Cordillera and Sub-Andean Zone fold and thrust belts (Figure 1). The high elevations and thick crust of the backarc region are related to the overall convergence of the Nazca plate and the South American plate but the exact origin of the thick crust remains enigmatic. Recent seismic studies consistently reveal crustal thicknesses of 60-75 km and very slow bulk velocities of approximately 6.0 km/s, however, investigators disagree on the cause of the slow velocities: melt or composition? We combine receiver function analysis and regional broadband waveform modeling to determine the average crustal velocities, crustal Poisson's ratio, and crustal thicknesses across the width and along the length of the Altiplano in order to constrain the formation of this over-thickened crust.

CONCLUSIONS

We have modeled the full waveforms from 8 intermediate depth (100 –260 km) earthquakes (m_b=5.3-5.9) recorded at regional distances by the BANJO and SEDA portable seismic networks from those stations located within or near the Altiplano (Figure 1). We used a grid search and forward modeling technique for 92 event-station paths to constrain four parameters of the Altiplano lithosphere; crustal thickness, average crustal velocity, and crust and upper mantle Poisson's ratio. The models that provide the best overall fit between the data, and synthetic seismograms are characterized by a slow average crustal P-wave velocity (5.75-6.25 km/sec), crustal thicknesses of 60-65 km, a crustal Poisson's ratio of 0.25, and a mantle Poisson's ratio of 0.27–0.29. We have also constructed stacks of receiver functions for each station to investigate variations in crustal thickness and mid-crustal structure in the vicinity of each station (Figure 2). Thick crust, 60-75 km, exists beneath both the Western and Eastern Cordilleras and beneath the Altiplano (60-65 km thick). We do not see any evidence for a high velocity lower crust. We observe a weak low velocity zone that can be traced across the entire width of the Altiplano at a depth of 15 to 20 km. The weak mid-crustal low velocity zone may mark the decoupling layer between the brittle upper crust and more ductile weak lower crust.

The low crustal velocities and Poisson's ratio are consistent with a felsic quartz-rich composition for the bulk of the thickened crust (Christensen, 1996; Rudnick and Fountain, 1995). This would imply that the crust is near the solidus and very weak in the deepest portion of the crust (Bills et. al., 1994). Hence, we might expect some melt in the lower crust. We have compared our crustal velocities and Poisson's ratio with a summary of existing laboratory and theoretical results on the effects of partial melt on seismic velocities compiled by Makovsky and Klemperer (1999). This suggests that there is less than a few percent of partial melt in the Altiplano crust. This observation is in contrast to the northern Tibetan Plateau, where several lines of evidence, including a Poisson's ratio of 0.33, indicates >5% partial melt in the lower crust (Owens and Zandt, 1997). We would suggest that there has not been sufficient time for the Altiplano crust to melt if much of the shortening occurred post-Oligocene (Allmendinger et. al, 1997; Lamb et. al, 1997). We do observe some locally strong low velocity zones under the western and Eastern Cordilleras that may be related to some localized zones of partial melt in those regions. The low velocity zone beneath the Western Cordillera is probably related to the active volcanic arc associated with the subduction zone. The low velocity zone beneath the western edge of the Eastern Cordillera corresponds to the location of the large Los Frailes ignimbrite field. This Altiplano-Eastern Cordillera region also corresponds to a region of high attenuation for Lg propagation (Baumont et al., 1999) and to a low velocity region in the upper mantle at the base of the crust where localized delamination may have occurred (Myers et al., 1998).

The low average crustal velocities, low crustal Poisson's ratio and the lack of a high velocity lower crust suggests a very weak lower crust and reaffirms our earlier conclusion that the thick crust is primarily the result of tectonic shortening rather than magmatic addition or underplating. We find no evidence of a high-velocity lower crust suggesting one of two possibilities: (1) most of the continental crust was predominately of a

felsic quartz-rich, composition prior to the shortening and uplift, or (2) the original mafic lower crust was either pushed to depths where it transformed to eclogite facies and has seismic velocities consistent with the mantle, or was delaminated. This second scenario would imply much more tectonic shortening than observed in the geologic record.

REFERENCES

Allmendinger, R., T. Jordan, S. Kay and B. Isacks, The evolution of the Altiplano-Puna plateau of the central Andes, *Annu. Rev. Earth Planet. Sci.*, 25, 139-174, 1997.

Baumont, D., A. Paul, S. L. Beck, and G. Zandt, The attenuation of Lg waves in the Bolivian Altiplano as a marker of strong crustal heterogeneity, submitted to *J. Geophs. Res.*, 1999.

Bills, B.G., S.L.d. Silva, D.R. Currey, R.S. Emenger, K.D. Lillquest, A. Donnellan, and B. Worden, Hydro-isostatic deflection and tectonic tilting in the central Andes: Initial results of a GPS survey of Lake Minchin shorelines, *Geophys. Res. Let.*, 21, 293-296, 1994.

Christensen, N., Poisson's ratio and crustal seismology, *J. Geophys. Res.*, 101, 3139-3156, 1996.

Lamb, S., L. Hoke, L. Kennan and J. Dewy, Cenozoic evolution of the central Andes in Bolivia and northern Chile, in Orogeny Through Time, edited by J.-P Burg, and M. Ford, Geological Society Special Publication No. 121, pp. 237-264, 1997.

Makovsky, Y. and S. L. Klemperer, Measuring the seismic properties of Tibetan bright spots: evidence for free aqueous fluids in the Tibetan middle crust, *J. Geophys. Res.*, 104, in press. 1999.

Myers, S., S. Beck, G. Zandt, T. Wallace, Lithospheric-scale structure from tomographic images of velocity and attenuation for P- and S-waves, *J. Geophys. Res.*, 103, 21,233-21,252, 1998.

Owens T., and G. Zandt, Implications of crustal property variations for models of Tibetan plateau evolution, *Nature*, 387, 37-43, 1997.

Rudnick, R., and D. Fountain, Nature and composition of the continental crust: A lower crustal perspective, *Rev. of Geophys.*, 33, 367-309, 1995.

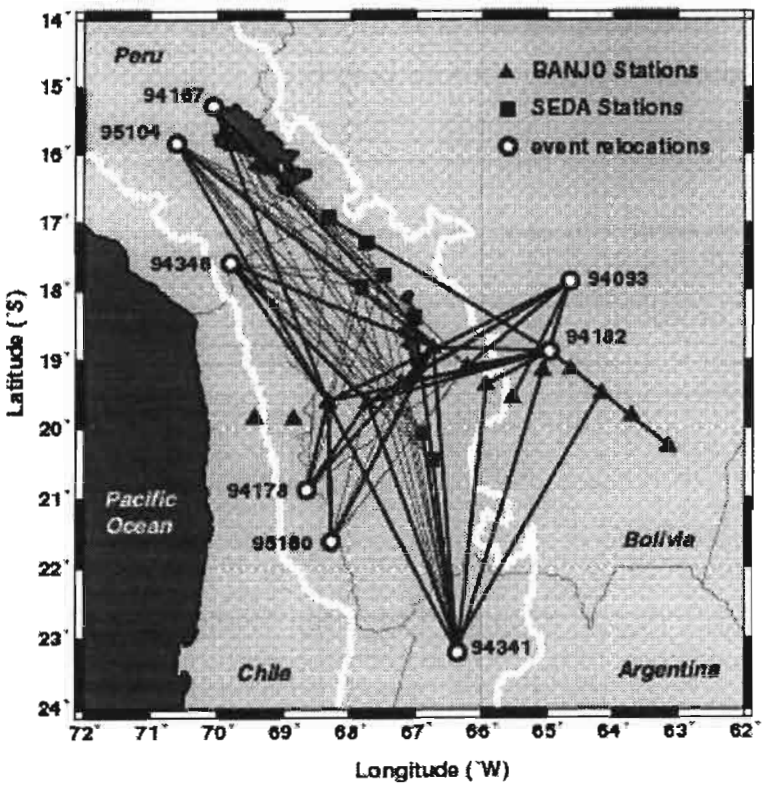

Figure 1. Map of the central Andes showing the BANJO and SEDA seismic stations and the source-station paths used in our regional broadband waveform grid search. The 3600 m contour is shown in white to represent the approximate outline of the Altiplano.

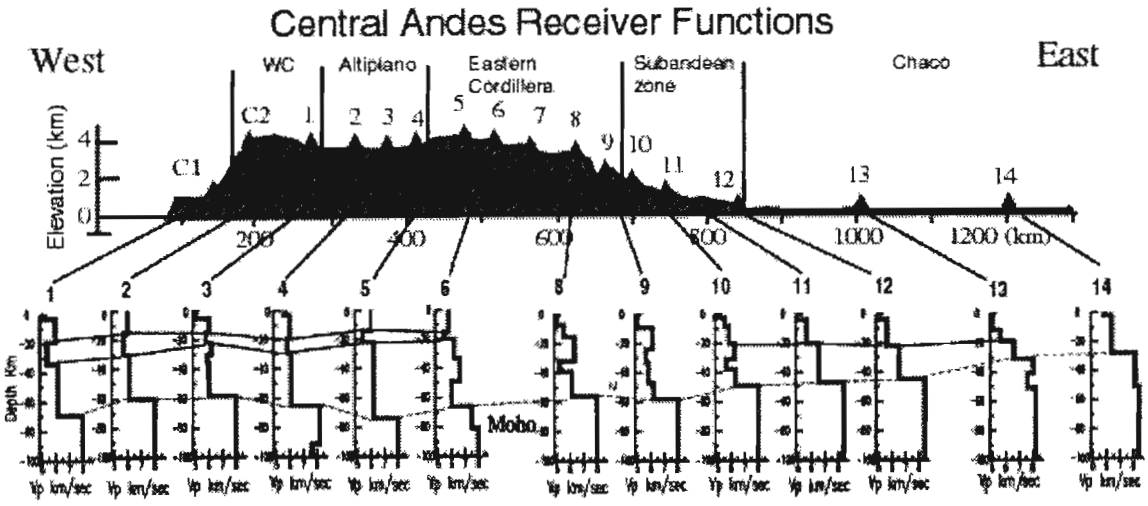

THE TECTONIC EVOLUTION OF THE MESOZOIC AND CENOZOIC AUSTRAL BASIN OF SOUTHERN SOUTH AMERICA

C. Mike BELL (1), Rita de la CRUZ (2) and Manuel SUÁREZ (2)

(1)Cheltenham and Gloucester College of Higher Education, Francis Close Hall, Swindon Road, Cheltenham GL50 4AZ, U.K. E-mail mbell@chelt.ac.uk
(2)Servicio Nacional de Geología y Minería, Santa Maria 0104, Santiago, Chile. E-mail msuarez@SERNAGEOMIN.cl

KEY WORDS: Southern South America, Andes, Tectonics, Mesozoic, Austral Basin, Subduction

ABSTRACT

The Austral Basin of Patagonia in southern Argentina and Chile extends for about 1400 km from north to south and 500 km from west to east. It is one of an extensive system of Mesozoic and Cenozoic back-arc sedimentary basins related to the evolution of the Andean orogenic belt (Riccardi, 1988). The basin developed on continental crust, with an oceanic back-arc basin along its southwestern margin, the Rocas Verdes Basin (Dalziel *et al.*, 1974), between late Jurassic and Cenozoic times (Biddle *et al.*, 1986). The predominantly clastic sedimentary fill reaches a maximum of over 7000 m, and the basin produces significant oil and gas in both Argentina and Chile. The Austral Basin formed adjacent to an orogenic belt produced by the eastward subduction of the Pacific plate beneath the South American continental margin. The basin is subdivided into a northern section, the Aysén Basin, and a much larger and longer-lived southern section, the Magallanes Basin. The Magallanes Basin shares a comparable geological evolution with the offshore Malvinas Basin (Galeazzi, 1998). In both basins late Jurassic to early Cretaceous crustal extension and silicic volcanism gave way to Cretaceous regional subsidence, followed by mid to late Cretaceous and Tertiary strike-slip faulting and compression, accompanied by pull-apart and foreland basin development. The late Paleozoic and Mesozoic geological history of the southern Andes and the Antarctic Peninsula are marked by closely comparable events. The Antarctic Peninsula originated in Jurassic times as an ensialic island arc to the southwest of the southern Andes (Grunow *et al.*, 1992). In the mid-Cretaceous this island arc became detached from South America and migrated towards the southeast on a major strike-slip fault system (Cunningham, 1993).

The geology of the southern Andes and the Austral Basin shows evidence for distinct geographical segmentation (Suaréz, 1976; Ramos, 1989) resulting from tectonic processes on different sections of the active margin. Three major Cretaceous and Tertiary segments are recognised with boundaries at about 50°S and 52°S. The 50°S boundary, marking the transition from the Magallanes to the Aysén Basin, coincides with the northern margin of the Rocas Verdes ophiolites. These ophiolites formed the floor of a back-arc basin produced by splitting and extension of the continental margin in late Jurassic-early Cretaceous times (Dalziel *et al.*, 1974).

Although radiometric evidence from the Patagonian batholith indicates that magmatic activity continued throughout the Cretaceous there is no obvious record of volcanic activity in the form of a westward thickening volcanic wedge in the area between 50° and 52°S. This indicates that the magmatic arc formed an offshore volcanic chain in this area. By contrast, to the south of 52°S, early Cretaceous turbidites were derived from an uplifted calc-alkaline volcanic source to the southwest and seismic sections show a westward thickening volcanic wedge of Turonian age wedge (Mella, 1996).

The early Cretaceous of the Aysén Basin, in the area north of 50°S, was marked by gentle subsidence of the back-arc continental margin, possibly related to thermal sag following Jurassic extension and silicic volcanic activity. In the mid-Cretaceous uplift and extensive silicic volcanism was associated with a magmatically active continental margin. Although the Tertiary fold and thrust belt (Ramos, 1989) penetrates into the south of the region, there is little evidence for the development of a foreland basin. Tertiary deposition was restricted to small basins formed by local subduction-driven tectonic processes.

The Magallanes Basin exhibits two main phases of sedimentation in the zone between 50° and 52°S. The first phase, which continued throughout the Cretaceous, was characterised by regional and long-lived basin subsidence in the form of gentle westward flexure of a broad back-arc area. The second phase which started in latest Cretaceous and early Tertiary times produced foreland subsidence related to a fold and thrust belt. During the first phase the continental margin subsided in pace with slowly accumulating deep marine sediments, derived from a low, deeply-weathered continental area to the northeast. The basin floor sloped gently southwestwards into a back-arc basin floored by the Rocas Verdes ophiolites. Coarse-grained volcaniclastic deposits, derived from an arc to the southwest, are present in the Rocas Verdes basin, on South Georgia and in the Larsen Basin (now situated to the east of the Antarctic Peninsula). The latter probably formed the southwestern section of the back-arc basin. Initial stages of subsidence during the early Cretaceous may have been related to thermal decay (Suárez & De La Cruz, 1994). However, the long time span of more than 70 million years of relatively constant conditions indicates that thermal decay

alone is insufficient to explain the basin subsidence. Foreland basin subsidence related to the development of an orogenic belt in the west is also not a likely mechanism for a number of reasons. Firstly the early Cretaceous successions appear to lack the asymmetrical infill characteristics of a foreland basin, although the thickness of these units have yet to be determined in detail due to their strong deformation. Secondly there is no westward thickening or coarsening volcanic wedge, except in the southernmost region, and thirdly no evidence of deformation in the west. It therefore seems probable that the subsidence was produced by a combination of thermal sag and the gravitational effects of subducted lithosphere, or dynamic coupling between the downgoing oceanic plate and the overlying continental plate (De Celles & Giles, 1996). In latest Cretaceous and early Tertiary times sedimentation in the area between 50° and 52° underwent a fundamental change, as evidenced by the data of Biddle *et al.* (1986) and Mella (1996) which show the characteristic profile of a foreland basin, implying thrusting and uplift in the west, associated with the development of a Tertiary fold and thrust belt (Ramos, 1989).

The geology of the zone south of 52°S has been dominated by left-lateral strike-slip deformation since mid-Cretaceous times (Cunningham, 1993). During the past 84 Ma, transform motions have caused east-west strike-slip separation and north-south divergence, related to the opening of the Scotia Sea, between southern South America and the northern Antarctic Peninsula. Mid-Cretaceous times in this region were marked by a major deformational event which has been called the Andean orogeny. This event is envisaged as the development of a sinistral strike-slip plate boundary cutting the southwest of the continental margin. Sections of the plate boundary were deformed and uplifted whilst other sections subsided as deep pull-apart basins. The Tertiary subsidence of the area south of 52°S was the combined product of transtensional pull apart and foreland basin subsidence related to the development of the fold and thrust belt.

The Malvinas Basin shows a similar record of geological events to the central area of the Austral Basin. A late Jurassic-Cretaceous sag phase lasting 70 Ma was characterised by broad regional subsidence with some displacement along Jurassic master faults related to differential sediment loading and compaction (Galeazzi, 1998). A major change in the tectonic regime from gentle regional subsidence to transtension occurred in the late Cretaceous. The unconformity marking the boundary between Mesozoic and Tertiary deposits probably reflects a change from late Cretaceous strike-slip dominated tectonics to Tertiary compression. Northward-directed compression, with the development of a compressive foredeep trough, was dominant by the end of the Eocene.

The Mesozoic and Tertiary subsidence of the Austral Basin can be best explained in terms of three distinct phases. The first phase, related to the gentle subsidence of the southwest dipping continental shelf, was

probably driven in part by thermal decay following Jurassic volcanism. The long time span and great width of the basin suggests that subsidence was also produced by the gravitational effects and dynamic coupling associated with subduction of the oceanic plate. In late Cretaceous times a second phase of subsidence was initiated in the south of the basin as the Antarctic Peninsula volcanic arc became detached from the continental margin on a transform fault system. Strike-slip faulting produced transtensional pull-apart subsidence. The third phase was the formation of a foreland basin related to an early Tertiary fold and thrust belt which deformed the basin infill.

REFERENCES

Biddle, K.T., Uliana, M.A., Mitchum, R.M., Fitzgerald, M.G. & Wright, R.C. (1986) The stratigraphic and structural evolution of the central and eastern Magallanes Basin, southern South America. *Special Publication International Association of Sedimentologists*, **8**, 41-61.

Cunningham, W.D. (1993) Strike-slip faults in the southernmost Andes and the development of the Patagonian orocline. *Tectonics*, **12**, 169-186.

Dalziel, I.W.D., De Wit, M.J. & Palmer, K.F. (1974) Fossil marginal basin in the southern Andes. *Nature*, **250**, 291-294.

Galleazzi, J.S. (1998) Structural and stratigraphic evolution of the western Malvinas Basin, Argentina. *American Association of Petroleum Geologists Bulletin*, **82**, 596-636.

De Celles, P.G. & Giles, K.A. (1996) Foreland basin systems. *Basin Research*, **8**, 105-123.

Grunow, A.M., Dalziel, I.W.D., Harrison, T.M. & Heizler, M.T. (1992) Structural geology and geochronology of subduction complexes along the margin of Gondwanaland: New data from the Antarctic Peninsula and southernmost Andes. *Geological Society of America Bulletin*, **104**, 1497-1514.

Mella, P.E. (1996) Evolución y geología general de la cuenca de Magallanes, entre Seno Skyring y plataforma Springhill, XII Region, Chile. Unpublished report, Universidad de Concepcion.

Ramos, V.A. (1989) Andean foothills structures in northern Magallanes Basin, Argentina. *American Association of Petroleum Geologists Bulletin*, **73**, 887-903.

Riccardi, A.C. (1988) *The Cretaceous System of southern South America*, Geological Society of America Memoir **168**.

Suaréz, M. (1976) La Cordillera Patagónica: su división y relación con la Península Antárctica. *Anales del Instituto Patagonia*, **7**, 105-113.

Suárez, M. & De La Cruz, R. (1994) Estratigrafía mesozoica de Aisén nororiental (45_-46_ Lat. S). *Actas VII Congreso Geológico Chileno, Concepcíon*, Vol. **1**, 538-542.

A GRAIN-SIZE CLASSIFICATION OF MINERALS FROM IGNEOUS AND METAMORPHIC ROCKS UNDER THE STANDARD PETROLOGICAL T.L. MICROSCOPE – WHY SHOULD THIS BE DONE?

Ludwig BIERMANNS

Universität Tübingen, Institut und Museum für Geologie und Paläontologie, Sigwartstraße 10; D - 72076 Tübingen; EU. (e-mail: < Biermanns@hotmail.com >, < biermanns@yahoo.com >, or < biermanns@netscape.net >.)

KEY WORDS: igneous rocks; metamorphic rocks; petrology; T.L. microscopy; grain-size classification; grain-size diameter.

INTRODUCTION

Investigations on plutonic, volcanic and metamorphic rocks, very frequently, also comprise studies on grain sizes. While, for field studies, a grain-size classification is defined, attributions for grain sizes by means of microscopical studies have not been made so far. A suggestion for delimitations of the grain sizes into different classes which might be most suitable for investigations with the standard petrological T.L. (= transmissive light) microscope, is in the focus of this contribution. A grain-size classification of a diameter from 3 200 µm to 12.5 µm as well as naming of the grain-size classes which seem to be most suitable for the studies under the petrological microscope, are discussed in detail. Also the problems with extremely fine-grained minerals, and with those which typically show elongated or irregular shapes, form a part of the article.

A GRAIN-SIZE CLASSIFICATION UNDER THE PETROLOGICAL T.L. MICROSCOPE

For investigations of plutonic, volcanic and metamorphic rocks, studies on grain sizes with the microscope are frequently of major significance. Also different projects which are done within the framework of the Andean geodynamics, are based on microstructural studies of igneous and metamorphic rocks. Up to now, however, no common grain-size classification has been defined for these rock groups which could be applied to the research under the standard petrological T.L. microscope.

With the microscope, only a limited area of the rock in the thin section to be investigated is in the petrologist's field of observation. With a magnification of 31.25 x, some 35 to 40 mm^2, with a magnification of 125 x, ± 2.5 mm^2, and with a magnification of 312.5 x, finally, merely 0.35 to 0.4 mm^2 are in the field of view under the microscope (tab. 1).

Under the microscope, of course, the mineral grains appear to be much bigger than they are in reality. The grain-size classification which is applied to field studies nowadays, however, is given e.g. by Whittin & Brook (1983); Allaby, A. & Allaby, M. (1991; cf. tab. 2). However, the grain-size attribution used in the field, cannot be applied to investigations with a standard microscope. From a grain size of < 1 mm, investigations in the field begin to be very difficult, mineral identification, in most cases, is not any longer possible, even though a lens is used. From this grain size, studies with the petrological microscope are indispensable where, i.a., a more exact classification of the different minerals and, consequently, a more detailed determination of the rock to be investigated is feasible than with the simple field methods.

A grain-size classification should be defined which is suitable for investigations of igneous and metamorphic rocks with the microscope under minor total magnification, between ca. 30 and 150 x, because under major total magnification, it is hardly, or not possible at all to get a general impression on

magnification:				Field of view:		
ocular:	objective:	total magnification:	magnifiction factor, based on the magnification of 31.25 x:	radius [mm]:	area [mm^2]:	area [%]:
12.5 •	2.5 =	31.25 x	0	3.5	38.485	100
12.5 •	10 =	125 x	4	0.9	2.545	6.61
12.5 •	25 =	312.5 x	10	0.35	0.385	1.06
12.5 •	40 =	500 x	16	0.225	0.159	0.41
12.5 •	100 =	1 250 x	40	≈ 0.113	≈ 0.040	≈ 0.104

Tab. 1: Field of view in dependence upon the magnification. For a grain-size classification under the standard petrological T.L. microscope [Zeiss, Oberkochen, Germany, as an example], a minor magnification should be applied. The data on the size of the microscopic image which is given in mm^2, with increasing magnification, give an impression on its rapid decrease. With magnifications of 500 and 1 250 x, merely conoscopic images are possible as well.

the grain sizes of a rock in the thin section. A table on grain-size delimitations from > 3 200 µm (very coarse-grained) to < 12.5 µm (extremely fine-grained) which is subdivided into several grain-size classes (tab. 3), seems to be most suitable.

The delimitation factor for a grain-size class is four if we go from the finer to the coarser granularity, and it marks the boundary between two grain-size classes. For example: 50 µm is the delimitation from "very fine-grained" to "fine-grained" (cf. tab. 3). An example of the grain-size class from 12.5 to 50 µm will explain this: if 12.5 µm is multiplied by four, the result is 50 µm. The same also applies to the following grain-size ranges. 50 µm, multiplied by four, gives 200 µm,etc. If several grain-size classes are combined to one interval, the delimitation factor increases by the mathematical power which corresponds to the number of the grain-size classes. If, e.g., the granularity has an interval from 50 to 3 200 µm, three different grain-size classes (fine-, medium-, coarse-grained) are passed. With this, the delimitation factor four is raised to the power of three with the result of 4^3 (scale of 4^x or x4 scale). The opposite way, from the coarser to the finer grain size, is characterized by the factor of one fourth.

For more detailed mineral investigations, in general, grain sizes of > 50 µm are necessary (crossed nicol prism). With decreasing grain sizes, it gets more difficult to determine a mineral. From < 10 µm, it is hardly, or even not possible at all to determine an unknown mineral grain, unless identification is possible by means of absolutely typical features, like crystal habit, twinning, refractive index, opake behavior, mineral or interference colours.

interval of grain-size diameter (grain-size class):	classification:
> 30 mm	very coarse-grained
5 - 30 mm	coarse-grained
1 - 5 mm	medium-grained
< 1 mm	fine-grained
minerals, only identified under the petrological T.L. microscope	microcrystalline
minerals, not identified under the petrological T.L. microscope	cryptocrystalline
no grains present	glassy (hyaline), effectively, a grain size of zero.

Tab. 2: Grain-size classification for igneous and metamorphic rocks used in the field (Aubouin et al., 1981: 406; Whittin & Brook, 1983; Castro-Dorado, 1989: 38; Allaby, A. & Allaby, M., 1991).

interval of grain-size diameter:		classification:	
> 3 200	µm	very coarse-grained	
800 - 3 200	µm	coarse-grained	
200 - 800	µm	medium-grained	microcrystalline
50 - 200	µm	fine-grained	
12.5 - 50	µm	very fine-grained	
< 12.5	µm	extremely fine-grained (cryptocrystalline)	
glassy (hyaline)		no mineral grains present	

Tab. 3: Proposed grain-size classification for investigations of plutonic, volcanic and metamorphic rocks under the standard petrological T.L. microscope. If the magnification is 31.25 or 125 x (tab. 1), minerals, with grain sizes of > 800 µm which are in a finer grained matrix, appear to be porphyric already (cf. plate 1). The term "microcrystalline" is representative for the grain-size classes where the individual minerals can be identified under minor magnification with crossed nicol prism. For a more detailed grain-size classification of the minerals, an ocular micrometer, or an object micrometer should be used (cf. Kerr, 1977: 27).

Problematic for the investigations on grain sizes are minerals with irregular (e.g. ilmenite), or elongated grain shapes (micas, chlorites, serpentines, amphiboles, pyroxenes). In this case, a grain-size classification should be made with regard to the crystallographic a, b and c axes where the length and breadth of the minerals should be given. Also ductile mineral deformations which frequently occur in micas, chlorite and serpentines, internal grain boundaries, typical of quartz in metamorphic rocks, and fissuring, or even cataclastic deformations which are often observed from olivine, the pyroxenes, amphiboles and garnets, also make grain-size classifications difficult under the microscope.

Point counting gets more difficult when the grain size of the mineral is < 10 µm, for the standard cross table, in its turn, only has an interval of 10 µm, what means that, with a grain size of < 10 µm, there exists the danger for the mineral of not being under the cross wire. It is not counted then and, as a consequence, with a decreasing diameter, the danger for the mineral increases not to be recorded by means of this method. From a grain size of < 5 µm, determination of an unknown mineral is virtually impossible by optical methods with a standard microscope! With a grain-size diameter of < 5 µm, the mineral is normally not identified any more if it is not directly at the upper surface, of the thin section. In this context, it should be realized that the thin section normally has a thickness of 25 to 30 µm! This fact makes it quite understandable that a mineral with such a minor diameter is frequently not even found.

In order to prevent confusions in the grain-size classification, the additive "under the microscope" should be used. If, e.g., the grain sizes of the minerals vary between 400 and 1 200 µm, the author should write: " ... the minerals are medium to coarse-grained under the microscope ...". In this way, it is clear that the attribution of the grain sizes is referred to investigations with the microscope and not to field studies. Numerical grain-size values, of course, also can be used.

For microscopic researches on sedimentary rocks, however, this classification should not be applied, because there already exist different particle-size classifications used for this rock group worldwide.

Summarizing, a common grain-size classification which could be applied to studies with the microscope, has not been defined so far, and the following clues are applied to the presented method:

-- A grain-size classification for igneous and metamorphic rocks aims at grain-size delimitations which are suitable for investigations with the standard petrological T.L. microscope.
-- A minor microscopical magnifiction, between ± 30 and 150 x and, if necessary, the use of the crossed nicol prism is suggested for grain-size classification and point counting.
-- Six grain-size classes, from "very coarse-grained" (> 3 200 µm) to "extremely fine-grained (crypto-crystalline)" (< 12.5 µm) should be applied. The attribution "amorphous, (hyaline)" means that no minerals are present (tab. 3).
-- The grain-size classes are based on the scale of 4^x (x4 scale) where the factor of four, in its turn, is

based on the boundary between two different grain-size classes.

-- Minerals with irregular or elongated crystal habit make an exact grain-size classification difficult. Similar problems also come up with ductile and brittle mineral deformations.
-- For more detailed studies of the minerals under microscope, grain sizes of > 50 µm are required.
-- As the standard cross table has an interval of 10 µm, point counting of the minerals gets more difficult with a grain size of < 10 µm.
-- If grain-size investigations are based on microscopical studies, the author should add "...under the microscope..." to show that the grain-size classifications are based on microscopical researches.

Terminating, the presented grain-size classification cannot be applied to sedimentary rocks, because there already exist different particle-size classifications for this rock group used wordwide.

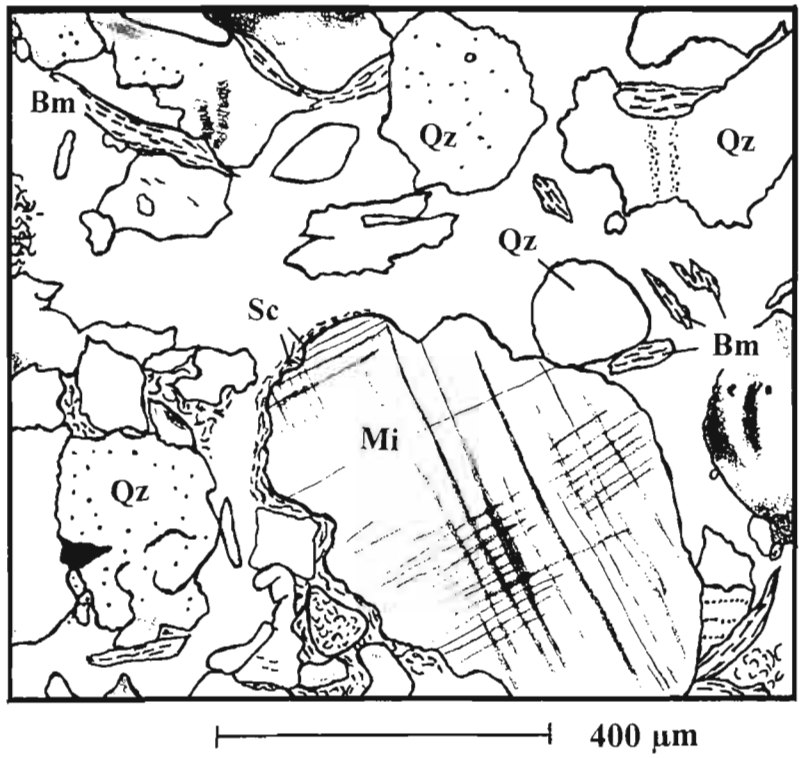

Plate 1: Quartzite. A broader variation in the grain size from ca. 500 to < 10 µm which gives a medium- to extremely fine-grained impression under the microscope, is characteristic of this object. A grain-size attribution of the black micas is difficult because of their elongated habit. The microcline (cross-hatched mineral) has a length of some 600 µm and an approximate breadth of 400 µm .
Locality: Road Salta - Jujuy, some 12 km from Salta and some 4 km north of the place of La Caldera; NW Argentina. Age: Devonian [Mojotoro Formation]. Magnification: 10 x 10; crossed nicol prism.
Mi = microcline; **Qz** = quartz; **Sc** = sericite; **Bm** = black mica.

SELECTED REFERENCES:

Allaby A. & Allaby M. 1991. The concise Oxford dictionary of earth sciences. - 410 p.; Oxford University Press; Oxford, New York.

Bates R.L. & Jackson J.A. (eds.) 1980. Glossary of Geology. - 751 p.; American Geological Institute; Falls Church, Virginia; USA.

Aubouin J., Brousse R. & Lehman J.-P. 1981. Tratado de geología. Tomo I. Petrografía. - 602 p.; Ediciones Omega; Barcelona.

Castro-Dorado A. 1989. Petrografía básica. Texturas, clasificación y nomenclatura de rocas. - 143 p.; Editorial Paraninfo; Madrid.

Kerr P.F. 1977. Optical mineralogy. - 492 p.; Mc Graw-Hill Book Company; New York, St. Louis, San Francisco, Auckland, Bogotá, Düss eldorf, Johannesburg, New Delhi, Singapore, Sydney.

Tröger W.E. 1979. Optical determination of rock-forming minerals. Part 1. Determinative tables. - 188 p.; Schweizerbart Publ.; Stuttgart.

Whitten D.G.A. & Brooks J.R.V. 1983. A dictionary of geology. - 495 p.; Hazell Watson & Viney Ltd.; Aylesburg, Bucks, Great Britain.

Nd and Pb isotopes as tracers of plate tectonic assemblages: evidence for Ordovician arcs and terranes in NW-Argentina and N-Chile?

B. BOCK(1), BAHLBURG, H.(2), WÖRNER, G.(1), and ZIMMERMANN, U.(3)

(1) Geochemisches Institut, Goldschmidtstr.1, D-37077 Göttingen
(2) Geol.-Pal. Instiut, Correnssstr. 24, D-48148 Münster
(3) Geol.-Pal. Institut, Im Neuenheimer Feld 234, D-69120 Heidelberg

KEY WORDS: Nd- and Pb-Isotopes, Paleogeographic Reconstructions, NW-Argentina, N-Chile

INTRODUCTION

Differences in radiogenic isotopes have been used in the Andes to define isotopic domains and to delineate terrane boundaries (Aitcheson et al., 1995). Either the change in isotope compositions in basement rocks or the appearance of exotic material in sedimentary rocks permit the identification of terranes and help to constrain the timing of the amalgamation of different continental blocks. The nature of these terranes and domains, the relationship to Laurentia and the timing of the amalgamation was investigated with Nd- and Pb-isotopes in Ordovician to Permian rocks for the Southern Central Andes.

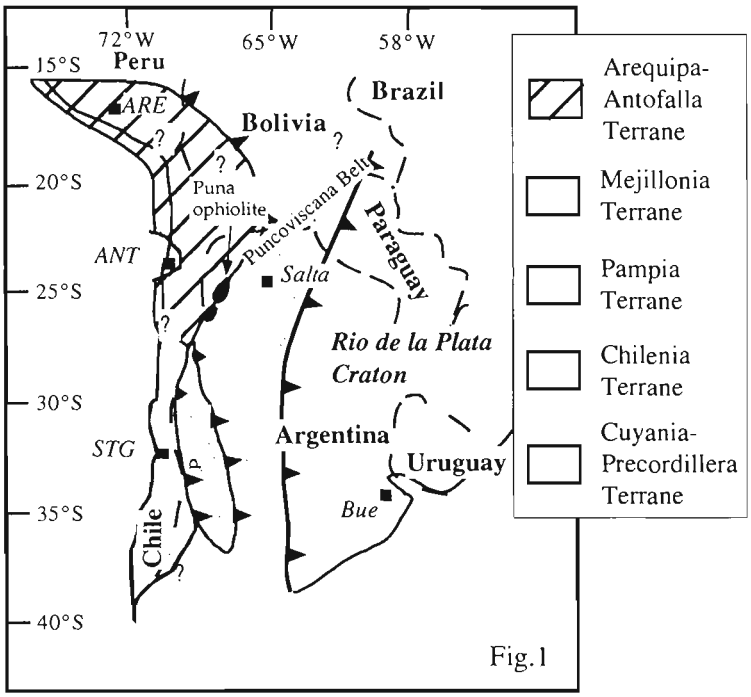

Fig.1

Figure 1 shows a possible terrane assemblage modified from Bahlburg and Hervé (1997).

Contrasting models for the Paleozoic evolution of the Gondwana margin have been

proposed ranging from (1) ensialic development (Damm et al., 1994) to (2) exotic terrane assemblages (Ramos, 1988) to (3) more or less continuous subduction (Coira et al., 1982). In case of an ensialic development, isotope compositions can be expected to be rather homogeneous whereas variable compositions and a juvenile component would be typical for a subduction regime and the presence of an arc. The Precordillera, a former part of Laurentia, is recognized (besides major lithologic differences) by relatively unradiogenic Pb isotope compositions and Nd model ages of about 1.3 to 1.6 Ga (Kay et al., 1996). Another possible terrane for collision with Gondwana is the Arequipa-Antofalla Terrane (AAT). This terrane is tagged with Nd model ages of about 2.0 Ga and relatively high $^{208}Pb/^{204}Pb$ ratios at given $^{206}Pb/^{204}Pb$. Pb isotopes further permit the identification of four crustal domains along the western margin of South America: (1) the Northern Altiplano, (2) the Southern Altiplano, (3) the Eastern Cordillera and (4) the Jurassic coastal domain (Aitcheson et al., 1995). According to Bahlburg et al. (1998) the Late Proterozoic-Early Cambrian Puncoviscana Fm. was deposited in a foreland basin contemporaneously with the Pampean Orogeny. It is overlain with an erosional unconformity by the Late Cambrian Mesón Group which may record a brief interval of tectonic quiescence. The Nd isotopes of these formations are representative of the detritus derived from the east (Gondwana) prior to the onset of Ordovician tectonic and magmatic activity. The ε_{Nd} values of these rocks are rather homogeneous and fall in a range from -9.7 to -5.4 at 450 Ma (shaded field in Fig. 2) with a mean of ε_{Nd} (450 Ma) = -7.0 and T_{DM}'s of about 1.7 Ga. During the Early Ordovician the basin deepend (more in the west than in the east) and immature volcaniclastic rocks (Volcanosedimentary Successions) were deposited in the western part of the basin.

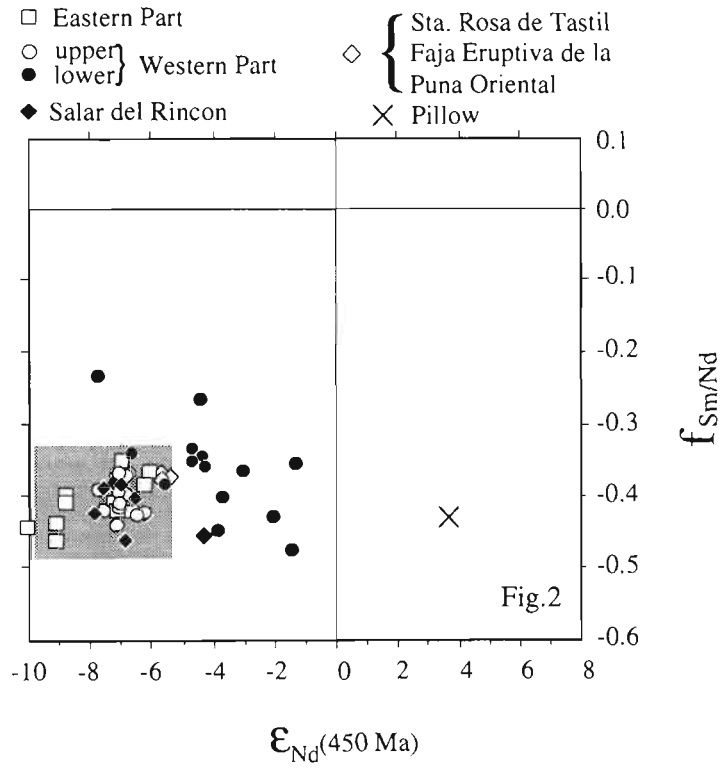

The Arenigian sedimentary rocks of the western part show variable Nd isotope compositions (ε_{Nd} (450 Ma) from -7.8 to -1.3; Fig.2) and indicate the contribution from a juvenile source. However, the existence of layers with a purely 'continental' signature, the restriction of the juvenile layers to a short stratigraphic interval, as well as the complete absence of such material in the overlying sedimentary rocks leads us to suggest that this juvenile source was only of minor importance. The sedimentary rocks of the Puna Turbidite Complex which overlie the Volcano-sedimentary Successions show again homogeneous Nd isotope compositions with a mean ε_{Nd} (450 Ma) = -7.0. The sedimentary samples of the eastern part of the Puna carry Nd isotope compositions indistinguishable from the underlying rocks (ε_{Nd} at 450 Ma = 10.1 to -6.1;

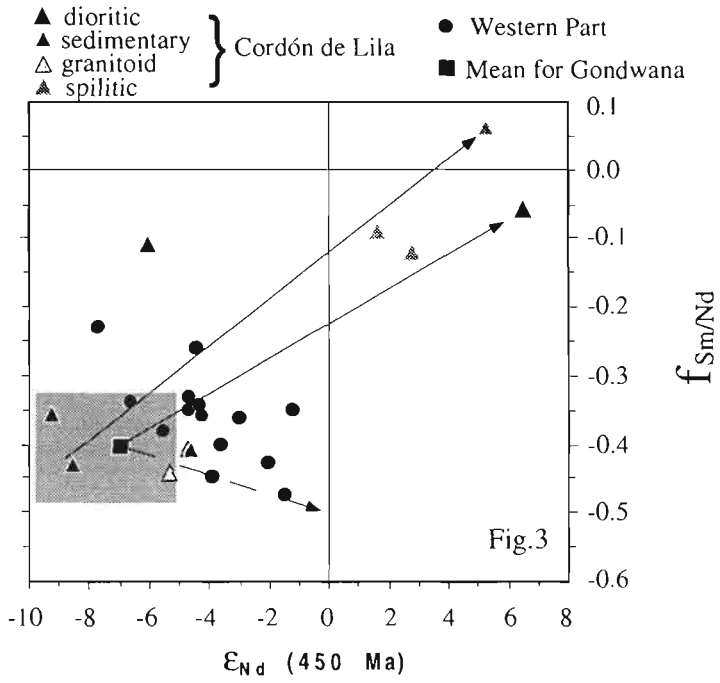

Fig.2). This indicates that the sources remained constant with no Ordovician juvenile input. The Cambrian granitoid Santa Rosa de Tastil (ca. 530 Ma; Damm et al. 1994) intruded into the Puncoviscana Fm. and is commonly interpreted as post-orogenic granitoid. We analyzed its Nd isotopes and it falls within the field defined by the pre-Ordovician sedimentary rocks (ε_{Nd} at 450 Ma = -5.4; Fig.2). Furthermore, we analyzed samples of the Faja Eruptive de la Puna Oriental which were previously interpreted as an Ordovician arc. Their Nd isotope composition is indistiguishable from the older granitoid Santa Rosa de Tastil and again falls within the range defined by the continental sedimentary rocks with ε_{Nd} at 450 Ma = -5.7. This indicates that the Faja Eruptiva de la Puna Oriental was most likely not the result of subduction. Another rock type that was formerly taken as evidence for subduction are pillows exposed in the eastern part of the Northern Puna. However, these pillows show a clear intra-plate signature in their trace elements (enriched LREE and HFSE). At the same time their isotopes are rather juvenile (Fig.2). These characteristics are better explained as the result of magmatism in an extensional environment.

Sedimentary rocks from the Salar del Rincon area (Early Tremadocian to Silurian) also fall within the ε_{Nd} range of pre-Ordovician rocks (mean ε_{Nd} at 450 Ma -7.1; Fig.2). One sample with a more juvenile Nd isotope composition is a dacitic dike (ε_{Nd} at 450 Ma = -4.4). Juvenile detritus observed in the Volcanosedimentary Successions of the western Puna did not reach this part of the basin. However, an arc component may be expected more likely here considering the proposed presence of an Ordovician arc in the Famatina. Nd isotopes of those rocks wre analyzed by Pankhurst et al. (1998) and they determined them to have ε_{Nd} (450 Ma) values in the range of -7.7 to -4.5 showing a major amount of crustal contamination. This leads to the question whether this proposed Ordovician arc incorporated any significant amount of juvenile material at all. The only undifferentiated juvenile material encountered in this study is exposed in the Ordovician part of the Cordón de Lila (Fig.3). However, even in this outcrop we found Ordovician sedimentary rocks that are of continental provenance according to their Nd isotopes. This indicates that the continental source(s) was never far and that the juvenile component never dominated the crustal input. The chemical compositions of the rocks with juvenile Nd isotope compositions do not have an intra-plate character (enriched LREE and HFSE) as the pillow of the eastern Puna. In fact, they show geochemical characteristics that cannot uniquely be attributed to a tectonic setting but are permissive for arc as well as MORB origin.

The observed range in Nd isotope compositions is accompanied with a range of Sm/Nd ratios (Fig. 3). If the range in Nd isotope compositions is due to mixing of a component derived from Gondwana (ε_{Nd} (450 Ma) = -7.0, $f_{Sm/Nd}$ = -0.4) and a primitive component such as observed in the Cordón de Lila then the mixtures should follow trends similar to the ones shown in Figure 3 (solid arrows). However, such mixtures are only able to explain some sedimentay samples. Two samples plot the left of these trends with negative ε_{Nd} (450 Ma) and only slightly negative $f_{Sm/Nd}$. They may be affected by REE mobility or show the effects of enrichment of a REE-rich phase. Other samples plot to the right of these trends. They may be explained by the presence of another juvenile but differentiated (low $f_{Sm/Nd}$) component (dashed arrow in Fig. 3). This observation is confirmed by the Th/Sc ratios which do not correlate with ε_{Nd} (450 Ma).

The Devonian sedimentary rocks from N Chile, that should reflect the detritus of newly arrived terranes or of deeper levels of the proposed Ordovician arc, show a small shift in ε_{Nd} (450 Ma) with a mean of -5.8. The Devonian sedimentary rocks of the Cordón de Lila exhibit a slightly more juvenile compositon. Their ε_{Nd} (450 Ma) fall in a range from -4.1 to -4.8. Permian rhyolites and a mafic dike of uncertain age from the Cordón de Lila as well as a Permian basaltic andesite from Peine are more juvenile with ε_{Nd} (450 Ma) ranging from +2 to +1.

On the basis on variations in Nd isotopes we selected some samples for Pb isotope analyses. The data are also fairly homogeneous and similar to the data of basement rocks from the Southern Altiplano (defined by Aitcheson et al. (1995)) with $^{206}Pb/^{204}Pb$ ranging from 18.18 to 22.63, $^{207}Pb/^{204}Pb$ ranging from

15.563 to 15.787 and $^{208}Pb/^{204}Pb$ ranging from 38.1 to 44.40. No correlation between geographic position and Pb isotope composition is observed.

The rather homogeneous distribution of our data during the Ordovician does not indicate isotopically distinct terranes in the study area nor do our data show major juvenile additions to the crust during the Paleozoic. Rather, they support the observations of Bahlburg et al. (1998) and Franz et al. (1999) who conclude that this area is one homogeneous continental block.

REFERENCES

Aitcheson S.J., Harmon R.S., Moorbath S., Schneider A., Soler P., Sori-Escalante E., Steele G., and Swain-bank I., 1995, Pb isotopes define basement domains of the Altiplano, central Andes. Geol. 23, 555-558.

Bahlburg H., Bock B., Zimmermann U., and Keppie D., 1998, The Paleozoic plate tectonic evolution of the Southern Central Andes in NW Argentina and N-Chile revisited: are there no allochthonous terranes left? ICGP Project 376, Oaxaca, Program and Abstracts, 9.

Bahlburg H. and Hervé F., 1997, Geodynamic evolution and tectonostratigraphic terranes of northwestern Argentina and northern Chile. GSA Bull., 109, 869-884.

Coira B., Davidson J., Mpodozis C., and Ramos V., 1982, Tectonic and magmatic evolution of the Andes in northern Argentina and Chile. Earth. Sci. Rev. 18, 303-332.

Damm K.-W., Harmon R. S., and Kelley S., 1994, Some Isotopic and Geochemical constraints on the Origin and Evolution of the Central Andean Basement (19° - 24°S), in: Reutter K.-J., Scheuber E., and Wigger P., (eds.), Tectonics of the southern Central Andes: structure and evolution of an active continental margin, Springer, Heidelberg.

Franz G., Lucassen F., and Trumbull R., 1999, The continental crust of the central Andes (21°-26°S) - The Petrological-Geochemical Perspective. EUG10, J. Conf. Abs. 4, 420.

Kay M.S., Orrell S., and Abbruzzi J.M., 1996, Zircon and Whole Rock Nd-Pb Isotopic Evidence for a Grenville Age and a Laurentian Origin for the Basement of the Precordillera in Argentina. J. Geol. 104, 637-648.

Pankhurst R.J., Rapela C.W., Saavedra J., Baldo E., Dahlquist J., Pascua I., and Fanning C.M., 1998, The Famatinian arc in the central Sierras Pampeanas: an Early to Mid-Ordovician continental arc on the Gondwana margin. in: The Proto-Andean Margin of Gondwana, Pankhurst and Rapela (eds.), Geol. Soc. Spec. Pub. 142, 343-367.

Ramos V.A., 1988, Late Proterozoic-Early Paleozoic of South America - a Collisional History. Episodes, 11, 168-174.

Tosdal R.M., 1996, The Amazon - Laurentian connection as viewed from the Middle Proterozoic rocks in the central Andes, western Bolivia and northern Chile. Tectonics, 15, 827-842.

Andean transpressive tectonics at the eastern edge of the Cordillera Oriental, Colombia (Chivor-Guavio area)

Yannick Branquet[1], Alain Cheilletz[1][2], Peter. R. Cobbold[3], Patrice Baby[4][5], Bernard Laumonier[6], Gaston Giuliani[4][1]

(1) Centre de Recherches Pétrographiques et géochimiques (CRPG-CNRS), BP 20, 54501 Vandœuvre-Lès-Nancy Cedex, France. E-mail: branquet@crpg.cnrs-nancy.fr
(2) Ecole Nationale Supérieure de Géologie (ENSG-INPL)
(3) Géosciences Rennes, Univ. de Rennes 1, 35 042 Rennes Cedex, France
(4) Institut de Recherche pour le Développement (IRD), 209-213, rue La Fayette, 75 480 Paris Cedex 10, France
(5) Petroproduccion, Apartado 17.12.857, Quito, Ecuador
(6) Ecole des Mines, 54042 Nancy, France

Introduction

The Cordillera Oriental of Colombia is considered to be an asymetric bivergent fold and thrust belt resulting from the Neogene inversion (Andean phase) of a thick Mesozoic and Tertiary back-arc basin with a predominant southeastward transport (Colletta *et al.*, 1990; Cooper *et al.*, 1995). The tectonic style of the chain implies both thick-skinned (e.g. compressional inversion of the Boyacá paleonormal fault) and thin-skinned tectonics. At present time, two important questions are debated : 1) the pre-Andean deformations and related unconformities that have been recognized from the Magdalena valley to the Llanos foothills (Casero *et al.*, 1997; George *et al.*, 1997; Schamel, 1991) ; 2) the role of strike-slip tectonics, recently evidenced in the southern domain of the chain (De Freitas *et al.*, 1997).

The Chivor-Guavio area we studied, located in the eastern edge of the Cordillera Oriental, provides good opportunities to answer these questions. In this area, field works and seismic interpretation have been untertaken in order to realized a cross-section from the « Las Juntas » crossroads in the Cordillera Oriental to the Llanos plain (Fig. 1).

Geometric and facies analysis along the cross-section Las Juntas-Llanos

Along the section from NW to SE we observe :

1) Along the Chivor dam, kinked folds with N30E axial trends and thrusts affecting the Early Cretaceous series ; 2) Hanging-walls of major basement-involved faults present series of en-echelon N50E-trending folds. En-echelon folding also affects the paleozoic rocks of the Quetame massif ; 3) NW-verging thrusts occur in the sedimentary cover but also transports westward the Quetame massif over Valanginian black shales ; 4) The western side of the Quetame massif shows dramatic eastward thickening and westward wedging in the Valanginian shales that suggests fault-controlled deposition above hanging-wall of basin-bounding master faults ; 5) The eastern part of the Quetame massif corresponds to a steep E-dipping panel of paleozoic sediments. Overlying this panel, a steeply dipping reverse sequence of pre-Oligocene sediments is limited eastward by a SE-verging

major accident (the Teasalia fault) that separates the Cordillera Oriental s.s. from the subandean Guavio foothills ; 6) The Guavio foothills are structured by the symetric Guavio anticline between the Nazareth and Rio Amarillo synclines. The eastern boundary of the foothills is the Agua Clara thrust, SE-verging ; 7) East of the Agua Clara thrust, the undeformed Llanos plain forms the western part of the Orinoco Quaternary drainage area.

Seismic interpretation

The seismic lines we studied show evidence of basement-involved NW-verging thrusts and well-individualized basement pop-up limited to the east by convex-upward reverse faults splaying off toward the surface. The bivergent transport, the pop-up, the downward convergence and the upward convex shape of faults stongly suggest basement-involved positive flower structure. Some of the kink and box-folds in the Early Cretaceous sediments correspond to fault-bend folding formed above decollements and ramps. The lower decollement is the contact between the basement and the Early Cretaceous sedimentary cover. The upper decollement would be located within black shales, limestones and evaporites forming the Berriasian Guavio formation. The ramps are thought to be parts of Early Cretaceous normal faults that are twisted and segmented during the basement-involved thrusting and folding. From the NW to SE, huge thickness variations of the Early Cretaceous series indicate important degree of fault-controlled sedimentation. The Tesalia fault appears as an anastomosed fault system, the faults converging downward. Steep reverse faults are implicated in the Agua Clara thrust system suggesting a basement-involved structure that is burried by a ramp linked to a major decollement at the base of the Turonian Chipaque (or Gacheta) formation.

Interpretation and discussion

Evidences of present-day dextral wrench tectonics are numerous (shallow-focus earthquakes, rivers shifting). The general morphology of the Cordillera Oriental also suggests that the Borde Llanero is a « dextral lateral ramp » of the chain, the frontal ramp being the thrusting front of the Sierra Nevada del Cocuy over the Llanos (Fig. 1). Moreover, the southward wedging of the Cordillera Oriental present important dextral wrench tectonics affecting the Garzon and Quetame massifs (Fig. 1).

In the Chivor-Guavio area, based on our observations, we propose that dextral transpressional tectonics is not only limited to present-day deformation but also occured during the entire Andean uplift of the Cordillera Oriental eastern edge. We interpret the Quetame massif as a serie of en-echelon basement pop-ups uplifted during transpressional Andean deformation. These pop-ups are linked to the en-echelon pattern of the Early Cretaceous normal faults which can be either segmented, or twisted, or then inverted (e.g. Tesalia fault) during the Andean transpression. This

transpressional thick-skinned tectonics is accomodated at the basement-cover interface and in the sedimentary cover by thin-skinned deformation.

Some of the en-echelon folds affecting the Paleozoic basement and its sedimentary cover suggest a sinistral strike-slip component. We interpret these folds as inherited folds from Paleozoic deformations, that were reactivated during Andean transpression. Because the developpement of these reactivated folds is controlled by some of the NW-verging thrusts, these thrusts are also thought to be reactivated Paleozoic thrusts. This is in accord with the Paleozoic history of the Borde Llanero that acted as a suture zone between the Guiana shield and an allocthonous continental microplate at the Ordivician-Silurian times (Suarez, 1990).

Conclusion

The Chivor-Guavio area is a key zone to understand the thick-skinned tectonics implied along the Colombian Borde Llanero. In this area, along a cross-section through the whole Borde Llanero, we identified basement-involved pop-ups related to a dextral transpressional inversion of an Early Cretaceous megahalf graben. This megahalf graben formed the eastern passive margin of the Colombian Cordillera Oriental back-arc basin. This transpression occured essentialy during the Andean orogeny (Middle Miocene to recent). Inherited structures from Paleozoic to Early Cretaceous are reactivated. The Early Cretaceous normal faults are reactivated in transpression and some of them were reused as ramps during Andean thin-skinned tectonics. The transpressional inversion of deep and steep basin bounding-master faults as the Tesalia fault is responsible for the upthrusting of the Cordillera Oriental above its eastern foothills. So, at least the southern part of the Borde Llanero can be regarded as a NNE-SSW-trending dextral transpressive belt.

We thank Ecopetrol for access to seismic data and Mineralco S.A. for logistical support. The study was supported by the French Ministry of Education, IRD and European Commission DG XII (grant CT 94-0098).

Casero, P., Salel, J. & Rossato, A., 1997. Multidisiplinary correlative evidences for polyphase geological evolution of the foot-hills of the Cordillera Oriental (Colombia), *in* VI Simposio Bolivariano, Exploracion Petrolera en las cuencas subandinas, Cartagena, Colombia, 14-17 Septembre, 1997, p. 100-118.

Colletta, B., Hebrard, F., Letouzey, J., Werner, P. & Rudkiewicz, J.-L., 1990. Tectonic and crustal structure of the Eastern Cordillera (Colombia) from a balanced cross-section, *in* Letouzey, J., ed., Petroleum and Tectonics in Mobile Belts, Technip, Paris, p. 80-100.

Cooper, M. A., Addison, F. T., Alvarez, R., Coral, M., Graham, R. H., Hayward, A. B., Howe, S., Martinez, J., Naar, J., Penas, R., Pulham, A. J. & Taborda, A., 1995. Basin development and tectonic history of the Llanos basin, Eastern Cordillera, and Middle Magdalena valley, Colombia. AAPG Bulletin, v. 79, no. 10, p. 1421-1443.

De Freitas, M. G., Françolin, J. B. L. & Cobbold, P. R., 1997. The structure of the axial zone of the Cordillera Oriental, Colombia, *in* VI Simposio Bolivariano, Exploracion Petrolera en las cuencas subandinas, Cartagena, Colombia, 14-17 Septembre, 1997, p. 38-41.

George, R. P., Pindell, J. L. & Cristancho, H., 1997. Eocene paleostructure of Colombia and implications for history of generation and migration of hydrocarbons, *in* VI Simposio Bolivariano, Exploracion Petrolera en las cuencas subandinas, Cartagena, Colombia, 14-17 Septembre, 1997, p. 133-140.

Schamel, S., 1991. Middle and upper Magdalena basins, *in* Biddle, K. T., ed., Active margin basins, AAPG *memoir*, vol. 52, p. 283-303.

Suarez, A. F., 1990. The basement of the eastern cordillera, Colombia: an allochtonous terrane in northwestern south America. Journal of South American Earth Sciences, v. 3, p. 141-151.

TECTONIC MODEL OF THE NORTH SUBANDEAN ZONE, ECUADOR.

Alfredo G. BUITRON P.(1)

(1) Escuela Politécnica Nacional, Dpto. de Geología, Quito-Ecuador (agbuitron@hotmail.com).

KEY WORDS : Subandean Zone, Napo Uplift, Orogenic wedge, Foreland system

INTRODUCTION

The Ecuadorian foreland system has different formational elements: orogenic wedge, wedge top, foredeep, forebulge, and backbulge (Fig.1), which are analized in this work from a tectonic-depositional and structural perspective. Futhermore, an evolutionary relationship between the tectonic system and the geodynamic regional events is established.

CONCLUSIONS

In the Late Cretaceous, the advance and eastward propagation of the orogenic wedge, which was composed by volcanic-sedimentary rocks of the Jurrasic Upano Unit and coeval volcanic deposits of the Misahuallí Formation, have been incorporating the sediments of the Cretaceous basin (Cretaceus Hollín and Napo Formations) that were forming the foredeep at that moment, and later the Maastrichtian-Paleocene Tena Formation as the wedge top of the system. The convex long shape of the Napo Uplift and the thinness and lack of deposition of the Tena Formation, indicate that the Napo Uplift was forming the forebulge during the Late Cretaceous. The geologic development of this Uplift had started 85 Ma ago, and had formed in principle "due to tectonic processes like flexular subsidence driven by sediment accumulation between the orogenic wedge and the forebulge, topographic loads, subduction loads, and the viscous coupling between

the subducted slabs and mantle wedge material beneath the outboard part of the overlying continent" (*). The tectonic processes for the develoment of the forebulge are related to the advance and forward propagation of the orogenic belt over a foreland basin system.

By the end of Eocene, the wedge top and foredeep had traveled eastward. These elements were represented by the coarse sediments of the Tiyuyacu Formation, whose depocenter was located on the eastern flank of the Napo Uplift. At this time (40 Ma), the Cretaceous sediments to the west of the Subandean Zone had already been incorporated in the Eocene orogenic wedge. Structural evidence suggests two additional important additional tectonic episodes, dated by fission track chronology at 20 and 10 Ma (**).

At the present time, the Subandean Zone forms the orogenic wedge, which has propagated to the east of the Napo Uplift. In the area of study, the present wedge top is represented by colluvial and alluvial terraces which form isolated Quaternary "piggy back" basins limited by the topographic front of the Eastern Cordillera and the Quaternary alkaline complex of the Sumaco and Cerro Negro - Pan de Azúcar volcanics. An uncomformity separates the current wedge top from the orogenic wedge. It demonstrates a strong erosion and a high rate of uplift in the Subandean Zone. The present orogenic wedge is conformed by the Upano Unit and Misahuallí, Hollín, Napo and Tena Formations on the Subandean Zone.

This tectonic-depositional model implies that the wedge top and foredeep, in the north of the Ecuadorian foreland basin, have traveled from the eastern flank of the Eastern Cordillera about 80-100 Km eastward, since the Late Cretaceous.

In the area of study, two principal zones with different degrees of deformation are observed. These zones are separated by the Cosanga Fault: to the west the rocks are very deformed, while eastward there is no internal deformation, the original sedimentary structures are subhorizontal, and are affected only by gently folding and inverse faulting (Fig.2). The difference in the degree of deformation between these zones is due to the most distorted zone formed an orogenic wedge at the end of the Eocene, while since the Eocene the less distorted zone has been incorporated progressively in this element of the foreland system. Hence, the degree of deformation increases from East to West. Thus, the tectonic structures found in the Napo Uplift, to the east of the Cosanga Fault, are younger than structures to the west.

Structural analysis allowed to model the Eocene orogenic wedge. In this way, west of the Cosanga fault a penetrative regional foliation S1 appears represented by a slaty cleavage o schistosity, which has been developed on the original stratification S0. S1 trends NNE-SSW to NE-SW, and dips steeply to the NW. With a similar tendency a second no penetrative foliation S2 appears. S1 and S2 are folded gently in decametric scale, while closed folds appear in centimetric and metric scale. Two important plastic deformation episodes are noted as given by the variation in the orientation of the centimetric fold axes, crenulation planes, and

inverse kink bands. Stereographic analysis shows compressional stresses, which rotated in a anticlockwise sense, from NW-SE to WSW-ENE, in moderate intervals smaller than 30°. In this way, NE-SW and NNE-SSW trending inverse faults, which comprise the tectonic system, change their style from pure compression to transpression with a dextral component.

The contacts between the litological formations are tectonic, since the sequences appear in lengthened and faulted strips with a NNE-SSW trends, forming thrusts sheets and splays of imbricate fans inside the thrust system, without showing evidence of horizontal displacement at depth. The thrust system is defined as an emergent type, with trailing imbricate fans. The thrust front is buried and there is evidence of slow stress relaxation. The detachment plane is 1-2 Km deep and is related to the rheologic-mechanical boundary between rocks of different competence, that is, between Cretaceous plastic sedimentary rocks and brittle Jurrasic rocks. The tectonic shortening is calculated in 52%.

Stratigraphically, the Upano Unit represents the western facies of the Jurrasic Misahuallí Formation. Furthermore, the Cosanga Fault divides the volcano-sedimentary rocks from pelitic schist within the Upano Unit.

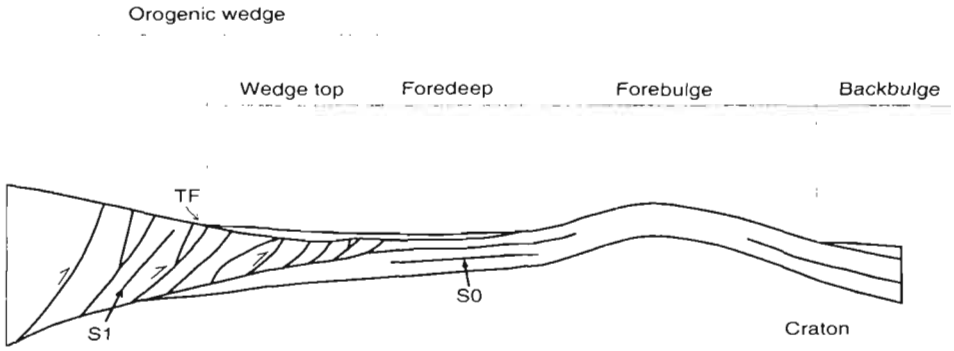

Fig.1. Schematic cross section of the foreland system showing its elements. The vertical scale is exaggerated.

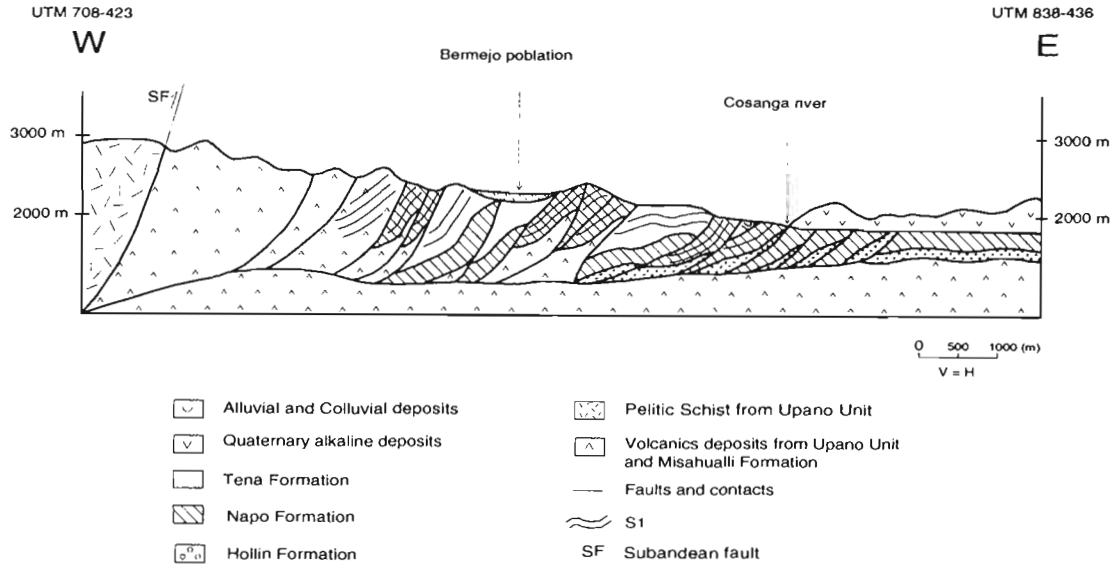

Fig.2. Geological section across the area of study.

REFERENCES

Boyer S.E. and Elliott D. 1982. Thrust Systems. A.A.P.G. Bulletin. Vol. 66. 1196-1230.

(*) DeCeles P.G. and Giles K.A. 1996. Foreland basin systems. Blackwell Science Ltd. Basin Research (1996) 8. 105-123.

Hall M. y Beate B. 1991. El volcanismo Plio-Cuaternario en los Andes ecuatorianos. Estudios de Geografía: El paisaje volcánico de la Sierra ecuatoriana, geomorfología, fenómenos volcánicos y recursos asociados. Quito-Ecuador. Vol.4. 5-17.

Jaillard E. 1997. Síntesis Estratigrafica y Sedimentológica del Cretácico y Paleógeno de la Cuenca Oriental del Ecuador. Informe final del convenio Orstom-Petroproducción. 164.

Litherland M., Aspden J., and Jemielita R. 1994. The metamorphic belts of Ecuador. Overseas memoir of British Geological Survey No.11.

Morley C.K. 1985. A Classification of Thrust Fronts. A.A.P.G Bulletin. Vol. 70. 12-25.

(**) Spikings R. 1999. Fission track data of samples of the Eastern Cordillera, Ecuador: in elaboration. ETH (Zurich).

White H.J., Skopec R.A., Ramírez F.A., Rodas J.A., and Bonilla G. 1995. Reservoir characterization of the Hollín and Napo formations, western Oriente Basin, Ecuador. A.A.P.G. Memoir 62. 573-596.

MANAGEMENT OF GEOSCIENTIFIC INFORMATION: THE WEBSITE OF THE SFB267 http://www.fu-berlin.de/sfb267

Heinz BURGER, Michael ALTEN and Sabine MOHR [1]

(1) Institut für Geologie, Geophysik und Geoinformatik, Malteserstraße 74-100, D-12249 Berlin, Germany, Email: hburger@zedat.fu-berlin.de

KEY WORDS: world wide web, information system, interdisciplinary research project, data catalog, geology, geophysics, Andes

INTRODUCTION

The "Collaborative Research Center 267" (SFB 267) entitled "Deformation Processes in the Andes" is an interdisciplinary research project which comprises about 120 scientists from three universities ("Free University of Berlin", "Technical University of Berlin", "University of Potsdam"), the "GeoForschungs-Zentrum Potsdam" and about 10 cooperating partner institutions (universities, geological surveys) in South America. It became soon apparent that communication within and between all working groups plays an important role in such a heterogeneous scientific environment. The WWW is a flexible tool for distributing information on various levels. Surprisingly most home pages provide only poor information beyond traditional lists of departments, staff members and recent publications.

The SFB267-website was designed to provide information on two levels: an intranet module for internal use (administration, exchange of data and ideas, discussion groups, announcement of colloquia/lectures) and an internet module as a source of information for the global scientific community presenting actual research activities, recent results, available maps and data, contact addresses to SFB-members etc. The combination of both tasks and the huge amount of data gathered during numerous geological and geophysical field campaigns require a careful design and permanent maintenance of the website.

This paper describes the concept of our information system, computer implementation and presents some information about experiences and problems.

Intranet functions of the website

The creation of the SFB267-information system started with a study of the administrative structure and scientific research proposals of all task groups. Next step was the design of a suitable web-representation of this structure, including traditional items (lists of staff, addresses etc.). The result was a tree like structure of the website see Fig. 1 (in reality, the pages are much more linked with each other).

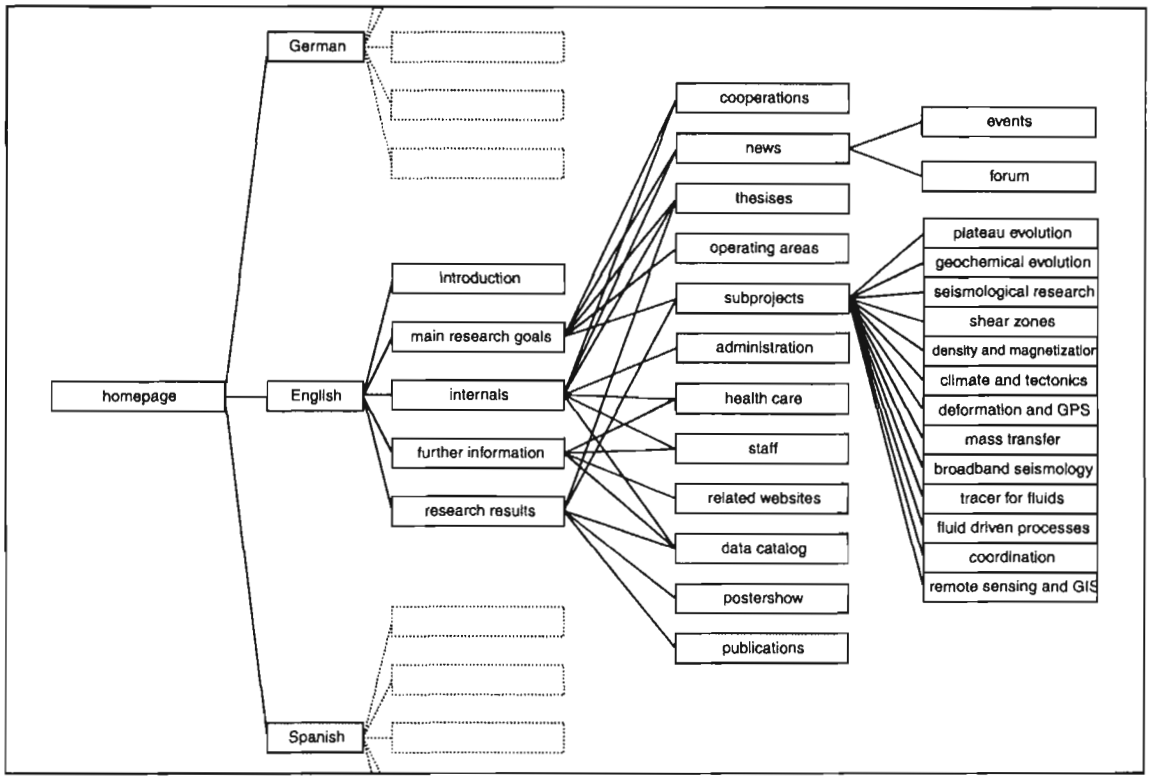

Fig 1: Simplified structure of the SFB 267 website

This part of the information system also serves as blackboard for the announcement of seminars, meetings, conferences, new hardware and software which can be used by all SFB-members. On-line forms for registration of field work, application forms for traveling funds, research grants etc. are distributed via the internal mailing lists. The intranet also serves as a forum for discussion of draft papers and preliminary research results. We hope that this part of the website will motivate scientists to present their results - even if they are preliminary - and to stimulate scientific discussions.

The logistic preparation of field work is supported by lists and previews of available road maps, geological maps and satellite imagery for each working area. A special service by the GIS-group is the

preparation of enlarged and spectral enhanced satellite images. These image maps have proven to be very useful for orientation in remote areas and as a medium for the documentation of spatial information gathered during the field work (e.g. identification of GPS-locations for geometric rectification of satellite images). A final check of the health service webpage is mandatory for 'flatlanders' working in remote areas between 3000m and 5000m above sea-level.

The website: An information gateway to the SFB267

The SFB-website should not only inform about structure and research goals of the research center but also serve as a guide to a huge amount of data obtained during the first and ongoing period of the project. The information system of the SFB267 includes various sources which may be of interest to visiting foreign scientists. For a website containing more than 250 pages navigation tools and tools for finding information are absolutely necessary. A website map and navigation bars on each page support navigation. In order to facilitate access to SFB267 information (a) full text retrieval and (b) spatial search tools were implemented which are able to search the existing web-pages and the databases as well. The full text search allows access to

- addresses of people
- participating institutions
- publications database
- data catalogue

From there other links may connect to personal home pages, on-line publications, posters etc. A special geoscientific problem is the implementation of spatial search via the web. The request is simple: The user should be allowed to draw a rectangular or a polygon as search window and the system should find and display all maps, texts and data related to the area chosen. A simple solution for this problem would be the combination of web-browser and limited GIS functionality (about 90% of GIS-functions are devoted to graphical editing and map design including map legend). Complexity and costs of commercial GIS or map-servers are prohibitive for such an approach. Other solutions are dependent on specific operating systems. The essential needs for spatial search are

a) georeferenced documents (texts, maps, satellite images)
b) point/line in polygon search tools

(An additional comfort would be buffering). A prototype for a spatial viewer with limited GIS-functionality is described in Kraak (1998). As long as we are waiting for a WWW-compatible GIS which supports more complex spatial queries we have realized spatial search requests by presenting clickable "image maps", i.e. maps are displayed at various scales and hyperlinks activate other maps or text documents. Hot spots on maps can be rectangles, polylines, symbols, map inlets etc. So users can get a

fast overview on research areas, location of geophysical transects or seismic nets, points where geologic age determinations are available etc.

Data catalog

During the first period of the Research Center SFB267 a wealth of geophysical, geological and geochemical data was gathered and stored in a comprehensive data base (S. Mohr & H.-J. Götze, 1998) Not all scientists allow an unrestricted access to their data. Therefore meta-information which describes type of data, location, date of processing, encoding format, and preliminary interpretation (graphical display of transects, compilations of seismic refraction profiles etc.) enable all visitors to get a clear impression about the quality and amount of data. Addresses and phone numbers are given which enable users to contact those scientists who are in charge of the corresponding data collection.

Implementation

The hardware platform of the webserver is a Pentium 133 PC with 64 MB RAM, 8 GB disk storage, Windows NT 4.0 operating system and Microsoft Internet Information Server 4.0 as webserver.
Fig. 2 gives an overview on the webserver structure and internet client server communication.

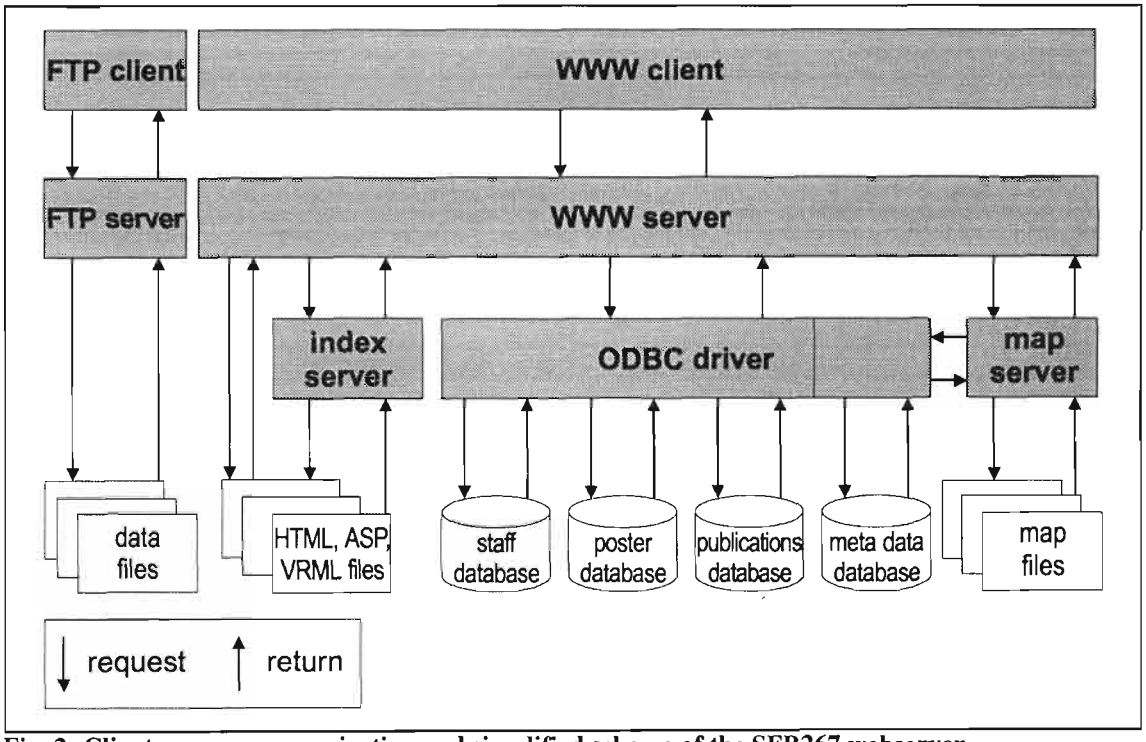

Fig. 2: Client-server communication and simplified scheme of the SFB267 webserver

Prominent features are an index server for text retrieval and the connection to several databases via ODBC (open database connector). In our case the database engine is Microsoft Access 97, other ODBC/SQL (standard query language) database engines can be connected.

We use the ASP (active server pages) technology from Microsoft to build pages with dynamically created contents at runtime. The ASP programming language is JScript - a Microsoft derivate of JavaScript which runs at the server platform (server side scripting). This approach was very time consuming during the development of the website, but we believe that it will save a lot of maintenance and administration efforts when established.

Actualization of the databases is done with the WWW browser interface We use the "forms" feature of HTML and the ODB connection of the server for writing-access (after author identification and permission control) and updating the databases. "Web weaving" is done with several tools: For ASP coding we use Visual InterDev 6.0 and Frontpage98 (Microsoft); HTML encoding is done with HoTMetaL 5.0 (Softquad) or simply with ASCII-Editor. The PDF (portable document format) poster files are generated with Acrobat 4.0 (Adobe) and for image conversion and composition we use Adobe Photoshop 5.0.2 and ImageStyler 1.0.

Concluding remarks

The website exists since June 1996 (since April 1999 located on an own server). In 1998 we had 26415 visits from outside the "fu-berlin.de" domain. About fifty percent of the total number of hits are from outside the German "DE" domain. The acceptance of the information system by SFB members was stimulated by international contacts and information requests from abroad. It increased significantly during the last years. A careful selection of keywords in the document meta-information of the website facilitates contacts via search machines.

Installation and maintenance of the website of an interdisciplinary research center is very time consuming if it contains more information than usual. Especially the creation of active server pages requires trained personal which can't easily be substituted after leaving.

It is our hope that the information service of the SFB267 website service will improve internal and international communication and exchange of expensive data. This can be seen as a contribution to parsimony by the scientific community.

References

Moor, S. & H.-J. Götze: The "Central Andes GIS", a comprhensive database for studies of deformation processes in the Central Andes.- http://earth.agu.org/eos_elec/96350e.html (March 1999).

Kraak, M.-J. & Rico van Driel (1998): Principles of hypermaps: - http://www.itc.nl/~kraak/hypermap/Hypermaps.html (March 1999).

EXTENSION IN THE SOUTHERN ANDES AS EVIDENCED BY AN OLIGO-MIOCENE AGE INTRA-ARC BASIN

W. Matthew BURNS(1) and Teresa E. JORDAN(1)

(1)Department of Geological Sciences, Cornell University, Ithaca, NY 14853-1504 USA
(mburns@geology.cornell.edu, tej1@cornell.edu)

KEY WORDS: Extensional basins, intra-arc basins, Southern Andes, Oligo-Miocene, Argentina, Chile

INTRODUCTION

The Late Oligocene-Early Miocene age Cura-Mallín Basin lies within the Southern Volcanic Zone of the Andes and in the adjacent Central Valley of Chile between approximately 36-38°S latitude (Fig. 1). The east-west extent reaches 200 km. The basin contains substantial thicknesses of volcanic and sedimentary strata (Niemeyer and Muñoz, 1983; Muñoz and Niemeyer,1984; Gutierrez and Minniti, 1985; Vergara et al., 1997) which, it is subsequently suggested, were deposited in an extensional volcanic arc with normal faults controlling subsidence.

Coincident with the development of the Cura-Mallín Basin, the convergence of the Nazca and South American plates became nearly trench-normal after a long period of high obliquity and the convergence rate nearly tripled (Pilger, 1984; Pardo-Casas and Molnar, 1987; Somoza, 1998). The geological evidence that the Late Oligocene and Early Miocene was a time of arc extension contradicts standard geodynamical models which correlate plate convergence rates to the state of stress in the overriding plate.

GENERAL BACKGROUND

The Cura-Mallín Basin is filled with volcaniclastic and lacustrine strata. Exposed sections of the basin fill range in thickness from less than 1000 to nearly 3000 m (Niemeyer and Muñoz, 1983; Muñoz and Niemeyer, 1984; Gutierrez and Minniti, 1985),but the base of the section is rarely observed. Two distinct depositional facies and a transitional hybrid between the two have been identified: a volcanic facies that consists of pyroclastic deposits with minor fluvial influence and a sedimentary facies that consists of fluvial and freshwater lacustrine deposits with minor pyroclastic input. The thickest known stratigraphic sections are composed of the sedimentary facies, but the volcanic and hybrid facies cover a larger area. Radiometric ages obtained for strata within the basin have established that most of the development of the basin occurred between 26 and 22 Ma (Jordan et al., unpublished manuscript).

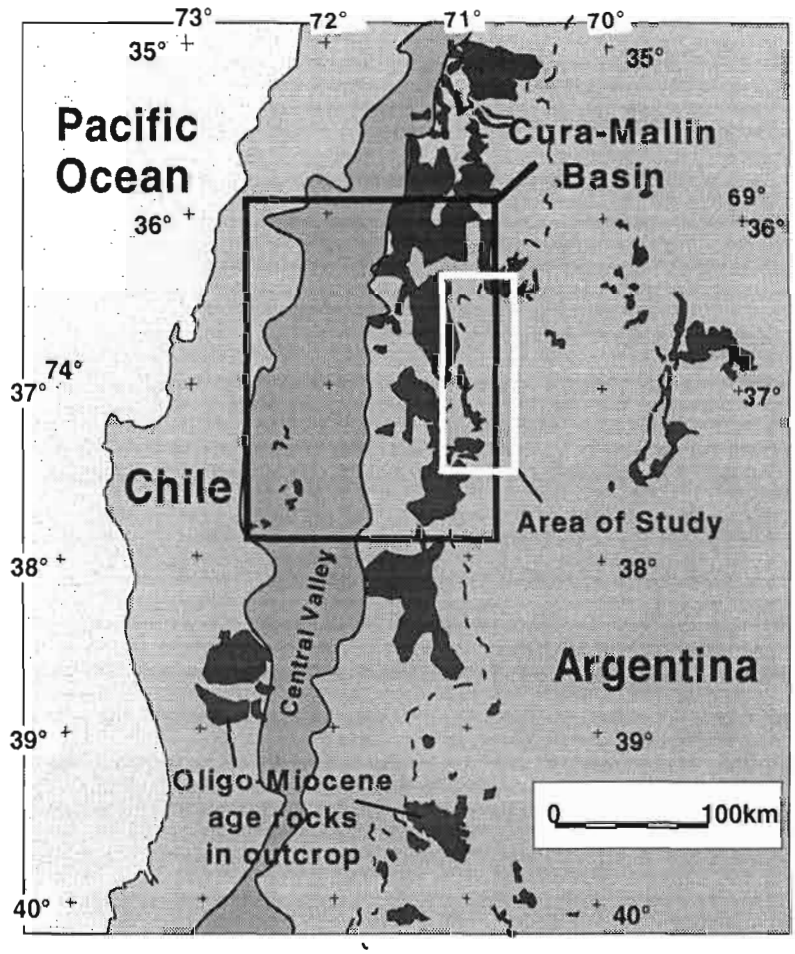

Figure 1. Location of Cura-Mallín Basin and other Oligo-Miocene rocks of the region (after Jordan et al., unpublished manuscript).

STRUCTURAL DEVELOPMENT OF THE BASIN

Seismic reflection data from the eastern flank of the basin in Argentina (Jordan et al., unpublished manuscript) and gravity and drilling data from the western flank in the Central Valley of Chile (Vergara et al., 1997) have been interpreted as showing basin-bounding normal faults controlling the distribution of Late Oligocene-Early Miocene strata, which were reactivated in a reverse sense during Late Miocene shortening. Small (offset < 3m) listric normal faults have also been observed within one of the basal outcrops of the sedimentary basin fill.

Stratigraphic relationships also suggest the presence of basin-bounding normal faults. In the Argentine portion of the basin, the sedimentary facies crops out in the eastern flank of the Andean Cordillera where it has been uplifted in the hanging wall of a reverse fault. The hanging wall of that normal fault exposes approximately 2800 m of Cura-Mallín strata, concordantly overlain by Middle Miocene volcanic rocks. However, in the footwall of the fault, no Cura-Mallín strata crop out and undeformed Eocene volcanic rocks are exposed 5 km east of the reverse fault. The rapid lateral transition from thick basin fill to strata predating the basin implies either strong differential subsidence by faulting during basin fill, or significant eastward transport of the Cura-Mallín strata by thrusting. The latter is unikely based on the seismic data and fold style.

Changes in section thicknesses suggest that subsidence within the basin was localized along individual faults. Thickness variations reflect position within footwall or hanging wall, proximity to a fault, and along-strike variations in fault displacement. The 200 km breadth of the basin fill implies that the Cura-Mallín basin consists of several interconnected depocenters each with its own controlling fault or faults.

TECTONIC SETTING OF THE BASIN

The reorganization of plate motions in the South Pacific (Tebbens and Cande, 1997) coincident with the initiation of the Cura-Mallín basin generated an increase in convergence rate of the Nazca and South American plates from near 5 cm/yr to almost 15 cm/yr and a rotation of the convergence vector from 50° obliquity to nearly trench normal (Pilger, 1984; Pardo-Casas and Molnar, 1987; Somoza,1998). Furthermore, the volcanism of the Cura-Mallín Basin represents the reinitiation of volcanism in this part of the Andes after a hiatus of approximately 15 m.y. (Jordan et al., unpubl. manuscript; Rovere, 1998). There is a probable causal relation between the increased convergence rate, a resultant increase in the flux of water into the asthenosphere, and the renewal of volcanic activity. However, geodynamical models indicate that the increase in convergence rate and reduction of obliquity would create a compressional regime in the overriding plate (Ruff and Kanamori, 1980; Peterson and Seno, 1984). This is in direct conflict with the geological evidence

from the basin for extension during this period of time. Therefore, it is necessary to examine the stress contributions from processes not included in the geodynamic models. One such source of stress is a change in thermal state. One hypothesis, to be tested by thermal studies in progress, is that heat flow in the South American lithosphere would have increased considerably due to the reinitiation of arc volcanism and the increase in asthenospheric flow caused by rapid subduction, causing doming and upper lithospheric extension.

REFERENCES

Gutiérrez, P. A., and Minniti, S., 1985, Reconocimiento geológico de las nacientes del Río Lileo (dept. Minas), provincia del Neuquén: YPF Informe (Comisión Geológica #1).

Jordan, T. E., Burns, W. M., Veiga, R., Pangaro, F., and Copeland, P., unpublished manuscript, Mid-Cenozoic intra-arc basins in the Southern Andes.

Muñoz, B. J., and Niemeyer R. H., 1984, Hoja Laguna del Maule, Regiones del Maule y del Bio Bio: Carta Geológica de Chile, Servicio Nacional de Geología y Minería, p. 98.

Niemeyer, R. H., and Muñoz, B. J., 1983, Hoja Laguna de la Laja, Región del Bio Bio: Carta Geológica de Chile, Servicio Nacional de Geología y Minería, p.52.

Pardo-Casas, F., and Molnar, P., 1987, Relative motion of the Nazca (Farallon) and South American plates since Late Cretaceous time: Tectonics, v. 6, p.233-248.

Peterson, E. T., and Seno,T., 1984, Factors affecting seismic moment release rates in subduction zones: Journal of Geophysical Research, v. 89B, p. 10233-10248.

Pilger, R. H. J., 1984, Cenozoic plate kinematics, subduction and magmatism: South American Andes: Journal of the Geological Society of London, v. 141, p. 793-802.

Rovere, E., 1998, Volcanismo jurásico, paleógeno y neógeno en el noroeste del Neuquén, Argentina: X Congreso Latinoamericano de Geología y VI Congreso Nacional de Geología Económica, Buenos Aires, v. 1, p.144-149.

Ruff, L., and Kanamori, H.,1980, Seismicity and the subduction process: Physics of the Earth and Planets International, v. 23, p. 240-252.

Somoza, 1998, Updated Nazca (Farallon) - South America relative motions during the last 40 m.y.: implications for mountain building in the Central Andean region: Journal of South American Earth Sciences, v. 11, p. 211-215.

Tebbens, S. F., and Cande, S. C., 1997, Southeast Pacific tectonic evolution from early Oligocene to Present: Journal Geophysical Research, v. 102, no. B6, p. 12061-12084.

Vergara, M., Moraga, J.,and Zentilli, M., 1997, Evolución termotectónica de la cuenca terciaria entre Parral y Chillán: analisis por trazas de fisión en apatitas: VIII Congreso Geológico Chileno, Antofagasta, v. 2, p.1574-1578.

SEISMIC SWARM IN QUITO (ECUADOR): TECTONIC OR VOLCANIC ORIGIN?

Alcinoe CALAHORRANO[1], Hugo YEPES[1], Bertrand GUILLIER[1, 2], Mario RUIZ[1], Mónica SEGOVIA[1], Darwin VILLAGÓMEZ[1] and Daniel ANDRADE[1]

(1) geofisico@accessinter.net. Apartado postal 2759, Quito-Ecuador
(2) bguillier@ednet.net. Apartado postal 2759, Quito-Ecuador

KEY WORDS: seismic swarm, inverse fault, volcanic activity, stress field, b-value, Ecuador

INTRODUCTION

The city of Quito (1.5 million pop.), Ecuador, located in the interandean valley, is limited on the west side by Guagua Pichincha Volcano and on the east side by a series of slopes aligned NNE, in accordance with the Andean trend. This latter morphological feature is the superficial expression of the Quito Active Fault System. Since June 1998, an anomalous increase of seismic activity was registered in the northern part of Quito, and two months later, an increase of volcanic and seismic activity at Guagua Pichincha Volcano (located 16 km SW of the swarm) was registered. Characterization and relationship between these two seismic activities are important to understand both processes and to advise people living in Quito and its surrounding areas

SEISMICITY

Since June 1998, a very intense seismic swarm of about 4000 events has been registered in Quito. During July 24 and October 31, the swarm shows an average of 40 events per day, and a maximum of 120 events daily, while in the first half of the year the average seismic activity was not bigger than 3 events per day. Two peaks of activity are clearly defined: the first between the end of the first days of July and September, and the second on October (figure 1a). The average magnitude was 2.7 while the

maximum calculated magnitude was 4.1. The seismic signals show frequencies from 1 to 12 Hz, with peaks at 2.3 and 3. 2 Hz on the nearest seismic stations. The total energy accumulated by the swarm, from June 6 1998 to the end of the year, shows two important increments related to the seismic peaks in August-September and October. (Figure 1b)

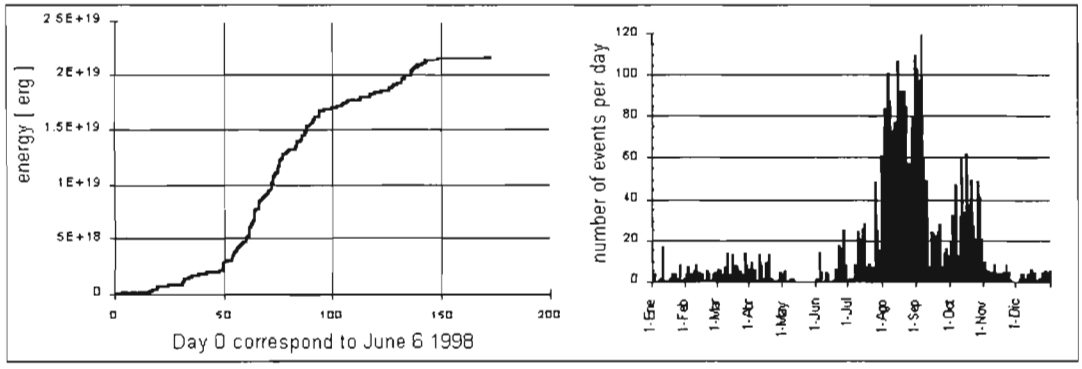

Figure 1 a Accumulated energy released in 1998 Quito Seismic Swarm, from Jun.6 to Dec. 31

Figure 1 b Number of events registered in 1998

DATA PROCESSING

The seismic data were processed using HYPOELLIPSE (Lahr, 1995) and a local velocity model. 2190 events from a total of about 4000 events were selected according to the following criteria: rms < 0.3, errx < 0.7, erry < 1.0 and errz < 2.0. A ratio Vp/Vs = 1.68 was determined using the P-P vs S-S diagram (Chatelain, 1978). The epicentral distribution presents a slight NW-SE orientation while depth foci are constrained between 5 and 15 km showing a possible plane dipping 40° to the W (Figure 2).

FOCAL MECANISMS

Geomorphological observations (Ego,1995; Yepes, 1995) suggest a NNE reverse active fault dipping to the west. This structure is supposed to be bifurcated and absorbed by a local sinestral fault in the northern part (Soulas et al., 1991). The focal mechanism, obtained for a 3.9 event occurred on October 11, shows a reverse movement The plane striking N136°E and dipping 41° to the SW roughly coincides with the weak orientation of the epicenters. It also shows a small left lateral component associated with this motion. The strike of this fault plane does not agree with the NNE-SSW trend of the main fault system, but it could be explained as the motion along a secondary branch of the Quito Fault as suggested by Soulas et al(1991). The main compression axis responsible for the seismic swarm coincides with the regional stress pattern (Guillier, non-published data), where the main compression axis ($\sigma 1$) has a ENE-WSW direction. A component of the volcanic stress generated inside Guagua Pichincha volcano could

also change the stress field in its surroundings. The magma chamber could also accounts for the occurrence of the seismic swarm, if the concurrent reactivation of the volcano is taken into consideration as well as the sort distance between the swarm and the caldera.

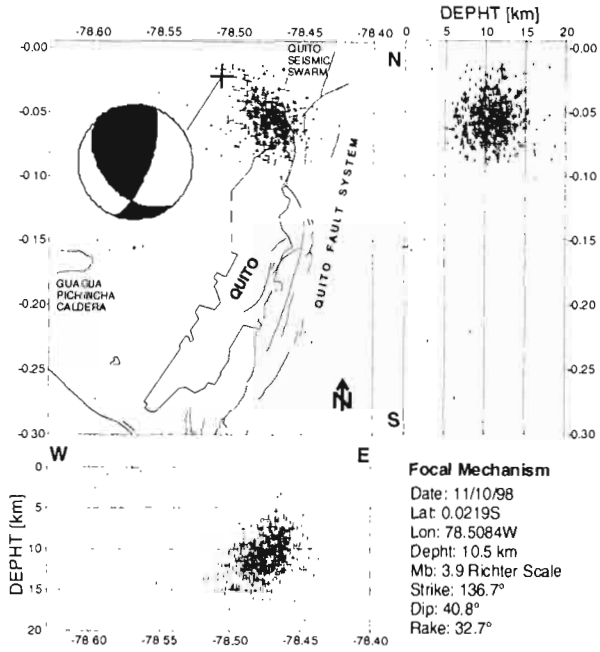

Figure 2. Swarm foci distribution and focal solution for 3.9 October event.

VARIATION OF THE b-VALUE

b-value were computed using windows of 200 events 25 % overlapped. For 1997 data, the observed value was 0.5340, while it was 1.467 and 1.07 for 1998 and 1999 respectively. In 1997 random distribution of seismicity without any evidences for a swarm is observed. In 1998 and 1999 the b-value increased, especially in 1998 when the swarm began. Temporal analysis of the b-value for 1998 shows two important increases around July 22 and September 10, with values that range from 1.2 to 1.7. The lower values correspond to the period of more seismic activity during August. Factors that could alter the b-value include increased heterogeneity of the material (Mogi, 1962) and increase in the stress field (Scholz, 1968; Wyss, 1973). Then, this parameter could be representing a newly fractured material or a variation in the stress field, explained equally well by the movement and cracking of the fault, and/or the increase of the gas pressure in the magma chamber underneath Guagua Pichincha.

CONCLUSIONS

An intense seismic activity was registered in the northern part of Quito since June 1998 to the present day. This type of activity was not observed before in this area, and presents two important peaks of around 40 events mb=2.0 or above per day, between July 24and October 31.

Epicentral distribution of the events shows a particular NW-SE orientation, while hypocenters suggest a plane dipping around 40 ° to W. The focal mechanism solution agrees with the rough swarm epicentral distribution and the regional compressive field. A possible compressional component coincident with the direction of Pichincha volcano is suggested, but additional focal mechanisms should be analyzed to better understand the stress fields in this area.

An important change in the b-value from 0.53 in 1997 to 1.467 in 1998 was observed. The appearance of the 1998 Quito seismic swarm could explain this difference by increases in the heterogeneity of the crustal materials (Mogi et al., 1992) and/or by variations in the stress field (Scholz, 1968; Wyss, 1973).

Both focal mechanism and foci distribution suggest that a structure striking NW-SE, could be the source of this seismic activity. This structure does not agree with the Quito Fault System trend, but it could be explained as a northern termination of the main structure with a NW-SE trend. Quito seismic swarm was initially attributed to the active Quito Fault System, corresponding to a tectonic origin. Nevertheless, the August 1998-March 1999 volcanic crisis at Guagua Pichincha, which presents b-value variations related with changes in the stress field beneath the volcano (Villagómez, this volume), could give new ideas about the origin of the swarm.

REFERENCES

BONILLA L.F., PEREZ V.H., SANCHEZ A., RUIZ M.,YEPES H. & CHATELAIN J.L., Análisis preliminar de la microsismicidad de la zona de Quito-Ecuador, período: 1988-1992, pp12-14.

CHATELAIN J.L., 1978, Etude fine de la sismicité en zone de collision continentale au moyen d'un réseau de stations portables: la région Hindu-Kush Pamir, Univ. Scient. Medic. de Grenoble, 219 p..

EGO F., 1995, Accomodation de la Convergence Oblique dans un chaine de type cordilleraine: les Andes d'Equateur, pp280.

LAHR J.C., 1995. HYPOELLIPSE/Version 3.0. A computer program for determining hypocenter, magnitiud and first motion pattern of local earthquake. U.S. Geol.Surv. Open-File Rep.95, 90p

MOGI K., 1962. Magnitud-frecuency relation for elastic shocks accompanying fratures of various materials and some related problems in earthquakes, Bull.Eathq. Res Inst., 40, pp831-853.

SCHOLZ C.H., 1983, The frecuency-magnitude relation of microfracturing in rock and its relation to earthquakes, Bull Seism. Soc. Am., 58, pp399-415.

SOULAS J.P., EGUEZ E., YEPES H., PEREZ V.H., 1991, Tectónica activa y riesgo sísmico en los Andes ecuatorianos y el extremo sur de Colombia, Bol.Geol. Ecuat., Vol2, No.1, pp3-11.

VILLAGOMEZ D., RUIZ M.,YEPES H., HALL M., GUILLER B., ALVARADO A., SEGOVIA M., CALAHORRANO A., VIRACUCHA D., 1999, Seismic Activity at Guagua Pichincha Volcano, Ecuador, this volume.

WYSS M.K., 1973, Towards a physical undestanding of the earthqauke frecuency distribution, Geophys.J.R. Astr. Soc, 31. 341-359.

YEPES H., EGUEZ A., BERNAL R.,SANTACRUZ., 1995, Seguridad Sísmica en las Escuelas, Evaluación del Peligro Sísmico, Instituto Geofísico-Escuela Politécnica Nacional, pp1-75.

FLUID INCLUSIONS STUDY IN MARTE PORPHYRY GOLD DEPOSIT, COPIAPO CHILE.

Eduardo CAMPOS(1)

(1) Departamento Ciencias de la Tierra, Facultad de Ciencias Quimicas, Universidad de Concepcion. Casilla 3-C, Concepcion, Chile. (camc@geo.vu.nl)
(2) Department of Earth Sciences, Faculteit der Aarwetenschappen, Vrije Universiteit Amsterdam. De Boelelaan 1085, 1081 HV Amsterdam, The Nederlands.

KEY WORDS: Porphyry gold deposit, boiling, final ice melting temperature, halite dissolution, Th.

INTRODUCTION

The Marte Porphyry Gold deposit (27°10'19" Lat S and 69°01'12" Long W) is located in the Andean Cordillera of the Atacama Region, northern Chile, and belongs to a Middle to Upper Miocene vulcano-plutonic arc. The mineralization occurred in a hornblende-biotite dioritic stock that has been divided into three sub-units: coarse-grained dioritic porphyry, fine-grained dioritic porphyry, and a microdiorite. The stock occurs at the intersection of two faults trending NNE-SSW and NW-SW respectively (Vila et al 1991).

Fluid inclusion studies were carried out on quartz vein in order to characterise the thermochemical nature of fluids associated with the formation of the stockwork. In order to establish the relative chronology of fluid-trapping events and to ensure paragenetic and spatial coverage of the paleo-hidrotermal system, 25 samples were collected along the total length of four drill cores, corresponding to different stages of quartz veins.

This study was carried out in the Laboratory of Microthermometry of the Department of Earth Sciences, University of Concepción, Chile. Heating and freezing runs were performed on a THMS-600 Linkam

nitrogen cooled stage, provided with a thermal control unit (TMS-90, TP-91). The temperature limits obtained are –190° and 600°C.

FLUID INCLUSION CHARACTERISTICS

All analysed inclusions were hosted by fine crystalline euhedral to subhedral crystals of quartz, rarely larger than 5 mm across. Nevertheless, despite the abundance of inclusions observed in these quartz crystals, only a small number of them were bigger than 7μ., therefore an extensive search was required to find good population of inclusions large enough to allow optical distinction of phases, and phase changes that could be definitively classified and measured to provide useful temperature and salinity data.

All measured inclusions were considered to be primary nevertheless, because recognisable crystal faces and growth zones are rarely observed, isolated inclusions or those forming irregular three dimensional groups within the quartz grains were classified as primary. Those located in trails defining intragranular planes were interpreted as pseudosecundary, and the ones along planes crosscutting grain boundaries were considered secondary (Roedder, 1984). In some cases distinction between primary and pseudosecundary inclusions was difficult to make.

Primary inclusions typically show ellipsoidal to negative crystal shapes that resemble doubly terminated quartz euhedrons with rounded crystal edges, whereas those of pseudosecundary or secondary origin are usually ellipsoidal to flat, irregularly shaped inclusions.

All fluid inclusions studied exhibit as visible phases, liquid, vapor, and in a lesser extend halite as daughter crystals. According to the number of phases present at room temperature it was possible to distinguish, three types of fluid inclusions

Type L liquid-rich (L+V), these are two phase inclusions in which the liquid is the dominant phase and the vapor bubble represent between 2 to 15 vol. % of total volume of the inclusion. These represent about 85 % of all measured inclusions.

Type G gas-rich (V+L), usually mono phase gaseous inclusions, some may contain very small quantities of liquid. Although they are abundant, no temperature measurement could be made on these inclusions.

Type B three phase liquid-vapor-solid inclusions (L+V+S). The aqueous phase is normally dominant, including a bubble (ca. 20 vol. %), and a halite daughter mineral (10-20% of the total volume). These represent about 15 % of all measured inclusions.

FLUID COMPOSITION

Despite the fact that all inclusions were frozen to -100°C, no phase changes occurred until the first melting of ice that occurred at temperatures higher than -20.8 °C . This suggests, but does not confirm the

predominance of NaCl, probably small amounts of KCl, and the absence of divalent salts in the aqueous fluids, and the system may be approximated by the NaCl-KCl-H2O system.

The salinities of fluid inclusions were calculated from final melting temperature of ice and temperature of halite dissolution. For final ice melting temperatures, 270 successful freezing runs were performed and yielded to a set of data which shows a wide range from -0.2°C to -22°C, indicating salinities between 0.9 and 23 Wt % NaCl equiv. (Fig. 1B). Salinity calculated from halite dissolution temperature shows a range between 28.5 to 45.6 wt % NaCl equiv.

Actual formation and melting of hydrate crystals were not visible under the microscope, in fact, clathration was defined only in few of the studied inclusions, generally by the occurrence of a double jerk of the vapor bubble during cooling or by a sudden jerk during warming above 0 °C .

Most fluid inclusions readily homogenise to liquid, only few to vapor. The homogenisation temperature falls roughly within a range of 180° to 400°C (Fig. 1A), providing a minimum estimates for vein formation temperatures. Within this wide range, two closely related population can be identified, one between 290° and 420°C, and the other slightly colder in the range of 180° and 320°C . The bimodal frequency distribution defined for the entire set of sample is (Fig. 1), can also be observed in the data from single sample.

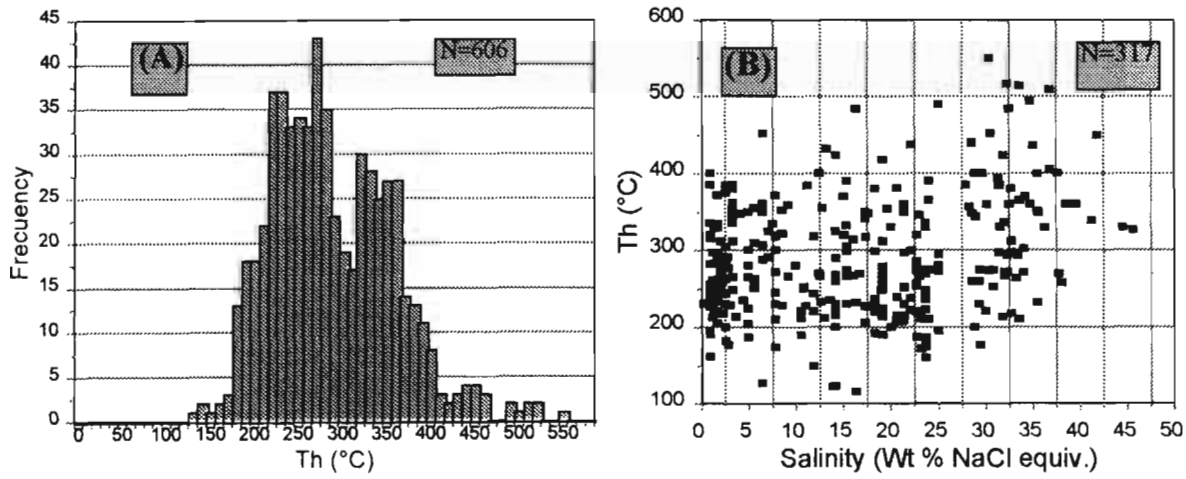

Fig 1. (A) Distribution of homogenization temperature. (B) Salinity vs homogenization temperature (Th).

The ubiquitous occurrence of both types L and G inclusions in all veins is a clear evidence for the presence of two immiscibility phases, vapor and liquid, due to boiling at the time of inclusion trapping. The boiling phenomena will also be the most probable reason for the large range of homogenisation temperatures observed on individual samples.

Even if there is no data available for vapor-rich inclusions, it is presumed that data gained from nearby liquid-rich inclusions adequately reflect the temperature and composition of the boiling fluids.

CONCLUSIONS

According to the data of fluid inclusions studied above, it can be concluded that solutions ranged in temperatures between 124° and 550°C showing a bimodal distribution, with a wide range of salinities of 0.9 to 45.6 wt % NaCl equiv.

On the basis of the microthermometric data, pressure values have been estimated between 120 to 140 bars under hydrostatic conditions.

Because the evidence of widespread boiling during inclusion trapping, it is presumed that the vapor pressure of the fluids closely approached the total pressure during the different stages of vein formation. In view of these no temperature correction due to pressure has been made.

Temperature-salinity diagram (Fig. 1B) shows a wide range of salinity, with a more restricted variation of homogenisation temperatures. This can be interpreted by continuous fracturing and vein opening that permitted recurring passage of fluids, which resulted in several stages of quartz vein formation resulted from many discreet hydrothermal pulses. Nevertheless a process involving fluid mixing and dilution between ascending, highly saline fluids typical of deeper magmatic hydrothermal enviroments such as porphyry metal deposits with less saline fluids from shallower environment, seems like a most plausible explanation.

REFERENCES

Roedder, E., 1984. Fluid inclusions., Mineral. Soc. Amer. Reviws in Mineralogy 12, 644 p.

Vila, T., Sillitoe, R., Betzhold , J., Viteri, E., 1991, The porphyry gold deposit at Marte,Northern Chile. Econ. Geol. v. 80. p 1271-1286.

CHARACTERIZATION OF FLUID INCLUSIONS FROM ZALDIVAR PORPHYRY COPPER, CHILE.

Eduardo CAMPOS(1) and Jacques R. L. TOURET (2)

(1) Departamento Ciencias de la Tierra, Facultad de Ciencias Quimicas, Universidad de Concepcion. Casilla 3-C, Concepcion, Chile. (came@geo.vu.nl)
(1, 2) Department of Earth Sciences, Faculteit der Aarwetenschappen, Vrije Universiteit Amsterdam. De Boelelaan 1085, 1081 HV Amsterdam, The Nederlands. (touj@geo.vu.nl)

KEY WORDS: SEM, Linkam stage, Raman spectrometry

INTRODUCTION

The Zaldivar mine, located 175 km SE of Antofagasta City, is part of a large Tertiary porphyry complex associated with the West Fissure structural system of northern Chile. The deposit is located at the intersection of two faults, one trending NW the other NE, and is centered in the NNE elongated Llamo Porphyry of Upper Oligocene age (Fig. 1). This is a light gray, green to "salt and pepper", granodioritic to dioritic intrusive with a marked porphyritic texture, with the phenocrysts representing between 25 to 40% and correspond to plagioclase, K-feldspar, biotite and rounded quartz phenocrysts. Strong phyllic and potassic hydrothermal alterations imprint these rock types. This unit is bisected by the N-S trending Portezuelo fault it intrudes andesite of the Augusta Victoria Formation (Upper Cretaceous-Lower Tertiary) and the Zaldivar porphyry, which is also of Upper Oligocene age (Fig. 1).

Samples from Llamo porphyry (Fig. 1) containing quartz grains as phenocrysts or in hydrothermal veins, both having a number of fluid inclusions, are currently being investigated in the Microthermometry laboratory of the Vrije University Amsterdam.

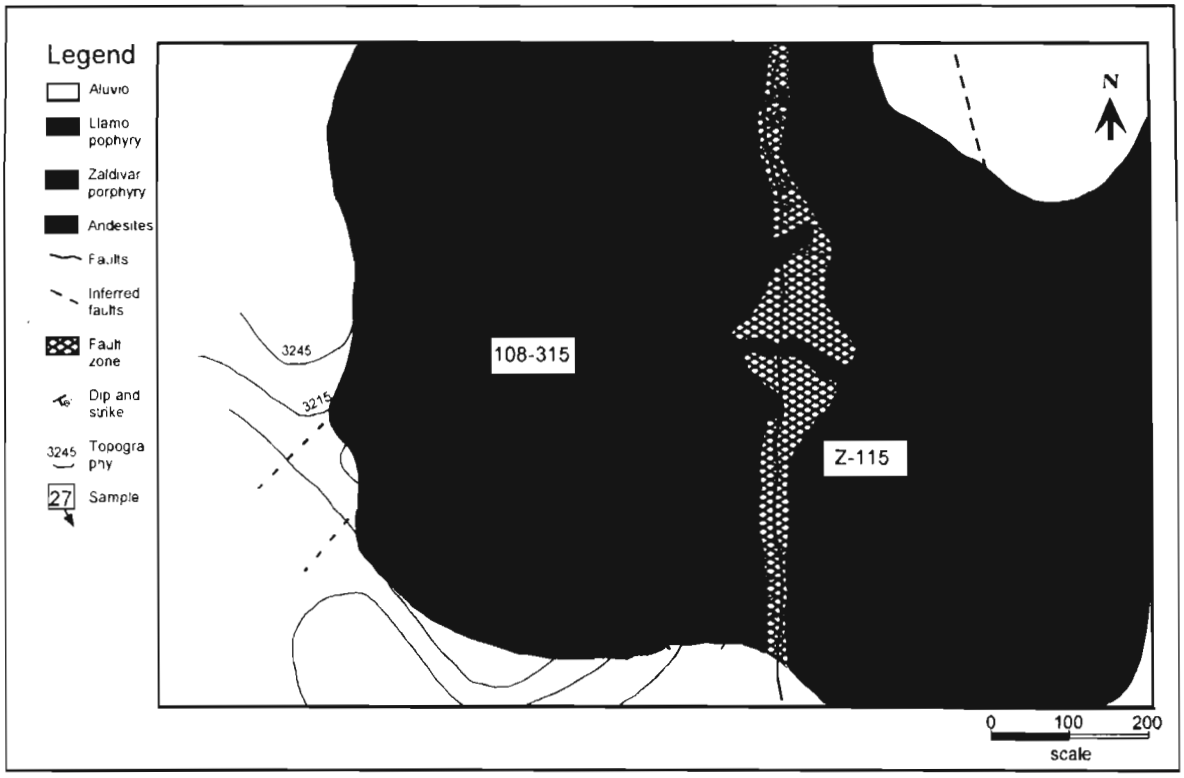

Fig 1. Local geology of Zaldivar Porphyry Copper

FLUID INCLUSIONS TYPES

Three different types of fluid inclusion classically described in Porphyry Copper Systems have been found usually closely associated to melt inclusions (Fig 2). Isolated inclusions or those forming irregular three-dimensional groups within grains (clustered) are classified as primary. Inclusion trails defining irregular planes crosscutting grain boundaries are considered to be secondary.

Type W: liquid-rich (L-V) inclusions (Fig. 2). Contains two fluid phases, a dominant liquid water solution and a vapor bubble, displaying a degree of fill between 90 an 70%. Some of these inclusions (less than 5%) may contain small opaques and/or transparent crystals as solid phase.

Type B: halite-bearing (L-V-S) (Fig. 2). Characteristically this type of inclusions contains a well-formed isotropic cubic halite crystal as an essential component in addition to the liquid phase and the bubble. Nevertheless, a number of other birefringent and opaques daughter minerals may also be present.

Type G: gas-rich (V-L) (Fig 2). Generally contains two fluid phases, with a dominant vapor phase representing more than 80 % of the total volume. In most of these inclusions, a thin rim of liquid is always visible. In same cases (less than 10%) a reddish or opaque and/or transparent daughter mineral is present.

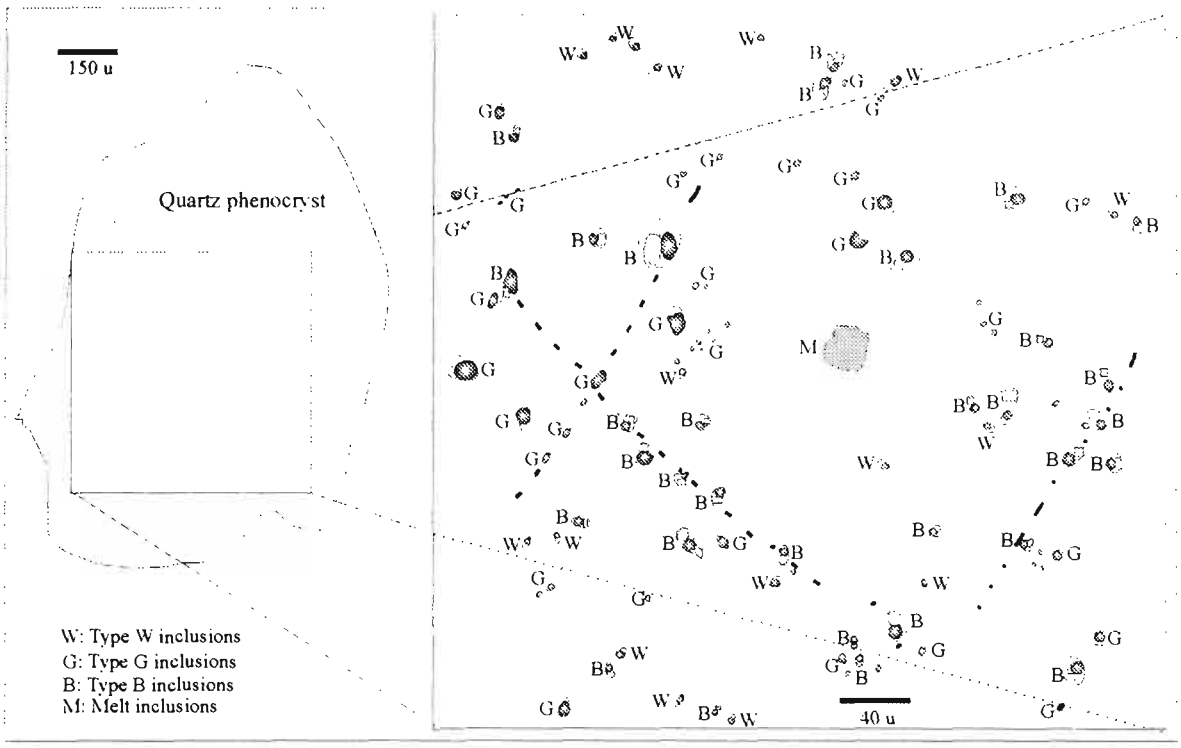

Fig.2. Quartz phenocryst showing the distribution of fluid and melt inclusions: The melt inclusions appear to be isolated among primary B and G inclusions, as well (broken lines) as pseudosecondary trails.

IDENTIFICATION OF DAUGHTER MINERALS

Daughter minerals are most commonly found and best developed in many type B inclusions. Nevertheless, they can also occur on type G and less frequently on type L inclusions. Halite is the most common daughter mineral, occurring as a colorless well formed isotropic cube and is a characteristic component of type B inclusions. The second most abundant daughter mineral is hematite, which is easily recognize under the microscope because it generally occurs as translucent reddish crystal. Depending upon the thickness may also occur as opaques.

In a number of inclusions, in particular type B, several opaque and semitransparent daughter minerals besides halite and hematite have been observed. These solid phases have been identified by SEM analysis on open fluid inclusions as iron oxide, mainly hematite and titanium-magnetite, silicates such as biotite, plagioclase, K-feldspar, sphene, zircon, while other minor components correspond to iron chloride, sylvite, and calcite.

Compositional analysis carried out on the walls of several inclusions indicates the occurrence of several elements such as S, Cl, Fe, Ti, and Ca.

FLUID COMPOSITION

Several inclusions specially type B, from both samples were analyzed by Raman spectrometry, but only on few of them traces of CO_2were found with no sight other components. An unknown single daughter

transparent crystal was also analyzed by Raman and the result indicates that correspond to a carbonate crystal most probably calcite

A wide range of initial melting temperatures from –70° up to –3°C were found mainly on primary type W and G fluid inclusions. From these values, it is possible to say that the fluids belongs to the system NaCl-$CaCl_2$-KCl-H_2O. The initial melting temperatures will vary depending on the presence and concentration of the different ions in the fluid of a given fluid inclusion, namely Na, K and Ca. Therefore, for temperatures between –75° to –50° besides Na, Ca will be an important component of the fluid. On the range -45° to –25° Na will be present with important amounts of K, and finally, on those inclusions with initial melting higher than –20°C, Na will be the only important ion on the fluid.

Final melting temperatures, together with halite dissolution give salinities in a range between 55.7 and 5 weight % NaCl equiv. In type G inclusions, homogenization is mostly to the gaseous phase, while for types W and B, homogenization is to the liquid phase. In all cases the temperatures are between 350° and 500°C.

From the relation of salinity and Th from the analyzed fluid inclusions, it is possible to recognize three types of hydrothermal fluids, a hot high salinity fluid (B), a low salinity hot fluid (W1), and a low salinity cold aqueous fluid (W2). Microthermometric data indicate that B and W_1 fluids were trapped at High temperature (about 500°C, roughly 200°C lower than magmatic temperatures). These fluids are assumed to be eventually of magmatic origin. The later, colder W_2 fluid, also low salinity aqueous, has a more problematic origin.

Type B and G inclusions shows an overlapping of homogenization temperatures in the range between 350° and 500°, being a good indication that boiling occurs, resulting in a strong compositional variation of fluid inclusions.

CONCLUSIONS

The original rock mineral assemblage is almost completely replaced by alteration minerals, marked also by hydrothermal quartz vein. However quartz phenocrysts preserve early, near magmatic features such as melt inclusions closely related to fluid inclusions classically described in Porphyry Copper Systems (coexisting vapor rich and highly saline brines).

Fluid types on igneous quartz phenocrysts and hydrothermal quartz are comparable. Low values of initial melting temperature, and the occurrence of different daughter minerals (mainly halite and sylvite, as well as calcite and anhydrite), indicates that the fluids involved in the ore deposit evolution correspond to the $NaCl$-KCl-$CaCl_2$-H_2O system, with small amounts of CO_2.

Discrete episodes of boiling have been recorded on a temperature range of between 350° and 500°.

No relation has been found so far between the fluid composition and Cu mineralization.

POST EOCENE DEFORMATIONAL EVENTS IN THE NORTH SEGMENT OF THE PRECORDILLERAN FAULT SYSTEM, COPAQUIRI (21°S).

Pedro CARRASCO (1), Hans–Gerhard WILKE (1) and Heinz SCHNEIDER. (1)

(1) Universidad Católica del Norte.(e-mail: hwilke@socompa.ucn.cl)

KEY WORDS: Central Andes, Precordilleran fault system, Tectonics, Transpression

INTRODUCTION.

The Precordilleran fault system of northern Chile (PFS), also known as West Fissure System (WFS), has been the subject of extensive research regarding its structural history and evolution. In light of these studies, several models of the kynematic histories of different segments of the PFS have been established. In this paper, we present the results of a study carried out in a segment of the PFS, between 20°52' - 21°00' S, in the area around Quebrada Copaquiri, Precordillera of the I Región de Tarapacá. Here, several structures indicate the existence of two deformational events of transpressive type, exhibiting left lateral and right lateral components succesively. These events postdate previous Eocene „Incaic" shortening related deformation. We examine the age constraints of these events and establish a comparison with other previously studied segments of the Precordillera, north and south of the area.

GEOLOGICAL - STRUCTURAL SETTING.

The most conspicuous feature of the area is the „main" trace of the PFS, which runs in an aproximate N-S direction through the central part of the mapped region, slightly deflecting to the NW at the northern end of the area. There is a marked difference in stratigraphic succession and structural style between the regions on both sides of the PFS main trace (fig. 1). The main sources of geological information for the area are Vergara & Thomas (1984) and Bogdanic (1990).

In the main trace of the PFS, the outcrops have suffered strong alteration effects, which conspires against the preservation of recordable structural features. Nevertheless, adjacent outcrops have well preserved structures, which generally trend obliquely to the PFS main trace. These include folds, foliations, brittle faults and thrusts. These structures define two distinct deformation events of transpressive type, which are radiometrically constrained to be post Eocene in time.

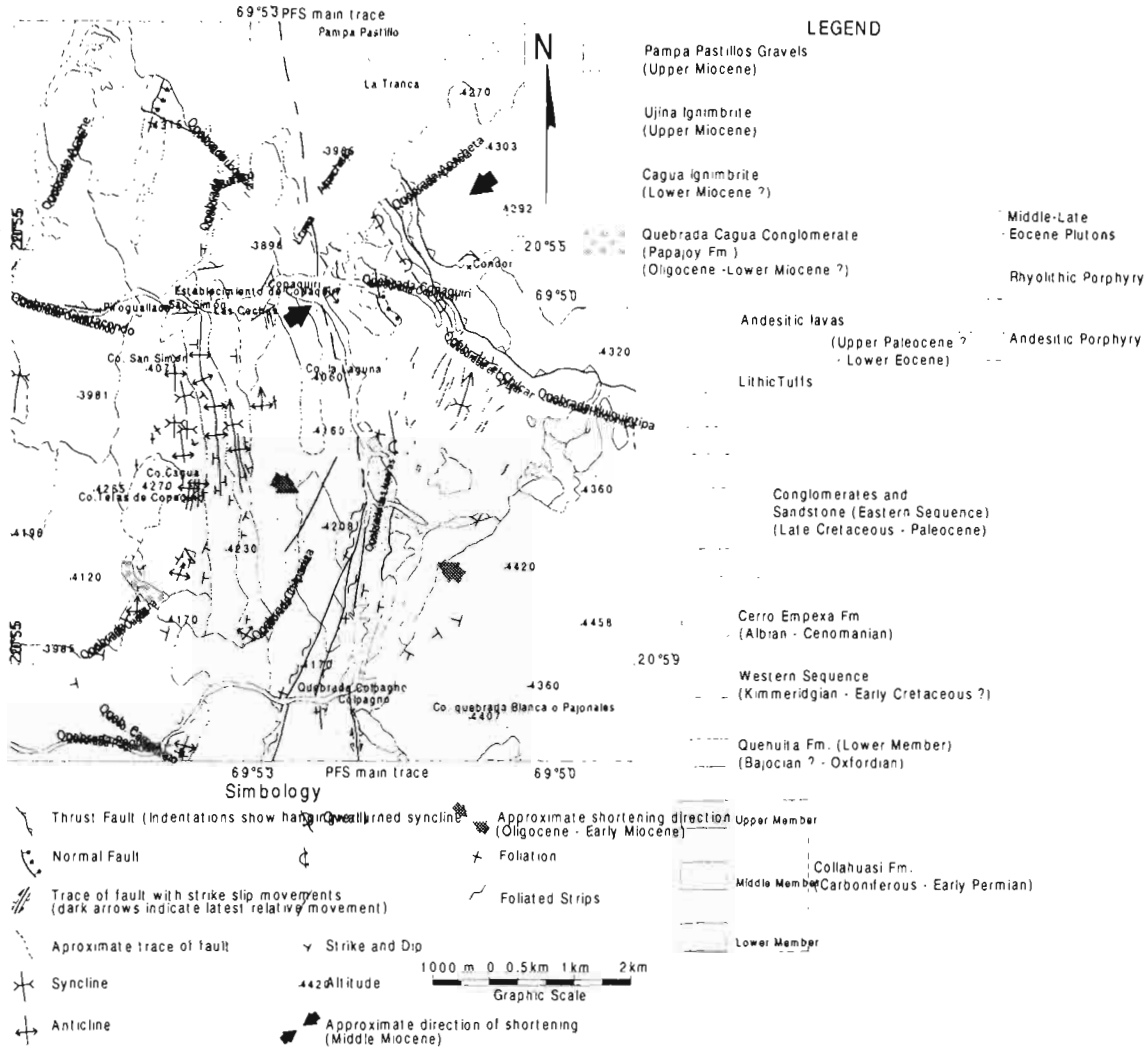

Fig. 1: Geological map of the studied area.

The first of these events shows a WNW – ESE shortening direction. Structures signaling this event occur on both sides of the PFS main trace. To the west, adjacent to Quebrada Las Letras, tuffs of the Cerro Empexa Fm. show NNE trending strips of intensely foliated rocks, that are several kilometres long and have a thickness of up to 20 - 30 m. These have a subvertical to steeply ESE - dipping attitude. Vertical thin sections on these rocks exhibit shear indicators (σ clasts, S-C style fabrics), indicating WNW vergent thrust of the eastern block.. Also affecting these rocks are brittle – ductile reverse faults and conjugate sets of brittle reverse faults with slickenside lineations. All of these features trend similarly in a NNE direction, and their kinematic indicators are consistent with a WNW –ESE shortening direction. West of the PFS main trace, rocks of the Eastern Sequence are folded into a wide syncline with a NNE – trending axis, that plunges gently in the same direction. These rocks are cut by an andesitic dyke swarm. The dykes trend in a NNE direction, and are tilted, dipping perpendicular to the strata on both sides of the

syncline. Consequently, they were emplaced prior to the deformational event. These dykes were dated by Hammerschmidt et al. (1992), yielding an ^{40}Ar-^{39}Ar age of 36,2 ± 0,6 Ma (biotite plateau age).

The second deformational event shows an aproximate SW –NE shortening direction. The structural features representing this event are mainly visible in the courses of Quebrada Apacheta and Quebrada El Chilcar. There, SW verging thrust faults put Paleozoic volcanics of the Collahuasi Fm. onto rocks of the Jurassic Quehuita Fm. and the Western Sequence, generating a series of SW verging folds affecting these latter sequences. The thrusts have variable dips (45°-55°) along their trace and trend in an approximate NW – SE direction, almost perpendicular to the trend of the previously described structures related to the first deformational event. The thrusts cut dykes and structures related to the first event. Other minor thrusts occur affecting the sedimentary sequences, showing small scale drag folds.

On the course of Quebrada Apacheta, a subhorizontal thrust fault was observed, exhibiting a 1,5 m thick gouge zone with S-C style planar fabrics, which are consistent with a NE vergence of the thrust, opposite to the previously described, high angle thrust faults. This thrust puts basal coraligenous banks of the Quehuita Fm. over andesitic lavas attributed to the paleozoic Collahuasi Fm., which could indicate a detachment of the sedimentary cover from the more rigid Paleozoic volcanics.

DISCUSSION.

The upper limit of the deformational events is constrained by undeformed deposits of the Ujina ignimbrite which yield a K-Ar biotite age of 9,0 ± 0,4 Ma (Vergara & Thomas, 1984). These exhibit only normal NW trending faults of post – Middle Miocene age, that affect also the gravel deposits of Pampa Pastillos. Consequently the age of the deformational events of interest here, can be broadly constrained to an Oligocene – Middle Miocene span.

Unfortunately, there is no direct field evidence in the area to constrain the age boundary between the two events. However, an attempt can be made to correlate these events with similar, previously described events in other segments of the PFS.

Oligocene sinistral movements of the PFS have been documented by Reutter et al. (1996) and Tomlinson & Blanco(1997), in the area of Chuquicamata and to the north. These authors also indicate a switch to dextral movements post – dating the sinistral event. According to the latter authors, this sinistral event must have predated deposition of the Huasco Ignimbrite (K-Ar biotite ages between 17,1 ± 0,8 and 14,6 ± 0,4 Ma; Vergara & Thomas, 1984).

Muñoz & Sepúlveda (1992), described NW trending structures, north of the present area, between 19° - 20°S, which were folded and thrusted showing a west vergence. They dated ignimbrites similar in age to the Huasco and Ujina ignimbrites of the present area, obtaining a K-Ar biotite age of 16,2 ± 0,2 Ma for the Tarapaca Ignimbrite, affected by the latter structures and an age of 8,2 ± 0,7 Ma for the overlying and undeformed Camiña Ignimbrite, thus constraining the age of deformation.

CONCLUSIONS.

The upper and lower age boundary of the two deformational events can be constrained on the basis of field observations and available radiometric data for the area. To constrain the limiting age between the two deformation events, we have relied on data from other studies outside the area. Nevertheless, on comparison the results seem consistent enough to hold true. On this basis, we can say that the first event correlates well with the already documented sinistral movements further south, around the area of Chuquicamata and can be assigned broadly an Oligocene – Early Miocene age. The structures clearly indicate strong shortening in a sinistral transpressive regime, so at least in this area a model of sinistral transtension (Reutter et al., 1996) is difficult to apply.

The second event is constrained to the Middle Miocene in age and reflects a dextral transpressive style deformation. The NW trending structures associated with this event mark the beginning of a deflection of structures in the Precordillera, as already pointed out by Muñoz & Sepúlveda (1992), and could represent a north end termination zone for strike slip movements of the PFS.

REFERENCES.

Bogdanic T. 1990. Kontinentale Sedimentation der Kreide und des Alttertiärs im Umfeld des Subduktionsbedingten Magmatismus in der chilenischen Präkordillere (21°-22°S). Berliner Geowiss. Abh., Reihe A, Band 123, 117 pp.

Hammerschmidt, K; Döbel, R. & Friedrichsen, H. 1992. Implication of ^{40}Ar-^{39}Ar dating of Early Tertiary volcanic rocks from the north – Chilean Precordillera. Tectonophysics, 202, pp. 55 – 81.

Muñoz N.; Sepúlveda P. 1992. Estructuras con vergencia al oeste en el borde oriental de la Depresión Central, Norte de Chile (19°15'S). Revista Geológica de Chile, Vol. 19, No. 2, pp. 241 – 247.

Reutter K. – J., Scheuber E., Chong G. 1996. The Precordilleran fault system of Chuquicamata, Northern Chile: evidence for reversals along arc – parallel strike – slip faults. Tectonophysics, 259, 213 – 228.

Tomlinson A., Blanco N. 1997. Structural evolution and displacement history of the West Fault System, Precordillera, Chile: Part 2, postmineral history. VIII Congreso Geológico Chileno. Universidad Católica del Norte. Actas, Vol. 3, pp. 1878 – 1882.

Vergara H., Thomas A. (1984). Hoja Collacagua, Región de Tarapacá Carta Geológica de Chile, No. 59. Servicio Nacional de Geología y Minería. 79 pp.

LAST MIOCENE-QUATERNARY STRATIGRAPHY AND TECTONIC OF THE EASTERN PART OF THE MADRE DE DIOS FORELAND BASIN (SE PERU)

José CARDENAS(1), Víctor CARLOTTO(2), Darwin ROMERO(2), Waldir VALDIVIA(2), Wilber HERMOZA(2), Luis CERPA(3), Omar LATORRE(2), Miriam MAMANI(2).

(1) Universidad Nacional San Antonio Abad del Cusco. (cardenas@inti.unsaac.edu.pe)
(2) Universidad Nacional San Antonio Abad del Cusco. (carlotto@chaski.unsaac.edu.pe)
(3) Universidad Nacional San Antonio Abad del Cusco. (geoloco@chaski.unsaac.edu.pe)

KEY WORDS : Last Miocene-Quaternary, stratigraphy, tectonic, Madre de Dios basin, SE Peru

INTRODUCTION

The north area of Madre de Dios Department (SE Peru) is located in the Amazon Plain (12° 00'- 12° 30' of south latitude, and 69° 80'- 70° 00' of longitude west; Fig. 1), and it corresponds to the eastern part of Madre de Dios foreland basin. This basin contains a sedimentary sequence of approximately 10,000 meters that has Paleozoic, Mesozoic and Cenozoic rocks. The study area corresponds to the Amazon occident, characterised for presenting a plain that varies between 200 and 400 m which is cut by big systems of rivers and vast areas of dissected lands. This has permitted to observe and study the Mio-Pliocene and Quaternary stratigraphic units, and also, the tectonic structures. These have allowed to interpret the evolution of this part of the basin in relation to tectonic events recognised in the subandine area.

STRATIGRAPHY

The oldest outcrops correspond to the upper part of the Ipururo Fm (♠ 80 m) (Palacios et al., 1996; Carlotto et al., 1998) whose observable lower part, is characterised by sandy sequences of fluvial origin (Fig. 2). A level of sandstones presents great quantity of trunks of trees of up to 4 m. of diameter, those that seem to indicate an important climatic crisis in this time.

The upper part of the formation is made up of bluish, gray and greenish clays of lacustrine environments (Fig. 2), where fossil remains of vertebrates faunas have been, particularly in the area of the Acre and Madre de Dios. The cheloniane fauna of the Southwest of the Amazon river, shows that these species are of sweet water, the one that can be comparable with the fauna of Huayquerian turtles of Urumaco-Venezuela (De Lapparent De Broin et al., 1993). As for the age, in the area of the Acre of the limit Peru-Brazil, the remains of fossils correspond to giant turtles coming from the Huayquerian stage (Last Miocene-Early Pliocene) (De Lapparent De Broin et al., 1993). On the other hand, works carried out by Frailey (1986) in the Madre de Dios river, have reported the presence of a new gender and proboscides species in the superior part of the Formation Ipururo and under the Madre de Dios Fm. This vertebrate has been dated in North America, as the Pliocene age. Based on this dating and field observations, the studied part of the Ipururo Fm would be of the Last Miocene-Early Pliocene age. This unit can be correlated with the Pebas Fm of Loreto (Northeast of Peru) and with the Charqui Fm of the Bolivian North Subandine, that also contains remains of vertebrates.

The Madre de Dios Fm (▲ 50 m) (Oppenheim, 1946; Campbell & Romero, 1989) overlies, in regional angular unconformity, to the Ipururo Fm (Carlotto et al., 1998). In this unit 3 members have been identified, composed by conglomerates, sands and clays of fluvial origin and of floodplain. It stands out the presence of a basal conglomerate that presents remains of plants of the species *Sapindus* sp. and a bivalve of the species *Corbula* (*Juliacorbula*) sp. that it indicates a Mio-Pliocene age (Romero: in Carlotto et al., 1998). The age of this formation outlines discrepancies, since initially it was considered of the last Neogene, without arguments; and later to the Pleistocene-Holocene, based on ^{14}C dating, that show uncertainties (Räsänen, 1991).

The Age of the Madre de Dios Fm was obtained for its stratigraphic position, the opposing fossils and the correlation with the Iñapari Fm of the Acre of Peru and Brazil. This last one contains giant turtles of the gender Chelonoia and probably a species of a *Podocnemidinae* that define the Huayquerian stage (De Lapparent De Broin et al., 1993). These data allow us attribute a late Pliocene-Pleistocene age. The Madre de Dios Fm is also correlated with the Tutuma Fm of the Bolivian Subandine North, the one that radicronologically has been dated in 3 Ma.

In the study area 3 groups of Terraces have been recognised. The estimate of their ages are based on dating previously attributed to other units (Räsänen, 1991). The Terrace T3 is of erosional type and it is assumed 176,000 year B.P.; the Terrace T2, possibly has an age between 40,000 and 32,000 years B.P.; and the Terrace T1 has probably been deposited among the last ones 10,000 and 5,000 years B.P.

TECTONIC

From the structural point of view, the study area has been divided in three domains (Fig. 1). The West Domain is characterised by the presence of not very deformed big folds of ONO-ESE

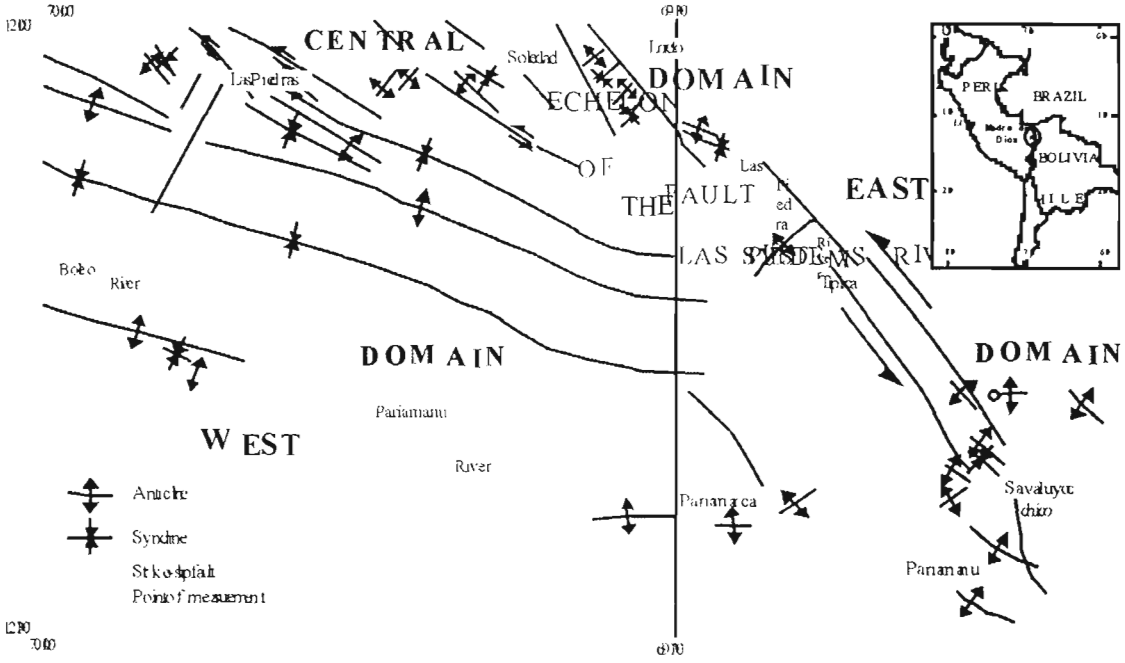

Fig. 1.- Structural sketch map of the study area.

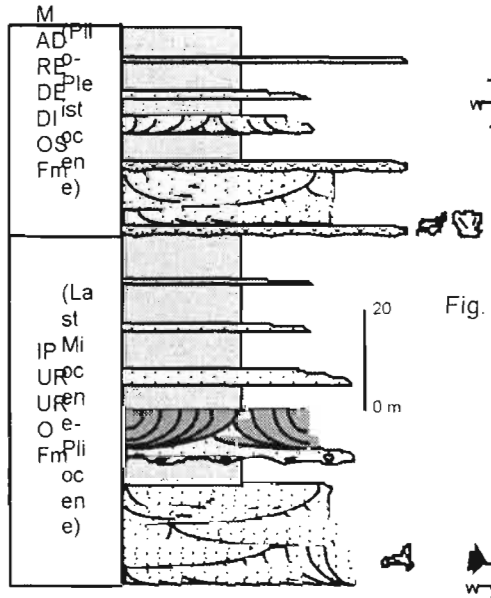

Fig. 2.- Stratigraphic Column

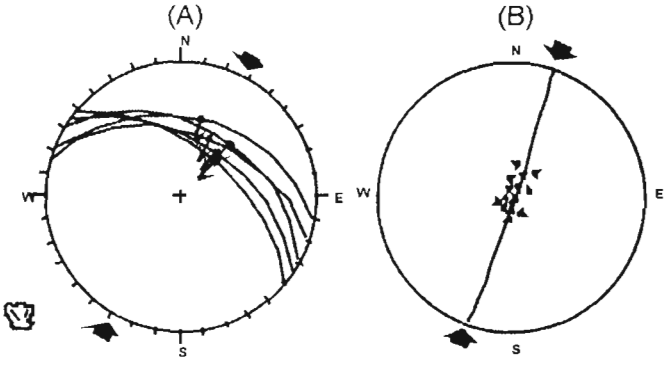

Fig. 3- (A) Inverse faults data (Wulff stereonet lower hemisph and (B) fold projection.

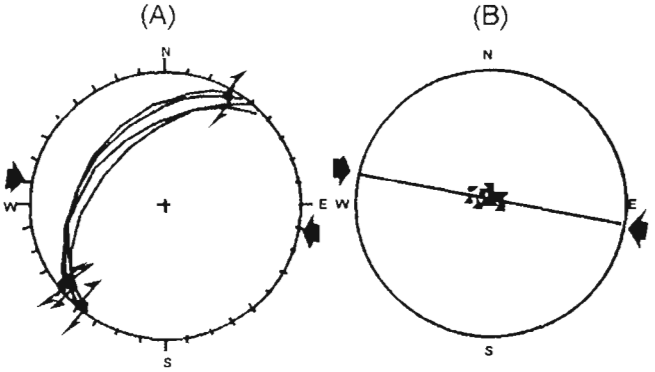

Fig. 3- (A) Strike-slip faults data (Wulff stereonet lower hemisph and (B) fold projection.

direction. They affect in more degree to the Ipururo Fm (Mio-Pliocene) and in smaller degree to the Madre de Dios Fm. These folds are also observed in the underground by the seismic reflection. The East Domain, differs because it is a little lower and possibly less deformed area. The limit between these two domains (Central Domain) is given for the echelon faults system of the Las Piedras river, the one that has had several times of deformation, controlling the formation and evolution of the Las Piedras river. The structural analysis of faults shows 3 systems: one of pure compression that corresponds to inverse faults with NE-SW shortening axis (Fig 3A), affecting to the Ipururo Fm and sealed by the Madre de Dios Fm; another of transpression that shows a E-W general shortening (Fig. 4A); and finally, one of constrictive compression, that seems to be the superposition of the previous systems. It has also been carried out the structural analysis of folds, where those of NO-SE direction affect to the Ipururo Fm (Mio-Pliocene), they have been originated by a NE-SW shortening (Fig. 3B) compatible with that of the inverse faults. This deformation relates it with the Quechua 3 tectonic crisis that seems to show in the Earliest Pliocene in the study area (♠ 4.5 Ma) which is continuous in the time, also deforming, in smaller degree to the Madre de Dios Fm. Later on, transpressional strike slip plays with E-W shortening axis, have originated NE-SW folds (Fig. 4B) that affect locally to the Madre de Dios Fm (Plio-pleistocene), along the faults system of the Las Piedras river. These deformations related to a change in the stress direction, have probably been produced by the Quechua 4 tectonic crisis of the late Pliocene-Quaternary (♠ 2.5 Ma). Finally, and for slight changes in the E-W stress (Early Pleistocene) a NE-SW transtension takes place, along the faults system of the Las Piedras river, and it will be the causing of the opening of the present depression for where this river flows. In fact, a NE-SO distension is also compatible with the E-O strike slip movements. The dating of this opening process is complicated because not having direct arguments, however it should be slightly previous to the formation of the Terrace T3, that is the late Pleistocene.

CONCLUSIONS

The deformation and the uplift of the subandine zone related to the Miocene-Pliocene tectonic (Quechua), developed a morphology with valleys that were filled in the late Miocene (ej. Valle de Quincemil). These deposits would be contemporary to the fluvial deposits of the Ipururo Fm of the low Amazonian region (Mio-Pliocene). The tectonic one that migrates from the West to the East, and shows that the Quechua 3 event of the Mio-Pliocene age, recently affects the study area during the Earliest Pliocene, producing NO-SE to ONO-ESE folds and inverse faults that affect to the Ipururo Fm.

After the maximum of this tectonic crisis, a peneplain of Pliocene-Quaternary age was formed. On this the Madre de Dios Fm is deposited, following the axes of the folds that continue still being deformed, very weakly and sealing the inverse fault. This is why the basal conglomerates of the Madre de Dios Fm are only in the depressions of the synclines.

The Quechua 4 tectonic crisis is more or less documented in the Andes and has happened at the end of the Pliocene. In the study area it takes place in the latest Pliocene or at the limit Plio-pleistocene. This event is characterised by sinistral-inverse faults, those that locally produce NE-SO folds, particularly along the system of the Las Piedras river. These strike slip faults that will control the fluvial evolution of Las Piedras river. In fact, later on to this tectonic crisis, the opening of the depression of the Las Piedras river takes place, and 3 stages of terraces can be seen. The Terrace T3 characterises a erosive peneplain, then, the Terrace T2 fill the depression. These two terraces reflect a uplift of the ensemble, perhaps controlled by quaternary movements. Between the deposit of the Terrace T1 and the present river bed, a difference is appreciated (slight subsidence of the area), since the Terrace T1 is inserted in the Terrace T2.

REFERENCES

Campbell, K. & Romero, L. 1989. La Geología del Cuaternario del Departamento de Madre de Dios. Bol. Soc. Geol. del Perú, 79, 53-61.

Carlotto, V., Cárdenas, J., Romero, D. Valdivia, W. & Jaimes, F. 1998. Geología de los Cuadrángulos de Soledad y Alegría, Hojas 25-x y 25-y, Boletin Ingemmet Nro 107, A: Carta Geol. Nac. 157p.

De Lapparent De Broin, F.; Bocquentin, J. & Negri, F. 1993. Gigantic Turtles (Pleurodira, Podocnemididae) from the late Miocene-Early Pliocene of South Western Amazon. Bull. Inst. fr. études andines 1993, 22 (3), 657-670.

Frailey, C.D. 1986. Last Miocene and Holocene mammals, Exclusive of the Notungulata, of the Rio Acre Region, Western Amazonian. Natural History Museum of the Angeles Country, Contribution in Science, 374, 46 p.

Oppenheim, V. 1946. Geological reconnaissance in Southern Perú. Bol. AAPG, Vol. 30, Nro. 2, p. 254-264.

Palacios, O.; Molina, O.; Galloso, A. & Reyna, C. 1996. Geología de los Cuadrángulos de Puerto Luz, Colorado, Laberinto, Puerto Maldonado, Quincemil, Masuco, Astillero y Tambopata, hojas: 26-u, 26-v, 26-x, 26-y, 27-u, 27-v, 27-x, 27-y. Bol. 81, Serie A, Ingemmet. 189 p.

Räsänen, M. 1991. History of the Fluvial and Alluvial landscapes of the Western Amazon Andean Foreland. II Biologica-Geographica-Geologica, 75, 16.p.

SEDIMENTARY AND STRUCTURAL EVOLUTION OF THE EOCENE-OLIGOCENE CAPAS ROJAS BASIN: EVIDENCE FOR A LATE EOCENE LITHOSPHERIC DELAMINATION EVENT IN THE SOUTHERN PERUVIAN ALTIPLANO

Victor CARLOTTO[1], Gabriel CARLIER [2], Etienne JAILLARD [3],
Thierry SEMPERE [2]and Georges MASCLE [4]

(1) Universidad Nacional San Antonio Abad del Cusco. Cusco. Peru.Carlotto@chaski.unsaac.edu.pe
(2) IRD (ex-ORSTOM). Apartado postal 18-1209. Lima 18. Peru. ird@chavin.rcp.net.pe
(3) IRD (ex-ORSTOM). Institut Dolomieu. 15 rue Maurice Gignoux. 38031 Grenoble. France
(4) Institut Dolomieu. 15 rue Maurice Gignoux. 38031 Grenoble. France

KEYWORDS: Eocene. Oligocene. Capas Rojas basin. Lithospheric delamination. Peruvian Altiplano

The Eocene-lower Oligocene Capas Rojas basin of the Cusco area is located at the northern end of the Altiplano. An important uplift of northern edge of the Western Cordillera around the Eocene-Oligocene boundary is documented by the evolution of the large Eocene-Oligocene Andahuaylas-Yauri batholith (Carlier et al., 1996).

Two sub-basins are recognised: the distal San Jerónimo sub-basin and the proximal Anta sub-basin (Fig. 1). Both sub-basins are separated by an important NNW-SSE strike-slip fault system (Accha-Huanoquite-Ccorca, Cusco-Sicuani, Sicuani-Ayaviri, and Lagunillas-Mañazo faults) that presumably controlled their evolution (Carlotto, 1998).

THE DISTAL SAN JERÓNIMO SUB-BASIN

The red beds deposited in the San Jerónimo basin unconformably overlie Paleocene and Eocene units (Jaillard et al., 1994). Near the top of the Capas Rojas (Fig. 2), a trachytic tuff is dated 29.9 ± 1.4 Ma (Carlotto et al., 1995; Carlier et al., 1996). The San Jerónimo red beds are thus Eocene and early Oligocene.

In the Cusco area, the San Jerónimo red bedsconsist of two thick formations: the K'ayra Formation (~3000 m) and the overlying Soncco Formation (~2000 m). Both are made up of silts, sandstones and conglomeratic sandstones of fluvial origin. Each consists of a coarsening-upward sequence that represents progradation of a fluvial system. Paleocurrents are directed toward the north in the K'ayra Formation and toward the northwest in the Soncco Formation. The finer upper part of the Soncco Formation indicates a significant change in the regional tectonic regime.

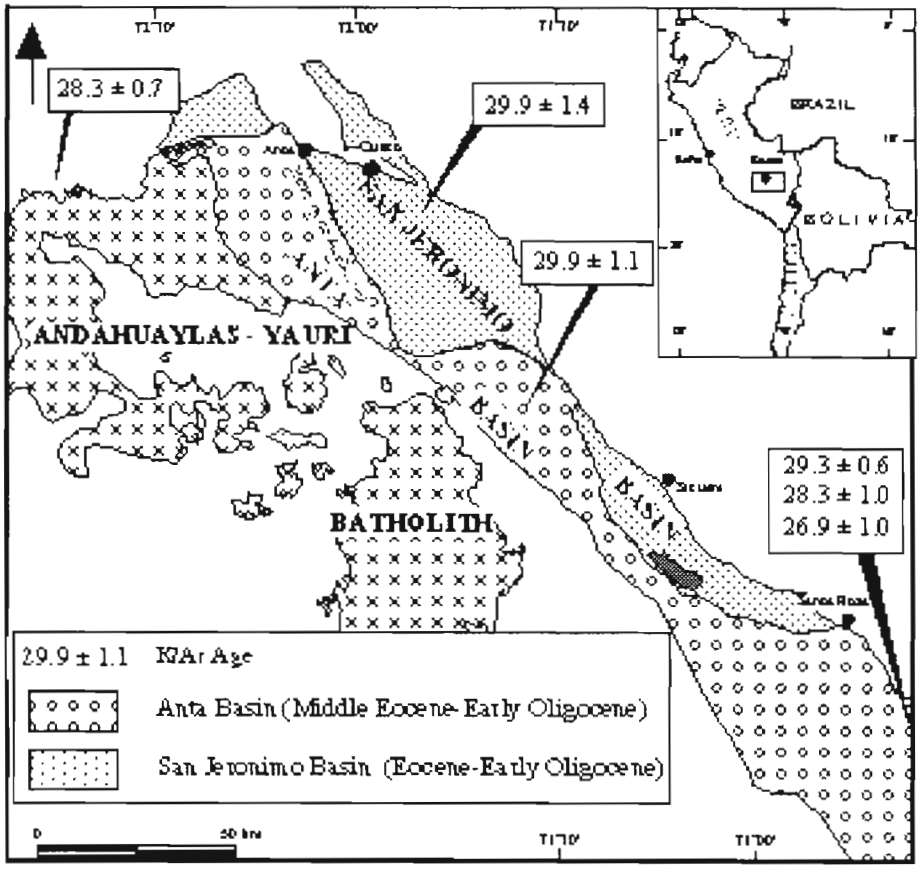

Fig. 1.- Structural sketch-map of the Cusco region,
showing the Anta (proximal) and San Jeronimo (distal) basins

THE PROXIMAL ANTA SUB-BASIN

The red beds of the Anta sub-basin unconformably overlie Cretaceous-Paleocene strata and Eocene intrusive rocks of the Andahuaylas-Yauri batholith (Carlotto, 1998). The lower and middle parts of the Anta red beds are thick (1500 m) and composed of conglomerates, breccias and sandstones (Fig. 2). These deposits are organized in coarsening-upward sequences interpreted to represent the superposition of syntectonic alluvial fans. The upper part of the Anta red beds (400m) comprises fluvial sandstones and mudstones associated with rare lacustrine limestones (Fig. 2). These deposits indicate a significant change of the regional tectonic conditions.

Calco-alkaline andesite and dacite flows intercalated in the middle Anta Formation are dated 38.4 ± 1.5 and 37.9 ± 1.4 Ma (Carlotto, 1998). The upper Anta Formation contains trachybasaltic flows dated 29.9 ± 1.1 Ma (Carlier et al., 1996; Carlotto, 1998). This magmatic activity implies that the red beds of the Anta basin were deposited during the late Eocene and early Oligocene. Consequently, the Anta Formation appears to be coeval with deposits in the San Jerónimo basin.

MAGMATISM

The trachybasaltic (46 wt% < SiO_2< 47 wt%; 5.6 wt% < K_2O+Na_2O < 5.7 wt%, 0.8 < K_2O/Na_2O < 0.9) and trachytic (SiO_2= 60.8 wt%; K_2O+Na_2O = 10 wt%; K_2O/Na_2O = 0.3) rocks intercalated in the upper part of the Anta and Soncco formations belong to alkaline series (Carlier et al., 1996). They are strongly enriched in LILE (Ba = 820-1750 ppm, Rb = 68-70 ppm), Sr = 1040-1110 ppm, La = 14.1-17.7 ppm) and depleted in HFSE (Nb = 6-7 ppm) and display low LILE/LREE ratios (Sr/Nd = 46-54, Ba/La = 48-124). In spite of their general depletion in HFSE, these rocks show low LILE/HFSE ratios (La/Nb = 2.4-2.5; Th/Nb = 0.3-1.0). Such geochemical characteristics are considered to reflect the composition of the subcontinental lithospheric mantle from which they originated (Kay et al., 1994; Comin-Chiaramonti et al., 1997).

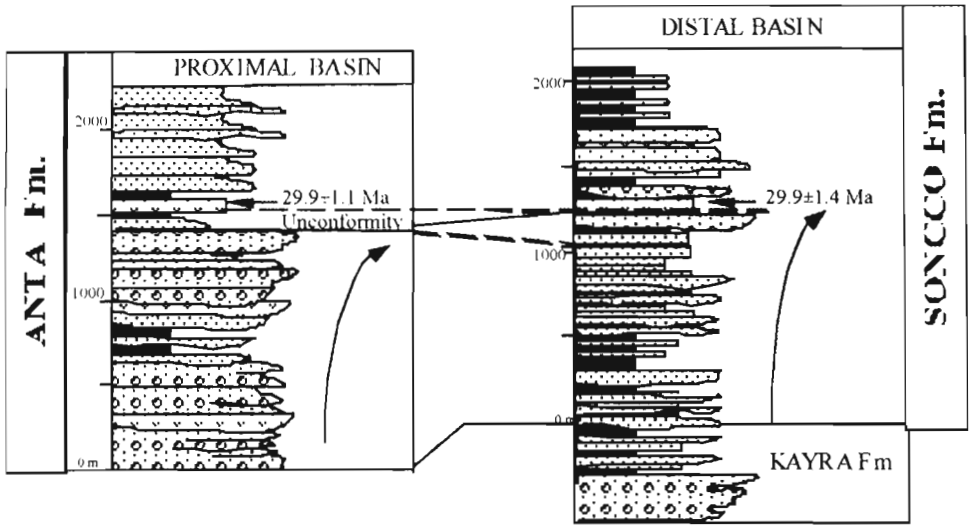

Fig. 2.- Stratigraphic columns of the Anta (proximal) and Soncco (distal) formations

UPLIFT AND TECTONIC

Calc-alkaline gabbroic cumulates form the main part of the northern rim of the Andahuaylas-Yauri batholith and are dated between 48 and 42 Ma (Carlier et al., 1996). They are intruded by granodioritic and dioritic subvolcanic stocks dated between 38 and 32 Ma (Carlier et al., 1996). These relationships document that a significant and rapid uplift (at least 5000 m) occurred along the northern rim of the Western Cordillera during the late Eocene and early Oligocene. The major shortening (up to 70%) documented at the Western Cordillera / Altiplano boundary is associated with this uplift (Carlotto, 1998). Erosion of reliefs produced by this uplift provided detritic material which filled the proximal Anta and distal San Jeronimo sub-basins. Deposition of the coarsening-upward Anta and Soncco formations was thus coeval with the compressional uplift of their source areas. In the upper Anta Formation (proximal sub-basin), thick alluvial fan deposits are overlain by strata of fluvial-lacustrine origin that include a trachybasaltic flow dated 29.9 Ma. In the Soncco Formation (distal sub-basin), a trachytic tuff also dated 29.9 Ma is associated with the sudden appearance of alluvial conglomerates in the succession.

DISCUSSION AND CONCLUSIONS

Rapid regional uplift and extension, accompanied by lithospheric thinning and increased magma production, have been recently recognised to indicate lithospheric delamination, i.e. rapid sinking of a lower lithosphere fragment into the asthenosphere (Bird, 1979; Kay et al., 1994). In the Cusco area, along the northern edge of the Western Cordillera, a significant late Eocene and early Oligocene thermal event

is documented by the existence of the Andahuaylas-Yauri batholith, which strongly suggests that advection of hotter asthenospheric mantle into shallow depths occurred in this area. The significant shortening associated with this thermal event also resulted in rapid uplift of the northern rim of the Western Cordillera. Erosion of this uplifted area generated the proximal coarse and distal fine deposits observed in the lower part of the Anta and Soncco formations, respectively. The upper part of each unit records an abrupt change in sedimentation, which is associated with a short middle Oligocene alkaline magmatic event: in the proximal Anta sub-basin, fine-grained strata abruptly overlie coarse-grained deposits; in the distal San Jeronimo sub-basin, alluvial conglomerates abruptly overlie fine-grained deposits. This sedimentary event is interpreted to reflect an isostatic rebound due to a change in the regional stress regime (see i. e., Heller et al., 1988). The coeval occurrence of alkaline suites demonstrates that the lithospheric mantle was involved in this process.

The abrupt changes in sedimentation recorded in the upper Anta and Soncco formations are reminiscent of a delamination process (Kay et al., 1994). As the Cusco area underwent rapid regional uplift and subsequent relative tectonic quiescence during the late Eocene - early Oligocene interval, we propose that a delamination process occurred in this area in the late Eocene. The characteristics of the coeval magmatic activity are in agreement with this hypothesis.

REFERENCES

Bird, P. 1979. Continental delamination and the Colorado Plateau. Journal of Geophysical Research, v. 84, 7561-7571.

Carlier, G., Lorand, J.-P., Bonhomme, M. & Carlotto, V. 1996. A reappraisal of the Cenozoic Inner Arc magmatism in the Southern Peru : Consequences for the evolution of the Central Andes for the past 50 Ma. III International Symposium on Andean Geodynamics, St Malo, France, Extended abstracts, ORSTOM, série "Colloques et Séminaires", p. 551-554.

Carlotto, V. 1998. Evolution andine et raccourcissement au niveau de Cusco (13-16°), Pérou: Enregistrement sédimentaire, chronologie, contrôles paléogéographiques, évolution cinématique. Ph.D. dissertation, University of Grenoble, France, 159p.

Carlotto, V., Carlier, G., Cárdenas, J. 1985. La edad de las Capas Rojas del Grupo San Jerónimo (Región de Cusco) y su significado tectónico. Seminario Taller de la Litósfera en los Andes Peruanos y sus márgenes, Lima, 2p.

Comin-Chiaramonti, P., Cundari, A., Piccirillo, E. M., Gomes, C. B., Castorina, F., Censi, P., De Min, A., Marzoli, A., Speziale, S. and Velázquez, V. F., 1997. Potassic and sodic igneous rocks from eastern Paraguay : their origin from the lithospheric mantle and genetic relationships with the associated Paraná flood tholeiites. Journal of Petrology, v. 38, 495-528.

Heller, L. P., Angebine, C. L., Winslow, S. N. & Paola, C. 1988. To phase stratigraphic model of foreland basin sequence. Geology, v. 16, 501-504.

Jaillard, E., Grambast-Fessard, N., Feist, M. & Carlotto, V. 1994. Senonian-Paleocene charophyte succession of the Peruvian Andes. Cretaceous Research, v. 15, p. 445-456.

Kay, S. M., Coira, B. and Viramonte, J., 1994. Young mafic back arc volcanic rocks as indicators of continental lithospheric delamination beneath the Argentine Puna Plateau, central Andes. Journal of Geophysical Research, 99, 24323-24339.

GIS ANDES:
A Metallogenic GIS of the Andes Cordillera

Daniel CASSARD(1)

(1) BRGM, Direction de la Recherche, Laboratoire de Géologie et Métallogénie
BP 6009, 3 av. Cl. Guillemin, 45060 ORLEANS Cedex 2 – France. E-mail: d.cassard@brgm.fr

KEY WORDS: Andes, GIS, Metallogeny, Ore deposits, Potential and favorability maps

INTRODUCTION :

GIS Andes is a homogeneous information system of the entire Andes Cordillera, covering an area of 3.83 million km² and extending for some 8500 km from the Guajira Peninsula (northern Venezuela) to Cape Horn (Tierra del Fuego). Conceived as a tool for both the mining sector, as an aid to minerals exploration and development, and the academic sector as an aid to developing new metallogenic models, GIS Andes is based on original syntheses and compilations (Cassard, 1998, 1999).

The different layers of the system, which can of course be combined in any way that the user sees fit, are both geographic and geologic (in the broad sense):

- Geographic — a DCW® geographic base;
- DEM — three digital elevation models with a structural analysis of the detailed topography;
- Imagery — SPOT 4 VEGETATION® satellite images;
- Geological synthesis — synthetic geological map of the Andes at 1:2,000,000 scale (Fig. 1);
- Geologic map coverage — more than 900 georeferenced maps;
- Seismic — more than 50,000 seismic records, with modelling of the subduction plane (Fig. 2);
- Volcanic — data on Holocene volcanism;

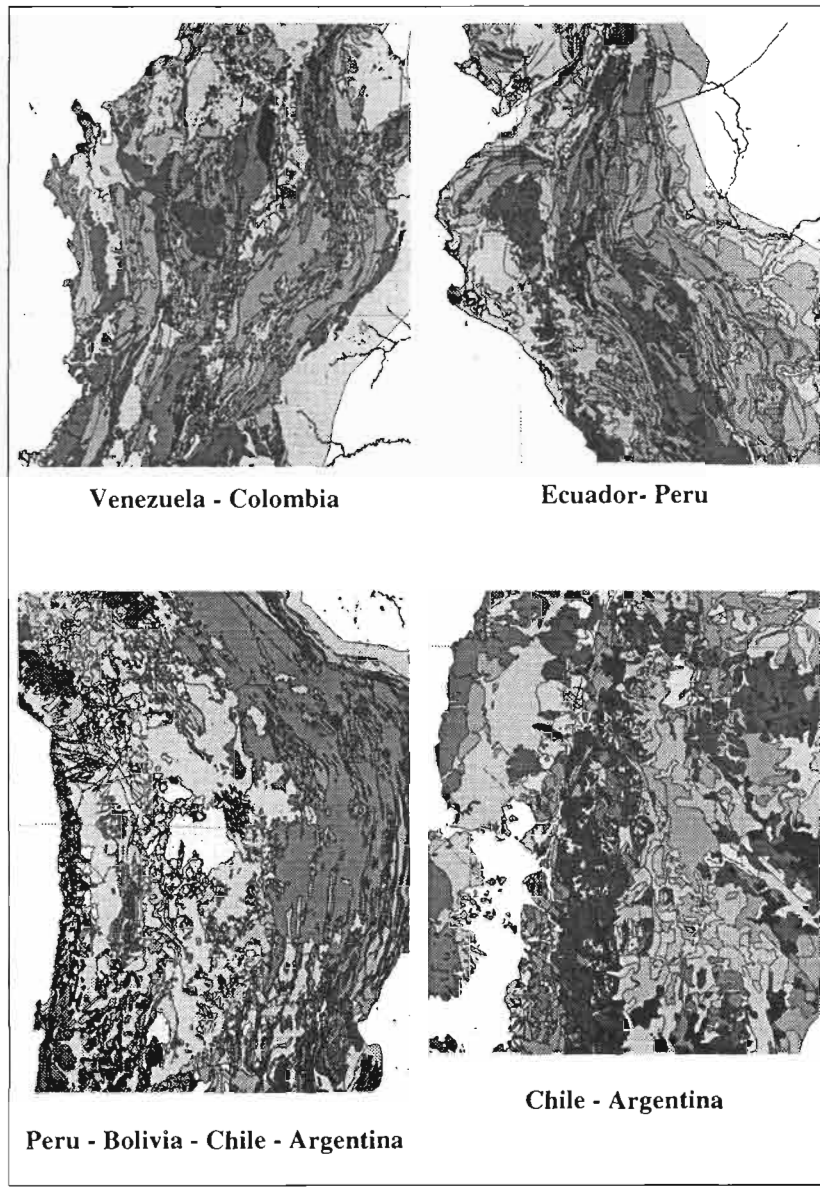

Figure 1: Extracts from the 1:2,000,000-scale geological synthesis

- Gravimetric — the Bouguer anomaly calculation; isostatic correction and corresponding residual anomalies; vertical gradient calculation and structural analysis; gravity modelling of the Nazca plate;
- Heat Flow — a base with 251 oceanic data and 239 continental data;
- Geochemistry — a geochemical database (3935 whole-rock analyses) from which it is possible, for example, to identify zones of adakitic magmatic activity – a new gold metallotect;
- Ore Deposits — linked to a Database under Access® and using a new metallogenic lexicon;
- Mineralogy, fluid inclusions, isotopes — data on the 350 main ore deposits of the Cordillera;
- Mining Districts and Provinces — location, main features, potential;

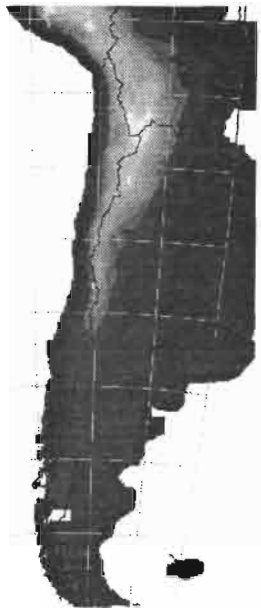

Bouguer anomaly

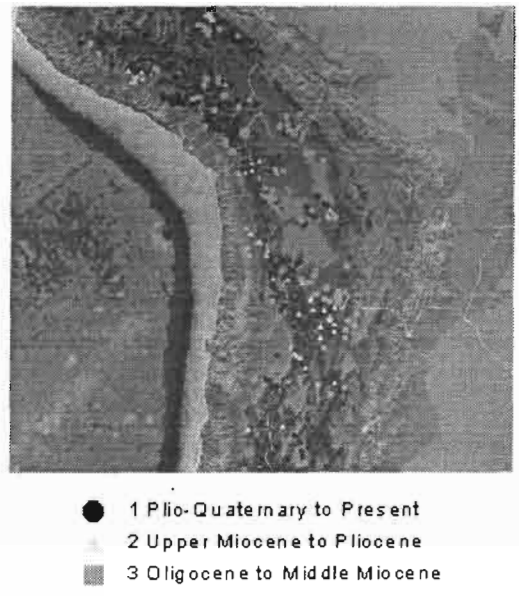

Adakitic magmatism

Holocene volcanism

Heat flow

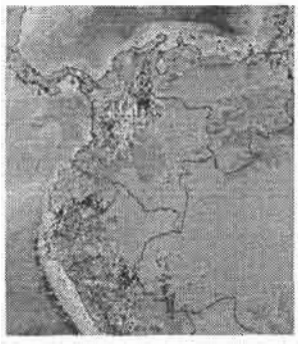

Seismic data: epicenter focal depth (km)

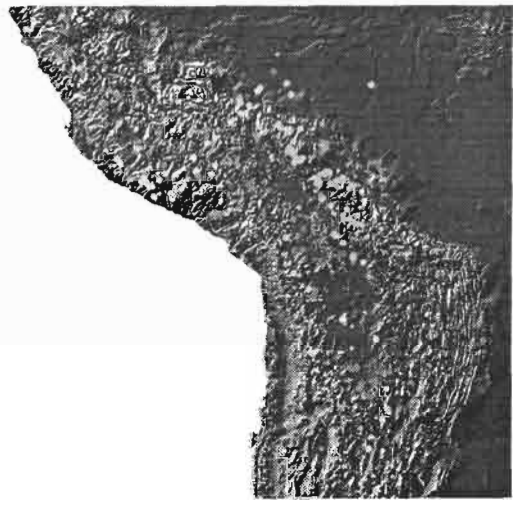

Ore deposits

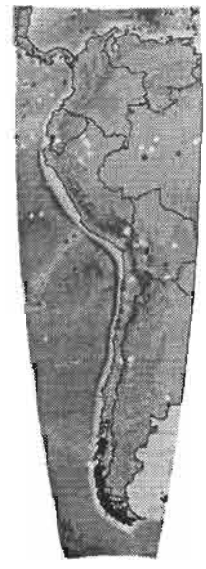

Figure 2: Extracts from different layers of the GIS Andes

- Geodynamic — the geodynamic evolution of the Andean margin with a series of palinspastic maps from 10 Ma onwards (developed in collaboration with IRD).

GIS Andes is a tool designed for creating maps of metallogenic potential, also known as favorability maps, for example:

(1) maps per substance(s) / age bracket / geologic setting: *e.g.* Au-Ag associated with Miocene volcanism taking into consideration the presence of adakites.
(2) maps of calc-alkaline formations for Au-Ag epithermal deposit exploration;
(3) maps of "sub-recent" deposits, created by combining data from the "Heat flow", "Gravimetric", "Geologic", and "Volcanic" (recent to present volcanic activity and geysers) layers: *i.e.* the combination of i) a thermal signature reflecting possible hydrothermal fluid circulation or magmatic activity, ii) a "light" body signature at depth, iii) a favorable geologic formation, and iv) evidence of recent volcanic activity and sub-recent hydrothermal fluid circulation.

GIS Andes is also designed for a more global approach to metallogeny. For example, 3D modelling of the subduction zone should be able to identify the influence of the Benioff plane geometry on the distribution of deposit types. It is hoped that this more "academic" approach will identify new regional metallogenic guidelines.

REFERENCES

Cassard, D., 1998. Projet PRD 406 Métallogénie Andes. Note BRGM DR/LGM/98 n° 486 DC, 26 p. (Unpublished.)

Cassard, D., 1999. GIS Andes on the web: http://www.brgm.fr/sigand

CRUSTAL-SCALE POP-UP STRUCTURE AT THE SOUTHERN ANDES PLATE BOUNDARY ZONE: A KINEMATIC RESPONSE TO PLIOCENE TRANSPRESSION

José CEMBRANO, Alain LAVENU, Gloria ARANCIBIA, Gloria LÓPEZ and Alejandro SANHUEZA.

Departamento de Geología. Universidad de Chile. Casilla 13518. Correo 21. Santiago de Chile.
e-mail address: jcembran@mail.cec.uchile.cl

Key words: Southern Andes, transpression, pop-up structure, ^{40}Ar-^{39}Ar dating, triple junction.

INTRODUCTION

The southern Andes plate boundary zone records a protracted history of bulk transpressional deformation during the Cenozoic. Transpression has been causally related to either oblique subduction or ridge collision (e.g. Hervé, 1976; Beck, 1988; Nelson et al. 1994; Cembrano et al. 1996). However, few structural and chronological studies of regional-scale deformation are available to support one hypothesis or the other.

The present work addresses along and across-strike variations in the nature and timing of plate-boundary deformation to better understand the Cenozoic tectonics of the southern Andes. A general objective was to gain insights into the geometry and kinematics of transpressional deformation at obliquely convergent plate margins. Five transects were mapped along the southern Andes, from 39°S to 46°S (Figure 1). Bulk mineral separates from high strain rocks with good field and microstructural kinematic constraints were selected for conventional furnace ^{40}Ar-^{39}Ar stepwise dating. Highly strained (dynamically recrystallized?) single minerals and/or mineral aggregates were dated in situ by using the laser technique on polished rock slabs.

KINEMATICS AND TIMING OF DEFORMATION

The northernmost, Liquiñe transect (39°S), documents ductile deformation of pre-Late Cretaceous age. Brittle deformation is represented by a regional, high angle, northeast-trending reverse fault that places greenschist facies mylonites against an undeformed Miocene granitoid. In contrast, Late Cenozoic brittle faulting of Cretaceous and Miocene plutons is well developed farther south at Reloncaví (41°S), where contractional and strike-slip kinematics are documented. At Hornopirén (42°S), Late Cenozoic ductile to brittle dextral strike-slip deformation along northeast striking shear zones was continuous from syntectonic pluton emplacement at 10 Ma, to low temperature, solid-state deformation at ca. 4.3 Ma. Brittle faults indicate that dextral strike-slip deformation remained active after 3 Ma. Puyuhuapi and Aysén transects (44-46°S), document a remarkable increase in the contractional component of ductile and brittle deformation. At Puyuhuapi (44°S), north-south trending, high-angle contractional ductile shear zones that developed from plutons, coexist with moderately dipping dextral-oblique shear zones in the wallrocks. In Aysén (45-46°), top to the southeast, oblique thrusting predominates to the west of the Cenozoic magmatic arc, whereas dextral strike-slip shear zones develop within it.

New ^{40}Ar-^{39}Ar data from mylonites and undeformed rocks from the five transects (Table 1) suggest that dextral strike-slip and contractional deformation occurred at nearly the same time but within

different structural domains along and across the orogen. For instance, ^{40}Ar-^{39}Ar laser dating on highly strained synkinematic biotite from plutonic rocks with S-C fabrics at 42°S documents dextral ductile shear at 4.3±0.3 Ma. Similar ages were obtained on both high strain pelitic schists with dextral strike-slip kinematics (4.4±0.3 Ma, laser on muscovite-biotite aggregates, Aysén transect, 45°S) and on mylonitic plutonic rocks with contractional deformation (3.8±0.2 to 4.2±0.2 Ma, fine-grained, recrystallized biotite, Puyuhuapi transect). Oblique-slip, dextral reverse kinematics of uncertain age is documented at the Canal Costa shear zone (45°S) and at the Queulat shear zone at 44°S. Published dates for the undeformed protholiths suggest both shear zones are likely Late Miocene or Pliocene, coeval with contractional and strike-slip shear zones farther north.

CONCLUSIONS

Coeval strike-slip, oblique-slip and dip-slip deformation on ductile shear zones of the southern Andes suggests different degrees of along- and across-strike deformation partitioning of bulk transpressional deformation. The long-term dextral transpressional regime appears to be driven by oblique subduction. The short-term deformation is in turn controlled by ridge collision from 6 Ma to present day. This is indicated by most deformation ages and by a southward increase in the contractional component of deformation. Oblique-slip to contractional shear zones at both western and eastern margins of the Miocene belt of the Patagonian batholith define a large-scale pop-up structure by which deeper crustal levels exposed in the Main Range have been differentially exhumed since the Pliocene. The overall geometry and kinematics of regional-scale shear zones obtained in three-dimensional analog and numerical models of transpression (e.g. Schreurs and Coletta, 1998; Braun and Beaumont, 1995) are strikingly similar to those we have described for the southern Andes plate boundary zone (Figure 2).

Acknowledgements

Fondecyt projects 1931096 and 1950497 funded field work in southern Chile. This work is part of the author's Ph.D. thesis at Dalhousie University, Canada. Peter Reynolds and Keith Taylor (Dalhousie University) are thanked for their help with the Ar-Ar age determinations. Professors Marcos Zentilli and Nick Culshaw read and made important contributions to the present work.

REFERENCES

Beck, M.E. 1988. Analysis of Late Jurassic-Recent paleomagnetic data from active plate margins of South America. *Journal of South American Earth Sciences*, 1: 39-52.

Braun, J. and Beaumont, C. 1995. Three-dimensional numerical experiments of strain partitioning at oblique plate boundaries: Implications for contrasting tectonic styles in the southern Coast Ranges, California, and central South Island, New Zealand. *Journal of Geophysical Research* 100, 18.059-18.074

Cande, S.C. and Leslie, R.B. 1986. Late Cenozoic tectonics of the Southern Chile Trench. *Journal of Geophysical Research* 91, 471-496.

Cembrano, J., Hervé, F. and Lavenu, A. 1996. The Liquine-Ofqui fault zone : a long-lived intra-arc fault system in southern Chile. *Tectonophysics* 259 (special issue on Andean Geodynamics), 55-66.

Hervé, M. 1976. Estudio geológico de la falla Liquiñe-Reloncaví en el área de Liquiñe; antecedentes de un movimiento transcurrente (Provincia de Valdivia). *I Congreso Geológico Chileno*, Actas, 1:B39-B56.

Nelson, E., Forsythe R. and Arit, I. 1994. Ridge collision tectonics in terrane development. *Journal of South American Earth Sciences*, 7, n° 3/4, 271-278.

Schreurs, G. and Colletta, B. 1998. Analogue modeling of faulting in zones of continental transpression and transtension. *In*: Holdsworth, R.E. Strachan, R.A and Dewey, J.F. (eds.) 1998. Continental Transpressional and Transtensional Tectonics. *Geological Society, London, Special Publications* 135, 59-79.

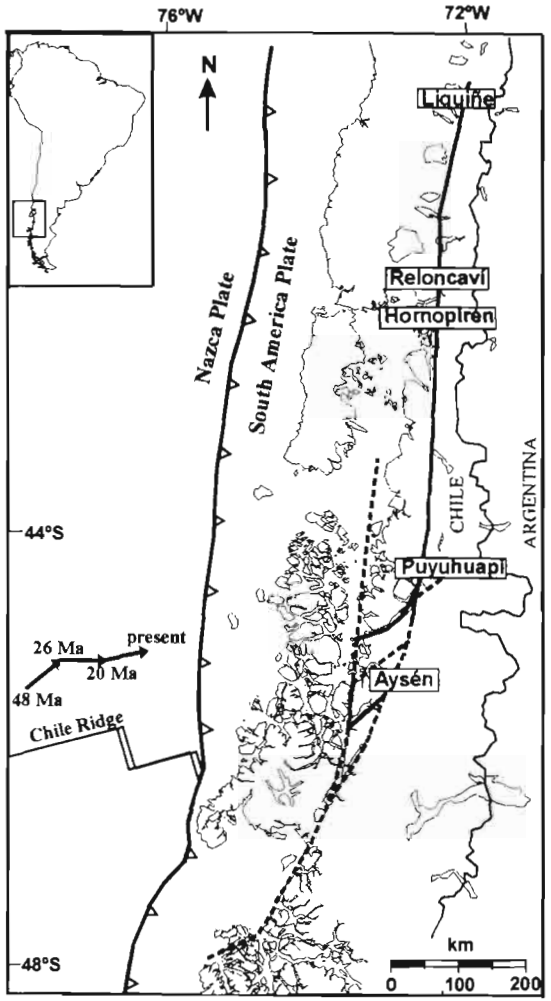

Figure 1. Geodynamic setting of Southern Andes plate boundary zone. Transect location is shown.

Sample	Transect	Rock type	Material	Age (Ma) ± 1σ
94JC54	Liquiñe	crosscutting dike	amp	100±2
94JC13	Hornopirén	S-C tonalite	bt (Laser spots)	4.35±0.05
95JC1	Puyuhuapi	mingled gd-diorite	bt	3.5±0.2
95JC1	Puyuhuapi	mingled gd-diorite	amp	20.2±0.2
95JC2	Puyuhuapi	mingled gd-diorite	bt	1.6±0.2
95JC4	Puyuhuapi	mingled gd-diorite	amp	37.4 ± 3
95JC4	Puyuhuapi	mingled gd-diorite	bt	5.3 ± 0.3
95JC6	Puyuhuapi	granodiorite	amp	14.4 ± 0.6
95JC6	Puyuhuapi	granodiorite	bt	14.4 ± 0.3
95JC12	Puyuhuapi	granodiorite	amp	discordant
95JC12	Puyuhuapi	granodiorite	bt	13.3 ± 0.2
96GA01	Puyuhuapi	mylonite	bt (bulk)	4.2 ± 0.2
96GA03	Puyuhuapi	mylonite	bt (bulk)	3.8 ± 0.2
95GA04	Puyuhuapi	mingled gd-diorite	bt (bulk)	4.2 ± 0.1
96GA26	Puyuhuapi	bt-ms schist	ms	6.2 ± 0.2
95JC14	Aysén	bt granite	bt	5.7 ± 0.2
95GA17	Aysén	schist	ms (bulk)	no result
95GA17	Aysén	schist	ms+bt bands (laser spots)	4.6-9.4Ma
95GA19	Aysén	schist	ms (bulk)	4-10Ma, 5.1± 0.2(tga)
95GA19	Aysén	schist	ms+bt bands (laser spots)	4.4 ± 0.3

Table 1. Summary of new ^{40}Ar-^{39}Ar age date for the studied transects

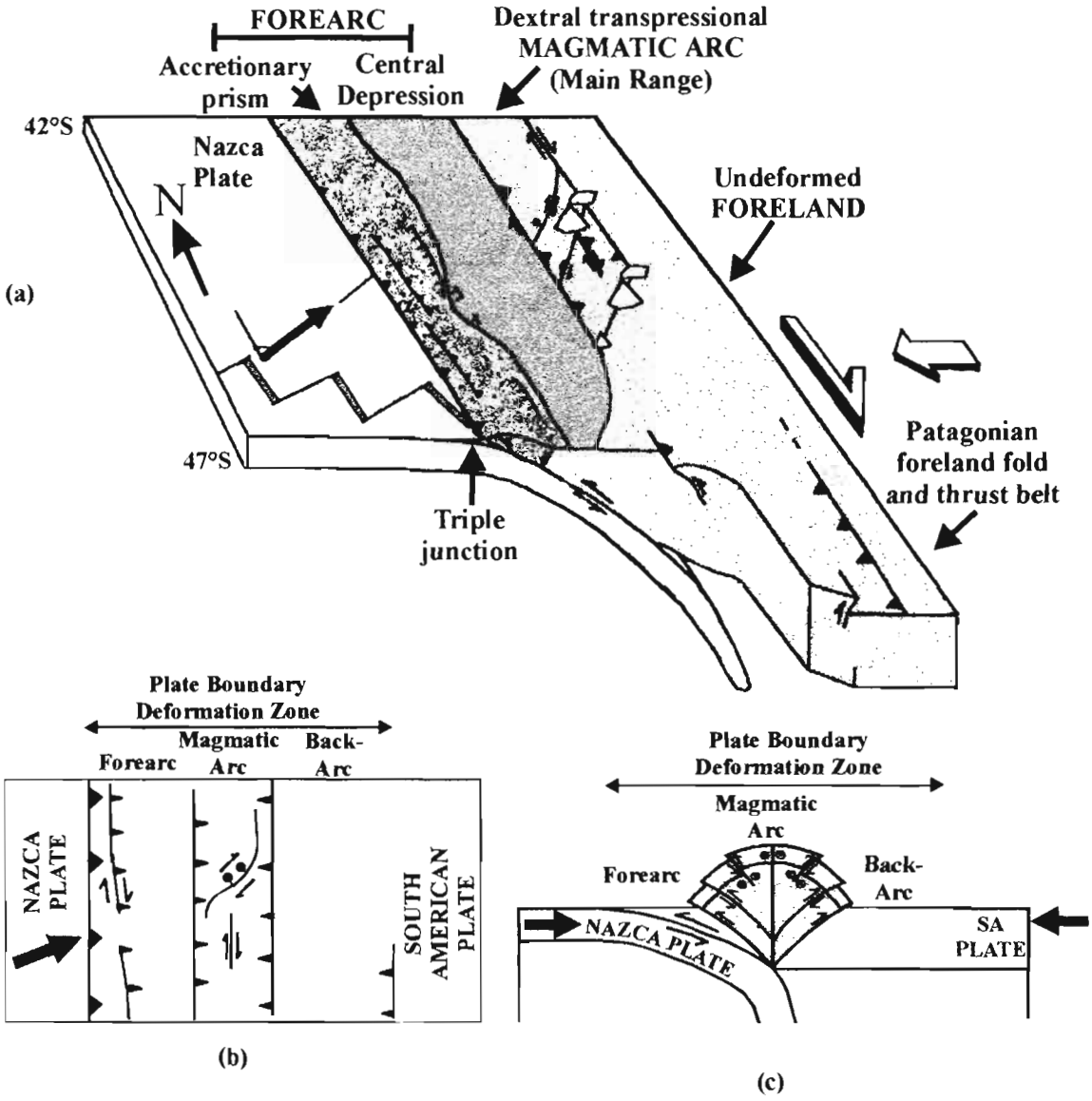

Figure 2. (a) Three-dimensional cartoon showing the regional-scale geometry and kinematics of deformation at the Southern Andes plate boundary zone; (b) Plan view of the plate boundary zone showing that transpressional deformation is mainly accommodated through regional-scale, east-dipping and west-dipping oblique-slip reverse shear zones flanking the Cenozoic plutonic belt of the North Patagonian Batholith; (c) Same as (b) but in sectional view.

OPPOSITE THRUST-VERGENCIES IN THE PRECORDILLERA AND WESTERN CORDILLERA IN NORTHERN CHILE AND STRUCTURALLY LINKED CENOZOIC PALEOENVIRONMENTAL EVOLUTION

Reynaldo CHARRIER(1-7), Gérard HERAIL(2-7), John FLYNN(3), Rodrigo RIQUELME(1-7), Marcelo GARCIA(4-7), Darin CROFT(5) and André WYSS(6)

(1) Departamento de Geología, Universidad de Chile; rcharrie@cec.uchile.cl.
(2) IRD, 209-213, Rue La Fayette, 75010 Paris,gherail@paris.ird.fr.
(3) The Field Museum of Natural History, Chicago, USA. flynn@fmppr.fmnh.org.
(4) SERNAGEOMIN. Av. Sta. María 0104, Providencia, Santiago, Chile. mgarcia@sernageomin.cl.
(5) The Field Museum of Natural History, Chicago, and University of Chicago, USA.
(6) Department of Geological Sciences, University of California Santa Barbara, USA wyss@magic.geol.ucsb.edu.
(7) Convenio IRD-Departamento de Geología, Universidad de Chile.

KEY WORDS: Altiplano, Chile, syntectonic sedimentation, Cenozoic paleoenvironment.

INTRODUCTION

Morphologic units in the northern Chilean Andes parallel one another and the offshore trench. These units are, from west to east: Coastal Cordillera, Central Depression, Precordillera, Western Cordillera and Altiplano (Fig. 1). The development of the west part of the Western Cordillera (Chapiquiña-Belén Ridge), in the Chilean Altiplano, was controlled by two diverging, trench-parallel systems of thrusts and folds, one located along the Precordillera and the other along the eastern side of the Western Cordillera. Although total shortening associated with these systems is only 12 to 14 km, their activity determined the development of fluvial and lacustrine basins which recorded the synorogenic paleoenvironmental evolution of this region. We describe here facies, geometry and chronology of the deposits associated with both systems and provide an explanation for the differing depositional environments developed on the Precordillera and the Western Cordillera.

STRUCTURE OF THE PRECORDILLERA AND WESTERN CORDILLERA

A compressive episode began in this part of the Andes during the Early Miocene (approx. 18 Ma). Along the Precordillera a west-vergent thrust system developed in normal sequence: the Belén-Tignámar and Copaquilla-Tignámar thrust faults. Coarse sedimenatry wedges were deposited proximal to these faults: the Joracane (18 to 16 Ma) and Huaylas (post-11 Ma to pre-5 Ma) Fms. Small displacements of parts of the Huaylas Ignimbrite (4.5 Ma), (which unconformably covers the Huaylas Fm.) suggest that compressive conditions lasted until the Pliocene. On the west side of the Chapiquiña-Belén Ridge an east-vergent thrust system caused the development of progressive unconformities and associated syntectonic sedimentary deposits, the Chucal Fm.

Syntectonic fluvial deposits along the Precordillera: Joracane and Huaylas Fms. Strong erosion of the relief generated by the activity of the Belén-Tignámar and the Copaquilla-Tignámar thrust-faults supplied abundant detrital fill for the depressed areas west of the faults. The Joracane Fm., close to the Belén-Tignámar fault, corresponds to coarse, proximal fluvial facies deposited by braided river systems with low sinuosity. No fossils (plants or animals) were reported from this unit.

The fluvial, upward fining and coarsening Huaylas Fm. is associated with the Copaquilla-Tignámar fault. The lower levels are composed of thin layers deposited in a flood plain environment. Grain size increases gradually upward ; near the top it contains 50 cm in diameter blocks. Lower layers tilt slightly to the west, while the upper levels are horizontal. To the east they locally cover the Copaquilla-Tignámar fault as well as the deformed late Oligocene?-early Miocene Lupica Fm. To the west they cover the scarps at the foot of the fault and they onlap the Oxaya Fm. at the east-flank of the Oxaya Anticline The thickness of the Huaylas Fm. varies considerably. It filled a network of west draining paleovalleys that reached the present Central Depression. The present topographic low in which most of the outcrops of the Huaylas Fm occur was never an endorreic basin. The lower levels contain fossil mammal remains (Notoungulates) (Bargo and Reguero, 1989; Salinas et al., 1991) of the Huayquerian (Salinas et al., 1991) South American Land Mammal Age (SALMA) of about 9 to 7 Ma (Flynn and Swisher, 1995).

Syntectonic fluvial and lacustrine deposits on the east side of the Chapiquiña-Belén Ridge: Chucal Fm. East of the Chapiquiña-Belén Ridge the Lupica Fm. is eastwardly deformed by a partially blind, east-vergent thrust system (Chucal thrust-system). This system, interpreted as a backthrusting of the west-vergent thrust system located along the Precordillera (Hérail et al., submitted), caused the development of progressive unconformities and associated syntectonic sedimentary deposits: lower member (post-21 Ma) and upper member (pre-11 Ma) of the Chucal Fm., that transitionally grades to the late to post-tectonic Lauca Fm. The uplift caused by the western fault (Chucal fault) of this system, exposed immediately west of the Chapiquiña-Belén Ridge, supplied the sediments that formed the Chucal Fm. and part of the Lauca Fm. The fluvial and lacustrine Chucal Fm. (Muñoz, 1991; Riquelme and Hérail, 1997) rest unconformably on the Lupica Fm. and is deformed by a growth fold. Although the Chucal and Lauca Fms. were deposited in fluvial and lacustrine environments, fluvial facies predominate in the Chucal Fm., while lacustrine environments

prevail in the Lauca Fm. The lower member of the Chucal Fm. begins with immature conglomerates composed of ignimbrite fragments, lavas of the Lupica Fm. and fluvial sandstones. Provenance is from the west and southwest. These are followed by siltstones, marls and limestones in decimeter thick layers deposited in flood plain and lacustrine environments. The lacustrine deposits contain well preserved plant stems and leaves. Vertebrate fossils have not been found in this sequence. The series continues with mudstones and siltstones deposited in a flood plain environment, and containing a rich mammal fauna. The upper member begins with a coarse fluvial sequence composed of green conglomerates, followed by sandstones and siltstones with limestone intercalations at the top, also deposited in flood plain and lacustrine (more restricted) environments ; it contains no mammal fossils. The sequence evolves upward toward higher energy deposits, which are also fossiliferous, and are covered to the west by the Chucal fault and to the east, in the basin, by the 11.2±0.5 Ma Chucal Ignimbrite. The Chucal Ignimbrite is covered by conglomerates composed of andesitic clasts, on top of which rests the Lauca Fm.

FOSSIL MAMMAL CONTENT

An extensive mammalian fauna has been recently recovered from the Chucal Fm. (Charrier et al., 1994a; Flynn et al., 1999). Specimens were collected from different stratigraphic levels. The current faunal list includes: hegetotheriine hegetothere, at least 2 mesotheriine mesotheres, toxodontid, macraucheniid litoptern, chinchillid rodent, armadillo, turtle carapace pieces, and several bird bones (large and small size).

Taxa in the assemblages found in northernmost Chile range elsewhere from Santacrucian to Chasicoan or Huayquerian, with most overlapping in the "Friasian". As these are the northernmost Cenozoic mammalian fauna(s) known from Chile, these assemblages from the Huaylas and Chucal Formations permit comparisons of an extensive latitudinal series (more than 30 degrees) of middle Cenozoic faunas from west of the Andean crest (Casamayoran? and "Tinguiririan" [pre-Deseadan, post-Mustersan] through Santacrucian and the type "Friasian"). The occurrence of these faunas at a critically important modern biotic disjunction (Atacama Desert – Bolivian Orocline bending axis), directly west of well known Cenozoic faunas from a variety of paleoelevations in the Altiplano and other regions of Bolivia, may allow assessment of the biotic history along an east-west transect from Chile to eastern Bolivia.

CONCLUSION

Tectonic evolution along the western Altiplano has occurred under prevailing compressive condition since 18 Ma creating a west-vergent thrust system and some east-vergent backthrusts associated with growth folds. These diverging systems generated an uplifted ridge located along the Precordillera and the present Western Cordillera. During development of these structures and uplift of the ridge, considerable amounts of syntectonic deposits containing mammalian remains accumulated at both sides of the ridge.

The west side of the ridge, was characterized geomorphologic conditions that favoring aridity and rapid drainage of rain and melt water toward the Central Depression, and explaining the relative scarcity of fossil faunas and the absence of fossil floras. On the east side, on the Chilean Altiplano, geomorphologic conditions favored the development of flood plains and shallow lakes with considerable accumulation of finer sediments containing abundant mammalian remains. This indicates that, as a consequence of the Middle Miocene tectonic activity, a partition of the environmental conditions occurred west and east of the present Western Cordillera. According to the paleofloras known from this Andean region, low altitudes in Chile (Charrier et al., 1994b and in Bolivia (Berry, 1919, 1922; Gregory-Wodzicki et al., 1998), this partition is better attributed to a topographic barrier, the Chapiquiña-Belén Ridge than to Andean uplift.

REFERENCES

Bargo, M.S. and Reguero, M.A., 1989. El primer registro de un mamífero fósil en el extremo septentrional de Chile. Ameghiniana, 26, 3-4, p.239.

Berry, E.W.1919. Fossil plants from bolivia and their bearing upon the age of uplift of the eastern Andes. proceeding U.S. National Museum, 54, 103-164.

Berry, E.W.1922. Late Tertiary plants from Jancocata, Bolivia. The John Hopkins University studies in Geology, 4, 145-202.

Charrier, R., Muñoz, N., Wyss, A., Flynn, J.J. and Hérail, G. 1994a. Hallazgo de un húmero de Toxodonte (Mammalia) en la Formación Chucal (Oligoceno Tardío-Mioceno Inferior) en el Altiplano de Arica, Chile. Proc. 7th. Congreso Geológico Chileno, Concepción, 430-433.

Charrier et al., 1994b. Edad y contenido paleoflorístico de la Formación Chucal y condiciones paleoclimáticas para el Oligoceno tardío-Mioceno Inferior en el Altiplano de Arica. Proc. 7th. Congreso Geológico Chileno, Concepción, 434-437.

Flynn, J.J., Charrier, R., Hérail, G., Croft, D. and Wyss, A., 1999. The first Cenozoic mammal fauna from the Chilean Altiplano. (Conferencia symposio sobre paleontología de Vertebrados, La Paz, Museo...)

Gregory-Wodzicki, K.M., McIntosh, W.C. and Velásquez, K., 1998. Climatic and tectonic implications of the late Miocene Jakokkota flora, Bolivian Altiplano. Journal of South American Earth Sciences, Vol. 11, N° 6, p. 533-560.

PROCESS OF FORMATION OF THE AU-AG SHILA-PAULA EPITHERMAL VEINS SYSTEM (SOUTHERN PERU)

Alain CHAUVET (1), Daniel CASSARD(2) and Laurent BAILLY (2)

(1) CNRS-UMR 6530, Université d'Orléans, BP 6759, 45067 Orléans Cedex 2, France - email: Alain.Chauvet@univ-orleans.fr
(2) BRGM, DR/LGM, BP 6009, 45060 Orléans Cedex 2, France - email: d.cassard@brgm.fr and l.bailly@brgm.fr

KEY WORDS : Peru, Shila Cordillera, Epithermal gold, Quartz veins, Structural control

INTRODUCTION

The Arequipa - Orcopampa area (southern Peru), about 600 km to the southeast of Lima, is characterized by several base- and precious-metal epithermal districts (Arcata, Caylloma, Madrigal, Orcompampa, Shila, Suykutambo) hosted by Neogene volcanics. A structural study of the Au-Ag mineralization of the Shila Cordillera is herein presented and discussed in order to understand the process of formation of this economic mineralization with respect to the Andean geodynamics.

GEOLOGICAL SETTING - The Shila low-sulphidation epithermal vein system is located in the western Cordillera, northwest of Arequipa. The veins are hosted by Early to Middle Miocene calc-alkaline Shila volcanic breccias and lavas. The mineralized veins generally (or 'vetas') trend east-west (Pillune, Sando Alcalde, Mina Paula), northwest-southeast (Apacheta, Colpa, Tocracancha), and exceptionally northeast-southwest (Apacheta, Puncuhuayca, Ampato)(Fig. 1a). The veins are generally thin (0.2 to 2.5 m) and steeply dipping (>75°) to the north or south. The gangue is siliceous or rich in rhodonite/rhodochrosite Adularia is commonly present. A complex sulphur-bearing paragenesis is observed. Most of the electrum is late.

STRUCTURAL FEATURES OF THE SHILA-PAULA VEIN SYSTEM - The vein system shows a general pattern characterized by the systematic association of a main vein (1-2 m thick) and thin open secondary fractures filled with euhedral quartz locally associated with sulphides (Fig. 1). The main vein commonly

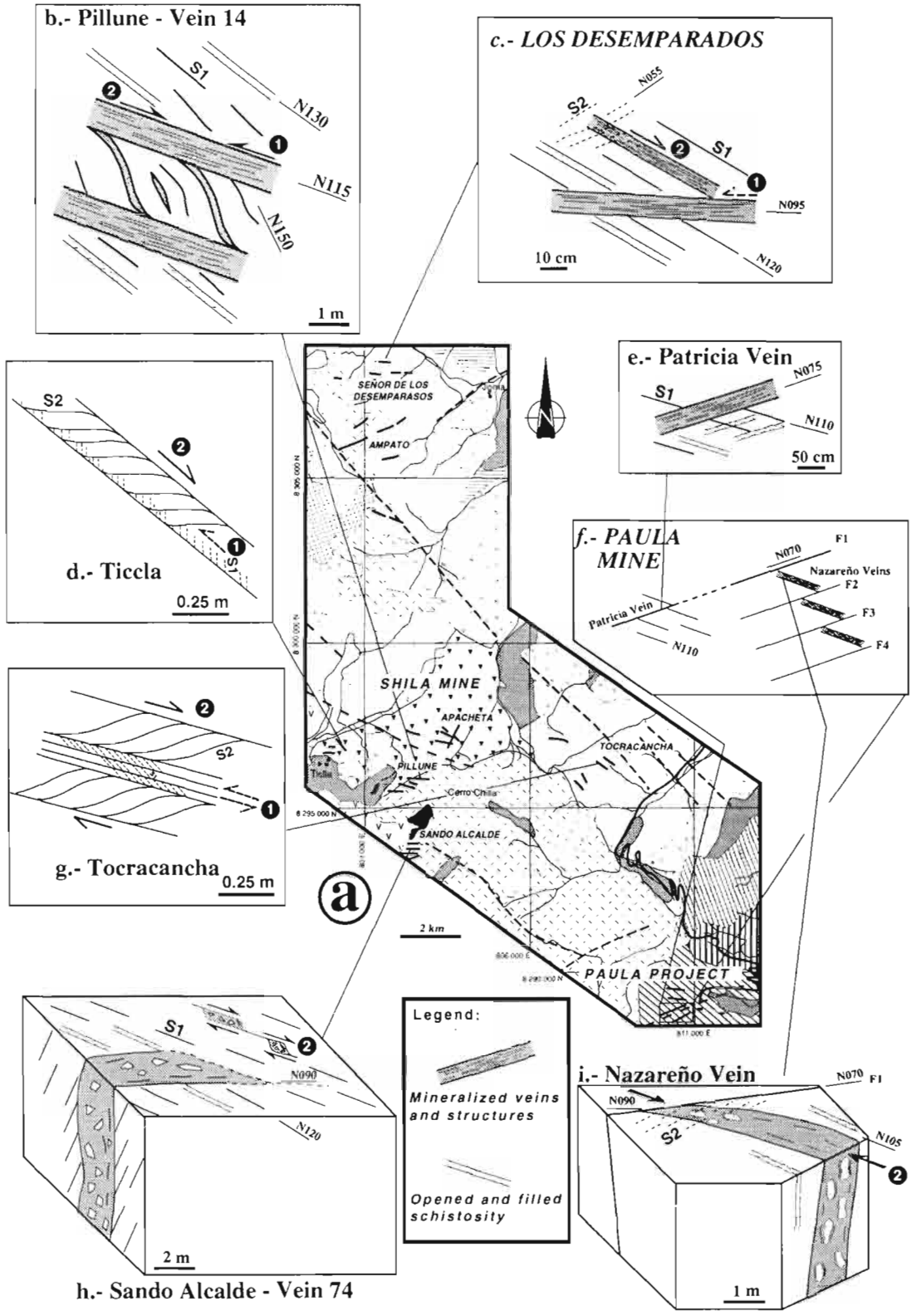

Fig. 1 - Examples of geometrical relationships between mineralized veins and structures

strikes N080-110°E, whereas the secondary fractures strike N120-135°E. This geometry, which is the most common case, is particularly well represented at Pillune, Sando Alcalde and Mina Paula - veta Patricia (Figs. 1b, e and h). It is interpreted as resulting from the superimposition of two deformation events. At this high structural level, the first event was characterized by sinistral movement that caused the development of major shear planes (oriented N080-110°E) associated with a crude S1 fracture schistosity, in places sigmoidal (oriented N120-135°E). Striae are not observed everywhere. The second event reactivated these two structure types. The major shear planes show evidence of dextral movement. Most of the S1 schistosity planes are reopened although some are locally affected by dextral shearing (pull-apart opening). Highly locally, the second deformation event caused S2 schistosity (Figs. 1c, d and g). When S1 and S2 are superimposed, sinistral-related S1 is systematically cut by dextral-related S2. In other words, the NE-SW to ENE-WSW shortening direction associated with sinistral displacement is earlier than the ESE-WNW to SE-NW shortening direction associated with dextral displacement (Fig. 1).

Vetas with orientations different to the considered trend present modified characteristics to the general framework. For exemple, in the Apacheta area, veta 2 trends N150°E and shows a few scarce secondary fractures without fill. Veta 22 (N040-060°E) is not associated with the secondary fractures and only shows evidence of sinistral movement. In the Mina Paula area, the Nazareño veta (N105°E) is intersected and offset by a group of approximately E-W-trending faults (F1 to F4 – Figs. 1f, i). No clear evidence of strike-slip deformation is noted on the walls of this thick brecciated structure which seems instead to have resulted from opening under stress during the second deformation event.

PROCESS OF FORMATION - The mineralization structures in the Shila-Paula area are interpreted as resulting from a process of reuse and reopening of the shear zones created during an earlier deformation

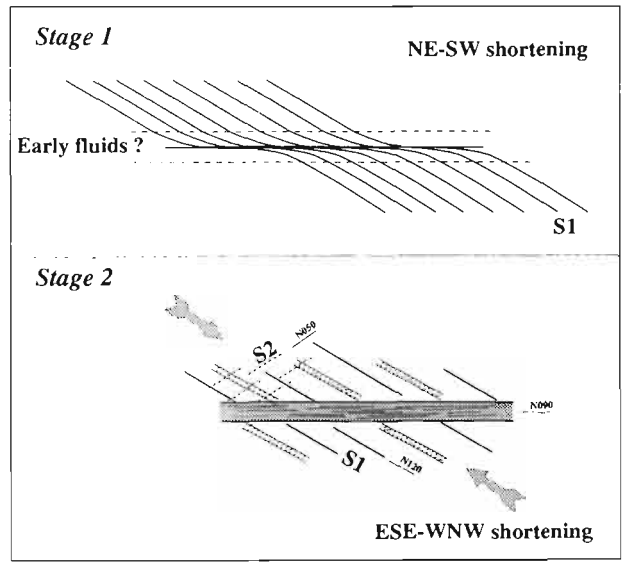

Fig. 2: Mineralization formation model.
Stage 1 - creation of E-W sinistral shear structures under NE-SW shortening direction. Development of N120E schistosity and possible emplacement of early hydrothermal fluids.
Stage 2 - SE-NW direction of shortening and reopening of the S1 schistosity assisted by hydrothermal fluids

event (Fig. 2). Stage 1 of this process consists in formation of the E-W sinistral shear zones under a NE-SW to ENE-WSW shortening direction, associated with the development of S1 schistosity globally oriented N120°E (Fig. 2a). During stage 2, these structures are reopened and receive mineralizing fluids, the circulation of which may have begun during stage 1. Reopening probably result from the joint action of tectonic stress (as evidenced by the local presence of S2 schistosity) and a high fluid pressure (fluid-assisted fracturing). The main veins are located along the ancient shear zones whereas the secondary fractures adopt the same direction as the earlier S1 schistosity (Fig. 2b). Such a mechanism offers the advantage of being able to account for most structures in the Shila-Paula mining district, despite certain specific zones (notably Apacheta) being difficult to integrate into this global framework (see above) and suggesting a rotation of the shortening direction, the causes of which are still unknown.

The ENE-WSW to NE-SW shortening direction adopted for the first deformation event agrees with paleo-stress field estimations for the considered area and period (Quechua II - Huaman, 1985; Soulas, 1977) and with the direction of convergence between the Nazca and South American plates (Pardo-Casas and Molnar, 1987). The second deformation event with a ESE-WNW to SE-NW shortening direction has never been described. It could be dated approximately at about 10 Ma because on the base of recent K-Ar datings of mineralized quartz vein-related adularia (Cassard et al., submitted). The regional scale of this event, which governed mineralization emplacement in the Shila-Paula district, remains to be verified.

ACKNOWLEDGEMENTS

This study was financed by a the BRGM-PRD 406 development project and by the Metallogenic research group (GDR). The authors would like to thank Jean-Marie Georgel and CEDIMIN SA for their friendly assistance and logistical support. Juan Rosas, Uberto Ruiz and Carlos Velasquez are particularly akknowledged.

REFERENCES

BLES, J.L., 1989. Contexte structural des minéralisations aurifères épithermales d'Orcopampa, Layo et Shila (Département d'Arequipa, Pérou). BRGM Report 89 PER 054 GEO, 61 p. (unpublished)

HUAMAN RODRIGO, D., 1985. Evolution tectonique cénozoïque et néotectonique du piémont pacifique dans la région d'Arequipa (Andes du Sud-Pérou). Thesis, Univ. Paris-Sud, Orsay, 220 p. (unpubl.).

PARDO-CASAS F. and MOLNAR, P., 1987. Relative motion of the Nazca (Farallon) and South American plates since late Cretaceous time. Tectonics, 6: 233-248.

SOULAS, J.P., 1977. Les phases tectoniques andines du Tertiaire supérieur, résultats d'une transversale Pisco-Ayacucho (Pérou central). C. R. Acad. Sci. Paris, Ser. D, 284: 2207-2210.

ORE AND ROCK LEAD ISOTOPE COMPOSITIONS WITNESS GEODYNAMIC EVENTS IN THE ECUADORIAN ANDES

Massimo CHIARADIA (1) and Lluís FONTBOTÉ (1)

(1) Département de Minéralogie, Université de Genève, Rue des Maraîchers 13, CH-1211 Genève 4, Switzerland; e-mail: chiaradi@sc2a.unige.ch and fontbote@sc2a.unige.ch

KEY WORDS: Lead isotopes, Ecuador, metallogeny, subduction, terranes

INTRODUCTION

Lead isotope compositions of magmatic rocks and ores of the Northern Andes may help to reveal whether and how subduction under a multiaccreted margin results in peculiar magmatogenic and metallogenic processes. In this contribution we discuss, in the frame of subduction-related geodynamics, 20 new Pb isotope results of Ecuadorian ores (Table 1) together with 54 data and geochemistry of 14 rocks previously analysed for isotopic compositions (Chiaradia and Fontboté, 1999).

Ecuador is composed of NNE-SSW trending microterranes which represent different geotectonic domains formed during the separation of the North and South American continents and successively reattached to the Amazon craton during subduction of the Pacific plate. From east to west the recognized microterranes (Figure 1), according to Litherland et al. (1994), are: i) *Salado*, a marginal arc basin composed of metamorphosed volcanic and volcaniclastic rocks of Upper Jurassic age with associated arc intrusives; ii) the continental *Loja* terrane composed of Paleozoic schists and gneisses; iii) *Alao*, a complete metamorphosed island arc sequence of Upper Jurassic age; iv) Guamote, a passive margin sedimentary sequence of material coming from the continental *Chaucha* terrane (v) which consists of Paleozoic sequences similar to those of the Loja terrane and is separated by an E-W trending ophiolitic belt from the *Amotape* continental terrane (vi) situated more to the South; vii) the Upper Cretaceous island arc of *San Lorenzo*, accreted against the Chaucha terrane during the Paleocene; viii) the *Macuchi* arc, established on the accreted San Lorenzo arc during the Eocene; and ix) the *Piñón* terrane, a slab of Cretaceous oceanic crust attached to the Macuchi arc.

We have analysed ores and rocks from the different terranes as subdivided above and ranging in age from Paleozoic to Miocene (Figure 1). For details of the analytical methods the interested reader can refer to Chiaradia and Fontboté (1999).

RESULTS AND DISCUSSION

In Ecuador five main time-related metallogenic events can be distinguished, of which we have analysed selected ores. The isotopic signatures of ores and associated magmatic rocks reflect different geotectonic and geodynamic scenarios changing through time and space (Figure 2a).

1) The *Jurassic skarns* of the Nambija district, emplaced at the *margin of the Amazon craton*, display a slight enrichment of thorogenic lead that reveals a lower crust component (not shown). Such a signature is also found in porphyry coppers of Colombia (Sillitoe and Hart 1989) situated in a similar context, at the margin of the Guyana shield, and in the inner deposits of Central Andes (e.g. Kontak et al. 1990).

2) The *Jurassic massive sulphide* of Minas Pilas, hosted by the island arc volcano-sedimentary sequence of the *Alao terrane*, displays a radiogenic signature identical to that of the host metavolcanic rock (Figure 2a). In the absence of continental crust underlying island arcs, this radiogenic signature could be related to assimilation of pelagic sediments dragged down by the subducting slab in the zone of generation of arc magmas, the mantle wedge, as ascertained by ^{10}Be systematics (Tera et al., 1984). The very high component of pelagic sediment lead (> 80%) necessary t

explain the isotopic composition of Jurassic magmas and associated ores could be related to the oblique and steep subduction of the Farallon plate from Jurassic to Paleocene (Daly 1989): this subduction style possibly limited the trench scraping of pelagic sediments at the trench in contrast with the orthogonal and shallow subduction style of the Central Andes. Also *Cretaceous massive sulphides* formed in the *San Lorenzo island arc* display radiogenic compositions that can be explained by a mechanism of pelagic sediment incorporation into the island arc magmas (Figure 2a).

Table 1. Isotopic compositions of ores measured during this investigation. Additional data plotted in Figure 2 are in Chiaradia and Fontboté (1999). Abbreviations: PY = pyrite; PO = pyrrhotite; MOL = molybdenite; STB = stibnite; CPY = chalcopyrite; SPL = sphalerite.

SAMPLE	*MINE*	*MINERAL*	*206/204*	*207/204*	*208/204*	*TERRANE*	*AGE*
PB801	CHAUCHA	PY	18.755	15.643	38.575	CHAUCHA	TERTIARY
PB800	FILO LARGO	MOL	19.039	15.684	38.989	CHAUCHA	TERTIARY
PB809	FILO LARGO	CPY	18.768	15.641	38.624	CHAUCHA	TERTIARY
PB806	MULUNCAY	CPY-SPL	18.991	15.661	38.862	CHAUCHA	TERTIARY
PB806	MULUNCAY	PY	18.879	15.657	38.776	CHAUCHA	TERTIARY
PB793	S.RAFAEL DE SHORO	PY	19.000	15.648	38.793	CHAUCHA	TERTIARY
PB795	EL TORNEADO	MOL	18.579	15.595	38.345	MACUCHI	TERTIARY
PB790	JUNIN	CPY	18.736	15.617	38.493	MACUCHI	TERTIARY
PB791	JUNIN	MOL	18.812	15.591	38.475	MACUCHI	TERTIARY
PB802	PONCE ENRIQUEZ	STB	18.683	15.629	38.543	MACUCHI	TERTIARY
PB804	PONCE ENRIQUEZ	STB	19.013	15.638	38.772	MACUCHI	TERTIARY
PB789	SIGCHOS	PY	18.898	15.631	38.651	MACUCHI	TERTIARY
PB798	S.BARTOLOMÉ	PY	19.373	15.706	39.125	ALAO	TERTIARY
PB794	LA PLATA	CPY	19.047	15.695	38.894	S. LORENZO	CRETACEOUS

PB803	COSANGA	PYRITE	18.561	15.634	38.504	TAHUIN	CRETACEOUS
PB805	PILAS	PY	19.262	15.703	38.993	ALAO	JURASSIC
PB808	CAMPANILLAS/NAMBIJA	CPY	18.462	15.622	38.421	AMAZON	JURASSIC
PB810	CAMPANILLAS/NAMBIJA	PY	18.353	15.582	38.263	AMAZON	JURASSIC
PB811	MINA REAL/NAMBIJA	PO	18.569	15.618	38.455	AMAZON	JURASSIC
PB799	PIUNTZA	PY-SPL	18.636	15.600	38.435	AMAZON	JURASSIC

3) The Cosanga *Cretaceous porphyry copper*, emplaced within the continental *terrane of Amotape*, bears lead that is less radiogenic than Cretaceous massive sulphides emplaced in the San Lorenzo arc (Figure 2a). A lower pelagic sediment component can be inferred from this signature and might be related to a different subduction style in the southern part of Ecuador where subduction, under continental crust, was more orthogonal and extension behind the trench was absent contrary to the north (Aguirre 1992). However, it is also possible that the pelagic sediment component in this ore be masked by incorporation of ^{207}Pb-poor lead from the lower continental crust.

4) *Tertiary ores* represent the most important and geographically widespread metallogenic event in Ecuador. This is related to subduction shallowing started in the Paleocene and to subduction of hot oceanic crust that produced magmatism across the whole section of the Ecuadorian Andes (Daly 1989). Tertiary ores are mostly *epithermal* volcanic-related ores and fewer *porphyry coppers* and as such are always strictly associated with coeval magmatism. Tertiary magmas display quite a large variation of $^{207}Pb/^{204}Pb$ values (Figure 2a), indicating a mixing between a primitive source, the mantle, and more radiogenic source(s). Lead isotope ratios of magmatic rocks are significantly correlated with typical lithophile elements like Si, Pb and U and anticorrelated with compatible mantle-enriched elements like Ca and calcophile elements like Cu. This indicates that mantle-derived Tertiary magmas assimilated acid crustal rocks in variable amounts probably depending on the type of terrane crossed (crustal, oceanic or transitional) and on the geodynamic style of magma emplacement.

Tertiary ores display a larger isotopic variability than Tertiary magmas. Ores of the *Chaucha continental terrane* overlap the most radiogenic compositions of the Tertiary magmatites suggesting derivation of their lead directly from associated magmas contaminated by upper crust rocks. Ores from the *Loja* and *Alao terranes* have similarly high $^{207}Pb/^{204}Pb$ ratios but, respectively, lower and higher $^{206}Pb/^{204}Pb$ values than Tertiary magmas. This pleads for remobilization of country rock lead from Paleozoic schists and Jurassic metavolcanites respectively in the Loja and Alao mineralisation. Finally, Tertiary ores emplaced in the *Macuchi arc* and at the transition between it and the continental Chaucha terrane bear the lowest $^{207}Pb/^{204}Pb$ and $^{206}Pb/^{204}Pb$ values of the Tertiary mineralisation phase. They partly overlap the lowest radiogenic compositions of Tertiary magmatites suggesting derivation of their lead from more primitive, less contaminated magmas with respect to mineralisation in the Chaucha terrane. However, some of the Tertiary Macuchi ores display even lower $^{207}Pb/^{204}Pb$ and $^{206}Pb/^{204}Pb$ values suggesting incorporation of higher amounts of mantle lead than the analysed magmas and variable amounts of continental crust lead.

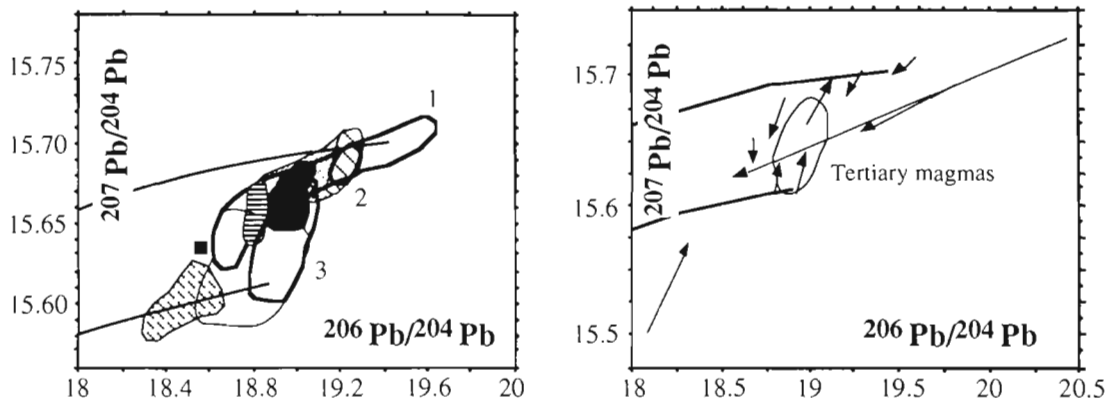

Figure 2a (left). $^{207}Pb/^{204}Pb$ vs. $^{206}Pb/^{204}Pb$ plot with the compositions of ores and rocks subdivided by terranes. Legend: ▨ =Tertiary Alao ores; ■ =Tertiary Chaucha ores; ▤ =Tertiary Loja ores; □ =Tertiary Macuchi/San Lorenzo and transitional crust ores; ▫ =Jurassic and Cretaceous massive sulphides; ▨ =Jurassic Nambija skarns; ■ =Cretaceous Cosanga porphyry Cu. Thick lines: 1=Paleozoic rocks of the Chaucha and Loja terranes; 2=Jurassic volcanic rock of teh Alao terrane; 3=Tertiary magmatites (all terranes). Figure 2b (right). $^{207}Pb/^{204}Pb$ vs. $^{206}Pb/^{204}Pb$ plot with residue-leach couples of analysed rocks (arrows go from residue to leach). Curves represent upper crust (upper) and orogen (lower) evolutions.

We can exclude that the radiogenic component of the Tertiary ores is mainly derived from subducted pelagic sediments for two reasons: i) most of the Tertiary ores have lower $^{207}Pb/^{204}Pb$ ratios than the Cretaceous and Jurassic massive sulphides and ii) Tertiary ores geographically very close to each other, but emplaced over terranes geotectonically different (i.e. Chaucha, Macuchi), display large variations of $^{207}Pb/^{204}Pb$ values that could hardly be explained by heterogeneities in the magma source region related to differential assimilation of pelagic sediments.

Separate analyses of leach and residue fractions of whole rocks allow identification of post-rock formation circulation of fluids (Chiaradia et al., in preparation). Almost all leach fractions of the rocks analysed converge towards the isotopic compositions of the Tertiary ores and residual fractions of Tertiary magmas (Figure 2b) suggesting extensive crustal circulation of magmatic fluids during the Tertiary.

CONCLUSIONS

Preliminary lead isotope data on ores and rocks of Ecuador reflect the complex geotectonic setting of the Northern Andes characterized by accretion of several terranes onto the craton margin and by a subduction style changing through time from oblique and steep to orthogonal and shallow. A very high (>80%) component of subducted pelagic sediment lead has possibly been recognized in Jurassic and Cretaceous ores and magmas formed in oceanic island arc settings and could be related to a limited trench scraping of sediments on top of the oceanic plate due to oblique and steep subduction style coupled with back-arc extension. This high pelagic component is absent in the Tertiary magmas and related ores possibly due to subduction orthogonalization and shallowing after separation of the Farallon plate into Nazca and Cocos. Subduction orthogonalization and shallowing could have caused a more efficient trench scraping of the pelagic sediments on top of the subducted

plate. Magmatism is an important source of metals in the Tertiary mineralisation phase as shown by the overlapping of isotopic signatures of magmatic rocks and many Tertiary ores. However, lead was probably remobilized from country rocks in ores of the Alao, Loja and Macuchi terranes. Isotopic compositions of rocks indicate nevertheless that areally extensive fluid circulation bound to magmatism occurred during the Tertiary at crustal level in Ecuador. Geochemical and isotopic compositional variations of Tertiary magmas are due to variable assimilation of upper crustal rocks as supported by the linear covariations of isotopic ratios and concentrations of compatible or incompatible elements.

REFERENCES

Aguirre L. 1992. Metamorphic pattern of the Cretaceous Celica Formation, SW Ecuador, and its geodynamic implications. Tectonophysics, 205, 223-237.

Chiaradia M. and Fontboté L. 1999. Preliminary new lead isotope data on ores and rocks of Ecuador: assessing metal sources in a complex subduction-related environment. In: Mineral deposits: from processing to processes, Proceedings of the 4th SGA and 10th IAGOD joint Meeting, London 22-25 August 1999, Balkema, Rotterdam.

Daly M.C. 1989. Correlation between Nazca/Farallon plate kinematics and forearc basin evolution in Ecuador. Tectonics, 8, 769-790.

Kontak D., Cumming G., Krstic D., Clark A. and Farrar E. 1990. Isotopic composition of lead in ore deposits of the Cordillera Oriental, Southeastern Peru. Economic Geology, 85, 1584-1603.

Litherland M., Aspden J. and Jemielita R. 1994. The metamorphic belts of Ecuador. Overseas Memoir 11, BGS, 147 p.

Sillitoe R.H., and Hart S.R. 1984. Lead-isotopic signatures of porphyry copper deposits in oceanic and continental settings, Colombian Andes. Geochim. Cosmochim. Acta, 48, 2135-2142.

Tera F., Brown L., Morris J., Sacks I.S., Klein J. and Middleton R. 1986. Sediment incorporation in island-arc magmas: inferences from ^{10}Be. Geochim. Cosmochim. Acta, 50, 535-550.

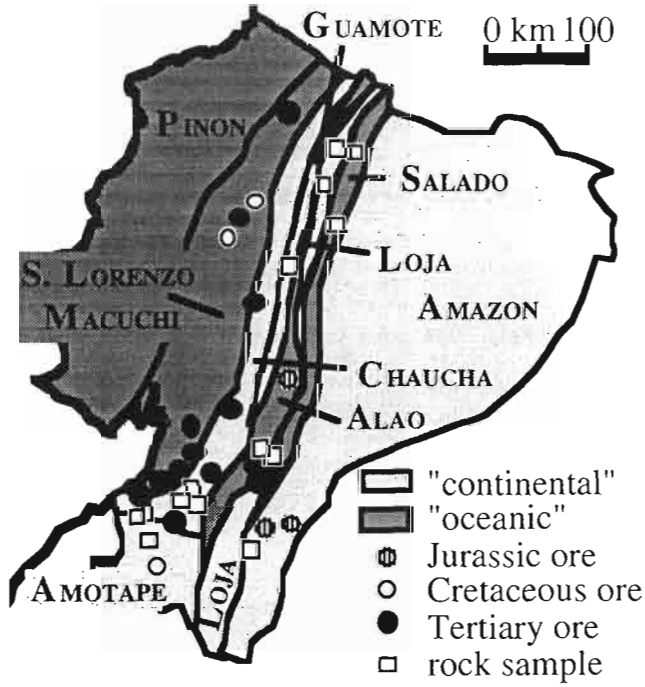

Figure 1. Geotectonic map of Ecuador (modified from Litherland et al. 1994) with location of analysed ores and rocks.

DESCRIMINATION OF EUSTATIC AND TECTONIC INFLUENCES IN THE ECUADORIAN ORIENTE BASIN FROM APTIAN TO OLIGOCENE TIMES

Frédéric CHRISTOPHOUL[1], Patrice BABY[2] and Celso DAVILA[2]

(1) Lab. de dynamique des bassins, 38 rue des 36 Ponts, 31400 Toulouse, France. geostruc@cict.fr.
(2) Convenio I.R.D.-Petroproducción, Apartado 17.12.857, Quito, Ecuador. pbaby@pi.pro.ec.

KEYWORDS: Tectonics, eustacy, sedimentation, retroforeland, Ecuador, Oriente Basin.

INTRODUCTION

The Ecuadorian Oriente Basin (Dashwood and Abbots, 1990) evolved from the peripheral eastern part of an old extensive back arc basin to a retroforeland basin system (DeCelles et Giles 1996). It is deformed by major compressive NNE-SSW wrench fault zones (Fig. 1), known from west to east as Subandean Zone, Sacha – Shushufindi Corridor and Capirón–Tiputini Inverted System (Baby et al., 1999). The filling of the Oriente Basin corresponds to 4 tectonosedimentary cycles ranging from Lower Cretaceous to Upper Oligocene (Fig. 2): Hollín Fm./ Lower Napo Fm. (Aptian to Turonian); Upper Napo Fm./ Tena Fm. (Turonian to Maastrichtian); Lower Tiyuyacu Mb. (Lower Eocene); Upper Tiyuyacu Mb./ Orteguaza Fm./ Chalcana Fm (Middle Eocene to Upper Oligocene). This study, realized as part of the research convention between I. R.D. and PETROPRODUCCION, is based on seismic, well logs and field data. It shows the main influence of each tectonosedimentary cycle in the Oriente Basin evolution.

CRETACEOUS CYCLES

The Hollín Fm./ Lower Napo Fm. tectonosedimentary cycle (Fig. 2) is characterized by a weak tectonic activity. Sedimentation is driven by eustatic variation, illustrated by the Hollín, 'T' and 'U' sedimentary cycles. These three cycles show the same evolution from the base to the top : valley incision, transgression traduced by estuarine deposits filling the incised valley (Hollín, 'T' and 'U' sandstones) and relative highstand by carbonated sedimentation (Lower Napo, 'B' and 'A' limestones). The effect of tectonism is recorded by extensive deformation between 'T' and 'U' cycles, identified at petroleum trap scale by sediment provenance modification and variations in 'U' cycle sediment thickness.

Upper Napo Fm./ Lower Tena Fm. cycle is characterized by a major compressive tectonic event (Fig. 3). Seismic sections show onlaps of 'M-2' sediments over the 'A' limestone in compressive structures. The 'M-2' sandstones correspond to a tectonically enhanced incised valley system which developed in eastern part of the basin. Tectonic uplift can also explain the erosion or non-deposition of 'M-1' sediments in the central part of the basin. This tectonic crisis is contemporaneous with an important continental hotspot volcanic activity (Barragan et al., 1999). Eustatic signature is still present but dominated by local compressive structures deformation. Laterally, equivalent slope facies known as 'Limón flysch', outcropping in the Subandean Zone and in the Ecuadorian Eastern Cordillera (Jaillard, 1997), show a deepening of the basin toward the west.

CENOZOIC CYCLES

The Lower Tena to Upper Tena transition is characterized by the basin emersion as show sedimentological evidences. Upper Tena Fm. shows an inversion in the basin polarity (sediments provenance from the East). It can be related with the onset of the Colombian Llanos foreland basin (Cooper et al., 1995), due to the subduction rate increasing (Pardo Casas and Molnar, 1987). This event can be interpreted as the retroforeland basin emersion.

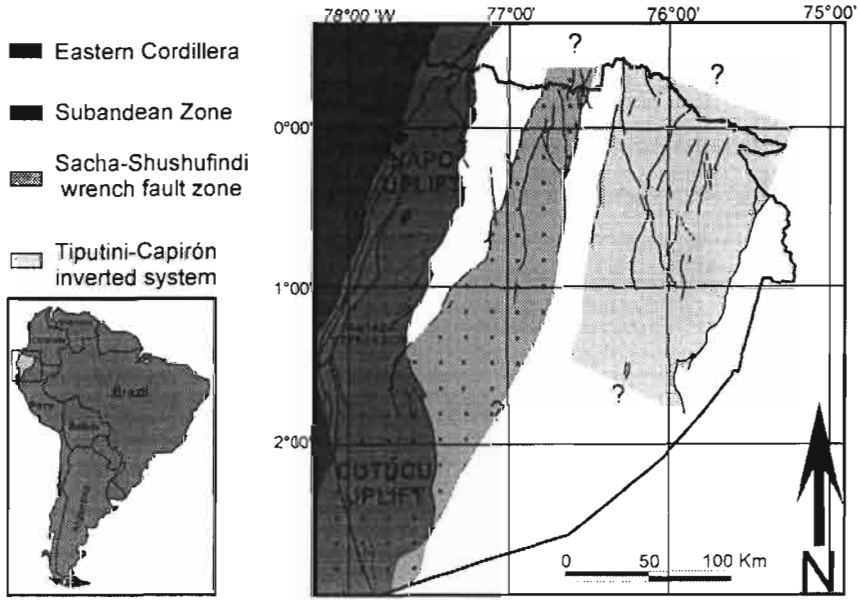

Fig.1 : Simplified structural map of the Oriente Basin. (Modified from Baby et al. 1998)

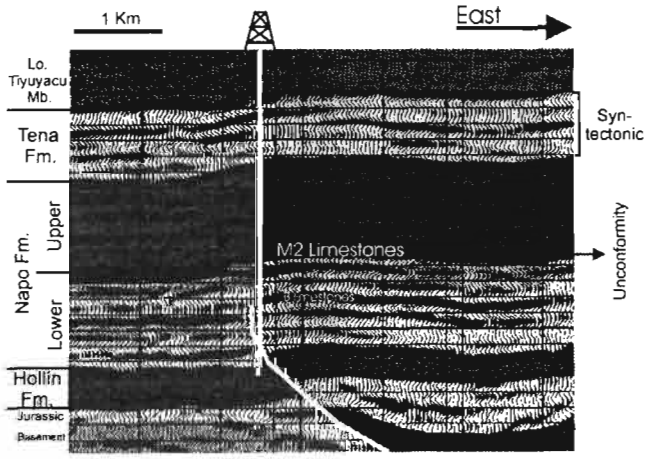

Fig.3 : Tectonic signature of Tena Fm. syntectonic sedimentation and Upper Napo Unconformity

Lower Tiyuyacu Mb. shows a superposition of thinning upward fluvial sediments characterized by a poor maturity of base conglomerates. Seismic sections reveal important thickness variation on compressive structures limbs (Fig. 4). A few progressive unconformities were identified in the basin

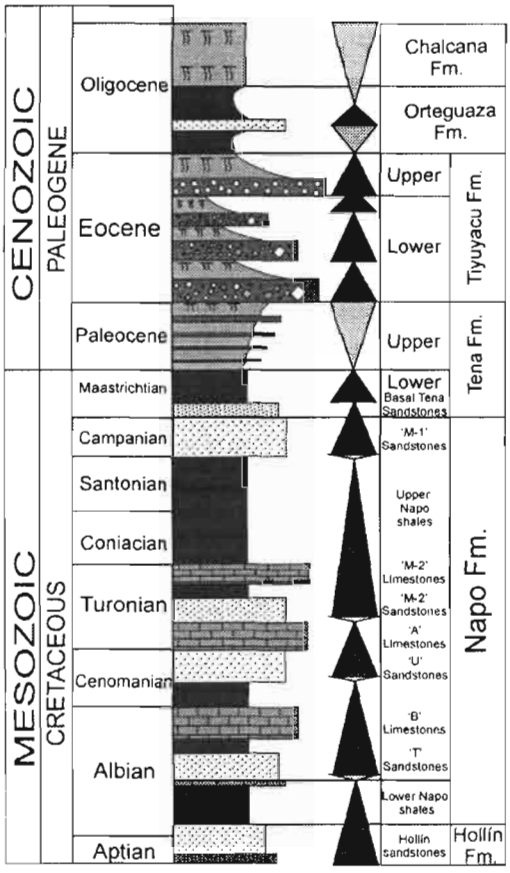

Fig. 2 : Stratigraphy of the Oriente Basin From Aptian to Oligocene

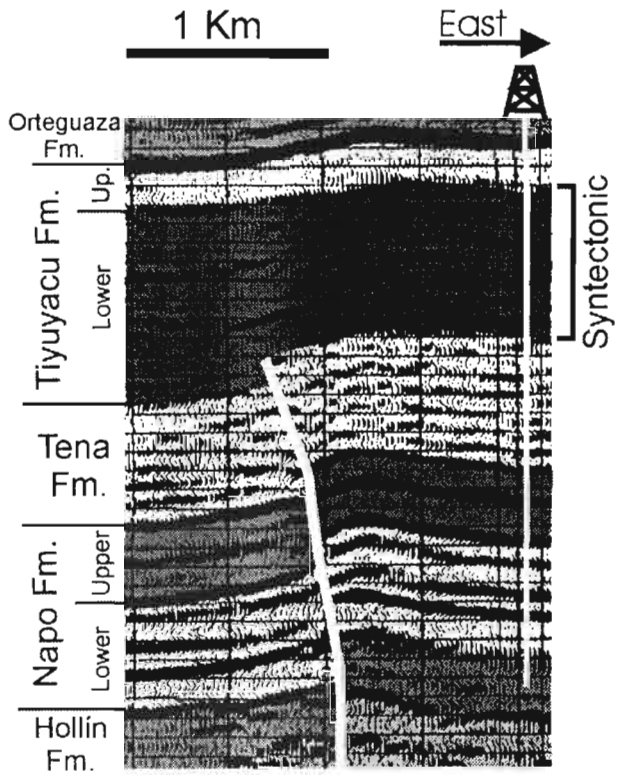

Fig. 4 : Seismic expression of syn-tectonic Tiyuyacu Fm.

western part. This member can be interpreted as syntectonic. Sedimentation is clearly driven by tectonics and each Lower Tiyuyacu Mb. sequence could be related to the growth of the orogenic wedge.

Upper Tiyuyacu Mb. / Orteguaza Fm. / Chalcana Fm. cycle shows no local tectonicdeformation. In seismic sections, no sediments thickness increasing and nor onlap have been identified near the compressive structures. Sedimentation is traducing a huge transgression-regression cycle independent of flower structures growing. Upper Tiyuyacu Mb. is an accumulation of fluvial deposits trapped in the basin by a base level rising with thinning upward stacking pattern. Orteguaza Fm. corresponds to fluvial, estuarine and shelf deposits (Tschopp, 1953) showing 2 transgressive-regressive cycles. The regression at the Orteguaza Fm. top goes on with the alluvial and fluvial Chalcana deposits. Tuffs identified in the Tiyuyacu Upper Mb have recorded a volcanic event related to the Upper Eocene Andean surrection.

Nevertheless, this tectonosedimentary cycle can be considered as syntectonic from stratigraphic and sedimentologic evidences : the Andean surrection increases the topographic load on the continental plate and therefore the subsidence, which produces more accommodation. This stage is expressed by retrogradation in the sediments stacking pattern (Upper Tiyuyacu Mb. and Orteguaza Fm. base). At the end of this stage, subsidence stops its increasing, the created relief is eroded and the accommodation vanishes. Sediments response is characterized by progradation (Orteguaza Fm. upper part and Chalcana Fm.). This transgression-regression evolution can be correlated with the tectonic stage of south Colombia (Casero et al., 1997). The apparent lack of deformation in this part of the basin is interpreted as the consequence of the far cratonward basin location and the subduction rate decreasing.

CONCLUSION

The Oriente Basin evolution from Aptian to Oligocene shows an Andean retroforeland onset in the Paleocene. Hollín / Lower Napo deposits shows an organization driven by eustacy. The basin inversion and its evolution to the foreland basin start during Upper Napo (Turonian-Maastrichtian). The basin emersion apparently occurred at the transition Lower Tena/Upper Tena (Paleocene). But, the Ecuadorian Oriente forms only one part of this foreland basin. In spite of no local deformation, Upper Eocene to Oligocene sedimentation must be considered as syntectonic. It is not directly related to local compressive structures, but to the Andean surrection. Sediments have an outer foredeep to forebulge depozones origin (DeCelles et Giles, 1999), and are driven by tectonics. This basin evolution is coherent with tectonic stages known northward in Colombia.

REFERENCES

Baby P., Rivadeneira M.,Christophoul F., Barragan R. 1999. Style and Timing of deformation in the Oriente Basin of Ecuador. ISAG 99, *This issue.*

Barragan R., Baby P. 1999. A Cretaceous Hot spot in the Ecuadorian Oriente Basin : Geochimical, Geochronological and Tectonic indicators. ISAG 99, *This issue.*

Cooper M .A., Addison F.T., Alvarez R., Coral M., Graham R.H., Hayward, A.B., Howe S., Martinez J., Naar J., Peñas R., Pulham A.J. and Tobarda A. 1995. Basin development and tectonic history of the Llanos basin, eastern cordillera, and middle magdalena valley, Colombia, *AAPG Bull.*, vol 79, n°10, pp1421-1443.

Dashwood M.F., Abbots J.L. 1990. Aspects of the Petroleum geology of the Oriente Basin, Ecuador, in Brooks J. Ed., Classic Petroleum Provinces, *Geological Society Special Publication*, n° 50 , pp89-117.

DeCelles P., Giles K., 1996. Foreland basin systems. *Basin Research*, n°8, pp105-123.

Jaillard E. 1997. Síntesis Estratigráfica y Sedimentológica del Cretáceo y Paleógeno de la Cuenca Oriental del Ecuador. Petroproducción-ORSTOM Edición, 164 p.

Pardo Casas F., Molnar P., 1987. Relative motion of the Nazca (Farallon) and South American plate since late Cretaceous time. *Tectonics*, vol. 6, n°3, pp 233-248.

MULTIFRACTAL ANALYSIS OF THE 1995 ANTOFAGASTA, NORTHERN CHILE EARTHQUAKE

Diana COMTE(1), Armando CISTERNAS(2), Louis DORBATH(3), Jaime CAMPOS(1), Jean Paul AMPUERO(4)

(1) Universidad de Chile, Casilla 2777, Santiago, Chile (dcomte@dgf.uchile.cl)
(2) IPGS, 5 rue Rene Descartes, 67084 Strasbourg Cedex France. (armando@sismo.u-strasbg.fr)
(3) IRD, 209-213, rue La Fayette, 75480 Paris-Cedex 10, Francia (louis@inti.u-strasbg.fr)
(4) IPGP, 4, Place Jussien F75252, Cedex 05, France

KEY WORDS: Self organising process, local networks, Northern Chile

INTRODUCTION

During the last decades there are several authors showing that the spatial distribution of earthquakes follows multifractal laws (e.g., Hirata and Imoto, 1991; Dongsheng et al., 1994), and the most interesting behaviour observed is the decreasing of the fractal dimensions before the occurrence of a big earthquake, and also before large aftershocks (e.g., Ouchi and Uekawa, 1986; De Rubeis et al., 1993; Legrand et al., 1996).

The 1995 Antofagasta, northern Chile earthquake (Mw=8.0)presented a privileged situation with respect to its location related with a permanent seismological network that was in continuous operation since 1991, permitting to follow the seismicity before, during and after the occurrence of the 1995 earthquake, we use the homogeneous catalogue of the Antofagasta network to study the multifractal analysis of the 1995 earthquake, following the same methodology described by Legrand et al. (1996) for the aftershock sequence of the 1992 Erzincan earthquake.

THE 1995 ANTOFAGASTA EARTHQUAKE

This event is located inside the coverage area of a telemetric seismological network (Figure 1) that is in operation since the end of 1990, through a joint cooperation project between the Institut de Physique du Globe de Strasbourg, Institut de Recherche pour le Développement (IRD, ex-ORSTOM) and the University of Chile for the study of the northern Chile seismic gap located immediately to the north of the 1995 rupture surface (Delouis et al., 1997). The most clear foreshock of the July 30, 1995 Antofagasta earthquake (Mw=8.0) was that occurred on December 10, 1994 (Mw=6.2), which presented the same hypocenter and thrust focal mechanism solution. The 1995 rupture extended over an area of 185x90 km^2 along the subduction interplate contact, between 10 and 50 km in depth. The major events

occurred during the first two weeks aftershock sequence were the August 2 (Mw=6.0), the August 3 (Mw=6.4), and the August 9 (Mw=5.5).

The seismic catalogue corresponding to the period of 1992 up to the second week of aftershocks of the 1995 earthquake, has a total of 1467 events with reliable hypocentral locations due to the coverage of the network. In order to work with a complete catalogue in magnitude, it was taken the data associated with the linear part of the Gutenber-Richter law, that is 1286 events with magnitudes greater than 2.8 and less than 6.0 (Figure 2), located inside of the rupture area of the 1995 Antofagasta earthquake (Figure 1).

METHODOLOGY

A full explanation of the theory can be found in Legrand et al. (1997). We will present a brief summary of the main equations used. The generalised correlation function used is defined as:

$$C_q(\varepsilon) = \left\{ \frac{1}{N} \sum_{j=1}^{N} \left[\frac{1}{N-1} \sum_{i=1, i \neq j}^{N} H\left(\varepsilon - \left\| X_i - X_j \right\|\right) \right]^{(q-1)} \right\}^{1/(q-1)}$$

and the generalised fractal dimension is done by:

$$D_q = \lim_{\varepsilon \to 0} \left(\frac{\log C_q(\varepsilon)}{\log(\varepsilon)} \right)$$

where D_q is the probability of occupation of the i^{th} box with size ε, and q is a positive real number corresponding to the order of the correlation dimension.

Considering that, the coverage of the permanent network of Antofagasta is good enough to obtain reliable hypocenters within the selected area, and that all the events considered in the catalogue have S wave readings, the calculations of spatial distances between earthquakes were done in 3D. We worked with a moving window containing a constant number of events in order to guarantee the preceise estimations of the fractal dimensions. After different trials, we choose 200 for the number of the data points in each windows. Two consecutive windows were shifted by 20 points (Legrand et al., 1996).

RESULTS

The $log_{10}C_q(\varepsilon)$ versus $log_{10}(\varepsilon)$ for each q and for the complete data set is shown in Figure 3. The linear part of the curves, for each q, fall between ε_{min} = 19 km and ε_{max} = 89 km; between these two values it can be observed different slopes of the curves suggesting a multifractal structure. The ε_{min} corresponds to the limit of hypocentral resolution of the permanent network, and the ε_{max} is smaller with the dimension of the selected area (km). Figure 4 show the spectrum of the generalised fractal dimension

versus q for the complete data set, with the corresponding error bars: it can be observed that an adequate precision of the fractal dimension D_q is obtained for q=25 so, the calculations stopped at this value. Figure 5 shows the evolution of the different generalised multifractal dimensions with respect to time. It can be observed that there is a clear increasing of D_q previous to the occurrence of the main foreshock of the 1995 Antofagasta earthquake, followed by a continuous decreasing of D_q up to the moment of the occurrence of the mainshock. The same behaviour is observed for the major aftershocks of the 1995 sequence, and it is also observed for every q value.

DISCUSSION

The multifractal analysis of the Antofagasta earthquake shows that there is a systematic decreasing of the fractal dimension with time before the occurrence of the mainshock and the major aftershocks, that can be observed for every q value. The decrease of the fractal dimension before the occurrence of a big earthquake has been noticed by several authors (e.g., De Rubeis et al., 1993; Legrand et al., 1996). The average amount of the estimated decreasing of the D_q value is almost the same for the 1995, Antofagasta and 1992 Erzincan earthquakes, even though both events are very different in their seismotectonic genesis, magnitude, depth, and number of aftershocks, suggesting that probably the multifractal analysis is independent of these parameters and that the whole processes involved in the nucleation of big earthquakes follow a global law that can be inferred from this kind of analysis.

Following Legrand et al (1996), these results emphasise the importance of applying multifractal analysis in the evolution of the spatio-temporal distribution of seismicity in relation to the occurrence of large earthquakes. However, it is important to point out that it is extremely necessary to have a complete and homogeneous catalogue of seismicity locally recorded in regions where large earthquakes are expected to occur.

ACKNOWLEDGEMENTS

This work was partially supported by CONICYT, Universidad de Chile and IRD, France.

REFERENCES

Delouis, B., T. Monfret, L. Dorbath, M. Pardo, L. Rivera, D. Comte, H. Haessler, J.P. Caminade, L. Ponce, E. Kausel and A. Cisternas, Bull. Seism. Soc. Am., 87, 427-445, 1997

De Rubeis, V., P. Dimitriu, E. Papadimitriou and P. Tosi, Geophys. Res. Lett., 20, 1911-1914, 1993.

Dongsheng, L., Z. Zhaobi and W. Binghong, Tectonophysics 233, 91-97, 1994.

Hirata, T. and M. Imoto, Geophys. J. Int., 107, 155-162, 1991.

Legrand, D., A. Cisternas, and L. Dorbath, Geophys. Res. Lett., 23, 933-936, 1996.

Ouchi, T. and T. Uekawa, Phys. Earth Planet. Int., 44, 211-225, 1986.

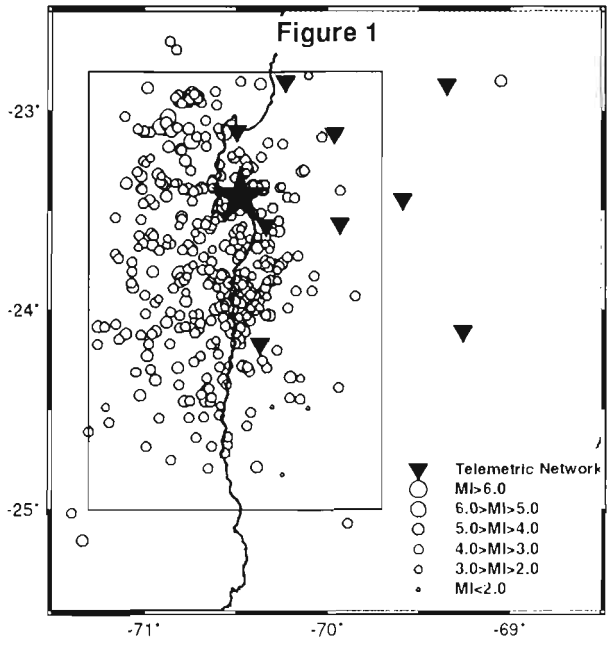
Figure 1
-23°
-24°
-25°
-71°
-70°
-69°
Telemetric Network
Ml>6.0
6.0>Ml>5.0
5.0>Ml>4.0
4.0>Ml>3.0
3.0>Ml>2.0
Ml<2.0

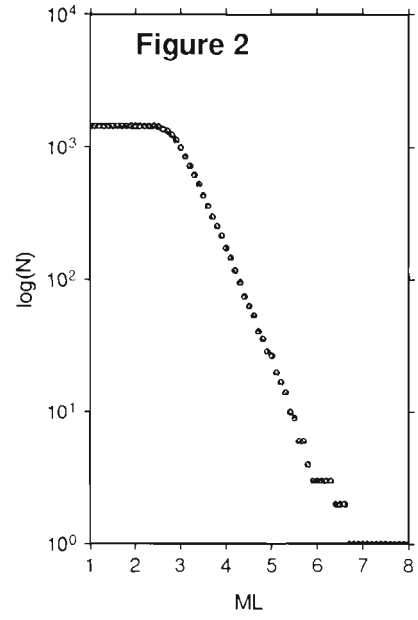
Figure 2
log(N)
ML

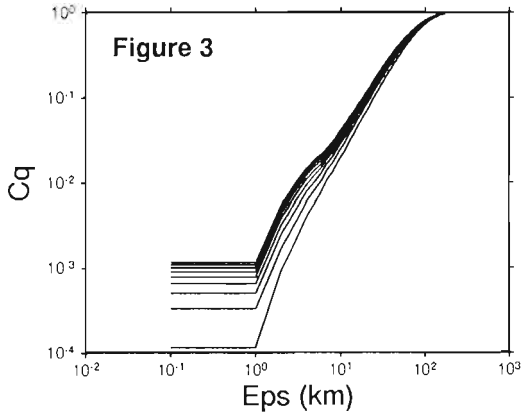
Figure 3
Cq
Eps (km)

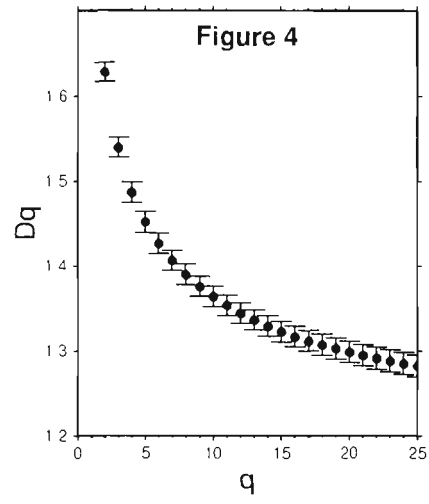
Figure 4
Dq
q

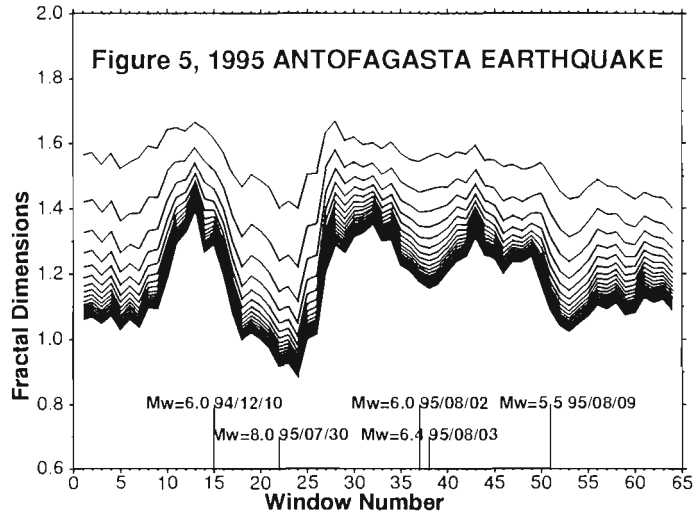
Figure 5, 1995 ANTOFAGASTA EARTHQUAKE
Fractal Dimensions
Window Number
Mw=6.0 94/12/10
Mw=6.0 95/08/02
Mw=5.5 95/08/09
Mw=8.0 95/07/30
Mw=6.4 95/08/03

A DOUBLE-LAYERED SEISMIC ZONE IN ARICA, NORTHERN CHILE

Diana COMTE(1), Louis DORBATH(2), Mario PARDO(1), Tony MONFRET(2), Henri HAESSLER(3), Luis RIVERA(3), Michel FROGNEUX(3), Bianca GLASS(4), and Carlos MENESES(4)

(1) Universidad de Chile. Casilla 2777. Santiago. Chile (dcomte (mpardo) @dgf.uchile.cl)
(2) IRD. 209-213. rue La Fayette. 75480 Paris-Cedex 10. Francia (louis@inti.u-strasbg.fr)
(3) IPGS. Université Louis Pasteur. 5 rue Rene Descartes. 67084 Strasbourg Cedex France.
(4) Universidad de Tarapacá. Campus Saucache. Casilla 6-D. Arica. Chile.

KEY WORDS: Subduction. Double-Layered Seismicity. Northern Chile

INTRODUCTION

A global view shows that seismicity along subduction zones usually delineates a single well-defined surface. with earthquakes distributed in depth from the surface down to several hundred kilometres. Since about two decades the existence of double seismic zones (DSZ) along localised segments of some subduction zones has been recognised. However only few of them have been studied in detail: beneath Honshu [e.g., Kawakatsu. 1986]. beneath Central and East Aleutians [e.g., Engdahl and Scholz. 1977; Abers. 1996] and beneath the Kuril-Kamchatka arc [e.g., Gorvatov et al., 1994; Kao and Chen. 1995]. They are characterised by a double-planed distribution of earthquakes. vertically separated by 20 to 40 km. at depths between 70 and 150 km. The upper plane seems to be just below the top surfaces of the subducting slab. and the lower plane is consequently within the subducted mantle. With the development of high quality global networks and the consequent improvements of waveform modelling. several DSZ have been identified during the past years. Most of them are defined by very few events spanning along hundreds of kilometres along the strike of the trench. and it is therefore almost impossible to asses the continuity or the segmentation of the phenomena. On the other hand. even if an unusual focal mechanism has been determined at intermediate depth in a subduction zone. it is also important to separate the double-layered seismic zones independently from stress-segmented criteria [Fujita and Kanamori. 1981]. In this work we present the results obtained using locally recorded events in the northern edge of the northern Chile seismic gap. along the Arica elbow.

DATA AND METHODS

The data used consisted of two sets: (1) from a telemetric short-period seismic network of 9 stations that has been operating since December 1994 as a joint research project among the U. of Chile.

the U. of Tarapacá, the IPG, Strasbourg, France and the IRD, France and (2) from a dense temporary seismic network (Figure 1), deployed from the coastline to the Altiplano from June to August, 1996. The second dataset contains ~1000 microseismic events while the first has about 3900 events.

The set of body-wave arrival times of microearthquakes recorded was used for preliminary hypocentral determination using a modified version of the HYPOINVERSE program. The crustal P-wave velocity model was the same flat layered model used by Delouis et al. [1996]. Each event is located with different trial depths (between 0 and 250 km, with an increment of 10 km), in order to minimise the effect of dependence of the final hypocentral determination with the initial trial solution. From the initial dataset, a subset of the best constrained hypocenters was selected to be used in a joint inversion for hypocentral locations and 3D body-wave velocity structure. The analysis of the hypocentral locations when 1D or 3D velocity models are used shows that, within the coverage of the network the epicentral differences reach maximum values < 2-3 km, and the average variations in depth are < 5 km. The improved ray geometry permits to determine single-event focal mechanisms using individual first motion polarity for some reliable events along the subducting plate. The polarity of each station was tested in laboratory and by comparing observed with expected first motion for teleseismic events.

RESULTS

Three cross sections along the average direction of the convergence of the Nazca plate beneath South America (N77°E) are shown in Figure 2; the half-width of the P1 to P3 profiles is 20 km. Some selected focal mechanisms are presented on Figure 3 (corresponding to the P2 profile, but with a half-width of 40 km) in a vertical back hemispheric projection along the convergence direction of the Nazca plate. Most earthquakes below 100 km depth lie in a single zone, about 10 km thick, that is almost planar down a depth of 150 km, dipping ~30° to the east. A second parallel planar zone 20-25 km beneath (perpendicular distance between both layers) is observed with fewer events and an average thickness of ~10 km (Figures 2 and 3). Fault plane solutions for these intermediate depth events vary significantly, even between nearby events, (for example events 9 and 10 in the shallowest layer, and events 20 and 21 in the deepest layer). Moreover, focal mechanisms of events located at approximately the same depth and the same distance from the trench can present opposite polarities observed in almost all the stations (for example events 12 and 14 in the shallowest layer, and events 21 and 22 in the deepest layer).

DISCUSSION

This work presents reliable data that show a double layered seismic zone in Arica, northern Chile located at depths between about 100 to 150 km, with compressional and tensional events at almost the same depth (Figure 3). The Arica DSZ can be observed mainly with microseismicity, therefore it is a phenomena that depends on the magnitude threshold used. Even though we are not able to define the genesis of the Arica

DSZ, there are some things that can be established: considering that the Arica DSZ is a localised phenomena in the northern Chile region, it seems to be independent of the age (84 My), the relative convergence rate (~8.3 cm/yr) and convergence direction (N77°E) of the subducting slab, because all of these parameters are almost the same along the whole northern Chile region. Moreover, the Arica elbow can not be responsible of the Arica DSZ, because no similar changes along the strike of the trench are observed in other well studied double seismic zones. In fact, it can be noted that the general patterns of the Arica DSZ are very similar with that observed in the Alaska Peninsula where no elbow is present [Abers, 1992, 1996]. Kao and Liu [1995] presented an interpretation for the seismogenesis of DSZ based on studies along the Kuril-Kamchatka and Japan subduction zones. Even that the general pattern of the stress distribution at intermediate depths is not so similar with that observed in the Arica DSZ, their hypothesis that microearthquakes in the upper portion of the top layer can be probably caused by conventional mechanisms such as dehydration of subducted materials and facies change from basalt to eclogite, whereas the lower layer could be associated with metastable phase transition, can not be rejected by our results. In the same way, the presence of melt-rich regions formed near of the mid-ocean ridges at the base of a thermal boundary layer, that occasionally crystallised into the plate without ascending to the surface proposed by Abers [1996] is still a viable alternative to explain the lower-zone seismicity.

ACKNOWLEDGEMENTS

This work was supported by FONDECYT N° 1961113 and IRD, France.

REFERENCES

Abers, G., Relationship between shallow- and intermediate-depth seismicity in the eastern Aleutian subduction zone, Geophys. Res. Lett., 19, 2019-2022, 1992.

Abers, G., Plate structure and the origin of double seismic zones. In Subduction: Top to Bottom, Geophysical Monograph 96, 223-228, 1996.

Delouis, B., A. Cisternas, L. Dorbath, L. Rivera, and E. Kausel, The Andean subduction zone between 22°S and 24°S (Chile): precise geometry and state of stress. Tectonophysics, 259, 81-100, 1996.

Engdahl, E.R. and C. H. Scholz, A Double Benioff Zone beneath the Central Aleutians: an Unbending of the Lithosphere. Geophys. Res. Lett., 4, 473-476, 1977.

Fujita, K., and H. Kanamori, Double seismic zones and stresses of intermediate depth earthquakes. Geophys. J. R. Astr. Soc., 66, 131-156, 1981.

Gorbatov, A., G. Suárez, V. Kostoglodov, and E. Gordeev, A double-planed seismic zone in Kamchatka from local and teleseismic data. Geophys. Res. Lett., 21, 1675-1678, 1994.

Kao, H. and W.-P. Chen, Transition from interplate slip to double seismic zone along the Kuril-Kamchatka arc, J. Geophys. Res., 100, 9881-9903, 1995.

Kao, H. and L. Liu, A hypothesis for the seismogenesis of a double seismic zone, Geophys. J. Int., 123, 71-84, 1995.

Kawakatsu, H., Double seismic zones: kinematics, J. Geophys. Res., 91, 4811-4825, 1986

FIGURE 1.- Spatial distribution of events and seismic stations.

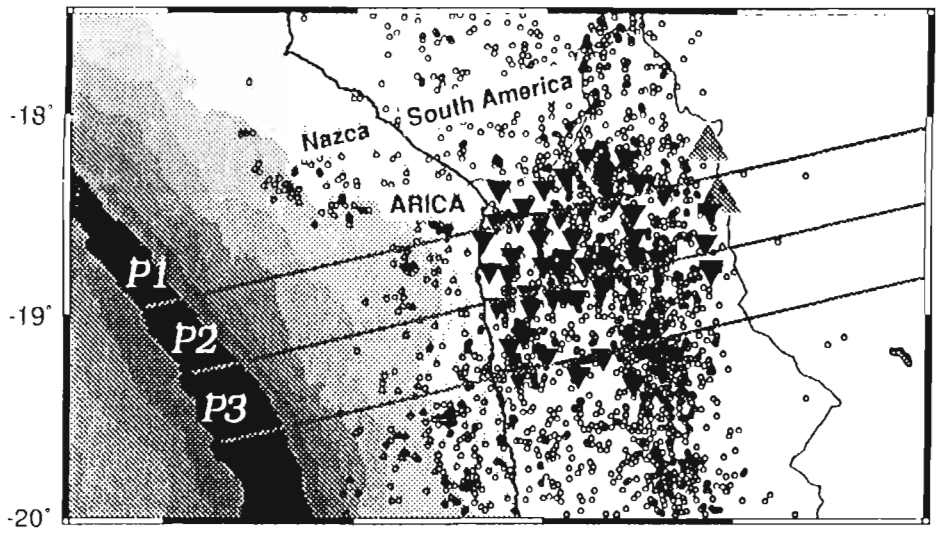

FIGURE 2.-

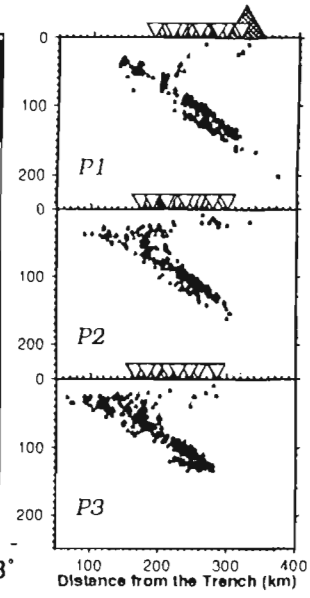

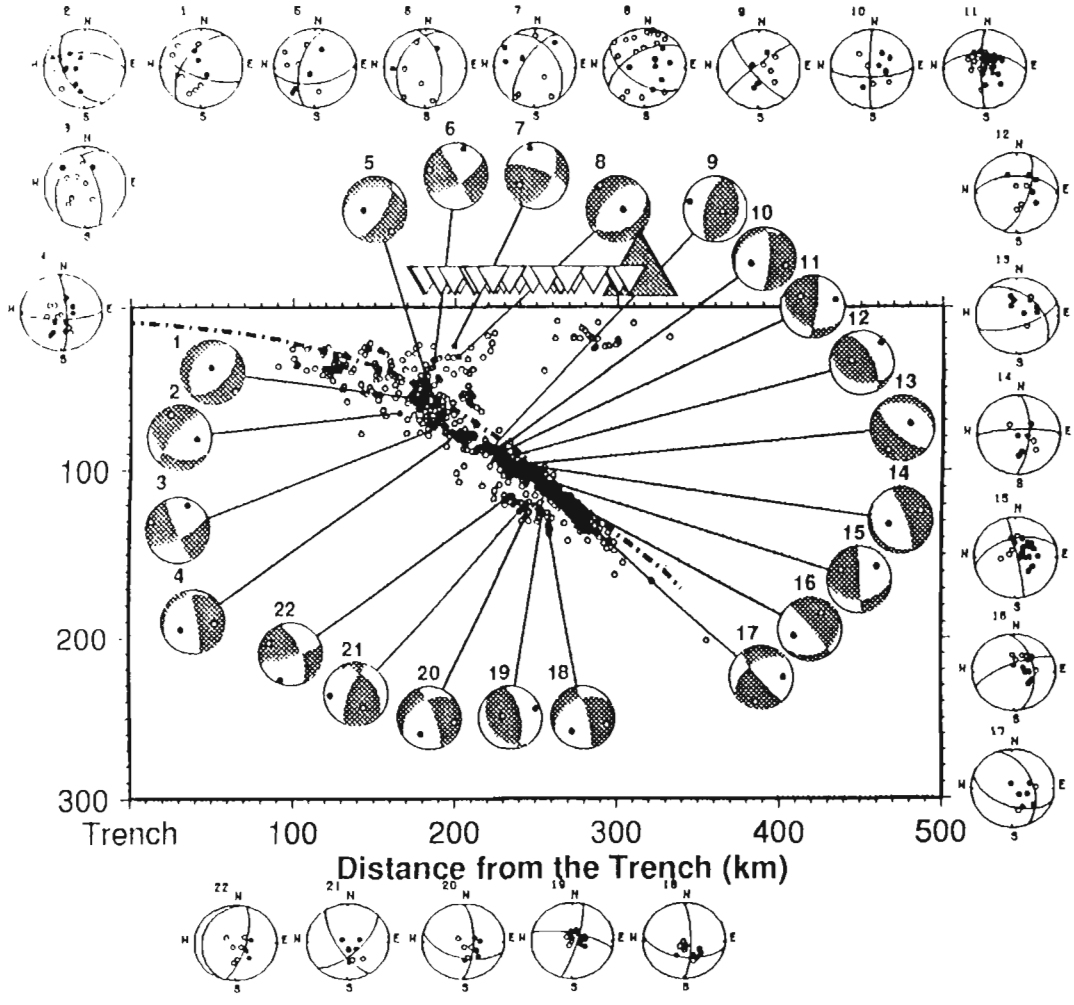

FIGURE 3.- Cross-section of reliable 3D hypocenters determined along the ±40 km wide P2 profile (Figure 1). Focal mechanism solutions projected on the vertical lower hemisphere are also shown. The lower hemispheric projection of each mechanism, with the first motion polarities is also shown. Projections of the seismic stations (inverted triangles) and active volcanoes (triangles) are also presented.

THE WADATI-BENIOFF ZONE AROUND COPIAPO, NORTHERN CHILE USING LOCALLY RECORDED DATA: PRELIMINARY RESULTS

Diana COMTE(1), Louis DORBATH(2), Bernard PONTOISE(2), Mario PARDO(1), Tony MONFRET(2), Henri HAESSLER(3), Yann HELLO(2), Yvan JOIN(2), Emilio LORCA(1), Alain LAVENU(2)

(1) Universidad de Chile, Casilla 2777, Santiago, Chile (dcomte @dgf.uchile.cl)
(2) IRD. 209-213, rue La Fayette, 75480 Paris-Cedex 10, Francia (louis@inti.u-strasbg.fr)
(3) IPGS, Université Louis Pasteur, 5 rue Rene Descartes, 67084 Strasbourg Cedex France.

KEY WORDS: Wadati-Benioff zone, Copiapó, Northern Chile

INTRODUCTION

The area studied is included in the rupture area of the last large earthquake that affected the region of Copiapó, northern Chile, namely the 1922, Atacama earthquake (Figure 1). The main seismotectonic characteristics of the studied area are: (1)The southern end of the Quaternary volcanic chain, that again reappears southward around 33°S. (2)The transition from normal to a subhorizontal subduction geometry. (3) An abrupt change in the bathymetry along the trench located south of 27°S.

The subduction process is able to generate large thrust events along the interplate contact in the Copiapó region. There are reports of two historical events with $M_S \geq 8.0$, the April 11, 1819 and the November 11, 1922 great earthquakes, with associated destructive tsunamis. However, they are not the only earthquakes that produced serious damages in the Copiapó region, in fact this zone has a very high seismic activity with at least eight events with magnitude $M_S \geq 7.5$ during the last 200 years. Moreover, the region of Copiapó had also experimented "swarm" periods of seismic activity, like that observed during July and August, 1973, without any large earthquake occurring before or after this period. Ten years later, the October 4, 1983 (M_S=7.4) thrust earthquake occurred re-rupturing the northern part of the great 1922 earthquake (M_S=8.5), remaining still intact its southern part.

The November 11, 1922 Atacama Earthquake.

Beck et al. [1997] determined the focal mechanism of the 1922 great earthquake using the available first motion polarities of the stations located at teleseismic distances, concluding that this event is an underthrusting earthquake. The duration and complexity of the 1922 source was constrained by the

inversion of the *P* wave record from the DNB station, where the focal mechanism was fixed with a shallow plane striking parallel to the trench and dipping 20° to the east. Beck et al. [1997] showed the difficult to determine the 1922 focal depth due to the long duration of the source (at least 75 sec), and they assumed a shallow depth (0-40 km) considering its local tsunami along the coast of 9 m and a far field tsunami in Japan of less than 50 cm [Lomnitz, 1971].

The 1973 Seismic "Swarm" Activity.

The 1973 swarm activity was an unusual increase of seismicity with magnitudes $5.0 \leq m_b \leq 6.0$ mainly observed during the months of July and August. Cifuentes [personal communication] relocated the 1973 "swarm" events recorded at teleseismic distances with respect to the greatest ones. The relocated longitude was the parameter that strongly changed, this behaviour is usual when only phases recorded at teleseismic distances are used, because of the smaller number of stations in the E-W azimuths. Cifuentes also modelled the *P* and *S* waveforms of the 1973 "swarm" events recorded in the long-period stations of the WWSSN. The majority of the events exhibits inverse or thrusting fault mechanisms, with an average depth of about 19 km. Cifuentes suggests that if the events of the 1973 seismic "swarm" were on the main thrust zone, it could indicate that the region to the north of the 1922 rupture zone was not ready to break in 1973. However, she also wondered whether the 1973 "swarm" events were not on the main thrust zone, they could be related with the deformation of the continental crust. Therefore, the sequence of events would indicate thrust motion along a series of high angle planes in a complex interface. But, considering the ability of the Copiapó region to generate great earthquakes like the 1922 one, if a geometrical complex interface exits there, it does not inhibit the nucleation of great earthquakes.

The 1983 Earthquake.

Mendoza [personal communication] analysed three events occurred in the region of Copiapó, the August 3, 1978 (M_S=6.7), the October 4, 1983 (M_S=7.4) earthquakes and its most energetic aftershock occurred on October 9 (M_S=6.3). He computed a JHD station adjustments and weights using the *P* wave arrival time data of the 1978 and the 1983 main shock and aftershock and, then they were used in a single-event computation of all the hypocenters with moderate magnitude seismicity (m_b>4.8) associated with the 1983 main shock. Mendoza concludes that the 1978 and the 1983 earthquakes represent two types of faulting occurring at virtually the same epicentre, but with different depths. The October 4, 1983 earthquake is a thrust faulting event that was followed by several aftershocks, including the M_S=6.3 one which has a thrust mechanism similar to that of the main shock. These two October 1983 earthquakes occurred at similar shallow depths (35 km) and are consistent with reverse slip along the interplate contact. The August 1978 earthquake was a normal faulting event that occurred within the downgoing slab as a result of extension in the direction of the plate dip.

LOCAL DATA AND PRELIMINARY RESULTS

Considering that the southern edge of the Copiapó seismic gap associated with the 1922 rupture zone had not been studied in detail with using locally recorded events, a temporary seismic network of 28 portable seismic stations in the area located between 26.5° and 28.5°S, along with 10 OBSs (Ocean Bottom Seismometers) located between the coast and the trench (Figure 1) were deployed between September and November, 1998. The use of the OBSs stations is particularly important due to the high seismic activity located close to the trench, so that a reliable control of the hypocenters recorded by the inland and the off-shore networks can be performed.

The inland network consisted in 11 vertical short period stations with EDA digital recorders, 8 three components short period stations with GEOSTRAS digital recorders, and 8 telemetric vertical short period stations that sent the signals to a central stations equipped with a three components seismometer. The telemetric network continuously recorded the microseismicity, and the EDA and GESOTRAS stations recorded the data using a trigger algorithm. The OBS stations were equipped with three components seismometer and they worked in continuous recording; the depth of the off-shore network was between 1300 and 4500 m.

The first 500 events recorded during the 1998 Copiapó field work are presented along a cross-section oriented normal to the trench with origin in 27°S (Figure 2), corresponding to about 15 days. The local data analysed show a clear tendency to a subhorizontal way of subduction; there is shallow seismicity that will be studied in order to see if it could correspond with some fault systems present in the region. It is interesting to point out that the events with depths >180km are all located between 27.5°S and 29.0°S, suggesting that at these latitudes the slab is still present in that depth range.

Finally, we just want to remark the importance to use locally recorded data to analyse detailed characteristics of the shape and the seismotectonic behaviours of the subducted Nazca plate along the South American margin. For instance, Cahill and Isacks (1992) using more than 20 years of events recorded at teleseismic distance had less resolution to follow the Wadati-Benioff zone in the region of Copiapó with respect to that obtained with some weeks of locally recorded microearthquakes.

ACKNOWLEDGEMENTS

This work was supported by FONDECYT N° 1981145 and IRD, France. We thanks to the Armada de Chile and SERNAGEOMIN for their valuable logistic support during the field work.

REFERENCES

Beck, S., S. Barrientos, E. Kausel and M. Reyes, 1997. In preparation.

Cahill, T. and B. Isacks, Seismicity and shape of the subducted Nazca plate, J. Geophys. Res., 97, 17,503-17,529, 1992

Lomnitz, C., Major earthquakes and tsunamis in Chile during the period 1535 to 1953. Geol. Rundsch, 59, 938-960, 1971

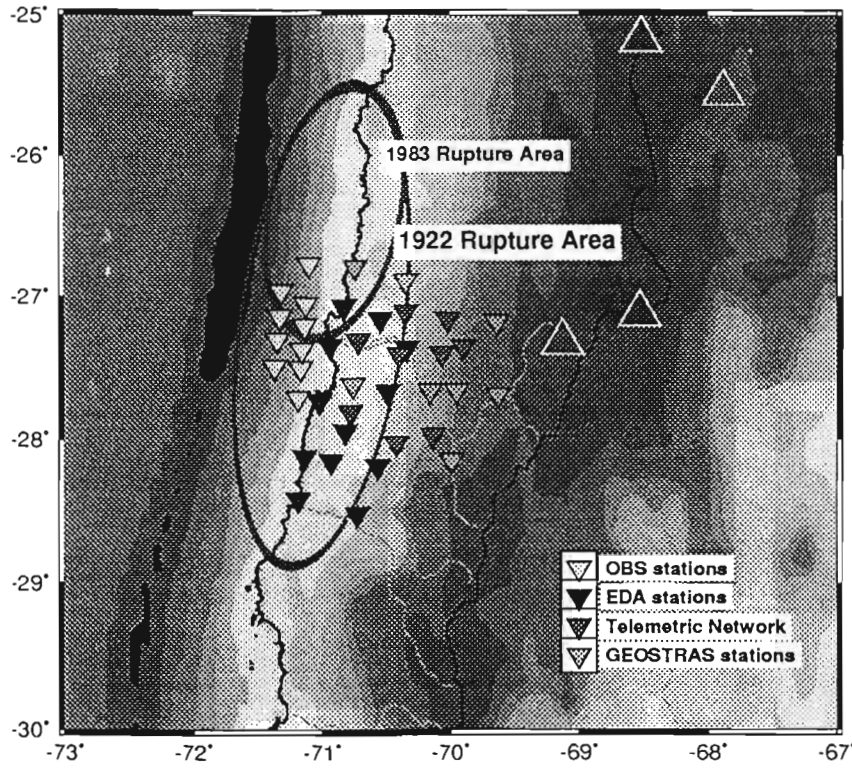

Figure 1.- Temporary inland and off-shore seismic stations (inverted triangles) around Copiapó region. The active volcanoes (triangles) and the estimated rupture areas of the 1922 and 1983 earthquakes (ellipses) are also shown.

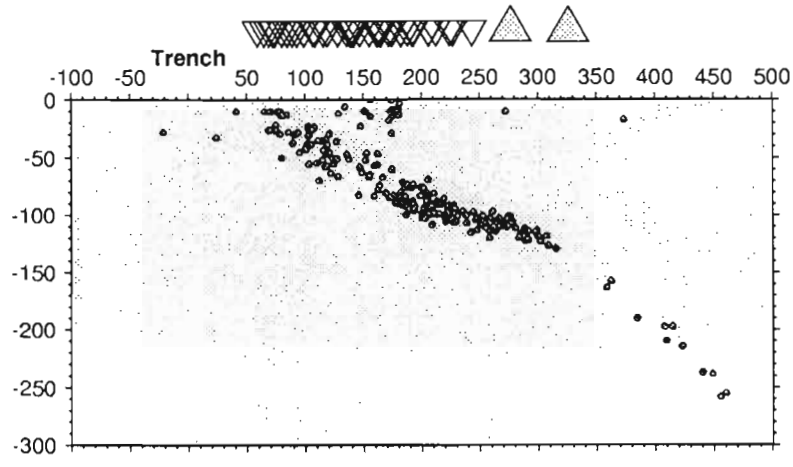

Figure 2.- Cross-section normal to the trench (27°S) with locally recorded data. The projection of the inland and off-shore stations (inverted triangles) and the active volcanoes is also shown

THE CRUSTAL STRUCTURE IN THE REGION OF THE 1997 CARIACO EARTHQUAKE, EASTERN VENEZUELA, BASED ON SEISMIC REFRACTION AND GRAVIMETRIC DATA

Rommel CONTRERAS (1), Michael SCHMITZ (2), Leonardo ALVARADO (2,3), Jesús CASTILLO (4), Stefan LÜTH (5)

(1) Universidad de Oriente, Cumaná, e-mail : rommel@re.udo.edu.ve
(2) Fundación Venezolana de Investigaciones Sismológicas, Caracas, e-mail:schmitz@funvisis.internet.ve
(3) Universidad Central de Venezuela, Facultad de Ciencias, Caracas, e-mail: joleonar@yahoo.com
(4) Universidad Simón Bolívar, Sartenejas, Caracas, e-mail: castillj@usb.ve
(5) Freie Universität Berlin, Fachrichtung Geophysik, Alemania, e-mail: stefan@geophysik.fu-berlin.de

KEY WORDS: Cariaco Earthquake, Aftershocks, Crustal Structure, Seismic Refraction, Gravimetry,

INTRODUCTION

The study region forms the easternmost part of the plate boundary between the Caribbean and South America plates with a relative plate motion of 1 to 2 cm/a. The July 9, 1997 Cariaco earthquake was located on the El Pilar Fault, a right lateral strike slip fault, which runs parallel to the southern border of the sedimentary basin of the Gulf of Cariaco. Damage was concentrated in the town of Cariaco, located in the western part of the valley, close to the Gulf of Cariaco, and surrounding villages, whereas Casanay, located close to the eastern end of the valley, suffered considerably less damage (figure 1).

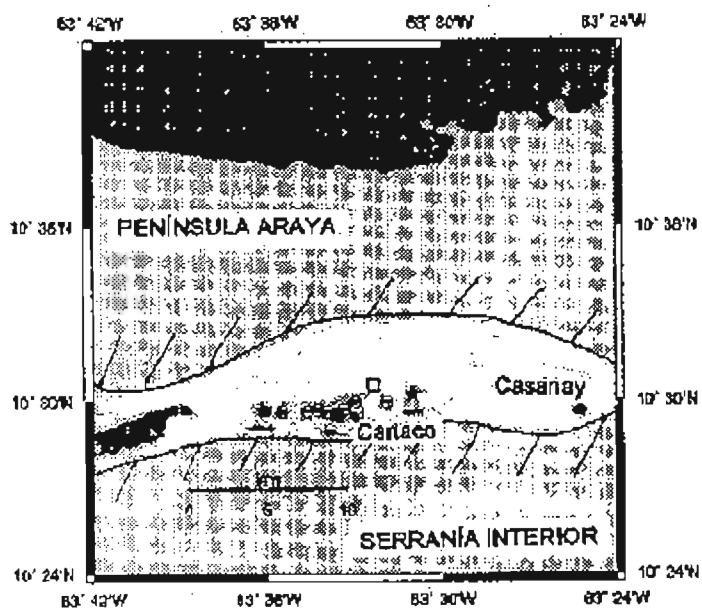

Figure 1. Map of the sedimentary basin of the Gulf of Cariaco (white), limited by the Araya Península (north) and the Interior Mountain Range (south). Station locations (circles) and shot-points (stars) of the record section displayed in figure 2, crossing the town of Cariaco; open square gives the location of the Cariaco earthquake. Caribbean Sea to the north and Gulf of Cariaco to the west (dark shaded areas).
We suppose that the damage pattern observed after the Cariaco earthquake is consistent with increasing thickness of unconsolidated, water saturated Quaternary sediments towards the Gulf of Cariaco in the west. The determination of the geometry of the sedimentary basin and the underlying basement structure are the main objectives of this study.

SEIMIC REFRACTION DATA

A net of 5 seismic refraction profiles crossing the Cariaco valley was realized in July 1998 for determination of the thickness of the Quaternary sediments. Profile lengths varied between 10 and 20 km, three of them within strike of the valley and two crossing perpendicular to the valley axis into the northern and southern, mainly Cretaceous, bedrock. 15 digital three component stations were deployed for recordings of detonations using between 5 and 20 kg of explosives each. Aftershock recordings, obtained by the international RESICA 97 ("Red Sismológica de Cariaco 1997") temporary deployment of 43 seismological stations, are used for the composition of seismic sections in order to know the basement structures and its seismic velocities.

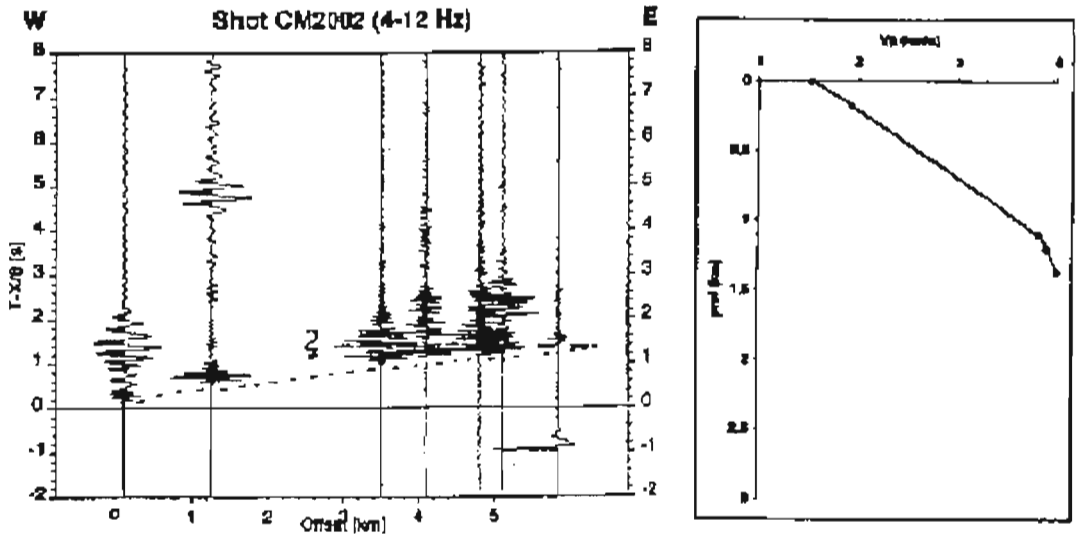

Figure 2. Seismic section of profile 2 (Campoma to Cariaco) with first arrivals from the sedimentary layers and a possible reflection from the base of the basin (left) and the corresponding velocity/depth – model (right).

CONCLUSIONS

Preliminary interpretations close to Cariaco (figs. 1 and 2) indicate up to 1.5 km thick Quaternary sediments with seismic velocities ranging between 1.5 and 3 km/s and bedrock velocities of more than 4 km/s. Available gravity data (Castillo et al., 1999) together with recent measurements will allow to model the density structure of the valley region using the seismic data as input.

Study partially funded by CONICIT S1-97002996 project.

REFERENCES

Castillo, J., Schmitz, M. , Alvarado, L., Lüth, S. y Sánchez, A., 1999. Determinación de la geometría de la Cuenca sedimentaria de Cariaco mediante el análisis de datos sísmicos de refracción y gravimétricos. VI Congreso Venezolano de Sismología e Ingeniería Sísmica, Mérida, 12 – 14 de Mayo de 1999, 5pp.

QUATERNARY DEFORMATIONS AND SEISMIC HAZARD AT THE ANDEAN OROGENIC FRONT (31°-33°, ARGENTINA): A PALEOSEISMOLOGICAL PERSPECTIVE

Carlos H. COSTA(1), Thomas K. ROCKWELL(2), Juan D. PAREDES(3) and Carlos E. GARDINI(4)

(1) Departamento de Geología, Universidad Nacional de San Luis, Chacabuco 917, 5700 San Luis, Argentina (costa@unsl.edu.ar)
(2) Department of Geological Sciences, San Diego State University, San Diego, CA 92182, U.S.A. (trockwel@geology.sdsu.edu)
(3) Departamento de Geología-INGEO, Universidad Nacional de San Juan-CONICET, Cereseto y Meglioli, 5400 San Juan (jparedes@unsj.edu.ar)
(4) Departamento de Geología, Universidad Nacional de San Luis-CONICET, Chacabuco 917, 5700 San Luis, Argentina (cgardini@unsl.edu.ar)

KEY WORDS: Central Andes, orogenic front, paleoseismology, neotectonics

INTRODUCTION

The primary zones of Quaternary deformation and seismogenic structures currently known in the argentinean territory between 31° and 33° South Latitude are located within a seismic belt defined between and including the Precordillera piedmont and the Western Pampean Ranges (Fig. 1). The most destructive earthquakes of the 20th century (M 7.4, 1944 San Juan and M 7.3 1977, Caucete) have been located within this region which not only concentrates the most significative records of historical and instrumental seismicity but also the most outstanding Quaternary deformations. The necessity of lengthening the short chronologic record provided by both historical and instrumental seismicity emphasizes the significance of paleoseismological studies focused on the dating and reconstruction of prehistorical seismic events.

The structural inhomogeneities along this latitudinal segment of the Precordillera foothills produce different surficial characteristics of Quaternary deformations. This, in turn, determines a variety of paleoseismic scenarios and accordingly different strategies to gather information on prehistorical earthquakes. North of 32° 15´, the main evidences of recent deformation are represented by west-verging thrusts in the Precordillera Oriental (Eastern Precordillera) related to deep, basement-involved faults of the Pampean foreland (Bastías et al., 1984; Comínguez and Ramos, 1990; Smalley et al., 1993). La Laja fault, whose last surface rupture took place during the 1944 San Juan earthquake, is the most conspicuous example among these structures. South of 32°15´, Andean deformation is influenced by pre-existing Mesozoic extensional structures and the primary faults verge east.

In this paper we examine two examples of Quaternary structures located within the refered region with the aim of illustrating different paleoseismic interpretations of active deformations.

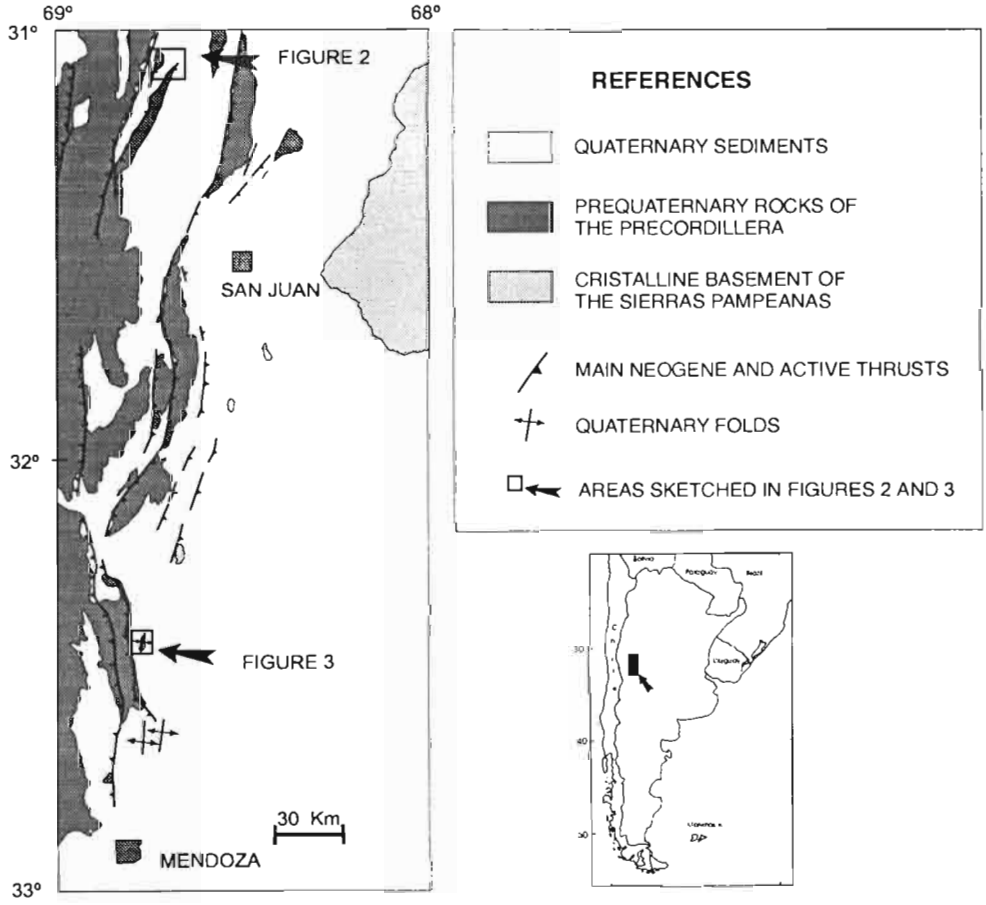

Figure 1: Location of main Neogene thrusts and folds in the Precordillera fold and thrust belt. Windows indicate location of Figs. 2 and 3.

BLANQUITOS-LOMAS DE LA DEHESA AREA, SAN JUAN PRECORDILLERA

Recent faulting is here characterized by a notorious linearity and parallelism of fault scarps affecting Quaternary bajadas in coincidence with bedding planes of the underlying Tertiary rocks. This is expresed by the west-verging Blanquitos, La Araña and La Bajada faults reverse faults (Bastías et al., 1984; Paredes et al., 1997), dipping 65°E to 70°E at surface (Fig. 2). These facts allow us to speculate that the refered structures are not primary rupture surfaces, but rather, a result of interbedding-slip. If so, there is probably a wide distribution of recent and ongoing fault displacements which should be expected along this area. This interbedding-slip could also be expressed as flexural-slip in secondary fractures associated to La Dehesa fault. Conversely, these faults may have a different geometry and much less individual displacement than the main shock source.

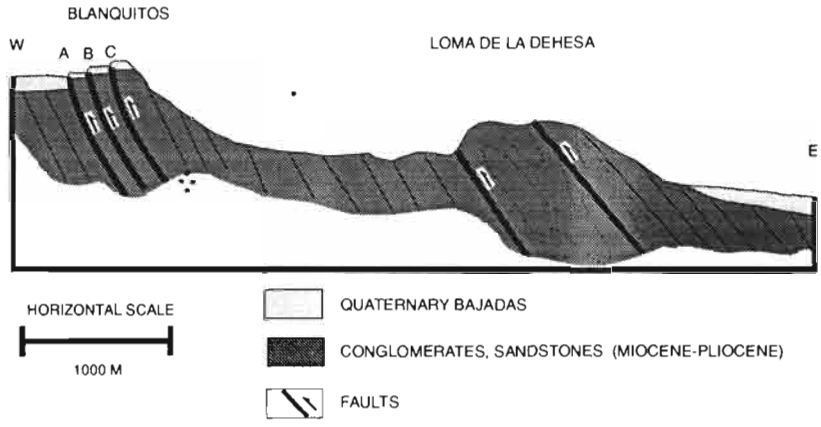

Figure 2: Simplified cross-section of Blanquitos-Loma de la Dehesa area. A. Blanquitos; B. La Araña and C. La Bajada faults. Modified from Paredes et al., 1997.

MONTECITO ANTICLINE, MENDOZA PRECORDILLERA

Quaternary thrusts at the Sierra de Las Peñas thrust front (Fig. 1) have not yet become fully emergent in the alluvial cover of the Andean piedmont and there is a remarkable interaction among fault propagation, alluvial sedimentation, stratal rotations and monocline scarp formation (Costa et al., in press). Eastward of the Las Peñas thrust, Quaternary fault-propagation folding have resulted in the development of the Montecito anticline, deflecting current fluvial systems and warping the piedmont alluvial cover. Offlap relationships among strata exposed at the western limb of Montecito anticline (Fig. 3) suggest an uplift rate higher than the sedimentation rate.

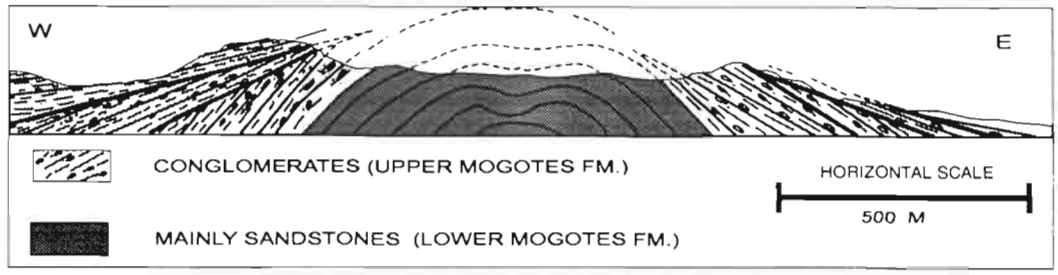

Figure 3: Sketched profile across the Montecito anticline showing offlaps relationships in the Upper Mogotes Formation (Pleistocene). Adapted from Costa et al., in press.

CONCLUDING REMARKS

The active front of the Central Andes in Argentina poses interesting challenges for reconstructing the Quaternary paleoseismic record. In the examples examined; an underestimation of the maximum event size would be obtained at the Blanquitos-La Dehesa area, if empirical relationships (i.e. rupture length and amplitude) were used for quantifying the surface slip data. This fact could also help to explain the 30 cm of instantaneous coseismic surface rupture of La Laja fault during the 1944 M 7.4 San Juan earthquake, which is minor than predicted by empirical data.

No surface ruptures have been identified at the Montecito anticline. Hence, some paleoseismological criteria such as the resolution of event horizons related to past surface ruptures are not useful for addressing these problems or they might provide misleading interpretations when attempting to reconstruct the paleoseismic record. However, coseismic folding could result in sudden changes in uplift rate vs sedimentation rate relationships, which in geomorphic settings with high sedimentation rates might give rise to a sequence of offlap, onlap and eventually overlap. It is understood that paleoseismic reconstructions in these settings may arise from careful descriptions of growth strata and progressive unconformities located at both limbs of Quaternary folds as well as from detailed geomorphologic mapping. Besides it would provide opportunities for testing suggested relatioships between folding and sedimentation (Burbank and Vergés, 1994) in active depositional systems.

REFERENCES

Bastías, H., Weidmann, N., y Pérez, M., 1984, Dos zonas de fallamiento Plio-Cuaternario en la Precordillera de San Juan. 9° Congreso Geológico Argentino Actas, 2, 329-341.

Burbank, D. and Vergés, J. 1994. Reconstruction of topography and related depositional systems during active thrusting. Journal of Geophysical Research. 99, 20.281-20.927.

Comínguez, A. y V. Ramos, 1990. Sísmica de reflexión profunda entre Precordillera y Sierras Pampeanas. 11° Congreso Geológico Argentino Actas 2, 311-314.

Costa, C., Gardini, C., Diederix, H. and Cortés, J., in press. The Andean Orogenic Front at Sierra de Las Peñas - Las Higueras, Mendoza, Argentina. Journal of South American Earth Sciences, 12.

Paredes, J. , Perucca L. y Tello, G – 1997. Fallamiento Cuaternario en el área Blanquitos, Departamento Ullum, San Juan, Argentina. 2° Jornadas de Precordillera Actas, 168-173.

Smalley, R. Jr., J. Pujol, M. Regnier, J.M. Chiu, J. L Chatelain, B.L. Isacks, M. Araujo and N. Puebla. 1993. Basement seismicity beneath the Andean Precordillera thin-skinned thrust belt and implications for crustal and lithosferic behavior. Tectonics, 12, 63-76.

CENOZOIC DEFORMATION AND TECTONIC STYLE OF THE PUNA PLATEAU (NORTHWESTERN ARGENTINA, CENTRAL ANDES)

Isabelle COUTAND (1), Peter COBBOLD (1), Annick CHAUVIN (1), Eduardo ROSSELLO (2), Oscar LOPEZ-GAMUNDI (3)

(1) Géosciences-Rennes (UPR-CNRS 4661), Université de Rennes I, 35042 RENNES cedex, FRANCE
Isabelle.Coutand@univ-rennes1.fr
(2) CONICET, Dpto de Ciences Geológicas, Universidad de Buenos Aires, 1428 Buenoa Aires, ARGENTINA
(3) Texaco Inc., International Exploration Division, 4800 Fournace place, Bellaire, 77401-2324 Texas, USA.

KEY WORDS : Puna plateau, intermontane basins, Cenozoic deformation, tectonic style.

INTRODUCTION AND GEOLOGICAL SETTING

The Puna plateau of Northwestern Argentina (22°00'S-26°30'S and 65°30'W-68°00'W) is the southernmost segment of the Central Andean high plateau (Fig. 1). It results from convergence between the oceanic Nazca plate and continental South America along an ENE-WSW direction, which has remained stable since about 49 Ma (*Pardo-Casas & Molnar, 1987*). The Puna plateau has an average elevation of 4400m. Its crust is up to 80 km thick (*Wigger et al., 1994; Beck et al., 1996*), mainly as a consequence of horizontal tectonic shortening (*Allmendinger et al., 1997; Lamb & Hoke, 1997*). The Puna plateau is a composite feature, where Precambrian and Paleozoic basement ranges, bounded by high-angle reverse faults, alternate with Cenozoic intermontane basins. Major thrusts, trending NNE-SSW, are distributed all over the plateau and verge alternatively eastward or westward. Our structural interpretation of the area is based on field observations, satellite imagery, kinematic analysis of fault data, measurements of Anisotropy of Magnetic Susceptibility (AMS) and analysis of seismic reflexion data.

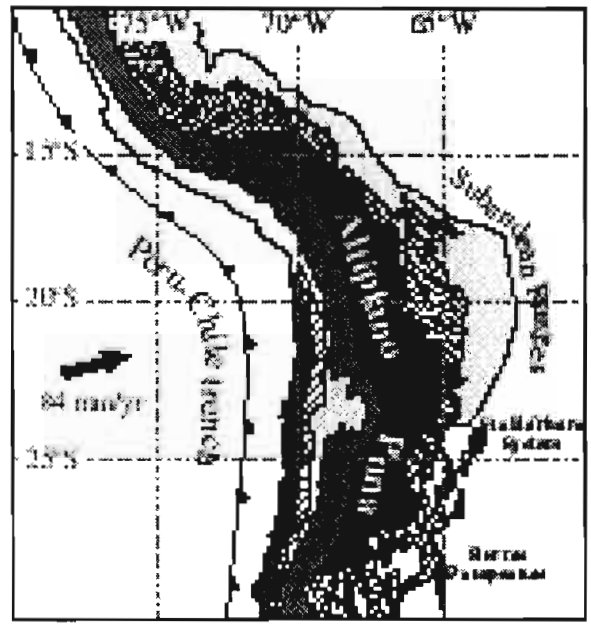

Fig.1 : Map showing the morpho-structural units of the Central Andes and the location of the Puna plateau.

FAULT KINEMATICS AND AMS DATA

In order to constrain the orientations of principal strains over the area, we have measured over 900 striated fault planes at 62 localities throughout the Puna and adjacent Eastern Cordillera. Localities are in Mesozoic and Cenozoic sedimentary cover, mainly along the edges of intermontane basins. A graphical and kinematic method has been used to analyze fault-slip data. On this basis, the principal directions of Cenozoic strain have rather uniform trends over the area. The longest axes of the strain ellipsoid ($\lambda 1$) are subvertical; the shortest ($\lambda 3$) are subhorizontal and trend WNW-ESE to NW-SE; the intermediate axes ($\lambda 2$) are subhorizontal and trend NNE-SSW to NE-SW. Thus the shortest axes are perpendicular to the major thrusts. Furthermore, the strain ellipsoids are of plane-strain shape. We infer that the thrusts are mainly dip-slip faults. The shortest axes are strongly oblique to the vector of relative motion between Nazca and South America. According to new paleomagnetic results obtained throughout the Puna (*Coutand, 1999; Coutand et al., in press*), fault blocks have been rotated clockwise about vertical axes. We attribute these rotations to scissoring on major thrusts and also to oroclinal bending of the orogen as a whole (*Coutand, 1999*). We have used the Anisotropy of Magnetic Susceptibility (AMS) at 28 sites (grouped into 10 localities) within Cenozoic red sediments across the Puna (*Coutand, 1999; Coutand et al., in press*), the northern bolivian Altiplano (*Roperch et al., submitted*) and the northern Sierras Pampeanas (*Aubry et al., 1996*). The AMS data show well-developed magnetic lineations, which are attributed in part to regional horizontal shortening (*Aubry et al., 1996; Coutand et al., in press; Roperch et al., submitted*). On removing tectonic rotations about vertical axes, inferred from paleomagnetic data, we obtain the shortening directions recorded by the sediments during their magnetization. These shortening axes form a radial pattern around the eastern edge of the Central Andes (Fig. 2). They trend WSW-ENE in northern Bolivia, along the axial plane of the Arica deflection; E-W, around 25°S; and NW-SE, along the southeastern edge of the Puna plateau. We attribute this pattern to an inhomogeneous stress field, reflecting the outwardly convex eastern side of the Central Andes.

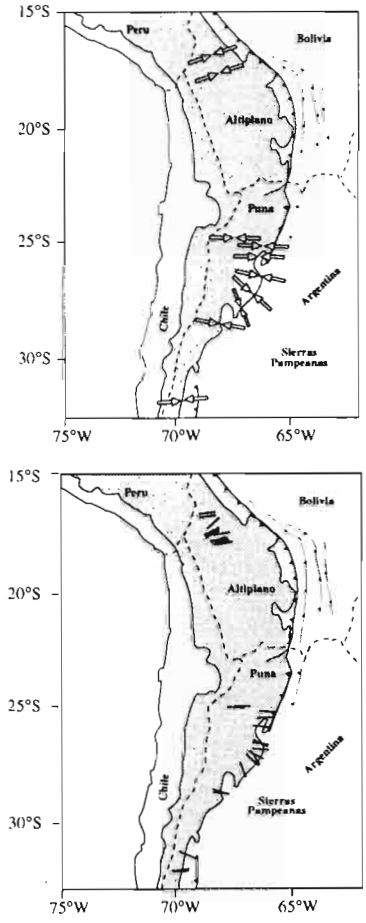

Figure 2: Central andean radial pattern of horizontal shortening axes deduced from AMS data. Black lines (white arrows) indicate the orientation of the intermediate axes of AMS tensors corrected from associated vertical-axes rotations, for each site (locality).

CROSS-SECTIONS BASED ON SEISMIC REFLEXION DATA

We have had access to industrial seismic reflexion data, acquired throughout internal basins of the northern Puna (from the Bolivian border to the Salinas Grandes). These data provide major constraints on basin structure and sediment chronology. Of greatest interest are two seismic lines, trending WNW-ESE across the Tres Cruces basin (Fig. 3). This basin is about 100 km South of La Quiaca and its sedimentary infill is of Mesozoic to Cenozoic age. At the base of the Cenozoic (Fig. 4) is the Casa Grande Fm., of Middle to Upper Eocene age (*Fernández et al., 1973*), where red sandstones and mudstones alternate, forming a sequence up to 800 m thick (*Boll & Hernández, 1985*). Unconformably overlying this is the Rio Grande Fm. (*Pascual et al., 1978*), an Oligocene sequence of conglomeratic and coarse-grained sandy layers, up to 2000 m thick (*Boll & Hernández, 1986*). It is unconformably overlain by the Pisungo Fm. (*Pascual et al., 1978*), a 2000 m thick sequence of alluvial fan deposits, Lower to Middle Miocene in age (*Boll & Hernández, 1986*). Unconformably overlying them again is the Sijes Fm. (*Turner, 1960*) a pyroclastic unit which is sealed at the top by the Pan de Azúcar dacites, dated at 12±2 Ma by K/Ar on whole rock (*Coira., 1979*). Seismic reflectors are constrained by surface outcrops. In addition, massive calcareous layers of the Maestrichtian Yacoraite Fm. (Balbuena Subgroup), which yield characteristically bold reflections, provide a template for our interpretation. We infer that the Tres Cruces basin has developed in the footwall of a major eastwards-verging thrust, which runs along the eastern edge of the Sierra de Aguilar (Fig. 5). There are large variations along strike. For example, fault-bend folds in the South (line 2) are not visible 15 km farther North (line 1). The progressive thickening of Cenozoic strata toward the thrusts and the marked upward increases in the dips of the thrusts provide evidence for synsedimentary thrusting. These features are observed in strata of the Casa Grande Fm., Upper Eocene in age (Fig. 5b). Thus compressional tectonics may have been ongoing as early as the Upper Eocene, in this eastern part of the orogen.

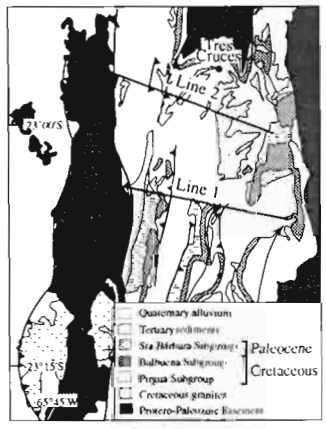

Figure 3: Geological and structural map of the Tres Cruces basin showing the approximate location of seismic lines n°1 and 2.

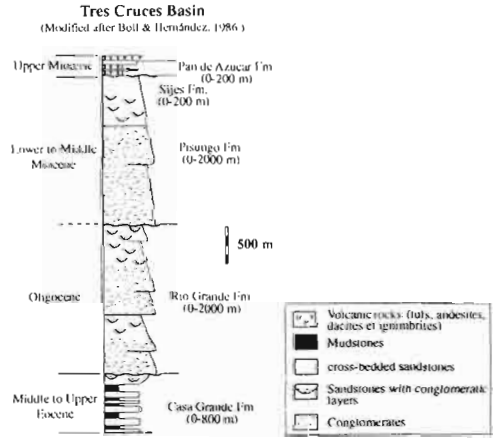

Figure 4: Stratigraphic column of the Cenozoic deposits of the Tres Cruces basin (excepted the Paleocene Sta Bárbara Subgroup).

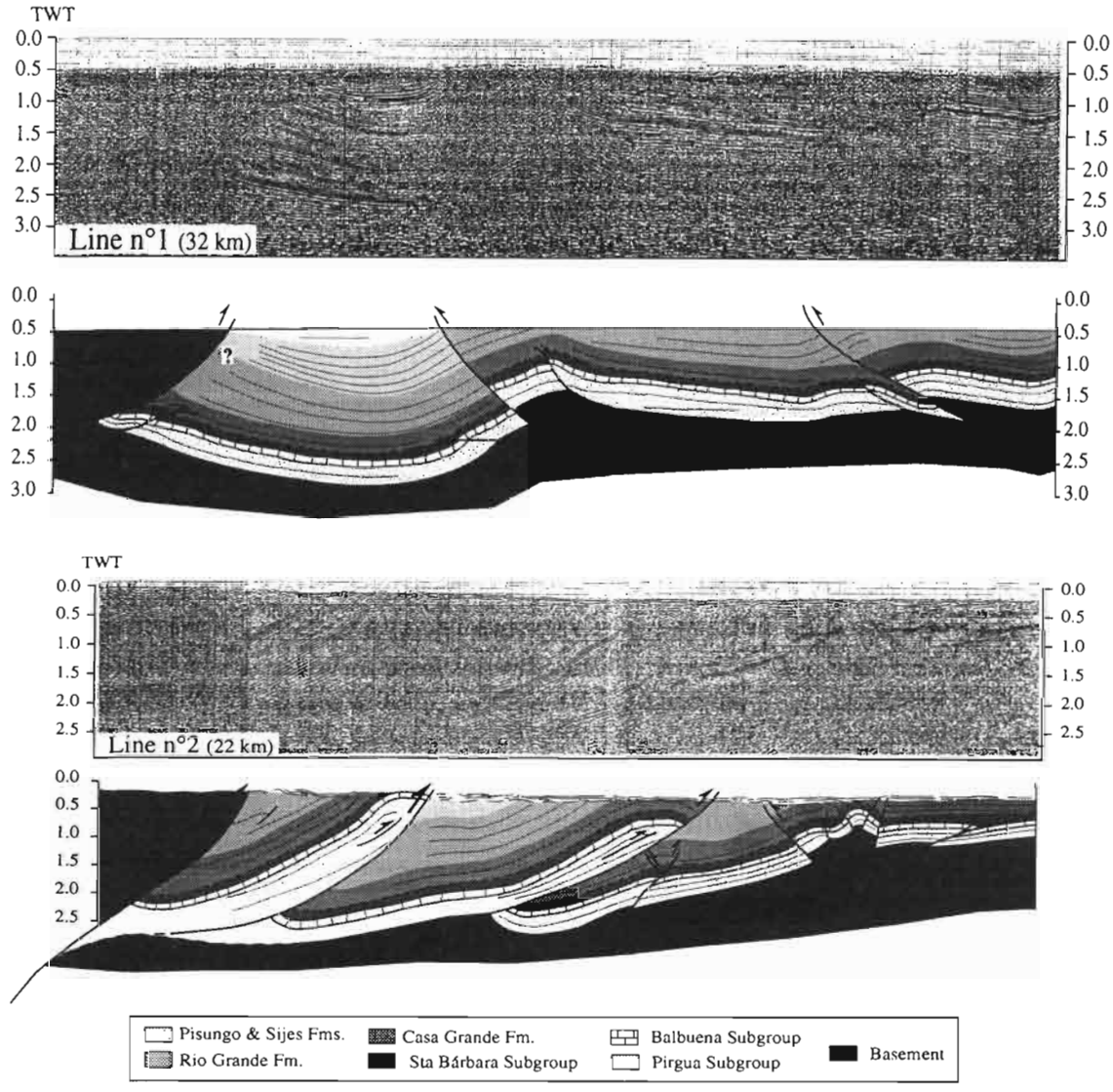

Figure 5: Seismic reflexion lines n°1 and 2 and their interpretations. Scaled in Two way Travel Time.

CONCLUSIONS

At the scale of the Central Andes, AMS data indicate that shortening axes form a radial pattern around the eastern edge of the orogen. This pattern is attributed to an inhomogeneous stress field, reflecting the outwardly convex eastern side of the Central Andes. At the scale of the Puna, field observations and analysis of fault-slip data indicate that thrusts are mainly dip-slip faults which do not show significant right-lateral strike-slip component, as classically expected for this part of the orogen. Finally, it has been suggested that shortening and thickening in the Puna accumulated mainly during the Neogene

(*Allmendinger et al., 1983; Jordan & Alonso, 1987*). According to our data, the process probably was underway as early as the Upper Eocene.

REFERENCES

Allmendinger, R. W., V. A. Ramos, T. E. Jordan, M. Palma, and B. L. Isacks, 1983, Paleogeography and Andean structural geometry, northwest Argentina: Tectonics, v. 2, p. 1-16.

Allmendinger, R. W., T. E. Jordan, S. M. Kay, and B. L. Isacks, 1997, The evolution of the Altiplano-Puna plateau of the Central Andes: Annu. Rev. Earth Planet. Sci., v. 25, p. 139-174.

Aubry, L., P. Roperch, M. d. Urreiztieta, E. A. Rossello, and A. Chauvin, 1996, Paleomagnetic study along the south-eastern edge of the Altiplano-Puna Plateau: Neogene tectonic rorations: J. Geophys. Res., v. 101, p. 17,883-17,899.

Beck, S. L., G. Zandt, S. C. Myers, T. C. Wallace, P. G. Silver, and L. Drake, 1996, Crustal thickness variations in the Central Andes: Geology, v. 24, p. 407-410.

Boll, A., and R. M. Hernández, 1986, Interpretacion estructural del area Tres Cruces: Boletin de Informaciones Petroleras, v. Tercera Epoqua, p. 2-14.

Coira, B. L., 1979, Descripción geológica de la hoja 3c, Abra Pampa, Buenos Aires, Servicio Geologico Nacional.

Coutand, I., P. Roperch, A. Chauvin, P. R. Cobbold and P. Gautier, Vertical-axis rotations across the Puna plateau (Northwestern Argentina) from paleomagnetic analysis of Cretaceous and Cenozoic rocks : J. Geophys. Res. (Accepted, March 1999).

Coutand, I., 1999, Tectonique Cénozoique du Haut Plateau de la Puna, Nord-Ouest argentin, Andes Centrales: Thèse de Doctorat, Université de Rennes, pp. 401.

Fernández, J., P. Bondesio, and R. Pascual, 1973, Restos de Lepidosiren Paradoxa (Osteichthyes, Dipnoi) de la F. Lumbrera (Eógeno, Eoceno) de Jujuy. Consideraciones estratigráficas, palcoecológicas y paleozoogeográficas: Ameghiniana, Buenos Aires, v. X, p. 152-172.

Jordan, T. E., and R. N. Alonso, 1987, Cenozoic stratigraphy and basin tectonics of the Andes Mountain, 20°-28° South latitude: Am. Assoc. Petrol. Geol. Bull., v. 71, p. 49-64.

Lamb, S., and L. Hoke, 1997, Origin of the high plateau in the Central Andes, Bolivia, South America: Tectonics, v. 16, p. 623-649.

Pardo-Casas, F., and P. Molnar, 1987, Relative motion of the Nazca (Farallón) and South American Plates since Late Cretaceous time: Tectonics, v. 6, p. 233-248.

Pascual, R., M. G. Vucetich, and J. Fernández, 1978, Los primeros mamíferos (Notoungulata, Henricosborniidae) de la Formación Mealla (Grupo Salta, Subgrupo Santa Bárbara). Sus implicancias filogenéticas, taxonómicas y cronológicas: Ameghiniana, v. XV, p. 366-390.

Turner, J. C. M., 1960, Estratigrafía de la Sierra de Santa Victoria y adyaciencas: Bol. Acad. Cienc. Córdoba, v. 41, p. 163-196.

Wigger, P., M. Schmitz, M. Araneda, G. Asch, and S. Baldzuhn, 1994, Variation in the crustal structure of the southern Central Andes deduced from seismic refraction investigations, in K. J. Reutter, E. Scheuber, and P. J. Wigger, eds., Tectonics of the Southern Central Andes: Structure and Evolution of an Active Continental Margin, Berlin, Springer-Verlag, p. 23-48.

AGE AND PETROLOGY OF TUSAQUILLAS PLUTONIC COMPLEX (CENTRAL ANDES): INFERENCES ON THE EVOLUTION OF CRETACEOUS RIFT IN NW ARGENTINA

Chiara CRISTIANI(1), Aldo DEL MORO(2), Massimo MATTEINI(3), Roberto MAZZUOLI(4) and Ricardo OMARINI(3)

(1) Minerogenesi e Geochimica applicata CNR, Via G. La Pira 4, 50121 Firenze (Italy)

(2) Geocronologia e Geochimica Isotopica CNR, Via Cardinale Maffi 36, 56127, Pisa (Italy)

(3) Facultad de Ciencias Naturales, UNSa, 4400, Salta (Argentina)

(4) Dipartimento di Scienze della Terra, Via S. Maria 53, 56100 Pisa (Italy) (mazzuoli@dst.unipi.it)

KEY WORDS: age, petrology, Tusaquillas, Pluton, Central Andes.

INTRODUCTION

A widespread magmatism related to a important extensional rift-type fracturing episodes affected South America continental plate from Upper Jurassic-Lower Cretaceous time (UJ-LC). The products of this alkaline magmatism constitute a belt that extends discontinuously with North-South direction from the Cordoba Province (Central Argentina; 32°S-64°W) up Velasco Province (South Bolivia; 18°S-62W) (Kay and Ramos, 1996; Fletcher and Beddoe-Stephens 1987). In the NW Argentina the UJ-LC magmatism is characterised by femic volcanic products and intrusive granitic and alkali-syenitic rocks (Viramonte and Rapela, 1991). The UJ-LC intrusive rocks, exposed on the Puna plateau (22-24°S, 65-67°W) are characterised by alkaline stocks, like Rangel, Hornillos and Fundiciones, and large calcalkaline batholiths, like Tusaquillas, Abra Laite and Aguilar. A geological sketch map of the Central-Eastern sector of the Puna plateau is show in figure 1 (modified after Reutter et al., 1994). According to

Viramonte and Rapela (1991) the intrusive products are linked to an early rifting stage (130-100 Ma). In this paper we present new geochemical and geochronological data on Tusaquillas Plutonic Complex (23°S-66°W) which is considered the most important intrusive body belonging to this rift-related magmatism. These data could contribute to the knowledge of the Mesozoic magmatism of the Central Andes that is of crucial importance to understand the geo-tectonic evolution of this sector of South America.

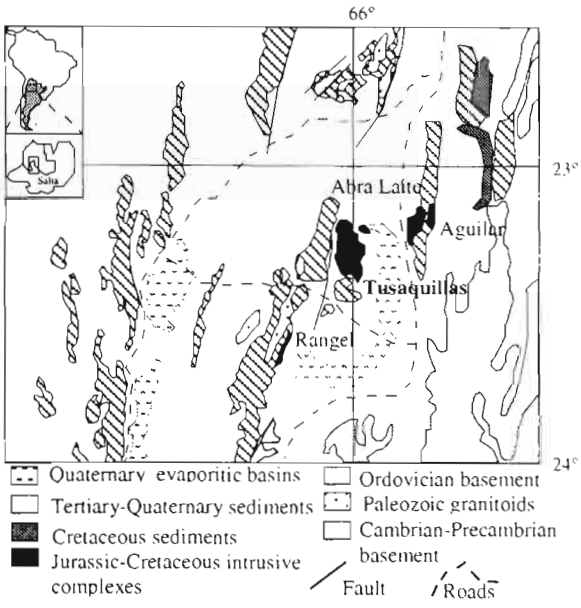

Fig. 1

Petrography and Geochronology of Tusaquillas Plutonic Complex

The Tusaquillas Plutonic Complex is constituted by intrusive bodies with different geochemical and petrological characteristics: (1) Tusaquillas Batholit (TB), characterised entirely by peraluminous granitic rocks ; (2) Castro Tolay Stocks (CTS), constituted mainly by basic-intermediate rocks and by granitic tabular intrusions. In the (Y+Nb) vs Rb and (Fe0tot/Mg0) vs (Zr+Nb+Ce+Y) discriminating diagrams (Pearce et al., 1984; Whalen et al., 1987) the TB rocks show S- and I-type granites features, whereas CTS products show within-plate and anorogenic characteristics. Representative Rb-Sr Tusaquillas Plutonic Complex ages, determined on the pairs biotite-whole rock, and the isotopic whole-rocks ratios of Sr and Nd are reported in tables 1 and 2.

Discussion and Conclusions

The new ages determination evidenced that the Tusaquillas Plutonic Complex emplaced in a range of time between 152 Ma and 140 Ma. The Palaeozoic ages reported for some of the CTS rocks (Zappettini 1989) must be therefore rejected. Up to now basic-intermediate intrusive rocks rift-related were not know in Central Andes. The younger age of Tusaquillas Plutonic Complex could be correlated with the eruptions of Paranà basaltic products, which occurred between 137 Ma and 127 Ma (Turner et al., 1994). Similar ages are reported for the emplacement of subvolcanic complexes of Damaraland in Namibia and some anorogenic complex in Namaqualand, South Africa (De Beer and Armstrong; 1998). The UJ-LC magmatism in South America, which extends from southern Brazil into Paraguay and Bolivia, is related to the South Atlantic opening. We suppose that also the Tusaquillas intrusive products and the UJ-LC

magmatism of NW Argentina are related to the opening phase of South Atlantic. The age, the within-plate and anorogenic features of the Hornillos and Rangel rocks (Menegatti et al., 1997; Rubiolo, 1997) suggest that these products are linked to the same rifting phase.

The low ($^{87}Sr/^{86}Sr$)i and preliminary ($^{143}Nd/^{144}Nd$)i values of basic rocks of CTS suggest a mantellic origin for these magmas (Tables 1 and 2). The relatively high values ($^{87}Sr/^{86}Sr$)i of granitic rocks of CTS could reflect a mixing or contamination process with crustal materials. All the chemical date and preliminary ($^{143}Nd/^{144}Nd$) i on the granites of TB suggest that these granites could have been originated for a partial melting process of continental crust. Tentatively we explain this partial melting process triggered by the intrusion in the crust of gabbroic subcrustal magma, during the Upper Jurassic-Lower Cretaceous rifting phase.

Samples		Rb (ppm)	Sr (ppm)	$^{87}Rb/^{86}Sr$	$^{87}Sr/^{86}Sr \pm 2SE$	Age±sd (Ma)	I.R. (150Ma)
Castro Tolay Stock							
T6	WR	27	426	0.18	0.70392±2	-	0.70353±2
T11	WR	202	354.0	1.65	0.70789±5	-	0.70437±6
	Bt	847	11.4	223.9	1.16450±3	145±1	
T30	WR	156	623	0.72	0.70732±1	-	0.70578±2
T31	WR	44	487.0	0.26	0.70450±1	-	0.70394±1
	Bt	271	24.2	32.48	0.77375±11	151±2	
T34	WR	155	347.0	1.29	0.71142±2	-	0.70866±3
	Bt	520	7.3	215.86	1.1750±1	152±2	
T36	WR	150	160.0	2.71	0.71220±2	-	
T70	WR	196	65.1	65.1	0.71822±3		
T73	WR	201	448	1.3	0.70706±1	-	0.70429±3
T79	WR	132	170	2.24	0.71798±4	-	0.71319±6
T83	WR	177	255	2.01	0.71378±2	-	0.70950±5
Tusaquillas Batholith							
T25	WR	362	16.6	63.66	0.82947±4		
T28	WR	456	14.0	96.03	0.93824±2	-	
	Bt	2412	2.9	4067.42	10.206±12	145±1	
T40	WR	420	27.7	44.23	0.78961±5		
T69	WR	430	15.2	83.15	0.87902±2	-	
	Bt	1781	12.0	471.6	1.6762±2	144±2	
T100	WR	329	34.0	28.19	0.76953±2	-	
	Bt	1401	5.8	808.91	2.3270±2	140±1	

Table 1: Representatives Rb-Sr ages and isotopic ratios for Tusaquillas Plutonic Complex rocks ($^{87}Sr/^{86}Sr$ initial values are calculated at 150 Ma).

Samples		Sm (ppm)	Nd (ppm)	$^{147}Sm/^{144}Nd$	$^{143}Nd/^{144}Nd$ ±2SE	eps Nd	I.R (150 Ma)
Castro Tolay Stock							
T11	WR	9.8	53.3	0.111	0.512617±10	1.23±.25	0.512508±12
T31	WR	5.7	25.4	0.136	0.512675±09	1.89±.25	0.512542±09
T34	WR	12.4	71.0	0.106	0.512389±10	-3.11±.24	0.512285±11
Tusaquillas Batholith							
T19	WR	6.8	30.7	0.134	0.512447±10	-2.52±.27	0.512316±15
T28	WR	3	11.4	0.154	0.512482±07	-2.32±.25	0.512326±09
T69	WR	4.5	17.2	0.158	0.512445±15	-3.03±.36	0.512290±13

Table 2: Representatives Sm-Nd isotopic ratios for Tusaquillas Plutonic Complex rocks ($^{143}Nd/^{144}Nd$ initial values are calculated at 150 Ma).

REFERENCES

Avila Salinas, W.A 1989. Fases diastroficas y magmatismo Jurasico-Cretaceo en Bolivia. Boletin del Servicio Geologico de Bolivia Serie A-Vol. IV, 1:47-68

De Beer, C.H. and Armstrong, R.A.1998. Age and Tectonic setting of a Mesozoic Anorogenic Complex West of Bitterfontein, Namaqualand, South Africa. Abstracts of International Volcanological Congress (IAVCEI), 15.

Fletcher, C.J.N. and Beddoe-Stephens, B., 1987. The petrology, chemistry and crystallization history of the Velasco alkaline province, eastern Bolivia. In: J.G. Fitton andB.G.J. Upton (Ed.^Eds.), Alkaline Igneous Rocks. Geological Society Special Publication, 403-413.

Kay, S.M. and Ramos, V.A., 1996. El magmatismo Cretacico de Las Sierras de Cordoba y sus implicancias tectonicas. XIII Congreso Geologico Argentino y III Congreso de Exploracion de Hidrocarburos, Actas III: 453-464.

Menegatti, N., Omarini, R., Del Moro, A. and Mazzuoli, R., 1997. El granito Alcalino de la Sierra de Rangel (Cretacico inf.) Provincia de Salta, Argentina. Actas VIII Congreso Geologico Chileno, II: 1379-1384.

Pearce, J.A., Harris, N.B.W. and Tindle, A.G., 1984. Trace element discrimination diagrams for the tectonic interpretation of the Granitic Rocks. J. Petrol., 25: 956-983.

Reutter, K.J., E. Scheuber and P.J. Wigger, 1994. Geological map of the Central Andes, between 20° and 26°S. In: K.J. Reutter, E. Scheuber and P.J. Wigger (Ed.^Eds.), Tectonics of Southern Central Andes.Structure and evolution of an Active Continental Margin. Springer-Verlag, Berlin, 121-139.

Rubiolo, D., 1997. Alkaline rocks in Central Andes from NW Argentina and Bolivia: tectonic implication. Actas VIII Congreso Geologico Chileno, II: 1379-1384.

Turner, S., Regelous, M., Kelley, S., Hawkesworth, C. and Mantovani, M. 1994. Magmatism and continental break-up in the South Atlantic: high precision ^{40}Ar-^{39}Ar geocronology. Earth and Planetary Science Letters, 121: 333-348.

Viramonte, J.G. and Rapela, C.W., 1991. Cretaceous rift of the northwestern Argentina and the northwestern limit of the pampean ranges.

Whalen , J.B., Currie, L.K. and Chappel, W.B., 1987. A-type granites: geochemical characteristics, discrimination and petrogenesis. Contrib. Mineral. Petrol, 95: 407-419.

Zappettini, E.O., 1989. Geologia y metalogénesis de la region comprendida entre la localidades de Santa Ana y Cobres, Pcias. de Jujuy y Salta. Rep. Argentina. In: (Ed.^Eds.), Univ. de Buenos Aires. Tesi Doctoral. Inedito:180p.

NEOGENE EVOLUTION OF THE MAIN ECUADORIAN FORE-ARC SEDIMENTARY BASINS AND SEDIMENT MASS-BALANCE INFERENCES

Yann DENIAUD [1], Patrice BABY [2], Christophe BASILE [1], Martha ORDOÑEZ [3], Georges MASCLE [1] and Galo MONTENEGRO [3]

(1) CNRS-UPRES 5025 – 15 Rue M. Gignoux 38031 Grenoble, FRANCE (ydeniaud@ujf-grenoble.fr ; cbasile@ujf-grenoble.fr ; gmascle@ujf-grenoble.fr)
(2) IRD - PETROPRODUCCION – Apartado 1712857 Quito Ecuador (pbaby@pi.pro.ec)
(3) PETROPRODUCCION - Via a Salinas km 6 ½ Guayaquil ECUADOR (cigq@telconet.net)

KEY WORDS : Fore-arc, Neogene, Ecuador, stratigraphy, sediment mass-balance

INTRODUCTION

The Ecuadorian fore-arc region, known as the physiographic "Coastal Region", is characterised during Neogene times by the development of four sedimentary basins that are from North to South : the Borbon basin, the Manabi basin, the Progreso basin and the Gulf of Guayaquil basin (fig. 1). All these basins are related to dextral shear affecting the coastal region in response to the oblique subduction at the Ecuadorian trench. In three of them (Manabi, Progreso and Gulf of Guayaquil), extensive hydrocarbon exploration and cartography have been carried out by different petroleum companies, Ecuadorian administration and authors (among others Faucher and Savoyat 1973 ; Baldock, 1982 ; Evans and Whittaker, 1982). This yields to numerous data upon the Neogene deposits of these basins although different stratigraphy and formations names were applied. We present and discuss in this paper the tectono-stratigraphic evolution and correlation, as well as the sediment mass-balance calculation, that we have inferred from our work as part of the cooperation convention between the Ecuadorian state petroleum company PETROPRODUCCION and the IRD (French Research Institute for the Development in cooperation).

NEOGENE FORE-ARC TECTONO-STRATIGRAPHY

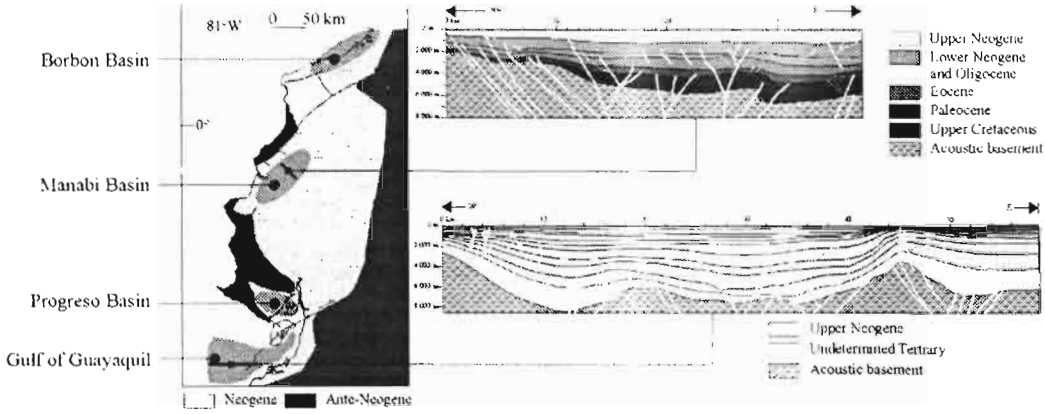

Fig 1 : Localisation and cross sections of the main Neogene Fore-arc Basins

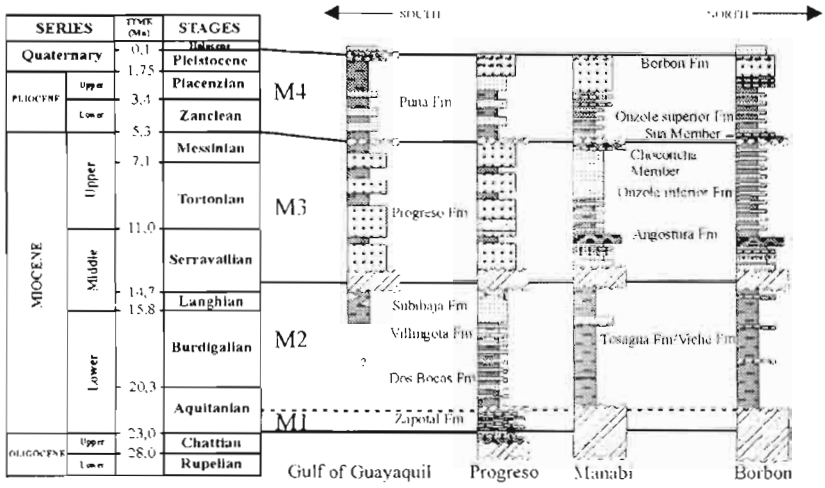

Fig 2 : Correlation between litho-stratigrafic columns of the main ecuadorian fore-arc basins

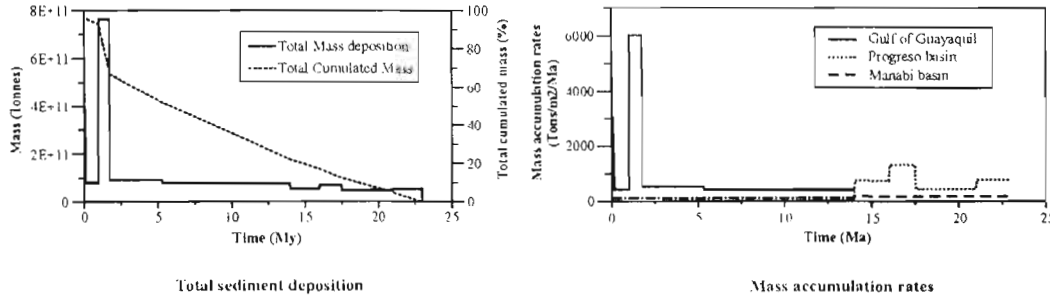

Fig 3 : Total net sediment deposition and Mass accumulations rates in the main Ecuadorian forearc sedimentary basins

The stratigraphy of the Ecuadorian fore-arc sedimentary basins may be divided in 4 mega-sequences, namely M1 to M4, separated by unconformity and possible hiatus (fig. 2). The M1 sequence is formed by conglomerate, sandstone and clay in granulometric decreasing sequences, and corresponds to the Zapotal Formation that is only known in the Progreso basin. His age is referred to the basal Lower Miocene. This sequence is related to the opening stage of the Progreso Basin in a close to North-South extensional trend. The M2 sequence is a rich clayey marine transgressive sequence that reaches 2000-3000 m in the Progreso basin (Dos Bocas, Villingota and Subibaja Formations); and 1000 m in the Manabi and Borbon basins (Tosagua and Viche Formations, respectively). M2 age ranges from the Lower Miocene (Biochronozone NN2) to the Middle Miocene (Biochronozones N9-N10). It corresponds to a generalized extension in the Coastal region. The M3 sequence is a thick sandy, silty and muddy sequence

ranging in age from the Middle Miocene (Biochronozone N9-N12) to the Upper Miocene (Biochronozone N16-N17). It corresponds to the Progreso Formation of the Progreso and Gulf of Guayaquil Basins. In the Progreso Basin, it is a regressive sequence formed by shore and beach sandy deposits ; whereas it corresponds in the Gulf of Guayaquil to a transgressive sequence marked by micro-conglomerate and sandy deltaic channel that pass upward to deltaic silty mud, and is linked to the first stage of opening of the Gulf of Guayaquil basin in a transtensive way along the Dolores-Guayaquil Megashear (Deniaud et al., 1999). The same double evolution can be seen in the Manabi and Borbon. In the Manabi Basin, M3 is a regressive sequence that starts with the sandy shore deposits of the Angostura Formation, is followed by the silty deposits of the Lower Onzole Formation, and ends with the 50 meters thick regressive sandy and conglomeratic Choconcha Member (Benitez, 1995). In the Borbon Basin, it forms a transgressive sequence starting with the sandy Angostura Formation and ending with the deepening up silty muddy Lower Onzole Formation (Evans and Whittaker, 1982). The M4 sequence corresponds, in the Progreso and Gulf of Guayaquil basins, to the Puna Formation which age ranges from the top Upper Miocene (Biochronozone N18) to, respectively, the top Upper Pliocene (Biochronozone N21) and the actual. In the Progreso basin it forms a regressive sequence of beach and swamp and deltaic muddy deposits that leads to the emergence of the basin, whereas in the Gulf of Guayaquil, it forms a thick sandy and muddy deltaic transgressive sequence directly related to the main opening stage of the Gulf of Guayaquil pull-apart basin (Deniaud et al, 1999). In the Manabi and Borbon basins, the M4 sequence corresponds to a regressive sequence which age ranges respectively from the Upper Miocene to the Lower Pleistocene (Biochronozones N18-N21) and from the Upper Miocene to actual. It is formed by the Upper Onzole and Borbon formations. In the Borbon Basin it starts with the transgressive sandy deposits of the Sua Member that disappear eastward. It is followed by the tuffaceous silty and muddy Upper Onzole Fomation that pass upward to the beach sand of the Borbon Formation. The Borbon Formation is diachronous with an age ranging from the Lower Pliocene to the Lower Pleistocene (Biochronozones N19-N22) in the Manabi

Basin and from the Upper Pliocene to Actual (Biochronozones N21-N23) in the Eastern Borbon basin where it forms a thick serie also referenced as Cachabi Formation.

SEDIMENT MASS-BALANCE METHODOLOGY

In order to better understand and constrain the evolution of the Neogene fore-arc basin dynamic, we intent to quantify the sediment mass deposition during Neogene time in the Gulf of Guayaquil, Progreso and Manabi basins. This quantification is based on close to 3000 km of seismic lines and wells that were re-interpreted. Seismic sections and well data are used together to construct time (double way travel time) maps of selected horizons at basin scale. Time maps are then converted into depth map using wells data and seismic velocity analysis. Sediment mass estimations are then derived at each point of the basin from the relationship (Métivier, 1996) :

$$M(dt) = (P_g*Z_2 + 0{,}43*P_g*3014*\exp(-Z_2/3014)) - (P_g*Z_1 + 0{,}43*P_g*3014*\exp(-Z_1/3014))$$

where M(dt) is the sediment mass in kg for the time interval dt related to the horizons depth Z_1 and Z_2, and P_g is the theoretical grain density of $2{,}7*10^3$ kg/m^3.

The integration on the basin area of the values obtained at each point provides the deposited mass of sediment for the considered time interval. This value can therefore be divided by the time interval and the basin area to obtain accumulation rates of sediment mass per square meters and time. Precision of the method depends on the accuracy of the time depth measurement, on the accuracy of the time to depth conversion law, on the accuracy of the mass estimation equation and on the accuracy of the horizon datation. It should be on the order of 20 % in the Gulf of Guayaquil and 40 % in the Manabi and Progreso basins. The application of this methodology to main Ecuadorian fore-arc basin is however restricted to the area where seismic sections are available. As seismic coverage do not exactly fit the extend of sedimentary basins, and as smaller contemporaneous basins were not surveyed, the total mass of sediment is certainly underestimated. Results of these calculations are shown in figure 3.

RESULTS AND CONCLUSIONS

The stratigraphy and sedimentological features as well as the sediments mass-balance of the main fore-arc basins of the Ecuadorian coastal region can be divided in a three-stage development history.

The first stage extends from the beginning of the Miocene to the Middle Miocene (ca 14 Ma). It is marked by the initiation of the Progreso Basin with the conglomeratic and sandy M1 sequence which marks the starting activity of the La Cruz and Carrizal Basin boarder faults; and by a widespread fine

marine transgressive sedimentation that affects the whole fore-arc area (sequence M2). The Manabi and Progreso basins show their highest mass accumulation rates during this time (fig. 3).

The second stage corresponds to the M3 sequence and extends from the Middle Miocene (ca 14 Ma) to the upper part of the Upper Miocene (ca 5,3 Ma, Biochronozone N18). It marks a major change in the dynamic of the Neogene fore-arc with a drastic change in the sedimentation of the whole fore-arc which turns to a marked sandy sedimentation with shallow water sedimentary structures. The mass accumulation rates show at this times the progressive ending activity of the Progreso and Manabi Basins and the coeval starting development of the Gulf of Guayaquil basin. An important transgression is also known in the Oriente basin of Ecuador at this time.

The third stage corresponds to the last sedimentary cycle that started at the beginning of the Pliocene and goes on actually. It is marked by a double evolution. In the Manabi, Progreso and West Borbon basins a regressive sedimentation took place during the Pliocene that led to the total emergence of these two basins. On the opposite the Gulf of Guayaquil and the eastern part of the Borbon basin undergo strong subsidence with the development of large deltaïc or shelf deposits. The main stage of sediment storage in the Neogene fore-arc basins takes place during this stage in the Lower Pleistocene and is coeval with the main stage of development of the Gulf of Guayaquil (Deniaud et al, 1999). The drastic rise of the sedimentary mass stored in the fore-arc basins at this time should be related to an increase of the sediment supply through the erosion of the Andean cordillera which start growing up around 9 to 8 My (Steinmann, 1997) and to the creation of a large space for the sedimentation in the fore-arc. The delay between the Andean cordillera uplift and the sediment storage in the fore-arc may be linked in part to sediment fore-arc bypass to the trench, in peculiar before the main development of the Gulf of Guayaquil Basin.

REFERENCES

Baldock J. W. 1982. Geologia del Ecuador: Boletin de la explication del mapa Geologico de la republica del Ecuador esc 1:100000. 70 p.

Benitez S. 1995. Evolution géodynamique de la province côtière sud-équatorienne au Crétacé supérieur Tertiaire. Géologie Alpine, Tome 71, 211 p.

Deniaud Y., Baby P., Basile C., Ordoñez M., Montenegro G., Mascle G. 1999. Ouverture et évolution tectono-sédimentaire du Golfe de Guayaquil : bassin d'avant-arc néogène et quaternaire du Sud des Andes Equatoriennes. Comptes Rendu de l'Académie des Sciences, Paris. 328,181-187.

Evans C. D. R. Whittaker J. E. 1982. The geology of the western part of the Borbon basin, North-West Ecuador. In: publ. Geol. Soc. London Spec., trench-forearc Geology, 10, p. 191-200.

Faucher B., Savoyat E. 1973. Esquisse géologique des Andes de l'Equateur. Revue de physique et de géologie dynamique, Paris. (2), vol XV, fasc 1-2, pp 115-142.

Métivier F. 1996. Volumes sedimentaires et bilans de masses en Asie pendant le Cénozoïque. PhD, University of Paris VII. 255 p.

Steinmann M. 1997. The Cuenca basin of southern Ecuador : tectono-sedimentary history and the tertiary Andean evolution. PhD, University of Zürich. 176 p.

NEVADOS DE CHILLAN AND ANTUCO VOLCANOES (SOUTHERN ANDES) REVISITED: A REMARKABLE EXAMPLE OF MAGMATIC DIFFERENTIATION THROUGH CLOSED-SYSTEM CRYSTAL FRACTIONATION.

Bernard DÉRUELLE [1] and Leopoldo LÓPEZ-ESCOBAR [2]

[1] LGIS - UPRESA CNRS 7047 - UPMC Paris & IUFM Versailles
Case 110, 4, place Jussieu, 75257 Paris Cedex 05 — France. deruelle@ccr.jussieu.fr
[2] Grupo Magmatico, Instituto GEA, Universidad de Concepción
Casilla 106, Concepción 3 — Chili. llopez@udec.cl

KEYWORDS : High-Al basalts, Andesites, Dacites, Crystal fractionation, Southern Andes, Magmatic petrogenesis.

INTRODUCTION

Nevados de Chillán (36°55' S) and the Antuco (37°30' S) strato-volcanoes belong to the Southern Volcanic Zone (SVZ) of the Andes. Post-caldera lavas from Nevados de Chillán are essentially andesites, dacites and rhyolites whereas lavas from Antuco are essentially high-Al basalts and andesites (Vergara and Katsui, 1969; Déruelle and Déruelle, 1974, Déruelle 1979, 1982; López-Escobar *et al.*, 1981).

Nevados de Chillán is composed of two adjacent stratovolcanoes located inside a caldera. Volcan Arrau appeared in 1973 (Déruelle, 1977; Naranjo et al., 1994). Only the post-caldera lavas are considered here. Antuco is a 130 000 year old stratovolcano (Vergara et al., 1985). Its summit collapsed in a caldera inside which a new cone appeared. Lava flows were emitted in 1853-63. Only the basalts are considered further.

MINERALOGY

Plagioclase is the dominant phenocryst phase. Its composition varies between An 85 (basalts) and An 30 (rhyolites). Phenocrysts of olivine (Fo 77-70) occur in basalts and basaltic andesites. Clinopyroxene is mostly present in andesites and orthopyroxene (En 48) in dacites. Magnetite is ubiquitous. Apatite occurs in andesites and dacites. No hornblende nor biotite were found.

GEOCHEMISTRY

Good correlations exist between SiO_2 and other major elements (except Ti and P) and correlations between trace elements present excellent linear trends (fig. 1); this is usually uncommon in lavas series from SVZ volcanoes. Sr-isotope ratios and $\delta^{18}O$ are similar for Antuco basalts (• 0.70375; 6.2, Harmon et al., 1984) and Nevados de Chillán andesites and dacites (• 0.70385; 5.6). The Sr- and Nd-isotope ratios (• 0.51287) for the Nevados de Chillán lavas are similar to those of basalts from oceanic islands.

MAGMATIC DIFFERENTIATION

The differenciation of the Nevados de Chillán lava series is remarkably well explained through

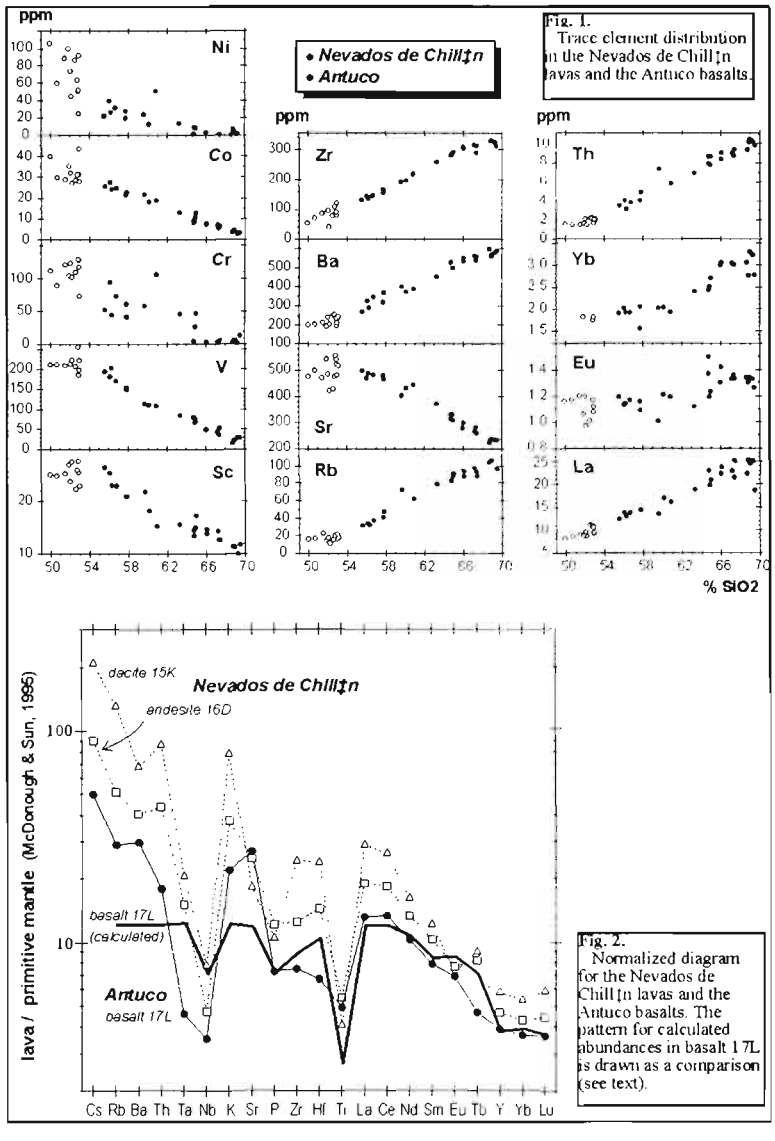

Fig. 1. Trace element distribution in the Nevados de Chillan lavas and the Antuco basalts.

Fig. 2. Normalized diagram for the Nevados de Chillan lavas and the Antuco basalts. The pattern for calculated abundances in basalt 17L is drawn as a comparison (see text).

fractionation of the mineral phases present as phenocrysts in the lavas. Dacitic magmas would have evolved from andesitic ones by fractionation of plagioclase (decrease in Al, CaO and Sr), pyroxenes (decrease in Sc) magnetite (decrease in Ti, Fe, V) and apatite (decrease in P). Nevados de Chillán andesites can be derived from Antuco basaltic magmas by fractionation of olivine (decrease in Mg and Ni), plagioclase and magnetite. Mass balance calculations (table) based on major elements are consistant which such an hypothesis. The mineral proportions calculated (Rayleigh fractionation) were used to model trace element distribution (table) using appropriate partition coefficients. The predominance of crystal fractionation in the differentiation of the lava series is noteworthy and illustrated in fig. 3 where the patterns for basalt, andesite and dacite are strictly parallel, incompatible elements being progressively more concentrated from basalt to dacite; these patterns intersect only for elements concentrated in mineral phases involved in the fractionation process (Sr, Ti, P for the dacite, and Eu).

ORIGIN AND EVOLUTION OF PRIMARY MAGMAS

Sr- and Nd- isotopic ratio values are among the most primitive of the SVZ (Déruelle et al., 1983; Harmon et al., 1984). Whilst crustal contamination is usually implied in the differentiation processes of SVZ lavas, it is ruled out for the magmatic evolution of the Nevados de Chillán lava series. Trace element mass balance modeling also suggests that the primary magmas were generated by fractional melting of a garnet peridotite mantle source. Ten percent partial melting (melting proportions: ol:cpx:opx—25:50:25) of a garnet-bearing peridotite mantle source (residual modal proportions: ol:opx:cpx:gt—58.5:25:15:1.5) of a similar chemical composition to the pyrolite model (MacDonough and Sun, 1995) can produce a primary magma whose evolution (5 wt % fractionations of cpx and olivine) can generate liquids of similar composition to that of Antuco basalts. This model is particularly satisfactory for rare-earth elements and Y (fig. 2). Nevertheless it is necessary to increase the concentrations of Rb, Sr and Ba by a factor of 2.3 and those of Th, K, Ti by factors between 1.5 and 1.8 to obtain conformity between the calculated and measured concentrations. Conversely, concentrations in Ta and Nb and Zr and Hf are between 3 and 1.5 times too high in the mantle source used. Selective contamination (Briqueu et Lancelot, 1979) of the mantle source by fluids from the subducted oceanic crust, or occurrence of phlogopite in the continental lithospheric mantle, may have influenced the genesis of Antuco primary basaltic magmas.

REFERENCES

Briqueu L. & Lancelot J.R., 1979. Rb-Sr systematics and crustal contamination models for calc-alkaline igneous rocks. Earth Planet. Sci. Lett., 43: 377-396.

Déruelle B., 1977. Sur l'activité récente des Nevados de Chillán (Chili central). C. R. Acad. Sc. Paris, 284: 1651-1654.

Déruelle B., 1979. Pétrologie d'un volcanisme de marge active: Atacama et Andes Méridionales. Thèse Doct. État, Univ.Paris XI, Orsay, 417 p.

Déruelle B., 1982. Petrology of the Plio-Quaternary volcanism of the South-Central and Meridional Andes. J. Volc. Geothermal Res., 14: 77-124.

Déruelle B. & Déruelle J., 1974. Géologie des volcans quaternaires des Nevados de Chillán (Chili). Bull. Volc, 38: 425-444.

Déruelle B., Harmon R. & Moorbath S., 1983. Combined Sr-O isotope relationship and petrogenesis of Andean volcanics of South America. Nature, 302: 814-816.

Harmon R.S., Barreiro B.A., Moorbath S., Hoefs J., Francis P.W., Thorpe R.S., Déruelle B., McHugh J. & Viglino J.A., 1984. Regional O-, Sr-, and Pb-isotope relationships in late Cenozoic calc-alkaline lavas of the Andean Cordillera. J. Geol. Soc. London, 141: 803-822.

López-Escobar L., Vergara M. & Frey F.A., 1981. Petrology and geochemistry of lavas from Antuco volcano, a basaltic volcano of the Southern Andes (37°25' S). J. Volc. Geothermal. Res., 11: 329-352.

McDonough W.F. & Sun S.-s., 1995. The composition of the Earth. Chem. Geol., 120: 223-253.

Naranjo J.A., Chávez R.M., Sparks S.J., Gilbert J. & Dunkley P., 1994. Nuevos antecedentes sobre la evolución cuaternaria del complejo volcánico Nevados de Chillán. 7° Congr. Geol. Chileno, Univ. Concepción, Concepción, 1: 342-345.

Vergara M. & Katsui Y., 1969. Contribución a la geología y petrología del volcan Antuco, Cordillera de los Andes, Chile Central. Univ. Chile, Fac. Cienc. Fís. Mat., Depart. Geol., Publ. 35: 25-47.

LOWER HOLOCENE PLINIAN ERUPTIONS OF COTOPAXI VOLCANO - ECUADOR

DESMULIER, F., (1), ROBIN, C., (2) and MOTHES, P., A., (3)

(1) Institut de Recherche pour le Développement (IRD-ex ORSTOM), A. P. 17-12-857, Quito, Ecuador, E-mail . desmulie@uio.satnet.net
(2) Institut de Recherche pour le Développement (IRD-ex ORSTOM), OPGC, 5 rue Kessler, 63038 Clermont-Ferrand, France, e-mail : robin@opgc.univ-bpclermont.fr
(3) Instituto Geofisico, Escuela Politecnica Nacional (IG-EPN), A. P. 17-01-2759, Quito, Ecuador, e-mail : geofisico@accesinter.net

KEY WORD : Ecuador, Cotopaxi volcano, Holocene, Rhyolitic, Plinian activity, volcanic hazards

INTRODUCTION:

Located 50 km south of Quito in the eastern Cordillera of the Andes, Cotopaxi, an ice-clad volcano (5890 m in elevation, Lat. : 0°68'S, Long. : 78°44'W) is one of the large Ecuadorian stratocones. The recent activity of this volcano is very explosive. During the Holocene, this volcano experienced large plinian events which have been responsible for the eruption of large volumes of tephras (ash, scoria, pumice), of andesitic and rhyolitic composition. The geologic description and physical studies of andesitic fallout deposits younger than 2000 y BP and of a giant rhyolitic lahar which occurred about 4500 y BP have been recently carried out (Barberi et al., 1995; Mothes et al, 1998). Nonetheless, the high rates of magma production related to intense and complex cycles of explosive activity during Lower Holocene of Cotopaxi's history and development remain little known. According to Hall and Mothes (1995), Cotopaxi is also remarkable for its bimodal activity, and approximately every 2000 years, during Late Pleistocene and Holocene, has produced large rhyolitic eruptions whose volumes exceed various km^3.

Field work carried out since November 1997 aims to characterize the nature and extent of voluminous tephra falls related to large explosive and silicic events which occurred during the Lower and Middle Holocene.

Summarized description of the deposits :

From about 9000 to 4500 y BP, the activity was strongly explosive. Especially, about 6000 y BP, four eruptive events were responsible for the deposition of thick, widely distributed, fallout pumice lapilli layers, rhyolitic in composition. These were also accompanied by large emissions of fine ash. Two lapilli layers (R1 and R2) were transported by dominant winds towards the west (Fig. 1), whereas the lapilli and

ash of the two other events were deposited towards the east. C14 datings show that these four major episodes occurred during a short time interval, i. e. at most over a few centuries. They represent the climatic eruptions of a discontinuous essentially acidic and explosive activity which started between 7000 and 9000 y BP and ended about 4500 y BP. Since 4500 y, Plinian fallout deposits at Cotopaxi are mainly andesitic in composition and are accompanied by andesitic lava and pyroclastic flows.

The good quality of outcrops allowed the recording of numerous key sections in the areas west of the volcano, as well as the elaboration of isopach and isopleth maps of each deposit (Fig. 1. and 2.). R1 and R2 layers are composite pumice and lithic lapilli deposits, several meters thick on proximal sections; They show a complex structure underlined by alternating beds more or less enriched in ash and/or lithics, as well successive normal and reverse grading.

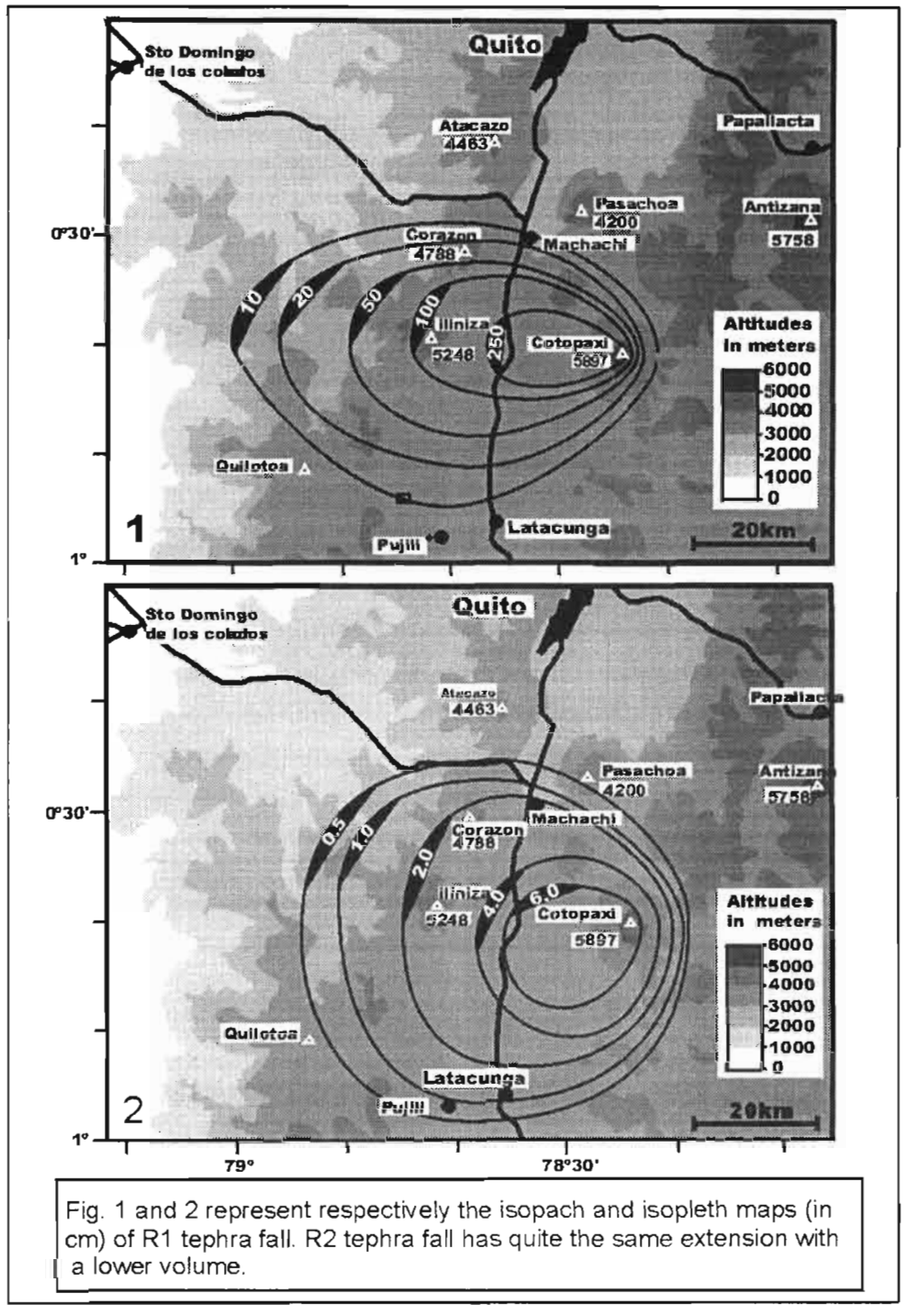

Fig. 1 and 2 represent respectively the isopach and isopleth maps (in cm) of R1 tephra fall. R2 tephra fall has quite the same extension with a lower volume.

Pyroclastic flows of rhyolitic composition (ash, pumice and obsidian blocks) were also emitted during the open-vent eruptions which occurred about 6000 y BP. These extended over the north, east and south-west sides of the volcano. Alternating with these large rhyolitic events, dome activity (rhyodacites) also occurred near or at the summit. During the whole period, from 9000 to 4500 y BP, very few products with an andesitic composition have apparently been erupted. This is demonstrated by subordinate andesitic ash and scoria layers within the thick sequence of rhyolitic fallout deposits that we studied (fig.3).

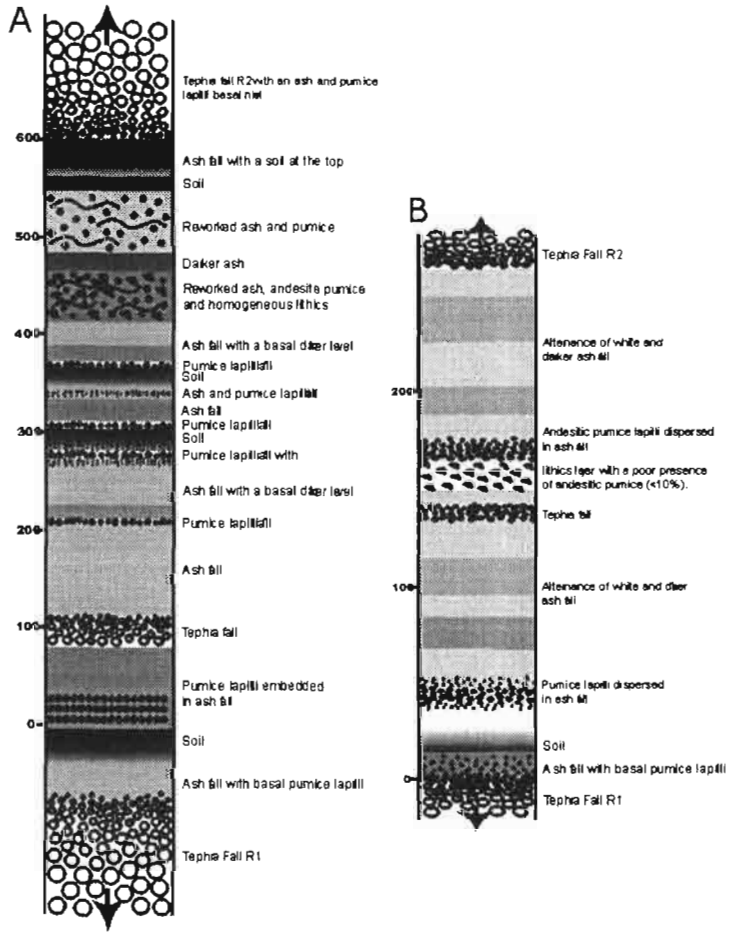

Fig. 3. A and B. Stratigraphic column of the events between R1 and R2. A is 5 km west from the volcano. B. is 15 km west from the volcano. Vertical scale in meters.

References :

Barberi, F., Coltelli, M., Frullani, A., Rosi, M., Almaeida, E., 1995. Chronology and dispersal of recently (last 5000 years) erupted tephra of Cotopaxi (Ecuador): implications for long-term forescating. J. Volcanol Geotherm Res 69: 217-239

Hall, M., L., Mothes, P., A., 1995. Bimodal nature of the eruptive history of Cotopaxi Volcano, Ecuador. Abstract IUGG XXI, General assembly, Boulder. Colorado, A452.

Mothes, P., A., Hall, M., L., Janda, R., J., 1998. The enormous Chillos Valley Lahar. An ash-flow generated debris flow from the Cotopaxi Volcano, Ecuador. Bull. Volcanol., 59: 233-244

Interrelations between the products of dome destruction and the related open-vent eruptions are observed in valleys at the base of the cone. On the contrary, distal tephra deposits (up to 40 km) only consist of fine ash.

Volumes for the R1 and R2 pumice lapilli layers are calculated to be 3.2 and 1.2 km^3 respectively (no DRE). Whereas an estimation of the total volume of tephras erupted during the 9000-4500 y BP period is around 14.3 km^3 (without considering the volume of pyroclastic flows). These values emphasize the large volume of fine ash produced, a striking characteristic of the rhyolitic sequence as a whole, which in turn indicates a high degree of magma fragmentation during the explosions.

CONCLUSION :

Cotopaxi Lower to Middle Holocene history is dominated by very explosive (Plinian) eruptions which produced large volumes of rhyolitic ash and pumice mainly deposited to the west of the volcano. The climactic phase of this activity occurred about 6000 y BP. A study of the deposits is in progress. It will allow an improved knowledge of the dynamic of this type of event, rare in andesitic stratocones. This study will be of great importance for increasing the knowledge of the hazards represented by Cotopaxi volcano, especially in the formation of large debris flows and tephra fallouts whose extension threatens cities in the Interandean Valley (Lasso, Latacunga and the urbanized zones south-east of Quito).

EVIDENCE FOR THE LATEST ORDOVICIAN/EARLY SILURIAN GLACIATION IN THE PERUVIAN ALTIPLANO: TECTONIC IMPLICATIONS

Enrique DIAZ-MARTINEZ(1), Harmuth ACOSTA(2), Rildo RODRIGUEZ(2),
Víctor CARLOTTO(2) and José CARDENAS (2)

(1) Instituto de Geología Económica (CSIC-UCM), Fac. CC. Geológicas, 28040 Madrid, Spain (ediaz@eucmax.sim.ucm.es)
(2) Universidad Nacional de San Antonio Abad del Cusco, Avda. de la Cultura s/n, Cusco, Peru (carlotto@chaski.unsaac.edu.pe)

KEY WORDS: Ordovician, Silurian, diamictites, glaciation, tectonism, Peru.

INTRODUCTION

Late Ordovician and Early Silurian glacial events have been extensively described and discussed in the literature. Late Ordovician glaciations are well documented in North Africa and Arabia, and Early Silurian glaciations have been reported from the Cape Basin (South Africa) and Brazilian intracratonic basins (Grahn & Caputo 1992). In the Central Andes, a diamictite unit is present near the Ordovician-Silurian boundary which has been traditionally used as a stratigraphic marker within the thick and otherwise monotonous Lower Paleozoic clastic sequences (Boucot 1988, Díaz-Martínez 1998). The diamictites are commonly interbedded with sandstones and shales, and frequently display slumps and contorted beds. The unit is known as San Gabán Fm. in Peru, Cancañiri Fm. in Bolivia, and Zapla Fm. in northern Argentina. The variable character of the underlying unconformity, and the common recycled character of most of the fossils found within these deposits, have led to strong discussions about its age (Suárez-Soruco 1995, and references therein). In Peru, the San Gabán Fm. has only been described for the central and southern Eastern Cordillera and Subandean regions (Laubacher 1974, Laubacher et al. 1982), whereas no evidence has ever been found of this unit in the Peruvian Altiplano (Laubacher et al. 1982, Boucot 1988, Ellison 1990, Suárez-Soruco, 1992).

The continental-scale diachronism and glacigenic character of these deposits have been used in Ordovician and Silurian paleogeographic reconstructions as evidence for the displacement of Gondwana across the pole. However, the ongoing discussion regarding their precise age and paleoenvironmental interpretation still does not allow for an integrated model of paleogeographic evolution. In an attempt to contribute to this model, in this work we present new evidence which confirms (a) the presence of the diamictite unit in the Peruvian Altiplano, and (b) its glacigenic character. At the same time, we draw conclusions on the tectonic implications of the presence of the San Gabán Formation in the Altiplano, both for Paleozoic and for Cenozoic tectonism.

STRATIGRAPHY AND SEDIMENTOLOGY

The diamictites of the San Gabán Fm. crop out at two stratigraphic sections near Ayaviri, in the Peruvian Altiplano (Fig. 1). The Huacacane section is located 14 km NNW of Ayaviri, with good outcrops on both sides of the strait formed by the Huacacane river between the Sullumara and Allcamarine hills. The Punco Punco section is located 7 km NNE of Ayaviri, with good outcrops along the eastern slope of the gorge, near the Morojullo hill. Both sections fall within the same structural block of Ordovician-Devonian rocks overthrust to the southwest (Fig. 1B). This tectonic block is morphologically part of the Peruvian high plains (Altiplano). However, our revision of its Paleozoic stratigraphy indicates that it is very similar to that of the Eastern Cordillera, and thus should be considered as part of the same tectonostratigraphic domain. For this reason, we have followed the lithostratigraphic nomenclature nowadays in use for the Late Ordovician and Silurian of the Eastern Cordillera: Sandia, San Gabán and Ananea Formations (Fig. 1C).

Above the quartzites and sandstones with mudstone and shale interbeds of the upper Sandia Formation, we found a heterogeneous unit with variable thickness (100-150 m) and composed of interbedded diamictites, mudstones and sandstones, which we correlate with the San Gabán Formation (Fig. 1C). The diamictite beds are characterized by frequent clasts of variable shape reaching up to 50 cm, and mostly composed of vein quartz or siliciclastic rocks (sandstone, mudstone, shale). The clasts are embedded in a muddy, structureless (massive) matrix with variable proportions of sand. Discontinuous deformed and contorted sandstone beds within the diamictites indicate their resedimented character, as a result of gravity-induced sediment mass transport. A few glacially-striated and faceted clasts were found, indicating a glacigenic influence in the origin of the resedimented material. The diamictites are interbedded with both massive and laminated mudstone and sandstone beds. Some of them may be large

slided slabs, although others seem to be continuous, indicating the superposition of several gravity flow events within the "normal" background marine sedimentation.

The contact of the San Gabán Diamictite Formation with the overlying dark shales of the lower Ananea Formation could not be seen. All three units lie conformable on each other, and are affected by very low grade metamorphism and development of cleavage.

DISCUSSION

This is the first time that the presence of the diamictite unit is mentioned in the Peruvian Altiplano. Our search for this unit in the classic section for the Ordovician-Silurian boundary of the Peruvian Altiplano (Chacas-Chagrapi area) was totally unsuccessful, coinciding with the observations of Laubacher et al. (1982). The Lower Paleozoic stratigraphy of the SW-verging thrust sheet north of Ayaviri demonstrates that the corresponding thrust plane should be considered as the boundary between the Altiplano and Eastern Cordillera tectonostratigraphic domains, and is probably a NW extension of the Coniri Thrust Fault, located on the Bolivian end of Lake Titicaca.

The precise age of the San Gabán Formation and its equivalents in Bolivia and Argentina is still under discussion. Some authors assign a late Ashgill (Hirnantian) age to all these diamictite units (Peralta & Baldis, 1990), whereas others assign a Llandovery age (Suárez-Soruco, 1995, and references therein), in accordance with what has been proved in Brazil (Grahn & Caputo, 1992). In Bolivia, these unit is interpreted as a result of several large-scale tectonically-induced resedimentation events in a deep marine offshore environment, with interbedded mud flows, debris flows and deformed slided slabs providing evidence for sediment instability and resedimentation of shallower facies (including glacigenic debris from a local glaciated source area). Tectonic deformation and its resulting relief are identified as the origin for the instability and local glaciation, respectively (Díaz-Martínez et al., 1996; Díaz-Martínez, 1997). In the case of the San Gabán Formation of the eastern Peruvian Altiplano, a similar age and interpretation seems appropriate.

Our findings suggest that the San Gabán Formation may also be present in other areas along the western margin of the Eastern Cordillera tectonostratigraphic domain, such as the Ananea region, where it may have been faulted at the type section (Laubacher et al., 1982; their Text-Fig. 4). These findings also indicate a pronounced tectonic shortening and compression along the fault zone between the Altiplano and Eastern Cordillera tectonostratigraphic domains.

CONCLUSIONS

The Lower Paleozoic stratigraphic sequence cropping out immediately to the north of Ayaviri (Peruvian Altiplano) belongs to the Eastern Cordillera tectonostratigraphic domain, and includes the Sandia, San Gabán and Ananea formations. Glacially-striated and facceted clasts found within the diamictites of the San Gabán Formation provide the first evidence for the late Ashgill-Llandovery glaciation in the Peruvian Altiplano, an area where this unit was previously considered not to be deposited. The marked difference between the Lower Paleozoic sequences of the Altiplano and Eastern Cordillera tectonostratigraphic domains suggests important tectonic shortening along the boundary fault zone.

ACKNOWLEDGEMENTS

This contribution results from a joint research project funded by the Spanish Government within the "Scientific Cooperation with Latin-America" Program, and from a cooperation agreement between the University of Cusco (UNSAAC) and the French Institute of Research for Development.

REFERENCES

Boucot A.J. 1988. The Ordovician-Silurian boundary in South America. In: L.R.M. Cocks & R.B. Rickards (eds.), A Global Analysis of the Ordovician-Silurian boundary. Bull. Br. Mus. Nat. Hist. (Geol.), 43, 285-290.

Díaz-Martínez E. 1997. Facies y ambientes sedimentarios de la Formación Cancañiri (Silúrico inferior) en La Cumbre de La Paz, norte de la Cordillera Oriental de Bolivia. Geogaceta, 22, 55-57.

Díaz-Martínez E. 1998. Silurian of Peru and Bolivia: recent advances and future research. Temas Geológico-Mineros ITGE, 23, 69-75.

Díaz-Martínez E., Limachi R., Goitia V.H., Sarmiento D., Arispe O. & Montecinos R. 1996. Tectonic instability related with the development of the Paleozoic forcland basin of the Central Andes of Bolivia. 3rd International Symposium on Andean Geodynamics, St.-Malo. Expanded abstracts, 343-346.

Ellison R.A. 1990. The geology of the Western Cordillera and Altiplano west of Lake Titicaca, southern Peru. British Geological Survey, Overseas Geology and Mineral Resources, 65, 39 p.

Grahn Y. & Caputo M.V. 1992. Early Silurian glaciations in Brazil. Palaeogeography, Palaeoclimatology, Palaeoecology, 99, 9-15.

Laubacher G. 1974. Le Paléozoique inférieur de la Cordillére Orientale du sud-est du Pérou. Cahiers d'ORSTOM, série Géologique, 6, 1, 29-40.

Laubacher G., Boucot A.J. & Gray J. 1982. Additions to Silurian stratigraphy, lithofacies, biogeography and paleontology of Bolivia and southern Peru. Journal of Paleontology, 56, 5, 1138-1170.

Palacios O., De La Cruz J., De La Cruz N., Klinck B.A., Allison R.A. & Hawkins M.P. 1993. Geología de la Cordillera Occidental y Altiplano al oeste del lago Titicaca - sur del Perú. INGEMMET, Boletín no. 42, Serie A (Carta Geológica Nacional), 257 p.

Peralta S.H. & Baldis B.A.J. 1990. Diamictitas del Ordovícico tardío sudamericano: correlaciones regionales y su relación con un evento glacial gondwánico. 4ª Reunión Argentina de Sedimentología, 3, 169-176.

Suárez-Soruco R. 1992. El Paleozoico inferior de Bolivia y Perú. In: J.C. Gutiérrez-Marco, J. Saavedra & I. Rábano (eds.), Paleozoico Inferior de Ibero-América, Univ. de Extremadura, 225-239.

Suárez-Soruco R. 1995. Comentarios sobre la edad de la Formación Cancañiri. Revista Técnica de YPFB, 16, 51-54.

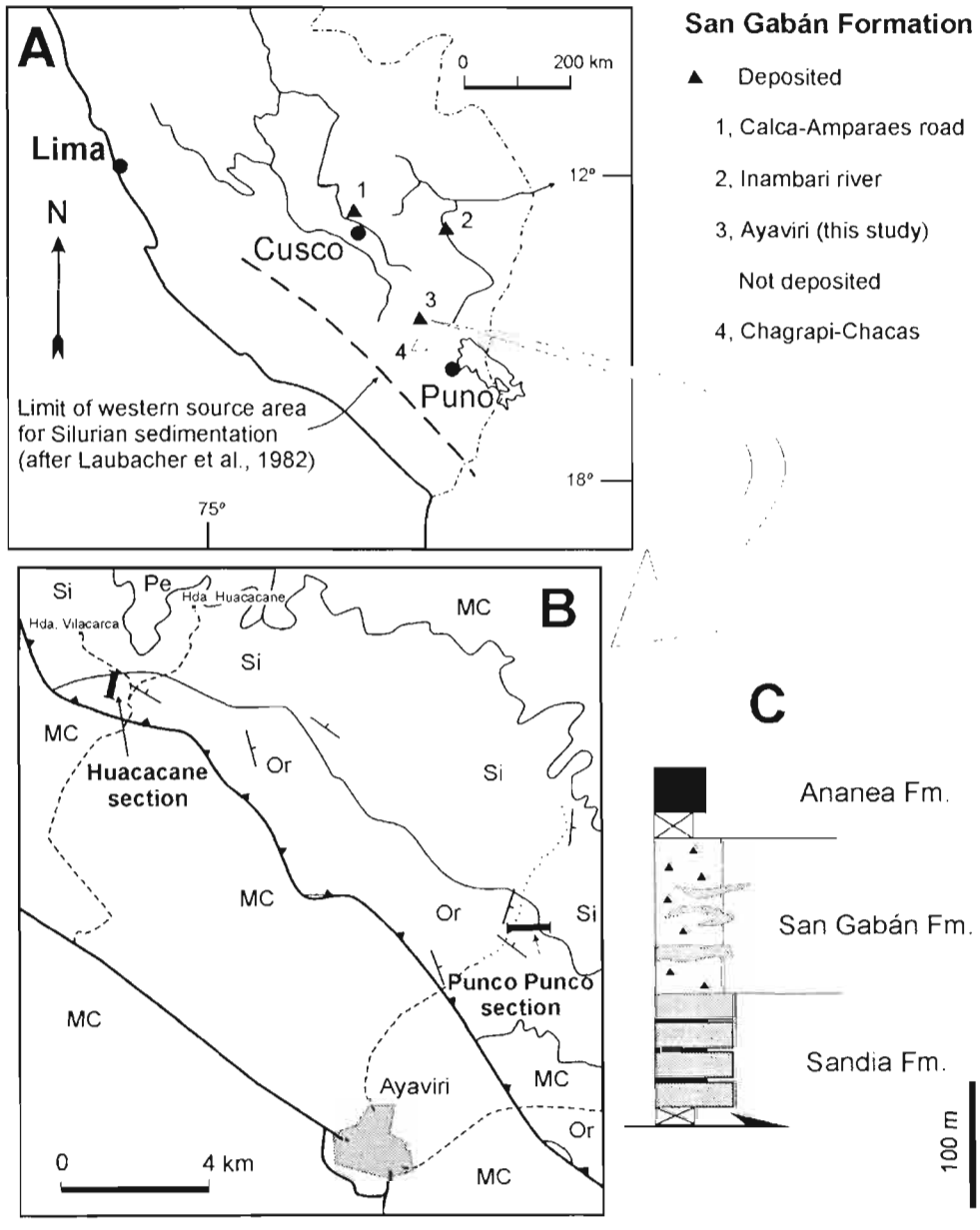

Figure 1: **A**, Main outcrops of the Ordovician-Silurian boundary, indicating where the San Gabán Formation was or was not deposited. **B**, Simplified geology of the Ayaviri area (after Palacios *et al.*, 1993): Or, Ordovician; Si, Silurian; Pe, Permian; MC, Mesozoic and Cenozoic. **C**, Simplified stratigraphic scheme for the Huacacane section.

$^{207}Pb/^{206}Pb$ AND $^{40}Ar/^{39}Ar$ GEOCHRONOLOGY OF THE COASTAL METAMORPHIC BELT BETWEEN 41°-42° S IN CENTRAL-SOUTH CHILE

Paul DUHART(1), Jorge MUÑOZ(1), Michael McDONOUGH(2), Mark MARTIN(3) and Michael VILLENEUVE(4)

(1) Servicio Nacional de Geología y Minería, Av. La Paz 406, Puerto Varas, Chile. sngmpv@entelchile.net
(2) Petro-Canada Oil&Gas, 150 – 6th Ave SW, Calgary, Alberta, T2P 3E3, Canada. mmcdonou@petro-canada.ca
(3) Massachusetts Institute of Technology, Cambridge, MA 02139-4307, USA. mwm@mit.edu
(4) Geological Survey of Canada, Rm 469, 601 Booth St., Otawa, Ontario K1A 0E8, Canada. mvillene@nrcan.gc.ca

KEY WORDS: geochronology, detrital circons, metamorphic muscovites, Bahía Mansa Metamorphic Complex, Coastal Range, Chile.

INTRODUCTION

The Coastal Metamorphic Basement complex between 41° and 42° S in south-central Chile includes pelitic to semipelitic schists that were tectonically intercalated with mafic schists and ultramafic bodies (Diaz *et al.*, 1988; Kato, 1985; Godoy and Kato, 1990) during Carboniferous-Triassic regional deformation and metamorphism (Munizaga *et al.*, 1988). This complex was recently named the Bahia Mansa Metamorphic Complex (BMMC) (Duhart *et al.*, 1998). Recognition of scarce blue amphiboles was interpreted as indicative of an accretionary subduction complex (Hervé, 1988). Blue amphiboles were almost totally destroyed by later metamorphic mineral growth related to prolonged deformation and metamorphism at green schist facies, ending at chorite grade (Kato, 1985; Hervé, 1988; Kato and Godoy, 1995; Duhart *et al.*, 1998). Previous Rb-Sr and K-Ar geochronology are representative of high pressure regional metamorphism and subsequent green schist facies and cooling to approximately 300° C during Triassic time. Preliminary U-Pb isotopic data obtained in detrital zircons collected from a metasandstone near Bahia Mansa constrain the maximum age for deposition to 275 Ma (Duhart *et al.*, 1997) and demonstrate a detrital component younger than previously considered (Duhart *et al.*, 1997).

DETRITAL ZIRCONS AND METAMORPHIC MUSCOVITES

Detrital zircons were separated from two samples from Río Capitanes and Lacui areas (XQ-0017 and XQ-0005, Figure 1A) for U-Pb dating, representing quartz-albite-muscovite and quartz-muscovite schists respectively, both with minor chorite. Both samples contain abundant grains of zircon with variable morphology and with size ratios from 2:1 to 3:1. Zircons typically show mechanical abrasion features, such as crystal faces partially or totally removed by transport processes, which clearly suggests detrital origin. A small amount of zircon of unknown origin have size ratios of 1:1 and crystals faces partially preserved. None of these zircons exhibit core-mantle relationships, a feature common in metamorphic zircons. In addition, muscovites from these two samples, which are concentrated in lepidoblastic bands, were dated by the K-Ar method.

$^{207}Pb/^{206}Pb$ DATING

Six rounded grains of zircons from sample XQ-0017 were analized, and four of them yielded concordant $^{207}Pb/206Pb$ ages of 369.2, 415, 422.7 and 504.1 Ma (fractions Z3, Z1, Z5 and Z6 in Figure 1B). The other two grains (Z2 and Z4) are discordant. Four of seven rounded grains of zircons from sample XQ-0005 gave concordant ages of 387.7, 468.4, 468.2 and 1116.2 Ma (fractions Z4, Z1, Z6 and Z3 in Figure 1C), and the others were discordant. Concordant ages in both samples represent the ages of the source of the sediments, and the younger age represents the maximum age for deposition. The discordant $^{207}Pb/^{206}Pb$ ages are interpreted as loss and/or inheritance of Pb, and do not represent the age of the source of the zircons.

K-Ar AND Ar/Ar DATING

Muscovite K-Ar ages for samples XQ-0017 and XQ-0007 are 235.5±5 and 220±6 Ma (Figure 1A). Ar/Ar step-heating ages for the same two samples were also determined. The age spectrum for XQ-0017 was determined twice, and each gave a well defined plateau. Both aliquots are concordant, allowing combination of the analyses in a single correlation plot (Figure 1D) which indicated an age of 230.0±3.2 Ma. Similarly, the correlation plot for sample XQ-0007 gave an age of 232.5±2.7 Ma (Figure 1E). Diamond simbols located to the right of the regression line in Figures 1D and 1E were not considered in the regression analyses because they may imply Ar loss mainly during low temperature steps, or non-radiogenic Ar. On this basis, sample XQ-0017 shows some evidence of minor Ar loss. On

the other hand, XQ-0007 shows an Ar loss pattern which could imply partial but important resetting. Both Ar-Ar ages should be considered as minimum cooling ages, and they do not represent the crystallization age during metamorphism.

DISCUSSION

The concordant $^{207}Pb/^{206}Pb$ zircon ages indicate that the deposition of sediments at the Río Capitanes and Lacui areas must be younger than 369.2 (late Devonian) and 387.7 Ma (middle Devonian), respectively. These ages do not restrict the age of the whole metamorfic complex, but indicate a sedimentary component younger than Devonian. As previously reported, a sedimentary component younger than 275 Ma (Permian) was recognized to the north in the Bahia Mansa Area (Duhart *et al.*, 1997), which is clearly a younger depositional component than that of the Río Capitanes-Lacui area. K-Ar ages for samples from the BMMC show a regional cooling near 300° C between 220 and 250 Ma after the main deformation and metamorphism event (Duhart *et al.*, 1997), which is confirmed by the Ar/Ar data reported for the Río Capitanes and Lacui areas.

Although confirmation is awaited, $^{207}Pb/^{206}Pb$ ages in detrital zircons from Río Capitanes and Lacui areas open the posibility for synchronous deposition with the Devonian shales from Buill (Fortey *et al.*, 1992).

Distinct depositional and metamorphic events are represented in the BMMC, traditionally considered on basis of structural and lithological criteria as coeval. Although penetrative greenschist grade metamorphism and deformation during Permian-Triassic time has obscured the Ar ages, new $^{207}Pb/^{206}Pb$ zircon ages indicate that more than one sedimentary protolith is represented in the metasedimentary rocks of the BMMC.

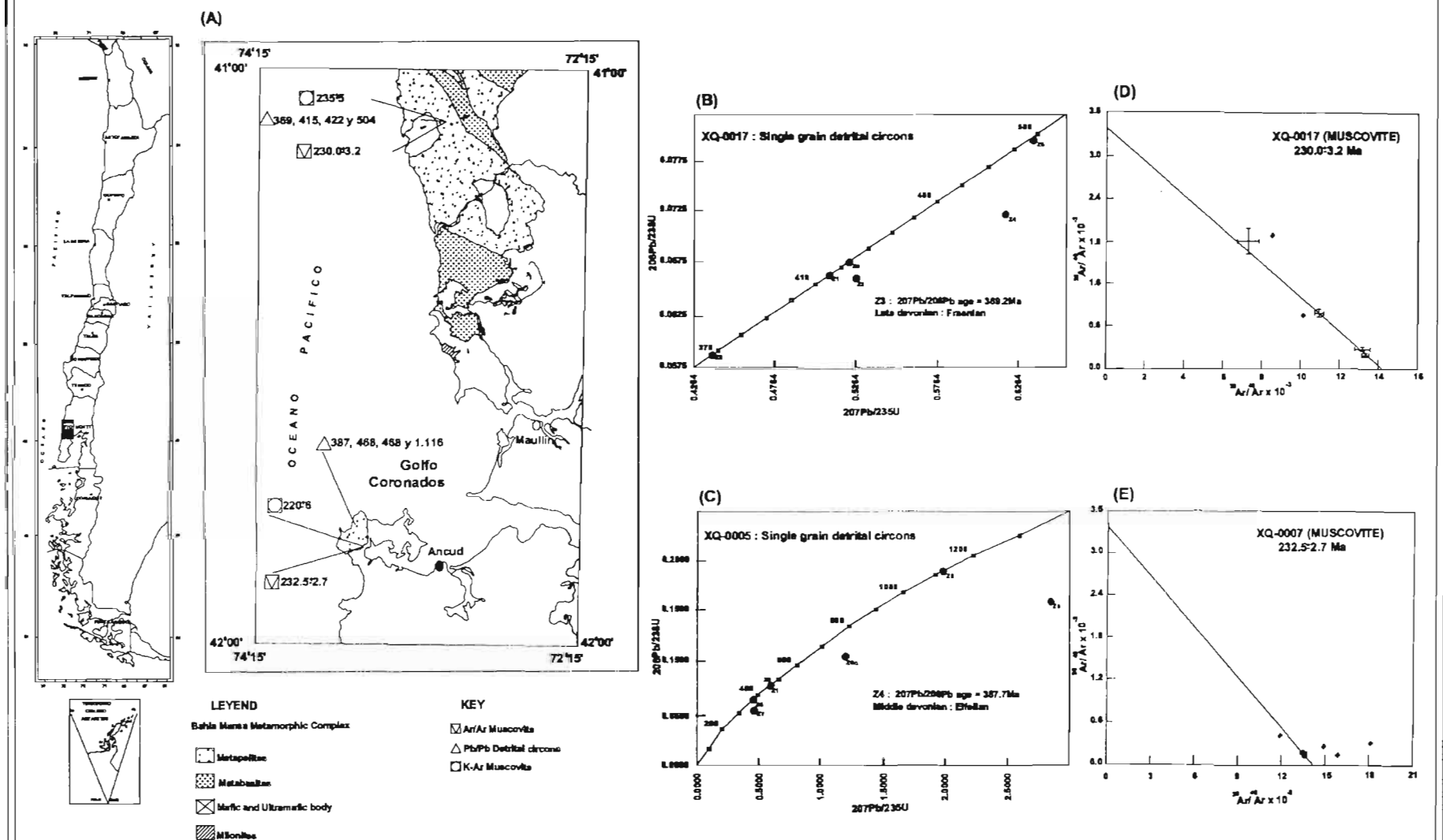

Figure 1. (A): Sketchmap showing the geology and geochronology of Bahia Mansa Metamorphic Complex between 41°- 42° S.; (B): Concordia - discordia diagram for sample XQ-0017.;(C): Concordia - discordia diagram for sample XQ-0005.; (D): Correlation plot for sample XQ-0017.; (E): Correlation plot for sample XQ-0007.

The available data for the BMMC are compared to Upper Triassic palaeontological evidence (Fang *et al.*, 1998) and detrital zircon data (Hervé *et al.*, 1998) from in the Los Chonos Metamorphic Complex. Available information distinguish Devonian to Triassic accretionary proccess for the CMBM (Duhart *et al.*, 1997) and upper Triassic-Jurassic accretion for the Los Chonos Metamorphic Complex (Hervé *et al.*, 1998).

REFERENCES

- Díaz, L.; Vivallo, W.; Alfaro, G.; Cisternas, M.E. 1988. Geoquímica de los esquistos Paleozoicos de Bahía Mansa, Osorno, Chile. *Congreso Geológico Chileno N°5*, 2, E75-E96.

- Duhart, P.; Martin, M.; Muñoz, J.; Crignola, P.; McDonough, M. 1997. Acerca de la edad del protolito del basamento metamórfico de la Cordillera de la Costa de la X Región: edades preliminares 207Pb/206Pb. *Congreso Geológico Chileno N°8*, 2, 1267-1274.

- Duhart, P.; Lara, L.; Pérez, Y.; Rodríguez, C.; Antinao, J.L.; Clayton, J.; McDonough, M.; Fonseca, E.; Muñoz, J. 1998. Geología Regional. *Estudio Geológico-Económico de la X Región Norte, Servicio Nacional de Geología y Minería*, Informe Registrado IR-98-15, 2(1), 244p.

- Fang, Z.J.; Boucot, A.; Covacevich, V.; Hervé, F. 1998. Discovery of Late Triassic fossils in the Chonos Metamorphic Complex, Southern Chile. *Revista Geológica de Chile*, 25, 165-173.

- Fortey, R.; Pankhurst, R.J.; Hervé, F. 1992. Devonian Trilobites at Buill, Chile (42°S). *Revista Geológica de Chile*, 19, 133-144.

- Godoy, E. and Kato, T. 1990. Late Paleozoic serpentinites and mafic schists from the Coast Range accretionary complex, central Chile: their relation to aeromagnetic anomalies. *Geol. Runds.*, 79, 121-130.

- Hervé, F. 1988. Late Paleozoic subduction and accretion in southern Chile. *Episodes*, 11, 183-188.

- Hervé, F.; Aguirre, L.; Godoy, E.; Massone, H.; Morata, D.; Pankhurst, R.; Ramirez, E.; Sepúlveda, V.; Willner, A. 1998. Nuevos antecedentes acerca de la edad y las condiciones P-T de los complejos metamórficos de Aysén, Chile. *In actas Congreso Latinoamericano de Geología N°10 y Congreso Nacional de Geología Económica N°6*, 2, 134-137.

- Kato, T. 1985. Pre-Andean orogenesis in the Coast Range of central Chile. *Geol. Soc. Amer. Bull.*, 96, 918-924.

- Kato, T.T. and Godoy, E. 1995. Petrogenesis and tectonic significance of Late Paleozoic coarse-crystalline blueschist and amphibolite boulders in the Coastal Range of Chile. *Int. Geol. Rev.*, 37, 992-1006.

- Munizaga, F.; Hervé, F.; Drake, R.; Pankhurst, R.J.; Brook, M.; Snelling, N. 1988. Geochronology of the Lake Region of South Central Chile (39°-42° S): preliminary results. *Jour. S. Amer. Earth Sci.*, 1(3), 309-316.

THE TATARA-SAN PEDRO VOLCANIC COMPLEX (36° S): IMPLICATIONS FOR ARC MAGMA GENESIS AND EVOLUTION IN THE SOUTHERN VOLCANIC ZONE (SVZ) OF THE CHILEAN ANDES

Michael DUNGAN (1)

(1) Département de Minéralogie, Section des Sciences de la Terre, Université de Genève, 13 rue des Maraîchers, 1211 Genève 4, Switzerland (michael.dungan@terre.unige.ch)

KEY WORDS: Andean volcanism, Southern Volcanic Zone, open-system magma evolution

INTRODUCTION

An investigation of the well exposed Tatara-San Pedro complex (TSPC; Singer *et al.*, 1997) has multiple goals: (1) develop a stratigraphic and geochronologic framework at a long-lived arc volcano on the basis of a multidisciplinary approach, (2) undertake petrologic modelling studies constrained by this framework, (3) assess the consequences of Quaternary glaciation for volcanic construction and erosion, and (4) contribute to the debate concerning the origin and evolution of arc magmas of the Andean SVZ (e.g., Davidson *et al.*, 1988; Singer *et al.*, 1995; Feeley and Dungan, 1996; Feeley *et al.*, 1997). This abstract focuses on the theme of point 4. Previous inferences based on along-arc geochemical reconnaissance investigations of SVZ centers (e.g., Hickey *et al.*, 1986; Hildreth and Moorbath, 1988; Tormey *et al.*, 1991) are discussed in light of the implications of the extraordinary diversity of evolved magmas at the TSPC.

TECTONIC SETTING AND ARC SEGMENTATION

The portion of the SVZ around 36° S has been referred to as "transitional" (Tormey *et al.*, 1991) between volcanoes built on thin crust south of 36° S, which display little evidence of crustal assimilation (e.g., Gerlach et al., 1988), and those north of 35° which have been built on thicker and older crust, and which are inferred to reflect increasingly large crustal contributions as a function of increasing crustal thickness (Hildreth and Moorbath, 1988). These inferences may need modification. The TSPC appears to mark an abrupt change in petrology from frontal arc centers south 36° S to a different behavior between 36-34.5° S, although there is little change in regional elevation or apparent crustal thickness in passing from the southern centers to the TSPC. This observation must be tested rigorously by detailed investigations of volcanic centers in the region 36-37° S, but it would appear that the arc segmentation scheme of Wood and Nelson (1988), which has been given a nomenclature in Fig. 1, deserves consideration as the geologic framework for SVZ volcanism. Fig. 2 (after Hildreth and Moorbath, 1988) illustrates the basis for treating the centers of each segment as a separate population; e.g., high Ce/Yb sets the TMS (33-34.2° S) apart and the LPS (36.2-40.5° S)has consistently lower abundances of LILE (Ba, K_2O).

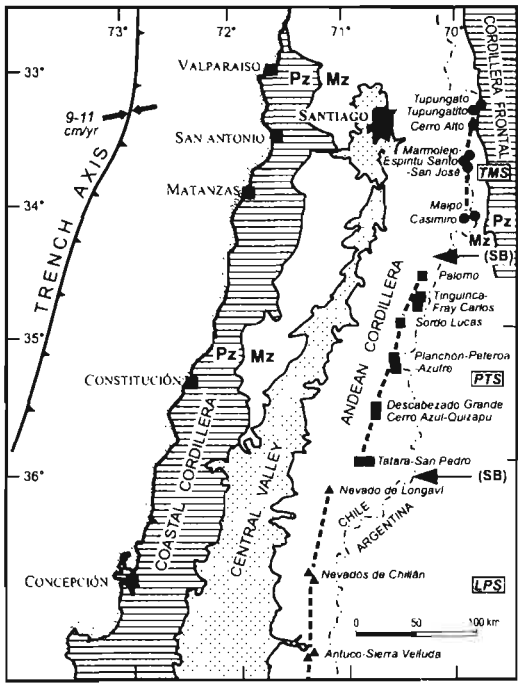

←**Figure 1:** Arc segmentation scheme of Wood and Nelson (1988) with inferred segment boundaries (SB): (TMS 33-34.2° S Tupungato-Maipo segment); (PTS 34.5-36° S Palomo-Tatara segment); (LPS 36.2-40.5° S Longavi-Puyehue segment). **Figure 2** (below): Comparison of the regression values at 57.5 wt. % SiO_2 (●-■-▲) of Hildreth and Moorbath (1988) defined by SVZ frontal arc centers between 33-38° S to the ranges of the same parameters at the TSPC (shaded band), which encompass nearly the total range of regression values for several parameters. The TSPC ranges correspond to the breadth of the envelopes surrounding the data arrays at 57.5 wt. % SiO_2 (column), which in general would not be characterized adequately by linear regressions.

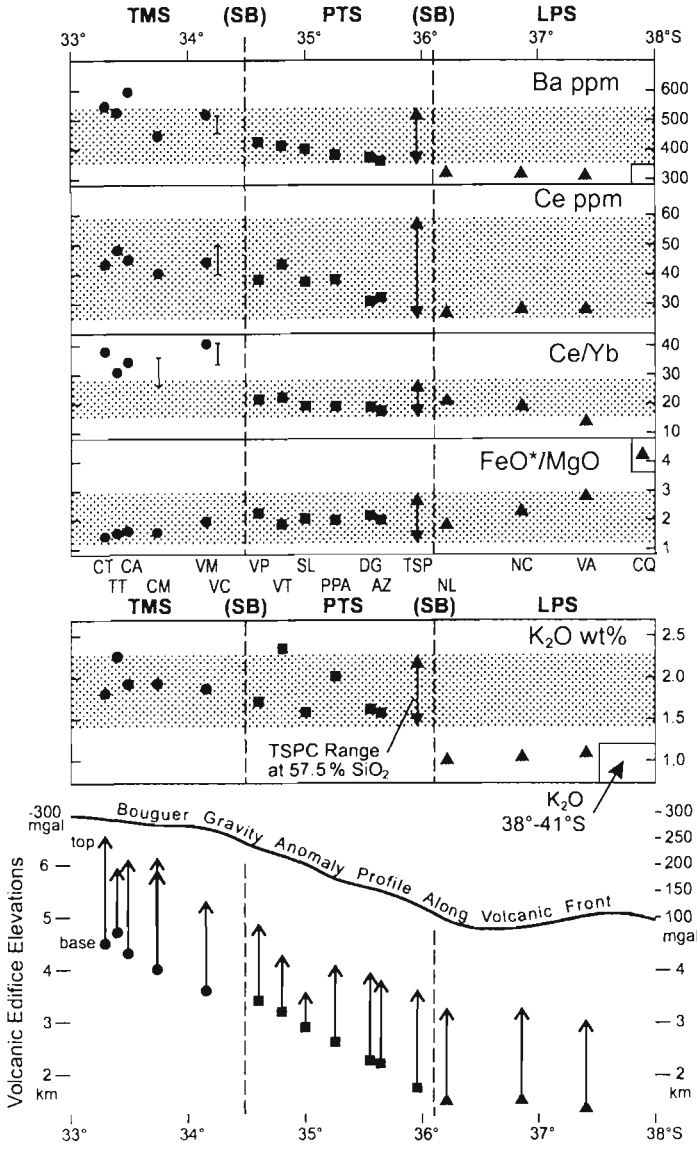

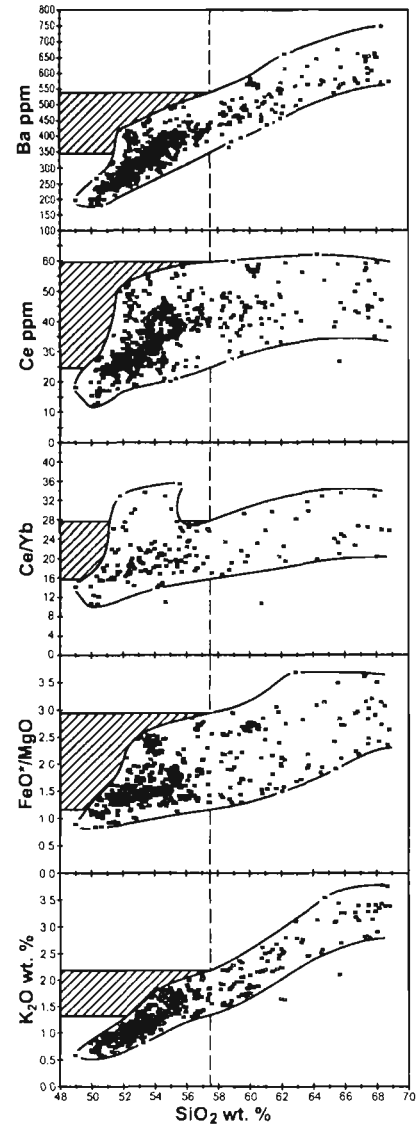

PROCESSES AND CONDITIONS OF MAGMA DIFFERENTIATION

SVZ stratocones south of 36.2° S are largely dominated by evolved magmas generated by low-pressure fractional crystallization. They are characterized by remarkably uniform tholeiitic (high FeO*/MgO) differentiation trends in which evolved magmas have low Sr and low Sr/Sc, indicating high plag/pyx in fractionating assemblages (evolved basalt rhyolite), and nearly constant incompatible trace element ratios, suggesting largely closed-system evolution after early modification of basalts during ascent to shallow levels (e.g., Gerlach et al., 1988). In contrast, TSPC lavas are extremely diverse for many trace element indices (Figs. 3-4; Barclay et al., 1999). Open-system evolution, involving both crustal assimilation and magma mixing, was far more important at the TSPC. Where fractional crystallization played a major role in the evolution of mafic TSPC magmas, mineral assemblages frequently had lower plag/(oliv+aug) than at more southerly centers. Interpretations of differentiation trends are complicated by uncertainties concerning compositions of parent magmas and assimilants, as well as the proportions of fractionating phases, but three suites (590 ka, 235 ka, 110 ka) of weakly contaminated mafic lavas are markedly different from those seen at more southerly centers such as Puyehue. The inferred range of TSPC basaltic parent magmas in Fig. 3 is based on relatively primitive magmas, moderately enriched in Ti, P, Nb, Zr, and LREE at the low-Sr end of the array and more evolved basalts with generally lower abundances of these same elements but with higher Sr-contents. The Sr-rich evolved basalts (7.5 and 6 wt. % MgO) and a suite of extremely Sr-rich basaltic andesites (4.5 wt. % MgO: up to 900 ppm) have sufficiently low Rb (7-12 ppm) to suggest minimal contamination. The combination of high Al_2O_3 and Sr, low Mg#, Cr, Ni, and Sc, and an absence of plagioclase phenocrysts in these mafic magmas is consistent with evolution by fractionation of an assemblage rich in olivine+augite (arrows in Fig. 3). High PH2O is suspected as a contributing causative agent for these trends, as the crust in this region is not exceptionally thick. Yet the suppression of Y-HREE in many evolved and contaminated TSPC magmas implies incorporation of crustal components with high Rb/Y, Ba/Y, La/Yb, Th/Yb, and low Y-HREE, which appear to record residual garnet at some stage. The latter may partly reflect the assimilation of basement granitoids at shallow levels (Figs. 3-4), as well as high-P open-system evolution.

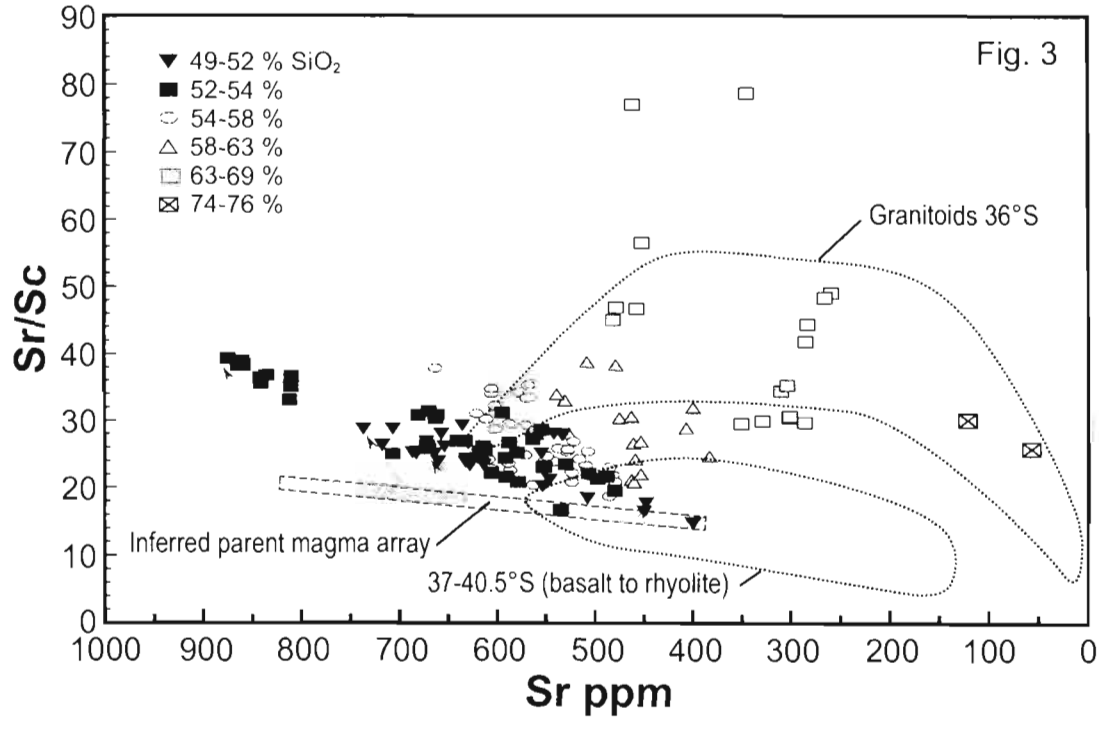

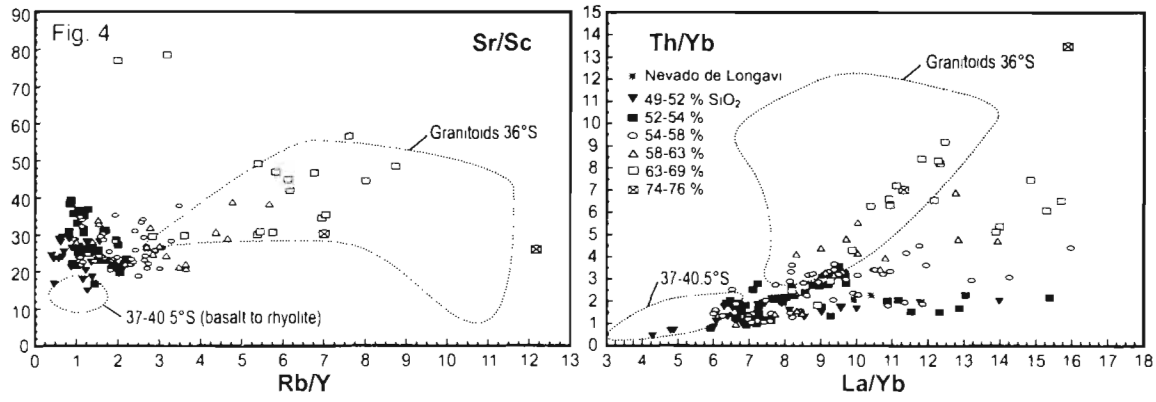

Figure 4: TSPC data (symbols coded for SiO_2 wt. %) compared to published data from the southern SVZ. The limited variations associated with largely closed-system differentiation contrast strongly with the TSPC.

Acknowledgements: We thank the many collaborators who have contributed generously to the Tatara-San Pedro project since 1984: L. Lopez-Escobar, G. Sanchez, J. Davidson, K. Ferguson, M. Colucci, R. Harmon, B. Singer, R. Thompson, L. Brown, J. Pickens, J.M. Rhodes, A. Wulff, F. Frey, T. Feeley, W. Hildreth, R. Drake, F. Costa, J. Lobato, and S. Nelson. Funding has been provided by the US NSF and the Swiss FNSRS.

Barclay, J., Marzoli, A., & Dungan, M. 1999. Magma evolution processes at the Tatara-San Pedro complex; 36° S, Southern Volcanic Zone (SVZ) Chile. *this volume.*

Davidson, J.P., Ferguson, K.M., Colucci, M.T., & Dungan, M.A., 1988. The origin and evolution of magmas from the San Pedro-Pellado volcanic complex, S. Chile: multiple sources and open system evolution: *Contr. Miner. Pet.* 100, 429-445.

Feeley, T.C., & Dungan, M.A., 1996. Compositional and dynamic controls on mafic-silicic magma interactions at continental arc volcanoes: evidence from Cordón El Guadal, Tatara-San Pedro Complex, Chile. *J. Pet.*, 37, 1547-1577.

Feeley, T.C., Dungan, M.A., & Frey, F.A. 1998. Geochemical constraints on the origin of mafic and silicic magmas at Cordón El Guadal, Tatara-San Pedro Complex, central Chile. *Contr. Miner. Pet.*, 131, 393-411.

Gerlach, D.C., Frey, F.A., Moreno-Roa, H., & López-Escobar, L. 1988. Recent volcanism in the Puychue-Cordon Caulle region, Southern Andes, Chile (40.5° S): Petrogenesis of evolved lavas. *J. Pet.*, 29, 333-382.

Hickey, R.L., Frey, F.A., Gerlach, D.C., & López-Escobar, L. 1986. Multiple sources for basaltic arc rocks from the Southern Volcanic Zone of the Andes (34°-41° S): trace element and isotopic evidence for contributions from subducted oceanic crust, mantle, and continental crust. *J. geophys. Res.*, 91, 5963-5983.

Hildreth, W., & Moorbath, S. 1988. Crustal contributions to arc magmatism in the Andes of central Chile: *Contr. Miner. Pet.*, 98, 455-489.

Singer, B.S., Dungan, M.A., & Layne, G.D. 1995. Textures and Sr, Ba, Mg, Fe, K, and Ti compositional profiles in volcanic plagioclase: clues to the dynamics of calc-alkaline magmas: *Amer. Miner.*, 80, 776-798.

Singer, B.S., Thompson, R.A., Dungan, M.A., Feeley, T.C., Nelson, S.T., Pickens, J.C., Brown, L.L., Davidson, J.P., & Metzger, J. 1997. Volcanism and erosion during the past 930 k.y. at the Tatara-San Pedro complex, Chilean Andes. *Geol. Soc. Amer. Bull.*, 109, 127-142.

Wood, C.A., and Nelson, K.L. (1988). Inter-segment variation of magmatic compositions in the Andes of Central Chile. AGU abs., EOS, 69, #44, 1494.

VOLCANOGENIC SEDIMENTATION MODEL FOR THE MIOCENE FARELLONES FORMATION, ANDEAN CORDILLERA, CENTRAL CHILE

Sara Elgueta(1), Reynaldo Charrier(2), Ramón Aguirre(3), Guy Kieffer(4) and Nicole Vatin-Perignon(5)

(1) Departamento de Geología, Facultad de Ciencias Físicas y Matemáticas, Universidad de Chile Plaza Ercilla 803, Santiago, Chile. selgueta@cec uchile.cl
(2) Departamento de Geología, Facultad de Ciencias Físicas y Matemáticas, Universidad de Chile Plaza Ercilla 803, Santiago, Chile. rcharrie@cec.uchile cl
(3) Departamento de Geología, Facultad de Ciencias Físicas y Matemáticas, Universidad de Chile Plaza Ercilla 803, Santiago, Chile.
(4) Département de Géographie et UPRES – A 6042 CNRS, Université Blaise Pascal, 29 Boulevard Gergovia, 63037 Clermont-Ferrant Cedex 1, France. gkieffer@cicsun.univ-bpclermont.fr
(5) Laboratoire de Géologie et UPRES – A 5025 CNRS, Université Joseph Fourier de Grenoble, 15 rue Maurice Gignoux, 38031 Grenoble Cedex, France. perignon@ujf-grenoble.fr

Key words: volcanogenic sedimentation, Farellones Formation, Tertiary/Miocene, Andes Cordillera, Central Chile

INTRODUCTION

A preliminary model of volcanogenic sedimentation and palaeogeographic evolution is presented for the Farellones Formation in the Andean cordillera between 33° 20' and 34° 00' S It is based on the sequential facies analysis of a representative composite sequence, and geological mapping at 1:25,000 scale, of the sector between the Maipo and Colorado rivers (Fig 1; Aguirre, 1999). This work is part of the on-going FONDECYT project N° 1970736, designed to understand the palaeoenvironments and palaeogeography of Tertiary formations in Central Chile.

The Farellones Formation was defined by Klohn (1960) and described in the Santiago 1:250,000 geological sheet by Thiele (1980). In the type section at Farellones it is a well-bedded sequence of continental volcanics 2,500m thick made up of massive to brecciated lavas of basaltic, andesitic and rhyolitic composition and minor quantities of fine grained to coarsely conglomeratic epiclastic sediments (Klohn, 1960).

In the study area, 30km south of Farellones, the sequence is 1,700m thick and overlies lavas of the Abanico Formation in apparent conformity or pseudoconformity (Aguirre, 1999). It is overlain by Pliocene volcanic and sedimentary deposits in angular unconformity. These units are the main components of the Andean Cordillera of this region.

A K/Ar age date on plagioclase within the study area gives a Lower Miocene age of 17.3 ± 0.2 m.a. age for the Farellones Formation (Drake et al., 1976); this broadly agrees with another in the Farellones area of 18.5 ± 0.2 m.a. (Drake et al., 1976).

SEQUENCE AND FACIES INTERPRETATION

The composite sequence is 1,400 m thick and was measured in a profile between Pata del Diablo and Cerro Puntilla de Lircan (Fig. 1). Three principal facies associations are recognized with no internal unconformities. They are similar to those described for the volcanoes of the southern Andes, particularly the facies associations observed at the Villarrica volcano (Clavero y Moreno, 1994). From the base upwards they are:

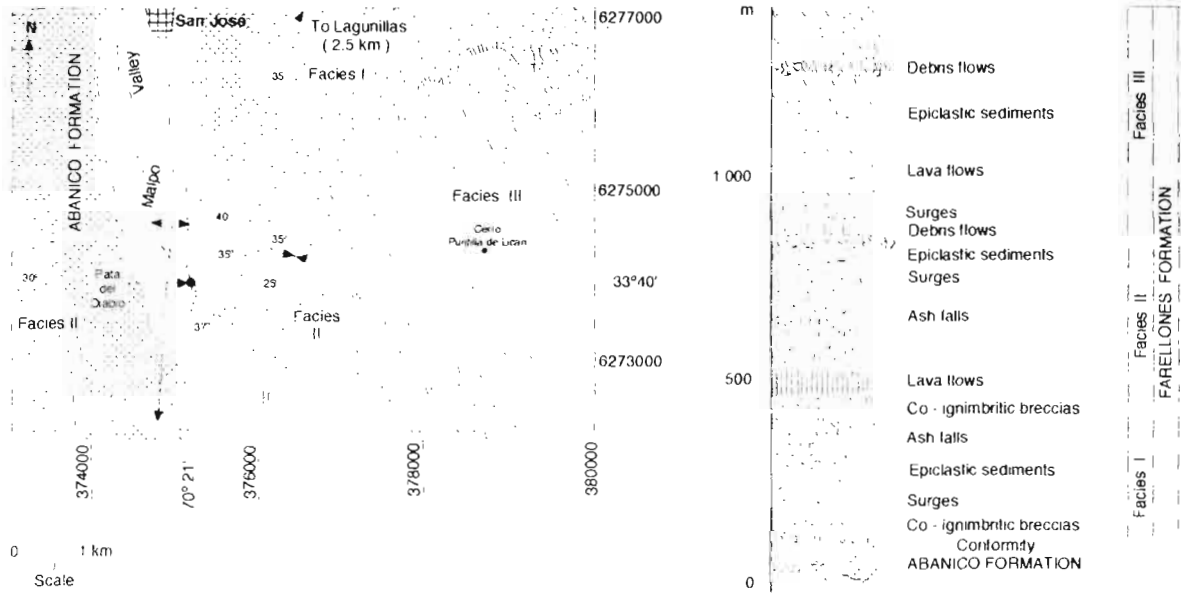

Fig 1: Schematic geological map showing distribution of main facies associations and measured composite sequence between Pata del Diablo and Cerro Puntilla de Licán, Maipo Valley

Facies Association I

The basal 300m consist of well-bedded pyroclastic deposits (beds of 0.5m to 3m) with minor intercalations of epiclastic sediments. The sequence is upward fining and bed-thinning upwards. In order of importance, the lithologies encountered are.

Ia) Lapilli tuffs with cognate, non-vesicular lithic clasts principally of andesitic and basaltic andesite composition, and to a lesser extent pumicitic and scoraceous fragments, has zeolite cement with little or no ash matrix. Occasionally larger (average 10cm) accidental lithic clasts of porphyritic andesite stand out. The majority of the beds are continuous, homogeneous to diffusely laminated, and show reverse or normal grading, other beds contain low angle cross-bedding, small erosive U-shaped channels, undulated surfaces (dune-bedding or antidunes), fluidization textures, impact sag structure and, possibly, accretionary lapilli. These lithologies have all the characteristics of surge deposits as have been recently reviewed by Carey (1991) and Druitt (1998) and are interpreted as pyroclastic base surge deposits (or wet surge deposits) with provenance, according to preliminary data, from a few kilometres to the north-east. They are best developed in the centre and upper parts of the sequence.

Ib) Coarsely bedded to massive fine pyroclastic breccias with very poorly sorted and chaotically arranged clasts which contain up to 70% lithic debris. The clasts are angular to sub-rounded, up to 10 cm in diameter, and composed of porphyritic to microcrystalline andesite and basaltic andesite; scoraceous and pumicitic fragments and fiammes occur in lesser amounts. Matrix (less than 30%) is composed of ash. Bombs averaging 35 cm in diameter occur occasionally, some are strongly flattened and indicate proximity to its source vent. These deposits are interpreted as pyroclastic flows and comparable to co-ignimbrite lag-fall breccias described by Cas and Wright (1987) and Branney and Kokelaar (1997), they are most common at the base of the sequence.

Ic) Fine to coarse ash and lapilli tuffs of lithic and lithic-crystal components, with subhedral feldspar and subordinate embayed quartz crystals making up the crystal fraction. Regular and continuous fine bedding is typical. The vertical grading pattern of these sheets suggests the collapse of a fluctuating high eruption column. The facies, most common towards the top of the sequence, is interpreted as the product of a major event: fallout tuffs (or air fall ash deposits) from a Plinian type eruption. The large volume of fine ash was generated contemporaneously with the pyroclastic flows and is likely to have been related to caldera formation (Druitt and Sparks, 1984).

Id) Epiclastic sediments: lithic and lithic-feldspar sandstones of coarse to medium grain size, submature to mature in texture and composed of volcanic lithic clasts and plagioclase crystals. Some horizons contain rare concentrations of crystals and pumice fragments towards the top. The facies occurs as sporadic intercalations throughout the sequence. These are interflow sediments interpreted to be derived from reworking of the contemporaneous volcanic deposits and redeposited in a fluvio-lacustrine environment (fluvial tuffs).

Facies Association II

This forms a sequence 550m thick, which overlies the previous facies association concordantly. The basal surface is abrupt and coincides with the arrival of massive pyroclastic flows and subordinate lava flows (together 140m thick). The pyroclastic flows are breccias very similar to those of Facies Association Ib (co-ignimbrite lag-fall breccias). The lava flows are thickly bedded, massive or autobrecciated and of andesite to basaltic andesite composition. Mapping shows a clearly increasing proportion of intercalated lavas to the north-east (Fig 1) In the middle of the sequence pyroclastic and epiclastic units very similar to those of the underlying sequence (Facies Ic and Id: wet surges, Plinian fallout deposits and fluvial tuffs) predominate. The upper part of the sequence consists of lavas with some intercalations of epiclastic breccias of large lava blocks (5-65cm) in a subordinate matrix of fine breccia and ash. Breccias are monolithologic and suggest that these deposits formed by rapid reworking of fresh primary material. Their position signifies proximity to eruption vents. These last units, which are 5 to 25m thick, are inferred to be lahars and/or other types of debris flows that may have been emplaced as a wet sediment gravity flow or landslide of water-saturated and occur intercalated with tuffs and other epiclastic sediments.

Facies Association III

This forms a sequence 450 m thick made up almost exclusively of massive to autobrecciated lava flows of andesite to basaltic andesite composition with an average thickness of 20 m. These blocky flows corresponded to the extrusion of several coulées often separated by thin beds of interflow epiclastic sediments (fine sandstone or siltstone). The other minor lithologies present are breccias of probable laharic origin, pyroclastic flows and air fall tephras. Contact with the underlying sequence is abrupt and conformable.

PALEOGEOGRAPHIC EVOLUTION

The greater part of the pyroclastic flows and surges of Facies Association I are considered to be related to phreatic and phreatomagmatic eruptions and were deposited in an intermediate position in relation to the central volcanic complex (Fig. 2). The emission of large quantities of pyroclastic material suggests that the initiation of sedimentation of the Farellones Formation corresponds to the collapse of a major volcanic centre and the probable formation of a caldera associated with high intensity eruptions. Facies Association II represents the beginning of a new phase of volcanic aggradation. Activity changed to eruption of dominantly andesitic lava flows and the construction of a new volcanic edifice closer to Lagunillas than the earlier one with intercalated lavas, pyroclastics and lahars. Facies Association III represents post-collapse evolution with an increase in volcanic activity in the area possibly, given the area covered and total thickness, by several centres of synchronous eruption

In this context, it is worth noting that the Farellones - rio Colorado area, 10-30 km north of Lagunillas, is characterized by lava flows which interdigitate with coarse pyroclastic and epiclastic deposits similar to those described here, together with shallow intrusive bodies (domes, dikes and sills). The strata are affected by angular intraformational unconformities caused by depositional-erosional processes rather than deformation. Preliminary work suggests that these are the remains of several eruptive centres which were active during deposition of the Farellones Formation. This volcanic complex would appear be the largest found in the region to date and could well have played a role in the deposition of part of the sequence described in this paper.

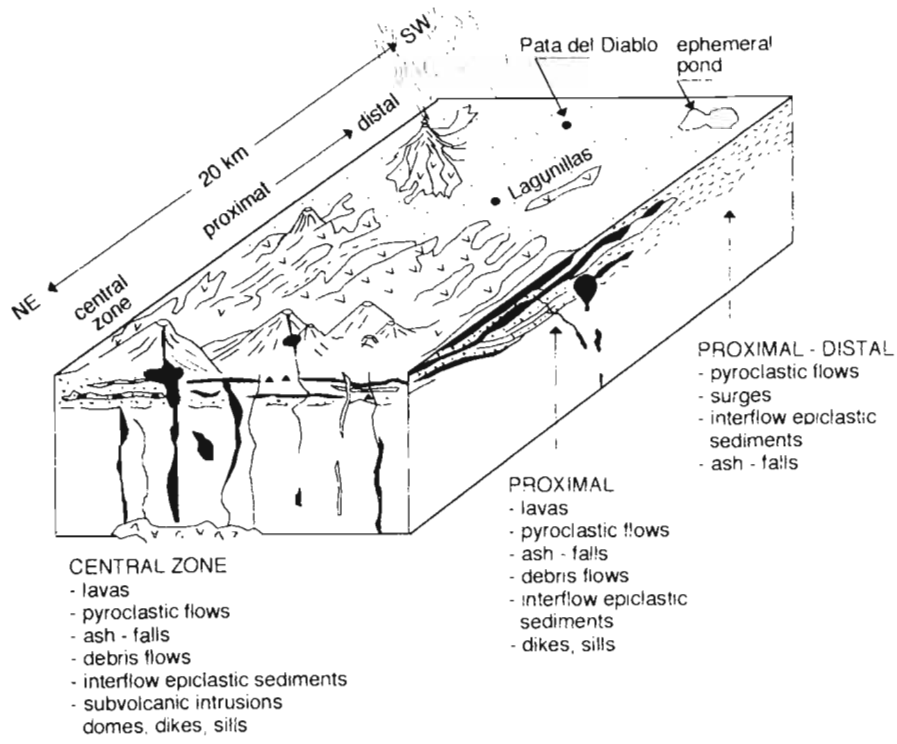

Fig. 2: Possible reconstruction of the palaeogeography, depositional conditions and facies relationships prevailing in the study area during the Farellones Formation.

REFERENCES

Aguirre R., 1999. Depositación y deformación de la secuencia volcánica terciaria en el sector cordillerano de Pata del Diablo, Cajón del Maipo, Región Metropolitana, Chile. Memoria para la obtención del Titulo de Géologo, Departamento de Geologia, Facultad de Ciencias Fisicas y Matemáticas, Universidad de Chile.

Branney M.J. and Kokelaar P., 1997. Giant bed from a sustained catastrophic density current flowing over topography : Acatlán ignimbrite, Mexico. Geology, 25, 115-118.

Carey S.N., 1991. Transport and deposition of tephra by pyroclastic flows and surges. In: Fisher R.V. & Smith G.A. (eds.). Sedimentation in volcanic settings. Soc. Economic Paleontologists and Mineralogists, Special Pub., 45, 39-57.

Cas R.A.F and Wright J.V., 1987. Volcanic successions, modern and ancient. Allen and Unwin , London.

Clavero J. and Moreno H., 1994. Ignimbritas Licán y Pucón: Evidencias de erupciones explosivas andesito-basálticas post-glaciales del volcán Villarrica, Andes del Sur, 39° 25' S. VII Congreso Geológico Chileno, 1, 250-254.

Drake R.E., Curtis G. and Vergara M., 1976. Potassium-Argon dating of igneous activity in the Central Chilean Andes, latitude 33° S. J. Volcanol. Geotherm. Res. 1, 285-295.

Druitt T.H., 1998. Pyroclastic density currents. In: Gilbert J.S. & Sparks R.S.J. (eds.) The physics of explosive volcanic eruptions. Geological Society, London, Special Pub., 145, 145-182.

Druitt T.H. & Sparks R.S.J., 1984. On the formation of calderas during ignimbrite eruptions. Nature, 310, 679-681.

Klohn C., 1960. Geología de la Cordillera de los Andes de Chile Central, Provincias de Santiago, O'Higgins, Colchagua y Curicó. Instituto de Investigaciones Geológicas, Santiago, Bol. N°8, 95 p.

Thiele R., 1980. Hoja Santiago, Región Metropolitana. Carta Geológica de Chile, Escala 1: 250.000. Instituto de Investigaciones Geológicas, Santiago, Carta N° 39, 51 p.

MONITORING GEOPHYSICAL AND GEOCHEMICAL DATA AT THE VOLCANO GALERAS, COLOMBIA

E. FABER(1), S. GREINWALD(2), D. PANTEN(3), G. G. VALENCIA(4), D. M. GÓMEZ(5), R. A. TORRES(6), C. MORAN(7) and A. O. ESTUPIÑAN(8)

(1), (2), (3) Federal Institute for Geosciences and Natural Resources, Stilleweg 3, 30655 Hannover, Germany (eckhard.faber@bgr.de)
(4), (5), (6), (7), (8) Observatorio Vulcanologico y Sismologico, Carrera 31 No. 18-07, Pasto, Colombia

KEY WORDS: Monitoring Volcanic Activity, Multiparameter Station, Electromagnetic Signals, Chemical Monitoring, Volcanic Hazards.

INTRODUCTION

For a better understanding of the activity and physics of active volcanoes the Federal Institute for Geosciences and Natural Resources (BGR) and the Instituto de Investigation en Geosciencias, Mineria y Quimica (INGEOMINAS) have started a new approach to set up a multiparameter monitoring station at the volcano GALERAS, located in the southern Andes of Colombia at the altitude of 4270 m. Although seismic broad band sensors are the main constituents of the station, other parameters like electromagnetic, thermographic and gas-geochemical data are or will be included. Data are measured close to or in the caldera and by radio telemetry transmitted for real time analysis. This contribution will focus on electromagnetic and geochemical equipment and preliminary results.

To monitor electromagnetic signals arising from internal activities of the volcano three stations have been set up. Two stations are located inside the caldera, a third one is set up at a distance of 5 km from the crater. At each station the horizontal electric field is measured in two orthogonal directions, and the vertical component of the magnetic field with an induction coil. Signals to be expected may be due to piezoelectric effects caused by mechanical vibrations of the ground and rock ruptures under high pressure. Low frequency electromagnetic signals may result from the flow of conducting liquids within the volcano or by the long term demagnetization of minerals by temperature changes. There are plans to extend the recorded signals to the horizontal components of the magnetic field to determine the resistivity of the

ground using magnetotelluric interpretation. First measurements show strong electrical noise at the stations inside the caldera probably due to a tv-transmitter located within a distance of 1 km to the crater.

For geochemical monitoring of gases escaping fumaroles a system has been designed to measure emitted

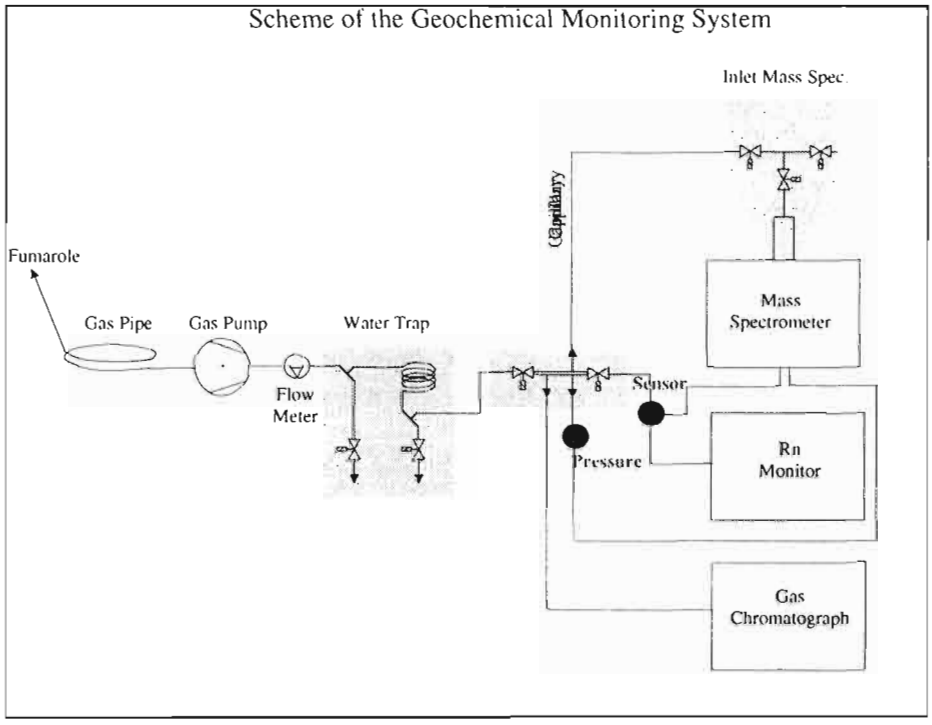

Fig. 1: *Schematic diagram of some components of the system for monitoring gases from volcanic fumaroles.*

gases in minute to sub-minute intervals. The instrument package, located near the fumarole, includes a mass spectrometer, radon units, gas chromatographs, and sensor based units, which are tested and optimised.

Also pipes and pumps are available to connect the analytical equipment to fumaroles over a distance of more than 1000 m. During three test campaigns different instrument set ups and pipe length are used. Depending on the local situation like power supply, weather conditions accessibility of the fumarole the instruments are installed close to the fumarole or in a distance of several hundred meters. According to this selection, components like CO_2, N_2, O_2, Ar, SO_2, H_2S, Rn, H_2 can be monitored, data gathered so far are characteristic for fumarolic gases. Radon readings are in good agremeent with conventional measurements.

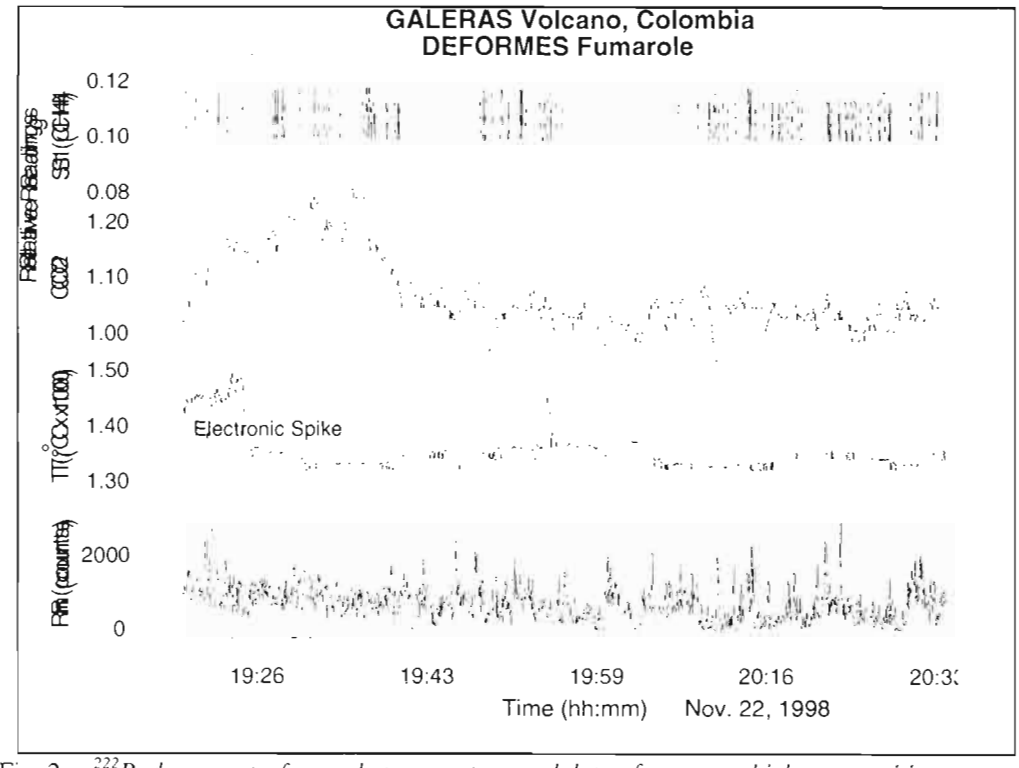

Fig. 2: *^{222}Radon counts, fumarole temperature and data of sensors which are sensitive predominantly for carbon dioxide and methane. Data were recorded every 5 seconds. Monitoring will be continued to make sure that the fluctuations are related to the fumarole, but are not technical artefacts.*

Conclusions

Volcanoes and fumaroles are the most hostile environments one can imagine for laboratory equipment. Therefore, we faced quite a lot of problems like strikes by lightning as well as stability and continuity of the instruments and resistance of the material inserted into the fumaroles used for the connection to the instruments. Nevertheless, we think that both the systems, electromagnetic and geochemical monitoring, have the potential to be used successfully for the monitoring of fumarolic emissions. Details will be presented.

THE NEOGENE TRANSPRESSIONAL ARCHITECTURE OF THE SANTA ELENA PENINSULA, ECUADOR: NEW INSIGHTS FROM SEISMIC DATA.

Fernando A. FANTIN [1], Patricio MALONE [2], Eduardo A. ROSSELLO [3] and Muriel MILLER [4]

(1) Compañía General de Combustibles S.A. A. Moreau de Justo N° 400, 1° (1107) BUENOS AIRES, Argentina. E-mail: fernando_fantin@cgc.com.ar
(2) Compañía General de Combustibles S.A. A. Moreau de Justo N° 400, 1° (1107) BUENOS AIRES, Argentina. E-mail: patricio_malone@cgc.com.ar
(3) CONICET-Depto. Cs. Geológicas, Universidad de Buenos Aires. Pabellón II, Ciudad Universitaria. (1428) BUENOS AIRES, Argentina. E-mail: rossello@gl.fcen.uba.ar
(4) Compañía General de Combustibles S.A. A. Moreau de Justo N° 400, 1° (1107) BUENOS AIRES, Argentina. E-mail: muriel_miller@cgc.com.ar

KEY WORDS: Tectonics, Transpression, Ancon Basin, Ecuador.

INTRODUCTION

The Peninsula of Santa Elena, located at the south-western coast of Ecuador, is an oceanic terrain accreted to the South America Plate margin by Late Cretaceous to Early Tertiary times. The Aptian to Albian oceanic rocks (Piñón Fm) are the basement of Upper Cretaceous-Paleogene sedimentary record that represents the development of successive fore-arc basins related with the syntectonic deformation generated by this subduction (see more details in Benítez, 1995; Jaillard *et al.*, 1995; Malone *et al.*, 1999). On this basement are developed fore-arc and slope basins (Shepherd & Moberly, 1981; Underwood & Bachman, 1982) with a complex evolutionary history, spans from the Cretaceous to the Eocene. The stratigraphic sequence of these basins is composed entirely by deep marine deposits, ranging from the Upper Cretaceous to the Upper Eocene. A thick sequences overlays the basement and is composed by hemipelagic silts, tuffs, volcanic breccias, turbidites and siliceous shales. The Upper Cretaceous Cayo Fm corresponds to an infill fore-arc sequence and would represent the erosion of a volcanic arc of islands (Chongón–Jama arc), present towards the eastern and north-eastern areas (Jaillard *et al.*, 1995). The Santa Elena Fm. (Upper Campanian-Upper Paleocene) is constituted by deep-water fine turbiditic deposits, slumps and siliceous and tuffaceous pelitic flows, associates with radiolarites. The Azúcar Gr. (Upper Danian-Upper Thanetian) is a thick sequence of turbiditic sandstone that constitutes the main oil reservoir of the area. Different sedimentary units of turbiditic and shallow marine deposits (Malone *et al.*, 1999) compose the Ancón Gr. (Middle Eocene). The subhorizontal Tablazo Fm (Pleistocene) overlay by angular unconformity on all the previous units and is composed by calcareous and bioclastic sandstones. Some present topographic highs

made by previous units (Asagmones, Chuculunduy, Baños de San Vicente, Azúcar hills) were islands during the sedimentation of this formation (Fig. 1).

Excepting cliffs and some quarries, outcrops in the region are scarce and no well exposed. Nevertheless, detailed structural works, surface mapping, electrical log correlation and the recent seismic surveys for oil prospecting acquired for **Compañía General de Combustibles S.A**. improve the structural knowledge of the subsurface geology of Santa Elena Peninsula. This current work shows new structural relationship into both Ancón (to the South) and Pacoa (to the North) oil producing basins taken from seismic surveying. The architecture of these basins was successively interpreted as a product of synsedimentary

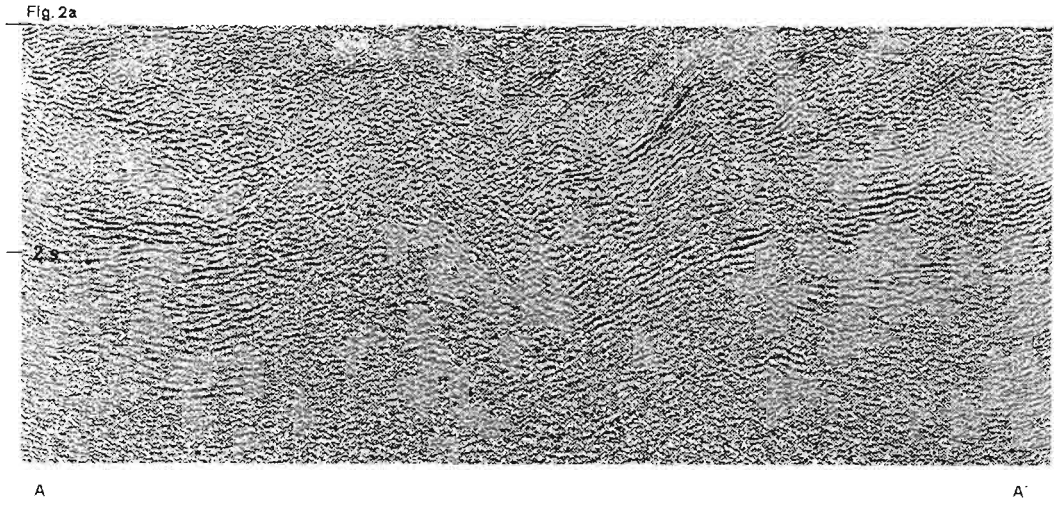

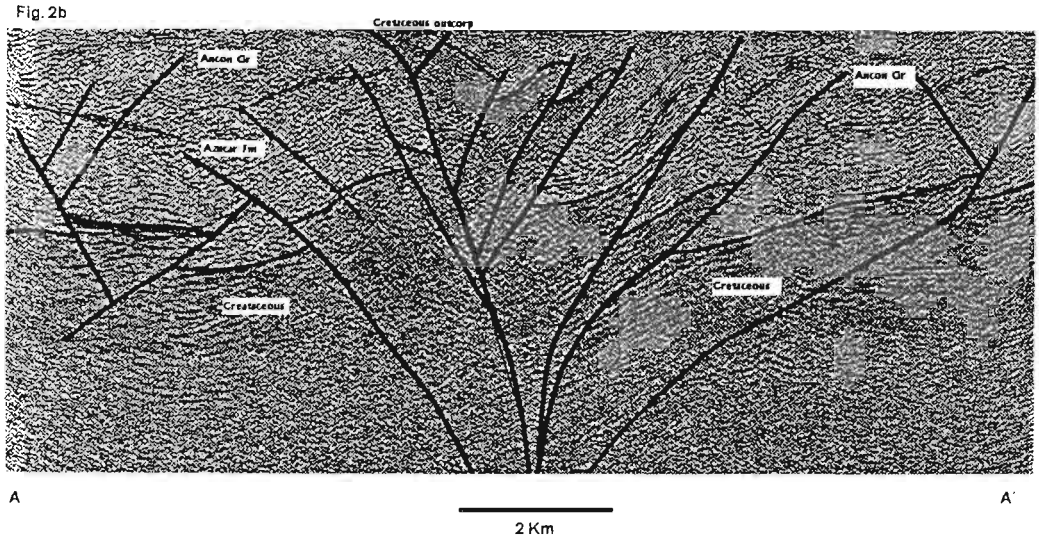

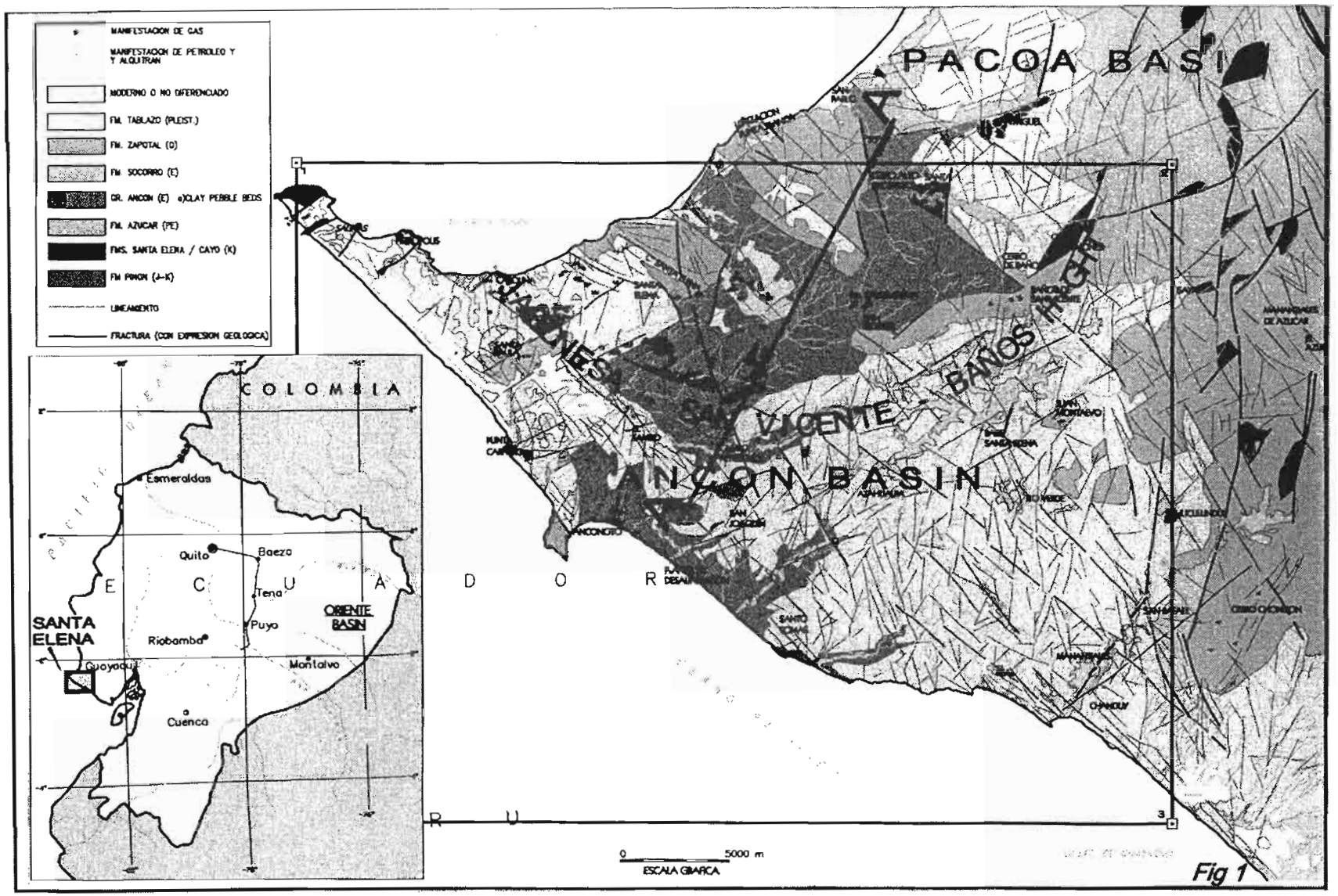
MANIFESTACION DE GAS
MANIFESTACION DE PETROLEO Y Y ALQUITRAN
MODERNO O NO DIFERENCIADO
FM. TABLAZO (PLEIST.)
FM. ZAPOTAL (O)
FM. SOCORRO (E)
GR. ANCON (E) a)CLAY PEBBLE BEDS
FM. AZUCAR (PE)
FMS. SANTA ELENA / CAYO (K)
FM PINON (J-K)
LINEAMIENTO
FRACTURA (CON EXPRESION GEOLOGICA)
PACOA BASI
ANCON BASIN
SAN VICENTE - BAÑOS HIGH
COLOMBIA
Esmeraldas
Quito
Baeza
Tena
Puyo
Riobamba
Guayaquil
Montalvo
Cuenca
SANTA ELENA
ORIENTE BASIN
E C U A D O R
0 5000 m
ESCALA GRAFICA
Fig 1

THE JAPONESA-SAN VICENTE BANOS HIGH

The **JSVBH** has been interpreted as a typical right-lateral transpressional structure characterized by a concentration of folds and inverse faults that lifted basement slides. Contraction in a NE-SW direction is evidenced by these subordinate structures. In plant view, it is possible to determine several syntectonic and antitectonic faults and folds, as well as, releasing and restraint steps and bendings of the main transpressional zone. The subsurface and surface expression of this structure is followed by over more than 5 km. wide and 30 km long (**Fig. 1**).

A seismic section, across the **JSVBH**, in the surroundings of Japonesa (Fig. **2a**, uninterpreted and **2b**, interpreted), exhibits a typical positive asymmetric flower structure (nomenclature in Biddle & Christie-Blick, 1985; Harding, 1990) involving basement formed by the Cretaceous Santa Elena Fm. Isolated outcrops of this formation express of the central uplifted portions of the **JSVBH**. The external and internal branches of the flower are steep and associated with reverse faults and thrusts that uplift slices of the Santa Elena Fm on the Ancón Gr. The tectonic vergence of the main structure is towards the South and it is probable that were a product of the reactivation of normal pre-existing faults.

Some isolate and small outcrops of the Santa Elena Fm, without clear connection with best known elements of this formation and located towards the northern border of the **JSVBH** (Fig. **1**) were considered as olistoliths by the authors. These hectometric blocks of the Santa Elena Fm. are subordinate competent units glided into non-competent rocks that form a discrete melange developed by imbricate faulting and gravitational gliding (Hsü, 1968). On the other hand this main structural feature has controlled and limited towards the north the Azúcar Fm. deposits in the Ancón basin. During the Neogene the **JSVBH** has been reactivated affecting the Ancón Group. The deformation is in accordance with the regional transpression generated by the main oblique subsidence of the Nazca Plate beneath the South America Plate. (Noblet *et al.*, 1996). More recent tectonics adjustments have affected the basin architecture generating little normal movements and inversion on the main structures involving the Pleistocene Tablazo Fm. deposits.

ACKNOWLEDGEMENTS

We acknowledge **Compañía General de Combustibles S.A**. for permitting the publication of this study. The CONICET and University of Buenos Aires, co-sponsored the work of EAR.

REFERENCES

Benítez, S.B., 1995. Evolution géodynamique de la Province cotière sud-Equatorienne au Cretacé Superieur-Tertiaire. Thèse Doctorale. Université Grenoble (France), 221p.

Christie-Blick, N. & K.T. Biddle, 1985. Deformation and basin formation along strike-slip faults. *In* Biddle, K.T. & N. Christie-Blick (eds.): Strike-slip deformation, Basin formation and sedimentation. Society of Economic Paleontologists and Mineralogists (Tulsa), Special Publication 37, 1-34.

Harding, T.P., 1990. Identification of wrench faults using subsurface structural data: criteria and pitfalls. American Association of Petroleum Geologists, Bulletin 74 (10), 1590-1609.

Hsü, K.J., 1968. Role of cohesive strength in the mechanics of overthrust faulting and landsliding. Geol. Soc. Am., Bull. 80, 927-952.

Jaillard, E., M. Ordoñez, S. Benítez, G. Berrones, N. Jiménez, G. Montenegro & I. Zambrano, 1995. Basin development in an accretionary, oceanic-floored fore-arc setting southern coastal Ecuador during Late Cretaceous-Late Eocene Time. In Petroleum basins of South America (Eds. A.J. Tankard, R. Suárez-Soruco & H.J. Welsink) American Association of Petroleum Geologists (Memoir 62), 615-631.

Malone, P., F.A. Fantin, EA. Rossello & M. Miller, 1999. Stratigraphic characterisation of the Ancón Group from the seismic data (Santa Elena Peninsula, Ecuador). *This volume.*

Noblet, C., A. Lavenu & R. Marocco, 1996. Concept of continuum as opposed to periodic tectonism in the Andes. Tectonophysics, 225, 65-78.

Roperch, P. F. Megard, C. Laj, T. Mourier, T.M. Clube & C. Noblet, 1987. Rotated oceanic blocks in Western Ecuador. Geophysical Research Letters, 14 (5), 558-561.

Shepherd, G.L. & R. Moberly, 1981. Coastal structure of the continental margin northwest Peru and southwest Ecuador. Geological Soc. Am. Memoir 154, 351-391.

Underwood, M.B. & S.B. Bachman, 1982. Sedimentary facies associations within subduction complexes. *In*: Legget, J.K. (Ed.) Trench-forearc geology. Geological Society Special Publication 10, 537-550.

ORIGIN OF CRYSTAL CLOTS AND THEIR ORTHOPYROXENE-TITANOMAGNETITE SYMPLECTITES IN LAVAS FROM THE LICANCABUR VOLCANO, SOUTH-CENTRAL ANDES

Oscar FIGUEROA [1] and Bernard DÉRUELLE [2]

[1] Departamento de Ciencias de la Tierra, Universidad de Concepción, Casilla 3-C, Concepción, Chile. e-mail: ofiguero@udec.cl

[2] IUFM Versailles and UPRESA CNRS 7047—UPMC Paris, case 110, 4, place Jussieu, 75257 Paris Cedex 05, France. e-mail: deruelle@ccr.jussieu.fr

KEY WORDS: Licancabur volcano, Crystal clots, Synneusis, Orthopyroxene-titanomagnetite symplectites.

INTRODUCTION

The Licancabur volcano (22°56' S, 67°53' W) is located in the Central Volcanic Zone of the Andes, on the Chilean-Bolivian boundary (fig. 1; Figueroa and Déruelle, 1996, 1997a, b). The lavas are mostly andesites s.s. (Figueroa and Déruelle, 1997a); only one basaltic-andesite and two dacites have been found. The texture of the lavas are porphyritic, seriate, glomeroporphyric and slightly vesicular. Andesite phenocrysts are plagioclase (Pl), orthopyroxene (Opx), clinopyroxene (Cpx) and Fe-Ti oxides (Ti-Mag). Some olivine (Ol) and hornblende (Hb) microphenocrysts are also present in some andesites. Phenocrysts of Hb (> 4.5 %) and rare biotite ones occur in the dacites. The groundmass has a hyalopilitic texture and contains microlites of Pl, Cpx, Ti-Mag, and pale brown glass. Some phenocrysts are not in equilibrium with their host lavas (Figueroa and Déruelle, 1997a, b).

THE CRYSTALS CLOTS

All the lavas contain crystal clots imparting to them a glomeroporphyritic texture. The size of the clots is around 2-3 mm in diameter, some ones being larger. The phenocrysts at the border of the clots are euhedral and have the same size as those found as isolated phenocrysts in the lavas whilst in the core of the clots are smaller (photo 1). The clots frequently contain interstitial glass with scattered tiny columnar pyroxene microlites (photo 2). The mineral phases present in the clots are the same as those found as isolated phenocrysts in the lavas. The modal composition of the clots is gabbroic (Pl + Cpx + Opx + Mag) but Cpx is more abundant than in the host lavas. Olivine and hornblende phenocrysts are sometimes present in the clots when these minerals also occur as isolated phenocrysts in their host lavas. Clots with predominant Pl phenocrysts coexist with others where Cpx predominates. The clots may simultaneously contain sieve-textured and limpid Pl phenocrysts. The phenocrysts at the border of the clots are often embayed and broken, some of them being partly separated from the clot. Some embayed Pl phenocrysts have a swallow-tail shape.

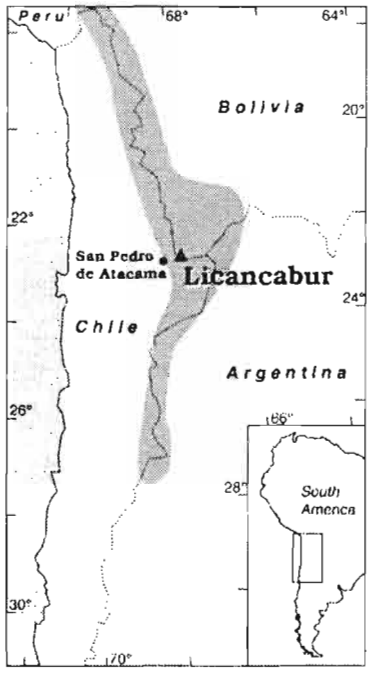

Fig. 1. Location of Licancabur volcano in the CVZ (shaded area).

Symplectites

Symplectites of Opx and Mag occur in the fine-grained part of the clots (photo 3). Similar symplectites commonly occur in intrusive and metamorphic rocks. Various hypotheses have been put forward to explain their origin (exsolution, eutectic reaction, interaction between adjacent phenocrysts during cooling, oxidation or replacement of Ol phenocrysts, deformation during growth (Barton and Van Gaans,

1988, Barton et al., 1991), but they cannot apply to Licancabur clots where rapid cooling facilitated fracturation of Opx phenocrysts and subsequent development of symplectites.

Origin of the clots

Some clots with a classical polygonal shape are undoubtedly related to the breakdown of high-Al amphibole (Stewart, 1975; Déruelle, 1979) and will not be considered here.

Photos (PPL).

1: Typical crystal clot with small crystals in the core and larger ones on the rim; x 4.

2: Core of one crystal clot showing rounded Pl, Opx, Mag, and glass with acicular crystals; x 10.

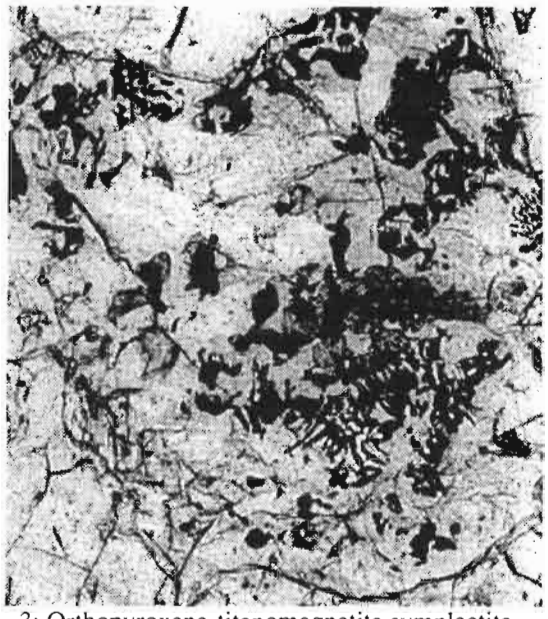

3: Orthopyroxene-titanomagnetite symplectite in the core of a crystal clot; x 10.

4: Monomineralic clot of sieve-textured plagioclase phenocrysts; x 4.

The clots and their host lavas are clearly of co-magmatic origin. Higher Cpx contents in the clots compared with that of their host lava attest for an early *in situ* origin. The crystal clots composed of a single mineral phase (photo 4) probably developped by synneusis —it means that two or more preexisting isolated phenocrysts, suspended in magma, may become attached to each other and grow as a unit if they accidentally meet in parallel or twinned orientation— as proposed for monomineralic clots observed in plutonic and volcanic rocks (Vance, 1969; Schwindinger and Anderson, 1989; Hogan, 1993). The genesis of clots with limpid and sieve-textured Pl phenocrysts conjointly observed in a same lava should have occurred during successive stages of the crystallization story of the magmatic liquid from which they originated.

Disaggregation of the clots may be responsible for the textural variety of isolated phenocrysts now observed in the lavas. Such an origin has been proposed to explain the phenocryst diversity in Mazama rhyodacites (Nakada et al., 1994).

Acknowledgements

This work has benefited of grants from ECOS U97-06 and Dirección de Investigación de la Universidad de Concepción (O.F.).

REFERENCES

Barton, M., Sheets, J. M., Lee, W. E. & Van Gaans, C. (1991). Occurrence of low-Ca clinopyroxene and the role of deformation in the formation of pyroxene-Fe-Ti oxide symplectites. Contrib. Mineral. Petrol., 108, 181-195.

Barton, M. & Van Gaans, C. (1988). Formation of orthopyroxene-Fe-Ti oxide symplectites in Precambrian intrusives, Rogaland, southwestern Norway. Amer. Mineral., 73, 1046-1059.

Déruelle, B. (1979). Pétrologie d'un volcanisme de marge active: Atacama et Andes Méridionales. Thesis Doct. État. Univ Paris XI, Orsay, 417 pp.

Figueroa, A. O. & Déruelle, B. (1996). Licancabur, an andesitic volcano of the South-Central Andes. *3rd Internat. Symp. Andean Geodynamics, Coll. Séminaires, ORSTOM*, 563-566.

Figueroa, O & Déruelle, B. (1997a). El volcán Licancabur (22°56' S, 67°53' W, Segunda región de Antofagasta): geología, petrografía y mineralogía. Actas VIII Cong. Geol. Chileno, 1, 322-326.

Figueroa, O & Déruelle, B. (1997b). Petrology of Licancabur volcano (Andes of Atacama): evidence of combined crystal fractionation and magma mixings. *Terra Abst. Terra Nova Suppl.*, 9, 1, 473-474.

Hogan, J. P. (1993). Monomineralic glomerocrysts: textural evidence for mineral resorption during crystallization of igneous rocks. J. Geol., 101, 531-540.

Nakada, S., Bacon, C. R. & Gartner, A. E. (1994). Origin of phenocrysts and compositional diversity in pre-Mazama rhyodacite lavas, Crater Lake, Oregon. J. Petrol., 35, 127-162.

Schwindinger, K. R. & Anderson, A. T. (1989). Synneusis of Kilauea Iki olivines. Contrib. Mineral. Petrol., 103, 187-198.

Shelley, D. (1993). Igneous and metamorphic rocks under the microscope. Classification, textures, microstructures and mineral preferred orientation. Chapman & Hill, London, pp. 445.

Stewart, D.C. (1975). Crystal clots in calc-alkaline andesites as breakdown products of high-Al amphiboles. Contr. Mineral. Petrol., 53, 195-204.

Vance, J. (1969). On synneusis. Contr. Mineral. Petrol., 24, 7-29.

DECOMPRESSION AT DECREASING TEMPERATURES IN ECLOGITE-FACIES METAPELITES (EL ORO METAMORPHIC COMPLEX, SW-ECUADOR): A RECORD OF FAST EXHUMATION RATES.

Piercarlo GABRIELE[1], Michel BALLEVRE[2], Etienne JAILLARD[3] and Jean HERNANDEZ[4]

(1) Institut de Minéralogie et Pétrographie, Université de Lausanne, BFSH2, 1015 Lausanne, Suisse Piercarlo.Gabriele@imp.unil.ch
(2) Laboratoire de Pétrologie, Géosciences Rennes (UPR CNRS 4661), Université de Rennes 1, 35042 Rennes Cedex, France. Michel.Ballevre@univ-rennes1.fr
(3) UPRES A-CNRS 5025,Université Joseph Fourier, Institut Dolomieu, 15 rue M. Gignoux, 38031 Grenoble Cedex, France. Etienne.Jaillard@ujf-grenoble.fr
(4) Institut de Minéralogie et Pétrographie, Université de Lausanne, BFSH2, 1015 Lausanne, Suisse Jean.Hernandez@imp.unil.ch.

KEY WORDS : Ecuador, Metapelite, Eclogite-facies metamorphism, Exhumation

GEOLOGICAL SETTING

The « El Oro province » is located in the south-westernmost Ecuador. The **El Oro metamorphic complex** (about 24000 km2) belongs to the displaced Amotape-Tahuin block (Mourier et al. 1988). The metamorphic complex comprises lithologies and assemblages, the ages of which range from the Palaeozoic to the Cretaceous, that are interpreted as a former accretionary prism (Aspden et al., 1995). According to the most recently published geological map (Aspden et al., 1995), this area is cross-cut by several E-W striking fault systems that subdivide the El Oro metamorphic complex in different smaller units.

The E-W-trending Raspas ophiolitic complex is bounded to the North and the South by the "La Palma - El Guayabo" and the "Tahuin Dam" faults, respectively. It consists of greenschists, serpentinised harzburgites, pelitic schists, blueschists and eclogites, described in detail first by Feininger (1980), and recently interpreted as a late Jurassic-early Cretaceous tectonic mélange representing an accretionary prism (Aspden et al., 1995). K-Ar data on phengite (132 ± 5 Ma, Feininger, 1980) suggests a Lowermost Cretaceous age for the high-pressure metamorphism (Duque, 1993).

The studied metapelites come from the « **La Chilca unit** », located in the northern part of the Raspas ophiolitic complex. K-Ar data on phengite (132 ± 5 Ma : Feininger, 1980) suggest a Lower Cretaceous age for the high-pressure metamorphism (Duque, 1993).

The aim of this paper is to present a revised P-T path for the Raspas complex, based on the garnet-bearing **metapelites**, in order to constrain their exhumation mechanisms.

PETROGRAPHY

The studied metapelites are medium- to coarse-grained graphite-bearing schists, where the high-pressure paragenesis consists of quartz, white mica, garnet , chloritoid, kyanite and rutile (98RR2 ; 98RR10 ; 98RR11 ; 98RR12 ; 97Ce5). The **white mica** defines the main schistosity which corresponds in the field to the regional schistosity. The phengite is idioblastic or sub-idioblastic and usually is concentrated in millimeter-thick layers alternating with **quartz**-rich, granoblastic layers. **Garnet** poikiloblasts contain inclusions of quartz, kyanite, chloritoid, rutile. The porphyroblasts overgrow an older schistosity mainly defined by minute graphite inclusions and showing isoclinal folds. The presence of rotational structures in porphyroblasts indicates that garnet growth was synkinematic with respect to the event that generated the older schistosity. Compared to the main schistosity (the phengitic one), the garnet is mostly pre-tectonic. Three different generations of **chloritoid** are identified, namely (1) relict xenoblastic crystals included in the garnet ; (2)-xenoblastic to sub-idioblastic crystals dispersed in the matrix and aligned along the main schistosity; and (3) - idioblastic chloritoids randomly oriented across the schistosity or pseudomorphing garnet. **Kyanite** is observed in the garnet and/or in the matrix. It often shows a reaction rim with chlorite and white mica, and also a pseudomorphic replacement by chloritoid and white mica. **Rutile** and **graphite** are the main accessories.

MINERALOGY

The chemical composition of garnet, white mica and chloritoid were determined using the wavelength dispersive electron microprobe (CAMECA SX50). Representative analyses are listed in **Table 1**. **Garnet** shows a regular decrease in Mn content and a regular increase in Mg content from core to rim. Average core and rim compositions are Alm60-62%, Sps6-7%, Prp2-4%,Grs22-24% and Alm59-64%, Sps0.3-1.5% Prp10-12%, Grs20-23%, respectively. **Chloritoid** inclusions in garnet cores and garnet rims have an XMg of 0.15 and 0.30, respectively. Matrix chloritoid has compositions similar the most magnesian inclusions in the garnet grains. Finally, the randomly-oriented grains in the matrix and the chloritoid grains pseudomorphing garnet are less magnesian (XMg = 0.21). **White micas** are phengitic

muscovites, with a relatively high Si content analyses (from 6.35 to 6.45 atoms p.f.u on the basis of 22 oxygens) and the Mg+Fe(tot) content vary between 0.35 and 0.55 atoms p.f.u..

Table 1 Representative chemical compositions for minerals in listed samples

Chloritoids				Garnets				White micas			
Sample	98RR2	98RR2	98RR2	98RR10	98RR10	97Ce5	97Ce5	98RR11	98RR12	98RR2	97 Ce 5
	Random	matrix	relic	rim	core						
Point n°	10	11	23	225	251	10	14	16	35	11	43
SiO2	24.39	24.09	24.10	37.79	37.29	37.58	37.14	47.04	47.64	47.73	48.52
TiO2	-	-	-	0.16	0.21	0.17	0.01	0.49	0.42	0.44	0.44
Al2O3	41.11	41.01	40.70	21.05	20.37	21.20	21.03	32.61	33.14	33.16	32.45
Cr2O3	-	-	-	0.02	0.00	0.00	0.00	0.00	0.03	0.05	0.06
FeO*	23.08	23.17	25.16	30.08	29.38	33.59	35.44	1.42	1.07	1.18	1.34
MnO	0.34	0.18	0.23	0.14	2.73	0.37	0.42	0.01	0.00	0.00	0.01
MgO	3.39	3.87	2.49	3.00	0.61	2.21	1.98	1.65	1.54	1.61	1.62
CaO	0.00	0.01	0.01	8.45	9.96	5.79	4.86	0.00	0.01	0.04	0.00
Na2O	0.06	0.00	0.03	0.00	0.00	0.04	0.01	1.14	1.16	0.93	1.21
K2O	-	-	-	-	-	-	-	8.77	8.79	8.81	8.94
Total	92.39	92.33	92.71	100.70	100.55	100.94	100.90	93.13	93.81	93.96	94.60

REACTION HISTORY AND P-T CONDITIONS

Microstructural relations and compositional data reveal that the assemblage chloritoid-kyanite-quartz was stable during garnet growth. Theoretical (e.g. Harte and Hudson, 1979; Vuichard and Ballèvre, 1988; Ballèvre et al, 1989) as well as calculated KFMASH (e.g. Powell and Holland, 1990) grids show that the assemblage Grt-Cld-Ky is stable within a narrow temperature range at high pressure. Specifically, the lower temperature limit is defined by the incoming of almandine + kyanite at the expense of Fe-chloritoid, and the upper temperature limit by the breakdown of chloritoid through the univariant reaction Cld = Grt + Chl + Ky.

The observed change of garnet and chloritoid chemistry records the progressive change in P-T conditions during garnet growth then resorption. Increasing Mg content from garnet core to garnet rim and correlative increasing Mg content of chloritoid (inclusions from garnet core to garnet rim, and matrix grains) indicate increasing temperatures during garnet growth. The same continuous reaction took place during garnet resorption, as indicated by the observed textures (garnet and kyanite pseudomorphs consisting of fine-grained chloritoid and quartz aggregates) and the decrease in Mg content of the late generation of chloritoid. The backreaction is incomplete, probably because H_2O was a limiting constituant during the retrograde history.

According to the KFMASH grids calculated by Powell et al (1998), the assemblage Grt-Cld-Ky is stable at higher pressures than 12 kbar, in the temperature interval 560-600°C. The Si content of phengite is

buffered at relatively low values by the assemblage Grt-Cld-Ky, but experimental data on the assemblage Alm-Ky (Massonne and Szpurka, 1997) indicates pressures of the order of 20 kbar (at 600°C).

IMPLICATIONS FOR THE EXHUMATION RATES

The observed decrease in temperature which follows peak pressure conditions provides severe constraints on the exhumation mechanism of the eclogite-facies rocks, because it means that a low geothermal gradient was still stable during exhumation. Such a process is consistent with an active setting, where subduction of relatively cold material continues below the accreted material during its exhumation, and/or that the exhumation rate, whatever its mechanism, is much faster that the thermal relaxation of the crust. This would explain the excellent preservation of the high-pressure paragenesis, except in the zones of ductile deformation that bound the Raspas Complex, which may have formed later during the final emplacement of the Raspas metamorphic rocks at high structural levels.

REFERENCES

Aspden, J. A., Bonilla, W., and Duque, P. 1995. The El Oro metamorphic complex, Ecuador: geology and economic mineral deposits. Overseas Geology and Mineral Resources, No. 67.

Ballèvre, M., Pinardon, J.-L., Kienast, J.-R., and Vuichard, J.-P. 1989. Reversal of Fe-Mg partinioning between garnet and staurolite in Eclogite-facies metapelites from the Champtoceaux Nappe (Britanny, France). Journal of Petrology, 30, 6, 1321-1349.

Duque,P. 1993. Petrology, metamorphic history and structure of El Oro Ophiolitic Complex, Ecuador. Second ISAG, Oxford (UK), 21-23 Sept. 1993, Extended Abstracts volume, 359-362.

Harte, B., and Hudson, N.F.C. 1979. Pelite facies series and pressures of Dalradian metamorphism in E-Scotland. In The Caledonies of the British Isles-Reviewed. Geological Society of London Special Publication, 8, 323-337. Blakwell Scientific Publications Ltd, Oxford.

Feininger, T. 1980. Eclogite and related high-pressure regional metamorphic rocks from the Andes of Ecuador. Journal of Petrology, 21, 1, 107-140.

Massonne, H.-J., and Szpurka, X., 1997. Thermodynamic properties of white micas on the basis of high pressure experiments in the systems K2O-MgO-Al2O3-SiO2-H2O and K2O-FeO-Al2O3-SiO2-H2O. Lithos, 41, 229-250.

Mourier, T., Laj, C., Megard, F., Roperch, P., Mitouard, P., and Farfan-Medrano, A. 1988. An accreted continental terrane in northwestern Peru. Earth and Planetary Science Letters, 88, 182-192.

Powell, R., and Holland, T. 1990. Calculated mineral equilibria in the pelite system, KFMASH (K2O-FeO-MgO-Al2O3-SiO2-H2O) American Mineralogist, 75, 367-380.

Powell, R., Holland, T., and Worley, B. 1998. Calculating phase diagrams involving solid solutions via non-linear equations, with examples using Thermocalc. Journal of Metamorphic Geology, 16, 577-588.

Vuichard, J.-P., and Ballèvre, M. 1988. Garnet-chloritoid equilibria in eclogitic pelitic rocks from the Sesia zone (Western Alps): their bearing on phase relations in high pressure metapelites. Journal of Metamorphic Geology, 6, 135-157.

AGE AND STRUCTURE OF THE OXAYA ANTICLINE: A MAJOR FEATURE OF THE MIOCENE COMPRESSIVE STRUCTURES OF NORTHERNMOST CHILE

Marcelo GARCIA (1), Gérard HERAIL (2), Reynaldo CHARRIER (3)

(1) SERNAGEOMIN. Av. Sta. María 0104, Providencia, Santiago, Chile. (mgarcia@sernageomin.cl.)
(2) IRD. 209-213 Rue La Fayette, 75010, Paris, France. (gherail@paris.orstom.fr.)
(3) Universidad de Chile. Casilla 13518, Correo 21, Santiago, Chile.

KEY WORDS: Central Andes, Miocene, anticline, Oxaya, tectonics.

INTRODUCTION

The Central Andes, with an elbow shape, forms the widest and highest segment of the Andean range. DeFm and uplift of this segment are mainly controlled by Neogene shortening, broadly documented in the Sierras Subandinas, Cordillera Oriental and Altiplano (references in Baby et al., 1997). In the Cordillera Occidental, northernmost Chile (Arica latitude), recent studies have shown that the Neogene shortening is mainly represented by a system of the Miocene west-vergent structures, locally associated with syntectonic sediments (Muñoz and Charrier, 1996; García et al., 1996; Riquelme, 1998). In the Belén region this system forms a narrow thick-skinned fold and thrust belt (García et al., 1996). To the west of the Belén Belt, lesser deFm structures (folds and flexures) represent an external and late activation of the compressive system. The major structure of this less deformed region is the gentle Oxaya Anticline (O.A.), which produces an important physiographical step from 2000 to 3600 m (Fig. 1). In this paper, we describe in detail the surface geometry, kinematics and chronology of the O.A., and propose a different interpretation to that of other workers (Muñoz and Charrier, 1996; Uhlig et al., 1996).

THE DEFORMED UNITS

In the O.A. region, an extensive Oligo-Miocene cover of volcanic and sedimentary deposits overlies a substratum of more deformed Mesozoic rocks. The substratum, exposed only in the Lluta, Cardones and Azapa valleys, is essentialy formed by folded Jurassic-Lower Cretaceous sedimentary series (Livilcar Fm; Muñoz et al., 1988), which are intruded by the Late Cretaceous-Paleocene "Lluta Intrusives" (Salas et al., 1966; Muñoz and Charrier, 1996).

The Oligo-Miocene cover has been grouped in the Azapa, Oxaya, El Diablo, Zapahuira and Huaylas Fms (Salas et al., 1966; Vogel and Vila, 1980; García, 1996; Parraguez, 1998). The Azapa Fm, which consists of fluvial gravels, includes a thick lower member (•400 m), limited to the east by the Ausipar Fault (Fig. 1) and a thin upper member (0-50 m) that overlies, to the west, the lower member and to the east the Mesozoic substratum. The Oxaya Fm, which conformably overlies the Azapa Fm and locally (to east) the substratum, is the most extensive unit in the region and is entirely involved in the O.A.. It is formed by large ignimbrite sheets, interbedded with minor sediments. These sheets form a broad ~1000 m thick ignimbritic plateau of strongly competent rocks. Several K-Ar radiosotopic determinations in the Oxaya Fm, indicate an age range from 25 to 19 Ma (García et al., this symposium). In the eastern Pampa Oxaya (Fig. 1), they are overlain by fresh black basaltic-andesite of the Zapahuira Fm, that yielded K-Ar ages of 15 to 12 Ma (García, 1996; García, in prep.). The Oxaya and Zapahuira Fms are covered by the fluvial deposits of the Lower Member of the Huaylas Fm (García, 1996). The lowermost sandstones of this member and both the Oxaya and Zapahuira Fms are tilted to the East due to folding of the O.A.. They are onlaped by gravels, which upward rapidly become horizontal, defining a smooth progresive unconformity (Fig. 1). In the lowermost Huaylas Fm, Bargo and Reguero (1989) and Salinas et al. (1991) reported the presence of Early Huayquerian (9-8 Ma) mammal rests. The upper Huaylas Fm contains a thin ignimbrite dated (K-Ar on biotite) in 8.7±1.0 Ma. To the west of the O.A., the Oxaya Fm is conformably overlain by the lower sandstones and upper gravels of the El Diablo Fm (Fig. 1). The gravels contain black andesite clasts of both lithology and age identical to the Zapahuira Fm. In the Moquella region (70 km south to the O.A.), the same El Diablo gravels are conformably covered by a lava flow dated in 8.4±0.6 Ma (mean age of two K-Ar determinations; Naranjo and Paskoff, 1985; Muñoz and Sepúlveda, 1992). These data implie than deposition of the El Diablo Fm ended between ~12 and ~8.4 Ma. All the described units are locally covered, to the east and west of the Oxaya Anticline, by the Huaylas Ignimbrite, an extensive pyroclastic flow dated in 4.4±0.3 Ma (mean age of six K-Ar determinations; Naranjo and Paskoff, 1985; Gardeweg et al., this symposium).

THE OXAYA ANTICLINE

The O.A. is a gentle and west-vergent assymetric fold, well exposed in the western part of the Pampa Oxaya, and mainly formed by ignimbrites of the Oxaya Fm (Fig. 1). Along strike (N30W) it can followed for ~50 km. The structure smoothly plunges to the south, whereas to the north it evolves to a

N20W trending monoclinal flexure (Fig. 1). The greater amplitude of the O.A. is observed in the proximity of the Azapa valley (section of Fig. 1), where the structure causes a change in altitude of ~1600 m. Extrapolating eastward the regional slope (1-2°W) of the top of the Oxaya Fm in the Central Depression, a 1100-1200 m vertical offset is obtained for the hinge region (Fig. 1). In this region, the assymetry of the fold is better observed: the western limb dips 12-18°, the eastern limb dips 7-8°. The anticline is also associated with a very open frontal syncline (Fig. 1). In the hinge zone of the O.A., buckling and strong competence of the rocks of the Oxaya Fm has caused normal faulting and grabens, wich are locally filled by the Huaylas Ignimbrite.

The O.A. was produced by the propagation and reactivation of an ancient thrust. This structure, the Ausipar Fault (Salas et al., 1966; Muñoz and Charrier, 1996; Parraguez, 1998), only exposes its trace in the Lluta valley. The Ausipar Fault dips 40-55°E in the floor of the valley where it juxtaposes the substratum with the lower Azapa Fm. Higher up it evolves to a subhorizontal thrust that propagates into the upper Azapa and lower Oxaya Fms and deforms the upper Oxaya Fm (Fig. 1). The existence of the lower Azapa Fm westward of the Ausipar Fault, and its absence to the east (over the substratum), indicate a major period of complexe faulting prior to the generation of the O.A.. This period is constrained between the deposition of the lower and upper members of the Azapa Fm, during the Oligocene.

AGE OF FOLDING

We here consider the ages of the non-folded and folded units in the flanks of the O.A.. On the eastern limb, the tilted lowermost Huaylas Fm (9-8 Ma) is unconformably covered by horizontal gravels, which have intercalated a 8.7±1.0 Ma ignimbrite. If we consider the analitycal error of this age, then its minimum age can be regarded as 7.7 Ma. Therefore, the age interval for folding in this area is between 9 and 7.7 Ma. On the western limb of the frontal syncline, the El Diablo and Oxaya Fms dip very gently to the west. The minimum age of the El Diablo Fm implies that folding occurred after ~12-8.4 Ma. In addition, the Huaylas Ignimbrite (~4.4 Ma) overlies the El Diablo Fm with strong erosion unconformity (Fig. 1) and also covers the anticline. Thus, the geometric relationships in the western side of the O.A. indicate that folding took place after ~12-8.4 Ma and much earlier than 4.4 Ma. This last interval of age is wider than that the one obtained at the eastern border of the anticline, but is very consistent, and contraints also the folding to the Late Miocene (~9-7.7 Ma).

CONCLUSIONS

The O.A. formed in the Late Miocene (~9-7.7 Ma). It was generated by the propagation and reactivation of the Ausipar Fault in a compresional environment. The O.A. representes an external and late activation, under conditions of lesser strain, of the Miocene west-vergent compressive system of the northernmost Chilean Andes (Arica latitude).

ACKNOWLEDGMENTS.

This contribution was supported by both the Geological Survey of Chile (SERNAGEOMIN) and IRD (ex ORSTOM). Text was revised and improved by Carlos Arévalo, Reynaldo Charrier, Estanislao *Pirzio* Godoy, Constantino Mpodozis and Andrew Tomlinson.

REFERENCES

Baby, P.; Rochat, Ph.; Hérail, G.; Mascle, G.; 1997. Neogen shortening contribution to crustal thickening in the back arc of the Central Andes. Geology, **25**, p. 883-886.

Bargo, M.; Reguero, M.; 1989. El primer registro de un mamífero fósil en el extremo septentrional de Chile. Ameghiniana, **26**, p. 239.

García, M.; 1996. Geología y estructura del borde del Altiplano occidental, en el área de Belén (Chile). Tesis de Magister y Memoria de Título, U. de Chile, 111 p.

García, M.; Hérail, G.; Charrier, R.; 1996. The Cenozoic forearc evolution in Northern Chile: The border of the Altiplano of Belén (Chile). Third ISAG, Saint Malo, France, p. 359-362.

García, M.; in prep. These de Doctorat. Universite de Grenoble, France.

Muñoz, N.; Charrier, R.; 1996. Uplift of the western border of the Altiplano on a west-vergent thrust system, Northern Chile. J. South Amer. Earth Sci., **9**, p. 171-181.

Muñoz, N.; Elgueta, S.; Harambour, S.; 1988. El Sistema Jurásico (Formación Livilcar) en el curso superior de la quebrada Azapa, I Región: Implicancias paleogeográficas. Actas V Congreso Geológico Chileno, Santiago, Tomo 1, p. A403-A415.

Naranjo, J., A.; Paskoff, R.; 1985. Evolución cenozoica del piedemonte andino en la Pampa del Tamarugal, Norte de Chile (18°-21° S). Actas IV Congreso Geológico Chileno, Antofagasta, V. 5, p. 149-164.

Parraguez, G.; 1998. Sedimentología y geomorfología producto de la tectónica cenozoica, en la Depresión Central, Pampa de Chaca, I Región de Tarapacá, Chile. Memoria de Título, U. de Chile, 108 p.

Salas, R.; Kast, R.; Montecinos, F.; Salas, I.; 1966. Geología y Recursos Minerales del Departamento de Arica, Provincia de Tarapacá. Inst. de Invest. Geol., Boletín 21, 130 p.

Salinas, P.; Villarroel, C.; Marshall, L.; Sepúlveda, P.; Muñoz, N.; 1991. *Typotheriopsis* sp. (Notoungulata, Mesotheridae), Mamífero del Mioceno Superior en las cercanías de Belén, Arica, Norte de Chile. Actas VI Congreso Geológico Chileno, Viña del Mar, p. 314-317.

Uhlig, D.; Seyfried, H.; Wörner, G.; Kohler I.; Schröder, W., 1996. Landscape Evolution in Northernmost Chile (18.5°-19.5°): its implication in the Tectonic, Sedimentary and Magmatism History of the Central Andes. Third ISAG, Saint Malo, France, p. 745-748.

OLIGO-MIOCENE IGNIMBRITIC VOLCANISM OF NORTHERN CHILE (ARICA REGION): STRATIGRAPHY AND GEOCHRONOLOGY

Marcelo GARCIA (1), Gérard HERAIL (2) and Moyra GARDEWEG (1)

(1) SERNAGEOMIN. Av. Sta. María 0104, Providencia, Santiago, Chile. (mgarcia@sernageomin.cl.)
(2) IRD. 209-213 Rue La Fayette, 75010, Paris, France. (gherail@paris.orstom.fr.)

KEY WORDS: Central Andes, Oligo-Miocene, volcanism, stratigraphy, geochronology.

INTRODUCTION

The Central Andes is a mountain range formed in an active continental convergent margin, generating large volume of subduction-related magmas. During the Late Cenozoic, the calc-alkaline emisions have been mainly concentred in the Cordillera Occidental of the Central Andes, whereas shoshonitic, alkalin and silicic back-arc magmas occur in the Altiplano and Cordillera Oriental (eg. Sébrier and Soler, 1991). Detailed studies about composition, distribution, age and tectonic environment of these rocks are scarce. In the Cordillera Occidental, along 500 km from North Chile to South Peru, large volume of ignimbrites, dated in 25 to 16 Ma, have been described (eg. Mortimer et al., 1974; Tosdal et al., 1981; Naranjo and Paskoff, 1985; García, 1996; Schröder and Wörner, 1996, Parraguez, 1998). We present here new data about the stratigraphy, K-Ar geochronology, petrography and the preliminary geochimistry of the 25-19 Ma ignimbritic volcanism of northernmost Chile (Arica region) (Fig. 1A). In this region, according to their degree of deformation and volume of sedimentary intercalations, the ignimbrites have been grouped in the two differnt units, that have been given different ages ranging from Cretaceous to Pliocene (Salas et al., 1966).

THE IGNIMBRITES OF THE ARICA REGION

The Oligo-Miocene (25-19 Ma) ignimbrites are subaerial, silica and K-rich and large in volume. They have been grouped in Oxaya and Lupica formations. The Oxaya Fm forms the western flanck of the Cordillera Ocidental, extending as far as the Pacific Ocenan by ~150 km, in gently folded beds. The

Lupica Fm, that outcrops immediately to the east, is strongly folded and thrusted such that the contact with Oxaya Fm is, in general, tectonic and thus their original relationships are masked.

Oxaya Formation. Is the more representative and extensive ignimbritic unit in Arica region, where conformably overlies and underlies sediments, respectively of the Azapa and El Diablo formations, respectively (Salas et al., 1966; Vogel and Vila, 1980; Parraguez, 1998). This succession unconformably covers to Mesozoic rocks. The Oxaya Fm (sensu García, 1996; Parraguez, 1998) is comprised of 4 to 6 welded, silicic, ignimbrite sheets, separated by minor sedimentary intercalations. West of the Oligo-Miocene arc the ignimbrites were deposited in alluvial pediment planes. Their thickness, welding and corseness systematicaly decrease westward. At the Pampa Oxaya, type locality of the formation, the sheets form a vaste and thick (~1000 m) plateau, although a more complete section is exposed in the Codpa-Sucuna region (Fig. 1B). The lower ignimbrites (25-24 Ma) are medium-volume, with the two oldest units (~25 Ma) exposed only in the Camarones valley, whereas an different ~24 Ma ignimbrite is exposed only in the Lluta valley. The thickest flow (200-600 m), a brown-colored unit named here Livilcar Ignimbrite (~23 Ma), is, however, only exposed in the Lluta and Azapa valleys. Over the Livilcar Ignimbrite we recognize a slightly thiner unit (~23 Ma, 50-150 m) characteristically pink in color. However, the most continuous and extensive deposit of the Oxaya Fm is a brown and grey-clored unit, that we designate Oxaya Ignimbrite (~21 Ma), with a mean thickness of 100 m, wich provides a superb regional stratigraphic marker. Only within the study area, it covers a surface of 15000 km^2, with a minimum estimated volume of 1500 km^3. Over the Oxaya Ignimbrite are scattered outcrops of thinner (<50 m), wedely distributed ignimbrites, grouped here as Sucuna Ignimbrite (~19 Ma). The large volume of some of these ignimbrites suggests they are very likely associated with large size collapse calderas, wich remain to be identified. Petrographically, these rocks are crystal-rich vitreous tuffs with scare volcanic lithics. They systematically contain crystal fragments of quartz (10-25%), sanidine (10-20%), plagioclase (3-10%), biotite (1-3%) and oxyhornblende (0-3%); pyroxene occur locally in Sucuna Ignimbrite. Chemical analyses of pumice clasts shows the composition to be high-silica (68-78% SiO_2), with dominant high-silica rhyolites.They show high-K calc-alkaline and dominant shoshonitic affinites (3-6% K_2O), with K_2O/Na_2O ratios ranging from 1 to 1,5.

Lupica Formation. Outcrops mainly in the Putre-Belén chaine (Fig. 1A), unconformably overlying the Belén Metamorphic Complex (Precambrian-Paleozoic) and covered by volcanics rocks and sediments of Miocene-Recent age (references in García, 1996). The Lupica Fm was tentatively assigned to the Cretaceous-Tertiary (Salas et al., 1966), however recent radioisotopic determinations indicate it to be Late Oligocene-Early Miocene in age (Aguirre, 1990; Muñoz and Charrier, 1996; García, 1996; Riquelme, 1998). From bottom to top, it comprised andesites and breccias, ignimbrites, sandstone and limestone, and andesites. This succession was deposited in a proximal volcanic-arc environment, locally extensional, with closed basins, where large volume of volcanoclastic and lacustrine sediments were accumulated (García, 1996). In the Belén-Lupica region is exposed one of its more representative sections (Fig. 1B), that in the middle part contains 4 to 5units of extensive welded ignimbrites, grey, brown, pink

and green in color. These tuffs show large mineral and chemical similarities to the Oxaya Fm ignimbrites, although locally exhibit strong hydrothermal alteration. The pyroxene and hornblende andesites and dacites of the Lupica Fm, with abundant plagioclase and absent sanidine, are dominantly calc-alkaline. The deformation of the Lupica Fm difficults to map the continuity of the ignimbrites, to separate them and to estimete their volume as in the Oxaya Fm.

GEOCHRONOLOGY

Recent radioisotopic determinations have been essential to our understanding of the age of the ignimbritic succession in the region. A compilation of 16 published and 27 new ages is summarized in Fig. 1C, all by the K-Ar method and mostly on biotite. The new values (Geochronology Laboratory of the SERNAGEOMIN) will be fully reported in García and Gardeweg, et al. (in prep.). For the ignimbrites of the Oxaya Fm 27 determinations indicate an age range from 25 to 19 Ma (Mortimer et al., 1974; Naranjo and Paskoff, 1985; García, 1996; Parraguez, 1998; this work). In the lower ignimbrites, the four existing data are close to ~25,5 Ma while other two values are identical to 23,7±0,8 Ma. The Livilcar and pink ignimbrites, that overlies it, yielded ages close to ~23 Ma. Eleven determinations in the Oxaya Ignimbrite yielded a weighted mean age of 21,3±0,7 Ma, whereas in the Sucuna Ignimbrite five data yielded a weighted mean age of 19,3±0,8 Ma. Sixteen age determinations on the Lupica ignimbrites of the Fm range from 25 to 18 Ma (Aguirre, 1990; Muñoz and Charrier, 1996; García, 1996; Riquelme, 1998; this work), values that closely match the ages for ignimbrites of the Oxaya Fm. In fact, two of the lowermost units are ~25,5 Ma, while in an intermediate ignimbrite in Chucal two results of ~23 Ma have been obtained in addition to an other age of ~23 Ma in Belén. Four scattered samples have ages close to 21 Ma, very similar to that of the Oxaya Ignimbrite. Finally, seven scattered determinations in upper flows yielded ages from 18,6 to 19,9 Ma, consistent with the ages of the Sucuna Ignimbrite.

CONCLUSIONS

In the Arica region, the large-volume Late Oligocene-Early Miocene ignimbrites occurs between 25 and 19 Ma. The western outcrops (Oxaya Fm) are weel preserved showing characteristicaly distals facies and mild defromation. In the eastern outcrops (Lupica Fm) the ignimbrites are intercalated with arc-lavas and sediments, and they are strongly deformed. The strong difference in the stratigrphy and deformation style reflects a difference in tectonic environement during deposition (plateau-type surface for Oxaya and intramontaneous basins for for Lupica) and a difference in strain of the deformation post-depositional, concentrated in the fold and thrust belt Belén (García, 1996). The dominantly shoshonitic character, in addition to the abundance of sanidine, suggests a back-arc origin for the ignimbrites.

ACKNOWLEDGMENTS.

This contribution was carried out through an agreement betheen the Geological Survey of Chile (SERNAGEOMIN) and ORSTOM, as part of the Multinational Andean Project (MAP). We are particularly grateful to Carlos Perez de Arce for his special efforts in obtaining the geochronologic data at the SERNAGEOMIN laboratories. Manuscript was revised and improved by Carlos Arevalo and Andrew Tomlinson.

REFERENCES

García, M.; 1996. Geología y estructura del borde del Altiplano occidental, en el área de Belén (Chile). Tesis de Magister y Memoria de Título, U. de Chile, 111 p.

García, M.; in prep. These de Doctorat. Universite de Grenoble, France.

Mortimer, C.; Farrar, E.; Saric, N.; 1974. K-Ar ages from Tertiary lavas of the northernmost Chilean Andes. Geol. Rundch., **63**, p. 484-489.

Muñoz, N.; Charrier, R.; 1996. Uplift of the western border of the Altiplano on a west-vergent thrust system, Northern Chile. J. South Amer. Earth Sci, **9**, p. 171-181.

Naranjo, J., A.; Paskoff, R.; 1985. Evolución cenozoica del piedemonte andino en la Pampa del Tamarugal, Norte de Chile (18°-21° S). Actas IV Congreso Geológico Chileno, Antofagasta, V. 5, p. 149-164.

Parraguez, G.; 1998. Sedimentología y geomorfología producto de la tectónica cenozoica, en la Depresión Central, Pampa de Chaca, I Región de Tarapacá, Chile. Memoria de Título, U. de Chile, 108 p.

Riquelme, R.; 1998. Evolución tectonosedimentaria post-oligocéna del borde occidental del Altiplano, entre Tignámar y el Salar de Surire, I Región, Chile. Tesis de Magister y Memoria de Título, U. de Chile, 123 p.

Salas, R.; Kast, R.; Montecinos, F.; Salas, I.; 1966. Geología y Recursos Minerales del Departamento de Arica, Provincia de Tarapacá. Inst. de Invest. Geol., Boletín 21, 130 p.

Schröder, W.; Wörner, G.; 1996. Widespread Cenozoic ignimbrites in N-Chile, W-Bolivia and S-Peru (17°-20°S/71°-68°E): Stratigraphy, extension, correlation and origin. Third ISAG, Saint Malo, France, 645-648.

Sébrier, M.; Soler, P.; 1991. Tectonics and magmatism in the Peruvian Andes from late Oligocene time to the Present. Geological Soc. of America, Special Paper 265, p. 259-278.

Tosdal, R. M.; Farrar, E.; Clark, A., H.; 1981. K-Ar geochronology of the late Cenozoic volcanic rocks of the Cordillera Occidental, southermost Perú. J. Volcanol. Geotherm. Res., **10**, p. 157-173.

Vogel, S.; Vila, T.; 1980. Cuadrángulos Arica y Poconchile. Región de Tarapacá. Carta Geol. de Chile. Instituto de Investigaciones Geológicas, N° 35, 24 p.

TO WHAT EXTENT DID THE POST 15 MA ARIDISATION OF CENTRAL SOUTH AMERICA MODIFY THE EVOLUTION OF THE CRUSTAL DYNAMICS OF THE BOLIVIAN ANDES

OUTLINE OF A RESEARCH PROPOSAL

Reinhard GAUPP(1), Fritz SCHLUNEGGER(1), Thomas JAHR(1)

(1)Friedrich-Schiller-Universität Jena, Institut für Geowissenschaften, Burgweg 11, D-07749 Jena
gaupp@geo.uni-jena.de, fritz@geo.uni-jena.de, jahr@geo.uni-jena.de

KEY WORDS: Bolivian Andes, climate and tectonics, surface erosion

INTRODUCTION

Coupled erosion/thermo-mechanical models for orogens reveal that surface processes exert a significant control on the exhumation pattern and the thermal evolution of mountain belts (Willett et al., 1993). This is the case because the crustal deformation of orogens appears to be controlled by the internal strength of the crust and the strenght of the décollement between the crust and the lithospheric mantle (e.g. Jaeger & Cook, 1969). According to Jaeger & Cook (1969) the strength of the crust and the décollement are dependent on temperature and the lithostatic pressure, both of which are modified to a great extent by surface erosion (Batt & Braun, 1997) and by the angle of subduction. Using these theoretical concepts, Schlunegger (1999) proposed that the shift from steady state of the Swiss Alps during the Oliogcene to a phase of constructive growth in the Early Miocene was controlled by the contemporaneous >50% reduction of surface erosion rates. Given this initial success, we decided to explore the extent of controls of surface erosion on strain partitioning in the Andean crust for an E-W transect that runs from Arica to Santa Cruz (18°S-21.5°S). Specifically, we speculate that the aridisation in South America which accelerated in the Miocene (δO^{18} from marine benthos, qualitative determinations of rates of supergene

weathering; Miller et al., 1987; Alpers & Brimhall, 1988) initiated the eastward shift of the location of major shortening (Lamb et al., 1997). This hypothesis is supported by (i) data from preliminary mass balance calculations in the west that indicate a >50% decrease of average erosion rates at ~15 Ma (Alpers & Brimhall, 1988), (ii) the eastward shift of the location of surface erosion at ca. 15/10 Ma (Lamb et al., 1997; Horton, 1998), and (iii) the contemporaneous eastward shift of the location of enhanced rates of thrusting (deformation of the Subandean Fold and Thrust Belt).

RESEARCH OBJECTIVES

A successful test of the extent of controls on strain partitioning in mountain belts requires (i) data to reconstruct the surface and the lithospheric mass flux in space and time, (ii) a process-oriented coupled erosion/thermo-mechanical model to simulate the interaction between surface and lithospheric forces, and (iii) parameters (e.g. erodibilities of bedrock, viscosity of the lithosphere, present-day heat flux) to calibrate the physical processes on the surface and in the lithosphere during the model runs.
Given these requirements we propose to (i) collect and process stratigraphic data in an effort to quantify the erosional mass flux, and (ii) develop a 2-dimensional coupled erosion/thermo-mechancial model with ABAQUS (software package). Both lines of data collection and data processing will be strongly linked with each other, because the model-oriented analysis will be calibrated with the observed erosional mass flux. On the other hand, the results of the numerical model will be useful to test the sensitivity of the geophysical input parameters, which in turn aids at focussing on further data collection.

Collection and processing of stratigraphic data

The stratigraphy oriented study comprises (i) mass-balance calculations of Late Oligocene to recent sedimentary basins that bear information on the surface mass flux, (ii) sedimentological and geochemical analysis of sandstones and mudstones to reconstruct temporal and spatial shifts of precipitation, and (iii) processing of digital elevational data to determine the kind of mass transfer (fluvial erosion, landslides, hillslope diffusion) and to estimate the size of the catchment areas.

Mass balance calculations

Thicknesses of temporally calibrated stratigraphic sections integrated across sedimentary basins allow determination of sediment flux. If the size of the drainage basin is known (what we intend to determine), then the supply rates of sediment can be converted into sediment yield.

There are five areas in the proposed study area that need to be considered for mass-balance calculations for the time interval between 25 Ma and the present (Lamb et al., 1997): the Precordillera of Chile, the Altiplano, the Eastern Cordillera, the Subandean Zone as well as the Foreland Basin. Detailed stratigraphic data were already collected and partly processed from the Late Oligocene basins within the Precoridillera of Chile by previous studies (Kött et al., 1995; Kohler, 1998; Gaupp et al., 1999). Temporally calibrated stratigraphic sections also exist in the Altiplano (unpublished oil company data) and the Eastern Cordillera (Horton, 1998), the Subandean Zone (research by J. Reynolds and R.M. Hernández) as well as in the Foreland Basin (unpublished oil company data). We propose to complete this dataset by seismo-stratigraphic analyses of available seismic sections especially from the Altiplano and the Foreland Basin. Thicknesses of other sections, located in the Subandean Zone, will be estimated to complete the stratigraphic dataset.

Geochemical analysis of sandstones and mudstones

We will collect sandstone and mudstone samples for microscopic analysis, geochemical and XRD analysis to gain information about the evolution of climate and weathering. For details of methodology refer to Gaupp et al. (1999).

Processing of digital elevational data

Digital elevational data will be combined with a digital interpretation of areal photographs. These data will be complemented with exisiting geological maps and stratigraphic data from the field and from seismic in an effort to estimate the volumes of deposited or eroded strata for different time intervals. Additionally, areal photographs allow identification of break-in-slopes of the topography that will be used to distinguish between areas of present-day and ancient erosion that develop if crustal uplift is more rapid than surface erosion (e.g. the present-day Swiss Alps). Furthermore, digital elevational data allow calculation of the slopes and curvatures of the topography. The combinations of this information enable us to reconstruct the long-term erosional processes.

Development of a coupled erosion/thermo-mechanical model

We propose to develop a two-dimensional coupled erosion/thermo-mechanical model with ABAQUS to simulate the evolution of the Bolivian Andes. Using this model, we will numerically explore the extent of controls of surface erosion on the eastward shift of the location of deformation. We propose to proceed according to Pope & Willett (1998). These authors simulated the crustal growth of the Bolivian Andes

using an ablative subduction model that solves for the thermal state and the strain rate pattern during crustal growth. There are three important input parameters to simulate the deformation of the crust: (i) crustal thicknesses and convergence velocities that determine the rate of crustal growth, (ii) initial geothermal gradient that will be modified as the Andes develop, and as subduction proceeds, and (iii) the viscosity of the crust that controls to a great extent the strain rate pattern within the crust. The parameters controlling erosion comprise the diffusivity coefficient (if erosion is simulated by diffusion) or a constant calibrating the bedrock erodibility (if erosion is simulated by advection). The surface mass flux that results from the model runs will be tested with the mass balance determined from the stratigraphic analyses. The calculated crustal deformation and the temperature field will be calibrated with the present-day heat flux, the results of deep seismic and gravity anomalies. These geophysical data are currently collected by the collaborating universites of Berlin (Freie Universität Berlin), Potsdam and the GFZ (Geoforschungszentrum Potsdam).

REFERENCES

Alpers C.N., Brimhall G.H. 1988. Middle Miocene climatic chnage in the Atacama Desert, northern Chile: Evidence from supergene mineralization at La Escondida. GSA Bulletin, 100, 1640-1656.

Gaupp R., Kött A., Wörner G. 1999. Paleoclimatic implications of Mio-Pliocene sedimentaion in the high-altitude intra-arc Lauca Basin of northern Chile. Palaeogeography, Palaeoclimatology, Palaeoecology, in press.

Horton B.K. 1998. Sediment accumulation on top of the Andean orogenic wedge: Oligocene to late Miocene basins of the Eastern Cordillera, southern Bolivia. GSA Bulletin, 110, 1174-1192.

Jaeger J.C., Cook N.G.W. 1969. Fundamentals of rock mechanics. Methuen & Co. Ltd., London, 513 p.

Kohler I. 1998. Syntektonische kontinentale Sedimentation auf der Westabdachung der Anden Nordchiles (18°-19°). Unpublished PhD thesis, university of Stuttgart, Stuttgart, 253 p.

Kött A., Gaupp R., Wörner G. 1995. Miocene to Recent history of the western Altiplano in northern Chile revealed by lacustrine sediments of the Lauca Basin (18°15'-18°40'S/69°30'-69°05'W). Geologische Rundschau, 84, 770-780.

Lamb S., Hoke L., Kennan L., Dewey J. 1997. Cenozoic evolution of the Central Andes in Bolivia and northern Chile. In: Burg J.P., Ford M. (eds) Orogeny through time. Geolocical Society Specical Publication, 121, 237-264.

Miller K.G., Fairbanks R.G., Mountain G.S. 1987. Tertiary oxygen isotope synthesis, sea level history, and continental margin erosion. Paleoceanography, 2, 1-19.

Pope D.C., Willett S.D. 1998. Thermal-mechanical model for crustal thickening in the central Andes driven by ablative subduction. Geology, 26, 511-514.

Schlunegger F. 1999. Controls of surface erosion on the evolution of the Alps: Constraints from the stratigraphies of the adjacent foreland basins. Geologische Rundschau, in press.

Fe AND Cu-Fe±Au MINERALIZATION IN THE COASTAL CORDILLERA OF CHAÑARAL, NORTHERN CHILE

Sergio GELCICH(1)

(1) Servicio Nacional de Geologia y Mineria, Chile, sgelcich@sernageomin.cl

KEY WORDS: CCIB, Fe and Cu-Fe±Au mineralization, metallogeny

INTRODUCTION

The Coastal Cordillera of northern Chile between 26° and 27° south latitude, hosts a great number of mineral deposits, in which the Fe and Cu-Fe±Au are the most important in terms of its historical production. The Fe deposits can be assigned to the Coastal Cordillera Iron Belt (CCIB). The Cu-Fe(Au) have not been integrated to a systematic characterization.

The CCIB is a 600 kilometer long metallogenic belt that runs parallel to the coast line with a general north south orientation (Espinoza, 1990). Without considering El Laco The CCIB hosts the largest iron deposits in Chile. In spite of the extent of the CCIB and the numerous ore bodies that it includes, there exist a poor geochronological control for the deposits and their host rock. A cretaceous age has been assigned for the whole mineralized belt, although this is based mainly on stratigraphic relationships of the host rock (exclusively granitoids and volcanic rocks), and some scarce radiometric ages.

This paper summaries the main characteristic of the Fe and Cu-Fe±Au deposits recognized in the area, in the framework of new geological data (stratigraphy, geocronology), allowing a discussion centered in the relationship between both deposit types and their age.

Geology

The Coastal Cordillera of Chañaral is characterized by the presence of igneous rocks which record the Jurassic to cretaceous igneous activity, associated to discrete magmatic arcs built on the continental margin.

Paleozoic metasementary rocks intruded by paleozoic to early early jurassic plutons formed the basement for the Jurassic and Cretaceous plutonic and volcanic rocks (Dallmeyer et al., 1996). The jurassic volcanics (La Negra Formation), are mainly andesitic lava flows, and they are overlained by the volcano-

sedimentary Punta del Cobre Formation (Late Jurassic-Early Cretaceous; Godoy, Lara, 1998, Lara and Godoy, 1998). Radiometric ages in the plutonic rocks define distinct episodes of magma emplacement between 202 to 103 Ma (Dallmeyer et al., 1996). Plutons are, in general, elongated in North-South direction and are limited by milonitic belts. These plutons show decreasing ages from West to East with Jurassic plutons close to the coast and Early Cretaceous to the east (Brown et al., Dallmeyer et al., 1996) (Fig. 1).

Brittlle deformation is overprinted to ductil one, definning the main branches of the Atacama Fault System (AFS), which have a NS general strike (Lara et al., 1996). The AFS separates the arc rocks in a Western and Eastern domain. Jurassic plutons are located at the Western Domain, and Cretaceous plutons, at the Estern Domain (Fig. 1).

The deposits

The Fe and Cu-Fe±Au deposits are mainly veins and irregular shaped bodies, hosted by plutonic and volcanic rocks. Both types occur close to each other. To the west of the AFS (Western Domain), the deposits are exclusively host in Jurassic plutonic rocks, whereas the deposits of the Eastern Domain are hosted by cretaceous granitoids and volcanic rocks (Fig. 1).

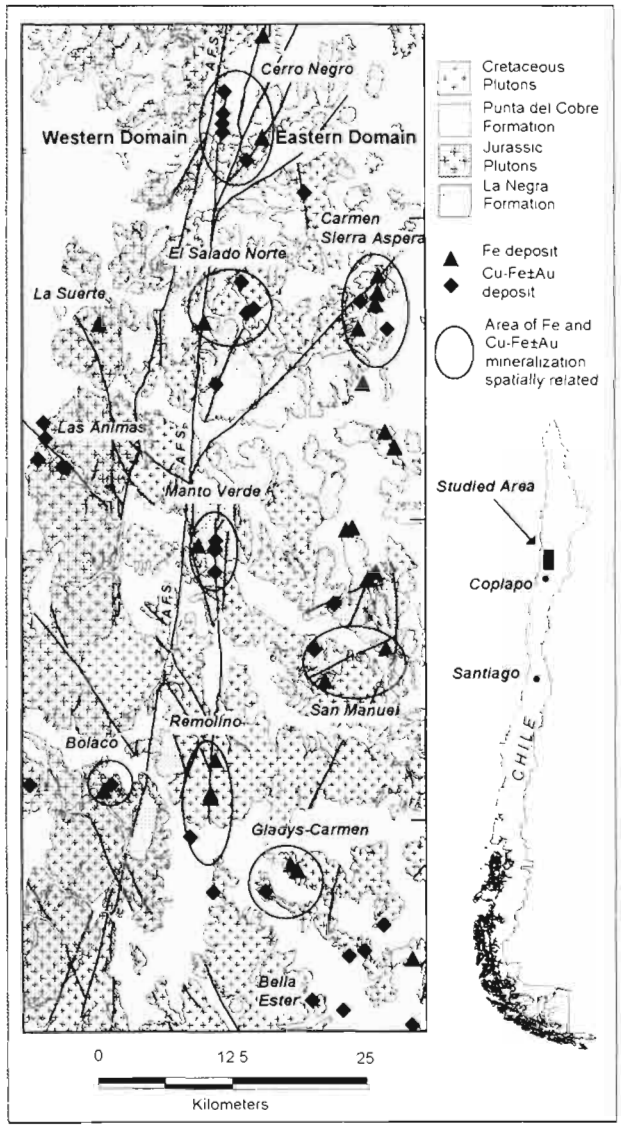

The iron deposits are magnetite-apatite type. They are formed by massive magnetite, apatite, minor sulfides and actinolite as main alteration mineral. Geochemical signatures of the magnetite are characterized by relatively high contents of V and low amounts of Cr an Ti (Gelcich 1998). Massive magnetites show dendritic and orbicular textures.

The Cu-Fe±Au deposits can be divided in two groups, depending of the dominant iron oxide (magnetite/hematite). Both types generally occur near massive magnetite bodies. The first group is defined by those deposits in which magnetite is the main iron oxide, with chalcopyrite, pyrite, quartz, calcite and actinolite. Alteration is restricted one to two meters besides the veins and is

Fig. 1 Geological map of the Coastal Cordillera in the studied area based on Godoy and Lara, 1998; Lara and Godoy, 1998. The main deposits (Fe and Fe-Cu±Au) are shown. Note the spatial relationship between both types, marked with ellipses.

vertically zoned, with actinolitized deep zones relative to upper K feldspar and biotite rich areas. The second group has an ore-gangue mineralogy composed by hematite (mainly especularite), chalcopyrite (generrally oxidized), calcite and tourmaline. Wallrock alteration is dominated by K feldspar and sericite. The deposits of this group occur only at the eastern Domain and are mainly hosted by volcanic rocks.

Age of the deposits

Although, there is still a poor geochronolgical control in the age of deposits, some remarks can be made on this matter. In the western domain, alteration biotite, associated to a magnetite-copper deposit (Las Animas District) had been dated in 162 Ma, giving the same age of the plutonic host rock, on the other hand the age of La Suerte, a massive Iron deposit has been estimated in 150 Ma according to cross relationship with basaltic dykes wich are cutting the plutonic host rock (Gelcich, 1998). In the AFS domain Cu-Fe±Au has been dated in the Manto Verde deposit by Ar-Ar method in sericite, giving an age of 117 to 121 Ma (Vila et al, 1996). In the Sierra Aspera district, a 114 Ma age was obtained in alteration actinolite associated with magnetite-coper deposits, very closed to the huge Carmen iron mine.

Genesis of the deposits

The genesis of the iron deposits of the CCIB is a controversial topic. Two main thesis had been proposed, a magmatic and an hidrothermal origin. The magmatic thesis is founded in the similarities (mainly textural, form and geochemistry) between the deposits of the CCIB and the El Laco district, where a pleistocene volcanic complex host magnetite-apatite bodies (very well exposed and conserved). There, ore bodies have been interpreted as lava flows, dykes and pyroclastic deposits. Therefore it explain the ocurrence of the iron deposits as the product of Fe rich magmas (or simply ore magma) that can solidify in upper crustal levels or extrude (Nystrom y Henríquez, 1994). The hydrothermal, point of view, explains textures and form of the bodies with replacement mechanism (Ruiz y Pebles, 1988; Bookstrom, 1994). Nevertheless, the magmatic thesis established in its wide context the ocurrence of intensive hidrothermal activity, associated with the emplaccement of Fe rich magmas and (Vivallo y Henriquez, 1997) that explain the occurrence of distinct kind of hidrothermal deposits.

Metallogenic model (Conclusion)

The geochemical signature and some textures described above for magnetites of the Iron deposits, allows to infer a Magmatic genesis for the Iron deposits, in the sense of Nyström and Henriquez, 1994. Condidering this fact, the spatial relationship between Fe and Cu-Fe±Au and the geocronological data, we can configure a regional metallogenic model for the study area in which episodic intrusions of orc magma (between the late Jurrassic and early Cretaceous) produced massive iron deposits (irregular and vein

form). Hidrothermal activity associated with the former generated the Cu-Fe±Au deposits (Fig. 2). The presence of magnetite or hematite as the main iron oxide in the later deposit was regulated by the oxygen fugacity (Fig. 2). Hematite bearing deposits, restricted to the AFS (Eastern Domain), represent upper crustal levels (relative to the western domain) where iron rich magma intrusion and hidrothermal activity, was canalized by the AFS structural framework.

The above suggest that the Fe and Cu-Fe±Au is recurrent trough time and that it is far from being a discrete event of the Early Cretaceous as sustained by the classic literature.

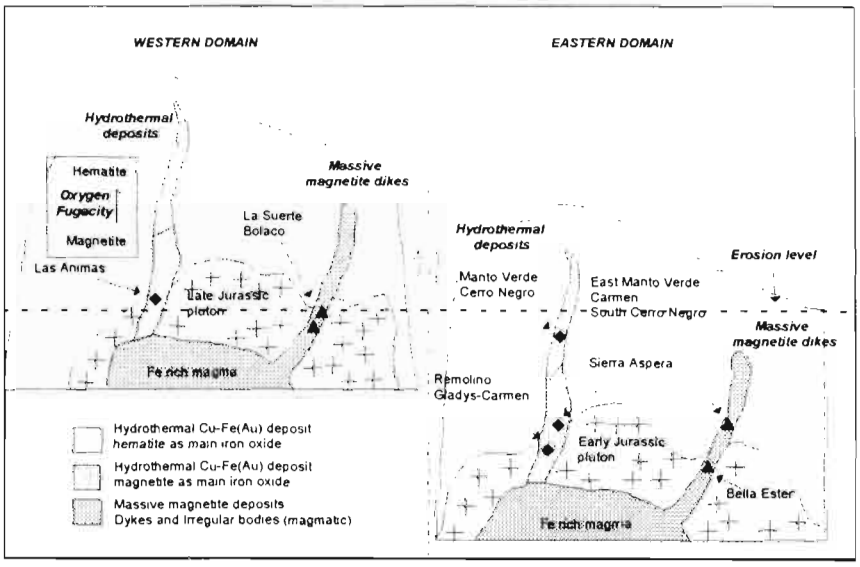

Fig 2. Genetic model for the Fe and Fe-Cu±Au mineralization. Both deposits types can be related to the intrusion of Fe rich magmas (Vivallo y Henriquez, 1997). Magnetite massive bodies represent the ore magma, magnetite(Cu±Au) and hematite(Cu±Au) deposits are associated with hydrothermal fluids related to the last stages of Fe magma intrusion.

REFERENCES

Bookstrom. A., 1995. Magmatic features of iron ores of the Kiruna Type in Chile and Sweden: ore textures and magnetite geochemistry – a discussion: Economic Geology. Vol. 90 p. 469-473.

Brown. M., Díaz. F., Grocott. J., 1993. Displacement history of the Atacama fault system 25°00'S-27°00'S. northen Chile. Geological Society of American Bulletin. v. 105. p 1165-1174.

Dallmeyer. R. D., Brown M., Grocott. J., Taylor. K., Treolar. J., 1996. Mesozoic Magmatic and tectonic Events within the Andean Plate Boundary Zone. 26°-27°30'. North Chile: Constraints from $^{40}Ar/^{39}Ar$ Mineral Ages. The Journal of Geology. volume 104. pp 19-40

Espinoza. s., 1990. The Atacama-Coquimbo ferriferous belt. northen Chile in Fontboté. L., Amstutz. G.C., Cardoso. M., Cedillo. E., and Frutos. J., eds., Stratabound ore deposits in the Andes: Berlin. Springer Verlag. p. 353-364.

Gelcich. S. 1998. Metalogénesis de los cuadrángulos El Salado y Quebrada Guamanga. Cordillera de La Costa. III Región. Master Thesis (Unpublished). Universidad de Chile. Departamento de Geología. 112 p., Santiago.

Godoy. E., Lara. L., 1998. Mapa Geológico de las Hojas Chañaral y Diego de Almagro. Servicio Nacional De Geología y Minería.

Lara. L., Godoy. E., 1998. Mapa Geológico de la Hoja Quebrada Salitrosa. Servicio Nacional de Geología y Minería.

Lara. L., Gelcich. S., Carrasco. J. & Diaz. A. 1996. Arc and forearc brittle deformation in tranpressive regimene of the lower Cretaceous. coastal range (26°-27°S). Chile: microtectonic antecedents. Third ISAG Simposium. St. Malo. pp 515-518.

Nyström. J., Henríquez. F., 1994. Magmatic Feature of Iron Ores of the Kiruna Type in Chile and Sweden: Ore Textures and magnetite Geochemistry. Economic Geology. vol 89. pp 820-839.

Ruiz. C. and Peebles. F. 1988 Geología y distribución de los yacimientos metalíferos chilenos. Santiago. editorial universitaria. 334 p.

Ruiz. C., Aguirre. L., Corvalán. J., Klohn. C., Klohn. E., and Levi. B., 1965. Geología y yacimientos metalíferos de Chile: Santiago. Chile. Instituto de Investigaciones Geológicas p. 305.

Vila. T., Lindsay. N., Zamora. R., 1996. Geology of the Manto Verde Cooper Deposit. Northen Chile: A Especularite-Rich. Hydrothermal-Tectonic Breccia related to the Atacama fault Zone. in "Andean Cooper Deposits: New Discoveries. mineralization. styles and metallogeny". Soc. Econ. Geologist. special publication N°5. Camus. F., Sillitoe. R.H., Peterson. R., Eds., 1996.

Vivallo. W., Henriquez. F., 1997. Relación genética entre los yacimientos estratoligados de Cu ("tipo manto"). de Cu-Fe+Au y de Hierro tipo Kiruna. In 8° Congreso Geológico Chileno. Antofagasta.

PETROGENETIC STUDY OF LAVAS ERUPTED THROUGH THE PERSISTANT EXPLOSIVE ACTIVITY OF THE NEVADO SABANCAYA VOLCANO, PERU (1990-1998)

Marie-C. GERBE (1) and Jean -Claude THOURET(2)

(1) Dept. Géologie-Pétrologie-Géochimie, Univ. Jean Monnet & UMR CNRS "Magmas et Volcans", F-42023 Saint Etienne, France (gerbe@univ-st-etienne.fr)
(2) IRD (ORSTOM), Instituto Geofisico del Peru, Calle Calatrava 216, Urb. Camino Real, La Molina Lima 100, Peru (jct@geo.igp.gob.pe)

KEYWORDS : Nevado Sabancaya, Peru, vulcanian activity, andesites, magma mixing, fractional cristallisation

INTRODUCTION :

Located within the Western Peruvian Cordillera (16°13'S, 71°51'W) in the Central Volcanic Zone, the Nevado Sabancaya volcano belongs to the group of active volcanoes of Southern Peru. Its Holocene activity is dominated by lava flows and lava domes, with few occurrences of pyroclastic deposits : one tephra layer was trapped in a proximal peat-bog attesting of a previous explosive activity about 8500 years ago (Juvigné et al., 1998). It presents a persistant explosive activity since the eruption of May 28, 1990, generating only air-fall tephra. The behaviour was increasingly explosive during the two first years, and was rather constant until late 1994, with hydromagmatic and moderate-magnitude vulcanian activity (Thouret et al., 1994). Since 1995, the frequency of explosions decreased gradually so that the time intervals between two events increased from 30 minutes to several hours. Since late 1997, the activity has been mainly phreatic (Bulmer et al;, 1997). The emission rate has decreased since 1994, with an overall increase of the juvenile component proportion through the eruption.

The erupted juvenile products consist of dark glassy, poorly vesiculated and highly porphyritic lavas of andesitic to dacitic compositions. They are characterized by high alkali-contents, and plot in the field of the high-K calc-alkaline series. The silica-content evolution is not linear through time : the 1990 lavas are

the most evolved (61 to 64 wt% SiO_2), then the composition drop down to 60-61.5 wt% SiO_2, and from 1994, it remains rather constant (61.5-62.5 wt% SiO_2). The juvenile facies emitted since 1992 eruptions contain rare nearly aphyric enclaves. These small enclaves range from 1 to 10 cm in size and exhibit a sharp boundary and some radial fractures. They are poorly vesiculated and exhibit microdoleritic textures. Their texture attests of their crystallization in the plumbing system. They are plagioclase- and amphibole-rich. They are characterized by lower silica-content (about 57 wt% SiO_2).

Lavas contain two types of plagioclase phenocrysts. Type A phenocrysts are optically unzoned, and have homogeneous oligoclase-andesine composition (An28-40). Type B phenocrysts are characterized by large homogeneous oligoclase-andesine cores coated with an inclusion-rich labradorite mantle (An 45-65) and a clear labradorite outer rim of a few micrometers. Microdoleritic enclaves contain optically unzoned homogeneous labradorite plagioclase (An45-60).

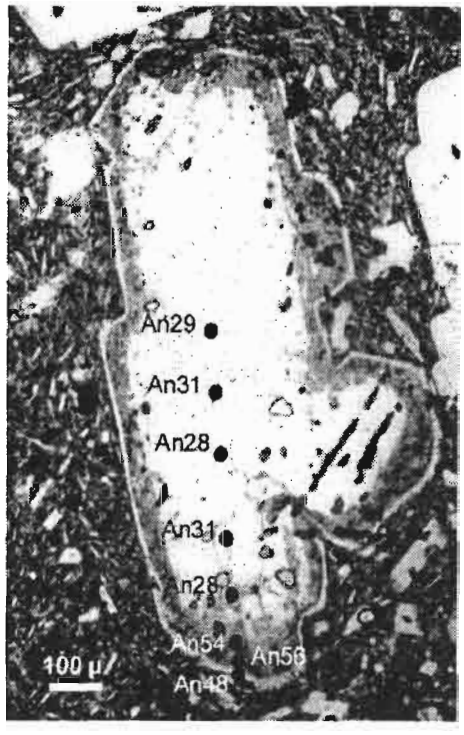

Type B plagioclase phenocrysts

Type B phenocrysts reverse compositional zoning may account for magma mixing processes. A dacitic magma in equilibrium with andesine plagioclase compositions has been mixed with inputs of an andesitic magma batch in equilibrium with labradorite plagioclase composition. All 1990-98 lavas contain both types of phenocrysts, but the first emitted dacitic lavas (about 64 wt% SiO_2) contain almost only type A plagioclase, suggesting that it might represent the dacitic component. Microdoleritic enclaves might represent fragments of the andesitic component crystallized in the plumbing system. These hypovolcanic rocks were carried up by magmas erupted during the actual eruption . Thus these enclaves do not give any evidence of a new magma injection prior to eruption that may have triggered off the actual volcanic crisis.

The overall series displays major and trace element trends and REE patterns, that might account for both fractional crystallization and magma mixing imprints: (i) The early emitted dacitic magmas might be derived from an andesitic magma batch similar in composition to the microdoleritic enclaves, by the

fractionation of plagioclase, amphibole, iron-titanium oxides and clinopyroxene; (ii) The intermediate lavas (60.5 to 62.5 wt% SiO_2), which exhibit mineralogical evidences of magma mixing might be issued from the mixing in variable proportion of the dacitic magma with an andesitic component.

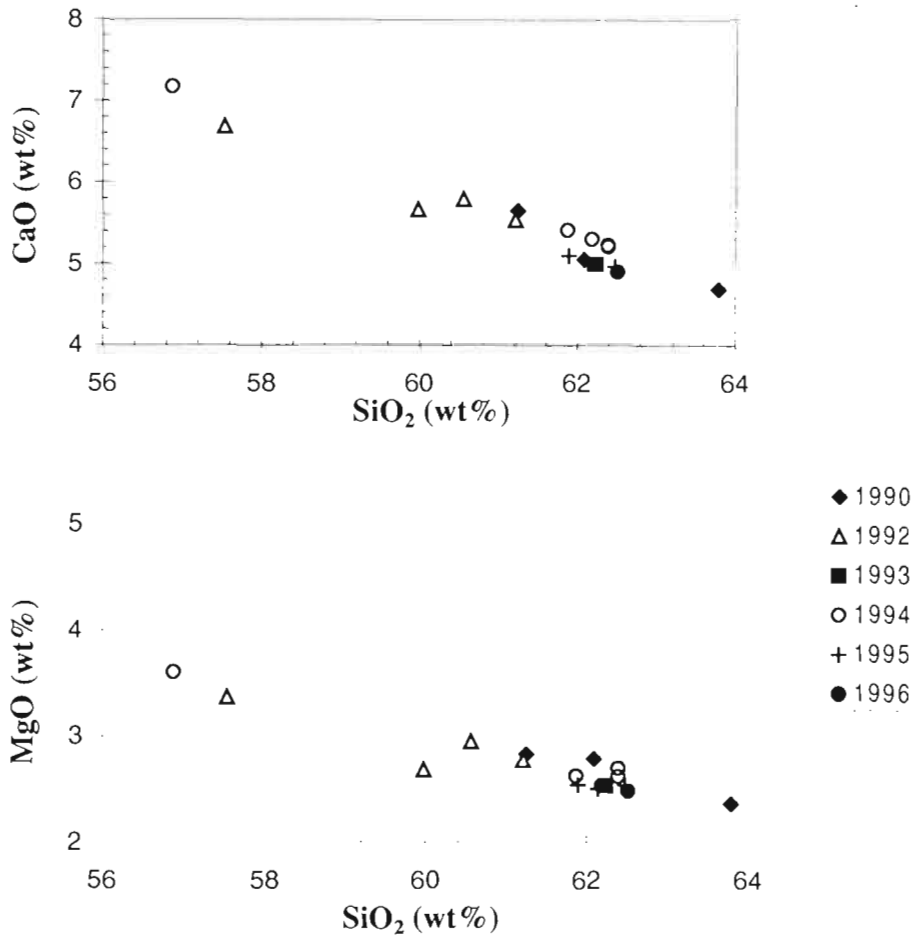

REFERENCES :

Thouret J-C, Guillande R, Huaman D, Gourgaud A, Salas G, & Chorowicz J, 1994. L'activité actuelle du Nevado Sabancaya (Sud Pérou) : reconnaissance géologique et satellitaire, évaluation et cartographie des menaces volcaniques. Bull. Soc. Geol. France, 165, 49-63 Bulmer M., Engle F., Johnston A., 1997. Nevado Sabancaya. Global Volcanism Network bulletin, 22, 7, 14-15. Juvigné E., Thouret J.C., Gilot E., Leclercq L., Gourgaud A., 1998. L'activité du volcan Nevado Sabancaya (Pérou) au cours de l'Holocène. Quaternaire, 9, 1, 45-51.

THE ALTO TUNUYAN NEOGENE FORELAND BASIN, MENDOZA, ARGENTINA

Laura B. GIAMBIAGI (1)

(1) Laboratorio de Tectónica Andina, Universidad de Buenos Aires, Argentina – IANIGLA-CRICYT (email Lgiambia@lab.cricyt.edu.ar)

KEY WORDS: ALTO TUNUYAN NEOGENE FORELAND, MENDOZA, ARGENTINA

INTRODUCTION

The Alto Tunuyán basin represents a Neogene foreland basin located between Cordillera Principal and Cordillera Frontal, from 33°30´ to 34° S latitude (Figs. 1A and 1B). The synorogenic units filling the basin comprise three Miocene formations which record alluvial and fluvial deposition. Each of these three units reflects a major phase in the basin development. The oldest unit, the Tunuyán Conglomerate, consists of up to 1,400 m of synorogenic coarse sediments deposited as a result of the exhumation of the Cordillera Principal. The lower 200 m of this unit contain clasts derived from the volcanic arc situated in Chile by this time, while the upper member is characterized by clasts derived from both the volcanic arc and the Mesozoic sequences of the Cordillera Principal. The Palomares Formation, unconformably overlying the former unit, consists of volcaniclastic and clastic sediments. This sequence, containing clasts derived from the eastern highlands, presents a maximum thickness of 200 m. The Butaló Formation, the youngest of the three units, records the final infilling of the intermontane trough between Cordillera Principal and Cordillera Frontal. It is separated from the underlying formations by an important angular unconformity. This unit has been correlated with the Papal Formation by Polanski (1964) and Perez et al. (1997).

During the Lower Miocene thrusting and uplift of the Aconcagua fold and thrust belt began, in the area today known as the Cordillera Principal (Ramos et al., 1996). The Alto Tunuyán foreland basin

formed in response to flexural subsidence driven by the topographic load of the adjacent thrust belt. Deformation and uplift of the volcanic arc, located on the western part of the thrust belt, generated a sediment source for the lower 200 m of the Tunuyán Conglomerate (Fig. 2A). As the deformation migrated progressively eastward, it envolved the Mesozoic sequences, the exhumation of which provided the material accumulated in the rest of the unit (Fig. 2B). The lower 1,000 m of this sequence were deposited in the foredeep depozone of the basin, while the upper 400 m show progressive unconformities recording accumulation in the frontal part of the orogenic wedge (wedge-top depozone). The transition from foredeep to wedge-top depozone strata marks the time at which an important thrust-front eastward propagation took place.

The angular uncomformity that separates the Tunuyán Conglomerate from the overlying Palomares Formation records a phase of deformation that is also recorded in the La Pilona-Tupungato area, between Mariño Formation and La Pilona Formation (Irigoyen et al., 1998). This tectonic event corresponde to the uplift of the crystalline basement of the Cordillera Frontal and the generation of a broken foreland basin as defined by Jordan (1995) (Fig. 2C).

Deposition of the Butaló Formation over the partially deformed broken foreland basin reflects accumulation during a period of tectonic quiescence and low exhumation of both Cordillera Principal and Cordilllera Frontal (Fig. 2D).

The uplift of the Cordillera Frontal generated a sticking point, preventing the propagation of the thrust belt towards the foreland. As a consequence, out of sequence thrusts developed in the Cordillera Principal and the basin was partially cannibalized (Fig. 2E).

REFERENCES

Irigoyen, M. V., V. A. Ramos and R. L. Brown, 1998. Magnetostratigraphy and 40Ar-39Ar dating of the Neogene synorogenic strata of northern Mendoza, Argentina: tectonic inplications. Actas X Congreso Latinoamericano de Geología y VI Congreso Nacional de Geología Económica, vol. II: 140. Buenos Aires.

Jordan, T. E., 1995. Retroarc foreland and related basin. En C. Spera y R. V. Ingersoll (Eds.): Tectonic of sedimentary Basins. Blackiwell Scientific: 331-362, Cambridge.

Pérez, J., G. Álvarez, A. Choncheyro, and V. A. Ramos, 1997. La Formación Papal: depósito sinorogénico de la cuenca de antepaís de Tunuyán, Mendoza, Argentina. Actas 8° Congreso Geológico Chileno (Antofagasta), 1: 568 – 572, Santiago.

Polanski, J., 1964. Descripción geológica de la Hoja 25 a-b - Volcán de San José, provincia de Mendoza. Dirección Nacional de Geología y Minería, Boletín 98: 1–92, Buenos Aires.

Ramos, V. A., M. Cegarra and E. Cristallini, 1996. Cenozoic tectonics of the High Andes of west-central Argentina (30-36° S latitude). Tectonophysics 259: 185-200, Amsterdam.

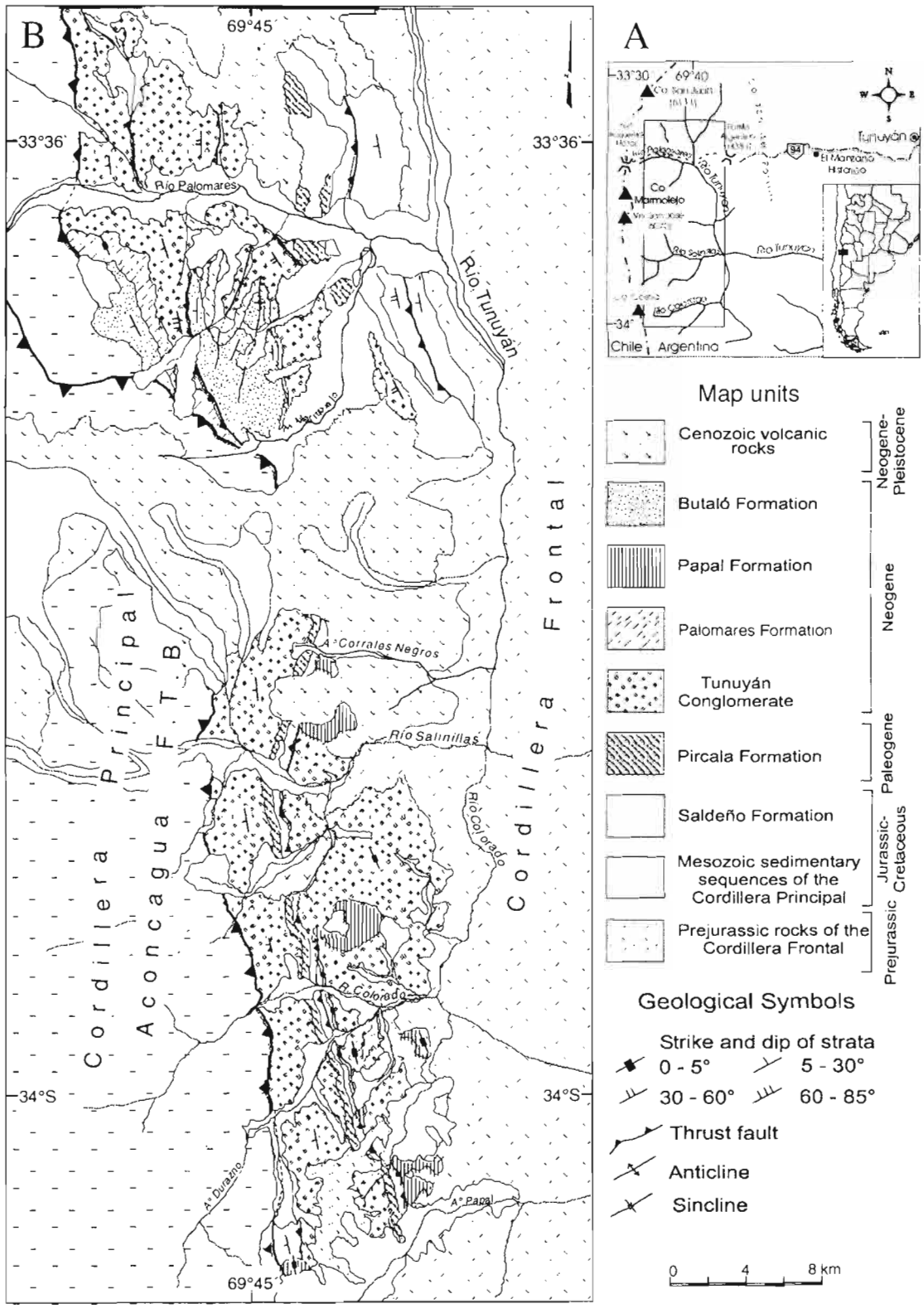

Figure 1: A) Location map of the Alto Tunuyán foreland basin, Mendoza, Argentina. B) Simplified geologic map of the basin, showing the distribution of Neogene strata.

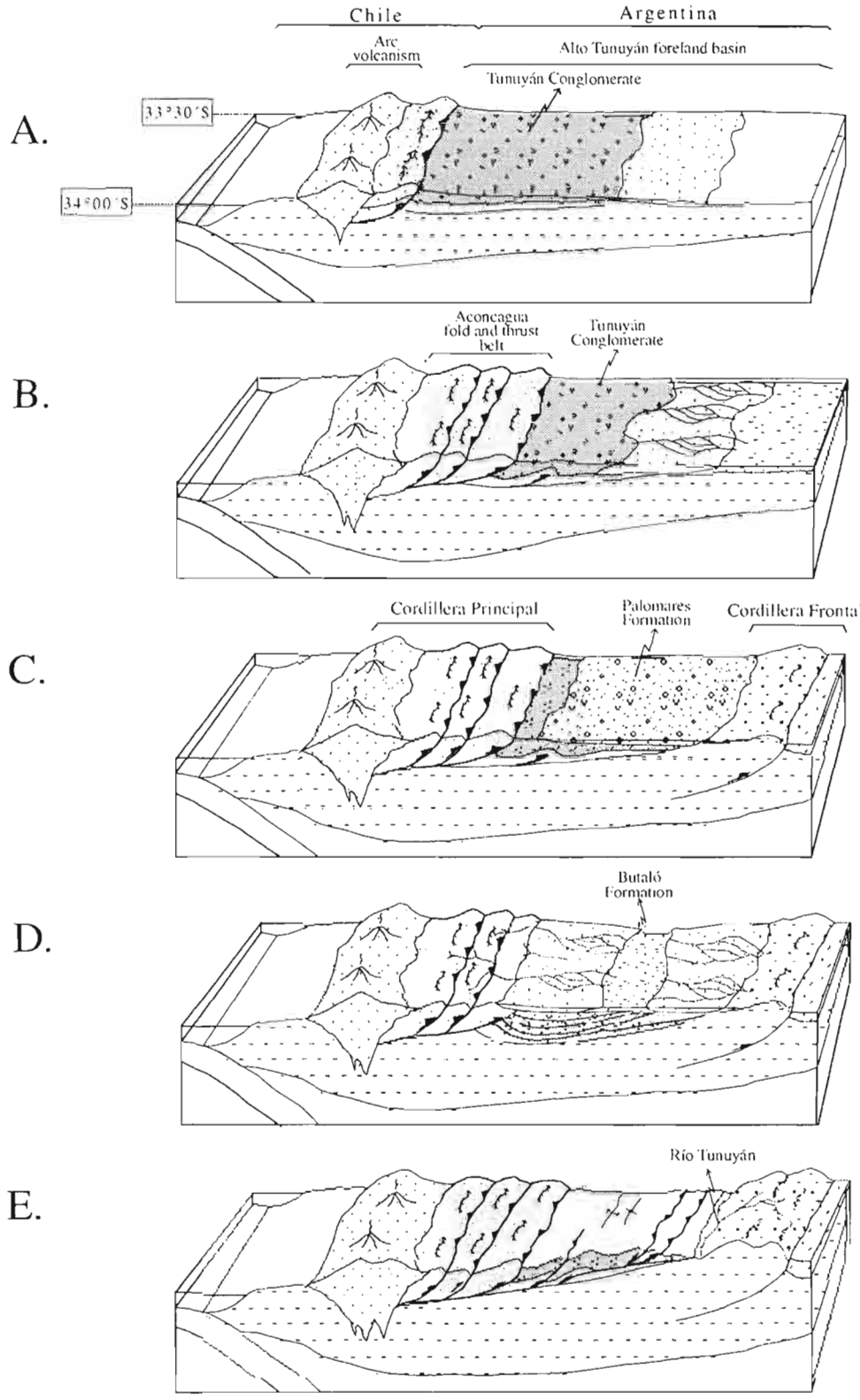

Figure 2: Schematic tectonic evolution model of the Alto Tunuyán foreland basin. A) Begining of deformation of the Aconcagua fold and thrust belt and generation of the foreland basin. Accumulation of the lower 200 m of the Tunuyán Conglomerate. B) Migration of the deformation towards the foreland and accumulation of the rest of the Tunuyán Conglomerate. C) Uplift of the Cordillera Frontal and deposition of the Palomares Formation in the broken foreland basin. D) Accumulation of the Butaló Formation during a period of tectonic quiescence. E) Cannibalization of the basin.

PARAMETERS CONTROLLING THE EXTREME PROPORTIONS OF THE CENTRAL ANDES

Peter GIESE(1), Klaus-J. REUTTER(1), Ekkehard SCHEUBER(1)

(1)Freie Universität Berlin, Institut für Geologie, Geophysik und Geoformatik
Malteserstr. 74-100, D 12249 Berlin, Germany (giese@geophysik.fu-berlin)

KEYWORDS: Central Andes, extreme properties, mid-Cretaceous superplume, hydration, climate

INTRODUCTION

The Cordilleran-type orogen of the Andes developed in the continental crust of the active South American margin as a consequence of its convergence with the SE Pacific oceanic plates and the uninterrupted subduction since at least 200 Ma. The Central Andes shows several unique features, e.g.: (1) The Altiplano-Puna-Plateau, which is 4 km high and 500 km wide, is the highest plateau in an ocean-continent convergence zone and the second highest plateau on Earth; (2) the plateau is underlain by a 70-km-thick crust; (3) although the structures of the plateau and its bordering regions are contractive and partly transpressive, the continental slope displays extensional and collapse structures indicating subduction erosion; (4) strong arc volcanism and plutonism during the last 200 My led to a considerable growth of crustal material, thus contrasting subduction erosion; (5) because of the extremely arid climatic conditions, the trench shows almost no sediments, and erosion in the mountain chain is at a minimum; (6) magmatism and hydrothermalism as well as the arid climate gave rise to large and very special metallic and non-metallic ore deposits. The subduction process was not steady during the last 200 My, but was subject to major changes in configuration of the oceanic plates, convergence rate and convergence obliquity. Besides the eastward migration of the volcanic arc during that time, three events can be recognised: (1) a first magmatic gap between 90 and 80 Ma; (2) a second magmatic gap between 35 and 25 Ma; and (3) widening of the volcanic belt over the Altiplano and Puna plateau to the Eastern Cordillera. Notwithstanding the long history, Central Andean plateau uplift, extreme crustal thickening, and increase in width of the mountain belt took place only during the past 25 My. The following questions may be posed: (1) What has triggered the change in Andean evolution? (2) Why did this development just

start at 20-25 Ma? (3) Which are the parameters controlling the formation of the extreme dimensions of the Central Andes?

SEAFLOOR SPREADING AND SUBDUCTION HISTORY

Seafloor spreading and the age of the subducting ocean floor are important parameters in the study of plate tectonic processes. An excellent basis for such studies is provided by the digital isochrons of the world's ocean floor published by Müller et al. (1997). The SE-Pacific and the bordering Andes are the

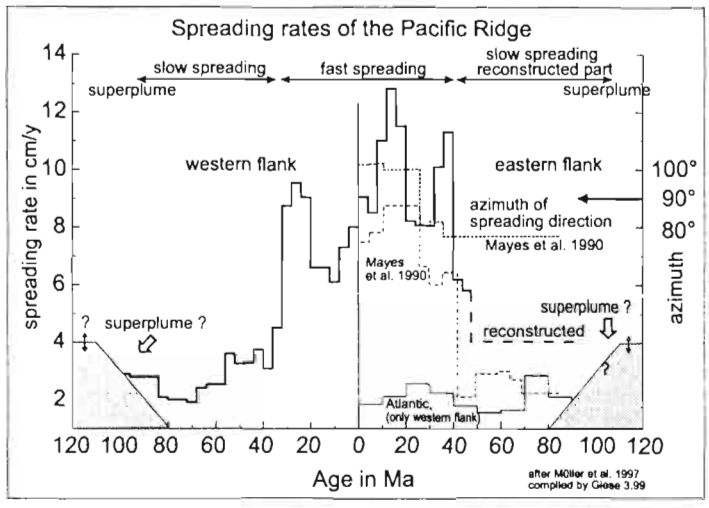

Fig. 1 Seafloor spreading rates for the western and eastern flank of the Pacific Ridge (Müller et al. (1997). In the last 45 My the average spreading rate is somewhat higher on the eastern flank (about 35%) than on the western flank. On the eastern flank between 55 to 108 Ma an average rate of 4 cm/a is estimated. The effect of the changing azimuth between 80° and 100° has been neglected.

only region on Earth where the evolution of an active continental margin can be related to spreading period since about 100 Ma ago. In Fig. 1 the spreading rates are displayed for both flanks of the Pacific Ridge between 15° to 30° S. The eastern flank shows a maximum age of 45 Ma, whereas on the western side the oldest oceanic crust has an age of about 110 Ma. On both flanks high spreading rates of 8-12 cm/a are recorded for the last 40 or 35 My. During this time the spreading rate on the eastern flank is, on an average, 35% higher than on the western side. Before 40 or 35 Ma the spreading rate was much lower, so the western flank shows a slow rate of 2-4 cm/y for the time interval between 110 and 40 Ma. The oceanic crust of the eastern flank older than 45 Ma is already subducted beneath the South America. If a reconstruction of that subducted crust is undertaken, symmetric spreading has to be assumed for the time prior to 50 Ma. From this observation another question arises: Which process is responsible for this dramatic change of the spreading rate within only a few million of years?

The isochrons of the western flank terminate at 110 Ma, a time which coincides with the activities of the mid-Cretaceous superplume (Larson 1991). This mid-Cretaceous magmatic pulse in the formation of oceanic crust, evidenced in the Pacific mainly by ridge and oceanic plateau generation, began almost at 120-125 Ma and then decreased until 80 Ma. Crustal thickness of oceanic plateaus exceeds that of normal

oceanic lithosphere due to a higher temperature and a higher degree of partial melting of the uprising mantle beneath the spreading zone. In the SW-Pacific relics of this superplume still exist, e.g. the Manihiki and the Ontong-Java plateau. As stated above, its eastern equivalent was subducted beneath Southern America. According to the differences of the spreading process, three types of oceanic crusts can be distinguished: (1) Slow-spreading crust with reduced to normal thickness of 4-8 km; (2) fast-spreading crust with normal thickness of 6-10 km, and (3) oceanic plateau crust with great thickness of 10-20 km. Slow-spreading crusts are more fractured and thus more hydrated by ocean-bottom metamorphism than fast spreading crusts. When these crustal types are subject to subduction, it is supposed that the higher buoyancy of a thick crust causes the subduction-dip angle to be lower than in the case of the subduction of a lithosphere with a thin crust.

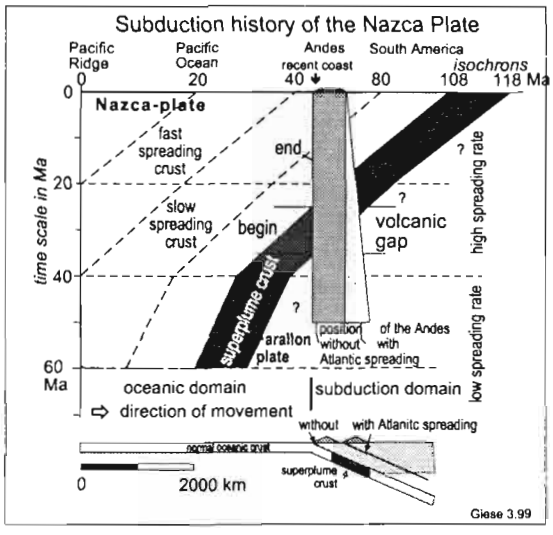

Fig. 2 Simplified reconstruction of the passage of the Nazca-Plate and the bordering superplume crust beneath the South American continent. Two version are displayed: (1) with a fixed position of the continent and (2) regarding the westward shift of South America due to the opening of the Atlantic. From this travel-path diagram it can be seen, that the superplume crust must have passed the western coast of South America between 35 and 20 Ma.

According to a speculative reconstruction of the subduction history of the Nazca Plate (Fig.1), the oceanic crust that was subducted beneath the South American plate in the course of the last 25 My had been generated between 110 and 45 Ma (Fig. 2). At about 35 Ma the eastern border of the superplume crust (age ~118 Ma) must have reached the trench. Assuming a reasonable width for the subducted oceanic plateau of 1000 km and a convergence rate of about 8-10 cm/a as deduced from Fig. 1, the subduction of the superplume plateau required about 10-15 My and was completed 25 to 20 Ma (age ~108 Ma). Thus, the subduction of the plateau coincided with the magmatic gap lasting from 35 to 25 Ma. The cessation of arc magmatism may be explained with a reduction of the slab-dip angle caused by a higher buoyancy which was conferred to the slab by the thick plateau crust. As a consequence the asthenospheric wedge between the plates became narrower, the corner flow was suppressed and the mantle of the upper plate cooled down to temperatures not sufficient for magma generation.

As a relic the normal oceanic lithosphere younger than that of the plateau continued to be subducted at slowly increasing angle for about 10-15 My, as evidenced by the broad volcanic arc which developed

during the Miocene between the Western Cordillera and the Eastern Cordillera. The observed retreat of the eastern limit of magmatism towards the volcanic front in the Western Cordillera during the past 10 My suggests an increase of the dip angle of the slab portion deeper than 100 km. This slab steepening may be related to the tendency of slow-spreading crusts to descend under moderate to steep angles.

DEVELOPMENT OF THE EXTREME PROPORTIONS OF THE CENTRAL ANDES

The considerations made above do not yet answer the question about the parameters controlling the formation of the extreme dimensions of the Central Andes. To begin with, the development of the magmatic arc during Miocene demonstrates that flat-slab subduction increases the width of the orogen. Furthermore, flat-slab subduction between 35 to 25 Ma (magmatic gap) did not generate magmas in the mantle of the upper plate, but it introduced fluids in a relatively wide area beyond the extinct magmatic arc. Fluids play an important role for a number of processes occurring in the upper plate as: (1) The formation of magmatism and volcanism and the convective heat transfer; (2) reduction of the rigidity and increase of the deformability of the lithosphere of the upper plate by magmatic processes and heating of the lower crust; and (3) hydration as partial serpentinization of the mantle wedge, causing a pseudo-crustal thickening. The amount of fluids released from the lower plate into the upper plate is controlled by numerous parameters. During the past 30-40 My a slow-spreading crust which was deeply fractured and thus highly hydrated by ocean bottom metamorphism was subducted. In addition fluid transport was increased when the convergence rate speeded up 40 Ma ago, and low-angle subduction distributed the fluids over a greater distance than before.. These parameters support the intense hydration of the upper plate with all the consequences, also for the tectonic behaviour of the upper plate. The optimal coincidence of these parameters must be seen as a very special situation.

The arid climatic environment, which exist at least since 100 Ma, is another very important parameter controlling the tectonic evolution of the Central Andes. The extreme arid conditions on their western flank reduce erosion to a minimum and thus the trench remains empty. Therefore no accretionary wedge is built up, but the continental margin is tectonically eroded. A consequence of long-lasting subduction erosion in Northern Chile was the stepwise eastward shift of the magmatic arc. The lack of mass removal by erosion does not allow a thinning of the crust and preserves its growing thickness.

CONCLUSIONS

The formation of the Central Andes was strongly controlled by the nature of the oceanic crust. The subduction of the abnormal mid-Cretaceous superplume crust influenced the formation of the young Central Andes. The high buoyancy of this thick oceanic crust caused a reduction of slab dip and interrupted the magmatic activity for at least 10 My. Coincidence of factors such as subduction of a hydrated slow spreading crust, a high

convergence rate, and a low-angle slab dip caused intense hydration of the upper plate mantle and controlled the Neogene tectonic and magmatic evolution of the Central Andes. Finally, arid climatic conditions prevented crustal thinning by erosional mass removal. "Deep wet and dry surface conditions" are responsible for the evolution of this extreme mountain belt.

REFERENCES

Larson, R.L. 1991 Latest pulse of Earth: Evidence for a mid-Cretaceous superplume. Geology 19,547-550.

Mayes, C., Lawer, L.A. and Sandwell, D.T. 1990. Tectonic History and New Isochron Chart of the South Pacific. J. Geophys. Res. 95, 6, 8543-8567.

Müller, R.D., Roest W.R,. Royer, J.-Y,. Gahagan, L. M. and J.G. Sclater, 1997. Digital Isochrons of the World's Ocean Floor. J. Geophys. Res., 102, B, 3211-3214.

NORTH-SOUTH STRUCTURAL EVOLUTION OF THE PERUVIAN SUBANDEAN ZONE

Willy GIL R. (1), Patrice BABY (2), René MAROCCO (1), Jean François BALLARD (3)

(1) IRD, Apartado 18-1209 Lima 18, Peru. ird@chavin.rcp.net.pe
(2) IRD. Apartado 17-10-7019, Quito, Ecuador. pbaby@pi.pro.ec
(3) ELF EP, Av. Larribau, 64000, Pau, France. Jean-Francois.Ballard@elf-p.fr

KEY WORDS: Subandean, Peru, thik-skin tectonics, thin-skin tectonics, inversion, paleogeography.

INTRODUCTION

The Peruvian Subandean zone corresponds to a foreland fold and thrust belt, whose structural geometry varies drastically from north to south. It constitutes the transitional zone between the Eastern Cordillera and the foreland basins of the Peruvian Andes (Marañon, Ucayali and Madre de Dios basins), and extends southward in Bolivia and northward in Ecuador (Fig. 1).

The northern part of the Peruvian Subandean zone (between lat. 4°S and 8°S) is formed by the Santiago and Huallaga Neogene basins. Its central part (between lat. 9°S and 11°S) comprises the Pachitea Neogene sub-basin, which prolongs to the south with the Ene basin. The southern Peruvian Subandean zone (between lat. 11°S and 14°S) extends from the southern extremity of the Ucayaly Basin to Bolivia.

This paper illustrates the north-south geometric evolution of the Peruvian Subandean zone and shows how the Paleozoic and Mesozoic paleogeographies have controlled the style of deformation. Serial balanced cross-sections construction has been possible due to field works, seismic reflection data and drilling information provided by petroleum industry.

DEFORMATION GEOMETRY AND KINEMATICS

In the northern part of the Peruvian Subandean, the section involved in deformation consists of metamorphic Precambrian rocks, and Triassic to Recent sedimentary rocks. The Santiago and Huallaga basins are deformed by diapirs, thrust sheets and tectonic inversions (Figs. 2A-2B). The diapirs and the

décollement of the thrust system developed in the Upper Triassic evaporites of the base of the Pucara Group. Thrust structures are locally deformed by deep positive inversions of Upper Triassic-Lower Jurassic normal faults. In the Huallaga Basin, horizontal shortening increases and the frontal fault

(Tarapoto Thrust) 30km overthrusts the Marañon Basin, which is deformed by wrench tectonics (flower structures) as the Oriente Basin of Ecuador (Baby et al., 1999). Apatite fission track analysis (Alemán and Marksteiner, 1997) shows that the uplift of the thrust belts which limit and deform the Santiago basin started at 10 Ma.

The central part corresponds to the Pachitea basin (Fig. 2C) which pinches out to the east on the Shira High limited by basement faults. The Hinterland (Subandean internal zone) is deformed by an important thrust system developed in a thick series of Paleozoic and Lower Mesozoic sediments. The main detachment is located in the base of the Upper Permian shales (Ene Fm.). A total horizontal shortening of 50% has been calculated in the internal Subandean zone from balanced cross-section construction (Fig. 2C). Neogene continental sediments are overthrusted and do not present strong thickness variations, which seems to show a very young age of the deformation (Gil, 1997).

The southern Subandean zone comprises the southern part of the Ucayali Basin and the north-western border of the Madre de Dios Basin which extends to Bolivia. It is deformed by a thrust system developed in a thick and continuous Paleozoic series (Figs. 2D-E). Total horizontal shortening is also of about 50%. The external zone is deformed by fault propagation folds, whereas the internal zone is structured by blind duplexes and Neogene piggyback basins, similar to the Alto Beni piggyback basin studied by Baby et al. (1995) in the northern Subandean zone of Bolivia.

PALEOGEOGRAPHIC CONTROL

Balanced cross-sections show that some Paleozoic and Mesozoic units wedge out to the east or despair abruptly in the thrust sheets of the hinterland. These drastic changes controlled the style of Subandean deformation.

Deformation of the northern Peruvian Subandean zone (Figs 2 A-B) was controlled by the inversion of an Upper Triassic-Lower Jurassic rift (Pucara Group) which extends to the north in the Oriente Basin of Ecuador (Baby et al., 1999). The presence of evaporites in the base of the Pucara Group induced the development of diapirs and an important detachment. Its pinching out to the east stopped the detachment propagation and provoked the formation of the Santiago Basin frontal triangle zone (Fig. 2 A).

In the central Subandean zone, the development of the hinterland thrust system was controlled by the appearance of the Permo-Triassic shales (Ene Fm.), which formed the sole thrust (Fig. 2 C). To the

east, the Ene Fm. disappears and the deformation is characterised by thick-skin tectonics and basement uplift (Shira High).

The southern part (Figs. D-E) is deformed exclusively by thin-skin tectonics. The thick and almost continuous series of Paleozoic sediments permitted the development of various detachments and duplexes in the internal zone. Similar paleogeography and thrust system geometry are known moreto the south in the northern Bolivian Subandean zone (Baby et al., 1995).

CONCLUSIONS

The Peruvian Subandean foothills is a transition zone where from north to south thick-skin tectonics is progressively replaced by thin-skin tectonics. This north-south evolution was controlled by the Triassic-Jurassic setting, which leaded rift systems oblique to the chain and a strong erosion of the Paleozoic sedimentary series. In the northern part, Triassic and Jurassic rift systems are inverted and their NNE-SSW orientation (oblique to the plate convergence) induced transpressive deformations. In the southern part, the Paleozoic series is poor eroded and permitted the development of thin-skin tectonics with 50% of horizontal shortening.

ACKNOWLEDGMENTS: Parts of this study have been possible due to research agreements IRD-PETROPERU (1993-95) and IRD-ELF EP (1997-99).

REFERENCES

Alemán, A., Marksteirner, R., 1997, Petroleum Systems and Structural Style in the Santiago Fold and Thrust Belt: A Salt Related Orogenic Belt: VI Simposio Bolivariano, Memorias-Tomo II, p. 171-186.

Baby, P., Colletta, B., Zubieta, D., 1995, Etude géométrique et expérimentale d'un bassin transporté: Exemple du bassin subandin de l'Alto Beni (Andes centrales): Bul. Soc. Géol. France, v. 166, p. 797-811.

Baby P., Rivadeneira M., Christophoul F., Barragán R., 1999. Style and Timing of Deformation in the Oriente Basin of Ecuador. ISAG 99, This issue.Gil, W., 1997, Importance du raccourcissement et influence des paléostructures dans le développement de la zone subandine du Pérou central: Mém. de DEA, Univ. Joseph Fourier (Grenoble), 24 p., 16 fig.

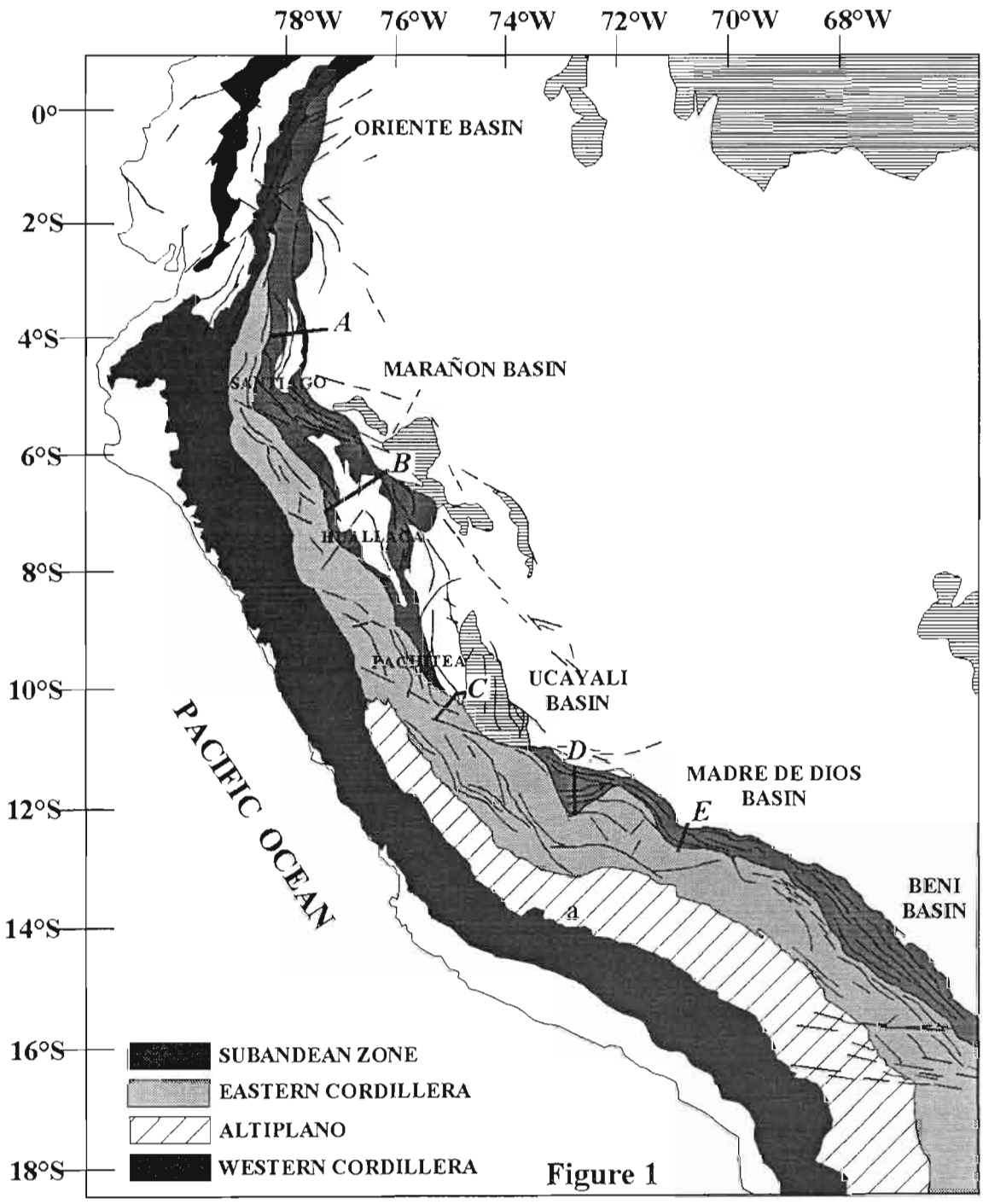
78°W
76°W
74°W
72°W
70°W
68°W
0°
2°S
4°S
6°S
8°S
10°S
12°S
14°S
16°S
18°S
ORIENTE BASIN
A
MARAÑON BASIN
SANTIAGO
B
HUALLAGA
PACHITEA
C
UCAYALI
BASIN
D
MADRE DE DIOS
BASIN
E
BENI
BASIN
a
PACIFIC OCEAN
SUBANDEAN ZONE
EASTERN CORDILLERA
ALTIPLANO
WESTERN CORDILLERA

Figure 1

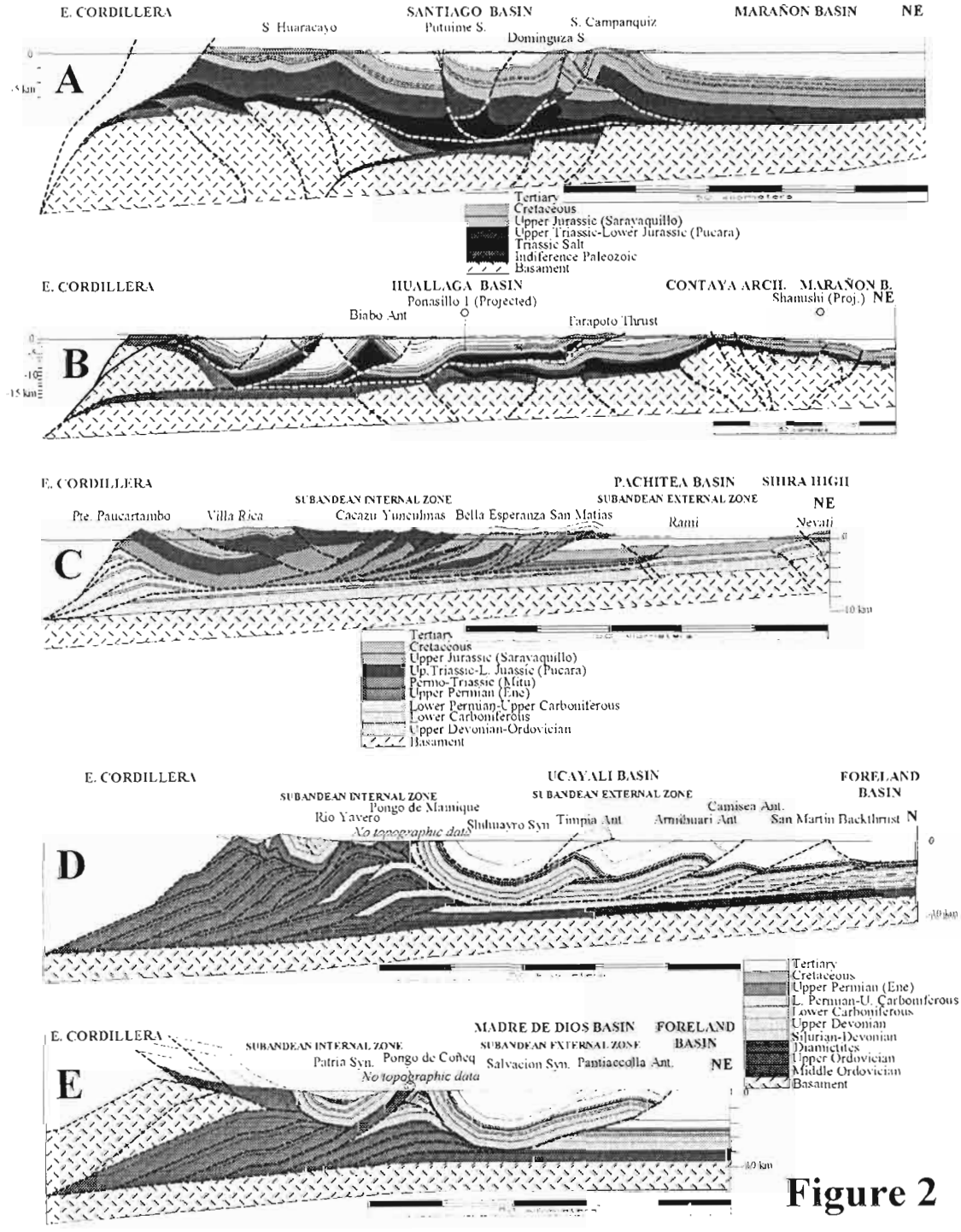
E. CORDILLERA
SANTIAGO BASIN
MARAÑON BASIN
NE
S. Huaracayo
Putuime S.
S. Campanquiz
Dominguza S.
A
Tertiary
Cretaceous
Upper Jurassic (Sarayaquillo)
Upper Triassic-Lower Jurassic (Pucara)
Triassic Salt
Indiference Paleozoic
Basament
E. CORDILLERA
HUALLAGA BASIN
CONTAYA ARCH.
MARAÑON B.
Ponasillo 1 (Projected)
Shanushi (Proj.)
NE
Biabo Ant
Tarapoto Thrust
B
E. CORDILLERA
PACHITEA BASIN
SHIRA HIGH
SUBANDEAN INTERNAL ZONE
SUBANDEAN EXTERNAL ZONE
NE
Pte. Paucartambo
Villa Rica
Cacazu Yuncuimas
Bella Esperanza
San Matias
Rami
Nevati
C
Tertiary
Cretaceous
Upper Jurassic (Sarayaquillo)
Up.Triassic-L. Juassic (Pucara)
Permo-Triassic (Mitu)
Upper Permian (Ene)
Lower Permian-Upper Carboniferous
Lower Carboniferous
Upper Devonian-Ordovician
Basament
E. CORDILLERA
UCAYALI BASIN
FORELAND BASIN
SUBANDEAN INTERNAL ZONE
SUBANDEAN EXTERNAL ZONE
Pongo de Manique
Rio Yavero
Shihuayro Syn
Timpia Ant.
Camisea Ant.
Armihuari Ant.
San Martin Backthrust
N
No topographic data
D
Tertiary
Cretaceous
Upper Permian (Ene)
L. Permian-U. Carboniferous
Lower Carboniferous
Upper Devonian
Silurian-Devonian
Diamictites
Upper Ordovician
Middle Ordovician
Basament
E. CORDILLERA
MADRE DE DIOS BASIN
FORELAND BASIN
SUBANDEAN INTERNAL ZONE
SUBANDEAN EXTERNAL ZONE
Patria Syn.
Pongo de Coñeq
Salvacion Syn.
Pantiacolla Ant.
NE
No topographic data
E

Figure 2

STRUCTURAL GEOLOGY OF THE SOUTHERN SUB-ANDEAN THRUST BELT, BOLIVIA. A NEW DEFORMATIONAL MODEL.

Raúl GIRAUDO (1), Rodrigo LIMACHI (2), Edgar REQUENA (3), Hugo GUERRA (4)

(1)Andina S.A., Santa Cruz, Bolivia (rgiraudo@email.ypf.com.ar)
(2)Andina S.A., Santa Cruz, Bolivia (rlimachi@email.ypf.com.ar)
(3)Andina S.A., Santa Cruz, Bolivia (erequena@email.ypf.com.ar)
(4)Andina S.A., Santa Cruz, Bolivia (hguerra@email.ypf.com.ar)

KEY WORDS: Fold belt, blind thrusting, duplex stacking.

INTRODUCTION

The Southern Sub-Andean zone of Bolivia is a thin-skinned fold-and-thrust belt, generally in-sequence system (Moretti et al, 1994; Roeder et al, 1995). Regional balanced cross-sections were prepared by integrating both surface and sub-surface geological data, supported by satellite imagery and regional seismic lines (Fig. 1).

As a result of this analysis, a new structural model was developed for the Southern Sub-Andean belt. Restoration of cross-sections indicates about 100 km (55 %) of shortening. Main decollement levels are located in the Silurian Kirusillas Formation and in the Devonian Los Monos Formation (Fig. 2). Equal Line Length Method was used to balance competent layers above and below the Los Monos shales which was considered as a plastic material and therefore balanced using the Equal Area Method (Mitra et al, 1989). Duplex geometry was modeled according to Suppe's Fault Bend Folding Method (Suppe, 1983).

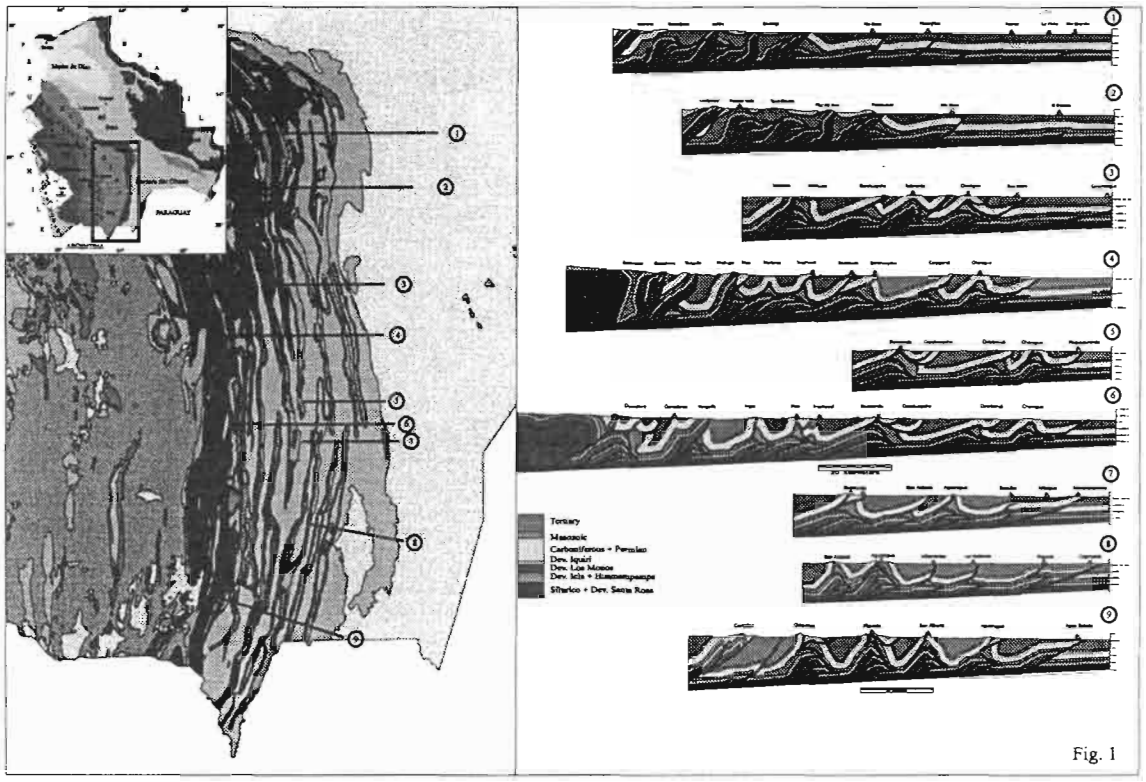

Fig. 1

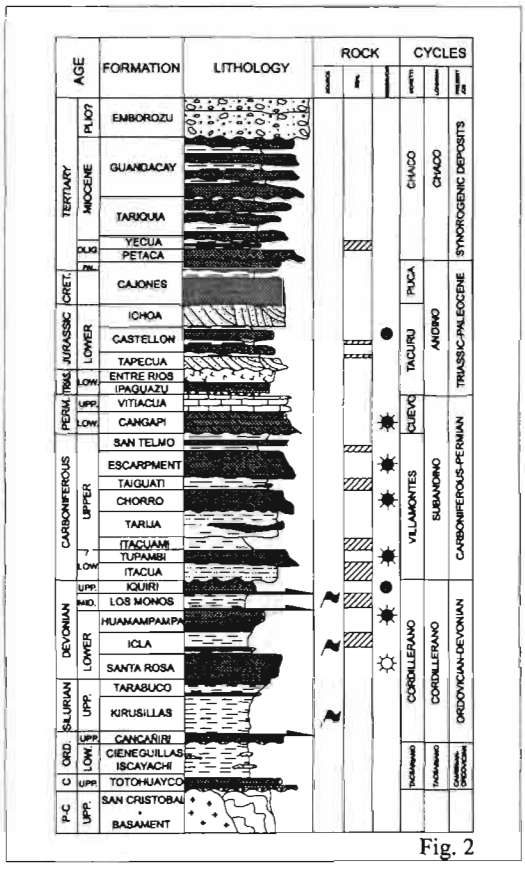

Fig. 2

Shortening, the result of the uplift of the Eastern Cordillera during the Oligocene, was transmitted to the foreland only through the basal shales of the Silurian Kirusillas Formation, being distributed in every structure of the Sub-Andean belt. Partial shortening was accommodated as a double triangle zone, with blind points located both at the base and top of the Devonian Los Monos Formation (Fig. 3).

Jones (Jones, 1991) points out that differential overburden loading controls the shape and location of ramps within a fold and thrust belt. In the outer Foothills and Chaco Plain, where overburden load was minor, faults from the basal Kirusillas detachment, ramping up through the entire section, predominate. In the Sub-Andean belt, excessive overburden originated high fluid pressures , high enough to

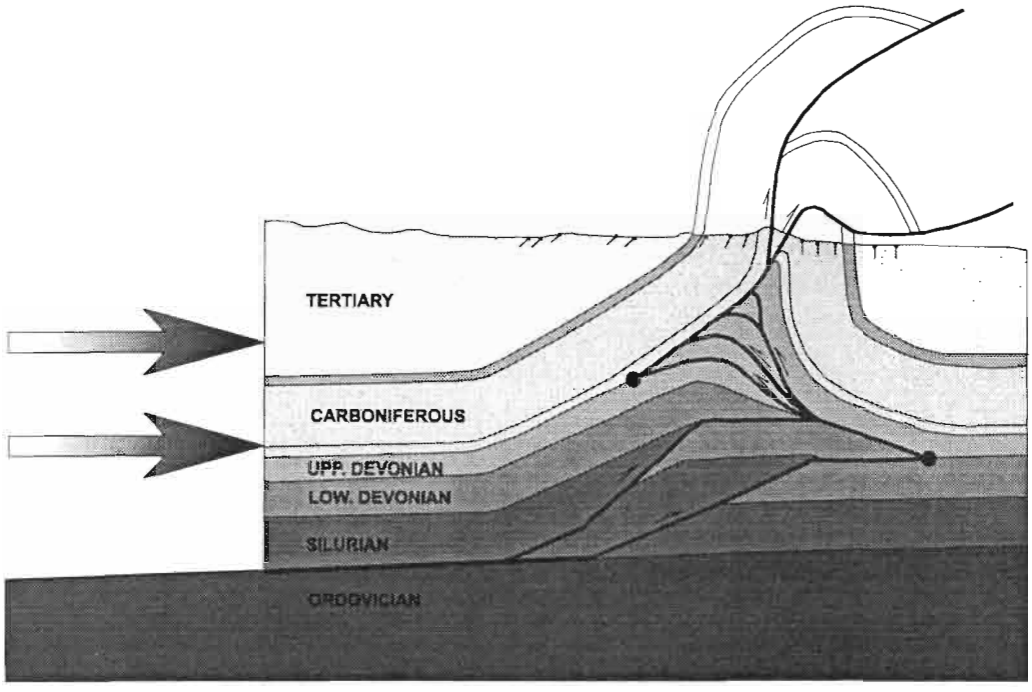

Fig. 3

lubricate movement and generate blind thrusting.

Out-of-sequence thrusting complicates the model even more. According to Coulomb's model (Davis et al, 1983), a typical fold and thrust belt has a triangular shape, a characteristic surface slope and a basal decollement dip. The wedge formed by pushing an initial layered sequence from behind such that thrusts propagate in sequence until a critical taper is attaincd; at such time, subsequent deformation involves transport of the whole wedge along the basal decollement; should surface slope is modified, the wedge will reply by generating out-of-sequence thrusting or back-thrusting in an attempt to recover pre-existing conditions.

CONCLUSIONS

Shortening was distributed all over the Sub-Andean belt through the basal shales of the Silurian Kirusillas Formation.

Every anticline is the result of partial shortening accommodation in a double triangle zone.

Shortening was not transmitted to the foreland by the Los Monos shales. Instead, passive-roof duplexes stack within this formation.

East-verging thrust faults originate from the upper blind point generating surface anticlines whose crests not always match sub-surface culminations.

Shape and location of ramps are controlled by the pressure regime developed within the Los Monos shales.

Out-of-sequence thrusting is the sedimentary prism's mechanical response to new lineaments developing in the foreland.

REFERENCES

-Davis D., Suppe J. and Dahlen A., 1983. Mechanics of fold belts and accretionary wedges. Journal of Geophysical Research, 88, 1153-1172.

-Jones P., 1991. Quantitative geometry of thrust and fold belt structures. The AAPG Bulletin, 68, 493-518.

-Mitra S. and Namson J., 1989. Equal-area balancing. American Journal of Science, 289, 563-599.

-Moretti I., Baby,P., Méndez E. and Zubieta D., 1994. Hydrocarbon generation in relation to thrusting in the Sub-Andean zone from 18 to 22° S, Bolivia. Petroleum Geoscience, 2, 17-28.

-Roeder D. and Chamberlain R.L., 1995. Structural geology of Sub-Andean fold and thrust belt in Northwestern Bolivia. In "Petroleum basins of South America. AAPG Memoir 62".

-Suppe J., 1983. Geometry and kinematics of fault-bend folding. American Journal of Science, 283, 7.

DIACHRONOUS DEFORMATION OF THE CENTRAL AND EASTERN ANDEAN CORDILLERAS OF COLOMBIA AND SYNTECTONIC SEDIMENTATION IN THE MIDDLE MAGDALENA VALLEY BASIN

Elías GOMEZ and Teresa JORDAN (1), Kerry HEGARTY (2), Shari KELLEY (3)

(1) Department of Geological Sciences, Cornell University, Ithaca NY 14853 (elias @ geology.cornell.edu, jordan@geology.cornell.edu)
(2) Geotrack International, 37 Melville Road, Brunswick West, Victoria 3055 Australia (mail@geotrack.com.au)
(3) New Mexico Tech, Department of Earth and Environmental Sciences, Socorro, NM 87801 (sakelley@ix.netcom.com)

KEY WORDS: Colombia, tectonics, sedimentation, geochronology, thermal history, AFTA

INTRODUCTION

The Late Cretaceous-Cenozoic Middle Magdalena Valley Basin (MMVB) of Colombia is filled with siliciclastic, syntectonic sediments. The Central Cordillera, to the west, supplied the majority of sediments and was the first-order control on accommodation. Deformation related to the Eastern Cordillera, to the east of the MMVB, created shorter wavelength variations in accommodation and was the primary control on unconformities that define the variable stratigraphic architecture. Deformation in each mountain system was diachronous along strike.

The Central Cordillera formed by transpressional strike slip deformation beginning in the Campanian (e.g. Pindell, 1993). Fission track cooling ages of the Mariquita stock, a Central Cordillera granitoid pluton, indicate slow cooling at rates of 2.8 °C/Ma between the Campanian (77.6±7.8 Ma, zircon) and the Oligocene (32.0±6.2 Ma, apatite), and 2.5 °C/Ma since the Oligocene. The Eastern Cordillera is considered to have formed dominantly as a consequence of E-W shortening during the Miocene-Pliocene as a doubly vergent thrust belt (Cooper et al, 1995).

Our results are based on integrated stratigraphic and structural analyses supported by the following data sets: 1) field information (source of stratigraphic sections with chronologic data for interbedded volcanic ashes, paleocurrent, facies, petrographic, geochemical and paleontological data), 2) thermal histories derived

from Apatite Fission Track Analyses (AFTA ®) and vitrinite reflectance studies, and 3) grids of seismic and well data.

UPPER CRETACEOUS-PALEOCENE

Southern MMVB: Maastrichtian unroofing of the Central Cordillera sourced quartzite and chert pebbles to ubiquitous braid delta deposits (Cimarrona Formation; Gómez and Pedraza, 1994). These conglomeratic deposits prograded eastward onto shallow marine mudstones (Umir Formation). Mild deformation in the basinal area controlled the distribution of Maastrichtian facies (Díaz, 1994). Paleocene eastward migrating deformation of the Central Cordillera tilted the mountain front alluvial fans (Hoyón Formation); the resultant sediment was deposited downfan as sheet and debris flows, which interfingered with alluvial plain muddy deposits (Seca and Guaduas Formations). Eastward progradation of alluvial fans is expressed as offlapping seismic reflections and radial eastward directed paleoflow patterns.

Northern MMVB: Northward propagation of the Central Cordillera uplift is registered by a delayed change to continental facies and Central Cordillera provenance, both of which are found in the Paleocene Lisama Formation. Absence of alluvial fans indicates a gentler topographic gradient of the Central Cordillera in this part of the MMVB.

EOCENE-EARLY MIOCENE

Communication between the MMVB and Llanos Basin to the east was partially interrupted by low, discontinuous hills (e.g. Gómez and Jordan, 1998), which resulted from incipient inversion of Mesozoic grabens in the area of the Eastern Cordillera. Stratal growth relations and time transgressive unconformities superbly illustrate this event. That the Central Cordillera was the main source area of sediments is indicated by syntectonic geometries, provenance, and paleocurrents.

Southern MMVB: Stratal growth geometries record progressive forelimb rotation of west vergent anticlines, which indicate that inclined shear was the likely mechanism of Paleogene deformation of the Eastern Cordillera. Northward-directed paleocurrents attest to the Eocene-Oligocene confinement of the MMVB between the Central and Eastern Cordilleras. Upper Oligocene-Lower Miocene strata finally overlapped the Eastern Cordillera uplift as the sedimentation sourced by the Central Cordillera overcame uplift rates of the eastern folds. Eocene-Lower Miocene basin fill also onlapped over the Paleocene alluvial fans and the pediment surface that resulted from erosional retreat of the Central Cordillera front.

Northern MMVB: Paleocene and older rocks were highly deformed during the Eocene as the Central Cordillera front propagated into the basin. Net westward retreat of the Central Cordillera front has created an eastward dipping unconformity, which is the base of the onlapping Eocene to Neogene sediments.

Chronology and kinematics of Eastern Cordillera deformation events in the northern MMVB are not the same as in the south. Paleocurrent and provenance analyses indicate that central areas of the Eastern Cordillera were uplifted during sedimentation of the lower part of the Eocene La Paz Formation. An event of westward thrust faulting of probable Eocene age has been also identified in the central part of the MMVB by Restrepo et al (1998). Paleocurrents and stratigraphic relations indicate that no barrier existed between the MMVB and Llanos Basin during the sedimentation of the upper part of La Paz and Esmeraldas Formations and lower part of the Mugrosa Formation, of probable Late Eocene-Oligocene age.

Westward migration of Eastern Cordillera deformation continued during the Oligocene-Early Miocene, as a series of fault propagation faults. AFTA and vitrinite reflectance results, and eastward thinning of Oligocene units (Mugrosa and Colorado Formations) constrain the age of the first uplift event of the foothills region to the time window 34 to 30 Ma. At this time, Cretaceous rocks began to cool from a maximum temperature of 180°C. Younger Upper Oligocene-Lower Miocene rocks preserve a syntectonic stratal record of instantaneous limb rotation, associated with layer-parallel shearing. Several oil producing anticlines, e.g. Provincia and Lisama, belong to this generation of folds.

An important implication arises from comparison of time constrains provided by AFTA results and growth strata: oil generation in Cretaceous marine rocks in portions of the Eastern Cordillera happened a long time before formation of Late Oligocene-Miocene anticlines, the oldest Tertiary traps preserved along the foothills. These data disprove older interpretations, which assumed that all foothills-synclines acted as oil-generation areas during the Neogene or are still areas of active hydrocarbon generation.

MIDDLE MIOCENE TO PLIOCENE

There was renewed deformation of the central part of the Eastern Cordillera during the Middle Miocene. Middle and Upper Miocene fluvial sediments were deposited by a northward-directed fluvial system, which was fed by the Eastern and Central Cordilleras. Sedimentation was contemporaneous with Central Cordillera volcanism between 10.92±0.11 and 6.2±0.4 Ma. Miocene sediments were originally deposited across the foothills area of the present Eastern Cordillera as indicated by AFTA calculations of the eroded sedimentary column and balanced structural sections.

Diachroneity of westward breakthrough of the Eastern Cordillera is indicated by the age of a second thermal event. Cooling from maximum paleotemperatures in the range of 110 to 120 °C started between 15 and 5 Ma in the southern part of the basin and between 5 to 0 Ma in the northern MMVB according to AFTA and vitrinite reflectance analyses. The main uplift of this mountain range and complete conversion of the MMVB into an intermontane basin occurred after 6.2±0.8 Ma.

DISCUSSION

A major feature of the MMVB is the east-dipping unconformity at the base of post-Paleocene strata caused by westward retreat of the Central Cordillera front. This unconformity is still under formation at the present mountain front. Former age assignments of this unconformity to the Paleocene-Eocene are oversimplified, as Eocene tectonism is not the only contributor in its formation.

The number, age and kinematics of Eastern Cordillera Tertiary deformation episodes vary along strike. Deformation did not proceed in a simple spatial sequence.

Paleogene subsidence of the MMVB was thought to be the result of flexure due to tectonic loading by the Eastern Cordillera (Gómez, 1997; Gómez and Jordan, 1998). Although this hypothesis must be tested, it is difficult that the incipient Eastern Cordillera Paleogene topography would have met the requirements of altitude, continuity, wavelength, and time duration that are required for important lithospheric flexure.

Two hypotheses, associated with deformation of the Central Cordillera, may explain the regional eastward dip of the unconformity at the base of post-Paleocene deposits: 1) Eastward propagation of the Central Cordillera eastern flank above a middle crustal detachment may have produced progressive eastward displacement of the region of maximum subsidence, and 2) West-vergent synthetic net shortening of the Central Cordillera orogen, associated with underthrusting of oceanic terrains, may have produced accommodation in a broad piggy-back-like region towards the east.

REFERENCES

Cooper, M. A., and 11 others., 1995 Basin development and tectonic history of the LLanos Basin, Eastern Cordillera and Middle Magdalena Valley, Colombia: AAPG Bulletin, V. 79 (10), p. 1421-1443.

Díaz, L., 1994. Reconstrucción de la cuenca del Valle Superior del Magdalena a finales del Cretácico. In: Etayo-Serna, Fernando, ed. Estudios Geológicos del Valle Superior del Magdalena, Chapter XI. Special Publication Universidad Nacional de Colombia-Ecopetrol. Bogotá, Colombia.

Gómez, E., and Pedraza, P., 1994. El Maastrichtiano de la región Honda-Guaduas, límite Norte del Valle Superior del Magdalena: Registro sedimentario de un delta dominado por ríos trenzados. In: Etayo-Serna, Fernando, ed. Estudios Geológicos del Valle Superior del Magdalena, Chapter III. Special Publication Universidad Nacional de Colombia-Ecopetrol. Bogotá, Colombia.

Gómez, E. 1997. Quantified Cenozoic evolution of the Middle Magdalena Basin (Colombia): Ages, paleogeography, and tectonics: AAPG Bulletin, V 81 (10), p.1774

Gómez, E., and Jordan, T., 1998. Relative timing of Cenozoic deformation of the Middle Magdalena Valley Basin and bounding mountain ranges, Colombia: AAPG/SEPM Annual Meeting Abstracts with Programs, Salt Lake City, Utah

Pindell, J.L., 1993. Regional synopsis of Gulf of Mexico and Caribbean evolution. In: Pindell, J. L. and Perkins, B. F., eds., 13th Annual Research Conference Proceedings, Mesozoic and Early Cenozoic Development of the Gulf of Mexico and Caribbean Region: SEPM Gulf Coast Section, p. 251-274.

Restrepo, P., Colmenares, F., Higuera, C., Mayorga, M., and Leal, J., 1998. Fold and thrust belt along the western flank of the Eastern Cordillera of Colombia; style, kinematics and timing constraints derived from seismic data and detailed surface mapping: AAPG Bulletin, V 82 (10), p.1956.

THE MULTI-PHASE MESO-CENOZOIC SLIP HISTORY OF THE ATACAMA FAULT SYSTEM, COASTAL CORDILLERA (21°-24° S), NORTHERN CHILE

Gabriel GONZÁLEZ, Jaime CORTÉS, Dan DIAZ, Baeza CLAUDIA, Heinz SCHNEIDER (1)

(1) Depto. Ciencias Geológicas, Universidad Católica del Norte,Casilla 1280 Antofagasta Chile

KEY WORDS: Atacama fault system, Kinematic history, Mesozoic-Cenozoic, Northern Chile

INTRODUCTION

The Atacama Fault System (AFS, Fig.1) is a significant regional structure in northern Chile, composed of discontinuos and overlapping faults that strike subparallel to the continental border. Several authors have interpreted the AFS to be a sinistral strike-slip fault formed in response to oblique subduction of the oceanic plate during the Early Cretaceous (Naranjo et al. 1984; Scheuber y Andriessen 1990). The northern part of the AFS -between Antofagasta and Iquique, is composed mainly of N-S trending faults and NW-SE splays whose younger activity exerts a strong control on the morphological features of the Coastal Cordillera. Our field observations indicate that the AFS has a very complicated multi-phase slip-history that started in the Early Cretaceous. In this contribution we focus on the kinematic of this slip-history. We report the results of extensive study of satellite images and detailed field observations concentrated in the northern part of the AFS. Three K-Ar radiometric ages in biotite from volcanic ashes were carried out to constrain the age of the younger deformations.

THE KINEMATIC SLIP HISTORY OF THE AFS

1. Early sinistral slip phase of the AFS

In many places in the Coastal Cordillera there are sinistral strike-slip faults that cut magmatic rocks which span from Late-Jurassic to Early-Cretaceous. This is the case of Caleta Coloso Fault, that displaces the intrusive contact between the Cerro Cristales Pluton and the Bolfin Complex (González, 1996). In the Sierra del Buey Muerto two Early-Cretaceous stocks are localized at the intersection of NW-trending sinistral splays and N-S faults, suggesting that the faulting occurred during or prior to the emplacement of

these intrusive bodies in Early Cretaceous times. Such supposed age for the sinistral motion agrees with ^{40}Ar-^{39}Ar datings on AFS-mylonites further south which shows that the initial sinistral strike-slip phases of the AFS was Early Cretaceous in age (Scheuber et al. 1995).

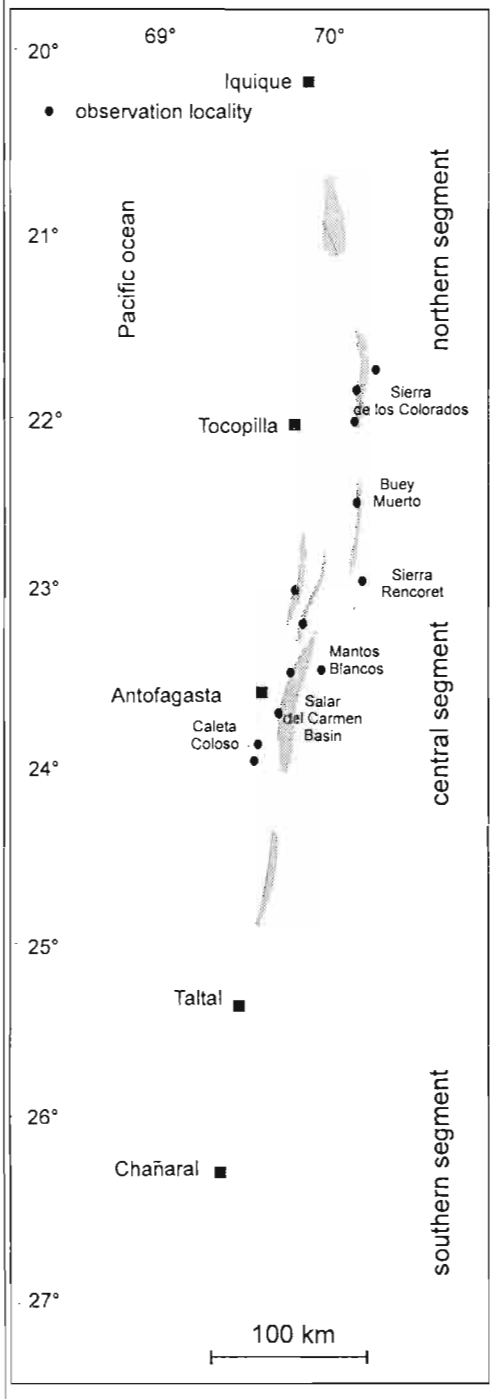

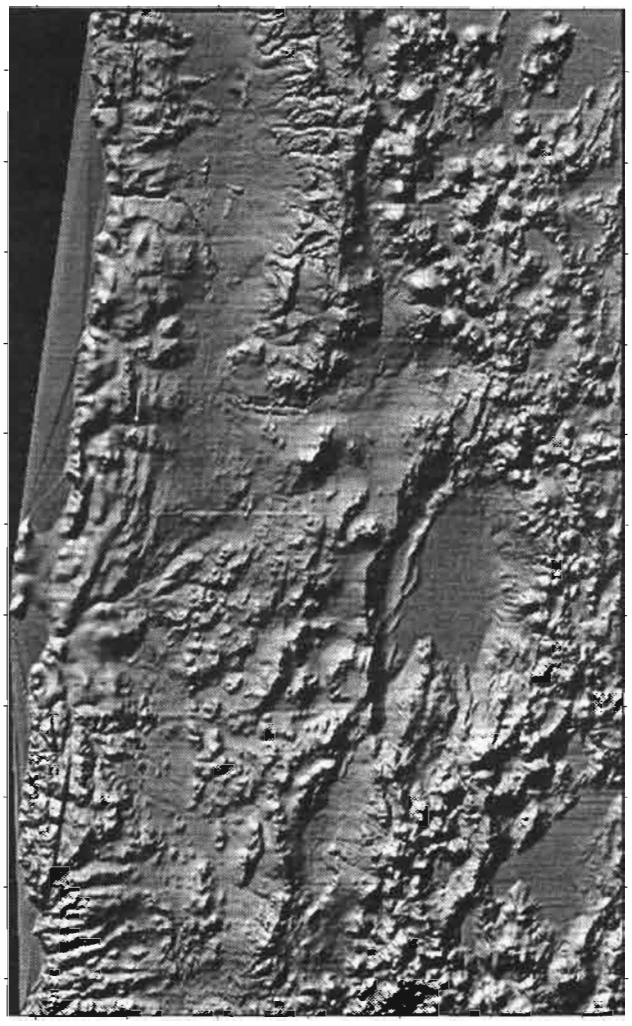

Fig. 1. Structural map of the Atacama Fault System along the Coastal Cordillera. Right side topographic model of northern Chile showing the strong structural control of AFS on the morphology of the Coastal Cordillera.

2. Dextral slip phase of the AFS

Between Sierra los Colorados and Mantos Blancos mine, well-developed large-scale sidewall ripout structures were found, some of which control the emplacement of quartz and carbonate veins. The geometry of the sidewall structures and the NE trending en-echelon veins indicate that the deformation took place in a dextral strike-slip regime. In Sierra los Colorados there is an important N-S fault zone with NE-SW trending subsidiary strike-slip faults with dextral and sinistral character. We interpreted these subsidiary structures as Riedel shear related to N-S dextral strike-slip along the N-S fault zone. In the same place, paleostress analyses using the slickenside lineations and kinematic indicators of the faults give an ENE-WSW shortening direction which is in agreement with such a N-S dextral motion. In Sierra del Buey Muerto, several small NNW-SSE trending thrusts related to the dextral strike-slip cut the NW-trending sinistral faults, indicating that the ENE-WSW shortening is younger than the sinistral strike-slip. We interpret these field relations as reversal of the AFS from sinistral to dextral slip. In the Mantos Blancos Mine we found the same cross-cutting relations: here there are NE-SW trending sinistral faults and NNE-SSW dextral faults that displace both older sinistral faults and the copper ore body. Paleostress analyses show that these faults were kinematically linked during a dextral slip phase with a NE-SW shortening direction. This dextral reversal represents an important tectonic phase superimposed on the previous sinistral deformation. As there are few age markers available, the time of this dextral phase is very difficult to constrain.

3. Extensional slip phase of the AFS

The majority of mountain ranges in the Coastal Cordillera are bounded by prominent scarps that face to the east and that reach elevations up to 100 m. A type of asymmetrical extensional deformation is suggested by the ocurrence of high-angle east-dipping faults that limit these east-facing range fronts. The faults produce west-tilted domino blocks that break an old topographic surface formed in the Oligocene-Early Miocene (Mortimer and Saric, 1975). Consequent east-side down movements can be inferred from the trapping of old gravels in the hangingwall of the faults. Fault planes related to this topography have been observed in few localities, where they show dip-slip lineations suggesting that the deformation took place in an extensional regime. Post-tectonic alluvial fan sediments covering the old gravels contain intercalations of volcanic ashes dated 5 to 3 Ma (K-Ar ages in biotite, this research), indicating that this extensional slip phase was probably active between the Early Miocene and the Upper Miocene.

Asymmetrical half-graben structures can be seen across the Coastal Cordillera to the subduction trench. They reflect very large extensional faults affecting the entire forearc of the Antofagasta area (Arabasz 1971; von Huene et al. 1995). According to Niemeyer et al. (1996) the activity of these extensional faults

was contemporaneous with the Miocene-Oligocene marine transgression that took place along the western edge of the Coastal Cordillera

4. Late slip phase of the AFS

Near Sierra Miranda the N-S trending faults bend into a NE-SW direction, here the subsidence along the faults was related to the formation of the Salar del Carmen basin. Along the western margin of the Salar del Carmen basin there are fault scarps 0.5-5 m height, that displace the surface of inactive alluvial fans. The offsets along these faults have locally both compressional and extensional character showing that strike-slip motion dominates the deformation of the salar margin. Ashes intercalated in the upper part of the fans give K-Ar ages of 5 Ma (this research), revealing that the strike-slip movements have a post Early Pliocene age. Younger fluvial channels and active alluvial fans cut these faults, indicating that these strike-slip movements are inactive today. However, another vertical displacements are still active as shown by the presence of small east side down offsets (10 cm) across N-S faults at the base of the youngest channels.

TECTONIC CONTROLS ON THE SLIP HISTORY OF THE ATACAMA FAULT SYSTEM

We explain the four phases of the slip history of the AFS by major changes of the convergent regime along the western margin of South America. The earlier slip-phase of the AFS occurred during the Early Cretaceous due to SE-directed subduction of the oceanic plate beneath South America. The reversal of motion along the AFS from sinistral to dextral slip indicates a major change in the orientation of the maximal horizontal stress (Shmax) from NW-SE to NE-SW. The timing of this change is difficult to constrains due to poor control on the age of the deformations. In Mantos Blancos mine the supergenic alteration cap is deformed by the dextral strike-slip motion. In this locality supergenic alunites were dated 14 $\pm$ 7 Ma (Chavez 1985). This age indicates that the dextral displacement was active in a post-middle Miocene time. However, in Sierra los Colorados, the occurrence of quartz and carbonate veins along the damage zone of N-S faults evidence that hydrotermal activity took place during dextral faulting. In the Coastal Cordillera magmatic heat supply for the hidrotermal activity is supposed active until to the middle part of the Cretaceous. Thus we interprete that the dextral strike-slip motion took place near the middle part of the Cretaceous, during the period of the magmatic cooling of the Coastal Cordillera. According to our data, dextral displacement along AFS ended with the extensional slip phase during the Miocene-Oligocene. Dextral deformation younger than 14 Ma, detected in Mantos Blancos Mine, represent the reactivation of the AFS under the same dextral kinematics.

The younger than 5 Ma extensional and contractional faults documented near the western side of the Salar

del Carmen are related to strike-slip displacements, the kinematic of this displacement is not clear. Armijo and Thiele reported sinistral displacements: we found evidence for dextral motions. The most recent activity along the AFS, given by the occurrence of small vertical offset of the youngest channels, which we interpret as extensional structures coupled with post-seismic deformation associated with the 1996 Antofagasta earthquake.

REFERENCES

Armijo R. & Thiele, R. (1990). Earth and Planetary Science letters, 98 , pages 40-61.

Chavez, W. (1985). Unpublished PH.D. tesis, University of California; Berkeley, USA.

González, G. (1996). Berliner Geowissenschaftliche Abhandlungen, Reihe A, Band 181.

Mortimer, C and Saric, N. (1985). Rev. Géomorphol. Dyn. 21. 162-170.

Naranjo, J. Hervé, Prieto, X. & Munizaga, F. (1984). Revista Comunicaciones, U de Chile, Vol. 34, p 57-66.

Niemeyer, H., González, G. & Martinez-De los Rios, E. (1996). Revista Geológica de Chile, Vol. 23, N°2, 165-186.

Scheuber, E. y Andriessen P. (1990). J. Struct. Geol., Vol 12, 243-257.

Scheuber, E. Hammerschmidt, K. and Friedrichsen; H. (1995). Tectonophysics Vol.250, 61-87.

Von Huene, R. Weinrebe, W. & Heeren, F (1995). Shipboard draft, 13 October 1995; Chapter 5. Geomar Kiel

THE GRAVITY FIELD, ISOSTASY AND RIGIDITY OF THE CENTRAL ANDES

Hans-Jürgen GÖTZE (1), Sabine SCHMIDT (1), Manuel ARANEDA (2), Guillermo CHONG D. (3), Michael KÖSTERS (1), Ricardo OMARINI (4) and José VIRAMONTE (4)

(1) Institut für Geologie, Geophysik und Geoinformatik, FU Berlin, Haus N, Malteserstrasse 74-100, D-12249 Berlin; hajo@geophysik.fu-berlin.de and schmidt @geophysik.fu-berlin.de
(2) Departamento de Geofísica, Universidad de Chile, Blanca Encalada 2355, Santiago (Chile); maraneda@dgf.uchile.cl
(3) Universidad Católica del Norte, Departamento de Ciencias Geológicas, Avd. Angamos 0610; Casilla 1280, Antofagasta, Chile; gchong@socompa.ucn.cl
(4) Instituto de Geología del Noroeste Argentino, Universidad Nacional de Salta, Buenos Aires 177, 4400 Salta, Argentina, geonorte@ciunsa.edu.ar

KEY WORDS: Gravity, Isostasy, Rigidity, Andes, Subduction zone

INTRODUCTION

The gravity field of the southern Central Andes and their eastern foreland between 20° to 30° S was investigated with regard to the isostatic state, the crustal density structure of the orogeny and the rigidity of the Andean Lithosphere (Götze et al., 1996, Kösters et al, 1997). Gravity data-base came from recent field data acquisition in the Central Andes and covers both the area of northern steep subduction zone and the flat slab area in the South (Araneda et al., this issue). All gravity data analysed in this paper were tied to the IGSN-71 gravity datum and terrain-corrected as well. Bouguer anomaly was evaluated using the sea level datum and a standard density of 2670 kg/m^3 for mass correction. Analysis of Andean topography bases on the 1 km x 1 km mean elevation data grid of the USGS and other sources. The gravity effect of the down going Nazca Plate was removed from both Bouguer and isostatic residual anomalies (Airy and Vening-Meinesz type) and then correlated with mean topographic heights to identify areas of disturbed isostatic equilibrium (Kirchner 1997; Götze and Kirchner, 1997). Additionally the balance of topographic surplus and deficit masses of the Andean root was estimated by applying Gauß´ theorem to the residual gravity field.

ISOSTATIC STATE

As can be expected from the principle of isostasy, isostatic anomalies close to zero dominate, however, clearly shifted to a small positive mean values. Most of the morphological Andean units close to an isostatic equilibrium. Differences were obtained in the Argentine Puna, the south-eastern foreland and along a large NW to SE striking zone crossing the volcanic arc. This structure can be linked to high density crustal remnants of Mesozoic rifting. A novel methodology (Lowry and Smith, 1995) for 2D modelling of lithospheric rigidity which can account for surface and subsurface loads were applied to both topography and gravity field. Rather low values (10^{22} to 10^{23} Nm) were obtained for the area of the inner mountainous basins and 10^{23} to $5x10^{23}$ Nm were observed for the back arc region which corresponds with an effective elastic thickness of 35 to 45 km (Kösters, 1999).

THE MODEL OF THE SUBDUCTED NAZCA PLATE AND MANTLE EDGE

The oceanic crust of subducting Nazca plate (30-40 My old age) is approximated by two crustal layers: basaltic layer 2 with density 2.8 g/ccm and gabbro layer 3 with density approx. 2 950 kg/m^3 (Orcutt, 1987; Johnson and Semyan, 1994). At the depth of approx. 20 km, layer 2 is shown to be wedged, because the pores in the basalts are thought to be mostly closed due to high pressure, and the density of these basalts and their following metamorphic changes must not strongly differ from those of the gabbro of the layer 3. The mantle part of Nazca plate is believed to be harzburgite grading with dept into spinel lherzolite with an average density approx.. 3 340 kg/m^3 (Cordery and Morgan, 1993). The boundary with the asthenosphere beneath Nazca plate near the western coast of South America has not been obtained using seismic methods. Its parameters corresponde to the age of the Nazca plate.

The most active area of continental and oceanic plates contact from the trench to volcanic arc is usually considered (Dumitru, 1991; Ponko and Peacock, 1995). The dehydration and different metamorphic transformations (basalt-eclogite is the most important from them) in the subducted oceanic crust are proposed here. Two results of these processes are the most important for the density modeling (Romanyuk, Götze and Halvorson, 1999):

(1) an increasing density into going down slab, and

(2) distortion of the mantle edge by the realized from slab water (?fluids?), causing a wet melting of mantle edge peridotites and forming a volcanic arc (Davies and Stevenson, 1992).

Three large parts into uppermost mantle beneath the Andean mountain belt are distinguished: the light mantle cones (3 200 kg/m ^{3}), the dense sinking root of the Andean lithosphere (3 400 kg/m^3), and "normal" continental mantle of the Brazilian craton (approx. 3 360 kg/m^3). The densities in the mantle at the 200-670 km depths were fixed in accordance of the standard columns proposed by (Dziewonski and Anderson, 1981, PREM-model) and (Lerner-Lam and Jordan, 1987, oceanic column).

REFERENCES

Araneda M. 1999. South Central Andes Gravity, New Data Base. ISAG 1999, this issue.

Cordery M..J. and Morgan J.P. 1993. Convection and Melting at Mid-Oceanic Ridges, J. Geophys. Res., V.98, N.B11, p.19,477-19,503.

Davies , J.H. and Stevenson D.J. 1992. Physical Model of Source Region of Subduction Zone Volcanics, JGR, V.97, N.B2, p.2037-2070.

Dumitru T.A., 1991. Effect of Subduction Parameters on Geothermal Gradients in Forearcs, with an Application to Franciscan Subduction in California, JGR, V.96, N.B1, p.621-641.

Dziewonski A.M. and Anderson D.L. 1981. Preliminary reference Earth model, Phys.Earth. Plan. Int., V.25, p. 297-356

Götze H.-J. and the MIGRA group 1996. Group updates the gravity data base in the Central Andes (20° - 29° S). EOS Transactions, American Geophysical Union, .Electronic Supplement, 5 pages. http://www.agu.org/eos_elec/95189e.html.

Götze H.-J. and A. Kirchner 1997. Gravity field at the South American active margin (20° to 29° S). Journal of South American Earth Sciences, vol. 10, no.2, pp. 179-188.

Johnson H.P. and Semyan S.W. 1994. Age variation in the physical properties of oceanic basalts: Implications for crustal formation and evolution, JGR., V.99, N.B2, pp.3123-3134.

Kirchner A. 1997. 3D-Dichtemodellierung zur Anpassung des Schwere- und des Schwerepotentialfeldes der Zentralen Anden. PhD Thesis FU Berlin, Berliner Geowiss. Abhandlungen, Reihe B, vol. 25, pp. 98 Kösters M., H.-J. Götze, S. Schmidt, J. Fritsch and M. Araneda 1997. Gravity Field of a Continent-Ocean Transition Mapped From Land, Air, and Sea. EOS, vol. 78, No. 2, pp. 13-16.

Kösters M. 1999. 3D-Dichtemodellierung des Kontinentalrandes sowie quantitative Untersuchungen zur Isostasie und Ridität der Zentralen Anden (20° - 26° S). PhD Thesis FU Berlin, Berliner Geowiss. Abhandlungen, Reihe B, vol. 32, pp. 181

Lerner-Lam A.L. and Jordan, T.H. 1987. How Thick Are the Continents?, J. Geophys. Res., V.92, N.B13, p.14,007-14,026.

Lowry A.R. and R.B. Smith 1995. Strength and rheology of the wetsern U.S. Cordillera. J. Geophys. Res., V. 100, N.B. 9, p. 17,947-17,963.

Orcutt J.A. 1987. Structure of the Earth: Oceanic Crust and Uppermost Mantle, Rev. Geophys., V.25, N.6, p.1177-1196

Ponko S.C. and Peacock S.M. 1995. Thermal modeling of the southern Alaska subduction zone: Insight into the petrology of subducting slab and overlying mantle wedge, JGR, V.100, N.B11, p.22,117-22,128.

Romanyuk T., H.-J. Götze and P.F. Halvorson, 1999. A density model of the Andean subduction zone. The Leading Edge, vol. 18, no. 2, p.264-268.

DEFORMATION PARTITIONING AT SUBDUCTION BOUNDARIES: AN EXAMPLE FROM THE NORTH CHILEAN ANDES (26°S - 30°S).

John GROCOTT (1), Graeme K. TAYLOR (2) and Carlos E. ARÉVALO (3)

(1) School of Geological Sciences, Kingston University, Kingston-upon-Thames, Surrey KT1 2EE, U.K.
(2) Department of Geological Sciences, Plymouth University, Plymouth, Devon PL4 8AA, U.K.
(3) Servicio Nacional de Geología y Minería, Avda. Santa Maria 0104, Providencia, Santiago, Chile.

KEY WORDS: Andes; northern Chile; deformation partitioning; advancing subduction boundary.

INTRODUCTION

Late Cretaceous deformation in the Coastal Cordillera of northern Chile (26°S-30°S) was partitioned into margin-parallel and margin-normal components. Margin-parallel displacement occurred on the Atacama Fault System, within the Early Cretaceous arc batholith, and on a fault system located at the eastern boundary of the Coastal Cordillera (Taylor et al. 1998; Arévalo 1999). The margin-normal component was taken up by strike-slip on NW-trending faults accompanied by vertical axis rotation of intervening fault blocks. Partitioning was in response to oblique convergence and coincided with a transition from a retreating to an advancing subduction boundary at the beginning of the Andean orogenic cycle.

STRUCTURE OF THE COASTAL CORDILLERA (26°S - 30°S)

The Coastal Cordillera in this sector comprises a Palaeozoic arc basement of mainly metasedimentary rocks deposited in a Devonian-Carboniferous forearc basin. The metasedimentary rocks were strongly deformed in a SW-vergent thrust system, prior to emplacement of granitic intrusions of Permian, Triassic and Lower Jurassic age. These large, sheet-like plutonic complexes were emplaced by roof uplift and floor depression, accommodated by dip-slip displacements on steeply-dipping faults. The structural

setting for the emplacement of the Permian and Triassic plutonic complexes is uncertain although Lower Jurassic plutonic complexes were emplaced during arc-normal extension (Grocott and Wilson 1997).

During Upper Jurassic and Early Cretaceous time a 75 km-wide, margin-parallel, arc-batholith was emplaced (Dallmeyer et al. 1996). Basaltic andesite dykes, and N-S elongate dioritic plutons, were intruded at c.154 Ma but the batholith consists largely of granitic rocks. It was constructed in two main phases; between 139 Ma and 125 Ma in the west ("western batholith"), and between 114 Ma and 106 Ma in the east ("eastern batholith"). Plutons were emplaced into N-S trending mylonite belts characterised by dip-slip and sinistral strike-slip displacements (Brown et al. 1993). This may be due to partitioning of sinistral transtension into arc-parallel and arc-normal components during emplacement. However, synplutonic dip-slip shear zones in host rocks may reflect roof uplift, or floor depression, associated with creation of room for the intrusion, and not regional deformation.

Unambiguous evidence for overriding plate extension during emplacement of the western batholith is given by volcanic, volcaniclastic and marine sedimentary rocks, deposited in an Upper Jurassic to Lower Cretaceous back-arc basin, now exposed in the eastern part of the Coastal Cordillera. Here, arc-volcanic rocks (Punta del Cobre Formation), overlain by an arc-volcanic and volcaniclastic sequence (Bandurrias Formation), pass laterally eastward into marine carbonates of the back-arc proper (Chañarcillio Group). Plutons of the eastern batholith were emplaced into volcanic and volcaniclastic sequences at the western margin of the back-arc. Synplutonic mylonite belts associated with emplacement of the eastern batholith were characterised by dip-slip and sinistral strike-slip displacements again consistent with partitioned sinistral transpression (Godoy et al. 1997). During emplacement of the eastern batholith, extension in the back-arc area stepped east leading to basin-and-range style extensional deformation in the Sierra de Fraga (Mpodozis and Allmendinger 1993) and contemporaneous deposition of the continental Cerillos Formation in a successor back-arc basin east of the Chañarcillio Group.

ARC-PARALLEL FAULT SYSTEMS

The Atacama Fault System (AFS) lies along the axis of the Upper Jurassic to Lower Cretaceous arc batholith. It is defined by a system of overstepping sinistral strike-slip faults, which rework belts of synplutonic mylonite associated with the construction of the western batholith. It is also defined by Kiruna-type Fe-Apatite mineralisation and its main activity was synchronous with the emplacement of the intrusions of the western batholith. The Central Valley Fault System (CVFS; Taylor et al. 1998) lies at the eastern margin of the eastern batholith and has similar attributes to the AFS although it has not figured so prominently in the literature (Arévalo and Grocott 1997; Arévalo 1999). Its initial activity was synchronous with emplacement of the eastern batholith but, together with the stratified rocks of the back arc immediately to the east, it was the locus of later, regionally important, sinistral transpression, which characterises the Coastal Cordillera/Precordillera boundary between 27°S and 30°S.

ROTATIONAL DEFORMATION

Vertical axis rotational deformation is often neglected in models of transpression and partitioned transpression. Abundant evidence of vertical axis rotation has been gathered through palaeomagnetic studies of the Andean margin of northern Chile, but rotational deformation has not been well integrated with other elements of the structural geology. In the Coastal Cordillera, at 26°S-30°S, vertical axis, clockwise rotations of 35°-45° are routinely determined for rocks from Early Jurassic to Early Cretaceous age (e.g. Randall et al. 1996 and references therein). Significantly, these rotations are present in rocks from both sides of the AFS and, although we are still assessing data, in younger rocks to the east of the CVFS as well. Hence, these rotations are not caused directly by displacements on the arc-parallel faults.

THE NW-TRENDING FAULT SYSTEM

A system of NW-trending, sinistral strike-slip faults is present throughout the Coastal Cordillera. The largest faults have a spacing of 10-15 km and displacements up to 10 km. Individual NW faults reveal evidence for older displacements, but the most obvious field relationship is that they cut, displace and rotate clockwise segments of the AFS. In contrast, NW faults appear to "sole" into the CVFS. In the Copiapó district, displacements on the NW faults are linked with displacements on the sinistral transpressional fault system that characterise the CVFS (Arévalo 1999). There is also abundant evidence, at outcrop-, map- and 1:2.000.000 landsat image-scale, that clockwise block rotation, and sinistral slip on NW-trending faults, were linked. Linkage between slip on NW faults and sinistral strike-slip and/or transpression on arc-parallel faults strongly implies that these fault systems and the vertical axis rotation are all elements of deformation partitioning in the Coastal Cordillera.

Assuming that the fault blocks were rigid and that blocks rotate "domino-style" by the same amount as the faults, block size and displacements in the Coastal Cordillera are consistent with only 20°-25° of the clockwise rotation observed. However, contractional structures within the fault blocks that are contemporaneous with slip on the NW faults shows that they have deformed internally during rotation. This favours a soft-domino model in which the amount of vertical axis rotation within fault blocks may exceed that dictated by slip and block width in a rigid block model.

RELATION OF NW-TRENDING FAULTS TO THE CVSZ

The Central Valley Fault System is a sinistral transpressional belt characterised by positive flower structures with near-perfect partitioning of the strike-slip component onto steep NNE-SSW trending faults and the dip-slip component on to WNW and ESE vergent thrust systems that root into strike-slip faults (Arévalo and Grocott 1997). NW-trending faults that transect the Coastal Cordillera interact with this system as strike-slip transfer faults. Sharp changes in the structural style of the thrust belts across NW-trending faults provide clear evidence that these fault systems were kinematically linked.

TIMING

The timing of the displacements on the CVFS and the linked displacements and rotations on the NW-trending fault system is constrained by a precise age for the emplacement of the eastern batholith at Copiapó ($^{40}Ar/^{39}Ar$ biotite age of 111 Ma; Arévalo 1999). The dated intrusion both pre-dates brittle strike-slip on the NW trending faults and the sinistral transpression on the CVFS. An upper bracket of 78 Ma is given by the age of shallow intrusive rocks within the sedimentary sequences that post-date the Cerillos Formation (K/Ar whole rock age, Arévalo unpublished data).

CONCLUSIONS

Deformation in the Andean margin in Upper Cretaceous time was partitioned between arc-parallel strike-slip, on margin-parallel faults, and arc-normal shortening, accomplished by vertical axis rotation of large-scale fault blocks. Vertical axis rotation was accommodated by a combination of sinistral strike-slip on NW-trending faults and internal deformation of the fault blocks during rotation. It is likely that this deformation reflects a transition from a retreating subduction boundary in the Early Cretaceous, associated with the emplacement of a magmatic arc during transtension and extension in the back-arc, to an advancing subduction boundary in the Late Cretaceous, in which oblique convergence was strongly partitioned into arc-parallel and arc-normal components in the overriding plate.

REFERENCES

Arévalo, C. 1999. The Coastal Cordillera/Precordillera boundary in the Copiapó area, northern Chile and the structural setting of the Candelaria Cu-Au ore deposit. *Unpublished PhD thesis.* University of Kingston, U.K.

Arévalo, C. & Grocott, J. 1997. The tectonic setting of the Chañarcillio Group and the Bandurrias Formation: a Lower Cretaceous sinistral transpressive belt between the Coastal Cordillera and the Precordillera, Atacama Region, Chile. *VIII Congreso Geologico Chileno, Actas* 3, 1604-1607.

Brown, M., Diáz, F. & Grocott, J. 1993 Displacement history of the Atacama Fault System 25° - 27° S. northern Chile. *Bulletin Geological Society of America* 105, 1165-1174.

Dallmeyer, R.D., Brown, M., Grocott, J., Taylor, G.K. & Treloar, P.J. 1996. Chronology of Mesozoic magmatic and tectonic events within the Andean plate boundary zone of northern Chile. *Journal of Geology* 104, 19-40.

Godoy, E., Lara, L. & Ugalde, H. 1997. La Falla Chivato: borde oriental del plutonismo asociado al sistema de falla Atacama. *VIII Congreso Geológico Chileno Actas* 3, 1604-1607.

Grocott, J. & Wilson, J. 1997. Ascent and emplacement of granitic plutonic complexes in subduction-related extensional environments. In: Holness, M. (ed.) *Deformation-enhanced fluid transport in the Earth's crust and mantle*, 173-195. Chapman and Hall.

Mpodozis, C. and Allmendinger, R.W. 1993. Extensional tectonics, Cretaceous Andes, northern Chile (27°S). *Geological Society of America Bulletin* 105, 1462-1477.

Randall, D.E., Taylor, G.K. & Grocott, J. 1996. Major crustal rotations in the Andean margin: Palaeomagnetic results from the Coastal Cordillera of Northern Chile. *Journal of Geophysical Research* 101, 15,783-15,798.

Taylor, G.K., Grocott, J., Randall, D.E. & Pope, A. (1998). Mesozoic fault systems, deformation and fault block rotation in the Andean forearc 25°-27°S: a crustal-scale strike-slip duplex in the Coastal Cordillera of Northern Chile. *Tectonophysics* 299, 93-106.

STEADY LONG-PERIOD ACTIVITY AT CAYAMBE VOLCANO, ECUADOR. LOCATION, SPECTRAL ANALYSIS AND CONSEQUENCIES.

Bertrand GUILLIER (1,2), Pablo SAMANIEGO (2,3), Mario RUIZ (2), Jean-Luc CHATELAIN (4), Michel MONZIER (1,2), Hugo YEPES (2), Claude ROBIN (3) and Francis BONDOUX (1,2).

(1) IRD, Quito, Ecuador ; BG : bguillier@eolnet.net, MM : michmari@orstom.org.ec, FB : nakamal@ecnet.ec
(2) Escuela Politéchnica Nacional, Quito, Ecuador ; PS : pablosam@hotmail.com
(3) Université Blaise Pascale, Clermont-Ferrand, France ; CR : robin@opgc.univ-bpclermont.fr
(4) Université Joseph Fourier, Grenoble, France ; JLC : Jean-Luc Chatelain@obs.ujf-grenoble.fr

KEY WORDS : Ecuador, Cayambe volcano, LP activity, VT activity, volcanic risk, seismology

INTRODUTION

A continuous monitoring of the Nevado Cayambe Volcano has started in 1988, with the installation of one vertical seismic station included in the Escuela Politecnica Nacional - Instituto Geofísico (EPN-IG) seismic array. Both LP and VT activities do not occur in swarm, but are continuous without period of complete calmness. From November 1997 to March 1998 a network of 3 to 5 stations (1 component, 1 Hz) has been installed to check out this activity. LP events were located in a N120 ellipse form, with a main axis of 8.5 km and a small one of 2.3 km (N30), between an elevation of 1 to 12 km depth beneath the bottom of the volcano. The VT events are mostly located in the northwestern flank of the volcano in column of 2 km diameter and concentrated at a depth from 3 to 9 km. From a total set of 1190 LP earthquakes located during the experiment, about 20% had a low-frequency content (< 2 Hz), 69% had a medium-frequency content (2 to 4 Hz) and 11% had a high-frequency content (4 to 6.5 Hz) (figure 1). Filtering of the mixed-frequency events waveform let suggesting that they are low-frequency events triggered by earthquakes, with a probable unique source.

DATA ACQUISITION AND LOCATION

The locations were performed using the Hypoinverse program (Klein, 1978), modified to run it on Macintosh platform and to automatically improve the earthquakes location, using time delay to take account of the station elevations (figure 2). We did a trial and error method to locate the earthquakes (both LP and VT) with a flat one-layered model computed with a P-wave velocity varying from 0.1 to 5.0 km/s, with a 0.1 km/s step. We have taken this approach because the velocity structure of the Cayambe Volcano is unknown and as the difficulties to use travel-time curves due to the emergent nature of the onset of LP P-waves.

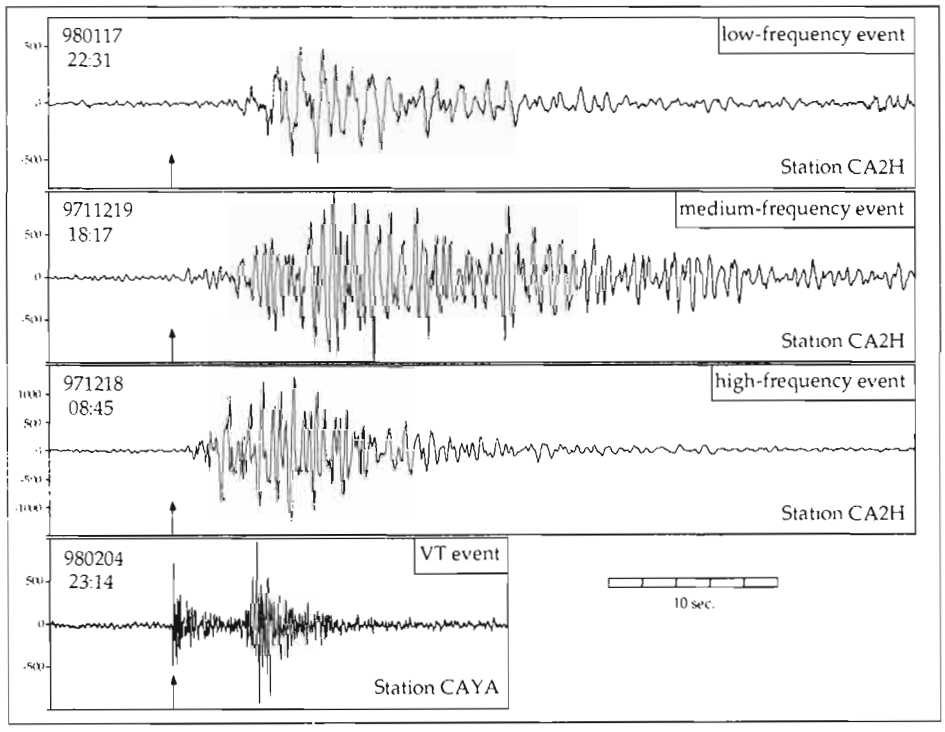

FIGURE 1 : Waveforms for a 4 different typical events on Cayambe Volcano. From the top to the bottom : 3 LP events (low, medium and high-frequency) and VT event.

We assumed that the best locations were found when a minimum was reached on each plots of average ERH, ERZ, RMS and Condition Number versus P-wave velocity. For both LP and VT events, the minimizations were converging for a P-wave velocity of 0.8 km/s. These very low P-waves velocities are in agreement with other observations for LP events (Chouet, 1981 ; McNutt, 1986) and for tremors waves assumed as sustained LP events (Aki, 1984 ; Gordeev et al., 1990). For VT events, the 0.8 km/s velocity is unknown, but if we assumed that the source is the same for LP and VT events, the velocities for both kinds of events have to be the same.

For LPs the criteria found for the selection of events are : (1) number of P+S arrival times • 5, (2) ERH•0.8 km, (3) ERZ•0.6 km, (4) RMS•0.25 sec., (5) Condition Number•25, that gave a final set of 875

LP events. For VTs, the same criteria are : (1) number of P+S arrival time•5, (2) ERH•0.6 km, (3) ERZ•0.7 km, (4) RMS•0.30 sec., (5) Condition Number•17, giving a final set of VT events of 90 from the initial set of 146 events.

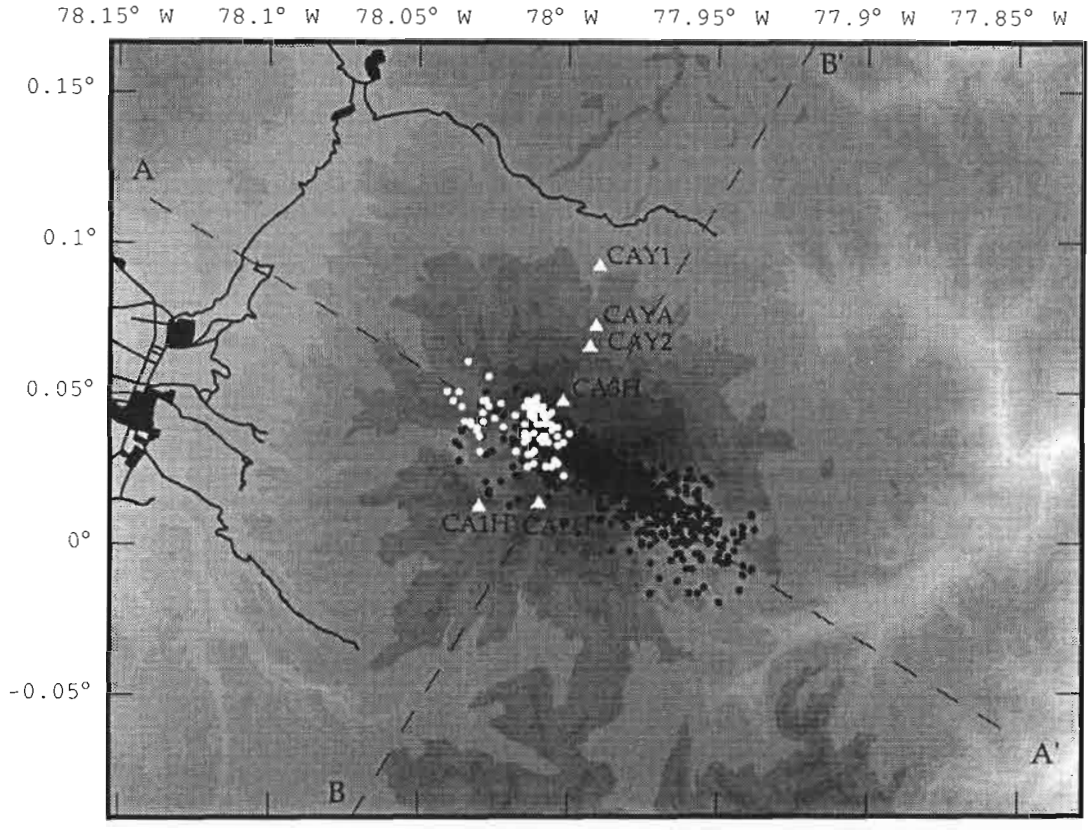

Figure 2 : Map showing the distribution of the selected LP events (closed circles) and VT events (open circles) . The stations used for the present study are shown by white triangle. The telemetred station of the EPN-IG is called CAYA ; CAY1 and CAY2 are portable stations when CA1H-CA2H and CA3H have been telemetred to Quito. A-A' and B-B' are cross-sections shown on figure 3.

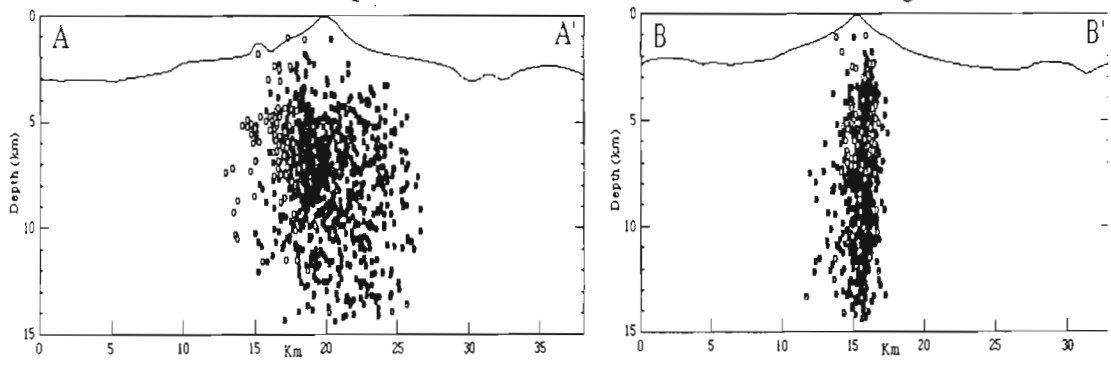

Figure 3 : N120 (A-A') and N30 (B-B') cross-sections of LP (closed circles) and VT (open circles) events selectionned as on figure 4.

CONCLUSION

The actual shallow LP-VT activity on Cayambe volcano is not occurring in swarm like a lot of volcanoes, but is a steady activity like in the Cotopaxi and Tungurahua Volcanoes. LP activity is concentrated in an ellipsoid form, with a major extensional axis (N120) compatible with the geometrical form of the volcano, the migration of the summital domes (migration westernward in a N110 direction) and the structural lineaments observed on the volcano which could be assumed as possible dike intrusions with a N110-120 direction (Samaniego, 1997). For VT events, they are located on the western flank of the volcano, near the last eruptive area of the volcano (youngest dome). For both LPs and VTs, the main concentration in activity is found between 4 and 8 kilometers depth, beneath the Cayambe volcano, compatible with the depth steady activity found in the Cotopaxi Volcano (Ruiz et al., 1998).

The Cayambe LP activity is classified by the spectrum content of the events : 20% of the events are real LP events with a low-frequency content (less than 2Hz), 69% have a medium-frequency content (2 to 4 Hz) and 11% a high-frequency content (4 to 6.5 Hz) giving possible crack size from 20 to 6 meters. The medium and high-frequency events, containing a low-frequency event triggered to a normal earthquake (VT ?) with a common P-wave arrival time and velocity, let suggest a real homogeneity of the source.

Moreover, this steady LP activity can not be assumed as a precursor eruption activity, but a residual one, due to the interaction between magma conduits and water system inducing pressure perturbations causing finally LP events as proposed by Chouet (1996).

REFERENCES

Aki K. 1984. Evidence of magma intrusion during the Mammoth Lakes earthquakes of May 1980 and implications for the absence of volcanic (harmonic) tremor. J. Geophys. Res., 89, 7689-7696.

Chouet B. 1991. Ground motion in the near field of a fluid-driven crack and its interpretation in the study of shallow volcanic tremor. J. Geophys. Res., 86, 5985-6016.

Chouet B. 1996. Long-Period volcano seismicity : Its source and use in eruption forecasting. Nature, 380, 309-316.

Gordeev EI, Saltykov VA, Sinitsin VI, Chebrov VN. 1990. Temporal and spacial characteristics of volcanic tremor wave fields. J. Volcanol. Geotherm. Res., 40, 89-101.

Klein FW. 1978. Hypocenter location progam Hypoinverse, U.S. Geol. Surv. Open File Rep., 78-694.

McNutt SR. 1986. Observations and analysis of B-type earthquakes, explosions and volcanic tremor at Pavlof Volcano, Alaska, Bull. Seism. Soc. Am., 76, 153-175.

Ruiz M, Guillier B, Chatelain JL, Yepes H, Hall ML and Ramon P. 1998. Possible causes for the seismic activity observed in Cotopaxi volcano, Ecuador. Geophys. Res. Lett., 25, 13, 2305-2308.

Samaniego P. 1997. Interactions entre les magmas adakitiques et calco-alcalins : géochimie des complexes volcaniques du Cayambe et du Mojanda-Fuya Fuya (Équateur). D.E.A., Université de Clermont-Ferrand II, 45 pp..

TECTONIC GEOMORPHOLOGY OF THE AMBATO BLOCK

(Northwestern Pampeanas Mountain Ranges, Argentina)

Adolfo Antonio GUTIÉRREZ(1)

(1) Facultad de Ciencias Naturales e Inst. Miguel Lillo. Univ. Nac. de Tucumán. Monteagudo 49. P 3ro. Dpto. B. (4000) San Miguel de Tucumán. Argentina. TE: 0381-4229797.
e-mail: terres@csnat.unt.edu.ar

INTRODUCTION

In the north end of the Pampeanas mountain ranges a group of mountain ranges oriented NNW-SSE es added to the Aconquija system –through the Tucumán Lineament (Mon. 1976)- mostly represented by the mountain ranges of Humaya, Loma Negra, La Carreta, Escaba, Santa Ana, Narváez, Potrerillos, Las Higueras, Los Pinos, Balcozna, Ambato, del Manchao, etc., which will be called –as a whole- the Ambato Block (Fig. 1).

Figure 2 is a detail of the North end of the Ambato Block. In it is summarized the geology of the whole area. In general, the metamorphic basement of the superior Precambrian-inferior Cambrian age is represented by schists and migmatites. The igneous body –of Paleozoic age- corresponds to the Aconquija system. In the intramountain basins, Tertiary sedimentites are preserved which belong to the Aconquija Group, Concepción Subgroup and Salta Group, Santa Bárbara Subgroup (Gutiérrez, et al., 1997). They stand on the peneplain of the basement dipping generally to the Southeast with variable inclinations, discordant with the plains of the regional faults. Over them there are important piedmont fanglomeradic deposits and loesoid slimes from the Quaternary.

González Bonorino (1950), among others, has expressed that the current morphology of the Pampeanas mountain ranges is due to Andean orogenic events. In the Ambato Block, the Andic structures have a marked direction NNW-SSE, opposite the structures located NW of the Tucumán Lineament (Gutiérrez, 1998).

Figure 1, result of the visual interpretation of the Landsat MSS 7 B & N, N° 13381, 1:250.000 image. It schematizes the structural design of the area. Morphologically, the group represents a faulted block by

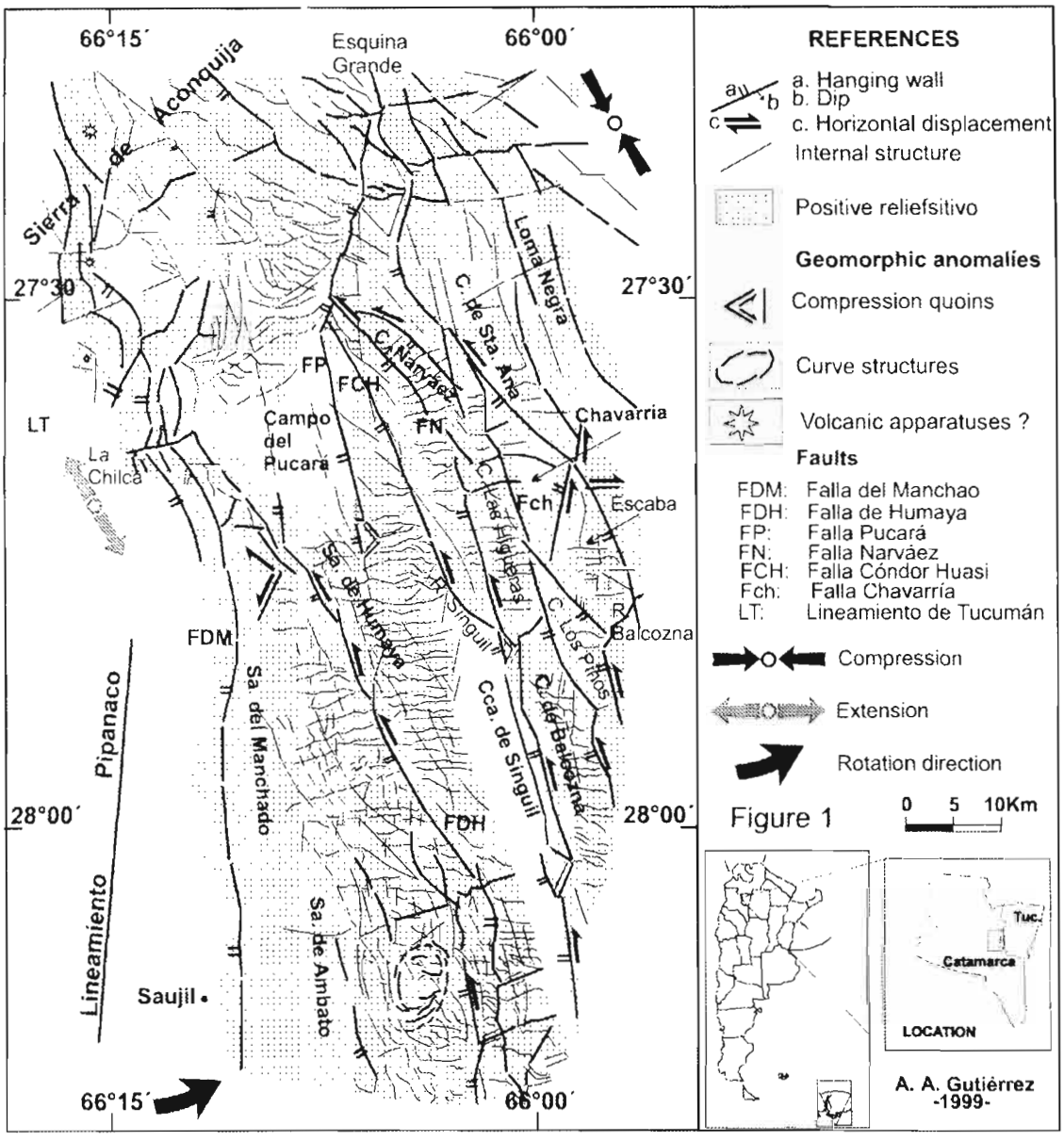

effect of the regional structures oriented NNW-SSE, limiting at the Western side of the mountain ranges. During the last phases of the Andic movement there is a raisin of the Ambato Block accompanied by a sinistral rotation. As a result of that, intramountain basins are originated, because of the breaking up and differential movement of minor blocks through the faults, which have had a double displacement component: vertical and horizontal. The inner structure of the basement –with a preferential ENE-WSW orientation- shows a close relation with a regional structures oriented NNW-SSE and the horizontal movements which have taken place.

The breaking apart and rotation of the block could have produced itself through an imaginary line oriented towards the Northeast, passing by the zone La Chilca and the North end of the Campo del Pucará, right South of the Tucumán Lineament. To the North of this line, the mountain ranges and the

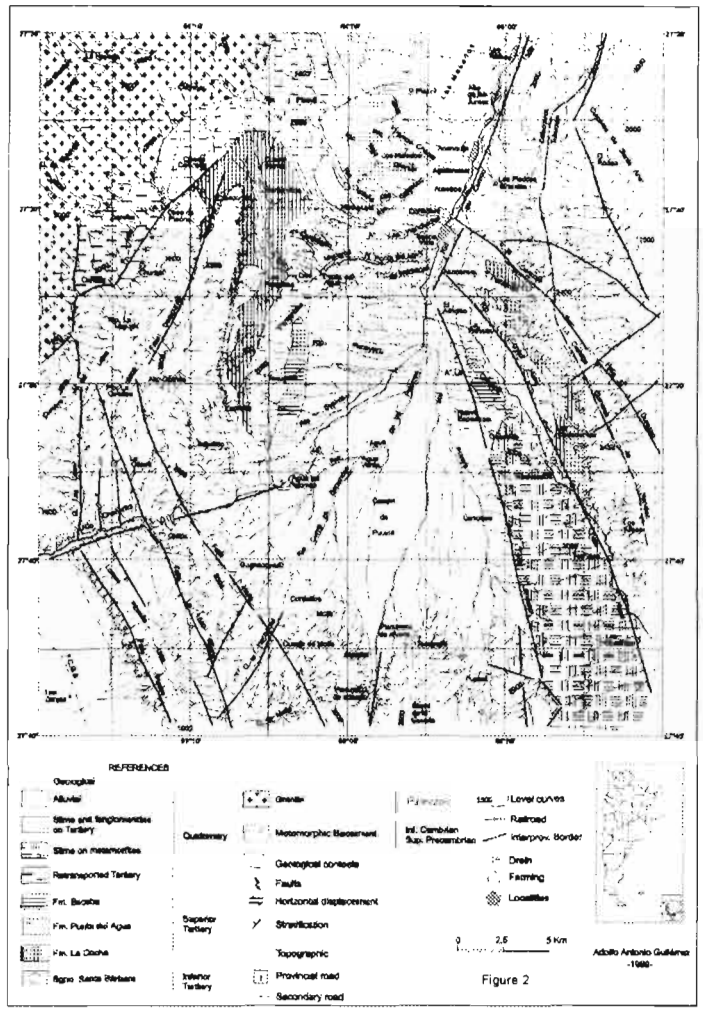

structures preserve their primitive submeridional orientation. The rotation of the block is expressed as a zone of extension in the zone of La Chilca and another of compression in the Northeast end, Esquina Grande. Originally, the Campo del Pucará basin drained towards the Southeast (Figs. 1 & 2). Later on, because of tectonic effects processes of drain capture ocurred, becoming Río del Campo or Pucará in the principal colector of the basin where the West draining rivers converge with a Northeast direction and with a Northwest direction those rivers which drain from the East. At the same time, Río del Campo has been captured by the Río Medina in the zone of Esquina Grande (Fig. 1). This last one drains its waters towards the East, as an affluent of the Río Sali, in the Tucumanian plains. Similar controls are observed in the rivers Sínguil and Balcozna, among others.

CONCLUSIONS

The Ambato Block has had complex movements due to the Andean tectonics. Towards the end of the Tertiary, the general uprising of the block in its Western end, with the peneplain tilting SSE is the result of the NW-SE stresses, generating NE-SW oriented structures.

Later on there is a sinistral rotation of the Ambato Block. The dominant stresses have a WNW-ESE trend. Then, intramountain basins are formed, where Tertiary sedimentites are preserved. Structures have horizontal as well as vertical movement, shifting their orientation towards NW-SE. In this rotation process of the Ambato Block, the differential movement of the minor blocks generates a dynamic draining system with capture effects.

In the Western sides of the mountain ranges there are fanglomerate deposits, as well as fault scarps in the Quaternary deposits, like in the basins of Singuil and Campo del Pucará, which show the current tectonics.

REFERENCES

González Bonorino, F. 1950. Descripción Geológica de la Hoja 13e Villa Alberdi (Tucumán-Catamarca). Dirección Nacional de Geología y Minería. Boletín N° 74. Buenos Aires, Argentina.

Gutiérrez, A. A., M. C. Alderete, P. Bortolotti y J. C. Porto. 1997. Correlación estratigráfica del Campo del Pucará (dist. Aconquija, prov. de Catamarca). VIII Congreso Geológico Chileno. Actas Vol. I, pp. 499-503. Antofagasta.

Gutiérrez, A. A. 1998. Análisis comparativo de estructuras planares y fotolineamientos en la sierra de Narváez (Tucumán-Catamarca). Acta Geológica Lilloana 18(1): 23-29. Tucumán, Argentina.

Mon, R. 1976. La tectónica del borde oriental de los Andes en las provincias de Salta, Tucumán y catamarca, Argentina. RAGA XXXI(2), pp. 65-72. Buenos Aires, Argentina.

FLAT SUBDUCTION BENEATH THE ANDES: SEISMOLOGICAL AND TOMOGRAPHIC CONSTRAINTS

Marc-André Gutscher (1), Wim Spakman (2) and Harmen Bijwaard (2)

(1) Lab. Geophys. et Tectonique, Univ. Montpellier II, F-34095 (e-mail: gutscher@dstu.univ-montp2.fr)
(2) Univ. Utrecht, NL-3584 Utrecht (wims@geo.uu.nl, bijwaard@geo.uu.nl)

KEY WORDS: flat subduction, plateaus, seismicity, tomography, Peru, Chile

INTRODUCTION

While the Peru and Central Chile flat slab segments (Fig. 1) were first discovered ca. 20 years ago (Barazangi and Isacks, 1976; Pilger, 1981; Hasegawa and Sacks, 1981), the debate continues as to the precise causes of flat subduction. Furthermore, it is uncertain if this is a unique "South American" phenomenon related to the Central Andes (Gephardt, 1994) or to unusual eastward directed mantle flow (Russo & Silver, 1996) or a fundamental process occurring worldwide today and widespread in early stages of the earth's history, contributing to the early stages of continental growth (Abbott et al., 1994).

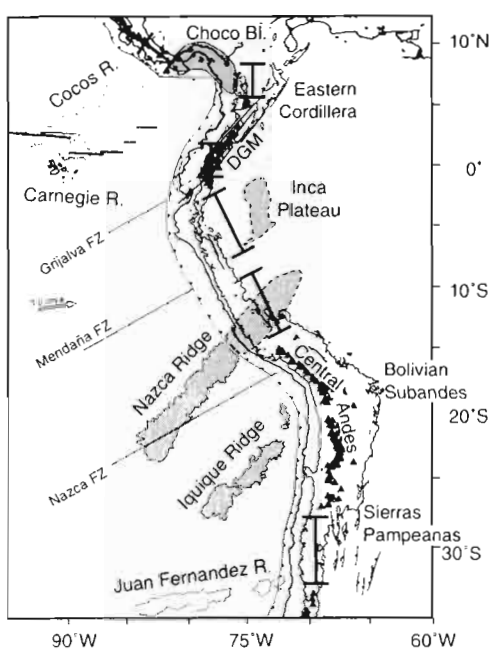

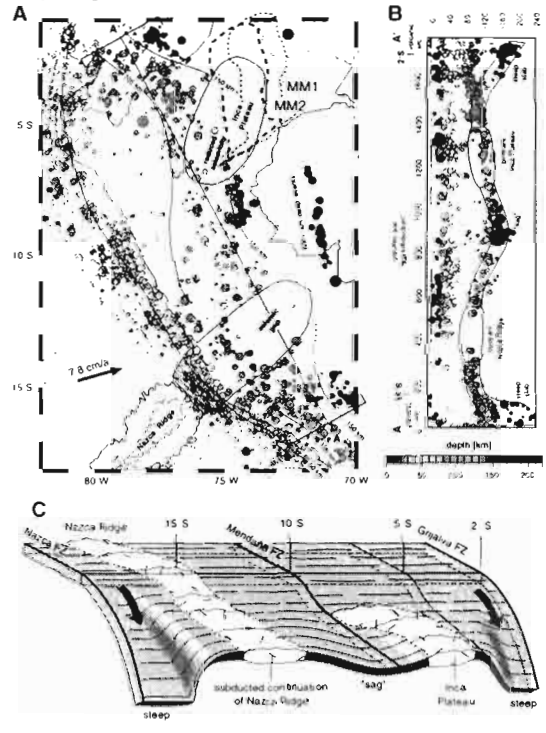

Figure 1 (left): Location map of western S. America showing the Andes (defined by 2000m contour), active volcanoes (triangles), oceanic plateaus (shaded gray) and associated flat slab regions.

Figure 2 (right): A: Peru area seismicity (1964-1995) **B:** Seismological cross-section **C:** Cartoon showing Peru flat slab segment, supported by Nazca Ridge to the south and Inca Plateau to the north.

In Peru and Central Chile, the Nazca Plate initially subducts at an angle of about 30 deg. down to a depth of ca. 100 km, then proceeds nearly horizontally for a distance of over 300 km before bending sharply and descending steeply (Hasegawa and Sacks, 1981; Smalley and Isacks, 1987). While, the subduction of Nazca Ridge correlates with the southern portion of the flat slab segment (Pilger, 1981; McGeary et al., 1985), its vast extent remained unexplained until recently.

PERU SEISMICITY AND FLAT SUBDUCTION

The spatial distribution of seismicity beneath Peru from 1964-1995 is shown in Figure 2a. Data are from a recent global hypocenter relocation effort (Engdahl et al., 1998). A NNW oriented seismological section beneath the Andes (Figure 2b) images the flat lying slab and associated volcanic gap from 2°S to 15°S (Barazangi and Isacks, 1976), flanked by steep slab segments with active arc volcanism on both ends. The intermediate depth seismic gap in the continuation of the subducting Nazca Ridge is a commonly observed effect when an oceanic plateau subducts beneath a convergent margin (McGeary et al., 1985). A lesser gap is situated between 5°S and 9°S (Fig. 2a) and coincides with the predicted position of the Inca Plateau based on kinematic reconstructions (Gutscher et al., subm.). A 20 - 40 km "sag" is located approximately mid way between 2°S and 15°S.indicating that the Nazca Plate is supported by two light bodies with an intervening lithospheric sag (Fig. 2b).

While the Peru and Chile flat slab segments are by far the best documented, there are several others worldwide (see Table 1). Flat subduction commonly inhibits active calc-alkaline volcanism, but adakitic volcanism (fusion of oceanic crust) may occur.

Table 1: Flat slab regions worldwide

Region	Length [km]	Associated Plateau(s) / Block	lithosphere age [Ma]	arc volcanism
Peru (2°S-15°S)	1500	Nazca Ridge, Inca Plateau	45-55	no (adakitic)
Chile (28-33°S)	550	Juan Fernandez Ridge	40-55	no (adakitic)
Ecuador (1°S-2°N)	350	Carnegie Ridge	20-30	adakitic
W. Colombia (6°N-9°N)	350	Choco Block	20-40	no
Costa Rica	350	Cocos Ridge	20-30	no / adakitic
Mexico	300	?	5-10	unusual
SW Japan	600	Izu Bonin Arc, Pal.-Ky. Ridge	15-25	adakitic
Cascadia (46-49°N)	350	Crescent Terrane	10-20	adakitic
E. Gulf of Alaska	500	Yakutat Terrane	45-60	no
(Solomon Islands?	>1000	Ontong Java Plateau?)		

total length 4750 - 6000(?) km which represents ca. 10% of all subduction zones

It has been suggested that the phenomenon of flat subduction is related primarily to the age of the subducting lithosphere and can only occur for young, buoyant lithosphere (Sacks, 1983). Seismological sections along the entire length of the Andes (three are shown in Fig. 3) and Table 1, demonstrate that age alone cannot be the primary controlling factor. Lithosphere as young as 15 - 25 Ma can subduct normally (steeply) and as old as 40 - 60 Ma can exhibit flat subduction.

Calculations of the density of oceanic lithosphere demonstrate that for reasonable crustal, mantle and asthenosphere densities, a 2 km high, 19 km thick oceanic plateau is sufficiently buoyant to support itself and a lateral slab of comparable width for lithospheric ages of 25 - 50 Ma, (those commonly encountered in known flat slab segments). For example a 200 km wide, 19 km thick plateau and 150 km of normal 50

Ma old oceanic lithosphere, taken together have a neutral buoyancy and will likely produce a 350 km wide flat slab segment. This agreess well with observed widths of flat slab segments listed in Table 1.

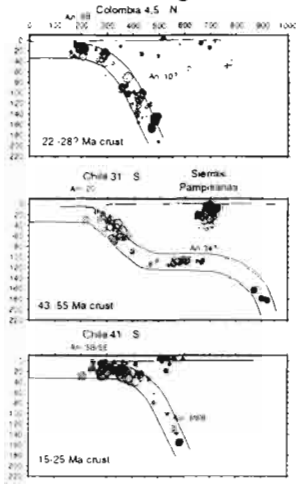

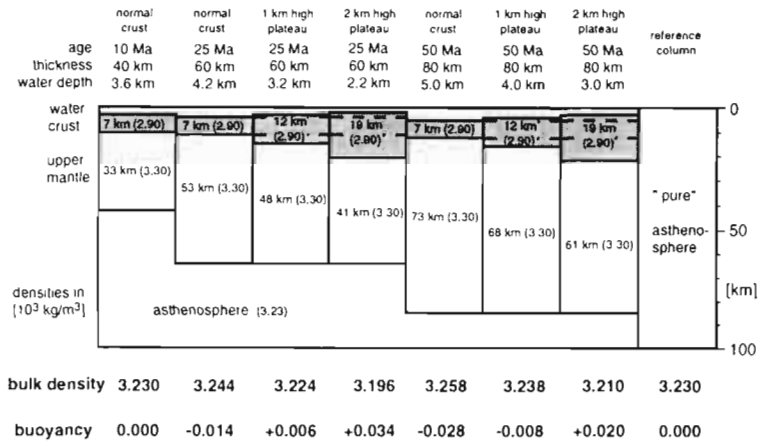

Figure 3 (left): Three E-W seismological sections showing contrasting styles of subduction and corresponding age of oceanic lithosphere. No correlation is apparent.

Figure 4 (right): Buoyancy of oceanic lithosphere as a function of age and crustal thickness.

TOMOGRAPHY AND THERMAL REGIME

A global tomographic velocity model (Bijwaard et al., 1998) was obtained by a travel time inversion of 82000 well constrained earthquakes hypocenters (Engdahl et al.,1998), using 7.6 million p arrivals with absolute residuals less than 7.5 s. The descending oceanic lithosphere can be seen as zones of higher seismic velocities due to the colder, denser material. The section beneath S. Peru / Bolivia (Fig. 5 top), images a typical steep slab segment, descending continuously and curving smoothly towards the 670 km discontinuity. .Near Nazca Ridge (Fig. 5 bottom) the slab proceeds horizontally for ca. 500km, undersliding the South American lithosphere before kinking sharply and descending almost vertically to the 670 km discontinuity.

The thermal and mechanical regimes associated with these two modes of subduction vary greatly. Steep subduction, is typically associated with a region of high heat flow in the back arc, where lithosphere is warmed by the underlying asthenosphere, possibly accentuated by convection in this upper mantly wedge (Fig. 6 top). In stark contrast, flat subduction cools and strengthens the overriding lithosphere (Spencer, 1994), but also shields the downgoing slab from two sided contact with the hot asthenosphere. This cooling delays temperature-dependent mineralogical phase changes, such as the basalt to eclogite transition, which can increase density by as much as 10%. Flat subduction is only possible if this transition is delayed, otherwise the slab will be too dense and collapse and sink under its own weight. This may occur at the landward termination of a flat slab segment, where the slab kinks steeply downwards. In some cases there is even evidence that slab detachment and sinking occurs.

Flat subduction transfers deformation several hundred km inland (into the back arc). This is believed to be the cause of the Sevier-Laramide uplifts in North America (Jordan et al., 1983; Spencer, 1994). This deformation can take 2 forms: block fault uplift - Sierras Pampeanas or transcurrent motion - Ecuador (DGM in Fig. 1) (Gutscher et al., in press).

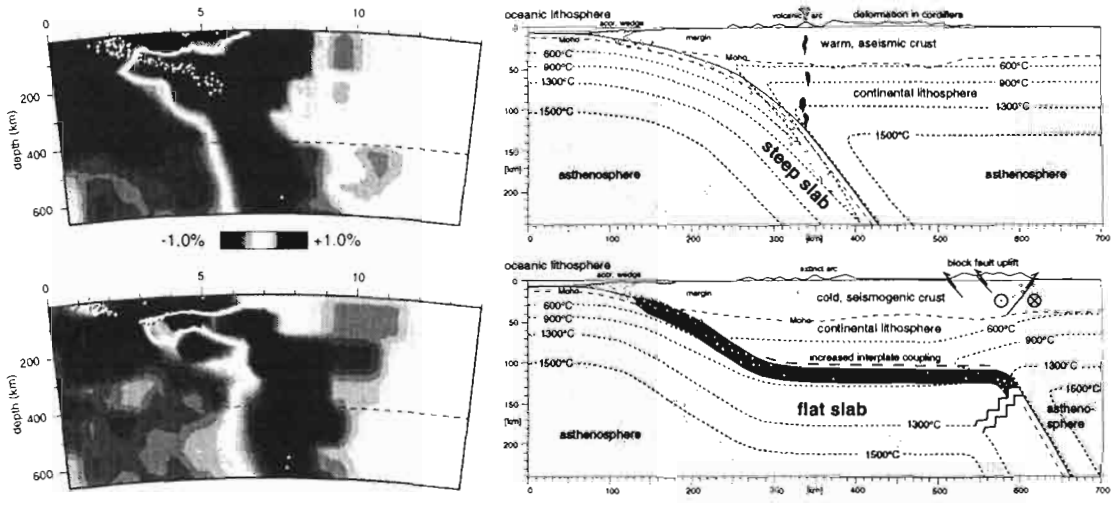

Figure 5 (left): Tomographic sections of steep subduction in S. Peru / Bolivia (top) and flat subduction in S. Central Peru along the Nazca Ridge trace (bottom). Earthquakes are small white circles.

Figure 6 (right): Effect of subduction style on overall thermal regime and upper plate deformation.

References

Abbott, D., Drury, R., Smith, W., 1994. Flat to steep transition in subduction style. Geology, 22, 937-940.

Barazangi, M. and Isacks, B., 1976. Spatial distribution of earthquakes and subduction of the Nazca plate beneath South America. Geology, 4, 686-692.

Bijwaard, H., Spakman, W., Engdahl, E.R., 1998. Closing the gap between regional and global travel time tomography. J. Geophys. Res., 103, 30055-30078.

Engdahl, E.R., van der Hilst, R.D., Buland, R., 1998. Global teleseismic earthquake relocation with improved travel times and procedures for depth relocation, Bull. Seism. Soc. Am., 88 722-743.

Gephardt, J.W., 1994. Topography and subduction geometry in the central Andes: Clues to the mechanics of a noncollisional orogen. J. Geophys. Res., 99, 12279-12288.

Gutscher, M.-A., Malavieille, J., Lallemand, S., and J.-Y. Collot, (in press). Tectonic segmentation of the North Andean Margin: Impact of the Carnegie Ridge collision. Earth Planet. Sci. Lett.

Gutscher, M.-A., Olivet, J.-L., Aslanian, D., Eissen, J.-P. and Maury, R., (subm.). Search for "lost Inca plateau": Flat subduction beneath Peru. (submitted to Science).

Jordan, T., Isacks, B., Allmendinger, R.W., Brewer, J.A., Ramos, V.A., Ando, C.J., 1983. Andean tectonics related to geometry of subducted Nazca plate. Geol. Soc. Am. Bull., 94, 341-361.

McGeary, S., Nur, A., and Ben-Avraham, Z., 1985. Spatial gaps in arc volcanism: The effect of collision or subduction of oceanic plateaus. Tectonophys., 119, 195-221.

Pilger, R.H., 1981. Plate reconstructions, aseismic ridges, and low-angle subduction beneath the Andes. Geol. Soc. Am. Bull., 92, 448-456.

Russo, R.M. and Silver, P.G., 1996. Cordillera formation, mantle dynamics, and the Wilson cycle. Geology, 24; 6, 511-514.

Sacks, I.S., 1983. The subduction of young lithosphere. J. Geophys. Res., 88, 3355-3366.

Smalley, R. and B. Isacks, 1987. A high resolution local network study of the Nazca Plate Wadati-Benioff Zone under Western Argentina. J. Geophys. Res., 92 13903-13912.

Spencer, J.E., 1994. A numerical assessment of slab strength during high- and low-angle subduction and implications for Laramide orogenesis. J. Geophys. Res., 99, 9227-9236.

METALLOGENY AND SEISMOTECTONIC PATTERN IN THE CENTRAL PART OF ANDEAN SOUTH AMERICA

Václav HANUŠ(1), Jiří VANĚK(1) and Aleš ŠPIČÁK(1)

(1)Laboratory of Global Tectonics and Metallogeny, European Centre Prague, c/o Geophysical Institute, Academy of Sciences of the Czech Republic, Boční II/1401, 141 31 Praha 4, Czech Republic (e-mail: als@ig.cas.cz)

KEY WORDS: Seismic pattern of Central Andes, subduction induced metallogeny, metallogeny controlled by seismic zones, cyclicity of subduction and metallogeny

INTRODUCTION

Systematic studies into the geometry of distribution of earthquake foci at convergent plate margins have shown that about one third of earthquakes do not geometrically belong to the Wadati-Benioff zone. It was proved that the earthquakes situated in continental wedges overlying active subduction zones are not distributed randomly being arranged in linear formations forming geometrically well definable seismically active fracture zones (Hanuš and Vaněk, 1977-78, 1987, 1992, 1996). The spatial correlation of the outcrops of these fracture zones with the distribution of large accumulations of metals, facilitated by advanced metalogenic and geochronologic evidence (Mapa Minero, 1966, Sillitoe, 1972, 1981, 1988, 1997, Ulriksen, 1990), made possible to speculate about the structural control of Andean metallogeny by seismically active fracture zones in the regions of Chile and Argentina between 18°S and 34°S.

CORRELATION OF DEPOSITS WITH SEISMICALLY ACTIVE FRACTURE ZONES

The occurrence of polymetallic, copper, gold, silver, tungsten, molybdenum and bismuth deposits and the system of seismically active fracture zones in the area 18°S-34°S and 65°W-71°W are shown in Fig. 1. The names and main parameters of individual fracture zones (azimuth, dip, maximum depth) are as follows: *Z1*- Carachas-Portillo F.Z., 0°, 65° to E, 80km, *Z2a* - Choquelimpie F.Z., 150°, 60° to NE,

100km, *Z2b* - Iquique F.Z., 165°, 45° to NE, 100km, *Z2c* - Domeyko F.Z., 170°, 50° to NE, 120km, *Z4a* - Río Blanco-Los Bayos F.Z., 0°, 85° to E, 100km, *Z6* - Farellones F.Z., 0° , 60° to E, 40km, *Y3* - Aconcagua F.Z., 45°, 50° to NW, 100km, *Y4* - Sierra del Volcán F.Z., 140°, 65° to NE, 70km, *Y5* - El Salvador F.Z., 100°, vertical, 200km, *Y6* - Maricunga F.Z., 100°, vertical, 190km, *Y9* - Jaroma F.Z., 60°, 50° to SE, 100km, *Y10* - Ujina F.Z., 100°, 60° to N, 100km, *Y11* - Tumbaya F.Z., 80°, 70° to NNW, 140km, *Y12* - Incahuasi-León Muerto F.Z., 90°, 65° to S, 100km. It should be noted that the reliability of the geometric parameters of the fracture zones (especially of the dip and depth) is limited by the accuracy of the ISC parameter determinations used in this study; however, it is evident that the fracture zones pass through the whole continental lithosphere.

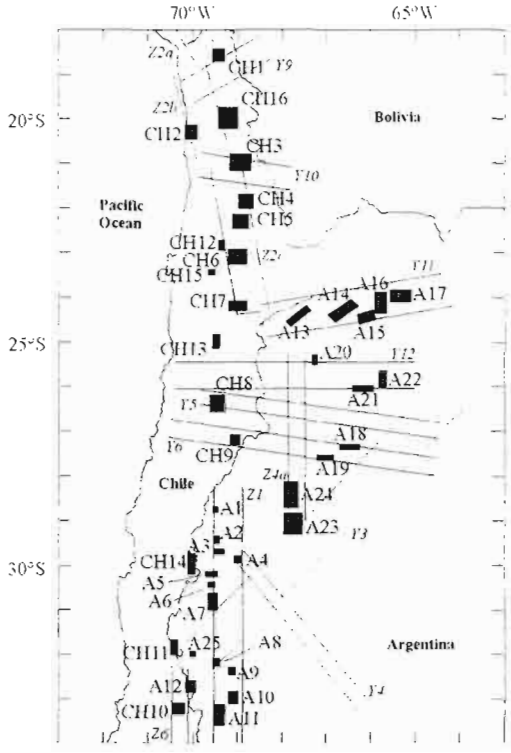

Fig. 1. Distribution of Andean mining districts, denoted by shaded quadrangles, in the framework of seismically active fracture zones (for names of fracture zones and mining districts see text).

The numbered quadrangles represent the following mining districts: CH1 - Belen-Choquelimpie, CH2 - Iquique, CH3 - Ujina, CH4 - San José del Abra, CH5 - Chuquicamata, CH6 - Caracoles, CH7 - La Escondida, CH8 - El Salvador-Potrerillos, CH9- Marte, CH10 - Farellones, CH11 - Los Pelambres, CH12 - Sierra Gorda, CH13 - Guanaco, CH14 - Indio, CH15 - Lomas Bayas, CH16 - Cerro Colorado, A1 - Cordillera de Carachas, A2 - Valle del Cura, A3 - Cordillera Nevada de Colangüil, A4 - Sierra del Volcán, A5 - Cordillera de Conconta, A6 - Cordillera de Olivares, A7 - Río Castano, A8 - Cordillera del Tigre, A9 - Cordillera Cortaderas, A10 - Guido, A11 - Cordón Portillo, A12 - Aconcagua, A13 - Taca-Taca, A14 - San Antonio de los Cobres, A15 - Meseta, A16 - Sierra de Chani, A17 - Tumbaya, A18 - Capillitas, A19 - Belen, A20 - Incahuasi, A21 - Cafayate, A22 - León Muerto, A23 - Los Bayos-El Tigre, A24 - Mogote Río Blanco. The graphical presentation of one of fracture zones - Domeyko F.Z. (Z2c) is shown in Fig. 2. For every fracture zone its trace in the map (a), the vertical section across (b) and along (c) the fracture zone with associated earthquakes are given. In the outcrops of the fracture zones the individual faults recorded in the geologic and tectonic maps are shown with the position of the individual mining districts. The faults observed on the surface roughly follow the azimuth of the respective fracture zone.

DISCUSSION

Figure 1 indicates that the most important mining districts in the Andean segment between 18°S and 34°S are situated in the outcrops of the seismically active fracture zones related to the present subduction of the Nazca plate. However, the distribution of mineral deposits is not strictly uniform in type, mineral contents and age. The majority of mineral deposits of porphyry copper type is situated in the Domeyko F.Z. (Z2c), Río Blanco-Los Bayos F.Z. (Z4a), Farellones F.Z. (Z6), in the east-west trending El Salvador F.Z. (Y5) and Maricunga F.Z. (Y6). Polymetallic deposits occur mainly in the Choquelimpie F.Z. (Z2a), Iquique F.Z. (Z2b) and Incahuasi-León Muerto F.Z. (Y12). Polymetallic vein deposits and Cu veins prevail in the Carachas-Portillo F.Z. (Z1).

The available ages of Tertiary magmatic rocks hosting mineral deposits (Sillitoe 1981, Davidson and Mpodozis 1991) can be arranged into four periods: A: Upper Miocene-Pliocene (13-4 Ma), B: Upper Oligocene-Middle Miocene (23-12 Ma), C: Upper Eocene-Middle Oligocene (44-28 Ma), D: Lower Paleocene-Upper Eocene (64-49 Ma). It appears that individual seismically active fracture zones are characterized by the occurrence of mineral deposits of different age.

The distribution of dated mineral deposits and sketches of metallogenic belts of different ages are plotted in the framework of the seismically active fracture zones between 18°S and 34°S in Fig. 3. It should be noted that this picture depends on the availability and accuracy of age determinations. This distribution of mineral deposits points to a spatial permanency of this system of fracture zones activated by the process of subduction in relation to the western margin of the South American continent since Lower Paleocene. However, small deviations of this system probably occurred during this time due to specific pecularities of individual subduction cycles.

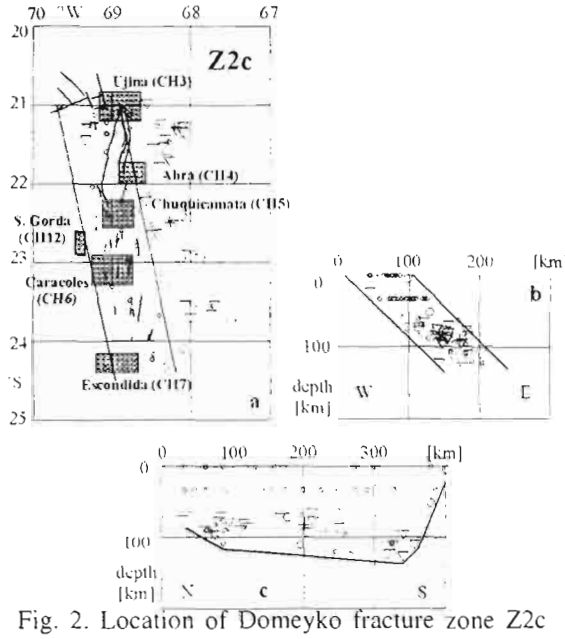

Fig. 2. Location of Domeyko fracture zone Z2c with associated earthquakes (a), transverse section (b) across and longitudinal section (c) along the fracture zone. Faults observed on the surface are denoted by lines in (a) and numbered mining districts by shaded quadrangles (for names of mining districts see text).

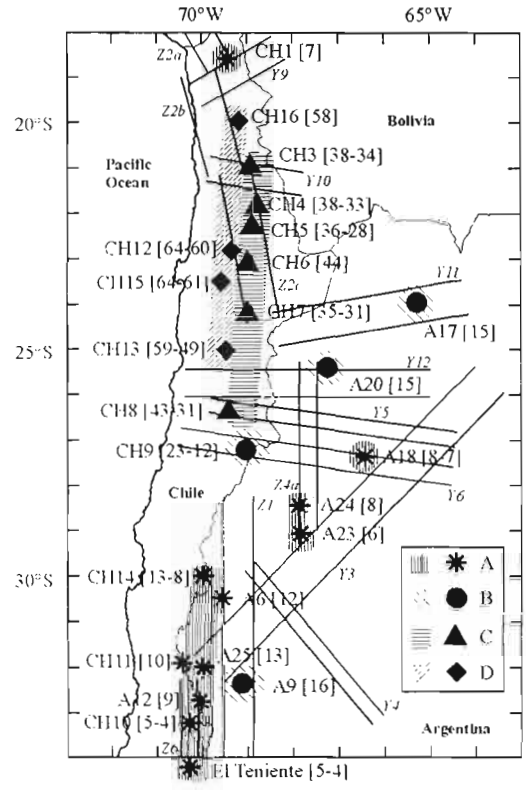

Fig. 3.Distribution of metallogenic belts and mineral deposits of different age in the framework of the seismically active fracture zones. Ages in Ma are given at individual mining districts in brackets. A: Upper Miocene-Pliocene, B: Upper Oligocene-Middle Miocene, C: Upper Eocene-Middle Oligocene, D: Lower Paleocene-Upper Eocene.

The hypothesis that the subduction runs in cycles connected with the formation of a system of successive downgoing slabs shifted several tens of km in or against the direction of the corresponding ocean floor spreading (Hanuš and Vaněk 1991, 1996) seems to have fundamental importance for the formation of large accumulations of metals at convergent plate margins. The continental lithosphere, moving against the direction of the ocean floor spreading, meets subduction zones of different age generated by subsequent cycles of subduction. It appears that the fracturing of the continental lithosphere near the convergent plate boundary, which is manifested by the above described seismically active fracture zones, remains preserved in time, being re-activated under favourable stress conditions by the sequence of subduction cycles of different age.

If we try to apply this hypothesis of cyclic development of subduction to the region of Andean South America between 18°S and 34°S, we come to the following model of the subduction history: The observed shape of the present Wadati-Benioff zone shows that in this region the maximum depth of penetration of the oceanic lithophere beneath the South American continent laterally varies up to 250-300 km (Cahill and Isacks 1992), which corresponds to a length of 600-700 km at the observed dip of the present subduction zone. Considering the rate of 6 cm/year for the subduction of the Nazca plate (Corvalan 1981), the duration of the present subduction would be 10-12 Ma. Because a completed cycle of subduction, given by the maximum depth of earthquakes of 600-650 km, corresponds to a length of about 1000 km for the subduction zone, the duration of one completed subduction cycle would be about 17 Ma at the above subduction rate of 6 cm/year. On the basis of these suppositions, the following model of the history of subduction cycles in the region considered may be constructed: subduction cycle (a): 12-0 Ma, subduction cycle (b): 29-12 Ma, subduction cycle (c): 46-29 Ma, subduction cycle (d): 63-46 Ma.
If we compare the history of subduction (a-d) with the periods (A-D) of endogeneous metallogeny, we see that this very simplified scheme surprisingly well agrees with the cyclic metallogenic development of the region based on radiometric dating. It should be noted that this model of the history of subduction of the Pacific floor beneath the South American plate is burdened by a number of unprovable suppositions as, e.g., length of paleosubduction zones, time of the South Farallon plate brake-up and subduction rates due to Cenozoic plate motions (Minster and Jordan 1978, Gordon and Jurdy 1986).It seems that the active fracture zones, penetrating the whole thickness of the continental lithosphere, effectuate a channeling of the ore-bearing solutions liberated by flow of volatiles from the subducting oceanic lithosphere. The repeated seismic activity seems to assure also the long-term permanent re-opening of the import paths for ore-bearing solutions and thus makes it possible to accumulate enormous amounts of metals in relatively restricted domains of the earth crust.

ACKNOWLEDGEMENTS

The present work has been performed in the framework of IGCP projects 345 "Andean Lithospheric Evolution" and 354 "Economic Superaccumulations of Metals in the Lithosphere". The financial support by the Grant Agency of the Czech Republic under Grant 205/95/0264 and by the Grant Agency of the Academy of Sciences of the Czech Republic under Grant A 3012805 is acknowledged.

REFERENCES

Cahill T. and Isacks B. L. 1992. Seismicity and shape of the subducted Nazca plate. J. Geophys. Res., 97, 17503-17529.

Corvalan J. (ed). 1981. Plate-tectonic map of the circum-Pacific region, southeast quadrant. American Assoc. Petroleum Geologists.

Davidson J. and Mpodozis C. 1991. Regional geological setting of epithermal gold deposits. Econ. Geol., 86, 1174-1186.

Gordon R. G. and Jurdy D. M. 1986. Cenozoic global plate motions. J. Geophys. Res., 91, 12389-12406.

Hanuš V and Vaněk J. 1977-78. Subduction of the Cocos plate and deep fracture zones of Mexico. Geofísica Internacional, 17, 14-53.

Hanuš V. and Vaněk J. 1987. Deep seismically active fracture zones in Ecuador and northern Peru. Studia Geophys. et Geod., 31, 8-25, 156-171.

Hanuš V. and Vaněk J. 1991. Paleoplates buried in the upper mantle and the cyclic character of subduction. J. Geodynamics, 13, 29-45.

Hanuš V. and Vaněk J. 1992. Seismotectonics of continental wedges overlying circum-Pacific subduction zones. Cas. Mineral. Geol., (Prague), 37, 277-287.

Hanuš V. and Vaněk J. 1996. Cyclic evolution of convergent plate margins indicated by time sequence of volcanism and subduction. Global Tectonics and Metallogeny, 5, 103-108.

Hanuš V., Špičák A. and Vaněk J. 1996. Sumatran segment of the Indonesian subduction zone: morphology of the Wadati-Benioff zone and seismotectonic pattern of the continental wedge. J. Southeast Asian Earth Sci., 13, 39-60.

Mapa Minero 1:750 000. 1966. Instituto Nacional de Geología y Minería, Buenos Aires.

Minster J. B. and Jordan T. H. 1978. Present-day plate motions. J. Geophys. Res., 83, 5331-5354.

Sillitoe R. H. 1972. A plate tectonic model for the origin of porphyry copper deposits. Econ. Geol., 67, 184-197.

Sillitoe R.H. 1981. Regional aspects of the Andean porphyry copper belt in Chile and Argentina. Transactions, Institution of Mining and Metallurgy, Section B 90, B15-B36.

Sillitoe R. H. 1988. Epochs of intrusion-related copper mineralization in the Andes. J. South Amer. Earth Sci., 1, 89-107.

Sillitoe R. H. 1997. Characteristics and controls of the largest porphyry copper-gold and epithermal gold deposits in the circum-Pacific region. Australian J. Earth Sci. 44, 373-388.

Ulriksen G. 1990. Mapa Metalogénico de Chile entre los 18°S and 34°S (1:1 000 000). Servicio Nacional de Geología y Minas - Chile, Santiago. Boletín No. 42, 1-112.

SUBDUCTION-RELATED GEOCHEMICAL AFFINITY OF EARLY CRETACEOUS VOLCANISM FROM NORTHERN LA SERENA, CHILE.

Laura B. HERNÁNDEZ(1), Osvaldo M. RABBIA(2) and Alejandro H. DEMICHELIS(3)

(1) (2) Grupo Magmático, Instituto GEA, Universidad de Concepción, Casilla 160-C, Concepción, CHILE. e-mail (1): lahernan@udec.cl; e-mail (2): rabbia@udec.cl
(3) Departamento de Geología, Universidad Nacional de Río Cuarto. Casilla Postal N°9, 5800 Río Cuarto, Córdoba, ARGENTINA. e-mail: ADEMICHELIS@exa.unrc.edu.ar

KEY WORDS: Central Chile, Coastal Range, Early Cretaceous, subduction volcanism, geochemistry.

INTRODUCTION

Early Cretaceous volcanic and sedimentary rocks in central Chile, form two north-south trending parallel belts. One is located in the present-day Coastal Range, and the other in the high Andes. They can be followed for more than 1000 km from Copiapó (27°S) to southern Santiago (34°S). These belts, have been interpreted as part of a synclinorium where thick sequences of volcanic and sedimentary rocks have deposited during the Mesozoic-Tertiary, in a asimetrical fashion. In general, the volcanics predominate in the western limb of this structure, while higher proportion of sedimentary rocks are found in the High Andes. (SERNAGEOMIN, 1982; Åberg et al., 1984; Aguirre, 1985).

An ensialic spreading-subsidence process with the development of an aborted marginal basin during the Lower Cretaceous, have been invoked to explain this regional feature (Levi and Aguirre, 1981; Levi and Nyström, 1982; Åberg et al., 1984). Even when the conclusions of these previous works have been extended to the whole central Chile (27°-34°), most of the information comes from an area near Santiago (ca. 33°S). Available geochemical data on Early Cretaceous volcanics northward to La Serena-Vallenar (28°-30°S) are more scarce and somewhat scattered.

Here we present new geochemical data on volcanic rocks from northern La Serena (600km north from Santiago), a region in north-central Chile that seems to have acted as a distinct paleogeographic and paleotectonic province during the Jurassic-Early Cretaceous (Sillitoe, 1974; Pincheira and Thiele, 1982; and Jensen, 1984).

GEOLOGY OF THE STUDY AREA

The studied area is located in the Coastal Range of north-central Chile (29°15´~29°25´S; 70°45`~71°20`W) 100 km north from La Serena. There, a thick sequence of Lower Cretaceous volcanic and volcaniclastic rocks with minor clastic sediments and marine limestone interbeddings, crops out. This sequence is known as Bandurrias Group (Moscoso et al., 1982). It correlates to the north, with Bandurrias Formation (Segestrom, 1964), and to the south with Arqueros and Quebrada Marquesa Fomations (Aguirre and Egert, 1965). The Bandurria Group rests unconformably on Triassic-Lower Jurassic marine sedimentary rocks. It is intruded by late Lower Cretaceous epizonal granitoids, and is unconformably overlain by subarerial Upper Cretaceous volcanic and sedimentary rocks (Cerrillos Formation). The Lower Cretaceous (Neocomian) age of the Bandurria Group have been determined in the study area by fossil content of the sedimentary rocks associated to the volcanics.

The studied rocks extend from the coast, where the westernmost and stratigraphically lowest part of the volcanic-sedimentary sequence crops out (Moscoso et al., 1982), toward the east, on Los Choros river valley, where the sequence extends up to the upper Cretaceous unconformity. A regional north-south trending fault separates western and eastern areas.

PETROGRAPHY AND GEOCHEMISTRY

Differences in petrography and geochemistry have been observed between the volcanics from the west and the east. In the *east*, all the rocks are porphyritic, some times amigdaloidal, with a phenocryst content up to 50%. Their mineralogy is rather homogeneous, consisting of phenocrysts of plagioclase, clinopyroxene, and Fe-Ti oxides. Locally, olivine and orthopyroxene (?) pseudomorphs can be observed. The intersertal groundmass is composed of microliths of plagioclase, clinopyroxene and Fe-Ti oxides. These rocks belong to the high-K calc-alkaline series, ranging in composition from basaltic andesites to dacites. The later, are ignimbritic flows located to the top of the sequence. Most of the basaltic andesites have high Al_2O_3 (> 17.4%), and low MgO (<5%), Cr (<60ppm) and Ni (< 60ppm). They show high LILE/HFSE (fig.1), high (La/Yb)n (3.9~8.4) and Eu/Eu*: 0.69-0.76. The dacitic ignimbrites show similar (La/Yb)n (4.5~4.6) but higher Eu/Eu* (0.47-0.50) as expected for more differenciated rocks. All rocks have Zr/Y >3.

In the *west*, the volcanic rocks are in general more basic than in the east. Their composition is restricted to the range basalt-andesite. The basalts here, are medium-K calc-alkaline high alumnina basalts. They are highly porphyritic, with fresh strongly zoned plagioclase and clinopyroxene phenocrysts. They also present olivine pseudomorphs and a ferromagnesian mineral highly altered to actinolite (?). Texturally, these rocks look more like subvolcanic intrusions than true lava flows. Al_2O_3 contents varies from 18.2~19.3%; MgO: <6.5%, Cr: variable from

43 to 146 ppm, and Ni: < 57 ppm. Their REE patterns show (La/Yb)n ranges from 3.2-3.7, and show almost no Eu anomaly (Eu/Eu*: 0.90-0.95). The basaltic andesites are medium-K calc-alkaline amphibole-bearing porphyritic volcanics with distinctive large amphibole phenocrysts (up to 5 cm). They also show high Al_2O_3 content (19.2%) and high Na_2O (4.2%). Their REE patterns show low (La/Yb)n (2.0) and Eu/Eu*: 0.96. The andesites, are highly porphyritic high-K calc-alkaline amphibole-bearing rocks. Their (La/Yb)n ranges from 6.4 to 6.7, and the Eu/Eu*: 0.57~0.62. In general, all these rocks present LILE/HFSE lower than those from the east (see fig.1); and Zr/Y >3.

The complicated outcrop pattern of the western volcanics, coupled with the lack of geochronological data, preclude yet the completly understanding of the relationships between all them. The ongoing research is being conducted to solve this problem.

DISCUSION AND CONCLUDING REMARKS

All the Lower Cretaceous volcanic rocks in central Chile are affected by low-grade metamorphism (Levi et al., 1989); then, it could be argued that the geochemical composition of the rocks consider here, have been changed. However, the extent in which this kind of non-deformative metamorphism can modify the original geochemistry is variable, controled in large extent by the permeability of the rock (Aguirre, 1988). In general, the samples selected for this study contain no visible veinlets or amigdules, and are incipient to faintly altered (e.g.: replacement of olivine, incipient alteration of plagioclase and a partial alteration of the groundmass minerals). The 80% of the studied rocks have LOI <2% and the remain 20% <3%. Therefore, besides being hydrated, the samples are probably relatively unmodified chemically, at least the basic volcanics. Furthermore, when comparison between "unaltered" and some more altered samples have been done for testing element mobilities, REE patterns remain almost unchanged. In the case of the MORB-normalized trace element patterns, changes are observed mainly in the LILE, although the general shape of the patterns mimics those of the "unaltered" samples.

The geochemistry of the studied volcanic rocks indicate that they originated in an arc environment. MORB-normalized trace element patterns for eastern and western volcanics (fig. 1) clearly show for both, the same distinctive spiked pattern with peaks in LILE (K, Rb, Ba, Th and in less extent Sr) and Ce, P and Sm; and trough in Ta-Nb, (Zr) and Ti.

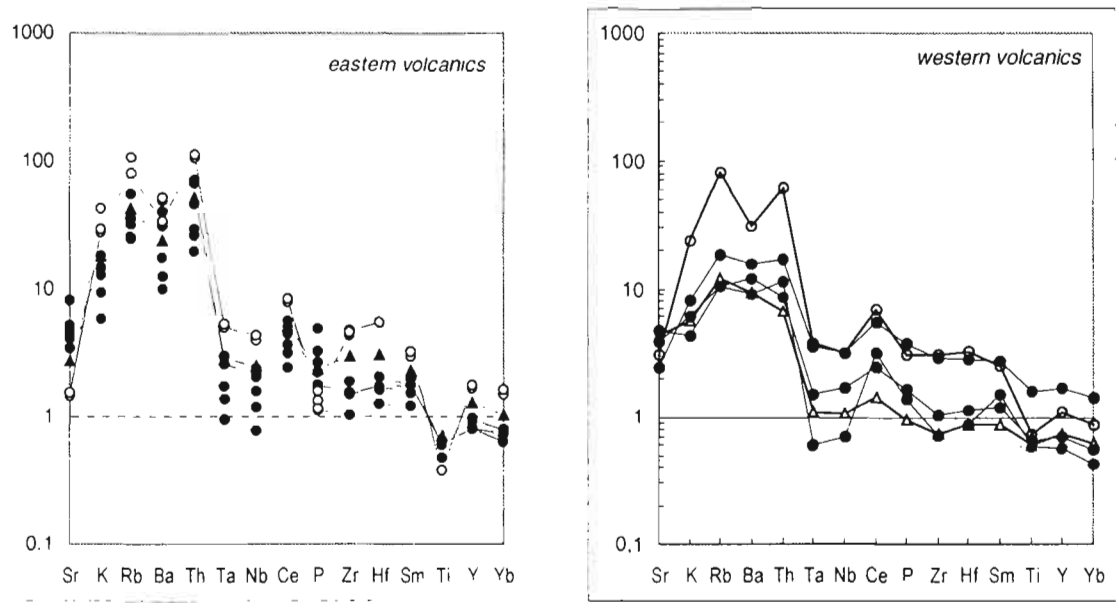

Fig. 1: MORB-normalized trace element patterns (normalizing values after Pearce (1983)) for representative eastern and western Lower Cretaceous volcanic rocks. *Eastern volcanics*: High-K calc-alkaline series: basaltic andesites (filled circles); andesites (filled triangle); dacitic ignimbrites (open circles). *Western volcanics*: medium-K calc-alkaline series: basalts (filled circles); basaltic andesite (open triangles); high-K calc-alkaline andesites (open circles).

They also show slightly higher concentrations of Ta and Nb relative to Zr and Hf, and of Zr and Hf related to Y and Yb, in the less differenciated rocks (this feature is enhanced with SiO_2 enrichment). The former features are considered to be characteristics of all subduction-related magmas, attesting to the involvement of subduction-zone fluids in Sr, K, Rb, Ba and Th in their petrogenesis; while the abundance relationship between Ta-Nb, Zr-Hf an Y-Yb have been attributed to the participation of the subcontinental lithosphere in the generation of the magmas (Pearce, 1983). Based on this diagrams, the subduction-zone component appears to be dominant the studied samples. The same conclusion can be drawn from Th/Yb and Ta/Yb bivariate incompatible elements diagrams (not shown). Here the samples develop two parallel trends. They plot mainly on the calc-alkaline field, above the depleted mantle-enriched mantle source array. In these trends, eastern and basic western rocks plot separately, being the later less enriched in Th respective to the former.

When Zr/Y vs Zr plot is considered, all samples having Zr/Y >3, plot on the continental arc field (Pearce, 1983), indicating the role of the subcontinental lithosphere. Here all the samples form one trend where the less evolved character of the western volcanics (they plot near the boundary between oceanic-continental arc fields) is again apparent. Arc affinity is also shown by all the rocks from basalt to dacites that plot well inside the field of volcanic-arc basalt inthe Th-Hf-Ta diagram (Wood, 1980).

Regarding to geochemical evolution with time, it can be said that, if the western rocks are effectively older than the eastern ones, and if all of them are Lower Cretaceous in age (Moscoso et al., 1982), the data should be suggesting that the rocks became more evolved with time to the east.

Finally, similar geochemical characteristics for rocks of the same age have been determined by Vergara et al. (1995) at the latitute of Santiago. Nevertheless, the geochemical variations in time of the volcanic rocks reflecting crustal attenuation as proposed by these authors, have not been tested yet in the study area, because chemical analyses from volcanics older and younger than Lower Cretaceous, were not done.

Further studies, should be done to clarifiy geochemical variations in time in north-central Chile.

ACKNOWLEDGEMENTS

This work was supported by the grant FONDECYT-CHILE N°1970875.

REFERENCES

Aguirre, L. 1985. The Southern Andes, In: Nair, A.E.;, Stehli, F.G. and Uyeda, S. eds., The ocean basins and margins, Volume 7A. The Pacific Ocean: New York, Plenum Press, 265-376.

Aguirre, L. 1988. Chemical mobility during low-grade metamorphism of a Jurassic lava flow: Río Grande Formation, Peru. Journal of South American Earth Sciences 1, 343-361.

Aguirre, L. and Egert, E. 1965. Cuadrángulo Quebrada Marquesa, Provincia de Coquimbo. Instituto de Investigaciones Geológicas, Carta Geológica. Chile N° 15, 92pp.

Åberg, G., Aguirre, L., Levi, B. and Nyström, J.O., 1984. Spreading-subsidence and generation of ensialic marginal basins: An example from the early Cretaceous of central Chile, *in* Kokelaar, B.P. and Howells, M.F., eds. Volcanic and associated sedimentary and tectonic processes in modern and ancient marginal basins: Geological Society of London Special Publication 16, 185-193.

Jensen, O.L. 1984. Andean tectonics related to geometry of subducted Nazca plate. Bulletin of the Geological Society of America, 95, 877-879.

Levi, B. and Nyström, J.O., 1982. Spreading-subsidence and subduction in central Chile: a preliminary geochemical test in Mesozoic-Paleogene volcanic rocks. III Congreso Geológico Chileno, 1, B28-B-36.

Levi B. and Aguirre, L. 1981. Ensialic spreading-subsidence in the Mesozoic and Palaeogene Andes of central Chile. Journal of the Geological Society of London, 138: 75-81.

Levi, B., Aguirre, L., Nyström, J.O., Padilla, H., and Vergara, M. 1989. Low-grade regional metamorphism in the Mesozoic-Cenozoic volcanic sequences of the central Andes: Journal of Metamorphic Geology, 7, 487-495.

Moscoso, R., Nasi, C., 1982. Hoja Vallenar y parte norte de La Serena, Regiones de Atacama y Coquimbo. Carta Geológica de Chile N°55, Escala 1:250.000. Servicio Nacional de Geología y Minería.

Pearce, J.A. 1983. The rol of the sub-continental lithosphere in magma genesis at destructive plate margins. In: Continental basalts and mantle xenoliths. C.J.Hawkesworth & M.J.Norry (eds.), 230-249. Nantwich: Shiva.

Pincheira, M., and Thiele, R., 1982. El Neocomiano de la Cordillera de la Costa al NW de Vallenar (28°15´ a 28°30´S): situación tectónica del borde occidental de la cuenca marina neocomiana tras-arco. III Congreso Geológico Chileno, Concepción, 1, A236-A261.

Segestrom, , K. 1968. Geología de las Hojas de Copiapó y Ojos del Salado, Provincia de Atacama. Instituto de Investigaciones Geológicas, Boletín N°24, 58p.

SERNAGEOMIN, 1982. Mapa Geológico de Chile: Santiago, Chile.Servicio Nacional de Geología y Minería, scale:1:1.000.000.

Sillitoe, R.H. 1974. Tectonic segmentation of the Andes: Implications for magmatism and metallogeny. Nature, 250, 542-545.

Vergara, M., 1972. Note on the paleovolcanism in the Andean Geosyncline from the central part of Chile: Proceedings, 24th International Geological Congress, Canada, 2, 222-230.

Vergara, M., Levi, B., Nyström, J.O. and Cancino, A. 1995. Jurassic and Early Cretaceous island arc volcanism, extension, and subsidence in the Coast Range of central Chile. Geological Society of America Bulletin, 107, 1427-1440.

Wood, D.A. 1980. The application of a Th-Hf-Ta diagram to problems of tectonomagmatic classification and to stablishing the nature of the crustal contamination of basaltic lavas of the British Tertiary Volcanic Province. Earth and Planetary Science Letters, 50, 11-30.

LATE PERMIAN SHRIMP U-Pb DETRITAL ZIRCON AGES CONSTRAIN THE AGE OF ACCRETION OF OCEANIC BASALTS TO THE GONDWANA MARGIN AT THE MADRE DE DIOS ARCHIPELAGO, SOUTHERN CHILE.

Francisco HERVE (1), Mark FANNING (2), John BRADSHAW (3), Margaret BRADSHAW (3) & Juan P. LACASSIE (1)

(1) Departamento de Geologia , Universidad de Chile , Casilla 13518, Correo 21, Santiago, Chile (fherve@cec.uchile.cl)

(2) PRISE, Australian National University, Canberra , Australia (Prise.Fanning@anu.edu.au)

(3) University of Canterbury, Christchurch, New Zealand (geology@csc.canterbury.ac.nz)

KEYWORDS: Late Paleozoic, southern Chile, accretion, detrital zircon ages, geochemistry

INTRODUCTION

The stratigraphy and structure of the Madre de Dios archipelago (49° to 52° S. Lat.), was studied by Forsythe and Mpodozis (1983) who distinguished: a) The Denaro Complex (DC) of metabasalt and chert , b) The Tarlton Limestone and c) The Duque de York Complex (DYC),of graywacke, siltstone, shale and conglomerate. These units are intruded by the South Patagonian Batholith (SPB).

The coeval late Carboniferous - earliest Permian Tarlton Limestone (Douglass & Nestell, 1976) and Denaro Complex, were deposited, after Ling et al, (1985), in a mid-ocean ridge environment and accreted to the Gondwana margin as alloctonous and exotic terranes before the Early Cretaceous intrusion of the SPB. In this context, the Duke of York complex was considered by Forsythe and Mpodozis (1983) as a continent derived detrital sequence unconformably deposited over the other stratified units, as they came to a position near to the continent. The three units were tectonically interleaved into the forearc of the South America plate during subduction processes.

The Denaro Complex is composed of metabasalts, often with pillow structures, and chert. The geochemistry of 10 samples of metabasalts of the Denaro complex indicates an E-MORB affinity,

broadly consistent with the tectonic setting suggested above. They have well preserved igneous textures, relic igneous clinopyroxene phenocrysts and microcrysts, completely albitized plagioclase, and a metamorphic overprint which includes chlorite, epidote, amphibole, pumpellyite, white mica , stilpnomelane and calcite. This suggests a low T, probably low P static metamorphism, which might have taken place in the mid ocean ridge where they were erupted.

The age of deposition of the. Duke of York complex is stratigraphically bracketed in time between the Early Permian age of the Tarlton limestones and the Early Cretaceous intrusion of the SPB. A paleokarstic surface, tectonically inverted , separates unconformably the DYC from the Tarlton Limestone at Seno Soplador. This erosional surface must have developed at or near sea level, or by dissolution at the CCD.

New detrital zircon SHRIMP U-Pb age determinations in two metasandstones of the DYC reveal a prominent late Early Permian population (ca. 270 Ma) of zircons of igneous derivation , together with late Proterozoic to early Paleozoic components.

CONCLUSIONS

This big peak of late Permian zircons can probably be interpreted as the first flush of detritus from a new igneous complex being developed in the continental margin, which might correspond to the widespread Permian Choyoi magmatic event in southwestern South America,. This interpretation implies that the oceanic assemblages were covered by the continent derived sediments of the Duke of York Complex , presumably near to the continental margin , already in the late-Permian.

ACKNOWLEDGEMENTS

Field an laboratory work was supported by Cátedra Presidencial en Ciencias and Fondecyt Grant 1980741 to FH. V. Ramos. A. Rapalini, D.Prior and G. López participated in the field work.

REFERENCES

Douglass, R.C. and Nestell, M.K. (1976) Late Paleozoic foraminifera from southern Chile.U.S. Geol.Surv. Special Paper, N 858, 49 p..

Forsythe, R. and Mpodozis, C. (1983) Geología del basamento pre-Jurásico Superior en el archipiélago Madre de Dios, Magallanes, Chile. Servicio Nacional de Geología y Mineria, Boletin N 39, 63 p., Santiago, Chile.

Ling, H.Y., Forsythe, R.D.,and Douglass, C.R.(1987) Late Paleozoic microfaunas from southernmost Chile and their relation to Gondwanaland forearc development. Geology, 13, 357 - 360.

OBLIQUE THRUSTING, STRIKE SLIP FAULTING AND STRAIN PARTITIONING IN THE BOOMERANG HILLS AREA, ANDEAN FOOTHILLS OF BOLIVIA.

Ralph HINSCH (1), Christoph GAEDICKE (1), Charlotte KRAWCZYK (1),
Gustavo REBAY (2), Raul GIRAUDO (2) and Daniel DemuRo (2)

(1) GeoForschungsZentrum Potsdam, Telegrafenberg, 14473 Potsdam, Germany; hinsch@gfz-potsdam.de;
(2) ANDINA S.A., Santa Cruz, Bolivia

KEY WORDS: Central Andes, Bolivia, Subandean, deformation front, strain partitioning

INTRODUCTION

The evolution of the Boomerang Hills is a key for understanding the style of deformation of the Subandean Ranges in the eastern area of the Bend in the Central Andes at 17°S. They form the topographic expression at the tip of the youngest thrust-sheet extending into the eastern foreland of the Andes. Because of its hydrocarbon potential, the area is densely covered by reflection-seismic profiles allowing the detailed investigation of the Andean deformation front in the subsurface. Preceeding publications already presented considerations for the evolution of frontal structures in the Subandean Belt in the region of the Bolivian Orocline (Baby et al. 1994, Welsink et al. 1995), but disregarded observable strike-slip faults. This work presents the first results of the interpretation of existing strike-slip faults, and discusses their role during the formation of this area.

REGIONAL SETTING

The recent deformation front of the Central Andes in the bend region at 17°S coincides with the northern limits of the Chaco Basin (Fig. 1). A Paleozoic wedge of siliziclastic sediment onlaps the submerged Brazilian Shield to the north. This sequence is topped above an angular unconformity by Cretaceaous sandstone and a Tertiary foreland basin succession. Both, onlapping and angular unconformities lead to rapid northward thinning of the Paleozoic wedge. The principal detachment horizon generally follows the

base of this wedge, which is mainly build up by dark shale of Silurian age. Further to the north, Cretaceous sandstone directly cover the Brazilian Shield, and no fundamental detachment is evolved.

The Subandean fold-and-thrust belt and the adjacent Foothills are the result of the youngest Andean deformation, which started in Oligocene (Sempere at al. 1990) and is still going on. The structural trend in the Boomerang Hills area is almost E-W and therefore oblique to the main shortening direction in the Subandean Zone, which is approximately NE-SW. This structural trend is defined by the south-dipping Brazilian Shield, which provides an oblique ramp for thrusting of the onlapping sedimentary wedge (Baby et al 1994). In the Boomerang Hills area, the young contractional deformation is characterized mainly by gentle folds formed above steps in the pre-shaped basement, and folds related to the tip of the detachment as well as reverse-faults (Welsink et al. 1995).

The interpretation of reprocessed seismic lines indicates the occurrence of a variety of sub-vertical faults. Like the reverse faults, these seem to branch off the detachment horizon, and are interpreted as second order strike-slip faults.

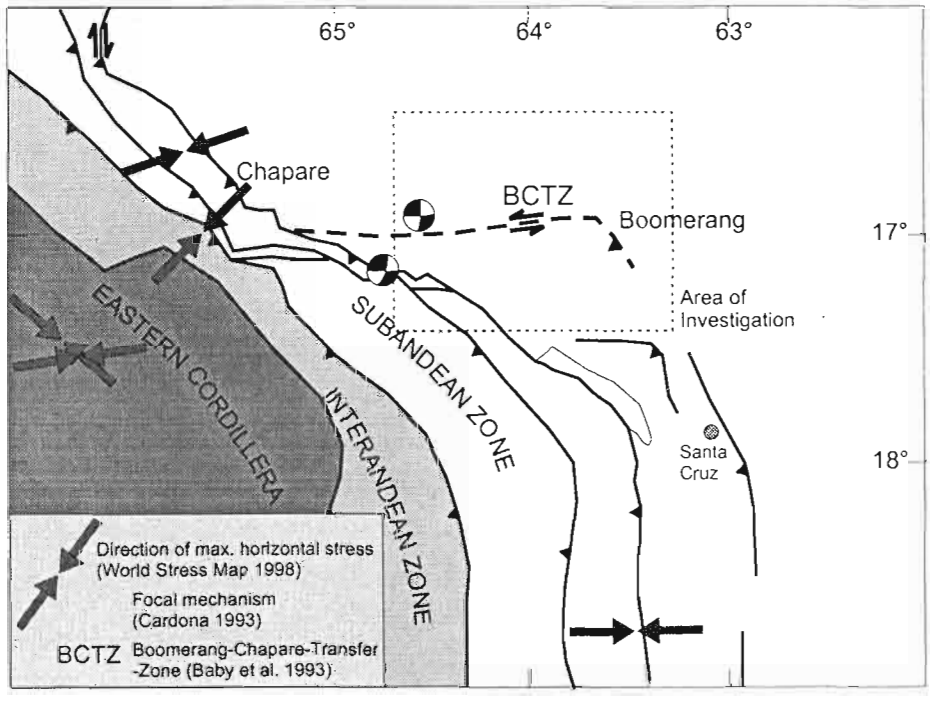

Fig. 1 Sketch-map of the bend region of the eastern Central Andes

RESULTS AND DISCUSSION

In order to receive additional information about the character of the strike-slip faults, the individual fault traces were analysed, correlated, and used to construct the 3D geometry of the fault surfaces. A preliminary map of correlated structures is displayed in Fig. 2.

On the basis of the observations a preliminary model for the evolution of Andean structures has been developed. This model explains the variety of structures as a result of oblique thrusting and pre-existing geometries forcing strain partitioning.

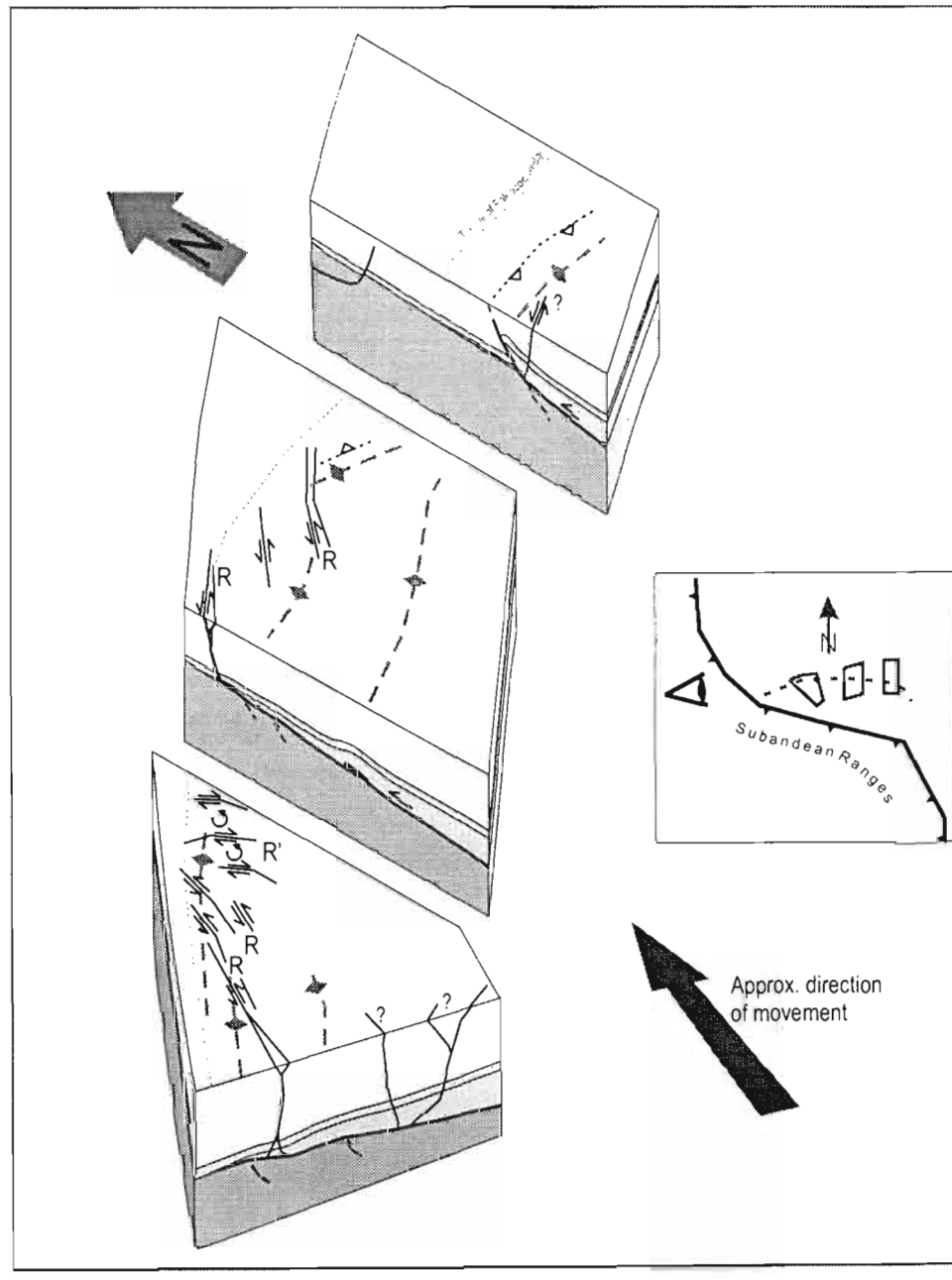

Fig. 2 Schematic correlation of observed structures. View from the west. R = Riedel shear faults, R' = anti-Riedel shear faults.

The regional direction of shortening is considered to be SW-NE to SSW-NNE. While thrusting of the sedimentary wedge is assumed to be roughly in the same direction, deformation at the limits of the thrust sheet is accommodated by a set of structures, indicating strain partitioning. Folds and reverse faults as well as strike-slip faults balance parts of the total movement of the thrust-sheet. This implies that all structures are connected with the detachment horizon below.

Two main domains can be distinguished:

1. Compressional structures dominate in the east. The detachment does not reach the tip-line of the Paleozoic wedge, and the deformation front trends E-W, paralleling the dipping basement.

2. In the western part of the area, the detachment front roughly coincides with the northern limit of the Paleozoic wedge, striking WSW-ENE.

Detaching of the Paleozoic wedge occurs until its very limits, suggesting that basal thrusting is limited by the distribution of Paleozoic shale. Hence the tip of the Paleozoic sediments roughly controls the Andean deformation front.

A remarkable feature in this area is the dominance of fold-axes parallel to the contours of the dipping basement, which are usually in an orientation vertical to the movement direction.

The interpretation that folds in this area are the result of steps in the basement (Welsink et al. 1995) may account for most of the structures. At the tip of the detachment, these folds have to accommodate compressional deformation. Because the tip of the detachment is constrained by the northern limit of the Paleozoic wedge, the fold axes have to develop in the same direction.

As a consequence of the WSW-ENE striking deformation front, the SW-NE orientated basal thrusting is accommodated predominantly by strike-slip faults, represented by the interpreted system of Riedel-shear faults. Especially for this region this purely thin-skinned model is only a preliminary adaptation, as some of the faults might be related to weak zones in the basement reactivated during Subandean thrusting.

CONCLUSION

In the investigated Boomerang Hills area, the front of Andean deformation reaches the northern limits of the Chaco Basin. The diversity of structures formed by the Andean deformation might be explained by oblique thrusting and a partitioning of strain forced by both, the geometry of the thrusted wedge as well as the pre-existing topography of the basement.

Minor strike-slip faults balance the oblique component of deformation which is not accommodated by the compressional structures.

Thin-skinned thrusting is limited by the distribution of incompetent strata. Ongoing deformation might result in a thick-skinned overprint. A thin-skinned to thick-skinned transition might be visible in the southwestern part of the investigated area, which will be investigated in the next future.

REFERENCES

Baby, P., Specht, M., Oller, J., Montemurro, G., Colleta, B., and Letouzey, J., 1994. The Boomerang-Chapare transfer zone (recent oil discovery trend in Bolivia): Structural interpretation and experimental approach, *in* Roure, F., Shein, V. S., and Skvortsov, I., eds., Geodynamic evolution of sedimentary basins: International Symposium, Moscow 1994, p. 203-218.

Baby, P., Guillier, B., Oller, J., and Montemurro, G., 1993. Modele cinematique de la Zone Subandine du Coude de Santa Cruz (entre 16°S et 19°S, Bolivie) deduit de la construction de cartes equilibrees.: Comptes Rendus de l'Academie des Sciences Paris, Serie II, v. 317, no. 11, p. 1477-1483.

Sempere, T., Herail, G., Oller, J., and Bonhomme, M. G., 1990. Late Oligocene-Early Miocene major tectonic crisis and related basins in Bolivia: Geology, v. 18, p. 946-949.

Welsink, H. J.,Franco, M., A., and Oviedo, G., C., 1995. Andean and pre-Andean deformation, Boomerang Hills area, Bolivia, *in* Tankard, A. J., Suárez S., R., and Welsink, H. J., eds., Petroleum Basins of South America, AAPG Memoir 62, p. 481-499.

EROSIONAL CONTROL ON THRUST BELT DEVELOPMENT IN THE BOLIVIAN ANDES

Brian K. HORTON(1)

(1)Department of Geology and Geophysics, Louisiana State University, Baton Rouge, LA, U.S.A.

KEY WORDS: Erosion, thrust belt, critical taper, Bolivia

INTRODUCTION

A pronounced along-strike erosional gradient exists in the modern central Andes, from a high-erosion region directly north of the 17.5°S bend in the Andes (Bolivian orocline) to a low-erosion region south of the bend. This study explores the hypothesis that this erosional gradient has significantly influenced thrust belt development since middle-late Miocene time, leading to fundamental differences in the geometry and kinematic evolution of the northern part of the Bolivian thrust belt versus the southern part of the belt. A synthesis of modern erosion data (precipitation, river discharge, and fluvial denudation rates), ancient erosion data (inferred from fission-track analyses and evaluations of sediment preservation potential), active rates of surface shortening (derived from GPS data), and Neogene thrust-belt kinematics (from structural analyses) supports a model in which the middle-late Miocene to Recent evolution of the thrust belt has been largely governed by maintenance of critical taper. In short, high erosion to the north has favored internal shortening and prevented significant thrust front advance (subcritical condition); low erosion to the south has promoted in-sequence thrusting and advance of the thrust front (critical condition).

EROSION DATA

Precipitation, river discharge, and fluvial denudation rates in the modern thrust belt north of 17.5°S are substantially higher than to the south. Two profiles across the central Andes (N and S) reveal a strong contrast in both topography and precipitation to the north and south (Fig. 1). As shown by Masek et al. (1994), maximum relief, average slope, and average precipitation are several times higher to the north than to the south (Fig. 1). Stations at the exit point of the Rio Beni from the northern thrust belt (site 1, Fig. 1) and

at the exit point of the Rio Pilcomayo from the southern thrust belt (site 2, Fig. 1) indicate nearly an order of magnitude higher river discharge to the north than to the south (Guyot et al., 1990; 1993). Clearly, the modern thrust belt is characterized by drastically different erosional regimes north and south of 17.5°S. This change in erosional character corresponds to the E-W-trending divide between the Amazon drainage basin (which encompasses the majority of northern South America) and the Parana drainage basin (covering much of southern South America). This erosional boundary in the central Andes therefore may reflect larger, continental or global scale patterns of atmospheric circulation.

Several lines of evidence suggest that the present-day erosional pattern has existed since about middle-late Miocene time. First, fission-track data from plutons in the Cordillera Real (site 3, Fig. 1) indicate rapid denudation rates (200–900 m/Myr) north of the bend, consistent with erosional removal of ~4–8 km of rock overburden, since ~10–15 Ma (Benjamin et al., 1987; Masek et al., 1994). Second, there has been enhanced preservation of erodible geologic features in the Eastern Cordillera south of the bend. The original volcanic morphology of the 16.2 Ma edifice Cerro Chorolque (site 4, Fig. 1) remains largely intact, a number of north-trending Miocene sedimentary accumulations are preserved (Fig. 1), and the late Miocene San Juan del Oro geomorphic surface persists over large areas of the Eastern Cordillera of southern Bolivia (Gubbels et al., 1993).

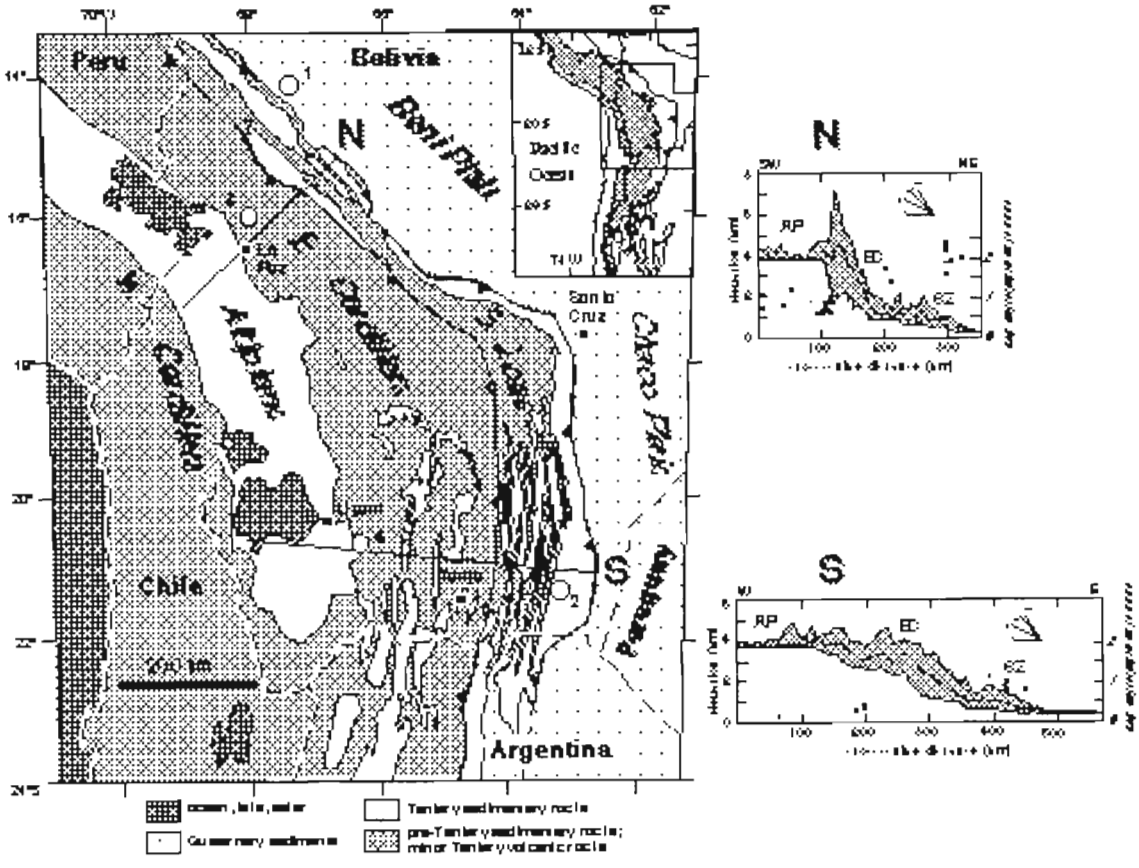

Figure 1. Geologic map of central Andes. Subandean Zone is situated between two major thrust faults: a frontal thrust to the east and the Main Andean thrust (or "Interandean Zone" of southern Bolivia) to the west. Note the greater amount of Tertiary sedimentary rocks within the Eastern Cordillera and Subandean Zone south of the 17.5° bend. Circles denote sites with denudation information (1, gauging station near Rurrenabaque; 2, gauging station at Villamontes; 3, Zongo and Huayna Potosi granites; 4, Cerro Chorolque). Inset map (upper right) shows areas above 3 km elevation, thrust front and basement uplifts. Topographic profiles N and S depict elevation data for 100-km-wide swaths (maximum, minimum, and swath-averaged elevations), highlighting the greater relief, steeper slope, narrower width, and higher precipitation (circles) to the north than to the south (modified from Masek et al., 1994).

GPS VELOCITY DATA

Active shortening within a thrust belt can potentially be monitored through GPS (Global Positioning System) velocity data from a collection of sites along a strike-perpendicular transect through the thrust belt. If a thrust belt is being internally shortened, the distance between adjacent sites will be decreased, and in turn, the site velocities with respect to the stable craton will be progressively lower toward the foreland. In contrast, if deformation is concentrated at or near the thrust front, the majority of sites across the thrust belt will show a relatively uniform velocity (i.e., no internal shortening). For the central Andes, GPS velocity data have been collected by Norabuena et al. (1998). Projection of their velocity data into two strike-perpendicular profiles, one north of the 17.5°S bend and one south of the bend, yields intriguing results regarding the distribution of active shortening in the central Andes (Fig. 2). Velocities across the northern profile indicate internal shortening within the Eastern Cordillera-Subandean Zone thrust belt (Fig. 2). For the southern profile, more or less uniform site velocities across the Eastern Cordillera and western Subandean Zone require no internal shortening over most of the thrust belt; however, the frontal 100 km of the Subandean Zone has no well-constrained velocity data (Fig. 2). Nevertheless, an important conclusion can be drawn for the southern profile based on the uniform velocities across the Eastern Cordillera-Subandean Zone boundary. This boundary is apparently one of the major structural elements of the thrust belt (Main Andean thrust to north, Interandean Zone to south) which accommodates nearly half of the total shortening in the thrust belt (Kley, 1996). To the south, the uniform GPS velocity data among all Eastern Cordillera sites and the ENRI (Entre Rios) site in the western Subandean Zone indicate that this structural system, as well as the entire Eastern Cordillera, are not undergoing internal shortening (Fig. 2b). In direct contrast, velocity data for the northern profile require internal shortening across the Eastern Cordillera-Subandean Zone boundary, suggesting that the Main Andean thrust (Roeder, 1988) may be accommodating active deformation.

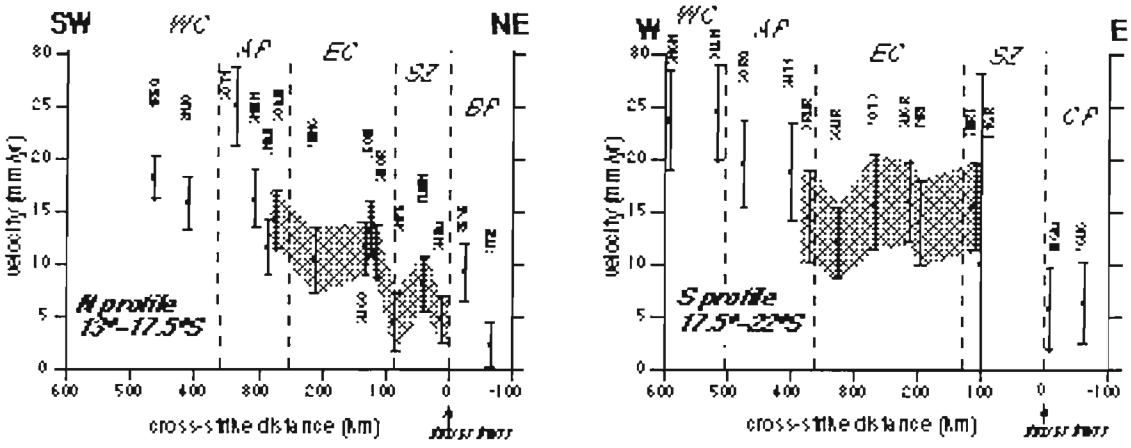

Figure 2. Surface velocity profiles (with error bars) for GPS sites across the central Andes, calculated from data in Norabuena et al. (1998). Sites north of the bend in the Andes (13°-17.5°S) are resolved into a strike-perpendicular profile trending 045°(NE-SW) at left. Sites south of the bend in the Andes (17.5°-22°S) are resolved into a strike-perpendicular profile trending 090° (E-W) at right. Shaded regions highlight the trends in surface velocities within the fold-thrust belt: variable velocities to the north and uniform velocities to the south. Abbreviations are as follows: WC, Western Cordillera; AP, Altiplano; EC, Eastern Cordillera; SZ, Subandean Zone; BP, Beni Plain; CP, Chaco Plain.

CRITICAL TAPER MODEL

Theoretical models state that a fold-thrust wedge strives for a stable or critical condition in which the net force driving the wedge forward—the sum of a gravitational body force and a horizontal compressive force—is exactly balanced by the basal-friction force resisting advance of the wedge (Davis et al., 1983). The critical condition is dependent on several mechanical properties of the wedge, including basal strength, internal wedge strength, basal pore-fluid pressure, and internal pore-fluid pressure. For a given set of these values, the critical condition will be attained only if the sum of surface slope (α) and decollement slope (β) reaches a specific value, or "critical taper." When changes in any of the geometric parameters (α and β) or mechanical parameters force the wedge out of the critical state into a "supercritical" or "subcritical" state, the wedge responds by deforming to alter its geometry (α and/or β) until the critical condition is regained. For instance, an orogenic wedge that becomes subcritical attempts to regain a critical state through internal deformation by out-of-sequence thrusting, synchronous thrusting, or duplexing. A major implication of this sort of thrust-wedge behavior is that processes, such as erosion, which reduce surface slope may ultimately tend to induce internal deformation within the wedge.

It is suggested here that erosion in the central Andes significantly modifies the geometry of the upper surface of the wedge, thereby affecting taper, and promoting subcritical conditions in the high-erosion thrust

belt to the north and critical conditions in the low-erosion thrust belt to the south. This is consistent with GPS velocity data suggesting internal shortening within the northern thrust belt and no internal shortening within the southern thrust belt (Fig. 2). It is also consistent with structural data for late Miocene and younger deformation within the Subandean Zone that indicate out-of-sequence deformation to the north (Roeder, 1988) and generally in-sequence thrusting to the south (Dunn et al., 1995; Kley, 1996).

CONCLUSIONS

Rapid denudation within the narrow (200-km-wide) northern thrust belt has apparently promoted a subcritical thrust-wedge condition in which internal contractional deformation is required to build taper prior to forward advance of the thrust belt. Modern surface velocities based on GPS data confirm that the northern thrust belt is currently experiencing internal shortening. To the south, a wider (350-km-wide) thrust wedge has expanded by continuous eastward migration of the thrust front with little or no internal deformation. Available GPS data reveal that the majority of the southern thrust belt is presently translating eastward without internal shortening, consistent with a critical wedge condition. The erosional gradient and associated variation in thrust-belt geometry and kinematics in the central Andes suggest that along-strike variations in long-term rates of erosion within an orogenic belt can potentially modify the tectonic processes associated with contractional mountain building.

REFERENCES

Benjamin, M.T., N.M. Johnson, and C.W. Naeser, Recent rapid uplift in the Bolivian Andes: Evidence from fission-track dating, *Geology, 15*, 680-683, 1987.

Davis, D., J. Suppe, and F.A. Dahlen, Mechanics of fold-and-thrust belts and accretionary wedges: *J. Geophys. Res., 88*, 1153-1172, 1983.

Dunn, J.F., K.G. Hartshorn, and P.W. Hartshorn, Structural styles and hydrocarbon potential of the Sub-Andean thrust belt of southern Bolivia, in *Petroleum Basins of South America*, edited by A.J. Tankard, R. Suárez, and H.J. Welsink, *AAPG Mem., 62*, pp. 523-543, 1995.

Gubbels, T.L., B.L. Isacks, and E. Farrar, High-level surfaces, plateau uplift, and foreland development, Bolivian central Andes, *Geology, 21*, 695-698, 1993.

Guyot, J.L., H. Calle, J. Cortes, and M. Pereira, Transport of suspended sediment and dissolved material from the Andes to the Rio Plata by the Bolivian tributaries of the Rio Paraguay (Rios Pilcomayo and Bermejo), *Hydro. Sci. J., 35*, 653-665, 1990.

Guyot, J.L., J.M. Jouanneau, J. Quintanilla, J.G. Wasson, Dissolved and suspended sediment loads exported from the Andes by the Beni river (Bolivian Amazonia), during a flood, *Geodinamica Acta, 6*, 233-241, 1993.

Kley, J., Transition from basement-involved to thin-skinned thrusting in the Cordillera Oriental of southern Bolivia, *Tectonics, 15*, 763-775, 1996.

Masek, J.G., B.L. Isacks, T.L. Gubbels, and E.J. Fielding, Erosion and tectonics at the margins of continental plateaus, *J. Geophys. Res., 99*, 13,941-13,956, 1994.

Norabuena, E., L. Leffler-Griffin, A. Mao, T. Dixon, S. Stein, I.S. Sacks, L. Ocola, and M. Ellis, Space geodetic observations of Nazca-South America convergence across the Central Andes, *Science, 279*, 358-362, 1998.

Roeder, D., Andean-age structure of Eastern Cordillera (province of La Paz, Bolivia), *Tectonics, 7*, 23-39, 1988.

CRETACEOUS AND TERTIARY TERRANE ACCRETION IN THE CORDILLERA OCCIDENTAL OF THE ECUADORIAN ANDES

Richard A. HUGHES (1) and Luis F. PILATASIG (2)

(1) British Geological Survey, Murchison House, West Mains Road, Edinburgh EH9 3LA, United Kingdom (r.hughes@bgs.ac.uk)
(2) CODIGEM, Casilla 17-03-23, Quito, Ecuador

KEY WORDS: Ecuador, accretion, terrane, Tertiary, Cretaceous

INTRODUCTION

Throughout most of Ecuador the Andean chain consists of two parallel ranges, the cordilleras Occidental and Real, separated by a central graben that is filled by Quaternary volcanosedimentary rocks. The eastern limit of the Cordillera Occidental is the active Pujil' Fault, the southern extension of the Cauca-Pat'a Fault, which can be traced for some 2000 kms through Colombia to the Caribbean (Litherland & Aspden 1992). Throughout much of the country the western limit of the Cordillera Real is the Baños-Peltetec Fault system (Litherland & Aspden 1992), the southern part of the equally extensive Romeral Fault.

The Cordillera Real consists of sub-linear belts of Palaeozoic to Cretaceous metamorphic rocks accreted mainly in the late Jurassic-early Cretaceous, intruded by early Mesozoic S- and I-type granitoids, and capped by Cenozoic to modern volcanics (Litherland et al., 1994). The Cordillera Occidental consists mainly of non-metamorphic, early to late Cretaceous oceanic crustal rocks (MOR basalts and peridotites), late Cretaceous marine turbidites, an Eocene marine turbidite basin fill sequence, a late Palaeocene-early Eocene basaltic-andesitic oceanic island arc sequence, and an Eocene-Oligocene terrestrial sequence. These are intruded by Eocene and younger I-type granitoids, with major late Eocene to Miocene and younger sub-aerial, calc-alkaline continental margin volcanosedimentary sequences, especially in the south.

A regional geological mapping programme, carried out over the past four years by the British Geological Survey and CODIGEM as part of a multilateral aid project, has identified two major terranes in the Cordillera Occidental. Within the older (Pallatanga) terrane, an assemblage of MOR basalts and peridotites with related fine-grained turbidites (the Unidad Pallatanga) represents an oceanic suite that consistently occupies a structural position along the eastern margin of the cordillera. In the same structural position is a locally exposed tectonic mélange (the Unidad Pujil'), which is believed to have formed in a suture zone, probably during the Campanian-Maastrichtian. The Unidad Yunguilla is a sequence of Maastrichtian, fine-grained, siliciclastic turbidites apparently deposited upon the oceanic crust of the Unidad Pallatanga. Most of the remainder of the Pallatanga

terrane consists of very thick Senonian and Campanian marine turbidites (the unidades Pilatón and Mulaute), derived mainly from basaltic-andesitic volcanic sources. Also present is a sequence of terrestrial sediments of late Eocene-early Oligocene age (the Unidad Silante), derived from a probably sub-aerial andesitic volcanic source.

The younger (Macuchi) terrane consists of an early Eocene (and possibly late Palaeocene) basaltic to andesitic volcanosedimentary sequence (the Unidad Macuchi), which hosts volcanogenic massive sulphide mineralisation. Unidad Macuchi turbidites contain early Eocene radiolaria (Eguez 1986). The sequence comprises pillow lavas, turbidites, debrites, hyaloclastites, thin limestones, and possible pyroclastic rocks. The facies indicate submarine eruption and deposition, with a sub-aerial environment for the possible pyroclastics. Most of the volcanic component consists of andesites or basaltic andesites, though some primitive basalts are also present. Geochemistry suggests an oceanic island arc setting, though a marginal basin setting cannot be ruled out.

Apparently common to both terranes is a mid to late Eocene marine turbidite basin fill sequence (the Grupo Angamarca). The geodynamic setting of the depositional basin of the Grupo Angamarca is unclear.

Evidence for the age of accretion of the older, Pallatanga terrane is largely indirect. (Aspden et al., 1992) suggested that the widespread resetting of K-Ar ages in the Cordillera Real to 85-65 Ma was caused by uplift resulting from the earliest stages of accretion of the Cordillera Occidental. This idea is supported by evidence of the deposition of very different Maastrichtian sedimentary facies on either side of the Cordillera Real, with marine turbidites (Unidad Yunguilla) to the west and red beds to the east (Tena Formation).

Stratigraphical and isotopic evidence suggests that the younger Macuchi terrane was accreted by the late Eocene. The Unidad Macuchi is intruded by a number of stitching, I-type granitoid plutons, the oldest of which has a K-Ar hornblende age of 38 ± 0.39 Ma. A strongly foliated dioritic intrusion from the suture zone which separates the two terranes gave a K-Ar hornblende age of 48 Ma. This age is believed to be reset, and probably indicates the early stages of the accretionary event in the mid Eocene.

The structure which separates the two terranes is a previously unrecognised, regionally important shear zone. All kinematic indicators within this anastomosing zone, including S-C mylonites, indicate dextral shear; it is believed that the Macuchi terrane was accreted during a dextral shear regime. Economically important gold and platinum deposits in the north of the country are probably related to the shear zone. Quilotoa, the only active volcano within the Cordillera Occidental, sits astride the zone, and it is probable that the structure provides a conduit for rising magma.

CONCLUSIONS

The Cordillera Occidental of Ecuador comprises two terranes accreted during two discrete events in the Maastrichtian and mid Eocene.

The older (Pallatanga) terrane contains an assemblage of MOR basalts and peridotites with related fine-grained turbidites, a tectonic mélange, late Cretaceous marine turbidites, and a sequence of late Eocene-early Oligocene terrestrial sediments. The widespread resetting of K-Ar ages in the Cordillera Real to 85-65 Ma, and

the deposition of different Maastrichtian sedimentary facies on either side of the Cordillera Real are believed to indicate a Campanian-Maastrichtian age of accretion for the older terrane.

The younger (Macuchi) terrane consists of an early to mid Eocene basaltic to andesitic island arc volcanosedimentary sequence. Stratigraphical evidence, late Eocene I-type stitching plutons, and a reset early-mid Eocene K-Ar age is believed to indicate that the Macuchi terrane was accreted by late Eocene times.

The suture which separates the two terranes is a broad dextral shear zone, of probable economic importance.

REFERENCES

Aspden, J.A., Bonilla, W. & P. Duque 1992. New geochronological control for the tectono-magmatic evolution of the metamorphic basement, Cordillera Real and El Oro Province of Ecuador. Journal of South American Earth Sciences, 6, 77-96.

Eguez, A. 1986. Evolution Cénozoique de la Cordillère Occidentale Septentrionale d'Equateur. Unpublished PhD thesis; Universite Pierre et Marie Curie, Paris.

Eguez, A. & J. Bourgois 1986. La Formación Apagua, edad y posición estructural en la Cordillera Occidental del Ecuador. Cuarto Congresso Ecuatoriano de Geolog'a, Minas y Petroleo, I, 161-178.

Litherland, M. & J.A. Aspden 1992. Terrane-boundary reactivation: a control on the evolution of the Northern Andes. Journal of South American Earth Sciences, 5, 71-76.

Litherland, M., Aspden, J.A. & R.A. Jemielita 1994. The metamorphic belts of Ecuador. Overseas Memoir 11. Keyworth: British Geological Survey.

THE GUAYAQUIL SEAWAY - LINKING THE PACIFIC OCEAN AND THE ECUADORIAN ORIENTE IN THE MIDDLE MIOCENE

Dominik HUNGERBÜHLER (1), Wilfried WINKLER (2), Michael STEINMANN (3), Dawn PETERSON (4) and Diane SEWARD (2)

(1) Shell Nederlandse Aardolie Maatschappij, 1950AA Velsen, Netherlands, Dominikh@compuserve.com
(2) Institute of Geology, ETH Zürich, 8092 Zürich, Switzerland, wilf@erdw.ethz.ch, diane@erdw.ethz.ch
(3) Matsag Perú S.A., Lima, Perú, msteinmann@glencore.com.pe
(4) California Academy of Sciences, San Francisco, USA, jurdyke@earthlink.net

KEY WORDS: Ecuador, Miocene, Guayaquil Seaway, marine transgressions, Andean uplift

INTRODUCTION

A series of Late Tertiary basin fills (Cuenca, Nabón, Girón-Santa Isabel, Loja, Malacatos-Vilcabamba, Catamayo-Gonzanamá) is situated in the Andes (Sierra) of southern Ecuador at altitudes of 1000 to 3000m above sea level. The basins show typical characteristics of intermontane basins, well known in the Andean domain. However, during the Middle Miocene all of these basins (excluding Nabón) were situated at sea level in a coastal plain environment at the western shoreline of the South American continent. The chronostratigraphy of the basement and basin fills and the timing of deformation has been established by more than 150 zircon fission-track age determinations on tephra layers (Hungerbühler et al., 1996). An apatite fission-track analysis allowed modelling of the thermo-tectonic history in the Cuenca basin and adjacent Cordilleras, yielding information about timing and rates of uplift and exhumation (Steinmann et al., in press). A paleontological study of ostracods and molluscs, combined with sedimentological analyses allowed identifying the prevailing depositional environments. The findings result in a paleogeographic reconstruction of southern Ecuador during the Late Tertiary, and the correlation of the studied basins in the Andean domain with coeval forearc and backarc basin series.

STRATIGRAPHY AND DEPOSITIONAL ENVIRONMENTS OF THE BASIN FILLS

The Miocene basin fills rest unconformably on volcanic rocks (Eocene to Early Miocene) and on metamorphic units (Paleozoic to Mesozoic). The fill sequences of the basins mentioned in the introduction, have variable ages from basin to basin, but generally cover a period between 15 to 8 Ma. Continuous volcanic activity in the Miocene within and outside the basins suggests an interarc setting. The development of the Miocene basins took place in two stages: **(1)** During a period of E-W oriented extension in the Middle Miocene, a series of basins developed in southern Ecuador. Large scale deltaic sedimentation prevailed in the Cuenca basin and coastal plain, lagoonal and lacustrine conditions occurred in the southern basins. This period is termed the *Pacific Coastal Stage* and lasted from 15 to 9.5 Ma. During this stage, two large marine embayments can be distinguished (Loja and Cuenca) which were separated by the Santa Rosa-Saraguro High (Fig. A). The reconstruction shows that the Ecuadorian Andes as we know them today did not yet exist at this time. Today only small remnants of the sediments deposited in the Loja Embayment are preserved. **(2)** After a period of deformation at 9-8 Ma, an *Intermontane Stage* occurred during 9-6 Ma. The 9-8 Ma deformation event involved surface uplift and regional E-W oriented compression, resulting in a basin inversion with large scale thrust faulting and folding of the coastal stage sediments and of basement rocks. In the Intermontane Stage, smaller individual basins developed within the former much bigger depositional area (Fig. B). Alluvial sedimentation (fluvial systems, alluvial fans, lakes) prevailed and coarse clastics represent the partly syntectonic fill.

LATE TERTIARY PALEOGEOGRAPHIC AND TECTONIC EVOLUTION

During 15 to 11 Ma marine trangressions occurred in the Cuenca and Loja Embayments from the west and northwest, respectively. In both embayments, continental sediments were derived from the developing Cordillera Real to the east and volcanic sources. During the Middle Miocene, the Cordillera Real in southern Ecuador had not yet developed as a prominent continuous mountain barrier. A marine branch, which is termed the Guayaquil Seaway, connected the Pacific Ocean via the Vilcabamba Inlet with the Oriente or Amazonian region of Ecuador and Peru (Fig. A). Ostracod and mollusc faunas in the Miocene basin series of southern Ecuador are similar to assemblages found in presumably Miocene deposits in the Oriente of Ecuador and the upper Amazon region of Peru, Colombia and Brazil. The faunal evidence combined with depositional facies and apatite fission-track data strongly suggest that faunal migration between the southern Ecuadorian basins and the Oriente occurred via marine inlets such as the Guayaquil Seaway. The appearance of two Caribbean ostracod taxa in the Middle Miocene sediments of southern Ecuador allows for some further speculations on faunal migration patterns.

The prominent change in depositional environments and sediment provenance at 9 Ma is coeval with the regional compressive deformation in southern Ecuador and surface uplift of the Cordillera Occidental and Cordillera Real. The uplift caused the closure of the Guayaquil Seaway (Fig. B). In the Ecuadorian Sub-Andean zone tectonic structures and facies developments are thought to have occurred coevally with the

uplift event in the Sierra at 9 Ma: (1) onset of Miocene deformation in the fold and thrust belt, (2) upthrusting of the Cutucú range which started to rise in the Late Miocene and (3) onset of coarse clastic sedimentation in the Sub-Andean zone, derived from the Cordillera Real (Chambira Fm.). The dominant western source area during the Intermontane Stage of the Cuenca basin indicates the rise of the Cordillera Occidental, which is also established by apatite fission-track data (Steinmann et al., in press). The apatite fission-track modelling implies a net surface uplift in the Cuenca area of 2700m, since 9 Ma (at a mean rate of 0.3 mm/y). The estimated vertical maximum rock uplift for the Cuenca area is 6100m and the exhumation 3400m. However, the strong tectonic activity and drastic change of depositional setting in the Late Miocene suggests that the major part of surface uplift occurred in the period from 9-6 Ma.

The coastal basins in the Loja and Cuenca Embayments were genetically linked with coeval coastal forearc pull-apart basin formation, which were controlled by dextral movement along the Dolores-Guayaquil Megashear (DGM, Fig A): the Manabí Basin in the north formed the continuation of the Cuenca Embayment, while the Progreso basin in the south represented the continuation of the Loja Embayment. The Manabí and Progreso basins were separated by the Chongón-Colonche High. The presented palinspastic reconstruction (Fig A) shows that the Santa Rosa-Saraguro High can be correlated with the Chongón-Colonche High in the coastal area of Ecuador. Continuing large scale dextral strike-slip movement along the DGM since the Late Miocene has displaced the coastal correlatives towards the north (Fig B). During this time, the Jambelí-Túmbez forearc pull-apart basin was formed and predominantly filled with the erosional products of the Cordillera Occidental which began to rise at 9-8 Ma. The formation of the Jambelí-Túmbez Basin most likely occurred coeval with the regional compressive deformation event in the Andean domain and the surface uplift of the Cordillera Occidental. The stratigraphic relationships reveal a Middle and a predominantly Late Miocene to Present activity of the DGM with a minimum right lateral displacement of 100 km since 9 Ma.

CONCLUSIONS

The Miocene basin formation in southern Ecuador occurred in the particular area of the triple point where the DGM intersects the Peruvian and Ecuadorian trenches. The important driving force for basin subsidence and extension was the NNE-directed dextral displacement of the coastal block along the DGM with respect to the Andean domain. The continental margin parallel extension in the Costa area decreased crustal thickness, and extension propagated into the Andean domain by margin-parallel halfgraben formation (extensional collapse) where marine the embayments could evolve. Local stronger extension may have opened the Guayaquil Seaway. In plate tectonic terms, the change from an extensional period from 15-10 Ma to compression at 9 Ma with associated uplift may be explained by a blocking of the retreat of the subducting Nazca plate hinge zone at around 9 Ma. This could have been caused by a slab break-off in the deeper part of the subduction zone. Related buoyant uplift (decrease of subduction pull) of the remaining slab and concomitant plate coupling may have driven regional uplift and compressional deformation in the Andean domain.

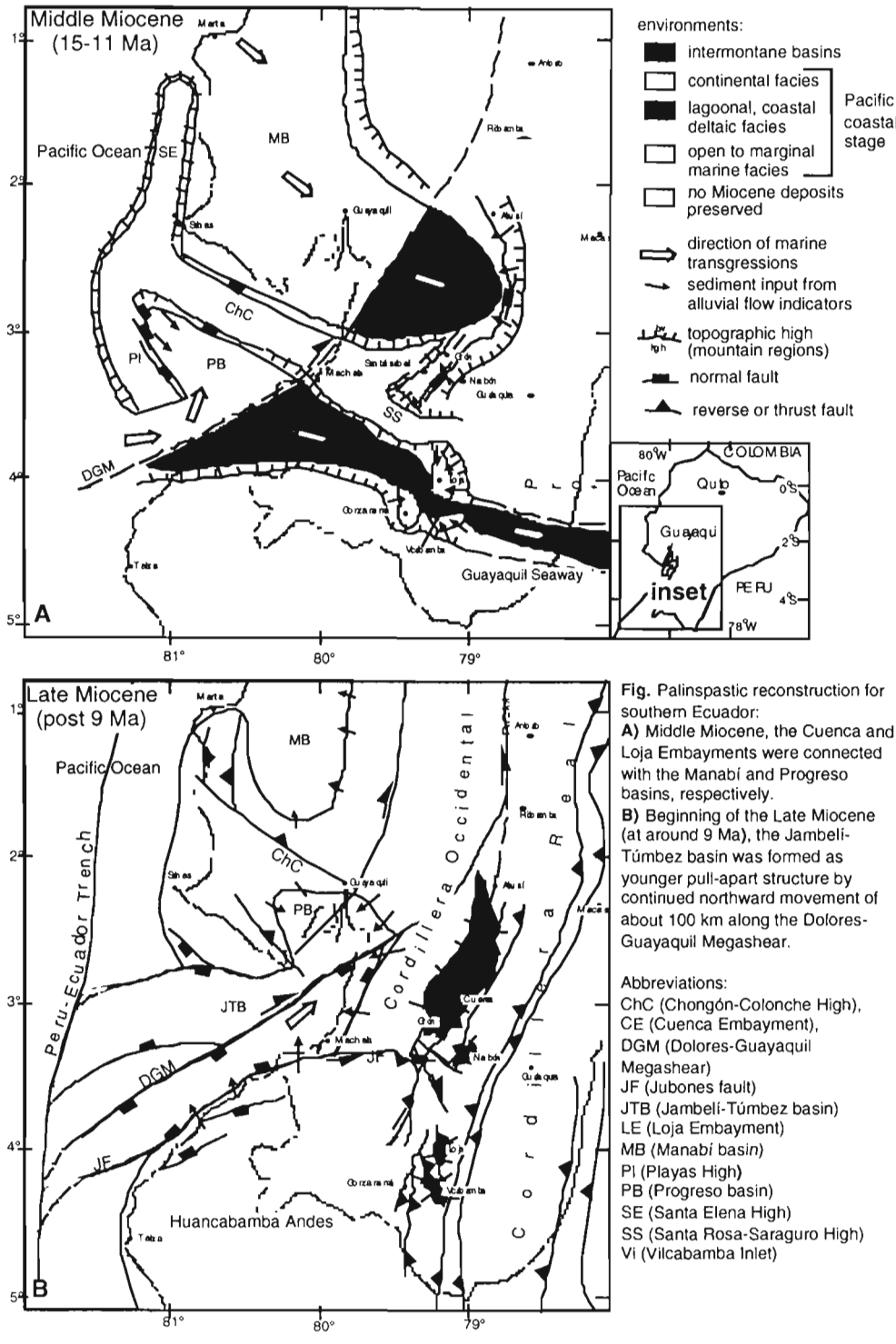

Fig. Palinspastic reconstruction for southern Ecuador:
A) Middle Miocene, the Cuenca and Loja Embayments were connected with the Manabí and Progreso basins, respectively.
B) Beginning of the Late Miocene (at around 9 Ma), the Jambelí-Túmbez basin was formed as younger pull-apart structure by continued northward movement of about 100 km along the Dolores-Guayaquil Megashear.

Abbreviations:
ChC (Chongón-Colonche High),
CE (Cuenca Embayment),
DGM (Dolores-Guayaquil Megashear)
JF (Jubones fault)
JTB (Jambelí-Túmbez basin)
LE (Loja Embayment)
MB (Manabí basin)
PI (Playas High)
PB (Progreso basin)
SE (Santa Elena High)
SS (Santa Rosa-Saraguro High)
VI (Vilcabamba Inlet)

REFERENCES

Hungerbühler D., Steinmann M., Winkler W. and Seward D., 1996. Neogene fission-track stratigraphy of southern Ecuadorian basins: Implications for regional tectonic history. 3rd ISAG, Saint-Malo, 387-390.

Steinmann M., Hungerbühler D., Seward D. and Winkler W., in press. Neogene tectonic evolution and exhumation of the southern Ecuadorian Andes: A combined stratigraphy and fission-track approach. Tectonophysics.

The study was supported by the Swiss Science Foundation grants No. 21-39134.93 and 20-45256.95.

THERMAL CONTROLS IN COMPRESSIVE ZONES. AN EXAMPLE FROM THE BOLIVIAN SUB ANDEAN ZONE

Laurent HUSSON and Isabelle MORETTI

In extensive area, the thermal field is controlled by crustal thinning and contingent transient perturbation due to sedimentation. In collisional areas, the thermal field is a much more complex combination of endothermic and exothermic parameters of various origins; their magnitudes, wavelengths and locations are closely linked to both global geodynamics and small-scale superficial phenomena. Fold and thrust belts constitute an additional problem for thermal studies, as available direct thermal data in these areas are all within the first 5 km; what's more, measured gradients are not representative of the whole front range since generally only anticlines are drilled.

THERMAL CONTROLS OVER THE THERMAL FIELD WITHIN COMPRESSIVE ZONES

These parameters can be classified as follows and an attempt to assess their relative importance is realised using numerical modeling.

The deep controls include mantellic and crustal contributions, and have a wide-scale surface signal.

Mantellic contributions are mainly due to the subduction type (continental or oceanic), which generate a possible cold or warm root beneath the orogen and induce vertical movements within orogens. The behaviour of the lithospheric mantle with regards to the crust (coupling or not) remains uncertain.

Crustal influences are of various types and include radiogenic production, phase changes during metamorphism, strain heating and frictional heating on the faults. Of these contributions, the last two are still much debated questions. Major thrusts and nappes have often been regarded as important advections of warm material over colder units. Nevertheless, as thrust velocities are not fast enough to counteract conduction, thrusting cannot be considered as an important transient control on the thermal field (Endignoux and Wolf, 1990); therefore, when the crust is involved, it reorganises the distribution of radiogenic elements within it. Crustal thickening increases the thickness of the radiogenic material, and thus the average heat flow. Nevertheless, this increase is not always well quantified. Indeed, radiogenic production is commonly described as an exponential decreasing function with depth (Cermak *et al.*, 1991) whereas, the deep boreholes drilled in Kula and Germany have not shown such a pattern (Kukkonen and Clauser, 1994).

The superficial controls include erosion, sedimentation, terrain effects (topography and surface temperatures) and meteoric water flow (Fig.1).

When erosion and sedimentation are slow, they do not disturb the thermal regime; however, these phenomena are often fast enough in compressive zones to induce major transient effects. In the foredeep, large sedimentation rates drastically decrease the gradient in the first few kilometres. This phenomenon is well known as the blanketing effect (Lucazeau & LeDouaran, 1985; De Braemaker, 1983). By contrast, erosion on the reliefs leads to a strong increase in the superficial gradient. Erosion and sedimentation act as major controls on the apparent thermal field: they both correspond to a competition between advection and conduction. In addition, the thermal impact of erosion and sedimentation are mutually enhanced as they have the same wavelength and opposite phase. Hence, the observed thermal field is a transient state governed by these superficial dynamic parameters.

Meteoric water circulation, driven by hydraulic charge within mountainous areas generates large scale fluid flow from the mountain belt to the foreland. This migration may affect hundreds of kilometres. Recharge can reach great depth and be fast enough to create a thermal disequilibrium between the cold down-flowing water and the warm surrounding rocks. Topography and thrusts induce abnormal pressures, which are generally negative if the foreland is well drained.

When the relief is uneven, topography also widely deviates the geothermal gradient up to depths of about 1500 m; the heat flow measured in the valleys is abnormally elevated whereas it is lowered over the highs. Up to shallow depth, contribution from the associated atmospheric gradient is to be taken into account as it lowers the aforesaid thermal impact of scarps.

The thermal field being usually observed at shallow depth, the measured signal is the sum of all these phenomena. Assessing these various parameters is a major academic and economic stake: the thermal signal used in geodynamics is the deep one and hence requires corrections from superficial effects. Temperature at a depth of up to 10 km and its evolution through time is a daily problem for economic geology.

This overview of the phenomena allows one to expect a contrasted heat flow profile through the belts: in the internal part of the orogen, crustal thickening and erosion should induce an elevated heat flow whereas in the foreland, a low heat flow is expected due to sedimentation. The data do not always follow such a simple pattern.

THERMAL PROFILES THROUGH MAJOR OROGENS

• The Apennines, due to their particular geodynamic setting, display a regularly increasing trend of the heat flow profile from the eastern subduction trench (40 mW/m^2) to the western back-arc opening (200 mW/m^2). The low heat flow is due to the thick recent sedimentary pile, whereas the elevated one is the result of lithospheric and crustal thinning. Tuscany features local extremely elevated anomalies (more than 400 mW/m^2), linked to the magmatism in this area.

• The Pyrenees display a surprising thermal profile: the external zones feature elevated heat flow, with maximum values located over the Ebro and Aquitaine forelands, reaching 180 mW/m^2, in spite of the sedimentary pile.

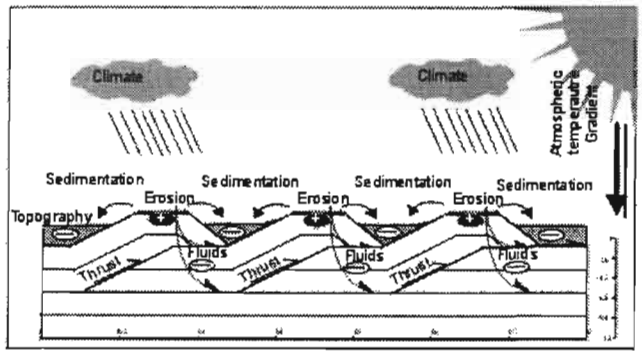

Fig.1: Various controls over a periodic system of fold and thrust belt. Positive and negative anomalies correspond to transient states due to erosion and sedimentation respectively. Meteoric fluid circulation also generate negative anomalies; terrain effects (topography and surface temperature variations) produce both positive and negative anomalies.

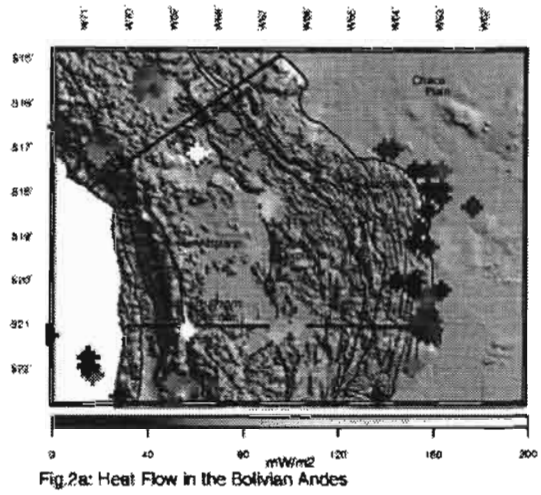

Fig.2a: Heat Flow in the Bolivian Andes

Fig.2a: Heat Flow data over the Central Andes
Fig.2b: Elevation, Moho depth, and Heat Flow Density data over the Northern (top) and Southern (bottom) Central Andes. Location of the traverses Fig.2a. (ETOP30 DEM).

Heat Flow

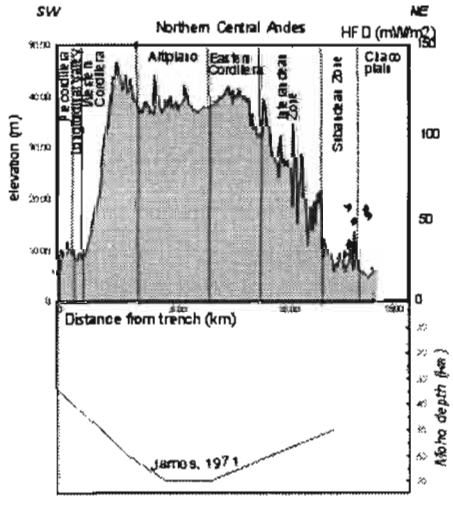

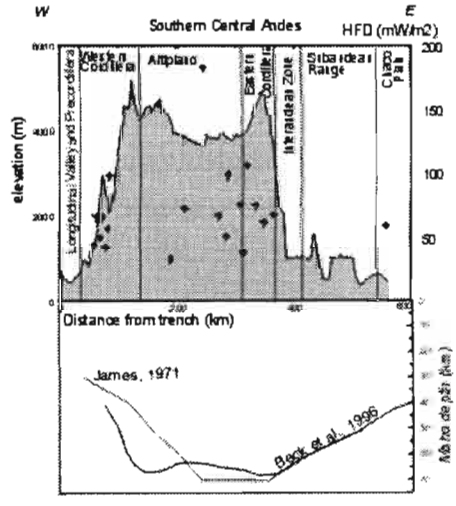

There is no blanketing effect in the Pyrenees since sedimentation is not active anymore. Another observation is the extremely fast lateral variations in the heat flow magnitude, which stressed the importance of local controls over the thermal field in this area. We have to note that the axial zone of the Pyrenees are poorly documented; no heat flow data are available on the area.

• The western Alps show a peculiar trend of the SN thermal profile: the heat flow increases from the very low values of the Po plain (30-40 mW/m^2) -due to the thick Plio-Quaternary sedimentary pile- to the very elevated heat flow in the Swiss molasse basin (up to 200 mW/m^2). Alpine external zones do not always display a high heat flow as southward in France the heat flow diminishes to medium values (60-70 mW/m^2). Internal zones do not show particularly high heat flow values. The causes of the elevated heat flow over the Swiss molasse is not yet clear but may be related to interaction with the Tertiary opening of the Rhine graben and Panonian basin.

• In spite of the small set of heat flow data in the Himalayas and Tibet, it appears that the heat flow drastically increases from the medium values of the Indo-gangetic plain to the High Himalayas and South Tibet (up to 380 mW/m^2). The extremely high heat flow is due to a particular crustal composition (thick, very radiogenic upper crust, mafic lower crust...Le Pichon *et al.*, 1997). In the very poorly documented North Tibet, the heat flow might be extremely low (40-50 mW/m^2).

• The Bolivian Andes broadly feature an increasing trend of the heat flow profile from the foreland Chaco plain to the Altiplano and the western Cordillera (Fig.2a). High sedimentation rates above the westward subduction of the Brazilian shield beneath the Andes lead to an important blanketing effect (40-50 mW/m^2). Crustal thickening (up to 60/70 km) and eventual lithospheric thinning can explain the elevated heat flow in the orogen (up to 180 mW/m^2). However, this heat flow trend is not obvious everywhere (Fig.2b), and local anomalies are to be taken into account over the Andes.

DISCUSSION AND APPLICATION TO THE SUBANDEAN ZONE

This overview of the thermal fields over the major orogens puts forward the fact that there is no standard thermal profile over collisional areas even if mountain belts always constitute warm areas.

Deep controls affect the superficial thermal field with wide wavelengths, whereas more superficial factors create local anomalies. Nevertheless, their magnitudes are of the same order, and the measured thermal regime is due to both, allowing for large variations of thermal fields between the orogens and local lateral variations.

As a consequence, maximum heat flows are not necessarily over internal zones, in spite of crustal thickening. What's more, external zone, including foredeeps, can display elevated heat flow values. We may note that the blanketing effect is only visible in extremely recent foreland (Po plain, Chaco plain...)where the sedimentation rate during the last 5 My has gone over 1mm/y. By contrast, in the Tertiary foreland such as the Alps or the

Pyrenees, the heat flows are high, which means that the blanketing is no longer the preponderent control over thermicity. Deep controls are significant in the western Apennines, the Altiplano and Eastern Cordillera, and in South Tibet. Important erosion rates leading to high heat flows over the High Himalayas have to be mentioned.

Hence it appears that each aforesaid individual parameter is to be assessed to understand the composite measured thermal signal. An application to the external inputs over the Subandean Bolivian range is realised as a forward model of superficial phenomena:

The thermal impacts of topography and erosion can be assessed from a DEM. Already published structural evolution (Baby et al., 1995, Moretti et al., 1996) and foreland basin stratigraphy are used to estimate the transient effect of sedimentation and erosion over the frontal thrusts and the Chaco plain. Numerical modeling (TEMISPACK software) is used to estimate fluid circulations within the frontal zone of the Bolivian Andes. The assessment of the thermal impact of external inputs over the frontal zone of the Bolivian Andes is thereafter used to invert the thermal signal and to restore the deep thermal field. Remaining thermal anomalies are thus interpreted from deep mantellic and crustal sources.

REFERENCES

Baby, P., Moretti I, B. Guillier, R. Limachi , E., Mendez ,J. Oller and M. Specht, 1995. Petroleum maturation versus thrust emplacement on the Bolivian foothills. In Petroleum of South America: AAPG Memoir 62 p 445-458.

Beck, S., Zandt, G., Myers, S.C., Wallace, T.C., Silver, P.G., Drake, L., 1996: Crustal thickness variations in the Central Andes; Geology, 24-5, pp. 407-410.

Cermak, V., Bodri, L., Rybach, L: Radioactive heat production in the continental crust and its depth dependence; in Cermak and Rybach (eds), Terrestrial heat flow and the lithosphere structure; Springer-Verlag, Berlin.

De Braemacker, J-Cl, 1983: Temperature subsidence and hydrocarbon maturation in extensional basins, a finite elements model; Bull. AAPG 67, 1410-1414.

Endignoux, L. and Wolf, S., 1990: Thermal and kinematic evolution of thrust basins: a 2D numerical model; in Letouzey (ed), Petroleum and tectonics in mobile belts; Technip, Paris.

James, D. E., 1971: Andean crustal and upper mantle structure; JGR 76/14, pp. 3247-3271.

Kukkonen, I. T. and Clauser, C., 1994: Simulation of heat transfer at the Kola deep-hole site: implications for advection, heat refraction and palaeoclimatic effects; Geoph. J. Int., 116, 409-420.

Le Pichon, X., Henry, P. et Goffé, B., 1997: Uplift of Tibet: from eclogites to granulites -implications for the Andean plateau and the Variscan belt; Tectonophysics 273, 57-76.

Lucazeau, F. and Le Douaran, S., 1985: The blanketing effect of sediments in basins formed by extension: a numerical model. Application to the Gulf of Lion and Viking Graben; Earth Pl. Sc. Let. 74, 92-102.

Moretti I., Baby P., Mendez E. and Zubieta D., 1996. Hydrocarbon generation in relation to thrusting in the Sub Andean Zone from 18 to 22°S, Bolivia. Marine and Petroleum Geology, v 2, 17-26.

STUDY OF THE CRUST ON THE PERUVIAN ANDEAN SECTION FROM GRAVITY DATA AND GEOID UNDULATIONS

Antonio Introcaso[1], and Iris Rosalia Cabassi[2]

(1) Facultad de Cs. Exactas, Ingeniería y Agrim., U.N. Rosario, Av. Pellegrini 250, 2000 Rosario, ARGENTINA.
(2) Facultad de Cs. Astronómicas y Geofísicas, U.N. La Plata, Paseo del Bosque s/n, 1900 La Plata, ARGENTINA.

KEY WORDS: Andes, Perú, Gravity, Geoid, Undulations

INTRODUCTION

The name of the Nazca section, here analysed, is due to the little Nazca City at the Pacific Coast in Peru. This section continues 250 km through Pacific Ocean, while on continental area it passes along Nazca, Pulquio, Chalhuanca, Abancay, Cuzco, Mazuco, until Puerto Maldonado into the Amazonian Basin (**Fig**. 1). The Nazca section crosses the coast, West Cordillera, the Altiplano, East Cordillera, and part of the Amazonian Basin.

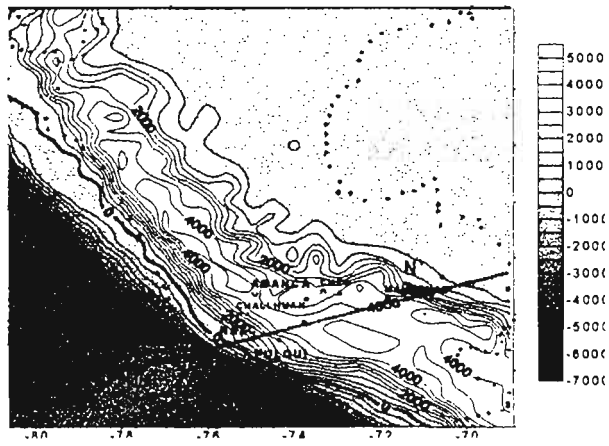

Fig. 1: Elevations Chart of Peru: Nazca Section analysed.

Bouguer anomaly on Peru-Chile trench is +220 mGal, +100 mGal near of the Pacific Coast, and from this border decreases gradually up to a minimum of –380 mGal beneath the West Cordillera (**Fig.** 2, bottom). It is possible to see that, although the topography is nearly symmetrical (**Fig**. 2, top), the Bouguer anomaly is not, showing an important gravity excess (about 120 mGal) beneath East Cordillera (**Fig**. 2, bottom). It is a clear indication of isostatic undercompensation. This result is confirmed by: 1) the expression of **AB** (mGal)= -25 –89 **H**(m) (**AB** is the mean Bouguer anomaly and **H** is the mean altitude), for the Peruvian Andes subdivided in squares of 1° x 1°, with standard deviation of 0.985 (*Cabassi and Introcaso*, 1997), and 2) the isostatic anomaly calculated using the Airy System, that has a 100 mGal excess (**Fig**. 3, top).

In order to study the crust structure from geoide undulations, a geoidal section is built. The residuals obtained (the difference between observed satellite geoide and topo-isostatic geoide) are consistent with the classical isostatic anomaly.

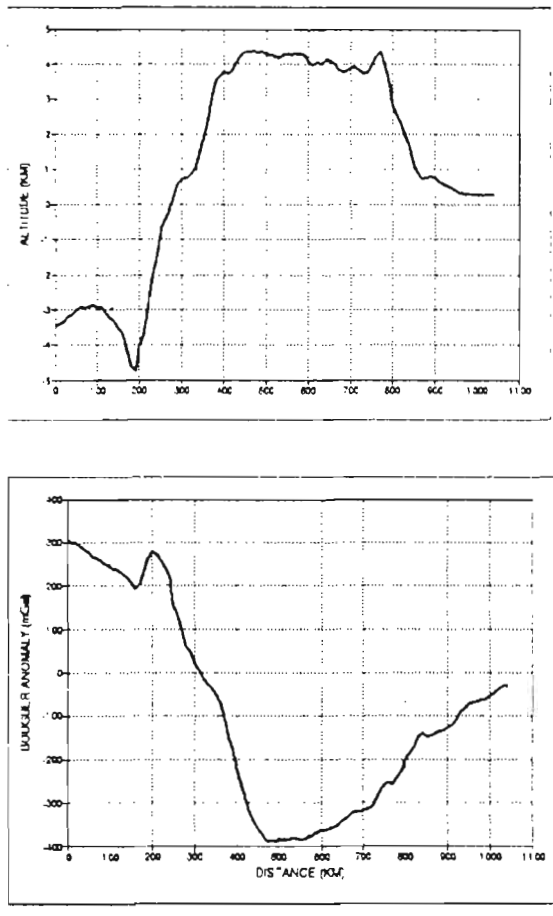

Fig. 2: Nazca Section. Top: Topography Bottom: Bouguer Anomaly

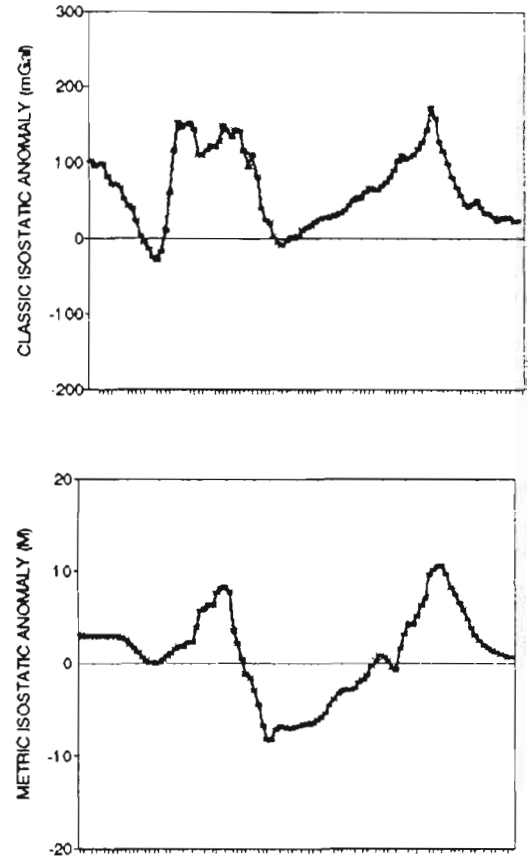

Fig. 3: Top: Classical Isostatic Anomaly Bottom: Metric Isostatic Anomaly

DATA ANALYSIS

Satellite geoide undulations had been computed based on a Harmonic Geopotential Model (*Yecai*, 1994). For removing intermediate to long wavelengths and so focusing the problem to (short) Andean wavelengths, a 4-degree spherical harmonic development was used. This value is consistent with the range (2 to 10) suggested by *Marsh and Martin* (1982) and *Sandwell and Renkin* (1988).

After obtaining the corresponding undulation for the Andean structure, it was compared with the calculated topo-isostatic geoide, using the Andean topography as an input signal (*Haxby and Turcotte*, 1978) or *Turcotte and Shubert* (1982) in the Airy System. *Dahlen* (1982) had affirmed that this approximation is excellent for wavelengths that are very little compared with the Earth ratio. The

resulting anomaly (**Fig**. 3, bottom), although in meters, keeps the features of the classical isostatic anomaly, since they were both obtained comparing the observed and computed anomalies from isostatically balanced models. The first one, using the geoide undulations in meters, and the latter, using gravity responses in mGal.

Comparing the results (**Fig**. 3), very good morphologic correlation between both isostatic indices was found.

Finally, two inversions were carried out: one from the regionalized Bouguer anomaly, and the other one from the satellite geoide undulations (in Andean wavelengths) (**Fig**. 4). Both of them result on a crustal model with a maximum thickness of 65 km beneath the West Cordillera, while beneath the East Cordillera, Moho computed using both methods rises revealing a deficit of compensating mass. Although there exist heat excess (*Kono et al.*, 1989), and shortening values we have obtained (*Cabassi and Introcaso*, 1997) are much higher than those proposed by *Sheffels* (1993), which is a necessary condition for delamination, this subject will not be dealt with in this short communication.

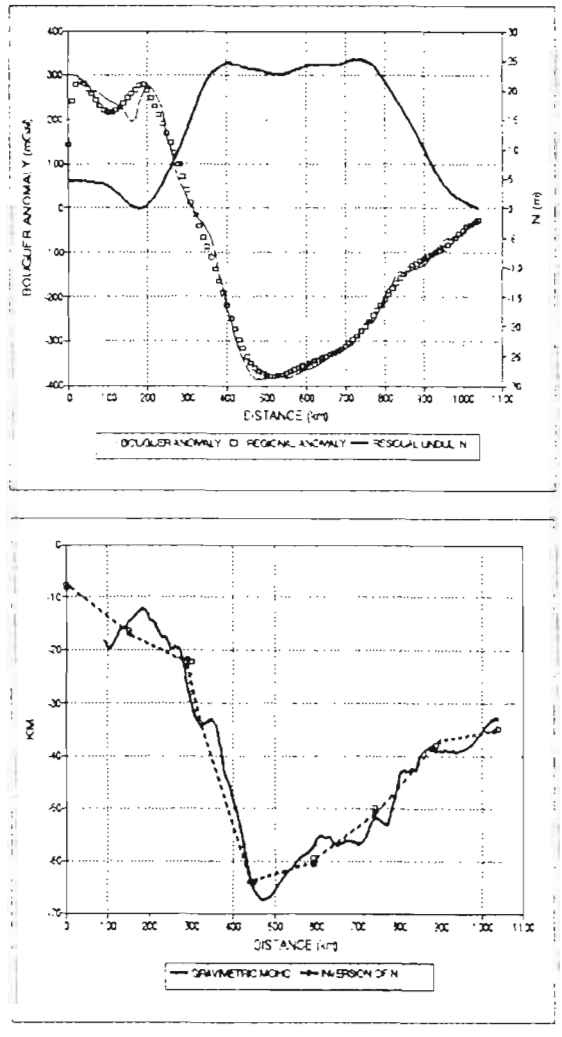

Fig. 4: Double Inversion Model (bottom) from Bouguer Anomaly (AB, mGal) and residual geoid undulation N(m) (top).

CONCLUSIONS

Nazca section corresponding to the Peruvian Andes was analysed, finding regionalized Bouguer anomalies with a minimum of -380 mGal beneath the West Cordillera, and only -260 mGal under the East Cordillera.. This last anomalous area was studied using both isostatic anomalies and classical inversion from Bouguer ones, and residual geoide undulations in Andean wavelengths, involving remove of the topo-isostatic effects.

Very good morphologic consistence in the isostatic state indices (undercompensation) was found using one method or the other. This reveals the importance of analysing the geoide undulations in the Andes to define the structure's features.

ACKNOWLEDGMENTS

This study had been supported by a Grant of the Agencia de Promoción Científica y Tecnológica. Project 07-00026-00508.

REFERENCES

Cabassi, I.R., and A. Introcaso, (1997): Análisis Gravimétrico y Acortamientos en la sección de Nazca (Andes Peruanos). *Rev., Asociación Argentina de Geofísicos y Geodestas (AAGG)*, San Juan, oct. 28-31, 1997, Argentina, 149-154.

Dahlen, F.A., (1982): Isostatic Geoid anomalies on a sphere. *Journ. Geoph. Res.*, 87, 3943-3947.

Haxby, W.F., and D.L. Turcotte, (1978): On isostatic geoid anomalies. *Journ. Geoph. Res.*, 83(B11), 5473-5478.

Kono, M., Y. Fukao, and A. Yamamoto, (1989): Mountain Building in the Central Andes. *Journ. Geoph. Res.*, 94(B4), 3891-3905.

Marsh, J.G., and T.W. Martin, (1982): The seasat altimeter mean sea surface model. *Journ. Geoph. Res.*, 87, 3269-3280.

Sandwell, D.T., and M.L. Renkin, (1988): Compensation of swells and Plateaus in the North Pacific: No indirect evidence for mantle convection. *Journ. Geoph. Res.*, 93, 2775-2783.

Sheffels, B.M., (1993): Has delamination of the lower lithosphere of the Central Andes ocurried?. *2nd. ISAG*, Oxford, U.K., 21-24.

Turcotte, D.L., and S. Schubert, (1982): *Geodynamics: application of continuum physics to geological problem*. Jhon Wiley, N.Y., 450 pp.

Yecai, L., (1994): Software GRAVT_GM, *Univ. Calgary, Alberta*, Canadá, modified from Dr. R. H. Rapp (*Reporte OSU*), Ohio State Univ., U.S.A.

CENTRAL ANDES: THE GRAVITY SIGNAL FROM THE SUBDUCTING SLAB

Carlos IZARRA(1), Nick KUSZNIR(1) and Huw DAVIES(1)

(1)Department of Earth Sciences, University of Liverpool, Liverpool L69 3BX, UK

KEYWORDS: Subduction, Gravity, Thermal Modelling, Isostasy

INTRODUCTION

Subduction at active continental margins, as exemplified by the subduction of the Nazca Plate under the Central Andes, is a fundamental process within plate tectonics. However there are many aspects of the subduction process which are poorly understood, for example the mass distribution, mass balance and dynamics of the subduction process. Gravity studies of the Central Andes have shown a residual isostatic anomaly less than 70mgal (Götze *et al.*, 1996; Kirchner *et al.*, 1996; Introcaso *et al.*, 1992, Kaban et al., 1999). On the other hand seismically determined crustal thickness indicates that the Central Andes are roughly in Airy isostatic equilibrium (Beck *et al.*, 1996). The combination of these observations suggests that the gravity signal from the subducting slab is small. Thermal modelling of the subducting slab under the Central Andes, assuming an isothermal asthenosphere wedge above the slab and neglecting phase transition, shows that the gravity effect from the slab exceeds 160 mgal. This discrepancy between the observed gravity anomaly of the subducted slab and that predicted from thermal models demands explanation and suggests that our understanding of the subduction process is incomplete. We believe that the resolution of this paradox lies not with the thermal model of the subducting slab, but with compensating mechanisms, either within or above the subducting slab, related to subduction dynamics.

References

Beck, S. L., G. Zandt, S. C. Myers, T. C. Wallace, P. G. Silver, and L. Drake 1996. Crustal-thickness variations in the Central Andes. *Geology*, v. 24, no. 5, 407-410.

Götze H.-J., S. Schmidt, A. Kirchner, M. Kösters, M. Araneda, and N. G. López 1996. Gravity field and geoid at the south American active margin (20° to 29° S). *Andean Geodynamics (ISAG96), extended abstracts*, St. Malo (France), 47-50.

Introcaso A., M. C. Pacino, and H. Fraga 1992. Gravity, isostasy and Andean crustal shortening between latitudes 30 and 35° S. *Tectonophysics*, 205, 31-48.

Kaban, M.K., Schwintzer, P, and Tikhotsky, S.A. 1999. A global isostatic gravity model of the Earth. Geophys. J. Int., 136, 519-536.

Kirchner A., H.-J. Götze, K. Lessel, and M. Schmitz 1996. A 3-D model for the central Andes based on joint interpretation of seismics and gravity. *Andean Geodynamics (ISAG96), extended abstracts*, St. Malo (France), 67-70.

LATE PALEOZOIC - EARLY MESOZOIC PLUTONISM AND RELATED RIFTING IN THE EASTERN CORDILLERA OF PERU

Javier JACAY(1), Thierry SEMPERE(2), Gabriel CARLIER(2), Víctor CARLOTTO(3)

(1)Universidad Nacional Mayor de San Marcos, apartado postal 3973, Lima 100, Peru
(2)IRD (ex-ORSTOM), apartado postal 18-1209, Lima 18, Peru (ird@chavin.rcp.net.pe)
(3)Universidad Nacional de San Antonio Abad del Cusco, Cusco, Peru (carlotto@chaski.unsaac.edu.pe)

KEY WORDS : Rifting, Early Mesozoic, Peru, Eastern Cordillera.

INTRODUCTION

Continental and marine sedimentary rocks of Permian, Triassic and Jurassic age have long been reported from central Peru (McLaughlin, 1924; Steinmann, 1929). These rocks traditionally form the Mitu and Pucará groups (Harrison, 1943, 1951; Jenks, 1951; Newell et al., 1953) and crop out nearly all along the Eastern Cordillera of Peru (Dalmayrac et al., 1980). The Mitu group furthermore includes volcanic rocks that are related to coeval granitoid emplacement, and records rifting processes of Late Permian-Triassic age (Mégard, 1978; Noble et al., 1978; Dalmayrac et al., 1980; Kontak et al., 1990; Rosas et al., 1997; Sempere et al., 1998).

Rifting initially produced grabens where locally >2000m-thick alluvial and lacustrine red deposits and evaporites accumulated above preserved Upper Paleozoic strata. Paleoenvironments include alluvial fans, streams, and (playa-)lakes. Limestones bearing Late Permian fusulinids are locally intercalated in the alluvial infill and record marine ingressions within some grabens (Laubacher, 1978). Abundant alkaline volcanic rocks were locally erupted in relation with plutonism at depth (Noble et al., 1978, Kontak et al., 1990).

In northern and central Peru, subsequent thermal sag permitted that the sea ingressed from the north along the rift axis (Fig. 1). The Pucará Group carbonates were deposited during the Norian-Liassic interval (Rosas and Fontboté, 1995). Numerous manifestations of basic alkaline volcanism are reported from the western Pucará basin (Kobe, 1995). In the eastern and southeastern Peru, time-equivalents deposits of the Pucará Group are in part represented by continental red beds (lower Sarayaquillo Fm; Mégard, 1978).

In southern Peru (Arequipa area), extension progressed during the Liassic and Dogger, and culminated in the Bajocian-Bathonian when a deep marine trough formed (Yura Group, Vicente et al., 1982; Sempere

et al., 1999). West of Lake Titicaca, synsedimentary extension is recorded, and basic sills intrude the Paleozoic and the Jurassic Muni Fm; the latter is transitionally overlain by the Lower Huancané Fm fluvio-eolian sandstones (Newell, 1949), which recalls the basalt-bearing Ravelo Fm of Bolivia. Fluvio-eolian sandstones occur in the Caycay Fm of the Cusco-Sicuani area, locally associated with alkaline basalts (Carlotto, 1998).

The roots of this late Paleozoic-early Mesozoic rift are exposed in the Eastern Cordillera and are mainly composed of Precambrian to early Paleozoic metamorphic rocks (Sempere et al., 1999). In central Peru, peridotite bodies occur in Precambrian metamorphic rocks, Mississippian plutons and at the Mitu/Pucará contact (Aumaître et al., 1977; Jacay, 1996; Mégard et al., 1996; Quispesivana, 1996). Given these geologic relationships, the peridotite bodies were possibly emplaced in the Jurassic in relation with major stretching and/or wrenching of the crust and with basic magmatism in this segment of the rift system. It is possible that in this segment rifting reached a state significantly more advanced than in other areas due to its earlier onset.

Numerous plutons also intrude the metamorphic basement exposed in the rift roots. They consist of a variety of granites, granodiorites and alkaline granitoids, which apparently display 2 clusters of ages: a large set of mainly northern plutons was emplaced during the Mississippian, and a larger one during the Late Permian and Triassic (Table 1; Fig. 1). This suggests that Late Permian-Triassic rifting was established along an area that had already been weak in the Mississippian.

Table 1: Ages obtained on Late Paleozoic - Early Mesozoic plutons in the Eastern Cordillera of Peru.

age (Ma)	method	dated	locality	composition	reference
359 ± 14	K/Ar	wr			Bonhomme et al., 1985
346.7 ± 7.3	K/Ar	B	Balsas	monzogranite to syenogranite	Sánchez, 1983
346 ± 10	K/Ar	B	Pacococha	adamellite	Maluski & Blatrix *in* Mégard, 1978
338 ± 8	K/Ar	B	Callangate-Enaben	granodiorite to monzogranite	Sánchez, 1995
331 ± 5	K/Ar	H		monzodiorite	Bonhomme et al., 1985
331 ± 20	K/Ar		Tambo-Perené	basalt	Martin & Paredes, 1977
330 ± 10	U/Pb	Z	Amparaes	orthogneiss	Lancelot *in* Marocco, 1978
329 ± 1	U/Pb	Z	Parcoy	granodiorite	Vidal et al., 1995
329 ± 10	K/Ar	B	Callangate-Enaben	granodiorite to monzogranite	Sánchez, 1995
321	Ar/Ar	B	Pataz	granodiorite to monzogranite	Schreiber et al., 1990
305	Ar/Ar	H	Pataz	granodiorite to monzogranite	Schreiber et al., 1990
294 ± 3	K/Ar	H	C° Pucará	essexite	Bonhomme et al., 1985
279.9 ± 3.3	K/Ar	wr	16°40'S, 68°36'W	basalt	Kontak et al., 1990
272 ± 10	K/Ar	H + B	C° Pucará, Juliaca	lava	Klinck et al., 1991
270	K/Ar	B	San Judas Tadeo	monzogranite	Kontak et al., 1985
262.9 ± 4.5	K/Ar	B	San Judas Tadeo	granodiorite	Kontak et al., 1985
260 ± 25	K/Ar	wr	hacienda Chorrillos	diorite	Rocha-Campos & Amaral, 1971
257 ± 3	U/Pb	Z	Quillabamba	granite	Lancelot et al., 1978
253 ± 11	K/Ar	M	Esquicocha	granite	Soler et al., 1990
251	K/Ar		Villa Azul	granite	Stewart et al., 1974
246 ± 10	Rb/Sr	B	Machu Picchu	granite	Priem *in* Egeler & De Booy, 1961
245 ± 11	K/Ar	B	Talhuis	quartz-diorite to granodiorite	Soler et al., 1990
244.9 ± 2.9	K/Ar	glass	16°40'S, 68°36'W	basalt	Kontak et al., 1990
238 ± 11	U/Pb	Z	Coasa	granite	Lancelot et al., 1978
238 ± 10	Rb/Sr	wr	La Merced	granite	Capdevila et al., 1977
236 ± 6	K/Ar	B	Huisaroque	tonalite	Klinck et al., 1991
235 ± 3	U/Pb	Z	Aricoma	granodiorite	Lancelot *in* Carlier et al., 1982
233 ± 10	K/Ar	B	Carrizal	tonalite / quartz-monzonite	Soler et al., 1987

230 ± 10	U/Pb	Z	Arcoma	granodiorite	Lancelot *in* Laubacher, 1978
227 ± 3	K/Ar	H		essexite	Bonhomme et al., 1985
225 ± 14.8	K/Ar	M	Arcoma	quartz vein	Kontak et al., 1990
222 ± 7	U/Pb	Z	Abancay	cataclastic ?granite	Lancelot *in* Carlier et al., 1982
216.8 ± 4.5	K/Ar	B	Arcoma	monzogranite	Kontak et al., 1990
216.2 ± 4.3	K/Ar	M	Coasa	granite	Kontak et al., 1990
211.0 ± 10.1	Rb/Sr	wr + B	Coasa	monzogranite	Kontak et al., 1990
210.9 ± 4.3	K/Ar	B	Coasa	monzogranite	Kontak et al., 1990
210.8 ± 4.2	K/Ar	B	Coasa	monzogranite	Kontak et al., 1990
210.7 ± 10.4	Rb/Sr	wr + B	Arcoma	monzogranite	Kontak et al., 1990
210.2 ± 4.2	K/Ar	B	Coasa	monzogranite	Kontak et al., 1990
209.3 ± 4.2	K/Ar	B	Coasa	monzogranite	Kontak et al., 1990
208.5 ± 2.6	Rb/Sr	wr + B	Coasa	monzogranite	Kontak et al., 1990
207.8 ± 4.4	K/Ar	B	Coasa	monzogranite	Kontak et al., 1990
207.7 ± 4.1	K/Ar	B	Coasa	monzogranite	Kontak et al., 1990
205.6 ± 10.3	Rb/Sr	wr + B	Coasa	monzogranite	Kontak et al., 1990
205.3 ± 4.2	K/Ar	B	Coasa	monzogranite	Kontak et al., 1990
204.5 ± 6.4	Rb/Sr	wr + B	Coasa	monzogranite	Kontak et al., 1990
204.1 ± 1.5	Rb/Sr	wr + B	Coasa	monzogranite	Kontak et al., 1990
202 ± 2	U/Pb	Z	San Gabán	gabbro to diorite and monzogranite	Kontak et al., 1991
199 ± 10	Rb/Sr	M	Limacpampa	monzogranite	Kontak et al., 1990
180	K/Ar	B	Macusani	syenite	Stewart et al., 1974
174.7 ± 3.6	K/Ar	B	Allincápac	syenite	Kontak et al., 1990
173.5 ± 3.1	K/Ar		Macusani	syenite	Kontak et al., 1985
133 ± 7	Rb/Sr	M	Gavilán de Oro	granite	Kontak et al., 1990
131 ± 5	K/Ar		Ayacucho	lava	Noble et al., 1978

REFERENCES

Aumaître, R., Grandin, G., Guillon, J. H., 1977. Données lithologiques et structurales relatives à un bloc précambrien surélevé de la Cordillère andine orientale (Pérou central). Les corps de roches ultrabasiques qui y sont présents. Bulletin de la Société Géologique de France, v. 19, p. 983-989.

Bonhomme, M. G., Audebaud, E., Vivier, G. 1985. K-Ar ages of Hercynian and Neogene rocks along an east-west cross section in southern Peru. Comunicaciones, Santiago de Chile, v. 18, p. 27-30.

Carlier, G., Grandin, G., Laubacher, G., Marocco, R., Mégard, F. 1982. Present knowledge of the magmatic evolution of the Eastern Cordillera of Peru. Earth Science Reviews, v. 18, p. 253-283.

Carlotto, V. 1998. Evolution andine et raccourcissement au niveau de Cusco (13°-16°S, Pérou). Thèse de doctorat, Université de Grenoble, France, 159 p. + figs.

Capdevila, R., Mégard, F., Paredes, J., Vidal, P. 1977. Le batholite de San Ramón, Cordillère Orientale du Pérou central. Geologische Rundschau, v. 66, p. 434-446.

Dalmayrac, B., Laubacher, G., Marocco, R. 1980. Caractères généraux de l'évolution géologique des Andes péruviennes. Travaux et Documents de l'ORSTOM, Paris, v. 122, 501 p.

Egeler, C.G., De Booy, T. 1961. Preliminary note on the geology of the Cordillera Vilcabamba (SE Peru), with emphasis on the essentially pre-Andean origin of the structure. Geologie en Mijnbouw, v. 40, p. 319-325.

Harrison, J.V., 1943. The geology of the Central Andes in part of the province of Junín, Peru. Quarterly Journal of the Geological Society of London, v. 99, p. 1-36.

Harrison, J.V., 1951. Geología de los Andes orientales del Perú central. Boletín de la Sociedad Geológica del Perú, v. 21, 97 p.

Jacay, J., 1996. Geología del cuadrángulo de Singa. Boletín INGEMMET, serie A, v. 67, 214 p.

Jenks, W.F., 1951. Triassic stratigraphy near Cerro de Pasco, Peru. Geological Society of America Bulletin, v. 62, p. 203-220.

Klinck, B. A., Allison, R. A., Hawkins, M. P., Palacios, O., De La Cruz, J., De La Cruz, N., 1991. Geología de la Cordillera Occidental y Altiplano al oeste del Lago Titicaca, Sur del Perú. Boletín INGEMMET, serie A, v. 42, 253 p.

Kobe, H. 1995. Componentes volcánicos, evaporíticos y sedimentos metalíferos en la parte occidental de la cuenca del Grupo Pucará, Perú central. Sociedad Geológica del Perú, volumen jubilar Alberto Benavides, p. 179-191.

Kontak, D.J., Clark, A.H., Farrar, E., Strong, D.F., 1985. The rift associated Permo-Triassic magmatism of the Eastern Cordillera: a precursor to the Andean orogeny. *In* Magmatism at a plate edge: the Peruvian Andes, W.S. Pitcher, M.P. Atherton, J. Cobbing, R.D. Beckinsale (eds.), Londres, p. 36-44.

Kontak, D. J., Clark, A. H., Farrar, E., Archibald, D. A., Baadsgaard, H. 1990. Late Paleozoic-Early Mesozoic magmatism in the Cordillera de Carabaya, Puno, southeastern Peru: Geochronology and petrochemistry. Journal of South American Earth Sciences, 3, 213-230.

Kontak, D. J.. Clark, A. H., Farrar, E., Tosdal, R. M. 1991. Geochronology and petrology of the San Gabán igneous complex of southern Peru: implications for Triassic-Jurassic felsic magmatism and Sn-W metallogeny in the Central Andes. Abstract, Geological Association of Canada.

Lancelot, J.R., Laubacher, G., Marocco, R., Renaud, U. 1978. U/Pb radiochronology of two granitic plutons from the Eastern Cordillera (Peru): Extent of Permian magmatic activity and consequences. Geologische Rundschau, v. 67, p. 236-243.

Laubacher, G., 1978. Géologie de la Cordillère Orientale et de l'Altiplano au nord et nord-ouest du lac Titicaca (Pérou). Travaux et Documents de l'ORSTOM, v. 95, 217 p.

Marocco, R. 1978. Un segment E-W de la chaîne des Andes péruviennes: la déflexion d'Abancay. Etude géologique de la Cordillère Orientale et des Hauts Plateaux entre Cuzco et San Miguel (Sud du Pérou, 12°30'S à 14°S). Travaux et Documents de l'ORSTOM, Paris, v. 94, 195 p.

Martin, C., Paredes, J. 1977. Données nouvelles sur le Paléozoïque de la zone subandine du Pérou central. Comptes Rendus de l'Académie des Sciences, Paris, série D, v. 284, p. 1647-1650.

McLaughlin, D.H., 1924. Geology and physiography of the Peruvian Cordillera, departments of Junín and Lima. Geological Society of America Bulletin, 35, p. 591-632.

Mégard, F., 1968. Geología del cuadrángulo de Huancayo. Boletín del Servicio Geológico, n° 18, 123 p.

Mégard, F., 1978. Etude géologique des Andes du Pérou central. Travaux et Documents de l'ORSTOM, París, v. 86, 310 p.

Mégard, F., Caldas, J., Paredes, J., De La Cruz, N., 1996. Geología de los cuadrángulos de Tarma, La Oroya y Yauyos. Boletín INGEMMET, serie A, v. 69, 279 p.

Newell, N.D., 1949. Geology of the Lake Titicaca region, Peru and Bolivia. Geological Society of America Memoir, v. 36, 111 p.

Newell, N.D., Chronic, J., Roberts, T. 1953. Upper Paleozoic of Peru. Geological Society of America Memoir 58, 276 p.

Noble, D.C., Silberman, M.L., Mégard, F., Bowman, H.R., 1978. Comendite (peralkaline rhyolites) in the Mitu Group, central Peru: Evidence of Permian-Triassic crustal extension in the Central Andes. U.S. Geological Survey Journal of Research, v. 6, p. 453-457.

Noble, D.C., McKee, E., Petersen, U., Alvarez, A., Yupanqui, M. 1995. The Cobriza copper skarn deposits, central Perú: Permian age, radiogenic lead, isotope composition and association with two-mica granite. Sociedad Geológica del Perú, volumen jubilar Alberto Benavides, p. 239-242.

Quispesivana, L. 1996. Geología del cuadrángulo de Huanuco. Boletín de INGEMMET, serie A, v. 75, 138 p.

Rocha-Campos, A. C., Amaral, C. 1971. K/Ar ages of igneous rocks of the Mitu Group, Huancayo region, central Peru. Boletín Paranense de Geociencias, v. 28-29, p. 3-7.

Rosas, S., Fontboté, L., 1995. Evolución sedimentológica del Grupo Pucará (Triásico superior-Jurásico inferior) en un perfil SW-NE en el centro del Perú. Sociedad Geológica del Perú, volumen jubilar Alberto Benavides, p. 279-309.

Rosas, S., Fontboté, L., Morche, W., 1997. Vulcanismo de tipo intraplaca en los carbonatos del Grupo Pucará (Triásico superior-Jurásico inferior, Perú central) and su relación con el vulcanismo del Grupo Mitu (Pérmico superior-Triásico). IX Congreso Peruano de Geología, p. 393-396.

Sánchez, A. 1983. Nuevos datos K/Ar en algunas rocas del Perú. Boletín de la Sociedad Geológica del Perú, v. 71, p. 193-202.

Sánchez, A. 1995. Geología de los cuadrángulos de Bagua Grande, Jumbilla, Lonya Grande, Chachapoyos, Rioja, -bamba y Bolívar. Boletín INGEMMET, serie A, n° 56, 285 p.

Schreiber, D.W., Fontboté, L., Lochmann, D. 1990. Geologic setting, paragenesis and physicochemistry of gold quartz veins hosted by plutonic rocks in the Pataz region. Economic Geology, v. 85, p. 1328-1347.

Sempere, T., Carlier, G., Carlotto, V., Jacay, J., 1998. Rifting Pérmico superior - Jurásico medio en la Cordillera Oriental de Perú and Bolivia. Memorias, XIII Congreso Geológico Boliviano, Potosí, v. 1, p. 31-38.

Sempere, T., Carlier, G., Carlotto, V., Jacay, J., Jiménez, N., Rosas, S., Soler, P., Cárdenas, J., Boudesseul, N. 1999. Late Permian-Early Mesozoic rifts in Peru and Bolivia, and their bearing on Andean-age tectonics. IV ISAG, Göttingen, this volume.

Soler, P., Bonhomme, M., 1987. Données radiochronologiques K/Ar sur les granitoïdes de la Cordillère Orientale des Andes du Pérou Central. Implications tectoniques. Comptes Rendus de l'Académie des Sciences, Paris, série II, v. 304, p. 841-845.

Steinmann, G., 1929. Geologie von Peru. Karl Winter, Heidelberg, 448 p.

Stewart, J. W., Evernden, J. F., Snelling, N. J. 1974. Age determinations from Andean Peru: a reconnaissance survey. Geological Society of America Bulletin, v. 85, p. 1107-1116.

Vicente, J.-C., Beaudoin, B., Chávez, A., León, I., 1982. La cuenca de Arequipa (Sur Perú) durante el Jurásico-Cretácico inferior. V Congreso Latinoamericano de Geología, v. 1, p. 121-153.

Vidal, C., Paredes, J., Macfarlane, A., Tosdal, R. 1995. Geología y metalogenia del distrito minero Parcoy, provincia aurífera de Pataz, La Libertad. Sociedad Geológica del Perú, volumen jubilar Alberto Benavides, p. 351-377.

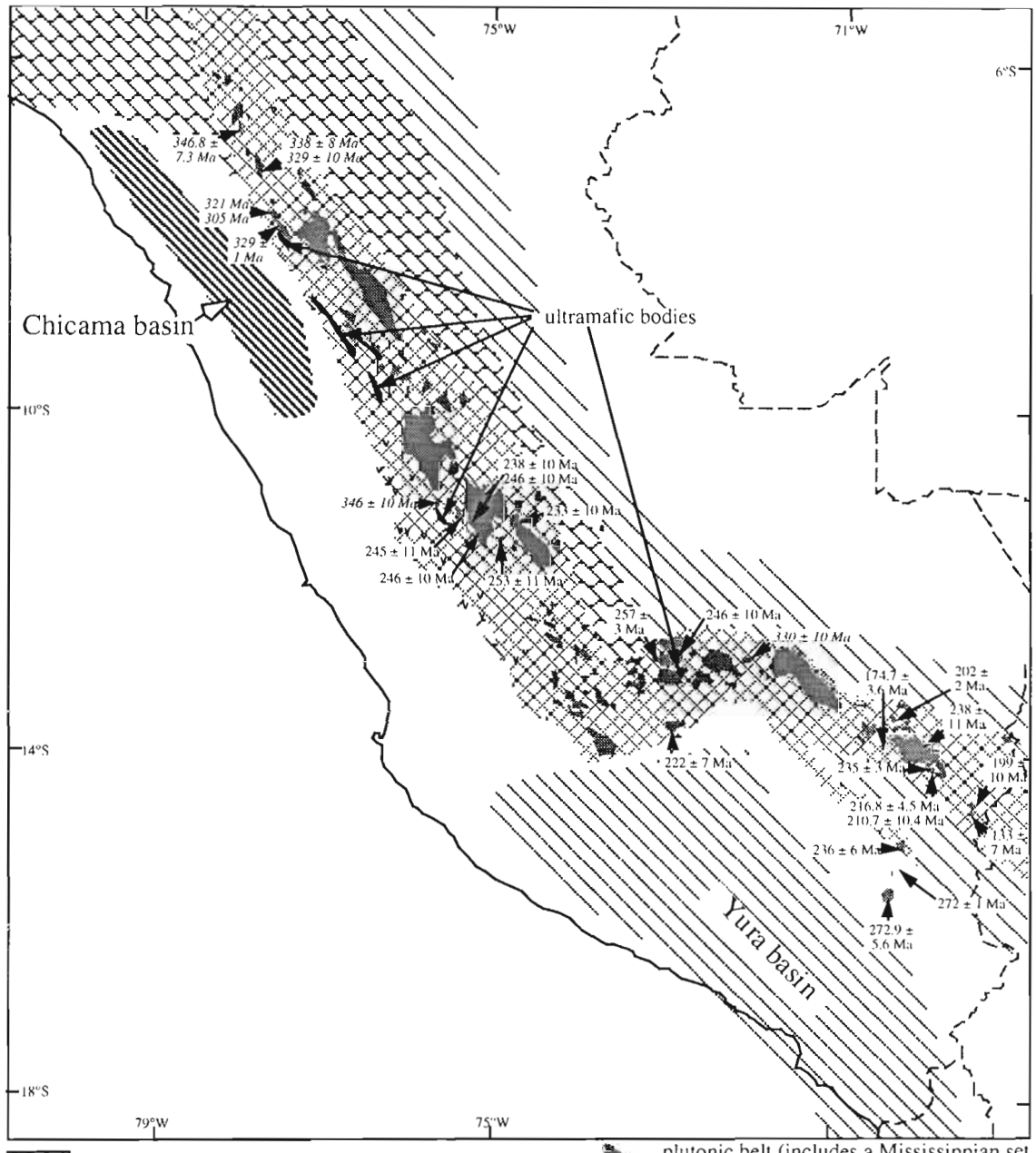

Figure 1. Selected Upper Paleozoic - Jurassic paleogeographic elements of Peru.

HERCYNIAN DEFORMATION AND METAMORPHISM IN THE EASTERN CORDILLERA OF SOUTHERN BOLIVIA

Volker JACOBSHAGEN (1), Joachim MÜLLER (1), Hans AHRENDT (2) and Klaus WEMMER (2)

(1) Freie Universität Berlin, FR Allgemeine Geologie, Malteserstr. 74-100, D - 1249 Berlin, Germany, (e-mail vojac@zedat.fu-berlin.de, and jotpecm@zedat.fu-berlin.de)
(2) Universität Göttingen, Institut für Geologie und Dynamik der Lithosphäre (IGDL), Goldschmidtstr. 3, D - 37077 Göttingen, Germany (e-mail kwemmer@gwdg.de)

KEY WORDS: Bolivia, Eastern Cordillera, Palaeozoic orogenesis, K/Ar dating, Ordovician schists

INTRODUCTION

The Eastern Cordillera of southern Bolivia belongs to the back-arc region of the Central Andes. It consists of a basement built up by more than 8000 m marine clastics of Cambro-Ordovician age, which is unconformably covered by Cretaceous redbeds with mafic volcanics in places and/or by late Tertiary continental deposits (Kley et al., 1997). The basement had already undergone a Palaeozoic orogenetic event, which is documented by a break of metamorphism between Ordovician and Cretaceous rocks and by low-angle unconformities at the base of the Cretaceous, that testify to flat, widespanned folds within the basement. The most obvious feature of the Palaeozoic orogenesis is, however, a slaty cleavage, which occurs everywhere.

Two Palaeozoic orogenies have been proposed to explain the pre-Cretaceous deformations of the basement. In Argentina, on one hand, the late Ordovician Oclóyic orogeny is believed to have caused the prevailing structures of the basement. Its age is well documented by stratigraphic gaps and/or unconformities and by radiometric data (e.g. Turner, 1960, Coira et al., 1982, Mon and Hongn, 1991). The later Chanic orogeny of late Devonian to Dinantian age seems to be of minor importance, there (Mon and Salfity,

1995). In Peru and Northern Bolivia, on the other hand, folding and cleavage of the Ordovician have been referred to an Eohercynian (i.e. Chanic) orogeny, whereas indications of Oclóyic deformations are unknown there (Dalmayrac et al., 1977, Martinez, 1980). In Southern Bolivia, however, neither stratigraphic nor radiometric data had existed up to now to fix the age of the main Palaeozoic orogeny. Nevertheless, Kley and Reinhardt (1994) had found indications of a Hercynian event: From geothermometric measurements of Ordovician rocks along a transsect Tarija-Tupiza-San Vicente they have concluded that these rocks had been overlain by 4-6 km of Palaeozoic sediments during metamorphism. At least parts of that cover must have been younger than Ordovician. Furthermore, tectonic deformations of Oclóyic age is highly improbable at least for the western part of that transsect, because Ordovician sequences there include Caradocian and perhaps even Ashgillian strata (Müller et al., 1996).

RADIOMETRIC DATATION

To define the age of Palaeozoic cleavage, phyllosilicates of 9 samples of fine-grained Ordovician rocks have been dated with the K/Ar method. Sample preparation and measurements were carried out in the IGDL laboratories, Göttingen University, following the procedures described in Wemmer (1991) and Ahrendt et al. (1996). From each sample the grain-size fractions <2 µm and <0.2 µm have been measured. The resulting experimental ages have been interpreted in relation to illite crystallinity data from the sample area. That procedure is based on the experience that, on one hand, during very low-grade metamorphism below the medium anchizone temperatures would not be sufficient to adjust all constituants of the <2 µm size fraction to that event, resulting in mixed ages of synkinematically grown and older detrital illites. In that case the age of metamorphism would most probably result from the <0.2 µm fraction, which is highly enriched in newly formed illites. If, on the other hand, metamorphism had surmounted the medium anchizone, its age can be expected from measuring the illites of the <2 µm fraction. On that base we achieved 7 ages in the range of 325-288 Ma. Taking the above mentioned detrital contamination into account, metamorphism has taken place at 310-280 Ma, i..e. from latest Carboniferous to Early Permian.

DISCUSSION AND CONCLUSIONS

Most of our data indicate that metamorphism and cleavage formation of the Ordovician rocks of Southern Bolivia have to be related neither to the Oclóyic nor to the Chanic orogeny, but, surprisingly, to late Hercynian processes. It seems to be difficult, at present, to interprete this result within the framework of the Central Andes.

Orogenetic activities of Late Carboniferous and Permian age are known from many regions of the Central Andes. Within the Chilean Precordillera, adjacent to southern Bolivia, considerable compressional deformations seem to have happened in early Late Carboniferous times (Toco event, Bahlburg and Breitkreuz, 1991), followed by post-orogenic intrusions at about 318 Ma. From Northern Argentina, an intra-Permian "San Rafael orogeny" is reported at about 265 Ma (Mon and Salfity, 1995). In Northern Bolivia, big stratigraphic hiatuses point to important tectonic activities in early Late Carboniferous as well as in Middle Permian times (Isaacson and Díaz Martínez, 1995).

It is certainly too early to draw out the geometries of late Palaeozoic orogens and their evolution in time and space for the Central Andes. Nevertheless, orogenies of Hercynian age are of a major importance, there, and should be more in the view of geologists. Anyway, for the Eastern Cordillera of southern Bolivia it should be taken into consideration that a distinct Chanic orogen might have been overprinted by late Hercynian geothermal orogenetic processes.

REFERENCES

Ahrendt H., Franzke H.-J., Marheine D., Schwab M., and Wemmer K. 1996. Zum Alter der Metamorphose in der Wippraer Zone/Harz - Ergebnisse von K/Ar-Altersdatierungen an schwachmetamorphen Sedimenten. Zeitschrift der Deutschen Geologischen Gesellschaft, 147, 39-56.

Bahlburg H., and Breitkreuz C. 1991. Paleozoic evolution of active margin basins in the southern Central Andes (northwestern Argentina and northern Chile). Journal of South American Earth Sciences, 4, 171-188.

Coira B., Davidson J., Mpodozis C., and Ramos V. 1982. Tectonic and magmatic evolution of the Andes of Northern Argentina and Chile. Earth-Science Reviews, 18, 303-332.

Dalmayrac B., Laubacher G., Marocco R., Martinez C., and Tomasi C. 1980. La chaîne hercynienne de l'Amérique du sud. Structure et évolution d'un orogène intracratonique. Geologische Rundschau, 69, 1-21.

Isaacson P. E., and Díaz Martínez E. 1995. Evidence for a middle-late Paleozoic foreland basin and significant paleolatitudinal shift, Central Andes. *In* Tankard A. J., Suarez S., R., and Welsink H. J., eds., Petroleum basins of South America. AAPG Memoir, 62: Tulsa, 231-249.

Kley J., and Reinhardt M. 1994. Geothermal and tectonic evolution of the Eastern Cordillera and the Subandean Ranges of Southern Bolivia. *In* Reutter K.J., Scheuber E., and Wigger P., eds., Tectonics of the southern Central Andes. Berlin (Springer), 155-170.

Kley J., Müller J., Tawackoli S., Jacobshagen V., and Manutsoglu E. 1997. Pre-Andean and Andean-age deformation in the Eastern Cordillera of Southern Bolivia. Journal of South American Earth Sciences, 10, 1-19.

Martinez C. 1980. Structure et évolution de la chaîne hercynienne et de la chaîne andine dans le nord de la Cordillère des Andes de Bolivie. Travaux et Documents d' ORSTOM, 119: Paris, 352 p.

Mon R. and Hongn F.D. 1991. The structure of the Precambrian and lower Paleozoic basement of the Central Andes between 22° and 32° S latitude. Geologische Rundschau, 80, 745-758.

Mon R. and Salfity J.A. 1995. Tectonic evolution of the Andes of northern Argentina. *In* Tankard A.J., Suarez S., R., and Welsink H.J. 1995, eds., Petroleum basins of South America, AAPG Memoir 62: Tulsa, 269-283.

Müller J., Maletz J., Egenhoff S., and Erdtmann B.-D. 1996. Turbiditas Caradocianas – (?)Ashgillianas inferiores en la Cordillera Oriental al sur de Bolivia: Implicaciones cinematicas. Memorias del XII Congresso Geologico de Bolivia – Tarija, Bolivia: 747-753.

Turner J.C.M. 1960. Estratigrafia de la Sierra de Santa Victoria y adyiencias. Boletin de la Academia Nacional de Ciencias, 41, 163-196.

Wemmer K. 1991. K/Ar-Altersdatierungsmöglichkeiten für retrograde Deformationsprozesse im spröden und duktilen Bereich - Beispiele aus der KTB-Vorbohrung (Oberpfalz) und dem Bereich der Insubrischen Linie (N-Italien). Göttinger Arbeiten zur Geologie und Paläontologie, 51: Univ. Göttingen, 61 pp.

STRUCTURAL AND ISOSTATIC MODELLING OF SERRANIA DEL INTERIOR THRUST BELT AND MONAGAS FORELAND BASIN: EASTERN VENEZUELA.

M.I. JACOME(1), N. KUSZNIR (1) and S. FLINT (1).

(1) Department of Earth Sciences, University of Liverpool, Liverpool L69 3 BX, UK; e-mail: cata@liv.ac.uk

KEY WORDS: Flexure, subsidence, Isostasy, thrust sheet loading, subduction dynamics.

INTRODUCTION

Geometrical structural modelling has been used by many workers to investigate the evolution of the Serrania del Interior thrust belt and the formation of the Monagas foreland basin. Flexural isostatic modelling indicates however that thrust-sheet loading predicted by these geometric models is insufficient to generate the observed subsidence within the Monagas basin deduced from seismic reflection and well data.

Based on earthquake and gravimetric evidence, we postulate that the additional subsidence in the Monagas basin is due to lithospheric deflection produced by NW dipping continental subduction of Trinidad and eastern Venezuela beneath the Caribbean Plate.

This work uses cross-section balancing and its flexural-isostatic response to generate a sequence of forward models from Cretaceous to present across the Serrania del Interior thrust belt to the Monagas foreland basin.

The predictions of these models are tested using stratigraphic, gravimetric and seismic data. Our objectives are to understand the processes responsible for the formation of the Monagas basin, to determine the contribution of thrust sheet loading, and to investigate the influence of other geodynamic processes (eg subduction).

Geological Setting.

The study area is located in NE Venezuela and covers an area of ~ 75,000 km^2. Four major tectonic features can be identify: the Serrania del Interior thrust belt (max. altitude of ~2300 m), the Monagas foreland basin (max. thickness ~ 11 km), the westward oceanic subduction zone of the Lesser Antilles, and northwest dipping continental subduction of the South American Plate under the Caribbean.

Eastern Venezuela has undergone complex tectonic interactions including the break-up of Pongea during the Jurassic, the development of northward dipping passive margin during the Cretaceous to Paleogene, and the formation of the Serrania del Interior transpressional thrust belt and the Monagas foreland basin during the Miocene. Thrusting and basin generation were produced as the result of the oblique convergence between the Caribbean plate and the South American plate. Present day configuration is shown in Figure 1. Five geological provinces can be identified: North of the El Pilar fault are the Araya-Paria Metamorphic and Oceanic igneous rocks, to the south uplifted and eroded passive margin sediments are exposed within the Serrania del Interior thrust belt, and in the southeast Pliocene to Pleistocene sedimentary rocks are found within the Monagas basin foothills and foredeep.

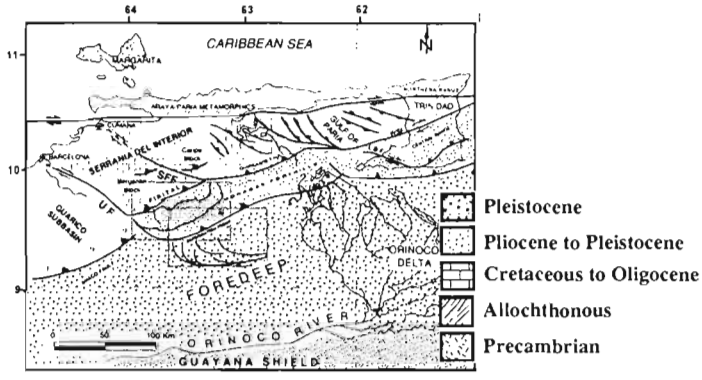

Figure 1. Geological Provinces in Eastern Venezuela (After Feo Codecido, Di Croce, 1995 and Hung, 1997)

Geodynamic modelling.

The flexural isostatic consequences of balanced section models prepared by other workers (Hung, 1997; Chevalier, 1995 and Passalacqua, et al., 1995) have been determined in order to understand the geodynamic evolution of the Monagas Basin and the Serrania Thrust belt (a selection of models are shown in Figure 2)

The modelling technique used combines flexural isostatic theory with cross-section balancing. Table 1 lists the different models examined, the values used for elastic thickness (Te) and shortening (S), and their outcome

Model Name	T_e (km)	S (km)	Comments	2xS(km)	Comments
Thick-Skinned Precambrian (Hung, 1997)	5, 15, **25**	16	Basin depth ~ 1.5 km	32	Basin depth ~ 3 km Basement exhumed in Serrania.
Thick and Thin-skinned Precambrian (Hung, 1997)	5, 15, **25**	35	Basin depth ~ 3 km .	70	Basin depth ~ 5 km . Basement exhumed in Serrania.
Thick and Thin-Skinned Palaeozoic or/and Jurassic (Chevalier, 1995)	5, 15, **25**	50	Basin depth ~ 2 km	100	Basin depth ~ 5 km . Palaeozoic exhumed in Serrania.
Thin-skinned Cretaceous (Hung, 1997)	5, 15, **25**	110	Basin depth ~ 3 km	---	---
Duplex structures (Hung, 1997)	5, 15, **25**	115	Basin depth ~ 4 km	---	---
Crustal Indenter (Passalacqua et al., 1995)	5, 15, **25**	70	Closest fit but still inadequate depth (~ 8 km).	---	---

Table 1. Results of numerical modelling for different geological hypothesis

Analysis of results and summary.

None of the previous proposed models can reproduce the observed geology. The observed depth of the Monagas foreland basin is 7 km greater than that modelled. In addition the modelled exhumation of passive margin sediments within the Serrania thrust belt is too great; no exhumation of basement rocks is observed within the Serrania. The flexural isostatic modelling indicates that thrust sheet loading alone is insufficient to generate the accommodation space within the foreland basin. The Crustal indenter model proposed by Passalacqua et al. (1995) gives the closest approximation to observation. This model, which incorporates an intracrustal load, gives an increased thickness (by 4 km) to the modelled depth of Monagas Basin, however it is still insufficient deep by 2-3 km.

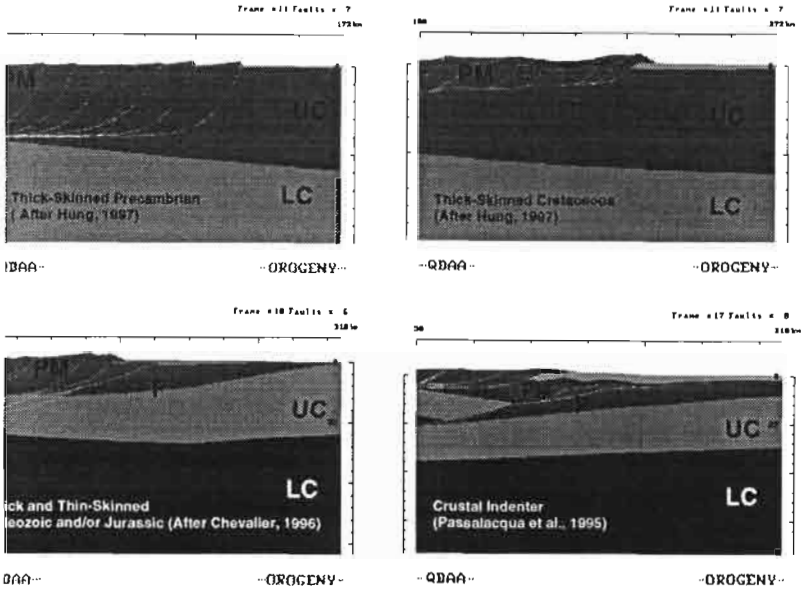

Figure 2. Reproduction of some of the geometrical models previously proposed. PM: Passive Margin, P : Palaeozoic, UC: Upper Crust and LC: Lower Crust.

The solution to the problem of insufficient modelled depth to the Monagas Basin using thrust sheet loading models may be due to the influence of subduction. Gravity data (Figure 3) shows a continuous negative anomaly extending from the Lesser Antilles subduction zone into the Monagas foreland basin. Besides Interpreted time isopach maps from Middle Miocene to Present have been produced to understand the variation of the depocenter in the basin. The axis of the depocenter changes direction from SW-NE to almost E-W during Pliocene and Pleistocene times, and is the result of the influence of the Lesser Antilles subduction zone. Based on this evidence we propose that subduction of the South American continental plate under the Caribbean generates additional subsidence within the Monagas Basin.

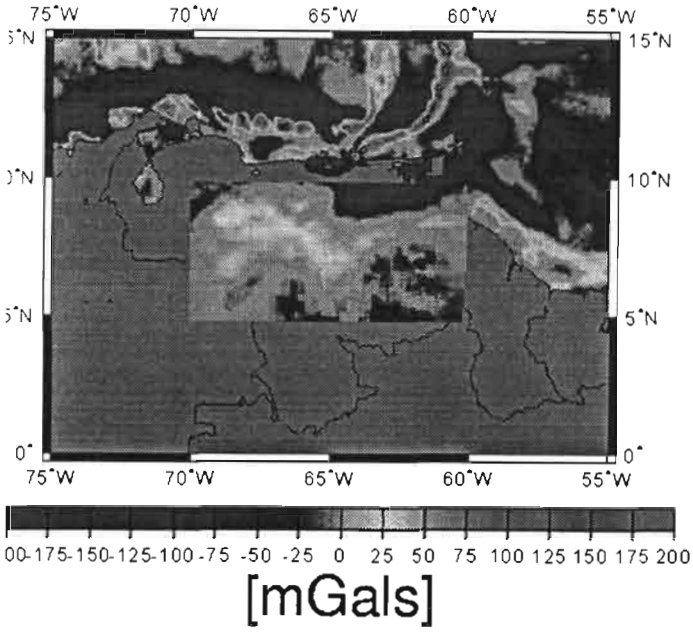

Figure 3. Bouguer Anomaly map (onshore) and Free air Anomaly map (offshore) of Eastern Venezuela and Lesser Antilles subduction zone.

Acknowledgements

This work forms part of MJ's PhD research and is funded by CONICIT, Venezuela. We are grateful to PDVSA , Simon Bolivar University and FUNVISIS for providing us with seismic, gravity and seismological data. The authors thank Felipe Audemard for his advice and encouragement, and Phil Nell for his technical support and assistance in the seismic interpretation.

Reference

- **Chevalier, Y., Gonzales , G., Mata, S., Santiago, N. and Spano, F., 1995,** Estratigrafia secuencial y tectonica del transecto El Pilar-Cerro Negro, Cuenca oriental de Venezuela: VI Congreso Colombiano del Petroleo, p. 115-125.
- **Di Croce, J., 1995,** Eastern Venezuela Basin: Sequence stratigraphy and structural evolution [Ph.D. thesis], Rice University, p. 67-165.
- **Feo-Codecido, G., Smith, F.D., Abound, N. and Di Giacomo, E., 1984,** Basement and Paleozoic rocks of the Venezuela Llanos basin, *in* Bonini, W. E., Hargraves, R,B. and Shagan, R., eds., The Caribbean-South American Plate Boundary and Regional Tectonics: Geological Society of America, M.162, p. 175-187.
- **Hung, E.J., 1997,** Foredeep and thrust belt interpretation of the Maturin subbasin, eastern Venezuela basin [Master Thesis], Rice University, p. 57-94.
- **Passalacqua, H., Fernandez, F., Gou, Y. and Roure, F., 1995,** Crustal Architecture and Strain Partitioning in the Eastern Venezuelan Ranges *in* Tankard, A.J., Suarez, R., and Welsink, H.J., Petroleum basins of South America: AAPG, M. 62, p.667-679.

CONTINENTAL TRIASSIC IN ARGENTINA: RESPONSE TO TECTONIC ACTIVITY

Uwe JENCHEN (1) and Ulrich ROSENFELD (2)

(1) Geologisch-Paläontologisches Institut der Universität, Corrensstraße 24, D-48149 Münster, Phone: +49/251/83-33956, e-mail: jenchen@uni-muenster.de

(2) Geologisch-Paläontologisches Institut der Universität, Corrensstraße 24, D-48149 Münster (corresponding author), Phone: +49/251/717480, Fax: -/-/83-33968

KEY WORDS: Triassic, sedimentary sequence, uplift, source of sediments, Argentina

INTRODUCTION

When the Proterozoic - Palaeozoic accretion processes at the Panthalassan margin of southern South America had come to an end, a number of rift basins developed in this region. They strike mainly NW to NNW, may have transtensional origin and, with the exception of the northernmost part, contain thick sequences of continental Triassic sediments (Fig. 1).

Especially in Central-West Argentina the Triassic graben fills overly a complex basement consisting of different terranes (RAMOS 1988). Thus the sediments comprise very different debris and the Triassic basins may undergo different evolutions according to the behaviour of the respective basement.

The stratigraphy of the Triassic strata is in principle well known (STIPANICIC 1983). Improvements are beeing elaborated by several working groups (e.g. ZAVATTIERI 1995).

SEDIMENTARY SEQUENCES

Obviously the Triassic continental sedimentation depends on wide spread uplift pulses of the respective hinterlands, which set in in the Early to Middle Triassic in Central-West Argentina, in the Middle and Late Triassic in the southern regions. In general uplift and beginning of sedimentation proceed from north to south in the course of time.

The sediments indicate fluvial facies ranging from alluvial fan to lacustrine and eolian facies. They form typical sedimentary sequences starting with high energy or relatively high energy resp. basal sediments and ending with low energy deposits. The sequences occur in large regional dimensions and in different smaller scales. ROSENFELD & VOLKHEIMER (1986) made an attempt to divide all the region on the basis of large sedimentary sequences. KOKOGIAN & MANCILLA (1989) set up a sequencial stratigraphy of the Triassic of the Cuyo Basin.

The large scale sequences may cover several lithostratigraphic formations. Its regional significance is best documentated by the Cacheuta Fm. (Carnian, Cuyo Basin, Potrerillos section) and its equivalents. The Cacheuta Fm. represents the upper member of a sequence and reflects a tectonically quiet state of the broader region.

Medium scale sequences form the lithostratigraphic formations or parts of it resp. Its distribution indicates also regional uplift pulses (North Patagonian Massif: Paso Flores, Comallo). Likewise volcanic activity induces sedimentary sequences (Deseado Massif: El Tranquilo Group).

Small scale sequences are the dominant sedimentary structures in most of the sediments. They appear in various types (FREY & ROSENFELD 1992, ZAVATTIERI, VOLKHEIMER & ROSENFELD 1994).

In the Marayes-Desagüadero Basin at least three, possibly four large sedimentary sequences are to be observed, in the Cuyo Basin regularly two. The Malargüe Basin indicates two sequences (HAUSCHKE 1989). In the North Patagonian Massif differences between sections indicate the existence of several small sedimentary basins. In the Deseado Massif the El Tranquilo section manifests a twofold uplift pulse, the upper one caused by volcanic activity. -- In general the Central-West Argentinian Triassic basins pass a more complicated evolution than the Patagonian ones.

PROVENANCE OF SEDIMENTS

Pebble analyses, modal analyses and, especially, geochemical analyses (JENCHEN 1998) yield reliable informations on the provenance of sediments and the state of the source areas.

Most of the sediments have undergone the first sedimentary cycle. The greater part is to be derived from definable stable blocks. Fossil magmatic arc provenances have been identified from the Marayes-Desagüadero Basin (Carrizal Fm., Carnian - Ladinian), from basal parts of the successions of the Cuyo Basin and the Malargüe Basin, and ? from the Deseado Massif (Canadon Largo Fm., Ladinian). In the Marayes-Desagüadero Basin these sediments originate from the Pampia terrane, in the Malargüe Basin, which is situated at the Patagonia terrane, from the Chilenia terrane. In the Cuyo Basin the position within the basin proofs to be decisive for the provenance of sediments: The more easterly sections receive its debris from the Precordillera terrane, the westerly ones from the Choiyoi Group of the Chilenia terrane. The isolated evolution of the Block of San Rafael causes specific local source conditions.

In contrast to Central-West Argentina transportation and sedimentation in Patagonia take place more uniform, uplift phenomena occur less pronounced. The sediments of the North Patagonian Massif indicate mostly a broad catchment area composed of different metamorphic rocks, plutonites and volcanics. The Los Menucos section shows local influences.

In the Deseado Massif pebble associations show the possibly largest transportation distances. The ?Triassic of the Austral Basin includes recycled sediments originating from a sedimentary, only weakly metamorphosed source area.

CONCLUSIONS

In Argentina the continental Triassic overlies a complex basement consisting of several terranes. The sediments originate from definable stable blocks and, partly, magmatic arcs. They form large scale and middle scale sedimentary sequences indicating uplift pulses of the respective hinterlands. The uplift pulses of the different terranes occured, with few exceptions, independently one from another and were a controlling factor for the evolution of the Triassic sedimentary basins.

REFERENCES

FREY, J.-W. & ROSENFELD, U. (1992): The strata of Potrerillos (Prov. of Mendoza/Argentina): A regionally typical profile of the continental Triassic in southern South America.-- Zbl. Geol. Paläont. I, 1991 (6): 1615-1632.

HAUSCHKE, N. (1989): Faziesanalyse kontinentaler triassischer Schichtfolgen im südlichen Südamerika mittels sedimentologischer und geochemischer Analysemethoden.-- DFG-Abschlußbericht: II + 78 S.; Münster.-- [Unveröff.]

JENCHEN, U. (1998): Fazies und Geochemie in kontinentalen Trias-Becken im westlichen Argentinien und in Patagonien (30° - 50° S).-- Diss. Univ. Münster: XXI + 261 S. + 344 S. Anhang; Münster [Unveröff.].

KOKOGIAN, D.A. & MANCILLA,O. (1989): Analisis estratigrafico secuencial de la Cuenca Cuyana. En: CHEBLI, G.A. & SPALLETTI, L.A. (Eds.): Cuencas Sedimentarias Argentinas.-- Serie Correlación Geologica, 6: 169-201; S.M.de Tucumán (Instituto Superior de Correlación Geológica)

RAMOS, V.A. (1988): Late Proterozoic-Early Paleozoic of South America - a collisional history.-- Episodes, 11 (3): 168-174; Ottawa.

ROSENFELD, U. & VOLKHEIMER, W. (1986): Classification of Triassic and pretransgressive Jurassic in western Argentina: An attempt.-- Zbl. Geol. Paläont. I, 1985 (9/10): 1309-1315.

STIPANICIC, P. N. (1983): The Triassic of Argentina and Chile. In: MOULLADE, M. & NAIRN, A. E. M. (Eds.): The Phanerozoic Geology of the World II, The Mesozoic, B: 181-199; Amsterdam (Elsevier).

ZAVATTIERI, A.M. (1995): Revisión de microfloras Triásicas de Argentina. Correlación.-- II. Reunión del Triásico del Cono Sur - 1995, Actas: 30-35.

ZAVATTIERI, A. M., VOLKHEIMER, W. & ROSENFELD, U. (1994): Palynology and facies of the Late Triassic of Comallo (Northern Patagonia, Argentina).-- Zbl. Geol. Paläont. I, 1993 (1/2): 133-154.

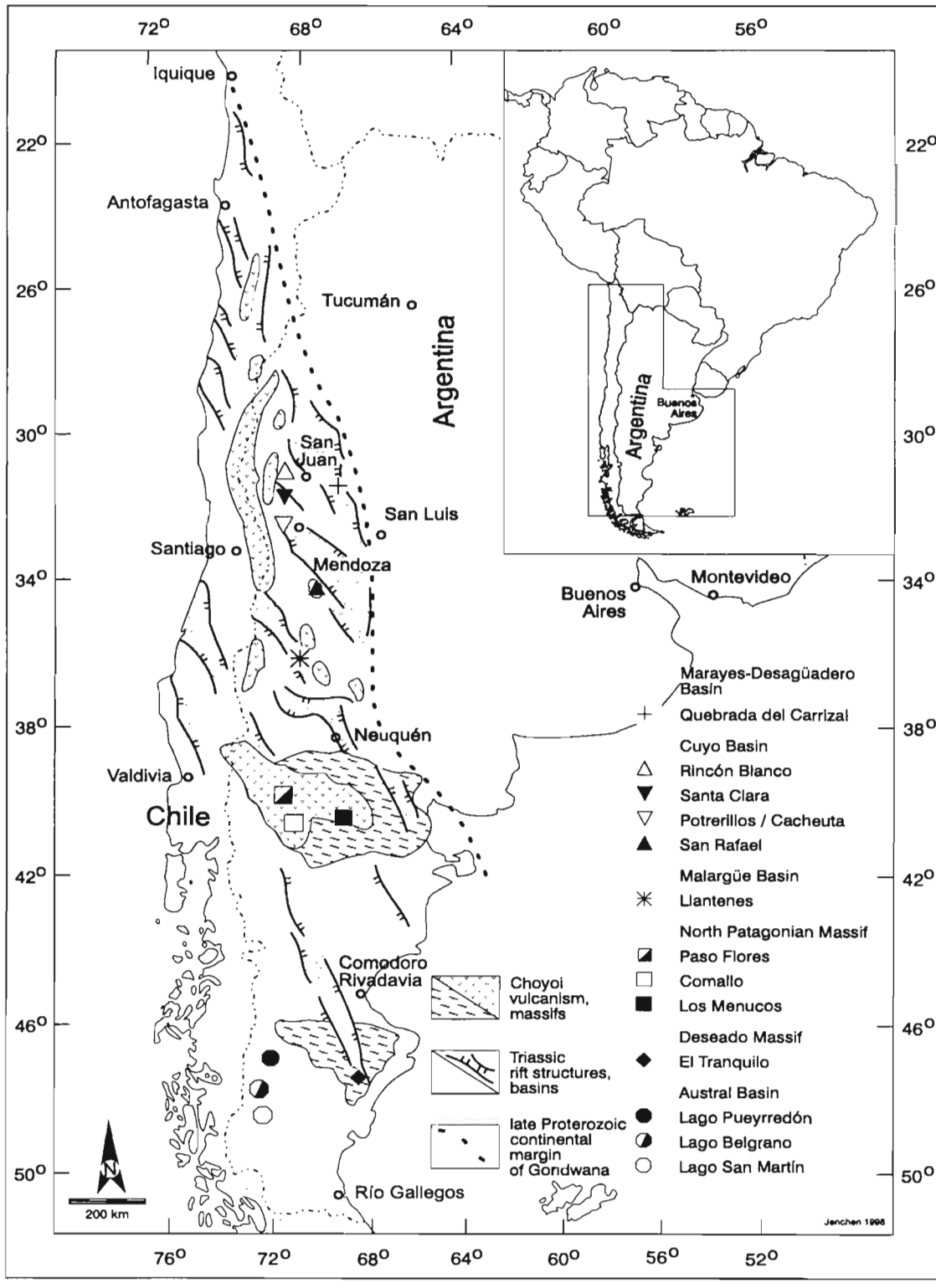

Fig. 1. Study areas and their position in the Triassic rift basins in southern South America (from JENCHEN 1998).

MICROGRAVITY AND GPS AT GALERAS VOLCANO, COLUMBIA: ESTABLISHMENT OF A NEW NETWORK AND FIRST MEASUREMENTS

Gerhard JENTZSCH(1), Marta CALVACHE(2), Arturo BERMUDEZ(3) and Milton ORDONEZ(4)

(1) Institut für Geowissenschaften, FSU Jena, Burgweg 11, D-07749 Jena
email: jentzsch@geo.uni-jena.de
(2) INGEOMINAS, Observatorio Vulcanológico y Sismológico de Pasto, Carrera 31#18-07, Pasto, Colombia, email: ovp@pasto.cetcol.net.co
(3) INGEOMINAS, Diagonal 53 # 34-53, Santafé de Bogotá, Colombia, email: abermu@esmeralda.ingeominas.gov.co
(4) INGEOMINAS, Observatorio Vulcanológico y Sismológico, Avenida 12 Octobre #15-47, Manizales-Caldas, email: opgi@col2.telecom.com.co

KEY WORDS: Physical volcanology, gravity variations, deformation, mass changes, microgravity network, gravity and deformation monitoring

INTRODUCTION AND THEORETICAL BACKGROUND

Galeras Volcano, South America's only IDNDR decade volcano, is situated near the city of Pasto in southern Columbia, about 100 km north of the equator. Galeras became well known after the unexpected eruption of January 14, 1992, which killed several people of a group of scientists visiting the crater.

In the frame of the cooperation between INGEOMINAS (Instituto de Investigaciones en Geociescias, Mineria y Quimica) and the German partner, the Federal Institute for Geosciences and Resources (BGR, Hannover) the monitoring will be improved by the installation of a multiparameter station (MP). This MP station comprises sensors for seismic, gaschemistry, electromagnetic, infra-sound, geodetic and meteorological observations near the crater. In a first step a new network of broad-band seismic stations and a continuously working gas probing equipment was installed. During repeated annual campaigns geoelectric and electromagnetic investigations are carried out (Seidl et al., 1998)

In parallel, microgravity and GPS measurements were prepared. The purpose of this work is to monitor mass and elevation changes. The advantage of gravity measurements repeated at identical points lies in the fact that no topographic corrections are needed. This increases the accuracy of the data to that of the measurements. Usually, a network consists of points / stations in the area of maximum changes connected to reference points where no changes are expected. The number and the distribution of the points are related to the expected changes and - of course - to the accessibility of the area.

In February 1998 the microgravity network was established around Galeras volcano (Jentzsch and Weise, 1998). This network consists of 30 stations: Two of them are used as remote references; there, the expected changes due to volcanic activities are thought to be neglectable. The road around Galeras is used for local points from where several profiles lead towards the summit; the most important profile connects Pasto (elevation 2,600 m) with the summit close to the active crater (4,200 m).

The theoretical background of elevation controlled microgravity measurements is described by Brown and Rymer (1991). The combination of gravimetry with, e.g., GPS is necessary because we observe two effects with opposite signs: Mass intrusion increases gravity, but the accompanying elevation change due to overpressure in the magma system reduces gravity. The ratio ('vertical gradient') $\Delta g/\Delta h$ contains information about the processes inside the volcano and their properties. In principle, the results of repeated measurements at the same points are compared, and changes are separated. Therefore, most of the usual corrections in gravity surveys are not needed here. Thus, we can work on the accuracy level of the gravimeter: The resolution of the gravity measurements is about $\pm$ 10 µGal ($\equiv \pm$ 100 nm/s²) equivalent to about 3 centimeters in height (free air gradient). The errors of the height control should be less, in the order of 1 centimeter or below. To increase the accuracy and the redundancy more than one gravimeter are used in parallel, and all the differences are measured several times in order to allow for a statistical analysis.

Microgravity studies have been successfully used e.g. at Poas volcano, Costa Rica (Rymer, 1991), at Campi Flegrei near Naples, Italy (Berrino and Corrado, 1991), and at Rabaul caldera (McKee et al., 1989). Co-author Jentzsch established a network at Mayon volcano, Philippines (Jahr et al., 1998), and he is involved in the monitoring of Merapi volcano, Indonesia (Gerstenecker et al., 1998).

MEASUREMENTS AND DATA

In September 1998 and March 1999 the first two campaigns were carried out. Prior to both campaigns the two available gravimeters were calibrated on the baseline Bogotá - Honda (elevation difference about 2,459 m; gravity difference: 553.473 mGal). This was done to adopt the calibration of our gravimeters to these low latitudes. In relation to the needed accuracy there exists a calibration problem: It is not possible to simply extrapolate the values obtained in Europe to areas close to the equator. Therefore, the existing calibration line Bogotá - Honda is of great importance to our work.

The network around Galeras comprises stations / points of altitudes between 1,549.11 m, in the west along the road around Galeras (BOMB), and 4,004.81 m as the uppermost point of the summit profile (TEL1), close to the rim of the volcano. The base station where we started and finished every day

is SANV, easy to access; the altitude is 2,621.34 m. All differences along the profiles and the road around Galeras as well as the connections to the reference points were measured at least three times.

Especially the elevation difference between SANV and TEL1 of 1,383.47 m along a very bumpy road causes problems: Due to the long time needed to drive up it is not possible to connect this point directly to other points of the network, esp. the reference stations. Therefore, the profile is only connected to the base station SANV. In order to improve the connection several ties are established between the uppermost points and the base station SANV as well as other points of the profile. The other profiles are dealt in the same way.

During the first campaign we used the LaCoste & Romberg gravimeter G 896 (Jena) and a SCINTREX gravimeter available by INGEOMINAS, whereas in the second campaign we used two L & R gravimeters (G 85 /Berlin and G 896). The L & R gravimeters are additional equipped with feedback systems and electronic levels (G 896 only). This reduces ambiguities considerably. Each data set consists of three independent gravity values (dial and feedback readings) measured consecutively, the altitude of the gravimeter above the plate of the point, and air pressure. The values are taken within five minutes at full minutes. Tidal corrections are applied in the field in order to avoid misreading.

FIRST RESULTS

The results are derived from several campaigns; i.e. to separate a change we need at least two campaigns. But, for a solid interpretation by numerical modeling more than two measurements are necessary. Therefore, in this paper we will only present some first results describing the quality of the data and the experiences gained at Galeras and the Bogotá baseline.

Now, we can report that the quality of the gravity data of the L & R gravimeters is in the expected order of about $\pm 10\,\mu$Gal or less. Unfortunately, the SCINTREX gravimeter caused some troubles during the first campaign; therefore we replaced it by a L & R gravimeter. Regarding GPS we are also working at the highest level of the resolution possible. Usually, standard software does not offer options necessary to fulfill our requirements. Therefore, different analysis packages are applied in order to achieve errors on the centimeter level.

CONCLUSIONS

Microgravity combined with GPS measurements is a good tool to understand the physics of a volcano. Although it is not possible to perform an on-line prediction we can contribute to the understanding of a

volcano considerably. Seismic monitoring is one of the best tools to predict eruptions, but from the gravity and deformation changes we can obviously derive information about the amount of mass movements and - thus - about the potential intensity of an eruption. With this information we may also get implications to the improvement of the assessment and the mitigation of volcanic hazards (Jahr et al., 1998).

At Galeras, the combination of different methods operating in a continuous mode (like monitoring of seismicity and gaschemistry) or applied repeatedly (like geosounding and electromagnetics) in connection with microgravity and GPS offers a good chance to improve the knowledge of this potentially dangerous volcano. Inspite of the rough transport conditions with off-road cars due to a soft support the vibrations were kept at a minimum such that the number of bad data is acceptable. It depends on the development of the volcanic activities how often these measurements will be repeated. To establish a base data set it seems reasonable to repeat the work every year.

REFERENCES

Berrino, G. and Corrado, G., 1991. Gravity changes and volcanic dynamics. Cahier du Centre Européen de Geodynamique et de Seismologie, Vol. 4, Proc. of the Workshop: Geodynamical Instrumentation applied to Volcanic Areas. Oct. 1 - 3, 1990, Walferdange, Luxembourg, 305 - 323.

Brown, G.C. and Rymer, H., 1991. Microgravity monitoring at active volcanoes: A review of theory and practice. Cahier du Centre Européen de Geodynamique et de Seismologie, Vol. 4, Proc. of the Workshop: Geodynamical Instrumentation applied to Volcanic Areas. Oct. 1 - 3, 1990, Walferdange, Luxembourg, 279 - 304.

Gerstenecker, C., R. Heinrich, G. Jentzsch, D. Kracke, G. Läufer, I. Suyanto, and A. Weise, 1998. Microgravity at Merapi volcano: Results of the first two campaigns. Deutsche Geophys. Ges., Sonderband III / 1998 (Herausg.: J. Zschau, M. Westerhaus), 61 - 64.

Jahr, T., G. Jentzsch, R.S. Punongbayan, U. Schreiber, G. Seeber, C. Völksen, and A. Weise, 1998. Mayon volcano, Philippines: Improvement of hazard assessment by microgravity and GPS - measurements? Seismological Press, Beijing, 599 - 608.

Jentzsch, G., and A. Weise, 1998. The microgravity network at Galeras volcano / Columbia. Deutsche Geophys. Ges., Sonderband III / 1998 (Herausg.: J. Zschau, M. Westerhaus), 57 - 59.

McKee, C., J. Mori, and B. Talai, 1989. Microgravity changes and ground deformation at Rabaul caldera, 1973 - 1985. In: Latter, J.H. (ed.), Volcanic Hazards, Assessment and Monitoring. Springer-Verlag, Berlin, 625 p.

Rymer, H., 1991. The use of microgravity for monitoring and predicting volcanic activities: Poas volcano, Costa Rica. Cahier du Centre Européen de Geodynamique et de Seismologie, Vol. 4, Proc. of the Workshop: Geodynamical Instrumentation applied to Volcanic Areas. Oct. 1 - 3, 1990, Walferdange, Luxembourg, 325 - 331.

Seidl, D., M. Calvache, D. Bannert, B. Buttkus, E. Faber, S. Greinwald, M. Hellweg and H. Rademacher, 1998. The Galeras multiparameter-station. Deutsche Geophys. Ges., Sonderband III / 1998 (Herausg.: J. Zschau, M. Westerhaus), 9 - 11.

STRUCTURAL STYLES OF THE FOLDED BOGOTA SEGMENT, EASTERN CORDILLERA OF COLOMBIA

Andreas KAMMER

Universidad Nacional de Colombia, Apartado 14490 Bogota (akammer@ciencias.ciencias.unal.edu.co)

KEY WORDS: Pure shear uplift, detachment folds, gravity glide.

INTRODUCTION

At its northern termination the Andean mountain system experiences a considerable fanning due to the ramification of the Eastern Cordillera from the Andean main trunk system. By its evolution within a Paleogene backarc basin of the ancestral Central Cordillera and its Pliocene uplift phase, the Eastern Cordillera classifies as an Andean foreland belt. Its trend parallel to the Colombian Caribbean coast is suggestive of a shortening brought about by a collisional event between Caribbean plate and Southamerican continent. This uniform pattern becomes disturbed in its northern part, where the Eastern Cordillera splits into a NNW trending range, which links to the Serrania de Perija, and the Merida Andes of Venezuela, the two embracing the Maracaibo basin and defining two sides of a fault-bounded, triangular shaped block, emplaced northward during the convergence with the Caribbean plate. This three-armed constellation dates back to the early Jurassic continental break-up, as evidenced by the trend of Jurassic half-graben and Triassic to Jurassic batholiths, and may have originated above an intracontinental hotspot. According to its orientation, each chain displays a distinct structural style.

This paper focuses on the structural evolution of the extensively folded Bogota segment of the Eastern Cordillera (fig. 1), which evolved along the southern arm of the above referred to rift system. It can be considered, to a first approximation, as an inverted structure of the early Jurassic rift system and a

Cretaceous to Paleogene intracontinental basin. It forms a broad axial depression between the Santander Massif to the north and the Garzon massif to the south and displays, by its NE- respectively N to NNW trending borders, a lozenge-shaped outline. Structurally, it can be divided into marginal highs and a central axial depression. The marginal highs display a characteristic relay pattern according to the orientation of the borders, they straddle: where the latter ones are NE-trending, as along the Middle Magdalena Valley and the Llanos foothills, they are right-stepping, whereas along the N-trending Upper Magdalena Valley, the structures are superseded in a left-stepping manner. Associating the right-stepping pattern with a dextral and the left-stepping pattern with a sinistral transpression, we may conclude about a general compression direction of 110°. In what follows, we outline characteristic properties of the structural elements of the Bogota segment and discuss some kinematic aspects, as revealed by selected cross-sections.

FOLDS

For descriptive convenience, we divide the folds into basement-involved first-order structures of continuities of more than 100 km, second-order folds of continuities of some tens of km and third-order fold trains of very restricted extensions. *First-order folds* are represented by the marginal antiforms referred to above (Quetame Massif, Villeta Anticlinorium), and by two further antiforms which extend from the spine of the Santander Massif into the Bogota segment (Floresta Massif and Guantiva-Arcabuco Anticline; fig. 1). These latter ones, together with the eastern border highs, display by their gently dipping western and steeply inclined to overturned eastern flanks a marked eastern vergence and represent sites of most intense compressive deformations, as evidenced by a steeply west dipping axial plane cleavage. In the southern Quetame Massif, an inverted limb of a marginal anticline defines the deformation front of the Eastern Cordillera, as a border fault is absent. A deformation contrast with the flat lying Llanos basement is obvious and may relate to the predominant phyllitic lithology of the Northandean basement. The granitic basement of the Guayana shield, on its turn, may have played the role of a rigid backstop. *Second-order folds* form highly cylindrical trains along the marginal, first-order antiforms or highly irregular trains with a varying vergence close to the axial depression. Their shapes and internal deformations vary according to their structural levels and reflect also the gross lithological change from shaley lower to sandy upper Cretaceous units. Within the upper Cretaceous sandstones, antiforms define relatively narrow structures, while its broad trough areas may be joined by smooth tangent planes, according to regional reference planes of detachment folds. Folding occurred at high structural levels by flexural slip. Toward lower structural levels, fold amplitudes decrease and a layer-parallel shortening is evidenced by an axial plane cleavage. *Third-order folds*, finally, compose disharmonic cascades and relate to flaps and minor slip sheets along flanks of second-order folds. By their consistent down-dip vergence they evidence a

gravity-driven collapse, as anticlinal hinges of second-order folds became subject to erosion.

CROSS SECTIONS

The fold style, as revealed by different cross sections, varies according to some simple parameters, such as the width of the axial depression, the thickness of the lower Cretaceous shaley units and the inclination of the flanks of the axial depressions. Fold trains display a regularly spaced pattern across the Tunja syncline, which is only 40 km wide and exhibits structural slopes in excess of 11° (section A-A', fig. 1). Vergence of the second-order folds opposes the structural slopes and fold amplitudes increase toward the synclinal depression. Above the strongly inclined western flank folds became locked, as evidenced by deformation zones originated by the migration of axial planes. A similar structural pattern repeats itself further south, as the axial depression widens to 150km and the lower Cretaceous sequence doubles its thickness to 5600m (section B-B', fig. 1). Still further south, the axial depression keeps its cross sectional dimension, but the lower Cretaceous shaley sequence reduces its thickness to 2600m. The axial depression is here unaffected by folds and, at the break between inclined flank and flat bottomed axial depression, a western fold marks a deformation front with respect to the second-order folding.

DISCUSSION

A particular feature of the structural styles observed so far is the lack of a deformational contrast between sedimentary cover and metamorphic basement. Folding is harmonic throughout the different structural levels and, as it decreases in amplitude and incorporates increasingly layer-parallel strains, renders deformation more homogeneous at low structural levels. Folding and deformation intensity are intimately related to uplift and point to a wholesale crustal thickening by a pure shear mechanism. As a consequence of the uniform shortening of lower ductile and upper brittle crust, thin-skinned thrust wedges are absent and foreland thrusts involve pre-Cretaceous basement. At the Llanos border the foreland belts become incorporated along-strike into folds of the Cordillera's main edifice, as a right-stepping release of a marginal high is completed.

A kinematic model best adjusts to the eastern flank of the Eastern Cordillera and takes account of the following stages: Marginal basement cored antiforms (embryonic first-order folds) become individualized since the early Oligocene and divide the hitherto intact foreland basin into an eastern foreland and a central intermontane successor basin. During the Pliocene shortening phase, uplift is intensified by a pure shear deformation, which leads to the formation of second-order folds at higher structural levels, where deformation becomes less penetrative. As the marginal highs acquire their present structural positions, the sediments undergo a widely distributed gravity glide which is facilitated by the shaley nature of the lower Cretaceous sequence and counteracted in the axial depression by a material transport from the opposed western border of the Eastern Cordillera. In the axial zone fold trains assume irregular, doubly plunging forms, and a late stage of fold amplification is assisted by a diapiric flow of probably overpressured shales into their cores, as erosion degraded their anticlinal hinges.

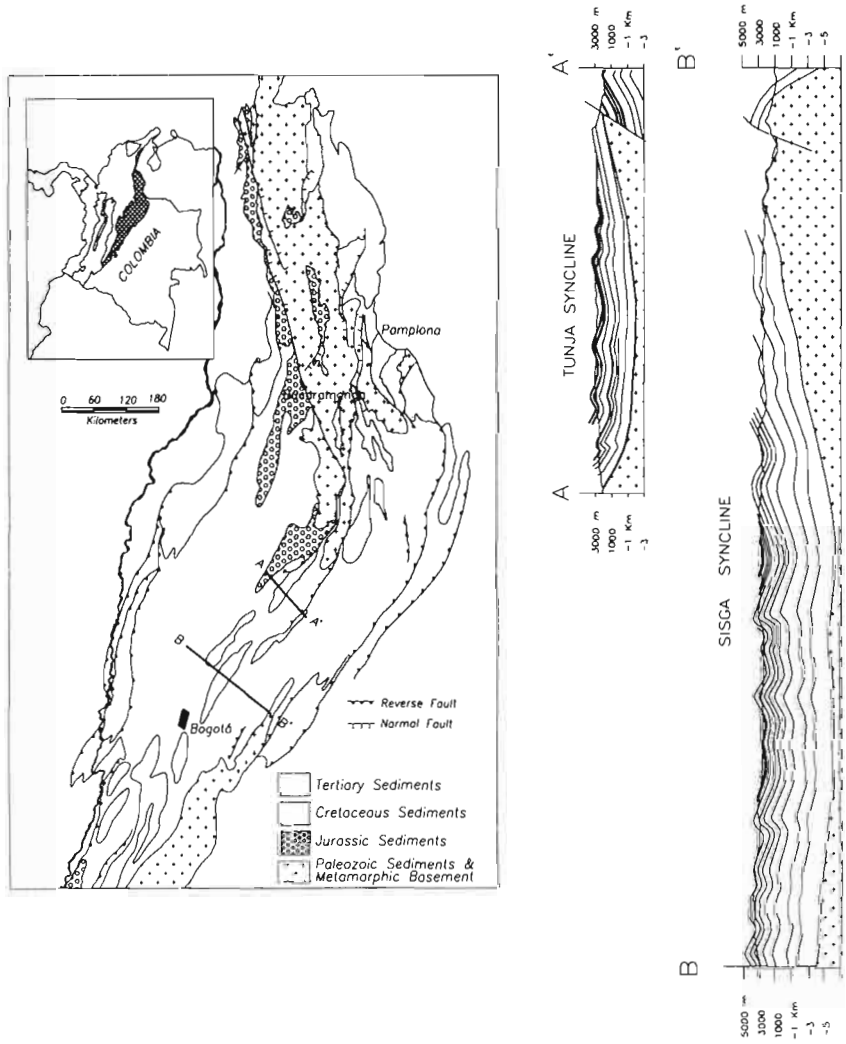

CHANGING SLAB DIP AND THE NEOCENE MAGMATIC / TECTONIC EVOLUTION OF THE CENTRAL ANDEAN ARC

Suzanne Mahlburg KAY

(1) Snee Hall, Cornell University, Ithaca, NY, 14853, USA, smk16@cornell.edu.

KEY WORDS: central Andes magmatism, slab geometry, continental lithosphere, arc migration, ignimbrite formation

INTRODUCTION

The Neogene magmatic and tectonic history of the central Andes reflects changes in the dip of the subducting Nazca plate and the thickness of the continental lithospheric mantle and crust. A model initially proposed by Isacks (1988) in which the slab has shallowed beneath the modern Chilean flatslab region (~28°S to 33°S), steepened beneath the northern Puna plateau (~22°S to 25°S), and remained in a transitional state beneath the intervening region (25°S to 28°S) (Fig. 1) is supported by spatial and temporal changes in Neogene magmatic and tectonic styles (e.g., Kay et al. 1999). The purpose here is to synthesize large scale continental lithospheric changes that complement proposed changes in slab geometry. Many important references not cited here can be found in Kay et al. (1999).

The best documented correlation between changing slab dip and central Andean Neogene tectonic and magmatic evolution is in the modern Chilean flatslab region (see Figs. 2a to d). In detail, shallowing of the

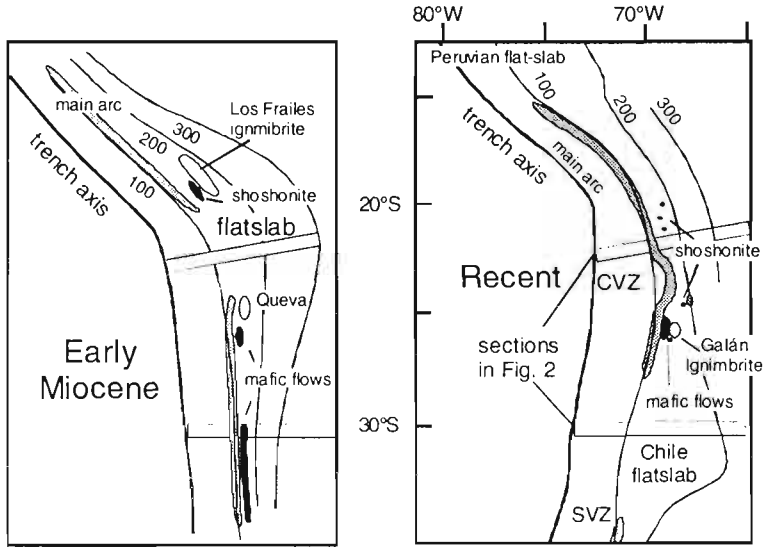

Figure 1 - Schematic cartoon showing changes in Neogene geometry of subducted plate. Contours to the Wadati Benioff zone from Isacks (1988). Magmatic features as discussed in text and in Kay et al. (1999). Lithospheric scale cross sections in Figure 2 are along linear gray regions. CVZ and SVZ are modern Central and Southern Volcanic Zone arc regions.

subducted plate can explain the general eastward broadening of subduction-related magmatism and deformation from the Main Cordillera to the Precordillera to the Sierras Pampeanas, termination of andesitic volcanism in the main Cordillera by ~ 9 to 10 Ma, virtual cessation of volcanic activity by ~ 6 Ma, initiation of Precordillera thrusting at ~ 18 Ma, and the uplift of the Sierra Pampeanas beginning at ~ 5-7 Ma. As emphasized by Kay and Abbruzzi (1996), shallowing of the subducting slab has led to crustal thickening beneath the main Cordillera, mechanical thinning of the continental lithosphere particularly beneath the main Cordillera and Precordillera, hydration of the continental lithosphere by fluids from the cooling subducting slab, and thinning of the asthenospheric wedge.

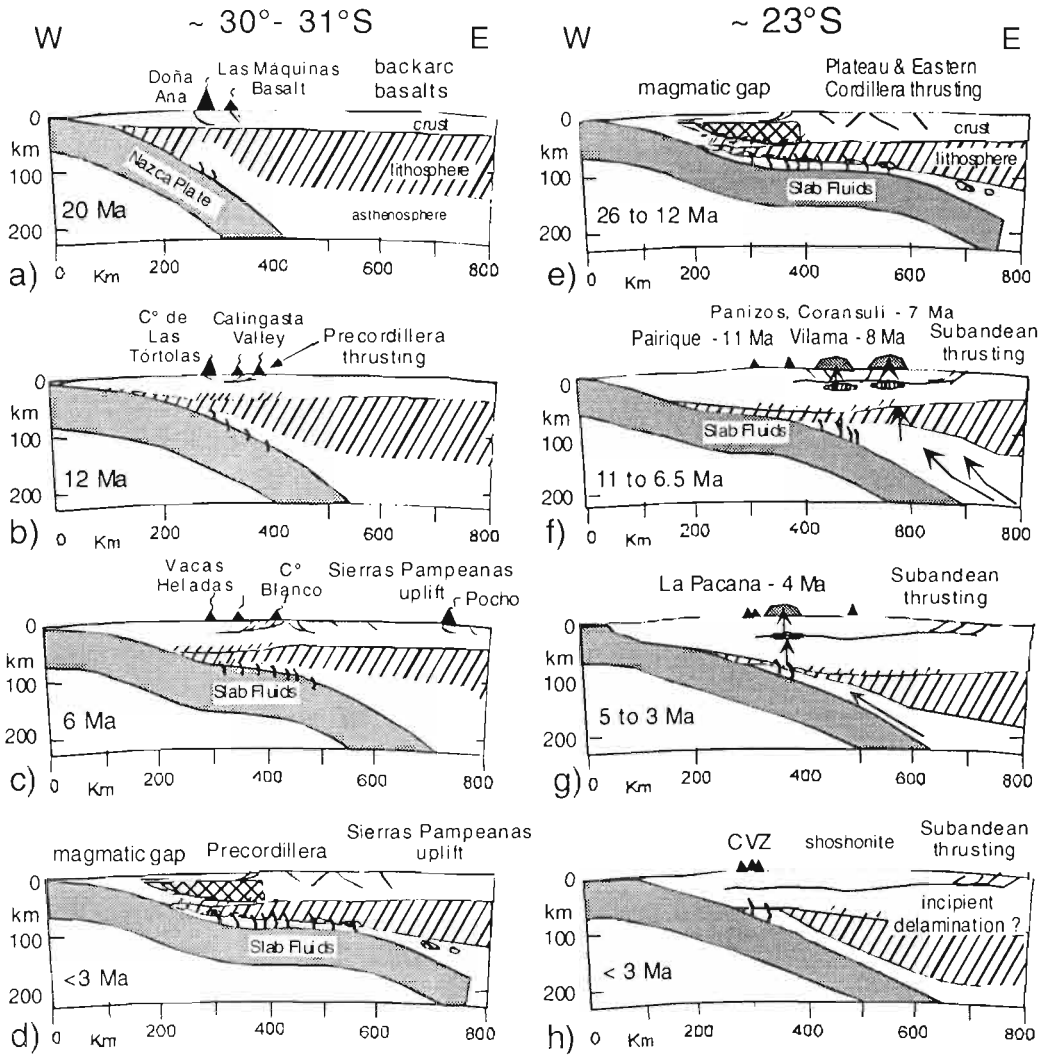

Figure 2 - Schematic cross sections showing evolutionary sequence for Neogene events over the Chilean flatslab (~30°-31°S) and northern Puna-southern Altiplano (~23°S). Place names refer to sites of Neogene magmatism and calderas (in f and g). See text

Evidence for contemporancous steepening of the subducting Nazca plate beneath the modern northern Puna and southern Altiplano plateau comes from Neogene geologic characteristics. Beginning in the Late Oligocene to

Middle Miocene, the presence of a shallowly dipping slab can account for widespread deformation and basin formation coupled with volcanic quiescence over the center and magmatism over the flanks of the flatslab (Figs. 1 and 2e). As in the modern Chilean flatslab region, a thin lithosphere hydrated by fluids from the cool shallow slab was particularly susceptible to deformation far to the east. A thin asthenospheric wedge prevented magmas from forming over the flattest part, whereas thicker asthenosphere under hydrated lithosphere on the margins of the shallow slab resulted in extensive melting and volcanic eruptions (e.g. Queva and Los Frailes in Fig. 1). Steepening of the slab in the Middle Miocene to Pliocene (Fig. 2f) resulted in an asthenospheric volume increase that led to melting of the overlying hydrated mantle wedge and lowermost crust. Evidence for steepening of the slab and melting comes from the emplacement of small stocks and domes across the backarc in the Middle Miocene, widespread eruption of huge ignimbrite sheets from calderas (e.g. Coranzulí, Panizos, Vilama-Curuto) in the Late Miocene (Fig. 2f), restriction of huge calderas (e.g. La Pacana) to the western plateau in the Pliocene (Fig. 2g), and concentration of magmatism in the modern Central Volcanic zone (CVZ) in the Western Cordillera by the Pleistocene (Fig. 2h). Geochemical data are consistent with erupted magmas being mixtures of mantle and deep crustal melts that accumulated at mid-crustal levels prior to emplacement as big ignimbrites sheets.

As the slab steepened, crustal deformation under the plateau essentially ceased and migrated eastward as the crust became increasingly melt-charged and yielded under compressional collapse (Isacks 1988). In detail, deformation is generally thought to have terminated beneath the plateau by the Late Miocene (~ 10-11 Ma) and to have begun in the Subandean belt before ~ 6 Ma. A feasible scenario is that Subandean thrusting primarily took place from 13 to 10 Ma with motion on major thrusts being genetically associated with the eruption of large ignimbrites. In essence, large fault motions and ignimbrite eruptions both would be linked to compressional horizontal failure in the crust. This failure would be a response to thermal weakening as critical volumes of magmas ponded below mid-crustal decollements. The principal plateau uplift and crustal thickening would be associated with these events. Resultant underthrusting of the Brazilian shield from the east and associated lithospheric cooling would lead to contemporaneous lithospheric thickening resulting in a thick crust over a relatively thick lithosphere (see Whitman et al. 1996). Geophysical studies (e.g., Myers et al. 1998) suggest that thickened backarc crust and lithosphere is starting to detach as expected in the early stages of delamination of thickened crust and continental lithosphere.

A persistent intermediate dip in the intervening region between the steepening slab to the north and the shallowing slab to the south is supported by a generally continuous magmatic record in the southern Puna (Fig. 1). The crustal deformational story is distinct from that to the north or south as a major foreland fold-thrust belt did not develop (Fig. 3), in part due to lack of a suitable sedimentary sequence. The magmatic story is also distinct as the arc front migrates ~ 50 km eastward in the Late Miocene to Pleistocene (8 to 2 Ma) as mafic flows erupt along normal and strike-slip faults in the backarc (Fig. 3). This period culminates with the last large Puna ignimbrite at Cerro Galán at ~ 2 Ma. The migration of the arc front from its pre 7 Ma to its post 4 Ma CVZ position along the Argentine border requires major adjustments in the continental lithosphere over an intermediately dipping slab. Compressional shortening necessitates crustal thickening which is best accommodated in the deep crust near the arc. The required

upper crustal shortening can potentially be compensated by subduction erosion at the continental margin, shortening in the forearc and arc crust, and reduced amounts of shortening in a poorly developed fold-thrust belt. Concentration of crustal thickening just behind the arc would facilitate Pliocene lithospheric foundering (delamination) of overly thick eclogitic facies lower crust and the attached lithosphere (e.g., Kay and Kay 1993). Continental lithospheric adjustments would produce the heterogeneous stress regime necessary for mantle-derived melts to erupt along extensional faults. Loss of continental lithospheric would increase asthenospheric wedge volume and facilitate the

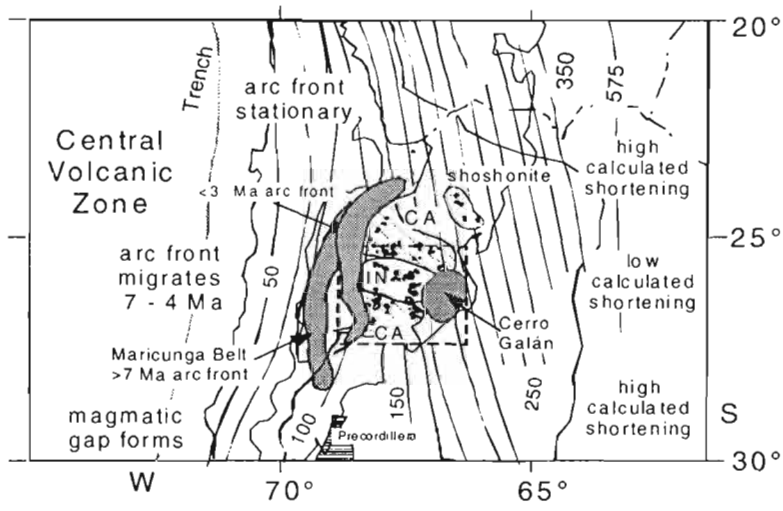

Figure 3 - Map showing zones of stationary and migrating arc fronts relative to regions of high and low calculated shortening in fold-thrust belts, backarc (CA-calc-alkaline, IN - intraplate) mafic lavas, delaminated zone (box), seismic contours and thinned lithosphere (gray) (Isacks 1988, Whitman et al. 1996). See text.

large scale lithospheric melting that culminated with the Cerro Galán ignimbrite. A thin lithospheric and thick asthenospheric wedge is consistent with the high average regional elevation, the abundance of mafic magmas, and the lack of earthquakes in the subducting slab beneath the southern Puna (c.g., Kay and Kay 1993, Whitman et al. 1996).

REFERENCES

Isacks, B.L., Uplift of the central Andean plateau and bending of the Bolivian orocline, *Journal of Geophysical Research*, *93*, 3211-3231, 1988.

Kay, R.., and S. Kay, Delamination and delamination magmatism, *Tectonophysics*, *219*, 177-189, 1993.

Kay, S.M., and J.M. Abbruzzi, Magmatic evidence for Neogene lithospheric evolution of the central Andean "flat-slab" between 30°S and 32°S, *Tectonophysics*, *259* (1-3), 15-28, 1996.

Kay, S.M., C. Mpodozis, and B. Coira, Neogene magmatism, tectonism, and mineral deposits of the Central Andes (22°S to 33°S), in *Geology and Ore Deposits of the Central Andes*, edited by B.J. Skinner et al.. Society of Economic Geologists, Special Publication number 7, in press, 1998.

Meyers, S., S. Beck, G. Zandt, and T. Wallace, Lithospheric-scale structure across the Central Andes of Bolivia from seismic velocity and attenuation tomography, *Journ.f Geophys. Research, in press*, 1999.

Whitman, D., B.L. Isacks, and S.M. Kay, Lithospheric structure and along-strike segmentation of the Central Andean Plateau: seismic Q, magmatism, flexure, topography and tectonics, *Tectonophysics*, *259* (1-3), 29-40, 1996.

METASOMATISM OF THE MANTLE WEDGE BELOW THE SOUTHERN ANDES

Rolf KILIAN (1), Christoph FRANZEN (2), Mario KOCH (2),
Charles R. STERN (3) & Rainer ALTHERR (2)

(1) Geologisches Institut, Universität Freiburg, Albertstr. 23B, 79104 Freiburg, Germany; kilianr@sun2.ruf.uni-freiburg.de

(2) Mineralogisches Institut, Universität Heidelberg, INF 236, 69120 Heidelberg, Germany; mkoch@classic.min.uni-heidelberg.de

(3) Department of Geological Sciences, University of Colorado CB-399; Boulder, CO 80309-0399, USA

KEY WORDS: Southern Andes, metasomatism, trace elements, mantle wedge

INTRODUCTION

Mantle xenoliths erupted during Late Miocene and Late Pleistocene at three different localities in the eastern range of the southern Andes (47-51°S) are complexly metasomatized. The aim of this study was to constrain chemical characteristics, time relations and types of metasomatic events. Cenozoic plate tectonics and chemical characteristics of magmatic rocks suggest that the mantle wedge below the southern Andes might have been modified by different magmatic and metasomatic processes. In the Paleogene oblique subduction associated with rare arc magmatism may have produced little contamination of the mantle. In the Lower Miocene (23-15 Ma) the convergence of the Nazca plate with the South American continent changed from oblique to more orthogonal direction and this could have caused an increasing slab dehydration and hybridization of the mantle wedge (Cande & Leslie 1986). Since the Upper Miocene, the subduction of the active Chile Ridge spreading center (15 Ma) caused the formation of a slab window below southernmost South America (48-52°S), enabling asthenospheric upwelling into a growing slab window and basalt formation (Gorring et al. 1997). During the Pliocene to Quaternary, the Antarctic plate was subducted very slowly (2-3 cm/a) and partially fused, forming adakitic slab melts which reached the surface and also contaminated the mantle wedge (Kilian & Stern 1999; Sigmarrson et al. 1998; Stern & Kilian 1996).

The petrography and texture of the xenoliths was investigated by microscope and electron microprobe analysis, including systematic core-rim-core electron microprobe line scans. Bulk major and trace element compositions of the xenoliths were investigated by XRF and ICP-MS. The trace element (Rb, Ba, Th, U, Pb, Sr, Nb, Ta, REE, Y, Zr, Hf and Sc) contents of clinopyroxene (cpx) and orthopyroxene (opx) grains, as well as fluid inclusions were analyzed at St. John´s Memorial University, Canada, using the technique described by Taylor et al. (1997).

OBSERVATIONS AND THEIR IMPLICATIONS

Mantle xenoliths from Pico Sur (49°S) are predominantly spinel peridotites that were ejected with enriched MORB-like basalts about 10-7 Ma ago. These basalts are likely to be formed at an early stage (15-7 Ma) of the slab window below the southern Andes (Gorring et al. 1997). Cpx cores in these lherzolites have preserved high U/Nb and La/Ta ratios when compared with typical cpx/melt partitioning in enriched MORB, suggesting an older slab-derived metasomatic event, probably in the Paleogene or Lower Miocene. Compared with the cpx cores, the trace element patterns of the cpx rims and some pyroxene-rich veins in these lherzolites are typical for a metasomatic overprint by enriched athenospheric mantle melts which can be related to the Upper Miocene slab window.

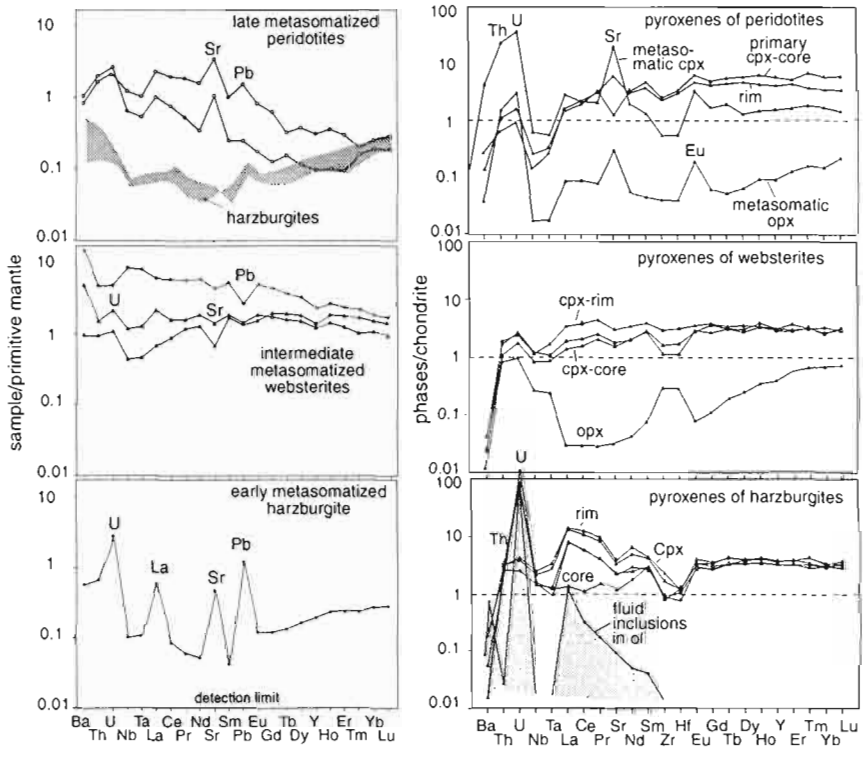

Fig. 1: Normalized trace element patterns for early, intermediate and late metasomatized peridotites, their pyroxenes and fluid inclusions.

Xenoliths from Cerro Donoso (51°S) were also ejected with OIB-like basalts about 15-10 Ma ago. They are mainly harzburgites with cpx showing a depletion of the middle REE compared to the HREE in chondrite normalized trace element patterns. These cpx also show extreme, but variable enrichment of the very light REE, U, as well as strongly pronounced negative anomalies of Nb and Ta. Such a strong enrichment of light REE and LIL elements and the relatively high U/Nb ratios along with negative anomalies of Nb and Ta are also typical for orthopyroxenes, suggesting a strong contamination by slab derived fluids which is not apparent in the host basalt (e.g. Elliot et al. 1997, Hawkeswoth et al. 1997).

Xenoliths from Cerro del Fraile (50°S) include harzburgites, lherzolites, websterites and pyroxenites. They were ejected with Pleistocene basalts, showing arc-related trace element signatures. Cpx and opx in harzburgites, some lherzolites and bulk harzburgitic xenoliths have normalized trace element patterns with extreme negative HFSE anomalies and a strong enrichment of U, Sr, Pb as well as very light REE similar to those observed in the Cerro Donoso mantle xenoliths. Th is also enriched, but not as much as U, resulting in relatively high U/Th ratios as it is typical for slab derived fluids (Elliot et al. 1997; Hawkesworth et al. 1997).

Olivine websterites and pyroxenites are commonly closely associated with the harzburgites and exhibit marble cake-like textures. Cpx trace element characteristics of these xenoliths do not show significant core to rim variations. The trace element patterns of pyroxenes and bulk xenoliths show only moderate enrichment of light REE compared to heavy REE patterns, no pronounced negative HFSE anomalies, but instead show negative Pb and Sr anomalies as it is typical for an enriched asthenospheric mantle and melts derived therefrom.

Some peridotite xenoliths contain veins and bulk compositions with high Sr/Y, La/Yb, and U/Nb ratios but low U/Th ratios. These trace element characteristics are typical for melts derived from eclogitic and plagioclase-free sources. Since this trace element enrichment is only partially equilibrated, it may be the youngest metasomatic event, related to the infiltration of slab-melts formed in the young and slowly subducted Antarctic plate (Stern & Kilian 1996).

CONCLUSIONS

An early metasomatic event has effected predominantely the harzburgitic mantle below the southern Andes. Hydrous fluids have carried significant amounts of U, La, Pb, and Sr, producing high U/Th, La/Nb and Pb/Ce ratios as it is typical for slab-derived fluids (Fig. 1). This metasomatism was probably related to the Paleocene to Lower Miocene subduction of the Nazca Plate below the southern Andes. Olivine websterites and pyroxenites form veins and agregates in the harzburgitic mantle, representing basalt infiltration and cumulate formation. These peridotites do not show the slab fluid signatures, but instead have an asthenospheric trace element pattern characterized by low La/Nb ratios and negative Pb and Sr

anomalies (Fig. 1). The genesis of these peridotite xenoliths may be related to the formation of a slab window in this region (10-5 Ma) which also cause a metasomatism of the lithospheric mantle of the back arc below Pali Aike (Stern et al. 1999). Some peridotite xenoliths contain glass veins and/or minerals formed by a modal metasomatism. Textural and chemical zoning patterns suggest that this was the youngest metasomatic event. The high Sr/Y, La/Yb and U/Nb ratios, as well as moderatly low U/Th ratios of these glass veins suggest infiltration of an adakitic melt formed in the eclogitic slab edge of the very young and slowly subducted Antarctic plate.

References

Cande S.C. & Leslie R.B. 1986. Late Cenozoic tectonics of the southern Chile trench. J. Geophys. Res., 91, 471-496.

Elliot T., Plank T., Zindler A., White W. & Bourdon B. 1997. Element transport from slab to volcanic front at the Mariana arc. J. Geophys. Res., 102, 14991-15019.

Gorring M.L., Kay S.M., Zeitler P.K., Ramos V.A., Rubiolo D., Fernandez M.I. & Panza J.L. 1997. Neogene Patagonian plateau lavas: Continental magmas associated with ridge collision at the Chile triple Junction. Tectonics, 16, 1-17.

Hawkesworth C.J., Turner S., Peate D., McDermott F. & Calsteren P.v. 1997. Elemental U and Th variations in island arc rocks: implications for U-series isotopes. Chem. Geol., 139, 207-221.

Kilian R. & Stern C.R. 1999. Constraints on the interaction between slab melts and the mantle wedge from adakitic glass in peridotite xenoliths. Eur. J. Mineral., submitted.

Sigmarrson O., Martin H. & Knowles J. 1998. Melting of a subducting oceanic crust from U-Th disequilibria in Austral Andean lavas. Nature, 394, 566-569.

Stern C.R. & Kilian R. 1996. Role of the subducted slab, mantle wedge and continental crust in the generation of adakites from the Andean Austral Volcanic zone. Contrib. Mineral. Petrol., 123, 263-281.

Stern C.R., Kilian R., Olker B., Hauri E. H. & Kyser T.K. 1999. Evidence from mantle xenoliths for relatively thin (<100 km) continental lithosphere below the Phanerozoic crust of southernmost South America. Lithos, accepted.

Taylor R.P., Jackson S.E., Longerich H.P. & Webster J.D. 1997. In situ trace-element analysis of individual silicate melt inclusions by laser ablation microprobe-inductively coupled plasma-mass spectrometry (LAM-ICP-MS). Geochim. Cosmochim. Acta, 61, 2559-2567.

"PETROGENESIS OF A MAFIC TO FELSIC PLUTONIC COMPLEX (COMPLEJO IGNEO POCITOS) AND ITS HOST ROCKS IN THE SOUTHERN PUNA OF NW ARGENTINA."

T. KLEINE (1,3), U. ZIMMERMANN (2), K. MEZGER (3), H. BAHLBURG (1) and B. BOCK (4)

(1) Geol.-Pal. Institut, Universität Münster, Correnstr. 24, 48149 Münster; Alemania, tkleine@nwz.uni-muenster.de, bahlbur@uni-muenster.de
(2) Geol.-Pal. Institut, Universität Heidelberg, INF 234, 69120 Heidelberg; Alemania, uzimmerm@ix.uni-heidelberg.de
(3) Institut für Mineralogie, Universität Münster, Correnstr. 24, 48149 Münster; Alemania, klaush@nwz.uni-muenster.de
(4) Geochemisches Institut, Goldschmidtstr.1, 37077 Göttingen; Alemania, bbock@ugcvax.dnet.gwdg.de

KEYWORDS: Complejo Igneo Pocitos, whole rock isotopes, U-Pb ages, petrogenesis

INTRODUCTION

Exposed Lower Ordovician sedimentary rocks in the southern Puna (NW Argentina, between 25°S and 26°S) are associated with mafic to felsic plutonic rocks (Complejo Igneo Pocitos) and mafic to ultra-mafic bodies (Complejo Basico Ojo de Colorados) (Zappettini et al. 1994). This association of sedimentary and mafic to ultra-mafic rocks was interpreted as an ophiolite sequence and as remnants of oceanic crust of an Ordovician ocean (i.e. Allmendinger et al. 1983). The supposed oceanic basin closed during the assumed collision of the Arequipa-Antofalla terrane with the western margin of Gondwana represented by the Pampia Terrane. This collision caused the Oclóyic Orogeny during the Upper Ordovician. The Pampia Terrane was amalgamated to Gondwana during the Lower Cambrian. The Complejo Igneo Pocitos has been interpreted as a syn-orogenic intrusion (Zappettini et al. 1994).

Recent fieldwork, petrological, geochemical and isotope data indicate a retro-arc basin position behind a volcanic arc (Puna-Famatinian-arc) for the Lower Ordovician sedimentary successions. This arc was

active from Tremadocian to Mid-Ordovician time. The volcanic arc as well as the retro-arc basin evolved on continental crust.

The oldest Ordovician unit (Tolar Chico Formation) is of Tremadocian age and comprises quartz-arenites with Th/Sc and La/Sc ratios typical for upper crustal compositions as well as REE patterns similar to PAAS. The overlying Tolillar Formation is composed of feldspar-rich massive sandstones, volcanogenic silt- and sandstones and greywackes. The occurrence of *Araneograptus murrayi* indicates an age for the sedimentation that coincides with the Tremadoc-Arenig boundary (Lancefield 2). The rocks have upper crustal trace element concentrations. Farther to the south in the central part of the Sierra Calalaste strongly volcanogenic greywackes (Diablo Formation) of Arenigian age interfinger with synsedimentary rhyolitic to andesitic lava flows.

In the south of the Salar de Pocitos, the Tolar Chico and Tolillar Formations are associated with mafic to ultra-mafic rocks (Complejo Basico Ojo de Colorados) of unknown age. The trace element composition of the latter indicate a calc-alkaline arc composition (Bahlburg et al. 1997).

The sedimentary rocks and mafic layers are isoclinally folded and verge in general to the west. The deformation occurred during the Upper Ordovician Oclóyic Orogeny. The sedimentary rocks have a metamorphic overprint corresponding to the pumpellyite-prehnite facies (after Warr 1996).

The mafic to felsic magmatic rocks of Complejo Igneo Pocitos intruded into gabbros leading to the formation of black-walls. The contact with the sedimentary rocks (only Tolillar Formation) is not exposed, but field data point to a discordant contact. The whole complex is lensoid with the long axes to the north and about 10 km to 4 km wide. The plutones show a distinct foliation from north to south, but no folding, because of their strong competence. There is no field evidence for folding caused by the Oclóyic Orogeny. The whole complex is intruded by several generations of dykes (east-west orientated) including rhyolites, aplites, basalts and pyroxenites. However, these dykes may be related to the Cretaceous Salta-rift (Salfity 1982).

Blasco et al. (1996) obtained a K/Ar age of 494 +/- 20 Ma for a hornblende separate and 470 +/- 17 Ma for a mixture of biotite+hornblende from the intermediate rock types of the Complejo Igneo Pocitos. The Tolillar Formation, which is affected by the intrusion, has a relative age of Lancefield 2 (Upper Tremadoc) at its base. This age can be correlated with the absolute age of 485 Ma (Gradstein & Ogg 1996).

The mafic to felsic magmatic rocks can be subdivided petrographically. They consist of diorite, monzonite and quartz monzonite and could point to different intrusive generations. Quartz is rare in all samples except in the quartz monzonite. The dominant phases are hornblende, plagioclase and alkalifeldspar. Some samples contain clinopyroxene in the matrix as well as inclusions in hornblende. Biotite is generally rare and occurs predominantly as a late growth along the rims of hornblende. Accessory phases include titanite (particularly in intermediate samples), apatite, zircon, allanite, magnetite and rare secondary hematite. The plagioclases show typical magmatic zoning. All magmatic rocks show signs of low temperature alteration, particulary sericitisation of feldspars. The primary mineral assemblages are

typical for magmatic rocks that were generated in an island arc setting. The strong enrichment in K as evidenced by the high modal abundance of K-feldspar indicates a tectonic setting quite distant from the trench. This interpretation is consistent with the trace element signatures that show pronounced negative Nb-Ta and Ti anomalies.

The detrital material of the Lower Ordovician to the Mid-Ordovician sedimentary rock successions was derived from a continental or continental island arc source. The Puna-Famatinian volcanic arc formed on continental crust and was active from Upper Tremadocian at least to Mid Ordovician time. The tectonic contact of the gabbroic with the sedimentary rocks is younger than the boundary Tremadoc-Arenig and older than the Oclóyic Orogeny. The intrusion of the Complejo Igneo Pocitos took place after this tectonic event and can be correlated with a subduction related setting, as deduced from the petrological data. In order to contrain further the sources for the magmatic suite Sr, Nd and Pb isotopes will be determined on the magmatic rocks. U-Pb ages for titanite will be used to date the intrusive bodies.

REFERENCES

Allmendinger, R.W., Ramos, V., Jordan, T.E., Palma, M. & Isacks, B.L. 1983. Paleogeography and Andean structural geometry, Northwest Argentina. Tectonics, 2 (1), 1-16.

Bahlburg, H., Kay, S.M. & Zimmermann, U. 1997. New geochemical and sedimentological data on the evolution of the Early Paleozoic Gondwana margin in the southern central andes. Geological Society of America Annual Meeting, abstracts with programs, A-378.

Blasco, G., Villar, L. & Zappettini, E.O. 1996. El complejo ofiolítico desmembrado de la Puna Argentina, Províncias de Jujuy, Salta y Catamarca. XIII Congreso Geológico Argentino y III Congreso de Exploración de Hidrocarburos, Actas, III, 653-667.

Gradstein, F. M. & Ogg, J. 1996. A Phanerozoic time scale. Episodes, 19 (1-2), 3-5.

Salfity, J. A. 1982. Evolución paleogeográfica del Grupo Salta (Cretacico-Eogenico), Republica Argentina. V Congreso Latino-Americano Geológico, Actas, I, 11-26.

Warr, L. 1996. Standardized clay mineral crystallinity data from the very low grade metamorphic facies rocks of southern New Zealand. European Journal of Mineralogy, 8, 115-127.

Zappettini, E., Blasco, G. & Villar, L.M. 1994. Geología del extremo sur del Salar de Pocitos, Provincia de Salta, Republica Argentina. VII. Congreso Geológico Chileno, Actas, I, 220-22.

TECTONIC EVOLUTION OF THE EASTERN CORDILLERA IN CARBONIFEROUS TO RECENT TIME, 23-24°S, NW ARGENTINA

Jonas Kley (1), Henning Kocks (1), Patricio Silva (1) and César R. Monaldi (2)

(1) Universität Karlsruhe, Geologisches Institut, P.O. Box 6980, D-76128 Karlsruhe, Germany (jonas.kley@bio-geo.uni-karlsruhe.de)

(2) Universidad Nacional de Salta-CONICET, Buenos Aires 177, 4400 Salta, Argentina

KEY WORDS: Eastern Cordillera, Subandean Ranges, rifting, tectonic inversion, displacement transfer, thrust kinematics.

INTRODUCTION

Neogene thrust belts on the eastern flank of the Andes in northern Argentina comprise the Eastern Cordillera and the easterly adjacent Subandean foothills. The high standing Eastern Cordillera is predominantly built of late Proterozoic to Ordovician strata covered unconformably by Cretaceous to Tertiary rocks. The topographically lower Subandean Ranges have a more complete and essentially conformable succession of Lower Paleozoic to Neogene strata. In terms of stratigraphy and structure, the Subandean Ranges north of 23°S differ strongly from the foothills segment south of 24°S (the Santa Barbara System; Rolleri, 1976). North of 23°S, Carboniferous to Jurassic(?) strata occur on top of a Devonian succession and beneath Neogene foreland basin strata. South of 24°S, rocks of the Cretaceous to Paleogene continental Salta rift overlie the Devonian and older strata and are topped by the Neogene foreland succession. The structural style is thin-skinned north of 23°S where the thrust belt is detached in Silurian strata (Aramayo Flores, 1989), but older rocks probably down to the crystalline basement are involved in the Santa Barbara System due to the inversion of Cretaceous normal faults (Monaldi and Kley, 1997; Salfity et al., 1993). In the segment we discuss here, between 23° and 24°S, Subandean foothill structures are conspicuously absent, with the Eastern Cordillera directly bordering the undeformed foreland (Fig. 1a). The Eastern Cordillera at this latitude also shows unusual features. Silurian to Carboniferous

(and Jurassic?) strata are preserved in the Cianzo area (Fig. 1b) and provide a rare glimpse of the geologic evolution in the Eastern Cordillera after Ordovician and before Cretaceous time. In the Quebrada de Humahuaca, deformation and sedimentation in a thrust-top basin of Neogene to Recent age record the evolution of the Eastern Cordillera during the last few Ma.

STRUCTURE AND KINEMATICS OF KEY AREAS

The Cianzo area. Silurian to Tertiary strata form the N-trending regional Cianzo syncline, which is cut in the north by the ENE-striking, steeply ESE-dipping Hornocal fault (Amengual and Zanettini, 1973). The Hornocal fault is an inverted Cretaceous normal fault (Salfity and Marquillas, 1994), which juxtaposes some 2 km of coarse synrift clastics in the south with no synrift strata at all in the north (Fig. 1b). Today, the Cretaceous strata are thrust on top of a several km thick succession of sandy and conglomeratic Tertiary strata. East of the point where the shallow dipping, N-striking Zenta thrust splays off the Hornocal fault, the latter has preserved its normal sense of displacement (Figs. 1b,d). There, Carboniferous strata show marked thickness variations across a subsidiary normal fault, suggesting Carboniferous synsedimentary normal faulting. Along trend with the Hornocal fault lies the southern boundary of thin-skinned foreland thrusting (Fig. 1a).

Quebrada de Humahuaca. Along the western flank of the Humahuaca valley, thin-skinned thrusting has imbricated rocks of the Salta Group in the footwall of a major E-directed basement thrust (Fig. 1b). Locally, the imbricated thrust stack was then refolded about E-trending axes, indicating N-S contraction. Both the early E-verging thrusts and the transverse structures are cut by a younger set of more steeply dipping, E-directed thrust faults (Fig. 1c). The structural relations of a tuff dated to about 3 Ma slightly north of our study area (Marshall et al. 1982) suggest that the first phase of W-E contraction and the phase of N-S contraction are older than 3 Ma, whereas the second phase of W-E contraction is younger. All three deformation phases appear to predate a final kinematic change from approximately W-E thrusting to a strike slip regime with SW-NE contraction at about 2 Ma (Marrett et al. 1994), in which the steeper thrusts of the second phase were locally reactivated as dextral strike slip faults.

CONCLUSIONS

The unusual features of the eastern Andes between 23° and 24°S are due to interaction of the Tertiary thrust front with inherited stratigraphic and structural features. Particularly important are ENE-striking normal faults that delimit the Cretaceous rift basin to the NW but show signs of early activity in Carboniferous time. Down-to-the-southeast offsets on these faults and erosion beneath the rift axis of the detachment horizon in Silurian shales caused the southward termination of Subandean thin-skinned thrusting (Cominguez and Ramos, 1995; Kley et al., 1999). Different from the Santa Barbara System south of 24°S, large-scale thrust reactivation of Cretaceous normal faults was inhibited by their strike at about 30-45° to the Tertiary contraction direction. This held back foreland deformation in the 23-24°S

segment, enforcing displacement transfer from thin-skinned Subandean thrusts to basement thrusts of the Eastern Cordillera. The ENE-striking normal faults controlled the location of the transfer zones. Very young deformation in the Humahuaca area is compatible with displacement transfer between the active Subandean deformation front and the Eastern Cordillera. Repeated rapid changes of the contraction direction may reflect partitioning of the regional convergence vector into E and N components as it rotated from E-W into SE-NW direction.

REFERENCES

Amengual R. and Zanettini J.C.M. 1973. Geología de la comarca de Cianzo y Caspalá (Provincia de Jujuy). Revista de la Asociación Geológica Argentina, 28, 341-352.

Aramayo Flores R.F. 1989. El cinturón plegado y sobrecorrido del Norte Argentino: Boletín de Informaciones Petroleras, 17, 2-16.

Cominguez A.H. and Ramos V.A. 1995. Geometry and seismic expression of the Cretaceous Salta Rift System, northwestern Argentina. *In* Tankard A.J., Suárez Soruco R. and Welsink H.J., eds., Petroleum Basins of South America, AAPG Memoir 62, Tulsa, 325-340.

Kley J., Monaldi C.R., and Salfity J.A. 1999. Along-strike segmentation of the Andean foreland: causes and consequences. Tectonophysics, 301, 75-94.

Marrett R.A., Allmendinger R.W., Alonso R.N., and Drake R.E. 1994. Late Cenozoic tectonic evolution of the Puna Plateau and adjacent foreland, northwestern Argentine Andes. Journal of South American Earth Sciences, 7, 179-207.

Marshall L.G., Butler R.F., Drake R.E., and Curtis G.H. 1982. Geochronology of Type Uquian (Late Cenozoic) Land Mammal Age, Argentina. Science, 216, 986-988.

Monaldi C.R. and Kley J. 1997. Balanced cross sections of the northern Santa Barbara system and Sierra de Zapla, Northwestern Argentina. VIII. Congreso Geológico Chileno, Actas I: Antofagasta, Chile, 180-184.

Rolleri E.O. 1976. Sistema de Santa Bárbara. Una nueva provincia geológica Argentina. Sexto Congreso Geológico Argentino, Actas 1, 239-255.

Salfity J.A. and Marquillas R.A. 1994. Tectonic and sedimentary evolution of the Cretaceous -Eocene Salta group basin, Argentina. *In* Salfity, J.A., ed., Cretaceous tectonics of the Andes. Vieweg, Braunschweig, 266-315.

Salfity, J.A., Monaldi, C.R., Marquillas, R.A., and Gonzáles, R.E., 1993, La inversión tectónica del Umbral de los Gallos en la Cuenca del grupo Salta durante la Fáse Incáica, XII. Congreso Geológico Argentino y II. Congreso de Exploración de Hidrocarburos, Tomo III: Mendoza, Argentina, 200-210.

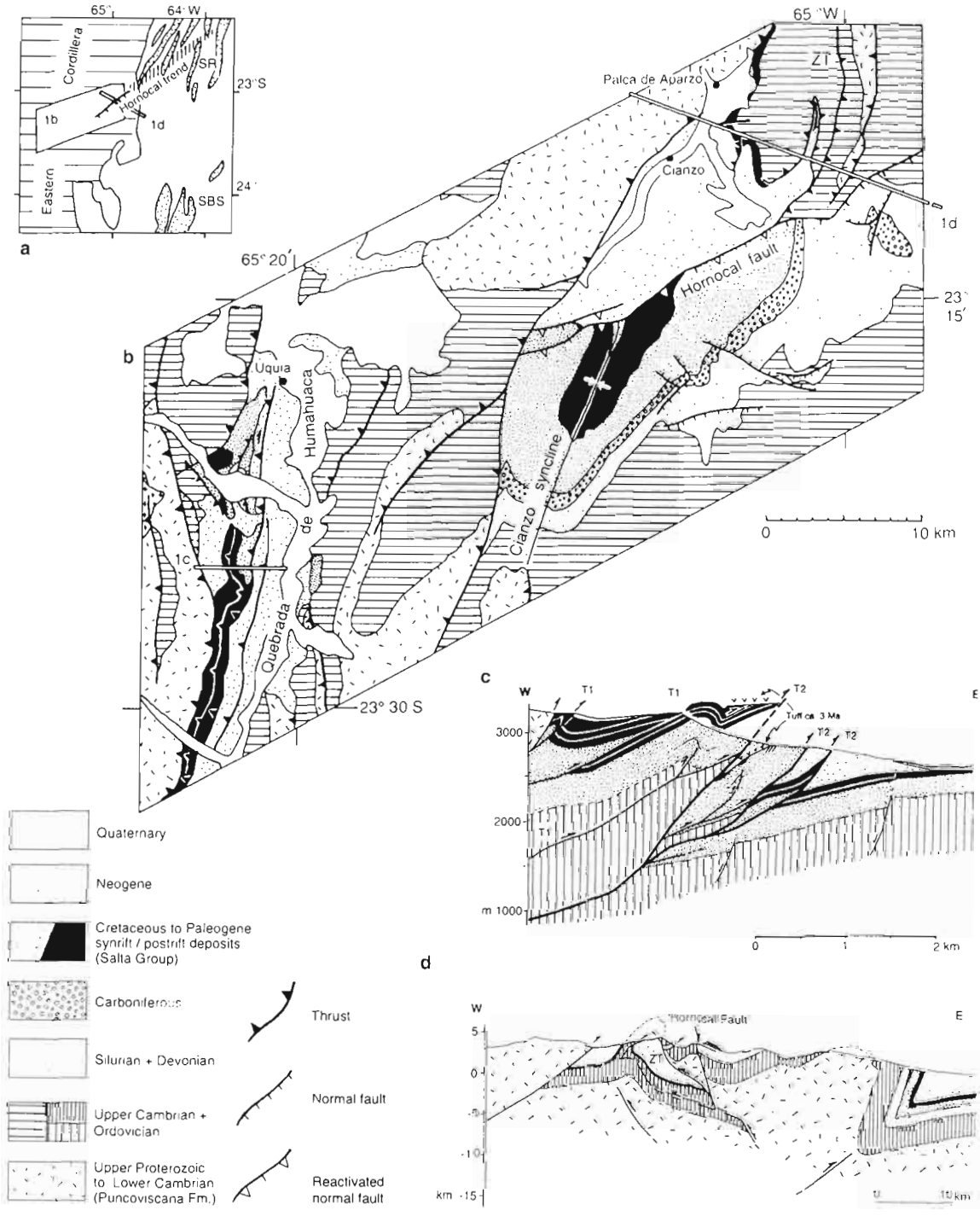

Figure 1. a) General setting of Eastern Cordillera, thin skinned Subandean Ranges (SR) and thick skinned Santa Barbara System (SBS) b) Geologic map comprising Cianzo and Quebrada de Humahuaca areas. ZT Zenta thrust c) Cross section through Humahuaca thrust zone with first and second phase thrusts (T1, T2) d) Cross section from the Cianzo area to the foreland.

EROSIVE MASS TRANSFER AT CONVERGENT MARGINS: CONSTRAINTS FROM ANALOG MODELS AND APPLICATION OF COULOMB WEDGE ANALYSIS

Nina Kukowski, Jürgen Adam, Jo Lohrmann

All at: GeoForschungsZentrum Potsdam, Telegrafenberg, D-14473 Potsdam, Germany (nina@gfz-potsdam.de)

KEY-WORDS: convergent margins, mass transfer modes, tectonic erosion, Coulomb analysis, analogue modelling, underplating

Non-accreting margins comprise more than half of the length of active convergent margins (von Huene & Scholl, 1991). However, mass transfer modes at erosive margins are not well understood. Seismic profiles across numerous margins give evidence for short term frontal tectonic erosion affecting accretionary complexes at the toe of the overriding continental forearc crust which may be caused by subducting asperities as seamounts or aseismic ridges and the rough surface of the subducting oceanic crust. Geological data infer long term frontal and/or basal erosion processes at non-accreting continental margins with significant trench retreat rates. Because this long term tectonic erosion occurs at the base of the forearc at greater depths, seismic imaging of related features is difficult. Thus, for a better understanding of erosive mass transfer at convergent margins it is necessary to combine the geological and geophysical data with mechanical concepts and analog models.

Actually, frictional wedge models concerning Coulomb plastic material provide the most actual physical concept for upper crustal deformation in convergent settings and allow to explore the dynamics, kinematics, mass transfer patterns and the controlling mechanism of exogenetic processes. In practise the capability of frictional wedge modelling is confirmed by numerous dynamic analyses of accretionary complexes and foreland thrust belts. For the study of the dynamics concerning long term erosive mass

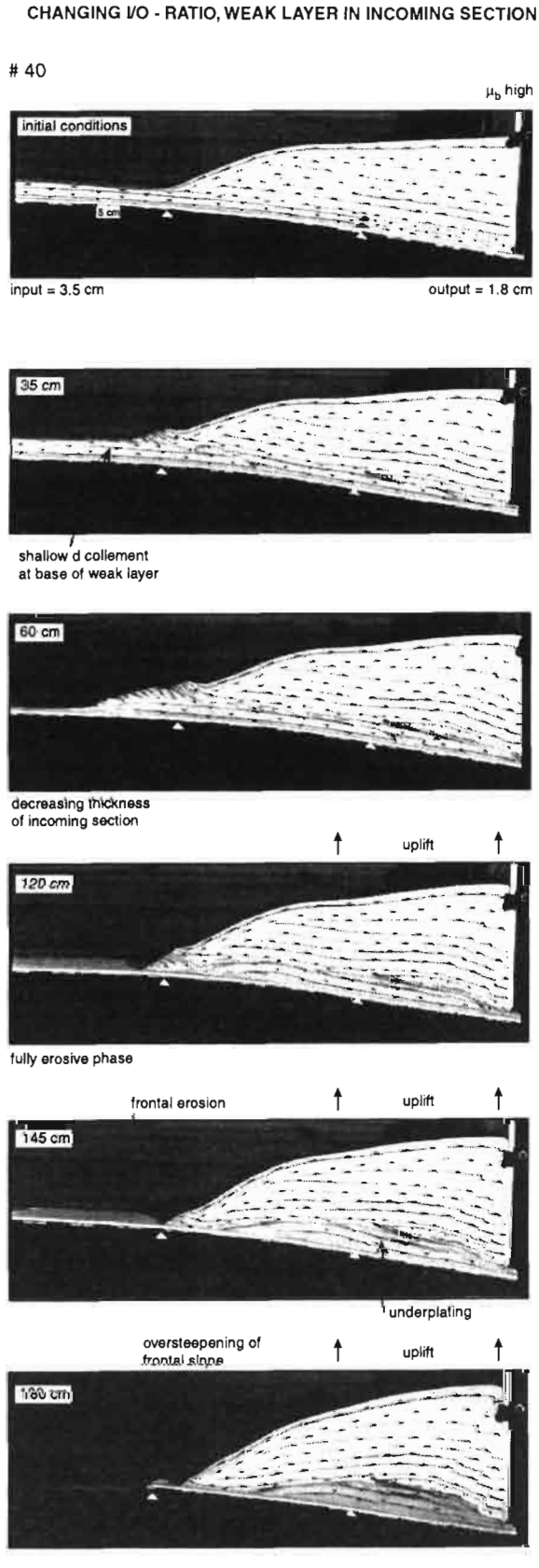

transfer at non-accretive convergent margins we apply scaled analog sandbox models and a critical taper frictional wedge concept to the entire brittle fore-arc crust.

Scaled sandbox experiments with different boundary conditions have shown that in the low basal friction case growth of the fore-arc dominantly occurs by frontal accretion of imbricate thrust slices, while high basal friction leads to a cyclic process alternating between frontal accretion and underthrusting of long undeformed units (Gutscher et al. 1996, 1998). Sandbox models with excess output (with a subduction window) provide insight in possible mass transfer modes at erosive margins (Kukowski et al., 1994, Gutscher et al., 1998). In the low basal friction case, basal erosion occurs in the footwall of a wedge-scaled out-of-sequence-thrust initiated on top of the subduction window located at the inner base of the deformable backstop. Trenchward overthrusting of the non erosive hangingwall block causes a pronounced fore-arc high with a leading depression. Tectonically eroded material will be removed from the arcward part of the accretionary wedge and from the adjacent backstop segment, both situated in the footwall block of the out-of-sequence-thrust, as shown by a significant decrease of the wedge geometry. This modeled deformation pattern images the formation of a fore-arc basin trapped between inner and outer fore-arc

Fig. 1: Several stages of the evolution of a sandbox experiment with decreasing input (change from accretive to erosive conditions)

highs. Contemporaneously, a frontal accretionary wedge may remain to exist or even grow, if there is some material supply indicating the simultaneity of frontal accretion and basal erosion.

In a high basal friction mode, nowhere significant growth is observed in the entire wedge. In sandbox models with heterogenous input and where a new basal decollement develops within the incoming sediment pile, frontal erosion and basal underplating may occur simultaneously (Fig. 1). Basal underplating then causes significant uplift and surficial extension of the continental margin. The combination of high basal friction and frontal erosion leads to an increasing taper and remarkable slope break of the frontal wedge. This characteristic topographic feature also is confirmed by bathymetric data of inner trench slopes at various erosive convergent margins. The results of the experiments imply that retreating margins may grow vertically to obtain a stable high frictional wedge geometry and therefore offer new concepts for the subduction of both, frontal and mid-arc material consisting of previously accreted sediments or framework rock of the fore-arc crust.

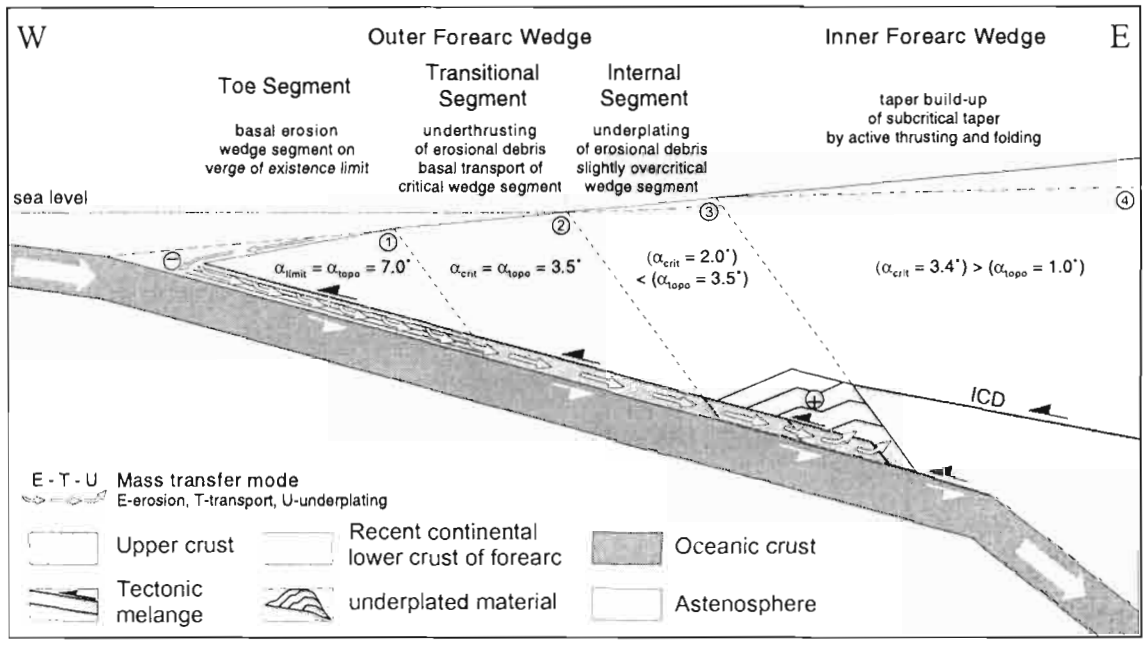

Fig. 2: Conceptual sketch of mass transfer modes active at the northern Chile margin

In terms of Coulomb wedge dynamics, frontal and basal erosion occur only under particular conditions. Frontal erosion will be triggered by the modification of the wedge shape due to variation of the wedge base by subducting topographic asperities of the oceanic crust shifting wedge dynamics into overcritical and subcritical states (e.g. Japan trench). Long term orogenic processes like mass transfer by basal erosion and underplating at non-accretive convergent margins is not restricted to the toe of the overriding plate but modify the entire fore-arc crust (e.g. Northern Chile) (Adam & Reuther, 1999).

Here enlarged frictional wedge analysis for the brittle fore-arc crust describes the active state of stress, mass transfer patterns, rheological conditions and dynamics controlling tectonic erosion. Progressive subduction processes and associated mass transfer shape the wedge geometry of the fore-arc system adjusting a dynamic equilibrium between internal deformation, basal erosion and surficial mass transfer (Fig. 2).

Therefore, at erosional convergent margins without significant recent variations of geodynamic or exogenetic factors, the fore-arc wedge geometry reflects the active dynamic processes and allows to analyse the rheological properties and dynamic processes of tectonic erosion. Ongoing basal erosion only occurs in high frictional Coulomb wedges at the verge of existence limit. In this case wedge internal detachments develop parallel to the locked subduction interface and material of the wedge base will be transported away by the subducting plate within a high strain deformation or melange zone. The process is comparable with the subduction channel model for sediment subduction. Changing rheological conditions with increasing depth (e.g. strain hardening, dewatering processes) control the unlocking of the subduction fault and re-entering of eroded material into the fore-arc wedge by underplating. These different modes of mass transfer by tectonic erosion, subduction and underplating are controlled by variations of the dynamic state within the fore-arc wedge system and are reflected by the actual wedge geometry and active deformation processes.

REFERENCES

Adam J. & Reuther C.-D. subm. Crustal dynamics and active fault mechanics during subduction erosion. Application of frictional wedge analysis onto North-Chilean Forearc. Tectonophysics.

Gutscher M.-A., Kukowski N., Malavieille J. & Lallemand S. 1998. Material transfer in accretionary wedges from analysis of a systematic seies of analog experiments. Journ. Struc. Geol.,20, 407-416.

Gutscher M.-A., Kukowski N., Malavieille J. & Lallemand S. 1996. Cyclical behavior of thrust wedges: Insights from high basal friction sandbox experiments. Geology, 24, 135-138.

von Huene R. & Scholl D. 1993. The return of sialic material to the mantle indicated by terrigeneous material subducted at convergent margins. Tectonophysics, 219, 163-175.

Kukowski N., von Huene R., Malavieille J. & Lallemand S. 1994. Sediment accretion against a buttress beneath the Peruvian continantal margin at 12°S as simulated with sandbox modeling. Geol. Rundsch., 83, 822-831.

IS BSR OCCURRENCE IN LIMA BASIN OFFSHORE CENTRAL PERU AN INDICATION FOR METHANE PRODUCTION BELOW THE GAS HYDRATE STABILITY ZONE ?

Nina KUKOWSKI (1) and Ingo A. PECHER (2)

(1) GeoForschungsZentrum Potsdam, Telegrafenberg, D-14473 Potsdam, Germany (nina@gfz-potsdam.de)
(2) Inst. for Geophysics, Univ. of Texas , 4412 Spicewood Springs Rd. , Austin, TX 78759-8500, U.S.A. (ingo@ig.utexas.edu)

KEY WORDS: convergent margins, reflection seismics, BSRs, tectonic erosion, subsidence, fluid flow

ABSTRACT

Bottom simulating reflectors (BSRs) identified in reflection seismic data are commonly associated with free gas beneath the base of the gas hydrate stability zone (BGHSZ) making them the most important indicator for gas hydrates. However, gas hydrates have been frequently found at locations which do not show a BSR. Recent studies have shown that hydrate formation is closely links to fluid advection and vertical tectonics. Therefore, a thourough understanding of these processes is required for gas hydrate quantification on a regional and global scale.

The convergent margins off Peru has been affected by the oblique subduction of Nazca Ridge (von Huene et al., 1996) which led to strong subsidence at a rate of about 500 m/my in Lima Basin. Due to high organic carbon content in the sediment, abundant methane for in situ gas hydrate formation should be available off Peru. On a large scale, BSRs offshore central Peru are present on the lower slope, where uplift is occurring at a rate of about 350 m/my (Pecher et al., 1996, von Huene & Pecher, 1999), whereas they are mostly absent on the upper slope in Lima Basin.

Fluid advection is thermally efficient at least in the neighbourhood of fault zones (Kukowski & Pecher, 1999). Stratigrafically elevated fluid flow apparently caused BSR occurrence above Seaward Ridge (Fig.1).

Tectonic subsidence leads to an increase of pressure and hence, a downward movement of the BGHSZ relative to the sediment column. Free gas at the BGHSZ is transformed to gas hydrates and thus is no longer available to cause the low-velocity layer that generates the BSR. BSRs have now been detected, however, in a small area in Lima Basin where erosion is taking place. Thermal accommodation to maintain a constant thermal gradient after erosion leads to cooling at a given point in the sediment. Erosion therefore, like subsidence, causes a downward movement of the BGHSZ with respect to the sediment column. The presence of BSRs and hence, most probably free gas, in an area of both subsidence and erosion, requires that a sufficient amount of gas has to be constantly supplied to the BGHSZ to sustain BSRs. Supply of free gas must offset the absorption of gas into the hydrate stability zone caused by the downward movement of its base.

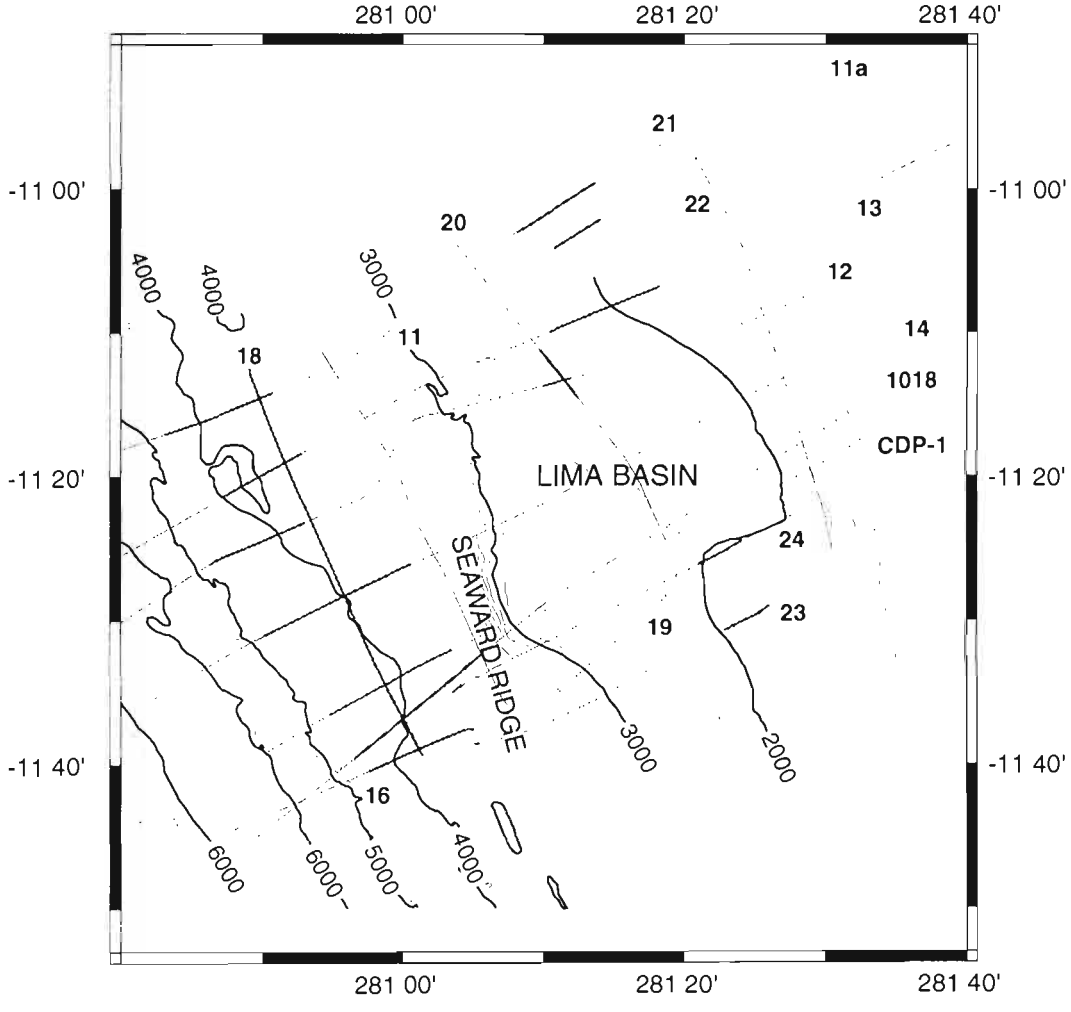

Fig. 1: BSR distribution offshore central Peru as indicated from reflection seismic data. Thick grey portions of seismic track lines indicate BSR identification.

Ocean Drilling Program Leg 112 showed that methane from gas hydrates off Peru is most probably of biogenic origin. Additional drilling would be required, however, to test whether methane from beneath the BGHSZ in this area in Lima Basin also is of biogenic origin. This would indicate considerable microbial production of methane deep in the sediment column beneath the hydrate stability zone.

REFERENCES

von Huene R., Pecher I.A., Gutscher M.-A. 1996. Material flux in the Peru subduction zone due to the subduction of Nazca Ridge and development of the accretionary prism. Tectonics 15, 19-33.

von Huene R., Pecher I.A. 1999. Vertical tectonics and the origins of BSRs along the Peru margin. Earth and Planet. Sci. Lett. in press.

Kukowski N., Pecher I.A. 1999. Thermo-hydraulic modelling of the accretionary complex off Peru at 12°S. - J. Geodynamics, Vol. 27, 373-402.

Pecher I.A., Minshull T.A., Singh S.C., von Huene R. 1996. Velocity structure of a Bottom Simulating reflector offshore Peru: Results from full waveform inversion. Earth and Planet. Sci. Lett. 139, 459-469.

NEW CONSTRAINS FOR THE AGE OF CRETACEOUS COMPRESSIONAL DEFORMATION IN THE ANDES OF NORTHERN CHILE (SIERRA DE MORENO, 21°-22°10' S)

Marco LADINO(1), Andrew TOMLINSON(1) and Nicolás BLANCO P.(1)

(1) Servicio Nacional de Geología y Minería, Avda Santa María 0104, Providencia, Santiago, Chile (email: atomlins@sernageomin.cl; nblanco@sernageomin.cl)

KEY WORDS: northern Chile, Sierra de Moreno, Cretaceous, shortening, syntectonic intrusion.

INTRODUCTION

In the Andean Precordillera of northern Chile previous authors have suggested that a regional tectonic shortening affected the area in the "middle" Cretaceous[7, 3]. However hard date concerning the nature and timing of this deformation were poorly constrained[4, 8, 10, 1]. We here summarize new radiometric data and geologic relations which, for the first time, indicate a late Early Cretaceous to middle Late Cretaceous age for deformation and uplift of Sierra de Moreno (21°-22°10'S) in the Precordillera of northern Chile.

REGIONAL GEOLOGY

The Sierra de Moreno is a NNE-trending mountain range occurring along the western margin of the Andean Precordillera of northern Chile (21°-22°10'S) and is composed of three structural domains limited by reverse faults (Fig. 1). From east to west, they are: 1) an eastern domain of Paleozoic basement blocks bound on the west by the west-vergent Sierra de Moreno, Quehuita and Choja reverse faults[5, 6, 9], which place the domain over 2) a central domain of strongly folded Jurassic and Lower Cretaceous sedimentary and volcanic rocks (Quinchamale Fm.[8] and Cuesta de Montecristo volcanic rocks[9], respectively) that at the southern end of the Sierra de Moreno is bound on the west by the west-vergent Barrera reverse fault, which places the domain over 3) a western domain of folded Upper Cretaceous and possibly Paleocene continental-facies rocks (Tambillo Fm.[8, 6]). East of the Sierra de Moreno, the Sierra del Medio is a fourth structural domain, which, from the conformity of the Jurassic to Eocene succession, appears to have largely escaped Cretaceous

deformation, but received epiclastic sediments (Tolar Fm.[1, 9]) derived from the uplift and erosion of the Sierra de Moreno. This fourth domain is separated from the Sierra de Moreno by the east-vergent Arca reverse fault (Fig. 1).

The Paleozoic rocks formed the basement of an ensialic back-arc basin that initiated in the Latest Triassic-Early Jurassic, with subsidence controlled by extensional tectonism[7]. During the Jurassic-Early Cretaceous, marine and later continental sedimentary rocks accumulated (Quinchamale Fm.) with volcanic rocks (Cuesta de Montecristo unit) being the last deposits of the succession[7, 1, 9]. The continental sedimentation was characterized by fluvial deposystems with sedimentary transport directions to the west[1]. Deformation and uplift of the Proto-Sierra de Moreno disrupted this pattern and produced two coeval alluvial basins flanking either side of the Sierra de Moreno (Fig. 1) and having opposing depositional slopes[1, 9, 5, 6]: one in a foreland position, with respect to the dominant structural vergence direction, ("Tambillo basin") with sedimentary transport directions to the west[1], and another basin in a hinterland position ("Tolar basin"), with transport directions to the east[1, 9]. The paleogeography suggests that initial Tambillo-Tolar sedimentation was syntectonic to the Cretaceous deformation, although it later continued accumulating as post-tectonic deposits during younger times[9].

CONSTRAINS ON THE AGE OF DEFORMATION

Barrera Quartz Monzonite: In Quebrada Barrera (Fig. 2) crops out a quartz monzonite emplaced at *ca.* 83-84 Ma (K/Ar amphibole and biotite ages[5, 6]). The body intrudes both the hanging wall and footwall blocks of the Sierra de Moreno Fault (SMF), postdating the majority of the displacement on the SMF, but a branch of the SMF also cuts the pluton (Fig. 2). In Jurassic-Lower Cretaceous epiclastic rocks west of the intrusion, a foliation associated with regional folding presents a metamorphic upgrade in the fabric mineralogy and texture as the intrusion is approached (from a spaced pressure-solution cleavage in mudstones to a penetrative schistosity in biotite schists), indicating the pluton was emplaced syntectonically to the shortening[5, 6]. The above indicate the Barrera Quartz Monzonite was emplaced at 83-84 Ma syntectonically to the shortening, but late in the displacement history of the SMF.

Tolar and Tambillo Formations: In the Sierra del Medio, in Quebrada Quinchamale (Fig. 1), an andesite clast in a conglomerate located at the base of the Tolar Formation yield a 109±4 Ma K/Ar biotite age[5, 9], providing a maximum age for the Tolar Fm. Sedimentary transport structures indicate clast derivation from the west, suggesting the likely source is the Cuesta de Montecristo volcanic unit in the Sierra de Moreno[6, 9]. In the San Lorenzo Anticline (Fig. 1) a rhyodacitic tuff interbedded in Tolar sandstones, 490 m above the base of the unit, yield a 77±3 Ma K/Ar biotite age[5, 9]. In the northern part of the central domain of the Sierra de Moreno, the Tambillo Formation unconformably overlies the Jurassic-Lower Cretaceous succession[9], and

between Quebradas Chug-Chug and Barrera (Fig, 2) it is intruded by sills with 61±1 Ma and 73±1.5 Ma K/Ar whole rock ages[5,6,2], indicating that at least in part the unit is also Upper Cretaceous. The data indicate that during the Late Cretaceous both sequences were deposited contemporaneously and that the beginning of sedimentation predates 73-77 Ma.

CONCLUSIONS

Based on the constrains discussed in this paper, deformation and uplift of the Andean Precordillera, at least in this part of northern Chile, relates to a phase of shortening that began after 109 Ma. An important component of this shortening, associated with displacement of the SMF, was largely over before 83-84 Ma, but shortening was ongoing at that time. The last displacement on the SMF is younger than this age.

Uplift of the Andean Precordillera in this part of northern Chile disrupted the pre-existing continental sedimentation patterns and generated two coeval Upper Cretaceous alluvial basins flanking either side of the Sierra de Moreno. Sedimentation in these basins is inferred to have been initially syntectonic to the Cretaceous deformation and radiometric data indicate that sedimentation began prior to 73-77 Ma.

REFERENCES

(1) Bogdanic, T. 1991. Evolución paleogeográfica del Cretácico-Terciario Inferior, entre los 21°-23° S, Región de Antofagasta, Chile. *In*: Congreso Geológico Chileno, N°6, Actas, Vol. 1, pp. 857-861, Servicio Nacional de Geología y Minería, Viña del Mar.

(2) Chong, G.; and Pardo, R., 1993. Geología del Districto de Chuquicamata, Segunda Región de Antofagasta (unpublished report). Superintendencia de Exploraciones y Desarrollo Geológico, CODELCO, Calama.

(3) Coira, B.; Davidson, J.; Mpodozis, C.; and Ramos, V. 1982. Tectonic and magmatic evolution of the Andes of northern Argentina and Chile. Earth Science Reviews, Vol. 18, pp 303-332.

(4) Ferraris, F. 1978. Hoja Tocopilla, Región de Antofagasta, Instituto de Investigaciones Geológicas, Mapas Geológicos Preliminares de Chile, N°3, 1:250.000 scale, 32 p., Santiago.

(5) Ladino, M.; Tomlinson, A.; and Blanco, N. 1997. Nuevos antecedentes para la edad de la deformación cretácica en Sierra de Moreno, II Región de Antofagasta-Norte de Chile. *In*: Congreso Geológico Chileno, N°8, Actas, Vol. I, pp. 103-107, Universidad Católica del Norte, Antofagasta.

(6) Ladino, M. 1998. Geología de la parte occidental de los cuadrángulos Quebrada Chug-Chug y Cerros de Montecristo, Región de Antofagasta, Chile. Universidad de Chile, Memoria de Título, 138 p., Santiago.

(7) Mpodozis, C.; and Ramos, V. 1989. The Andes of Chile and Argentina. Circum-Pacific Council for Energy and Mineral Resources, Earth Science Series, Vol. 11, pp. 59-90, Houston, Texas.

(8) Skarmeta, J.; and Marinovic, N. 1981. Hoja Quillagua, Región de Antofagasta, Instituto de Investigaciones Geológicas, Carta Geológica de Chile, N°51, 1:250.000 scale, 63 p., Santiago.

(9) Tomlinson, A.J.; Blanco, N.; Maksaev, V.; Dilles, J.H.; Grunder, A.; and Ladino, M. in prep. Geología de la Precordillera Andina de Quebrada Blanca-Chuquicamata, Regiones I y II (20°30'-22°30'). Servicio Nacional de Geología y Minería y Corporación Nacional del Cobre, Informe Registrado.

(10) Vergara, H.; and Thomas, A. 1984. Hoja Collacagua, Región de Tarapacá. Carta Geológica de Chile, N° 59, 1:250.000 scale, 79 p., Servicio Nacional de Geología y Minería, Santiago.

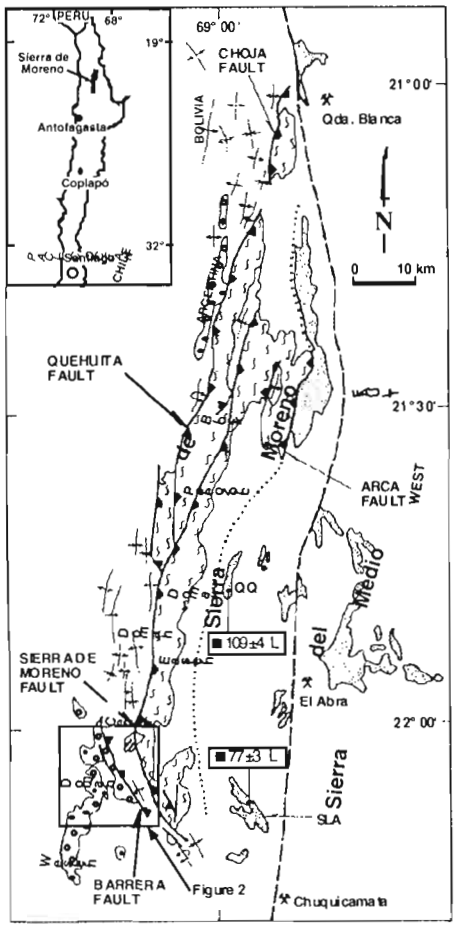

LEGEND

- Tambillo Formation: red sandstones and conglomerates on the west flank of the Sierra de Moreno, Upper Cretaceous - Paleocene?
- Tolar Formation: red sandstones and conglomerates on the east flank of the Sierra de Moreno, Upper Cretaceous - Lower Eocene
- Barrera Quartz Monzonite, 83-84 Ma
- Folds developed in Jurassic - Lower Cretaceous sequences
- Basement of Paleozoic granitoids and metamorphic rocks uplift in the Cretaceous
- K-Ar biotite

Figure 1: Simplified geologic map of the Chilean Precordillera north of Chuquicamata, with the location of the principal Cretaceous structures. The West Fault (Tertiary) is located only for reference. L: Ladino et al. (1997), QQ: Quebrada Quinchamale, SLA: San Lorenzo Anticline.

Figure 2: Geologic map of the southern end of the Sierra de Moreno, showing the contact relations between the Barrera intrusion and Cretaceous faults. Also shown are the principal structures in the area. L: Ladino et al. (1997), CP: Chong and Pardo (1993), SMF: Sierra de Moreno Fault.

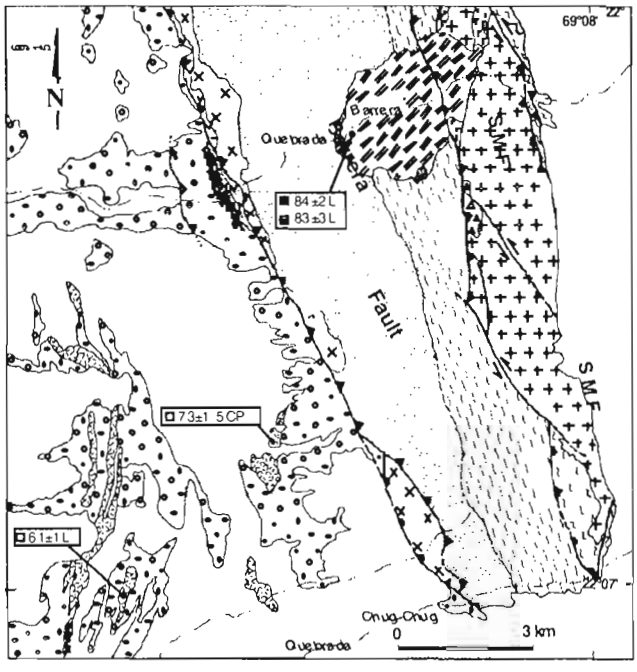

LEGEND

- Gravels, Miocene - Quaternary
- Hypabyssal andesitic and basaltic intrusions, 61-73 Ma
- Tambillo Fm., continental sedimentary clastic rocks, Upper Cretaceous - Paleocene?
- Barrera Quartz Monzonite, 83-84 Ma
- Contact metamorphosed sedimentary rocks
- Farellón Monzodiorite, late Early Cretaceous?
- Cuesta de Montecristo volcanic rocks, Lower Cretaceous?
- Quinchamale Fm., continental sedimentary rocks, Kimmeridgian - Lower Cretaceous?
- Quinchamale Fm., marine sedimentary rocks, Hettangian - Kimmeridgian
- Granitoids, Late Paleozoic
- Collahuasi Fm., rhyolites and sedimentary breccias, Upper Paleozoic
- Sierra de Moreno metamorphic complex, schists, Paleozoic
- Shear zone

■ K-Ar biotite, ■ K-Ar amphibole, ▫ K-Ar whole rock

FROM COMPRESSIONAL TO EXTENSIONAL TECTONIC REGIME AT THE FRONT OF THE PATAGONIAN ANDES, 46°S-47°S:

A response to the subduction of the Chile Spreading Ridge?

Yves LAGABRIELLE (1), Jacques BOURGOIS (2), Manuel SUAREZ (3), Rita DE LA CRUZ (3), Erwan GAREL (1), Olivier DAUTEUIL (4), Marc-André GUTSCHER (5).

(1) CNRS, UMR 6538, IUEM, Place Nicolas Copernic, 29280 Plouzané, France. E-mail : yves.lagabrielle@univ-brest.fr
(2) CNRS and UPMC, Laboratoire de Géodynamique, Tectonique et Environnement, Bte 119, 4 place Jussieu, 75252 Paris Cedex 05, France. E-mail : bourgois@ccr.jussieu.fr
(3) Servicio Nacional de Geología y Minería, Avenida Santa María 0104, Providencia, Santiago Chile, E-mail msuarez@SERNAGEOMIN.cl
(4) CNRS, UPR A4661 CNRS, Université de Rennes, Campus de Beaulieu, 35042 Rennes Cédex, France. E-mail : Olivier.Dauteuil@univ-rennes1.fr
(5) IRD, Centre de Brest, B.P. 70, F-29280 Plouzané, France. E-mail : magutsch@ifremer.fr

KEY WORDS : Patagonian Andes, recent-active extension, Miocene compression, ridge subduction

INTRODUCTION

Relationship between shortening, thickening and frontal convergence are well studied in regions where thrust faults are developed, that is far north and south of the Chile Triple Junction (CTJ) Andean transect. In contrast, implications regarding the processes of continental tectonics related to the subduction of the active spreading ridge are poorly investigated. In this paper, we report the results of preliminary geological work conducted in the region of Lake General Carrera, a major transverse structure of the Patagonian Andes, paralleling the direction of subducted transform of the oceanic lithosphere.

DISCONTINUITIES OF THE SOUTHERN ANDES AND RIDGE SUBDUCTION

The backarc fold and thrust belt of southernmost Patagonia is well developped south of the latitude of the CTJ, where it can be followed over few hundred of kilometers (Ramos, 1989, Ramos and Kay, 1992). This tectonic front appears to end between Lakes General Carrera and Cochrane close to the latitude of the CTJ region, also corresponding to a change in the thickness of the Miocene molasse. Immediately to the north of

Lake General Carrera (Lake Buenos Aires in Argentina), geological mapping did not allow yet to evidence any major thrust fault.

Kinematic analysis allowed to reconstruct the history of the subduction of the Chile ridge during the Neogene. A long segment of the Chile ridge met with the Chile trench west of Tierra del Fuego around 14 Ma ago (Cande and Leslie, 1986; Forsythe et al., 1986). Three short ridge segments were then subducted at 10 Ma, 6 Ma, and 3 Ma. The segment of the South Chile ridge (SCR) between the Taitao and the Darwin fracture zones (segment SCR 1) is presently being subducted and intersects the trench at 46°12'S. From our reconstruction based on magnetic anomalies collected during the CTJ cruise of R/V l'Atalante in 1997 (Bourgois et al., 1997), we are able to trace with more detail the prolongation of the main subducted oceanic features of the Chile Ridge under the continent. In particular, the trace of the Tres Montes fracture zone corresponds to the northern limit of the Golfo de Penas and is roughly parallel to the northern shore of Lake General Carrera. The projections of the subducted ridge segments SCR 0 and SCR -1 coincide respectively with the Ofqui Isthmus and a line joining the middle part of Lakes General Carrera and Cochrane. According to this peculiar position, geological investigations of the eastern part of the Cordillera in the region of Lakes General Carrera and Cochrane is supposed to provide pertinent informations regarding the neotectonic evolution of the frontal Patagonian Andes and its present-day state of stress, in relation with the subduction of active ridge and transform fault.

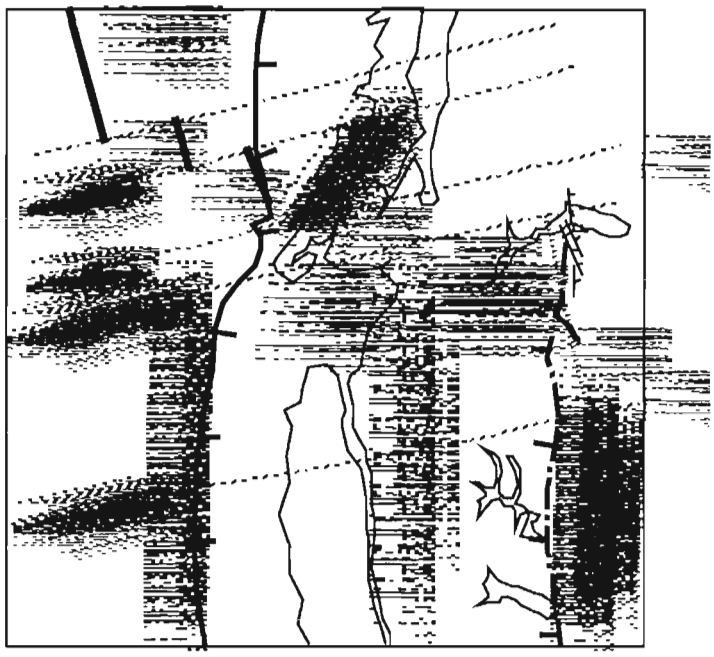

Fig. 1. Simplified map of the central Patagonian Andes showing the location of the patagonian thrust and fold belt to the east and the position of the subduction front to the west. The location of the fracture zones and spreading segments of the Chile ridge is shown (SCR 1, SCR 2) and the hypothetical position of the subducted segment SCR 0 and

SCR -1 is indicated (thick dashed lines). Recent or active normal faults observed in the region south of Lake General Carrera are indicated with their approximate orientation.

TECTONIC INVESTIGATIONS OF THE FRONT OF THE PATAGONIAN ANDES AT THE LATITUDE OF THE CHILE TRIPLE JUNCTION.

The continental region at the latitude of the CTJ is characterized by a relatively simple geological organization apparently devoid of major visible thrust fault. At a broad scale, Jurassic volcanics (Ibanez Group) and Cretaceous marine and continental stratas (Coihaique and Divisadero Groups) rest almost horizontally over the deformed basement (references in Suarez et al., 1996). However, compressional structures that accomodate E-W shortening are reported from Tertiary strata within uplifted basins representing molasse deposits (Cosmelli Basin, Cerro Rocoso Basin, and Balmaceda Basin: Prior et al., 1996; Ray, 1996; Flint et al., 1994; Suarez et al., 1996). Deformation is supposed to have occurred during the middle-upper Miocene (25-10 Ma). The links between this compressional evolution and the subduction of the active Chile spreading ridge, as well as the connection of the observed folds and thrust faults to the Patagonian foreland thrust have been discussed by few authors (Ramos and Kay, 1992; Flint et al., 1994; Suarez et al., 1996) but were studied in detail only in restricted areas.

Compressional Features

Verticalized volcanic rocks of the Ibanez group as well as basalts and strata of Eocene and Miocene age (Guadal formation), locally slightly overturned, can be followed along a N-S line from Rio Quebrada Chica (Ray, 1996) to Arroyo Marques, immediately south of the town of Chile Chico. This tectonic lineament marks the northern prolongation of the compressive front of the Patagonian Andes. South of Arroyo Quebrada Honda, rocks of Mesozoic and Cenozoic ages (formations Ibanez, Cerro Colorado, Estero los Flamencos tuffs; Eocene basalts; Guadal and Galera) are folded and verticalized, and show clear internal thrusts. Although a pre-Paleocene, probably Cretaceous contractional tectonism has also been identified in the region (Suarez and De La Cruz, 1996), the evidences for compressional tectonic events of upper Tertiary age are frequent in different transects between Arroyo Quebrada Honda and Arroyo Marques (Suarez and De La Cruz, in prep.). They include hectometric imbricated thrust faults affecting green-red Miocene marine stratas (levels with oysters, rynchonellids, etc.) of the so-called Guadal formation, well exposed in Rio la Horqueta. Adjacent continental strata assigned to the Galera Formation exhibit two different structural attitudes: steeply dipping (subvertical and even overturned beds) and horizontally-bedded. This may imply either folding and faulting of the same unit or an angular unconformity between a "lower" deformed Galera Formation and an "upper" undeformed Galera Formation. The latter suggests that the deformation apparently ceases progressively upper in the sequence in a similar way as described in the Cosmelli basin by Flint et al., (1994). This suggests that the contractional deformation occurred during the sedimentation, probably between the Middle Miocene and

the Upper Miocene (25-10 Ma), prior to the Upper-Miocene to Pliocene deposition of the flat-lying basaltic lavas of the Meseta Buenos Aires (Ramos and Kay, 1992; Suarez and De La Cruz, in prep.).

Therefore, the age of the Guadal and Galera formations is crucial for interpreting the tectonic evolution of the area. Flint et al. (1994) suggested an age younger than 17 Ma (late Lower Miocene) for the entire Guadal/Galera stratigraphy in the area south of General Carrera, on the basis of lithologic correlations with strata exposed in the Alto Rio Cisnes area, approximately 200 km to the north. However, recently Frassinetti and Covacevich (in press) proposed an Upper Oligocene-Lower Miocene (35-16 Ma), and probably a Lower Miocene age (26-16 Ma) for the Guadal Formation, in accordance with earlier studies (see Niemeyer et al., 1984). The Galera Formation, in turn, has been correlated with the Santa Cruz Formation, which includes fossil mammals of Santacrucian age (late Early Miocene-early Middle Miocene age : 18-15 Ma, Marshall and Salinas, 1990).
Consequently, if there is a contractional tectonic event during the deposition of the Galera Formation, this would have occurred sometime between 18 and 15 Ma, if the above correlations are correct. On the other hand, if the whole of the so-called Galera Formation was deformed, then this contractional tectonism took place after 15 Ma.

Extensional Features

Beside these evidences for contractional tectonics, numerous features demonstrate that important normal faulting and extension occurred in this region after the deposition of the Miocene molasse. Normal faults clearly crosscut Miocene stratas of the Guadal formation in Rio La Horqueta and at Loma del Rodeo, some kilometers south of Chile Chico.
In addition, field observations and aerial photo analysis reveal frequent evidences of post-glacial tectonics.
- The most striking features concern the deformation of young moraines crests, trending E-W, well exposed on the plateau immediately south of Chile Chico (1000 m). A N140 trending vertical fault cross cut the successives moraines crests and leaves a clear trace in the topography. Dextral strike-slip motion can be possible but the topographic offset also indicates that the eastern block is down-faulted. To the east, the morainic crests are abruptly cut along a normal fault with similar orientation. Close to this point, en échelon open fissures, locally 10-20 m wide, are observed on the plateau, within the Upper Jurassic basement rocks of the Ibanez formation. The envelop of the en échelon fissures is trending N140, parallel to the direction of the fault that cuts the moraines. The E-W trending border of the plateau, corresponding to the major scarp south-west of Chile-Chico, represents a vertical wall with the larger step of the studied area, corresponding to the southern boundary of the Lake General Carrera active rift zone.
- Normal faults with more than 10 m of vertical offsets have been observed in glacial sedimentary formations (tills). The amplitude of the vertical offsets and the presence of similar features cutting through Miocene stratas favours the hypothesis of regional tectonics rather than glacitectonics as a major cause of such features.

- Lacustrine sediments (varves) are well exposed along the road, west of Chile Chico. They are often tilted and locally show spectacular post-depositional listric faults. Such tilting can be either related to syn-glacial tectonics or to pure tectonic activity of the bed-rock. The abundance of evidences for very recent tectonic disturbances observed through out the entire region suggests that vertical displacement within the basement rocks can be responsible of most of the features observed in the varves of Chile Chico. Synsedimentary soft disturbance, "seismites", are repeatedly observed within the varve sequences.
- Recent scarps, 10-20 m high, are observed in the relatively flat areas immediately west of Chile Chico. They offset the glacier-related polished surface (roches moutonnées), and could thus represent again marks of post glacial tectonic activity.
- Six levels of low postglacial fluvial-lacustral terraces, with second-order sub-levels, are identified around the Lake General Carrera. One of the lower terrace is notched by well-developed ancient fluvial system (loops, captures and delta). The paleo-flowing orientation was approximately from west to east, thus revealing a regional paleo-slope dipping eastward. At present, the two mains rivers (Rio Jeinimeni and Los Antiguos) have a rotated northward drainage orientation. We may thus consider that important regional slope modification occurred very recently.

CONCLUSION

Our preliminary results of field investigations in the Patagonian Cordillera at the latitude of the Chile Triple Junction confirm that the northern prolongation of the Patagonian fold and thrust belt along the Andean front (Ramos, 1989) can be traced here. The amplitude of such a contractional tectonic in the area of the lake General Carrera remains an open question. Much more clear are the numerous evidences of recent and active extension found in this area which is undergoing a E-W trending stretching. We suggest that present-day active extension along the Andean front is the tectonic response to the presence of the Chile ridge spreading center at depth. Eastward progression of the buried spreading segment would drive the progressive shift from compression to extension. Local age constraints for these events are poor, but regional constraints discussed above suggest that compression stopped between at least before 8 Ma, whereas segment SCR -1 entered the trench around 6 Ma. These probable tectonic effects of ridge subduction have to be correlated with magmatic manifestations related to the development of an asthenospheric window below Patagonia (Ramos and Kay, 1992; Gorring et al., 1997). Pliocene and Holocene basaltic flows with transitional affinities are present in the region of Lake General Carrera, especially near Chile Chico, Rio Jeinemeni and Meseta Buenos Aires. Moreover, Holocene basaltic edifices with E-MORB affinities, similar to that emplaced at the Chile spreading center have been discovered recently in the valley of Murta on the northern side of Lake General Carrera (Demant et al., 1998).

Acknowledgments : this work was partially funded by FONDECYT project No 1960097, by the ECOS-sud Program, and by UMR-CNRS 6538, Brest.

REFERENCES

Bourgois et al., 1997. *EOS, Transactions, AGU. 78, 46.*

Cande and Leslie, 1986. *Journal of Geophysical Research*, 91, 471-496.

Coutand et al., 1996. *Extended Abstracts*, 3rd ISAG, St Malo, France, 331-334.

Demant et al., 1998. *Compte Rendus Académie des Sciences*, Paris, 327,795-801

Diraison et al., 1997. *Geology*, 25, 8, 703-706.

Flint et al., 1994. *Journal of the Geol. Soc. London*, 151, 251-268.

Frassinetti and Covacevich. *Bol., Servicio Nacional de Geologia y Mineria, Chile*, in press

Forsythe et al., 1986. *Geology*, 14, 23-27

Gorring et al, 1997. *Tectonics*, 16, 1, 1-17.

Marshall and Salinas, 1990. Revista Geologica de Chile, 17, 57-58.

Niemeyer et al., 1984. *Carta Geologica de Chile N° 60-61, SERNAGEOMIN, Santiago, Chile, 80p.*

Prior et al., 1996. *Extended Abstracts*, 3rd ISAG, St Malo, France, 461-464.

Ramos and Kay, 1992. *Tectonophysics*, 205, 261-282.

Ramos, 1989. *AAPG Bull.*, 73, 7, 887-903.

Ray, 1996. *PhD Dissertation*, University of Liverpool, Dept Earth Science, UK

Skarmeta, 1978. *Carta Geologica de Chile, N° 29. SERNAGEOMIN, Santiago, Chile*

Suarez et al., 1996. *XIII Congreso Geologico Argentino, Acta I*, 575-590

VOLCANISM AND TECTONICS OF THE PLEISTOCENE-HOLOCENE VOLCANIC ARC, SOUTHERN ANDES (40.5°-41.5°S)

Luis LARA (1), Hugo MORENO (2), Alain LAVENU (3)

(1) SERNAGEOMIN, Av.Santa María 0104. Santiago. Chile (lelara@sernageomin.cl)
(2) SERNAGEOMIN, Cerro Ñielol s/n. Temuco. Chile. (ovdassis@chilesat.net)
(3) ORSTOM, casilla 53390. Santiago. Chile (alavenu@dgf.uchile.cl)

KEY WORDS: Stratovolcanoes, monogenic cones, transverse chains, strain rate

INTRODUCTION

The volcanic arcs, especially those which are emplaced at convergent margins, present a complex configuration which is expressed in their geometry and temporal evolution of magmatism. Although volcanic arcs conform to a margin-parallel belt on a continental scale, these belts consist of many transverse chains that comprise different types of volcanic centres (stratovolcanoes, flank and monogenetic cones). This internal anisotropy can reflect, in the sense of Nakamura (1997), the overpressure of the regional stress field. However, Fedotov (1981) has analized these variations from the thermodynamic point of view relating the building of stratovolcanoes/monogenetic cones to the magmatic input rate from the asthenosphere. Takada (1994) developed an 'output stress' diagram which incorporates the combined effect of strain rate and magmatic input in volcanic regions of continental scale.

We document this effect in the Southern Andes, where the architecture of the volcanic arc includes NE-SW and NW-SE transverse chains of morphologically and geochemically heterogeneous volcanic centres. These transverse alignments are associated with a long-lived structural system.

VOLCANIC CENTRES AND STRUCTURES

This study relates to the arc segment between 40.5° and 41.5°S (FIG.1). It concerns the Carrán-Los Venados group, a chain of 70 basaltic cones and maars of N50E orientation; the Cordillera Nevada-Cordón Caulle- Puyehue volcanic chain, a line of colapsed stratovolcanoes, fissural vents of rhyolitic composition, and monogenetic cones; the Grupo Casablanca, a basaltic stratovolcano together with flank and monogenetic cones of NE-SW orientation; and the Osorno-Puntiagudo chain, a group of stratovolcanoes and cones of the same orientation. The Liquiñe-Ofqui Fault behaves as an axis of

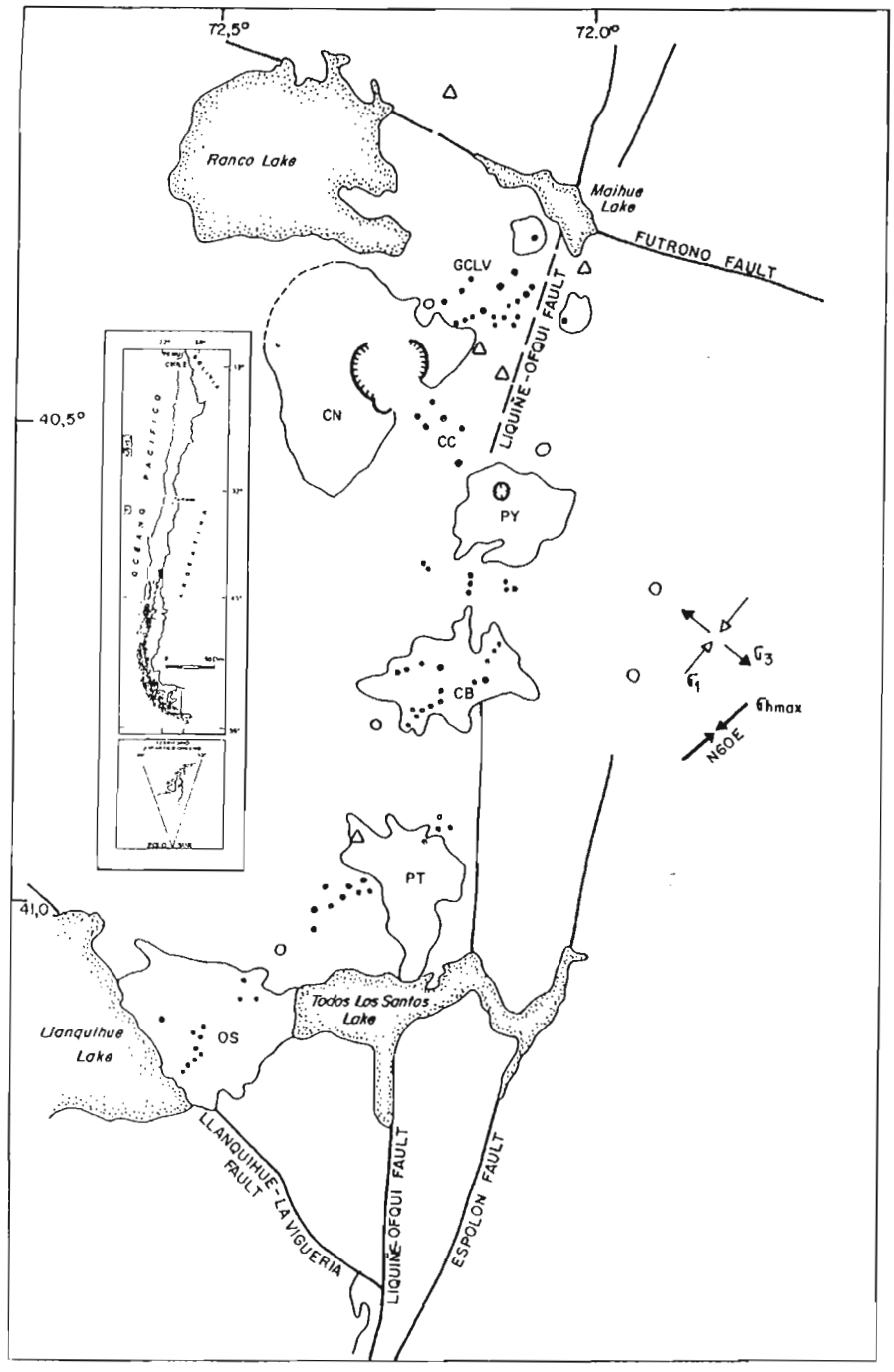

FIG.1. Volcanic centres and structures in 40.5°-41.5° segment of Southern Volcanic Zone. Chile.

Key: GCLV: Grupo Carrán-Los Venados; CN: Cordillera Nevada; PY: Puyehue; CB: Casablanca; CC: Cordón Caulle; PT: Puntlagudo; OS: Osorno.

- ○ Plio-Pleistocene volcanoes
- ● Holocene pyroclastic cones, domes and fissural vents
- →← Holocene σ_{hmax} axis
- →↕← Miocene-Pliocene σ_1-σ_3 axis (*e.g.*, Lavenu *et al.*, 1997)
- △ 1992-1995 crustal earthquakes (depth: 10-30 km; M:4.1-4.9)

longitudinal symmetry and in its trace are also located some of the centres which form the transverse chains.

The orientation of volcanic alignments is roughly coincident with structures recognized in the basement, but whose kinematics are only partially known in this area. The studied segment is delimited by a structure of N120E orientation, the Futrono Fault, which corresponds to a major limiting structure of the continental margin, and is possibly the western expression of the Gastre System (Coira *et al.*, 1975). The southern limit is the Llanquihue-La Viguería Fault of N40W orientation and unknown kinematics. The Liquiñe-Ofqui Fault (*e.g.*, Hervé, 1976; Cembrano y Hervé, 1993, Cembrano, 1996) is also exposed; the Miocene-Pliocene kinematics of this fault are consistent with a dextral transpressive regime (Lavenu *et al.*, 1997). Two crustal earthquakes located outside the segment are the sole record of the instantaneous deformation on this arc segment and their focal mechanisms (*e.g.*, Chinn and Isacks, 1983; Barrientos y Acevedo, 1992) are consistent with the inversion of mesoscopic structural data of basement rocks.

The present data show that the monogenetic cones, likewise the flank cones of the stratovolcanoes, are placed at a NE-SW orientation or isolated within the Liquiñe-Ofqui Fault. The stratovolcanoes are located in both NE and NW chains, and the more siliceous centres, although scarce, have a preferential NW orientation. In addition, although there no permanent seismic stations in the area, stations outside the zone have recorded five crustal earthquakes of 4.1-4.9 magnitude with depths between 10 and 30 km since 1995.

DISCUSSION

The above observations suggest important questions with respect to volcanic activity in the region. Cembrano and Moreno (1994) proposed a model of strain partitioning, and interpret the tranverse chains as expressions of compressive and extensional domains in the arc. Lavenu *et al.* (1997), in addition to proposing a partial strain partitioning model, suggest the coincidence of basement structures and volcanic chains. Alaniz-Alvarez *et al.* (1998) have shown, for the Transmexican Volcanic Belt, the importance of structural reactivation, and they explain the difference in volcanic morphology as a function of strain rate (desplacement) of pre-existing structures. In agreement with this model, we conclude that in the studied arc segment, the NE-SW structures are well-orientated for reactivation in the current regional stress field, whereas those of NW-SE orientation are misorientated in a factor of 0.23. As the strain rate is unknown in the volcanic arc, and the strain partitioning considerations have a strict value for pre-pliocene rocks, the relation between volcanism and deformation is still not well understood.

CONCLUSSIONS

The geometry and architecture of this volcanic arc segment show clearly the effect of the action of an homogeneous regional stress field upon the volcanic structures. At the same time, the pre-fractured nature of

the basement causes the preferential reactivation of NE-SW structures, leading to local distortions of the deformation regime. In addition, local factors such as weight and internal anisotropy of stratovolcanoes have an important effect on the force balance.

In the present study, we expect to bring together the record of mesostructural kinematics, to analyze the volcanic morphology and its relation to the deformation regime, and to design a field experiment of the record of natural crustal earthquakes in order to quantify the instantaneous deformation in this segment.

The above tools will allow us to develop a methodology of regional study of volcanological behaviour of an arc segment, and to develop individual models relating to the evolution and hazards associated with single volcanic centres.

ACKNOWLEDGMENTS

We are grateful to Fondecyt 1960885 grant and to S. Mathews for his comments.

REFERENCES

Alaniz-Alvarez, S., Nieto-Samaniego, A., Ferrari, L. 1998. Effect of strain rate in the distribution of monogenetic and polygenetic volcanism in the Transmexican volcanic belt. Geology,V.26,No.7, p.591-594.
Barrientos, S.; Acevedo, P. 1992. Seismological aspects of the 1988-1989 Lonqimay (Chile) volcanic eruption. Journal of Volcanology and Geothermal Research, No.53, p. 73-87.
Cembrano, J. y Hervé, F. 1993. The Liquiñe-Ofqui Fault Zone: a major Cenozoic strike slip duplex in the Southern Andes. ISAG No.2, Oxford. Editions de l'ORSTOM, p.175-178.
Chinn, D.; Isacks, B. 1983. Accurate source depths and focal mechanisms of shallow earthquakes in Western South America and the New Hebrides Island arc. Tectonics, V.2, No.6, p. 529-563.
Fedotov, S.A. 1981. Magma rate in feeding conduits of different volcanic centres. Journal of Volcanology and Geothermal Research, V.9, p.379-394.
Hervé, M. 1976. Estudio geológico de la Falla Liquiñe-Reloncaví: antecedentes de un movimiento transcurrente (Provincia de Valdivia). Congreso Geológico Chileno No.1, Actas v.1, p.B39-B56.
Nakamura, K. (1977). Volcanoes as possible indicators of tectonic stress orientation: principle and proposal. Journal of Volcanology and Geothermal Research No.2, p.1-16.
Takada, A. 1994. The influence of regional stress and magmatic input on styles of monogenetic and polygenetic volcanism. Journal of Geophysical Research, V.99, No.B7, p.13.563-13.573.

STRUCTURAL SETTING AND AGE OF THE COLOMBIAN EMERALD DEPOSITS: IMPLICATIONS FOR THE TECTONIC EVOLUTION OF THE CORDILLERA ORIENTAL

Bernard LAUMONIER [1], Yannick BRANQUET [2], Alain CHEILLETZ [2] & Gaston GIULIANI [2,3]

(1) Ecole des Mines, 54042 Nancy Cedex, France
(2) CRPG-CNRS, BP 20, 54501 Vandoeuvre-les-Nancy Cedex, France
(3) IRD, BP 20, 54501 Vandoeuvre-les-Nancy Cedex, France

The Cordillera Oriental of Colombia houses a unique type of emerald deposit entirely related to sedimentary rocks and tectonic-hydrothermal processes. But, quite surprisingly, there are two groups of such deposits that differ greatly by their structural setting and age. The western deposits (WD : Muzo and Coscuez deposits...) are located north of Bogotá, in the western part of the mountain belt, at some distance from the middle Magdalena basin. The eastern deposits (ED : Chivor deposit...) are located to the northeast of Bogotá, near the eastern border of the cordillera, not far from the Llanos basin. The deposits crop out in two anticlinoria resulting from the inversion of a Cretaceous subsident basin and its thrusting over both middle Magdalena and Llanos basins. The emerald deposits provide important clues to the tectonic evolution of the Eastern Cordillera.

Main common characteristics of the WD and ED are : (i) close linkage with evaporites (halite and gypsum/anhydrite) and black shales; (ii) Lower Cretaceous hosting rocks; (iii) a same mesothermal-sedimentary genetic model, involving generation of hot brines (280-300 °C) through evaporite dissolution by basinal waters, thermochemical sufate reduction, Na-Ca metasomatism of black shales (albitization and carbonatization), coeval leaching of beryllium and pyrite-calcite-dolomite-bitumen-emerald precipitation; (iv) intense hydro-thermal-tectonic breccias development. Hydrothermal breccias underline the tectonic contacts that acted as channels for the mineralizing fluids.

The WD are hectometer- to kilometer-sized, highly complex associations of thrusts, reverse faults, drag folds, ramp folds, duplexes, strike-slip and tear faults and flowers structures of varied orientations, all attesting a very heterogeneous compressive deformation of the mineralized Valanginian-Hauterivian series. At a larger scale, the deposits are disharmonic structures residing in the core of plurikilometer-sized, upright anticlines, regularly trending parallel to the belt, i. e. N20°E, and associated with a strong axial plane cleavage. These folds are linked to west-vergent reverse faults and, at this regional scale, the cordillera is an ordinary fold-and-thrust belt. Structural analysis shows that the small

deposits and the large anticlines are coeval. The overall structure implies a concealed décollement that probably is the evaporite level from which originated the mineralizing fluids. Logically, such a décollement must be also a major floor thrust along which the belt was thrusted, probably westward. Mineralization, and consequently the regional deformation, is dated by K/Ar and Ar/Ar methods at 38-32 Ma, i.e. Upper Eocene to lowermost Oligocene. Other data are consistent with this conclusion; for example, folding and thrusting is known to have occurred as early as Middle Eocene in the middle Magdalena area. Thus, in the WD area, the cordillera became a fold-and-thrust belt long before the Neogene Andean uplift.

The ED are scattered along a Berriasian-Valanginian stratigraphic level. This level contained evaporites, now largely dissolved and replaced by a huge hydrothermal breccia. Mineralization occured within or very close to the breccia level (here, contrary to the WD, source of and sink for the mineralizing fluids are coincident). All tectonic structures coeval with the mineralizing event are strictly linked to the breccia level and are extensional: normal faults and tension gashes associated with the collapse of the breccia level roof. At this time, the breccia level acted as a detachment, possibly gravity-driven owing to a favorable dip of tilted blocks. But it has not been possible to characterize the regional tectonic regime as extensional, though there is no clear evidence of any compressive structure at this time. Mineralization and related extensional structures are well dated by K/Ar and Ar/Ar methods at 65±3 Ma, i.e. the Cretaceous-Tertiary boundary. This time is also known as one of important reorganization of the basin extending over the easternmost cordillera and nearby Llanos basin. Later on, the mineralized stratiform level, together with the whole Cretaceous-Tertiary series, was passively folded and thrusted eastward by the Andean tectonics from Middle Miocene to Actual (Branquet et al., this volume). Here, contrary to the western zone, there is absolutly no link between this fold-and-thrust regional structure and the mineralizing event.

In summary, we propose that, in the Eastern Cordillera of Colombia, the fold-and-thrust belt formation is diachronous: (i) in the east, structuration began at the Cretaceous-Tertiary boundary with the tectonic event linked to the emerald mineralization, whereas the east-vergent fold-and-thrust belt formation is supposed to be not older than Middle Miocene; (ii) in the west, the west-vergent fold-and-thrust belt developed earlier, in Upper Eocene to lowermost Oligocene time. So, the east side story was very different from the west side story.

This study was supported by the French Ministry of Education (MSER fellowship) and European Commission DG XII (grant CT 94-0098), with the help of MINERALCO SA and emerald mining companies.

Reference:

Branquet, Y., Laumonier, B., Cheilletz, A., Giuliani, G. 1999. Emeralds in the Eastern Cordillera of Colombia: two tectonic settings for one mineralization. *Geology*, in press.

QUATERNARY EXTENSIONAL DEFORMATION AND RECENT VERTICAL MOTION ALONG THE CHILEAN COAST (BETWEEN 23°S and 47°S)

Alain Lavenu[1, 2], Carlos Marquardt[3], Diana Comte[4], Mario Pardo[4], Luc Ortlieb[5], Tony Monfret[5]

(1) IRD-Chili, casilla 53 390, correo central, Santiago 1, Chile. (alavenu@dgf.uchile.cl)
(2) Departamento de Geología, Universidad de Chile, casilla 13518, Santiago, Chile.
(3) SERNAGEOMIN, Av. Santa María 0104, Santiago, Chile (cmarquar@sernageomin.cl)
(4) Dpto. de Geofísica, Universidad de Chile, casilla 2777, Santiago, Chile. (dcomte(@dgf.uchile.cl; mpardo@dgf.uchile.cl)
(5) IRD, 209-213, rue La Fayette 75480 Paris cedex 10, France. (Luc.Ortlieb@bondy.ird.fr)

Key Words : neotectonics, sismotectonics, uplift, co- /post-seismic extensional deformation, Andes

INTRODUCTION

Along the South American Pacific margin are located various regions with uplifted Quaternary marine terraces in Ecuador, Peru and Chili for example. These coastal features result from the interaction between the subduction process and the continental deformation of the fore arc region. These South American coastal terraces are generally submitted to extensional deformation, mostly because they lie over the subducted plate without lateral constrains. However, the direction of the extensional deformation is variable. In areas of oblique convergence and relatively wide coastal zone (comprised between trench and Western Cordillera) the direction of extensional deformation stays orthogonal to the direction of plate convergence in Ecuador (Dumont *et al.* 1997) and in Southern Peru (Sébrier *et al.*, 1985). In Chile, where there is a narrow belt between the trench and the Main Cordillera, the vertical uplift motion of the coast line is documented by numerous Quaternary uplifted terraces. Moreover, the Coastal region is submitted to an extensional deformation normal to the margin and roughly parallel to the convergence direction. On the contrary, south of 33° Lat. S., the inner part of the fore arc (Central Depression) is submitted to a N-S compressional deformation (Lavenu and Cembrano, 1999) (Figure). North of 33° lat. S., between the Coastal range and the Main range, the Quaternary deformation is not documented.

Extensional deformation of the uplifted terraces

In the northern part of Chile (Mejillones Peninsula, Hornitos, Antofagasta) (Ortlieb *et al.*, 1996) Quaternary marine terraces indicate a regional uplift, and along the Atacama Fault Zone, numerous active faults show recent ruptures. The fault motion is essentially vertical with an E-W trending extensional deformation (Delouis, 1996). Nevertheless Armijo and Thiele (1990) described left lateral offsets.

In the coastal area of Caldera, Quaternary marine terraces also indicate a regional uplift linked to the subduction process (Ortlieb, 1995; Marquardt *et al.*, th is Symposium; Marquardt and Lavenu, this Symposium). Active crustal normal faults cut these Quaternary terraces (<220 000 años).Neotectonic field studies demostrate that the movement is essentially vertical, without lateral motion, and the extensional deformation direction is E-W trending.

In the Río Limari/Altos de Talinay zone, uplifted Quaternary marine terraces (the oldest are dated in300 kyr) are also affected by normal faults, parallel to the coast and trending approximately N-S (Ota *et al.*, 1995).

In the Arauco Peninsula, southern part of Central Chile, field works permited to observe uplifted supposed Quaternary marine terraces. A kilometric normal fault, trending N10, affects the Plio-Quaternary deposits. This fault is the result of an ESE-WNW trending extensional deformation, similar to the Caldera and Mejillones deformations.

Seismotectonics and co- y/o post-seismic vertical motion

During this century Chile has been affected by one event with magnitude about 8, in average each ten years. The May 22, 1960 is one of the type example that reflects the strongly coupled seismogenic interplate contact associated with the subduction of the oceanic Nazca plate beneath the South American plate and it is the largest earthquake ever instrumentally recorded. In general, it is difficult to estimate the vertical and horizontal motions of the historical earthquakes that occurred along the Chilean trench, however, some of them has detailed reports: The 1822 Central Chile earthquake produced an uplift of 1.2 m and 0.9 m in the shoreline near Quintero and Valparaíso, respectively. The 1835 Concepción earthquake (Ms~8, 8¼) indicating that the Santa María Island (just north of the Arauco Peninsula) was uplifted by about 3 m, Quiriquina Island by 2.5 m and Talcahuano, in the bay of Concepción, by about 1.5 m (Barrientos, 1991). During the 1837 Valdivia earthquake (Ms~8), which is comparable with the 1575 and 1737 earthquakes and smaller than the 1960 one, crack openings were observed in Chiloé Island and Lemus Island was uplifted by about 2.5 m (Barrientos, 1991). The 1906 Valparaíso large earthquake (Ms=8.6, Gutenber and Richter, 1954) produced an uplift of the coast reaching between 40 and 50 cm in the Zapallar-Quintero (32.5°S) and Pichilemu-Llico (34.5°S) areas. There are reports that the 1928 Talca (Ms=8.4, Richter, 1958) produced an uplift in the coastal locality of Putú (35.3°S). There are no information that 1939 Chillán earthquake produced coastal elevation changes, agreeing well with the study of Campos and Kausel (1990) suggesting that this is a normal faulting event. The 1960 event ruptured more than 900 km, from the Arauco Peninsula (37.3°S) to the Taitao Peninsula (46.8°S); remarkable land level changes were observed over and area of 200x1000 km², the city of Valdivia subsided by about 2 m and the Guafo and Guamblin Islands were uplifted by more than 4 m (Plafker and Savage, 1970). Near the Laguna San Rafael dead forest attests of post-sismic subsidence and uplitf of this area. The 1985 Central Chile earthquake (Mw=8.1) generated a permanent uplift of the shoreline of 11 and 28 cm in Valparaíso and San Antonio (Comte *et al.*, 1986). The recent

1995 Antofagasta earthquake (Mw=8.0) had the maximum ground acceleration of 29%g in the E-W direction, and the maximum vertical offset recognized was 20 cm (Delouis et al., 1997). Over the zone of coastal uplift, E-W extension in the continental crust is expected.

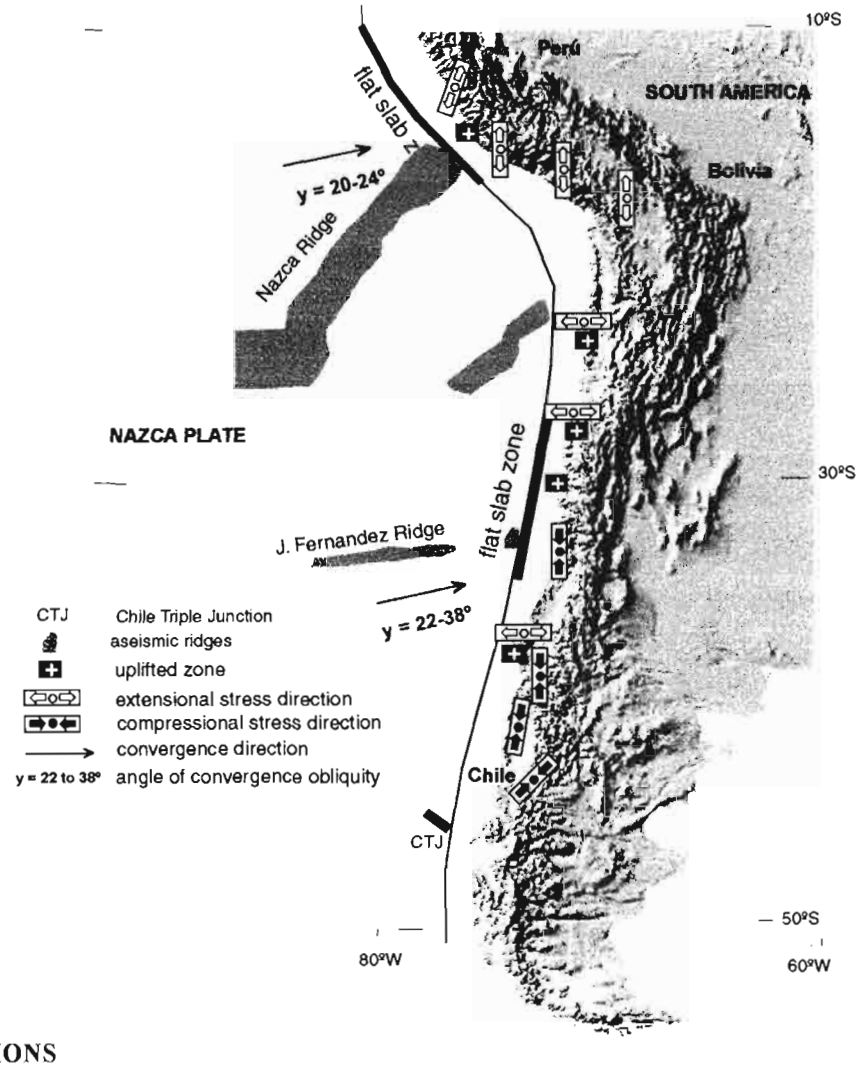

CONCLUSIONS

The partition of the deformation across the plate boundary zone shows that the tectonic regime of the Quaternary is more complex than previously recognized (e.g. Dewey and Lamb, 1992). Along the coast and within the main range of Perú as well in the Bolivian Altiplano and Western Cordillera, the extensional deformation is interpreted as resulting from an acomodation of the rising topography, related to body forces. The E-W trending stress is $\sigma 3$ (Horizontal minimum principal stress, or tensional deviatoric stress), $\sigma 2$ is N-S trending (intermediate deviatoric stress) and $\sigma 1$ is vertical (maximum principal stress or compressional deviatoric stress) (Sébrier et al., 1985). Along the Chilean Coast, the Quaternary tectonic regime is extensional and of a ~ E-W direction. This deformation characterizes the westernmost portions of the continental forearc, close to the trench axis (~ 80 km). This deformation does

not appear to be directly linked to boundary forces due to the convergence, but could be the consequence of co- or post-seismic crustal bending with subduction-related earthquakes. It could be topographic accomodation to the uplift of this part of the coast (body force due to topography): $\sigma 3$ is striking E-W, $\sigma 2$ is striking N-S, and $\sigma 1$ is vertical. The uplifted terraces, located over a crustal bulge due to the subduction, are related to the E-W stretching.

References

Armijo R., Thiele R. 1990. Active faulting in northern Chile: ramp stacking and lateral decoupling along a subduction plate boundary? Earth and Planet. Sci. Lett., 98, 40-61.

Barrientos, S., 1991. Large events, seismic gaps, and stress difussion in Central Chile. In Tectonic of the southern Central Andes, K. –J. Reutter, E. Scheuber, and P. J. Wigger Editors, 111-117.

Campos, J. and E. Kausel, 1990. The large 1939 intraplate earthquake of southern Chile, Seismol. Res. Lett., 61, 43.

Comte, D., A. Eisenberg, E. Lorca, M. Pardo, L. Ponce, R. Saragoni, S.K. Singh, and G. Suarez, 1986 The 1985 Central Chile earthquake: A repeat of previous great earthquakes in the region ?, Science, 233, 449-452,.

Delouis B., 1996. Subduction et déformation continentale au Nord-Chili. Thèse, Université Louis Pasteur, Strasbourg.

Delouis, B., T. Monfret, L. Dorbath, M. Pardo, L. Rivera, D. Comte, H. Haessler, J.P. Caminade, L. Ponce, E. Kausel, and A. Cisternas, 1997. The Mw=8.0 Antofagasta (Northern Chile) earthquake of 30 July 1995: A precursor to the end of the large 1877 gap, Bull. Seism. Soc. Am., 87, 427-445.

Dewey J.F., Lamb S.H. 1992. Active tectonics of the Andes. Tectonophysics, 205, 79-95.

Dumont, J.F., Alvarado, A., Guillier, B., Lavenu, A., Martinez, C., Ortlieb, L., Poli, J.T., Labrousse, B., 1997. Coastal morphology as related to geodynamics in Western Ecuador: preliminary results. In Late Quaternary Coastal Tectonics, London, O-07, INQUA Commission on Neotectonics and Geological Society, London.

Gutenberg, B. and C. F. Richter, 1954. Seismicity of the earth and associated phenomena, Princeton University Press, 310 pp,.

Lavenu A., Cembrano J., 1999. Compressional- and transpressional-stress pattern for Pliocene and Quaternary brittle deformation in fore arc and intra-arc zones (Andes of Central and Southern Chile). Journal of Structural Geology, in press.

Marquardt C., Lavenu A. 1999. Quaternary brittle deformation in the Caldera area, northern Chile (27°S). This symposium.

Marquardt C., Ortlieb L., Lavenu A., Guzman N. 1999. Recent vertical motion and Quaternary marine terraces in the Caldera area, northern Chile (27°S). This symposium.

Ortlieb L., Zazo C., Goy J.L., Hillaire Marcel C., Ghaleb B., Cournoyer L. 1996. Coastal deformation and sea level changes in northern Chile subduction area (23°S) during the last 330 ky. *Quatern. Sci. Rev.*, 15: 819-831.

Ortlieb L., in collab. with J.L. Goy, C. Zazo, Cl. Hillaire-Marcel & G. Vargas, 1995. *Late Quaternary coastal changes in northern Chile*. Guidebook for a fieldtrip, II annual meeting of the International Geological Correlation Program, Project 367 (Antofagasta, 19-28 Nov. 1995), ORSTOM, Antofagasta. 175 p.

Ota Y, Miyauchi T., Paskoff R., Koba M. 1995. Plio-Quaternary marine terraces and their deformation along the Altos de talinay, noerth-central Chile. Rev. Geol. de Chile, 22, 1, 89-102.

Plafker G., and J. Savage, 1970. Mechanism of the Chilean earthquakes of May 21 and 22, 1960, Geol. Soc. Am. Bull., 81, 1001-1030.

Richter, CF, 1958. Elementary Seismology. Freeman, San Francisco, 768 pp,.

Sébrier, M., Mercier, J.L., Mégard, F., Laubacher, G., Carey-Gailhardis, E., 1985. Quaternary normal and reverse faulting and the state of stress in the central Andes of southern Peru. Tectonics, 4, 7, 739-780.

COMPETITION BETWEEN MAGMA FLOW AND SUBDUCTION RELATED STRESSES IN A DOLERITIC DYKE COMPLEX LOCATED CLOSE TO THE SUBDUCTION OF THE CHILE RIDGE (PATAGONIA). AN AMS AND STRUCTURAL STUDY.

Jean-Pierre LEFORT (1), Tahar AÏFA (2) and Francisco HERVE-ALLAMAN (3)

(1) Tectonophysics, Géosciences-Rennes, Institut de Géologie, Campus de Rennes-Beaulieu, 35042, Rennes-Cédex, France. e-mail: lefort@univ-rennes1.fr
(2) Geophysics, Géosciences-Rennes, Institut de Géologie, Campus de Rennes-Beaulieu, 35042, Rennes-
Cédex, France. e-mail: aifa@univ-rennes1.fr
(3) Departamento de Geologia, Facultad de Ciencias Fisicas y Matematicas, Universidad de Chile, Dario Urzua 1625, Santiago de Chile, Chile. e-mail: fherve@tamarugo.cec.uchile.cl

KEY WORDS: Chile, Patagonia, Dykes, Subduction,Tectonics, AMS.

INTRODUCTION

A doleritic dyke complex intruding the Paleozoic Chonos metamorphic complex, the Tertiary Traiguen volcano-sedimentary Formation and the North Patagonian Batholith (Hervé, 1993) has been studied, using AMS and structural techniques, in the restricted area of Magdalena Island. A few whole rock dates have been already published on the Chonos Archipelago and on the Ayssen area, they suggest a Miocene age for most of the mafic dykes (Pankhurst and Hervé, 1994). However, in the same zone, at Pitipalena, a few dykes, as young as 3.6 to 5.6 Ma, are known. At the time of the main dykes emplacement (17 to 14 Ma?), the Chile oceanic ridge was just beginning to dock with Southern America (Gorring et al., 1997).This collisional event started 800 kilometers south of the studied area. Since that time, the triple junction resulting from the subduction of the Chile ridge beneath Southern America has been sliding in a northward direction. This movement resulted from the Nazca and Antarctic plates oblique subduction. After marine magnetic studies (Tebbens and Cande, 1997), the azimuth of convergence of the oceanic plates did not change between 20 Ma and the present time, it is approximately oriented N75°.

At Magdalena Island, most of the doleritic dykes are trending in a N30° direction (Hervé, 1993) . As a consequence, the stress developed by the subduction process cannot be directly responsible for the opening of these dykes. However, if we consider at the same time: 1/ the many faults cutting across the Chonos Archipelago, oriented in the same direction as the N30° dyke set; 2/ the many macroscopic evidences of dextral transtension in the N30° dykes; 3/ the existence of the N10° dextral Liquine-Ofqui shear zone and of its satellite, the Moraleda Canal fault, at the Eastern edge of the Chonos Archipelago

and 4/ the azimuth of the Pacific subduction, a general kinematic model can be proposed. This model suggests that the Triple Junction behave like an indenter which collided against a crustal segment unconfined to the West. The general pattern mimics exactly an analogic model already developed by Davy and Cobbold (1988) using quartz sand, ethyl cellulose, silicone putties, powdered galena and glucose syrup.

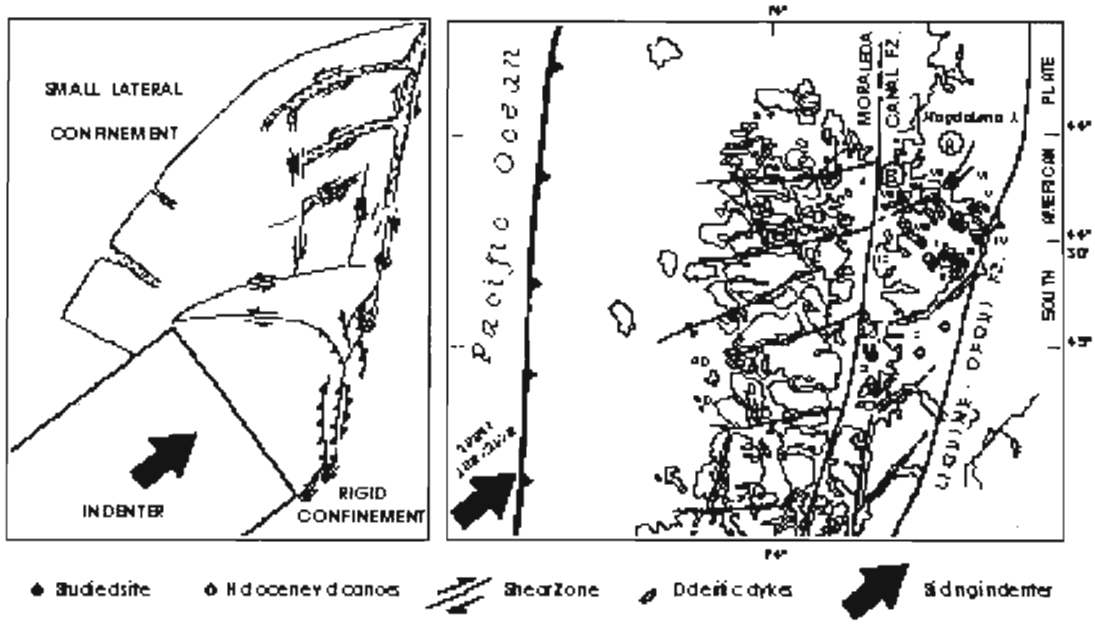

Indentation of the Chonos Archipelago

The results of the study of the anisotropy of the magnetic susceptibility (AMS) show steep and shallow dipping inclinations of the main or intermediate components of the anisotropy tensor. The vertical and sub-vertical plunges are almost certainly, as already observed elsewhere in various dyke swarms (see Aïfa, Lefort and Hervé, companion paper), associated with the magma flow (Mushayanddebvu et al., 1995). This result is not unexpected since the sampling was made in a Tertiary volcanic arc, probably characterized by magma chambers at depth. However, and contrary to the usual results, the magma flow is not only associated with the maximum of anisotropy (K_1), but in some places with the intermediate value (K_2).

Comparisons between the direction of the dykes and the direction of the shallow dipping components of the anisotropy tensor, show that most of the N30° and some of the East-West trending dykes are oriented the same as their K_1 or K_2. Because these directions are associated with the shortening direction which was responsible for the opening of the dykes, they can be interpreted as the result of the regional stress (Mushayanddebvu et al., 1995). This proceeding is only valid if a vertical or subvertical plunge is already observed in the same dyke, since horizontal flows oriented in the same direction as the dyke are also known in dykes located at a far distance from the magma chamber (Smith, 1987).

CONCLUSIONS

If the indenter tectonic model is correct, the N30° and submeridian dykes must be younger that 17 to 14 Ma? since the indenting process was located too far from Magdalena Island at that time. They may show the same age as the Pitipalena dykes which have been dated at 3.6 and 5.6 Ma, a period of time where the indenter was located closer to the studied area. The 17 to 14 Ma? dykes are usually oriented differently. In any case, the dykes are all younger that 17 Ma, age of the Magdalena granodiorite, since they all cut across the granodiorite.

The main conclusion which can be deduced from the AMS study, is that there has been, in this particular area, a competition between the stress associated with the indenting process and the stress associated with the magma flow, since K_1 represents, either the flow or the stress. It is difficult to assume that K_1 was associated with a stronger stress than K_2, since the mechanism responsible for the alignment of the magnetic minerals is different in the flow and in the tectonic processes. However, since we know that the variations of the stress associated with the subduction is a slow changing process, the shift from K_1 to K_2 was probably related with a rapid modification in the flow propagation (Lister, 1995). The few other dyke directions and components of the anisotropy tensor which do not fit with this general pattern are probably associated with dykes which predate the indenting episode.

shallow K1 or K2 (N30°±10°)	steep K1 or K2 (random)	shallow K1 or K2 (N30°±10°)	steep K1 or K2 (random)
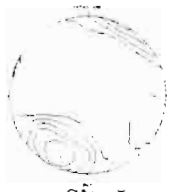			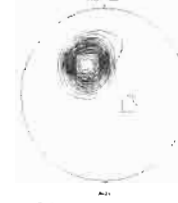
Site I	Site I		Site VIIA

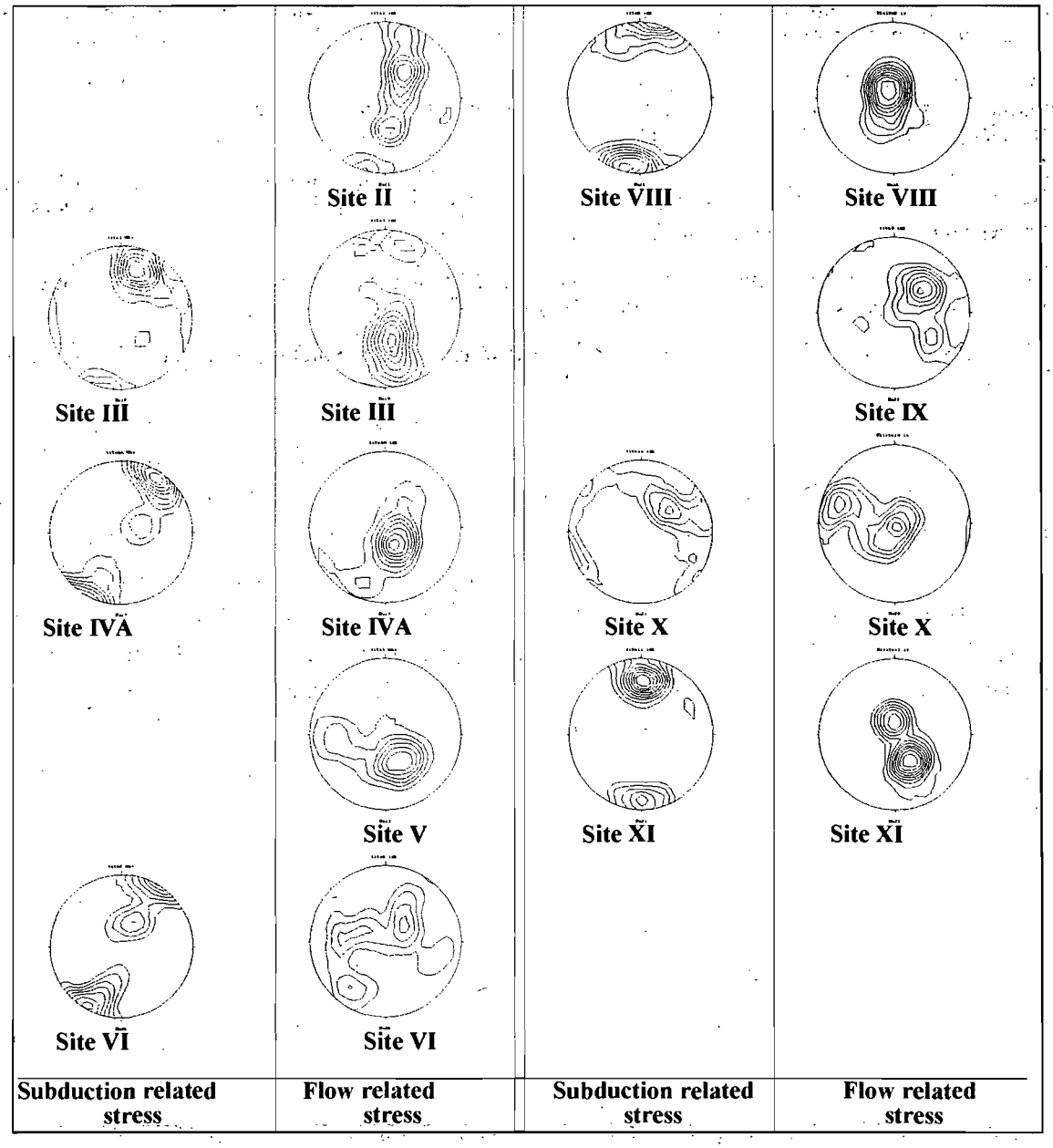

Competition between subduction and flow related stresses

REFERENCES.

DAVY PH. and P.R. COBBOLD 1988. Indentation tectonics in nature and experiment. 1. Experiments scaled for gravity. Bull. Geol. Inst. Univ. Uppsala, N.S. 14, 129-141.

GORRING M.L., KAY S.M., ZEITLER P.K.RAMOS V.A., RUBIOLO D., FERNANDEZ M.land PANZA J.L., 1997. Neogene Patagonian Plateau Lavas: Continental magmas associated with ridge collision at the Chile Triple Junction. Tectonics, 16:1-17.

HERVE F. 1993. Paleozoic metamorphic complexes in the Andes of Aysen, Chile (West of Occidentalia). First Circum-Pacific and Circum Atlantic Terranes Conference, Proceedings:64-65, Guanajuaato, Mexico.

LISTER J.R. 1995. Fluid-mechanical models of the interaction between solidification and flow in dykes. Physics and chemistry of dykes. G. Baer and A. Heiman (eds). Balkema A.A., Rotterdam:115-124.

MUSHAYANDDEBVU M.F., BATES M.P. and JONES D.L. 1995. Anisotropy of magnetic susceptibility results from Mashonaland doleritic sills and dykes of Northern Zimbabwe. Physics and chemistry of dykes. G. Baer and A. Heiman (eds). Balkema A.A., Rotterdam:151-164.

PANKHURST R.J. and HERVE F. 1994. Granitoids age distribution and emplacement control in the North Patagonian batholith in Aysen (44°-47° S). 7° Congreso Geologico Chileno, Actas, II:1409-1413, Concepcion.

SMITH R.P. 1987. Dyke emplacement at Spanish Peaks, Colorado. Mafic dyke swarms. H.C. Halls and W.F. Fahrig (eds). Geol. Ass. Can. Sp. Issue, 34:47-54.

TEBBENS S.F. and CANDE S.C. 1997. Southeast Pacific tectonic evolution from early Oligocene to Present. Journ. Geoph. Res., 102, 6:12061-12084.

ELECTRICAL CONDUCTIVITY BENEATH THE TUZGLE VOLCANO AND ITS SURROUNDING SHOSHONITIC VOLCANIC CENTERS, NW ARGENTINA

P. LEZAETA(1) and H. BRASSE(1)

(1)Fachrichtung Geophysik, FU Berlin, Malteserstr.74-100, D-12249 Berlin;
e-mail: pamela@geophysik.fu-berlin.de

KEY WORDS: Magnetotellurics, electrical conductivity, Puna, partial melts, asthenosphere.

INTRODUCTION

Magnetotelluric (MT) measurements were carried out in 1989 within the frame work of the Research Group " Mobility of Active Continental Margins" in the Southern Central Andes. In the present work, 7 stations located on the backarc subduction zone of the Andean system in NW Argentina at latitudes 23.5°S - 24.5° S –between the Puna and Eastern Cordillera (66.5°W - 67.5°W)– are analysed in order to obtain a two dimensional (2D) electrical conductivity model of the underground. Data quality was satisfactory in the period range 90-7000 s, thus allowing investigation depths between 5 and 80 km. The 80 km long profile extends in WNW-ESE direction mainly along the El Toro lineament, between the Tuzgle volcano and the city of Salta (Fig. 1). A 2D electrical model of an E-W profile between Salta and the Chaco was previously obtained (Fig.3; Lezaeta, 1995), i.e., eastward of the actual study area (transect B in Fig.1). In this previous model, a good deep conductor uprising in direction to the Puna was interpreted as an upraise of the asthenosphere. Hereby it seems reliable to associate the good conductors at lower crust and upper mantle depths traced in both models with the Puna volcanism.

Geological setting

Crustal depths vary between 65 and 50 km (e.g., Isacks, 1988) from W to E along the MT profile with average regional elevations of 3.5 km, reaching a maximum of 5.5 km at the top of the Tuzgle volcano.

This region belongs to the recent seismic gap in the down-going slab located ~200 km above the Wadatti-Benioff zone (Cahill, 1990).

The study area comprehends an active volcanic history since the Cretaceous. The most recent magmatism associated to a backarc source started about 2 Ma ago, namely the Tuzgle and shoshonitic magmas and the Tocomar ignimbrite (Fig.1). The Tuzgle magma presents a mixture of mantle and crust-end members activity (Coira & Kay, 1993) whereas shoshonitic lavas are characterised by an enriched mantle composition with lower crustal contamination. Tuzgle volcanism is linked in time with young thrust faulting to the North, while the nearby shoshonitic centers and the Tocomar ignimbrite are connected with El Toro NW-trending sinistral strike-slip fault (e.g., Coira & Kay, 1993; Fig.1). An hypothesis for the late Pliocene to Recent Tuzgle volcanic evolution is that it developed in two different mantle precursor sequences; an older with highest melting rate and silicic composition and a younger of basaltic andesitic components with lower flux of magma (Coira & Kay, 1993). The magma chamber for the Tuzgle eruption would have been originated at mid-crust decollement levels (20-25 km depth; Cahill, 1990) or alternatively at approx. 15-18 km depth beneath the sole of one of the NS thrust faults (Coira & Kay, 1993). Additionally, Tuzgle is described as the only major back-arc Quaternary stratovolcano of the Central Andes (Coira & Kay, 1993).

2D electrical model

After dimensional analysis and data decomposition (Chave & Smith, 1994), the original data coordinate system (NS) was rotated 15° cw. with respect to the north – the 2D strike of the regional electrical structure – and therefore the profile trending is N15°W (transect A in Fig.1). A previous analysis made on the vertical to horizontal magnetic field components for this data set (Blumensath, 1996) showed a similar orientation for the lateral conductivity variations. Then a 2D model was obtained by inverting the horizontal electric and magnetic field components through a relaxation field gradient code (Mackie et al., 1997), starting with a homogenous half-space. More weight on phase data was considered in the inversion in order to reduce static telluric distortions.

The good conductor tracing vertically from shallow depths until 35-40 km depth on the western border of the model (Fig. 2) is spatially correlated with a west-verging thrust fault to the south of sites Sab and Mun. Immediately west of sites Sab and Sep the east verging thrust fault next to the Tuzgle volcano is located (Fig. 1). In addition there are two shoshonitic volcanoes (SE of Tuzgle) extending immediately to the west of site Sab. The deep conductor traced between Cue and Ima with its top layer at 45-60 km depth (Fig.2) is located NE beneath La Poma shoshonitic center (Fig.1). The corresponding depths are in the transition zone between the lower crust and upper mantle according to the crustal thickness of the region (e.g., Isacks, 1988). A complex of east and west verging thrust fault systems are also surrounding this area, crossing the MT profile as well.

Another MT investigation realised in the Precordillera fault system has revealed high conductivity zones (Echternacht et al., 1997) which may be interpreted as salinary fluids ascending through the fault planes. High conductivity zones found at depths of 20-30 km beneath the Western Cordillera – the magmatic arc – are possibly explained as zone of partial melts (Schwarz & Krüger, 1997) related to the magmatic evolution, which is also supported by laboratory experiments (Schilling et al., 1997).

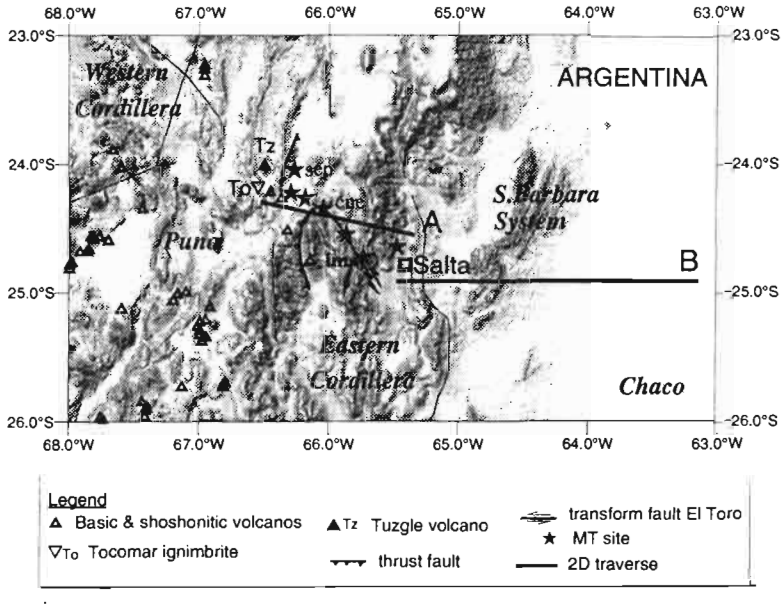

Fig. 1: Map of the Southern Central Andes showing MT site locations, the transverse for the 2D modelling (thick lines), geological units, the Recent volcanism in the study area, main thrust faults and El Toro lineament.

Conclusions

- The thrust faults linked with the magmatic evolution of the Tuzgle volcano are possibly connected with high conductivity zones (HCZ). The conductors (<30 Ωm) at upper crustal levels (until depths of thrust fault soles) can be caused by salinary fluids ascending through the fractures, whereas the HCZ at approx. 20-40 km depth beneath the Tuzgle and its surrounding shoshonitic centers may be explained as crustal partial melts.

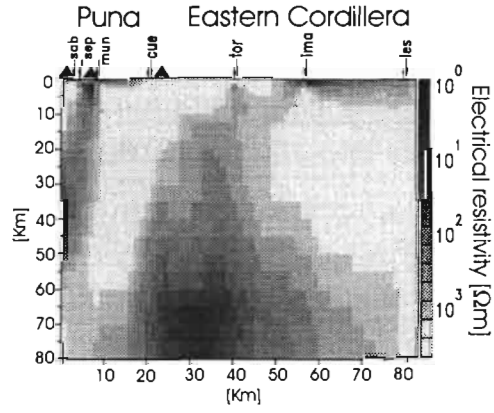

Fig.2: 2-D inversion result of traverse A. Dark triangles represent the location of recent volcanoes projected on the profile.

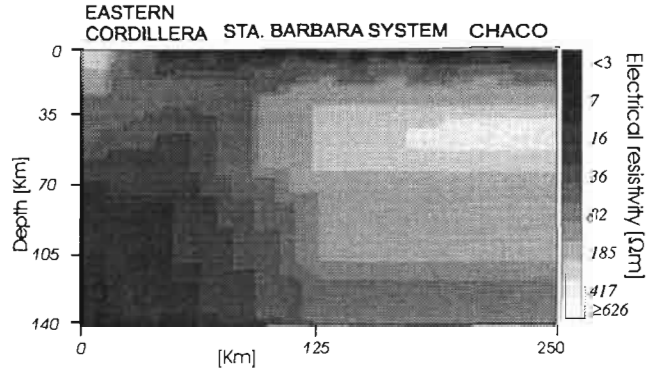

Fig.3: 2-D model of traverse B.

- The HCZ traced at the lower crust–upper mantle transition zone (45-60 km depth) is probably revealing partial melts associated to the Recent Puna magmatism.

- The HCZ extending in depth can be connected with the ductile thinned lithosphere as was suggested by several authors (e.g., Whitman et al., 1992) and additionally supported by another 2D electromagnetic model to the east (Fig.3; Lezaeta, 1995) where an upraise of the asthenosphere in direction to Puna was interpreted (Lezaeta & Muñoz, 1996). This is also supported by the increasing E-to-W surface heat flow of the area (>100 mW/m²; Hamza & Muñoz, 1997).

References

Blumensath, S. (1996): Über die Entzerrung elektromagnetischer Daten – Anwendung auf ein 3D-Modell und auf Meßdaten aus Argentinien, Dipl.-Arbeit FR Geophysik, FU Berlin, 78 pp.

Cahill, T. (1990): Earthquakes and tectonics of the Central Andean subduction zone. PhD Thesis, Cornell Univ., Ithaca, NY.

Chave, A.D. & Smith, J.T. (1994): On electric and magnetic galvanic distortion tensor decompositions, *J. Geophys. Res.*, **99**, B3, 4669-4682.

Coira, B. & Kay, S.M. (1993): Implications of Quaternary volcanism at Cerro Tuzgle for crustal and mantle evolution of the Puna Plateau, Central Andes, Argentina, *Contrib. Mineral Petrol.*, **113**: 40-58.

Echternacht, F., Tauber, S., Eisel, M., Brasse, H., Schwarz, G. & Haak, V. (1997): Electromagnetic study of the active continental margin in northern Chile, *Phys. Earth Planet. Int.*, **102**, Nos. 1-2, 69-88.

Hamza, V. M. & Muñoz, M. (1996): Heat flow map of South America, Geothermics, 25, 599-646.

Isacks, B. (1988): Uplift of the Central Andean plateau and bending of the Bolivian Orocline, *J. Geophys. Res.*, **93**: 3211-3231.

Lezaeta, P., (1995): Inversión y Modelo Bidimensional de Observaciones Magnetotelúricas en el Chaco Argentino. Tesis de Magister en Geofísica, Universidad de Chile, Santiago. 182 pp.

Lezaeta, P & Muñoz, M. (1996): Analysis, inversion and modelling of magnetotelluric observations between the Cordillera Oriental and El Chaco (NW Argentina). In *Géodynamique Andine*, Third Int. Symp. Andean Geodynamics, Saint-Malo, France, pp. 79-82.

Mackie, R.L., Rieven, S. & Rodi, W. (1997): Users Manual and Software Documentation for 2D-Inversion of Magnetotelluric data, MIT, Earth Resources Laboratory, Cambridge, Massachusetts.

Schilling, F.R., Partzsch, G.M., Brasse, H. & Schwarz, G. (1997): Partial Melting below the Magmatic Arc in the Central Andes Deduced from Geoelectromagnetic Field Experiments and Laboratory Data, *Phys. Earth Planet. Int.*, **103**, Nos. 1-2, 17-32.

Schwarz, G. & Krüger, D. (1997): Resistivity cross section through the southern central Andes as inferred from magnetotelluric and geomagnetic deep soundings, *J. Geophys. Res.*, **102** , No. B6 , 11957-11978.

Whitman, D., Isacks, B.L., Chatelain, J.L., Chiu, J.M. & Perez, A. (1992): Attenuation of high frequency seismic waves beneath the central Andes plateau: Evidence for along-strike changes in lithospheric thickness, *J. Geophys. Res.*, **97**, No. B13, 19929-19947.

ANTUCO VOLCANO: ONE OF THE ISOTOPICALLY MOST PRIMITIVE STRATOVOLCANOES OF THE SOUTHERN ANDES (37°25'S)

Silke LOHMAR (1a), Leopoldo LÓPEZ-ESCOBAR (1b), Hugo MORENO (2) and Bernard DÉRUELLE (3)

(1) Magmatic Group. Instituto de Geología Económica Aplicada, Universidad de Concepción. Casilla 160-C. Concepción, Chile. e-mail (1a): slohmar@udec.cl e-mail (1b): llopez@udec.cl
(2) Observatorio Volcanológico de los Andes del Sur (OVDAS). Servicio Nacional de Geología y Minería. Cerro Ñielol s/n. Casilla 23 D. Temuco, Chile. e-mail: ovdassis@chilesat.net
(3) LGIS-UPRESA-CNRS 7047. UPMC, 4 Place Jussieu 75257. Paris, Cedex 05. Francia. e-mail: deruelle@ccr.jussieu.fr

KEY WORDS: Volcanism, Quaternary, Geochemistry, Southern Andes, Central-south Chile.

INTRODUCTION

The Antuco volcano is a composite, compound stratovolcano, located in the Southern Volcanic Zone (SVZ) of the Chilean Andes at 37°25'S. The volcanic activity at Antuco extends to 130 ka (Upper Pleistocene; Moreno et al., 1986). Two main units are distinguished at this volcano: 1) a primary edifice (Antuco 1) whose evolution ended ca. 9.7 ka ago with the formation of a 4 km diameter avalanche caldera, with a westward opening, and 2) a younger eruptive cone (Antuco 2) nested in the caldera (Vergara and Katsui, 1969 and references therein).

The Antuco volcano is emplaced on basement consisting of Miocene stratified rocks and Pleistocene-Quaternary volcanic rocks from the neighbouring Sierra Velluda volcano. To date, the Antuco volcano has been considered a basaltic stratovolcano (Vergara and Katsui, 1969; López-Escobar et al., 1981). This

classification is valid, only in the case of Antuco 2, and based on our preliminary studies, lavas from Antuco 1 vary in composition from basalt to silicic andesite.

The caldera formation was probably caused by a Bandai type catastrophic phreatomagmatic eruption, followed by: a) a voluminous debris-avalanche (>5 km^3) that dammed the Laja lake, increasing the water level to 100 m above the current water line and b) lateral blasts that generated wet basaltic ash pyroclastic surges (Thiele et al., 1998 and references therein). Following this catastrophic eruption, the activity of Antuco built: a) the current, almost perfect, 1000 m high, basaltic to basaltic-andesite cone, called Antuco 2, and b) several satellite cones (Moreno et al., 1986 and references therein). For the past 9.7 ka, Antuco 2 eruptions have produced lava, debris and at least three pyroclastic flows. The existence of pyroclastic flow deposits younger than 9.7 ka implies that Antuco 2 volcano has also had violent eruptions, in spite of the mainly basalt to basaltic-andesite composition.

Documentation of eruptions at Antuco 2 only started in 1739. At least 17 eruptions are documented, the last one being in 1911. These eruptions have been strombolian in nature, emitting aa-type basaltic to basaltic-andesite lava flows and scoria through the central crater, satellite cones and lateral fissures. Currently, Antuco 2 has weak fumarolic activity through a small pyroclastic cone, called Sombrerito (Little Hat), nested in the main crater (Petit-Breuilh, 1994).

The aim of this work is to present preliminary petrographic and geochemical data on this Southern Andean stratovolcano and discuss the genesis and evolution of its magmas.

PETROGRAPHY

Antuco 1 lavas range in composition from basalt to silicic andesite, with olivine basalts and basaltic andesites being the most abundant lithologies. In contrast, Antuco 2 lavas are, mainly basalts and basaltic andesites. Independent of the unit to which they belong, Antuco basalts and basaltic andesites are porphyrytic, with little vesiculation, and contain phenocrysts of predominantly plagioclase, and lesser olivine and clinopyroxene. Orthopyroxene is observed in some basaltic andesites. Plagioclase phenocrysts are strongly zoned (center=An 80-76; rim=An 75-65) and occassionally contain glass and inclusions of groundmass minerals. The groundmass is composed of plagioclase microlites and grains of olivine, clinopyroxene, opaque minerales and variable amounts of glass. Texture varies from intergranular to intersertal, and locally pilotaxitic.

Antuco 1 andesites are also porphyrytic and contain phenocrysts of strongly zoned plagioclase and lesser clinopyroxene, orthopyroxene and olivine. The groundmass is composed of plagioclase microlites, grains of olivine, clinopyroxene and opaque minerales, and glass. Texture varies from pilotaxitic to intergranular. All Antuco 1 silicic andesites exhibit flow textures.

The Antuco 1 lithological sequence is intruded by dykes whose composition is more silicic than these lavas. These dykes contain plagioclase and amphibole.

GEOCHEMISTRY AND PETROGENESIS

Antuco 1 lavas vary in SiO_2 content from 51 to 60 %. The SiO_2 range is, however, more restricted in the case of Antuco 2 lavas (50 to 53 %). Independent of their age, Antuco basalts are relatively poor in MgO, Ni and Cr, but are comparatively rich in Sr. Their $^{87}Sr/^{86}Sr$ ratios are among the lowest of the SVZ of the Andes (0.70369-0.70391) and the $^{143}Nd/^{144}Nd$ ratios are relatively high (0.512808-0.51239). These values are similar to those of the oceanic islands of the Nazca plate. The $^{87}Sr/^{86}Sr$ ratios are practically equal within the basalt-andesite range.

The REE patterns (La = 15-20 x chondrites; Yb = 8-10 x chondrites; no Eu anomaly) of the basalts are consistent with an origin of 9-10 % partial melting of a garnet peridotite mantle source having: i) a chemical composition similar to that of the silicate Earth of MacDonough and Sun (1995), and ii) a modal composition equal to: 58.5 % olivine + 0.25 % orthopyroxene + 0.15 % clinopyroxene + 0.015 % garnet. The percentages of melting would be: olivine : orthopyroxene: clinopyroxene: garnet = 1 : 1 : 2 : 0. As a result of this melting process, a primary magma is generated. Fractionation of olivine (5 %) + clinopyroxene (5 %) yields a residual magma analogous to the Antuco basalts. However, Rb, Sr and Ba in the MacDonough and Sun (1995) model are insuficient to explain the content of these elements in the Antuco basalts. It is thus neccessary to multiply these abundances by 2.3, suggesting that the mantle source of Antuco magmas is enriched in these incompatible trace elements, probably by fluids originating from the subducted lithosphere.

CONCLUSIONS

Two main units are distinguished at Antuco volcano: a primary edifice (Antuco 1) whose evolution extended from 130 ka to 9.7 ka ago and concluded with the formation of a caldera, and a younger eruptive cone (Antuco 2) nested within the caldera.

Antuco 1 lavas range in composition from basalt to andesite, while Antuco 2 lavas are mainly basalts and basaltic andesites. Antuco basalts are relatively poor in MgO, Ni and Cr, indicating that the Antuco basaltic magmas are not primary, experiencing fractionation of olivine and pyroxene prior to emplacement. Their relatively high Sr contents suggest that the fractionation of clinopyroxene was more important than that of plagioclase and that the magmas probably evolved at a relatively high pressure. The

$^{87}Sr/^{86}Sr$ ratios of these basaltic magmas are one of the lowest while the $^{143}Nd/^{144}Nd$ ratios are one of the highest in the SVZ of the Andes.

The most silicic rocks are linked to the most basic by a crystal fractionation process dominated by olivine and clinopyroxene in the basalt-basaltic andesite transition and by plagioclase in the basaltic andesite-andesite transition. The fact that the silicic rocks have practically the same Sr isotopic ratios than the basic counterparts indicates that crustal contamination was not significant in the evolution of Antuco magmas.

ACKNOWLEDGEMENTS: This work was funded by FONDECYT Grant 198-0136, had the collaboration of project ECOS-FONDECYT C97U04 and is part of the Volcanic Risk Program of SERNAGEOMIN -Chile.

REFERENCES

López-Escobar, L.; Vergara, M.; Frey, F. 1981. Petrology and chemistry of lavas from Antuco volcano, a basaltic volcano of the Southern Andes (37°25'S). Journal of Volcanology and Geothermal Research, 1, 329-352.

McDonough, W.F.; Sun, S.-S. 1995. The composition of the Earth. Chemical Geology, 120, 223-253.

Moreno, H.; Lahsen, A.; Varela, J.; Vergara, M. 1986. Edades K-Ar de rocas volcánicas cuaternarias del Grupo Volcánico Antuco-Sierra Velluda, Andes del Sur, 37°27'S. Comunicaciones, 36, 21-25.

Petit-Breuilh, M.E. 1994. Actividad volcánica y cronología eruptiva histórica del volcán Antuco (37°24'S-71°22'W), Chile. Revista Geográfica de Chile Terra Australis, 39, 79-102.

Thiele, R.; Moreno, H.; Elgueta, S.; Lahsen, A.; Rebolledo, S.; Petit-Breuilh, M. E. 1998. Evolución geológico-geomorfológica cuaternaria del tramo superior del valle del río Laja. Revista Geológica de Chile, 25, 229-253.

Vergara, M.; Katsui, Y. 1969. Contribución a la geología y petrología del volcán Antuco, Cordillera de los Andes, Chile Central. Departamento de Geología, Universidad de Chile, 35, 25-47.

BASIC TO INTERMEDIATE MIDDLE JURASSIC VOLCANISM IN THE NORTH PATAGONIAN MASSIF: DYKE SWARMS OF THE SIERRA DE MAMIL CHOIQUE.

Mónica G. LÓPEZ DE LUCHI (1) and Augusto E. RAPALINI (2)

(1) Centro de Investigaciones en Recursos Geológicos, J. Ramírez de Velasco 847, 1414, Buenos Aires Argentina . e-mail: deluchi@mail.retina.ar
(2) Laboratorio de Paleomagnetismo "D.A. Valencio", Dpto. Cs. Geológicas, Univ. de Buenos Aires,Pabellón II, Ciudad Universitaria, 1428, Buenos Aires, Argentina. e-mail: rapalini@gl.fcen.uba.ar

KEYWORDS: dyke swarms, basic-intermediate volcanism, Middle Jurassic, Patagonia

INTRODUCTION

Although basic to intermediate dyke swarms are common in the North Patagonian Massif (NPM) they have only been studied in the Sierra de Mamil Choique (SW Rio Negro Province, López de Luchi and Rapalini, 1997) and no precise relation with the major volcanic events that characterize the Mesozoic and Tertiary magmatism of Patagonia have been proposed. In this paper the geochemical characterization of the Sierra de Mamil Choique dyke swarms is presented in order to elucidate the significance of the dykes in the Jurassic evolution of Northern Patagonia (Fig. 1).

Middle Jurassic volcanism represent a major magmatic event in the evolution of Patagonia (Lesta and Ferello 1972, Page and Page 1993, Pankhurst and Rapela 1995 and references therein) and has been separated in two complexes, the (178-183 Ma) Marifil for the eastern sector of NMP (Rapela and Pankhurst 1993) and the (168-170 Ma) Chon Aike for the eastern sector of the Deseado Massif (DM) (Pankhurst et al. 1993). Basic to intermediate volcanism is principally developed towards the west of these areas, Central Volcanic Belt (Page and Page 1993) and is represented by Taquetren and Cañadon Asfalto Formation and the Lonco Trapial Group in MNP that cover the span from 180-136 Ma and by the 156.7 Ma Bajo Pobre Formation in DM, that have been regarded as essentially contemporaneous with the Chon-Aike Formation (Pankhurst

and Rapela 1995). North-south migration of volcanic activity have been defined for the acid volcanism. A western migration of the volcanic activity with younger more basic compositions have been proposed (Pankhurst and Rapela 1995). The Jurassic silicic volcanic rocks of the Marifil and Chon-Aike complexes posseses uniform Sr and Nd isotopic compositions, that indicate a Late Proterozoic low Rb/Sr mafic lower crustal source (Pankhurst and Rapela 1995). These authors assigned the extensive lower crustal melting event represented for the above mentioned complexes that are located east of 68° W to an extensional tectonic setting associated with the rifting and incipient break up of Gondwana. The mesosilicic to basic volcanic rocks of the Central Volcanic belt (180-136Ma) have been assigned to an eastern branch of the Jurassic Volcanic Arc (Page and Page 1993) or to an extensional setting for the Bajo Pobre Formation (Pankhurst and Rapela 1995)

GEOLOGICAL AND GEOCHEMICAL CHARACTERIZATION

The Sierra de Mamil Choique (41° 40'-41° 55'S and 70°-70° 33'W) dyke swarms are part of the Central Volcanic Belt and are intruded in a WNW-NW belt (in three systems 260°-270°, 280°-290° and 300°-310°) in the Paleozoic Mamil Choique Granitoids and the Permian La Pintada Granite (Fig.1). Dykes are made up by dark green to greenish gray porphyric to aphyric rocks. TAS classification distinguish two series: **series 1** composed of subalkaline basalts, basaltic andesites and dacites and **series 2** composed of alkaline trachyandesites and basaltic trachyandesites (Fig. 2a). Phenocryst phases are: **clinopyroxene-plagioclase± clinoamphibole** for series 1 and **plagioclase-clinoamphibole±biotite** for series 2. Series are essentially metaluminous and plot in the calcalkaline field in AFM diagram. Serie1: is composed by medium-K calcalkaline basalts and basaltic andesites with a somewhat restricted silica range from 49-54% and high-K mildly peraluminous dacites with silica content around 62-63%. TiO2, Fe2O3t, MgO and CaO present negative slopes against silica, Al2O3 shows a scattered pattern against silica; Na2O show a positive slope and K2O a smooth negative correlation. Serie2: is composed of high-K trachyandesites and basaltic trachyandesites that cover the span from 52 to 60% SiO2. Absolute values for MgO, CaO are lower and Na2O, K2O higher than in series 1 Correlations are similar to those depicted by the Serie 1 except for Al2O3 that shows a scattered pattern and K2O that presents a positive slope. Mean Rb, Ba, Zr values are higher than in series 1 and Sr and Cr are lower.

Rb, Zr and Ba patterns parallezise trends depicted by K2O in both series but Sr show positive slope against silica in serie 1. K/Rb varies between 180-220 for serie 1 and are higher between 260-280 for series 2. Rb/Nd varies from 1.2-2 in series 1 to 2-3.6 in series 2; Zr/Y varies from 6 to 11 (Fig.2b). LREE/HREE are sligthly higher in series 2 with $(La/Lu)_N$ 8 for series 2 and 6 for the basalts of series 1. Chondrite normalized REE patterns show relatively smooth slopes(Fig.2).

DISCUSION AND CONCLUSIONS

These dykes represent two magmatic series being the alkaline series 2 sligthly older than series 1(López de Luchi and Rapalini 1997 A progressive higher degree of partial melting of a source undergoing decompression would be in accord with the smooth slopes of the REE for series 1 and the higher LREE/HREE for series 2. Zr/Y 6-11 are typical of intraplate basalts. Normalized patterns for the more primitive types within each series indicate a melt in equilibrium with clinoamphibole and magnetite in series 1 and plagioclase+clinoamphibole for series 2. Within each series fractional crystalization is responsible for gradually steeper slopes of the REE. Crystallization in both series is controlled essentially by clinoamphibole+-magnetite with plagioclase in the more evolved terms of series 1. An extensional setting in an incipient intracratonic rift stage has been proposed for Middle Jurassic times for the Somoncura Cañadón Asfalto basin (Figari and Courtade 1993, Cortiñas 1996). The marked structural control of the dyke swarms in a belt that parallelizes regional lineaments that were active during Paleozoic and early Mesozoic time agrees with the regional data indicating that initial rifting of Gondwana has been controlled for preexisting crustal discontinuities.

K/Ar ages, 168.4±3.5 Ma for series 1 basalts and 172.7±4.5 Ma for series 2 indicate a volcanic event in the Bajocian-Bathonian contemporaneous with the Lonco Trapial Group and sligthly older than Cañadón Asfalto Formation. The calculated values are coincident with the age assigned to Chon Aike Formation (López de Luchi and Rapalini 1997). Paleomagnetic pole for these dykes is particularly coincident with the paleomagnetic pole from the Chon-Aike lavas at Estancia La Reconquista (Vilas 1974). This suggests a temporal correlation between the intrusion of the Mamil Choique dykes and the extrusion of the Chon Aike lavas.Thus, these poles may indicate the ≈ 170 Ma pole for South America.

In synthesis, regional, structural and petrological evidences for the Middle Jurassic dyke swarms of the Sierra de Mamil Choique point to an extensional intracratonic setting. A model is proposed in which the alkaline and medium-K series could be related by different degrees of partial melting of a progressive shallowing source. North-south/east-west migration with younger units to the south and to the west has been proposed for the Jurassic volcanism of the MNP and DM; age and paleomagnetic data indicate that basic to mesosilicic activity starts at the same time than silicic magmatism in the DM. Progressive rifting of Gondwana could have allowed the ascent of primitive magmas that migth represent the advective heat source for the lower crustal melting that originated the more silicic eastern volcanism. The relation of this intracratonic setting with the initiation of the activity of the active Pacific margin remains unclear.

This work was partially financed by a grant from Fundación Antorchas: Estudio paleomagnético y petrográfico-petrológico de la Formación Mamil Choique, Río Negro y Chubut Director: A. Rapalini. A. González from CIRGEO helped us with the illustrations.

REFERENCES

Cortiñas J 1996. La Cuenca de Somoncura-cañadón Asfalto: sus límites, ciclos evolutivos del relleno sedimentario y posibilidades exploratorias. Actas 13° Congreso Geológico Argentino,1: 147-163, Buenos Aires.

Figari E and Courtade S 1993. Evolución tectosedimentaria de la Cuenca de Cañadón Asfalto, Chubut, Argentina. Actas 12° Congreso Geológico Argentino, 1: 66-77, Mendoza

Lesta P. and Ferello R.1972.Región extrandina de Chubut y Norte de Santa Cruz. In: Geología Regional Argentina, Leanza A.F.(ed) pp 601-654. Academia Nacional de Ciencias, Córdoba, Argentina

López de Luchi M.G. and Rapalini A.E. 1997. Jurassic dyke swarms in the Sierra de Mamil Choique, North Patagonian Massif: Lithology, Age and Paleomagnetism. Simposio Final IGCP Project 345. Lithospheric Evolution of the Andes, Actas 8° Congreso Geológico Chileno ,3:1674-1679., Antofagasta, Chile

Page R. and Page S.1993.Petrología y significado tectónico del Jurásico volcánico del Chubut Central, Revista de la Asociación Geológica Argentina, 48,1:41-58.

Pankhurst R. J. and Rapela C.R. 1995. Production of Jurassic rhyolites by anatexis of the lower crust of Patagonia. Earth and Planetary Science Letters, 134: 23-36.

Pankhurst R.J., Sruoga P. and Rapela C.W. 1993. Estudio geocronológico Rb-Sr de los complejos Chon-Aike y El Quemado a los 47°30'L.S. 12 Congreso Geológico Argentino, Actas 4: 171-178, Buenos Aires.

Rapela C.W. and Pankhurst R.J. 1993.El volcanismo riolítico del noreste de la Patagonia: un evento meso-jurásico de corta duración y origen profundo, 12_Congreso Geológico Argentino, Actas, 4: 179-188, Buenos Aires

Vilas J. F. 1974. Palaeomagnetism of some igneous rocks of the middle Jurassic Chon-Aike Formation from Estancia La Reconquista, Province of Santa Cruz, Argentina. Geophysical Journal of the Royal Astronomical Society, 39: 511-522.

Figure 1: Geological skecht of the Sierra de Mamil Choique showing the distribution of the Jurassic dyke swarms.

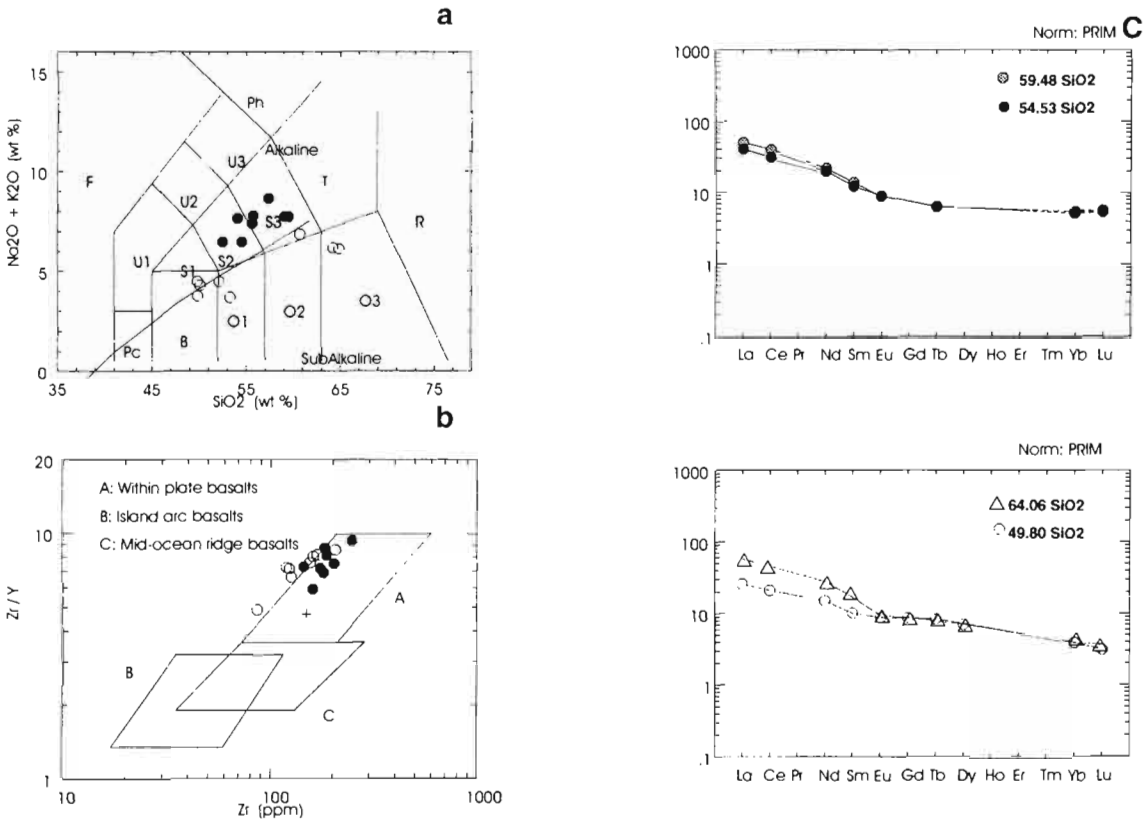

Figure 2: **a**) TAS classification of dykes from Series 1 and 2, **b**) Zr/Y vs. Zr diagram showing the location of samples from series1 and 2, all the samples plot in the within-plate basalt field, **c**) Chondrite normalized patterns for series 2 basaltic tranchyandesites and trachyandesites and **d**) chondrite normalized patterns for series 1 basalts and dacites. Note the slightly defined Eu anomaly for the dacites indicating plagioclase fractionation. Normalization factors from NEWPET v:94. Symbols: open circle: series 1; filled circle: series2 in a and b

THERMOCHRONOLOGICAL EVOLUTION OF A DEFORMED TONALITE OF THE NORTH PATAGONIAN BATHOLITH, SOUTHERN ANDEAN MARGIN

Gloria LÓPEZ[*], *Dave PRIOR*[**] *and Simon KELLEY*[***]

[*] Departamento de Geología, Universidad de Chile. Casilla 13518 Correo 21, Santiago, CHILE
e-mail address: glopez@cec.uchile.cl
[**] Department of Earth Sciences, University of Liverpool. Liverpool L69 3BX, UK.
[***] Department of Earth Sciences, Open University. Milton Keynes MK7 6AA, UK.

Key words: Southern Andes, microstructure, excess argon, $^{40}Ar/^{39}Ar$ dating

INTRODUCTION

The timing of the latest transpressional deformation event along the arc zone of the southern Andean margin has been restricted to the Mio-Pliocene. This has been based on argon dating techniques, which have not taken into account how deformation could affect the way in which argon has moved through the rocks and minerals. The potential problem of age variations due to excess argon and/or heterogeneous argon distribution can be reassessed using high spatial resolution analyses in individual grains with control of their microfabric and location of argon measurements with the aim to reassess the deformation history of the rocks (e.g. Kelley et al, 1994; Reddy et al, 1996; Pickles et al, 1997).

A deformed tonalite from a meter-wide ductile shear zone of the North Patagonian Batholith of the Southern Andes has been studied by using SEM and $^{40}Ar/^{39}Ar$ laserprobe techniques. We described the microstructure and argon distribution in the rock and grain network to constrain the absolute age of deformation and thermal history of the rock.

GEOLOGICAL SETTING

The southern Andes accommodate transpressional dextral deformation along the Liquiñe Ofqui Fault Zone (LOFZ), an intra-arc Cenozoic duplex developed mainly within the Meso-Cenozoic North Patagonian Batholith(NBP)(Cembrano et al, 1996) and which development has been driven either by oblique subduction or ridge collision (Nelson et al 1994; Cembrano, 1998). Ductile dextral shear occurred during late Miocene-Pliocene time (13-3 Ma) with brittle shear occurring after 3 Ma (Cembrano, 1998).

Pliocene transpressional deformation event along the magmatic arc is related to ridge collision during the last 6 Ma (Nelson et al, 1994; Cembrano, 1998).

A tonalitic pluton of the BNP located at 42°S and which is spatially related to one of the main traces of the LOFZ has parallel magmatic fabric and subsolidus fabric indicating dextral shear. Solid-state deformation of plagioclase by extensive fracturing and quartz/biotite by crystal plasticity shows that deformation occurred under low greenschist facies conditions (Simpson, 1985; Lonka et al, 1998). The emplacement age is 9.9 Ma (U-Pb) and single crystal total fusion Ar-Ar ages of biotite range from 8.7 to 3.6 Ma reflecting solid-state deformation and/or cooling following deformation (Cembrano, 1998). Previous high resolution laser dating of a deformed sample from this unit constrained the age of a regional deformation event that took place between 6 and 4.3±0.3 Ma linked to subduction of consecutive segments of the Chile Ridge (Cembrano, 1998).

SAMPLE PREPARATION

The sample was prepared as a 6-cm square, 9-mm thick section to produce a 30 μm thin section and 2mm thick section. The thin section was studied under the light optical microscope and the SEM. The thick section was analysed by using SEM obtain a picture montage of the slab made up with backscatter atomic number contrast and forescatter orientation contrast images (Prior et al, 1996). For Ar methodology, the thick section was then prepared as 1 cm square, 250 μm thick polished section. Following irradiation, the sample was loaded into an ultra-high vacuum laser port with polished side up and observed using a CCD camera mounted onto a microscope through which the infrared laser beam was also directed onto the sample surface.

SAMPLE DESCRIPTION

The sample is a coarse-grained protomylonitic hb-bt tonalite. The schistosity is defined by aligned plagioclase crystals, flattened interstitial quartz and aligned aggregates of hornblende and biotite with grain sizes ranging from 0.1 to 5.5 mm. Centimetre-spaced shear bands transect the main foliation indicating dextral shear sense. Relatively less deformed specimens have a set of short shear bands nucleated within mafic (hb+bt) domains with a similar orientation. Shears bands show subhorizontal stretching lineations.

SEM work has revealed a complex intragrain structure of the igneous minerals. Hornblende shows corroded boundaries, fractures, fluid inclusion trails and a complicated intragrain structure. Structure of hornblende consists of different and separate domains with sharp and/or diffuse boundaries and with/without intradomain variations apparently randomly distributed. They also have inclusions of biotite and feldspar. Plagioclase behaviour is brittle with frequent fluid inclusion trails and no intragrain

variations, whereas K-feldspar shows a complex structure similar to that developed in amphibole. Biotite is intergrowth with amphibole, shows frequent subgrains and large grains pass laterally to smaller grains towards the border suggesting grain size reduction. Larger biotite shows small amount of slip along their basal cleavage, which is parallel to the main foliation. Quartz shows an heterogeneous fabric with a wide range of crystal sizes ranging from < 0.1-2.5 mm. Grain size decreases towards the shear bands. Larger grains show irregular grain boundaries with undulose extinction and elongate subgrains, which pass laterally into domains of smaller dynamically recrystallized grains. Subgrains have elongate shape oriented parallel to the external foliation.

RESULTS

Fifteen analyses of biotite and amphibole were extracted using the focussed infrared laser producing melt pits around 100-150 microns in diameter. As a rough guide, the laser pits are as deep as they are wide. The analyses of amphiboles yielded ages in the range 49.9±0.3 Ma to 280±1.6 Ma. Laser pits in biotites yielded ages in the range 3.7±0.1 Ma to 10.3±0.5 Ma. All Ar-Ar analyses yield information not only on the age but also the chemistry of the analysed sample, in particular the Ca/K ratio of the analysed volume can be determined rapidly from the $^{37}Ar/^{39}Ar$ ratio. Biotites generally have little or no calcium and thus yield very low $^{37}Ar(Ca)/^{39}Ar(K)$. Amphiboles have much higher $^{37}Ar/^{39}Ar$ ratios and tend to be more variable reflecting Ca and K zonation what explains amphibole analyses yielding ratios of 2.9 to 12.7. The analyses of biotite however show a range of $^{37}Ar/^{39}Ar$ values indicating that in fact despite the intention to analyse pure biotite, amphibole was also involved in many of the analyses. Clearly although the surface of the rock slice was biotite, at depth the laser was also melting amphibole. A mean of the younger ages yields 4.5±0.5 Ma. Although there is a good correlation between $^{37}Ar/^{39}Ar$ and age, there are high 37Ar/39Ar analyses, which yield low ages and samples with low $^{37}Ar/^{39}Ar$ yielding ages significantly older than 4.5 Ma. There is no obvious correlation between position relative to the shear bands and the age produced from biotites. The SEM montage seems to show that some are in the shear band and yield ages ranging from 4.3±0.3 Ma to 8.5±0.4 Ma. Whereas those analyses out of the shear yield ages in the range 3.7±0.1 Ma to 10.3±0.5 Ma.

CONCLUSIONS

High spatial resolution $^{40}Ar/^{39}Ar$ investigation in hornblende and biotite of a deformed tonalite shows heterogeneous age distribution within the rock and individual grains. Hornblende yielded ages between 49.9±0.3 Ma to 280±1.6 Ma, older than the known emplacement age of the original igneous precursor (9.9 Ma), reflecting diffusion of excess into the grain network. The excess argon component in amphibole has also an heterogeneous distribution. Biotite mixture with amphibole yielded ages in the range 3.7±0.1 Ma to 10.3±0.5 Ma. The relationship between amphibole and biotite is likely to be complex

and probable related to subgrain sizes. Younger ages are relate to a more pure biotite content or little (or no) excess argon content in amphibole. Thus either the subgrain size controlling the ages is not related to the shears bands and the sample cooled relatively slowly through biotite closure, or more likely the dominant cause of age variations is excess argon leaking from the amphiboles during deformation and rapid cooling. This would cause a variable picture of excess argon in the biotites depending upon supply of excess and removal along the subgrain boundary network. Deformation and subgrain formation may have occurred above the closure temperature what is quite possible given the poor constraints on deformation temperature i.e. low greenschist facies. The temperature subsequently dropped rapidly through the closure temperature, quenched the microstructure and kept the age difference of grains of different sizes (and therefore different closure temperatures) similar. Therefore, apparent ages represent cooling rather than deformation ages.

Acknowledgements. This work was funded by FONDECYT project 1950497 under which the first author is a graduate student. Comprehensive review by José Cembrano is gratefully acknowledged.

REFERENCES

Cembrano, J., Hervé, F. And Lavenu, A. 1996. The Liquiñe-Ofqui fault zone: a long lived intra-arc fault system in southern Chile. Tectonophysics., 259, p.55-66.

Cembrano J. 1998. Kinematics and timing of intra-arc deformation, southern Chilean Andes. Ph.D. thesis (Unpublished), Dalhousie University, Canada, 231 p.

Kelley, S.P., Arnaud, N.O. and Turner, S.P. 1994. High spatial resolution $^{40}Ar/^{39}Ar$ investigations using an ultraviolet laser probe extraction technique. Geochimica et Cosmochimica Acta , 58, p.2519-3525.

Lonka, H., Schulmann, K. and Venera, Z. Ductile deformation of tonalite in the Suomusjärvi shear zone, south-western Finland. Journal of Structural Geology, 20, p.783-798.

Nelson, E., Forsythe, R. and Arit, I. 1994. Ridge collision tectonics in terrane development. Journal of South American Earth Sciences, 7, N°3/4, p.271-278.

Pickles, C., Kelley, S.P., Reddy, S.M. and Wheeler, J. 1997. Determination of high spatial resolution argon isotope variations in metamorphic biotites. Geochimica et Cosmochimica Acta, 61, p. 3809-3833.

Prior, D, Trimby, P. and Weber, U. 1996. Orientation contrast imaging of microstructures in rocks using forescatter detectors in the scanning electron microscope. Mineralogical Magazine, 60, p.859-869.

Reddy, S.M., Kelley, S.P. and Wheeler, J. 1996. A $^{40}Ar/^{39}Ar$ laser probe study of micas from the Sesia Zone, Italian Alps: implications for metamorphic and deformation histories. Journal of Metamorphic Geology. 14, p.493-508

Simpson, C. 1985. Deformation of granitic rocks across the brittle-ductile transition. Journal of Structural Geology, 5, p.503-511.

A CHAOS OF LEAD IN THE BASEMENT OF THE CENTRAL ANDES (18°-27°)?

Friedrich Lucassen[1, 4], Raul Becchio[2], Russell Harmon[3] and Gerhard Franz[1]

[1] Fachgebiet Petrologie, Technische Universität Berlin, Ernst Reuter Platz 1, EB15, 10623 Berlin, Germany; email: luca0938@mailszrz.zrz.tu-berlin.de
[2]Universidad Nacional de Salta, GEONORTE y CONICET, Buenos Aires 177, 4400 Salta, Argentina
[3]U. S. Army Research Office; P.O. Box 12211; Research Triangle Park, NC 27709-2211, USA.
[4]Mineralogisches Institut, Universität Münster, Corrensstrasse 24, 48149 Münster, Germany

Keywords: Central Andes, Palaeozoic basement, crustal composition, Pb and Nd isotopes

INTRODUCTION

The Palaeozoic metamorphic - magmatic basement of the Central Andes in northern Chile and NW Argentina (18-27°S) comprises magmas of variable ages (e.g. Damm et al. 1994) and high grade metamorphic rocks (Lucassen et al., 1996; Becchio et al., 1997). Major magmatic pulses in the Palaeozoic occur in the Cambrian, in Mid-Ordovician to Silurian and in Carboniferous to Permian. The main phase of metamorphic crystallization at high temperature was at ca. 500 Ma. The bulk of the magmatic and metamorphic rocks has granitoid composition. We investigated chemical and isotopic composition (Nd, Sr, Pb) of the metamorphic basement in northern Chile and NW Argentina and Late Palaeozoic granitoids in northern Chile. Isotopic composition (Nd, Sr, Pb) of (meta)intrusions from the distinct magmatic pulses were investigated and to some extent published before by Damm et al. (1994). A detailed presentation and interpretation of this data set together with the new and data from the metamorphic basement is still lacking. Lead isotope ratios on feldspars indicate a wide range of composition in rocks with ages > 500Ma and a more restricted composition in the younger rocks.

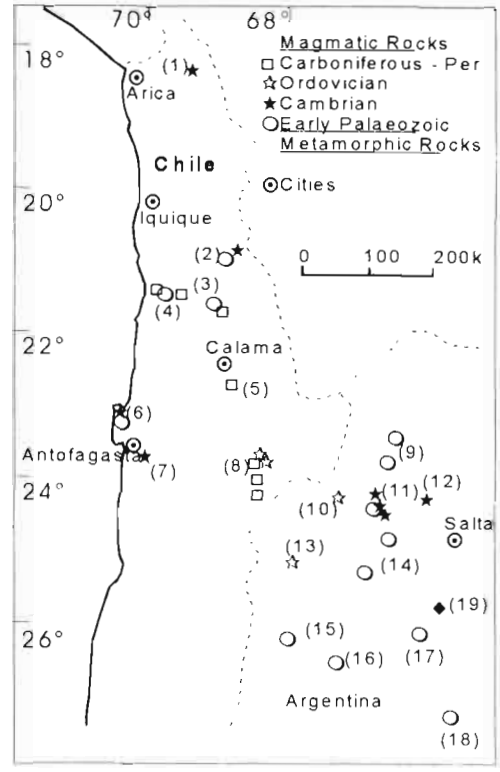

Figure 1 shows the approximate distribution of sample locations of magmatic rocks (Damm et al., 1994; our data) and Early Palaeozoic metamorphic rocks. (1) Belén; (2) Sierra de Moreno - Qda. Choja; (3) Sierra de Moreno - Qda. Arcas; (4) Rio Loa Cañon; (5) Sierra de Limón Verde; (6) Peninsula Mejillones; (7) Salar de Navidad; (8) Cordón de Lila; (9) Calderas de Coranzuli and Ramadas; (10) Sierra de Macón; (11) Qda. Tajamar, Salar Centenario and Diablillos; (12) Santa Rosa de Tastil; (13) Arita; (14) Salar Hombre Muerto; (15) Salar de Antofalla; (16) Sierras El Jote - El Peñon; (17) Sierra de Quilmes; (18) Cumbres Calchaquies - Sierra de Aconqija; (19) Qda. Las Conchas lower crustal xenoliths (Lucassen et al., 1999).

ND, SR AND PB ISOTOPES

All Pb isotope ratios were measured on feldspar separates and approximate the lead isotope composition at the time of magmatic or metamorphic crystallization. The Cambrian intrusions show a considerable spread in their Pb isotope ratios (Figs. 2, 3) from unradiogenic to radiogenic. The Ordovician intrusions are variable in their $^{207}Pb/^{204}Pb$ at moderate variation of $^{206}Pb/^{204}Pb$. The Early Palaeozoic high grade metamorphic rocks, Late Palaeozoic granitoids from northern Chile and lower crustal granulite xenoliths from the Salta Rift system (Lucassen et al., 1999) define a restricted field of Pb isotope composition and only four samples from the Sierra de Limón Verde plutonic complex (Permian) have distinctly lower $^{206}Pb/^{204}Pb$ ratios. The age of the Belén granitoids is somewhat uncertain (Ordovician?, Cambrian?). Their Pb isotope ratios plot into or close to the compositional field of Proterozoic gneisses from the Arequipa Massiv and their $^{207}Pb/^{204}Pb$ ratios are distinct from all other samples.

Most time corrected $^{143}Nd/^{144}Nd_{500Ma}$ ratios (Fig. 4) of rocks from the different magmatic pulses are between 0.5116 and 0.5120 and resemble the spread of values measured in the Early Palaeozoic high grade metamorphic basement of NW-Argentina and northern Chile.

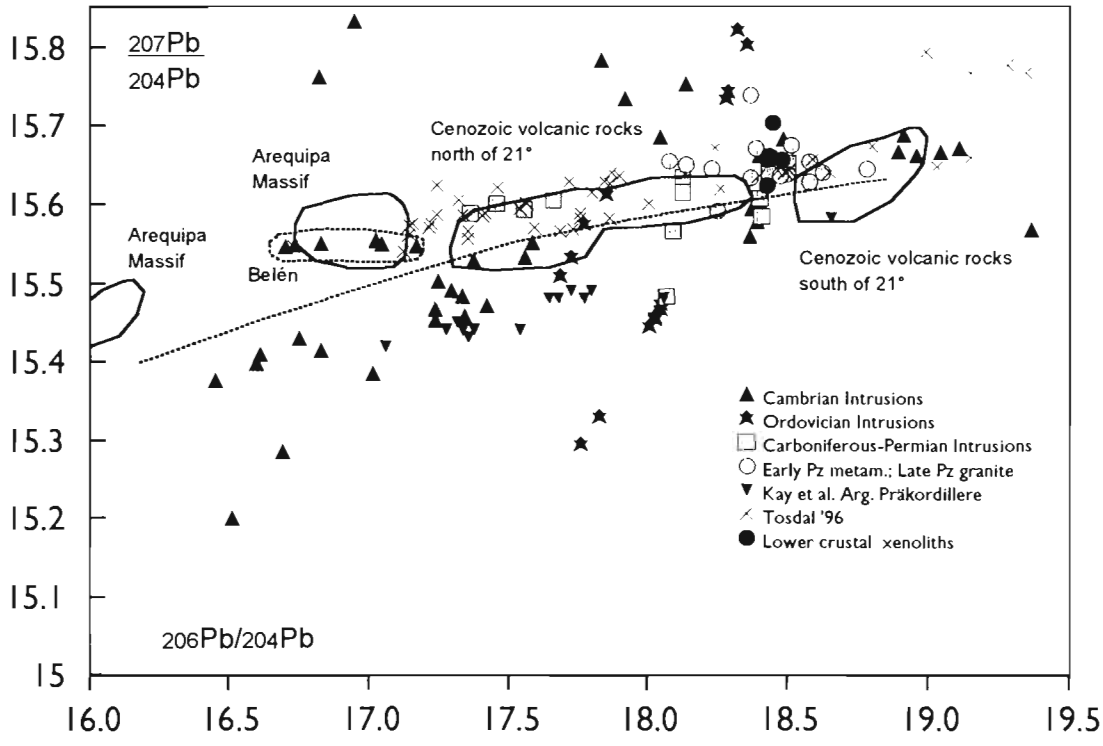

Figure 2 $^{207}Pb/^{204}Pb$ - $^{206}Pb/^{204}Pb$ ratios of Cambrian, Ordovician and Carboniferous to Permian intrusions and Early Palaeozoic metamorphic rocks. Average crustal lead development line from Stacey and Kramer (1975). Metamoprhic rocks from the Argentine Precordillera with a 'Laurentian' lead signature (Kay et al., 1996) and the Arequipa Massif (Tilton and Barreiro, 1980) are whole rock all other samples are feldspar separates. Whole rock analysis of various Pre-Mesozoic rocks from Bolivia and northern Chile from Tosdal (1996). Lower crust xenoliths: Lucassen et al.(1999). Composition of Cenozoic volcanic rocks north and south of 21°S: Wörner et al. (1994).

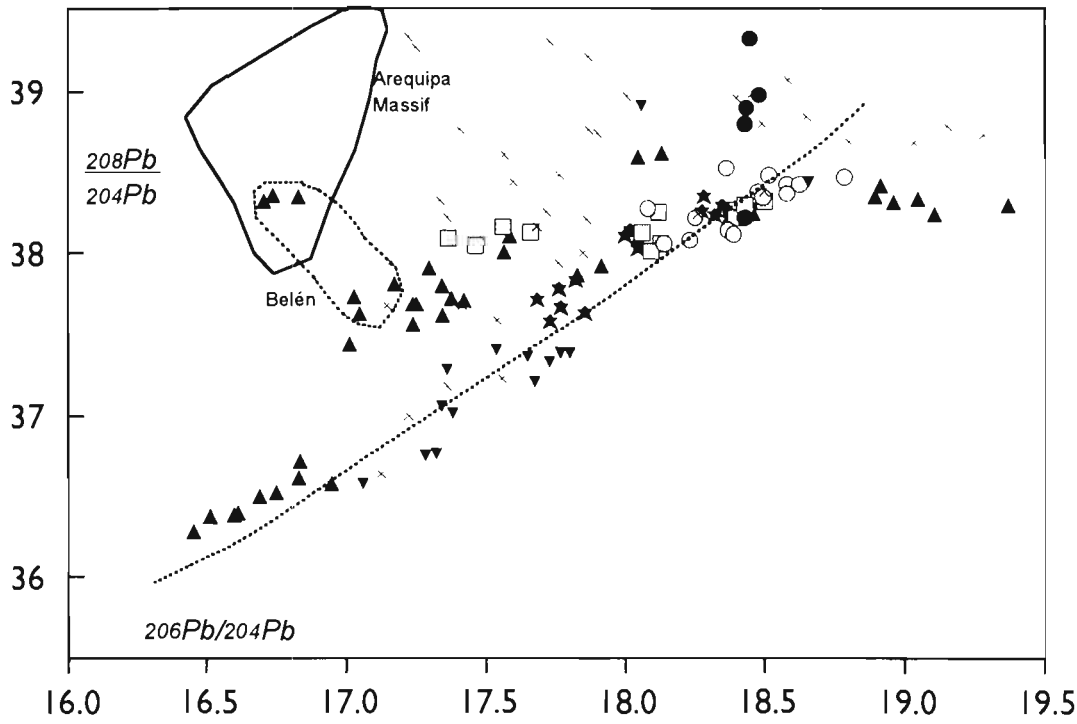

Figure 3 $^{208}Pb/^{204}Pb$ - $^{206}Pb/^{204}Pb$ ratios. Symbols as in Figure 2.

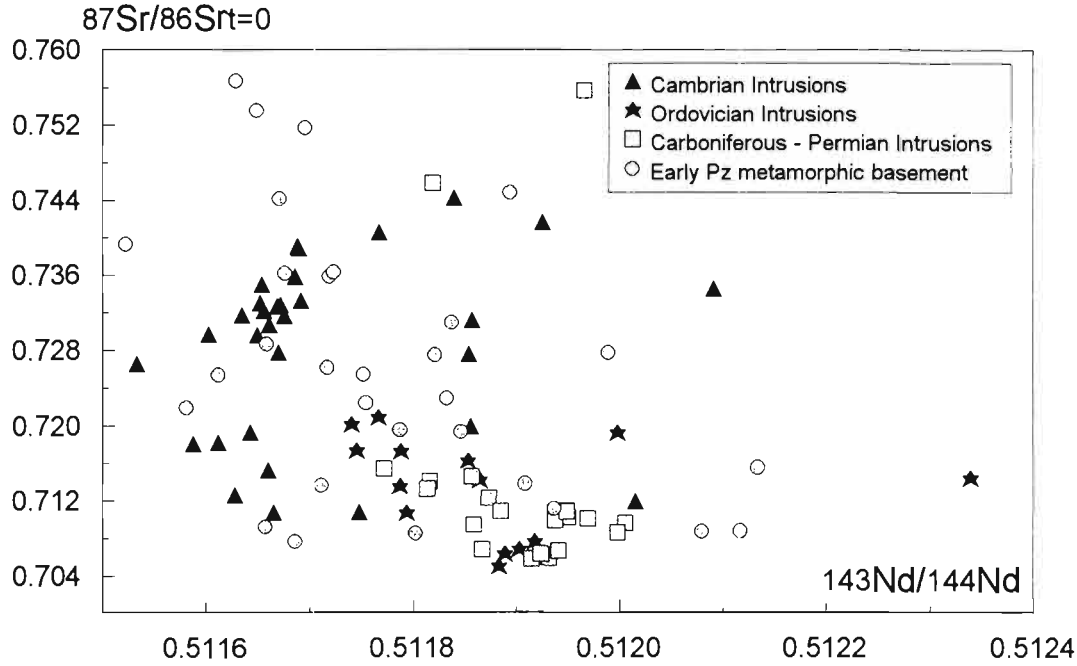

Figure 4 $^{87}Sr/^{86}Sr$ - $^{143}Nd/^{144}Nd$ ratios of Cambrian, Ordovician and Carboniferous to Permian intrusions and Early Palaeozoic metamorphic rocks. Sr ratios are present day values, all Nd ratios are recalculated to 500 Ma.

DISCUSSION AND SPECULATION

Isotope signatures are used to differentiate between the contributions of different sources to the respective sample. The Nd isotope ratios of the magmatic and metamorphic basement are rather homogeneous and no major influence of a depleted mantle source is seen in the magmatic rocks. Evolved magmatic rocks from an enriched mantle source or with major contribution of the latter could possibly not be distinguished by any of the used isotope systems. However, mafic rocks typical for large scale melting in the mantle lithosphere are absent in the Palaeozoic. Therefore, it is plausible to explain the Nd (and Sr) isotope composition of the Palaeozoic basement with recycling of the existing crust as the dominating process.

Lead isotope signatures in evolved plutonic rocks intruding into a continental crust reflect the signature of this crust even in mantle derived magmas. The Cambrian magmatic rocks have highly variable Pb isotope ratios indicating a heterogeneous Pb signature in the sampled crust including values considered to be typical for 'Laurentian' lead (Fig. 2, 4; e.g. Kay et al., 1996). The $^{207}Pb/^{204}Pb$ and $^{206}Pb/^{204}Pb$ signature should be preserved in the melt region, because uranium is commonly extracted from the source during melting under more or less hydrous conditions. The subsequent Ordovician and Late Palaeozoic magmatic pulses, however, have a far more restricted lead isotope composition with $^{206}Pb/^{204}Pb$ ratios similar to those from the high grade metamorphic basement. We speculate that a Proterozoic crust (21-27°S) with heterogeneous lead isotope ratios and homogeneous Nd isotope ratios was largely homogenized during the 500 Ma high grade metamorphism: Cenozoic volcanic rocks south of 21° S (Wörner et al., 1994) do not show any influence of the unradiogenic lead composition obvious in the Cambrian magmatic rocks. In Belén the lead isotopic signature is similar to the signature of the Proterozoic Arequipa Massif.

REFERENCES

Becchio, R, Lucassen, F., Franz, G. and Viramonte, J. 1997). Condiciónes de P-T del basamento metamorfico de alto grado. Borde oriental de la Puna Austral, Argentina. 8. Congreso Geologico Chileno, Antofagasta, Chile, Vol. III, 1220-1224.

Kay, S.M., Orrell, S. & Abbruzzi, J.M. 1996. Zircon and whole rock Nd-Pb evidence for a Grenville age and a Laurentian origin for the basement of the Precordillera in Argentina. Journal of Geology, 104, 637-648.

Lucassen, F., Wilke, H.G., Viramonte, J., Becchio, R., Franz, G., Laber, A., Wemmer, K. and Vroon, P. 1996. The Paleozoic of the Central Andes (18°-26°S) - a metamorphic view. Third International Symposion on Andean Geodynamics, St Malo, France, Abstract Volume, ORSTOM editions, Paris: 779-782.

Lucassen, F., Lewerenz, S., Franz, G., Viramonte, J. and Mezger, K. 1999. Metamorphism, isotopic ages and composition of lower crustal granulite xenoliths from the Cretaceous Salta Rift, Argentina. Contrib. Mineral. Petrol. ,134, 325-341.

Stacey, J. S. & Kramers, J. D., 1975. Approximation of terrestrial lead isotope evolution by a two-stage model. Earth and Planetary Science Letters, 26, 207-221.

Tilton, G. R. & Barreiro B. A., 1980. Origin of lead in Andean calc-alkaline lavas, southern Peru. Science, 210, 1245-1247.

Tosdal, R. M., 1996. The Amazon-Laurentian connection as viewed from the Middle Proterozoic rocks in the central Andes, western Peru and northern Chile. Tectonics, 15, 827-842

Wörner, G., Moorbath, S., Horn, S., Entenmann, J., Harmon, R., Davidson, J. & Lopez-Escobar, L. 1994. Large- and fine-scale geochemical variations along the Andean Arc of Northern Chile (17.5°-22°S). In: Reutter, K. J., Scheuber, E. & Wigger, P. J. (eds.) Tectonics of the Southern Central Andes. Springer. Heidelberg, pp. 77-92.

ISOTOPIC COMPOSITION OF LATE MESOZOIC MAFIC ROCKS FROM THE ANDES (23 - 32°S) - HOW HETEROGENEOUS IS THE MANTLE SOURCE?

Friedrich Lucassen[1, 4], Monica Escayola[2], Rolf L. Romer[3], José Viramonte[2] and Gerhard Franz[1]

[1] Fachgebiet Petrologie, Technische Universität Berlin, Ernst Reuter Platz 1, EB15, 10623 Berlin, Germany; email: luca0938@mailszrz.zrz.tu-berlin.de
[2]Universidad Nacional de Salta, GEONORTE y CONICET, Buenos Aires 177, 4400 Salta, Argentina
[3]GeoForschungsZentrum Potsdam, Projektbereich 4.2, Telegrafenberg, 14473 Potsdam, Germany
[4]Mineralogisches Institut, Universität Münster, Corrensstrasse 24, 48149 Münster, Germany

Keywords Mesozoic mantle derived magmas, Nd-Sr-Pb isotopes, mantle source, crustal contamination

GEOLOGICAL BACKGROUND

Mafic magmatism of Jurassic and Cretaceous age in South America (21 - 27°S) occurs in three distinct 'first order' tectonic settings from the active margin in the West to the passive margin in the East. (1) The Jurassic active continental margin was located at the present Pacific Coast line of northern Chile (Fig.1). The magmatic arc shifted gradually ca. 150 - 200 km inland during the Cretaceous. In the Jurassic a large volume of mantle derived magma intruded or extruded in the Chilean Coastal Cordillera (e.g. Rogers and Hawkesworth, 1989; Lucassen and Franz, 1994). (2) Further to the East from Bolivia to central W-Argentina a continental rift system developed from Mid-Cretaceous to Early Tertiary (Fig.1). The distinct stages of syn- to post rift sedimentation are contemporaneous with phases of minor mafic volcanism especially during the synrift stage (e.g. Viramonte et al., in press). These volcanic rocks bear xenoliths from the upper mantle and the lower crust. (3) In the Paraná region, south Brazil (Fig.1), continental flood basalts of mainly tholeiitic composition extruded during a short period in the Early Cretaceous related to the opening of the South Atlantic (e.g. Hawkesworth et al., 1992). Mafic potassic magmatism in the Paraná region occurs in the Late Cretaceous (Gibson et al., 1996). It has similar ages as the synrift volcanism in the Cretaceous rift system. The Pre-Mesozoic continental crust as a possible contaminant of the mafic, mantle derived magmas can be regionally separated into a Proterozoic metamorphic - magmatic basement of the stable cratonic areas of the Brazilian Shield and metamorphic - magmatic - sedimentary basement of latest Proterozoic - Early Palaeozoic in NW Argentina and northern Chile (Lucassen et al., 1996; Becchio et al., 1997). The isotopic composition of the Early Paleozoic basement points to a Proterozoic protolith of these rocks (ca 32°S: Rapela and Pankhurst, 1998; 21 - 27°S: Lucassen et al., 1999; our unpublished data). The major reorganization of the crust at the western edge of the continent with widespread crustal derived magmatism during Palaeozoic implies also a major reorganization of the whole lithosphere of this section. A major reorganisation of the whole lithosphere seems also likely during the vast Mesozoic mantle derived magmatism in the Coastal Cordillera.

Our ongoing study of Mesozoic mantle derived rocks focus on three areas, the Jurassic magmatic arc south of Antofagasta with a minimum age of ca 150 Ma (Lucassen and Franz, 1994; Lucassen and Thirlwall, 1998), the Cretaceous rift magmatism from Qda. Las Conchas

near Cafayate (Viramonte et al., in press; Lucassen et al., 1999), and Sierras Los Cóndores at the latitude of Córdoba (Viramonte et al., in press). We present new data on the chemical and Nd, Sr, and Pb isotope composition of the magmatic rocks. Preliminary data of mantle xenoliths are also included. Detailed account to the geological situation and age relations at the sample sites is given in the references above.

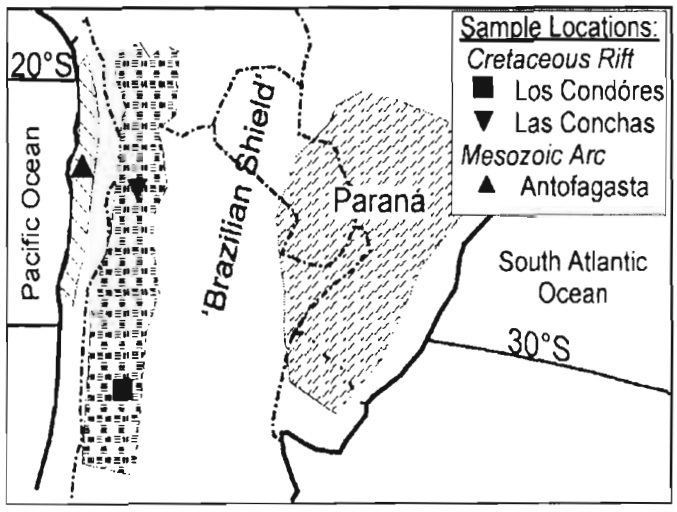

Figure 1 Map showing the approximate distribution of the three main Mesozoic provinces of mantle derived magmatism and the approximate position of our sample areas. The Jurassic magmatic arc is at the Chilean Pacific Coast, the Cretaceous rift related sedimentary basins are in and east of the Cenozoic Andes, the Paraná volcanism is in south-east Brazil and surrounding areas. The precise extension of Proterozoic cratonic basement to the west is unknown, however, ages of the basement in NW-Argentina and northern Chile are mainly (Early) Palaeozoic.

RESULTS

Most volcanic rocks of the Las Conchas area are basanites. Samples from Los Cóndores cover a wide range of composition from basanite to basaltic trachyandesite but no differentiation trend is observed in the TAS classification. The Jurassic (meta)intrusions from the Coastal Cordillera follow a calcalkaline differentiation trend in the compositional fields of basalt and basaltic andesite. The three rock suites are also different in their REE with the highest La/Yb ratios in the Los Cóndores samples and distinctive lower values in the Las Conchas basanite at similar La/Sm ratios and flat REE pattern in the calcalkaline rocks of the Coastal Cordillera.

Nd and Sr isotope ratios (Fig.2) are recalculated to 90 Ma, the age of extrusion of the Las Conchas basanite (Lucassen et al., 1999. The bulk of the Las Conchas basanite samples have similar compositions and plot in the depleted mantle field. One clinopyroxene (cpx) sample from the Las Conchas mantle xenoliths plots close to the depleted mantle field, the other cpx plots close to the Las Conchas basanite. The Jurassic (meta)intrusions have a very small range of composition and plot between the Las Conchas basanite and the depleted mantle (DM) and Pacific N-type MORB (PNM). The Los Cóndores volcanic rocks have distinctly lower $^{143}Nd/^{144}Nd$ ratios and higher $^{87}Sr/^{86}Sr$ ratios,both similar to those of

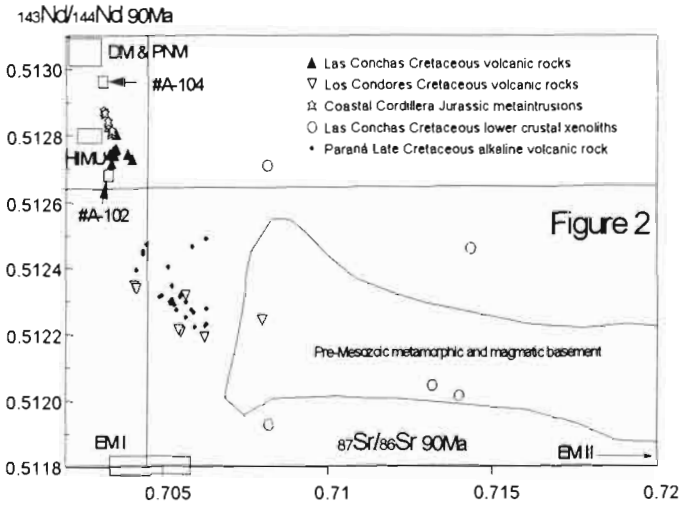

Figure 2 $^{87}Sr/^{86}Sr$ and $^{143}Nd/^{144}Nd$ ratios recalculated to 90 Ma. Paraná Late Cretaceous alkalic volcanic rocks (Carlson et al., 1996; Gibson et al., 1996); DM, HIMU and EM I, EM II fields (Zindler and Hart, 1986); Pacific N-type MORB (PNM; Saunders et al., 1988); Pre-Mesozoic basement and lower crustal xenoliths (Lucassen et al., 1999; our unpublished data). Discussion in the text.

Cretacious alkalic magmas from the Paraná area (Carlson et al.,1996; Gibson et al., 1996). Pb isotope ratios (Figure 3) distinguish between the more radiogenic Las Conchas basanite and the less radiogenic samples of the Los Cóndores volcanic rocks and Jurassic (meta)intrusions. The Las Conchas mantle xenoliths are similar to the basanite as sample #A-102, which also has similar Nd and Sr isotope ratios, or they are different as sample #A-104 which has Nd, Sr, and Pb isotope ratios similar to PNM or DM. The Pb isotope ratios of the Los Cóndores and Jurassic samples are similar to some of the Paraná Late Cretaceous alkalic rocks (Carlson et al., 1996). The difference between a depleted mantle source and an enriched mantle source can not be seen by the similar Pb isotope ratios, though the Nd and Sr isotope ratios of the Los Cóndores volcanic rocks and the Jurassic metaintrusions are very different.

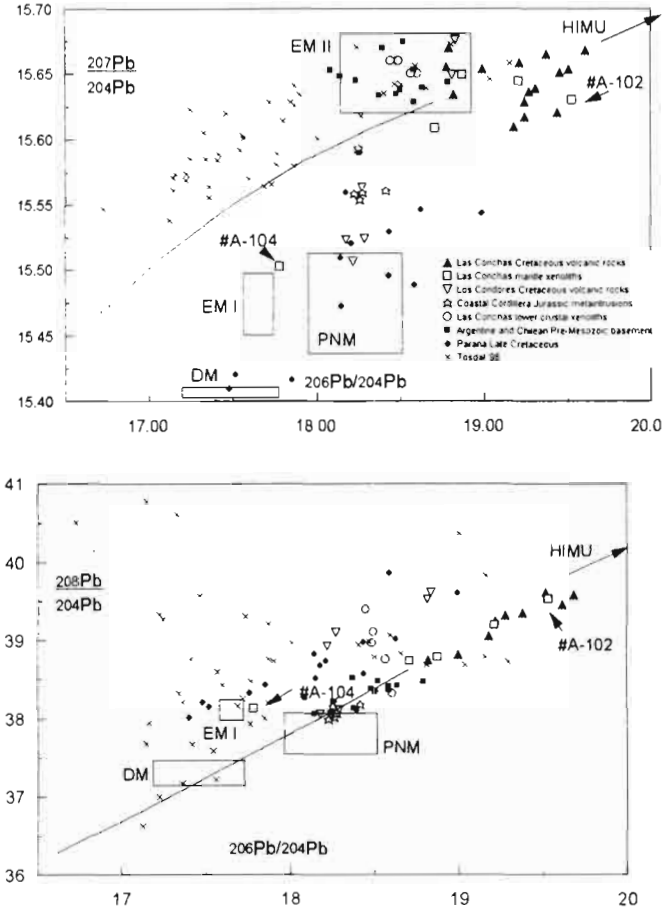

Figure 3 $^{207}Pb/^{204}Pb$ - $^{206}Pb/^{204}Pb$ and $^{208}Pb/^{204}Pb$ - $^{206}Pb/^{204}Pb$ present day ratios. Different sources as in Fig.2. Data from the Pre-Mesozoic basement and lower crust (Tosdal, 1996; Lucassen et al., 1999; our unpublished data) from the Paraná Late Cretaceous alkalic magmas (Carlson et al., 1996). Discussion in the text.

DISCUSSION: SOURCE COMPOSITION OR CRUSTAL CONTAMINATION

Possible contaminants of the Las Conchas basanite from upper and lower crustal sources (Tosdal, 1996; Lucassen et al., 1999; our unpublished data) are shown in Figures 2 and 3. The Nd and Sr isotope composition of the Sierra de Córdoba Pre-Mesozoic basement (in: Pankhurst and Rapela, eds, 1998) near to Los Cóndores is very similar to the compositional field of the basement in Figure 2 (no comparision can be made in Fig.3, because Pb data are not available). The Nd and Sr ratios of all but one magmatic sample are distinct from the field of Pre-Mesozoic basement and felsic lower crustal xenoliths (Fig.2). Since REE content (40 to 100 ppm in most samples) and Sr content (500 - 3000 ppm) are high in the Las Conchas and Los Cóndores volcanic rocks compared to typical values of the local basement (Nd < 20 - 30 ppm; Sr < 200 ppm), significant contamination of the Nd and Sr isotope systems by this basement should be seen in major and trace element composition of the volcanic rocks, e.g., if a mixing of a depleted mantle source magma and the Pre-Mesozoic basement is assumed. This is not the case. The Jurassic (meta)intrusions have the lowest REE content (Nd ~10 ppm) of the investigated rocks and contamination by the Pre-Mesozoic basement should be seen in the Nd isotope ratios of the (meta)intrusions which, however, are very homogeneous in their Nd isotopic composition.

The lead isotope system of mantle derived rocks is assumed to be very sensible to crustal contamination. The $^{207}Pb/^{20}4Pb$ versus $^{206}Pb/^{204}Pb$ ratios of the Pre-Mesozoic basement and the lower crustal xenoliths samples (Fig. 3) are distinct from most samples of the magmatic rocks and mantle xenoliths from Las Conchas, Los Cóndores and Coastal Cordillera. Dominance of crustal lead composition in most magmatic and xenoliths samples is unlikely. The majority of the Las Conchas basanite Pb isotope ratios point to a mixture of a HIMU type source and DM for the primary magma as represented by mantle xenoliths #A-104 and #A-102. The group of basanite samples, situated in an array towards the field of crustal lead composition is assumed to be contaminated by crustal material.

Beyond this speculation about contamination or mixing processes it can be resumed: The Cretaceous mantle in the Las Conchas area was heterogeneous on a local scale with a HIMU and a DM component, as seen in the basanite and the xenoliths. On a regional scale, the volcanic rocks of the Creatceous Rift system sampled an enriched mantle type in the Los Cóndores area with Nd, Sr and Pb isotopic composition similar to the composition of Cretaceous alkalic magmas from the Paraná area where a Proterozoic lithospheric mantle below the Brazilian Shield is assumed (Carlson et al., 1996; Gibson et al., 1996). The Jurrassic magmatic arc magmas have the isotopic signature of a depleted mantle source perhaps similar to the source of the Pacific N-type MORB. The isotopic composition of the mantle was rather variable in Late Cretaceous at the edge of the Andean orogeny.

ACKNOWLEDGEMENTS

This research is a result of Sfb 267 "Deformation processes in the Andes". We thank the Deutsche Forschungsgemeinschaft for financial support. F.L. acknowledges Bundesanstalt für Arbeit.

REFERENCES

Becchio, R, Lucassen, F., Franz, G. and Viramonte, J. 1997. Condiciones de P-T del basamento metamorfico de alto grado. Borde oriental de la Puna Austral, Argentina. 8. Congreso Geologico Chileno, Antofagasta, Chile, Vol. III, 1220-1224. **Carlson, R.W., Esperanca, S. and Svisero, D.P., 1996**. Chemical and Os isotopic study of Cretaceous potassic rocks from southern Brazil. Contrib. Mineral. Petrol., 125, 393-405. **Gibson, S.A., Thompson, R.N., Dickin, A.P. and Leonardos, O.H. 1996**. Erratum to 'High-Ti and low-Ti mafic potassic magmas: Key to plume-lithospere interaction and continental flood-basalt genesis'. Earth Planet. Sci. Lett., 141, 325-341. **Lucassen, F. and Franz, G., 1994.** Arc related igneous and metaigneous rocks in the Coastal Cordillera of northern Chile/Region Antofagasta. Lithos 32, 273-298. **Lucassen, F. and Thirwall, M.F. 1998**. Sm-Nd formation ages and mineral ages in metabasites from the Coastal Cordillera, northern Chile. Geologische Rundschau, 86, 767-774. **Lucassen F, Wilke HG, Viramonte J, Becchio R, Franz G, Laber A, Wemmer K, Vroon P. 1996**. The Paleozoic of the Central Andes (18°-26°S) - a metamorphic view. Third International Symposion on Andean Geodynamics, St Malo, France, Abstract Volume, ORSTOM editions, Paris: 779-782 **Lucassen, F., Lewerenz, S., Franz, G., Viramonte, J. & Mezger, K. 1999**. Metamorphism, isotopic ages and composition of lower crustal granulite xenoliths from the Cretaceous Salta Rift, Argentina. Contrib. Mineral. Petrol. ,134, 325-341. **Pankhurst, R.J. and Rapela, C.W., eds, 1998**. The Proto-Andean margin of Gondwana. Geological Society, London, Special Publications, 142. **Saunders, A.D., Norry, M.J. and Tarney J. 1988**. Origin of MORB and chemically depleted mantle reservoirs. In: Menzies, M.A. and Cox, K.G. eds. Oceanic and Continental Lithosphere: Similarities and Differences, J. Petrol., Special Volume, 415-445. Tosdal, R. M., 1996. The Amazon-Laurentian connection as viewed from the Middle Proterozoic rocks in the central Andes, western Peru and northern Chile. Tectonics, 15, 827-842. **Viramonte JG, Kay SM, Noviski I, Becchio R, Escayola M (in press)** Cretaceous rift related magmatism in south-central south America. South Am J of Earth Sci **Zindler, A. and Hart, S.R., 1986**. Chemical geodynamics. Ann. Rev. Earth. Planet. Sci., 14, 493-571.

CONTRIBUTION OF SELF-POTENTIAL AND SOIL-TEMPERATURE SURVEYS FOR THE INVESTIGATION OF STRUCTURAL LIMITS AND HYDROTERMAL SYSTEM ON UBINAS VOLCANO (PERU)

MACEDO SÁNCHEZ O. (1), FINIZOLA A. (2,3), GONZALES K.(1), and RAMOS D. (1)

(1): Instituto Geofísico del Perú, IGP-Arequipa, Urb. La Marina B-19, Cayma, Arequipa-PERU - E-mail: omacedo@geo.igp.gob.pe - Tel/Fax: (51) 54-251373
(2): Universite Blaise Pascal, OPGC-CNRS, UMR6524-CRV, 5 rue Kessler, 63038 Clermont-Ferrand (France) - E-mail: finizola@opgc.univ-bpclermont.fr - Tel: (00-33)-4-73-34-67-44
(3) IRD - (ex-ORSTOM) UR6 (France)

KEY WORDS : Self-Potential, Soil-Temperature , Ubinas volcano , South Peru

INTRODUCTION

Ubinas strato-volcano (16° 22' S, 70° 54' W, 5672 m) is the most active volcano of Peru; it has been reported 23 minor eruptions since 1550. This volcano has been built upon the Altiplano and the Cordillera Occidental and its truncated appearance is due to a broad summit crater or caldera of 1,2 km wide. The south part of the caldera contains a pit funnel-shaped crater (600 m in diameter, 300 m deep), where a permanent fumarolic activity take place. Increasing gas emission has been reported since late in 1995. White and bluish steam commonly rose 100-500 m over the summit and some times these gases reach filling completely the entire caldera in a few hours.

Observations and thermic measurements realized at the bottom of the pit crater revealed the presence of six zones, located near the walls, emiting gases with strong pressure and high temperatures, until 444° C. These fumeroles constitute the unique rising gas evidence over the entire volcanic edifice.

Detailed Self-potential (SP) and soil-temperature measurements has been carried out inside the summit caldera's floor. SP and thermic maps show no significative anomaly in the caldera. (Figs. 1a, 1b).

Thermic results seems to show an absence of comunication between hydrothermal system of today's active crater and the caldera's floor. SP results show no evidence of gas rising organization inside the caldera.

Four long radial SP profiles were also measured over the entire volcanic edifice (Fig. 2). The SP versus elevation profiles show a common pattern on active volcanoes: the lower part is characterised by inverse relationship between SP and elevation whereas it inverts in its higher parts (Fig.3). This lower part is interpreted by normal hydrogeological model, whereas the upper part is a signature of an hydrothermal system (Zhody et al:, 1973; Corwin & Hoover, 1979; Anderson & Johnson, 1978; Fournier, 1989).

On the map of the area, the limit between these two parts (hydrogeological and hydrothermal) shows a circular shape of approximatively 6 km wide. These results can be interpreted a signature of a deep structural limit of an older great caldera.

CONCLUSIONS

Self-potential and soil-temperature results results suggest that Ubinas hydrothermal system is in over-pressure state having difficulties to evacuate the enormous volume of superficial water infiltrated in the caldeira. Also, results of self-potential long profiles over the entire volcanic edifice show the signature of an old great caldera of circular shape and 6 km wide.

REFERENCES

Anderson L.A. and Johnson G.R., 1978. Some observations of the self-potential effect in geothermal areas in Hawaii and Nevada. Geothermal Ressources Council Transactions, 2, 9-12.

Corwin R.F. and Hoover D. B., 1979. The self-potential method in geothermal exploration. Geophysics, 44-2, 226-245.

Fournier C., 1989. Spontaneous potentials and resistivity surves applied to hydrogeology in a volcanic area: case history of the Chaine des Puys (Puy-de-Dome, France). Geophysical Prospecting 37, 647-668.

Zhody A.A.R., Anderson L.A. and Muffler L.J-P., 1973. Resistivity, self-potential and induced polarisation surveys of a vapor dominated geothermal system. Geophysics, 38-6, 1130-1144.

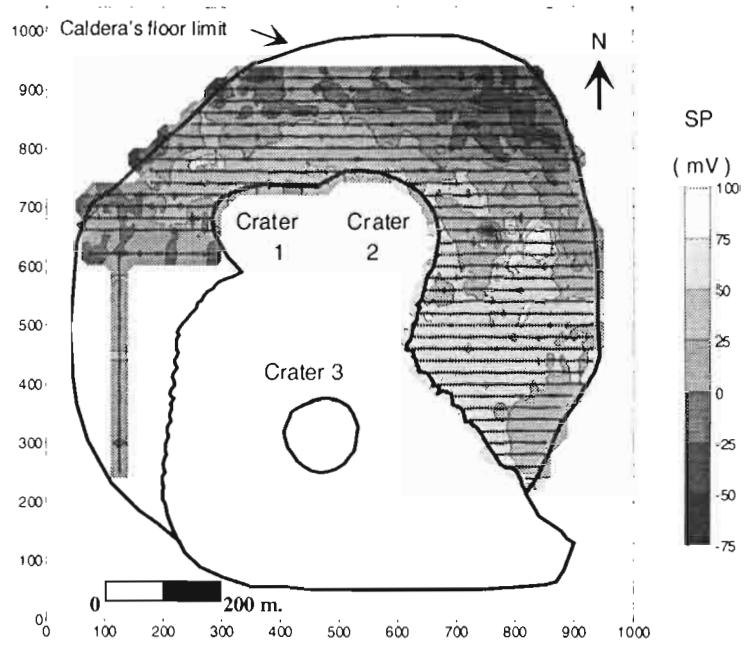

Fig. 1a.- Self-potential map of Ubinas's caldera.

Crosses: location of measurement stations

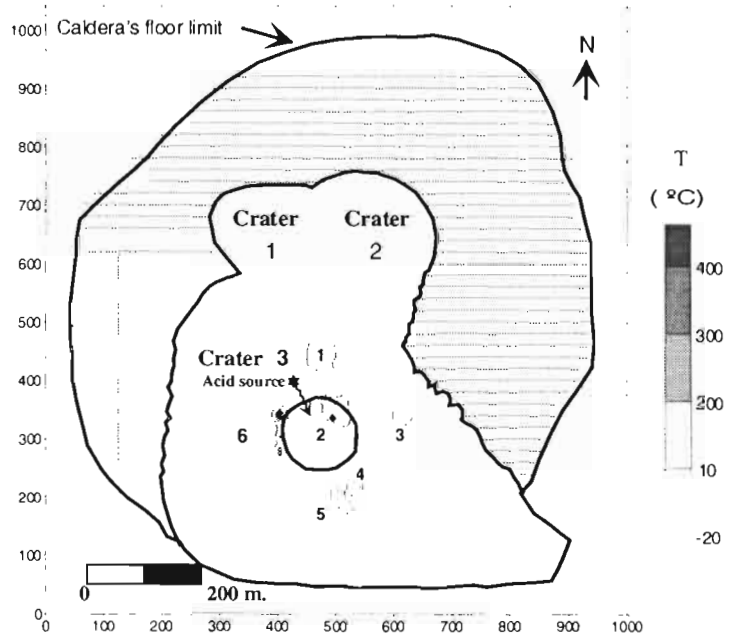

Fig. 1b.- Infra-red thermic map of Ubinas's caldera.

Crosses: location of measurement stations

1,2,3,4,5 and 6: permanent fumarolic zones

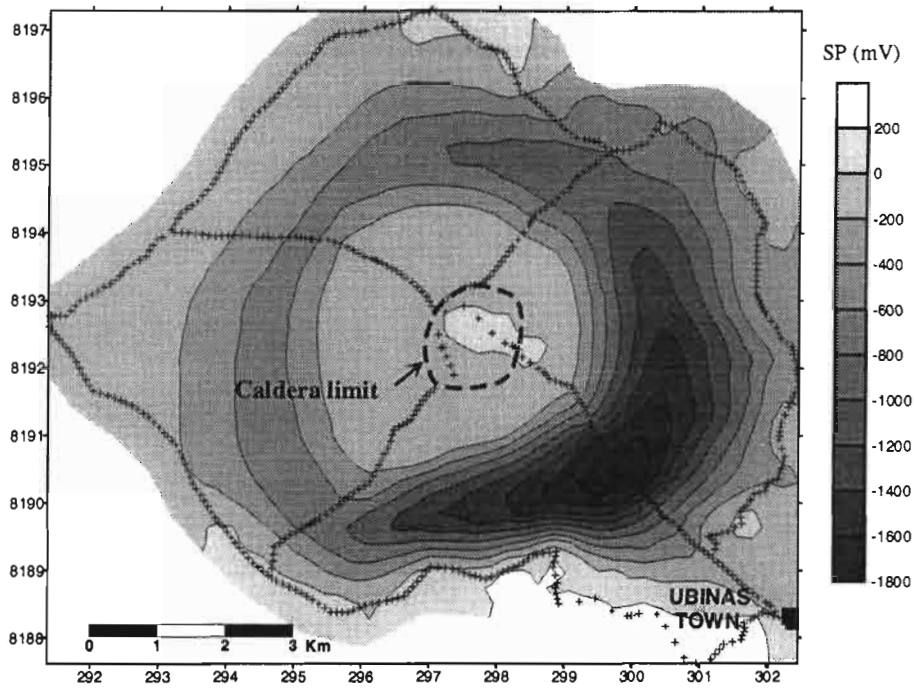

Fig. 2.- Self-potential map of Ubinas volcano

Crosses: location of SP measurement stations

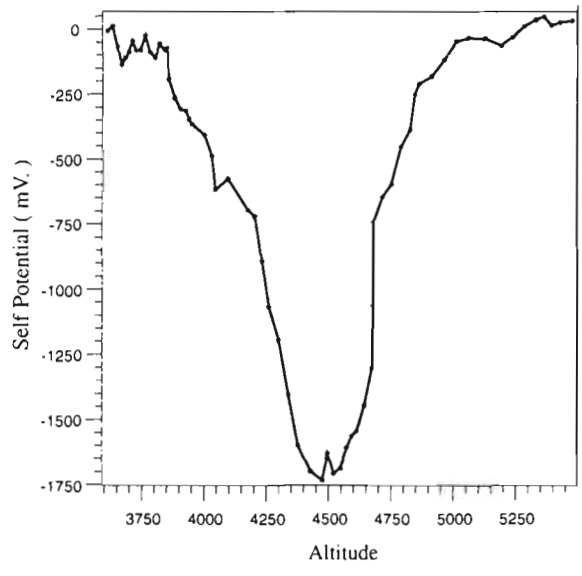

Fig. 3. Example of Self-potential profile obtained at Ubinas volcano, (SE profile).

THE RASPAS METAMORPHIC COMPLEX (SOUTHERN ECUADOR): REMNANT OF A LATE JURASSIC-EARLY CRETACEOUS ACCRETIONARY PRISM. GEOCHEMICAL AND ISOTOPIC CONSTRAINTS

Jean-Louis MALFERE [1, 2], Delphine BOSCH [2], Henriette LAPIERRE [1], Etienne JAILLARD [1, 3], Richard ARCULUS [4] and Patrick MONIE [2].

(1) UPRESA 5025-CNRS, UJF, 15 rue Maurice Gignoux, F. 38031 Grenoble, France. Malfere@ujf-grenoble.fr.
(2) ISTEEM UMR5567-CNRS, Université Montpellier II, Place Eugène Bataillon, F. 39095 Montpellier, France.
(3) IRD, Dept. RED, 209-213 rue Lafayette, 75840 Paris cedex 10, France
(4) Department of Geology, Australian National University, Canberra, ACT 0200, Australia

KEYWORDS : High-pressure rocks, Raspas complex, isotope geochemistry, N-MORB and OIB sources, Ecuador.

INTRODUCTION

Along the western boundary of the Eastern Cordillera of north-central Ecuador, a major fault system marks the suture of the Amotape-Chaucha Terrane (Litherland et al., 1994), and extends northwards into Colombia. Dextral transcurrent motion associated with clockwise rotation (Mourier et al., 1988), which was concurrent or subsequent to subduction-accretion of the Amotape-Chaucha Terrane, has resulted in the exhumation *en bloc* of previously subducted portions of this terrane (El Oro Metamorphic Complex) which comprises exotic blocks of eclogite-blueschist-amphibolite known as the Raspas Complex (Duque and Feininger (1974; Figure 1). Arculus *et al.* (1999) demonstrated that the basalts and gabbros have N-MORB and oceanic plateau affinities while the pelitic schists represent crust-derived sediments.

MAJOR, TRACE ELEMENT AND ISOTOPIC CHEMISTRY

On the basis of major, trace element and isotopic geochemistry, two groups of meta-igneous rocks can be recognized. The first, composed of eclogite, garnet-amphibolite and one meta-gabbro exhibits E-MORB affinities; the second group, comprising greenschist- and amphibolite-facies basalts and gabbros is similar to N-MORB.

The relatively high MgO (7 to 8%) and TiO_2 (1.5 to 2.2 %) contents of the eclogites and N-MORB type basalts indicate that they do not represent strongly fractionated melts. The gabbros differ from the basalts by lower TiO_2 (0.4 to 0.8 %) and higher Al_2O_3 (~17 %) contents, suggesting that they contain cumulus plagioclase. In contrast, the high MgO (10.36 %) and Cr (542 ppm) of the garnet amphibolite indicate that the protolith of this rock was a clinopyroxene cumulate gabbro. The harzburgites are characterized by high MgO (~ 37 %) and Cr (2280 to 2614 ppm) correlated with very low Al_2O_3 (< 3 %). The major- and trace-element chemistry of the pelitic schists is very homogeneous. Variations in Zr content are interpreted as reflecting the presence of detrital zircon.

The rare earth element (REE) pattern of the eclogite is clearly distinct from the other basalts of the Raspas Complex in that it is enriched in light REE (LREE) relative to heavy REE (HREE) [$(La/Yb)_n$ = 1.15; $(La/Sm)_n$ = 1.0] while the other basalts are depleted in LREE [0.55 < $(La/Sm)_n$ = 0.9] (Figure 2). The gabbros differ from the basalts by lower REE abundances (~ 10 times the chondritic abundances), lower (La/Yb)n ratios (0.55 to 0.6; with the exception of 97CE19), and Eu positive anomalies (Figure 2). The Nd-to-Ln_n spectrum of the harzburgites are within the general range expected of refractory ultramafic lithologies (Figure 2). However, two features may reflect a more complex origin: i) enrichments of La, Ce and Pr relative to MREE; ii) a positive Eu anomaly (Eu/Eu*=1.76). Both features might result from original veining by melt-related material.

The REE_n abundances of the pelitic schists (Figure 3) resemble those of bulk continental crust. All these rocks are LREE enriched relative to HREE [4.27 < $(La/Yb)_n$ < 5.82]. There is no indication in these high-grade pelitic rocks of bulk or differential selective loss of REE. Noteworthy in this respect is absence of selective loss of the light REE compared with medium to heavy REE.

The N-MORB-normalised, extended trace element abundances of the varied mafic-ultramafic lithologies are informative (Figure 2). For greenschist-facies rocks, with the exception of Rb and Ba (on one sample of metagabbro) and Pb (in both meta-basalts and gabbros), overall abundances are relatively unfractionated. Likewise, smooth relative enrichments in certain LILE of the eclogite (Th, U, Nb, Ta, and Pb) are consistent with faithful preservation of original E-MORB or OIB abundances. Conversely, abundances of Rb, Ba, and Sr are significantly depleted compared with fluid-immobile LILE. Garnet amphibolite differs from the eclogite in that it shows significant depletion in Nb and Ta and compared to the gabbros, and is enriched in Th and U. However, this rock shows Like the greenschist-facies samples and the harzburgites, this rock is relatively enriched in Pb. While Ba is below detection limit (5 ppb) and

may have been lost from the serpentinite, there are no apparent losses of Rb, Th, U, and Sr. An absence of Ba loss distinguishes the preserved harzburgite differs from the serpentinized samples.

ISOTOPE RESULTS

The isotope compositions of Sr, Nd and Pb were determined on samples from same data set, including whole-rocks and separate minerals. All the isotopic compositions have been corrected for "in situ" decay using an age of 150 Ma for the basic and ultrabasic rocks and 123 Ma for the sedimentary rocks.

The metabasalts clearly show a N-MORB affinity with εNd values ranging between +10 and +11 and $(^{87}Sr/^{86}Sr)i$ ranges from 0.70306 to 0.70310 (Figure 4). The two gabbroic samples are different. One sample (Ce13) has a depleted signature similar to the metabasalts (εNd=+10, $(^{87}Sr/^{86}Sr)i = 0.70396$) and probably originated from a N-MORB type reservoir. The second one (Ce19) presents a significantly different signature with a higher $(^{87}Sr/^{86}Sr)i$ ratio (0.70507) and a lower Nd composition (εNd=+7) suggesting a more enriched origin similar to E-MORB or OIB. The distinction between the two gabbroic samples agrees quite well with the conclusions previously proposed on the basis of REE and trace element distributions. The composition of sample Ce19 falls in the same domain as the garnet amphibolite and the eclogite whole-rocks in Fig 4 .

The Sr and Nd isotopic compositions of the garnet amphibolite and the eclogite are more enriched and are located on an intermediate position between N-MORB and OIB (Figure 4). The slightly elevated $(^{87}Sr/^{86}Sr)i$ ratios of these rocks suggests seawater alteration. For the eclogite sample, we also determined the isotopic compositions on separated clinopyroxene (omphacite) and amphibole (barroisite). The slightly elevated $(^{87}Sr/^{86}Sr)i$ ratios (0.70649) determined for the whole-rock compared to the mineral separates (0.70307 and 0.70391 for clinopyroxene and amphibole, respectively) clearly suggest a limited impact of this late low temperature hydrothermal event.

The two ultrabasic samples yield εNd ratios in agreement with an origin from a depleted reservoir. The serpentinite (Ce14) yields a more elevated $(^{87}Sr/^{86}Sr)$ ratio (0.70407) than the fresh one which has a lower $(^{87}Sr/^{86}Sr)i$ ratio (0.70378).

The pelitic schists exhibit the most radiogenic Sr isotopic compositions $(^{87}Sr/^{86}Sr)i > 0.715$ with εNd values ranging between -6 and -8. These isotopic compositions clearly suggest a continental crustal affinity: the source could have been old detrital sediments with ages ranging from 0.6 to 1.0 Ga.

Pb isotopic compositions are reported in the $^{207}Pb/^{204}Pb$ vs $^{206}Pb/^{204}Pb$ and $^{208}Pb/^{204}Pb$ vs $^{206}Pb/^{204}Pb$ diagrams (Figure 5). The distribution of the analytical points defines three distinct groups of samples. The first, constituted by the metabasalts, one metagabbro (Ce13) and one harzburgite (Ce15), has very low ratios corresponding to an origin from a depleted or N-MORB type reservoir. The second group of samples has more radiogenic $(^{206}Pb/^{204}Pb)i$ and $(^{208}Pb/^{204}Pb)i$ ratios that overlap the OIB or E-MORB domains. This group includes eclogite, harzburgite, the second metagabbro (Ce19) and the garnet

amphibolite. These rocks probably come from a more enriched source than the metabasalts and the gabbros Ce13. Moreover, they show pervasive hydrothermal alteration. The metagabbro Ce19 has an elevated ($^{207}Pb/^{204}Pb$)i ratio compared to the eclogite and harzburgite whole-rocks. This can be explained by a contribution either of small quantities of a sedimentary component (pelagic?) or of old continental crust. The third group of samples, composed of the three pelitic schists, displays a range of Pb ratios that clearly reflect their origin from old crust. The clear distinction between the present data set and the Hispaniola samples supports different origins and precludes, for the Raspas Complex rocks, a similar hotspot contribution. Compared to the 123 Ma Ecuadorian samples, the first Raspas group is less enriched but the second one is similar, which could be interpreted as involvement of the same components (Figure 5; Lapierre et al., 1999).

CONCLUSION

The major-, trace-element and Nd, Sr, Pb isotopic compositions of metamorphosed igneous and sedimentary components of the Raspas Complex define three groups of samples. The meta-basalts, one gabbro (Ce18) and the harzburgites have depleted characteristics corresponding to a N-MORB type reservoir. The eclogite, another gabbro (Ce19) and the garnet amphibolite present strong affinities with a more enriched source similar to that of OIB or E-MORB. Finally, the pelitic schists clearly come from old continental crust probably of Proterozoic or Archaean age (> 0.6 Ga). Pervasive hydrothermal alteration is clearly seen in the oceanic plateau rocks. The distinct origins for these rocks from a restricted area of the El Oro district supports the hypothesis of an accretionary prism including an exotic block of eclogite-blueschist-amphibolite.

REFERENCES

Arculus, R. J., Lapierre H, and Jaillard E., 1999, A geochemical window into subduction-accretion processes: the Raspas Metamorphic Complex, Ecuador, *Geology*, in press.

Duque, P., and Feininger, T., 1974, Eclogitas y esquistos azules de la Provincia de El Oro, Ecuador, *Memorias Simposio sobre ofiolitas*. Universidad Nacional Medellín, Colombia, 35-38, abstr.

Lapierre, H., Bosch, D., Dupuis, V., Polvé, M., Maury, R.C., Hernandez, J., Monié, P., Yeghicheyan, D., Jaillard, E., Mercier de Lépinay, B., Mamberti, M., Desmet, A., Keller, F. and Sénebier, F., 1999, Multiple plume events in the genesis of the peri Caribbean Cretaceous oceanic plateau province, *J. Geophysical Research*, in press.

Litherland, M., Aspden, J.A., and Jemielita, R. A., 1994, The metamorphic belts of Ecuador, British Geological Survey, *Overseas Memoir* No.11.

Mourier, T., Laj, C., Mégard, F., Roperch, P., Mitouard, P., and Farfan-Medrano, A., 1988, An accreted continental terrane in northwestern Peru., *Earth Planet. Sci. Lett.*, 88, 182-192.

Sun, S-S., and McDonough, W. F., 1989, Chemical and isotopic systematics of oceanic basalts: implications for mantle composition and processes, *in* Saunders, A.D., and Norry, M.J., eds., Magmatism in Ocean Basins: *Geol. Soc. London, Spec. Publ.* 42, 313-345.

STRATIGRAPHIC CHARACTERIZATION OF THE ANCÓN GROUP FROM THE SEISMIC DATA (SANTA ELENA PENINSULA, ECUADOR)

Patricio A.MALONE(1), Fernando A. FANTIN(2), Eduardo A.ROSSELLO(3) and Muriel MILLER(4)

(1) Compañía General de Combustibles S.A., Alicia Moreau de Justo N° 400, 1° (1107) Buenos Aires. Email: patricio_malone@cgc.com.ar
(2) Compañía General de Combustibles S.A., Alicia Moreau de Justo N° 400, 1° (1107) Buenos Aires. Email: fernando_fantin@cgc.com.ar
(3) CONICET-Depto. Cs. Geológicas, Universidad de Buenos Aires. Pabellón II, Ciudad Universitaria. (1428), Buenos Aires. Argentina. Email: rossello@gl.fcen.uba.ar
(4) Compañía General de Combustibles S.A., Alicia Moreau de Justo N° 400, 1° (1107) Buenos Aires. Email: muriel_miller@cgc.com.ar

KEY WORDS: Stratigraphy, turbidites, fore-arc basin, Andes, Ecuador

INTRODUCTION

The Ancón Basin is located in the southwestern coastal area of Ecuador in a geologic unit denominated as Santa Elena uplift and has had a complex evolutionary history. Deep marine deposits, spans from the Cretaceous to the Lower Tertiary (Paleocene-Eocene), compose the sedimentary sequence. The coastal area of the southwest of Ecuador has been defined as an oceanic terrain (Jaillard *et al.*, 1995), accreted to the South-American plate in the Paleocene. The sedimentary record represents the development of successive fore-arc basins related with the deformation generated by the subduction of Nazca-Farallón Plate beneath the South-American Plate. Recent seismic surveys for oil prospecting acquired for **Compañía General de Combustibles S.A.** allows depict the structural and stratigraphic framework of the subsurface geology of Santa Elena Peninsula (Fig. 1). This current work shows new stratigraphic relationship between the different units of the Eocene sequence denominated Ancón Group.

GENERAL STRATIGRAPHY OF THE AREA

The stratigraphic sequence of Santa Elena's Peninsula is compound entirely by deep marine deposits. The age of the sequences ranges from the Upper Cretaceous to the Upper Eocene. The basement of Santa

Elena basin is conformed by oceanic floor (Piñón Fm) that includes basalt and andesitic lavas. A new Middle Jurassic (180 ± 11 Ma) K/Ar whole rock age has been given of this complex taken in basandesitic rocks from outcrops in Puerto Lucia, Santa Elena Peninsula. Thick Upper Cretaceous sequence overlays the Piñón Fm. composed by hemipelagic silts, tuff, volcanic breccias, turbidites and siliceous shales. This lithologic association has been denominate Cayo Fm that corresponds to an infill fore-arc sequence of a Cretaceous marginal basin and it would represent the erosion of a volcanic arc of islands (Chongón–Jama arc), present in the eastern and north-eastern area of the Santa Elena Peninsula.

Toward the west the facies change to a typical deep marine ones, composed by pelagic silts and shales with tuffs, radiolarites and chert, showing an intense tectonic deformation evidenced by imbricate faulting, folds and development of penetrative cleavages. This sequence has received the name of Santa Elena Fm (also called Carolina Cherts, Wildflysh, etc.) and its geotectonic setting would correspond to the accretionary prism. In the Paleocene the uplift and the consequent erosion of the volcanic arc of islands takes place, being developed a shelf-slope system tract and submarine basin floor fan that conform the sedimentary cycle of the Azúcar Fm. (see Fig 3a). These turbiditic fans systems are composed by mid to coarse turbiditic sandstones and conglomerates (upper to middle fan lobes facies) that constitute the main reservoir of the oil fields in the Peninsula de Santa Elena. These sequences include shaly sandstones and mudstones (overbank bank and slope apron facies). The stratigraphic thickness of the Azúcar Fm. is considered in approximately 3,000 m in the area of Ancón, diminishing toward the West and to the North. In the Early Eocene, a tectonic reactivation took place which determines unconformity at the top of Azúcar Fm. and the growth of the pre-Ancón Gr. structures and the formation of narrow slope basins that receive turbidites and debris flow deposits (Passage Beds and Clay Pebble Beds formations). These sequences present variable thickness (varies among 0 and 1,000 m), and show syntectonic sedimentation and Neogene reactivation (Fantin *et al.*, 1999). Continuous this cycle with the deposition of the Socorro Fm with laminate shales and fine turbidites corresponds to outer platform. Lastly the cycle culminates with shallow marine deposits (shales and silts) of the Seca Fm. deposits of the Punta Ancón and Zapotal formations.

ANCÓN GROUP STRATIGRAPHY

The silicoclastic sequence of Eocene age outcrops on the cliffs to the south of the Ancón Field. In the Ancón Field, this sequence unconformable overlay on the Azúcar Fm, while to the north lying upon Cretaceous rocks. This sequence has been classically subdivided in different units: Clay Pebble Beds, Socorro, Seca and Punta Ancón formations. Benítez (1995) includes Passage Beds Fm. in the lower section of the Ancón Gr. The sedimentary cycle of the Ancón Gr. begins with submarine lobes that filled elongated intra-slope basins (Underwood *et al.*, 1982) limited by reverse faults, product of compressive stress field due to the oblique convergence of the Nazca-Farallón plate below South-American Plate. This

turbiditic deposit has been denominated generically as Passage Beds (Marchant, 1956) in the subsurface in the oil field of Ancón. This beds shows quick lateral variation of thickness, losing it toward the structural highs of Azúcar Fm., which have controlled the sedimentary development of the Eocene sequence. In seismic sections (**BB´** type section, Fig. 1; location in Fig 3.b), two sequences can be defined and characterised by different seismic facies **A** and **B,** that they can be subdivided into two sub-sequences (see Fig. 1 and Fig. 2). The lower one ($\mathbf{A_1}$), deposited in the depocenters axis of the narrow slope basins (see Fig 3.b), overlying in unconformity to the top of Azúcar Fm., internally it does not exhibit continuous reflectors. This feature is interpreted as chaotic deposits, product of submarine debris flows, possibly associated to synsedimentary tectonic activity. This movements could be associated with latest activity of the Early Eocene tectonic phase, that cause the growth of the structures of the Azúcar Fm. Using the turbidites facies model of Walker & Mutti (1973) and Mutti & Ricchi-Lucchi (1975) this unit would be conformed by chaotic horizons (Type F) and pelitic-arenaceous turbidites (Type D). The upper sub-sequence ($\mathbf{A_2}$) overlays to the previous one in apparent paraconformity and laterally overlays in unconformity on the Azúcar Fm., being observed an on-lap relationship concerning previous structural highs of the Azúcar Fm on which are wedging. This height had worked as submarine ridges, which controlled the turbiditic sedimentation. Seismically it is characterised by the presence of sub-parallel continuous reflectors that constitute turbiditic cycles, which have been able to correlate with electric log in the sub-surface of the Ancón Field, where constitute a secondary reservoir. Lithologically are composed by cycles of arenaceous and pelitic-arenaceous turbidites (Type C and Type E). Occasionally, these cycles can be separated by thin mudstones units, interpreted to record of relative sediment stability in the source area. The unitary thickness of these cycles varies among 200 to 300 m and occasionally shows coarsening-up and thickening-up patterns in electrical logs. Toward the top of this sub-sequence, in the north area of the Ancón Field, an increase on the frequency and thickness of the sansdtones bodies can be noticed. This arenaceous turbidites, locally denominated Santo Tomás Sandstones (by the geologists of the former **AEO** Oil Company) constitute the secondary importance reservoir. It has been interpreted as amalgamated submarine channels deposits and they would determine the culmination of turbiditic Passage Beds's cycle with the participation of upper to middle channalized fan facies. Due to the active geotectonic setting of the youngest units of the Eocene sequence, that could directly trigger submarine slides and gravity flows, we can interpret that this turbidite system has been tectonically controlled. This reason can explain the quick change on thickness and lateral facies variation in Passage Bed. Therefore a vertical and lateral transition exists in Passage Beds between chaotic mudstones product of mass removal and classic turbiditic deposits. Over Passage Bed's sequence described above, the sedimentation continuous with the deposit of the Socorro-Seca-Punta Ancón cycles (**B**), with a progressive shallower sequence a progradant sequence can be observed which overlay on unconformity upon, partly on the Azúcar Fm., in the structural highs, and lay on the Passage Beds toward the basins depocenters. This sequence is divided in two sub-sequences, the lower one ($\mathbf{B_1}$) exhibits wedge geometry with sub-parallel very well defined

reflectors, which presents a down-lap relationship at the base. Lithologically is composed by pelitic turbidites, slope shales and mudstones (Type D and E). This succession was described as Socorro Fm and Seca Fm. Also in other sectors they can accompany chaotic deposits of submarine slides and debris flows that have been denominated as Clay Pebble Beds and they would correspond to slumps deposited at the base of the slope (Type F). Culminating the Eocene sedimentary cycle ($\mathbf{B_2}$) appears the shallow marine sub-sequence with wedge geometry that shows a divergent configuration of not very marked seismic reflectors.

After Late Eocene, a dextral transpressive tectonic regime deformed the Paleogene sequence and rotated clock-wise (Roperch *et al.*, 1987) reactivating older structures (see reverse faulting in Fig 1).

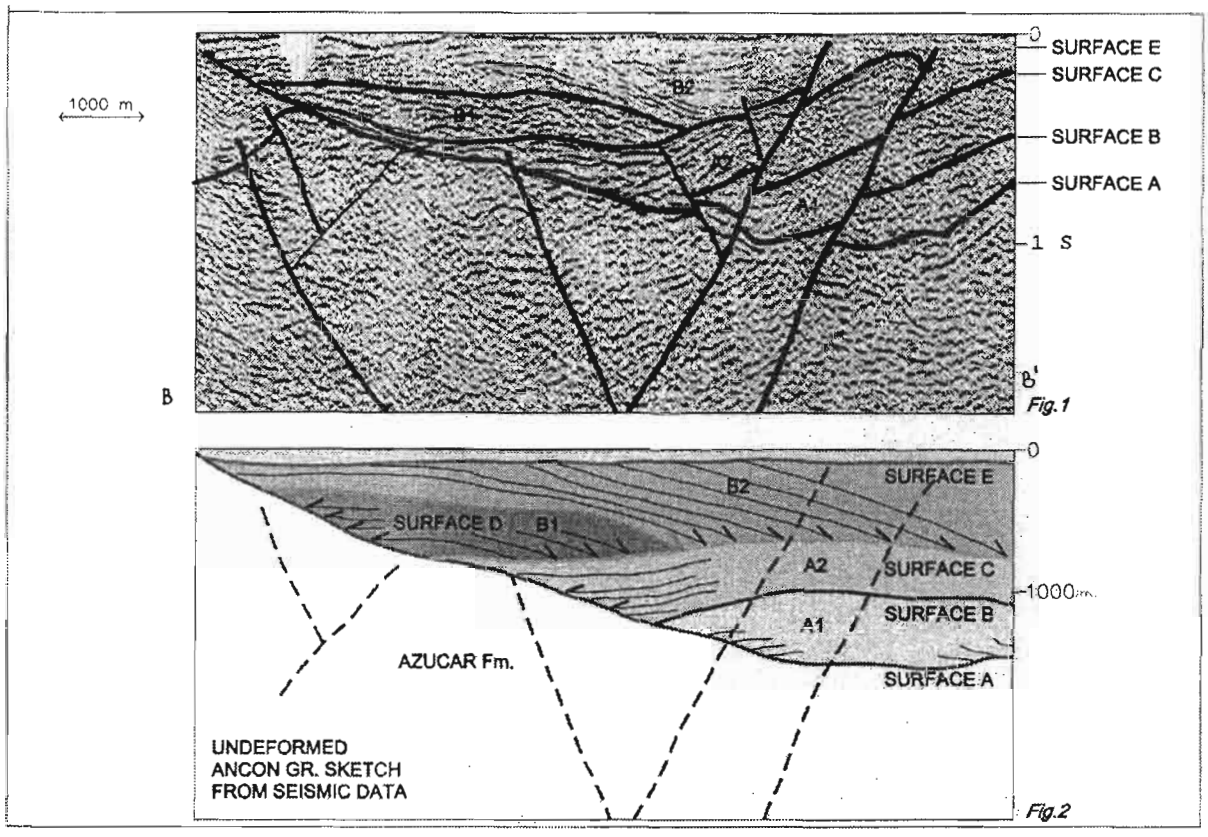

ACKNOWLEDGEMENTS

We acknowledge **Compañía General de Combustibles S.A.** for permitting the publication of this study. The INGEIS (Buenos Aires) has done the K/Ar datation.

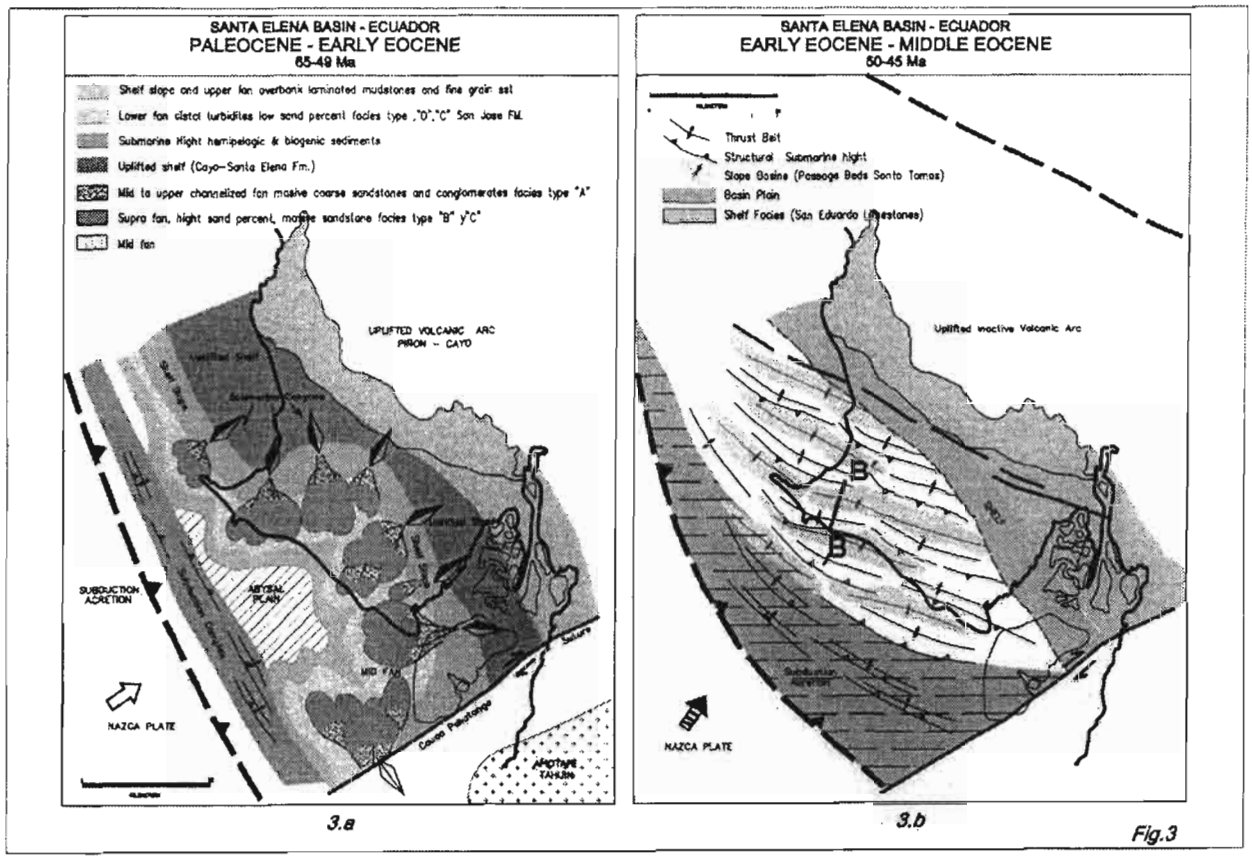

REFERENCES

Benítez, S.B., 1995. Evolution géodynamique de la Province cotière sud-Equatoriennc au Cretacé Supcrieur-Tertiaire. Thèse Doctorale. Université Grenoble (France), 221p.

Fantin, F.A., P. Malone, E.A. Rossello & M. Miller, 1999. The Neogene transpressional architecture of the Santa Elena peninsula, Ecuador: new insights from seismic data. *This volume*.

Jaillard, E., P. Soler, G. Carlier & T. Mourier, 1990. Geodynamic evolution of the northern and central Andes during early to middle Mesozoic times: a Tethyan model. Journal Geological Soc. London, 147, 1009-1022.

Jaillard, E., M. Ordóñez, S. Benítez, G. Berrones, N. Jiménez, G. Montenegro & I. Zambrano, 1995. Basin development in an accretionary, oceanic-floored fore-arc setting: southern coastal Ecuador during Late Cretaceous-Late Eocene Time. In Petrolcum basins of South America (Eds. A.J. Tankard, R. Suárez-Soruco & H.J. Welsink) American Association of Petroleum Geologists (Memoir 62), 615-631.

Marchant, S., 1961. A photogeological analysis of the structure of the western Guayas Province, Ecuador; with discussion of the stratigraphy and Tablazo formation. Q. Journal Geol. Soc. 117, 215-232.

Mutti, E. & Ricci-Lucci, F. 1975. Turbidites facies and facies association. 9th Int. Congress of Sedimentology, Nice.

Roperch, P. F. Megard, C. Laj, T. Mourier, T.M. Clube & C. Noblet, 1987. Rotated oceanic blocks in Western Ecuador. Geophysical Research Letters, 14 (5), 558-561.

Underwoood, M.B. & S.B. Bachman, 1982. Sedimentary facies associations within subduction complexes. In: Legget, J.K. (ed) Trench-forearc geology. Geological Society Special Publication 10, 537-550.

Walker, R. G. & Mutti, E. 1973. Turbidite facies and facies association. In: Turbidites and Deep Water Sedimentation. Pacific Sec., Short Course, Soc. Econ. Paleotol. Mineral. 119-58

PETROGRAPHY AND GEOCHEMISTRY OF THE DOÑA JUANA VOLCANIC COMPLEX SOUTHWESTERN COLOMBIA

MARÍN, M.(1), MOLINA, M.(1), ORDÓÑEZ,O.(2) and WEBER, M(1).

(1) Faculty of Mines, National University, Medellín-Colombia
(2) Geochronologic Laboratory, Geoscience Institute - University of Brasilia-Brasile-mail:mimarin@andromeda.unalmed.edu.co, ordonez@unb.br, wweber@epm.net.co

KEY WORDS: Colombia, Doña Juana volcano, Northern Volcanic Zone, geochemistry, subduction Nazca plate, active volcanism.

INTRODUCTION

The Doña Juana Volcanic Complex is located in southwestern Colombia figure 1, and is part of the southern Central Cordillera. It reaches 4250 m of altitude, at the exact coordinates of 1°28 ' N and 76° 55 ' W. This volcano comprises a 4 km wide caldera, which opens towards the northwest and the southwest. In this caldera lies a central 750 m high cone, with a crater of 500 m in diameter (Ramirez, 1982).

The Doña Juana volcano registered its last active period about 100 years ago, between 1897 and 1906. This activity was characterized by the formation of a dome in the central part of the crater, accompanied by base-surge deposits, pyroclastic flows and mudflows, associated strong seismic activity (Ramírez,1982; Méndez,1989).

TECTONIC SETTING AND REGIONAL GEOLOGY

The active volcanism within the Andes is divided into three zones (Thorpe *et al.*, 1982), a Northern Volcanic Zone (NVZ), a Central Volcanic Zone (CVZ), and Southern Volcanic Zone (SVZ). Although there exits a considerable amount of information about the SVZ and CVZ, little is known about the processes and magma formation of the NVZ, especially in Colombia.

The recent volcanism in the Colombian Andes is part of the Northern Volcanic Zone (NVZ), characterized by the collision of the South American, Nazca and Caribbean plates and the Panamá block. The subduction of the Nazca oceanic plate beneath the Andes generates the magmas that form the volcanic complexes and cenozoic intrusions of the Central and Western Cordilleras and Cauca-Patía graben of Colombia. According to Aspden *et al.*(1987) the current activity is probably the continuity of the magmatic event that generated the volcanism of the Miocene-Pliocene, registered in the Colombian Andes. The recent magmatism of the Northern Andes is mainly of explosive type, with its largest expression represented by more than 55 volcanoes (ca. 15 are considered active). These are located roughly at a horizontal distance of 200 Km from the Colombia-Ecuador-trench, where the oceanic Nazca plate is subducted beneath the South America plate. The quaternary volcanoes of Colombia are associated to distention zones of the Romeral faults system (Cepeda, 1987). The petrography and geochemistry of these Colombian volcanic rocks indicate an active calc-alkaline volcanism.

The Doña Juana volcanic complex is located in the Central Cordillera, which is made up of Precambrian-Paleozoic metamorphic and igneous crystaline basement, that comprises gneisses, schists and phyllites (Arango and Ponce, 1982). The complex is bordered to the west by the Romeral faults system, which separates rocks of continental affinity to the east from rocks of oceanic affinity to the west.

Here we present new geochemical and Sr-Nd isotopic data determined for representative samples of the Doña Juana volcanic complex. The aim is to characterize the magma that forms this volcano, as well as to compare these results with those available from other volcanoes in the NVZ.

GEOCHEMISTRY AND ISOTOPE ANALYSES

Whole-rock geochemical (major and trace elements and REE) and isotopic (Sr-Nd) data of lavas representative of the volcanic complex were obtained at the Institute of Geosciences of the University of Brasilia.

Major and trace Elements and REE

The Doña Juana volcanic rock data presented here falls within of the traqui-andesite range, with variations to dacite and andesite, according to the chemical classification and nomenclature of volcanic rocks of the diagram TAS (Le Bas *et al.*, 1986).

Figure 2 shows the sub-alkaline trend of the Doña Juana volcanic complex rocks (Gill, 1981). The analyzed samples show a SiO_2 variation between 60.5 and 65.23 for the central cone and 60.5.2 and 64.17 towards the north near the town of La Cruz, and an alkalis (Na2O+K2O) variation between 6.26 and 7.98, showing a calc-alkaline character for these rocks, characteristic of an active continental margin. Figure 3 shows a typical trend for NVZ calc-alkaline rocks with a characteristic LREE-enrichment in the Doña Juana volcanic evolution. This trend is constant except for sample DJ-14, which is less enriched in REE compared to the other samples.

Isotope geochemistry

The $^{87}Sr/^{86}Sr$ ratios (0.7041 to 0.7045) obtained in this study fall within the NVZ volcanics rocks ratios ($^{87}Sr/^{86}Sr$ <0.7055; Marriner and Millward 1984, Francis *et al.* 1977), and are certainly different from those known from the north of Chile and south of Peru which show $^{87}Sr/^{86}Sr$ ratios between 0.7055 to 0.7072 (e.g., Francis *et al.* 1977; Thorpe *et al.* 1982).

The $^{143}Nd/^{144}Nd$ ratios are high and show little variation (0.51275 to 0.51281). The positive ε_{Nd} values (figure 4) suggest a depleted source for the magmas of the volcanic complex. The Sr-Nd isotopes indicate the dominance of a mantle source for these magmas, although assimilation and contamination with crustal rocks is probable, which is suggested by preliminary T_{DM} values. These indicate contamination of a Paleozoic basement.

REFERENCES

- ARANGO, J & PONCE, A., 1982. Mapa geológico del departamento de Nariño y memorias, Ingeominas, Bogotá.
- ASPEN, J. A. & McCOURT, W. J. & BROOK, M., 1987. Geometrical control of subduction –related magmatism: the Mesozoic and Cenozoic plutonic history of western Colombia. Journal of the Geological Society, London, 144, 893-905.
- CEPEDA, H., 1987. Vulcanismo moderno en los Andes de Colombia. Informe IR-53. Ingeominas, Medellín.
- EVENSEN, N. M.; HAMILTON, P. J. & O'NIONS, R. K., 1978. Rare-earths abundances in chondritic meteorites. Geochimica et Cosmochimica acta, 42: 1199-1212.
- FRANCIS, P. W., MOORBATH, S. & THORPE, R. S., 1977. Strontium isotope data for Recent andesites in Ecuador and North Chile. Earth and Planetarry Science Letters, 37, 197-202
- LE BAS, M. J.; LE MAITRE, R. W.; STRECKEISEN, A.; ZANETTIN, B., 1986. A Chemical classification of volcanic rocks based on the total Alkali-Silica diagram. Journal of Petrology, 27(3): 745-750.
- MARRINER, G. F. & MILLWARD, D., 1984. The petrology and geochemistry of Cretaceous recent volcanism in Colombia: The magmatic history of an accretionary plate margin. Journal of the Geological Society, London, 141, 473-486.
- MÉNDEZ, R.A., 1989. Catálogo de los volcanes activos de Colombia. Bol. Geol. V30, No. 3, Ingeominas, Bogotá, 75 p.
- RAMIREZ, C., 1982. El Vulcanismo neogénico y cuaternario en Colombia: Cronología y Caracterización químico-petrográfico, unpublished Bsc thesis, Universidad Nacional de Colombia, Bogotá.
- RAMIREZ, J., 1975. Historia de los terremotos en Colombia; IGAC, Bogotá, 250 p.
- STEIMLE, U., 1989. The Doña Juana volcano, Departamento de Nariño, Southern Colombia, unpublished Bsc thesis, Eberhard Karls Universität, Tübingen, 92 p.
- THORPE, R. S., FRANCIS, P. W & L. O'CALLAGHAN, 1984 Relative source composition, fractional crystallisation and crustal contamination in the petrogesis of Andean volcanic rocks. Phil. Trans. R. Soc. Lond. A310, 675-92.

QUATERNARY BRITTLE DEFORMATION IN THE CALDERA AREA, NORTHERN CHILE (27°S)

Carlos MARQUARDT(1) and Alain LAVENU(2)

(1) SERNAGEOMIN Chile, Av. Santa María 0104, Santiago (cmarquar@sernageomin.cl)
(2) IRD, casilla 53 390, correo central, Santiago1, Chile (alavenu@dgf.uchile.cl)

KEY WORDS: Neotectonics, extensional deformation, uplift, marine terrace.

INTRODUCTION

Even though evidence of young brittle deformation is well preserved in several localities of the coastal belt south of Caldera (27°-27°15'S), the only reference available regarding faulting in the area is found in Mortimer (1969), who describes a Neogene reverse fault followed by normal reactivation SE of Morro Copiapó (figure 1). Deformation is characterised by variously oriented high angle normal faults. They show centimeter to meter long displacements in sedimentary layers associated to Quaternary marine terraces and, occasionaly, originate scarps that may be well distinguished from marine cliffs.

We thus infer the normal faults present in the southern part of the area based on the fact that they cut old beach-ridges and other shorelines, specially those more oblique to the fault traces. A second criterium we have applied considers the fact that, in contrast to marine cliffs, the base of fault scarps shows a variable elevation, refered to sea-level.

Two case studies have been selected in order to better describe the geometry, kinematics and age of these faults : the Calderilla and Bahía Inglesa localities.

CALDERILLA

One N10°E and three N60°E trending normal faults outcrop in the area between Caldera and Bahía Inglesa. Fault planes are well exposed only in the major one from the second set, whose base scarp varies from sea level up to 45 m above it. In figure 2 we describe the following three profiles, located in figure 1, along this fault :

Profile A.- two normal faults are exposed at a elevation of 9 m, one km inland northeast from Bahía Inglesa. They offset both the base of the sedimentary cover and erosional unconformities within littoral and continental unconsolidated sediments with an age range from Neogene to Quaternary. These N72°E/66°N and N81°E/64°N trending faults suggest an hemigraben related to NNW-SSE extension. The small western antithetic normal fault in the hanging wall may reflect minor rigid block rotation.

Deformation took place after deposition of the sedimentary cover, whose age is given by that of the marine terrace (Qm), formed at 125 kyr (Marquardt *et al.*, 1999).

Profile B.- a branched normal fault that crops out at 13 m a.s.l. displaces at least 3 m the base of the Quaternary shallow marine sediments (outside from figure 2B). The fault seems to be sealed by eolian and aluvial deposits, yet the development of a superficial scarp favours their involvement in the deformation.

The NE-SW trend of this fault suggests a NW-SE extensional deformation. As shown in the same figure, 10 m southeast of this structure a set of four small reverse faults may be related to footwall rigid rotation.

Profile C.- 2.5 km northeast of the previous profile and 10 m southeast from the main fault trace (figure 2C); we recognise two secondary SE dipping normal faults. A small NW dipping reverse fault is associated to one of them. Because no scarp is preserved in the loose overlying sands, faulting seems to have displaced only the marine deposits, assigned here to the 220 kyr (I.S. 7) marine high stand. Their offset is less than a meter and their trend once more suggests a NW-SE extensional deformation.

Age of deformation may here be somewhat older than in profile 2A, considering the age assigned to the only markers clearly displaced.

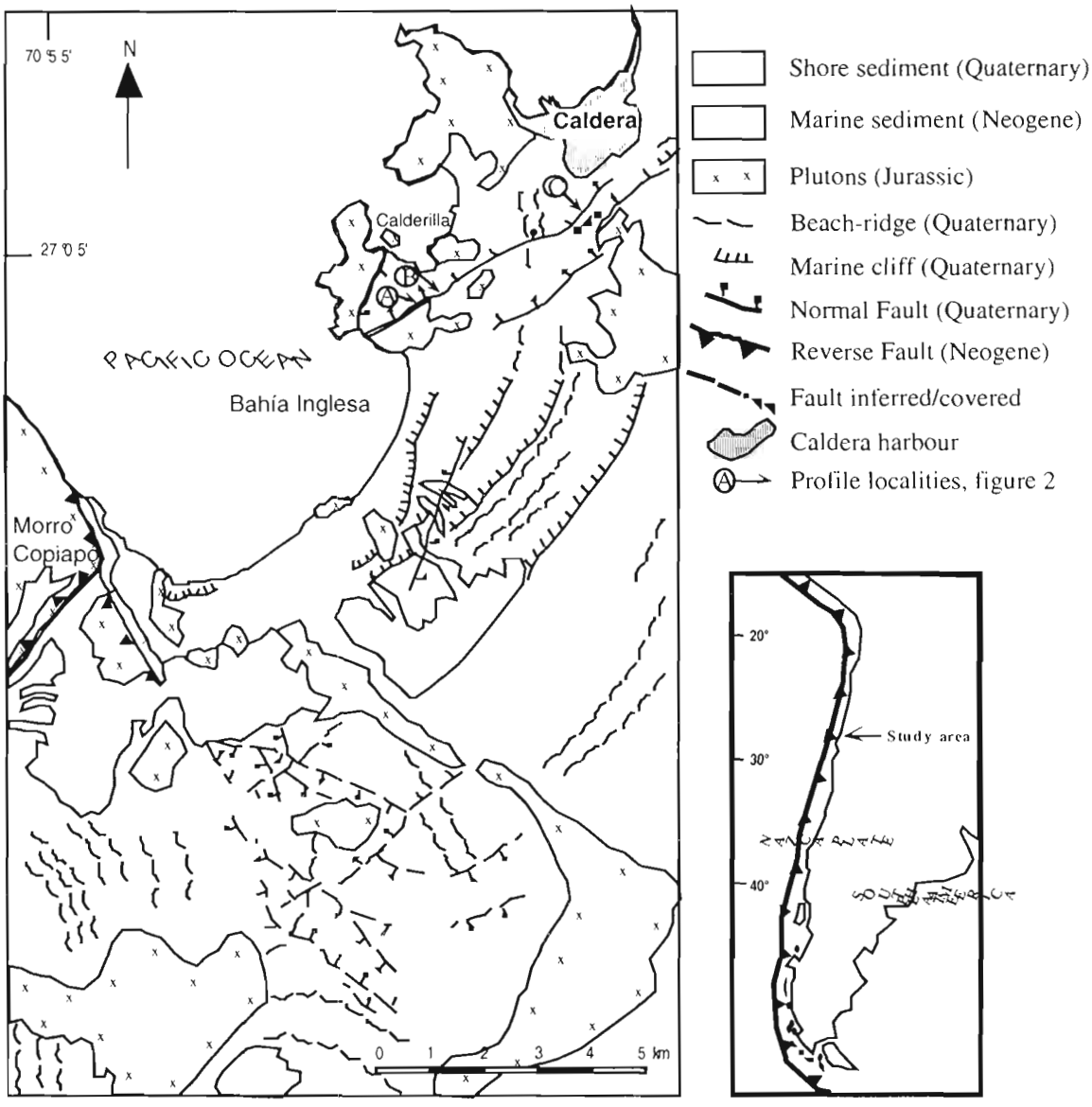

Figure 1.- Geologic sketch map showing the main structure of the coastal south Caldera harbour.

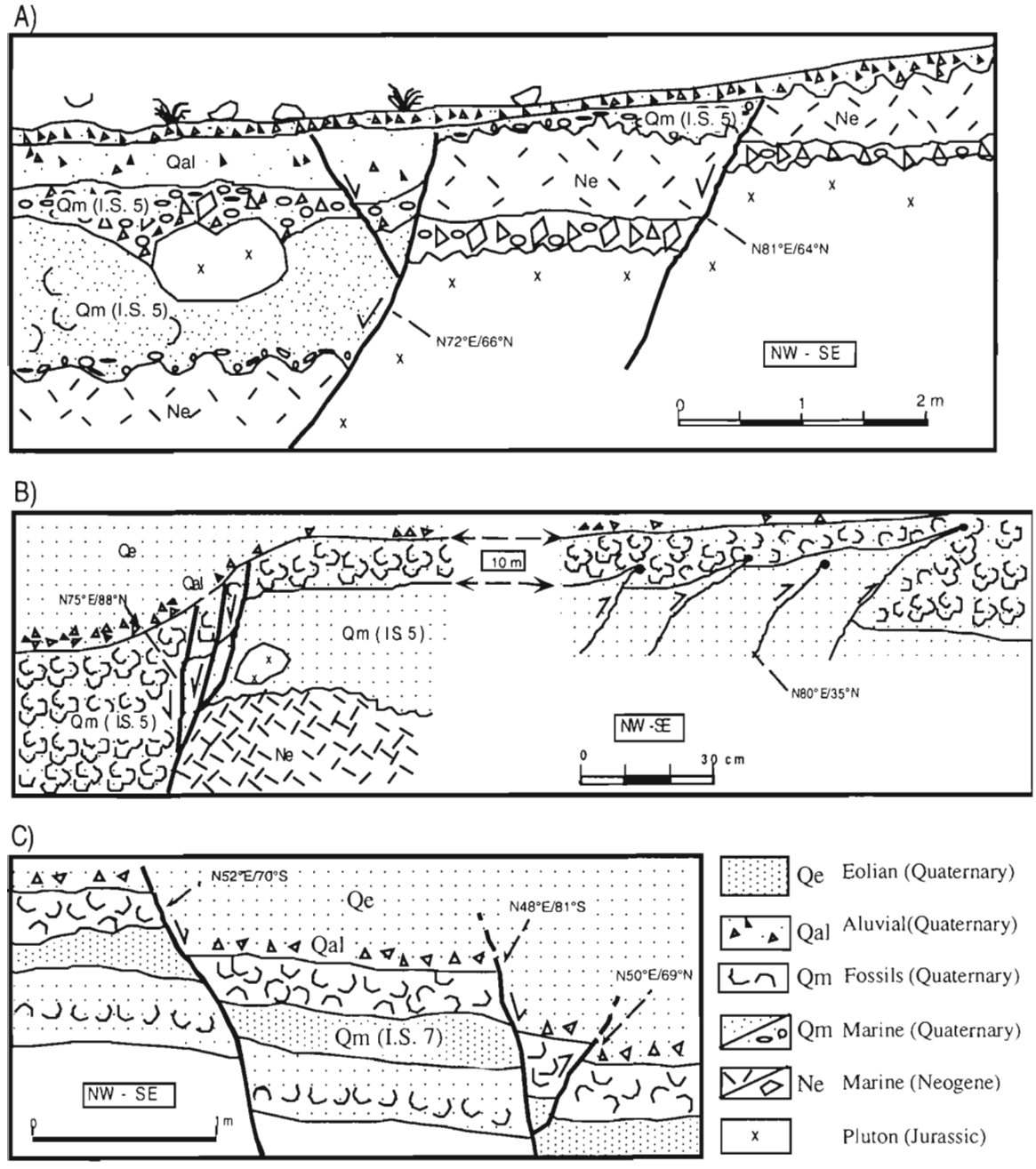

Figure 2.- Profile along the same normal fault scarp, inland Calderilla.

BAHIA INGLESA

A NNE-SSW trending normal fault scarp, subparallel to a marine cliff whose base lies at 30 m a.s.l., develops 2 km east of Bahía Inglesa.

The fault scarp faces westward in its northern half and eastward in the southern one, showing that the structure corresponds to a scissor fault (figure 3). A small graben is developed westward of the northern section. Vertical offsets range from 4 m down to half a meter in the vertical dipping central zone. A WNW-ESE extensional deformation, younger than 125 kyr (age of the displaced marine sediments) may be infered for this structure.

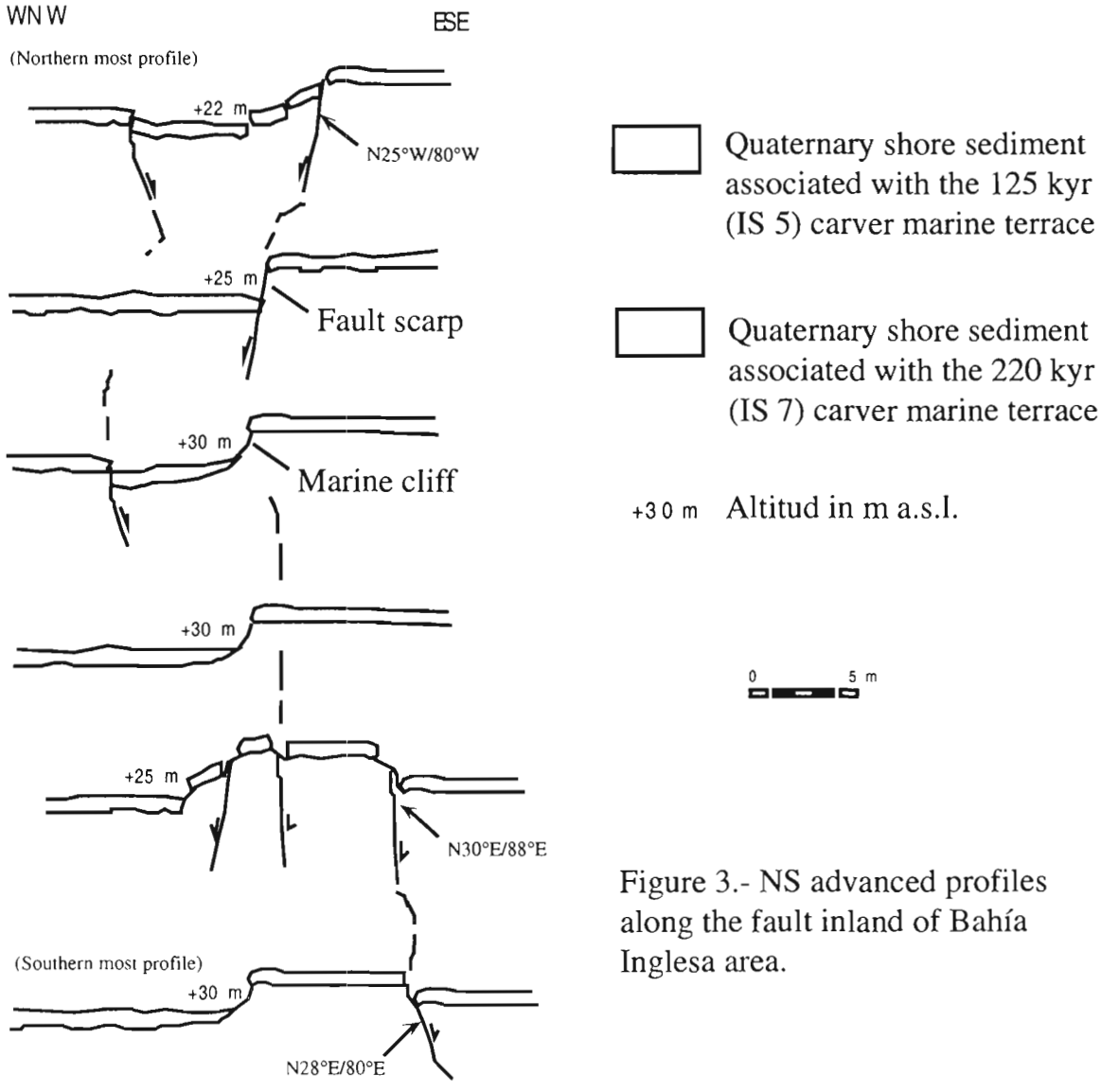

Figure 3.- NS advanced profiles along the fault inland of Bahía Inglesa area.

CONCLUSIONS

In the coastal belt between 27° and 28°S evidence of neotectonic activity is recorded by :

- Quaternary marine terraces uplifted at various heights under 200 m a.s.l.
- brittle deformation found in the terrace sediments close to Caldera (27°00' to 27°15' S).

The brittle deformation is recorded by probably coseismic normal faults that may be related to reactivation of preexistent structures. Based on their trend and the age of the sediments involved in the deformation, we propose that extensional deformation took place after 220 kyr
(most likely after 125 kyr), with a WNW-ESE to NNW -SSE trend. Extension may have resulted from uplift and trenchward migration of the coast.

The "major" faults show a maximum vertical displacement of 4 m. Normal and reverse cm scale faults, associated to rigid block rotation, are recognized in both their foot and hanging walls.

ACKNOWLEDGEMENTS

This study was supported by the chilean Servicio Nacional de Geología y Minería, as a part of its "Geological Mapping of the Atacama Fault System and Coastal Belt between 26° and 28°S", a project carried out with Estanislao Godoy , to whom we acknowledge his help in both field work and discussion of the text.

REFERENCES

Marquardt, C., Ortlieb, L., Guzmán, N. and Lavenu, A., 1999. Recent Vertical Motions and Quaternary Marine Terraces in the Caldera Area. (This Simposium).

Mortimer, C., 1969. The Geomorphological Evolution of the Southern Atacama Desert, Chile. A thesis submitted to the University of London for the Degree of Philosophy. Departament of Geology, University College London.

RECENT VERTICAL MOTION AND QUATERNARY MARINE TERRACES IN THE CALDERA AREA, NORTHERN CHILE (27°S)

Carlos MARQUARDT(1), Luc ORTLIEB(2), Alain LAVENU(3), Nury GUZMAN(4)

(1) SERNAGEOMIN Chile, Av. Santa María 0104, Santiago (cmarquar@sernageomin.cl)
(2) IRD, 32 Avenue Henri Varagnat, F-93143 Bondy-Cédex, France (Luc.Ortlieb@bondy.ird.fr)
(3) IRD, casilla 53 390, correo central, Santiago 1, Chile (alavenu@dgf.uchile.cl)
(4) FAREMAR, Univ. de Antofagasta, casilla 170, Antofagasta, Chile (nuryguzman@yahoo.com)

KEY WORDS: Neotectonics, forearc, marine terraces, uplift, Quaternary, Chile.

INTRODUCTION

The main sequence of marine abrasion terraces along the coastal belt of northern Chile, between 27°-28°S, was carved during the last million year or so. Detailed mapping and a morphostratigraphic study of these marine terraces provide new data for assessing the style and rates of Quaternary deformation. In a second contribution within this symposium Marquardt and Lavenu (1999) discuss the recent brittle deformation registered by the area, and emphasize its extensional character.

THE COASTAL BELT IN THE CONTEXT OF THE CENTRAL ANDES

In the Caldera area (27°-28°S), the coastal belt is a narrow portion of land, 1 to 3 km wide, located between the coastline and the Coastal Cordillera (figure 1). It represents the westernmost emerged forearc morphostucture of the Central Andes and includes a sequence of marine terraces preserved up to an altitude of about 300 m a.s.l.

With respect to the morphostructure of the Norte Grande, fully developede at the latitud of Antofagasta (23°S), the Norte Chico shows some differences (figure 1): (a) the coastal belt reaches a much larger width (up to 15 km) than to the north; (b) the Coastal Scarp (which limits the coastal belt from the Coastal Cordillera north of 30°S) of the Norte Grande is replaced by a gently sloping surface covered by aluvial and eolian sedimentary deposits; (c) a transitional zone between the northern intermediate depression and the transversal valleys develops towards the east; and (d) the mesozoic backarc basin rocks and the Puna plateau disappear southward. At the latitude of the study area there is a

transitional zone between the inclined subduction segment to the north and the subhorizontal subduction segment to the south, without active volcanism betwen 28° and 33°S.

ELEVATION, INFERRED AGE AND LATERAL CORRELATION OF THE MARINE TERRACES

The best preserved marine terraces are located up to an altitude of ~250 m a.s.l. The terraces with associated Pleistocene marine deposits are preserved at ~200 m a.s.l. and they are identified mainly by *Argopecten purpuratus* and *Concholepas concholepas*. Over 200 m a.s.l. and up to ~350 m., coastal marine deposits, assigned to Pliocene because of the presence of *Chamys* spp., *Ostreas* spp. and other extinct species, do not correspond to marine terraces deposits s.s. but rather to basin margin sediment (Herm, 1969).

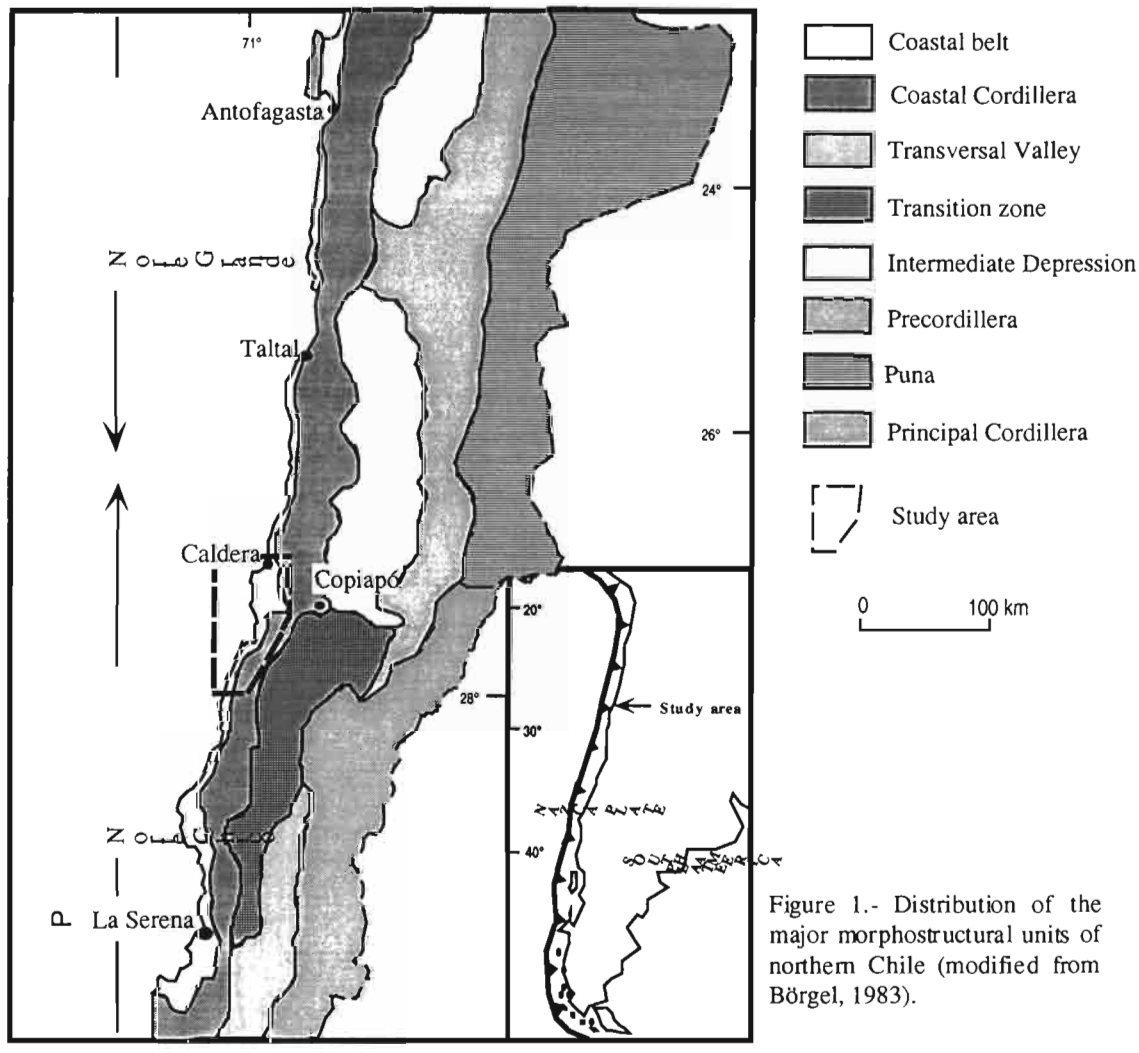

Figure 1.- Distribution of the major morphostructural units of northern Chile (modified from Börgel, 1983).

Based on our morphostratigraphic analisis of the Quaternary marine terraces sequences, we propose the Caldera succession as the type sequence (figure 2). East of Caldera, the altitudes reached by the maximum of the transgression responsible for each marine terrace average +3, +25, +44, +110, +162 and +200 m a.s.l. These altimetric values have an instrumental error of ±5 m and a possible error of about ±10 m in the evaluation of the position of the trace of the transgression maximun.

Age estimation of the terraces is based on : (a) A few geochronological results in the vicinity of Caldera (Radtke, 1987; Leonard, 1994). (b) The hypotesis that warm water mollusc (such as *Donax peruvianus* and *Trachycardium procerum*) may be assigned to a warmer interglacial stage (isotopic stage, i.s., 11) at about 430 kyr (Ortlieb *et al.*,1995; 1996b; 1997). (c) Lateral and vertical correlations between the traces of the successive transgressions corresponding to the Middle and Late Pleistocene sea level variations, as they area known worldwide.

Consequently the age estimations proposed for our type sequence are deduced from that of the last major Quaternary highstands of sea level : ~6 (middle Holocene), ~100 (isotopic substage 5c?), ~125 kyr (i.s. 5e), ~210 (i.s. 7), ~330 (i.s. 9) and ~430 kyr (i.s. 11) (figure 2). By geologycal mapping and lateral correlations, we inferred the chronostratigraphical "age" of the other remnants of the terraces in the southern part of the study area (figure 3).

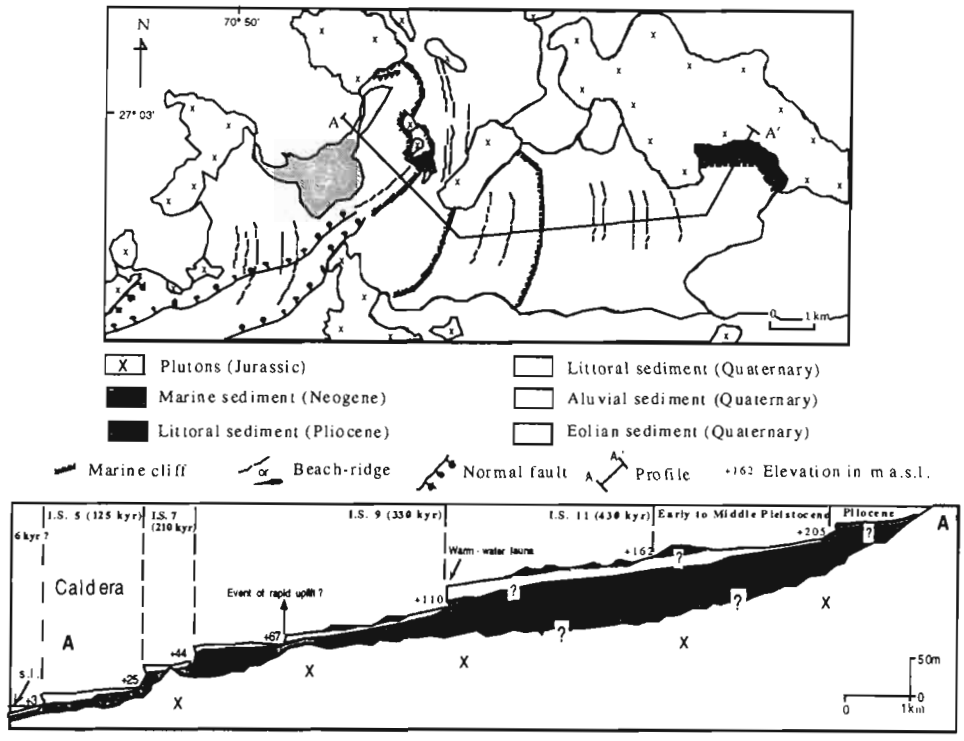

Figure 2. Marine terraces and associated deposits in the Caldera area.

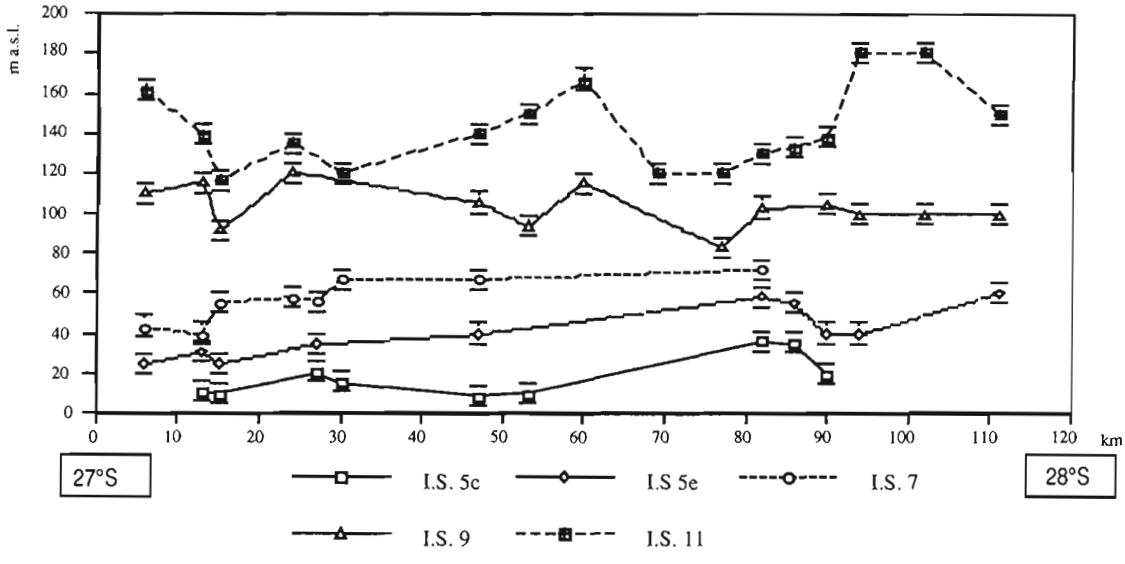

Figure 3.- Vertical and lateral distribution of the remmants of the transgressive maxima of the Middle and Late marine terraces in the Caldera area. Elevations are in m a.s.l.. Age estimation for each terrace should be considered as hypothetical (see text).

CONCLUSIONS

The hypothetical ages of the terraces, mainly deduced from geometrical considerations and from assumptions regarding the faunal composition of 430 ka deposits, lead us to estimate local and regional uplift rates for the last half-million years. The whole set of data obtained in the Caldera area thus suggest that the uplift rates varied in the range of 0.4 to 0.2 m/ky during the last 0.5 My. In a similar way than what was done in Baja California (Ortlieb, 1991) or in California (Hanson *et al.*, 1994), an elevation vs. inferred age plot (figure 3) shows important deformation patterns. The uplift rates varied through time and within the study area, even if part of the observed lack of parallelism between the inferred correlation lines (figure 3) may be attributed to local faulting activity (see Marquardt & Lavenu, 1999).

The Caldera area was submitted to uplift motions which compare with those determined in the Hornitos-Mejillones area (23°S), and are much higher than those calculated for the southeastern rim of the Antofagasta bay (Ortlieb et al., 1995, 1996a, 1997).

ACKNOWLEDGEMENT

This study was supported by the Chilean Servicio Nacional de Geología y Minería, as a part of its "Geological Mapping of the Atacama Fault System and Coastal Belt between 26° and 28°S", a project supervised by Estanislao Godoy. We thank E. Godoy for his help in the field and in the preparation of this work.

REFERENCES

Börgel R. 1983. Geografía de Chile, Tomo II: Geomorfología. Instituto Geográfico Militar.

Hanson K., Wesling J., Lettis W., Kelson K., Mezger L. 1994. Correlation, ages, and uplif rates of Quaternary marine terraces: South-central coastal California.I.B. Alterman, R.B. McMullen, L.S. Cluff andD.B. Slemmons(eds.). Seismotectonics of the Central California Coast Range: Boulder, Colorado, Geological Society of America, Special Paper 292, 45-71.

Herm D. 1969. Marines Pliozän und Pleistozän in Nord und Mittel Chile unter besonderen Berücksichtigung der Entwicklung der Mollusken-Faunen. Zitteliana (München), 2, 1-159.

Leonard E.M., Muhs D.R., Ludwig K.R., Wehmiller J.F. 1994. Coral Uranium-series ages and mollusc amino-acid ratios from uplifted marine terrace deposits, Morro de Copiapó, north-central Chile. AMQUA (American Quaternary Association Program and Abstracts), 13th Biennal Meeting, 223.

Marquardt C., Lavenu A. 1999. Quaternary Brittle Deformation in the Caldera Area, Norther Chile (27°S). (This simposium)

Ortlieb L. 1991. Quaternary vertical movements along the coasts of Baja California and Sonora. In: The Gulf and Peninsular province of the Californias, J.P. Dauphin & B.R.T. Simoneit (eds.), Amer. Assoc. Petrol. Geol. Mem. 47: 447-480.

Ortlieb L. in coll. with Goy J.L., Zazo C., Hillaire-Marcel Cl., Vargas G. 1995. Late Quaternary Coastal Changes in Northern Chile. Guidebook for a fieldtrip, II annual meeting of the International Geological Correlation Program, Project 367 (Antofagasta-Iquique, 23-25 nov. 1995). ORSTOM, Antofagasta, 175 pp.

Ortlieb L., Zazo C., Goy J.L., Hillaire-Marcel C., Ghaleb B. & Cournoyer L. 1996a. Coastal deformation and sea level changes in northern Chile subduction area (23°S) during the last 330 ky. Quatern. Sci. Rev., 15: 819-831.

Ortlieb L., Díaz A. & Guzmán N. 1996b. A warm interglacial episode during oxygen isotope stage 11 in Northern Chile. Quatern. Sci. Rev., 15: 857-871.

Ortlieb L., Guzman N., Marquardt C., Vargas G. 1997. El Cuaternario marino del norte de Chile: revisiones cronológicas e identificación posible de depósitos de 400 ka. VII Congreso Geológico Chileno, vol. 1, 371 - 375.

Radtke, U., 1989. Marine Terrassen und Korallenriffe. Das Problem der Quartären Meeresspiegelschwankungen erläutert an Fallstudien aus Chile, Argentinien und Barbados. Düsseldorfer geographische Schriften, Heft 27, 245p.

THE CENTRAL ATLANTIC CONTINENTAL FLOOD BASALT PROVINCE, AND POSSIBLE RELATIONSHIP WITH TRIASSIC-JURASSIC MAGMATISM IN THE ANDES

Andrea Marzoli (1), Paul R. Renne (2), Enzo M. Piccirillo (3), Marcia Ernesto (4)

(1) Departement de Mineralogie, rue des Maraichers 13, 1211 Genève, Switzerland (Andrea.Marzoli@terre.unige.ch)

(2) Berkeley Geochronology Center, 2455 Ridge Road, Berkeley, 94709 CA, USA (prenne@bgc.org)

(3) Dipartimento di Scienze della Terra, Universitá di Trieste, via Weiss 8, 34127 Trieste, Italy (picciril@univ.trieste.it)

(4) Instituto Astronômico e Geofísico, Universidade de São Paulo, C.P. 9638, 0165-970 São Paulo, Brazil (marcia@iag.usp.br)

Keywords: Continental Flood Basalts; Mantle Plume; Triassic-Jurassic; Geodynamics.

The Central Atlantic Magmatic Province (CAMP) is defined by dikes, sills and rarely preserved lava flows of low-TiO_2 tholeiitic basalt that occur in once-contiguous parts of North America, Europe, Africa, and South America (Fig. 1). Poor outcrops, weathering, subsequent continental dispersal, and a paucity of reliable geochronologic data have hindered recognition of the spatial and temporal patterns of CAMP magmatism. New $^{40}Ar/^{39}Ar$ and U/Pb ages, and paleomagnetic data from Africa, North and South America (e.g., Sebai et al., 1991; Deckart et al., 1997; Marzoli et al., 1999), indicate that in those continents the magmatism occurred over a narrow time interval with peak activity at 200 Ma over an area of at least 6 million km^2 producing ca. 2-3 million km^3 of basaltic lavas. Such a brief duration and large aerial extent is

similar to those of other CFB provinces, such as the Siberian traps and the Paranà. As with other CFB provinces, CAMP is associated with continental break-up (i.e., the disruption of Pangaea), ocean-formation (i.e., the opening of the central Atlantic Ocean; Withjack et al., 1998), and with a mass extinction event (i.e., the Triassic-Jurassic boundary).

New $^{40}Ar/^{39}Ar$ data presented herein extend the CAMP much farther south and west in South America than has been previously recognised and firmly establish this province as the largest CFBP known on Earth. According to previous K/Ar dating, Late Jurassic to Cretaceous high-TiO_2 (HTi) tholeiitic basalts (e.g. Sardinha and Ceará-Mirím dyke swarms) are restricted to the Atlantic margin in Eastern Brazil, and may be related to the opening of the South Atlantic, while a belt extending from the Mato Grosso region to the Amazonian and Parnaiba basins in Central and Northern Brazil, respectively, is dominated by Low-TiO_2 (LTi) tholeiitic basalts of mainly Jurassic age. These LTi tholeiites affect Archean-Early Proterozoic cratonic (e.g. Guyana and Amazonia cratons) areas and Late Proterozoic to Phanerozoic basins (e.g. Maranhão basin). Dike and sill intrusions are strongly prevalent in the cratonic crustal settings, while lava flows are mostly preserved in the younger basins. Jurassic LTi rocks from Brazil have similar compositions to CAMP magmatic rocks from N-America and W-Africa, and have generally relative variable trace element and Sr-Nd isotopic compositions. For example ε_{Sr} ranges from -18 to +179 and ε_{Nd} ranges from +6 to - 6, suggesting contributions of heterogeneous sources in the petrogenesis of these rocks.

We dated fresh LTi tholeiitic dikes, sills and lava flows from the Amazonian, Roraima, Maranhão, Amapa, Ceara and Anari and Tapirapuã regions of North and Central Brazil via $^{40}Ar/^{39}Ar$ incremental heating with a resistance furnace and Ar-ion laser using analytical procedures described elsewhere. Ages were calculated relative to an age of 28.02 Ma for the Fish Canyon sanidine (FCs) neutron fluence monitor.

The new $^{40}Ar/^{39}Ar$ data allow definition of an Earliest Jurassic (191- 203 Ma) LTi tholeiitic province extending from central Brazil to northern Brazil. All available radioisotopic dates for the CAMP plot between 191 and 205 Ma, with a mean value of 199.1 ± 1.7 Ma, and the peak at 200 Ma. The available data clearly show that tholeiitic dikes, sills and lava flows from Brazil are similar in age to those of the CAMP in Africa and North America. Therefore, considering geochemical and geochronological data, it is clear that the CAMP includes the widespread Triassic-Jurassic magmatism in Brazil and had a total extension of ca. 6000 by 3000 km. Moreover, the geochronological data suggest that this widespread magmatism was produced in a relatively short time interval with a peak at ca. 200 Ma. Similarly widespread and short-lived tholeiitic magmatism characterises other well-studied continental flood basalts provinces.

Extension of the CAMP magmatism to a much larger portion of South America than previously recognised, and the evidence of a brief, widespread and intense magmatic event, has several important

geodynamic implications. It may be suggested, for example, that widespread plume-related magmatism in north-eastern South America and the associated continental extension and break-up may have increased eastward subduction of the Pacific oceanic plate under the western margin of the South American (Guyana shield). This may then have triggered the Triassic-Jurassic magmatism along the convergent margin from Colombia to Ecuador, Chile and Patagonia at ca. 200 Ma (Jaillard et al., 1990; Pankhurst, 1990; Parada, 1990; Aspden et al., 1992; Dörr et al., 1995).

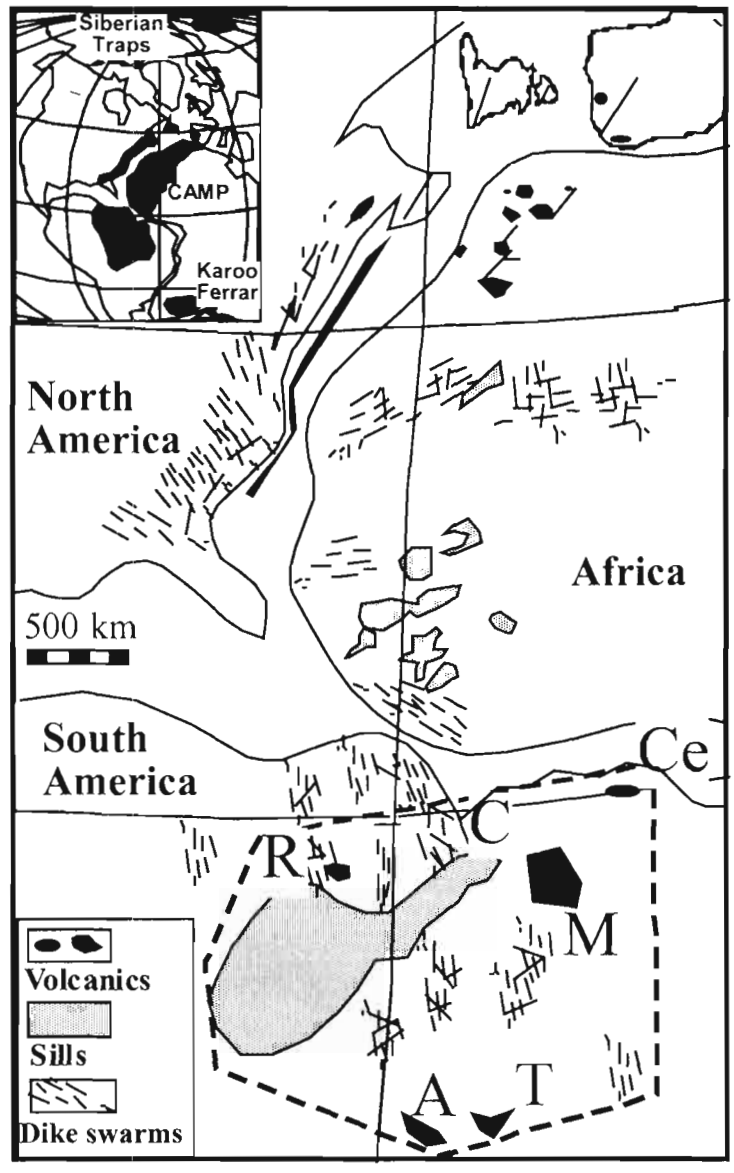

Fig. 1: Sketch map of CAMP in a Pangaea reconstruction at ca. 200 Ma ago.

References

Aspden J. A. and Litherland M. 1992. The geology and Mesozoic collisional history of the Cordillera Real, Ecuador. Tectonophys, 205, 187-204.

Deckart K., Féraud G. and Bertrand H. 1997. Age of Jurassic tholeiites of French Guyana, Surinam and Guinea: implications for the initial opening of the Central Atlantic ocean. Earth Planet. Sci. Lett., 150, 205-220.

Dörr W., Grösser J. R. Rodriguez G. I. and Kramm U. 1995. Zircon U-Pb age of the Paramo Rico tonalite-granodiorite, Santander Massif (Cordillera Oriental, Colombia) and its geotectonic significance. J. S. Am. Earth. Sc., 8, 187-194.

Jaillard E., Soler P., Carlier G. and Mourier T. 1990. Geodynamic evolution of the northern and central Andes during early to middle Mesozoic times: a Thethyan model. J. Geol. Soc. L., 147, 1009-1022.

Marzoli A., Renne P. R., Piccirillo E. M., Ernesto M., Bellieni G. and De Min A. 1999. Extensive 200-Million-Year-old Continental Flood Basalts of the Central Atlantic Magmatic Province. Science, in press.

Pankhurst R. J. 1990. The Paleozoic and Andean magmatic arcs of West Antarctica and southern South America. In: Plutonism from Antarctica to Alaska (Kay, S. M., and Rapela, C. W., eds.) Geol. Soc. Am. Spec P., 241, pp1-8.

Parada M. 1990. Granitoid plutonism in central Chile and its geodynamic implications. Ibidem, pp. 51-66.

Sebai A., Féraud, G. and Bertrand, H. 1991. $^{40}Ar/^{39}Ar$ dating and geochemistry of tholeiitic magmatism related to the early opening of the Central Atlantic rift. Earth Planet. Sci. Lett., 104, 455-472.

NEW INSIGHTS INTO THE STRUCTURE OF THE UPPER PALAEOZOIC / MESOZOIC ACCRETIONARY WEDGE COMPLEX OF THE COASTAL CORDILLERA OF CENTRAL AND SOUTHERN CHILE

Hans-J. MASSONNE(1), Lydia HUFMANN(1), Paul DUHART(2), Francisco HERVÉ(3) and Arne P. WILLNER(4)

(1) Institut für Mineralogie & Kristallchemie, Univ. Stuttgart, Azenbergstr. 18, D-70174 Stuttgart, F.R.G. (imima@po.uni-stuttgart.de)
(2) SERNAGEOMIN, Puerto Varas, Av. La Paz, 406, Chile
(3) Departamento de Geologia, Universidad de Chile, Casilla 13518, Correo 21, Santiago de Chile, Chile
(4) Institut für Mineralogie, Ruhr-Universität, D-44780 Bochum, F.R.Germany

KEY WORDS: metapsammopelite, phengite, accretionary wedge, tectonics, Chilean Coastal Cordillera, Chiloé

INTRODUCTION

Similar to paired metamorphic belts, the metamorphic basement within the Coastal Cordillera of Chile south of 32°S can be divided into a series of low grade metamorphic rocks locally containing obvious high-pressure, low-temperature rocks such as glaucophane schists and a series east of it with intermediate to high grade rocks metamorphosed under low pressure conditions (Gonzalez Bonorino & Aguirre, 1971; Aguirre et al., 1972). In the westerly series metagreywackes and metapelites dominate. Subordinate are greenschists, which partly show relic pillow structures and MORB signature. Intercalated are lenses of serpentinite, massive Fe-Cu-Zn-sulphides and metacherts. The thick clastic sequences are probably of Late Palaeozoic sedimentary age. Metamorphic ages are at least not older than Carboniferous younging towards the south (Hervé, 1988).

NEW PETROLOGICAL RESULTS ON HIGH-PRESSURE METAMORPHISM

The low-grade metapsammopelites of the Coastal Cordillera of Chile south of 32°S contain the mineral assemblage chlorite, phengite, quartz, albite with biotite occassionally present. Greenschists are also characterized by a common mineral assemblage: albite, chlorite, epidote, Ca-amphibole with minor

phengite and quartz. In spite of these ordinary assemblages it was demonstrated by Massonne et al. (1996) that the investigated rocks generally experienced an early high-pressure metamorphic event, because the cores of the potassic white micas often showed Si contents per formula unit close to 3.5. Applying phengite geothermobarometry (see e.g. Massonne, 1995), these mica compositions point to metamorphic pressures between 6 and 8 kbar, which were reached at temperatures between 300° and 400°C. Peak metamorphic temperatures can, however, exceed this range and be clearly different among the metasediments of the low grade belt (Willner et al., 1999a). The common phengite compositions are those with Si contents around 3.3 p.f.u. being the result of a fairly penetrative equilibration at greenschist facies conditions. In metabasites the additional observation of amphibole cores enriched in sodium corroborates the early low-temperature, high-pressure nature of the rocks. Since these results were obtained only from several rocks of coastal outcrops, e.g. from Pichilemu or Mehuin, further efforts were made to confirm this picture. Now, we can add several new localities within the Coastal Cordillera where both rock types show the above signature. These are in the Chonos Archipelago (Willner et al., 1999a), on Chiloé and on the mainland, e.g. near Bahia Mansa (Lange & Willner, 1997). Under these circumstances, the idea that the low grade metapsammopelitic series is part of an accretionary prism (Hervé, 1988; Massonne et al., 1996) must be considered as broadly proven.

STRUCTURAL INFORMATION ON THE ACCRETIONARY WEDGE COMPLEX

The abundant coastal outcrops of the Chonos Archipelago and the southern shore of Chiloé facilitate the study of cross-sections through the N – S trending accretionary belt whereas on the mainland the poor outcrop situation inland generally does not allow this. However, these coastal outcrops are hardly accessible. Nevertheless, we can report here valuable structural information on this accretionary wedge complex by two more or less W – E directed cross-sections. One is located at the southern coast of Chiloé between Isla Quilan and the southeastern edge of Isla de San Pedro. The length of this section is approximately 50 km. The other section being 25 km in length starts at the issue of Rio Abtao into the Pacific ocean and ends 12 km NW of Castro. The corresponding inland outcrops through the Cordillera de Piuchen are poor but surprisingly almost continuous.

On Chiloé the thick clastic sequence of the accretionary wedge complex is subdivided into two similar portions by the intercalations of metabasites. This is similar in the Chonos Archipelago and possibly for the mainland parts of the accretionary wedge complex as well, where it is, however, hard to prove. For instance, at Pichilemu, where blueschists undoubtedly occur in coastal outcrops, a significant part of the western portion of the accretionary wedge complex must have been eroded following the above conclusion. Especially at the southern shore of Chiloé along the Canal Guamblad the metabasic intercalations show clear evidence for the first foliation plane crosscutting the metabasite-metasediment

boundary significantly. Provided that such boundary planes can be related to the former strata, the first compression was directed more or less perpendicular to it and might represent the stage of separation of the clastic cover from the oceanic crust that was further subducted. A second more weakly pronounced foliation plane rather caused crenulation. Sometimes it is missing in dekameter thick metabasic intercalations. The crenulation cleavage planes show the same strike but a significantly different orientation compared to the first foliation plane. This situation can be explained by back-thrusts which, thus, can be related to the stacking of the metasediments within the accretionary prism. Only these two foliation planes surprisingly in almost equal appearance occur in metasediments of the westernmost portion of the W – E cross-section along the southern shore of Chiloé. This pattern is unique in the entire accretionary wedge complex along the Coastal Cordillera probably due to the fact that the corresponding area is the westernmost portion of the accretionary wedge complex preserved at all. Towards the east, shear planes develop with centimeter to decimeter distance and subparallel strike to the previous foliation planes. Further to the east these grade into very tight folds. For instance, in the Canal Guamblad area these folds are thoroughly developped and appear at the first glance as tight isoclinal folds. There, this third deformation event is clearly discernable in the metabasic rocks as well. This type of deformation is related to further compression but with a considerable strike-slip component. We believe that an oblique subduction was responsible for that. A special tectonic feature that was so far only observed in southern Chiloé is related to a discrete, slightly dipping foliation plane with spacings in the decimeter to meter range. Corresponding folds could not be detected so far. This fourth stage of deformation probably also caused the present strike of the early foliation planes to be NW – SE trending whereas in other parts of the accretionary wedge complex the N – S trend is obvious. Maybe this zone in southern Chiloé marks the southern border of one of the partial complexes in which the entire accretionary belt of the Chilean Coastal Cordillera is subdivided. This idea is also the result of the view that the entire belt has a non-contemperaneous nature (Willner et al., 1999b).

CONCLUSIONS

Our new petrological results confirm that the Upper Palaeozoic / Mesozoic metamorphic rocks of the Chilean Coastal Cordillera have experienced similar metamorphic conditions at high pressures and low temperatures. Under these circumstances, the idea that the thick clastic sequence is part of an accretionary prism is broadly proven. Results on the tectonics that effected the low grade metapsammopelites were mainly obtained along a W – E profile along the southern shore of Chiloé and are compatible with this view. Similar tectonic structures were reported for other accretionary wedge complexes with oblique subduction, for instance, by Wallis (1998). With additional data to be obtained in

the future we are confident that we can resolve the formation of the Chilean accretionary wedge complex in detail which is unique due to its wide extension.

ACKNOWLEDGMENTS

The above research was financially supported by governmental agencies of Chile (CONICYT, FONDECYT, Catedra Presidential) and by the German Ministry of Education and Research.

REFERENCES

Aguirre L., Hervé F. and Godoy E. 1972. Distribution of metamorphic facies in Chile: an outline. Krystallinikum, 9, 7-19.

Gonzalez Bonorino F. and Aguirre L. 1970. Metamorphism of the crystalline basement of Central Chile. J.Petrol., 12, 149-175.

Hervé F. 1988. Late Paleozoic subduction and accretion in Southern Chile. Episodes, 11, 183-188.

Lange S. and Willner A.P. 1997. Genese und metamorphe Fluidentwicklung von Coticules (Spessartinquarzite) in einem jungpaläozoischen Akkretionskeil im südlichen Zentralchile. Ber. Dt. Mineral. Ges., Beih. Eur. J. Mineral., 9, No. 1, 215.

Massonne H.-J. 1995. III. Rhenohercynian Foldbelt, C. Metamorphic units (Northern phyllite zone), 4. Metamorphic evolution. In: Dallmeyer R.D., Franke W. and Weber K. (eds.) Pre-Permian geology of central and eastern Europe, 132-137, Springer, Berlin.

Massonne H.-J., Hervé F., Muñoz V. and Willner A.P. 1996. New petrological results on high-pressure, low-temperature metamorphism of the Upper Palaeozoic basement of Central Chile. Troisième Symp. Int. sur la Géodynamique Andine, Saint-Malo (France), Ext. Abstr., 783-785.

Wallis S. 1998. Exhuming the Sanbagawa metamorphic belt: The importance of tectonic discontinuities. J. metamorphic Geol., 16, 83-95.

Willner A.P., Hervé F. and Massonne H.-J. 1999a. Pressure-temperature evolution of two contrasting high pressure – low temperature belts in the Chonos Archipelago, Southern Chile. J. Petrol. submitted

Willner A.P., Massonne H.-J. and Hervé F. 1999b. Comparison of the PTd-evolution of HP/LT metamorphic rocks occurring in the South Shetland Islands and along the Coastal Cordillera of Chile. 8th Int. Symp. Antarctic Earth Sci., Wellington, Abstr. Vol.

EXPLORATION OF THE NORTHERN PART OF THE SOUTHERN PATAGONIAN BATHOLITH, SOUTHERN CHILE, COMBINING SPECTRAL AND HYPERSPECTRAL SATELLITE DATA WITH GROUND THRUTHING METHODS

Hans-J. MASSONNE(1), Jörg-U. MOHNEN(1), Hans-Georg KLAEDTKE(2), Alfred KLEUSBERG(2) and Francisco HERVÉ(3)

(1) Institut für Mineralogie & Kristallchemie, Univ. Stuttgart, Azenbergstr. 18, D-70174 Stuttgart, F.R.G. (imima@po.uni-stuttgart.de)
(2) Institut für Navigation, Universität Stuttgart, Geschwister-Scholl-Str. 24D, D-70174 Stuttgart, F.R.G.
(3) Departamento de Geologia, Universidad de Chile, Casilla 13518, Correo 21, Santiago de Chile, Chile

KEY WORDS: Patagonian Batholith, Chile, satellite data, image processing, inventorization

INTRODUCTION

The southern Patagonian batholith forming the coastal ranges of Southern Chile between the latitudes 47°S and 55°S is the relic of an eroded magmatic arc that was formed by the subduction of oceanic lithosphere of the Antarctic Plate underneath the South American continent in Cretaceous to Tertiary times (e.g. Bruce et al., 1991). The present magmatic arc that can be located by a few recently active volcanoes has moved eastwards by some tens of a kilometer. Plutonic rocks ranging from gabbros to granites are the dominating rock type. Minor metamorphic rocks mostly metasediments are also present. Due to its inaccessibility the various rock types of the vast regions of the southern Patagonian batholith were so far mainly explored by some expeditions. Therefore, our knowledge about the geology of this region is very poor compared to other areas of our planet.

PETROLOGICAL UNDERLAY

A new set of geological field expeditions have been launched under the responsibility of F. Hervé in 1998 to investigate coastal outcrops of some areas in the northern portion of the southern Patagonian batholith in more detail. Spotwise field studies and rock sampling actions are conducted to finally come

up with structural, petrological, geochemical, chronological and other sort of data for specific rock types. This bundle of studies should lead to a comprehensive understanding of the evolution of this fossil magmatic arc. The precise identification of the locality of rock specimens is allowed by GPS data.

Using the available geological information such as those shown in the 1 : 1.000.000 Geology Map of Chile and reported in the literature (e.g. Weaver et al., 1990) specific spots were selected for the detailed investigations. It turned out that even the detailed literature has to be revised in regard of the outcropping rock type. Incorrect identification of sample spots or rock types are probably responsible for that. Until now, more or less all kind of rocks appearing in the target area were collected at georeferenced localities. The sampled plutonic rocks cover all sorts of gabbros, diorites, tonalites, granodiorite and granites. Magma mingling, plutonic portions with high amounts of xenoliths, alteration zones and boundaries between plutonic bodies and those due to fault zones were detected. Abundant vein systems are related to dolerites and lamprophyres. Aplitic dykes are relatively rare. Metamorphic rocks are mainly metapsammopelites that show a very similar appearance mainly concerning layering and structural style as the low grade ones from the Palaeozoic/Mesozoic accretionary wedge complex occuring in the coastal ranges north of the southern Patagonian batholith where the Nazca plate is subducted under the South American continent. In spite of these similarities, the metapsammopelites of our study area are broadly effected by contact metamorphism. Sometimes relatively large minerals, such as andalusite, have unorientedly grown in the generally fine grained metasediments. Among the metasediments, greenschists can appear as relatively rare interlayers.

INVENTORIZATION USING SATELLITE DATA

Georeferenced Landsat5-TM data were processed and analyzed for the northern part of the southern Patagonian batholith. The selected area ranges roughly between the latitudes 47.5°S and 50.5°S. This region has, so far, been classified and inventorized into glaciated regions, water, regions covered with primary growth forests and barren regions. Presently, we are attempting to subdivide the latter regions at least into two main rock classes, which are plutonic rocks ranging from gabbros to granitoids and metapsammopelitic rocks showing variable mineral assemblages due to different degrees of contact metamorphism. These attempts imply the consideration of vegetation covering a significant portion of the various rock types. For that purpose, our georeferenced field data were taken into account. Furthermore, programs were used to detect tectonic lineations from optical imagery (Mohnen et al., this volume).

FUTURE OUTLOOKS

In addition to Landsat5-TM data, similar optical satellite data, hyperspectral satellite data of relatively high resolution as well as radar data and possibly geomagnetic data will be processed and analyzed for the above mentioned region. These new data treated as overlays in Arc-Info format and processed with ER-Mapper will help to subdivide the rock classes considerably. A digital elevation model will be additionally included.

The natural vegetation in the vast region of our study, which is unlike many regions in Europe and North America, might even facilitate this task because different vegetation types can be related to some extent to different rock types. Moreover, we believe that this treatment could guide us to valuable mineral deposits, which does not seem to exist in our study area. However, the southern Patagonian batholith shows potential for mineral exploration and was so far only neglected for exploration purposes due to its inaccesibility and remoteness (Nelson, 1996).

ACKNOWLEDGMENTS

The above research was financially supported by governmental agencies of Chile (CONICYT, FONDECYT, Catedra Presidential) and by the German Ministry of Education and Research.

REFERENCES

Bruce R.M., Nelson E.P., Weaver S.G. and Lux D.R. 1991. Temporal and spatial variations in the southern Patagonian batholith; Constraints on magmatic arc development. Geol. Soc. Am. Spec. Papers, 265, 1-12.

Mohnen J.-U., Klaedtke H.-G. and Massonne H.-J. 1999. Geomorphology, pattern recognition of textures, tectonic lineation analysis and material classification using optical satellite imagery on the Patagonian batholith, Southern Chile. This volume

Nelson E.P. 1996. Suprasubduction mineralization: metallo-tectonic terranes of the southernmost Andes. Geophys. Monograph 96, Subduction: Top to Bottom, Am. Geophys. Union, 315-329.

Weaver S.G., Bruce R., Nelson E.P., Brueckner H.K. and LeHuray A.P. 1990. The Patagonian batholith at 48°S latitude, Chile; Geochemical and isotopic variations. Geol. Soc. Am. Spec. Papers, 241, 33-50.

GEOPHYSICAL STUDIES OF COTOPAXI VOLCANO, ECUADOR : SEISMICITY, STRUCTURE AND GROUND DEFORMATION.

Jean Ph. MÉTAXIAN (1,2), Mario RUIZ (2), Alexandre NERCESSIAN (3), Sylvain BONVALOT (3,4), Patricia MOTHES(2), Germinal GABALDA(4), Francis BONDOUX(1,2), Pierre BRIOLE(3), Jean-Luc FROGER(5) and Dominique RÉMY(4)

(1) IRD, Apartado postal 17-12-857, Quito, Ecuador, E-mail: jpmetaxi@uio.satnet.net
(2) Instituto Geofisico, EPN, Campus Ing. José Rubén Orellana R., Apartado 2759, Quito, Ecuador, E-mail : geofisico@accessinter.net.
(3) Institut de Physique du Globe de Paris, 4 place Jussieu, 75005 Paris (France)
(4) IRD, Lab. de Géophysique, 32, av. Varagnat, 93143 Bondy (France), E-mail : bonvalot@bondy.ird.fr
(5) Université Blaise Pascal, CRV, 5 rue Kessler, 63038 Clermont-Ferrand (France)

KEY WORDS : Cotopaxi, seismicity, LP, glacier, structure, gravity, GPS, ground deformations.

INTRODUCTION

Cotopaxi volcano (5897 m) lies in the Cordillera Real, 60 km south of Quito. This andesitic stratovolcano, with a base diameter of 25 km and almost 3000 m of relief, is covered by an icecap on the uppermost 1000 m of the cone. It is one of the most active volcanoes of Ecuador; the most recent eruptions occured in 1742-44, 1768 and 1877. In a stratigraphic study covering the last 5000 years, Barberi et al. (1995) calculated an average eruption reocurrence interval of 117 years. In the last eruption, huge debris flows were generated as a result of ash flows melting the icecap. Mothes (1992), and Hall and Mothes (1997) reported that in the eruption of 1877, the debris flow arrived at the ocean in 18 hours, covering a distance of 326 km. An event of similar magnitude, if it were to occur today, would directly affect more than 80 000 people (Hall and Mothes, 1997, Mothes et al., 1998).

Cotopaxi volcano has been monitored by the Instituto Geofìsico of the Escuela Politécnica Nacional (IGEPN) with one seismograph since 1977 and with four permanent telemetered one-component seismic stations since 1989. Deformation studies using a laser EDM on radial lines started in 1987 (WOVO, 1994). Between August 1996 and June 1997, we operated an array of 12 additional seismic stations (Figure 1). This work was accomplished in the framework of collaboration between ORSTOM and the IGEPN. The goal was to characterise and analyse the nature of the volcano's seismic activity and to perform a preliminary study of the internal structure of the volcano. Geodetic, gravity and microgravity studies were also carried out at Cotopaxi in the frame of this research program with the aim to study ground deformation and internal changes related to the volcanic activity. In this summary, we present a synthesis of the preliminary results of the seismological experiment made in 1996-97 and of the geodetic and gravity data gathered in October 1996.

Description of the SEISMOLOGICAL experiment and data ACQUISITION

The experiment was carried out in two phases. First we installed some stations on the volcanic cone varying at azimuths and distances from the crater and other stations in a wide area around the volcano, up to 20 km distance from the crater, to do the structural study (Figure 1). In a second phase, we moved part of the equipment closer to the crater in order to register in geater detail the volcanic activity concentrated below the summit area. One station was installed along the edge of the crater on a rock base at an elevation of 5820 m.

The array was composed of 3 RefTek stations employing Mark Products L4-3D seismometers, one Leas station equipped with a Mark Products L4C seismometer and 8 telemetered stations divided in two groups of four stations comprising sub-arrays which had separate reception and acquisition units. Three other Leas stations worked occasionally between March and June 1997. One of these stations was equipped with a Guralp 40T seismometer, and the others with Mark Products L4C vertical seismometers. The data were registered on 500 Mb hard disks with the RefTek stations and on 170 Mb PCMCIA disks with the Leas stations, both at 100 samples/sec. The acquisition, digitalization and storage of the telemetered data was performed at the same sample rate with the program ACQ (Fréchet and Glot, 1994).

Characteristics of the seismic activity

The local activity associated with Cotopaxi volcano represents roughly 2000 events per month. We categorize for the 10 month period three main classes of local seismicity :

1) About 100 well located volcano-tectonic events. The volcano-tectonic hypocenters are located 2-10 km under the summit and are distributed under the volcano's flanks and the crater.

2) Clear long-period-type event (LP) with emergent first arrival waves detected by all of the array and with a low frequency spectral content (3 Hz). About 500 LP events occured each month, although only 70 have identifiable phases, as the emergent first phase makes these events difficult to locate. The LP activity is superficial (< 2 km under the summit), concentrated under the crater and may be associated with transport of fluids and vaporisation of water in conduits beneath the crater. The source of water is prabably the glacier, which could explain the permanent and constant LP activity.

3) Earthquakes with a typical LP signature (emergent onset and low frequency spectra) for the events registered at the stations located below the glacier and with a volcano-tectonic signature (impulsive onset and dominant frequency at 6 Hz) for data registered at the summit station. This grouping comprises 75% of the seismic activity at the volcano. Comparatively, the wave amplitude is ten times greater at the summit than 2 km lower and proximal to the glacier. The P wave arrival time difference between the summit and a second station at 3 km distance is between 2 - 3 seconds. Most of these events are not registered by the IGEPN's permanent seismic array which is located nearer to the base of the volcano and that has a distance to the summit (7 km. This clearly implies that the source of this type of event is superficial, close to the summit and the propagation occurs in a superficial, very slow medium. These events could be associated with glacier motions. They are similar to events observed in Cascades volcanoes partially covered by an icecap (Mount St Helens, Mount Baker and Mount Rainier) and are interpreted by Weaver and Malone (1976, 1979) as icequakes. The Cotopaxi events have similar characteristics as those observed on these volcanoes, i. e., initial detection and higher amplitude at the higher station, impulsive initial waves at the summit station becomes emergent at the bedrock stations located at the base of the glacier, strong dispersion effect. Araujo and Métaxian (1999, this volume) show, by comparison between events registered on ice and on bedrock, that part of this seismic activity has a glacier origin. The model proposed by Weaver and Malone to explain the mechanism of glacier earthquakes is sliding of ice over bedrock. Neave and Savage (1970) suggest that icequakes appear to originate from extensional faulting near the surface of the glacier. The model proposed by Araujo and Métaxian (1999, this volume) is ice cracks. The observation of multiple icequakes, registering tens to hundreds of similar events each month, seem to support this hypothesis.

We also registered 1000 regional tectonic events of which half originated from the Pisayambo seismic concentration and from the region of Pujili, situated respectively 35 km south and 45 km southwest of Cotopaxi. Most of the activity is situated at less than 20 km depth. There are few events originating from the west or north except superficial activity from the Quito area (< 10 km) and Guagua Pichincha volcano.

Preliminary results of the structural study

A prelimirary processing was performed using the volcano-tectonic events located inside the array at a maximum depth of 10 km. A joint inversion of the P wave arrival times and velocities fixed from an average linear velocity model adapted from other andesitic volcanoes show for the superficial layer (-6 to 0 km depth) a low velocity anomaly centered on the volcanic cone and a positive anomaly situated in the southern part of the volcano, corresponding to an old volcanic structure or proto Cotopaxi, named Morurco. Between 0 and 4 km depth, we observe a positive anomaly centered under the volcanic cone. Our goal is to process regional seismic events located in a radius of 100 km around the volcano, using the arrival times at 12 seismic stations of the IGEPN's array situated in this area. This extended array will allow for greater precision in locating the regional tectonic events in order to perform ray tracing between the tectonic sources and the Cotopaxi array stations.

PRELIMINARY RESULTS OF THE Geodetic and gravity sTUDIES

In november 1996, we set up a repetition network of 18 GPS stations distributed from the base of the volcano up to 4850 meters (Figure 2). The GPS and microgravity observations were performed in a differential mode using dual frequencies Ashtech Z12 surveyor receivers and Scintrex CG-3M micro-gravity meters. For this network, we also reoccupied 4 GPS stations determined in 1993 by the USGS as well as some of the IGEPN's EDM bases. In addition, SAR interferometry using ERS satellite images is also used to evaluate the ability of the interferometric method to produce coherent interferograms for ground deformation measurements on Cotopaxi volcano. The results of the GPS and microgravity surveys as well as SAR interferometric studies are discussed here in relation with other geophysical data in terms of baseline measurements for monitoring of the volcanic activity.

REFERENCES :

Barberi, F., M. Coltelli, A. Frullani, M. Rosi, and E. Almeida, Chronology and dispersal characteristics of recently (last 5000 years) erupted tephra of Cotopaxi (Ecuador): implications for long-term eruptive forecasting, J. Volc. Geoterm. Res., 69, 217-239, 1995.

Fréchet, J. et J. P. Glot, Programme ACQ, Laboratoire de Géophysique Interne et Tectonophysique, Université Joseph Fourier et C. N. R. S Observatoire de Grenoble, 1994.

Hall, M. L., and P. Mothes, Cotopaxi volcano, Ecuador : mitigation of debris flow impact ñ daunting task ?, IAVCEI News, No : 3, 1997.

Mothes, P. A., Lahars of Cotopaxi volcano, Ecuador : hazard and risk evaluation, Geohazards ñ Natural and Man-Made, Eds : McCall, Laming and Scott, Chapman and Hall, London, pp 53-63.

Mothes, P. A., M. L., Hall, and R. J., Janda, The enormous Chillos Valley Lahar : an ash-flow-generated debris flow from Cotopaxi Volcano, Ecuador, Bull. Volcanol., 59, 233-244, 1998.

Neave, K. G., and J. C. Savage, Icequakes on the Athabasca Glacier, J. of Geophys. Res., 75, 1351-1362, 1970.

Weaver, C. S., and S. D. Malone, MT. Saint Helens seismic events : Volcanic earthquakes or glacial noises ?, Geophysical Research Letters, Vol. 3, No. 3, 197-200, 1976.

Weaver, C. S., and S. D. Malone, Seismic evidence for discrete glacier motion at the rock-ice interface, Journal of Glaciology, Vol. 23, No. 89, 1979.

World Organisation of Volcano Observatories, Directory of volcano observatories 1993-1994, WOVO, IAVCEI, UNESCO, Paris, 1994.

GEOMORPHOLOGY, PATTERN RECOGNITION OF TEXTURES, TECTONIC LINEATION ANALYSIS AND MATERIAL CLASSIFICATION USING OPTICAL SATELLITE IMAGERY ON THE SOUTHERN PATAGONIAN BATHOLITH, SOUTHERN CHILE

Jörg-U. MOHNEN(1), Hans-Georg KLAEDTKE(2) and Hans-J. MASSONNE(1)

(1) Institut für Mineralogie & Kristallchemie, Univ. Stuttgart, Azenbergstr. 18, D-70174 Stuttgart, F.R.G.
(2) Institut für Navigation, Universität Stuttgart, Geschwister-Scholl-Str. 24D, D-70174 Stuttgart, F.R.G.

KEY WORDS: Patagonian batholith, Chile, satellite data, image processing, tectonic lineation

INTRODUCTION

The region of the southern Patagonian batholith in Southern Chile has been eroded since its magmatic origin in the Cretaceous and Tertiary. The geomorphic development along this active continental margin through continued subduction of the Antarctic plate under the South America continent is dominated by the emplacement of a variety of batholiths over extended time periods. The basement into which the magma has been intruded into, consists mainly of a sequence of metapsammopelites. In addition to these lithological changes, the area is subdivided by major tectonic lineations.

We are in the process of building an optical image database from a variety of satellite sensor data platforms (Massonne et al., this volume). As our primary base dataset, we use the Landsat5-TM data with a resolution of circa 30 by 30 meters and a total geographically corrected image extent of circa 200 by 600 km lying between the latitudes 46°S and 51°S. GPS measurements made in the study area during the past two years are used in georeferencing these initial satellite data (Massonne et al., this volume). We have performed system and terraine corrections on this primary Landsat5-TM database, i.e. destriping, color balancing and mosaicing. We first present a classification of the predominant material found in our primary database. Clouds, ice, water, barren rock and vegetation will be statistically assessed and quantized. This primary Landsat5-TM database will be synthesized with more recent optical and hyperspectral images through a process called datafusion.

From recent field work and ground truthing in Patagonia (Massonne et al., this volume), we are able to subdivide regional plutonic and metasedimentary bodies through pattern and texture recognition (see Haralick, 1986). The metasediments with their foliation patterns can be distinguished from granitoids using self-developed algorithms and compared with subjective inspection. Regional faulting is another endogenic pattern we will examine in this study. Not only do they reveal tectonic sutures and major extensional and compressional regimes, they help in confining major crystalline boundaries mentioned above.

Yet another result from this study is the problem of seperating dikes from these regional faulting patterns. Since dike swarms intrude both metasediments and granatoid bodies, and since they seem to have less of a resistance to erosion than there host rock, it is sometimes very difficult to assess whether the lineation is a dike or a fault. In our ground truthing, we have studied both types and hope to be able to distinguish these two patterns using our past ground truthing experience. We proceed with the second derivative method for edge detection (Nevatia, 1986). Many methods relying on a first derivative method for edge detection fall short of expectation due to ramp characteristics in satellite imagery caused by lighting from one single source which is sunlight. For ideal results, use of a second derivative method suggested here eliminates this difficulty. In the process of cluster coding our binary image as the input file is subjected to cluster coding or vector quantization (see Gonzalez, 1986) and recognition. Using ER-Mapper, we convert the vector files to AutoCad (*.dxf) and then use a batch-wizard running on Windows-NT through ER-Mapper. The results are rather impressive and can be viewed as rose diagrams. We will subdivide the vast training region into several quadrants which depict general tectonic lineations.

We will present our results above by comparing them with past literature where geological maps have been published. Using ER-Mapper, AutoCad and Arc-Info, we generate overlays and raster data which will synthesize all applicable information into a coherent body of information. In some cases, we will show the presence of possible multiple granitoid bodies which have not yet been mapped, and subsequently, have been termed the southern Patagonian batholith on a regional scale.

REFERENCES

Haralick R.M. 1986. Statistical image texture analysis. In: Young T.Y. and Fu K.-S. (eds.) Handbook of pattern recognition and image processing, 247-279, Acad. Press, Orlando, Florida.

Gonzalez R.C. 1986. Image enhancement and restoration. In: Young T.Y. and Fu K.-S. (eds.) Handbook of pattern recognition and image processing, 191-213, Acad. Press, Orlando, Florida.

Massonne H.-J., Mohnen J.-U., Klaedtke H.-G., Kleusberg A. and Hervé F. 1999. Exploration of the northern part of the southern Patagonian batholith, Southern Chile, combining spectral and hyperspectral satellite data with ground thruthing methods. This volume.

Nevatia R. 1986. Image segmentation. In: Young T.Y. and Fu K.-S. (eds.) Handbook of pattern recognition and image processing, 215-231, Acad. Press, Orlando, Florida.

PHANEROZOIC PALEOGEOGRAPHY AND GEOLOGIC EVOLUTION OF COLOMBIA

Jairo MOJICA (1)

(1) Departamento de Geociencias. Universidad Nacional de Colombia, Apartado 14490, Bogotá- Colombia . E-mail: jmojica@usanet.com and jairomojica@hotmail.com

KEYWORDS: Colombia, Phanerozoic Episodes, Paleogeography, geological evolution

INTRODUCTION

The present geological configuration of Colombia may be considered as the result of the development of two provinces with different age and types of basement. The limit between them is the Romeral-Dolores Fault System (RDFS), which according to Case et al. (1971) separates the continental crust (here called Eastern Colombian Province, ECP) from the oceanic crust (here called Western Colombian Province, WCP). The first one comprises the sector between the western edge of the Guyana Shield and the RDFS. The second one is the region between such fault system and the Pacific Coast.

The Proterozoic igneous-metamorphic basement has yielded radiometric ages between 1600? and 700 Ma and constitutes the ECP (Priem et al., 1989; Ordoñez, 1997). The basement is unconformably cover by different Phanerozoic sediment sequences separated by non-deposition intervals and erosion events. The WCP is composed essentially of oceanic diabases, basalts and ultramafites, as well as deep-water sediments of Cretaceous age (Etayo-Serna et al.1982). Rocks of the WCP crop out in the eastern edge of the Cauca Valley, the Western Cordillera, and the Baudó Range.

During the last two decades and taking into account geographical criteria and local characteristics of the sedimentary cover, several authors have proposed that the present tectonic configuration of the country has resulted from the accretion of different suspect terranes, each one of them delimited by master faults (paleosutures). Ingeominas (1983) proposed thirty-four terranes, reduced to five by Restrepo and Toussaint (1988). Forero (1990) difference only three suspect terranes, referred by him as to the Eastern South American Province (ESAP), the Central Andean Province (CAP) and the Western Province (WP). According to those

authors, the only autochthonous block is the one located eastward of the Borde Llanero Fault System (BLFS) which includes the pericratonic area and the western edge of the Guyana Shield.

According to Forero (1990), the CAP extends between the BLFS and the RDFS, and is an allochthonous terrane accreted to the ESAP during the Silurian (Caledonian Orogeny), as a result of the collision between the eastern portion of North America and northwestern corner of old South America. Forero (1990) also assumed that the WP (partially coinciding with the Western Andean Terrane, or WAT of Restrepo and Toussaint, 1988) is an allochthonous terrane, attached to the CAP along the RDFS during the Paleocene. However, the Caledonian Orogeny in the northwestern corner of South America probably did not take since: *a*) the BLFS do not present typical properties of a paleosuture, e.g. the presence of ophiolitic complexes. *b*) There is no evidence of real orogenic events, since the Cambro-Ordovician sediments do not show regional-metamorphic effects, or association to large coeval intrusions. *c*) In comparison to the overlying Meso and Cenozoic cover, the Paleozoic sediments do not show differences in the type and intensity of folding. *d*) The Paleozoic sediments do not include molasses as those belonging to the Cenozoic Orogeny and occupying large areas of the ECP. *e*) The supposed Cambro-Ordovician age of the Quetame, Cajamarca, Ayurá-Montebello and similar Groups, on which the idea of the Caledonian Orogeny is based, has not yet been proved. Furthermore, the stratigraphic relationships observed at several places indicate that these groups represent pre-Devonian, even Pre-Cambrian rocks. Almost the same objections can be argued (especially those from *a* to *d*) against a currently supposed Hercynian Orogeny in Colombia.

PALEOGEOGRAPHY AND GEOLOGICAL EVOLUTION

The reconstruction of 23 paleogeographic maps (Figs. 1 and 2) elaborated with the most recent information (up to 1998), evidences that the geological history of the northwestern corner of South America has been determined mainly by two fundamental facts:

1. The consolidation of a Proterozoic platform extending as far as to the RDFS. Several tectonic events affected this crustal block during the Phanerozoic. The deformation has been concentrated in a mobile belt located between the eastern flank of the Central Cordillera and the BLFS (active since the Early Devonian). The present Central Cordillera domain shows a persistent positive tendency on the above-mentioned maps. This fact would explain the generalized absence of Phanerozoic cover, as well as the local exposures of the Precambrian basement, studied and dated by Ordoñez (1997). Consequently, we deduce that this region constitute an autochthonous province since the Proterozoic.

2. The uplift and integration to the continent of the WCP, presumably occurred during the Early Tertiary. In this sense, this block would be the only allochthonous (or para-allochthonous) terrane in the northwestern corner of South America.

The analysis and comparison of the here reconstructed maps permit us to establish following four major evolution episodes in the considered area.

Paleozoic episodes. They are represented by four major transgression- regression sedimentary cycles occurred during Upper Cambrian, Middle Ordovician, Early to Middle Devonian and Carboniferous-Middle Permian times. They are separated by non-deposition events corresponding to: a) Early Ordovician, b) Late Ordovician to latest Silurian, c) Latest Devonian to Early Carboniferous. The deposition cycles permitted the accumulation of mainly shallow marine and lagoonal sediments. The Paleozoic sediments exposed within the ECP show moderate thickness and high diagenesis but no regional-metamorphic effects. Consequently, Mojica and Villarroel (1990) interpret the Paleozoic tectonics in terms of distensional (taphrogenic) and epeirogenic processes influenced by eustatic sea level changes. Between the Late Permian and the Early Triassic occurred a generalized uplift and erosion.

Triassic-Jurassic episodes. In the ?Middle Triassic, began a volcano-sedimentary cycle (Luisa, Payandé and Saldaña Formation and similar) extending up to the Middle Jurassic and including and short-lived ingressions along narrow corridors. During the Late Jurassic, sedimentation was restricted to a small triangle between the Gulf of Maracaibo and the Floresta Massif. This area was infilled with thick red-bed sequences (Girón Group in northeastern Colombia, Seco Conglomerate in the Perijá Range). At the same time, in the Guajira Peninsula developed an E-W trending trough that preserved red-beds in the lower levels and shallow marine sediments (limestones) toward the top. As in other regions of South America, the tectonic regime during the Triassic - Jurassic has been assumed to be extensional, and leading to the development of a supracontinental graben or aulacogen that has been interpreted as being produced by of the separation between South and North America. Consequently, the accumulation of the Triassic-Jurassic volcano-sedimentary sequences, locally cut by granodioritic intrusive bodies, is supposed to have occurred in grabens or halfgrabens trending parallel to the present cordilleras.

Cretaceous episodes. Thy are represented by a mainly marine cycle initiating in a small depocenter (Cundinamarca Basin), gradually expanded toward NE and SW, and encompassing nearly all the country during the Late Cretaceous. As in the Triassic-Jurassic, the tectonic regime is supposed to have been extensional, but with graben structures migrated eastward. Small gabroid bodies were intruded locally into the Early Cretaceous sediments. At the Early Paleocene, began a regression phase, initiated near the present forking zone of the Central and Eastern Cordilleras, and divergently moving toward NE and SW. Consequently, large blankets of diachronic coal-rich, lagoon-like and fluvial sediments (Guaduas Group and similar) were deposited.

Tertiary episodes. During this Sub-era, occurred the first real Andean Orogenic Cycle in Colombia during the Phanerozoic. The movements initiated in the Paleocene, in form of light uplifting in the present Central Cordillera domain. They became more vigorous during the Late Paleocene and the Early Eocene. At the same time, the neighboring region located eastward suffered a compressive phase, resulting in strong folding and a conspicuous regional unconformity.

During the Late Eocene, the Oligocene and the Middle Miocene, continued the uplifting in Central Cordillera and large portions of the Subandean Zone, the Eastern Cordillera and the Magdalena and Cauca Valleys were infilled with huge volumes of continental molasses (Gualanday, Honda Groups, etc.). The upper parts of the Miocene ones contain the first records of the explosive volcanic events that have been active until present.

The uplifting of the Eastern Cordillera began in the Late Miocene and it became a new source for the Neogene molasses now cropping out in the Magdalena Valley and Subandean the Zone. The Late Miocene movements changed drastically the drainage patterns, causing the establishment of the Magdalena, Orinoco and Amazons fluvial systems. During the Pleistocene, the Eastern Cordillera raised quickly and reached its present topographic levels. The Late Miocene-Pleistocene tectonic regime was frankly compressional and lead to tectonic inversion of the preexisting structures (Cooper et al., 1995). Shortening of the sedimentary cover up to 60 km has been estimated in both sectors. As a consequence, fold- and faulting structures, including detachment zones with tectonic transport toward the Magdalena Valley and the Subandean Zone were produced.

The uplifting of Baudó Range occurred in the Pleistocene. The Atrato -San Juan Basin existed during the whole Cenozoic times. It is infilled with several thousand meters of sediments, deposited in alternating deep and shallow-water environments.

REFERENCES

-Case, J.E., Durán L.G., Lopez, A. & Moore, W.R. 1971: Tectonic investigations in western Colombia and Panama. Geol. Soc. Amer. Bull., 82, 2685-2904.

-Cooper and eleven other. 1995. Basin development and tectonic history of Llanos Basin, Eastern Cordillera and Middle Magdalena Valley, Colombia. Bull. Am. Assoc. Petrol. Geol. 79, 1421-1443.

-Etayo-Serna, F., Parra, E. and Rodriguez, G. 1984. Análisis facial del „Grupo Dagua" con base en sucesiones aflorantes el oeste de Toro (Valle del Cauca). Geología Norandina, No. 5, 3-12.

-Forero, A. 1990. The basement of the Eastern Cordillera, Colombia: An allochthonous terrane in northwestern South America. Jour. South Am. Earth Sc., 3, 141-151.

-Ingeominas. 1983. Mapa de terrenos geológicos de Colombia. Publ. Esp. No.14

-Mojica, J. & Villarroel, C. 1990. Sobre la distribución y facies del Paleozoico Inferior sedimentario en el extremo NW de Suramérica. Geología Colombiana, No.17, 219-226.

-Ordoñez, O. 1997 O Pré-Cambriano na parte da Cordilheira Central dos Andes Colombianos. Master Thesis, Universidade de Brasília.

-Priem, H.N.A., Kroonenberg, S., Boelrijk, N.A. & Hebeda, E.H. 1989: Rb-Sr and K-Ar evidence for the presence of a 1.6 Ga. basement underlying the 1.2 Ga. Garzón-Santa Marta granulite belt in the Colombian Andes. Precambrian Research, 42, 315-324.

-Restrepo, J.J. and Toussaint, J.F. 1988. Terranes and continental accretion in the Colombian Andes. Episodes 11, 189-93.

NORMAL FAULTING AND MAJOR ROCK SLIDES IN THE NORTH PAMPEAN RANGES OF ARGENTINA

Ricardo MON(1)

(1) Facultad de Ciencias Naturales, Univ. Nac. Tucumán, Miguel Lillo 205, 4000 Tucumán, Argentina.

KEY WORDS: normal faults landslides uplifting neotectonics

INTRODUCTION

The Sierras Pampeanas in central Argentina are a series of mountain ranges formed by huge crystalline blocks bounded by faults. This morphotectonic province extends from 26° to 33° S. Southward of 28°S it belongs to the deformed Andean foreland (Jordan & Allmendinger, 1986) and is separated from the main Andean chain by N-S elongated continental basins. Northward of 28° it is incorporated into the Andean chain. Since Gonzalez Bonorino (1950) most workers accepted that the range bounding faults are reverse, almost vertical near the surface and concave-upward at depth.

The aim of this paper is to show that in some areas of the Sierras Pampeanas a significant portion of the faults are normal and that there is a gradual transition from kilometric-scale gravitational rock slides to major blocks separated by normal faults similar to large landslides. This structural situation is particularly well illustrated in the mountains situated eastward of the Salar Pipanaco between 27° 30' and 28° 10' S (Fig.1). They were first elevated to the surface and tilted according to the model of Gonzalez Bonorino (1950) but afterwards or simultaneously segmented by normal faults. The presence of normal faults in the Sierras Pampeanas was recognized by early workers such as Beder (1920), Gross (1948) and Schlagintweit (1954), but later some of their observations were forgotten.

STRUCTURE

The ranges represented in the map of Fig.1 consist of a series of tilted fault blocks, where the range-bounding faults are at their west borders. The topographic profile of the ranges is asymmetric with steep west slopes coinciding with the fault scarps. The gently dipping east slopes coincide with a partially eroded pre-Cenozoic erosional surface, which at some places is almost intact. This east-dipping erosional surface is frequently disrupted by west-dipping well conserved fault scarps.

The normal fault block structure is well represented in the relief and the connection between structure and relief is obvious. The normal faults are Upper Pleistocene or even younger. The fault surfaces themselves crop out only exceptionally; in these cases they are vertical or dipping steeply to the west (Fig.2).

Along the major fault scarps there are wedges, 4-6 km long and 2-3 km wide, with a triangular appearance on the map, which have slid down. They obey the same principles as rock slides, recognized on the slopes of mining and civil engineering works and well described by Hoek and Bray (1977). In the sites 1,2 and 3 (Fig. 1) there are good examples of this kind of structure. Figure 3 shows a detailed map of one of them, on the west slope of the La Carreta range. The descending movement of the wedge affected Pleistocene beds and produced an anomaly in the drainage. The movement of the normal fault blocks (Fig. 1) are probably major landslides following the same model.

At some places major landslides affecting Pleistocene beds penetrate along the trace of the faults in crystalline basement, which demonstrate the gravitational origin of some of the faults affecting the crystalline basement. A good example of this situation is found on the west slope of the Narvaez range, Fig. 4. There the Las Lagunas fault, which corresponds to a major landslide involving Pleistocene beds, penetrates southward into the basement, separating two basement blocks. The slide closed some ravines, causing small natural dams. Moreover the fault association illustrated in Fig. 4 gives the image of a giant landslide affecting the west slope of this part of the Narvaez range.

According to the cross-section of Fig.2, the blocks which have slid along normal faults are not necessarily at lower topographic levels; in most situations they are at higher levels. In spite of this, there are major blocks which have descended hundreds of meters below their original position along a sliding surface. Among them the most conspicous is that corresponding to the Lomas Picasas (Fig.5). This block is about 10 km long and 2-3 km wide and has it slid at least 800 m down the slope, along a 35° sloping surface (Fig.6). On the north-east slope of the block which slid there are remnants of the original Quaternary cover, with big rounded boulders of pegmatites and quartz attaining 0.6 m in diameter. These beds are similar to those represented in the south part of Campo Pucará. The Lomas Picasas block was part of it before it slid down. There is no evidence to allow the establishment of the velocity of the slide, which is not extremely recent, because the sliding surface is partially eroded.

DISCUSSION

The structure of the 27°30-28°S stretch of the Sierras Pampeanas results from two faulting episodes. The first one corresponds to an east-dipping inverse range-bounding fault running at the west border of the mountains which uplifted and tilted a basement block. The second one, clearly extensional, disrupted it generating narrow slices and wedges, ranging from a few kilometers to tens of kilometers, separated by normal faults. The first compression event was probably related to the 2-3 Ma Diaguita Orogeny which culminated 1.2 Ma ago (Gonzalez, 1995). The activity of the second event is still younger; it involved loess deposits which, according to Sayago (personal communication), are upper Pleistocene or Holocene.

It is not easy to find arguments to explain the origin of the extensional faults. In spite of this, the regional tectonic setting suggests that crustal extension could not be completely excluded. The ranges are flanked by two continental basins (Fig.7): to the west is the Salar Pipanaco, a topographic depression with internal drainage and a salt flat. To the east is a similar depression almost closed, the Tucumán basin which is filled with a thick sequence of Quaternary deposits. The origin of the lattter one has been postulated as extensional, according to gravimetric investigations by Pomposiello et al. (1993). The origin of the Salar Pipanaco depression is still poorly understood. Further geophysical investigations are necessary in this area to solve these significant questions.

Young vertical uplifting is well documented for the whole region, where meandering valleys have deeply dissected in the basement by cutting Quaternary beds. Moreover there are remnants of fluvial Quaternary deposits at high positions in the mountains, completely isolated from their original areas. It still remains an open question wether differential vertical uplifting could produce upper crustal bending and wether such bending could be responsible for the extensional stresses generating the normal faults. If the reverse fault surfaces are not strictly cylindrical, spatial problems leading to the deformation of the hanging fault block could arise during displacement. Such deformations could be another hypothetical cause of the normal faults affecting the hanging blocks.

Preliminary observations in other areas of the Sierras Pampeanas, such as the west border of the Sierra Grande of Córdoba, have shown that the extensional structures could have a wider distribution. The young tectonic evolution of the Sierras Pampeanas have some complexities that with the present day information can only be glimpsed at.

REFERENCES

Beder R. 1920. Ensayo de un diagrama de la estructura tectónica terciaria de la sierra de Córdoba. In Windhausen (Ed), 1931 Geología Argentina II . p.172. Buenos Aires.

Gonzalez O. 1995. Descripción geológica de la Hoja 2766 II, San Miguel de Tucumán. Secretaría de Minería. Buenos Aires. Inédito.

Gonzalez Bonorino F. 1950. Algunos problemas geológicos de las Sierras Pampeanas. Revista Asociación Geológica Argentina V. 82-110.

Gross W. 1948. Cuadro tectónico del valle de la Punilla. Revista Asociación Geológica Argentina VII.

Hoek E. & Bray J. 1977. Rock slope Engineering. The Institution of Mining and Metallurgy. 197 pp. London.

Jordan T. & Allmendinger R. 1986. The Sierras Pampeanas of Argentina: a modern analogue of Rocky Mountains foreland deformation. American Journal of Science 286. 737-764.

Pomposiello M.C., Mon R. & Diaz M.T. 1993. The gravity field of the Tucumán plain and its implications in the Structural Geology. Géodynamique 6. 3-8.

Schlangintweit O. 1954. Una interesante dislocación en el Potrero de Garay, Córdoba. Revista de la Asociación Geológica Argentina 3. 135-153.

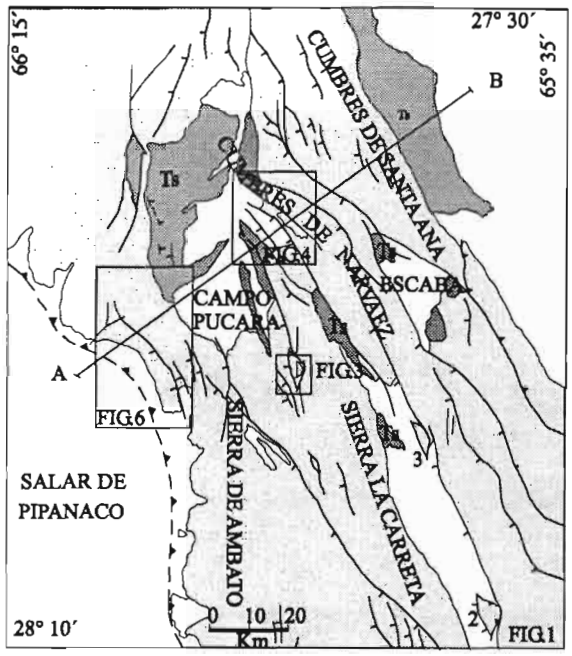
66° 15′
27° 30′
65° 35′
B
CUMBRES DE SANTA ANA
CUMBRES DE NARVAEZ
ESCABA
CAMPO PUCARA
FIG4
FIG5
FIG6
A
SIERRA DE AMBATO
SIERRA LA CARRETA
SALAR DE PIPANACO
28° 10′
0 10 20
Km
FIG1

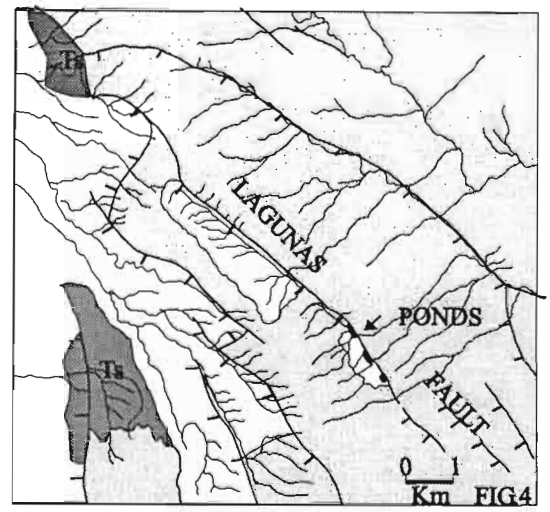
LAGUNAS
PONDS
FAULT
0 1
Km
FIG4

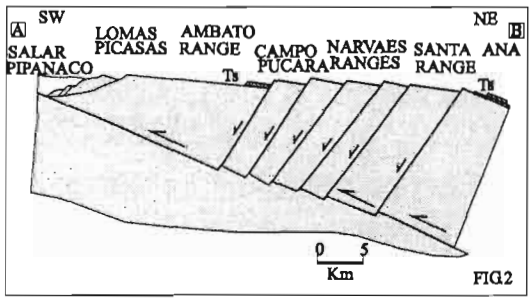
SW
NE
SALAR PIPANACO
LOMAS PICASAS
AMBATO RANGE
CAMPO PUCARA
NARVAES RANGES
SANTA ANA RANGE
0 5
Km
FIG2

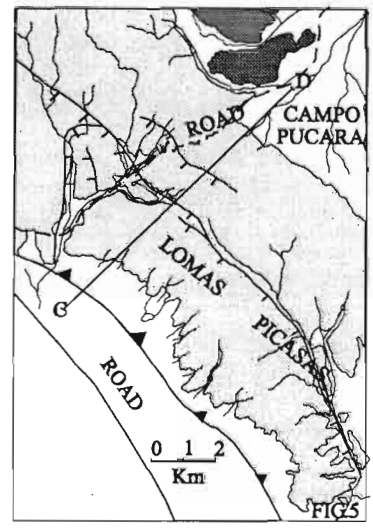
ROAD
CAMPO PUCARA
LOMAS PICASAS
ROAD
0 1 2
Km
FIG5

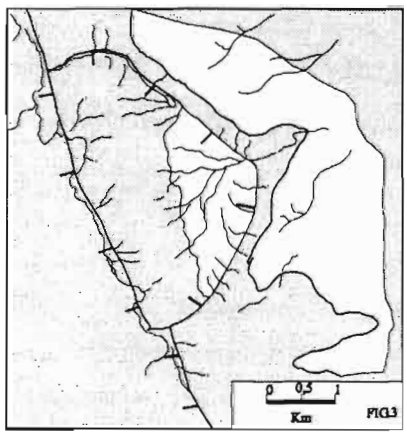
0 0,5 1
Km
FIG3

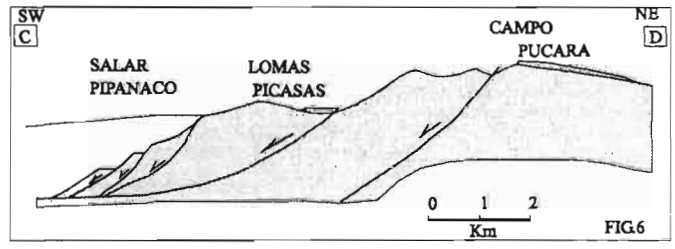
SW
NE
SALAR PIPANACO
LOMAS PICASAS
CAMPO PUCARA
0 1 2
Km
FIG6

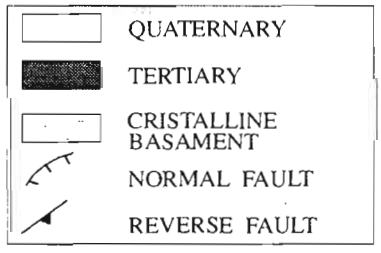
QUATERNARY
TERTIARY
CRISTALLINE BASAMENT
NORMAL FAULT
REVERSE FAULT

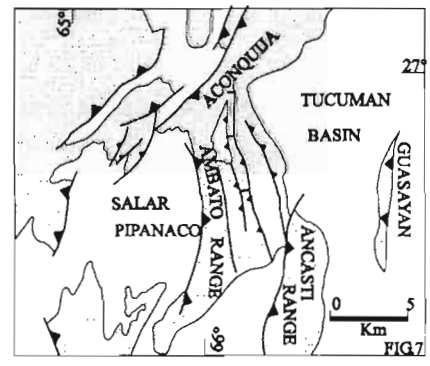
65°
ACONQUIJA
27°
TUCUMAN BASIN
GUASAYAN
AMBATO RANGE
SALAR PIPANACO
ANCASTI RANGE
66°
0 5
Km
FIG7

GEOCHEMISTRY AND TECTONICS AT THE SOUTHERN TERMINATION OF THE NORTHERN VOLCANIC ZONE (RIOBAMBA VOLCANOES, ECUADOR); PRELIMINARY RESULTS

M. MONZIER (1-3), C. ROBIN (2), M.L. HALL (3), J. COTTEN (4) and P. SAMANIEGO (2-3)

(1) Institut de Recherche pour le Développement (IRD, previously ORSTOM), A. P. 17-12-857, Quito, Ecuador (michmari@orstom.org.ec)
(2) IRD, Université Blaise Pascal, 5 rue Kessler, 63038, Clermont-Ferrand cedex, France, (robin@opgc.univ-bpclermont.fr)
(3) Instituto Geofisico, Escuela Politecnica Nacional (IG-EPN), A. P. 17-01-2759, Quito, Ecuador (geofisico@accessinter.net)
(4) UMR 6538, Université de Bretagne Occidentale, B.P. 809, 29285, Brest, France (Jo.Cotten@univ-brest.fr)

KEY WORDS: Andean NVZ, arc termination, low-Y volcanics, infracrustal AFC processes

INTRODUCTION:

The Riobamba volcanoes constitute the southern termination of the NVZ. To the south, active volcanism is absent along a 1600 km long segment of the Andes (Fig. 1A-B). This work presents preliminary geochemical data for these volcanoes and relates them to an unusual underlying slab and the complex seismo-tectonics of the continental crust in the area.

SEISMOTECTONICS:

In the Riobamba area, the main Ecuadorian arc becomes frontal and Sangay volcano lies unusually eastward (Fig. 1C). Contrary to southern Colombia and Ecuador, beneath which intermediate depth seismicity is almost absent, a strongly seismogenic slablet dipping • 35° towards N58°E is present under the Sangay area at • 130 km beneath the volcano (Fig. 1D). The N58°E boundary between this slablet to the south and the weakly seismogenic slab to the north reflects a sharp change in the thermal characteristics of the subducted oceanic crust, and corresponds to a tear running from the Grijalva Fracture Zone (GFZ; Fig. 1B), that separates the young (<24 My) crust subducted under Colombia and Ecuador, from older crust (>32 My) beneath southern Ecuador and northern Peru (Monzier et al., 1999). To the

south, another N58°E boundary probably separates this slablet from the shallow dipping slab which is typical of southern Ecuador and northern Peru. Due to the convergence motion between the Nazca and South America plates (• 8.0 cm/y in a direction • N80°E; De Mets et al., 1990), the N58°E tear in the slab slowly sweeps the area. Calculations show that this tear was under the Chimborazo-Puñalica area • 1.35 My BP and under the Calpi-Tungurahua area • 0.7 My BP; it is presently under Tulabug-El Altar volcanoes and will be under Sangay in • 1.16 My (Fig. 1D). These calculations neglect, among other factors, the dextral strike-slip motion between the North Andean Block and the rest of South America. The southern termination of the NVZ -which is oriented • N148°E in contrast with the usual N30°E orientation of the Ecuadorian arc- is exactly perpendicular to the N58°E dipping Sangay slablet. Thus, to a large extent, the volcanic history of the termination has been controlled by the southeastward migration of this narrow piece of old oceanic crust, bounded to the North by the GFZ but also cut by numerous secondary fracture zones parallel to the GFZ.

RIOBAMBA VOLCANOES:

Plio-Quaternary volcanoes are located on the edges or in the middle of the Riobamba pull-apart basin (a segment of the Interandean Valley), with the exception of El Altar and Sangay, which are clearly located in the Eastern Cordillera of Ecuador (Fig. 2A-B). In addition to the old and eroded Igualata and Huisla edifices, four major Pleistocene volcanoes developed in the area, as well as several smaller volcanic cones. The Chimborazo complex formed first by effusive eruptions (acid andesites), then by explosive activity (dacite-rhyolite); some 35,000 y BP, this volcano experienced cone collapse and a large-scale debris avalanche. Post-collapse activity ended with eruptions of basic andesites before 11,000 y BP (Clapperton, 1990; Kilian et al., 1995). The Tungurahua complex is composed of three successive volcanic edifices, the first two of which were partially destroyed by sector collapse. The last collapse event occurred • 3,000 years ago, preceding the construction of the present cone, which is dominated by basic andesites (Hall et al., 1999). Over the past 500,000 y, the Sangay volcanic complex also has had three successive andesitic edifices. The two former cones have been largely destroyed by sector collapses. The present edifice is active at least since 14,000 y BP (Monzier et al., 1999). Finally, El Altar volcano consists of subglacial andesite breccias, with the remnants of a shallow (< 3 km) magma chamber, including a large rhyolitic body and a subordinate diorite body. Its development ended with the cataclysmic evisceration of this chamber (probably accompanied by sector collapse) that resulted in caldera formation; subsequent glacial erosion has deeply eroded the edifice (Monzier et al., in prep.). Other volcanic centers of the Riobamba area include the small cones of Calpi and Tulabug. For all the Riobamba edifices, extensive geochemical sampling is currently done or in progress.

CHARACTERISTICS OF RIOBAMBA VOLCANICS AND DISCUSSION:

A striking feature of the Riobamba volcanics is that basic rocks are more abundant here than in the rest of the NVZ (Fig. 2C). This may be explained by the fact that most of the these volcanoes are associated

with a large pull-apart basin, bounded by major N22°E strike-slip faults oblique to the regional N-S orientation of the Cordillera, and profusely cut by transverse faults. Such a faulted crustal structure provides pathways for rising magmas and thus limits the effect of upper crustal fractionation processes. Except for this feature, Riobamba volcanics are not significantly different from other NVZ arc rocks, showing the usual enrichment in incompatible elements as the distance to the trench increases. All share similarly low Y and HREE contents (Fig. 2D). However, Riobamba volcanics dont show the marked decrease in Y and Zr (Fig. 2E) frequently observed for differentiated rocks from the rest of the arc, and certainly caused by upper crustal amphibole fractionation. By contrast, and except for the most evolved compositions, Y contents remain almost constant and Zr clearly acts as an incompatible element in Riobamba volcanics. For the Sangay suite, the low concentration in Y, as well as the presence of Sr-rich andesites, can be explained by AFC processes occuring at the base of a 50 km-thick crust, where basaltic melts pond and assimilate remelts of previously underplated, compositionally similar basaltic material (Monzier et al., 1999). Similar AFC processes probably affect other magmas of the southern termination, as indicated, for example, by samples from Tulabug, that comprise basalts (53% SiO_2 & 725 ppm Sr) associated with Sr-rich andesites (58% SiO_2 & 1000 ppm Sr, but not plagioclase cumulative). Furthermore, partial melting of altered Cretaceous MORB, tectonically accreted to the lower crust, was proposed by Kilian et al. (1995) to explain the genesis of some Sr-rich andesites from the Chimborazo complex. Thus, AFC processes seem to be active at the base of the crust beneath most Riobamba volcanoes. Work is currently being done to constrain these processes and better understand the magmatic evolution of the whole area.

REFERENCES

Clapperton, C. M., 1990. Glacial and volcanic geomorphology of the Chimborazo-Carihuairazo Massif, Ecuadorian Andes. Transactions of the Royal Society of Edinburgh: Earth Sciences, 81: 91-116.

DeMets C., Gordon, R.G., Argus, D.F. and Stein, S., 1990. Current plate motions. Geophys. J. Int., 101: 425-478.

Droux, A. and Delaloye, M., 1996. Petrography and geochemistry of Plio-Quaternary calc-alkaline volcanoes of southwestern Colombia. Journal of South American Earth Sciences, 9, 1/2: 27-41.

Hall, M.L., Robin, C., Beate, B., Mothes, P. and Monzier, M., 1999. Tungurahua Volcano, Ecuador : structure, eruptive history and hazards. J. Volcanol. Geotherm. Res., in press.

Kilian, R., Hegner, E., Fortier, S. and Satir, M., 1995. Magma evolution within the accretionary mafic basement of Quaternary Chimborazo and associated volcanoes (Western Ecuador). Revista Geologica de Chile, 22, 2: 203-218.

Monzier, M., Robin, C., Samaniego, P., Hall, M.L., Cotten, J., Mothes, P. and Arnaud N., 1999. Sangay volcano, Ecuador: structural development, present activity and petrology. J. Volcanol. Geotherm. Res., in press.

Monzier, M., Andrade, D., Cotten, J., Hidalgo, S., Robin, C. and Witt, C., in prep. El Altar caldera (Ecuador): subglacial andesitic volcanism and caldera formation by evisceration of a shallow rhyolitic magma chamber. J. Volcanol. Geotherm. Res., ...

GEOCHEMISTRY OF TRIASSIC VOLCANIC ROCKS FROM THE COASTAL RANGE, CENTRAL CHILE.

Diego MORATA, Luis AGUIRRE, Marcela OYARZÚN and Mario VERGARA (1)

(1) Departamento de Geología. Facultad de Ciencias Físicas y Matemáticas. Universidad de Chile. Casilla 13518, Correo 21, Santiago, Chile. E-mail: dmorata@cec.uchile.cl

KEY WORDS: Geochemistry, Sr-Nd isotopes, petrogenesis, Triassic magmatism, Coastal Range, central Chile.

INTRODUCTION

The Coastal Range in central Chile is mainly composed of Meso-Cenozoic igneous and sedimentary rocks deposited on a pre-Mesozoic crystalline basement. The Triassic units are represented by the El Quereo and Pichidangui Formations; only the latter contains significant volumes of volcanic and subvolcanic rocks. The only geochemical information concerning the volcanic rocks from these units (major and trace elements) is found in Vergara *et al.* (1991) and Cancino (1992). Here we present the first isotopic (Sr and Nd) data about the volcanic rocks from the Pichidangui Formation (31°56'-32°20' Lat S) for which a bimodal magmatism has been already described (Vergara *et al.* 1991). In particular, the relationships between acid and basic volcanic rocks and their paleotectonic and petrogenetic implications will be discussed.

GEOLOGICAL CONTEXT AND PETROGRAPHY

The Pichidangui Formation, an isoclinal sequence 4000 to 5000 m thick dipping 15 to 25° to the east-southeast, was deposited in a subaquatic environment varying in time from predominantly marine to paralic, temporary continental conditions being apparent (Vergara *et al.*, 1991). The formation consists of acid and

basic lava flows with interbedded shales containing a Middle to Late Triassic marine fauna; numerous basic dykes and sills intrude this unit. Charrier (1979) suggested deposition in a Triassic graben for the strata of the Pichidangui Formation, probably caused by shearing between the Gondwana continent and a major block located to the west. Mpodozis *et al.* (1988) included all the upper Paleozoic-Triassic magmatic rocks of central-northern Chile in a Pacific margin magmatic belt of Gondwanaland. More recently Vergara *et al.* (1991), based on major and trace element chemistry, interpreted the volcanic rocks of the Pichidangui Formation as belonging to a volcanic arc floored by a quasioceanic crust. Petrographic characteristics of the acid and basic rocks are also in Oyarzún *et al.* (1997)

GEOCHEMISTRY OF THE IGNEOUS ROCKS

Thirteen fresh and slightly altered samples (five basic and eight acid rocks) were selected for chemical analysis (ICP-AES, Department of Geology, University of Chile). Nd and Sr isotopic analyses of 8 samples were performed in a TIMS at the Centro de Instrumentación Científica, University of Granada, Spain. The chemical analyses confirmed the bimodality already described for these rocks which is characterized by the presence of trachybasalt, traquiandesitic basalt and andesitic basalt whereas the acid rocks correspond to rhyolites. Al_2O_3 values range between 13.83 and 15.52% in the basic types and 11.20 to 15.19% in the acid rocks. The *[mg]* value (=Mg/(Mg+Fe^{2+})) is *c.* 0.53 in basic rocks. The Al_2O_3 values of the basic rocks as well as the projection of both the basic and acid rocks into the FeO/MgO *vs* SiO_2 diagram indicate a tholeiitic affinity.

The trace element chemistry of the basic rocks shows a general enrichment in incompatible elements compared to N-MORB with Rb ≥ Th and decreasing in values from Ta to Yb. A similar pattern has been established for the acid rocks characterized by a strong enrichment (> 10 times the normalized values) in K_2O, Rb, Ba and Th (Rb ~ Th) and strong negative anomalies in P_2O_5 and TiO_2. In these acid rocks neats negative Ta and Nb anomalies are present. With the exception of the strong P_2O_5 and TiO_2 anomalies in the acid rocks, the patterns of both compositional groups are quite similar, with general higher values in the acid rocks.

The REE patterns for the basic rocks show enrichment in LREE of 20-50 times the chondrite values and of *c.* 20 times for the HREE and the absence of Eu anomaly. Mean values for the ratios $(La/Lu)_n$, $(La/Sm)_n$ and $(La/Ce)_n$ are 2.24, 1.23 and 1.04 respectively. The acid rocks have higher total REE, 60 to 100 times the chondritic values for the LREE and 20 to 50 times for the HREE. A strong negative Eu anomaly (Eu/Eu* = 0.51) is observed. Mean values for the ratios $(La/Lu)_n$, $(La/Sm)_n$ and $(La/Ce)_n$ are 3.71, 2.30 and 1.14 respectively.

The initial isotopic compositions were calculated to 220 Ma for basic and acid rocks. The $(^{87}Sr/^{86}Sr)_i$ ranges from 0.704095 to 0.705959 in the former and from 0.699722 to 0.710328 in the latter. The

$(^{143}Nd/^{144}Nd)_i$ varies from 0.512761 to 0.512859 in the basic rocks and from 0.512110 to 0.512512 in the acid types.

DISCUSSION AND CONCLUSIONS

Basic and acid rocks plot in the "within plate" field of various discrimination geotectonic diagrams, consistent with the geodynamic extensional setting already proposed by Charrier (1979) for the Triassic units in the Coastal Range of central Chile. A well defined bimodal magmatism with tholeiitic affinity is firmly established. The similarities in trace element and REE patterns can be interpreted as a genetic link between the basic and acid rocks. Low *[mg]*, Cr and Ni values in the basic rocks indicate the absence of primary mantle-derived liquids and, consequently, a previous olivine (and/or clinopyroxene?) fractionation. Ca-rich plagioclase fractionation, previous to the genesis of the acid rocks, is suggested by the strong negative Eu anomaly observed in these rocks. Differences in trace element ratios in basic and acid rocks could be due to the action of other petrogenetic processes accompanying fractional crystallization. Thus, the neat Ta and Nb negative anomalies in the acid rocks together with their higher contents of Th and La/Nb, could be interpreted as a crustal component in their genesis. This model is strongly supported by the isotopic data (Fig.1) which show εNd in basic rocks ranging from 5.0 to 3.3 consistent with the presence of a minor crustal component whereas in the acid types εNd is in the interval 3.1- (-4.8) indicating a higher rate of crustal contamination. This contamination process is here envisaged as due to crustal extension during Triassic times which permitted the ascent of mantle material and its interaction with the granitoids which make up part of the Paleozoic basement exposed in the region (curve A, Fig.1). Curve B in Fig.1 was modelled for comparison using an standard value for the upper continental crust to show the effect of contamination with a more Sr-radiogenic end term. In both trends, the crustal component is higher than 10% but lower than 15% for the basic rocks and still higher for the acid types.

ACKNOWLEDGMENTS

This work has been supported by the FONDECYT Project 1961108. We thank F. Bea (University of Granada, Spain) for analytical facilities in the isotopic analyses.

Figure 1.- $(^{87}Sr/^{86}Sr)_i$ vs εNd_t (calculated to 220 Ma) for the Triassic volcanic rocks of the Coastal Range in central Chile. Symbols as follows: full squares= basic rocks; full circles= acid rocks; open triangles= Carboniferous granitoids (Santo Domingo Complex, Parada et al., 1999). Values for the depleted mantle (DM), prevalent mantle (PREMA) and mantle array (shaded area) taken from Rollinson (1993). UCC= Upper Continental Crust ($^{87}Sr/^{86}Sr$ = 0.7369; Sr = 160 ppm; $^{143}Nd/^{144}Nd$ = 0.51212; Nd = 31 ppm) from Faure (1986). Path A= mixing model between PREMA and Carboniferous granitoids; path B= mixing model between PREMA and UCC. Compositional intervals in both paths are indicated by crosses.

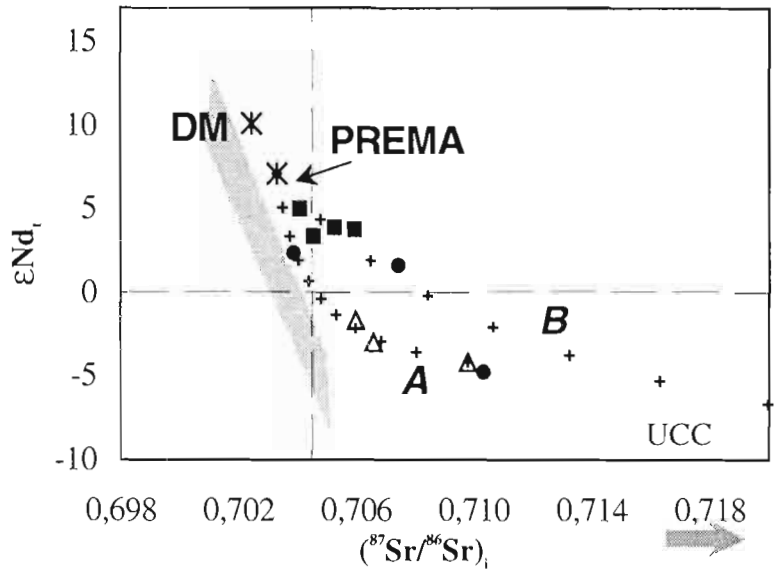

REFERENCES

Cancino A. 1992. *Memoria de Título, Universidad de Chile* (inédita), 259 p.

Charrier R. 1979.. *Comunicaciones*, 26, 1-37.

Faure G. (1986). *Principles of Isotope Geology*. John Willey & Sons, 589 p.

Mpodozis C., Kay S., Nasi C., Moscoso R. and Cornejo P. 1988. *Comunicaciones*, 39, 268.

Oyarzún M., Aguirre L. and Morata D. 1997. *8° Congreso Geológico Chileno, Actas* vol. II, 1424-1428.

Parada M.A., Nyström J.O. and Levi B. 1999.. *Lithos*, 46, 505-521.

Rollinson H. 1993. *Using geochemical data: evaluation, presentation, interpretation*. Longman Scientific & Technical, 352 p.

Vergara M., López-Escobar L. and Cancino A. 1991. *Geological Society of America, Special Paper* 265, 93-98.

CRETACEOUS TO PALEOGENE GEOLOGY OF THE SALAR DE ATACAMA BASIN, NORTHERN CHILE: A REAPPRAISAL OF THE PURILACTIS GROUP STRATIGRAPHY

Constantino Mpodozis[1], César Arriagada[2], Pierrick Roperch[3]

(1) Servicio Nacional de Geología y Minería, Santiago, (cmpodozi@sernageomin.cl)
(2) Departamento de Geología, Universidad de Chile, (carriaga@quad.dgl.uchile.cl)
(3) IRD/Dep. de Geología, Universidad de Chile (properch@dgf.uchile.cl)

Keywords: Purilactis Group, Salar de Atacama, Northern Chile

INTRODUCTION

The transient subsiding Salar de Atacama basin in Northern Chile is one of the largest negative topographic anomalies occurring along the western slope of the Central Andes. More than 6.000 m of Cretaceous-Oligocene sedimentary sequences, described in the literature under the name of "Purilactis Group" (Charrier and Reutter, 1994; Hartley et al., 1992), form most of the basin fill. Although recognized at the subsurface in the Toconao 1 well (Muñoz et al, 1997) the main outcrops of the Purilactis Group occur at the El Bordo Escarpment, a prominent 120 km long, NS cliff confining the basin to the West, and forming the western edge of the (Late Paleozoic) basement block of the Cordillera de Domeyko (Figure 1a). Numerous publications have described the stratigraphy of the Purilactis Group. However, because of the lack of fossiliferous horizons and/or interbedded volcanics suitable for dating, many doubts concerning nomenclature, internal stratigraphical architecture and age, still remain. An ongoing tectonic and paleomagnetic study (see Arriagada et al, this volume) that includes the classical localities of Barros Arana and El Bordo on the western border of the Atacama basin has permitted to obtain new K-Ar ages in previously undated volcanic horizons. This, and the restudy of outcrops to the east, south and north of the Salar de Atacama (Poquis, Quebrada Pajonales, Agua Colorada, Ayquina, Tuina etc).allows to propose a new stratigraphic system for the Purilactis Group.

A Revised Stratigraphy for the Purilactis Group

Figure 1b is an integrated stratigraphic column for the Purilactis Group assembled according to the observations and new data collected along the El Bordo Escarpment. Part of the evidence and new data supporting the proposed stratigraphic system can be summarized as follows:

1) Lower units of the Purilactis Group include the classical Tonel and Purilactis formations (Dingman, 1963). East of Cerro Quimal, the Tonel Formation unconformably overlies the Paleozoic basement of the

Cordillera de Domeyko. There, 60 m of basement-clast breccias are covered by finely bedded red sandstones, and near the top (Cerros de Tonel) massive evaporite horizons were deposited in a playa-lake environment (Hartley et al, 1992). A faulted (détached) unconformity marks an abrupt upwards transition to the Purilactis formation proper that is a sequence of 2800 m of sandstones, red mudstones and minor conglomerate deposited in proximal fluvial, alluvial fan lobes and lacustrine environments (Hartley et al., 1992). Paleomagnetic studies indicate the prevalence of rocks exhibiting only normal polarity (Arriagada et al, this volume) suggesting that both units could have been deposited during the long Cretaceous Normal Chron (119-84 Ma).

2) Proximal alluvial fan coarse-grained conglomerates with volcanic and granitoid clasts up to 1 m in diameter occur at the core of the Barros Arana Syncline ("upper Purilactis formation," Dingman, 1963, "Cinchado formation", Hartley et al., 1992) which is here refered to as the Barros Arana Strata (Figures 1). These units testify to a drastic change in sediment energy transport that could be associated with uplift of the adjacent Cordillera de Domeyko. At Cerros de Ayquina, aprox. 45 km to the north, these units rest directly on top of the Paleozoic basement. They could be, in part, equivalent to the red beds of the Tolar-Tambillos formations, which have been interpreted as syn-post orogenic deposits associated with a regionally significant Late Cretaceous compressional event that occurred between 109-83 Ma (Ladino et al., this volume).

3) South of Cerro Quimal, (Cerro Totola, Cerro Negro, Cerro Pintado, Figure 1) a 800 m thick sequence of basaltic andesitic lava flows interbedded with welded rhyolitic ignimbrites, and coarse volcaniclastic sediment (Cerro Totola Strata) rests unconformably over older Cretaceous units. Nine new K/Ar ages (whole rock, amphibole and biotite) between 70-65 Ma indicate a Maestrichtian age. Further south, in Cerro Pintado, the same lavas are interbedded with red sandstones, conglomerates and impure, marine, bioclastic limestones. The latter could represent the westernmost exposures of marine sediments that record the regionally widespread Maestrichtian transgression of the Salta Group (Lecho and Yacoraite formations Salfity et al, 1985).

4) A Paleocene-Eocene clastic sequence ("Orange Unit") unconformably overlies the Cerro Totola lavas in the southern El Bordo Escarpment area. This fining upward sequence begins with aprox. 400 m of conglomerates that is succeeded by 500 m of semiconsolidated sandstones alternating with thin evaporite (gypsum) beds. Near Pan de Azúcar, 50 km south of the Salar de Atacama, this unit includes andesitic lava horizons that have been dated (K-Ar) at around 57-58 Ma (Gardeweg et al 1994). This sequence can be correlated with the Chojfias formation of the Zapaleri-Poquis region and the Santa Bárbara Subgroup on the Argentine Puna (Salfity et al., 1985).

5) A more than 1000 meter thick section of Eocene (Oligocene?) conglomerates, (Loma Amarilla strata) that rests on top of the "Orange Unit" east of Cerros Negros (Figure 1) represents one of the more regionally important map-scale units of the Purilactis Group. Internal progressive unconformities occur in

the basal part of the sequence where very coarse conglomerates alternate with tuffaceous horizons dated (K-Ar, 39Ar/40Ar) between 42-39 Ma (Ramírez and Gardeweg 1982, Hammerschmidt et al 1992). Mpodozis et al (1993) suggested that these deposits could be syntectonic to the Eocene "incaic" deformation. This event was associated with left lateral transpression, clockwise block rotations and generalized uplift of the Cordillera de Domeyko basement block (Mpodozis et al, 1993, Arriagada et al, this volume). Although still poorly studied, small outcrops of volcaniclastic conglomerates near Cerro Negro could represent sediments associated with the reactivation of Incaic faults. These outcrops could represent the youngest unit of the Purilactis Group (Cerro Puntiagudo Strata, Figure1)

Discussion and Conclusions

The Purilactis Group is a stratigraphic succession of seven regionally distinguishable, map-scale, sedimentary and volcanic sequences generally bounded by angular and/or erosional unconformities. Available radiometric ages suggest a Lower Cretaceous to Oligocene (?) age for the Purilactis Group as a whole. Despite formal nomenclature differences, the stratigraphic section along the El Bordo Escarpment is consistent with the stratigraphy of the deep Toconao 1 well in the central Atacama basin (Muñoz et al, 1997). However, only the uppermost units of the Purilactis Group are present in the well, where Cerro Totola strata equivalents rest directly over Paleozoic basement. This sequence shows that partially overlapping depocenters were formed during the complex evolution of the Atacama-Purilactis basin. This revision of the Purilactis Group stratigraphy provides a new framework to constrain paleogeographic interpretations and/or regional correlations for the Cretaceous-Paleogene of the Central Andes.

Acknowledgments: Research funds provided by FONDECYT, Chile (grant 1970002) and the cooperative program IRD/Departamento de Geología, Universidad de Chile. Published under the auspices of the Subdirección de Geología, SERNAGEOMIN.

REFERENCES

Charrier, R., Reutter, K. 1994. Tectonics of the Southern Central Andes, Springer Verlag, Berlin Heidelberg, New York.
Dingman, R. J., 1963. Cuadrángulo Tulor: Carta Geológica de Chile N°11 (1:50.000), p. 1-35, Santiago.
Gardeweg, M., Pino, H., Ramírez, C. F., Davidson, J. 1994. Servicio Nacional de Geología y Minería, Documentos de Trabajo, N°7 (1:100.000), Santiago.
Götze, H-J., Lahmeyer, B., Schmidt, S., and Strunk, S. 1994. Tectonics of the Southern Central Andes.
Hammerschmidt, K., Döbel, R., Friedrichsen, H. 1992. Tectonophysics, v. 202, p. 55-81.
Hartley, A., Flint, S., Turner, P., Jolley, E. J. 1992. Journal of South American Earth Sciences, v. 5 (3/4), p. 275-296.
Mpodozis, C., Marinovic, N., Smoje, I. 1993. Second Symposium International Géodynamique Andine, p. 225-228., ORSTOM.éditions, Paris.
Muñoz, N., Charrier, R., Reutter, J-K. 1997. VIII Congreso Geológico Chileno, v 1, p 195-199, Antofagasta.
Ramírez, C. F., Gardeweg, M. 1982. Carta Geológica de Chile N°58 (1:250.000), p. 1-121, Santiago.
Salfity, J., Marquillas, R., Gardeweg, M., Ramírez, C., Davidson, J. 1985. IV Congreso Geológico Chileno, v. 4, 1 654-1 667, Antofagasta.

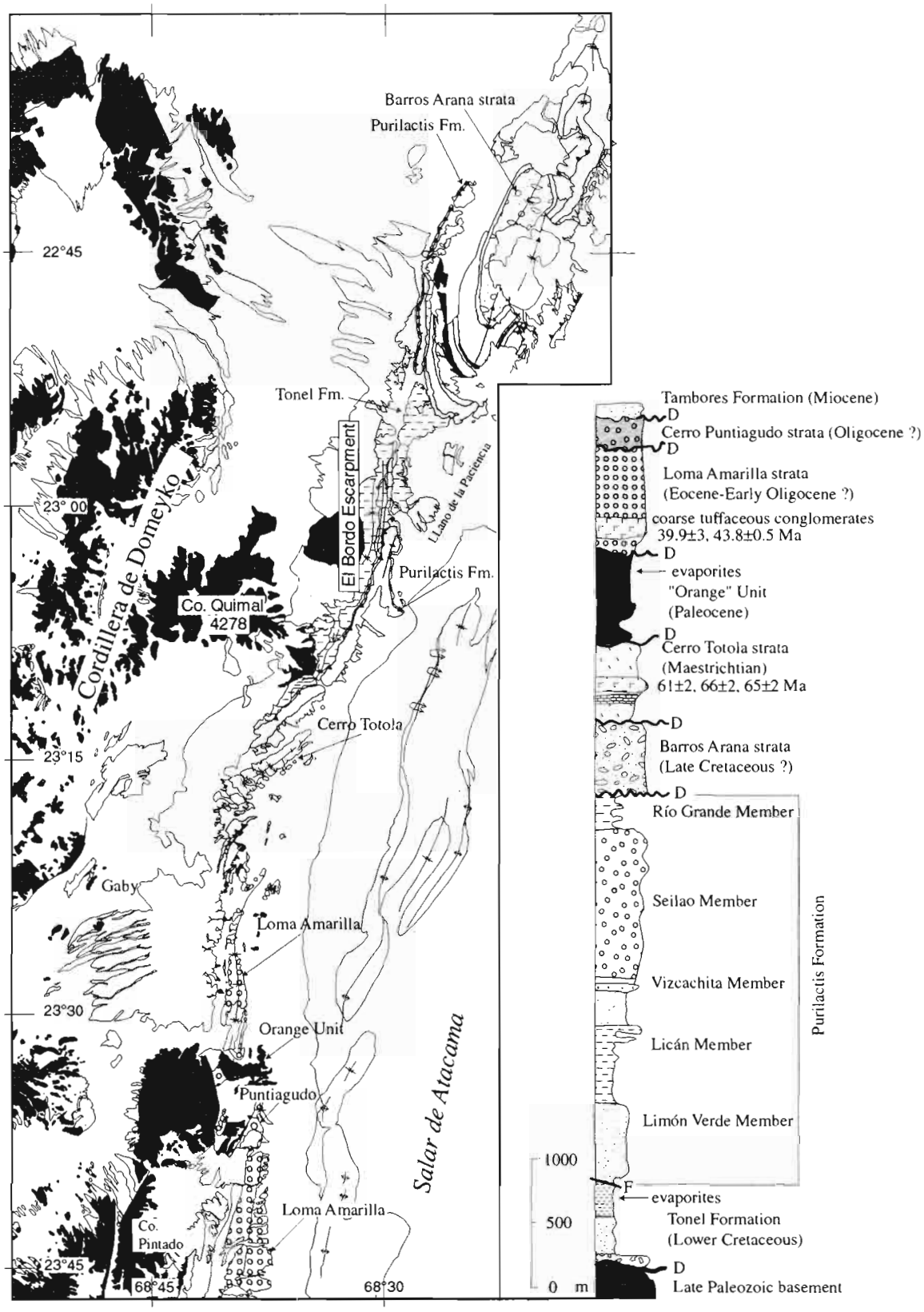

Figure 1: Simplified geological map and stratigraphic section of the El Bordo Escarpment area.

OLIGOCENE-EARLY MIOCENE COASTAL MAGMATIC BELT IN SOUTH-CENTRAL CHILEAN ANDES (37°- 44° S)

Jorge MUÑOZ(1), Rosa TRONCOSO(1), Paul DUHART(1), Pedro CRIGNOLA(1), Lang FARMER(2), Charles STERN(2)

(1)Servicio Nacional de Geología y Minería, Av. La Paz 406, sngmpv@entelchile.net, Puerto Varas, Chile
(2)University of Colorado, Boulder, CO 80309, sternc@stripe.colorado.edu, farmer@cires.colorado.edu,USA

KEY WORDS: Tertiary, Andes, arc magmatism, tectonism, geochronology, petrogenesis

INTRODUCTION

Oligocene-early Miocene magmatism and associated sedimentation in south-central Andes between 37° and 44° S were developed along the Central Valley and on the Coastal Cordillera as far west as along the coastal line in Chile, herein referred as the Coastal Magmatic Belt, and also along the Main Andean Cordillera and to the east in the Argentine extra-Andean region (Figure 1). Oligocene-early Miocene Coastal Magmatic Belt developed in association with late Oligocene continental and late Oligocene-middle Miocene marine sedimentary sequences, although the peak of the magmatic activity ended prior to rapid subsidence associated with the peak of the Miocene marine sedimentation.

TECTONIC SETTING

Oligocene-early Miocene Coastal Magmatic Belt developed during a regionally widespread episode of late Oligocene-Miocene extensional tectonism, related to a major plate reorganizations in the southeast Pacific (Tebbens and Cande, 1997) and to an increase in plate convergence rates below southern Andes (Pardo-Casas and Molnar, 1987), producing changes in the geometry of plate subduction (Frutos and Cisternas, 1994). Convergence rates remain relatively high and without major changes during the late Oligocene-early to middle Miocene (Pardo-Casas and Molnar, 1987). Approximately north-south and northwest trending normal and strike slip faults systems (Figure 1) were active during the Oligocene-early Miocene, generating a proto-

Central Valley and controlling the emplacement of magmatism and location of sedimentary basins. Northwest trending strike slip faults represent old structures probably actives also during Paleozoic and Mesozoic times. Large and deep positive magnetic and gravity anomalies recognized below the Central Valley between 40° and 42° S (Figure 1) are interpreted as produced by deep mafic intrusion and lithosphere mantle upwelling generated during extension. Magmatic discontinuities in the Coastal Magmatic Belt are recognized between Temuco and Bahía Capitanes and Ancud and Castro (Figure 1) and are coincident with uplifted tectonic blocks corresponding with Paleozoic to Triassic metamorphic rocks (Duhart *et al.*, 1999) and limited by northwest trending strike slip faults.

PETROGRAPHY

Lava flows, pyroclastic flows, volcanic breccias, domes, necks, sills and dikes ranging from basaltic to dacite-rhyolitic are represented in the Coastal Magmatic Belt, although silicic compositions are better represented in pyroclastic rocks and domes which are locally volumetrically important. Main exposures are in the areas Los Angeles-Temuco, along the coastal line at Bahía Capitanes and Estaquilla-Caleta Parga, Ancud and south of

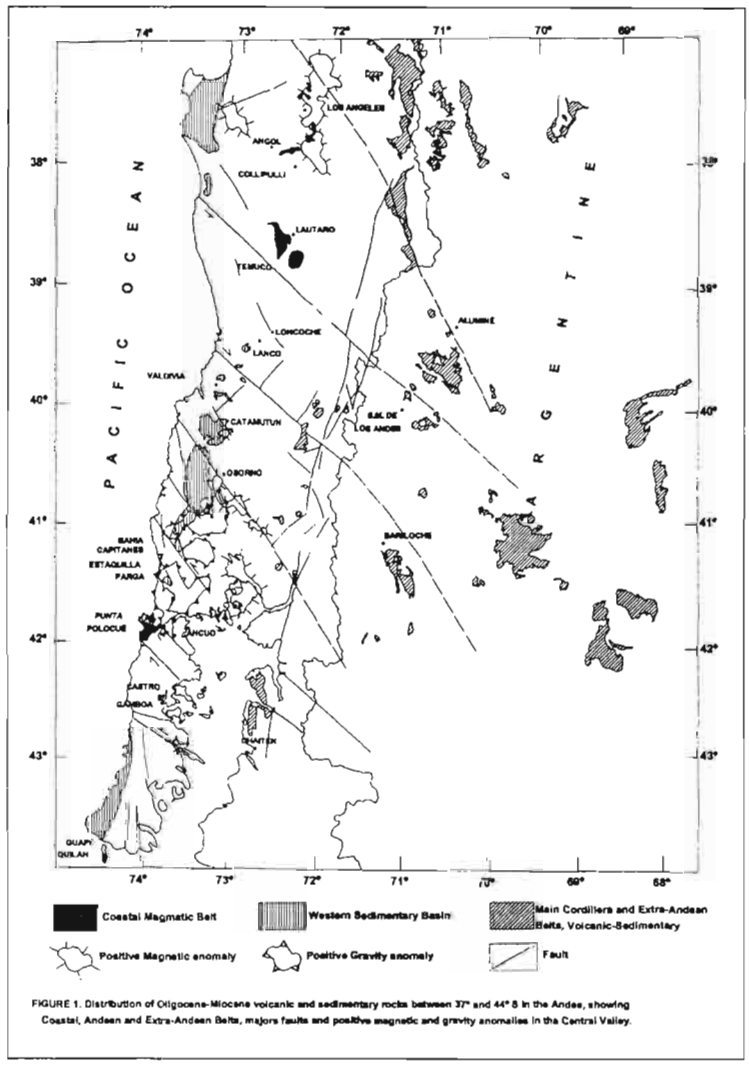

FIGURE 1. Distribution of Oligocene-Miocene volcanic and sedimentary rocks between 37° and 44° S in the Andes, showing Coastal, Andean and Extra-Andean Belts, majors faults and positive magnetic and gravity anomalies in the Central Valley.

Castro (Vergara and Munizaga, 1974; Valenzuela, 1984; Stern and Vergara, 1992; Alfaro *et al.*, 1994; Troncoso *et al.*, 1994; Muñoz *et al.*, 1997; López y Vergara, 1997) and in Guapi Quilán islands south of Chiloé (Figure 1). Porphyry to aphanitic clinopyroxene and clinopyroxene-olivine basaltic andesites and clinopyroxene andesites are the dominant lithologies, but also amphibole dacites, amphibole-orthopyroxene-clinopyroxene andesites and two pyroxenes andesites and olivine-clinopyroxene basalts are respectively represented in the Temuco and Parga areas. Fluidal glassy clinopyroxene dacitic lavas and domes are also represented at Capitanes and Estaquilla areas. Pyroclastic rocks are banded crystal to lithic tuffs with plagioclase, andesitic fragments, ash, brown glass and local minor quartz, locally interbeded with continental and marine sedimentary rocks. Volcaniclastic sandstone are composed by plagioclase, ash and volcanic fragments in a carbonate matrix. Coarse porphyry quartz-biotite dacitic dikes and sills are emplazed in metamorphic rocks near Castro and microporphyry clinopyroxene-olivine basalts to porphyry dacites are distributed in some of the Guapi Quilán islands immediately south of Chiloé Island.

GEOCHRONOLOGY

Available K-Ar data for samples from the Coastal Magmatic Belt from Los Angeles to Chiloé range between 37 and 20 Ma (Vergara and Munizaga, 1974; García *et al.*, 1988; Stern and Vergara, 1992; Cisternas and Frutos, 1994; Muñoz *et al.*, 1997; López and Vergara, 1997). Oldest K-Ar were obtained in a dacite south of Castro (37.2±1.2 Ma), in basaltic andesites from Bahía Capitanes (32.9±1.0 and 27.5±1.0 Ma) and in andesites north of Temuco (28.1±1.1 Ma). However, most of the K-Ar ages are in the range 20-27 Ma. K-Ar ages of 20.7 and 21.6 Ma were reported in two samples collected in the Colegual 2 drill hole completed by ENAP (Vergara and Munizaga, 1974; McDonough *et al.*, in prep.). A late Oligocene U-Pb age (23.5±0.5 Ma) was obtained in zircons collected from an ash fall deposit between two coal layer interbeded with continental sedimentary rocks along the Central Valley north of Osorno, at the Catamutún coal mine (Elgueta and Urqueta, 1998). K-Ar data confirm the Oligocene-early Miocene age for the Coastal Magmatic Belt and evidence an important peak during the Oligocene-Miocene limit.

PETROCHEMISTRY

Rocks range from basaltic to rhyolitic in composition and are generally subalkaline in character although a few mildly alkaline basaltic rocks occur along the coast at Bahía Capitanes, Caleta Parga and Ancud.

For mafic rocks, rare-earth-elements (REE) display light-rare-earth (LREE) enrichment relative to heavy-rare-hearth (HREE) with La/Yb ranging between 4 to 7. Alkali-earth-elements are variably enriched relative to LREE, with Ba/La ranging between 8 to 34 which spans the range between oceanic island and convergent plate boundary magmas. Also, high-field-strength elements such as Nb are variable depleted relative to REE, with La/Nb ranging from 1 to 2.5, which also spans the range from oceanic island to convergent plate boundary magma types. Sr and Nd isotopic ratios for mafic rocks vary from more primitive than any modern Andean magma erupted at the same latitude to similar to recently erupted magmas in the southern Andes. The data suggest variable sources for mafic magmas. Dacites and rhyolites have more radiogenic Sr and Nd isotopic composition possibly reflecting crustal contamination.

DISCUSSION

The Coastal Magmatic Belt between 37° and 44°S is interpreted as the Oligocene-early Miocene volcanic front and, as indicated by structural and geophysical interpretations, magmatism was related to crustal extension, crustal thinning and mantle upwelling. Synchronic volcanism north of 36°S have also been related to crustal extension and thinning (Thiele *et al.*, 1991; Vergara *et al.*, in press). Chemical and isotopic data suggests an anomalous volcanic front with diverse sources for the magmas, such as both non-modified oceanic type asthenospheric mantle and asthenosphere variably contaminated by subduction processes, as well as intra-crustal assimilation. Oligocene-early Miocene magmatism, extensional tectonism, crustal thinning and mantle upwelling in this portion of the southern Andes are associated to major plate reorganization in the southeast Pacific.

REFERENCES

Alfaro, G.; M. Vukasvic; R. Troncoso; M.E. Cisternas, 1994. Aeromagnetometría en la ubicación de cuerpos volcánicos en el ambito de la Cordillera de la Costa Sur: El volcanismo Terciario de Punta Capitanes, Decima Región. *In* Séptimo Congreso Geológico Chileno, 1, 556-561. Concepción.

Cisternas, M.E.; Frutos, J. 1994. Evolución tectónico-paleogeográfico de la cuenca terciaria de los Andes del sur de Chile (37°30'-40°30' L.S). *In* Séptimo Congreso Geológico Chileno, 1, 6-12. Concepción.

Duhart, P.; Muñoz, J.; McDonough, M.; Martin, M.; Villeuneve, M. 1999. $^{207}Pb/^{206}Pb$ and $^{39}Ar/^{40}Ar$ geochronology of the Coastal Metamorphic Belt between 41°-42° S in Central-South Chile. 4th International Symposium on Andean Geodynamics. Göttingem, Germany.

Elgueta, S.; Urqueta, J. 1998. Sedimentología y estratigrafía de las cuencas terciarias en la Región de Los Lagos (39°-42° S), Chile. *In* SERNAGEOMIN, 1998. Estudio Geológico-Económico de la X[a] Región Norte. IR-15-98, 6 Vols., 27 mapas. Santiago.

García, A.; Beck, M.E.; Burmester, R.F.; Munizaga, F.; Hervé, F. 1988. Palaeomagnetic reconnaissance of the Región de Los Lagos, southern Chile, and its tectonic implications. Revista Geológica de Chile, 15, 1, 13-30.

López, L; Vergara, M. 1997. Eocene-Miocene longitudinal depression and Quaternary volcanism in the southern Andes, Chile (33°-42.5° S): a geochemical comparison. Revista Geológica de Chile, 24, 2, 227-244.

McDonough, M.R., Herrero, C.; van der Velden, A.; Martin, M.; Villeuneve, M. in prep. La interpretación sísmica y el desarrollo tectónico de la Cuenca Osorno-Llanquihue, X Región, Chile: una cuenca asimétrica.

Muñoz, J.; Duhart, P.; Crignola, P.; Farmer, L.G.; Stern, C.R. 1997. The mid tertiary coastal magmatic belt, south-central Chile. *In* Octavo Congreso Geológico Chileno, 3, 1694-1698. Antofagasta.

Pardo-Casas, F.; Molnar, P. 1987. Relative motion of the Nazca (Farallon) and South America plates since Late Cretaceous time. Tectonics, 6, 6, 223-248.

Stern, C, Vergara, M., 1992. New age for the vitrophyric rhyolite-dacite from Ancud (42°S), Chiloé, Chile. Revista Geológica de Chile, 19, 261-272.

Tebbens, S.F.; Cande, S.C. 1997. Southeast Pacific tectonic evolution from early Oligocene to Present. Jour. Geophy. Res., 102, B6. 12,061-12,084.

Thiele, R.; Beckar, I.; Levi, B.; Nystrom, J.O.; Vergara, M. 1991. Tertiary Andean volcanism in a caldera-graben setting. Geologische Rundschau, 80, 179-186.

Troncoso, R.; M.E. Cisternas; G. Alfaro; Vukasovic, M. 1994. Antecedentes sobre volcanismo Terciario, Cordillera de la Costa, X Región, Chile. *In* Séptimo Congreso Geológico Chileno, 1, 205-209. Concepción.

Valenzuela, E., 1982. Estratigrafía de la boca occidental del canal de Chacao, X Región, Chile. *In* Tercer Congreso Geológico Chileno, 1, A343-376. Concepción.

Vergara, M.; F. Munizaga, 1974. Age and evolution of the upper Cenozoic volcanism in central-south Chile. Bull. Geol. Soc. Am., 85, 603-606.

Vergara, M.; Morata, D.; Hickey-Vargas, R.M.; López, L. in press. Geoquímica de las rocas volcánicas del Terciario del área de Colbún, Precordillera de Linares, Chile Central (35°35`-36°60`S). Revista Geológica de Chile.

TECTONOPHYSICS OF THE ANDES REGION: RELATIONSHIPS WITH HEAT FLOW AND THE THERMAL STRUCTURE

Miguel Muñoz

International Heat Flow Commission (IASPEI)

KEY WORDS: Crust and Upper Mantle Temperatures; Seismic Activity in the Continental Crust; Allochtonous Terrains; Transient Component of Heat Flow.

INTRODUCTION

Surface heat flow in the Andes region is very variable spanning the whole range of values observed in continents (including the characteristic ones of cratonic areas). While in most cases in the Andes heat flow can be related to processes occurring in environments of active tectonics, there are some areas where anomalously low heat flow could indicate old aged allochtonous terrains accreted to the continent.

The variable thermal structure beneath the Andes has a clear manifestation in the seismic activity observed in the continental crust and upper mantle. Whereas the areas of high heat flow have only shallow seismic activity of low magnitude, the areas where the geotherm is low or "normal" may be subjected to earthquakes of intermediate magnitude with foci in the crust and uppermost mantle.

In this contribution some previous results are revisited and new observations and inferences are presented. The main sources of heat flow data are found in Muñoz and Hamza (1993) and Hamza and Muñoz (1996).

Geotherms are generally computed in zones far from the oceanic trench (200-300 km) where the thermal structure of the continental crust and uppermost mantle is not significantly perturbed by processes occurring in the Wadati-Benioff zone. A depth dependent thermal conductivity and an exponential model of radiogenic heat production are assumed. Surface heat production data are available only for some areas in Chile; in other areas, different values of radiogenic heat production have been assumed according to the geological setting. An iteration procedure is followed for constructing the geotherm of the middle and lower crust. The relevant thermophysical parameters are considered in this procedure. The same is done for computing geotherms of the uppermost mantle and when high temperatures are reached the heat transfer due to radiation is taken into account.

GEOTEMPERATURES AND MEAN GRADIENTS

The temperature in the crust-mantle boundary ranges from about 300° C to 800° C, reaching in some areas values of 1000° C - 1100° C (in the Altiplano and the southern volcanic zone). Low mean geothermal gradients in the crust (8 - 12 °C/km) are characteristic of large areas in the Peruvian Andes, Norte Chico (Chile), Sierra Pie de Palo and Central Cordillera (Argentina). Mean gradients of intermediate magnitude (12 - 15 °C/km) are characteristic in zones of Venezuela, Colombia, Ecuador, Altiplano (Bolivia - Chile), southwestern Peru and central Chile. Excepting hot spring areas and zones very close to active volcanoes, high mean gradients (20 - 30 °C/km) are obtained in the Colombian cordilleras and in the south volcanic zone and Patagonian Cordillera.

High gradients are principally due to transient phenomena and not to heat generated by radioactive elements. At the present time no high value of radiogenic heat production has been obtained in granites of the Andes region. Erosion seems to be an important factor involved in the removal of crustal radioactive sources (Muñoz, 1991).

Hot spring areas are encountered in large areas of the Andes, but in many cases geothermal exploration is not enough developed as to consider them for energy utilisation. A brief state of the art concerning geothermal fields is presented.

THERMAL CONTROL OF SEISMOGENIC ZONES

Rheological regimes are strongly dependent on the characteristic geotherm and gravity stratification of the upper tectonosphere. Brittle and ductile behaviours of the Andean crust and upper mantle are studied in the frame of the Anderson-Sibson faulting theory and Dorn's formulation of non-linear rheology. Low and "normal" heat flow areas where the characteristic geotherm is not high may be subjected to earthquakes of intermediate magnitude with foci in the middle and lower crust. The geotemperature generally imposes a cut-off to the seismic activity. Earthquakes of this class can be generated in mountain zones of Colombia and Ecuador, large cordilleran areas of Peru, surrounding areas of the Altiplano, Norte Chico (Chile), Central Precordillera (Argentina), Cajón del Maipo and central cordilleran zone in Chile. The south volcanic zone is free from this class of earthquakes.

LOW HEAT FLOW IN THE CENTRAL PRECORDILLERA OF ARGENTINA

Anomalously low heat flow in the Central Precordillera of Argentina could be explained by considering it as an allochtonous terrain derived from the present southeastern region of North America. Geological and palaeontological studies regarding the Central Precordillera as an allochtonous terrain derived from Laurentia are fully presented in Astini et al. (1996). In southeastern United States heat flow is anomalously low in a band of the Central Appalachians and in Alabama, increasing -yet under the continental mean- in the region of Texas (Blackwell et al., 1991). To the north, in New York, anomalously low heat flow is associated to low radiogenic heat production in the basement of Grenville age (Birch et al., 1968). Low heat flow in areas of the Appalachians could have a similar cause or could be due to regional redistribution of heat by large-scale underground water flow. It has not been possible to differentiate between these two hypotheses (Smith et al., 1981; Blackwell et al., 1991). In the eastern Canada there is also low heat flow in the Grenville terrain and it is inferred that at least in part this is associated with a crust where radiogenic heat production is low (Marechal et al., 1989). In the Precordillera of Argentina, the exposed basement of Grenville age (Astini et al., 1996), the low heat flow and the seismic activity observed in the middle and lower crust (Smalley and Isacks, 1990) are certainly indicating low radiogenic heat production in the crust. Other processes are surely less important for explaining anomalously low heat flow in this area.

It is not clear whether the low heat flow pattern observed in other areas of the Andes could have an explanation similar to the one proposed to the Precordillera of Argentina. The continental terrains recognized may be shuffled and reworked South American crust (Richards and Coney, 1991).

HEAT FLOW IN THE SOUTHERNMOST ANDES AND AREAS OF THE PATAGONIA

Recent observations in lakes Carrera and Cochrane (Chile - latitudes 46.5° S - 47.2° S approx.) show that the regional heat flow is 97 $\pm$ 15 mW/m2. These results agree with inferences made earlier (Hamza and Muñoz, 1996). Close to the eastern limit of the Cenozoic arc and farther eastward there are large units of Pliocene and Quaternary alkali basalts overlying the subalkaline tholeiitic basalts (Stern et al., 1990). Near the heat-flow sites the principal lava outcrops are the areas of Meseta Buenos Aires (close to Chile Chico) and Meseta de la Muerte. A radiometric age for lavas of Meseta Buenos Aires is 4.4 My -age of other outcrops is generally less than this value (Skewes and Stern, 1979). Lavas of these Mesetas correspond to "cratonic" basalts in the work of Stern et al. (1990). In opposition to "transitional" basalts, the "cratonic" lavas are formed by relatively low degrees of partial melting of heterogenous lower continental lithosphere and/or asthenosphere. No evidence of 'slab-derived' components is observed in the "cratonic" Patagonian basalts (Stern et al., 1990). It can suggested that a

convection process -manifesting a thermal perturbation of the mantle- is associated to the formation of these basalts. This should be a process connected to the tectonic evolution of the whole southermost region of the continent and which most recent activity is represented in the Palei Aike field (52°). The rather high heat flow is caused by thermal perturbations in the mantle. The thermal transients are very young, and then it can be expected a large transient component in the total heat flow.

REFERENCES

Astini R.A., Ramos V.A., Benedetto J.L., Vaccari N.E. and Cañas F.L., 1996. La Precordillera: un terreno exótico a Gondwana. XIII Congreso Geológico Argentino y III Congreso de Exploración de Hidrocarburos, Argentina, Actas, Vol. 5, 293-324.

Birch F., Roy R.F. and Decker E.R., 1968. Heat flow and thermal history of New York and New England. In: Zen E., White W.S., Hadley J.B. and Thompson J.B., Jr., (Eds.), Studies of Appalachian geology: Northern and maritime, Interscience, New York, 437-451.

Blackwell D.D., Steele J.L. and Carter L.S., 1991. Heat-flow patterns of the North American continent; A discussion of the Geothermal Map of North America. In: Slemmons D.B., Engdahl E.R., Zoback M.D. and Blackwell D.D., (Eds), Neotectonics of North America, Geological Society of America, Decade Map Volume 1, Boulder, Colorado, 423-436.

Hamza V.M. and Muñoz M., 1996. Heat Flow Map of South America. Geothermics, vol. 25, 599-646.

Marechal J.C., 1989. New heat flow density and radiogenic heat production data in the Canadian Shield and the Quebec Appalachians. Canadian Journal of Earth Sciences, vol. 26, 845-852.

Muñoz M., 1991. Radiogenic heat production and erosion process in central Chile. Intern. Meeting on Terrestrial Heat Flow and the Structure of the Lithosphere, Bechyne Castle, Czech Rep., Book of Abstracts, p. 60.

Muñoz M. and Hamza V.M., 1993. Heat flow and temperature gradients in Chile. Special Issue Studia Geophys. et Geod., Prague, vol. 37, 315-348.

Richards D.R. and Coney P.J., 1991. Andean suspect terranes. Comunicaciones, Dep. Geología, Univ. de Chile, Santiago, N° 42, 194-198.

Skewes M.A. and Stern C.R., 1979. Petrology and geochemistry of alkali basalts and ultramafic intrusions from the Palei-Aike volcanic field in southern Chile and the origin of the Patagonian plateau lavas. J. Volcanol. Geotherm. Res., vol. 6, 3-25.

Smalley R. and Isacks B.L., 1990. Seismotectonics of thin- and thick-skinned deformation in the Andean foreland from local network data: evidence for a seismogenic lower crust. J. Geophys. Res., vol. 95, 12,487-12,498.

Smith D.L., Gregory R.G. and Emhof J.W., 1981. Geothermal measurements in the southern Appalachian Mountains and southeastern Coastal Plain, American Journal of Science, vol. 328, 282-298.

Stern C.R., Frey F.A., Futa K., Zartman R.E., Peng Z. and Kyser T.K., 1990. Trace-element and Sr, Nd, Pb, and O isotopic composition of Pliocene and Quaternary alkali basalts of the Patagonian plateau lavas of southernmost South America. Contrib. Mineral. Petrol., vol. 104, 294-308.

ANOMALIES OF THE GEOMAGNETIC VARIATION FIELD IN THE ANDES (30° - 34° S) AND THEIR TECTONOPHYSICAL SIGNIFICANCE

M.MUÑOZ***, E.BORZOTTA*, I.I ROKITYANSKY**, H. FOURNIER* & M.MAMANI*

*Departamento de Geofísica, IANIGLA-CRICYT, Casilla 330, Mendoza, Argentina
**Institute of Geophysics, Ukrainian Academy of Sciences, POB 338/7, Kiev, Ukraine
***Jorge Matte 2005, Santiago, Chile

KEY WORDS: Geomagnetic Anomalies, Conductors in the Lithosphere, Andean Conductivity Anomalies.

INTRODUCTION

The anomalies of the geomagnetic variation field are related to regional changes of the electrical resistivity and to the existence of conductivity anomalies (CA) in the crust and upper mantle. The study of the resistivity distribution has geodynamical implications by means of the description of melting and suture zones, large fracture systems, etc.

Starting from the observations of the geomagnetic variation field carried out in 1962 in Peru and Bolivia by U. Schmucker and collaborators with the support of the National Science Foundation and the cooperation of the Carnegie Institution of Washington (Schmucker et al., 1964), a considerable amount of geoelectromagnetic research has been done in the Andes region. During 1972, a magnetic variometer array was operating in the area between 30° - 34° S and 68.5° - 71.5° W from about the Rio Bermejo and Beazley basins in Argentina to the coast of Chile (Aldrich et al., 1978). The Z-D transfer function for the period T= 128 min indicated a complex conductivity structure in the eastern part of this area. Also, it was suggested the existence of a conductor SW of the array and a deep conductor beneath the Andes (Aldrich et al., 1978). Later, the set of data was reprocessed (Robertson, 1985) and according to the study of the induction vectors no evidence was found of a feature similar to the "Andean anomaly" discovered by U. Schmucker in Peru. However, it was suggested the existence of a high conductivity zone south of latitude 34° S (Robertson, 1985). Meanwhile, in a pers. comm. (1983) reported in Rikitake and Honkura (1985), L.T. Aldrich indicated that more detailed analyses show a far more complex distribution of transfer functions than earlier.

These results encouraged us to reprocess a part of the magnetograms obtained by L.T. Aldrich and collaborators in 1972. Taking into account the proximity of the Pacific ocean, we preferred not to use induction vectors as they are strongly perturbed by the coast effect. This is the geomagnetic effect of the concentration of electrical currents induced in the sea water where conductivity is higher than in the solid surrounding media. Besides perturbations due to the coast effect, if there are in the area several CA close to each other the induction vectors may give a wrong description of conductivity anomalies.

DATA ANALYSIS

The reprocessed magnetograms correspond to observations from a magnetic array of three profiles crossing the Andes cordillera. The positions of 15 variometers recording the horizontal (H and D) and the vertical (Z) components of the geomagnetic field are shown in Fig. 1 (solid circles). We used selected sections of the magnetograms from the original records. These are published in Robertson (1985) where the selected magnetograms were magnified in photographic paper and the components H, D and Z were digitized taking 4 samples per minute. The original records correspond to observations carried out in April, May and June 1972 (L.T. Aldrich and coll.).

In this work, geomagnetic events corresponding to different periods were examined and their amplitude for every recording site in the array was determined. The amplitude obtained for each site and period was normalized to the average amplitude for the given period (H/Ho, D/Do, Z/Zo). For H and D components with period T, the average value in the whole area of the event considered was taken as an estimate of the "normal" geomagnetic variation field (GVF). This is the field that it would exist if no lateral variations of resistivity and CA were present in the studied area. The departure from the average value for a given site (and period) was taken as constituing the anomalous geomagnetic variation field (AGVF). The AGVF is extensively discussed in Rokityansky (1982). For Z usually it is not possible to follow the same procedure as before: when geological heterogeneities are present, the Z variation field is very anomalous whenever its average amplitude in the whole area is normally near zero. But in our case the array is located near the Pacific ocean, and then there is a coast effect detectable generally with the same sign in all sites. This makes possible to obtain an average value for Z and to normalize amplitudes in the same way as was done with the horizontal components.

The AGVF for H and D was considered as constituted by two parts: i) A part produced by the lateral variation of resistivity in the lithosphere; ii) A second part due to CA which are produced by elongated bodies having high conductivity -generally, these anomalies are observable with different intensity in H and D according to the strike of the anomalous structures (ie., a CA lying approximately in NS direction will produce an anomalous field stronger in D). For describing conductivity anomalies it was necessary to estimate a common coast effect for the three profiles -this is possible because the Pacific ocean has an almost uniform depth in this region.

CONCLUSIONS AND BRIEF DISCUSSION

The following conclusions can be drafted (see also Fig. 1):

1. The regional electrical conductivity drastically changes at about the NS trace crossing the Iglesia, Calingasta and Uspallata basins. The electrical conductivity is lower westward. This can be related to a basement with different composition at both sides of this trace -possibly corresponding to different allochtonous terrains (e.g., Ramos et al., 1984; Astini et al., 1996)- or to the profuse Neopaleozoic magmatism in the Frontal Cordillera and westward from it (e.g., Llambías et al., 1987). A combination of these causes can also be envisaged.

2. There is a conductivity anomaly (CA) contiguous to the Precordillera and lying close to the border between the areas of different resistivity described firstly. It is a deep-seated anomaly (intermediate or deep zones of the lithosphere) and the nature of conductivity should be ionic. A critical point is its presumable similarity with the case observed in North America regarding the CA of Sierra Nevada and Rio Grande (Schmucker, 1964).

3. A CA is detected beneath the Principal Cordillera and lying at intermediate depth. It is probably produced by the fault system including the Santa Cruz and Mondaquita faults with NS strike in direction to the Frontal Cordillera.

4. A CA in the zone of Rio Bermejo, lying approximately in NS direction. Because of scarce data, its location is more uncertain -especially southwards in the western flank of the Pie de Palo block. It can be a superficial anomaly produced by ionic current channeling through thick sediments.

5. In the area of Valparaiso in the coast of Chile a deep-seated anomaly is detected also. North of this area it lies offshore, and inland to the south. It is contiguous to the western margin of the Andean Mesozoic geosynclinal basin. The question whether this CA can be related to electronic conductors (e.g., graphite) or to ionic currents in weakened zones of fractures remains unclear.

REFERENCES

Aldrich L.T., Bannister J.P., Casaverde R.M. and Triep E.G., 1978. Anomalous electrical conductivity structure in central Chile. Carnegie Inst. Washington Yearbook, 77, 543-548.

Astini R.A., Ramos V.A., Benedetto J.L., Vaccari N.E. and Cañas F.L., 1996. La Precordillera: un terreno exótico a Gondwana. XIII Congreso Geológico Argentino y III Congreso de Exploración de Hidrocarburos, Argentina, Actas, Vol. 5, 293-324.

Llambías E.J., Sato A.M., Puigdomenech H.H., and Castro C.E., 1987. Neopaleozoic batholiths and their tectonic setting. Frontal range of Argentina between 29° S and 31° S. X Congreso Geológico Argentino, Actas, Vol. IV, 92-95.

Ramos V.A., Jordan T.E., Allmendinger R.W., Kay S.M., Cortés J.M. and Palma M.A., 1984. Chilenia: un terreno alóctono en la evolución paleozoica de los Andes centrales. IX Congreso Geológico Argentino, Actas, Vol. II, 84-106.

Rikitake T. and Honkura Y., 1985. Solid Earth Geomagnetism. Terra Scientific Publishing Company, Tokyo, 384 pp.

Robertson R.A., 1985. Estudio geomagnético de los Andes centrales. Depto. Geofisica, Univ. de Chile, Santiago, 179 pp.

Rokityansky I.I., 1982. Geoelectromagnetic Investigation of the Earth's Crust and Mantle. Springer Verlag, Berlin, 381 pp.

Schmucker U., 1964. Anomalies of geomagnetic variations in the southwestern United States. J. Geomagn. Geoelec., XV, 193-221.

Schmucker U., Hartmann O., Giesecke Jr A.A., Casaverde M. and Forbush S.E., 1964. Electrical conductivity anomalies in the earth's crust in Peru. Carnegie Inst. Washington Yearbook, 63, 354-362.

Fig. 1. (see next page)
Left: Map of the studied region showing the observation sites (solid circles). FLOR, ALUM, REAL and USPA sites are located close to the trace through the Iglesia, Calingasta and Uspallata basins.
Right: Electrical conductivity anomalies (CA). **a:** Principal Cordillera CA; **b:** Precordillera CA; **c:** Rio Bermejo anomaly; **d:** Valparaiso anomaly. Some other conductivity features are shown also.

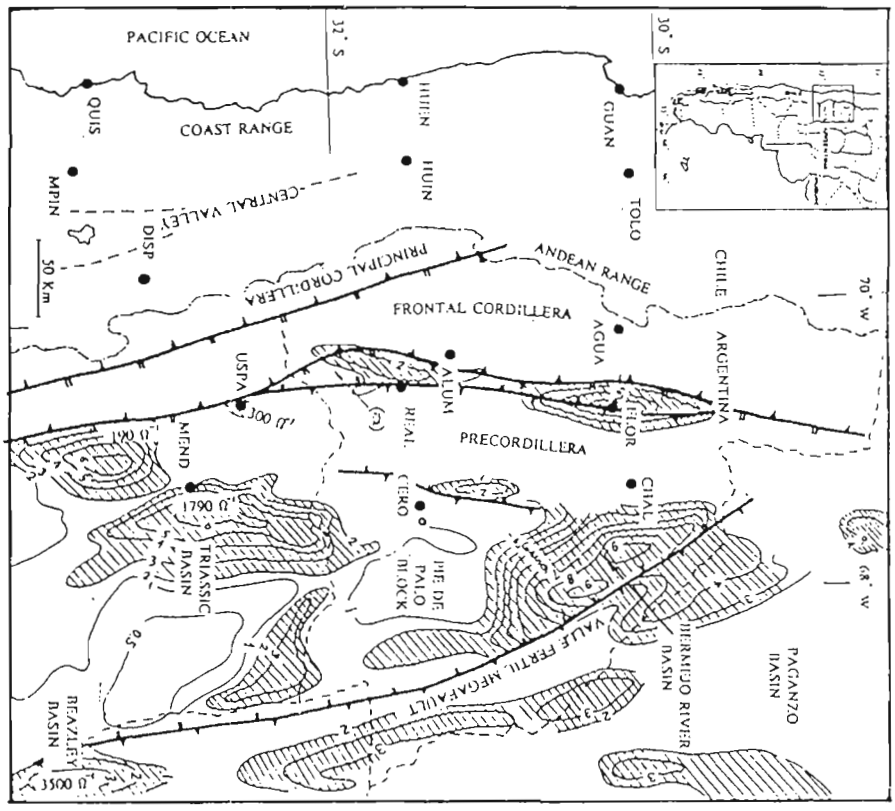
PACIFIC OCEAN
32° S
30° S
QUIS
COAST RANGE
HUEN
GUAN
MPIN
HUIN
TOLO
CENTRAL VALLEY
DISP
50 Km
PRINCIPAL CORDILLERA
ANDEAN RANGE
CHILE
70° W
FRONTAL CORDILLERA
AGUA
USPA
ALUM
ARGENTINA
3000 m
PRECORDILLERA
MEND
CHAL
CUEKO
1790 m
TRIASSIC BASIN
PIE DE PALO BLOCK
68° W
VALLE FERTIL-MEGAFAULT
DIAMANTE RIVER BASIN
PAGANZO BASIN
BEAZLEY BASIN
3500 m

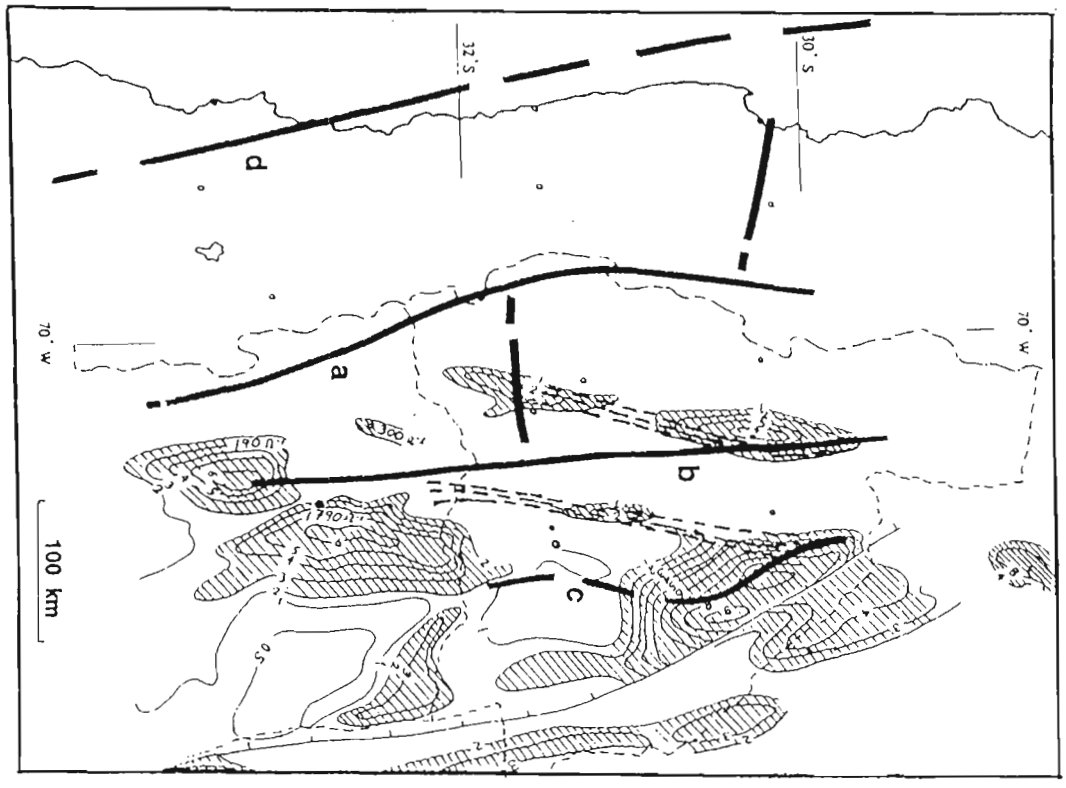
32° S
30° S
70° W
a
b
c
d
100 km

HEATFLOW, TEMPERATURE AND BATHYMETRY OF LAGO GENERAL CARRERA AND LAGO COCHRANE, SOUTHERN CHILE.

Ruth E. MURDIE(1), David T. PUGH(2) and Peter STYLES(3), Miguel MUñOZ(4)

(1) Department of Earth Sciences, Keele University, Staffordshire ST5 5BG, U.K.
r.e.murdie@keele.ac.uk
(2) Southampton Oceanography Centre, Empress Dock, Southampton SO14 3ZH, U.K.
David.T.Pugh@soc.soton.ac.uk
(3) Department of Earth Sciences, Liverpool University, Liverpool L69 3BX, U.K. sr15@liverpool.ac.uk
(4) formerly of Departamento de Geofisica Universidad de Chile, Casilla 2777, Santiago, Chile

KEY WORDS: heatflow, ridge subduction, sediment temperature probe, thermal modelling,

INTRODUCTION

We have undertaken a survey of heatflow in the sediments of two deep lakes, in Southern Chile, Lago General Carrera (LGC) at 46°30'S and Lago Cochrane at 47°12'S, using traditional marine techniques, adapted for working from small boats. These lie onshore of the Chile Triple Junction where the subduction of the Chile Rise has been proceeding for the past 14 My, (Cande et al., 1987) as successive sections of the oceanic spreading centre have been taken into the Peru-Chile Trench. The aim of the survey was to use heatflow measurements to see if the subduction of the Chile Rise had left a thermal imprint across the South American Continental Margin.

Field Measurements

Bathymetric maps of both lakes were made using an echo sounder with G.P.S. navigation. To estimate the seasonal temperature stability in the bottom water of the two lakes, measurements were made early in December 1996, and February 1997.

A special self-contained sediment temperature probe was designed and built so that it could be deployed off any boat. It was constructed from hollow stainless steel tubing containing 5 temperature loggers at various intervals along its depth and an inclinometer to determine the angle of penetration of the probe.

Sediment samples, for water content, were collected by trapping mud in transverse holes set at frequent intervals along the probe. The probe was lowered into the water to within 50m of the bottom and then allowed to free fall. It was left in the sediments long enough for the heat energy produced on entry of the probe into the sediments to dissipate, and for the temperature loggers to come to thermal equilibrium with the surrounding sediments.

Data reduction and corrections

The main corrections applied to sediment temperatures were for seasonal bottom water temperature variations (Pugh, 1977), topographic corrections using Jeffrey's methods (Jessop, 1990) and sediment blanketing, using the method of Lachenbruch and Marshall (1966). In the absence of heavy coring gear, sediment thermal properties had to be estimated from the measured water content of the samples along the probe. Possible effects of decadal and longer-term bottom water temperature changes have not been eliminated as no long term water temperatures have been made in this area.

Results

Bathymetry

The bathymetric surveys of Cochrane showed that the lake appears to be made up of a series of small deep basins of just over 200m in the western end. After crossing a shallow sill, corrected depths of 460m were surveyed in the central basin.

LGC is divided into two main basins, both with relatively flat sedimentary plains, separated by a shallow sill at Fachinal (46°33'S 72°13'W). The central area has an average maximum depth of about 400m. As it narrows at 72 13'W, it shoals considerably and the lake floor has a rough hummocky topography. The lake deepens sharply westwards of the Fachinal sill to a flat basin with the floor lying at a maximum corrected observed depth of 586m. This places LGC as the deepest lake yet measured in South America

Sediment temperature measurements

Heatflow values were obtained for eight stations, three in Cochrane and five in LGC. The overall regional average of 102 ± 15 mWm^{-2} is significantly higher than the global average of 62 mWm^{-2} (Jessop, 1990) and the average for South America of 63mWm^{-2} (Hamza and Muñoz, 1996). There is no significant horizontal gradient in the values within each lake, nor any significant difference between the two lakes.

Why is Lago General Carrera so deep ?

The complex regional geological evolution of the region has influenced the depth and orientation of these great lakes. The topography makes it clear that the principal mechanism of excavation of both

lakes, has been glacial erosion. However, deep scouring has been enhanced by tectonic uplift of the region, due to the approach of the Aluk-Farallon ridge during the Eocene and then since 14 Ma, the approach from the south, of the Chile Rise. The subsequent filling of the basin is a result of subsidence again after the passage of the ridge segments. The subduction of the Chile rise, has also resulted in differences in geology north and south of LGC although no major faults trending east-west have been found in the region. To the south of LGC, compression, associated with the approach of the raised topography of the Chile Rise, was accommodated by shortening in the back arc region (Ramos, 1989). To the north, it is taken up by strike slip along the Liquiñe-Ofqui fault (Ray 1996, unpublished thesis. University of Liverpool). LGC lies at the boundary between these two deformation regimes. The extreme depth of the lake may be due to a fundamental tectonic influence.

Modelling of thermal structure and heatflow of the region

Finite difference and element models have been used to investigate which factors influenced the production of these high heatflow values in this area. Factors we consider are

1) the age of the subducting plate which is well constrained in this area. The main effect of this is seen in the heat flow offshore, although slight variations (up to 15mW/m^2) would be noticed up to 150km onshore.
2) The dip of the slab which is not well defined as there is very little seismicity from this area. Estimates in the dip of the slab range from 15° from seismic data at the triple junction to 25° estimated from the position of the old volcanic arc to 35° in the back arc. This has an effect of up to 40 mW/m^2.
3) The velocity of the subducting plates which is well constrained to be 90mmyr^{-1} for the Nazca plate and 20mmyr^{-1} for the trailing Antarctic plate. However this has negligible effect on heatflow.
4) Thickness of the continental lithosphere. There is very little handle on the thickness of the lithosphere in this region so we selected values between 125 and 50 km This is the factor so far that has the greatest effect on the heat flow which would be measured on the continent.

Other effects which are being considered, but are harder to model include areas of high degrees of partial melting of mantle peridotite as observed corresponding to projections of subducted fracture zones further north under the South American margin (Onuma and López-Escobar 1987) and the existence of profuse Pliocene and Quaternary Basalts in the Patagonian Plateau, which could possibly have been produced by a thermal perturbation (Gorring et al 1998).

Conclusions

We have successfully made 8 measurements of heat flow in sediments of deep Andean lakes. The effects of ridge subduction should be noticeable from the heat flow signature up to 150 km inland of the trench. However, early attempts at modelling show that it is hard to conclusively say that the values we have measured show the additional heat input from the ridge or a thermal perturbation rather than just the effects of subducting of young, shallowly dipping oceanic crust.

Acknowledgements

The work for this research was funded by NERC grant number GR9/02567. Field work was carried out with Ian Waddington. We are grateful for logistical support provided by the Armada de Chile and Carabineros de Chile.

References

Cande, S.C., R.B. Leslie, J.C. Parra, and M. Hobart. 1987. Interaction between the Chile Ridge and Chile trench: geophysical and geothermal evidence. Journal of Geophysical Research 92: 495-520.

Goring M.L., Kay S.M. Zeitler P.K. Ramos V.A. Rubiolo D. Fernandez M.I. & Panza J.L. 1997 Neogene Patagonian plateau lavas: Continental magmas associated with ridge collision at the Chile Triple Junction. Tectonics 16: 1-17

Hamza, V.M. and M. Muñoz 1996. Heat flow map of South America. Geothermics 25: 599-646.

Jessop, A.M. 1990. Thermal Geophysics. Elsevier pp.306.

Lachenbruch, A.H. and B.V. Marshall. 1966. Heat flow through the Arctic Ocean Floor. The Canada Basin-Alpha Rise Boundary. Journal of Geophysical Research 71: 1223-1248.

Onuma N. & López-Escobar L. 1987 Possible contribution of the asthenosphere below the subducted oceanic lithosphere, to the genesis of arc magmas: Geochemical evidence from the Andean southern volcanic zone (33-46°S. Journal of Volcanology and Geothermal Research 33: 283-298.

Pugh, D.T. 1977. Geothermal gradients in British lake sediments. Limnology and Oceanography 22: 581-596.

Ramos, V.A. 1989. Foothills structure in the Northern Magellanes Basin, Argentina. Bulletin of the American Association of Petroleum Geologists. 73: 887-903.

NEW CONSTRAINTS ON THE CRETACEOUS-TERTIARY DEFORMATION IN SIERRA DE MORENO, PRECORDILLERA OF THE SEGUNDA REGION DE ANTOFAGASTA, NORTHERN CHILE.

Claudio NICOLAS (1), Hans-G. WILKE (1), Heinz SCHNEIDER (1) & Friedrich LUCASSEN (2)

(1) Departamento de Ciencias Geológicas, Universidad Católica del Norte, Casilla 1280, Antofagasta, Chile (hwilke@socompa.cecun.ucn.cl)
(2) Fachgebiet Petrologie, Sekr. EB 10, Technische Universität Berlin, Strasse des 17. Juni 135, 10623 Berlin, Germany (luca0938@mailszrz.zrz.tu-berlin.de)

KEY WORDS: Central Andes, Precordillera, Peruvian Phase, Incaic Phase, Post-tectonic intrusions

INTRODUCTION

The deformation events ocurred in Late Cretaceous – Early Tertiary are not well dated in the studied area. In the present paper new data are contributed regarding the structural configuration and the tectonic regime during this time-span.

GEOLOGICAL SETTING

The geology of the chilean Precordillera, specifically in Sierra de Moreno, has a wide stratigraphic record ranging from the Early Paleozoic to recent time (fig. 1). The distribution as well as the surface exposure of the geological units present a strong structural control, signaled by N-S trending reverse faults and, to a lesser extent, normal faults.

The tectonic events of interest here are separated in two major phases, one of Late Cretaceous age and the other of Paleogene age.

LATE CRETACEOUS DEFORMATION

In the study area the rocks of the Quinchamale Fm. are intruded by a plutonic stock , here named Barreras Granite, constituted of diorite, monzodiorite, monzonite and monzogranite. This pluton yields K/Ar ages in hornblende and biotite of 83±3 and 84±2 Ma respectively (LADINO et al. 1997) and a K/Ar biotite age

of 82±6 Ma (LUCASSEN & FRANZ 1997). The geochemical characteristics of the Barreras Pluton show an alcaline evolutionary trend with low silica content and Sr 87/86 ratios of 0,704550 – 0,704669 and Nd 144/143 ratios of 0,512471 – 0,512505. This defines a mantle source for the melt ruling out a volcanic arc affiliation.

The intrusive contact between the Barreras Granite and the Quinchamale Fm. is well exposed in the middle course of Quebrada Barreras. Here, abundant decimetric to metric sedimentary xenoliths are observed. These are part of partially digested strata, originated by the intrusion dynamics of the pluton. These xenoliths are of elongated shape with their principal axes oriented in a vertical position defining N-S trending planes similar to the trends of the unaffected sedimentary strata. On the basis of this we assume that the pluton intruded a previously deformed, folded or at least strongly tilted sedimentary sequence.

The intrusion generated an extensive contact aureole consisting in intensive silicification and metamorfic development of biotite and epidote. Those define a foliation subparallel to the contact of the intrusion. The pluton itself does not exhibit any ductile deformation.. The foliation is due to intrusion effects rather than to a regional metamorphic event.

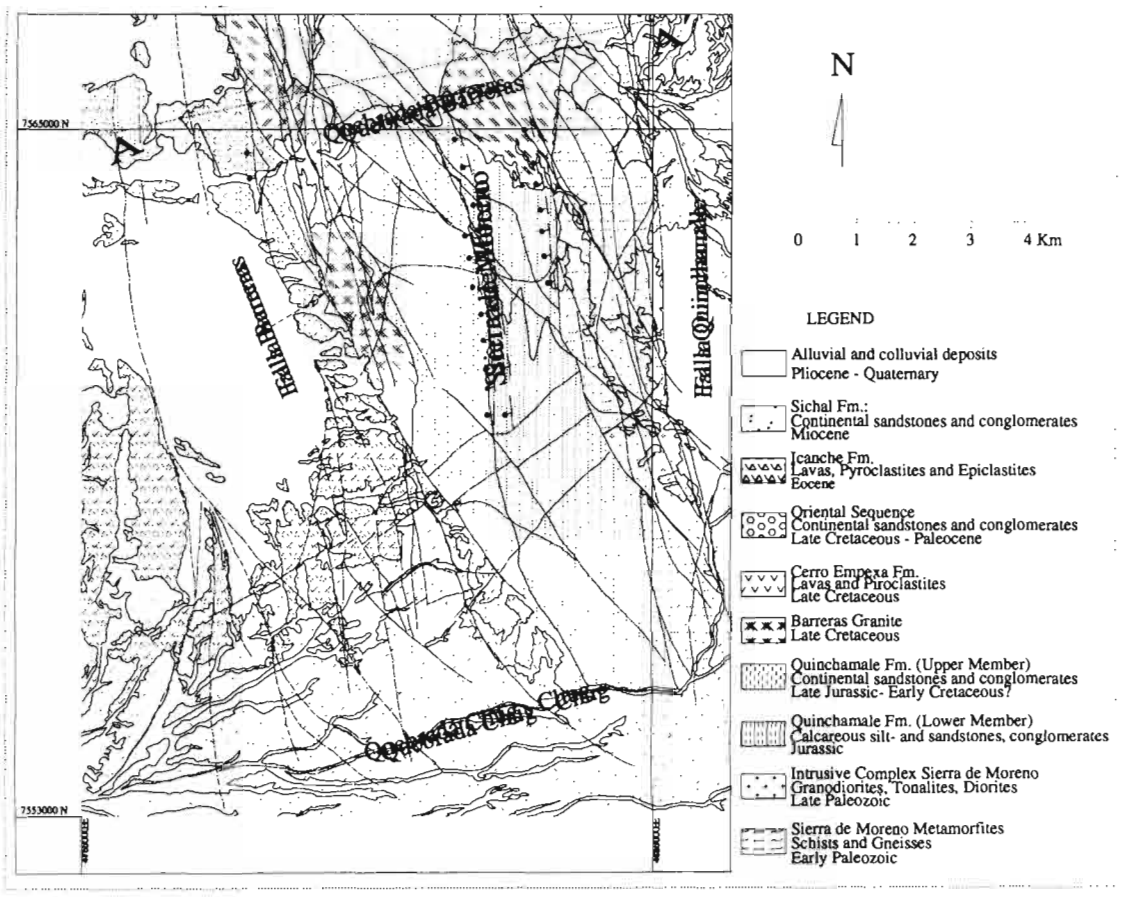

Fig. 1: Geological map of the study area. The line A-A' indicates location of profile shown in fig.2

Small outcrops of lavas of the Cerro Empexa Fm., comformably overlying the Quinchamale Fm., occur north of Quebrada Chug-Chug. That means that the deformation must have ocurred after the deposition of these volcanics. The age of the Cerro Empexa Fm. has been discussed by BOGDANIC & DÖBEL 1990. They restrict the possible formation age of this unit to 123 Ma – 94 Ma. This time span is in agreement with the radiometric age of 109 Ma obtained on an andesitic clast from rocks of the Eastern Sequence (LADINO et al. 1997).

According to the preceding arguments the deformation of the Mesozoic sequence ocurred after, at minimum, 109 Ma and before 84 Ma corresponding to the Peruvian Tectonic Phase (STEINMANN in MAKSAEV 1979).

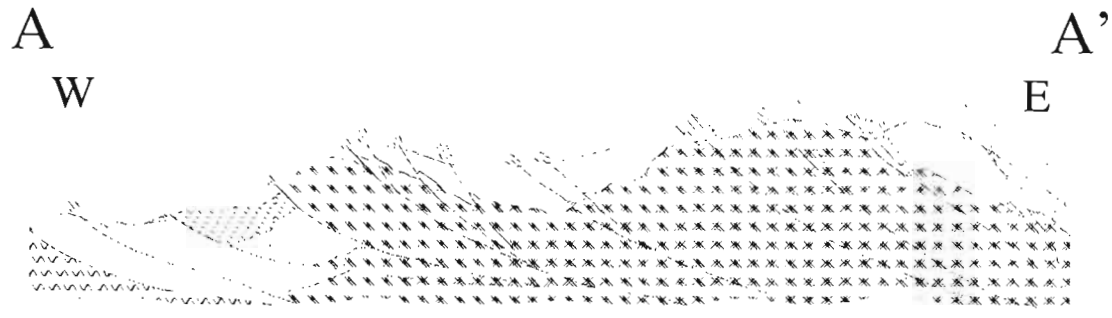

Fig. 2: Schematic cross section along Quebrada Barreras, showing tulip-like structures with decreasing dips towards the west. For simbols refer to fig. 1

PALEOGENE DEFORMATION

This event is characterized by a strong refolding of the Mesozoic sequences and by the thrusting of metamorphic units and intrusives of Paleozoic age over Jurassic units on the eastern flank of Sierra de Moreno, and thrusting of Jurassic sedimentary rocks, Cretaceous volcanics and intrusives over Late Cretaceous-Paleogene volcanic and sedimentary units in the western flank (figs.1, 2).

The thrust faults strike in a N-S to NNW direction, dipping 40° to 75° to the east. The presence of drag faults indicate associated dextral transcurrence. Although on the southend of Sierra de Moreno there are few sinistral transcurrent movements. A similar situation has been described by SCHEUBER et al. 1994, REUTTER et al. 1996.

The geometry of these thrusts corresponds to an en-echelon array on the east flank and to a subparallel array on the west flank. The subparallel arrangement of the fault traces disappears towards the south in the Quebrada Chug-Chug area, where a series of ramifications can be observed. This can be interpreted in terms of a horse splay terminal (fig. 1), which in cross section would constitute a tulip structure (fig. 2). This tulip-like structure, with decreasing dips toward the west flank of Sierra de Moreno, would be the cause of structural repetition of units, such as the Lower and Upper Members of the Quinchamale Fm.
On the basis of contact relationships, these thrust faults can be attributed to the eocene Incaic tectonic phase. The thrusts, which have a horsesplay-type geometry are probably associated to a major structure, which corresponds to the Barreras fault in the study area, and in more general terms forms part of the Precordilleran Fault System.

CONCLUSIONS

On the basis of the previously exposed arguments, we propose the existence of two separate events of deformation for the area. The first of Late Albian to Santonian folded the mesozoic sequences. Intrusion of the Barreras Granite was post-tectonic to this event. The cooling of the Barreras Granite must have ocurred during a period of tectonic quiescence evidenced by a lack of ductile deformation structures. The second deformational event, attributed to the Incaic tectonic phase, generated a series of reverse faults with dextral transcurrent components. The geometry of these faults is interpreted as a tulip structure.

REFERENCES

BOGDANIC, T. & DÖBEL, R. 1990: Cretaceous and early Tertiary in northern Chile between 21° and 23°S. – Symposium International „Géodynamique Andine„, Grenoble, 245-248.
LADINO, M., TOMLINSON, A.& BLANCO, N. 1997: Nuevos antecedentes para la edad de la deformación cretácica en Sierra de Moreno, II Región de Antofagasta, Norte de Chile. - Actas VIII Congreso Geológico Chileno, vol. I., 103-107, Antofagasta.
LUCASSEN, F.& FRANZ, G. 1997: Crustal recycling of metamorphic basement: late Proterozoic granites of the Chilean Coast Range and Precordillera at ~22°S. - Actas VIII Congreso Geológico Chileno, vol. II, 1344-1348, Antofagasta.
MAKSAEV, V. 1979: Las fases tectónicas incaica y quechua en la Cordillera de los Andes del Norte Grande de Chile. - Actas II Congreso Geológico Chileno, vol. I., B63-B77, Arica.
REUTTER, K.-J., SCHEUBER, E. & CHONG, G. 1996: The Precordilleran fault system of Chuquicamata, Northern Chile: evidence for reversals along arc-parallel strike-slip faults. - Tectonophysics, 259, 213-228.
SCHEUBER, E., BOGDANIC, T., JENSEN, A. & REUTTER, K.-J. 1994: Tectonic development of the North Chilean Andes in relation to plate convergence and magmatism since the Jurassic. - In:. Reutter, Scheuber & Wigger (eds.) Tectonics of the southern Central Andes. 121-139. Springer.

Geochemical Evolution of Neocomian Volcanism S of Vallenar, Chile.

Nova A.[1] and Cisternas, M.E.[2]

1. Institut für Allgemeine und Angewandte Geologie. Ludwig Maximilians Universität.

2. Instituto de Geología Económica Aplicada GEA. Universidad de Concepción.

The Las Cañas sector, located south of Vallenar, Chile, exhibits excellent exposures of volcanic, volcano-clastic and marine-carbonate rocks (Fig. 1). The rock sequence is considered representative of the Neocomian arc - back-arc pair.

The Neocomian sequence at Las Cañas has been subdivided into four stratigraphic unit Unidad Volcánica Inferior and three carbonate rocks units, which belong to the Nantoco, Totoralillo and Pabellón formations [4]). The Unidad Volcánica Inferior can be correlated with the Punta del Cobre Formation near Copiapó by its stratigraphic position [6].

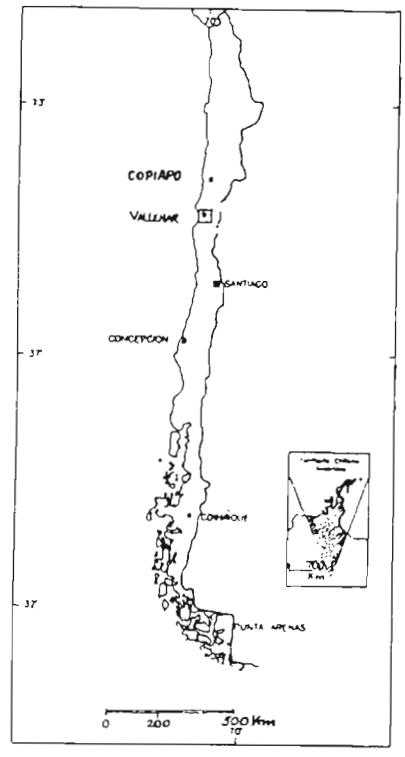

Fig. 1. The studied sector.

Structurally, this sequence forms NNE-SSW belts, which are intensively folded and tilted. In the west, the sequence is limited and unconformably overlain by Tertiary gravel deposits. In the east, it is cut by dioritic to monzodioritic intrusive rocks and underlies unconformably volcaniclastic conglomerates of the Cerrillos Formation (Upper Cretaceous).

The REE patterns of the volcanics rocks at Las Cañas shows similarities with those of the Andean Quaternary arc at 37-41.5°S which erupted in a continental arc environment (Table 1; Figs. 2, 3).

Table 1. Major and trace elements abundance for laves in study.

	AN-7	AN-17	AN-55
Unit	U. Volc. I.	Nantoco	Totoralillo
UTM-E	332.050	332.400	333.150
UTM-N	6.811.100	6.810.030	6.808.850
SiO_2	50,16	58,63	50,06
TiO_2	0,91	1,63	0,68
Al_2O_3	18,02	15,78	15,47
Fe_2O_{3tot}	9,97	8,27	6,30
MnO	0,26	0,30	0,20
MgO	6,58	1,95	1,42
CaO	6,31	4,81	11,09
Na_2O	4,16	7,38	6,00
K_2O	1,94	1,39	1,89
PsO_5	0,11	0,18	0,06
LOI	3,74	1,98	8,83
TOTAL	102,16	102,30	102,00
Y	21,00	31,70	13,30
Zr	73,00	139,80	63,81
La	9,72	14,93	9,01
Ce	22,09	33,61	16,84
Pr	2,53	4,01	1,64
Nd	13,31	21,54	8,10
Sm	3,17	5,43	2,00
Eu	1,07	1,69	0,69
Gd	3,39	6,09	2,25
Tb	0,51	0,86	0,36
Dy	3,18	5,89	2,36
Ho	0,66	1,17	0,48
Er	2,00	3,63	1,62
Tm	0,29	0,51	0,25
Yb	1,587	3,42	1,70
Lu	0,33	0,59	0,29

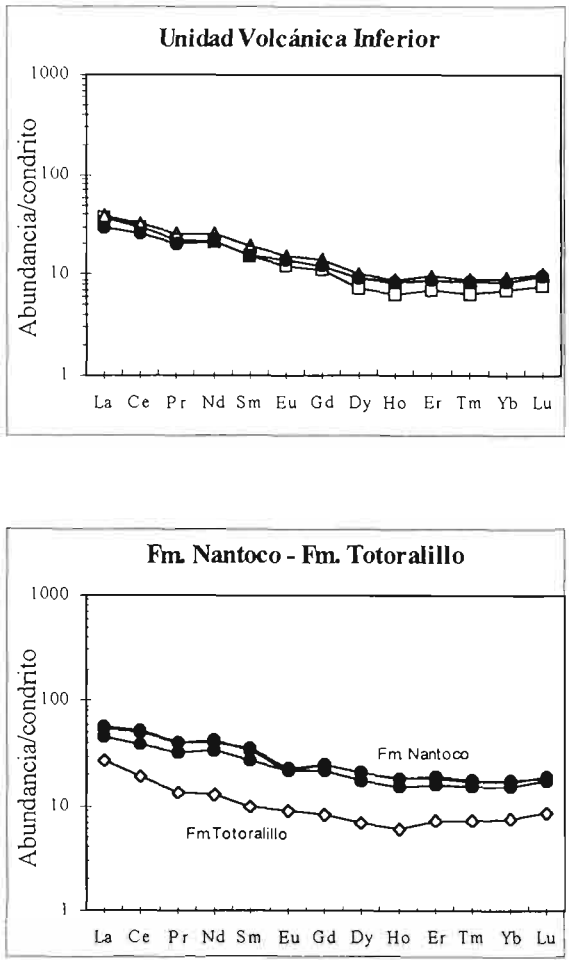

Fig. 2. Nakamura condrite (1974) [3] normalized spider diagrams for Lavas from the Las Cañas sector.

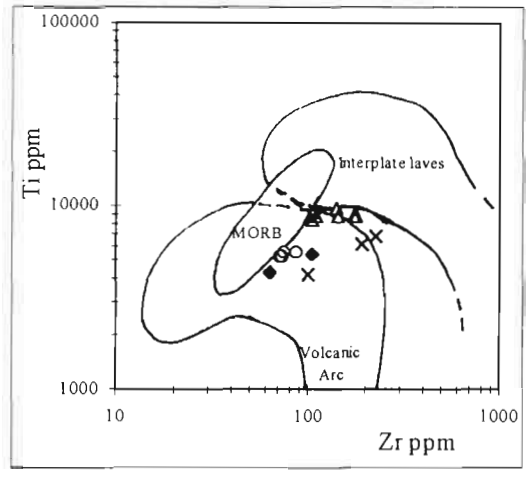

Fig. 3. Volcanic rocks of the Las Cañas sector plot in the field of arc lavas (Diagram of Pearce, 1982 [5]).

Simbology Las Cañas sector:
o: Unidad Volcánica Inferior, Δ: Fm. Nantoco, ♦: Fm. Totoralillo, x: Dykes.

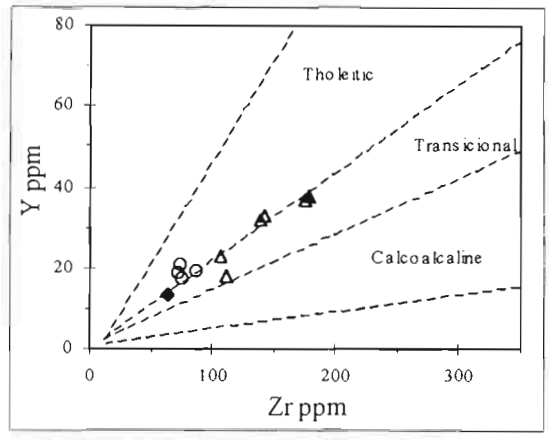

Fig. 4. Volcanics rocks of Las Cañas plot in the field of tholeitic to calcoalkaline trend (Diagram of Maclean and Barret, 1993 [1]).

Simbology Las Cañas sector:
o: Unidad Volcánica Inferior, Δ: Fm. Nantoco, ♦: Fm. Totoralillo, x: Dykes.

Las Cañas sector lavas range from basalt to silica-andesite in composition, they belong to the subalkaline magmatic series, and show tholeiitic to calc-alkaline affinities (Figs. 4, 5).

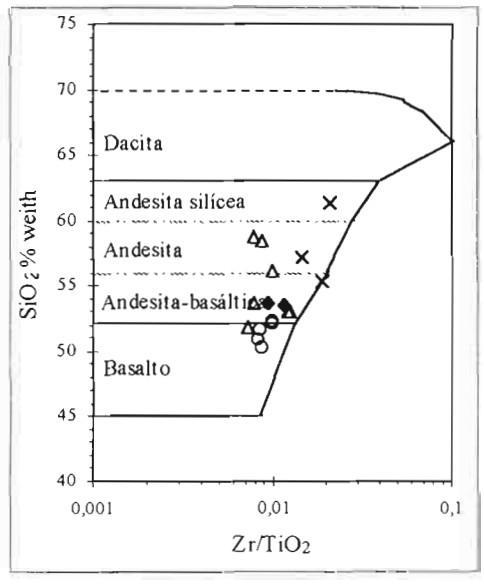

Fig. 5. Discrimination diagrams of Las Cañas (Diagram of Winchester und Floyd, 1977 [7]).

Simbology Las Cañas sector:
o: Unidad Volcánica Inferior, Δ: Fm. Nantoco, ♦: Fm. Totoralillo, x: Dykes.

Finally, there exist a stratigraphical correlation consistent with the geochemical characteristics between the basalts from the Unidad Volcanica Inferior at Las Cañas and those from the Unidad Lavas Superiores belonging to the Punta del Cobre Fm in the Copiapó area [2, 4]). This supports a genetic analogy for both units. This is particularly significant for mineral exploration since the Punta del Cobre Fm at Copiapó is considered an important Cu metallotect.

Acknowledgments

This work was suppörted in part by the Instituto de Geología Economica Aplicada GEA, Universidad de Concepción (Chile) and by the Institut für Allgemeine und Angewandte Geologie, Ludwig Maximiliams Universität (Germany). We thank Prof. Dr Hubert Miller for helpful discussions in these abstract.

References

[1] Maclean, W. H. and Barret, T. J. 1993. "Lithochemical tecniques using inmobile elements." *Journal of geochemical exploration*, Vol. 48, pp. 109-133.

[2] Marschik, R. 1996. "Cretaceous Cu (-Fe) mineralization in the Punta del Cobre belt, northern Chile." Ph.D. Thèse. *In* Terre & Environment. Vol. 5, 198 pp. *Université de Genève*. Genève, Suisse.

[3] Nakamura, N. 1974. "Determination of REE, Ba, Fe, Mg and K in carbonaceous and ordinary chondrites." *Geochimica et cosmochimica acta*. Vol. 38, pp. 757-775.

[4] Nova, A. 1997. "Estudio petroquímico de las volcanitas neocomianas en el sector de Quebrada Las Cañas. III Región de Atacama. Chile." Memoria de Título (Inédito), *Universidad de Concepción, Departamento de Geología*, 133 pp. Concepción. Chile.

[5] Pearce, J. 1982. "Trace element characteristics of lavas from destructive plate boundaries." *In* Andesites (Thorpe, R.S.; editors). Willey, Chichester, pp.525-548. London. United Kingdom.

[6] Segerstrom, K. and Parker, R. 1959. "Geología del cuadrángulo Cerrillos, provincia de Atacama." *Instituto de investigaciones geológicas. Carta geológica de Chile*. Vol. 3, N°2, 33 pp. Santiago. Chile.

[7] Winchester, J. and Floyd, P. 1977. "Geochemical discrimination of different magma series and their differentiation products using inmobile elements." *Chemical geology*. Vol. 20, pp. 325-343.

TECTONIC STYLE, DEFORMATION, AND ACTIVE PROCESSES AT THE CENTRAL ANDEAN MARGIN - CONSTRAINTS FROM ANCORP'96

Onno ONCKEN(1), and ANCORP Research Group

(1) GeoForschungsZentrum Potsdam, Telegrafenberg A17, D-14473 Potsdam, Germany, oncken@gfz-potsdam.de

KEY WORDS: Seismology, Reflection Seismics, Central Andes, Subduction zone, Active Processes, Deformation

ABSTRACT: The Central Andes are characterised by substantial crustal thickening with plateau formation above a moderately dipping subduction zone with a high subduction rate and tectonic erosion at the Pacific continental margin. A 400 km long deep seismic reflection profile and integrated geophysical experiments across the Central Andes along with surface-based studies yield new constraints on accumulation and partitioning of deformation. The data also provide unexpected evidence that the hypocentres of earthquakes are offset into the oceanic mantle from the reflection image of the plate boundary. Most geophysical features are probably caused by fluid- and melt-associated petrological processes driven by active subduction.

INTRODUCTION

The deep structure of active orogenic belts, particularly that of active subduction orogens is only known from very few geophysical studies like the INDEPTH study across Tibet and the Vancouver island experiment across the North American margin which is the only integrated geophysical survey across a complete active continental margin encompassing the offshore and the onshore parts of the plate margin. In 1996 a joint German-Chilean-Bolivian group conducted the geophysical experiment ANCORP'96 in the southern central Andes at 21°S (ANCORP research group, 1999). The experiment consisted of an

active reflection and refraction seismic component and a passive seismological network recording the local seismicity and teleseismic events. It continued an earlier offshore-seismic survey (CINCA'95) designed to image the subduction erosion processes operating at the Chilean margin at this latitude. ANCORP was conceived to image the subduction zone and the upper plate structures from the coast to the eastern border of the Altiplano in order to image subduction zone processes and the internal architecture of the Andean crust.

RESULTS

The Andes are the Earth's largest active subduction-controlled orogen with a length of 7500 km and a width of up to 800 km in their central parts. In their central parts, their evolution is controlled by subduction of the oceanic Nazca plate (recent convergence rate: 8.5 cm/a), active arc magmatism in most segments of the overriding plate, substantial continental thickening, and by highly arid conditions with very minor erosional removal into the trench. As evidenced by marine reflection profiles collected by CINCA in 1995 (between 19 and 26° S), features suggesting tectonic erosion are particularly well developed offshore. The eastward migration of the volcanic front from the Coastal Cordillera during the Jurassic to its present position in the Western Cordillera indicates that more than 200 km of continental material in an E-W section have been tectonically eroded and subducted. Uplift of the central Andean cordillera, however, only commenced in early Tertiary times and resulted in a broad mountain belt with the world's second largest plateau, the Altiplano/Puna situated at an average elevation of 4000 m between the volcanic Western Cordillera and the Eastern Cordillera. Formation of this plateau and the contribution of different processes (crustal shortening, magmatic addition, mantle delamination and hydration) are a matter of debate. As with all young orogenic belts, surface data on crustal deformation substantially underrate the shortening needed to explain actual crustal thicknesses.

ANCORP imaged the subduction of the Nazca plate beneath the central Andes as a reflective zone from 40 km (below the coast) to 80 km depth (below the Precordillera) with the deepest so far acquired reflections from a subduction zone. Towards depth, the Nazca reflector is increasingly offset above the Wadati-Benioff zone along with increasing downdip reflection intensity before breakdown below 80 km. Offshore wide angle data acquired during the CINCA experiment allow to link the Nazca reflector with the oceanic crust and subduction shear zone. Our preferred model explains the lower Nazca reflector as a fluid trap located at the front of recent hydration of the forearc mantle by fluids being supplied from dehydration of the subducting Nazca plate oceanic crust.

The subduction shear zone here is nearly a-seismic. Intermediate-depth earthquakes are offset downdip from the Nazca reflection by some 20 km into the oceanic mantle and cluster at some 100 km depth below the western Cordillera, the active magmatic arc. They are probably associated with intraplate

dehydration embrittlement. The higher parts of the Nazca reflector are probably controlled by deformation and elongation of the oceanic and tectonically eroded rocks at the blueschist transition which still occurs in the brittle field as shown by distributed friction-controlled seismicity.

Above the breakdown of the Nazca reflector a particularly bright reflection at some 20 km depth below the Precordillera is revealed (Quebrada blanca bright spot) with a reflection coefficient of similar strength as the Nazca reflection. Trapped fluids are again suggested to be the most likely cause for this reflection. The prevailing temperatures at this depth suggest that hydration of the rocks and destruction of permeability are probably controlled by retrograde metamorphism with chlorite formation at the amphibolite-greenschist facies boundary. The involved fluids are derived from the subduction zone as evidenced by a subvertical zone of high electric conductivity linking the two strong reflection sequences in the forearc along a major fault zone (West Fissure).

The magmatic cordillera and the backarc area below the Altiplano are nearly as reflective as the forearc, with a band of distributed reflectivity at some 15-25 km depth. A Moho can nowhere be observed at the base of the Andean crust. Some single shotgathers below the Precordillera and further east suggest minor reflectivity down to about 20 sTWT (60-70 km). Since the Moho is well identified at this depth below the Altiplano in wide angle observations and in receiver functions from teleseismic data, which both employ low frequency-long wavelength signals with a lower resolution capacity, the crust-mantle boundary probably has a transitional nature with a width of several km. Receiver function data, however, show a deep Moho at c. 70 km under the entire Altiplano from the Precordillera to the Eastern Cordillera along with a weakly W-dipping mid-crustal converter. This observation may suggest underthrusting of the Brazilian shield substantially further west than suggested from published balanced sections. The frequency-dependant Moho image may be due to active processes which obscure a sharp crust-mantle boundary like hydration of mantle rocks (in the cooler parts of the plate margin system), magmatic underplating and intraplating under and into the lowermost crust, partial melting, etc.

The mid-crustal reflection band under the Altiplano is linked to a low velocity zone, a high conductivity zone, and is associated to a strong P-to-S converter with negative impedance contrast at the base. Similar to the Tibetan plateau, these observations would suggest that the entire plateau is underlain by a fluid- or melt-enriched zone at the above depth. Deformation in the Altiplano, as seen from surface data, industry reflection lines, and section balancing is rooted at this level and does not seem to penetrate into the deeper crust. Moreover, analysis of high-resolution industry data clearly indicates that crustal shortening is stronger in the subsurface than that observed at surface. Taking into consideration distibuted shortening in the sedimentary cover, non-plane strain related to orogen-parallel material transport, and the methodological pitfalls of balancing techniques in uneroded orogens, actual crustal shortening is estimated to be substantially higher than previously suggested, more closely agreeing with values obtained from crustal scale area balancing.

The style of deformation across the Central Andean belt varies in a very specific way: Unstable extension and subsidence in the offshore forearc, strike-slip in the coastal Cordillera with mainly reactivation of earlier structures, a transition from localised shortening to transtension with uplift at the western Altiplano boundary that also reactivated earlier features, distributed thick-skinned shortening of the Altiplano area, thin- to thickskinned shortening and pop-up deformation of the Eastern Cordillera, thinskinned foreland imbrication in the Subandean belt. This distribution of styles is suggested to be basally-driven, i.e. by the existence and properties of a decollement level at some depth. While such a level exists in the Subandean zone (weak sediments) and the Altiplano (mid-crustal zone of partial melt), no such level is apparent in the forearc area. Here, a mechanically strong plate-interface controls subduction erosion along with extensional collapse of the uppermost crust, necessitating a decoupling in the deeper crust. The onshore forearc lacks a decollement and only shows evidence of deeply rooted deformation along reactivated basement structures. This typically Andean pattern of orogen-wide strain partitioning between forearc, arc and backarc is probably largely controlled by the actual temperature field, the compositional properties of the involved crust and the amount of erosive material transfer from the continent to the trench.

CONCLUSIONS

ANCORP'96 is the first section to produce a high resolution deep image of an active continental margin. Most reflectivity can be seen to be linked to active processes which involve the release, trapping, or consumption of fluids. This result is in contrast to seismic sections across most fossil mountain belts which usually can be interpreted in terms of structure and lithological contrasts only. Here, active petrological processes driven by active subduction are the probable causes for the most conspicuous features seen in the section. Thus, reflection seismic techniques have an unexpected potential to image ongoing intralithospheric processes at active margins. Integration with results from passive imaging techniques, details from industry seismic sections, and general methodological considerations suggest that plateau formation and crustal thickening are mostly controlled by tectonic shortening.

REFERENCES

ANCORP Research Group, 1999. Seismic reflection image of the Andean Subduction Zone Reveals Offset of Intermediate-Depth Seismicity into Oceanic Mantle. Nature, 397, 341-

NEW U-Pb AGES AND Sr-Nd DATA FROM THE FRONTAL CORDILLERA COMPOSITE BATHOLITH, MENDOZA: IMPLICATIONS FOR MAGMA SOURCE AND EVOLUTION

Helen M. ORME (1) & Michael P. ATHERTON (2)

(1) School of Geological Sciences, Kingston University, Penrhyn Road, Kington-Upon-Thames, Surrey, KT1 2EE, UK. <h.orme@kingston.ac.uk>
(2) Department of Earth Sciences, University of Liverpool, Brownlow Street, Liverpool, L69 3BX, UK. <mikea@liv.ac.uk>

KEY WORDS: Frontal Cordillera, U-Pb dates, Sr-Nd data.

INTRODUCTION

Palaeozoic granitic and associated acid volcanic rocks of the Frontal Cordillera Composite Batholith (FCCB) of Mendoza Province (Argentina) belong to one of the least studied segments of the pre-Andean Frontal Cordillera (FC), yet they record an important, but still poorly understood, episode of large-scale silicic magmatism related to the final assembly and initial break-up of the Gondwanan margin of the Pangaea supercontinent. The FC is a remnant of a Palaeozoic orogen which has since been partially covered by the sediments and volcanics of the Cenozoic, and suffered tectonic rejuvenation during the Andean Orogeny.

GEOLOGICAL SETTING

The Frontal Cordillera Composite Batholith (FCCB) is made up of granitic plutons cropping out with a N/S strike over the entire length (>800km) of the Frontal Cordillera (FC) from Argentina to northern Chile, between latitudes 27° - 36°46'S. The FC today is sandwiched between the Precordillera to the east, the Principal Cordillera of Chile to the south-west and the Coastal Cordillera of Chile to the north-west. Boundaries are east directed thrust fronts developed during the more recent Andean Orogeny.

The batholith consists of granites, granodiorites and tonalites, that crop out in various N/S striking cordones or chains in Argentina and Chile. The volcanic rocks associated both spatially and temporally with the FCCB are the Choiyoi Formation (Rolleri & Criado Roque, 1969). The succession consists of mainly andesitic and dacitic lavas, tuffs and breccias with later sub-volcanic porphyry rhyolite bodies. The exact relationship between the FCCB and the Choiyoi volcanics is a matter of debate (Polanski, 1958; Caminos, 1979).

In the south of the FCCB there have been two major isotopic dating studies, using the K-Ar method (Dessanti & Caminos, 1967) and the K-Ar plus Rb-Sr method (Caminos et al, 1979). The results prompted the subdivision the FCCB in this region into three magmatic cycles: ~400-300 Ma (Silurian to Lower Carboniferous), 275 ± 30 Ma (Lower Permian) and 225 ± 20 Ma (Triassic) (Caminos et al, 1979). More recent workers have divided the intrusion of the batholith into two distinct phases that occurred between the Lower Carboniferous and the Mid Triassic with associated eruptive events (Ramos, 1993).

RESULTS

- The seven FC stocks studied are I-type metaluminous, calc-alkaline granitic plutons. The Boca del Rio, Cacheuta and Cerro Médanos stocks crop out along the río Mendoza ~50km west of the city of Mendoza; Cerro Arenales stock crops out in cordón del Plata 10km to the west, and Cerro Bayo, Punta Negra and Punta Blanca stocks crop out in cordón del Portillo, 35km to the west of Tunuyán. They range in composition from granodiorites to monzogranites to syenogranites The stocks contain typical metaluminous modal mineralogies of plagioclase, quartz and K-spar, with amphibole and biotite. In addition, the granodiorite stocks contain primary clinopyroxene, mostly in the form of secondary polycrystalline amphibole clots. Accessory phases include magnetite, zircon, titanite, apatite and allanite, which are characteristic of I-type rocks. With the exception of Punta Blanca stock, the plutons are high-K and plot with alkalic trends on the TAS diagram. Contact relationships between the granitic

stocks and the Choiyoi volcanics, long thought to be their effusive equivalents, are intrusive, suggesting that the volcanic rocks are older, though chemically similar to the granites.

- P-T data from amphiboles suggest depths of emplacement of less than 10km. The Boca del Rio, Cerro Arenales, Cerro Bayo and Punta Blanca stocks all contain amphiboles which crystallised within 3-4km of the surface; this indicates that whilst the stocks are not sub-volcanic, emplacement occurred relatively near the surface.

- The FCCB differs from typical I-type granites batholiths, such as the Coastal Batholith of Peru (Atherton et al, 1979), in some crucial respects: 1) they are high-K (with the exception of Punta Blanca stock), 2) alkali feldspar crystallised early in the more evolved stocks, as indicated by Ba and Sr depletion with increasing SiO_2, geochemical modelling and quaternary diagrams, 3) the stocks contain high Ba and intermediate Sr, with U and Th enrichment in the leucocratic stocks of Cacheuta, Cerro Arenales and Punta Negra, and 4) the stocks form part of a batholith in which granites predominate over granodiorites and tonalites (granites / granodiorites + tonalites = 4.5; Caminos, 1965). Typical I-type Cordilleran batholiths e.g. the Coastal Batholith of Peru, are predominantly tonalitic to granodioritic (granites / granodiorites + tonalites = 0.01; Wilson, 1989).

- On an εNd_t vs. $^{87}Sr/^{86}Sr_i$ diagram, FCCB granites show a trend of radiogenic Sr enrichment (from ~0.7045 to ~0.7095) with fairly constant εNd_i (~2.5 - 3.5). Binary mixing and AFC was modelled using a MORB-type magma (the most basaltic dyke in the area) with various examples of South American basement and enriched mantle compositions. Simple binary mixing required the addition of >60% EMII to generate the most evolved FCCB granite composition, which is unrealistic. Binary mixing with basement rocks and AFC trends with the same contaminants do not approach that of the FCCB rocks. This suggests that the isotopic variations of the FCCB plutons are the result of heterogeneities in the source, rather than later high level processes.

- Three stocks, Cerro Médanos, Cerro Bayo and Punta Blanca, were dated by the U-Pb zircon method. These are the first such dates for any plutons of the FCCB. Punta Blanca stock was found to be 276 Ma old, Cerro Médanos stock 263 Ma old, and Cerro Bayo stock 262 Ma old. All of these ages are in the Lower Permian. These dates differ from those in the literature (291 Ma by K-Ar and 264 Ma by Rb-Sr; 271 Ma by K-Ar; and 244 Ma by K-Ar and 404 Ma by Rb-Sr, respectively). This is interpreted to be the result of disruption of the K-Ar and Rb-Sr decay schemes by the alteration and deformation experienced by these stocks.

- The granitic rocks of the southern FC are mineralogically and geochemically similar to the so-called subalkaline potassic plutons of the Ballons Massif, France (Pagel & Leterrier, 1980). Other plutons of this type include the "monzonitic" Tak Batholith, Thailand (Mahawat et al, 1990) and the monzonite

suites of Patagonia (Rapela & Pankhurst, 1996). These plutons have been likened to the volcanic shoshonitic associations with high K_2O/Na_2O and high Ba, Sr, U and Th contents, which are formed over active continental margins.

REFERENCES

Atherton, M. P., McCourt, W. J., Sanderson, L. M., & Taylor, W. P., 1979. The geochemical character of the segemented Peruvian Coastal Batholith and associated volcanics, *in*: Atherton. M. P., & Tarney, J., *eds*, Origin of granite batholiths: Geochemical evidence. Shiva Publishing Ltd, Cheshire, 148pp.

Caminos, R., 1965. Geología de la vertiente oriental del cordón del Plata, Cordillera Frontal de Mendoza. Rev. Asoc. Geol. Arg., Bs. As., 20 (3), 351-392.

Caminos, R., 1979. Cordillera Frontal, *in* Turner, J. C. M., ed., Segundo Simposio Geología Regional Argentina: Córdoba, Argentina, Academia Nacional de Ciencias, 1, 397-454.

Caminos, R., Cordani, U. G., & Linares, E. 1979. Geología y geocronología de las rocas metamórficas y eruptivas de la precordillera y cordillera frontal de Mendoza, República Argentina. II Congreso Geológico Chileno, Actas, 43-60.

Mahawat, C., Atherton, M. P., and Brotherton, M. S., 1990. The Tak Batholith: the evolution of contrasting granite types and implications for tectonic setting. J. Southeast Asian Earth Sci., 4 (1), 11-27.

Pagel, M., & Leterrier, J., 1980. The subalkaline potassic magmatism of the Ballons Massif (Southern Vosges, France): shoshonitic affinity. Lithos, 13, 1-10.

Polanski, J., 1958. El bloque Varisco de la Cordillera Frontal. Asociacion Geológica Argentina, Revista XII (3), 165-195.

Ramos, V. A., 1993. Interpretacion Tectonica. XII Congreso Geológico Argentino y II Congreso de Exploración de Hidrocarburos (Mendoza), *in* Ramos, V. A., ed., Geología y Recursos Naturales de Mendoza, Relatorio I (7), 65-78.

Rapela, C. W., & Pankhurst, R. J., 1996. Monzonitic suites: the innermost Cordilleran plutonism of Patagonia. Trans. R. Soc. Edinburgh Earth Sci., 87, 193-203.

Rolleri, E. O., & Criado Rocque., 1969. Geología de la provinvia de Mendoza. Cuart. J. Geologíca Argentina Acta, 2, 1-60.

Wilson, M., 1989. *Igneous Petrogenesis*. Chapman & Hall, London. 466p.

EPISODIC SILICIC VOLCANISM IN PATAGONIA AND THE ANTARCTIC PENINSULA: PLUME AND SUBDUCTION INFLUENCES ASSOCIATED WITH THE BREAK-UP OF GONDWANA

R.J. PANKHURST (1, 2), T.R. RILEY (1), C.M. FANNING (3) and S. P. KELLEY (4)

(1) British Antarctic Survey, NERC Isotope Geoscience Laboratories, Keyworth, Nottingham NG12 5GG, UK. Fax: +44 (0)115 936 3302;e-mail: r.pankhurst@bas.ac.uk
(2) British Antarctic Survey, High Cross, Cambridge CB3 0ET, UK; t.riley@bas.ac.uk
(3) Research School of Earth Sciences, The Australian National University, Canberra ACT 0201, Australia; prise.fanning@anu.edu.au
(4) Department of Earth Sciences, The Open University, Milton Keynes MK7 6AA, UK; s.p.kelley@open.ac.uk

KEY WORDS: Ignimbrites, U–Pb Zircon, Jurassic, Patagonia, Antarctic Peninsula

INTRODUCTION

Jurassic magmatism in western Gondwana constituted the most voluminous episode of continental volcanism in the Phanerozoic era. During Early–Middle Jurassic time, some 2½ –3 million km^3 of basalt and, to a lesser extent, rhyolite were erupted onto the supercontinent in its early stages of break-up. Recent high-precision geochronology (U–Pb and Ar–Ar) has shown that much of the basalt volcanism occurred during a very short period around 183–184 Ma ago, but comparable studies of the silicic volcanism have so far been lacking.

The Jurassic silicic volcanic rocks of the Chon Aike province of Patagonia and the similar sequences of the Antarctic Peninsula Volcanic Group, together with related sub-volcanic granitoids, constitute one of the largest silicic igneous provinces known (see review by Pankhurst et al. 1998). Knowledge of the timing and nature of this volcanism is crucial to assessing its role in the rifting and break-up of Gondwana. Key questions concern whether silicic and mafic magmatism were synchronous, the previously observed evidence for westward migration of volcanism, and the significance of petrogenetic models for the generation of the magmas. New geochronological data obtained by Rb–Sr whole-rock, SHRIMP U–Pb zircon, and ^{40}Ar–^{39}Ar feldspar methods are presented for these rocks.

RESULTS

All three geochronological methods are capable of equivalent precision, but only the U–Pb method has yielded consistently reliable results for dating the crystallization of these ignimbritic rocks. Rb-Sr is prone to hydrothermal resetting in the analysed material and Ar–Ar is affected both by this and, apparently, by initial excess ^{40}Ar. U-Pb SHRIMP dating of such rocks is both precise and reliable; obviously volcanic zircon forms were selected (usually with axial gas tubes), and it was possible to target only the cleanest parts of such crystals, clear of cracks and inclusions.

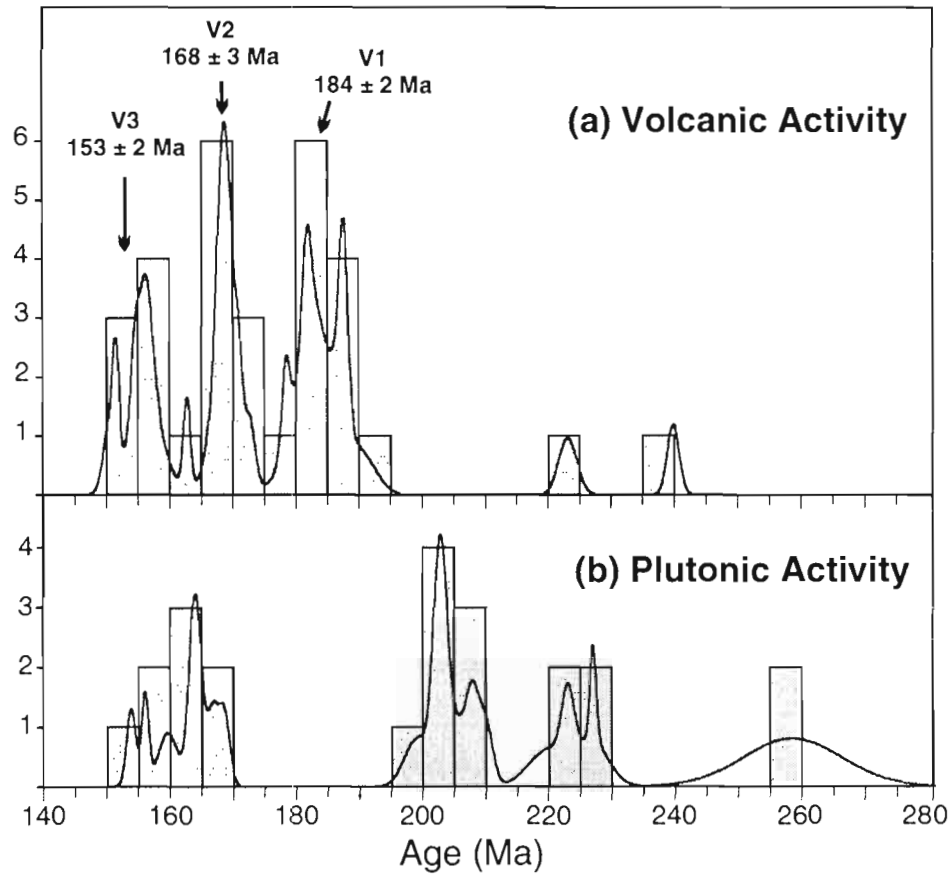

Figure 1. Histograms and cumulative frequency curves for the ages of silicic volcanism (top) and plutonism (bottom) in Patagonia and the Antarctic Peninsula.

The results show that the silicic volcanism occurred over an extended period of time (*c.* 185–155 Ma), but was apparently concentrated in three main episodes, termed V1 = 184 ± 2 Ma, V2 = 168 ± 3 Ma and V3 = 153 ± 2 Ma (Fig. 1a). The first of these essentially coincides with the Karoo plume-related mafic magmatism of South Africa and the widespread Ferrar mafic magmatism of Antarctica and

Tasmania. The silicic products of V1 have „within-plate" geochemical affinities, i.e. a tendency to high Nb and Zr contents. They also have quite strongly negative εNd_t values of –4 to –9,and are interpreted as lower crustal melts. The two subsequent episodes, V2 and V3, exhibit progressive migration of activity towards the Pacific margin of Gondwana, merging into initiation of a subduction-related arc centred on the Andes. The chemistry of these V2 and V3 rhyolitic ignimbrites is more characteristic of destructive plate margins as shown by their lower Nb and Zr contents and less strongly negative εNd_t values of –2 to –5 (Fig. 2).

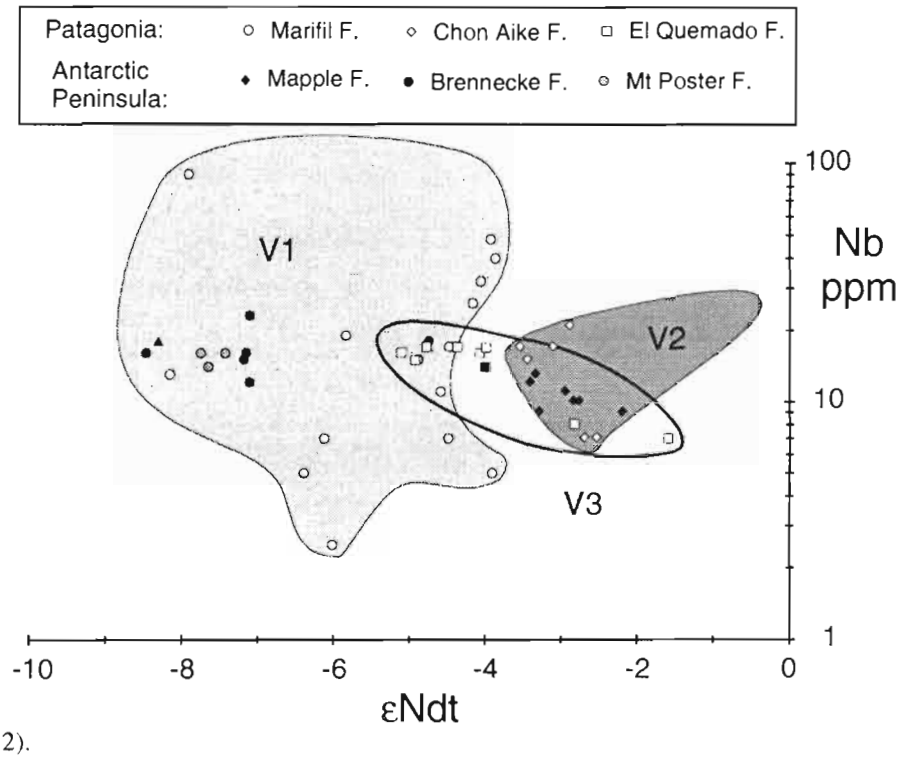

Figure 2: Geochemical distinction between the three episodes of volcanism defined in the text.

Ignimbrites erupted during previously identified Permian and Triassic silicic igneous cycles also show within-plate characteristics, so that the V1 event cannot be uniquely attributed to the effects of the Karoo plume. The overall pattern of Mesozoic activity in the region suggests episodic alternation of subduction-dominated (plutonic) and extension-dominated (volcanic) tectonics at the continental margin over a period of 100 Ma, finally leading to opening of the South Atlantic Ocean.

CONCLUSIONS

The Jurassic volcanic province of Patagonia and the Antarctic Peninsula is now revealed as a complex polygenetic one, formed by multiple events by and generated by a variety of magmatic processes. Discrete episodes reflect changes in the tectonic regime of Gondwana break-up, apparently involving the alternation of extension and compression related to subduction at the Pacific margin. The Early Jurassic extensional phase coincided with uprise of the Karoo mantle plume. All these events preceded Early Cretaceous separation and opening of the Atlantic Ocean.

REFERENCES

Pankhurst, R.J., Leat, P.T., Sruoga, P, Rapela, C.W., Márquez, M., Storey, B.C. and Riley, T.R. (1998). The Chon-Aike silicic igneous province of Patagonia and related rocks in West Antarctica: a silicic LIP. *Journal of Volcanology and Geothermal Research*, **81**, 113-136.

THERMOCHRONOLOGY OF THE LOWER CRETACEOUS CALEU PLUTON IN THE COAST RANGE OF CENTRAL CHILE: TECTONO-STRATIGRAPHIC IMPLICATIONS

Miguel A. PARADA(1) and Paula LARRONDO(1)

(1)Departamento de Geología, Universidad de Chile. Casilla 13518, correo 21, Santiago, Chile
maparada@cec.uchile.cl

KEY WORDS: Thermochronology, Lower Cretaceous, Coast Range, central Chile

INTRODUCTION

The Caleu pluton, located in the Coast Range of central Chile (33° S - 71° W), is a zoned body emplaced into an eastward dipping thick pile of flood basalts and intermediate lava flows of the Lower Cretaceous Veta Negra Formation. Three lithological zones are recognized in the pluton: (1) hornblende-pyroxene gabbro zone (GB zone), (2) hornblende-biotite tonalite zone (TO zone) and (3) biotite-hornblende granite zone (GR zone). The contact between the GB and TO zones is gradational suggesting an origin from a common magma chamber. The rocks of the GR zone intrude rocks of the TO zone.

The aim of this study is to provide evidence, from hornblende and biotite ^{40}Ar-^{39}Ar and apatite fission track dating of the Caleu pluton, about the tectono-stratigraphic processes that took place during a clue period (Lower Cretaceous) of the Andean geological evolution in central Chile.

GEOCHRONOLOGICAL RESULTS

Four samples were selected for ^{40}Ar-^{39}Ar and fission track dating (Table 1). Sample 97018-3 was taken from the GB zone near the transition to the TO zone. Samples 970524-3 and 970121-4 were collected from the TO zone but separated 1,100 m in the vertical sense from each other. Sample 970616-1 is representative of the GR zone.

Sample (zone)	Hornblende*	Biotite*	Apatite**	Elevation (m)
970118-3 (GB)	117.0 ± 1.0	100.9 ± 0.8	92.7 ± 6.2	1,400
970524-3 (TO)	109.5 ± 1.1	98.7 ± 0.9	95.7 ± 6.2	1,975
970121-4 (TO)	110.1 ± 1.6	98.1 ± 0.8	90.4 ± 7.6	875
970616-1 (GR)	102.8 ± 0.9	93.9 ± 0.9	82.0 ± 5.6	1,100

Table 1. Geochronological data in Ma. * ^{40}Ar-^{39}Ar; ** Fission track

The ^{40}Ar-^{39}Ar analyses were performed at the Geochronological Laboratory of Standford University. The Ar spectra of the analyzed samples yielded weighted mean plateau ages. The apatite fission track ages were obtained at Dalhousie University Fission Track Laboratory. The apatite of all four samples contained abundant confined fission tracks and pass the chi-square test at 95 % confidence level.

IMPLICATIONS CONCERNING THE AGE OF THE VETA NEGRA FORMATION

The Veta Negra Formation, into which the Caleu pluton was emplaced, represents one of the most intensive volcanic events of the Andes of central Chile. Its 10,000 m thick pile of volcanic strata and continental sedimentary intercalations was deposited in extensional intra-arc subsiding basins (Vergara et al., 1995). The Veta Negra Formation was deposited during the Barremian - Albian interval (124 - 98 Ma) because it overlies the Hauterivian Lo Prado Formation and is locally intruded by a Cenomanian granitoid pluton (Vergara et al., 1995). However, the oldest age reported here for the Caleu pluton constraints the upper age limit of the Veta Negra Formation deposition to 117 Ma (see Table 1). Furthermore, the age of this formation could be even older if one takes into account that, according to preliminary paleomagnetic results (Roperch, oral com.), the Caleu pluton is not tilted despite the homoclinal disposition of the Veta Negra Formation. It is interesting to note that an age of 119.4 ± 1.2 Ma has been obtained on fresh plagioclase phenocrysts from a Veta Negra volcanic rock sample (Féraud et al., 1998).

The rate of subsidence for the Veta Negra Formation that can be calculated dividing its thickness by its age, is of about 1.4 mm/yr, which is substantially larger than the previous estimations (0.25 mm/y; Vergara et al., 1995).

RATE OF UPLIFT-EROSION OF THE CALEU PLUTON

The uplift-erosion rates were determined by two methods: 1) the mineral pair method, which utilizes the difference between cooling ages of two different minerals (using either hornblende and biotite ^{40}Ar-^{39}Ar ages or apatite fission track ages) from a single sample; 2) the relief method that uses the differences in cooling ages for a single mineral from two samples collected at different elevations. For the uplift-erosion calculation using the first method, a low geothermal gradient (Aberg et al., 1984; Vergara et al., 1994) of 25 °C/km is assumed. During the 117-100 Ma interval, the uplift-erosion rates were about 0.6 mm/yr and increased significantly to about 1.0 mm/yr around 100 to 93 Ma. Uplift-erosion rates decreased to *c.* 0.7 mm/yr from 93 to 82 Ma. The weigthed mean rate of uplift-erosion is 0.7 mm/yr for the time elapsed between the setting of the hornblende ^{40}Ar-^{39}Ar and apatite fission track 'clocks'. This value can be reduced if the time of the pluton emplacement (currently unknown) and/or a higher thermal gradient are considered. Moreover, uplift-erosion rates of the Caleu pluton of 0.17 and 0.25 mm/yr were obtained using the hornblende ^{40}Ar-^{39}Ar and apatite fission track ages and pressure estimate of hornblende cristalization (2 kb) of two samples from the TO zone (samples 970524-3 and 970121-4).

For the calculation based on the relief method, the apatite fission track ages of samples 970524-3 and 970121-4 (collected at 1,975 and 875 m, respectively) were considered. The uplift-erosion rate thus calculated is about 0.2 mm/yr.

DISCUSSION

The rates of 0.17 - 0.25 mm/yr for the Caleu pluton are comparable with the rate of erosion of >0.3 mm/yr obtained for the Veta Negra Formation before the deposition of the overlying syntectonic Las Chilcas Formation (Vergara et al., 1995). The comparatively high rate of uplift-erosion for the 100-93 Ma interval (*c.* 1.0 mm/yr) could indicate an orogenic peak yielding a tectonic relief and the subsequent formation of molassa type deposits represented by the thick conglomerates with abundant volcanic fragments that characterize most of the Las Chilcas Formation. Consequently the deposition of the Las Chilcas Formation should have ocurred during that interval. This age for the Las Chilcas conglomerate is compatible with the Mid-Albian (107-102 Ma) age for the limestone intercalations (Polpaico limestone) at the lowermost levels of the Las Chilcas Formation deduced from marine planktonic microfossils (Martínez-Pardo et al., 1994). The paleogeographic reconstruction inferred by Martínez-Pardo et al., (1994) from the Polpaico limestones, indicates a shallow marine platform open to the Pacific Ocean and connected southeastward with the Neuquén basin. Therefore,

the observed peak in the rate of uplift-erosion of the Caleu pluton may be associated with the closure of the Early Cretaceous subsiding volcano-sedimentary intra-arc basins, the beginning of arc/orogene construction and the deposition of the Las Chilcas molasse.

The apatite fission track thermochronological results of 82-96 Ma obtained for the Caleu pluton would confirm that the age of 93.1 ± 0.3 obtained on secondary adularia in the Veta Negra Formation (Féraud et al., 1998), represents an age of burial metamorphism since at that time the pluton was at *c.*100 °C, which is lower than the temperature of formation for secondary adularia.

ACKNOWLEDGEMENTS

This study was financed by the FONDEF Project 1033 and DTI Project E3306

REFERENCES

Aberg G., Aguirre L., Levi B., Nyström J.O. 1984. Spreading-subsidence and generation of ensialic marginal basins: an example from the early Cretaceous of central Chile. In: Kokelaar, B.P., Howells, M.F. Volcanic and Associated Sedimentary and Tectonic Processes in Modern and Ancient Marginal Basins. The Geological Society, Spec. Pub. 16, pp. 185-193.

Féraud G., Aguirre L., Vergara M., Morata D., Rolinson D. 1998. ^{40}Ar-^{39}Ar data on primary and secondary minerals of a volcanic series affected by burial metamorphism: example of a Cretaceous Andean extensional basin. Mineralogical Magazine, 62A, 444-445.

Martínez-Pardo R., Gallego A., Martínez-Guzmán R. 1994. Middle Albian marine planktonic microfossils from the Santiago basin, central Chile: their depositional and paleogeographic meaning. Revista Geológica de Chile, v. 21, pp. 173-187.

Vergara M., Levi B., Nyström J.O., Cancino A. 1995. Jurassic and Early Cretaceous island arc volcanism, extension, and subsidence in the Coast Range of central Chile. Geological Society of America Bulletin, v. 107, pp. 1427-1440.

THE PUNITAQUI EARTHQUAKE OF 14 OCTOBER 1997 (Ms=6.8): A DESTRUCTIVE INTRAPLATE EVENT IN CENTRAL CHILE

Mario PARDO(1), Diana COMTE(1) and Tony MONFRET(2)

(1) Departamento de Geofisica, U. de Chile, Casilla 2777, Santiago, Chile (mpardo, dcomte @dgf.uchile.cl)
(2) IRD, 209-213, rue La Fayette, 75480 Paris-Cedex 10, France (monfrett@faille.unice.fr)

KEY WORDS: Seismotectonic, Seismicity, Subduction, Central Chile

INTRODUCTION

On October 15, 1997, a magnitude Ms=6.8 earthquake stroke central Chile producing important damages into the Punitaqui-Ovalle region, located about 100 km south of Coquimbo city. Even though it magnitude was moderate, the reports indicate that eight people died, almost 5000 houses collapsed and about 16000 houses were strongly damaged. The earthquake was followed by many aftershocks for several months, being the most important the one which occurred on November 3, 1997 (Ms=6.2), with epicenter located inland similar to the main shock, but at a shallower depth.

About two months before this seismicity, a swarm type activity of thrust events occurred offshore central Chile, between 30°S and 30.8°S, during July and August. At least 13 shallow thrust earthquakes (mb≥4.9) were reported in the Harvard CMT catalogue (HCMT), with two of them with maximum magnitude mb=5.8. Although their hypocenters were located close to the cities of Coquimbo and La Serena, low damages and intensities were reported there.

Due to the lack of local seismological stations in the region, outside the coverage area of the seismological network that the University of Chile operates about 250 km to the south, it was not possible to accurately locate the hypocenters of these events. For that reason, we relocate the hypocenters determined from records of stations at teleseismic distances, in order to study this earthquake and its possible relation to the precedent swarm type activity.

SEISMOTECTONIC SETTING

The studied seismicity is located within the rupture zone of the large April 6, 1943 Illapel earthquake (Ms=7.9) (Kelleher, 1972) (Figure 1). According to historical reports, it has been affected by at least other

two important earthquakes, on July 8, 1730 (M~8.7), and on August 15, 1880 (M~7.7). The 1943 event generated a local tsunami of 4.5 m (Beck et al., 1998). To the south, this region is limited by the 1971 Aconcagua (Ms=7.5) and 1906 Valparaíso (Ms=8.3) earthquakes rupture zones (Kelleher, 1972; Malgrange et al., 1981; Korrat and Madariaga, 1985) and to the north by the 1922 Copiapó (Ms=8.3) seismic event (Beck et al., 1998). These are thrust events related to the subduction of the Nazca plate beneath the overriding South American plate.

The region is included into the zone (27°S-33°S) where the dip of the subducted slab becomes nearly horizontal at depths of 100-120 km, for more than 250 km beneath the Andes and Argentina, before reassuming its descent into the mantle (Cahill and Isacks, 1992). This nearly horizontal slab geometry characterized the general tectonic of the zone: a strongly coupled interplate contact, a highly compressed continental crust with back-arc crustal shortening and seismic activity in Argentina, and absence of active Quaternary volcanism.

DATA AND ANALYSIS

The data used correspond to the hypocenters reported by ISC of earthquakes with magnitude mb>5, occurred in the region between 1964 and 1996, and the arrivals time of P, pP and S waves from the earthquakes occurred during 1997, with more than 15 of these phases reported by NEIC. The focal mechanisms of the events between 1977 and 1997 were obtained from the HCMT catalogue.

The P, pP and S waves arrival times, were used to relocate the 1997 hypocenters using the Joint Hypocenter Determination technique, JHD (Dewey, 1971). The largest 21 earthquakes were used as calibration events to determine the time residual correction matrix to be applied to the rest of the 1997 events. A total of 152 events were relocated (Figure 1-B).

The relocated seismicity during 1997 shows two clusters. The first one is located offshore between 30°S and 30.8°S, corresponding to the offshore swarm type activity during July and August, with at least 13 events with magnitudes $4.9 \leq mb \leq 5.8$. The second one is located inland between 30.8°S and 31.3°S, corresponding to the Punitaqui earthquake sequence (Figure 1-B). These clusters in seismicity occurred in zones where, at least since 1964, very low seismicity was observed (Figure 1-A). At the plate interface between the shallow offshore activity and the Punitaqui seismicity, not important earthquakes occurred during 1997 (Figure 1-C), suggesting that this part of the interplate contact was not seismically activated and that it is strongly coupled.

The Punitaqui earthquake mainshock was relocated at 31.02°S, 71.21°W, and 67 km of focal depth, differing on about 35 km from the hypocenter obtained from the central Chile local network located ~250 km to the south (30.74°S, 71.33°W, 52 km). The largest aftershock was relocated at 30.84°S, 71.26°W and depth of 52 km. Though these earthquakes have similar epicenters, the focal mechanisms indicate that the mainshock was an intraplate event within the subducted slab with an almost vertical fault plane related to downdip tension, while the largest aftershock corresponds to an interplate event with reverse faulting related to compression along the plate interface (Figure 1-C).

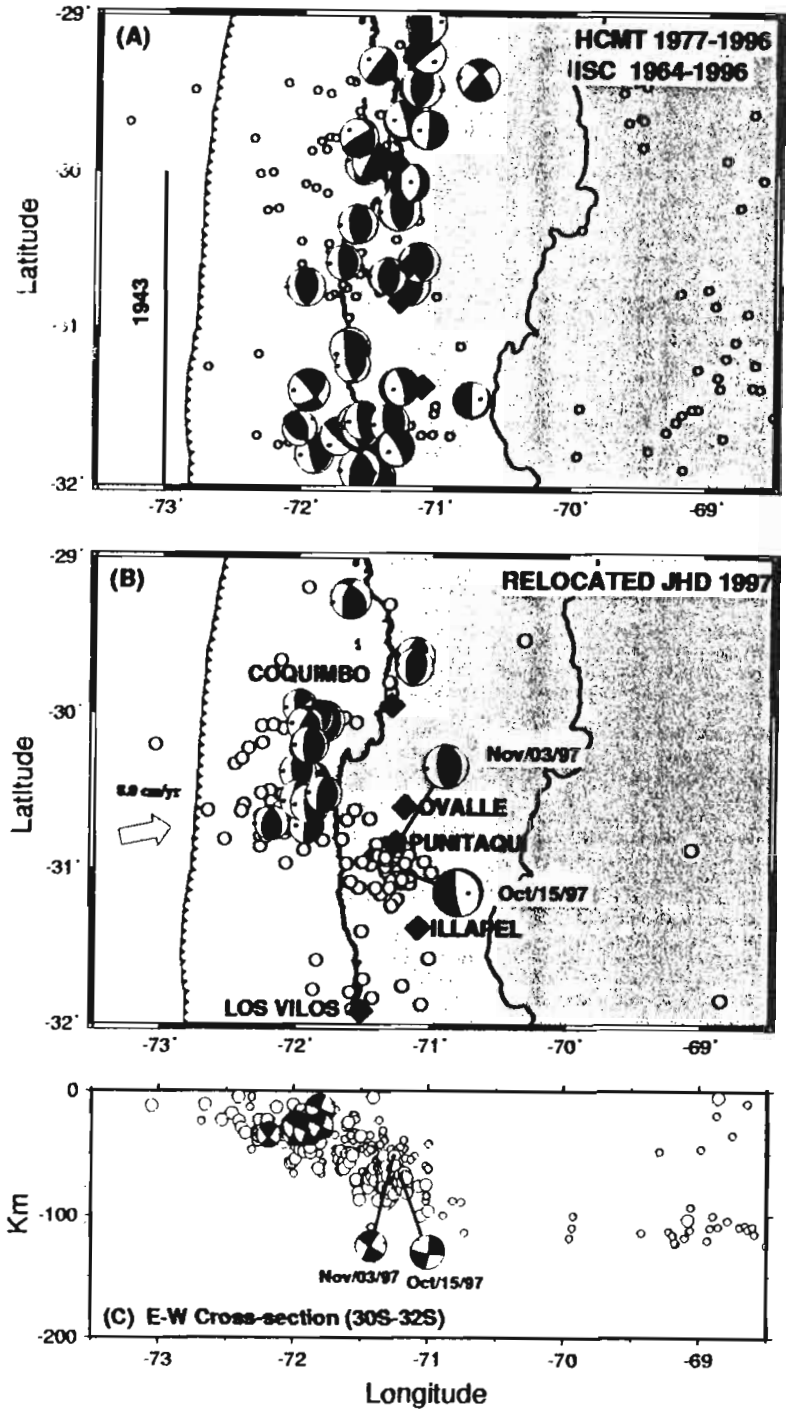

Figure 1.

(A) Epicenters for the indicated time periods before 1997, reported by the ISC with magnitude mb>5, with focal mechanisms from the HCMT catalogue on lower hemispheric projection with size proportional to the magnitude and showing P and T axis (black and white dots), Also are shown the 1943 earthquake rupture length, the trench and the Chile-Argentina border line.

(B) Relocated epicenters using the JHD method of all the events, mb>5.0, reported by NEIC during 1997. Focal mechanisms are from the HCMT catalogue, as in Fig 1-A. The Punitaqui mainshock and its largest aftershock are indicated. Solid diamonds indicate some cities in the zone. The arrow shows Nazca-South America convergence direction.

(C) East-West cross-section of the seismicity presented on Fig. 1-A and B, between 30°S and 32°S, using the same symbols. Focal mechanisms are on lateral back hemispheric projection.

Though the magnitude of the intraplate Punitaqui earthquake was moderated (Ms=6.8), the structures in the zone were highly damaged as the result of the strong ground motion and also site-amplification effects. In contrast, the offshore thrust events (mb≤5.8) that occurred about two months before, produced almost no damages and were felted with low intensities at populated cities located at similar hypocentral distances than the structures that collapsed with respect to the Punitaqui earthquake. This suggests that the potential of

damage or strong ground motion, of intraplate earthquakes is higher than the one of thrust events. Other destructive intraplate earthquakes have been observed along the Chilean subduction zone, as the downdips 1939 Chillan earthquake (Ms=7.8) and the 1965 Aconcagua earthquake (Ms=7.5), which occurred at similar depths than the Punitaqui earthquake, and the 1950 Calama earthquake (Ms=8.0) at a depth of 120 km.

CONCLUSIONS

The Central Chile subduction zone, corresponding to the rupture zone of the last large thrust earthquake occurred in this region in 1943 (Ms=7.9), was partially activated during 1997. The shallowest part of the Nazca–South America interplate contact was activated on July and August, by an offshore swarm type seismicity with thrust events in the magnitude range $4.9 \leq mb \leq 5.8$. On October 15, an intraplate tensional event (Ms=6.8) occurred downdip, below the village of Punitaqui, generating many compressional aftershocks that activated the deepest part of the interplate contact. Not important earthquakes occurred at the central part of the interplate contact indicating that the interacting plates are strongly coupled in this region.

The Punitaqui earthquake generates unexpected damages for an event of this magnitude. The large damages produced by this moderate size intraplate tensional earthquake, along with the observation of other destructive intraplate tensional events in Chile, suggests that these type of earthquakes have a higher potential of producing strong ground motion than the thrust type events.

ACKNOWLEDGEMENTS: This study is supported by FONDECYT 1990355 and IRD-France projects.

REFERENCES

Beck S., S. Barrientos, E. Kausel and M. Reyes, 1998. Source characteristics of historic earthquakes along the Central Chile subduction zone. *J. South Am. Earth Sc.*, in press.

Cahill, T., and B. Isacks, 1992. Seismicity and shape of the subducted Nazca plate. *J. Geophys. Res.*, **97**, 17503-17529.

Dewey, J., 1971. Seismicity studies with the method of Joint Hypocenter determination. *Ph.D. Thesis, U. California, Berkeley.*

Kelleher J. A., 1972. Rupture zones of large South American earthquakes and some predictions. *J. Geophys. Res.*, 77, 2087-2103.

Korrat I. and R. Madariaga, 1986. Rupture of the Valparaiso (Chile) gap from 1971 to 1985. in *Earthquake Source Mechanism , Geophysical Monograph 37, Am. Geophys. Union, Washington, D.C.*, 247-258.

Malgrange M., A. Deschamps and R. Madariaga, 1981. Thrust and extensional faulting under the Chilean coast: 1965, 1971 Aconcagua earthquakes. *Geophys. J. R. Astr. Soc.*, **66**, 313-331.

WHITNESSES OF AN ACCRETED OCEANIC TERRANE IN EARLY EOCENE DEPOSITS OF NORTHERN PERU : TECTONIC IMPLICATIONS

Laurence PECORA [1,2], Étienne JAILLARD [1,3] and Henriette LAPIERRE [4]

(1) Institut Dolomieu, 15 rue Maurice-Gignoux, 38031 Grenoble Cedex, France.
(2) Géosciences Rennes, Campus de Beaulieu, 35042 Rennes Cédex, France.
(3) IRD (anciennement ORSTOM), CS 1, 211 rue La Fayette, 75480 Paris Cedex 10, France, ejaillar@ujf-grenoble.fr
(4) UPRES A 5025, Institut Dolomieu, 15 rue Maurice-Gignoux, 38031 Grenoble Cedex, France, lapierre@ujf-grenoble.fr.

KEYWORDS : accretion, oceanic terranes, Eocene, North Peru.

INTRODUCTION - GEOLOGICAL FRAMEWORK

Northwestern South America is made of accreted oceanic terranes, some of which are assumed to have been subsequently displaced along major dextral wrench faults (McCourt et al., 1984; Aspden & Litherland, 1992; Toussaint & Restrepo, 1994; Litherland et al., 1994; Aspden et al., 1995; Cosma et al., 1998; Jaillard et al., 1999). However, such movements are difficult to demonstrate and quantify.

Western Ecuador comprises oceanic and continental terranes accreted to the south-american margin (Litherland et al., 1994; Cosma et al., 1998). These terranes include oceanic plateaus overlain by island arc series of Cretaceous age (Goossens & Rose, 1973; Kehrer & Van der Kaaden, 1979; Lebrat et al., 1987; Cosma et al., 1998, Reynaud et al., 1999). They were accreted in the Late Cretaceous (Faucher & Savoyat, 1973; Kehrer & Van der Kaaden, 1979; Lebrat et al., 1987) and in the Late Paleocene (~ 57 Ma; Jaillard et al., 1997; Cosma et al., 1998). In southern Ecuador (Guayaquil area), the latter event is locally marked by strong deformations which affect early Late Paleocene cherts and are concealed by unconformable, coarse-grained quartz-rich turbidites of latest Paleocene age (Jaillard et al., 1997).

In the Paita area (northern Peru, fig. 1), unconformable transgressive forearc deposits of latest Cretaceous age rework the metamorphic and sedimentary Paleozoic basement (Fig. 2; Jaillard et al., 1999). The unconformably overlaying coarse-grained conglomerates (Mogollón Fm), of latest Paleocene-earliest Eocene age (~ 56-52 Ma, Morales, 1993), contain boulders of mafic magmatic rocks, whereas such boulders are lacking in the underlying deposits. The petrographic and geochemical study of five of these boulders indicates that some of them are of oceanic origin, thus indicating that an accretion occurred in Northwestern Peru by the Paleocene-Eocene boundary.

PETROGRAPHY AND GEOCHEMISTRY OF MAGMATIC ROCK BOULDERS FROM THE MOGOLLON FORMATION (PAITA BASIN)

Petrography and mineralogy

All the samples are affected by a low grade metamorphism. Plagioclase is sometimes altered in sericite while clinopyroxene is entirely replaced by pale green actinolitic hornblende and actinolite. Amphibole is replaced by chlorite and epidote.

Microdiorites are highly phyric with plagioclase and clinopyroxene phenocrysts enclosed in a matrix entirely crystallised into actinolite and chlorite. The plagioclase clusters in glomeroporphyritic aggregates. When preserved, it shows andesine to labradorite compositions. Fe-Ti oxides (5 %) are enclosed in the phenocrysts or present in the groundmass. The gabbro exhibits a cumulate texture with plagioclase (labradorite) as cumulus and clinopyroxene as intercumulus. The crystallization of the abundant Ti-rich magnetite begins after the plagioclase and continues while the clinopyroxene precipitates. Finally, the granophyre is characterized by a pegmatitic texture with plagioclase laths embedded by quartz. Amphibole and epidote are in accessory.

On the basis of the Fe-Ti oxides in the sequence of crystallisation, microdiorites show calc-alkaline affinities while the gabbro is tholeiitic.

Geochemistry

Gabbro and microdiorites have low TiO_2 contents (< 1.5 %). Microdiorites are markedly depleted in Light Rare Earth Elements (LREE) relative to Heavy (H) REE [$0.13 < (La/Yb)_{cn} < 0.76$], whereas the gabbro is slightly enriched in LREE relative to HREE [$(La/Yb)_{cn} = 2.21$] (fig. 4A). The granophyre has the highest $(La/Yb)_{cn}$ ratio (4.3) (fig. 3).

The microdiorites, the gabbro and the granophyre show features of subduction-related rocks because they exhibit the classic Nb and Ta negative anomalies, relative to N-MORB. Both rocks are depleted in Zr and Hf relative to N-MORB. However, the gabbro differs from the microdiorites by the absence of the Ti negative anomaly (relative to N-MORB; Fig. 4B). The granophyre differs from the gabbro and microdiorites by higher contents in large ion lithophile elements (LILE), Th, Zr and Hf (fig. 4B). Finally, the gabbro and microdiorites cluster in the oceanic arc tholeiite field defined by Pearce et al. (1984) while the granophyre falls in the shoshonitic domain (fig. 3).

CONCLUSIONS, TECTONIC IMPLICATIONS

Petrographic and geochemical studies indicate that the microdiorites derived from a calc-alkaline magma depleted in incompatible elements. The gabbro differs from the diorites only by its tholeiitic composition. Therefore, these rocks emplaced most probably in an intra-oceanic island arc setting. The

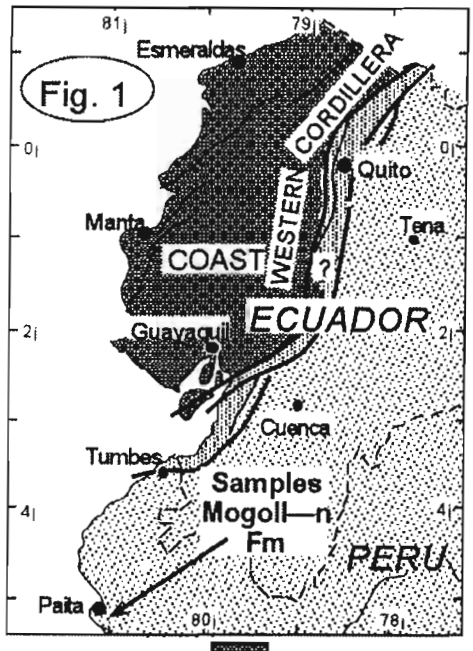

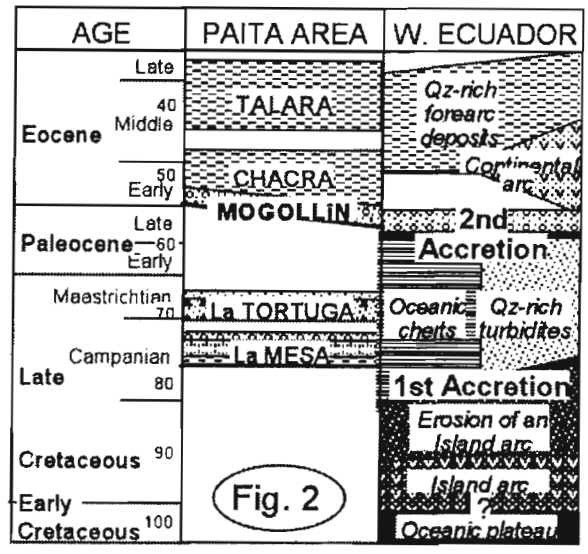

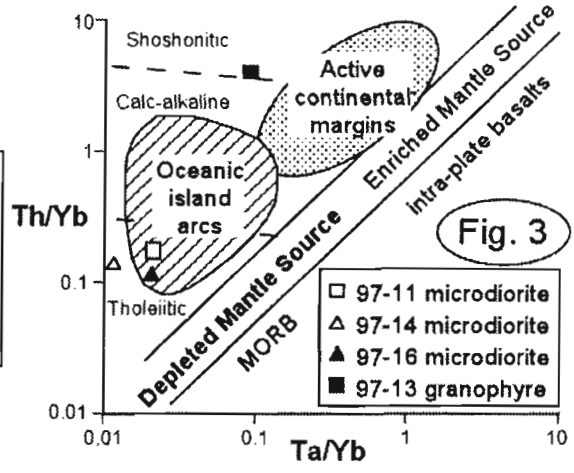

Fig. 1 : Structural sketch of NW Peru and Ecuador.
Fig. 2 : Stratigraphic sketch of NW Peru and Western Ecuador
Fig. 3 : Th/Yb vs Ta/Yb diagram for some boulders of the Mogoll—n Fm

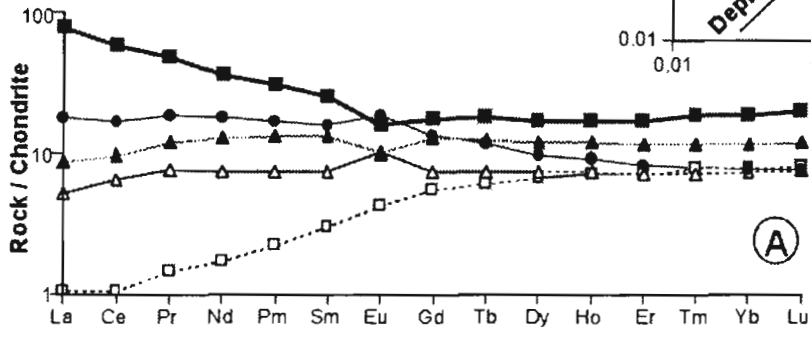

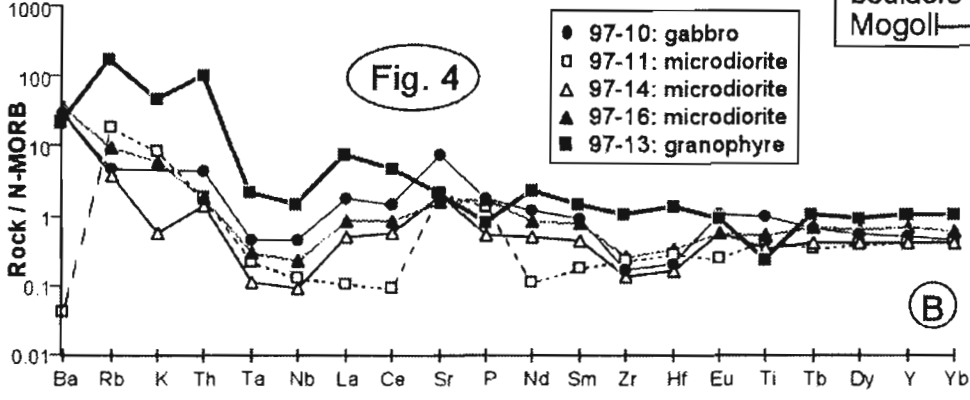

Fig. 4 : Normalized spidergrams of some boulders from the Mogoll—n Fm.

granophyre is significantly enriched in LILE, Th, LREE, Zr and Hf. It may derive either from an evolved island arc, or from an active margin magmatism.

The first appearance of island arc-deriving boulders in the latest Paleocene-earliest Eocene unconformable conglomerates of the Paita area confirms that collision of an oceanic terrane occurred in the Late Paleocene, and indicates that it took place in northern Peru. Since the closest oceanic terrane crops out presently south of Guayaquil, *i.e.*, 250 km north of Paita, it shifted NNE-ward along dextral wrench faults at a minimal average rate of 4.5 mm/year, since the Paleocene-Eocene (~ 55 Ma).

Such dextral wrench movements are documented since the Miocene, and an average rate of 2.5 mm/yr has been estimated for the Quaternary (Lavenu et al., 1994). This rate accounts for only 75 to 200 km since the Paleocene-Eocene boundary. Our data suggest, therefore, that dextral movements began well before the Miocene, and/or that the displacement rate was significantly higher than that calculated for recent times.

REFERENCES

Cosma (L.), Lapierre (H.), Jaillard (E.), Laubacher (G.), Bosch (D.), Desmet (A.), Mamberti (M.), Gabriele (P.), 1998 - Pétrographie et géochimie des unités magmatiques de la Cordillère Occidentale d'Équateur (0°30'S) : implications tectoniques. *Bull. Soc. géol. Fr.*, 169 : 739-751.

Faucher (B.), Savoyat (E.), 1973 - Esquisse géologique des Andes de l'Équateur. *Rev. Géogr. Phys. Géol. Dyn.*, 15 : 115-142.

Goossens (P.), Rose (W.), 1973 - Chemical composition and age determination of tholeiitic rocks in the basic Cretaceous Complex, Ecuador. *Geol. Soc. Am. Bull.*, 84 : 1043-1052.

Jaillard (E.), Mascle (G.), Benítez (S.), 1997 - Les déformations paléogènes de la zone d'avant-arc sud-équatorienne en relation avec l'évolution géodynamique. *Bull. Soc. Géol. France*, 168 : 403-412.

Jaillard (É.), Laubacher (G.), Bengtson (P.), Dhondt (A.), Bulot (L.), 1999 - Stratigraphy and evolution of the Cretaceous forearc "Celica-Lancones Basin" of southwestern Ecuador. *J. South Am. Earth Sci.*, 12, in press.

Kehrer, W. & Van der Kaaden, G., 1979. Notes on the Geology of Ecuador with special reference to the Western Cordillera. *Geol. Jahrbuch*, B **35**, 5-57.

Lavenu, A., Noblet, C. & Winter, T., 1994. Neogene ongoing tectonics in the southern Ecuadorian Andes. Analysis of the evolution of the stress field. *J. Struct. Geol.*, **17**, 47-58.

Lebrat, M., Mégard, F., Dupuy, C. & Dostal, J., 1987. Geochemistry and tectonic setting of pre-collision Cretaceous and Paleogene volcanic rocks of Ecuador. *Geol. Soc. Amer. Bull.*, **99**, 569-578.

Litherland, M., Aspden, J.A. & Jemielita, R.A., 1994. The metamorphic belts of Ecuador. British Geological Survey, *Overseas Memoir* **11**, 147 pp., Brit. Geol. Surv. publ..

McCourt, W.J., Aspden, J.A. & Brook, M., 1984. New geological and geochronological data from the Colombian Andes: Continental growth by multiple accretion. *J. geol. Soc. London*, **141**, 831-845.

Morales, W. (1993).- Reinterpretación geológica del area de Lagunitos (NW Perú) en base a sísmica reflexión. *3rd INGEPET*, INGP-055, 1-19, Lima.

Pearce, J.A., Harris, N.B.W. & Tindle, A.G., 1984. Trace element discrimination diagrams for the tectonic interpretation of granitic rocks. *J. Petrol.*, **25**, 956-983.

Reynaud, C., Jaillard, É., Lapierre, H. & Mascle, G.H., 1999. Oceanic plateau and island arcs of Southwestern Ecuador : their place in the geodynamic evolution of northwestern South America. *Tectonophysics*, in press.

Toussaint, J.-F. & Restrepo, J.J., 1994. The Colombian Andes during Cretaceous times. in: J.A. Salfity, ed., *Cretaceous tectonics in the Andes*, 61-100, Earth Evol. Sci., Fried. Vieweg & Sohn, Braunschweig-Wiesbaden.

MECHANISM AND CONSEQUENCES OF TECTONIC EROSION IN THE FOREARC OF NORTHERN CHILE (20-22°S)

Klaus PELZ (1) and Onno ONCKEN (1)

(1) GeoForschungsZentrum Potsdam, Telegrafenberg, D-14473 Potsdam
(pelz@gfz-potdam.de, oncken@gfz-potsdam.de)

KEYWORDS: Tectonic erosion, 2-D Modelling, 3-D Modelling

INTRODUCTION

For some time, the Central Andes plate boundary in Northern Chile has been suggested to be a margin controlled by tectonic erosion (Rutland, 1971), although the precise mechanism still is a matter of debate. Whereas accretionary growth at an active margin is evident from the accreted material itself, tectonic erosion has to be inferred from indirect evidence (Oncken, 1998). Tectonic erosion at convergent plate margins produces distinct kinematic patterns in the forearc of a plate margin (Von Huene & Scholl, 1991, Lallemand et al, 1994). The present contribution focusses on constraints on the mechanism and precise geometry of tectonic erosion derived from detailed field studies in the Coastal Cordillera of northern Chile and interpretation of wide-angle and reflection-seismic data from the CINCA offshore seismic experiment.

NEOGENE TO RECENT KINEMATIC

The North Chilean forearc consists of several morphotectonic units: offshore forarc, Coastal Cordillera, Longitudinal valley and Precordillera. In this study we focus on the offshore forearc and the Coastal Cordillera, which exhibit the most conspicuous features of subsidence and uplift respectively that may be related to material transfer mode. Both units consist mainly of plutonic, volcanic and sedimentary rocks of a Jurassic to Early Cretaceous Arc system, that intruded or covered a Paleozoic basement and are overlain by an incomplete succession of Cretaceous to Recent deposits. From both surface geology and seismic data we suggest four distinct N-S trending trench parallel kinematic domains (fig. 1): (a) the steep offshore Fore-Arc (6-12°); (b) the outer rise; (c) the Coastal Cordillera (CC) west of the Atcama Fault Zone (AFZ); (d) the CC east of the AFZ.

Neotectonic structures in the offshore forearc (a) indicate E-W extension with collapse toward the trench. Miocene to Pleistocene deposits of less than a few hundred meters are cut by trench dipping normal faults. Subaerial deposits in the Miocene sequence drilled as deep as 1800m (4000m?) water depth suggest a high rate of subsidence since deposition. On Mejillones Peninsula, marine sediments of the same age, controlled by NW-SE trending normal faults show post-Pleistocene compressional overprint in a NE-SW direction. Uplift of Pleistocene beach deposits up to 300m above sealevel (Niemeyer et al, 1996) show this domain to be uplifted. Seismic and bathymetric data north and south of Mejillones reveal the continuation of this topographic high into the offshore forearc forming an outer rise(b) with reduced subsidence.

The CC forms a topographic high (1000-1500m) bounded by the coastal escarpment, a trench dipping normal fault overprinted by collapse structures, and the Longitudinal Valley. Within the CC, the generally N-S trending AFZ separates two kinematic domains. Neogene to Recent kinematic of the AFZ is mainly dextral with a high amount of dip-slip. West of the AFZ (c) predominantly uplift occurs along with dextral strike-slip motion along N-S directed faults. Alluvial sediments representing an Early Miocene peneplanization are cut by the coastal escarpment in the west showing some 1000 to 1500m minimum vertical offset. To the east the amount of vertical offset along the east dipping AFZ since the Oligocene reaches up to 1100m (Reijs & McClay, 1998). The kinematic domain east of the AFZ (d) is mainly characterized by E-W trending normal faults resulting in N-S directed extension and subsidence with respect to the western part of the CC. These faults are dipping both towards north and south forming scarps up to 250m. South of Iquique the AFZ is split up into several branches and changes general strike direction from N-S to NW-SE. Crosscutting relationships between the AFZ and the N-S trending coastal escarpment indicate a younger age of the latter and its eastward propagation.

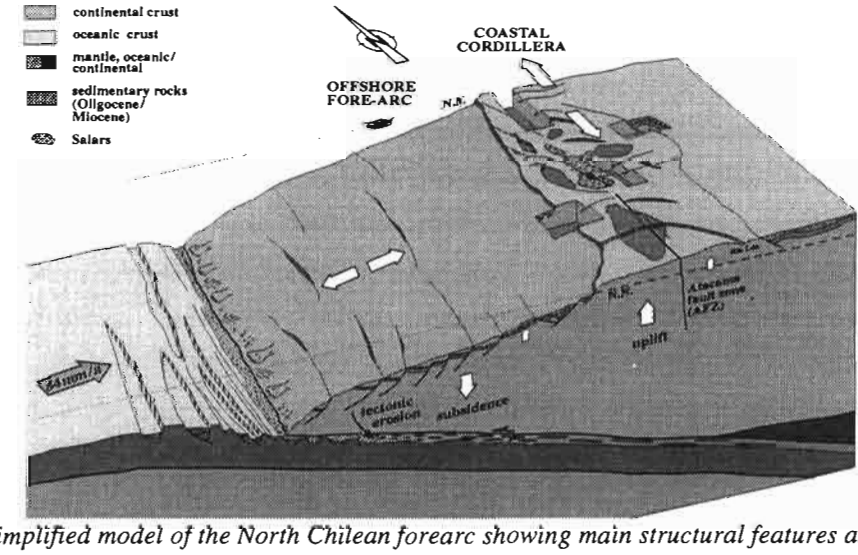

Fig. 1. Simplified model of the North Chilean forearc showing main structural features and kinematic domains.

2-D MODELLING

The North Chilean convergent plate margin is a non-accreting margin characterized by tectonic erosion. Rock material is removed from the upper plate and transported to greater depths (Von Huene & Scholl, 1991). Since the Jurassic, some 200-300 km of continental crust has been removed. From kinematic analyses of the forearc we suggest that subsidence of the offshore forearc is governed by basal tectonic erosion whereas uplift of the onshore region is mainly a consequence of transport of tectonically eroded material beneath the forearc wedge. There is no evidence of underplating.

The demonstrated contrast between subsidence and uplift is the key point to the problem. Quantification of upper plate material loss is based on differential vertical movement of different domains. In order to quantify the amount of tectonic erosion since the Early Miocene a simplified geometrical forward modelling approach was used.

To obtain the geometry of the initial (Early Miocene) wedge a crustal scale cross section was constructed restoring the known vertical displacement along the normal faults. In order to simulate effects of spatial limited tectonic erosion we separate the forearc into two domains: the upper part of the subduction zone where tectonic erosion affects the forearc and the lower part of the subduction zone where no material transfer between upper and lower plate occurs.

The process of tectonic erosion is then modelled incrementally: (1) In the upper part of the subduction zone the basal detachment between the subducting slab and the overriding upper plate is locked and a new detachment forms within the upper plate. In the lower part the basal detachment keeps its position at the continent/oceanic crust interface. The transition between the upper and lower part is marked by a ramp. The tectonically eroded layer is therefore bounded by the newly formed detachment, the old detachment and the ramp. (2) In the next step the upper plate material beneath the newly formed basal detachment is transported to greater depths with the downgoing slab. The overriding upper plate reveals domains of uplift and subsidence due to the ramp flat geometry of the detachment. Domains of subsidence and uplift can directly be correlated with domains where tectonic erosion affects the upper plate (material loss) and domains with no material transfer between upper and lower plate respectively. (3) After the tectonically eroded material has been transported to greater depths a new detachment is constructed in the upper plate marking the next increment of tectonic erosion.

According to this modell the amount of subsidence in the forearc is directly correlated to the amount of the removed material. Furthermore the CC is interpreted as an antiform above the ramp of the downgoing lower plate. From crustal scale cross sections in the North Chilean forearc we deduce a minimum upper plate material loss due to basal tectonic erosion of 190km² since the Early Miocene, which is equivalent to a length of 10 km of forearc crust. This allows us to place further constraints on the geometry and parameters of the forearc system.

The parameters controlling the amount of eroded upper plate material are: (i) subduction velocity v (transport velocity of eroded material); (ii) geometry of tectonically eroded layer given by the length l of

the layer and its thickness (=distance d of the upper plate detachment to the continent/oceanic crust interface; (iii) number of increments i and (iv) time t. Subduction velocity v of 84mm/a (DeMets et al, 1990) provides a "conveyor belt" of 1680km length since Early Miocene(t=20 Ma). The length l of the eroded layer at each increment is constrained by the recent geometry of the subsiding offshore forearc being at least 100km, which corresponds to the part of the forearc affected by tectonic erosion. To accomplish the boundary condition of 190km² material loss since Early Miocene, combinations of i and d can vary from i=1 with d=1,9km to i=16 with d=0,12km. If i<16, the process of basal tectonic erosion is discontinuous.

Wide-angle seismic data and geological observations in the North Chilean forearc support the discontinuous nature of basal tectonic erosion through time.

3D-MODELLING

Long wavelength topographic culminations (2000m) and depressions (800m) of the CC indicate along strike variation of the above process similar as the refraction seismic data. Oblique subduction geometry and spatial distribution of layers of tectonically eroded material lead to orogen parallel material transport (out-of-section movement) within the forearc of Northern Chile. On the base of topographic and kinematic data an attempt was carried out to correlate laterally varying topographic and kinematic domains with the geometry of these tectonically eroded layers. Applying the modell described above we are able to predict deformation patterns in the forearc depending on the choosen detachment geometry. Several iteration steps have to be carried out with changing the detachment geometry to fit observed kinematic and topographic information. In summary thin elongate slabs seem to be detached and removed down the subduction zone parallel to the plate kinematic vector leading to elongate ramp antiforms (=CC) with temporally varying amplitude.

CONCLUSIONS

The Neogene to Recent kinematic picture of the North Chilean forearc is mainly governed by basal tectonic erosion under the offshore forearc. Based on field observations and seismic data a model has been developed to show the mechanism and geometry of basal tectonic erosion. Vertical movement of distinct kinematic domains provides indirect evidence to infer the geometry of tectonically eroded layers. Oblique subduction geometry and oblique geometry of the tectonically eroded layers result in an orogenparallel component of material flux. This flux is probably discontinuous involving major slabs (of crushed and fragmented upper plate material) transported toward depth. The zone controlled by tectonic

erosion largely coincides with the zone of seismic coupling between both plates, suggesting that the strength of this part of the subduction zone controls the site of material abrasion.

REFERENCES

DeMets, C., Gordon, R.G., Argus, D.F., & Stein, S. (1990). Current Plate Motions. Geophys. J. Int., 101, 425-478.

Niemeyer, H., Gonzalez, G. & Martinez-De Los Rios, E. (1996). Evolución tectónica cenozoica del margen continental activo de Antofagasta, norte de Chile. Rev. Geol. de Chile, 23, 2, 165-186.

Lallemand, S., Schnürle, P., & Malavieille, J. (1994). Coulomb theory applied to accretionary and nonaccretionary wedges: possible causes for tectonic erosion and/or frontal accretion. J. Geophys. Res., 99, 12,033-12,055.

Oncken, O. (1998). Evidence for precollisional subduction erosion in ancient collisional belts: The case of the Mid-European Varsicides. Geology, 26, 12, 1075-1078.

Reijs, J. & McClay, K. (1998). Salar Grande pull-apart basin, Atacama Fault System, northern Chile. In: Holdsworth, R.E., Strachan, R.A. & Dewey, J.F.(eds) 1998. Continental Transpressional and Transtensional Tectonics. Geol. Soc., London, 135, 127-141.

Rutland, R.W.R. (1971). Andean orogeny and ocean floor spreading. Nature, 233, 5317: 252-255.

Von Huene, R. & Scholl, D. (1991).Observations at convergent margins concerning sediment subduction, subduction erosion, and the growth of continental crust. Rev. of Geophysics, 29, 279-316.

GEOMORPHIC EVOLUTION OF SALINAS GRANDES-QUEBRADA DE HUMAHUACA SECTOR, IN RELATION WITH TECTONIC SETTING AND CLIMATE, NORTHWESTERN ARGENTINA

Fernando X. PEREYRA (1) and TCHILINGUIRIAN, Pablo (2)

(1) Dpto. de Cs. Geológicas, FCEyN-Universidad de Buenos Aires, C. Universitaria, Pabellón II, 1428 Buenos Aires. E-mail fxp@gl.fcen.uba.ar
(2) IGRM-SEGEMAR, Avda. Roca, 657, piso 8, Buenos Aires

KEYWORDS: geomorpholgy-tectonic setting-Northwestern Argentina-geomorphic evolution

INTRODUCTION

Main pourpose of present contribution is to characterize geomorphology of a sector of Northwestern Argentina (NOA region) located beetween 23° and 24°S and 65° and 66°W. The relationships beetween regional geomorphic evolution and tectonic setting is particullarly considered, specially the structural variability (space and temporal) and tectonic evolution. Finnaly, close relations beetween past climate variations and geomorphic evolution are also considered. Studied area shows a strong climatic gradient, with cold-arid high mountain climate west and humid subtropical to east, this gradient could be also verified in north-south direction but with less intensity. This strong climatic gradient had undergone important waverings in the past, thus sectors that today are semiarid were in the past humid, so relictic geomorphic features are frequent in the studied area. The studied area is located encompasing three morphostructural domains: from west to east, Puna, Cordillera Oriental and Sierras Subandinas (figure 1). Is located in a north-south back-arc fold and trhust belt (F&TB) related to Andean Orogeny pulses. The deformation front migrated from Puna region to east of Sierras Subandinas, and probably begun in Miocene (Vervoort et al., 1995), continuing to present times. Nowadays, compressive strenght is restricted to Sierras Subandinas, while Puna and Cordillera Oriental shows some evidences of extension and normal reactivation of older thrust faults (Bianucci et al., 1987; Salfity et al., 1984 & Cortes et al., 1987). Older Cordillera Oriental F&TB is thick skinned type meanwhile eastern Sierras Subandinas F&TB is thinn skinned. Current Andean Orogeny broke up a pre-existent regional planation surface at least of pre-Miocene age. Remmanant of that surface could be observed in some sectors of Sierra Alta (western Cordillera Oriental). In Late Pliocene-Pleistocene, ongoing tectonics

(Diaguita Phase) resulted in backthrust formation in Cordillera Oriental (for example in western flanks of Sierra Alta and Sierra de Aguilar).

DISCUSSION

The structural style resulted in a north–south elongated basin and ranges relief, with basement ranges in the west and Late Paleozoic, Mesozoic and particularly Tertiary rocks ranges in the east. Main acting geomorphic process is fluvial. Nevertheless, above montioned structural differences resulted in heterogeneities in fluvial process action and consequently, in landforms and geomorphic features. In western zone, the absence of a strong Quternary compressive strength, resulted in the formation of large intermontane basins filed with Pliocene evaporitic materials covered by piedmont deposits. So, in Salinas Grandes area, at least three main Piedmont agradation levels (bajadas) could be recognized. Older level was probably formed in Late Pliocene-Ealy Pleistocene and later was disected and strongly eroded. During tectonic calm periods, probably after main Diaguita Phase, pediment levels were built in friable tertiary outcropping rocks. Two pediment levels were observed in depression located east of Sierra de Aguilar.

In the Quebrada de Humahuaca two fluvial agradation levels were formed. Particullarly, in creeks with headwaters in Cordillera Oriental, like Volcán, Coiruro, Purmamarca, Yacoraite, alluvial fans were built due to fluvial and mass wasting actions. Río Grande river is a subsequent river that collects water from eastern side of Cordillera oriental. At least two terraces levels cuold be recognized, specially in Maimará. A relative sequence of terraces and alluvial fan formation was done, based on soil development. To the east, in Sierras Subandinas, drainage pattern is totally different due to predominance of Tertiary outcropping rocks. Main rivers developed alluvial fans that by coalescence formed one bajada level. In Quebrada de Humahuaca, pediments (also developed in Tertiary sedimentites) were formed near Humahuaca-Huacalera, in Abra de Cianzo-Zenta and near Purmamarca-Tumbaya. A deformation sequence of mountain ranges was established based on geomorphic features like sinuosity of mountain ranges fronts and valleys, alluvial fans and pediments characteristics (using parameters proposed by Bull, 1986 and Bull & Mc Fadden, 1977). Straighter so newer mountains fronts correspond with backthrust.

Another important structural feature are transversal structures to north-south F&TB. These structures were older than Andean Orogeny a were reactivated by the latter. Strike slip resulted of reactivation of the old structures and consequent formation of transtesional basins, like the sector located north to Humahuaca, were the Quebrada de Humahuaca tectonic valley wided over. Old drainage pattern of this sector evidenced the presence of a local close basin. Transversal structures are also important in controlling the basin integration. Is very likely that Casa Grande depression was originally a small close basin. By headwater erosion related to ongoing tectonic movements of transversal structures, Yacoraite river produced the capture of Casa Grande area drainage integrating this basin to Río Grande basin. The same ocurred with Tres Cruces basin and in La

Quiaca, north of studied area, which by captures was integrated to Bermejo river basin. Neotectonics evidences affecting piedmont agradation levels, pediments and fluvial terraces are widespread distributed features.

Saline depressions, with lacustrine deposits and playa environments are important features in Puna region, due to tectonic evolution (distensive stresses after compression and reactivation of transversal structures that reasulted in formation of small transtensional basins). In Salinas de Guayatayoc-Salinas Grandes, saline deposits ocuppy a large area of 70 km length and 35 km wide. Several levels of paleocoast could be recognized in both depressions. Margins of saline deposits are partially covered by aeolian deposits. This formed extensive dune fields with longitudinal and parabolic dunes. Dunes covered piedmont drainage also. These dunes were formed due to Middle-late Holocene aridization of NOA region. Accordig to Irgazabal (1991) a strong regional dessication followed Tardiglacial, particularly after 8000 yrs. AP. Anthropogenic activities during past 2000 years probably had also impacted in extension of dune fields. Volcanic landforms, though very important in NOA Region, in studied area, are restricted to Puna environment.

Extenssion of glaciation in the studied zone is restricted to higher zones, generally 4500 m or more. Best exposures and preserved landforms are located in Nevado del Chani range, and belong to a spacially restricted valley glaciation. Moraines were also recognized in Sierra de Aparzo and Sierra de Zenta. Dry climate and heights of mountain ranges are probably main causes of limited importance of glaciar process. There is no datations of morenic deposits in NOA region, but because of landform preservation and correlating with Northern Chile moraines in Laco region (Gardeweg et al., 1997) is possible to atributed this features to Last Glaciation. Comparatively large glacier features in Cordillera Oriental than in Puna is probably linked with influence of wetter winds from east. Criogenic features, old and inactive rock glaciers, gelifluction lobes and criplanation surfaces could be recognized in mountain zones higher than 4000 m. Old glacier valleys in southwestern sector of studied zone, in Sierra Alta and south of Sierra de Zenta, presented this criogeneic features associated with moraines deposits. Is probable that glaciations (widespread distributed in Altiplano of Bolivia and ranges of that region, Clapperton, 1993) had indirected influenced on piedmont agradation level formation. Glaciation periods in NOA region are related with wetter conditions, so that bajada levels could be formed. In Salinas Grandes basin levels 2 and 3 could be correlated with Penultime and Last glaciation respectively. Large detritic covered slopes, sparce vegetation, high dipping slopes and earthquakes, antrhopogenic action and fluvial erosion acting as triggering mechanisms, are responsible of extensive distribution of mass wasting processes in studied area. Main features could be observed in Quebrada de Humahuaca, tectonic valley. In Volcan river basin several debris flows were recognized in the past affecting comunication lines and population (Chayle & Agüero 1987 and González Díaz et al., 1993). Complex forms predominates, generally with a first slide movement and a second debrisflows stage. In Sierras Subandinas, debris avalanches that graded to debrisflows are frequent features.

REFERENCES

Bianucci, H., C. Fernández Garrasino y E. Sanchez, 1987. Corriemientos de bajo ángulo entre La Quiaca y Abra Pampa. 10° Congreso Geológico Argentino, Actas I:165-168.

Bull, W. y L. Mac Fadden, 1977. Tectonic geomorphology north and south of the Garlock Fault, California. En D. Doehring (ed.) Geomorphology of Arid Regions, 115-138. Binghampton.

Bull, W., 1986. relative rates of long term uplift of mountain fronts. U.S. Geological Survey, Open File Report 87:192-202.

Clapperton, Ch., 1993. Quaternary Geology and Geomorphology of South America. Elsevier, Amsterdam, 779 pp.

Cortés, J., M. Franchi y F. Nullo, 1987. Evidencias de neotectónica en las Sierras de Aguilar y del Tanque, Cordillera Oriental y Puna Jujeña. 10° Congreso Geológico Argentino, Actas I:239-242.

Chayle, W. y Aguero, P., 1987. Características de remoción en masa en la cuenca del río Grande. Revista del Instituto de Geología y Minería N°7:107-121.

Gardeweg, M.; R. Steve, J. Sparks y S. Matthews, 1997. La evolución del volcán Lascar y su relación con el clima del Pleistoceno superior-Holoceno de los Andes Centrales. 8° Congreso Geológico Chileno, Actas 1:327-331, Antofagasta.

González Díaz, E., L. Fauqué y F. Pereyra, 1991. utilidad del mapeo geomorfológico en la toma de decisión. Una traza alternativa para el FFCC Belgrano en la quebrada de Humahuaca. Revista de la Asociación Argentina de Geología Aplicada a la Ingeniería, Tomo 7:133-145.

Irgazabal, A., 1991. Morfología de las provincias de Salta y Jujuy. Revista del Instituto de Geología y Minería, N°8:97-132.

Salfity, J., E. Brandan, C. Monaldi y E. Gallardo, 1984. Tectónica compresiva cuaternaria en la Cordillera Oriental, latitud de Tilcara. 9° Congreso Geológico Argentino, Actas II:427-434.

Vanderoort, D., T. Jordan; P. Zeitler y R. Alonso, 1995. Chronology of internal drainage development and uplift, southern Puna Plateau, Argentine Central Andes. Geology 23 N°2:145-148

THE VOLCANIC SERIES OF THE CORDILLERA DE LAS YARETAS, FRONTAL CORDILLERA (34°S) MENDOZA, ARGENTINA

Daniel J. PÉREZ (1) and Lidia I. KORZENIEWSKI (1)

(1) Laboratorio de Tectónica Andina, Dpto. Geología, Universidad de Buenos Aires, daniel@gl.fcen.uba.ar

KEYWORD: High-Andes, Magmatic arc, volcanic deposits, Frontal Cordillera, Yaretas.

INTRODUCTION

The objective of the present contribution is to give new geochemistry and radiometric date, about the early defined Eocene Volcanic Serie of the Cordillera de las Yaretas (Polanski, 1964). New radiometric date indicated that this serie is Middle Miocene, and is located in the Frontal Cordillera at 34°S-69°30'W, in Mendoza province, Argentina (see Figure 1).

The stratigraphic section in the mentioned area starts with the supposed Eocene Volcanic Association, which is composed by andesites and basalts, and lies over the eruptive neopaleozoic rocks and sedimentites of Saldeño Formation (Maastrichtian-Paleocene). This volcanites developed the efusive centers of La Paloma, Colorado and Mesón de Hierro (see Figure 1).

The series continues with agglomerates of cerro La Paloma, that concordantly overlie the Eocene volcanites. This agglomerates extend between La Paloma and Colorado creek, are subhorizontally stratificated and the andesites and basalt clasts have petrografic relation whit the supposed Eocene Volcanic Association.

The sequences finish with the Pliocene volcanic association, composed by olivine basalts and hornblendic andesite dikes. This association are represented by La Paloma Stock and Meson de Hierro creek (see Figure 1).

The geochemistry analysis of the Yaretas Volcanic Complex, show the compositional variation of silica (46-55%) which locate it between andesites and basaltic andesites, aluminum values between with 15-17%, and potassium ones between 1,5-3,3%, and iron oxides with 3,9-10,3% (see Figure 2a). This geochemistry characteristics are related to alkaline a subalkaline rocks and calcoalkaline, showing arc magmatism (see Figure 2b).

In addition this Volcanic Complex have high Ba/La ratios (31,8-24,7) and La/Ta ratios (29,7-39,8), low La/Yb ratios (7,3-12,2), and medium to low La/Sm ratios (2.7-6.6) (see Figure 2c). This geochemistry

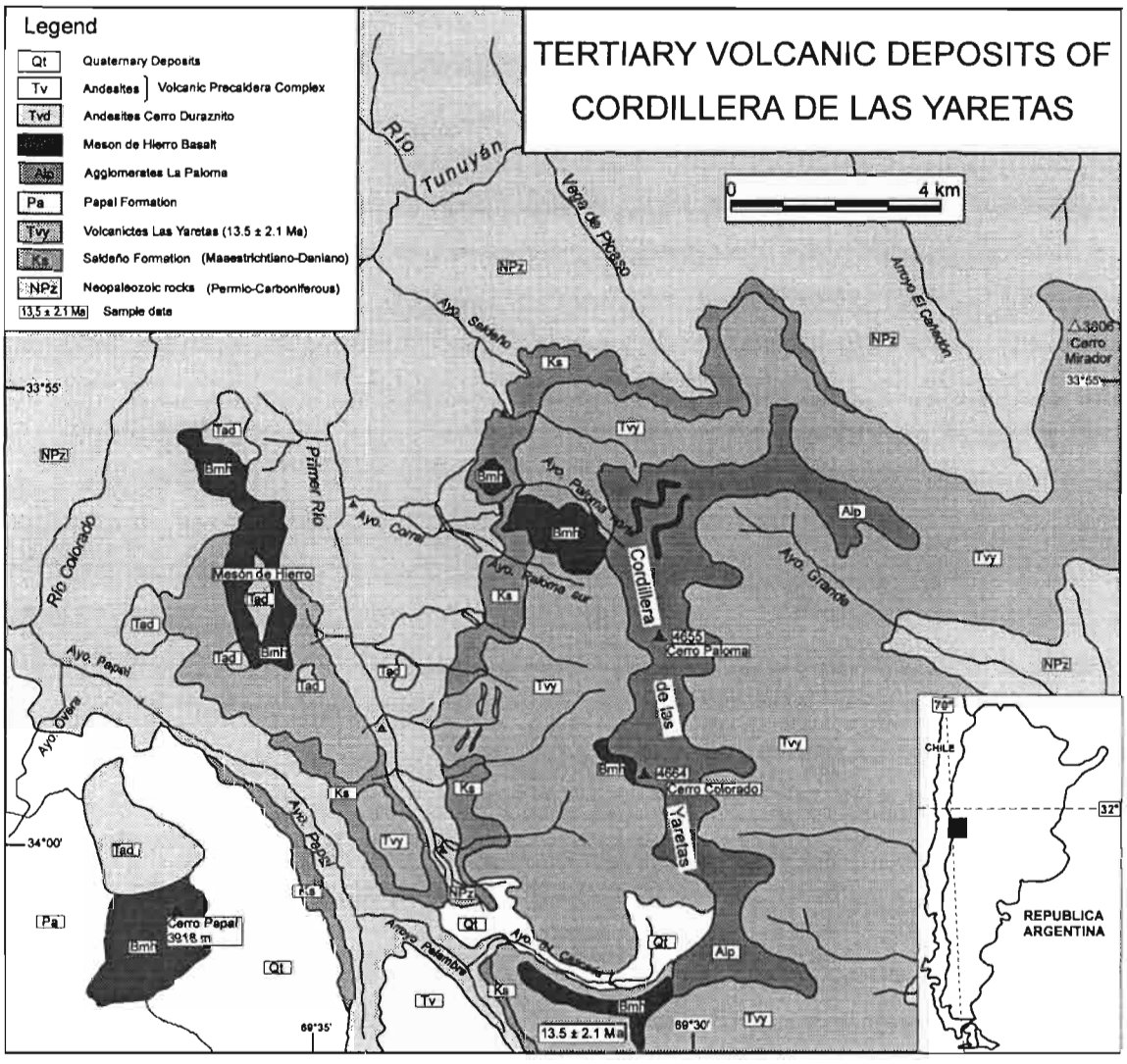

Figure 1: Map of Cordillera de las Yaretas

features allow us to define this rock as a calcoalkaline series developed on magmatic arc (see figure 2d). However, a datation on this supposed Eocene volcanic association, by K/Ar method, has give an age of 13,5 ± 2,1 Ma.

CONCLUSIONS

The volcanites of Yaretas Complex present similar emplacement characteristics as the Maqui Chico and Sewell groups of the Teniente Complex, located in Chile, westward of the studied area (Kay et al., 1999). All the mentioned features suggest that the Volcanic Yaretas Complex, was developed at the same time that the basal members of the Teniente Complex, between Middle Miocene and Pleistocene.

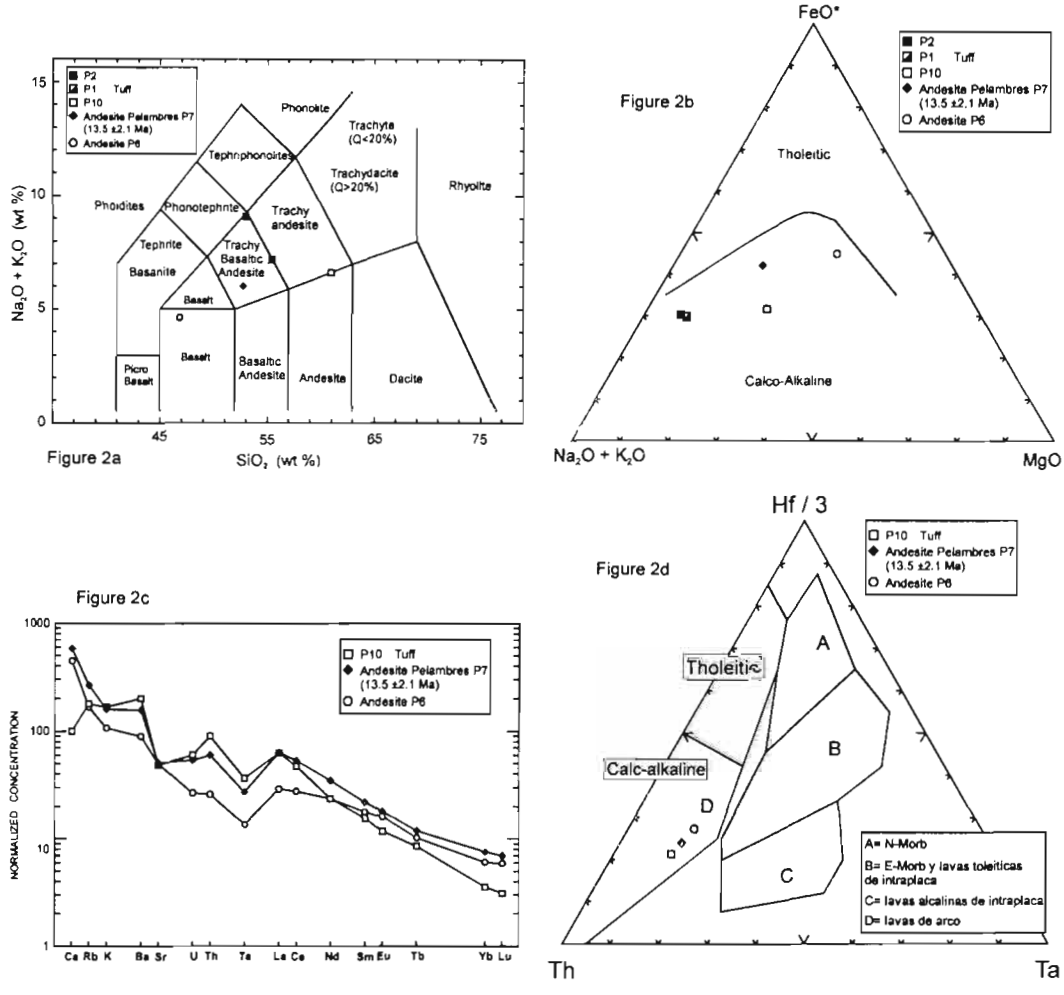

Figure 2a-d: 2a) geochemistry classification and nomenclature of volcanic rocks, by TAS diagram, total alkalis versus silica (Le Maitre et al., 1989). 2b) AFM diagram and limits between calcoalkaline and tholetic rock (Irvine y Baragar, 1971). 2c) distribution of trace element plots normalized to chondrite by Kay et al. (1987a). 2d) Wood diagram showing the magmatic arc association.

REFERENCES

Kay, SM., C. Mpodozis, B. Coira, 1999. Neogene magmatism, tectonism, and mineral deposits of the central Andes (22°S-32°S). Society of economic geology. Special Publication. Edited by Brian Skinner et al. In press.

Polanski, J., 1964. Description geologic de la Hoja 25a Volcán San José, provincia de Mendoza. Dirección Nacional de Geología y Minería, Boletín 98:1-94.

Kay, S.M., Maksaev, V., Mpodozis, C., Moscoso, R., y Nasi, C., 1987a. Probing the evolving Andean litosphere: Mid-late Tertiary magmatism in Chile (29°-30,5° S) over the zone of subhorizontal subduction. Journal of Geophysical Research, 92:6173-6189, Washington.

LAST INTERGLACIAL VOLCANIC SEDIMENTS AT THE COAST OF VALDIVIA, SOUTH OF CHILE

Mario PINO Q. (1)

(1) Instituto de Geociencias, Universidad Austral de Chile. Casilla 567, Valdivia, Chile (mpino@uach.cl)

KEYWORDS: Fluviomarine terraces, pyroclastic fluxes, Andean vulcanism, Chile.

INTRODUCTION

All the people who visits the Valdivian coast for the very first time, wonder about the dark grey colour of the sandy beaches. Most of the components of those beaches are volcanic, and due to the presence of the Costal Range composed by metamorphic rocks, it is difficult to establish an obvious relationship with the Andean volcans, and to understand how that volcanic material has come to the coast.

Near to the coast of Valdivia (*ca.* 38° 30' - 40° south), and in the vicinty of the mouth of the river estuaries, outcrops a well developed fluviomarine terrace (Brüggen, 1945; Fuenzalida *et al.*,1965; Pino, 1987; Rojas, 1990). The surface of the terrace is almost 15 m above present sea level, but there are a lot of sectors with heights ranging between 10 and 60 m, due to a block neotectonics (Illies, 1970). The faults that controled the blocks (with patterns N-S and NE – SW) also controls the creeks orientation (Grupo de Estudios Urbanos, 1997). Due to the altitude of the terrace and stratigraphical observations, Lauer (1968) and Illies (1970) have suggested an interglacial Riß – Würm age.

Along this 160 km of coast, it is possible to recognize two different facies. The first one has an autochtonous origin, because it is composed by coarse sediments derived from the local metamorphic basement, interbedded with fine sand and silt, peats and coquinas. The fossil invertebrates of the coquinas indicate a subtropical association (Alvarez & Gallardo, 1996). The wood of the peats indicate the presence of an evergreen forest (*Nothophagus* sp. and *Fizroya cupresoides*). An infinite C^{14} age > 50.000 years B.P was

obtained on one *Fitzroya* sample. This facies had a restricted areal development related to old little rivers and estuaries.

The second facies has been interpreted as allochtonous, because the sediments are composed only by volcanic sand with a >15% volcanic ash matrix. The matrix has been suffering an intense weathering that resulted in clay, in a sort of secondary cement. This second facies dominate and is present not only along that entire coast segment, but also near the most important rivers, up to 15 km from the present mouth (Fig. 1). The aproximate volume of this volcanic sand contrains 4.5 km^3. When the volcanic sandstone overlay the peat – muddy facies, you can often recognize flame estructures.

The content of volcanic ash in the sandy facies decrease from north to south. Near the mouth of the Imperial river estuary (northern limits of the outcrops) the volcanic ash is present not only in the matrix of the sandstone, but also conform layers of pure ash, with a biocoenosis of estuarine invertebrates. The postglacial Sollipulli, Sierra Nevada and Llaima volcans are located in the basin of the Imperial river (Fig. 1).

The sandstone is composed by fragments of andesite, basalt, orthopyroxene, plagioclase, hornblende, olivine and magnetite, and ocasionally it is possible to recognize large fragments of pumice. Most of the orthopyroxene cristals, and some of the hornblende, plagioclase and magnetite are not rounded, but keep the euhedral forms. Olivine and orthopyroxene are frequent products of the basaltic and dacitic postglacial volcanism (Naranjo & Moreno, 1991; Moreno et al., 1994), but it has not been possible to associate the volcanic sandstone with a particular volcanic event until now, because the preglacial volcanic rocks have been covered or destroyed by the last glaciation deposits

CONCLUSIONS

The mineralogical composition of the sandy facies, the high amounts of fine volcanic matrix, the absence of roundness of some of the volcanic minerals, the presence of pumice and the flame structures at the base of the sandy bodies, indicate a mechanism of a rapid and massive transport in a mixture of water and ash, from one of the Andean volcans towards the coast, in a kind of hyperconcentrated sand flux. That mechanism of transport is well known in other much younger volcanic collapses around this region, that has produced a wide variety of lahars and turbulent wet pyroclastics fluxes (Naranjo et al.,1993; Thiele et al., 1998). But this is a very first report of a pyroclastic deposit near the Pacific coast in the south of Chile. Finally, the volcanic sandstone is the source of the dark sandy beaches in this area.

REFERENCES

Alvarez R & Gallardo C. 1996. Faunistic and paleoenvironmental characterization of quaternary fossiliferous beds at rio Tornagaleones (Bahia de Corral, Valdivia) Revista de Malacología Médica y Aplicada, 4° Congreso Internacional de Malacología Médica y Aplicada, Vol 8, N° 1, p120.

Brüggen J. 1945. Miscelánea geológica de las provincias de Valdivia y Llanquihue. Revista Chilena de Historia y Geografía 2: 90-113.

Fuenzalida H.; Cooke R.; Paskoff R.; Segerstrom K. & Weischet W. 1965. High stands of Quaternary sea level along the chilean coast. Geological Society of America. Special Paper 84: 473-496.

Grupo de Estudios Urbanos. 1997 . Estudio del Medio Fisico : Plan Seccional Costero Niebla - Los Molinos - San Ignacio, Comuna de Valdivia. Infome Final, Instituto de Geociencias, Universidad Austral de Chile, 68 pp, 3 mapas.

Illies H. 1970. Geología de los alrededores de Valdivia y Volcanismo y Tectónica en márgenes del Pacífico en Chile meridional. Universidad Austral de Chile. Instituto de Geología y Geografía. 64 p.

Naranjo J.; Moreno H. 1991. Actividad explosiva postglacial en el volcán Llaima, Andes del Sur. Revista Geológica de Chile 18, n° 1, 69-80

Naranjo J.; Moreno H.; Emparan C. & Murphy M. 1993. Volcanismo explosivo reciente en la caldera del volcán Sollipulli, Andes del Sur (39°S). Revista Geológica de Chile 20 n° 2, 167-191.

Pino M. 1987. Stratigraphie, Granulometrie und Schwermineral Analyse der miozänen silikoklastischen - Ablagerungen der Provinz Valdivia, Südchile. Inaugural - Dissertation zur Erlangung des Doktorgrades. WWU Münster, 209 p.

Rojas C. 1990. La terraza fluvial de "Cancagua" en la ciudad de Valdivia: Nuevos antecedentes estratigráficos y granulométricos. Revista Geográfica de Chile "Terra Australis" 32:7-24.

Thiele R.; Moreno H.; Elgueta S; Lahsen A.; Rebolledo S & Petit-Breuilh M.E. 1998. Evolución geológica – geomorfológica cuaternara del tramo superior del valle del río Laja. Revista Geológica de Chile 25 n° 2, 229-253.

Fig. 1: location map of the last interglacial terrace. The most probably source of the volcanic sand facies are the Sierra Nevada, Llaima or Sollipulli volcans.

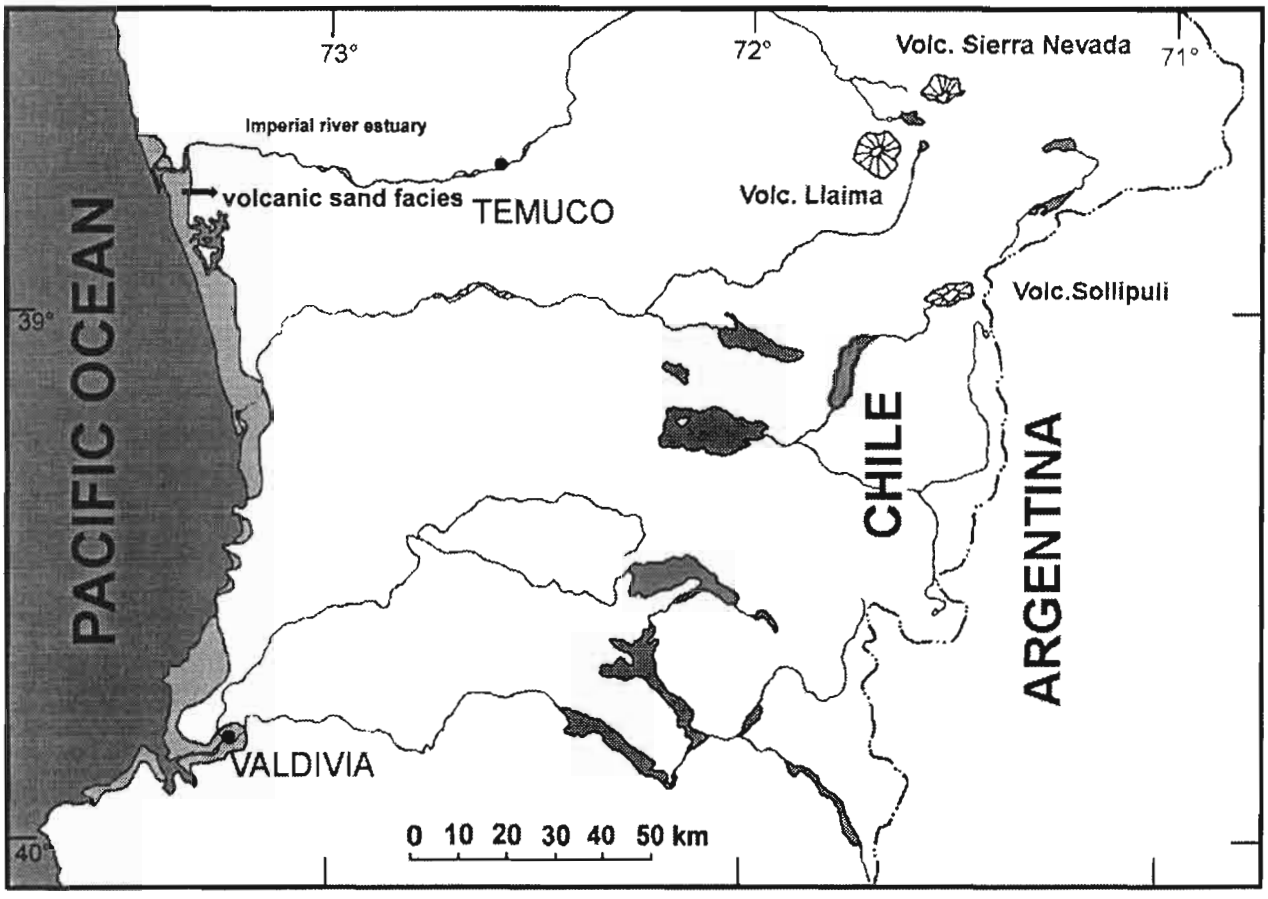

SEDIMENTARY REGISTER OF THE CENOZOIC DEFORMATION OF THE WESTERN BORDER OF THE ALTIPLANO IN THE NORTHERN CHILE (REGION OF TARAPACÁ, 19°00' - 19°30')

Luisa PINTO [1], Gérard HERAIL [2] and Reynaldo CHARRIER [3]

(1) Departamento de Geología, Universidad de Chile, Casilla 13518, Correo 21, Santiago. (lpinto@cec.uchile.cl, rcharrie@cec.uchile.cl)
(2) IRD. 209-213 Rue La Fayette, 75010, Paris, France. (gherail@paris.orstom.fr)
(1) and (2) Convenio IRD- Departamento de Geologia de la Universidad de Chile.

KEY WORDS: Altiplano, Chile, supply source, flexure, syntectonic, Miocene.

INTRODUCTION

Along the west side of the 3.500 - 4.500 m high Altiplano plateau, in northern Chile between 15° and 27° South latitude, there are thick Early to Late Miocene sedimentary series that register the tectonic evolution of the plateau. In this paper we describe: a) the substratum of the sedimentary series, b) a regional flexure (Moquella Flexure), which is part of the west-vergent thrust system (Muñoz and Sepúlveda, 1992; Muñoz and Charrier, 1996; García et al., 1996) and is well exposed in the Moquella region (19°08'-19°27'S / 69°20'-69°50' W), c) the geometry, composition and fabric of the associated syntectonic deposits, and intend to establish the chronology of the described events, and to reconstruct the tectonic evolution of this region and its implications for the uplift of the Altiplano.

THE DEFORMED SERIES

a) *The substratum*. The substratum consists of folded mesozoic continental sedimentary deposits with some andesitic intercalations intruded by rhyolitic and granodioritic stocks, correlated with the Cretaceous Cerro Empexa Formation (Camus and Fam, 1971) and the late Oligocene ? - early Miocene Altos de Pica Formation an equivalent of the Oxaya Formation (Montecinos, 1963), which unconformably covers the Mesozoic rocks.

The Altos de Pica Formation (Galli and Dingman, 1962) forms in the study region an approximately 400 thick series composed of ash tuffs with polymictic volcanic intercalations of conglomerates and sandstones. K/Ar age determinations on biotite from two tuffs in the upper levels of the unit gave 21.7 ± 0.6 Ma (Naranjo and Paskoff, 1985) and 19.3 ± 0.8 Ma (Pinto, in publication). North of the study region an ignimbrite in the lower levels of the Altos de Pica Formation gave a 25 Ma age (García and Hérail, this symposium).

b) *Moquella Flexure* (or monoclinal: see Muñoz and Sepúlveda, 1992; Muñoz and Charrier, 1996). Deformation in the Altos de Pica Formation and older units in this region corresponds to the west-verging and N20°W trending Moquella Flexure (Fig. 1). This structure, exposed along 13 km between Suca (in the North) to Retamilla (in the South) valleys, deforms a regional gently west dipping slope formed by the top the Altos de Pica Formation. The throw along this flexure of ca. 300 m generated a depressed area to its west side that was filled by the products of the erosion developed on the east side of the flexure. The lowermost layers of the Altos de Pica Formation exposed in the core of the flexure form a chevron fold, suggesting the existence of an east-dipping thrust fault in the underlying Mesozoic substratum. The northward prolongation along strike coincides with the Ausipar Fault (Muñoz and Charrier, 1996; García and Hérail, this symposium), indicating its close association to the west-vergent thrust system exposed along the west border of the Altiplano.

c) *The syntectonic deposits.* In the zone we differenciated on the basis of their distribution, composition and grain-size three westward fining units associated to activity of the Moquella Flexure. These units were deposited on the front west side of this structure.

The basal unit or **Latagualla Formation** (Pinto, in publication) is composed in the lower levels by matrix supported, polymictic volcanic conglomerates, and sandstones, whereas in the well stratified upper levels it is composed by rhyodacitic volcanic sandstones. Abundant pumice matrix is present throughout the sequence. Acidic components in this unit were originated by erosion of the Altos de Pica Formation. To the West, the Latagualla Formation forms an approximately 300 m thick sedimentary series. The thickness decreases to the East, where it overlies the flexured Altos de Pica Formation (Fig. 1). An ignimbritic deposit intercalated in the upper levels of the Latagualla Formation gave a 16.2 ± 0.7 Ma age (Muñoz and Sepúlveda, 1992).

The second unit, overlying the Latagualla Formation, is the **Transition Sequence** (Pinto, in publication) composed by a lower volcanic member that interfingers with an upper sedimentary member. The volcanic member, exposed to the east of the Moquella Flexure (Fig. 1), corresponds to a 200 m thick and 16.3 ± 0.6 Ma old (Muñoz and Sepúlveda, 1992) rhyodacitic ignimbrite. The ca. 80 m thick sedimentary member, located to the west of the Moquella Flexure (Fig. 1), is composed by very fine conglomerates and sandstones composed by pumice and andesite fragments.

The third unit or **El Diablo Formation** (Tobar et al., 1968) overlies the Transition Sequence and corresponds to a sequence of predominantly very coarse andesitic gravels and scarce gravelly sands. This deposits forms a wedge: the thickness of which decreases from West to East from ca. 300 m to 0 m next to the flexure (Fig. 1); in addition, from North to South its thickness increase from 50 m to 300 m. Before deposition of the El Diablo Formation strong erosion affected the Latagualla Formation in the south part of the study

region. The lower layers of the El Diablo Formation form successive systems of westward prograding alluvial fans. The upper layers of the El Diablo Formation, that fill-up the depressed area west of the Moquella Flexure, are in onlap the west-dipping slope of the flexure and cover the East side of this structure (Fig. 1). K-Ar age determinations on an andesitic lava that overlies the El Diablo Formation (Fig. 1) gave 9.0 ± 1.0 Ma (Naranjo and Paskoff, 1985) and 8.2 ± 0.5 Ma (Muñoz and Sepúlveda, 1992). This lava is slightly eroded to the East of the Moquella Flexure, suggesting a slight activity of the flexure after 9 Ma.

CONCLUSION: SEQUENCE OF THE DEFORMATION

The deformation in the western border of the Altiplano at 19°15' S is represented by the Moquella Flexure which was active between 19 Ma and 9 Ma. Its activity is represented by the following syntectonic deposits: Latagualla Formation, Transition Sequence and El Diablo Formation. The compositional differences in these units indicate different source rocks for the sediments.

The first phase of deformation (ca. 19 Ma) flexured the Altos de Pica Formation, generating an uplifted relief to the East that represented the source of the sediments accumulated in the depressed area developed to the west of the flexure. The Latagualla Formation was generated during this phase (ca. 19-16 Ma). The second phase (ca. 16 Ma) is represented by a rhyodacitic and andesitic volcanic activity that generated the volcanic deposits covering the relief formed in the first phase that since then has been eroded. The erosion of these volcanic deposits provided the components of the Transition Sequence. Finally, deposition of the El Diablo Formation (ca. 16-9 Ma) was characterized by a great supply of andesitic component coming from andesitic volcanic centers located to the East. The higher volume of materials represented by the El Diablo Formation relative to the Latagualla Formation (Fig. 1), that indicates a higher storage capacity of the depressed area to the west of the flexure, and the high energy environment represented by the lower levels of El Diablo Formation suggest the existence of a higher period of activity along the Moquella Flexure, shortly after 16 Ma, while the onlap geometry of the upper levels suggests a later slowing of the deformation near 9 Ma.

The Moquella Flexure like was produced by the activity of a blind west-vergent thrust fault affecting to the Mesozoic substratum.

REFERENCES

Camus, F., Fam, R., 1971. Programa de exploración de yacimientos tipo "Porphyry Copper": Proyecto Camiña y Quebrada Manujna.SERNAGEOMIN, Chile, Inédito 0279, 22 p.

Galli, C., Dingman, I., 1962. Cuadrángulos Pica, Alca, Matilla y Chacarilla, *con un estudio sobre los recursos de agua subterránea.* Provincia de Tarapacá. Escala 1:50.000. I.I.G., Carta Geológica de Chile, Vol. III, Nos 2, 3, 4 y 5, 125 p.

García, M., Hérail, G., Charrier, R., 1996. The cenozoic forearc evolution in northern Chile: The border of the Altiplano of Belén (Chile). Third ISAG, St Malo (France), p. 359 - 362.

Montecinos, F., 1963. Observaciones de Geología en el Cuadrángulo Campanani, Depto. de Arica, Provincia de Tarapacá. Memoria de Título, Depto. de Geología, Universidad de Chile, 109 p.

Muñoz, N., Sepúlveda, P., 1992. Estructuras compresivas con vergencia al oeste en el borde oriental de la Depresión Central, Norte de Chile (19°15'S). *Revista Geológica de Chile*, Vol. 19, N° 2, p. 241 - 247.

Muñoz, N., Charrier, R., 1996. Uplift of the western border of the Altiplano on a west-vergent thrust system, Northern Chile. *Journal of South American Earth Sciences*, Vol. 9, Nos 3/4, p. 171 - 181.

Naranjo, J.A., Paskoff, I., 1985. Evolución cenozoica del piedemonte andino en la Pampa del Tamarugal, norte de Chile (18° - 21°S). IV Congreso Geológico Chileno, Vol. 4, p. 149 - 165.

Pinto, L., 1999. Evolución tectónica y geomorfológica de la deformación cenozoica del borde occidental del Altiplano y su registro sedimentario entre los 19°08'-19°27'S (Región de Tarapacá, Chile). Memoria de Título y Tesis de Grado de Magister, Mención Geología. Departamento de Geología, Universidad de Chile.

Tobar, A., Salas, I., Kast, I., 1968. Cuadrángulos Camaraca y Azapa, Provincia de Tarapacá. Escala 1:50.000. I.I.G., Carta Geológica de Chile, N° 19 y 20, 20 p.

RAPID TECTONIC UPLIFT AS REVEALED BY PEDOLOGIC CHANGES: THE OÑA MASSIF, SOUTHERN PART OF CENTRAL ECUADOR.

Jerôme POULENARD(1), Theofilos TOULKERIDIS(2) and Pascal PODWOJEWSKI(3)

(1) CPB-CNRS, Vandoeuvre les Nancy, France, poulenar@cpb.cnrs-nancy.fr
(2) CGS-CNRS, Strasbourg, France, theo@illite.u-strasbg.fr
(3) IRD (previously ORSTOM), Quito, Ecuador, podwo@orstom.org.ec

KEY WORDS : Tectonic uplift, Soils, Ultisols, Andisols, Ecuador

INTRODUCTION

Tectonic uplift rates are usually determined by radiogenic dating and also combined fission-track dating of apatite and zircon (Spikings et al., 1998). Here, we present with a new approach how pedological changes may reveal uplift rates in our studied case of an ultisol which has been formed in situ above of rocks of the Oña Massif in the southern part of central Ecuador (Fig. 1). The Oña Massif which is located 50 km south of Cuenca has an altitude of 3000m and is covered by a high altitude grassland, the so-called Páramo. There the soils are up to 6m thick and overlie Miocene flows being dacitic and rhyolitic in composition of which effusion took place above of Miocene marine sediments. The soils are red in colour at their base and yellow on their top and were considered as humults (humiferous ferrallitic soil). Their upper organic horizons are black, 40cm thick, and have andic-like properties such as (a) high C contents (12 to 8 g/100g), (b) low bulk density (0.6), (c) a water retention at 0.3 kPa of 60g/100g, and finally (d) a (Al+1/2 Fe) oxalate extract being between 1.1 to 1.3%. The lower yellow and red horizons contain (a) much lower C contents, (b) a bulk density of 1.2, (c) a water retention at 0.3 kPa of 35g/100g and (d) a (Al+1/2 Fe) oxalate extract less than 0.4%. These upper-organic horizons have been compared to andisols (melanocryand) of the Cajas Massif located 50km north of the Oña massif, formed above of recent volcanic ashes (> 10,000 years B.P.) which were previously thought to have been originated by the active volcanoes of Sangay and/or Tungurahua, both located more than 100 km north of the Oña Massif (Fig. 1). Resistant relicts from weathering of a parent-rock suite such as the presence of coarse-grained quartz (>2mm in diameter) in these black horizons cast doubt on the origin of the recent ash deposits from sources that far away. An additional fact to the mentioned doubt is the clay-mineral composition which is

predominantly made up by kaolinite with small amounts of chlorite as the exclusive clay component in the organic part of that horizons, while the lower yellow horizons is exclusively made up of kaolinite with small amounts of goethite. Geochemical determinations based on rare earth elements confirm the uniformity of the whole profile with Eu/Eu* of 1.15±0.05, Ce/Ce* of 0.67±0.31 and Gd_N/Yb_N of 3.84±0.33 strongly implying not to have any contribution of volcanic ash deposits compared to such as the andosolic profile of the Cajas Massif with Eu/Eu* of 0.97±0.03, Ce/Ce* of 1.08±0.07 and Gd_N/Yb_N of 1.55±0.10.

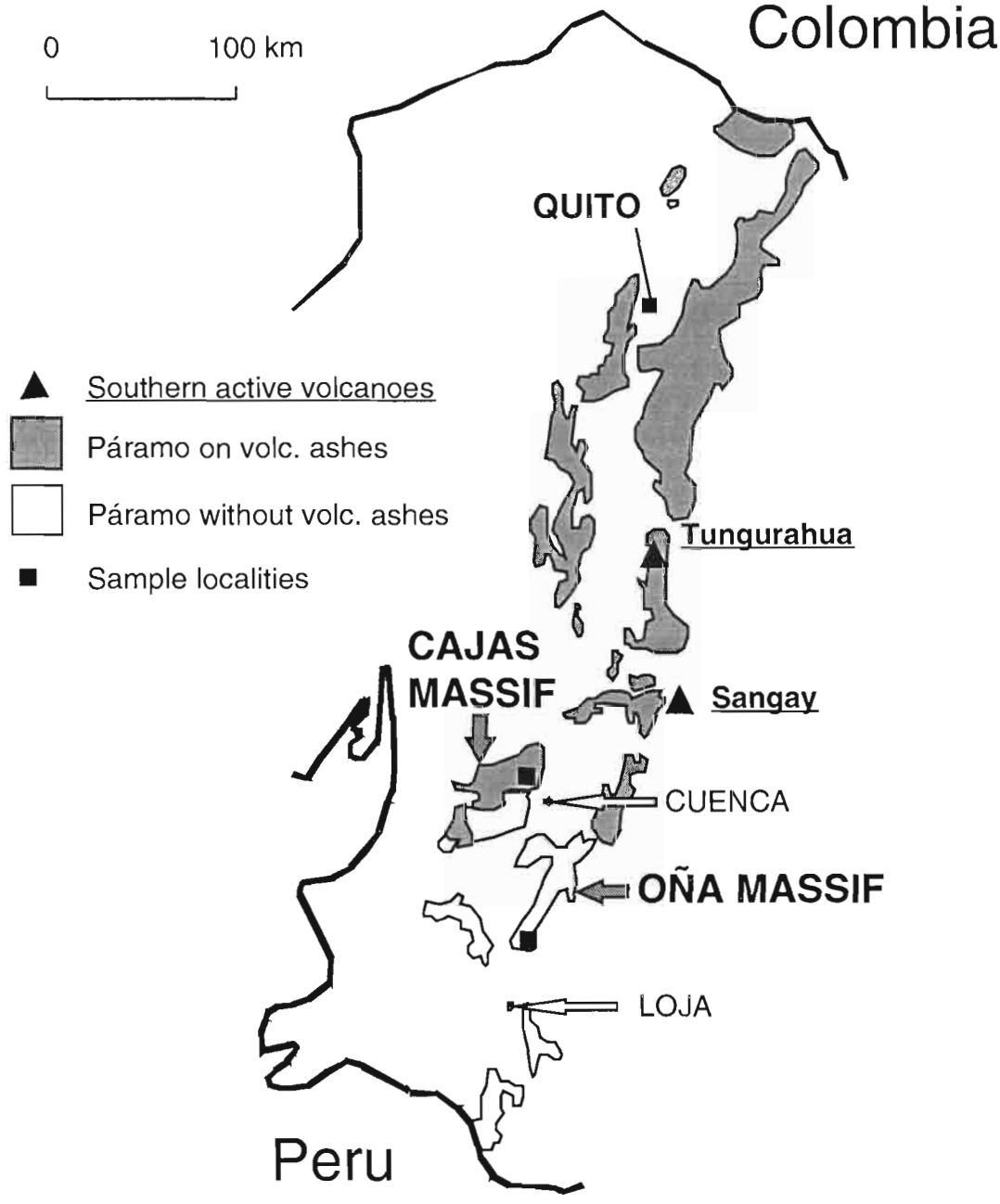

Fig. 1: Distribution of the Pàramo in Ecuador and sample localities.

A major climatic change might be a possible explanation for this major change in the pedological outcome. The evolution of this ultisol into andisols could be the result of rapid tectonic uplift of this area accompanied with weak erosional process of the soils due to the absence of strong slopes on the top of this

massif. The high uplift rate is hereby explained by the limited formation of kaolinite. Kaolinite can only be formed with an average temperature far above 20°C (Tardy, 1993; Segalen, 1994). In past time the massif was close to sea level with an annual average temperature of 25°C, high annual average temperature favoured exclusively neoformation of kaolinite derived out of Si and Al-rich solutions. Considering the mechanical erosion rate and a temperature decrease of -0.6°C per 100m, while soils are now located at 3000m height with an average annual temperature around 12°C a calculated uplift rate fits with previously obtained data with independent methods of the same area to be higher than 0.6 mm/year. Nowadays average annual temperature became lower, kaolinite becomes unstable, favouring the presence of oxides, goethite and amorphous components which dominate the present stage. These amorphous components associated with lower temperature and low pH values (<5.0) also limit presently the carbon mineralization.

This proposition is also confirmed by the orientation of south-west trending altitudinal winds which carry high amounts of fine volcanic ash from the active volcanoes of Tungurahua and Sangay. They generally affect with that spreading mainly areas such as the Cajas Massif or west-Saraguro which are located in the direction of these winds, while the massifs located to the south remain unaffected from these emissions.

REFERENCES :

Segalen, P., 1994: Les sols ferrallitiques et leur répartition géographique. Tome 1 - Intro-duction générale les sols ferrallitiques: leur identification et environnement immédiat. Editions de l'ORSTOM, Paris, 198pp.

Spikings, R., Ruiz, G., Winkler, W. and Seeward, D. 1998: The geodynamic history of the Cordillera Real and Oriente foreland basin, Ecuador. Abstract, 16th Latin American Symposium, Bayreuth, Germany.

Tardy, Y., 1993: Pétrologie des Latérites et des Sols Tropicaux. Masson, Paris, 459pp.

RELATIONSHIPS BETWEEN EARTHQUAKES AND THE PENINSULAS IN THE BIOBIO REGION, SOUTH CENTRAL CHILE

Jorge QUEZEDA FLORY (1)

(1) Universidad de Concepcion. Casilla 3-C Concepcion, Chile. Email jquezad@udec.cl

KEY WORDS: Coastal Seismicity, Barrier, Peninsula

INTRODUCTION

The Biobio region of Chile is located between 36.0 ¼ and 38.4¼ Lat S. in western South America. The seismicity of this area is distributed mainly in the coast, offshore and in the Coastal Cordillera. This seismicity is generate mainly by the subduction of Nazca Plate under South American Plate. The rate of convergence is approximately 9 cm per year. Focal mechanisms are not well determined due to the lack of stations. Some of then are thrust, like May 21st, 1960 of 7,5 magnitude in the Arauco Peninsula. From comparatives topografic profiles before and after the 1960 May 21st earthquake, there are an uplift of 2 meters in coastal areas and Mocha Island and it increases to south beneath the sea, to the east there are negative changes. Between 1939 and 1975, nine earthquakes over 7 magnitude took place in the Biobio Region (Fig. 1), mostly offshore with depths of 20-30 km but two earthquakes had 60 km of depth beneath the shoreline. North of this area the seismicity is located uniformly from the coast to the Andes Cordillera, but from Biobio Region to south it is located in the coast area; in the central valley is absent and a little one is located in the Andes Cordillera at 100 km of depth. Historical earthquakes of magnitude over 7 in Concepcion area like 1570, 1657, 1751 and 1835, producing big tsunamis and changes in the landscape with an uplift in the coastal area of 2 meters in average. This earthquakes are located near Tumbes Peninsula.

From PDE, SISRA and NEIC catalogs (1), the main earthquakes of magnitude

4.0-6.9 are located in the coast from 36.0 Lat. S until 38,4 Lat. S., between Tumbes Peninsula and Mocha Island. Other earthquakes are located in the Cordillera de la Costa-Central Valley border. Like January 24th 1939 Chillan Earthquake, normal faulting intraplate at 100 km of depth (4) and Angol May 10th 1975, earthquake at 30 km of depth, both with 7,8 magnitude. The geomorphologic units in this area are a) Peninsulas and Islands: Peninsulas of Arauco, Hualpen, Tumbes and Coliumo and the islands of Quiriquina, Santa Maria and Mocha; b) Coastal Plains; c) Coastal Cordillera: Nahuelbuta Cordillera; d) Central Valley and e) Andes Cordillera. (Fig. 1). The geologic structure is mainly graben and horst (Fig. 2). The horst are the blocks of Andes Cordillera, Coastal Cordillera, Peninsulas and Islands and the grabens are the Central Valley and the Coastal Plain. It is not well known the kind of border of this structures but it is infered north-south normal faults. Some earthquakes produces movements of these faults like Chillan, 1939 when the western and eastern borders of Coastal Cordillera moved one meter. The Andes Cordillera is made of volcanic and granitic rocks, mainly Cenozoic, the Coastal Cordillera is made of metamorphic and granitic rocks of Carboniferous age; in the western border and the peninsulas and island, there are sedimentary rocks from Cretaceous to Late Tertiary age. The Central Valley is a filled basin with 2000 m of glacial, volcanic and fluvial sediments. The Coastal Plains are made by 100 m of sandy sediments, mostly made of basalts from Antuco Volcano that collapsed around 9.000 years ago.
The shoreline of the Biobio region go to west due to the peninsulas of Arauco and Hualpen-Tumbes ones and the islands of Mocha, Santa Maria and Quiriquina. In these areas, the epicenters of great earthquakes are located. Another example of this situation, are in Antofagasta in northen Chile when the epicenter of the earthquake of July 30th, 1995 of 7,8 magnitude was in the Mejillones Peninsula (23¼ Lat.S). This case is well studied (4) and the rupture began in this peninsula towards the south up to 180 km. In the case of the earthquake of May 21st 1960, the epicenter is in the Arauco Peninsula and the aftershoks, some of them of 6 and 7 magnitude, are distributed towards the south and the next day earthquake of Valdivia in May 22nd, are located 250 km to south. These earthquakes had a total moment magnitude Mw= 9,5. Another example of seismicity related with western peninsulas are the swarms of earthquakes of 4 and 5 magnitude in La Serena in central-north Chile (30¼Lat S) in 1997 and 1998. In this case, the epicenters are located near the Tongoy Peninsula. In the Biobio Region, the most part of smaller and biggest earthquakes are located near the Tumbes and Arauco Peninsulas. This close relationship can be explained by the effect of barrier of this peninsulas and coastal islands and their deeper structures can be asperities that traps the movement of the Nazca Plate and are points of nucleation or concentration of energy in the Wadatti-Benioff zone that can be released during great earthquakes. This accumulative energy produces smaller but increasing deformation in the western border of the South American Plate, like a fold with horizontal shortening in east-west direction. When an earthquake takes place, the fold can dissapear with horizontal extention in east-west direction producing the movement to west and up of the western border of the South American Plate. This movement is the source of the tsunamis after the earthquakes. These explains the uplift in the coastal areas and the subsidence in the Coastal Cordillera and

Central Valley in thrust earthquakes along Wadatti-Benioff zone. In this case, it is very difficult to find evidence of fault rupture in surface because it had NNE strike and dip around 20¼ towards east and reaches the earth surface under the sea near the trench. Normal faulting earthquakes like Chillan 1939, produces another kind of movements (Fig.2). The faults that separate the Coastal Cordillera and peninsulas are moving. In summary, the landscape in the Biobio region of Chile, like Coastal and Andes Cordillera, Peninsulas, Coastal Plains and Central Valley are been built up to today by the earthquakes.

REFERENCES

(1) Askew, B.; Algermissen, S.; 1985. Catalog of Earthquakes for South America. V.1. Description of the Catalog and National Reports. CERESIS. Lima, Perœ. 191 pp.

(2) Barrientos, S.; Ward, S.; Lorca, E.; 1988. El terremoto de 1960 en el sur de Chile y sus deformaciones cuasi permanentes. V Congreso Geol—gico Chileno. Santiago, Chile. Tomo II. PP F 133-F 151. (3) Beck, S.; Barrientos, S.; Kausel, E.; Reyes, M.; 1998. Source characteristics of historic earthquakes along the central Chile subduction zone. Journal of South American Earth Sciences. Vol 11 N¼2. PP 115-129. (4) Campos, J.; Ruegg, J.; Barrientos, S.; Kausel, E.; Delouis, B. 1997. Proceso de ruptura del terremoto del 30 de julio de 1995 en Antofagasta. VIII Congreso Geol—gico Chileno. Universidad Cat—lica del Norte. Facultad de Ingenier'a y Ciencias Geol—gicas, Departamento de Ciencias Geol—gicas. Antofagasta, Chile. PP 1751-1754.

(5) Dewey, J.; Lamb, S.; 1992. Active tectonics of the Andes. Tectonophysics 205. Amsterdam, The Netherlands. PP 79-95. (6) Ponce, L.; San Mart'n, C.; Kausel, E.; 1994. Caracter'sticas de la Sismicidad (1965-1993, Mb>4.7) asociada a la brecha s'smica "Pichilemu-Concepci—n". VII Vongreso Geol—gico Chileno. Universidad de Concepci—n, Departamento de Ciencias de la Tierra, Concepci—n, Chile. PP 689-694.

(7) Saint Amand, P.; 1961. Observaciones e interpretacion de los terremotos Chilenos de 1960. Comunicaciones de la Escuela de Geologia A–o 1 Numero 2. Universidad de Chile Facultad de Ciencias F'sicas y Matem‡ticas. 53 pp.

MAMMAL FOSSILS IN THE REGION OF CUZCO

Jose Angel RAMIREZ PAREJA(1)

(1) e-mail: libero@amauta.rcp.net.pe
e-mail: jarp@chaski.unsaac.edu.pe

INTRODUCTION

Mammal fossils have been encountered over the passed decades in a number of fossil rich localities in the province of Cusco. An important collection of the material studied is currently stored in the Natural History Museum of the Nacional San Antonio University of Cusco. Scientific interest is currently focussed on the relation between the fossil collection and other recently discovered fossil occurrences (on a local and regional scale).

Previous studies

Early studies of fossil mammals in the region of Ayusbamba (Paruro) were conducted by Herbert and Eaton (1914). Carlos Kalatovich already mentioned the presence of a Gliptodon in the Valley of Cusco (1955). The author of this abstract performed various studies on mammal fossils encountered in the region (1958).

Localities and material

So far ten fossil localities have been discovered, the most important of which are localized in the Cusco Valley and Aysbamba. The samples collected contain abundant fossils and even comprised a complete gliptodon skeleton.

Geology

The fossils are located in sedimentary deposits representing a continental environment. These deposits form part of the Quaternary San Sebastian Formation which primarily consists of fluvioglacial limestones, clays, sands and gravels. In the Cusco Valley, the formation reaches a thickness of 120 meters.

Systematics

The following species have been determined:

Orden EDENTATA
Megatherium americanum Cuvier 1800, encountered in the Cusco Valley.
Gliptodon clavips Owen 1838, Cusco Valley
Scelidotherion sp. Owen 1840

Orden Litopterna
Macrauchenia patachonica Ameghino 1840, Cachimayo Cusco Valley
Scelidotherion sp. Owen 1840

Orden Litopterna
Macrauchenia patachonica Ameghino 1840, Cachimayo Cusco Valley

Orden Proboscidea
Cuvieronius hyodon Fichc 1929 and Simpson and Paula Couto 1955, Ayusbamba (Paruro).

Orden Perysodactyla
Equus andium Branco; Various localities among which Ayusbamba, Cachimayo and Kayra.
Parahiparion sp. Ameghino 1904; Ayusbamba and Anta.

Orden Artiodactyla
Mazama (Protomazama) anadina Spillmann 1931; Cachimayu Cusco Valley

Fossil ages

Herbert and Eaton (1914) considered an age of 100.000 years for the Mastodont fossiles of Ayusbamba. A specialized team headed by Dr Robert Bouchez (1984) of the University of Grenoble determined an age of 1.1 Ma for the same material using the RPE spectrometric method.

Discussion

The fossils have been discovered in sedimentary deposits of lower and middle Pleistocene age. Recently, a systematic revision of the species has been made.

Problems to be addressed

-Why did mammals migrated from the low lying terranes of the continent towards the Andes Cordillera?
-Could the climatic changes that occurred at the beginning of the Quaternary have played a major role?
-How could the migration of gliptodonts and other heavy animals be explained with reference to natural barriers such as topography and height.
-The fossils are presently encountered at heigths of 3-4000 meters. The difference between present height and the height at the time of migration is most probably very small.

CONCLUSIONS

1. The mammal fossil fauna that has been studied corresponds to the lower to middle Pleistocene. Possibly, some species have survived until the upper Pleistocene.
2. Fossil ages dated by radiometric methods suggest 1.1 Ma for the oldest fossils.
3. Species that are known today migrated into the Andes Cordillera in subsequent waves and during different moments during the lower and middle Pleistocene.

REFERENCES

Bouchez Robert (1984) According to a specialist team: E. Lopez Carranza. Department of Physics of the University of Lima; J.L. MA, Laboratorium of Archeological Research, ISN University of Grenoble; J. Amosse of the Dolomieu Institute of Geology, Univ. of Grenoble, A. Cornu, Analytical Service Studies, CEN Grenoble. , J. Diebolt, Analytical Service Studies, CEN Grenoble; H.D. Lumley Institute of Paleontology Humaine, Paris; J.A. Ramirez Pareja, Universidad National de San Antonio Abad del Cusco, Cusco Peru; C. Guerin, Department of Sc. De la Terre, Univ. Lyon. Dating by spectrometry of fossil dental email in the range of 50.000 years and a few million years.

Herbert, G.E, Eaton, F. (1914) Geological reconnaissance of the Ayusbamba fossil beds (Peru) and vertebrate fossils from Ayusbamba. The Am. Mus. Jl. of Science – Vol. XXXVII

Hoffsteter, R. (1981) Historia biogeografica de los mamiferos terrestres sudamericanos. Seperata de Acta Geologica Hispanica Nro. 1-2 tomo 16

Kalafatovich, V.C. (1955) El fossil de Gliptodonte Hallado en el Cusco. Revista de la Univ. del Cusco, No 108

Ramirez Pareja Jose Angel (1958) Mamiferos Fosiles del Departamento del Cusco. Tesis para optar al Grado de Doctor en Ciencias Biologicas. Universidad Nacional San Antonio Abad del Cusco-Peru

THE ANDES OF NEUQUÉN (36°38° S): EVIDENCE OF CENOZOIC TRANSTENSION ALONG THE ARC

Victor A. Ramos and Andrés Folguera

Laboratorio de Tectónica Andina, Universidad de Buenos Aires, Ciudad Universitaria, Pabellón II, (1428) Buenos Aires, Argentina (email: andes@gl.fcen.uba.ar)

KEY WORDS: Volcanic arc, extension, caldera collapse, neotectonic, wrenching.

INTRODUCTION

The Andean Cordillera is characterized by a discrete segmentation along strike, controlled by different tectonic settings, the crustal composition, and the mechanics of adjacent oceanic attributes. These distinctive features are expressed in the resulting topography. An outstanding example of these controls is the segment of the Andes that corresponds to the Cordillera Neuquina (36°-38°S). This segment has low elevation, a crustal thickness less than 45 Km, and the topography is dominated by oblique NW fault-bounded blocks.

Detail studies on the present volcanic arc have shown that the major NW trend have evidence of left-lateral strike-slip, as well as extensional components (Folguera and Ramos, 1999). This major northwest wrenching associated with subordinated ENE minor faults have produced a series of rhombohedric structures, interpreted as pull-apart basins, as the Agrio Caldera (González Ferrán, 1995). This structure is a collapse caldera controlled by the NW and ENE faults, developed between 2.6 and 1.6 Ma. Major normal faults associated with the caldera show dominant extensional dip-slip component in the ENE trend. Within these pull-apart basins there are secondary faults which show minor folds and thrusts associated with conspicuous strike-slip components. This kinematics is affecting the Pliocene and Quaternary volcanics, and either postglacial lavas, that have been cut by ENE normal faults (Folguera and Ramos, 1999). There are NE trending faults related to minor folds, with reverse slips, that put Holocene alluvial deposits on the Pleistocene volcanics (Figs. 1 and 2).

DISCUSSION

The partitioning of the stress in the Andes between 46° and 39°S is heavily controlled by

the right-lateral displacements of the Iquiñe-Ofqui fault (Hervé, 1988, Dewey and Lamb, 1992, Cembrano et al., 1996, 1997). Recent studies have shown that this situation can be extended across the Andes to the foothills as far as to the Ñirihuau and Ñorquinco basins (Diraison et al., 1998). This tectonic setting is the result of the interaction of oblique subduction along the margin, and the dominant NNE trend of the Iquiñe-Ofqui fault (Cembrano et al., 1997). This partition is confirm by the right-lateral strike-slip focal mechanisms along a NNE trending fault associated to the basement of the of the Lonquimay and Hudson volcanoes (Lavenu et al., 1997).

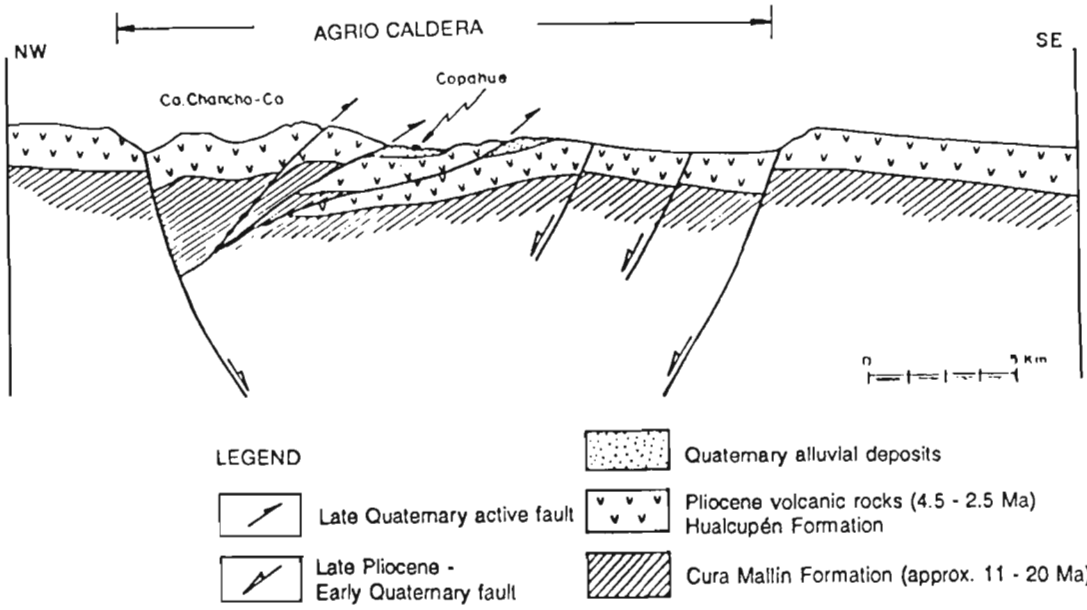

Figure 1: Longitudinal section in a NW-SE direction of one of the pull-apart basins, corresponding to Agrio Caldera (37° 45'S).

However, the Andes north of 38°S are dominated by conspicuous NW trending fault-bounded blocks as the Pino Hachado-Copahue High. These features are inherited at least from Oligocene times, when a backward migration of the volcanic front towards the trench produced a series of NW trending half-graben system (Vergara et al., 1997 a,b). This system controlled the major depocenters of the Cura Mallín basin, at both slopes of the Main Cordillera. These northwest trending lineaments show evidence of left-lateral displacements across the Neuquén basin (Ramos, 1978).

The analysis of the structure of the volcanic arc show that important contraction is accommodated through left-lateral strike-slip of NW trending faults. As a result of these displacements a series of minor pull-apart basins, link to minor normal faults, were formed during Quaternary times, as the Agrio Caldera. Progressive deformation within these basins reactivated the previous faults as reverse faults and folds affecting up to the Quaternary alluvial deposits.

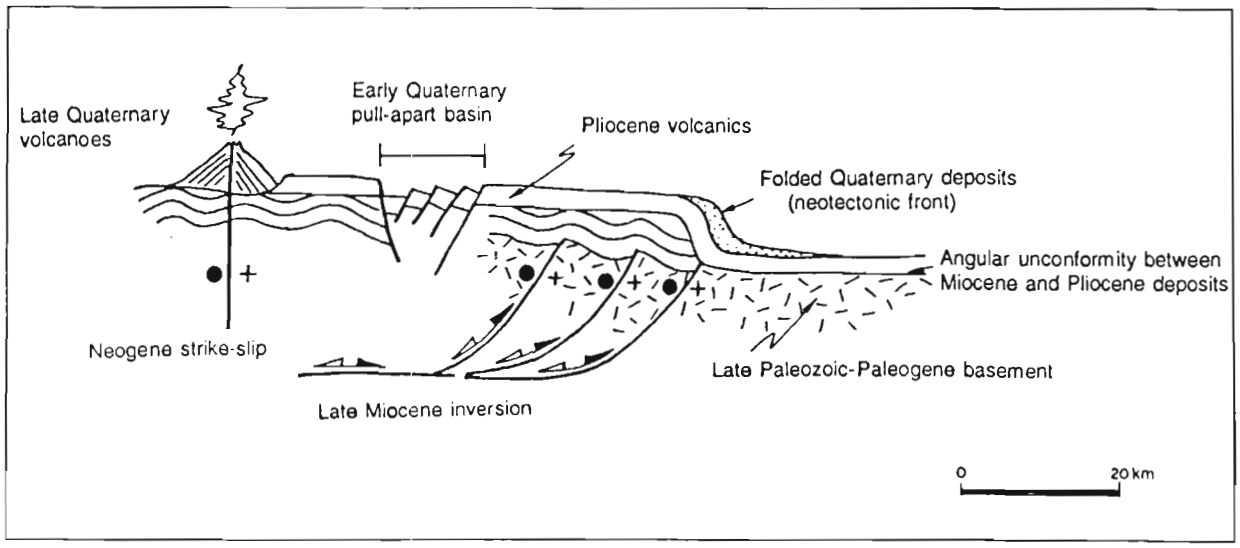

Figure 2: Transverse section of the volcanic arc that shows left-lateral strike-slip, as well as contractional reactivation of previous normal faults, that folds the Pliocene volcanic rocks and the Quaternary alluvial deposits.

CONCLUSIONS

Stress partitioning as the result of oblique convergence between the Nazca and South America plates is controlled by major preexisting discontinuities. South of 39°S is well known that most of the structures are dominated by right-lateral wrenching of northeast structures as the Iquiñe-Ofqui fault system. North of 38°, where major crustal discontinuities are produced by NW-trending fault-bounded blocks, stress partitioning produced dominant left-lateral wrenching. This strike-slip faults produced a series of transtensional features, as the Agrio Caldera, and other pull-apart basins. As a result of progressive deformation within these basins are presently developed minor contractional structures.

ACKNOWLEDGEMENTS

The field studies were funded by projects PIP 4162 of CONICET and UBACYT EX-132.

REFERENCES

Cembrano, J., Hervé, F., and Lavenu, A., 1996. The Liquiñe Ofqui fault zone: a long-lived intra-arc

fault system in southern Chile. Tectonophysics 259: 55-66.

Cembrano, J., Lavenu, A., Arancibia, G., Sanhueza, A. And Reynolds, P., 1997. Coeval transpressional and transtensional magmatic arc tectonics in the Southern Andes. VIII° Congreso Geológico de Chile, Actas III: 1613-1616, Antofagasta.

Dewey, J.F. y S.H. Lamb, 1992. Active tectonics of the Andes. Tectonophysics 205: 79-95.

Diraison, M., P.R. Cobbold, E.A. Rossello, And A.J. Amos, 1998. Neogene dextral transpression due to oblique convergence across the Andes of northwestern Patagonia, Argentina. Journal of South America Earth Sciences, 11(6): 519-532.

Folguera, A. and Ramos, V.A., 1999. Control estructural del volcán Copahue: implicancias tectónicas para el arco volcánico cuaternario (36°-39°S). Asociación Geológica Argentina, Revista (in press), Buenos Aires.

González Ferrán, O., 1995. Volcanes de Chile. Instituto Geográfico Militar, 1-640, Santiago.

Hervé, F., 1988. Late Paleozoic subduction and accretion in Southern Chile. Episodes 11(3):183-188.

Lavenu, A., Cembrano, J., Arancibia, G., Deruelle, B., López Escobar, L., and H. Moreno, 1997. Neotectónica transpresiva dextral y volcanismo: Falla Iquiñe-Ofqui, Sur de Chile. VIII° Congreso Geológico de Chile, Actas I: 129-133.

Ramos, V.A. 1978, Estructura, in Geología y Recursos Naturales del Neuquén: VII° Congreso Geológico Argentino, Relatorio, p. 99-118.

Vergara, M., López Escobar, L. and Hickey-Vargas, R., 1997a. Geoquímica de las rocas volcánicas miocenas de la cuenca intermontana de Parral y Ñuble. VIII° Congreso Geológico Chileno, Actas II: 1570-1573, Antofagasta.

Vergara, M., Moraga, J. and Zentilli, M., 1997b. Evolución termotectónica de la cuenca terciaria entre Parral y Chillán: análisis por trazas de fisión en apatitas. VIII° Congreso Geológico Chileno, Actas II: 1574-1578, Antofagasta.

PRELIMINARY PALEOMAGNETIC EVIDENCE FOR A VERY LARGE COUNTERCLOCKWISE ROTATION OF THE MADRE DE DIOS ARCHIPELAGO, SOUTHERN CHILE.

Augusto E. RAPALINI (1), Francisco HERVÉ (2) and Victor A. RAMOS (3) .

(1) Laboratorio de Paleomagnetismo Daniel Valencio, Departamento de Ciencias Geológicas, FCEyN, Universidad de Buenos Aires, Pab.2, Ciudad Universitaria, 1428, Buenos Aires, Argentina. rapalini@gl.fcen.uba.ar
(2) Departamento de Geología y Geofísica, Universidad Nacional de Chile, Santiago, Chile. fherve@tamarugo.cec.uchile.cl
(3) Laboratorio de Tectónica Andina, Departamento de Ciencias Geológicas, FCEyN, Universidad de Buenos Aires, Pab.2, Ciudad Universitaria, 1428, Buenos Aires, Argentina. andes@gl.fcen.uba.ar

KEY WORDS: Paleomagnetism, Southern Andes, tectonic rotation, Chile

INTRODUCTION

The Madre de Dios archipelago is located around 50.5° S in southernmost Chile (Fig.1). Its more relevant geologic characteristic is the presence of exotic Late Paleozoic successions. According to Forsythe and Mpodozis (1987) the stratigraphy of the area comprises four major units (Fig.1):

1. The Denaro Complex, mainly composed of submarine tholeitic basalts, cherts and limestones, interpreted as remnants of paleooceanic floor.
2. The Tarlton Limestone, massive limestones with Late Carboniferous to Early Permian fusulinids.
3. The Duque de York Complex, made up of thick sequences of flyschoid sediments.
4. The Patagonian Batholith that was emplaced in the previous units and has been dated between 132 and 120 Ma approximately (Halpern, 1973).

The three pre-Cretaceous units are tectonically disrupted and juxtaposed in what has been called as a „macromelange" (Forsythe and Mpodozis, 1987).

In order to determine the paleogeographic position and provenance of the Denaro Complex and Tarlton Limestone rocks, a paleomagnetic study was initiated in these two units. Sampling was done during a twelve-day field work in the Madre de Dios and Diego de Almagro archipelagos in July 1997.

PALEOMAGNETIC STUDY

One hundred and thirty oriented samples were collected with a portable drilling machine at 19 sites: 14 in Madre de Dios and 5 in Diego de Almagro. Fourteen sites were located in limestones and five in basaltic pillow lavas. The distribution of the sampling localities in Madre de Dios are shown in Fig.1. Although laboratory procedures are yet unfinished, preliminary results from over 60% of the samples suggest that final results will not substantially change the preliminary conclusions. Samples analyzed were submitted to stepwise AF and thermal cleaning. Demagnetization steps reached up to 140 mT and 690°C. In a few cases detailed thermal cleaning was applied to samples previously AF demagnetized. Samples from limestones exposed in Diego de Almagro (AL1 to AL5) and Isla Guarello, in Madre de Dios, (MD6 and MD7), showed extremely weak NRM intensities (<10 μA/m). Most remaining samples presented complex magnetic behaviours with generally two or three partially overlapped magnetic components. A preliminary analysis shows no evidence of preservation of the primary remanence in most sites. However, a consistent magnetic component apparently carried by magnetite was isolated at seven sites in Madre de Dios. This component was found both in basaltic lavas and in limestones of the Denaro Complex and Tarlton Fm in different localities. Preliminary *in situ* mean site directions of this component are shown in Fig.2. They were calculated on the basis of 3 to 5 samples per site. This component presents both polarities and is clearly postectonic (99% confidence). Mean direction from these seven sites is: Dec. 244.9°, Inc. 76.4°, α95: 6.8°. This direction is not consistent with any expected Mesozoic or Cenozoic direction for the study area.

Although the age of the isolated remanence is still uncertain, it must postdate the main folding and thrusting events. According to Forsythe and Mpodozis (1987) the pre-Late Jurassic units underwent two tectonic phases, the second one of possible Late Jurassic age, although a younger age cannot be ruled out. This indicates that the postfolding remanence was acquired in Cretaceous or younger times. Considering that the South American reference pole from Early Cretaceous to Recent times has not changed considerably (e.g. Beck, 1998), the remanence age is not critical for a tectonic interpretation of the paleomagnetic data. The presence of both polarities indicate that magnetization was not acquired during the Cretaceous Normal superchron. This constrains the age of magnetization either to the Early Cretaceous or the latest Cretaceous to Recent times. Values of rotation and paleolatitude anomaly with their corresponding errors were calculated according to Beck (1989). They do not differ substantially regardless the reference pole used. Using the latest Cretaceous (~70 Ma) Patagonian basalts pole (Butler et al., 1991) as the reference pole, the following values are obtained:

Rotation: 97.2°± 25.5° (ccw)

Paleolatitude Anomaly: 7.5°± 6.5° (Northward displacement)

The paleomagnetic data obtained so far indicate a very large ccw rotation of a large area of the Madre de Dios archipelago. The paleolatitude anomaly suggests a marginally significant northward displacement. Selection of different reference poles (Early Cretaceous, Recent) produces slightly larger values of rotation and paleolatitude anomaly. Minimum size of the rotated block exceeds 30 km (distance between sampling localities). The rotation took place after the main deformational events that folded and thrust the pre-Late Jurassic rocks. The age of rotation and the tectonic mechanism that caused it are under investigation.

ACKNOWLEDGMENTS

Field work was supported by Catedra Presidencial de Ciencias to FH, laboratory studies were supported by UBACyT grant AX002 to AR.

REFERENCES

Beck, M. E. Jr., 1989. Paleomagnetism of continental North America; Implications for displacement of crustal blocks within the Western Cordillera, Baja California to British Columbia. Geol. Soc. Am. Mem. 172, 22, 471-492.

Beck, M.E. Jr., 1998. On the mechanism of crustal block rotations in the central Andes. Tectonophysics, 299, 75-92.

Butler, R.F., Hervé, F., Munizaga, F., Beck, M.E., Burmester, R., Oviedo, E., 1991. Paleomaagnetism of the Patagonian Plateau Basalts, southern Chile and Argentina. *J. Geophys. Res., 96*, 6023-6034.

Forsythe, R. and Mpodozis, C., 1987. El archipiélago Madre de Dios, Patagonia Occidental, Magallanes: rasgos generales de la estratigrafía y estructura del „basamento" pre-Jurásico Superior. *Revista Geológica de Chile, 7*, 13-29.

Halpern, M., 1973. Regional Geochronology of Chile south of 50° latitude. *Geol. Soc. Am. Bull., 84*, 2407-2422.

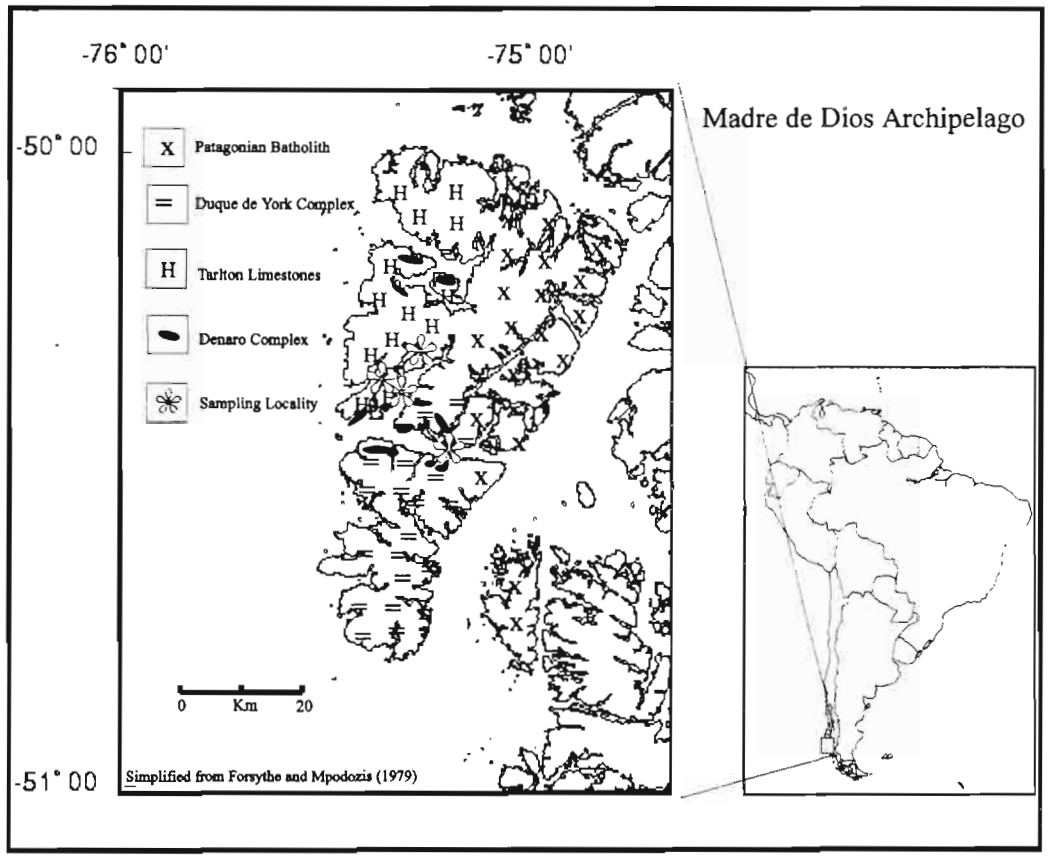

Fig.1: Simplified geologic map of the madre de Dios Archipelago and location of paleomagnetic sampling localities.

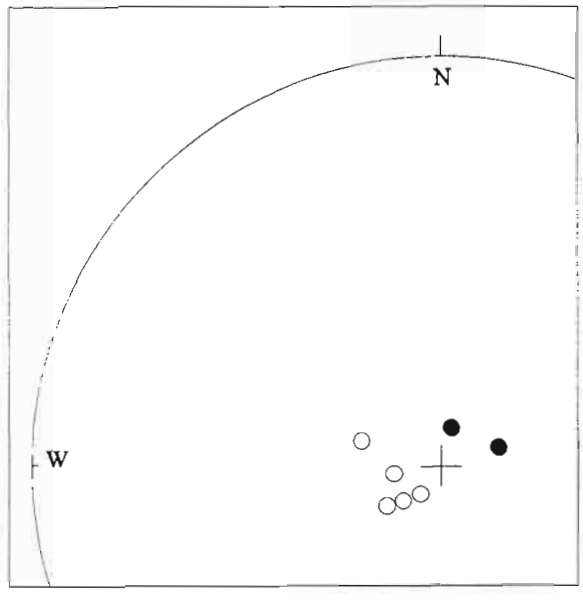

Fig.2: In situ mean site directions of the post-folding remanence isolated at Madre de Dios.

MODELS FOR SUBDUCTION EROSION OF NORTH CHILE

CINCA Working Group

(1) Author for correspondence: Christian Reichert, BGR, POB 510153, D-30631 Hannover, Germany (christian.reichert@bgr.de)

KEY WORDS: subduction erosion, mass balancing, North Chile, Central Andes

INTRODUCTION

The comprehensive off- and onshore geoscientific CINCA survey in North Chile yielded the following basic results: deep fracturing of the oceanic crust along the outer trench slope with almost no overlying sediments; deep and thorough strongly extensional regime of the continental wedge associated with thinning toward the trench; slumping and creeping at the slope surface, and especially a horizontal morphotectonic tripartition of the slope; identification of four lithostratigraphic or/and tectono-structural units with a frontal wedge of disordered debris nature characterized by low seismic velocities; recurring uplift processes associated with the outer structural high beneath the upper slope; the uppermost ca. 10 m of slope seafloor are formed by hemipelagic sediments of Neogene age apart from rare locations at the outer structural high where rocks similar to those of the Coastal Cordillera were dredged; evidence of strong continuous slope subsidence by lithofacies analyses; no accretionary wedge is formed. Under the assumption that the original thickness of the continental paleo-crust was between 25 and 35 km and that the average eastward trench migration is around 1 mm/a (Scheuber et al., 1994), we consider two possible models of subduction erosion. **Model A** is based on the observation that the open inter-horst volumes at the surface of the subducting crust provide a minimum transport capacity of 56 km^3 per Ma and per km trench length for removal of rock material creeping and slumping from the surface of the continental slope

(v. HUENE et al., 1999). More than enough space is provided to remove the entire crust by filling the inter-horst gaps at the subduction front. However, this implies continuous uplift of ca. 0.34 mm/a and exhumation of even Moho levels after only about 100 Ma from the beginning of subduction erosion. Thus presently considerably deeper portions of the upper mantle should be involved in the erosion at the top side of the slope but no corresponding geological samples have been recovered. Instead, at particular locations associated with steep scarps at the outer structural high where seismic unit CM2 (CM: Chile Margin) obviously crops out, samples typical of the Coastal Cordillera were dredged. It cannot be decided whether these rocks are autochthonous or allochthonous. If the former applies, seismic unit CM2 could represent the western extension of the La Negra Formation (Jurassic volcanism of the Coastal Cordillera). This is also supported by comparison of observed thicknesses that also on land vary up to 10 km thickness.

All datable geological sediment cores taken from the uppermost continental slope surface at widely spread locations (penetration < 10 m) give ages not older than middle Miocene (NN4-NN5, ca. 15 Ma). Multi-channel seismic (MCS) data show a transparent zone of about 1 km thickness below the sea bottom of the continental slope similar to a draping. Simple calculation yields that the complete cover containing about 80 km^3 per km trench length would be removed by erosional processes at the top side of the continental wedge within less than 10 Ma. Thus, the geological results preclude abundant mass wasting from the top side of the continental slope.

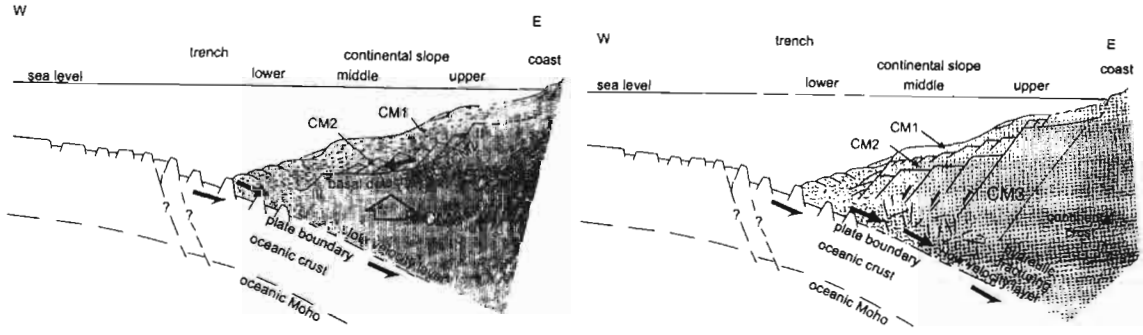

Model A Model B

An alternative model is provided by erosion at the front and along the base of the continental wedge (**Model B**). Here, the surface of the slope remains relatively undisturbed apart from the normal extensional faults and tilted blocks that in this interpretation are the expression of large vertical and relatively small lateral movements. The pronounced morphotectonic tripartition shows that the middle slope with a width of ca. 50 km extension obviously plays a particular role. Compared to the outer structural high, stronger subsidence of the middle slope than of the upper slope is demonstrated by the seismic and bathymetric data which can be best explained by more pronounced erosion at the base of this portion. Restora-

tion of the CM2/CM3 boundary yields that an extension of approximately 5 km is produced by fault-related decomposition over a length of about 50 km during some 50 Ma.

Balancing of all effects that can contribute to the total erosional volume leads to the equation:

$$V_{tot} = TCW + FSU + MS_{pl} + DCUM_{pl}$$

with V_{tot} =: total volume (must add up to ca. 35 $km^3\ Ma^{-1}$ per km trench length); TCW =: top side of the continental wedge (CM1 and CM2); FSU =: frontal slope unit (chaotic debris masses with low seismic wide-angle/refraction velocities; see Fig. 5.3); MS_{pl} =: middle slope basis (plate boundary); $DCUM_{pl}$ =: deep crust/upper mantle at the plate boundary east of the middle slope; all per km trench length. TCW is estimated to be ca. 1 $km^3\ Ma^{-1}\ km^{-1}$ from the previous considerations (about 0.5 $km^3\ Ma^{-1}\ km^{-1}$ by decomposition extension and probably another 0.5 $km^3\ Ma^{-1}\ km^{-1}$ by slumping and creeping). FSU could theoretically be as big as V_{tot} since the open volumes provided by the inter-horst gaps of the down-flexing oceanic crust are capable to remove even more volume. But this has already been ruled out when considering model A. Thus a mechanism is required that prevents filling the entire gaps. It seems likely that the high prominent horsts on the top of the oceanic crust will be destroyed under the increasing load and compression at a certain distance from the trench. Weak seismic indications of their morphology we detect still at the boundary between lower and upper slope in the MCS data. This is in congruence with the bathymetric observations (v.HUENE et al., 1999). Beneath the middle slope the reflected energy from the plate boundary is very weak. This might be due to the strongly disrupted overburden or due to decreasing velocity contrasts. However, where detected, the strong morphology of the oceanic crust has disappeared and a band of low-frequency subparallel reflections becomes visible. Thus, we feel that the horsts are ground or razed approximately beneath the boundary between lower and upper slope when they come into contact with the base of seismic unit CM3. Their remnants are being mixed with the sedimentary infill of the inter-horst gaps forming a melange that is subducted as an interlayer at the plate boundary. The surplus of inter-horst sediments is scraped or squeezed out and recycled to the frontal slope sedimentary unit until an appropriate balance is reached.

The observed constant total thickness of seismic units CM1 + CM2 + CM3 at the boundary to the frontal slope unit of around 5 km on all CINCA profiles, other constraints and considerations on the pronounced middle slope terrace lead to a stepwise estimation for the required terms:

TCW = ca. 1 $km^3\ Ma^{-1}\ km^{-1}$; FSU = ca. 5 $km^3\ Ma^{-1}\ km^{-1}$; MS_{pl} = ca. 14 $km^3\ Ma^{-1}\ km^{-1}$;

$DCUM_{pl}$ = ca. 15 $km^3\ Ma^{-1}\ km^{-1}$. In total about 35 $km^3\ Ma^{-1}\ km^{-1}$.

The intense fracturing of the oceanic crust comprises also very deep levels and allows seawater to penetrate also into the upper mantle of the Nazca Plate. Suffering increasing pressure from the overburden this chemically unbound water is expelled into the overlying plate by closing pores and fissures thus initiating 'hydraulic fracturing' at the base of the upper plate. This process is probably strongly supported by

'dilatational brecciation' beneath the middle slope where extensional normal faults reaching most likely down to the base of seismic unit CM3 are observed. In turn, these alterations at the base of the middle slope facilitate the erosional process and therefore the dominant morphology of this part of the continental wedge develops. In deeper levels the majority of pores and fissures is depleted and erosion changes from low compression to high compression beneath the outer structural high. Slight changes in the stress regime could result in the 'elevator' effect observed in geological samples at the Iquique block.

CONCLUSIONS

The strongly and deeply fractured Nazca Plate enables fluids to percolate and reach even the upper oceanic mantle. Hydration and destabilization of the percolated rocks is implied. In conjunction with the high convergence rate and the sediment starved deep trench along with strong surface morphology a high capability is provided to remove continental rocks. Also on the continental wedge - mainly beneath the middle slope - strong extensional fracturing occurs destabilizing the rocks down to the base of the plate. During the subduction process the increasing pressure expels fluids from the down-going plate into the overlying plate increasing the destabilization of its base by hydration and hydraulic fracturing. The major part of erosion takes place at the base of the overlying plate (Model B) due to geological results and some basic considerations. Balancing of mass removal according to model B reveals the particular role of the middle and frontal slope units. However, the discussed models and interaction of processes are still highly speculative. Uncertainties exist whether the major reflections represent lithostratigraphic or tectono-structural boundaries or both. This is essential with respect to the top side erosion component at the continental slope and the amount of lateral displacement in conjunction with the poor coverage and depth penetration of geological sampling. Therefore, further seafloor sampling and drilling is required. Moreover, comparison with areas further south that are subject to different conditions should mutually yield more insight into the respective subduction processes and the dependencies they are influenced by.

REFERENCES

v.Huene R., Weinrebe W., Heeren F. 1999. Subduction erosion along the North Chile margin. Geodynamics, 345-358.

Scheuber E., Bogdanic T, Jensen A., Reutter K.J. 1994. Tectonic development of the North Chilean Andes in relation to plate convergence and magmatism since the Jurassic. In: Reutter K.-J., Scheuber E., Wigger, P.J. (ed.) Tectonics of the Southern Central Andes - Structure and Evolution of an Active Continental Margin. Springer-Verlag, Berlin-Heidelberg-New York, 121-139.

Andean deformation mechanisms in the eastern Puna, NW Argentina

Ulrich Riller [1], Manfred Strecker[2] and Onno Oncken[3]

[1] Geoforschungszentrum Potsdam, Telegrafenberg C, 14473 Potsdam, Germany

[2] Institut für Geowissenschaften, Universität Potsdam, Potsdam, Germany

Horizontal crustal shortening, tectonic underplating, addition of voluminous magmas and climatic relationships are currently considered as prime mechanisms controlling the formation of the central Andean plateau. A field-based study of first-order structures in the Calchaquies River valley (Fig.1) was conducted to assess the tectonic component in the formation of the plateau. In this area, Precambrian to Cambrian low-grade metasedimentary rocks form the basement to Cretaceous/Paleocene rift sediments and Miocene continental red beds. Buckle folding of the rift sediments around dominantly north-south trending, orogen-parallel axes involved ignimbrite layers, most likely 12 to 8 Ma in age, and accounts for subhorizontal shortening during Andean (post mid Miocene) deformation. The unconformity at the base of overturned rift sediments is unstrained and indicates that Precambrian basement rocks were folded along with their cover rocks. Amplitudes of first-order folds are in the order of 0.5 to 1.5 km. This provides strong evidence for thick-skinned tectonism and possibly substantial crustal thickening during an early stage of Andean deformation. By contrast, the contact between basement rocks and Miocene red beds is characterized by high-angle reverse faults which formed at a later stage of Andean deformation. Displacement magnitudes on the fault surfaces as indicated by drape folds in red beds are generally less than 50 m and suggest that reverse faulting was of minor importance during Andean deformation. Thus, major crustal thickening may have been achieved by thick-skinned tectonism during an early stage of Andean orogenic activity.

The fold pattern in Cretaceous and Tertiary strata of the Calchaquies River valley indicates that horizontal shortening was accompanied by a strong component of left-

lateral shear on N-S striking discontinuities, e.g., the valley-bounding faults. In particular, folds in Miocene redbeds trend NE-SW (Fig. 1a) and are characterized by high interlimb angles. By contrast, folds in Cretaceous strata are tight to recumbent and subparallel to N-S striking master dislocations. Thus, progressive deformation in the Calchaquies River valley was characterized by tightening of folds and counterclockwise rotation of fold axes which is characteristic for left-lateral transpression. Such deformation can also be inferred in areas where hinge zones of first-order folds are not apparent. For example, in the northernmost part of the valley, the curvature of bedding plane trajectories of inclined Cretaceous strata (Fig. 1b) indicates a counterclockwise rotational component corresponding to left-lateral strike shear on N-S striking faults. Left-lateral transpression in the eastern Puna may be related to an overall clockwise rotation of the Puna if such rotation was accomplished by flexural slip on major discontinuities (Fig. 2).

Fig. 1. Geology and structure of the Valles Calchaquies. (a) Note the obliquity of fold axial trends between Miocene and Cretaceous strata. (b) Sigmoidal bedding plane trajectories in the northern portion of the Calchaquies River Valley

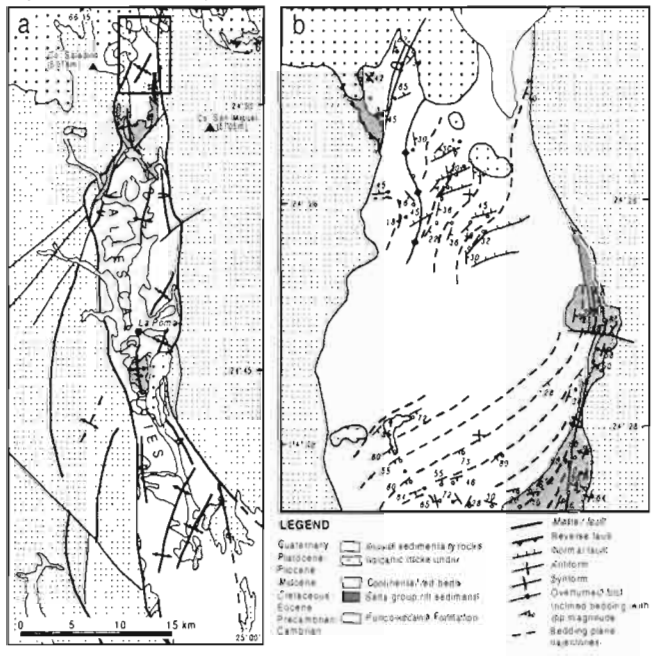

Fig. 2. Tectonic model explaining left-lateral transpression in the Calchaquies River valley by flexural slip due to bending of the Andean orogen.

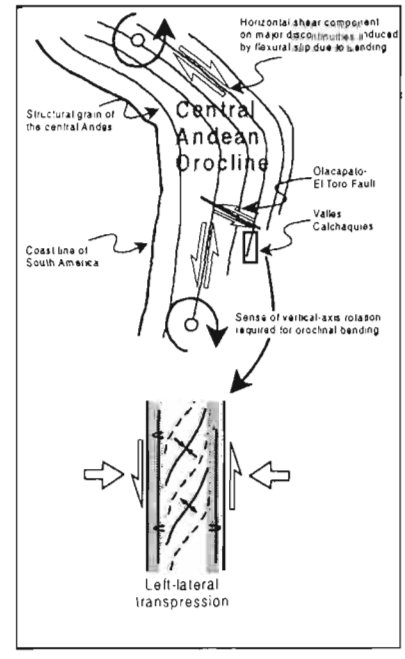

Structures indicating horizontal extension are seen sporadically in the northernmost portion of the Calchaquies River valley but are most likely linked kinematically to the NW-SE striking Olacapato - El Toro fault, a left-lateral master fault in the central Andes (Fig. 2). This fault along with its conjugate branches appear to transect structures that led to crustal thickening and indicate a component of orogen-parallel horizontal extension in the Puna. In models explaining the curvature of the Andean orogen by bending, N-S stretching and strike-slip faults serving as transfer zones between domains undergoing different amounts of transverse shortening are required in the outer arc of the orogen to maintain strain compatibility during oroclinal bending. Thus, left-lateral transpression in the south limb and strike-slip faults in the hinge zone of the orocline may well be kinematically related and may indicate that bending of the Andean orogen occurred at an advanced stage of crustal thickening. Our hypothesis can be tested by examining e.g. the structure in the inner arc of the orocline and in the Altiplano area where horizontal N-S shortening and a dextral component of orogen-parallel strike-shear should be apparent, respectively.

THE ORIENTE BASIN: AN OPTIMUM TECTONIC - SEDIMENTARY ENVIRONMENT FOR CRUDE GENERATION AND ACCUMULATION

Marco V. RIVADENEIRA M. (1), Patrice BABY (1)

(1) Convenio Petroproducción-IRD. Apartado 17-10-7019, Quito, Ecuador. pbaby@pi.pro.ec

KEY WORDS: Oriente Basin, Ecuador, sedimentation, tectonic, crude.

INTRODUCTION

The Oriente basin, Ecuador, constitutes the most prolific segment of the Putumayo-Oriente-Marañon oil province. In December of 1997, total original reserves was of 6,124 million barrels of crude. This great oil accumulation is product of the tectonic–sedimentary evolution between the Cretaceous and the present time.

THE SHALY AND CALCAREOUS CRETACEOUS LITHOFACIES (SOURCE ROCKS)

The potential and active source rocks were deposited on a cretaceous platform, in a shallow and half restricted enviroment, with void to scarce presence of bioturbation and pellets. The Napo black shales and interbedded limestones (Basal Napo Shale, "B" and "U" Limestones, "U" and "M1" Shales -Fig. 1), deposited under partially anoxic conditions, constitute rich, potential and active source rocks, whose organic matter content is increased toward the W, reaching the higher values in the NW zone of the basin (greater than 2% of Total Organic Carbon content). Turonian limestones ("A" and "B" Limestones -Fig. 1), comprise mainly black and gray mudstones and wackestones, deposited on a carbonate shelf under quiet waters with partially restricted circulation that create anoxic conditions in certain areas. This conditions change gradually appearing benthic communities. At the end of Turonian time, the basin emersion occurred (Jaillard E., 1997). The Turonian limestones thickens toward the WSW, reaching 400-450'.

THE APTIAN-CENOMANIAN SANDSTONES (MAIN OIL RESERVOIRS)

In Late Aptian-Early Albian Hollin basin had a SW- NE orientation, and were deposited quartzose, massive, cross-bedded sandstones with interbedded silty and clayey layers with amber, coal and plant remains in the middle and uppermost section. In the depocenter at the SW of the basin, sedimentary thickness surpass 500', and the section progressively thins toward the eastern-northeastern flank of the basin, until disappearance (Fig. 2). These sediments express a fluvial enviroment, type braided, with channel facies and minor overbank levee and crevasse splay. Thereafter, over a regional condensation surface, were deposited glauconitic calcareous sandstones, interbedded with calcareous black shales of the uppermost Lower Albian (Basal Napo Sandstone) in an estuaries and tidal flats environment.

The Upper Albian "T" and Cenomanian "U" sandstones (Fig. 1) consist of quartzose sandstones, in part glauconitic, which were deposited in predominantly fluvial enviroment to the east basin border, ranging westward and vertically to estuaries and deltas with tidal influence. To the westernmost, it was a domain of a well-developed shelf enviroment with glauconitic sandstones, muds and limes. The "T" and "U"

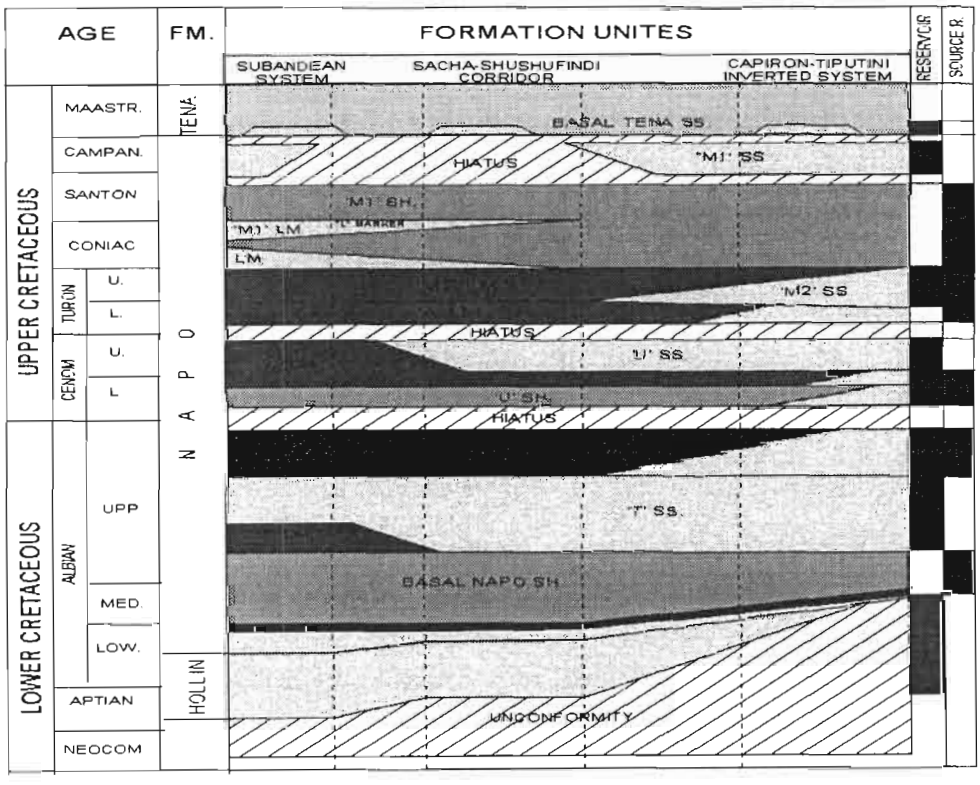

sandstone basin axis change of an SE-NNW (Fig. 3) to the E-W orientation respectively (Fig. 4). The "T" sandstone thins to the NE and disappears (Fig. 3).

Fig. 1. Generalized time-space distribution of the Cretaceous stratigraphic units showing major source rocks and reservoir intervals (Petrocanada, 1987; Jaillard E., 1997; Christophoul F., 1999).

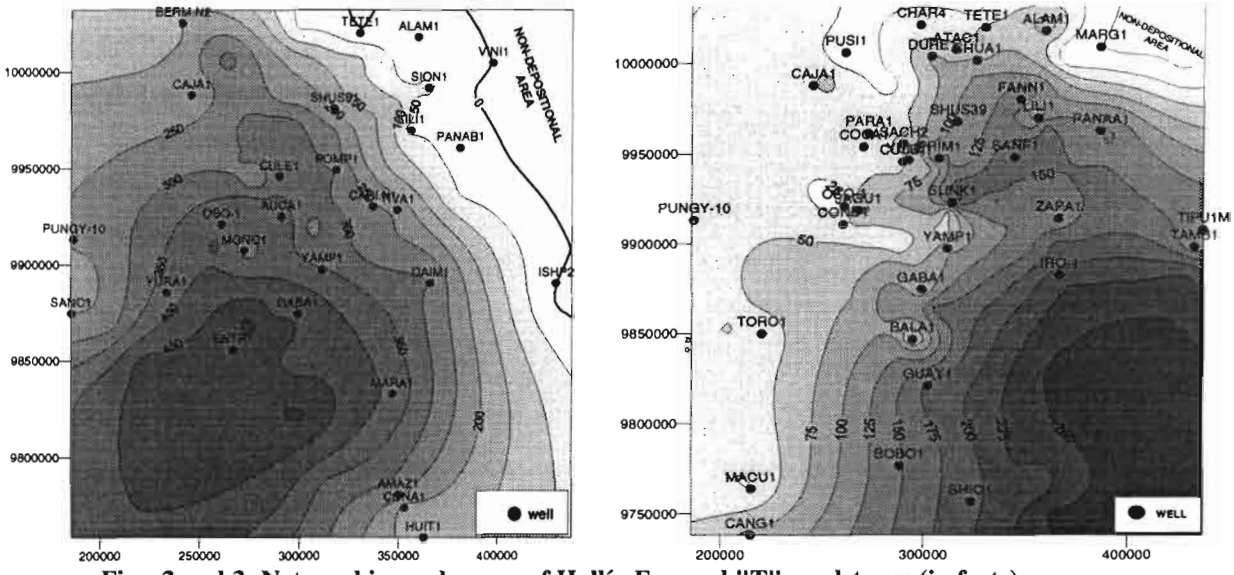

Figs. 2 and 3: Net sand isopach maps of Hollín Fm. and "T" sandstones (in feets).

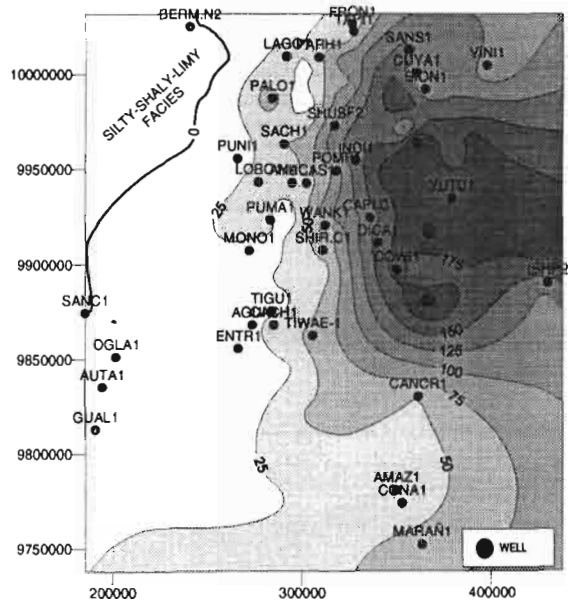

Fig. 4. Net sand isopach map of the "U" sandstone (in feet).

STRUCTURAL TIMING

Two transpressive stages are responsible for the formation of the anticlines (Baby et al., 1999) which constitute the oil fields:

- the first is developed between the Late Turonian and the Maastrichtian times, and corresponds to the Peruvian phase, which *forms the first oil structures* of the basin (Fig. 5), and, is responsible for the uplift of local structures located in the zone of the current Napo Uplift and Pastaza Depression, and
- the second during the Lower to Middle Eocene, contemporary with the Incaic phase, is responsible for the *final formation of the more oil productive structures* (Fig. 5) and the integrated system: *Andean mountain chain – foreland basin.*

ORIENTE BASIN OIL SYSTEM

The Oriente Basin of Ecuador had a propitious time-space evolution for the generation and accumulation of oil.

- First, the *Hollin-Napo is a "correct" interstratified sequence* of potential and active source rocks (shales and limestones) and reservoirs (sandstones), developed as a result of cyclic sedimentary basin evolution in short transgressive-regressive events.
- Second, the presence of an *" intra-continental hot spot"* (Barragán R., 1999), during nearly all the Cretaceous, creates favorable thermal conditions that accelerate the maturation of the shales and limestones of Basal Napo and the "T" and "U" sequences, which in the Eocene, due to the subsidence of the basin by effect of the raising of the Andes, enter to the zone of "mesocatagenesis" and expel hydrocarbons (Bernal C., 1998).
- Third, *the structural timing*, when at the beginning of the Upper Eocene, most of the Oriente basin anticlines were formed, before the expulsion and migration of crude.
- Fourth, *the structures were preserved*, preventing the remigration and destruction of the accumulated crude, with exception of the fields of the Subandean zone, deformed and in same cases destroyed

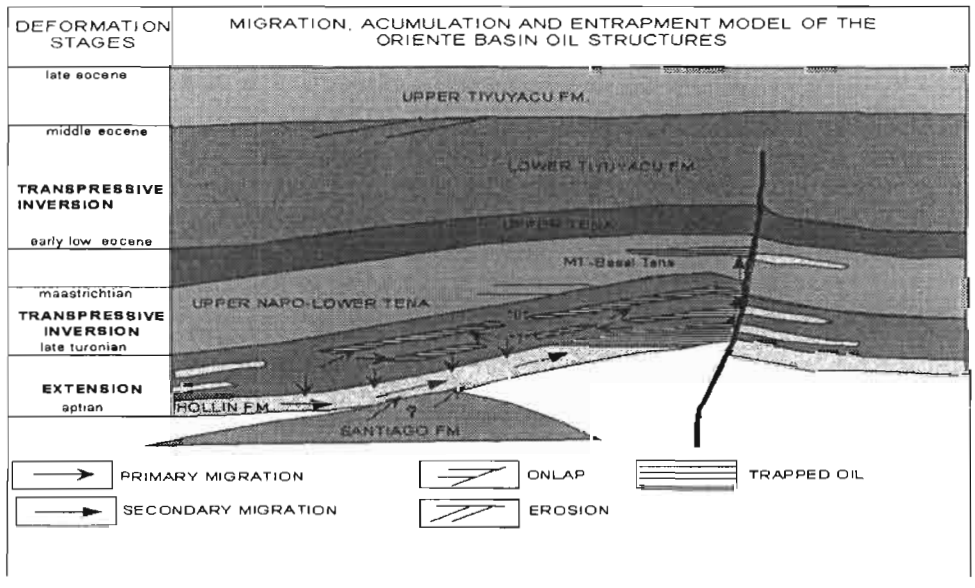

(Fields of the Napo Anticline) by effect of the strong erosion, as a result of the Quechua tectonic crisis of the Andean orogeny.

Fig. 5. Schematic model of trap formation, migration and accumulation of HC in the Oriente Basin

POINTS IN DISCUSSION

1. The role of the black shales and limestones of the Jurassic Santiago formation (Fig. 5), as potential source rocks of part of the Oriente crude (Investigation to be developed within the Petroproduccion-IRD Project).
2. A secondary hydrocarbon migration with two stages: - a first lateral migration trough the Hollín sandstones, and - a second vertical hydrocarbon migration within the structures, across the faults, redistributed to the upper reservoirs (Fig. 5).
3. The presence or absence of crude in Hollín sandstones in the fields of the basin. The analyses of the tectonic evolution of each field will allow to explain that.

REFERENCES

Baby P., Rivadeneira M., Christophoul F., Barragán R., 1999. Style and Timing of Deformation in the Oriente Basin of Ecuador. ISAG 99, This issue.

Barragán R. And Baby P. 1999. A Cretaceous hot spot in the Ecuadorian Oriente Basin: Geochemical, Geochronological and Tectonic indicators. ISAG 99, this issue.

Bernal C. 1998. Modelo Teórico de Generación y Migración de Hidrocarburos de la Formación Napo en la Cuenca Oriente Ecuador. Tesis de grado. Archivo Petroproducción. 99 p.

Jaillard E. 1997. Síntesis Estratigráfica y Sedimentológica del Cretaceo y Paleógeno de la Cuenca Oriental del Ecuador. Petroproducción-ORSTOM edition 164 p

THE BAJO DE VELIS-SAN FELIPE-YULTO MEGAFRACTURE (SAN LUIS, ARGENTINA): AN EXAMPLE OF ANDEAN REACTIVATION OF A RECURRENT CRUSTAL DISCONTINUITY

Eduardo A. ROSSELLO (1), Mónica G. LOPEZ DE LUCHI (2), Armando C. MASSABIE (3) & Claude A. LE CORRE (4).

(1) CONICET-Depto. Cs. Geológicas, Universidad de Buenos Aires. Pabellón II, Ciudad Universitaria. (1428) BUENOS AIRES, Argentina. E-mail: rossello@gl.fcen.uba.ar
(2) CONICET-CIRGEO. Ramírez de Velazco 847. (1414) BUENOS AIRES, Argentina. E-mail: DELUCHI@mail.retina.ar
(3) Depto. Cs. Geológicas, Universidad de Buenos Aires. Pabellón II, Ciudad Universitaria. (1428) BUENOS AIRES, Argentina. E-mail: armando@gl.fcen.uba.ar
(4) Université de Bretagne Sud. 1, rue de la Loi, 56000 VANNES, France. E-mail: Claude.Le-Corre@univ-ubs.fr

KEY WORDS: TECTONIC REACTIVATION, PAMPEAN RANGES, SAN LUIS, ARGENTINA.

INTRODUCTION

In the Cenozoic foreland of the Cordillera de los Andes foreland basins up to 600 km wide are controlled by major faults that results from the reactivation of older discontinuities. In the eastern flank of the Sierras of San Luis, in the typical background of the Sierras Pampeanas, a major Neogene NNE lineament is recognised; it extends about 200 km and is expressed for the submeridional alignment of blocks of crystalline basement that were peneplanized during the Cenozoic. This lineament initially described by Criado-Roqué et al (1981) and is here named Bajo de Velis-San Felipe-Yulto (BV-SF-Y) megafracture (Fig.1)

The Sierras Pampeanas are separated in two morphostructural units, the eastern and western Pampeanas on the basis of their different tectonic evolution, ages and lithology. The Sierras of San Luis at the southern end of the eastern Sierras Pampeanas are made up for Late Proterozoic to Early

Carboniferous basement. This crystalline basement constitutes the foreland of the Cordillera de los Andes that is characterised by en echelon and subordinate blocks produced by Andean NNE-SSW faulting

Metamorphic and igneous units and several tectonomagmatic events have been distinguished. Essentially the metamorphic rocks appear as NNE belts of micaceous schists, gneisses and migmatites. Metamorphic grade varies from medium to locally high for the presence of the sillimanite-garnet paragenesis. These belts alternate in the central and western sector of the Sierras with low-grade belts of phyllites, acid metavolcanics and fine grained chlorite bearing schists.

During the (500-330 Ma) Famatinian Cycle, granitoids that are separated in pre-Famatinian, Famatinian and post-Famatinian (Dalla Salda et al., 1998) or early, syn and post orogenic with reference to the Ocloyic Phase of the Famatinian Cycle, have been intruded (Llambías et al., 1998).

The upper limit of the metamorphic-igneous evolution of the basement of the Sierras of San Luis is marked for the beginning of the sedimentation in the Late Carboniferous.

THE BAJO DE VELIS-SAN FELIPE-YULTO MEGAFRACTURE

This BV-SF-Y megafracture is a major morphotectonic feature that exhibits evidences of several types and intensities of tectonic activity during: i) Ordovician-Silurian, ii) Devonian-Early Carboniferous, iii) Late Carboniferous-Permian, and iv) Neogene. Initially, during the Ordovician, the BV-SF-Y megafracture separates domains with ductile deformation in medium grade metamorphic rocks with development of folds, axial plane cleavage and a dominant NNE regional foliation. On the other hand, this fracture limits toward the east a folded belt of hectometric pegmatoids that show sinistral displacements toward the main plane of the discontinuity. During Devonian-Early Carboniferous, the BV-SF-Y megafracture is intruded along about 20 km by the Batolito of Renca; their diametrical position suggest a possible regional control of their location, favoured by local releasing bend or step of its main trace. In the Late Carboniferous-Permian, the BV-SF-Y acts as an extensional fault controlling toward the east the sedimentation of the continental Neopaleozoic basin of Bajo de Velis. In the Batolito of Renca a NNE kilometric wide belt of fine grained porphyric syenogranitic dykes and cataclastic breccias cemented by white quartz are associated with the inferred trace of the lineament. Finally, during the Neogene, the BV-SF-Y megafracture reacts to the Andean deformation developing the alignment of eastern tilted blocks of the Paleozoic basement with antithetic hectometric scarps and elongated depressions filled by loessic sediments.

Between the above described several periods of tectonic activity the BV-SF-Y megafractures experiences important processes of isostatic recovery as indicated by thermobarometric data with the consequent erosions and sedimentations. The magnitude of the several controlled processes indicates a longeve tectonic activity during almost the entire Paleozoic that has involved different crustal levels.

Andean deformation took advantage of this deep structure in order to express itself with transpressive character to more than 500 km east of the active subduction.

ACKNOWLEDGEMENTS

This study was founded by: the Project: PICT 97 07-00000-00539: Mecanismos de emplazamiento, evolución petrotectónica y caracterización geoeconómica del Batolito de Renca, San Luis, Argentina, the CONICET and the University of Buenos Aires.

REFERENCES

Criado-Roqué, P., C. Mombr' & V.A. Ramos, 1981. Estructura e interpretación tectónica. 8° Congreso Geológico Argentino (San Luis), Relatorio, 155-192.

Dalla Salda, L. H.; López de Luchi, M. G.; Cingolani, C. & Varela, R., 1998. Laurentia-Gondwana collision: the origin of the Famatinian-Appalachians Orogenic Belt: In Pankhurst R. J. and Rapela C.W. (eds.): The Proto-Andean Margin of Gondwana Geological Society Special Publication N° 142: 219-234, London.

Llambías E.J., Sato A:A, Ortiz Su·rez A. & Prozzi C. 1998. The granitoids of the Sierra de San Luis. In Pankhurst R. J. and Rapela C.W. (eds.): The Proto-Andean Margin of Gondwana Geological Society Special Publication N° 142: 325-341, London.

Figure 1: Geological sketch of the Sierra de San Luis showing the main Andean reactivated faults modified after Criado Roque et al. (1981).

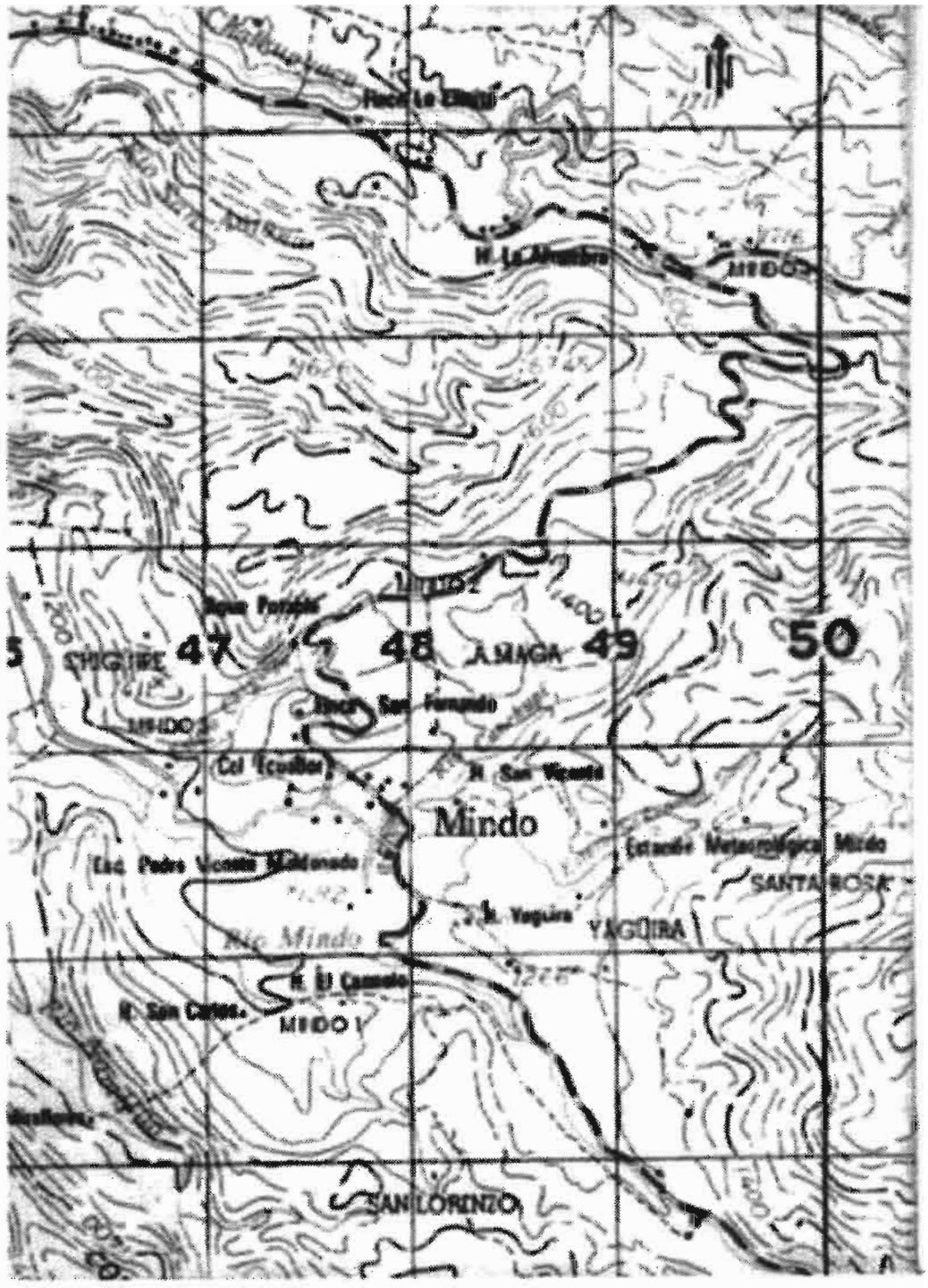

TECTONIC AND SEDIMENTARY EVOLUTION OF CENOZOIC BASINS IN THE EASTERN CORDILLERA, NW-ARGENTINA (22° - 23°S)

Daniel RUBIOLO (1,2), Raúl SEGGIARO(1,4), Roberto RODRIGUEZ(3), Alfredo DISALVO(5) and David REPOL(1)

(1) Instituto de Geología y Recursos Minerales. Servicio Geológico Minero Argentino (SEGEMAR).Avda. J.A. Roca 651, piso 10. (1322) Buenos Aires. Argentina. e-mail: drubio@secind.mecon.ar
(2) Consejo Nacional de Investigaciones Científicas y Técnicas
(3) Instituto Tecnológico Geominero de España. C/Rios Rosas 23. 28003 Madrid. España
(4) Universidad Nacional de Salta. Buenos Aires 177. (4400) Salta. Argentina
(5) Compania General de Combustibles. Buenos Aires. Argentina

KEY WORDS: Cenozoic. Eastern Cordillera. Tectonic. Magmatism. Argentina

INTRODUCTION

The Eastern Cordillera between 22° and 23° S of northernwest Argentina exhibits an E-verging basement-involved thrusts linked to the Subandean belt. During Cenozoic times the sedimentary basins were developed under thecontrol of this type of thick skinned structure (Rubiolo, et al., 1997).

A view of regional geological structure, sedimentary Cenozoic deposits and the arc magmatic units allow us to present a schematic evolution of the cenozoic basins. The sedimentary deposits of Pozuelos basin, Tres Cruces basin, Santa Victoria Range and Western Subandean Ranges basin are considered (Fig. 1 and 2).

The Tres Cruces basin presents Cretaceous to Eocene synrift and postrift deposits (Salta Group). They are covered by a Paleogene initial stage of a foreland basin (Casa Grande and Rio Grande Formations) and it ends with an overfilling stage during Lower Miocene (Pisungo Formation) (Boll & Hernandez, 1986). At the Pozuelos basin, the Moreta and Cara-Cara Formations represents typical piggyback deposits (Cladouhos, 1994; Gangui &Götze, 1996; Gangui, 1998). During the Middle Miocene

the orogenic front migrated towards the east elevating the Sierra de Santa Victoria. The Tres Cruces basin, which was formerly a foreland basin is incorporated to the orogenic system and continued its evolution as a piggyback basin. Consequently in the subandean area a new foreland basin was developed starting with an underfilling stage (Tranquitas Formation), followed by a prograding sequence (Terciario Subandino Inferior y Medio) and during the Upper Miocene-Lower Pliocene an overfilling stage is built (Terciario Subandino Superior and Simbolar Formation) (Hernandez et al., 1996). An important crustal Eastern Cordillera during Upper Miocene.

Since Eocene times three compressive stages in the evolution of the orogenic front are recognized, with alternating periods of tectonic calm (Fig. 3). The periods of tectonic activity at the orogenic front are equivalent to the Eocene Inca, Middle Miocene Pehuenche and Upper Pliocene Diaguita orogenic phases. However, there is no evidence of the Upper Miocene Quechua movements at the orogenic front. During Upper Miocene, tectonic activity developed through out-of-sequence thrusts behind the orogenic front. This event produced crustal thickening in the Puna with important volcanics and ignimbritic sequences (Coira & Kay, 1993). Upper Pliocene to Pleistocene became a period of tectonic activity at the orogenic front.

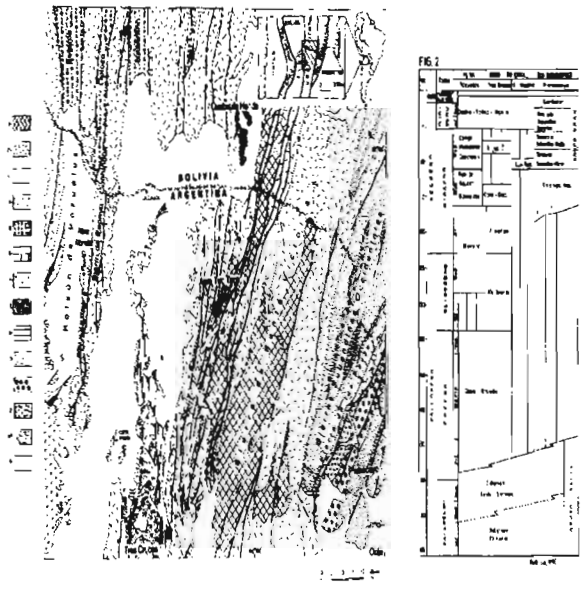

Fig. 1: Geologic map of the Eastern Cordillera between 22° and 23° S and cenozoic basins. 1-Eastern Cordillera Basement: Puncoviscana Formation and Cañaní Granite (Precambrian to Lower Cambrian). 2-Lithologic Units Pre-Salta Group (Upper Cambrian to Jurasic). 3-Salta Group (Cretaceous to Lower Eocene). 4-Casa Grande, Río Grande and Pisungo Formations (Middle Eocene to Lower Oligocene). 5-Moreta and Tupiza Formations (Upper Oligocene to Lower Miocene). 6-Cara Cara

Formation (Middle Miocene). 7-Volcanics and pyroclastics flows (Middle to Upper Miocene). 8-Tuc Tuca and Quebrada Honda Formations (Upper and Middle Miocene). 9-Tranquitas Formation (Middle Miocene). 10-Terciario Subandino Inferior y Medio (Upper Miocene). 11-Terciario Subandino Superior (Upper Miocene to Pliocene). 12-Simbolar Formation (Pliocene to Pleistocene).13-Tafna, Uquía and Casira Formation (Pliocene to Pleistocene) 14-Quaternary deposits

Fig. 2: Chronostratigraphic chart of Eastern Cordillera's Cenozoic Basins between 22° and 23°S.

Fig. 3: Schematic tectosedimentary evolution for cenozoic basins of Eastern Cordillera between 22° and 23°S: A) Upper Eocene to Lower Oligocene: Period of tectonic activity at the orogenic front. B) Upper Oligocene to Lower Miocene: Period of tectonic calm at the orogenic front. C) Middle Miocene: Period of tectonic activity at the orogenic front. D) Upper Miocene to Lower Pliocene: Period of tectonic calm at the orogenic front, but tectonic activity development of out of sequence thrust behind the orogenic front. This produces crustal thickening of the Puna and the Eastern Cordillera and extensive volcanic activity in the Puna. E) Upper Pliocene to Pleistocene: Period of tectonic activity at the orogenic front.

REFERENCES

Boll, A. y Hernandez, R., 1986. Interpretación Estructural del área Tres Cruces (Provincia de Jujuy, Argentina). Boletín de Informaciones Petroleras, 3, N°7.

Cladouhos, T.T., Allmendinger, R.W., Coira, B., Farrar, E., 1994. Late Cenozoic deformation in the Central Andes: Fault kinematics from the northern Puna, northwest Argentina and southern Bolivia. Journal of South American Earth Sciences, 7(2):209-228.

Coira, B.& Kay, S. M., 1993. Magmatismo y levantamiento de la Puna, su relación con cambios en el ángulo de subducción y en el espesor cortical. 12° Congreso Geológico Argentino y 2° Congreso de Exploración de Hidrocarburos, Actas, 3:308-319.

Gangui, A., 1998. Seismic stratigraphy of the Pozuelos Basin, Northern Puna, Argentina. 10° Congreso Latinoamericano de Geologia y 4° Congreso Nacional de Geologia Económica, Actas, 1:12-17.

Gangui, A., Götze, H. J., 1996. The deep structure of the northern Puna, Argentina – Constrains From 2D seismic data and 3D gravity modeling. 13° Congreso Geológico Argentino y 3° Congreso de Exploración de Hidrocarburos, Actas, 2:545-565.

Hernandez, R. M., Reynolds, J., Disalvo, A., 1996. Análisis tectosedimentario y ubicación geocronológica del Grupo Orán en el río Iruya. Boletín de Informaciones Petroleras, Marzo, 1996:80-93.

Rubiolo, D.G., Gallardo, E . Seggiaro, R., Turel, A., Disalvo, A., Coira, B., Ramallo, E., Sandruss, A., Godeas, M., Sanchez, M.C., 1997. Hoja Geológica La Quiaca (2366-II y 2166-IV), escala 1:250.000. Instituto de Geología y Recursos Minerales (IGRM), Servicio Geológico Minero Argentino (SEGEMAR), inédito; Buenos Aires.

APATITE AND ZIRCON FISSION TRACK ANALYSIS OF THE ECUADORIAN SUB-ANDEAN (NAPO) ZONE: A RECORD OF THE ORIENTE GEODYNAMICS SINCE EARLY JURASSIC

Geoffrey RUIZ, Richard SPIKINGS, Wilfried WINKLER, and Diane SEWARD

Geological Institute, ETH-Zenrum, CH-8092 Zürich, Switzerland
(ruiz@erdw.ethz.ch, spikings@erdw.ethz.ch, @erdw.ethz.ch, seward@erdw.ethz.ch)

KEY WORDS: Sub-Andean Zone, Oriente, Ecuador, thermochronology, geodynamics

INTRODUCTION

We present several working hypotheses involving different methodological approaches to reveal the geodynamic development of the Ecuadorian Oriente Foreland Basin. The early Oriente Basin formed during a distensive tectonic regime within the Tethyan spreading system (upper Triassic-lower Jurassic Santiago Fm.), and latter evolved in a retro-arc foreland basin system, associated with a NW oriented subduction (Upper Santiago Fm., Chapiza Fm. and its associated calc-alkaline volcanic Misahualli unit, Romeuf et al., 1997).

The actual northern Oriente Foreland Basin can be divided into two zones based on variations in elevation, structural style and sedimentary thickness: (1) the proximal foreland basin is composed of steeply dipping thrust slices and a series of frontal foothill highs (Napo antiform), which together define the Sub-Andean Zone (SAZ). Six lithologic units ranging in age from early Jurassic to Eocene, the Misahualli volcanic unit, the Abitagua batholith, and the sedimentary Hollin, Napo, Tena and Tiyuyacu Formations are at least contained, (2) the distal Oriente Basin is at a lower elevation, flat lying and essentially undeformed. It is bordered by the Guyana and Amazon Shields to the east. Metamorphic complexes of these shields define the basin basement.

The geodynamic development of these terranes during periods of orogenesis is poorly understood. An alternative approach to analyse and quantify the sedimentological, structural and tectonic

history of the Oriente Basin system is to examine the thermal history across the northern Sub-Andean Zone using apatite and zircon fission track methods. The techniques provide quantification of the thermal history of the regions over the temperature ranges of ≈370-180 (zircon, Yamada et al. 1997) and 110-60°C (apatite).

CONCLUSIONS

Preliminary results from apatite and zircon indicate an early Jurassic depositional age (185 Ma) of the Misahualli volcanics. Thermal modelling on apatite from Misahualli unit beneath the prominent Hollin (Aptian-Albian)-Misahualli unconformity suggests uplift at ≈145-125 Ma, and sedimentary burial at ≈100-90 Ma . These records could be correlated with one of the main Andean tectonic collision event, the Peltetec event (Litherland et al. 1994) and the subsequent cover by the Hollin and Napo Formations, respectively.

The conspicuous unconformities between the lower Jurassic Misahualli volcanics (185 Ma) and the oil-bearing Hollin and Napo Formations (upper Aptian-Campanian, 115-90 Ma (White et al. 1995), according to the apatite fission track modelling results suggest a pre-Maastrichtian development of the foreland basin althought traditionally, the continental Tena Fm. has been used to correlate the onset of retro-arc foreland basin formation in the Maastrichtian (70 Ma). These results together with subsidence history analysis are used to test different foreland basin models, e.g DeCelles & Giles, 1996 and Catenuanu et al., 1997, in order to refine the chronology of the development of the Oriente Foreland Basin during Jurassic and Cretaceous time.

REFERENCES

Catuneanu, O., Beaumont, C., Waschbusch, P. 1997. Interplay of static loads and subduction dynamics in foreland basins: Reciprocal stratigraphies and the "missing" peripheral bulge. Geology, 25, 1087-1090.

DeCelles, P.G., & Giles, K.A., 1996. Foreland Basin Systems. Basin Research, 8, 105-123.

Litherland, M., Aspden, J.A., and Jemielita, R.A., 1994. The metamorphic belts of Ecuador, British Geological Survey, Overseas Memoire, 11, 147 pp.

Romeuf, N., Münch, P., Soler, P., Jaillard, E., Pik, R., Aguirre, L., 1997. Mise en évidence de deux lignées magmatiques dans le volcanisme du Jurassique inférieur de la Zone subandine équatorienne. C.R. Acad. Sci. Paris, t. 324, série II a, 361-368.

White, H.J., Skopec, R.A., Ramirez, F.A., Rodas , J.A., Bonilla, G, 1995. Reservoir characterization of the Hollin and Napo Formations, Western Oriente Basin, Ecuador. In Tankard, A.J., Suárez S, R., Welsink, H.J., Petroleum basins of South america: AAPG Memoir, 62, 573-596.

Yamada, R., Tagami, T., Nishimura, S., and Ito, H., 1996. Annealing kinetics of fission tracks in zircon: an experimental study. Chemical Geology, 122, 249-258.

Supported by Swiss Science Foundation grant no. 21-050844.97.

SEISMIC ACTIVITY IN TUNGURAHUA VOLCANO: CORRELATION BETWEEN TREMOR AND PRECIPITATION RATES

Mario RUIZ (1), Minard HALL, Pablo SAMANIEGO, Andrés RUIZ, Darwin VILLAGÓMEZ

(1) geofisico@accessinter.net

KEY WORDS: Tremor, spectra, precipitation, hydrothermal system

INTRODUCTION

Tungurahua volcano is a young active stratovolcano located in the central zone of the Cordillera Real of Ecuador. The main historic eruptions occurred in 1773, 1886 and 1916-1918. Some of these eruptive events were preceded by earthquakes, underground noises, and small steam columns (Hall & Vera, 1985). Shortly before the 1916 eruption, Martínez (1932) reported prolonged low frequency subterranean noises that were heard in villages around the volcano, sometimes followed by weak oscillatory quakes which often increased in intensity as the volcanic activity progressed.

Tungurahua volcano shows a low level of activity for discrete seismic events. The monthly number of local earthquakes has remained at less than 16 since 1989. The majority of A and B type events are located beneath or very near the edifice at depths between 2 and 12 km. In October 1994 and September 1998, swarms of more than 100 events with magnitudes less than 2.5 were registered. However, it is noticeable that an increment of the b value from 0.62 (σ = 0.06) for the period June 1989-December 1990 to 1.25 (σ = 0.10) for the period June-November 1995. This increment was followed by sudden decrease until September 1998 with a b-value of 0.54 (σ = 0.08). The b-value was computed using a least squares method over 100 event windows overlapped 50%. The behavior of the b value may be related to an increase in the degree of heterogeneity and crack density in the medium under a constant stress field (Mogi, 1967) or to a gradual decrease in stress field intensity with negligible differences in heterogeneity and rigidity of the medium (Gesta & Patané, 1983).

TREMOR ACTIVITY

Beginning in 1993, tremor activity has been frequently detected in Tungurahua volcano. In April 1994, an important increase of tremor activity began with amplitude of 7.1μm/s registered in a seismic station at 3.1 km from the crater on June 10, 1994. High tremor amplitudes remained until September 1994. Tremor activity continues at present although with less amplitudes. Peaks with amplitudes larger than 7μm/s were detected on 10 June 1994, 2 and 8 July 1997, and 21 April and 28 June 1998.

The tremor source was estimated to be 1 to 2 km under the volcano's summit by Ruiz et al (1994), using an analysis of attenuation of seismic signals at 5 different places located along a radial profile over the same lava flow during the high amplitude episode of May 1994. Tremor signals registered at different distances (from 3.1 to 6.8 km to the crater) and elevations (3300 to 1500 m) were used to calculate the reduced displacement (RD), assuming that the tremor source is located beneath the crater. The depths that gave the minimum residual error in the RD calculation were at 1 to 2 km under the volcano's summit and were considered the tremor's source. With this source depth, a maximum RD of 6.7 cm^2 was calculated using the formula of Fehler (1983) for surface waves. In comparison with RD values from other volcanoes, this value is relatively small (McNutt, 1992).

Between May 1994 and July 1996, the daily fundamental frequency (frequency of larger tremor signal as read on analog records) falls in the range of 1.4-2.2 Hz. Spectra of tremor signals registered at MSON station during the period of greatest tremor activity generally shows a monochromatic pattern with a 1.6 Hz band-width, a maximum amplitude at 1.56 Hz, and secondary peaks at 1.99, 1.40, 2.26 and 1.19 Hz. This tremor also shows a monochromatic pattern in other seismic stations, however this is less clear at stations located farther from the crater where the tremor amplitude is diminishing.

CORRELATION BETWEEN TREMOR AND PRECIPITATION

A temporal correlation is observed between the volcanic tremor and both the seasonal as well as the short period variation in precipitation. Comparing the accumulated precipitation over biweekly periods and the energy release of the tremor (Figure 1), a strong positive correlation is found for the periods of March 1994 - September 1995 and August 1996 - August 1997. Low correlation is found between October 1995 and July 1996. There is a peak in tremor energy released for the first two weeks of July 1997, which is coincident with a peak in the precipitation rate of 212 mm for those fifteen days, the highest rate in the six years analyzed.

Banks et al. (1990) believes that sufficient number of correlations exists between precipitation, ash eruption, deformation, and periods of seismic activity to suggest that rainfall should

be considered in forecasting activity at volcanoes that are in states of unrest and thus could be influenced by the relative small stresses associated with precipitation. Thus, eruptions could be influenced by high loading rate or perhaps a threshold peak of loading. Following the November 12, 1985 eruption of Nevado del Ruiz, the energy released by low-frequency events generally followed fluctuations in precipitation with a 30- to 45-day phase shift (Banks et al., 1990). Other factors that may influence these observations could be the widespread generation of steam as well as the associated vibrations due to flashing.

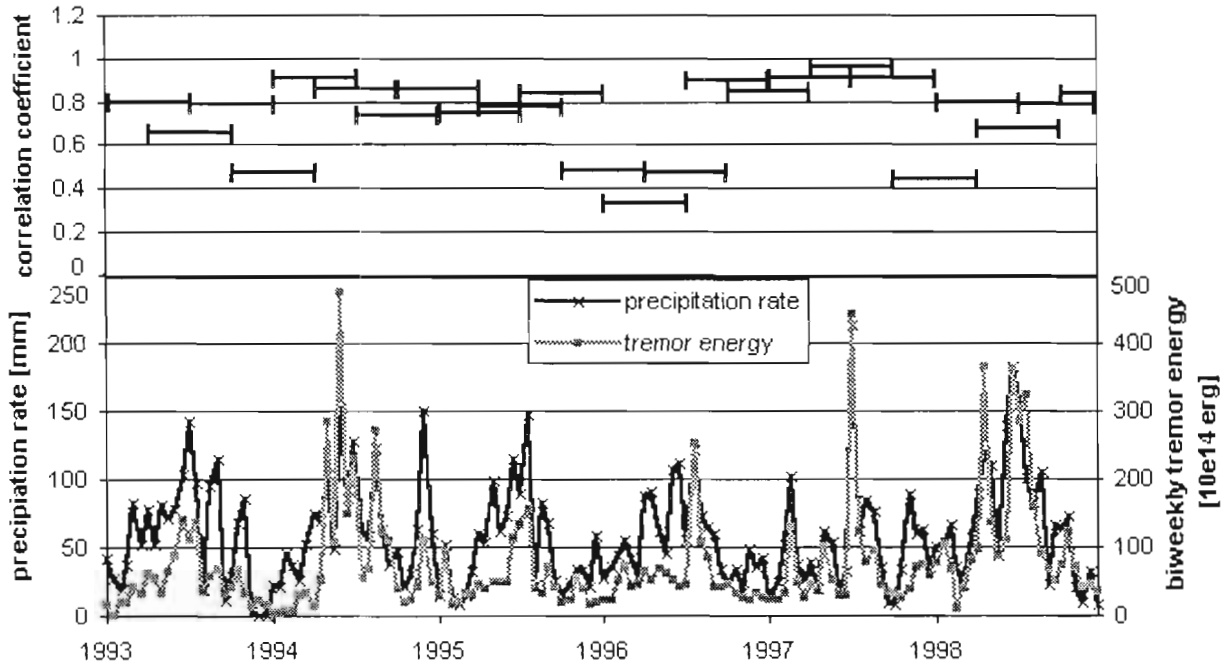

Figure 1. Correlation between biweekly accumulated precipitation (grayed line) on the north flank of Tungurahua and tremor energy release (black line) between 1993 - 1998. The correspondent correlation factors were computed using 6 months windows with an overlap of 50% are shown in the upper part of the figure.

CONCLUSIONS

Until we carry out detailed studies of stress field variations in Tungurahua, we conclude that occurrence of seismic swarms and the increase in the *b* value may suggest that a magmatic component may be responsible for the observed tremor. However, the correlation between precipitation and released tremor energy, the shallow location of the tremor source, and the low RD values of the tremor are more in agreement with an active hydrothermal system. The existence of numerous hot springs at Tungurahua supports this interpretation.

REFERENCES

BANKS N., C. CARVAJAL, H. MORA, and E. TRYGGVASON (1990): Deformation Monitoring at Nevado del Ruiz , Colombia - October 1985-March 1988, *J. Volcanol. Geotherm. Res.*, **41**, 269-296.

FEHLER M. (1983): Observations of Volcanic Tremor at Mt. St. Helens volcano, *J. Geophys. Res.*, **88**, 3476-3484.

GESTA S. and G. PATANE (1983): Variations of b Value Before the Etnean Eruption of March 1981, *Pageoph*, **121**, No.- 2, pp. 79-87.

HALL M. and R. VERA (1985): Actividad volcánica del volcán Tungurahua: sus peligros y riesgos volcánicos. Monografía de Geología N.- 4, *Revista Politécnica*, **XI**, 91-144.

MARTINEZ N. (1932): Las grandes erupciones del Tungurahua, In *Pioneros y Precursores del Andinismo Ecuatoriano*, Tomo I, Colección Tierra Incógnita N.- 11, Ed. Abya-Yala, Ecuador, 281 p.

McNUTT S. (1992): Volcanic Tremor, Encyclopedia of the Earth System Science, Academic Press, Inc., USA, 417-425.

MOGI K. (1967): Earthquakes and Fractures, *Tectonophysics*, **5**, 35-55.

RUIZ M., D. VIRACUCHA, H. YEPES, J. AGUILAR, M. Hall, P. MOTHES, and J.L. CHATELAIN (1994): Seismic Activity of Tungurahua Volcano: Analysis of Long Sustained/ Tremor. *in Abs. I Regional Seismological Assembly in South America*, Brasilia, Brazil, 114.

SHEAR WAVE SPLITTING IN THE REGION OF THE CHILE MARGIN TRIPLE JUNCTION

Raymond M. RUSSO (1) and Ruth E. MURDIE (2)

(1) Department of Geological Sciences, Northwestern University, Evanston IL 60208, USA.
ray@earth.nwu.edu
(2) Department of Earth Sciences, Keele University, Staffordshire, ST5 5BG, UK.
r.e.murdie@keele.ac.uk

KEY WORDS: shear wave splitting, anisotropy, mantle flow, slab window,

INTRODUCTION

Shear wave splitting results when shear waves pass through anisotropic media. Initially linearly polarised shear waves are split into orthogonally polarised fast and slow waves separated by a time delay (e.g., Silver and Chan, 1991). Splitting principally occurs in the upper mantle where lattice preferred orientation of olivine crystals in aggregates is the primary source of anisotropy (Nicolas and Christensen, 1987). The fast polarisation direction is aligned with the principle axis of extensional finite strain of the olivine. The delay time is dependent upon the length of the wave travel path through the anisotropic medium and on the strength of the fabric within it. Measurements of shear wave splitting have been used to deduce the degree and orientation of upper mantle anisotropy, and hence the direction of upper mantle flow beneath the receiver. Here, we examine seismic data gathered at sites in southern Chile where the Chile Rise subducts beneath South America. Shear wave splitting observations of mantle flow here are of potentially great interest in that they may uniquely delineate asthenosphere-lithosphere interaction in a complex and interesting tectonic environment.

The Chile Margin Triple Junction at 46.5 S, 75.5 W, is the best documented extant example of subduction of an active mid ocean ridge (e.g., Cande et al., 1987). Studies of ridge subduction invoke the concept of a 'slab window' (e.g., Dickinson and Snyder, 1979; Ramos and Kay, 1992; Thorkelson and Taylor, 1994; Gorring et al., 1997). Implicit in this idea is the assumption that spreading between the two sides of the subducted ridge continues after subduction, but that no new lithosphere is formed after subduction, leading to a progressively widening, mantle-filled gap between the two edges of the former ridge. Obviously, formation of a slab window of this type requires a highly mobile fluid mantle to fill the increasing volume of the window.

Shear-Wave Splitting Measurements

We used two seismic phases (SKS and ScS/PcS) to deduce the anisotropy of the mantle in the region of the Chile Margin Triple Junction. We used the method of Silver and Chan (1991) to determine splitting parameters, phi (fast polarisation azimuth) and delta t (the delay time). Several of the measurements were 'nulls', indicating that there is either no splitting or that the fast or slow polarisation azimuths are parallel or perpendicular to the phase polarization.

At station MURT, three ScS phi measurements have polarization azimuths in the northwest quadrant. Two of the measurements are very similar (phi's of 353+-5 and 350\+-15, delta t's of 1.4+-0.1 and 0.9+-0.8), but the third is quite different (phi = 306, delta t = 0.6+-0.8). All three measurements were made on ScS phases, which means that complications from source-side splitting are a possibility. However, a fourth measurement, a clear observation of splitting of an SKS phase has a phi direction of 297+-4 and a delta t of 3.3+-0.4 s. The consistency of the two groups of phi directions obtained for these measurements is reasonably good evidence that the measurements are accurate in fast angle estimation. Two other readings at MURT are nulls from an SKS phase and a PcS phase. Neither phase carries source-side splitting information and both have potential phi directions close to N-S, similar, within estimated errors, to the slightly west of north phi directions of the events mentioned above.

For station NORT, closer to the coast than station MURT, we have a single measurement, an SKKS phase from the Kurile Islands. The phi is 348+-3, and delta t is 1.3+-0.1, similar to one group of the consistent measurements and the nulls at MURT. The other measurement at NORT is a null with possible phi angles to the northwest and northeast. This null derives from an ScS phase, and given the consistency of the null and the measurement phi directions, it is unlikely that this ScS phase carries a significant source-side signal.

Station ORIE lies about 30 km south of NORT. We made two measurements on ScS phases recorded at this station. The first event gives a phi of 23+-13 and a delay time of 1.3+-0.1 s, and the second event is a null with possible fast directions trending N-S. The measurement and the null are reasonably consistent in indicating a N-S phi azimuth for this station.

Discussion

Of the six measurements we made, three have phi azimuths just west of north, and two to the northwest. The null measurements all have one of two possible splitting fast axes trending N-S, generally consistent with co-located observed measurements. Our data set is limited in both number of events and in recording frequency of the seismometers, and therefore this splitting data set can only be regarded as very preliminary. Nevertheless, the overall consistency of the measurements is encouraging: most of the fast axis measurements lie parallel to the trend of the Chile Rise, and the nulls are either parallel or perpendicular to the orientation of the Chile-Peru trench. The second, north western phi direction we obtain at station MURT probably results from a superposition of differently deformed mantle beneath that station.

Although the data set is small, there does appear to be a consistent fast polarisation direction sub-parallel to the trend of the ridge segments of the Chile Rise, and to the subduction trench. This result is counter to expectations based on assumed two-dimensional flow fields at spreading ridges, and also does not fit models of mantle deformation in a decoupling asthenosphere, which should yield fast anisotropy axes parallel to absolute plate motion (Russo and Okal, 1998). Both these processes, assuming splitting results primarily from development of moderate lineation fabrics of upper mantle olivine, should result in generally east-west mantle flow and phi directions. The slab window could act as a pathway for sub-Nazca slab mantle to flow eastward. It is possible that the NW-SE trending fast polarisation directions we observed at station MURT indicate mantle flow towards the southeast, potentially through the well-developed slab window beneath that station.

The ridge-axis parallel fast polarisation directions could be considered odd if flow in the vicinity of the ridge is assumed to be strictly two-dimensional. Normally, fast axes of anisotropy should trend in the spreading direction at a mid ocean ridge. However, studies of ophiolites commonly show evidence for along-axis asthenospheric flow (Nicolas and Boudier, 1995), and such flow has been inferred from seismic studies of mid ocean ridges (Blackman et al., 1993). Alternatively, asthenospheric upwelling at the site of the subducted mid ocean ridge may continue after subduction, although new crust is no longer formed. Thus, mantle flow in the vicinity of the ridge could be predominantly two-dimensional upwelling

overturning to flow perpendicular to the ridge, and the splitting we see could be due to magma-filled dikes or cracks trending along the ridge segments (Gao et al., 1997).

CONCLUSIONS

Although our data are preliminary, we have found two consistent fast polarization directions of splitting in the region where the Chile Ridge subducts beneath South America. These measurements show that there is anisotropy within the mantle in the region of the Chile Triple Junction. Near the coast, the dominant orientation of the splitting appears to lie parallel to the subducted portions of the Chile Rise. This splitting fast-axis direction may reflect either three-dimensional flow, including a significant along-axis component, at the subducted spreading ridge; or the effects of ridge-aligned pockets of melt. Inland, we find two splitting fast-axis directions, one parallel to the subducted Chile Rise ridge segments, and a second trending NW-SE. We infer that upper mantle deformation in the vicinity of a well developed slab window is complicated and may involve two superposed directions of upper mantle deformation.

REFERENCES

Blackman, D. K., Orcutt, J. A., Forsyth, D. W., and Kendall, J.-M., 1993. Seismic anisotropy in the mantle beneath an oceanic spreading centre, Nature, 374, 824-827.

Cande, S. C., Leslie, S. D., Parra, J. C., and Hobart, M., 1987. Interaction between the Chile Ridge and the Chile Trench: Geophysical and geothermal evidence, J. Geophys. Res., 92, 495-520.

Dickinson, W. R., and Snyder, W. S., 1978. Geometry of subducted slabs related to San Andreas transform, J. Geol., 87, 609-627.

Gao, S., Davis, P. M., Liu, H., Slack, P. D., and Rigor, A. W., 1997. SKS splitting beneath continental rift zones, J. Geophys. Res., 102, 22,781-22,797.

Gorring, M. L., Kay, S. M., Zeitler, P. K., Ramos, V. A., Rubiolo, D., Fernandez, M. I., Panza, J. L., 1997. A slab window origin for Neogene Patagonian plateau lavas (46.50 to 49.500S), Tectonics, 16, 1-17.

Nicolas, A., and Boudier, F., 1995. Mapping oceanic ridge segments in Oman ophiolite, J. Geophys. Res., 100, 6179-6197.

Nicolas, A., and Christensen, N. I., 1987. Formation of anisotropy in upper mantle peridotites: A review. In: Composition, Structure and Dynamics of the Lithosphere-Asthenosphere System, Geodynam. Ser. Vol. 16 (eds. Fuchs, K., and Froidevaux, C.) (Am. Geophys. Union, Washington, D.C.) pp. 111-123.

Ramos, V. A., and Kay, S. M., 1992. Southern Patagonian plateau basalts and deformation: backarc testimony of ridge collisions, Tectonophys., 18, 261-282.

Russo, R. M., and Okal, E. A., 1998. Shear wave splitting and upper mantle deformation in French Polynesia: Evidence for small-scale heterogeneity related to the Society hotspot, J. Geophys. Res., 103, 15,089-15,107.

Silver, P. G., and Chan, W. W., 1991. Shear wave splitting and subcontinental mantle deformation, J. Geophys. Res., 96, 16,429-16,454.

Thorkelson, D. J., and Taylor, R. P., 1989. Cordilleran slab windows, Geology, 17, 833-836.

GEOCHEMISTRY OF CAYAMBE AND MOJANDA-FUYA FUYA VOLCANIC COMPLEXES: EVIDENCES FOR SLAB MELTS - MANTLE WEDGE INTERACTION?

P. SAMANIEGO[1, 2], H. MARTIN[2], C. ROBIN[3], M. MONZIER[4], J-Ph. EISSEN[5], M.L. HALL[1]

(1) Instituto Geofisico, Escuela Politecnica Nacional (IG-EPN), A.P. 17-01-2759, Quito, Ecuador. (samanieg@opgc.univ-bpclermont.fr; pablosam@hotmail.com).
(2) CNRS, UMR 6524, Université Blaise Pascal, 5 rue Kessler, 63038, Clermont-Ferrand cedex, France. (martin@opgc.univ-bpclermont.fr).
(3) IRD, Université Blaise Pascal, 5 rue Kessler, 63038, Clermont-Ferrand cedex, France. (robin@opgc.univ-bpclermont.fr).
(4) Institut de Recherche pour le Développement (IRD), A.P. 17-12-857, Quito, Ecuador. (michmari@orstom.org.ec).
(5) IRD, UMR 6538, Université de Bretagne Occidentale, B.P. 809, 29285, Brest, France. (eissen@ifremer.fr)

KEY WORDS: Andean NVZ, Ecuador, adakites, mantle wedge processes.

INTRODUCTION

The Northern Andean volcanic zone results from the subduction of the Miocene (12 - 22 Ma) Nazca plate beneath the South-American continental lithosphere. The Quaternary Ecuadorian Volcanic Arc (about 50 edifices) extends from latitude 1°N to 2°S. The main part of this arc has been developed facing the Carnegie Ridge which represents the trace of the Galapagos hotspot across the Nazca Plate. This ridge has been subducting for 6-8 Ma to a position beneath the Andes 300-400 km from the trench (Gutscher *et al.*, accepted). Volcanoes from this arc are distributed following four alignments lying on the Western Cordillera, the Interandean Valley, the Eastern Cordillera and the Back-arc Region (Fig. 1). Recent regional and detailed volcanological works carried out by the Geophysical Institute of the National Polytechnic School at Quito and the IRD show that several large edifices, such as Cayambe and Mojanda-Fuya Fuya, present distinct magmatic series, either with classic calc-alkaline characteristics or with a "adakite-like" feature. The purpose of this paper is to present and discuss these characteristics in order to constrain and understand the petrogenesis process of the Ecuadorian volcanic rocks.

GEOLOGICAL SUMMARY OF THE VOLCANOES

The Mojanda-Fuya Fuya volcanic complex is located in the Interandean Valley, 50 km NNE of Quito. After Robin et al. (1998), the complex consists of an eastern edifice, the Mojanda stratovolcano (MOJ) and a more recent edifice, the Fuya Fuya (FF), built over the western flank of this stratovolcano. Mojanda is formed by lava flows and pyroclastic flow deposits whose composition varies from mafic andesite to dacite (55-67% SiO_2, recalculated as anhydrous). The volcanic units from Fuya Fuya are basal andesite lava flows and subsequent dacitic lava flows, domes and related pyroclastic flow deposits emplaced after a large sector collapse. The whole magmatic FF series is restricted to 61-68% SiO_2. The last domes of this complex are late Pleistocene to Holocene in age.

The Cayambe volcanic complex is located in the Northern Cordillera Real, 30 km E of Mojanda-Fuya Fuya. It mainly consists of a western lavic edifice, the Old Cayambe (VCAY), consisting of former basic andesites to younger dacites (56-68 % SiO_2). Barberi *et al.* (1988) report an K/Ar age of 0.25 ± 0.05 Ma for these dacites which end the volcanic activity of this edifice. The Nevado Cayambe (NCAY) is built upon the eastern remnants of the Old Cayambe structure, probably after a caldera collapse. Nevado Cayambe consists of basal andesitic lava flows (58-63 % SiO_2) overlain by a still active summit dacitic dome complex (63-68 % SiO2) which was the source of several recent pyroclastic flows (Samaniego et al., 1998). Lastly, a small parasitic cone, the " Cono de La Virgen " (CLV) was emplaced on the east flank of NCAY and emitted Holocene andesitic lava flows (59-60 % SiO_2).

MAGMATIC SUITES

As a whole, compared to the Mojanda-Fuya Fuya rocks, the Cayambe volcanics are alkali, LILE, HFSE and LREE enriched (Fig. 2). Such eastward enrichment is classic in the Andean subduction context and has been already noted for Ecuador (Barberi *et al.*, 1988; Barragan *et al.*, 1998).

However, based on major and trace element analyses, two distinct magmatic series can be distinguished in both volcanoes. Whereas the VCAY and MOJ volcanic rocks define a classical calc-alkaline trend, rocks from the young NCAY and FF edifices belong to magmatic suites with distinct geochemical characteristics. They are characterised by the lack of mafic andesites, as well as a HREE and Y depletion with related high La/Yb and Sr/Y ratios (Fig. 2 and 3). In addition, CLV's rocks are high-K andesites, strongly enriched in LREE, LILE and relatively MgO- and HFSE-rich.

In addition, the whole suites of both volcanic complexes show a significant MgO, Ni and Cr enrichment compared to "normal" andesitic suites. Their Sr and Nd isotopic ratios are similar and close to the MORB values, suggesting no contamination by the highly radiogenic upper continental crust.

On the other hand, the two series are mineralogically different: in the NCAY and FF suites, amphibole is omnipresent, whereas in VCAY and MOJ it is in subordinate amounts and only in the more evolved laves (>63 % SiO_2).

GEOCHEMICAL MODELLING AND DISCUSSION

Modelling based on both major and trace element behaviour has been performed on these suites. This procedure shows that the fractional crystallisation in the upper crust can account for the geochemical diversity of the volcanics (line 1a and 1b, Fig. 3). For both low-Y (or adakite-like) NCAY and FF series, the fractionation of amphibole, plagioclase, clinopyroxene and magnetite explains the whole compositional variations. In the same way, the fractionation of plagioclase, ortho- and clino-pyroxene and magnetite accounts for some characteristics of the VCAY and MOJ suites. In addition, geochemical modelling shows that it is impossible to relate low-Y and classic calc alkaline rocks by fractional crystallisation.

In order to understand the HREE and Y depletion of the subduction-related volcanic rocks, two models have been proposed: (1) partial melting of the basaltic oceanic crust leaving an eclogitic residue (the adakitic model); or (2) assimilation of lower crustal silica-rich melts. In fact, geochemical modelling shows that partial melting of an enriched MORB source leaving an eclogitic residue (cpx + gt +/- hb) may explain low HREE and Y contents (line 2a and 2b, Fig3). On the other hand, the volcanic arc is located too far from the trench (250-300 km), the slab is apparently too deep under the volcanoes (> 100 km) and the arc is built over a thick continental crust. This argues against the adakitic model and suggest a explanation by lower crustal assimilation. Thus, the two hypotheses (slab melting or lower crustal assimilation) are currently debated.

The anomalous high MgO, Ni and Cr concentrations; as well as the anomalous geochemical characteristics of the CLV volcanics (strongly incompatible elements enriched and weakly enriched in MgO) may be explained by interaction between slab-derived silica-rich partial melts and the mantle wedge. This model for magnesian andesite generation was proposed by Kay *et al.* (1993) and Yogodzinsky *et al.* (1995). The enrichment in transition elements as well as "magmatic" metasomatism of the mantle wedge could result from the mixing between hypothetical slab-derived melts (aprox. 5-15 % partial melting) and the depleted mantle wedge (line 4, Fig. 3). Therefore, a different degree of mixing between a "low-Y end-member" and a "mantellic end-member" (line 5, Fig. 3) could account for the parental magmas of each series. Such a model has been proposed by Yogodzinski *et al.* (1998) to explain the genesis of Aleutian high-magnesian andesites.

Whatever the correct hypothesis, the genesis of these magmas implies an anomalous thermal regime either in the subduction plane or in the mantle wedge and lower crust. The high density of

volcanoes in Ecuador, the large width of the volcanic arc (120-150 km) and the intermediate seismicity gap (70-220 km) along the Benioff plane that caracterizes the Ecuadorian subduction system (Gutscher *et al.*, accepted) argue for the presence of an anomalous high thermal regime, and may be due to the subduction of the Carnegie Ridge. This ridge is younger and thus hotter than the Nazca lithosphere, and its subduction could be responsible for additional stress heating in the subduction zone.

CONCLUSION

On the basis of available data, the low-Y and HREE contents of the NCAY and FF suite, show that there is a intervention of silica-rich basaltic melts via slab partial melting or infra-crustal assimilation. On the other hand, the enrichment in MgO, Ni and Cr for all rocks and the peculiar chemical compositions of CLV volcanics are evidence for a small degree of slab partial melting and an intense interaction between slab-derived silica-rich melts and the mantle wedge. In addition, the slab melting hypothesis is supported by recent geophysical data corroborating the subduction of a hot and young oceanic slab. Detailed petrological studies in those two volcanic complexes are in progress, in order to decide between the two hypotheses.

REFERENCES

Barberi F., Coltelli M., Ferrara G., Innocenti F., Navarro J.M., et Santacroce R. (1988) Plio-Quaternary volcanism in Ecuador; *Geol. Mag.*, 125,1, pp. 1-14.

Barragan R., Geist D., Hall M.L., Larson P. and Kurz M. (1998) Subduction controls on the compositions of the lavas from Ecuadorian Andes. *Earth Planet. Sci. Lett.* 154, 153-166.

Gutscher M.A., Malavielle J., Lallemand S. and Collot J.Y. (accepted) seismotectonics of the North Andean margin: Impact of the Carnegie Ridge collision. *Earth Planet. Sci. Lett...*

Kay M.S., Ramos V.A. and Marquez M (1993) Evidence in Cerro Pampa volcanic rocks for slab-melting prior to ridge-trench collision in South America. *J. Geol.*, 101, 703-714.

Samaniego P., Monzier M., Robin C. and Hall M.L. (1998) Late Holocene eruptive activity at Nevado Cayambe volcano, Ecuador. *Bull. Volcanol.* 59:451-459.

Robin C., Hall M.L., Jimenez M., Monzier M. and Escobar P. (1998) Mojanda Volcanic Complex (Ecuador): development of two adjacent contemporaneous volcanoes with contrasting eruptive styles and magmatic suites. *J. South Am. Earth. Sci.* Vol. 10; No. 5-6, 345-359.

Yogodzinsky G.M., Kay R.W., Volynets O.N., Koloskov A.V. and Kay S.M. (1995) magnesian andesite in the western Aleutian Komandorsky region: Implications for slab melting and processes in the mantle wedge. *Geol. Soc. Am. Bull.*; vol. 107; No. 5; 505-519.

Yogodzinsky G.M. and Kelemen P.B. (1998) Salb melting in the aleutians / implications of an ion probe study of clinopyroxene in primitive adakite and basalt. *Earth Planet. Sci. Lett.* 158, 53-65.

TECTONIC AND GRAVITATIONAL STRAIN FLUCTUATIONS AND EARTHQUAKES IN NORTHERN CHILE

Karl Heinz SCHÄFER(1)

(1) Karl Heinz Schäfer, Abt. Geologie, Universität Bayreuth, D-95440 Bayreuth, E-mail: khschafer @ uni bayreuth.de

KEY WORDS: Strainmeters, tectonic stress, earth-tides, strain fluctuations, Chile

ABSTRACT

Five strainmeters measured with high acuracy (10^{-10} m/m) since 1988 between Iquique, I. Region and Ovalle, IV.Region (1150 km N-S-distance) horizontal rock strain in three directions (N-S, NE-SW, E-W). Four sites are located in the coastal cordillera (Iquique, Copiapo, La Serena, Ovalle) and two sites are in the western high cordillera (magmatic arc), in Contacto (W of Vicuña) and in Queltehues (SE of Santiago). Tectonic and earth-tide strain has been recorded in different stratigraphic, petrologic and structural rock bodies.

In *Iquique (MacIver)* largest horizontal srain of all strainmeter sites has been measured from April 1990 to October 1993. The E-W wire length (5 m) of the strainmeter decreased by - 49,2 µm/m, the NE-SW-wire (5m) shortened by -24,3 µm/m and in N-S contraction was -2,4 µm/m (fig. 1).

In *Copiapo (UDA)* strain was recorded from Sept. 93 to Sept 96 revealing extension of 0,6 µm/m in the E-W-direction, compression of -0,6 µm/m in the NE-SW-direction and of -0,4 µm/m in N-S.

300 km south of Copiapo a strainmeter recorded in *La Serena (Brillador)* from April 91 to March 1993 extensional strain (0,75 µm/m) in the E-W-direction and 0,82 µm/m in the NE-SW-direction, while in the N-S-direction compressive strain was -0,53 µm/m.

In the mine of *Contacto* a strainmeter records since 1988 horizontal strain along 10m N-S-, NE-SW- and E-W-directions. From initial recordings in Feb. 1988 to Sept. 1996 all three horizontal distances exhibit continuously increasing compressive strain. The maximum horizontal strain (-17,2 µm/m), followed by medium horizontal strain in the NE-SW-direction (-12,1 µm/m). In the N-S-direction minor compressive strain (-0,2 µm/m) or no strain was measured. Since 1991 horizontal N-S-strain increased to -3,0 µm/m.

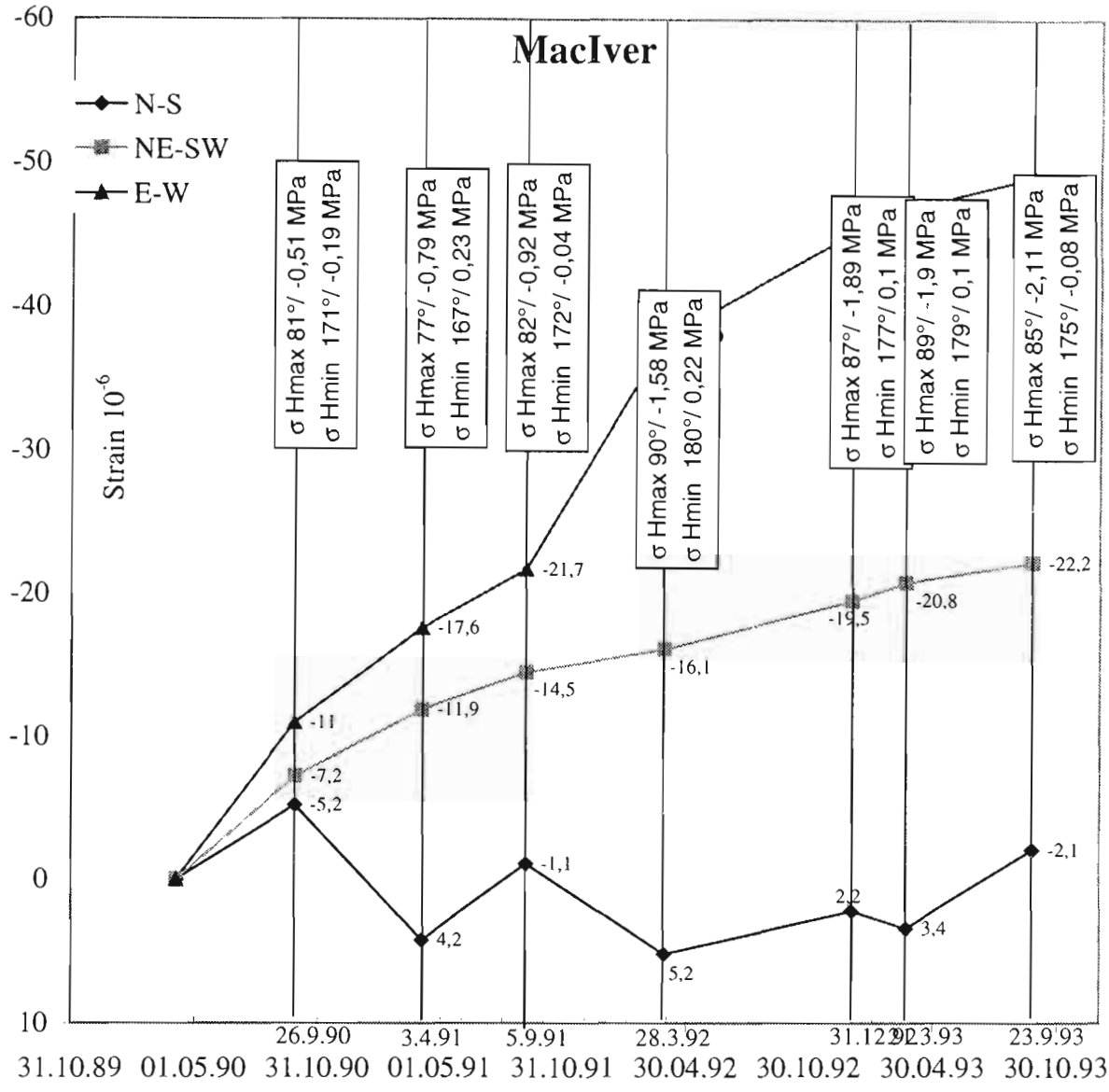

Fig. 1 In Iquique (mine MacIver) largest horizontal strain of all strainmeter sites was recorded to be compressive in

all directions , -49,2 µm/m in E-W, -24,3 µm/m in NE-SW, and -2,4 µm/m in N-S.

On 10.04.98 horizontal in situ stress was determined in the mine of Contacto. SHmax (in situ) revealed compressive stress of 61,7 Mpa in N 60° E, while SHmin (in situ) showed tensile stress of -8,1 Mpa in E 60 ° S. Since Feb. 1988 horizontal fluctuating compressive stress (SHmax fluct) of 2,9 Mpa in N 82° E and fluctuating tensile stress of 0,4 Mpa in E 82 ° S is superimposed on the horizontal in situ stresses.

In *Ovalle* (mine *Cocinera*) a strainmeter of 10m-extensions recorded from Feb. 1988 to March 1997 in the N-S-, NE-SW- and E-W-directions. Until May 1995 horizontal N-S-strain was tensile (1 µm/m), while NE-SW-strain was compressive (-25,5 µm/m) until April 93 and E-W horizontal strain was compressive (-29,8 µm/m) until

March 1997. Maximum horizontal compressive strain (EHmax fluct) changed from E-W- to NE-SW-direction between June 88 and March 91 at Cocinera and between Dec. 92 and Sept. 96 at Contacto.
In the lab tunnel *Queltehues* of the University of Chile a 5m-strainmeter was installed from August 1990 to Sept. 1991 recording horizontal E-W-strain fluctuation that did not exceed 0,1 µm/m. No tectonic horizontal strain was measured in the NE-SW- and N-S-directions. All three directions revealed earth-tide strain achieving maximum values of $1,5 \times 10^{-7}$ m /m in the E-W-direction corresponding to a vertical earth-tide movement of 1,50 m.

The semidiurnal main moontide (M_2) in addition to the semidiurnal main suntide (S_2) have generated maximum horizontal earth-tides of $1,2 \times 10^{-7}$ m/m in Contacto and in Cocinera in the horizontal directions with the respective largest tectonic compressive strain (E-W or NE-SW).

Strain measurements in Cocinera and Contacto revealed strain fluctuations from March to June 1988 and in November 1991 that initiated in both mines synchronously . In Cocinera and in Contacto, being 85 km apart, compressive strain decreased in the E-W- and in the NE-SW-directions synchronously and increased simultaneously initiating eventually local earthquakes (M 3,8 to M 5,2). The epicenters of those earthquakes cluster around Cocinera and Contacto.

The rhythmic sequence: stalling stress - earthquake - stress increase is also recorded with the strainmeters in Copiapo (UDA) and in Iquique (MacIver).

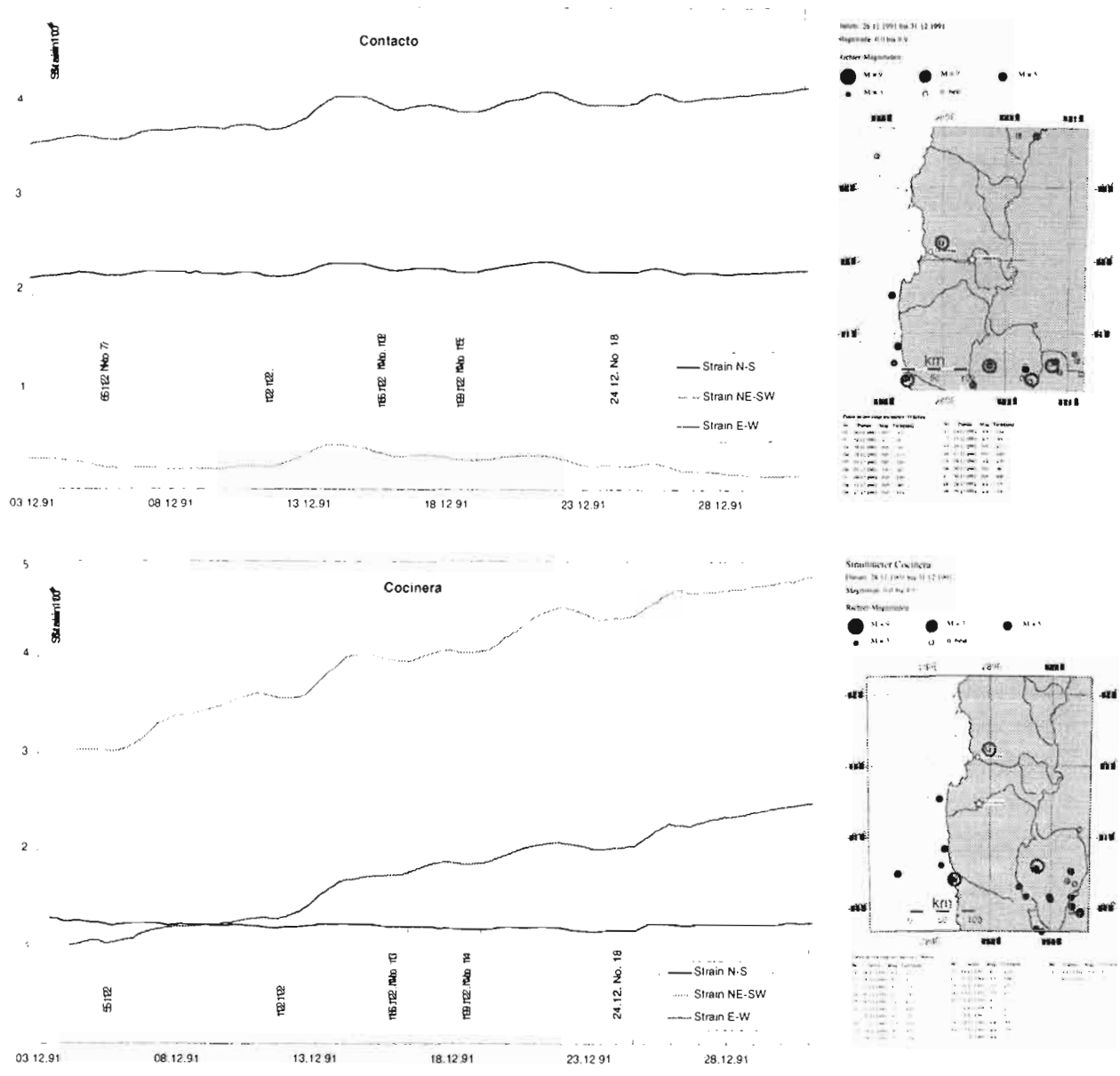

Fig. 2 In Cocinera and in Contacto, being 85 km apart, horizontal strain fluctuated in all directions synchronously

revealing the occurrence of local earthquakes that cluster around the strainmeter sites

There is evidence of the rhythmic sequence: stalling stress - earthquake - stress increase.

REFERENCE

Schäfer, K.H. & Dannapfel, M. (1994): State of In Situ Stress in Northern Chile and in Northwestern Argentina.- In: Reutter, K.-J., Scheuber, E., & Wigger, P.J. (eds): Tectonics of the Southern Central Andes: 103-110, Berlin (Springer).

RECENT CRUSTAL TILT BETWEEN THE SALAR DE ATACAMA AND THE VOLCANO LASCAR IN NORTHERN CHILE.

Karl Heinz SCHÄFER

Karl Heinz Schäfer, Abt. Geologie, Universität Bayreuth, D-95440 Bayreuth.
E-mail: khschafer @ uni-bayreuth.de

KEY WORDS: Tilt, Salar de Atacama, Lascar, Chile

Tilt is measured in semiannual intervals since 1993 between the Salar de Atacama (2310 m asl) and the volcano Lascar (5641 m asl) located 37 km to the east. The Salar de Atacama is the largest of six basins within the Preandean depression bordered to the west by the Precordillera and to the east by the magmatic arc.
The Preandean depression and the magmatic arc are underlain by a high conductivity zone and a seismic low velocity zone at crustal depth of 10 to 30 km. The load of sedimentary and volcanic deposits on the crust results in crustal subsidence. Since the Oligocene continental sediments with evaporites more than 3000 m thick have been deposited in the Salar de Atacama.

From January 1993 to April 1994 nine tiltmeters have been installed in one-meter-deep boreholes between Tumbre and the intersection of roads 23/B-355. Crustal tilt, created by the active Lascar to the east of the tiltmeters and induced to the west by the subsiding Salar de Atacama, should be determined. The boreholes are in Pliocene ignimbrites that dip 2° W between Tumbre and new Talabre and dip 5° W between new Talabre and the Salar de Atacama. Seasonally and daily temperature changes cause rock stresses that have been measured and logged during 18 months. No earthtide tilt could be recorded.
After the installation of the tiltmeters in January 1993 and after the first tilt measurements in March 1993 occurred the largest historical eruption of Lascar from 18-20 April 1993. The total volume of erupted material, excluding material injected into the stratosphere, was estimated to be 0.1 km^3. 90% of it was proximal air fall.

The tiltmeters at Tumbre and at ancient Talabre (fig. 1) recorded during one year after the eruption of Lascar (from 04/93 to 04/94) a continuous subsidence to the southeast. This is suggested to be due to magma deficit within the magma chamber during and after the eruption and the consequent collapse of the volcanic edifice and ist surrounding area. From ancient Talabre to the eastern margin of the Salar de Atacama depression tiltmeters record permanent subsidence to the west and southwest since 1993 (fig.2, fig.3).

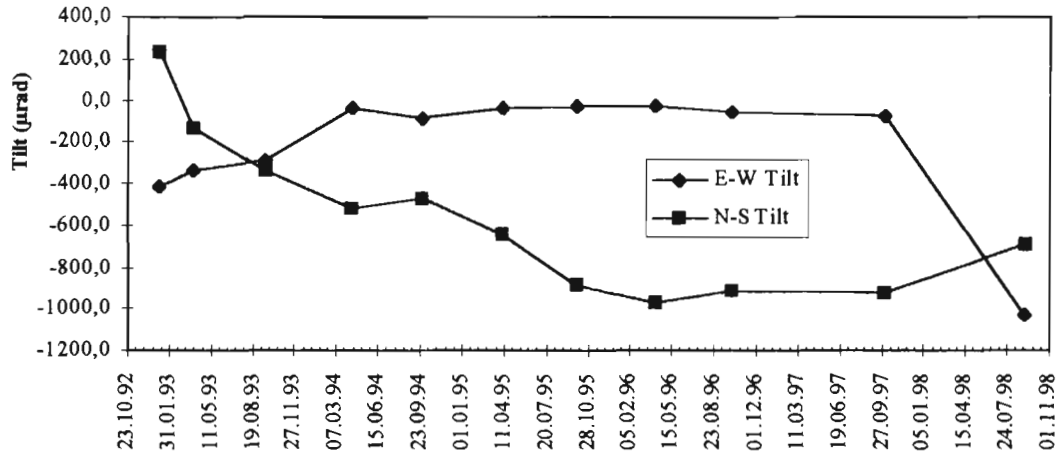

Fig.1 From 09.01.93 to 13.04.94 tilt data of Tumbre and ancient Talabre (tiltmeter No. 16) reveal prominent subsidence to the southeast due to magma deficit within Lascar's magma chamber during and after the eruption and the consquent collapse of the volcanic edifice and ist surrounding area. Most of the recorded period is characterized by subsidence to the southeast that is interupted shortly by minor subsidence to the northwest.

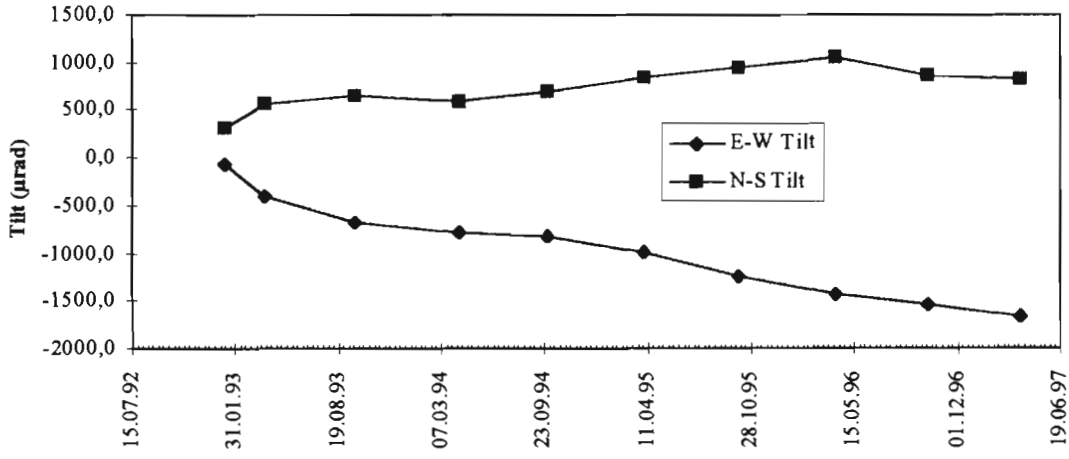

Fig.2 During the entire recording period of more than four years at the new Talabre site (tiltmeter No. 18) there is a permanent strong tilt revealing subsidence to the westnorthwest.

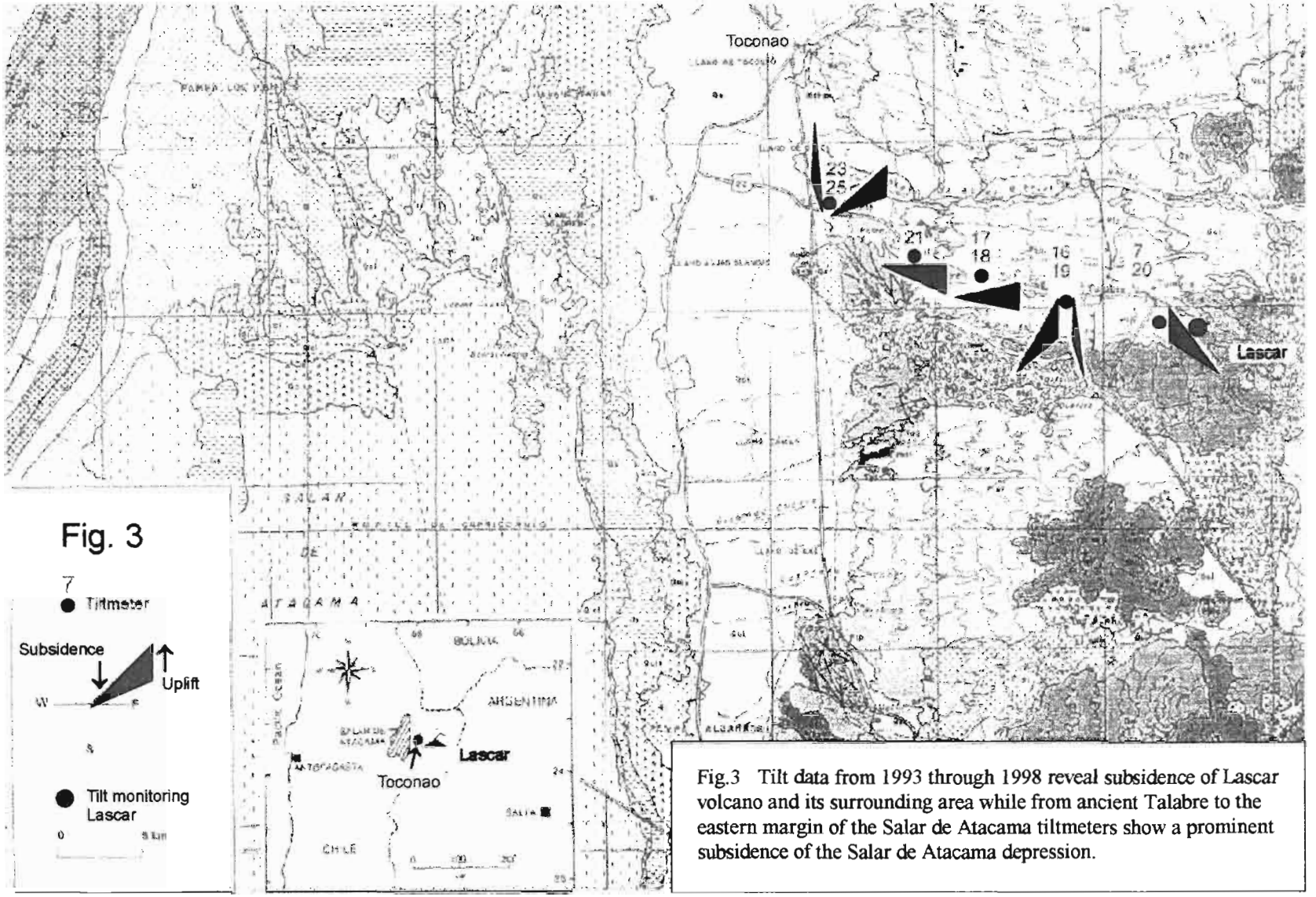

Fig.3 Tilt data from 1993 through 1998 reveal subsidence of Lascar volcano and its surrounding area while from ancient Talabre to the eastern margin of the Salar de Atacama tiltmeters show a prominent subsidence of the Salar de Atacama depression.

At the western border of the Salar de Atacama, borehole tiltmeters installed at the same latitude (23° 20' S) as those of the eastern side of the Salar de Atacama have recorded subsidence to the eastnortheast. Since September 1994 two tiltmeters are recording at the northwest-flanc (4239 m asl) of Lascar. The eastwest-component changed abruptly on 15.10.1994 to a striking uplift in the west which continued until 13.11.1994 yielding a tilt of 1580 µrad within one month. There was a minor eruption on 13.11.94 (fig.4) ejecting a brownish column 700 m above the crater. The next day (14.11.94) previous southwest-uplift changed to southeast-uplift which is indicative to a forthcoming eruption.

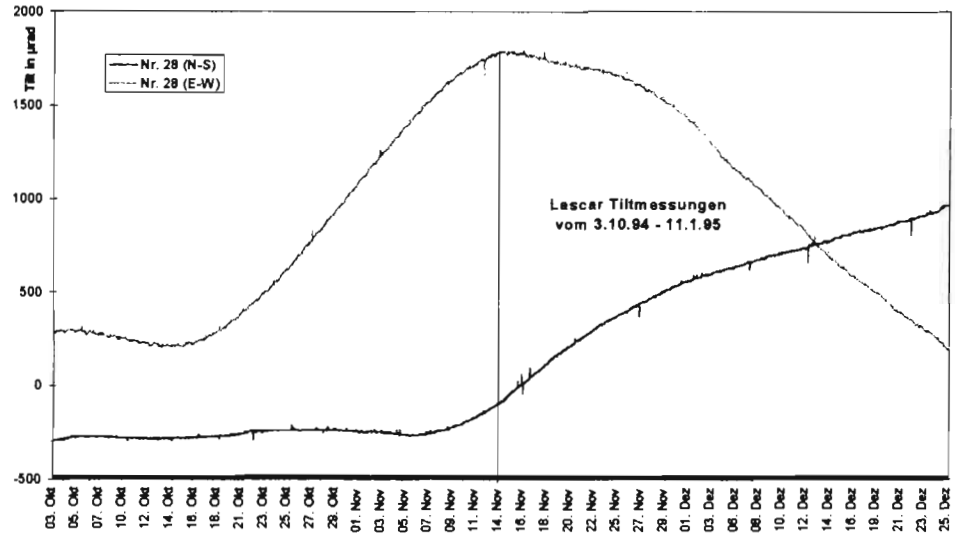

Fig.4 Tiltmeters at the northwest-flanc of Lascar (red dot at fig.3) show a northeast-subsidence from 03.10.94 until the event of an eruption at 13.11.94. After the eruption of 13.11.94 the northwest-flanc of Lascar experiences a northeast-subsidence (or southwest-uplift) i.e. a steepening of the northwest-flanc.

REFERENCES

Schwarz, G., Chong Diaz, G., Krüger, D., Martinez, E., Massow, W., Rath, V., & Viramonte, J. (1994): Crustal High Conductivity Zones in the Southern Central Andes.- In: Reutter, K.-J., Scheuber, E., & Wigger, P.J. (eds): Tectonics o the Southem Central Andes: 49-67, Berlin etc. (Springer).

Wigger, P.J., Schmitz, M., Areneda, M., Asch, G., Baldzuhn, S., Giese, P., Heinsohn, W.-D., Martinez, E., Ricaldi, E., Röwer, P., & Viramonte, J. (1994): Variation in the Crustal Structure of the Southern Central Andes Deduced from Seismic Refraction Investigations.- In: Reutter, K.-J. Scheuber, E., & Wigger, P.J. (eds): Tectonics of the Southern Central Andes: 23-48, Berlin etc. (Springer).

Wilkes, E., & Görler, K. (1994): Sedimentary and Structural Evolution of the Salar de Atacama Depression.- In Reutter, K.-J., Scheuber, E., & Wigger, P.J. (eds): Tectonics of the Southern Central Andes: 171-188, Berlin etc. (Springer).

Ramirez, C.F., & Gardeweg, M. (1982): Carta Geologica de Chile No 54, Hoya Toconao, 1:250.000, Geologia de la Hoya Toconao.- 117 S., Santiago (Sernageomin).

Silva De, S.L., & Francis, P.W. (1991): Volcanoes of the Central Andes.- 216 S., Berlin etc. (Springer).

Bull. Volcanol. (1993) 55 : 455

3D DENSITY MODELLING, ISOSTATIC STATE AND RIGIDITY OF THE CENTRAL ANDES

Sabine SCHMIDT (1), Hans-Jürgen GÖTZE (1), Andreas KIRCHNER (2) and Michael KÖSTERS (3)

(1) Institut für Geologie, Geophysik und Geoinformatik, FU Berlin, Haus N, Malteserstrasse 74-100, D-12249 Berlin; schmidt@geophysik.fu-berlin.de and hajo@geophysik.fu-berlin.de
(2) Shell International Exploration and Production B.V., 2280 AB Rijswijk, Netherlands (formerly at 1)
(3) Sonnenweg 5, D-30171 Hannover (formerly at 1)

KEY WORDS: Density modelling, Isostasy, Rigidity, Central Andes, Subduction zone

INTRODUCTION

On the base of some 15 000 reprocessed gravity observations in the Central Andes we established a 3D density model which is constrained by other geophysical data sets of the region. Onshore the Bouguer anomaly drops down to a regional minimum of about - 4500 $\mu m/s^2$ in the area of the recent volcanic arc, related to both (1) crustal thickening by isostatic compensation and (2) low density material of the volcanic arc. The effect of isostatic compensation of topography and intra crustal loads was calculated assuming a Vening-Meinesz model with the following parameters: density contrast of the earths mantle and crust Rho = 350 kg/m^3, a normal crustal thickness of 35 km and a flexural rigidity of 10 exp. 23 Nm. 2D calculations of rigidity results in normal values in the fore and back arc area but extreme low values in the area of the high intra mountainous basins. Local minima along the recent volcanic arc point to domains of partly molten material (10 to 15 % of melts) at depths of 10 - 15 km and light volcanic material close to the Andean surface. Both was tested by depth estimations in the wave number domain. The maximum-type geoid in the Central Andes mainly reflects the topographic edifice. It rises from some 20 m in the Pacific area up to a 50 m high in the centre.

RESIDUAL GRAVITY FIELD AND GEOLOGICAL INTERPRETATION

The Central Andes segment between 20°S to 28°S shows an anomalous gravity field which consists of numerous local and regional components and fits in the morphostructural units in most cases (Götze et al. 1994, 1996; Götze and Kirchner 1997; Omarini et al. 1999). Three distinct anomalous domains have been

observed (Gangui 1998):

(1) A prominent continuous positive N-S anomaly is located along the Chile margin mostly parallel to the axis of the exposed outcrops of the Coastal Cordillera.

(2) A regional gravity high with NW-SE trend extends from the northern Domeyko Cordillera to the Fiambala Ranges. These extremely high residual gravity reflects the density of a Precambrian - Early Paleozoic basement beneath the Western Cordillera (e.g. Götze and Kirchner, 1997).

(3) Another NNE-SSW anomaly is located eastward to the present magmatic arc and covers the entire Eastern Cordillera. Its western border extends beneath the Puna Plateau and is rather well correlated with the boundary between Puna and the Eastern Puna Mylonite Zone. The eastern border is interpreted by Götze et al. (1994) as a transition zone between different crust types represented by the Eastern Cordillera and the Subandean foreland. This distinctive signature probably mark the west-dipping suture zone between the Brazilian craton and the Puncoviscana belt.

Earlier gravity interpretations (Strunk 1990; Omarini and Götze 1991) postulated the presence of a dense bodies with a calculated rock density of 2 960 kg/m^3 below the Eastern Cordillera (6-8 km up to 24 km). In the northwestern portion of the inferred Puncoviscana belt boundaries there is a relatively shallow highly positive anomaly of more than 300 µm/s^2. Gravity modelling (Gangui and Götze 1996) shows the presence of high density bodies with a calculated density of 2 950 kg/m^3 and thicknesses of about 8 km in the basement below a sedimentary and volcanoclastic Ordovician cover. As reported there this gravity anomaly is caused by assuming a continent-continent accretion of a Late Ordovician magmatic arc. It is believed that the existence of similar gravity anomaly pattern in an adjacent Precambrian-Lower Cambrian terrane strongly suggests that the positive gravity is caused by older structures, which had been overprinted by the Cretaceous rift orogeny. The presence of a decollement level in the upper crust, clearly seen also in reflection seismic data (Gangui and Götze, 1996), appears to be an attractive explanation since it allows for of large scale sub horizontal displacements of the middle crust towards the east. Thus, the pronounced gravity bodies (e.g. massive granulites e.g. xenoliths) within Cordillera Oriental of Salta and Jujuy may be ascribed to the mechanical processes involved in the consolidation of the Puncoviscana belt during collision in the Late Proterozoic. In this context some important conclusions can be established here (Omarini et al, 1999; Gangui, 1998):

(1) The regional geology and geophysical signature is dominated by a linear NNE-SSW trend of granites and volcanic rocks related to the accretion of a linear volcanic belt and terrane. Their juxtaposition with Palaeoproterozoic cores indicates substantial crustal mobility.

(2) In the major Puncoviscana belt there are many individual crustal blocks whose boundaries coincide with gradients between major elongated, subparallel, positive and negative anomalies. This is not what we would expect if the Puncoviscana belt comprised a number of accreted terranes with

separate histories. This can be better explained by structures being formed while younger crust was thrusted against older lithosphere.

(3) Outside of the Puncoviscana belt, another anomalous gravity trend coincides with relicts of the Late Ordovicean structures from magmatic Ocloyic episodes of the Famatinean belt.

(4) In the pre-Andean rift of the Northwestern Argentina (Jurassic-Cretaceous boundary), the intrusion and extrusion of igneous bodies correlate with positiv gravity signature. Hence, it seems reasonable that the rocks of the pre-Mesozoic basement were modified by reworking during the Jurassic-Cretaceous crustal extension. The gravity pattern has also been overprinted by rock-density signature of the Puncoviscana belt.

(5) During the Andean cycle (post-Inca phase from Middle Eocene), major over plating events played an important role in the formation and evolution of the lower crust. The present Andean magmatic arc is characterizes by extreme negative gravity. Positive gravity anomalies are strong at the recent Pacific margin and have a north-south trend. A previous interpretation of this anomalies has been given by Götze et al. (1994) and Götze and Kirchner (1997).

REFERENCES

Gangui A.H. 1998. A combined structural interpretation based on seismic data and 3D gravity modeling in the northern Puna/Eastern Cordillera, Argentina. PhD Thesis, Berliner Geowiss. Abhandlungen, Reihe B, vol. 27, pp. 176.

Gangui A. and Götze H.-J. 1996. The deep structures of the Northern Argentina: constrains from 2D seismic data 3D gravity modelling. XIII Congr Geol Arg, 5(2):545-565.

Götze H.-J., B. Lahmeyer S. Schmidt and S. Strunk 1994. The lithospheric structure of the Central Andes (20-26S) as inferred from interpretation of regional gravity. In: Reutter K, Scheuber E, Wigger P (Eds) Tectonic of the Southern Central Andes. Springer Verlag, 7-23.

Götze H.-J. and the MIGRA group 1996. Group updates the gravity data base in the Central Andes (20° - 29° S). EOS Transactions, American Geophysical Union, Electronic Supplement, 5 pages. http://www.agu.org/eos_elec/95189e.html.

Götze, H.-J., and A. Kirchner, 1997: Gravity field at the South American active margin (20° to 29° S). Journal of South American Earth Sciences, vol. 10, no.2, pp. 179-188.

Omarini R.H. and H.-J. Götze 1991. Central Andes Transect, Nazca Plate to Chaco Plains, South- western Pacific Ocean, Northern Chile and Northern Argentina. Copublished by Inter-Union Comm Lithos and Am. Geophys. Union Washington, pp. 30.

Omarini R., H.-J. Götze, R.J. Sureda, A. Seilacher and F. Pflüger, 1999. Puncoviscana folded belt in NW Argentina: testimony of Late Proterozoic Rodinia fragmentation and pre-Gondwana collisional episodes. Geologische Rundschau, 1999 (in press).

Strunk S 1990. Analyse und Interpretation des Schwerefeldes des aktiven Kontinentalrandes der Zentralen Anden, (20°-26° S), PhD Thesis, Berliner Geowiss Abhandlungen, Reihe B. vol. 17, pp.135.

ASSESSMENT OF THE DEPTH OF INTRACRUSTAL MELT GENERATION AND MAGMA STORAGE ZONES IN THE CENTRAL ANDES- INSIGHTS FROM IGNIMBRITE PETROLOGY AND GEOCHEMISTRY

Axel K. SCHMITT, Robert B. TRUMBULL, Jan M. LINDSAY and Rolf EMMERMANN (1)

(1) GeoForschungsZentrum Potsdam, Telegrafenberg 14473 Potsdam, Germany. axelk@gfz-potsdam.de; bobby@gfz-potsdam.de; kiwi@gfz-potsdam.de; emmermann@gfz-potsdam.de

KEY WORDS: ignimbrite, crustal melting, Nd-Sr-isotopes, AFC, upper crustal magma chamber

INTRODUCTION

Information on the location, amount and physical properties of partial melts in the crust is needed to understand the interplay of magmatism and tectonics in orogenic belts. Using the Neogene ignimbrite province of the Altiplano-Puna plateau in the central Andes as an example, this study presents estimates of compositional properties and pressure-temperature conditions of crustal magma at the site of melt generation and in pre-eruptive magma storage zones, and compares these results with present-day geophysical observations.

The Altiplano-Puna plateau between 21-24¡ S was the focus of intensive felsic volcanism during the late Neogene and Pleistocene. The most important expression of this activity is a group of composite caldera centers known as the Altiplano-Puna Volcanic Complex (APVC, de Silva, 1989), which erupted large sheets of ash-flow tuffs and felsic lava domes between 10 and 1 Ma. Single eruptive units from these calderas commonly exceed 1000 km^3. Felsic magmatism began after a period of crustal shortening and thickening 20-15 Ma ago, and reached total volumes greater than those of the contemporaneous andesitic arc magmatism. This sudden onset of ignimbrite activity is a first-order feature reflecting a marked change in the thermal and structural state of the Andean crust.

Compositionally, the majority of juvenile rocks (pumice samples) are homogeneous, metaluminous to weakly peraluminous, high-K dacites and rhyodacites (SiO_2 = 63-69 wt.%) with high concentrations of phenocrysts. Rhyolitic compositions are also present but the vast majority of ignimbrites belongs to the crystal-rich, monotonous intermediate type. Initial Sr-Nd isotopic ratios from the ignimbrites ($^{87}Sr/^{86}Sr$ = 0.7085 to 0.7132, εNd = -6.7 to -8.9) differ significantly from coeval arc-andesites and indicate a major

crustal contribution in the source magmas (Figure 1). Bimodal andesitic-dacitic pumice distributions are present within some eruptive units. Although volumetrically minor, the andesitic pumices are important because they provide evidence for magma mingling (chamber recharge?) and a potential role of andesites in the genesis of the intermediate ignimbrites.

Pre-eruptive temperature and pressure estimates for the ignimbrite-forming dacitic magmas derived from mineral equilibria are 780-820¡C (Fe-Ti oxides) and 100-200 MPa (Al-in-hornblende). Pre-eruptive melt water contents of 3.5-4.5 wt.% were measured on melt inclusion glasses in quartz phenocrysts. Subtracting the contribution of observed hydrous and anhydrous phenocrysts, the total water content of typical bulk magma is estimated at 2-3 wt.%. These values constrain the conditions of crystal growth and equilibration of ignimbrite source magma in upper-crustal chambers (depth 4-7 km) whose volumes must be several 1000 km^3.

The ignimbrite-forming magmas in the APVC have long been considered as products of crustal melting but few attempts have previously been made to quantify the crustal contribution. Recent progress in understanding the crustal structure and basement geology of the Central Andes, combined with better constraints on the melting process of different protoliths from experimental studies makes it possible to reassess the genesis of the APVC ignimbrites. Petrologic and isotopic studies of basement exposures (Lucassen et al. in prep.) in the area of the APVC reveal a compositionally uniform felsic upper crust metamorphosed in the Early Paleozoic at high-T, medium-P conditions. Proterozoic protoliths (T_{DM} Nd-model ages 1.6 - 2 Ga) were recycled in the Early Paleozoic and again during Late Paleozoic orogenesis (300 Ma granites). Mafic lithologies (amphibolites) are rare. Seismic and gravity data also indicate a quartzo-feldspathic composition throughout the crust with no evidence for a lower crust dominated by mafic minerals (Beck et al. 1996). This is supported by the presence of lower-crustal xenoliths of felsic granulite which have been reported from the Cretaceous Salta Rift.

If, as seems likely, the Central Andean basement is dominated by quartzo-feldspathic rocks like those presently exposed, it is unlikely that the large-volume ignimbrites represent pure crustal melts. Dehydration melting experiments show that biotite-bearing felsic protoliths yield highly silicic, iron and magnesium-poor and strongly peraluminous compositions which do not match those of the large-volume dacitic ignimbrites. Experimental melting of quartz-amphibolite yielded low degrees (<20 wt.%) of high-Si melts which also differ greatly from the compositions observed in the APVC. Furthermore, if the ignimbrites are products of either bulk or partial melting of Paleozoic felsic crust, their moderately radiogenic $^{87}Sr/^{86}Sr$ ratios (0.7085 to 0.7095) demand a low time-integrated Rb/Sr ratio in the source. This is not consistent with the exposed basement compositions and it is difficult to imagine a source rich enough in biotite to generate abundant dehydration melts and at the same time having a low bulk Rb/Sr ratio. Felsic granulites like the Salta Rift xenoliths do not have the appropriate bulk composition to be fertile sources for dehydration melting.

Several lines of evidence therefore suggest that the APVC ignimbrites are not pure crustal melts. The fact that arc andesites also erupted during the lifespan of the ignimbrite province makes it reasonable to propose that andesitic magmas provided the heat for crustal melting and that the ignimbrites are hybrid magmas (see also de Silva, 1989). The feasability of this hypothesis was demonstrated from thermal modelling by Laube and Springer (1997). Geochemical modelling using appropriate crust and arc andesite endmembers (relatively uncontaminated basaltic andesite and average Paleozoic granites from the Central Andes) yields ratios of crustal melts to andesitic material between 1 (mixing) and 1.5 (AFC), which are consistent with major element compositions assuming mixing between a basic andesite and a rhyolitic haplogranitic melt.

The depth of the melting and assimilation zone can be estimated from the following geochemical arguments. (1) biotite dehydration melting reactions produce garnet above 1000 MPa and orthopyroxene at lower pressures. The ignimbrites show no evidence of the heavy REE-depletion which dehydration melt reactions in the garnet- stability field would produce; thus, we conclude that the zone of melting is above appoximately 30 km. (2) The crystallizing mineral assemblage from andesitic melts is pressure-sensitive, with higher ratios of Cpx/Plag at higher pressures. Because these two minerals have different mineral-melt distribution coefficients for Sr and Nd, bulk D values are also pressure sensitive. Using MELTS thermodynamic modelling, the bulk D-values for Nd and Sr were calculated as a function of pressure and the results were used to model Sr and Nd-isotope AFC trends. Low-pressure (<700 MPa) fractionational crystallization is plagioclase dominated and leads to low bulk D_{Sr} –values. The expected depletion in Sr, however, is not seen in the ignimbrites, and isotopic and trace element compositions of the ignimbrites are only matched by AFC models for conditions >700 MPa.

CONCLUSIONS

The arguments outlined above yield a rough depth estimate of between 20 and 30 km for the interaction zone between mantle-derived basic magmas and crustal partial melts. Combining this with the unambiguous evidence for pre-eruptive residence in an upper-crustal magma chamber (7-4 km), we conclude that large quantities of felsic magmas must have traversed 10-20 km of continental crust before they reached their shallow storage sites. Geophysical anomalies (low v_p, high v_p/v_s-ratio, high electrical conductivity) presently observed in the mid crust below the Altiplano-Puna plateau have been interpreted to represent a zone of partial melting with a top at about 19 km depth (Schmitz et al. 1997, Schilling et al. 1997). Our estimates for the source depths of the Neogene-Pleistocene ignimbrite magmas are in good agreement. An important implication of this is the persistence since perhaps the Late Miocene of a thermal anomaly and partial melting zone within the thick central Andean crust which is fed by continuous magma supply from ongoing subduction.

REFERENCES

Beck S., Zandt G., Myers S. C., Wallace T. C., Silver P. G., Drake, L. 1996. Crustal thickness variations in the central Andes. Geology, 24, 407-410.

de Silva, S. L. 1989c. Altiplano-Puna volcanic complex of the central Andes. Geology, 17, 1102-1106.

Laube, N., Springer, J. 1998. Crustal melting by ponding of mafic magmas; a numerical model. Journal of Volcanology and Geothermal Research, 81, 19-35.

Lucassen, F., Franz, G., Thirlwall, M. & Metzger, K. (in preparation). Upper Palaeozoic granites in the Coastal Cordillera and Precordillera of N-Chile (21¡S): their genesis and formation on the Pacific margin in the central Andes.

Schilling F.R., Partzsch G.M., Brasse H., Schwarz G. 1997. Partial melting below the magmatic arc in the central Andes deduced from geoelectromagnetic field experiments and laboratory data. Physics of the Earth and Planetary Interiors, 103, 17-31.

Schmitz, M., Heinsohn, W. D. & Schilling, F. R. 1997 Seismic, gravity and petrological evidence for partial melt beneath the thickened central Andean crust (21-23¡ S). Tectonophysics, 270, 313-326.

Trumbull, R. B., Wittenbrink, R., Hahne, K., Emmermann, R., BŸsch,. W., Gerstenberger, H., Siebel, W. Evidence for Late Miocene to Recent contamination of arc andesites by crustal melts in the Chilean Andes (25–26¡S) and its geodynamic implications. Journal of South American Earth Sciences. In press.

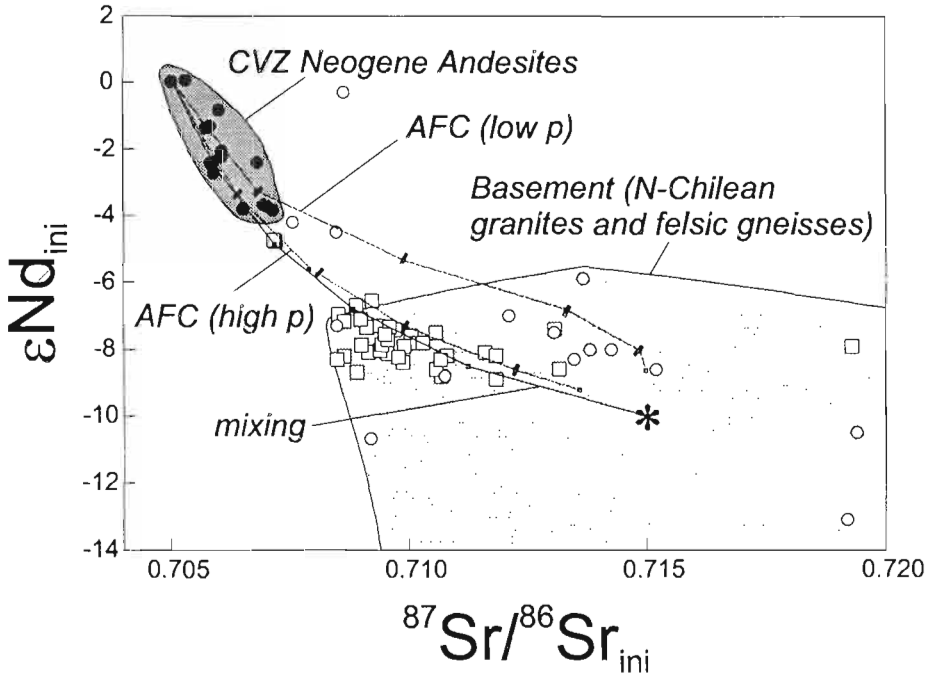

Figure 1: Initial Sr- and Nd isotopic composition of APVC ignimbrites (open squares) with mixing and AFC-trends (dashed line = low P; dotted line = high P). CVZ andesite data (shaded field with filled circles) from Trumbull et al. (in press); Paleozoic basement data (shaded field with open circles) from Lucassen et al. (in prep.)

THE CRUSTAL STRUCTURE AND ISOSTATIC BALANCE OF THE GUAYANA SHIELD, VENEZUELA

Michael SCHMITZ (1), Daniel CHALBAUD (2), Jesús CASTILLO (2), Carlos IZARRA (2,3) and Stefan LÜETH (4)

(1) FUNVISIS, Fundación Venezolana de Investigaciones Sismológicas, Apto. Postal 76880, Caracas 1070A, Venezuela, e-mail: mschmitz@funvisis.internet.ve
(2) Universidad Simón Bolívar, USB, Sartenejas, Caracas, e-mail: castillj@usb.ve
(3) University of Liverpool, Great Britain, e-mail: cizarra@liverpool.ac.uk
(4) Freie Universität Berlin, FUB, Germany, e-mail: stefan@geophysik.fu-berlin.de

KEY WORDS: Seismic Refraction, Crustal Structure, Moho, Isostasy, Guayana Shield.

INTRODUCTION

The Guayana Shield is an elevated plain consisting mainly of Precambrian rocks up to 3.6 Billion years and an average height of 1.200 m with high plains ("Tepuys") reaching up to 3.000 m high. Gibbs and Barron (1993) indicate that this old shield region or at least part of it should have elevated during Mid-Tertiary, possibly as a consequence of an hot-spot or a thermal anomaly. The principal objective of the ECOGUAY project is to contribute data on the crustal structure and thickness, in order to better understand the geological evolution of the craton in northeastern Southamerica. We present preliminary results of a combined geophysical study integrating seismic refraction, gravimetric and magnetic data. The study aimed to determine the crustal structure, its thickness and the isostatic balance of the Guayana Shield in southeastern Venezuela.

SEISMIC DATA

Field work was done within the scope of the ECOGUAY project (Estudios de la Estructura Cortical del Escudo de Guayana) in June 1998. We obtained 7 seismic refraction profiles of up to 250 km length, using the blasts of the iron mines in Ciudad Piar (Quadrilátero San Isidro) as energy source (shot list see Schmitz et al., 1999). The seismic data, actually in processing, show a good signal to noise ratio up to the end of the profiles – only the profiles that extended northwards into the Eastern Venzuelan Basin are more noisy due to the Quarternary sediments north of the Orinoco river.

The seismic sections were obtained by "scrolling" with the available 13 seismological stations (11 PDAS 100 and 2 ORION, all equipped with Mark 3-D, 1Hz seismometer) along the profile, as seen for profile 100 in figure 1. In the seismic section of profile 100 in the eastern part of the Guayana Shield, first arrivals can be distinguished with a good signal/noise ratio up to 250 km distance (figure 2). The first arrivals of the basement (P_g) are observed around 0 up to 170 km distance. P-velocities increase from 6.0 km/s at the surface to 6.6 km/s at 30 km depth. The reflections from the upper mantle (P^M) are observed at 170 – 120 km distance. The crust – mantle boundary (Moho-discontinuity) is calculated to 45-48 km depth with a velocity of 8.2 km/sand an average crustal velocity of 6.6 km/s. First arrivals of waves that passed through the upper mantle (P_n) are observed between 190 and 250 km distance.

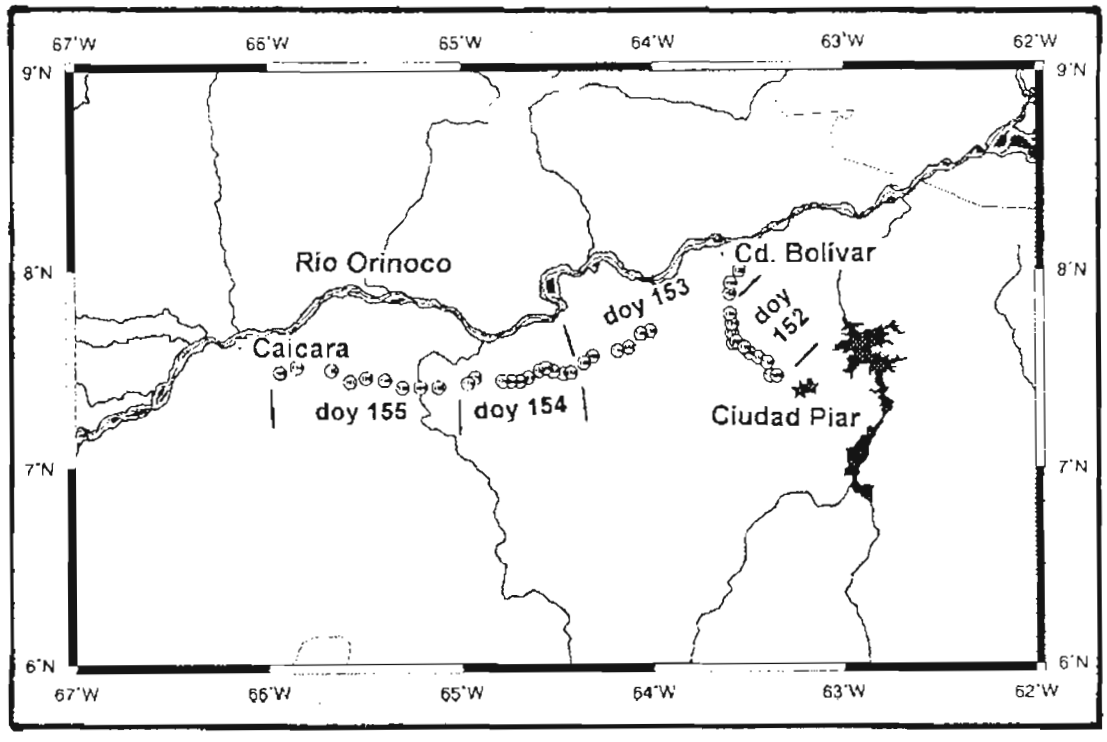

Figure 1. Location map of profile 100 (Ciudad Piar to the west). The record section was recorded during 4 days (doy 152-155); stars = shotpoints; circles = recording points.

GRAVIMETRIC AND MAGNETIC OBSERVATIONS

About 300 new gravimetric data were obtained in order to complement the existing gravity data base at Simon Bolívar University. The Bouguer anomalies vary from 50 mGal in the north of the study region to values of –40 mGal in the south (Schmitz et al., 1999). The free air anomalies generally vary between –10

and 10 mGal, only in the extreme south values of 150 mGal are obtained. Along the e-w profile (see figure 1) the Bouguer anomaly drops from 35 mGal in the west to –15 mGal at Ciudad Piar (km 300) and –30 mGal further east (figure 3). The magnetic data obtained during field work is actually in processing.

Figure 2. Record section of profile 100 (Ciudad Piar – west) with reduction time of 6 km/s (above) with the velocity model and raytracing (center) and the calculated arrivals (below).

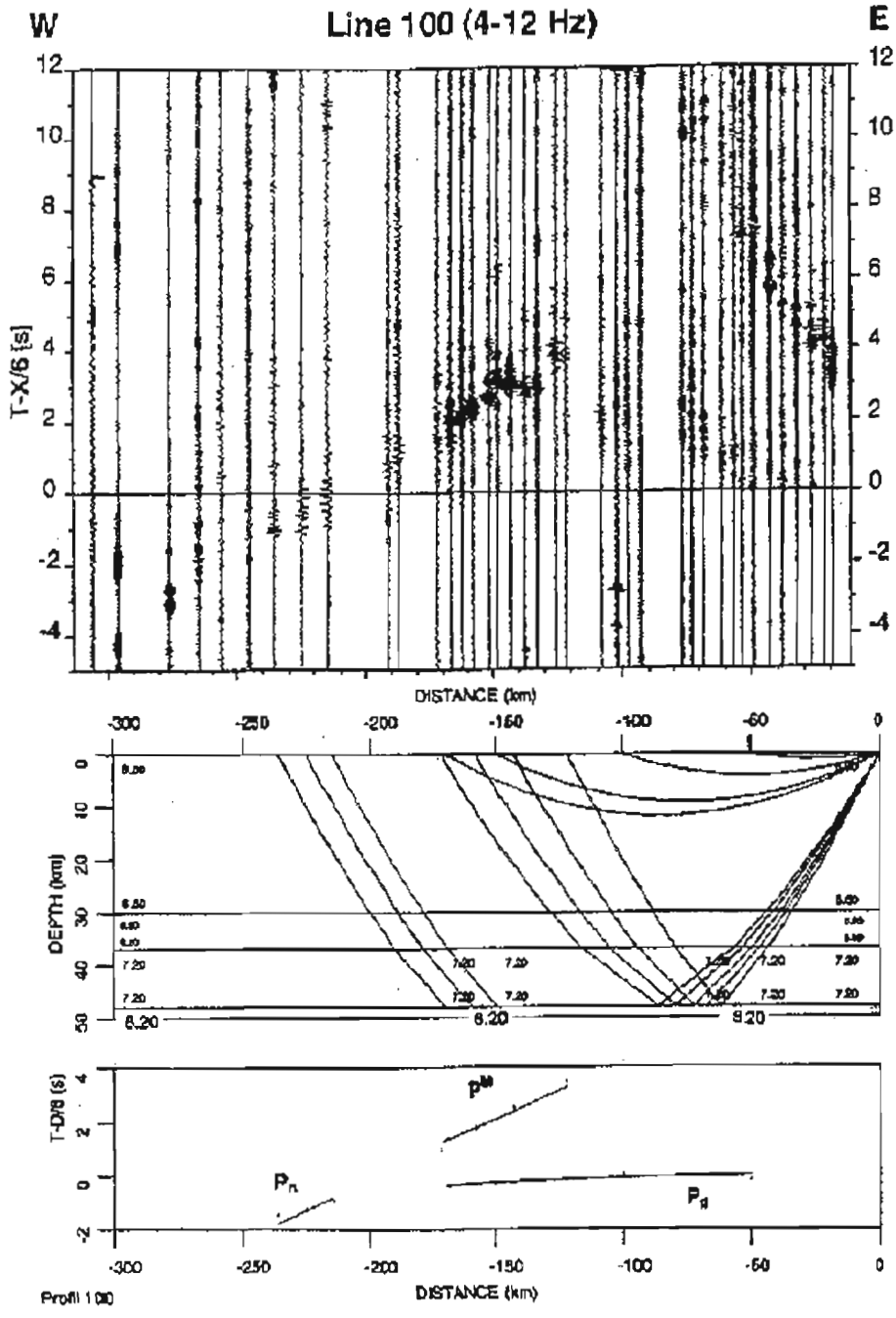

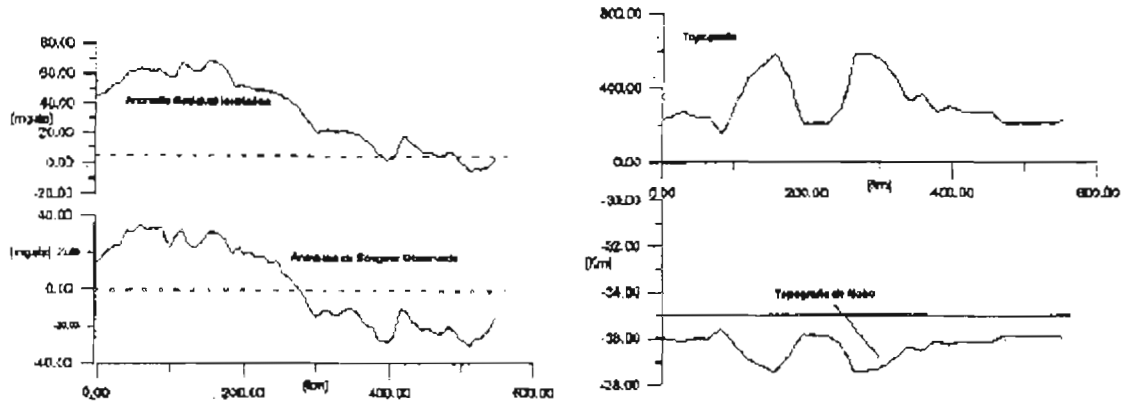

Figure 3. Gravimetric and topographic sections along profile 100 from 66° W to 61° W (see figure 1) with the residual isostatic anomaly (USB gravity database) based on a 35 km Moho-depth (upper left), the Bouguer anomaly (lower left), the topography after ETOPO5 (upper right) and the isostatic Moho (lower right).

CONCLUSIONS

Based on the analysis of profile 100 in the western part of the Guayana Shield crustal thickness must be considered 45 – 48 km with subcrustal velocities of 8.2 km/s and an average crustal velocity of 6.6 km/s. These values are in agreement with observations for other shield regions (Mooney et al., 1998). The northeastern part of the Guayana Shield is composed of Arquean crust (Imataca Province), while the Cuchivero Formation of Lower Proterozoic age is exposed in the western part. The profile analysed up to the date crosses the border between the two provinces, but samples within the Arquean crust. Nevertheless, the obtained crustal thickness of 45-48 km would indicate a thickened crust typical for Proterozoic provinces, as indicated by similar studies by Durrheim and Green (1992) for the Kapvaal Carton and worldwide observations (Mooney et al., 1998). The two units may be connected by a broad transition zone e.g. an inclination of the Moho towards the west. The results are still too preliminar to discuss the isostatic balance and the elevation history of the Guayana Shield. Nevertheless, the hight crustal thickness of more than 45 km and the upper mantle velocities of 8.2 km/s do not support thermal anomalies as the isostatic support of the high elevations of the Shield. Vdovin et al. (1999) indicate a reduced velocity beneath the Guayana Shield based on the analysis of the dispersion of surface waves beneath Southamerica. The complete set of geophysical data obtained during the ECOGUAY project hopefully will unable us to identify with more detail the crustal thickness and upper mantle velocities in order to clarify the isostatic state of the shield crust. Project financed by CONICIT No. S1-97002996.

REFERENCES

Durrheim, R.J. and Green, R.W.E., 1992. A seismic refraction investigation of the Archean Kaapvaal Craton, South Africa, using mine tremors as the energy source. Geophys. J. Int., 108, 812-832.

Gibbs, A.K. and Barron, C.N., 1993. The Geology of the Guayana Shield. Oxford University Press, Oxford, pp. 258.

Mooney, W.D., Laske, G. And Masters, G., 1998. CRUST 5.1: A global crustal model at 5o x 5o. JGR, 103, 727-747.

Schmitz, M. , Castillo, J., Izarra, C., Lüth, S., DaSilva, A. And Chalbaud, D., 1999. Mediciones sísmicas de refracción, gravimétricas y magnéticas en el Escudo de Guayana. VI Congreso Venezolano de Sismología e Ingeniería Sísmica, Mérida, 12-14 de Mayo de 1999, 5pp.

Vdovin, O., Rial, J.A., Levshin, A.L. and Ritzwoller, M.H., 1999. Group-velocity tomography of South America and the surrounding oceans. GJI, 136, 324-340.

ELECTRICAL CONDUCTIVITY ANOMALIES AROUND THE ANCORP-PROFILE: AN OVERVIEW OF NEW RESULTS

K. SCHWALENBERG(1), P. LEZAETA(2), W. SOYER(2) and H. BRASSE(2)

(1) GFZ Potsdam, Telegrafenberg, D-14473 Potsdam; e-mail: katrin@gfz-potsdam.de
(2) Fachrichtung Geophysik, FU Berlin, Malteserstr. 74-100, D-12249 Berlin

KEY WORDS: electrical conductivity, magnetotellurics, Central Andes

INTRODUCTION

Magnetotelluric (MT) measurements in North Chile and South Bolivia were carried out within the framework of the Collaborative Research Program (SFB 267) "Deformation Processes in the Andes" to investigate the electrical conductivity structure of the Central Andes between 20°S and 21°S. Previous studies further south revealed several high conductivity zones (HCZ) especially below the volcanic arc of the Western Cordillera (Schwarz & Krüger 1997), which were interpreted as zones of partial melts by Schilling et al. (1997). It was already then believed that large fault systems, especially the Atacama Fault in the Coastal Cordillera, could be imaged as good conductors. Data quality and lacking station density did not permit a quantitative interpretation at that time, however. Consequently, in addition to tracing the "magmatic arc conductor" towards the north our new investigations concentrated on the study of several prominent fault systems: the already mentioned Atacama Fault, the Precordilleran Fault System (Falla Oeste) and the Uyuni-Keniani-Fault in the Bolivian Altiplano.

THE DATA BASE

The locations of the newly measured MT sites in the Central Andes are displayed in Fig. 1. An already existing profile at 20°S (Echternacht et al. 1997) passing the town of Pica was extended into Bolivia until the shores of the Salar de Uyuni, thus crossing the whole Western Cordillera. A second profile was set up along 21°S from the Pacific Coast to the eastern margin of the Altiplano following the ANCORP seismic reflection line (ANCORP Working Group 1998). In the forearc intermediate sites were operated in order to account for three-dimensional structures discovered earlier by Echternacht et al. (1997).

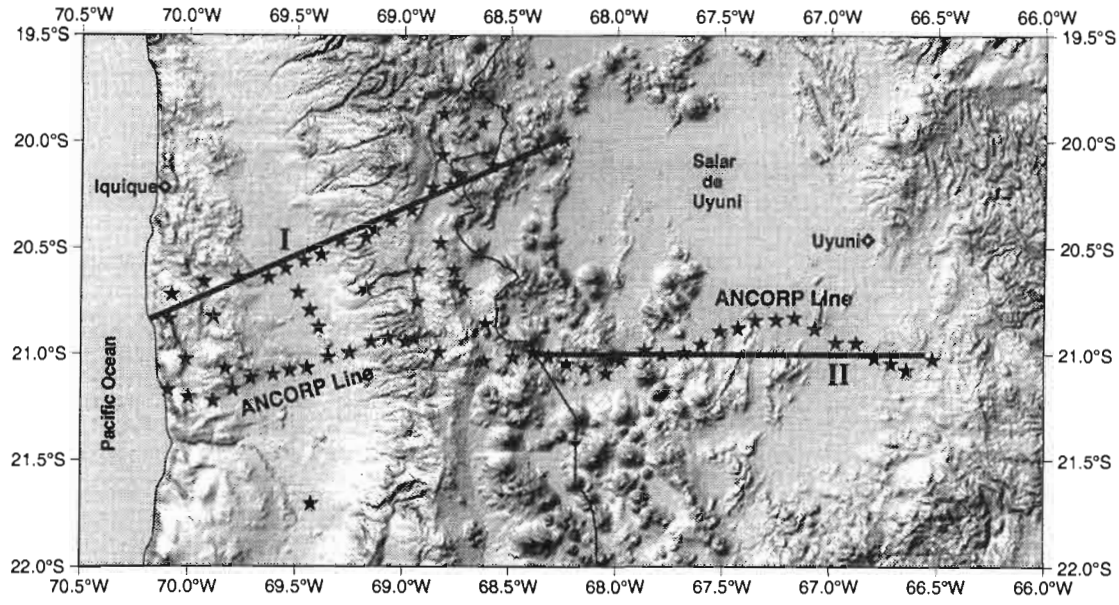

Fig. 1: Shaded relief map of the western Central Andes showing locations of newly measured MT sites. I and II refer to profiles or profile segments which where interpreted by 2-D inversion.

Spacing between stations was on the average 10 km and the data were registered in a period range from 10-10.000 s, yielding an approximate penetration depth from 5-100 km, depending on the subsoil conductivity.

In the following we present two-dimensional models of profile segments I and II (Fig. 1). Data are severely distorted by surficial inhomogeneities especially in the Coastal Range and restrict a simple two-dimensional approach. There are also clear indications of deep-seated three-dimensional structures in the Preandean depression on profile I, the whole Coastal Cordillera and on the eastern Altiplano. Thus 2-D models may only serve as a first step in evaluating the whole complex data set. However, the discovered conductivity anomalies are so prominent that they produce a "zero-order effect" in the magnetotelluric transfer functions and more sophisticated interpretation should not alter significantly the overall image achieved so far.

2-D INTERPRETATION

A 2-D inversion code (Mackie et al. 1997) was applied using a homogeneous halfspace as a starting model. By adapting error bounds for apparent resistivities and phases the weight of phase data (reflecting the actual induction process) was enhanced during inversion; static distortion of apparent resistivity curves could thus be minimized.

An inversion result of data from profile I is presented in Fig. 2. It confirms a model achieved earlier by Echternacht (1998) for the Chilean part of the profile and displays a prominent zone of enhanced

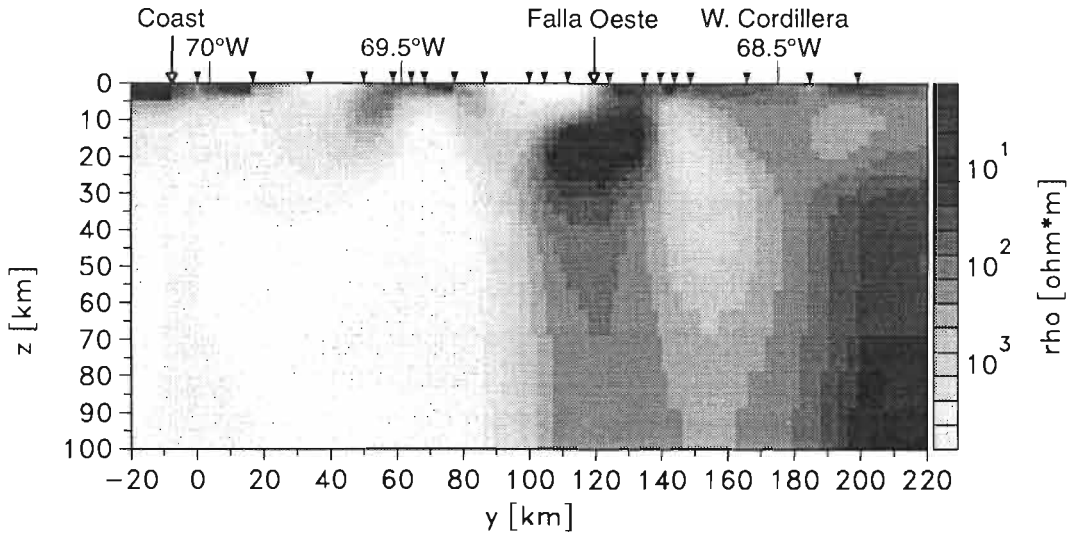

Fig. 2: 2-D inversion result of profile I.

conductivity below the Precordilleran Fault system. Although the depth extent of this anomaly is not well resolved, an extension to lower crustal levels is required by the data. The spatial correlation of this HCZ with the Falla Oeste hints at ascending salinary fluids as a possible cause of the high conductivities (about 1 S/m), a model that was also inferred from the interpretation of seismic reflection data along the ANCORP profile 60 km further south (Sobolev, pers. comm.; ANCORP Working group 1998).

It is now clear from modelling results of both profiles I and II that the HCZ below the magmatic arc detected further south vanishes to the north of parallel 21°S. This remarkable result, which is in accordance with seismological observations regarding the spatial distribution of seismic absorption (Haberland 1999), correlates with the "Pica gap", a region without recent volcanism. However, along profile II itself volcanism is still active or at least fumarolic (manifested e.g. in Irruputungu and Olca volcanoes) . Apparently these volcanoes lack a broader feeding zone in the deeper crust, as was inferred from the investigations further south (Schilling et al. 1997).

Inversion results of profile segment II are shown in Fig. 3 (the processing of the whole data set is still under way, since measurements in the Chilean sector were completed only recently in the beginning of 1999). Besides the bad or at least "normal" conductor beneath the Western Cordillera, a broad HCZ is modelled below the central part of the Altiplano with resistivities as low as 1 Ωm or even less. Unfortunately, the conductor do not permit a resolution of its actual depth extent – much longer periods would have to be analyzed to achieve a sufficient penetration depth of the electromagnetic fields (which would require a quasi-observatory operation of stations beyond the capabilities of a field campaign). The data would be equally fitted by a model that restricts the high conductivities to the middle or lower crust. Taking into account the high heat flow on the Altiplano (with 120 mW/m^2 the highest in the Central Andes), a partially molten domain at depths of 10-20 km and below is the most plausible explanation of

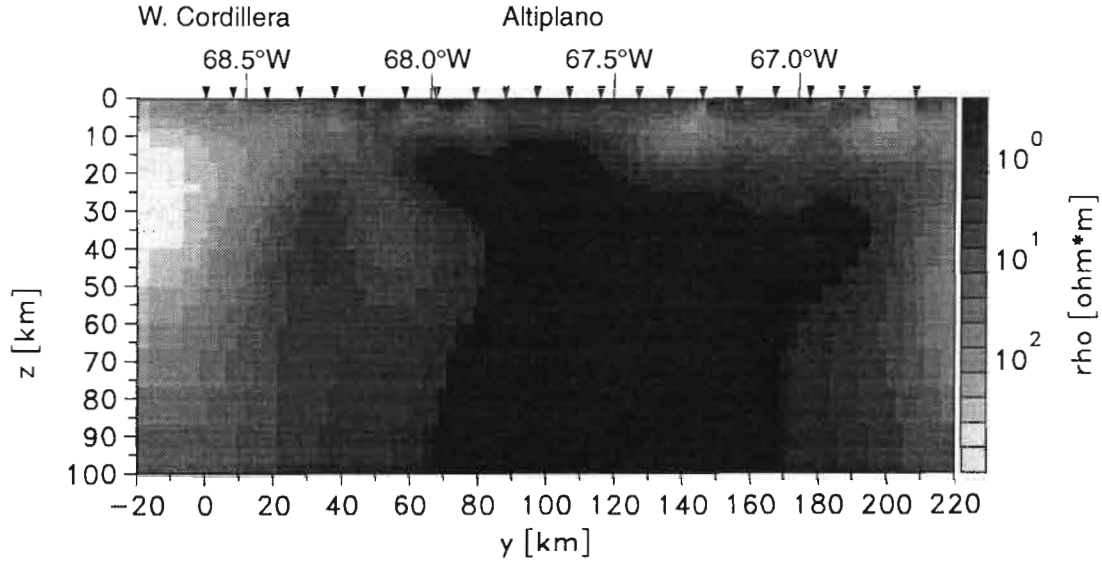

Fig. 3: 2-D inversion result of profile segment II.

the HCZ. A recent re-interpretation of the ANCORP reflection data (Stiller & Lühr, pers. comm.) yields a diffuse but distinguished reflection pattern in the middle crust with it's lateral extent coinciding with the HCZ. A certain negative correlation exists concerning the isostatic residual gravity field, however, which shows *positive* values of about 40 mgal in the same area.

The Uyuni-Keniani Fault is not imaged as a good conductor as was initially assumed. The pattern of induction arrows (derived from an analysis of the ratio: vertical to horizontal magnetic field components) and the already mentioned three-dimensionality of the MT data in this region require a 3-D approach; an obvious and necessary task for the further interpretation of this data set.

CONCLUSIONS

- The magmatic arc between 20°S and 21°S is not connected with a highly conductive zone which is dominant further south and is believed to be caused by partial melts.
- A good conductor below the Altiplano may indicate – together with other geophysical observations – a zone of partial melting in the middle crust .
- Below the Falla Oeste the resistivity model shows a good conductor that could be explained by ascending fluids.

REFERENCES

ANCORP Working Group (1998): Seismic reflection image revealing offset of Andean subduction-zone earthquake locations into oceanic mantle, Nature, **397**, 341-344.

Echternacht, F., Tauber, S., Eisel, M., Brasse, H., Schwarz, G. & Haak, V. (1997): Electromagnetic study of the active continental margin in northern Chile, Phys. Earth Planet. Int., **102**, Nos. 1-2, 69-88.

Echternacht, F. (1998): Die elektrische Leitfähigkeitsstruktur im Forearc der südlichen Zentralanden bei 20°-21° S, abgeleitet aus magnetotellurischen und geomagnetischen Sondierungen, Diss. Freie Universität Berlin.

Haberland, C. (1999): Die Verteilung der Absorption seismischer Wellen in den westlichen zentralen Anden, Diss. Freie Universität Berlin.

Mackie, R.L., Rieven, S. & Rodi, W. (1997): Users Manual and Software Documentation for 2D-Inversion of Magnetotelluric data, MIT, Earth Resources Laboratory, Cambridge, Massachusetts.

Schilling, F.R., Partzsch, G.M., Brasse, H. & Schwarz, G. (1997): Partial Melting below the Magmatic Arc in the Central Andes Deduced from Geoelectromagnetic Field Experiments and Laboratory Data, Phys. Earth Planet. Int., **103**, Nos. 1-2, 17-32.

Schwarz, G. & Krüger, D. (1997): Resistivity cross section through the southern central Andes as inferred from magnetotelluric and geomagnetic deep soundings, J. Geophys. Res., Vol. **102** , No. B6 , 11957-11978.

THE AUGUST 4, 1998, BAHIA EARTHQUAKE (Mw=7.1): RUPTURE MECANISM AND COMMENTS ON THE POTENCIAL SEISMIC ACTIVITY

SEGOVIA M.(1), PACHECO J. (2) , SHAPIRO N.(1,2), YEPES H.(1), GUILLIER B.(3), RUIZ M.(1), CALAHORRANO A.(1), ANDRADE D, EGRED J.(1)

(1) Instituto Geofísico, EPN, Quito-Ecuador
(2) Instituto de Geofísoca, UNAM, México DF, México
(3) IRD, Quito-Ecuador

KEY WORDS: Ecuador, subduction, rupture

INTRODUCTION

In front of the Ecuadorian coast, the Nazca plate subducts beneath the South America plate. This kind of limits between plates fail repeatedly in large earthquakes, moreover, important topographic features like the Carnegie Ridge in the Nazca Plate may produce strong coupling and the behavior of energy release may be very complex. So, studying these events is important to know about the recurrence of great earthquakes.

At 18:59, august 4 1998 (UT), an earthquake of magnitude 7.1 (Mw) shock the coast of Ecuador. The hipocenter was located by the National Network of Seismographs (NNS) of the Instituto Geofísico of the Escuela Politécnica Nacional, 10 km north to Bahía (Figure 1). The focal depth was estimated to be equal 20km. This event has a precursor (Mw=5.4) which occurred 1 hour and 24 minutes before the main shock. Therefore, the population was alerted and the number of casualties was small, while the damage was very important in several modern buildings in Bahía, where intensities of VIII were reported (Figure 1). Most of the small towns of the region were isolated because of landslides and interruptions of the telephonic communication. The event did not produce a notable tsunami. Only a small water rise (30 cm) was registered in Manta, 80 km south of the epicenter.

The Bahía earthquake is the strongest seismic event occurred in Ecuador during last 19 years. It was recorded by short-period seismographs of the NNS and numerous broad-band stations of the IRIS network. This data set allows a quantitative analysis of the rupture process.

LOCAL DATA

The NNS is operating since 1987. The network consists of 35 1Hz, telemetric stations. Seven of them are located in the coastal area. It allows to record and locate seismic events with magnitudes larger than 3.8. The seismic activity in the region surrounding the epicentral area of the Bahía earthquake is shown in Figure 2. It can be seen that an important number of small earthquakes occurred from May to July 1998 just south to the epicentral zone of the august 4 earthquake. During August–December 1998, 800 aftershocks were recorded by permanent stations of the NNS and two portable seismographs installed in the region of Bahía. Filled circles in Figure 2 show 30 best located aftershocks. It gives us possible limits of the area ruptured by the Bahía earthquake. Large ellipses in Figure 2 show rupture areas estimated for three large earthquakes close to the Ecuadorian coast during last 50 years. It can be seen that the aftershocks of the 1998 Bahía earthquake are located in the southern segment of the zone ruptured by the 1942 earthquake. Therefore, the northern segment remains probably loaded and next large coastal earthquake can be expected in this region. Comparing the affected zones by large events of 1942,1958 and 1979 (Kanamori and McNally, 1982; Mendoza and Dewey, 1985; Swenson and Beck, 1996) is easy to see that there is a zone of relatively quiescence (Figure 2).

TELESEISMIC INVERSION

We used the algorithm proposed by Nábêlek (1984) in order to estimate the source mechanism and rupture duration. This method is based on the inversion of teleseismic P and SH waves. We used broadband records of the 19 IRIS stations (Table 1) with epicentral distance lying between 30° and 90°. Original velocity records (LHZ, LHN, and LHE channels) were rotated to the great circle path and integrated to the ground displacement. Time windows of ~50s containing direct P and S waves were selected for the inversion. The results are presented in Figure 3. The obtained fault orientation (ϕ=9, δ=14.5, λ=110) is close to this reported by Harvard. Source mechanism corresponds to a subduction thrust earthquake with a weak dipping angle. Very similar mechanisms were reported for previous strong earthquakes occurred in the Ecuadorian coast region. We have also tried to invert details of the source time function using the broad band records of P waves (BHZ channels, 20 samples per second). However, our tests have shown that source complexity cannot be resolved. Visual analysis of seismograms shows certain directivity toward the north-west.

CONCLUSIONS

The Ecuadorian coast was affected by large thrust earthquakes and now with the local monitoring it is possible to locate and follow the small and medium seismic activity which may be precursor of a great earthquakes. The event of august 4, 1998 is a shallow thrust earthquake with an energy release of 10 s. The source mechanism obtained is consistent with what we know about the subduction in front of the coast and with other large events in the zone. The seismic moment (2.92e26 dyn-cm) differs in a range of 45% this is accepted if we consider that the present analysis was made with the P and SH waves and not with surface waves as Harvard do. This event affected the southern part of the 1942 rupture zone and it is possible to expect other large event in the near future.

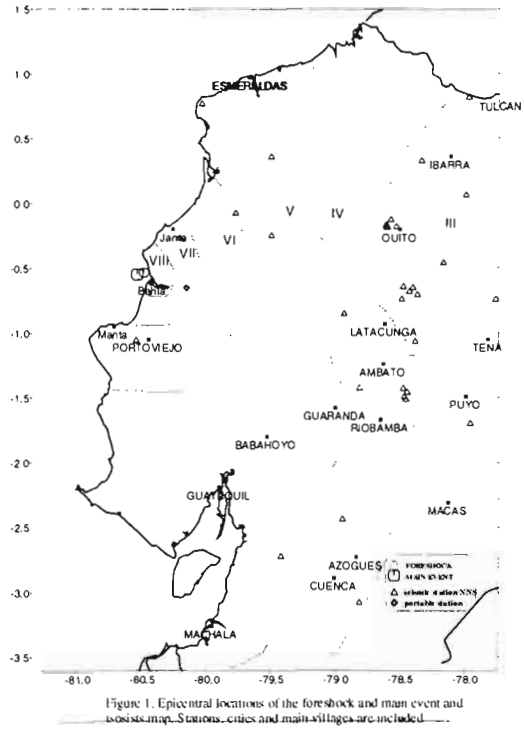

Figure 1. Epicentral locations of the foreshock and main event and isosists map. Stations, cities and main villages are included.

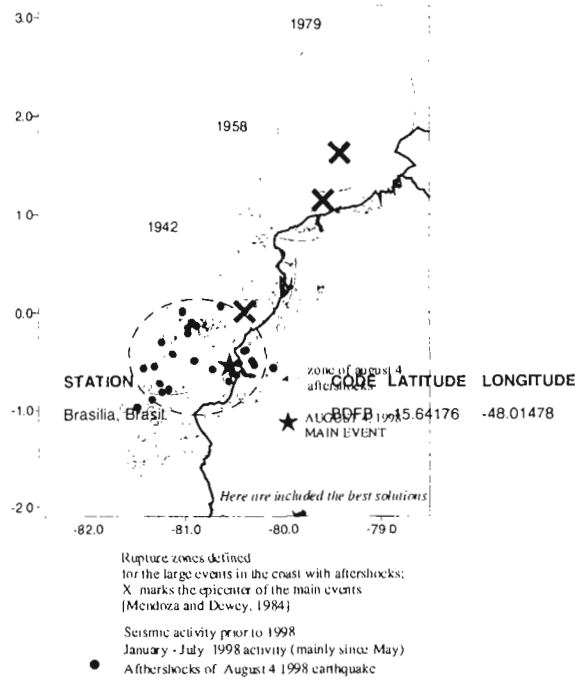

Figure 2. Relation between the past events and the instrumental seismicity

Cathedral Cave, Missouri, EU	CCM	38.0557	-91.2446
Standing Stone, Pennsylvania, EU	SSPA	40.6401	-77.8914
Paso Flores, Argentina	PLCA	-40.73277	-70.55083
Alburquerque, New Mexico, EU	ANMO	34.9462	-106.4567
Harvard, Massachusetts, EU	HRV	42.506	-71.558
Tucson, Arizona, EU	TUC	32.3096	-110.7846
Columbia College, California, EU	CMB	38.035	-120.385
Mount Kent, East Falkland Is.	EFI	-51.6753	-58.0637
Flin Flon, Canada	FFC	54.725	-101.9783
Corvallis, Oregon, EU	COR	44.5857	-123.3032
Butt Crater, Ascension Is.	ASCN	-7.9397	-14.3601
Dimbokro, Costa de Marfil	DBIC	6.67016	-4.8565
San Pablo, España	PAB	39.5458	-4.3883
Hawaii, Kipapa, EU	KIP	21.4233	-158.015
Kodiak Is., Alaska, EU	KDAK	57.7828	-152.5835
Eskdalemuir, Scottland, UK	ESK	55.3167	-3.205
College Outpost, Alaska, EU	COLA	64.8738	-147.8511

Table 1. Seismic stations used in the present analysis

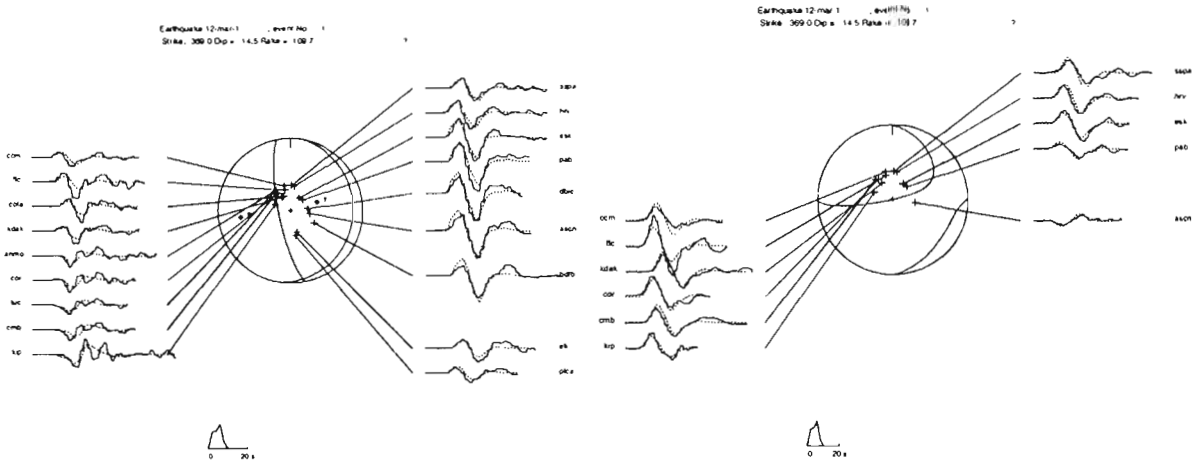

Figure 3. Comparison between the observed (solid lines) and theoretical seismograms (dashes lines) for the best fit model obtained by the simultaneous inversion of P and SH waves.

REFERENCES

Kanamori, H., and McNally, K., 1982, *Variable rupture mode of the subduction zone along the Ecuador-Colombia coast*, Bulletin of the Seismological Society of America, Vol. 72, No. 4, pp. 1241-1253.

Mendoza C. and Dewey J., 1984, *Seismicity associated with the great Colombia-Ecuador earthquakes of 1942,1958 and 1979: implications for barrier models of earthquake rupture*, Bulletin of the Seismological Society of America, Vol. 74, No. 2, pp. 577-593.

Nábêlek (1984) in Escobedo D., 1997, *El sismo del 9 de octubre de 1995 en Colima, un estudio telesísmico*, Tesis Msc., UNAM, CU, 66p. and Suárez G. y Nábêlek J., 1990, *The 1967 Caracas earthquake: fault geometry, direction of rupture propagation and seismotectonic implications*, Journal of Geophysical Research, Vol. 95, No. B11, pp. 17459-17474.

Swenson , J. and Beck S., 1996, *Historical 1942 Ecuador and 1942 Peru subduction earthquakes, and earthquakes cycles along Colombia-Ecuador and Peru subductions segments*, PAGEOPH. Vol . 146, No.1, pp. 67-101.

ACKNOWLEDGMENTS

The work performed in the Laboratorio de Geofísica in the UNAM, Mexico was supported by IRD-Quito.

EARLY MIOCENE SUBVOLCANIC STOCKS IN THE CENTRAL CHILEAN ANDES: A CASE OF SLAB MELTING?

Daniel SELLÉS MATHIEU (1)

(1) SERNAGEOMIN, Chile dselles@sernageomin.cl

INTRODUCTION

Several small stocks of andesitic to dacitic composition cut Tertiary volcanic strata along the western foothills of the Andean range near Santiago (33°-34°S). These stocks were analyzed by major and trace elements, including REE, as part of the author's thesis during the development of the "Hoja Santiago" project carried out by SERNAGEOMIN.

K-Ar and $^{40}Ar/^{39}Ar$ ages of these stocks indicate a lowermost Miocene age (20-18 Ma, Gana and Wall, 1997), immediately postdating the volcanic activity of the wall rocks (known as Abanico Fm), and previous or simultaneous to an eastward shift of the magmatic front. The geochemistry of the volcanic host rocks is consistent with a pyroxene peridotite source, and eruption through a thin crust under an extensional regime (Nyström *et al.*, 1993). In contrast, the stocks that cut these rocks show evidence of garnet as a refractory phase in their source region, which cannot be related to crustal thickening due to temporal proximity with previous thin crust conditions.

Several key geochemical features of these bodies are consistent with those of 'adakites' as defined by Defant and Drummond (1990), including high La/Yb ratios, positive Eu/Eu*, high Sr/Y, and low Y content. Such features indicate, roughly, dehydratation melting of amphibole+plagioclase with a garnet±clinopyroxene restite. Even though these data alone are not sufficient for deducing slab melting, alternative garnet bearing source regions fail to fit available data.

Slab melting requires special thermal conditions such as subduction of young slab or high shear heating. These conditions cannot be clearly stated for this time and position, but geochemical features of host volcanic rocks give a clue to hypothesize an explanation.

The Abanico Fm. calalkaline volcanics, formed under a period of low convergence rate during the Eocene to lowermost Miocene, exhibits the most MORB-like isotopic composition in

the whole Andean Orogenic Cycle in Central Chile (Nyström *et al.*, 1993). Sellés (1998) identified a group of aphanitic lava flows, dated at 26 to 23 Ma (Gana and Wall, 1997), intercalated with typical porphiritic andesites of this formation. These aphanitic flows are somewhat different from the rest of Abanico Fm. in their geochemical trends. They have a clear tholeiític differentiation trend and no amphibole fractionation, which is indicative of low magmatic $P(H_2O)$, which in turn can be related to even slower plate convergence rates (Ballhaus *et al.*, 1990). Moreover, a non-depositional gap, possibly between 23 and 21 Ma, is inferred from environmental changes revealed by plant remains contained in strata immediately below and above these lavas (Sellés and Hinojosa, 1997). This hiatus could be indicating paucity in volcanic activity and possibly no subduction at all. It is proposed, then, that during this low (or null) convergence period the downgoing slab could have experienced enough heat transfer as to mimic thermal regimes in young slabs, and to make melting possible as the slab reaches the stability limit of hornblende when normal rate subduction is resumed.

LATE PERMIAN-EARLY MESOZOIC RIFTS IN PERU AND BOLIVIA, AND THEIR BEARING ON ANDEAN-AGE TECTONICS

Thierry Sempere(1), Gabriel Carlier(1), Víctor Carlotto(2), Javier Jacay(3), Nestor Jiménez(4), Silvia Rosas(5), Pierre Soler(6), José Cárdenas(2), Nicolas Boudesseul(1)

(1) IRD (ex-ORSTOM), apartado postal 18-1209, Lima 18, Peru (ird@chavin.rcp.net.pe)
(2) Universidad Nacional de San Antonio Abad del Cusco, Cusco, Peru (carlotto@chaski.unsaac.edu.pe)
(3) Universidad Nacional Mayor de San Marcos, apartado postal 3973, Lima 100, Peru
(4) Universidad Mayor de San Andrés, casilla 6568, La Paz, Bolivia (nesjim@kolla.net)
(5) Sociedad Geológica del Perú, Arnaldo Márquez 2277, Lima 11, Peru
(6) IRD (ex-ORSTOM), 211 rue Lafayette, 75480 Paris cedex 10, France (soler@paris.orstom.fr)

KEY WORDS: Rifting, Permo-Triassic, Peru, Bolivia, Andean tectonics.

Rifting in Peru and Bolivia

Late Permian-Triassic rifting (Fig. 1) is recognized in the Eastern Cordillera of Peru (Laubacher, 1978; Noble et al., 1978; Mégard, 1978; Dalmayrac et al., 1980; Rosas and Fontboté, 1995; Rosas et al., 1997; Jacay et al., 1999) and proved to have extended into Bolivia in the Jurassic (Sempere et al., 1998). The rifting zone appears to coincide with the axis of the Eastern Cordillera in both countries. Rifting produced subsident grabens in which the Mitu Group red alluvial deposits and volcanics accumulated over preserved Late Paleozoic strata, and generated a thermal sag that progressively expanded the basin. Predominantly alkaline volcanic rocks were erupted, in relation with pluton emplacement at depth. Plutons from the Eastern Cordillera of southern Peru have a signature similar to those in the Oslo graben, an aborted rift system in Norway (Kontak et al., 1985). Most plutons are cut by younger basic dykes. South of 17°S, the rifting zone is characterized by elongated swarms of basic dykes and sills that intrude mainly Paleozoic rocks. When Mesozoic strata occur in such areas, basaltic flows, sills and/or dykes are generally also observed in the Mesozoic. In Bolivia, a basanite dyke intruding Ordovician rocks (Tawackoli, 1997) and a tholeiitic sill of large areal extension intruding Mesozoic strata (Sempere et al., 1998) were respectively dated 184 ± 4.9 Ma and 171.4 ± 4.2 Ma.

Mitu paleoenvironments include alluvial fans, rivers and (playa-)lakes. In southern areas, red continental strata overlie volcanic flows that in turn overlie the Late Permian-Triassic Ene (=Vitiacua, =Chutani) Fm. In Bolivia, infills of coeval grabens characteristically include a basal unit, generally no

more than several tens of m thick, consisting of alluvial pale sandstones and/or reddish conglomerates, which is transitionally overlain by a thick red mudstone unit of alluvial to lacustrine origin. This succession is postdated by the fluvio-eolian Ravelo Fm. Eolian sandstones, locally associated with basalts, are also found in the Lower Huancané Fm northwest of Lake Titicaca (Newell, 1949) and in the Caycay Fm of the Cusco area (Carlotto, 1998). In the Peruvian Oriente, red alluvial and eolian strata (Sarayaquillo Fm) grade westwards into the Pucará Group carbonates, which reflect a transgression that initiated in the Norian and progressed from north to south following the Mitu rift axis (Mégard, 1978; Rosas et al., 1997; Sempere et al., 1998). Basalts with within-plate signature commonly occur in the Pucará Group (Rosas et al., 1997).

In southern Peru, the Yura basin apparently originated by rifting in the Liassic (Marocco and Delfaud, 1986). The succession in the Arequipa area begins with thick lavas and subordinate continental deposits (Chocolate Fm) that resemble those of the Mitu Group, suggesting development of similar processes. Transgressive shallow-marine limestones of Toarcian-Bajocian age (Socosani Fm) overlie the Chocolate Fm (Vicente et al., 1982), just as the Norian-Liassic Pucará Group overlies the Mitu Group in the Eastern Cordillera of central Peru. These relationships and the occurrence of Sinemurian marine intercalations in the upper Chocolate Fm suggest that rifting developed in this area later than in the East--ern Cordillera. Rifting culminated in the late Bajocian-Bathonian with considerable downwarp of the Arequipa region (Vicente et al., 1982).

Deposits typical of the Yura basin are known in the Lagunillas area (15°50'S, 70°30'W), i.e. at the Western Cordillera-Altiplano transition. To the NE, outcrops at Las Huertas and Cerro Sipín (Newell, 1949), and at Yanaoco on the NW corner of Lake Titicaca (Sempere and Carlotto, unpublished), form a series of localities where a limestone-bearing unit overlies the Paleozoic basement, documenting a transgression that developed in a NE shallow-marine extension of the Yura basin.

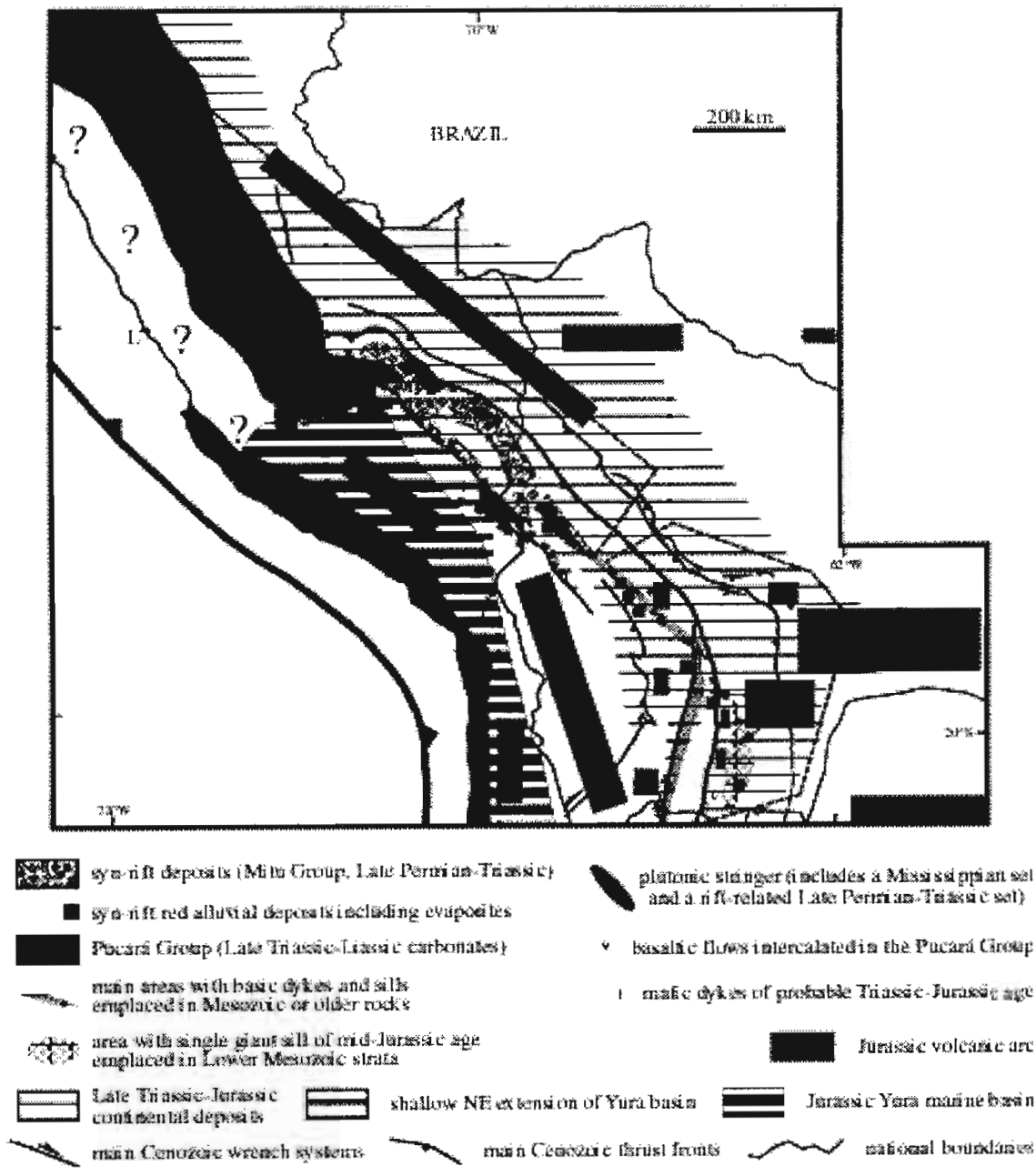

Figure 1: Principal Early Mesozoic geologic elements of central Peru and Bolivia. The axis of the eastern, Late Permian-Middle Jurassic, rift system is defined by the Mitu group, coeval granitoids, and basic dyke swarms, and approximately coincides with the axis of the Eastern Cordillera of Peru and Bolivia. Cities: C: Cochabamba, Cu: Cusco, L: Lima, P: Potosí, SC: Santa Cruz, Tu: Tupiza.

Latest Jurassic - earliest Cretaceous tectonics

The Eastern Cordillera of central Peru is traditionally believed to have behaved as a structural high since the Late Triassic (Mégard, 1978, 1987; Dalmayrac et al., 1980; Jaillard, 1994), in part because in this area the onlapping Cretaceous deposits are much thinner than to the west. The reconstruction of a Late Permian - Middle Jurassic rift system along the same area implies instead that absence of Late Triassic - Jurassic deposits reflects uplift and erosion during the latest Jurassic-earliest Cretaceous. In central Peru, this uplift is documented by the Copuma (Jacay, unpublished) and Upper Sarayaquillo conglomerates that overlie Lower to Middle Jurassic strata respectively west and east of the "Marañón geanticline"; the former unit underlies the Lower Cretaceous Goyllarisquizga Fm with an angular unconformity. Uplift of this previously rifted area points to coeval incipient rift inversion.

At the Altiplano-Western Cordillera transition (15°47'S, 70°36'W), a locally angular unconformity separates the Saracocha conglomerates and overlying transgressive Cretaceous strata from underlying marine strata of Jurassic age (Newell, 1949; Carlotto and Sempere, unpublished). A post-Dogger, pre-Tithonian, unconformity was also identified in coastal southern Peru (Rüegg, 1961). Reliable data document that the Tithonian-Berriasian interval was a period of marked tectonic instability (Mégard, 1978; Laurent, 1985; Jaillard, 1994) that was postdated by northeasterly onlap of late Early Cretaceous strata.

In Bolivia, a tectonic event was assigned to the Kimmeridgian on the basis of tentative correlation with the Kimmeridgian-age Araucan event known in the greater Neuquén basin of Argentina and Chile (Sempere, 1994). However, current research definitely shows that Mesozoic Bolivia was connected to eastern Peru, and not to southern basins. The late Early Cretaceous onlap developed on the erosional surface that separates the Serere Group from the overlying Puca Group. Evident correlation with Peru shows that this unconformity must be of latest Jurassic-earliest Cretaceous age.

Influence on Andean tectonics

Reconstruction of rifted areas in the Andes of Peru and Bolivia sheds some light on the structure and building history of the Andes at these latitudes. In the Yura basin, Late Cretaceous-Early Paleogene compressional tectonics (Vicente, 1989) probably resulted from inversion of the southwestern Jurassic rift. The Eastern Cordillera of Peru and Bolivia appears to result from inversion of the eastern rift. Compressional failure of this rift system in the late Oligocene explains the apparent jump in shortening location observed by Sempere et al. (1990). The Altiplano, which underwent little Cenozoic surface shortening, appears as a paleogeographic block that was limited by 2 rift systems during most of the Mesozoic (Fig. 1). In the central and northern Oriente region of Peru, Cenozoic structures proceed from reactivation of preexistent faults (Laurent, 1985). In the Eastern Cordillera of central Peru, ultramafic rocks, including peridotites, occur mainly within locally high-grade Precambrian metamorphics but are possibly of Early Mesozoic age (Sempere et al., 1998; Jacay et al., 1999); in any case, these occurrences suggest that rift inversion uplifted relatively deep levels of the lithosphere in this area.

Because rift inversions can affect different structural depths, the amount of inversion-derived uplift can also be perceived from the distribution of Late Paleozoic-Triassic granitoids. Exposed granitoids nearly disappear north of 6°S, although the rift system continues into the Ecuadorian foreland basin (P. Baby, pers. com.), suggesting that shortening in the Eastern Cordillera considerably decreases north of this latitude. Shortening and/or depth of rift inversion in the Eastern Cordillera apparently also decrease southeast of 17-18°S, where exposed granitoids disappear and only basic dyke swarms crop out, because this segment of the Eastern Cordillera, although of tectonic origin, is geomorphically not a true, high and narrow, cordillera but a broad highland region affected by large-scale erosional surfaces.

Many thrusts in the Eastern Cordillera probably originated by compressional reactivation of earlier normal faults. The geometry of the Late Permian-Jurassic rift faults presumably determined the vergence of many Andean-age thrusts, as SW(resp. NE)-vergent thrusts are predominant southwest (resp. northeast) of the rift axis. In the N-trending segment of the Eastern Cordillera, south of 19°S, tectonic displacements were possibly more transpressional, reactivating ancient wrench faults.

REFERENCES

Carlotto, V. 1998. Evolution andine et raccourcissement au niveau de Cusco (13°-16°S, Pérou). Thèse de doctorat, Université de Grenoble, France, 159 p. + figs.

Dalmayrac, B., Laubacher, G., Marocco, R. 1980. Caractères généraux de l'évolution géologique des Andes péruviennes. Travaux et Documents de l'ORSTOM, Paris, v. 122, 501 p.

Jacay, J., Sempere, T., Carlier, G., Carlotto, V. 1999. Late Paleozoic - Early Mesozoic plutonism and related rifting in the Eastern Cordillera of Peru. IV ISAG, Göttingen, this volume.

Jaillard, E. 1994. Kimmeridgian to Paleocene tectonic and geodynamic evolution of the Peruvian (and Ecuadorian) margin. *In* Cretaceous tectonics of the Andes, J.A. Salfity (ed.), Vieweg, p. 101-167.

Kontak, D.J., Clark, A.H., Farrar, E., Strong, D.F. 1985. The rift associated Permo-Triassic magmatism of the Eastern Cordillera: a precursor to the Andean orogeny. *In* Magmatism at a plate edge: the Peruvian Andes, W.S. Pitcher, M.P. Atherton, J. Cobbing and R.D. Beckinsale (eds.), Londres, p. 36-44.

Laubacher, G. 1978. Géologie de la Cordillère Orientale et de l'Altiplano au nord et nord-ouest du lac Titicaca (Pérou). Travaux et Documents de l'ORSTOM, v. 95, 217 p.

Laurent, H. 1985. El pre-Cretáceo en el Oriente peruano: su distribución y sus rasgos estructurales. Boletín de la Sociedad Geológica del Perú, v. 74, p. 33-59.

Marocco, R., Delfaud, J. 1986. L'évolution du secteur de Cuzco-Arequipa (Pérou) expliquée à la lumière du modèle de rift continental. Abstract, XI Réunion Annuelle des Sciences de la Terre, Clermont-Ferrand, France, p. 121.

Mégard, F. 1978. Etude géologique des Andes du Pérou central. Travaux et Documents de l'ORSTOM, Paris, v. 86, 310 p.

Mégard, F. 1987. Cordilleran Andes and marginal Andes: a review of Andean geology north of the Arica elbow (18°S). *In* Circum-Pacific orogenic belts and evolution of the Pacific ocean basin, J.H.W. Monger & J. Francheteau (eds.), American Geophysical Union, Geodynamic Series, v. 18, p. 71-95.

Newell, N.D. 1949. Geology of the Lake Titicaca region, Peru and Bolivia. Geological Society of America Memoir, v. 36, 111 p.

Noble, D.C., Silberman, M.L., Mégard, F., Bowman, H.R. 1978. Comendite (peralkaline rhyolites) in the Mitu Group, central Peru: Evidence of Permian-Triassic crustal extension in the Central Andes. U.S. Geological Survey Journal of Research, v. 6, p. 453-457.

Rosas, S., Fontboté, L. 1995. Evolución sedimentológica del Grupo Pucará (Triásico superior-Jurásico inferior) en un perfil SW-NE en el centro del Perú. Sociedad Geológica del Perú, vol. jubilar A. Benavides, p. 279-309.

Rosas, S., Fontboté, L., Morche, W. 1997. Vulcanismo de tipo intraplaca en los carbonatos del Grupo Pucará (Triásico superior-Jurásico inferior, Perú central) y su relación con el vulcanismo del Grupo Mitu (Pérmico superior-Triásico). IX Congreso Peruano de Geología, p. 393-396.

Rüegg, W. 1961. Hallazgo y posición estratigráfico-tectónica del Titoniano en la costa del sur del Perú. Boletín de la Sociedad Geológica del Perú, v. 36, p. 203-208.

Sempere, T. 1994. Kimmeridgian? to Paleocene tectonic evolution of Bolivia. *In* Cretaceous tectonics in the Andes, J.A. Salfity (ed.), Vieweg, p. 168-212.

Sempere, T. 1995. Phanerozoic evolution of Bolivia and adjacent regions. *In* Petroleum Basins of South America, A.J. Tankard, R. Suárez-Soruco, y H.J. Welsink (eds.), AAPG Memoir 62, p. 207-230.

Sempere, T. 1999. Discussion of "Sediment accumulation on top of the Andean orogenic wedge: Oligocene to late Miocene basins of the eastern Cordillera, southern Bolivia" (Horton, 1998). Geological Society of America Bulletin, in press.

Sempere, T., Hérail, G., Oller, J., Bonhomme, M.G. 1990. Late Oligocene-early Miocene major tectonic crisis and related basins in Bolivia. Geology, v. 18, p. 946-949.

Sempere, T., Carlier, G., Carlotto, V., Jacay, J. 1998. Rifting Pérmico superior - Jurásico medio en la Cordillera Oriental de Perú y Bolivia. Memorias, XIII Congreso Geológico Boliviano, Potosí, v. 1, p. 31-38.

Tawackoli, S. 1997. Andine Entwicklung der Ostkordillere in der Region Tupiza (Südbolivien). Ph.D. dissertation, Freie Universität Berlin, 116 p.

Vicente, J.-C., Beaudoin, B., Chávez, A., León, I. 1982. La cuenca de Arequipa (Sur Perú) durante el Jurásico-Cretácico inferior. V Congreso Latinoamericano de Geología, v. 1, p. 121-153.

Vicente, J.-C. 1989. Early Late Cretaceous overthrusting in the Western Cordillera of southern Peru. *In* Geology of the Andes and its relation to hydrocarbon and mineral resources, G.E. Ericksen, M.T. Cañas and J.A. Reinemund (eds.), Houston, v. 11, p. 91-117.

NEOGENE SILICIC MAGMATISM IN THE SOUTHERN CENTRAL ANDES: NEW ASPECTS OF IGNIMBRITE FORMATION

Wolfgang SIEBEL (1), Wolfgang SCHNURR(2), Knut HAHNE(1), Bernhard KRAEMER(2), Robert B. TRUMBULL(1)

(1) GFZ Potsdam, Telegrafenberg, 14743 Potsdam; siebel@gfz-potsdam.de
(2) FU Berlin, Malteserstr. 74–100, 12249 Berlin; schnurr@zedat.fu-berlin.de

KEY WORDS: Arc magmatism, Andes, Ignimbrites, Isotope System, Salar de Antofalla, Salar de la Isla

INTRODUCTION

Neogene volcanism in the central Andes is characterized by composite andesite-dacite strato-volcanoes and by large amounts of coeval, felsic ignimbrites. A number of studies have focussed on the large volume, crystal-rich dacite-rhyodacite ignimbrites and concluded that these rocks were formed dominantly by melting of the crust (e.g., Francis & Hawkesworth 1994). Less attention has been spent on the smaller occurrences of crystal-poor rhyolitic ignimbrites. This study presents geochemical and isotopic data of several small volume (<10km^3) and moderate volume (<100 km^3) rhyolitic ignimbrite sheets from the southern central Andes between 25°20´ – 26°30´ S and 67°30´ – 69°30´ E. Our goal was to constrain the petrogenesis of this type of calc-alkaline magmatism and in particular, to assess its relationship with the arc andesite-dacite volcanoes and with the large-volume intermediate ignimbrites (> 100 km^3). The ignimbrites studied occur in the active volcanic arc around the Salar de la Isla area (SIS) in Chile, and behind the arc in the Salar de Antofalla area (SAF), Argentina. Both areas are underlain by exessively thick continental crust of 50 – 70 km. With the exception of the early Miocene Rio Frio ignimbrite (SIS) the ignimbrites erupted between 13 Ma and Recent.

RESULTS

The rhyolitic ignimbrites in both areas are characterized by initial $^{87}Sr/^{86}Sr$ ratios (0.7066 to 0.7090) and •Nd(t) values (–2.4 to –5.1) that are significantly different from those of the intermediate, caldera-sourced ignimbrites of Co.Galán ($^{87}Sr/^{86}Sr(t)$ = 0.7107 to 0.7117, •Nd(t) = –7.6 to –9.5, Francis et al., 1989) and LaPacana ($^{87}Sr/^{86}Sr(t)$ = 0.7084 to 0.7132, •Nd(t) = –6.8 to –8.9, Siebel et al. 1998), which have been interpreted to represent dominantly crustal melts. Since Co. Galán is located in the SAF area close to the rhyolitic ignimbrites we have studied, it is unlikely that the isotopic differences observed are due to different crustal compositions.

The isotopic composition of the SIS and SAF ignimbrites resemble those of the younger (10 Ma to Recent) arc andesites in the same area. This similarity suggests that the ignimbrite magmas may have formed directly by differentiation from an intermediate precursor without a major input from crustal melting. Major and trace element data from the andesites and ignimbrites define differentiation trends which can be reproduced by a fractionation crystallization model. The modelling shows that about 40–50% fractional crystallization of an uncomtaminated arc andesite magma can produce the ignimbrite compositions.

One striking feature of the Neogene arc volcanic centers in the SIS area is a systematic variation in chemical and isotopic composition with age. The younger andesites and dacites (10 Ma to Recent) have higher Rb, Cs and Th contents, higher initial $^{87}Sr/^{86}Sr$ and $^{206}Pb/^{204}Pb$ ratios and lower •Nd(t) values which are interpreted as reflecting a greater degree of crustal contamination of these magmas compared with andesites from older (20 to 10 Ma) centers (Trumbull et al., 1999). The SIS and SAF ignimbrites show no such change in composition with age. Furthermore, there is a geographic variation in composition between the andesite-dacite stratovolcanoes in the arc (SIS) and backarc (SAF) areas (Wittenbrink & Kraemer, 1996). Apart from differences in Nb and Ta concentrations, we observed no corresponding change in composition between the rhyolitic ignimbrites in the SIS and SAF areas. The fact that the ignimbrites in both the arc and backarc areas have isotopic compositions which suggest an affinity to arc andesite magmas might be interpreted to indicate that the SAF ignimbrites were derived from the main arc further west, but geologic field evidence rules out long-range transport for many of the localities.

CONCLUSIONS

Highly silicic, relatively crystal-poor ignimbrites are widespread in the southern CVZ, both in the main arc and back-arc settings. These ignimbrites are geochemically more differentiated than the large, crystal-rich intermediate ignimbrites such as those from the Co. Galán, La Pacana and Panizos calderas (Francis et al., 1989; de Silva, 1987; Ort et al., 1996), but their Sr and Nd isotopic compositions more

closely resemble those of coeval andesite volcanoes of the active cordillera. Based on this observation and supporting geochemical modelling, we argue that ignimbrite formation in the central Andes can be related to two different petrogenetic processes. Whereas the SIS and SAF-type rhyolitic ignimbrites were generated from an arc andesitic magma by fractional crystallization with relatively minor crustal contamination, the large-volume ignimbrite magmas of Galán type are dominantly crustal melts. Radiogenic isotope ratios have proven to be an effective means for distinguishing between these two different types of ignimbrites.

REFERENCES

deSilva, S.L. 1987. Large volume explosive silicic volcanism in the central Andes of N. Chile. Unpublished PhD thesis, Open University, U.K. 409 pp.

Francis P.W., Hawkesworth C.J. 1984. Late Cenozoic rates of magmatic activity in the central Andes and their relationship to continental crust formation and thickening. J Geol Soc London, 151, 845–854.

Francis P.W., Sparks R.S.J., Hawkesworth C.J., Thorpe, R.S., Pyle D.M., Tait S.R., Mantovani M.S., McDermott F. 1989. Petrology and geochemistry of volcanic rocks of the Cerro Galán caldera, northwest Argentina. Geol Mag, 126, 515–547.

Ort M.H., Coira B.L., Mazzoni M.M. 1996. Generation of a crust-mantle magma mixture: magma sources and contamination at Cerro Panizos, central Andes. Contrib Mineral Petrol, 123, 308–322.

Siebel, W., Trumbull, R.B., Lucassen, F., Emmermann, R., Haase, G., Hahne, K., Kraemer, B., Lindsay, J.M., Schmitt, A., Schnurr, W., Wolter, M. 1998. Isotopic contrasts in Neogene ignimbrites from the central Andes (23°S–27°S): source heterogeneity or different petrogenesis? Terra Nostra, 98/5, 152.

Trumbull R.B., Wittenbrink R., Hahne K., Emmermann R., Büsch W., Gerstenberger H., Siebel W. 1999. Evidence for Late Miocene to Recent contamination of arc andesites by crustal melts in the Chilean Andes (25–26°S) and its geodynamic implications. J South Am Earth Sci., in press.

Wittenbrink R., Kraemer B. 1996. Variation in time and space of magmagenesis of Neogene to Recent volcanic rocks in the southern Central Volcanic Zone (CVZ) of the Andes (24°–26°S, 67°–69°W). V.M. Goldschmidt Conference, Heidelberg, 31. 3. - 4.4., J Conf Abstracts, 1 (1), 682.

DOMAINS WITH UNIFORM STRESS IN THE WADATI-BENIOFF ZONE OF ANDEAN SOUTH AMERICA

Alice SLANCOVÁ, Aleš ŠPIČÁK, Jiří VANĚK and Václav HANUŠ (1)

(1) Geophysical Institute, Academy of Sciences of the Czech Republic
Boční II/1401, 141 31 Praha 4, Czech Republic, Fax: +420-2-71761549, e-mail: alice@ig.cas.cz

KEY WORDS: state of stress, Andean Wadati-Benioff zone, focal mechanisms

INTRODUCTION

Focal mechanisms of earthquakes are indicators of stresses acting in the lithosphere. Variations of focal mechanisms are probably connected with changes of the state of stress. Focal mechanisms in the Wadati-Benioff zone (WBZ) dominantly show the following pattern: firstly, either P-axes (represent compression) or T-axes (represent extension) are parallel to inclined WBZ; secondly, deep parts of WBZ undergo slab-parallel compression; thirdly, intermediate parts of WBZ undergo either a slab-parallel compression or extension depending on the studied region (Isacks and Molnar, 1971). This general pattern is disturbed in some parts of WBZ, where the plunge of the above mentioned axes differs from the dip of WBZ, and very often the focal mechanisms indicate strike-slip faulting or a combination of normal or reverse and strike-slip faulting.

The aim of our work is to determine the detailed variations of stress in the Andean Wadati-Benioff zone in the latitude range 10°N-40°S. The work is based on the analysis of the distribution of seismic activity and on the orientation of P- and T- axes. By a thorough analysis of the distribution of earthquake foci we separated events that form WBZ, and studying focal mechanisms we defined groups of events where earthquake foci with similar focal mechanisms occurred. Such groups are taken as basic units - we call them domains - for further determination of the state of stress in WBZ. Because P, B and T axes of fault plane solutions are only an approximation of the principal stress axes, we used the method of Gephart and Forsyth (1984) for estimating the state of stress in individual domains.

DATA AND METHOD

For the analysis of the distribution of seismic activity, International Seismological Centre (ISC) data for years 1964-95 were used. The stress distribution in WBZ was studied by means of P- and T- axes from the Harvard Centroid Moment Tensor Solutions (HCMT) for years 1977-1997. Altogether 700 events with HCMT were available for the whole Wadati-Benioff zone in the ISC magnitude range 4.7-6.9.

To distinguish between earthquakes occurring in the downgoing oceanic lithosphere and those situated in the overlying continental wedge, 170 vertical cross-sections perpendicular to the axis of the Peru-Chile trench were used. The width of these swaths was 0.25°-0.5° (approx. 30-50 km). Comparing the neighbouring cross-sections, the dip of WBZ was estimated; it was also possible to distinguish between earthquakes occurring in the downgoing oceanic lithosphere and those situated in the overlying continental wedge. Only seismic events occurring in WBZ are depicted in the map of epicentres (Fig. 1).

The state of stress in the descending lithosphere was estimated by the method of Gephart and Forsyth (1984) based on fault plane orientations and slip directions as indicated by fault plane solutions. The method enables (a) to determine the orientation of principle stress components $\sigma 1$ (maximum

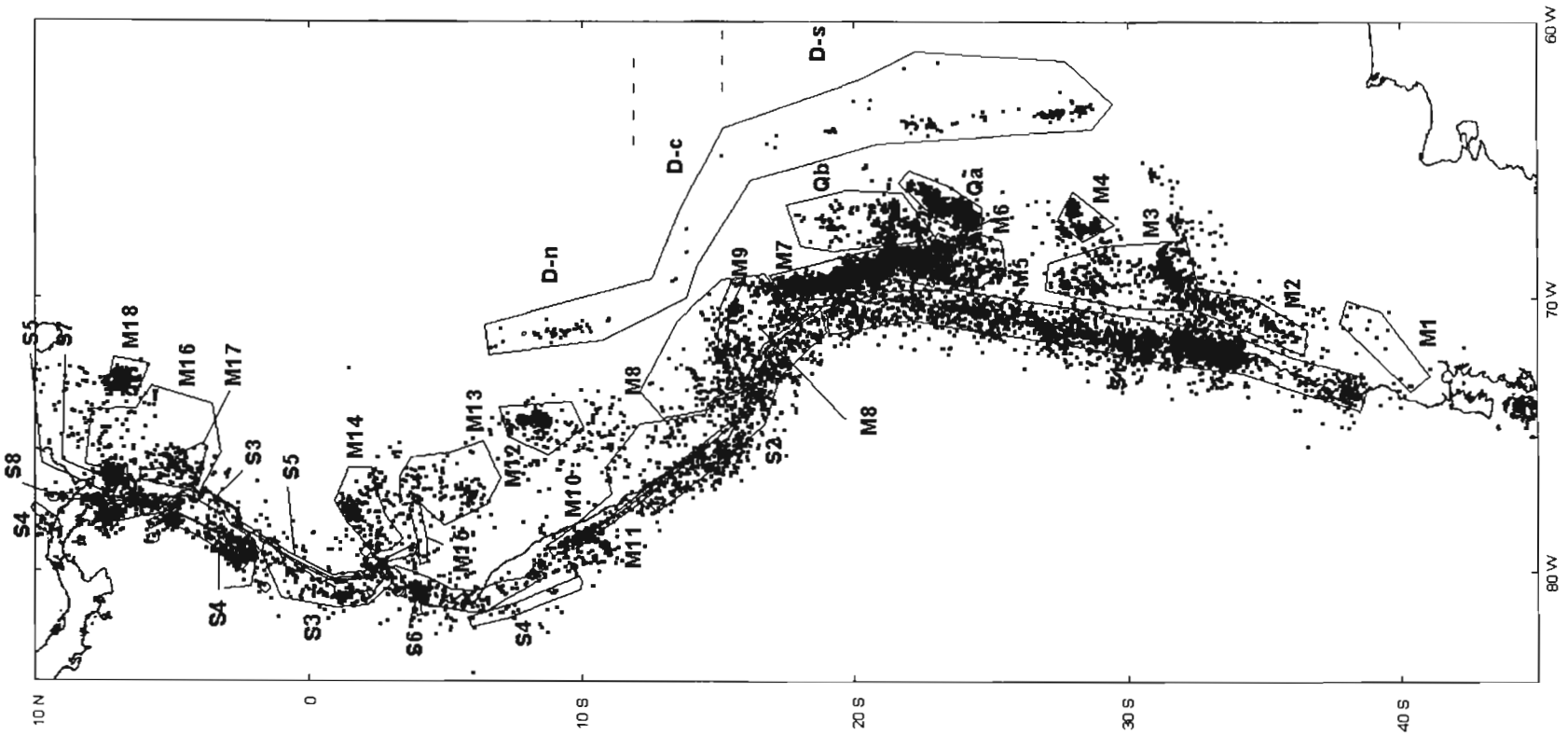

Fig. 1. Distribution of epicentres of earthquakes located in the Wadati-Benioff zone during the period 1977-1995. Zones S1-S8, M1-M18, Q (Qa and Qb), D denote domains with uniform state of stress. Isolated individual events shown by circles are grouped in domain S9 which probably represents the state of stress on fault structures. Areas that are not included in any domain do not contain a sufficient number of earthquakes with available focal mechanisms.

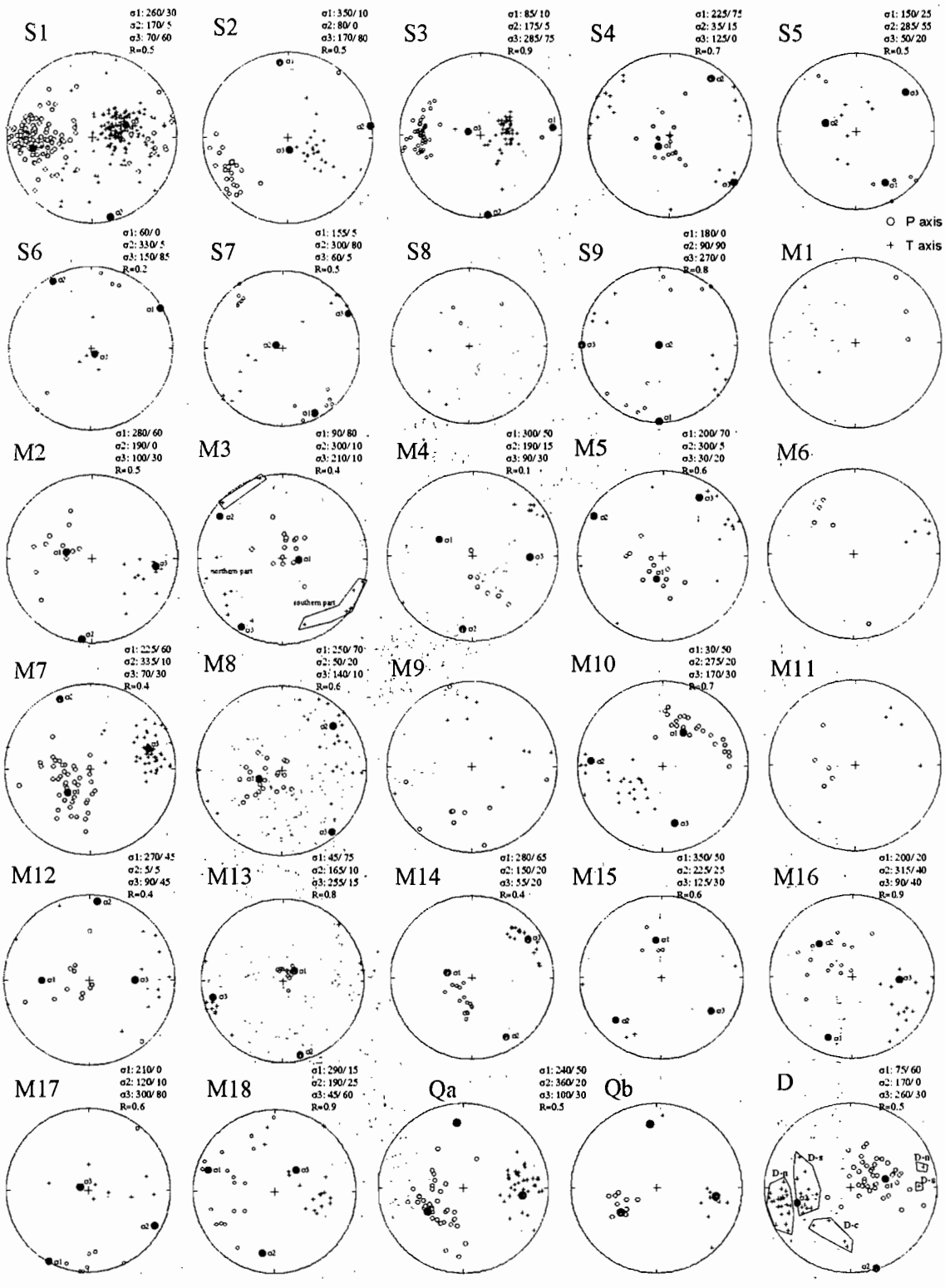

Fig. 2. P and T axes of focal mechanisms in the stereographic projection to the lower hemisphere for each domain. The determined principal stress axes σ1, σ2 and σ3 are denoted by black dots in the graph and its position in rounded angles is given in the left top corner of each graph.

compression), $\sigma 2$ (medium compression), $\sigma 3$ (minimum compression), (b) to determine the parameter $R = (\sigma 2-\sigma 1) / (\sigma 3-\sigma 1)$ relating the principal stress magnitudes ($R \in \langle 0,1 \rangle$, for R=1: $\sigma 2=\sigma 3$, for R=0: $\sigma 2=\sigma 1$), and (c) to discriminate the fault plane from the auxiliary plane.

RESULTS

The events with the similar orientation of P- and T- axes were grouped together in 30 individual domains (Fig.1). In each domain, the events show a similar tectonic pattern which differs from the neighbouring domains (Fig.2). The state of stress was determined in domains with sufficient amount of data. According to plunges of principal stress axes it is suitable to distinguish four main parts of WBZ: 1) depth range 0-100 km, domains S1-S9, 2) depth range 50-200 km, domains M1-M18, 3) depth range 200-300 km, domain Qa and Qb, 4) depth greater than 500 km, domain D. The azimuth of $\sigma 1$ is in the direction of the Nazca or Cocos plate motion for most domains.

The state of stress in the depth range 0-100 km is characterized mainly by long domains S1, S2 and S3 that follow the west margin of the South American continent. The plunge of $\sigma 1$ is 10°-30° to W, of $\sigma 3$ 60°-90° to E, focal mechanisms show reverse faulting. The state of stress is changed in smaller domains as S4, characterized by normal faulting, or in domains S5, S7, S9, characterized by strike-slip faulting and in domains S6, S8 where the compression does not act in the W-E direction.

The state of stress in the depth range 50-200 km varies accordingly to variations of the dip of WBZ. The $\sigma 1$ axis is perpendicular to the plane of WBZ, the $\sigma 3$ axis is parallel to the dip of WBZ. The faulting is normal. This pattern is well seen in domains M2, M3, M5, M7, M8, M11-M14, M16, M18. Significant strike-slip component appears in domains M4, M6, M15. The $\sigma 1$ axis parallel to the dip of WBZ is typical for domains M1 and M10. The compression in the N-S direction is evident in domains M9 and M17.

Only domain Q (Qa and Qb) represents the state of stress in WBZ in the depth range 200-300 km. The faulting is normal. The plunge of $\sigma 1$ is 50° to W and is nearly perpendicular to the slab, while the plunge of $\sigma 3$ is 30° to E and is parallel to the slab.

The depth range 500-600 km is characterized by domain D. The plunge of $\sigma 1$ is 60° to E, of $\sigma 3$ 30° to W. This large domain is stress stable from 6°S to 40°S, even though changes of stress with the curvature of the domain might be expected.

The state of stress in the Andean Wadati-Benioff zone keeps the general pattern of stress observed in subduction zones (Isacks and Molnar, 1971). Changes in this stress pattern could be caused by a reactivation of faults in WBZ (M6, S6, S9), by local variations of the shape of the subduction zone (M9, M17) or by an atypical contact with surrouding medium (M10).

Acknowledgements: The present work has been performed in the framework of IGCP project No. 345 „Andean Lithospheric Evolution". The financial support of Grant Agency of the Czech Republic under Grant 205/95/0264 and of the Grant Agency of the Academy of Sciences of the Czech Republic under Grant A3012805 is acknowledged.

REFERENCES

Gephart, J. W. and Forsyth, D. W. 1984. An improved method for determining the regional stress tensor using earthquake focal mechanism data: application to the San Fernando earthquake sequence. J. Geophys. Res., 89, 9305-9320.

Isacks, B. and Molnar, P. 1971. Distribution of stresses in the descending lithosphere from a global survey of focal mechanisms solutions of mantle earthquakes. Rev. Geophys. Space Phys., 9,103-174.

NEW PALEOMAGNETIC DATA FROM NORTHERN CHILE: FURTHER SPATIAL-TEMPORAL CONSTRAINTS ON TECTONIC ROTATIONS IN THE REGION.

R. SOMOZA(1) and A. TOMLINSON(2)

(1) Departamento de Geología, FCEyN, Universidad de Buenos Aires, Argentina.
(2) Servicio Nacional de Geología y Minería, Santiago, Chile.

KEY WORDS: Paleomagnetism, Tectonics, Rotations, Northern Chile

INTRODUCTION

Paleomagnetic studies in northern Chile have shown the systematic presence of clockwise vertical-axis rotations from 28/30°S to 22°S. On the other hand, counterclockwise tectonic rotations are found in northernmost Chile (near 19°S) and further north along the Peruvian margin (Fig. 1). The origin of this orogen-scale pattern of rotations remains controversial. Proposed tectonic models comprise small-block rotations in response to margin-parallel shear related to oblique convergence, oroclinal bending of the Central Andean forearc linked to Late Cenozoic differential shortening in the eastern foreland thrust belt or a combination of both these mechanisms.

However, several aspects of the paleomagnetic data set in Figure 1 remain poorly constrained. For instance, the location and nature of the boundary between clockwise and counterclockwise rotations in northern Chile are unknown. The spatial distribution of paleomagnetic data from previous studies leave the boundary to being poorly constrained to a gap between 22°S and 19°S (open symbols in Figure 1). In this study we present new data which reduce the amount of gap (shaded symbols near Pica in Figure 1). Another poorly know feature is the tim-

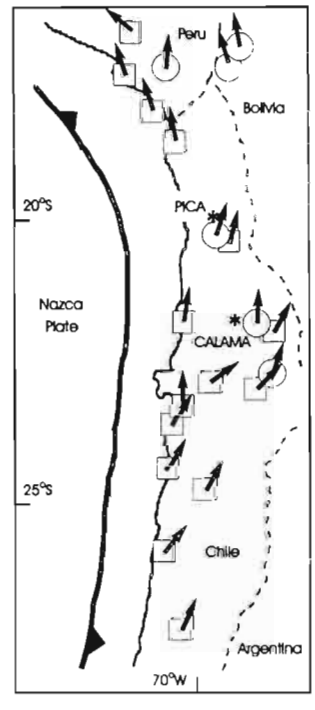

Figure 1. Tectonic rotations in northern Chile and southernmost Perú. Squares (circles) indicate paleomagnetic data from Mesozoic-Lower Tertiaty (Upper Tertiary) rocks. Arrows indicate amount and sense of rotation. Data from this study are shaded.

ing of rotations. The Central Andean orogen has had a protracted evolution since the Mesozoic, thus the data in Figure 1 show the final state of a potentially long and complex rotation history with multiple superimposed rotational events. Most paleomagnetic studies in northern Chile have either assumed, without testing, that rotations is associated with the age of local deformation or not addressed the problem of timing. The timing of rotations can be constrained by sampling different levels of a single structurally coherent stratigraphic section. If the timing of the aquisition of remanence can be determined and is distinct for different units in the section, then a rotation history for the section is defined.

For this study we performed paleomagnetic sampling in two areas of northern Chile: near Pica (20°30'S) and east of Calama (at 22°S) (Fig. 1).

In the area of Pica (20°30'S, Figure 1), we sampled strongly folded rocks of the Upper Cretaceous Cerro Empexa Formation in both limbs of a N-S trending, kilometric scale syncline. We also sampled Upper Eocene dikes that cut the Cretaceous section, and uppermost Oligocene to Lower Miocene (24-21 Ma) levels of the nearly flat-lying Altos de Pica Formation which unconformably overlie the Cretaceous rocks. Thus, 36 block samples were taken from different Cretaceous sedimentary beds in both limbs of the syncline. Nine samples were taken from two Eocene andesitic dikes and baked host rocks in the eastern limb limb of the syncline. Sampling in the Lower Miocene rocks was more difficult due to the scarcity of fine-grained sedimentary beds. We took 80 samples from 12 different sedimentary beds and ignimbrite sheets. In this case, each stratigraphic level is considered as a single site. Paleomagnetic results are shown in Figure 2 (Pica). Cretaceous rocks from both limbs of the syncline show a high-temperature, normal-polarity component of magnetization carried by hematite (Fig. 2a, northern hemisphere). The ratio of the precision parameters ($k_{unfolded}/k_{in\text{-}situ} = 4$) indicates that this component is pretectonic at a 99% confidence level. On the other hand, samples from the eastern limb show an additional reverse-polarity component carried by magnetite, the direction of which is almost identical to the magnetization found in the dikes and baked sedimentary rocks (Fig. 2a, southern hemisphere). This strongly suggests that the reversed component in the Cretaceous rocks of the eastern limb was acquired during the Eocene intrusive activity. On the basis of regional geology we suggest that this remagnetization is posttectonic. Paleomagnetic behavior of most Lower Miocene rocks was straightforward. Normal and reversed polarities were found in the ignimbrites, whereas the few sampled sedimentary layers showed only reversed polarity (Fig. 2b). All the paleomagnetic directions obtained in the Pica area show similar declination anomalies, irrespective of the time of remanence acquisition (Fig. 2). This suggests that this area has undergone about 25° clockwise rotation after the Early Miocene. Thus, the rotation postdates major deformation in this area which folded the Cretaceous rocks prior to deposition of the Lower Miocene section, but it could be coeval and associated with major deformation further east in the Bolivian Altiplano.

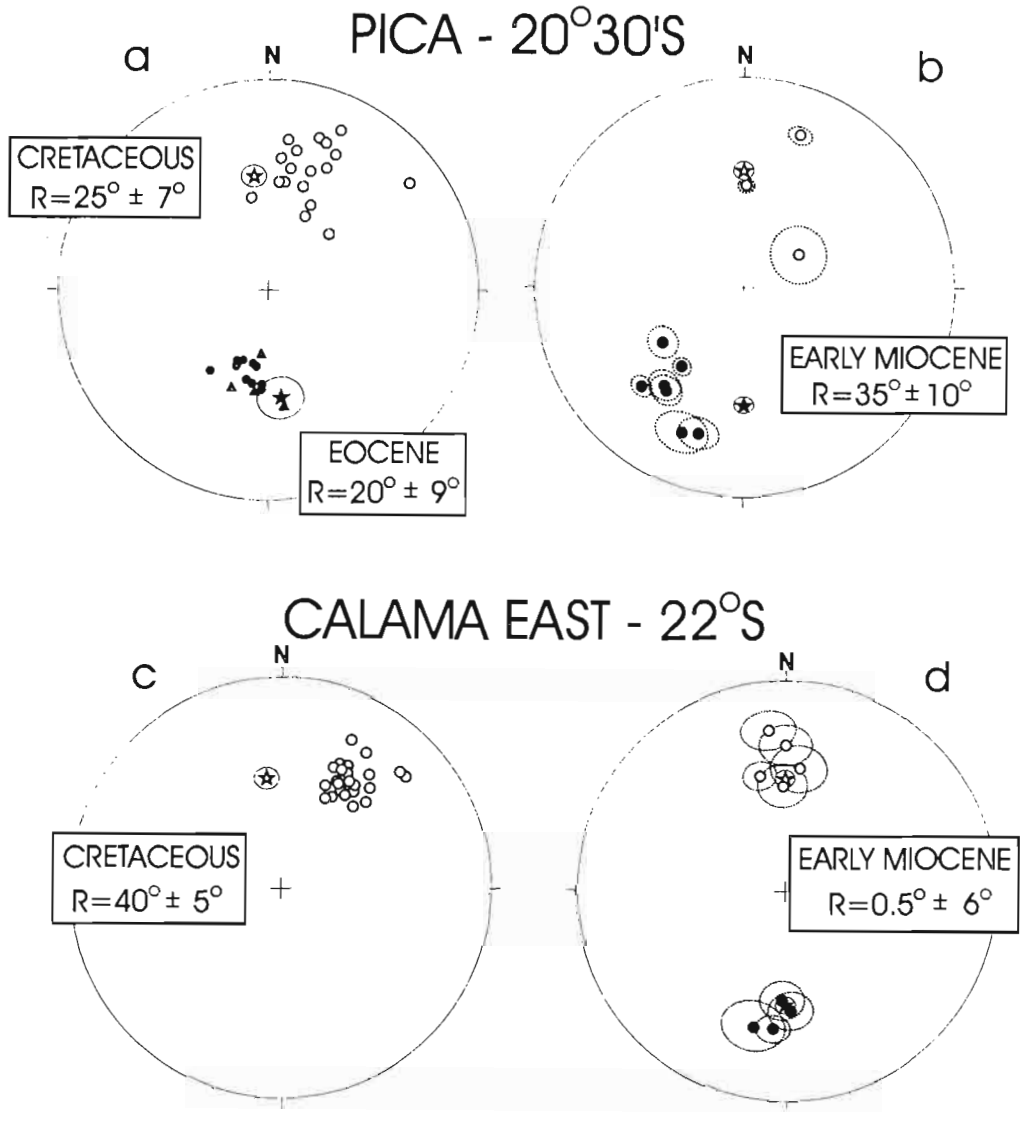

Figure 2. Paleomagnetic results and calculated rotations. Open (closed) symbols indicate projection onto the upper (lower) hemisphere. Stars indicate the expected paleofield direction at each locality for each particular time, shaded circle is the correspondent 95% confidence interval. Both normal and reversed expected directions are shown for the Early Miocene. Only the normal expected direction is shown for the Late Cretaceous, and the reversed expected direction for the Eocene (ca. 50 Ma).

a) Circles are the directions from samples of the Cretaceous Cerro Empexa Formation. Triangles are the directions from Upper Eocene dikes and baked sedimentary host rocks. In the northern hemisphere are the unfolded, high-temperature directions (interpreted as Cretaceous magnetizations) obtained from different samples in both the limbs of the syncline. In the southern hemisphere are the reversed components obtained from samples of the eastern limb and directions from dikes and baked host rocks (all interpreted as Eocene magnetizations). **b**) directions from sites of the Lower Miocene Altos de Pica Formation with their 95% confidence intervals. **c**) tilt-corrected directions from samples of the Cretaceous Purilactis Formation. **d**) directions from sites of the Lower Miocene rocks in the El Loa Formation and their 95% confidence intervals.

Note: the Eocene directions (remagnetization) are presented in geographical coordinates. The remainder results are referred to the paleohorizontal.

East of Calama (22°S, Figure 1) we sampled the Cretaceous Purilactis Formation in the footwall block of an Eocene thrust. The Eocene structures are covered by rocks of the El Loa Formation, which show a gentle westward dip. Early Miocene Ar/Ar biotite ages (20-19 Ma) were obtained from some tuffs of the El Loa Formation in this area. A total of 24 samples were taken from different fine-grained sedimentary beds of the Purilactis Formation, and a total of 78 samples, grouped in 9 sites, were taken from the overlying Miocene rocks. In the latter case, each site comprises stratigraphically closely spaced fine-grained beds which are separated from the next site by a several meter thick succession of coarse-grained layers. The Cretaceous rocks show a single, normal-polarity component carried by hematite (Fig.2c). The Lower Miocene rocks also display univectorial behavior with both normal and reversed polarities (Fig. 2d), and magnetite as the main carrier. The tilt-corrected mean-direction of the Cretaceous rocks indicates a clockwise rotation of about 40°, whereas paleomagnetic data from the Lower Miocene rocks do not show evidence of rotation. This implies that the tectonic rotation in the Cretaceous section is older than Late Cenozoic and may have occurred during the major Eocene deformation in the area.

Our results indicate that:

1) clockwise tectonic rotations are present in northern Chile as far north as 20° 30'S (Pica area), suggesting that the location of the boundary between clockwise and anticlockwise paleomagnetically detected rotations in the Central Andean forearc is restricted to a narrow region of 1.5° latitude or less.

2) clockwise tectonic rotations in northern Chile occurred at different times in different localities, and may be related to both local deformation (rotation in the Cretaceous rocks of the Calama basin area) and far-field deformation (Miocene of Pica).

3) there is at least one region (the Miocene Calama basin) which has not experienced paleomagnetically resolvable rotation during the Late Cenozoic, suggesting that any large-scale rotation of northern Chile related to crustal shortening on the eastern side of the Central Andes is either very low or nonuniform.

This research was funded by FONDECYT grant # 1970002.

SALAR DE ANTOFALLA:
Transpressive Regime in the Argentine Puna.

José Angel SOSA GÓMEZ

(1) Universidad Nacional de Tucumán Sosago@csnat.unt.edu.ar

ABSTRACT

The Salar de Antofalla is a north-south depression in the northwest Puna plateau in the Argentine Province of Catamarca. It is an endorheic basin located in a intraarch position.

The morphology of the salar is unique in the Puna; its length reaches 140km the brightest section is 10km in a shape like a streached "Z". The volcanic chain represented by many volcanic strata is well developed in the W margin, although the E margin volcanic activity is fissural. The emphasis of these interpretation is a strike-slip structural environment in response to the salar shaped morphology.

Most of the endorheic basins in the Puna are developed in depressions linked to reverse faults in the case of the Salar de Antofalla. It was developed in a simultaneously compressive and dextral strike slip regimen which, uplifted the ordovician Sierra de Calalaste in the E boundary of the salar, and folded whith heterogeneous trend the tertiary continental pile. The length of the fault zone is not restricted to the Puna area; it extends with an N-S trend over 800km. In the San Juan Province it is named "Sistema del Tigre" (Bastías et ali 1987).

In the Antofalla area the fold train azimuth in the tertiary strata range obliquely with a NW-SE trend in a discrete pattern "en echelon", one of these structure is the depression Salar del Fraile, it correspond to an strongly eroded anticline.

The structural mapping reveals recent extensive fault regimen, which strikes N-S. The areal coexistence of different structures would be a prediction for the conceptual model of the origin of the Salar de Antofalla in a transpressive regime linked with subduction. Basin evolution must have started in the Neogene, represented in clastic and salt deposits and is continuous at present. Focal mechanism solution for the earthquake of 1973, eastern of the salar, indicated the motion was right-lateral strike slip with N-S extention (Chinn and Isaks 1983).

REFERENCES

Bastías, H. y Bastías,J.1987 Fallamiento rumbo deslizante en el borde oriental de los Andes entre los 32° y 26``de latitud S. Actas X Congreso Geológico Argentino Tucumán

Chinn,D.S. and Isacks,L. 1983 Accurate source depth and focal mechanisms of shallow earthquakes in western South America and in the New Hebride Island. Arch. Tectonics 2(6):529-563.

MORPHOLOGY OF THE WADATI-BENIOFF ZONE AND SEISMOTECTONIC PATTERN OF THE ANDEAN LITHOSPHERE IN THE ARICA ELBOW REGION

Aleš ŠPIČÁK, Václav HANUŠ, Jiří VANĚK and Alice SLANCOVÁ (1)

(1) Laboratory of Global Tectonics and Metallogeny, European Centre Prague, c/o Geophysical Institute, Academy of Sciences of the Czech Republic, Boční II/1401, 141 31 Praha 4, Czech Republic (e-mail: als@ig.cas.cz)

KEY WORDS: Andean South America, Arica Elbow, morphology of the Wadati-Benioff zone, seismotectonics, fracture zones in the continental lithosphere

INTRODUCTION

For the study of the geometry of distribution of earthquake foci in the Arica Elbow region International Seismological Centre (ISC) data (Regional Catalogue of Earthquakes 1964-93) and relocated events by Engdahl et al. (1998), representing revised ISC data for strong earthquakes, were used. The above region was covered by 22 vertical cross sections perpendicular to the axis of the Peru-Chile trench. In these sections the earthquakes which belong to the Wadati-Benioff zone were separated from those situated in the continental wedge. The detailed analysis of the distribution of earthquakes allowed us to derive a fingerlike shape of the lower part of the Wadati-Benioff zone below the aseismic gap (Hanuš et al. 1999) and to delineate seismically active fracture zones in the continental wedge (Vaněk et al. 1999).

MORPHOLOGY OF THE WADATI-BENIOFF ZONE

Geometrical parameters of the Wadati-Benioff zone were estimated from vertical cross sections showing the depth distribution of earthquake foci situated in the Wadati-Benioff zone between 17°S and 23°S (for details see Hanuš et al. 1999). The dip and thickness are practically constant in all sections, whereas the length and depth of penetration considerably vary from north to south. The length shows small changes around 350 km in the northern sections, expressive length oscillations between 350 and 750 km in the

central sections and a constant value of about 650 km in the southern sections. A similar behaviour with a smaller amplitude can be observed for the depth of penetration.

To visualize the shape of the slab, ISC data for the period 1964-93 and relocated earthquake foci (Engdahl et al. 1998) were projected on the upper surface of the slab. The picture obtained on the basis of the relocated data is given in Fig. 1. It follows from this picture that the slab is continuous above the aseismic gap. However, the distribution of earthquake foci in the lower part of the slab under the aseismic gap in the central part of the Arica Elbow region seems to show that the seismic activity is concentrated into several radial strips which can be interpreted as six separated lobes of different lengths.

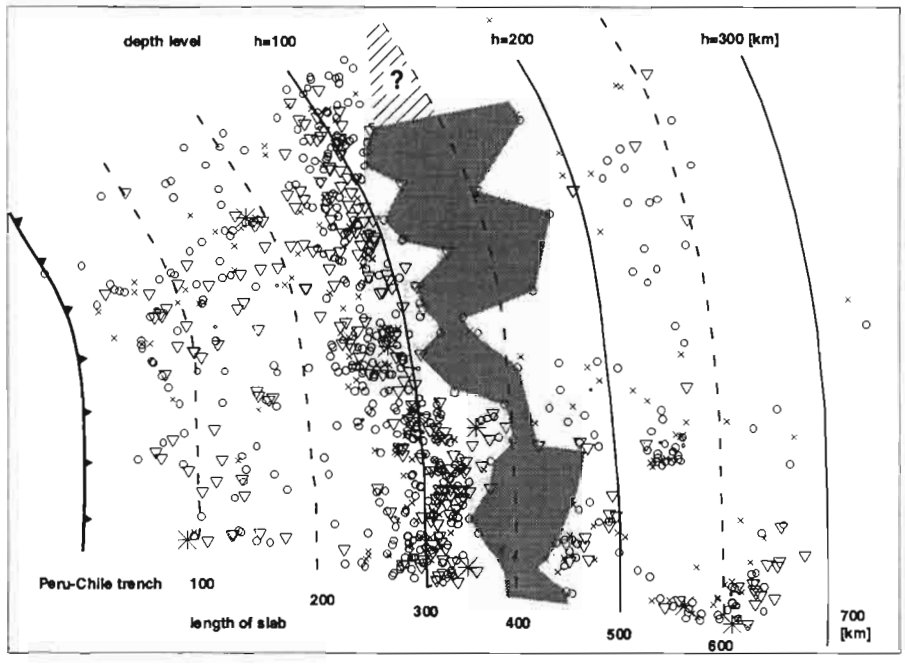

Fig. 1. Map of Engdahl et al. (1998) foci of Wadati-Benioff zone earthquakes projected on the surface of the slab; shaded area represents the shape of the Wadati-Benioff zone constructed on the basis of the distribution of earthquakes and dark shaded area the aseismic gap. Symbols of earthquakes with ISC magnitude m_b: ∘ ≤ 4.0, x = 4.1 - 4.5, ○ = 4.6 - 5.0, ∇ = 5.1 - 6.0, ✱ = 6.1 - 7.0.

The detailed delineation of individual lobes in the lower part of the slab based on the distribution of earthquake foci is a delicate problem depending on the accuracy of location of individual events. To test the reliability of our solution based on all ISC Wadati-Benioff earthquakes, we constructed the images based on ISC events with number of P arrivals n≥25, n≥40, and on the relocated Engdahl et al. (1998) data (see Figs. 9-11 in Hanuš et al. 1999). In all cases the fingerlike shape of the slab remains preserved with the same maximum length of individual lobes. The distance of the tips of the neighbouring lobes, greater than 50 km, safely exceeds the accuracy of teleseismic locations of earthquakes.

To check the reality of the fingerlike shape of the lower part of the Wadati-Benioff zone, in view of the continual process of the Nazca plate subduction with preserved slab thickness, the areas of the slab surface above and below the aseismic gap were estimated. The area of the lobes, which represent in our interpretation the subducted oceanic plate between the slab length of 500-600 km, is practically the same as the area of the corresponding along-strike strip of the slab between 200 and 300 km. The ratio of both areas was found to be 1.004. In the case of an uninterrupted continuous shape of the slab below the aseismic gap, this ratio would be 1.272, which would require a substantial increase of the area of the surface of the slab in the process of its penetration in the concave-seaward segment of the plate margin in the Arica Elbow region. Every hypothesis favouring the lateral continuity of the lower part of the Wadati-Benioff zone in the Arica Elbow region should consider this fact.

SEISMICALLY ACTIVE FRACTURE ZONES

In the Arica Elbow region eleven seismically active fracture zones were delineated (Fig. 2). The names and main parameters of individual fracture zones (azimuth, dip, maximumu depth) are as follows: Z2a - Choquelimpie F.Z., 150°, 60° to NE, 100km, Z2b - Iquique F.Z., 165°, 45° to NE, 100km, Z2c - Domeyko F.Z., 170°, 50° to NE, 120km, Z3 - Pichanal F.Z., 180°, 40° to W, 110km, Z7 - Santa Cruz F.Z., 180°, 55° to W, 70km, Z8 - Río Ichilo F.Z., 130°, 45° to SW, 70km, Z12 - San Antonio F.Z., 180°, 70° to W, 105km, Z13 - Dragones F.Z., 180°, 50° to W, 90km, Y8 - Tocalaya F.Z., 45°, 60° to SE, 75km, Y9 - Jaroma F.Z., 60°, 50° to SE, 100km, Y10 - Ujina F.Z., 100°, 60° to N, 100km. As an example, the graphical presentation of the Domeyko fracture zone Z2c is given in Fig. 3. The pattern of the seismically active fracture zones combined with focal mechanisms of earthquakes occurring in individual fracture zones allows us to study the contemporary tectonic processes in the continental wedge above the subduction zone in the Arica Elbow region.

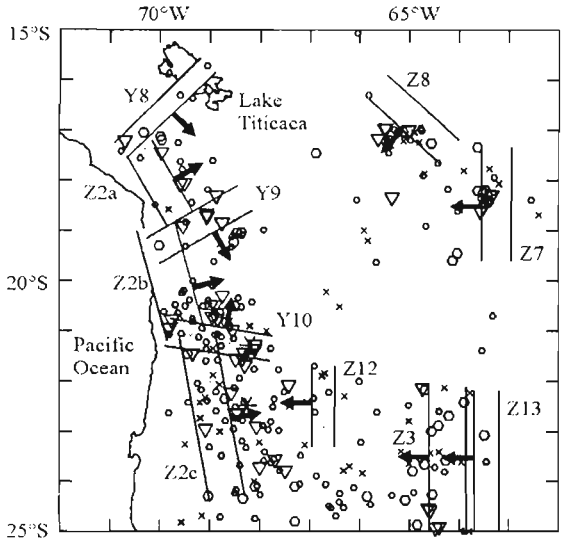

Fig. 2. Scheme of seismically active fracture zones near the Arica Elbow region and distribution of epicentres of earthquakes occurring in the continental lithosphere; arrows indicate the inclination of individual fracture zones. Symbols of earthquakes as in Fig. 1.

The dominant active tectonic feature in the continental lithosphere appears to be the fracture system Z2. The system located at the western boundary of the Andes is divided by the transverse Jaroma fracture zone Y9 and Ujina fracture zone Y10 into three fracture zones, characterized by a gradually changing strike (Z2a, Z2b, Z2c). The Iquique fracture zone Z2b between the Jaroma fracture zone Y9 and Ujina fracture zone Y10 is shifted to the west. All the mentioned fracture zones are well documented in geologic maps (Mapa Geológico de Chile 1982, Ulriksen 1990). Fracture zones Z2a, Z2b, Z2c are inclined to the northeast similarly as the subduction zone; however, their dip between 45° and 60° is greater than the average dip of 28° for the Wadati-Benioff zone. The existing fault plane solutions indicate normal faulting with strikes of fault planes near to the strike of fracture zones. The Choquelimpie fracture zone Z2a is limited in the north by the transverse Tocalaya fracture zone Y8, the northeastern continuation of which can be the seismically inactive Lineamiento Consata (Lineamientos etc. 1979). The only fault plane solution available for transverse fracture zones, situated in the Jaroma fracture zone Y9, indicates left-lateral strike-slip faulting.

The position of the Jaroma fracture zone Y9 corresponds to the northern boundary and the position of the Ujina fracture zone Y10 to the southern boundary of the fingerlike structure of the lower part of the Andean subduction zone (compare Fig. 1). It means that the transition zone in the Arica Elbow region is characterized in the continental lithosphere by the domain surrounded by the Iquique fracture zone Z2b, Jaroma fracture zone Y9 and Ujina fracture zone Y10. This domain covers an inter-Andean basin with large lakes (Lago de Poopo, Lago de Coipasa) and salars (Salar de Coipasa, Salar de Uyuni). The northeastern continuation of the Jaroma fracture zone Y9 is formed by seismically inactive Lineamiento Santa Rosa Machacamarca (Lineamientos etc.1979).

The fracture zones Pichanal Z3, Dragones Z13, Santa Cruz Z7 and Río Ichilo Z8 appear to have a similar tectonic function. They are located at the easternmost boundary of the Andes, inclined to the west (Z3, Z13, Z7) or to the southwest (Z8) below the Andean mountain range under angles between 40° and 55°.

The Santa Cruz fracture zone Z7 and the Río Ichilo fracture Z8 are well documented in Mapa Geológico de Bolivia (1978). The existing fault plane solutions in these fracture zones indicate reverse faulting with strikes of fault planes near to the strike of fracture zones.

The area of the inter-Andean basin between the fracture system Z2 and the fracture zones Santa Cruz Z7, Río Ichilo Z8 appears to be seismically almost inactive excepting isolated events near N-S trending faults between Oruro and Independencia, between Sucre and Colquechaca and eastwards of Uyuni. Fracture zone Z12 is in continuation of a graben structure near San Antonio de Lípez, dips steeply to the west and the only fault plane solution indicates normal faulting. The results of stress analysis show that the stress regime at the eastern boundary of the Andes is different from that at seismically active fracture system Z2 in the west. Also fault plane solutions point to a different type of tectonic movements at the western and eastern boundaries of the Andes. It seems that the block of the continental lithosphere in the Arica Elbow region between the fracture system Z2 and the fracture zones Santa Cruz Z7 and Río Ichilo fracture zone Z8 behaves like a rigid body and tilts to the west due to the movement of the subducting oceanic plate.

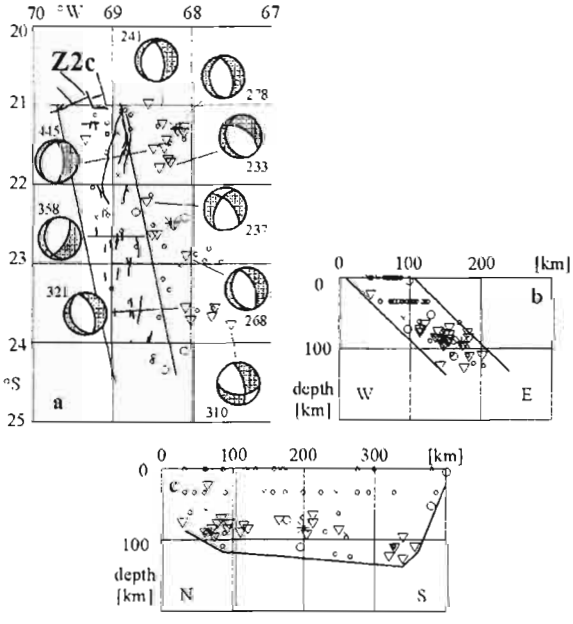

Fig. 3. Location of the Domeyko fracture zone Z2c with associated earthquakes (a) transverse section (b) across and longitudinal section (c) along the fracture zone; faults observed on the surface are denoted by lines in (a). Fault plane solutions are lower focal hemispheres of Harvard solutions, black represents compressional first motion arrivals, white represents dilatational arrivals. Symbols of earthquakes as in Fig. 1.

Acknowledgements: The present work has been performed in the framework of IGCP project No. 345 "Andean Lithospheric Evolution". The financial support of the Grant Agency of the Czech Republic under Grant 205/95/0264 and of the Grant Agency of the Academy of Sciences of the Czech Republic under Grant A3012805 is acknowledged.

REFERENCES

Engdahl E.R., van der Hilst E.D. and Buland R., 1998: Global teleseismic earthquake relocation with improved travel times and procedures for depth determination. Bull. Seism. Soc. Amer., 88, 722-743.

Hanuš V., Slancová A., Špičák A. and Vaněk J., 1999: Discontinuous nature of the lower part of the South American Wadati-Benioff zone in the Arica Elbow region. Studia Geophys. et Geod., 43, 163-184.

Lineamientos y cuerpos intrusivos de los Andes Bolivianos (1:1 000 000), 1979. Servicio Geológico de Bolivia, La Paz..

Mapa Geológico de Bolivia (1:1 000 000), 1978. Yacimientos Petrolíferos Fiscales Bolivianos y Servicio Geológico de Bolivia, La Paz.

Mapa Geológico de Chile (1:1 000 000), 1982. Servicio Nacional de Geología y Minería, Santiago.

Mapa Geológico de la República Argentina (1:2 500 000), 1982. Servicio Geológico Nacional, Buenos Aires.

Regional Catalogue of Earthquakes 1964-94, International Seismological Centre, Edinburgh and Newbury.

Ulriksen C. G., 1990: Mapa Metalogénico de Chile entre los 18° y 34°S (1:1 000 000). *Boletin No. 42*, Servicio Nacional de Geología y Minería, Santiago.

Vaněk J., Hanuš V., Slancová A. and Špičák A. 1999. Seismically active fracture zones in the continental wedge above the Andean subduction zone in the Arica Elbow region. Studia Geophys. et Geod., 43 (in print).

LOW TEMPERATURE THERMOCHRONOLOGY OF THE NORTHERN CORDILLERA REAL, ECUADOR: INSIGHTS INTO TERTIARY TECTONICS

Richard SPIKINGS, Diane SEWARD and Wilfried WINKLER (1)

(1) Geologisches Institut, ETH-Zentrum, Zürich CH-8092, Switzerland. spikings@eurasia.ethz.ch

KEY WORDS: Fission-track dating, thermochronology, exhumation, Cordillera Real, Ecuador

INTRODUCTION

The poly-deformed Cordillera Real in Ecuador (Figure 1) originated during the early Cretaceous accretion of allochthonous terranes at ~140 Ma, otherwise referred to as the 'Peltetec event' (e.g. Litherland et al., 1994). Progressive cratonward migration of arc-orogenic elements (e.g. Litherland and Aspden, 1992) and unroofing of the orogen since the Peltetec event has lead to the current exposure of greenschist and lower grade facies metamorphic rocks . However, the post-Peltetec evolution of the orogen is only loosely constrained by a series of partially and completely reset K/Ar ages (e.g. Litherland et al., 1994).

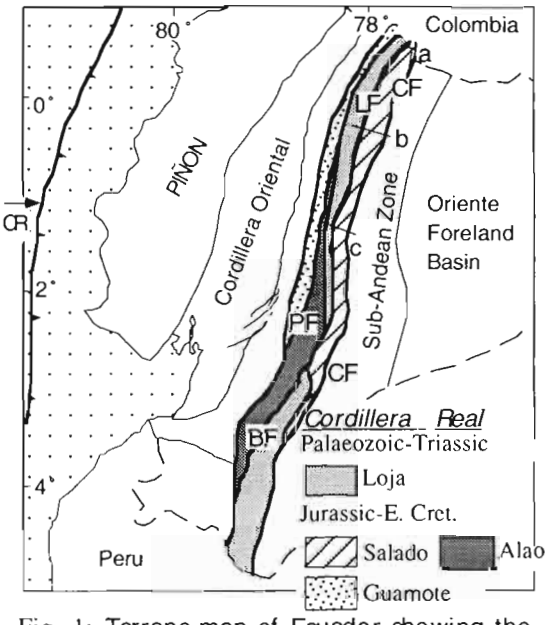

Fig. 1: Terrane map of Ecuador showing the main tectonic divisions of the Cordillera Real . The Ecuador trench is shown. PF: Peltetec Fault, BF: Baños Fault, LF: Llanganates Fault, CF: Cosanga Fault, CR: Carnegie Ridge. Labels a,b,c identify the three sample traverses.

We present zircon and apatite fission track (ZFT and AFT respectively) data from three traverses across terranes of the northern Cordillera Real (a, b, c; Figure 1) that provide a quantitative framework for the post-Palaeocene tectono-thermal evolution of the orogen. Such a framework provides constraints on the unroofing history of the orogen, as well as intra-orogen fault displacements.

RESULTS AND INTERPRETATION

AFT ages range between 41 and 8 Ma (Figure 2) suggesting the present land surface was cooling through the ~ 110°C isotherm during and prior to this time period. A majority of mean track lengths are < 14 μm and have standard distributions > 1.4 μm. These results record a protracted cooling history below ~ 110°±10°C. However, several samples, with AFT ages that cluster at 9 – 20 Ma and ~ 40 Ma have mean lengths of ~≥14 μm (Figure 2) which suggests that significant cooling events occurred at these times.

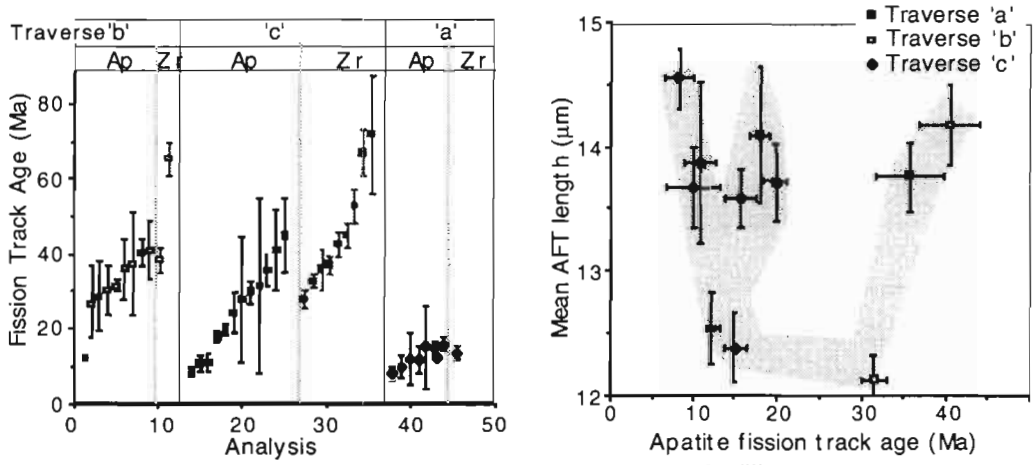

Fig 2: ZFT and AFT age and length data from three traverses across the Cordillera Real

The Misahualli Unit in far northern Ecuador yields concordant ZFT and AFT ages of ~12 Ma suggesting the region cooled rapidly through ~290 – 60°C at this time. Additionally, particular samples from the Salado and Loja terranes in the centrally located terranes yielded concordant ZFT and AFT ages at ~40 and ~20 Ma within a 1σ error (Figure 2), which suggests that these samples also cooled rapidly through ~290 – 60°C at the time indicated by the fission track ages.

The wide variation in AFT data does not follow a coherent relationship (Spikings et al., in prep.) with apatite composition. This suggests the variation is a consequence of widely varying temperature (T) – time (t) paths, between different regions of the Cordillera during the Cenozoic. Additionally, the wide variation in T-t paths between samples throughout the Cenozoic has dissected any coherent relationship that may have existed between elevation and AFT age. Therefore, the samples have been modelled (e.g. Gallagher, 1995) to derive T-t histories for particular samples.

This study assumes that all cooling was a result of crustal exhumation. However, cooling may also be related to thermal relaxation following periods of igneous activity and the exhumation depths and rates reported here should be considered as maximum values (calculated using a geothermal gradient of

30°C/km; Figure 3). Three distinct periods of increased exhumation rates can be identified. However, not all the sampled fault blocks were exhumed during every period.

0 – 12 Ma

All regions were exhumed at relatively high rates during this period (Figure 3). The rates were highest at ~9 and ~5 Ma when they peaked at ~1.3 km/Ma in the Salado terrane of far northern Ecuador, and proximal to the Baños Fault in more central regions.

Exhumation at this time can be correlated with terrigenous alluvial fan development within the Inter-Andean and Foreland basins. Additionally, high rates at ~9 Ma may be synchronous with subduction of the Carnegie Ridge (e.g. Daly, 1989) as well as increased half spreading rates within the equatorial Atlantic (e.g. Brozena, 1986).

15 – 25 Ma

Fault bounded units from the far northern traverse (a), and a traverse (c) between the towns of Baños and Puyo were exhumed at average rates of ~<0.3 km/Ma although local variations are observed (Figure 3). However, a fault bounded unit of deformed Misahualli volcanic rocks may have been exhumed at rates of ~≤1.2 km/Ma as a result of compressional reactivation of the La Sofia Fault.

Increased exhumation rates are not observed within structural units intersected by a traverse between the towns of Quito and Baeza. This may be an artefact of sampling density although it is more likely to be a consequence of relative tectonic stability in this region at this time.

Miocene thrusting of the Cordillera Real (Pasquaré, 1990) and high rates of exhumation of the Inter-Andean Quingeo Basin at ~18 Ma (Steinmann et al., 1999) are consistent with tectonic instability within the Cordillera Real. Prograding of coarse siliciclastic sediments (Chalcana Fm.) within the Foreland Basin was probably in response to an elevating Cordillera to the west.

43 – 30 Ma

Concordance between AFT and ZFT ages suggests various faulted units of the Cordillera were exhumed at rates between ~0.4 and >1 km/Ma in central regions of Ecuador (Figure 3). The highest rates occur within granitic bodies.

This time period corresponds with sedimentation of coarse clastics into the foreland basin (Figure 3; Tiyuyaku, Orteguaza Fms.). Additionally, the oceanic Piñon terrane accreted onto the Pacific margin at this time, in response to changing plate convergence kinematics (e.g. Jaillard et al., 1995).

CONCLUSIONS

1. The Cordillera Real has been exhumed by 4 – 8 km since ~40 Ma. Greatest amounts of exhumation occurred in far northern Ecuador, possibly as a result of reactivation of the La Sofia Fault during ~15 – 25 Ma; high rates are also observed proximal to the Baños Fault since ~9 Ma.

2. Periods of exhumation correlate with foreland and inter-andean sedimentary Fms. However, they extend for longer periods than tectonic 'phases' postulated by other authors (Figure 3), suggesting that compressional phases may have persisted for longer periods than previously thought.

REFERENCES

Brozena J.M., 1986. Temporal and spatial variability of sea-floor spreading processes in northern South Atlantic. Journal Geophysical Research 1, 497 – 510.

Daly M.C. 1989. Correlations between Nazca/Farallon plate kinematics and forearc basin evolution in Ecuador. Tectonics (8) 4, 769 – 790.

Litherland M. and Aspden J.A. 1992. Terrane boundary reactivation: a control on the evolution of the Northern Andes. Journal of South American Earth Sciences, 5, 71 – 76.

Litherland M., Aspden J.A. and Jemielita R.A. 1994. The metamorphic belts of Ecuador. British Geological Survey Overseas Memoir 11.

Noblet C., Lavenu A. and Maroco R., 1996. Concept of continuum as opposed to periodic tectonism in the Andes. Tectonophysics, 255, 65-78.

Steinmann GT., 1929. Geologie von Peru. Karl Winter, Heidelberg, 488 pp.

Steinmann M., Hungerbühler D., Seward D., and Winkler W. 1999. Neogene tectonic evolution and exhumation of the southern Ecuadorian Andes. Tectonophysics, in press.

Yamada R., Tagami T., Nishimura S., and Ito H. 1996. Confined fission-track length measurement of zircon: assessment of factors affecting the palaeotemperature estimate. Chemical Geology, 122, 249-258

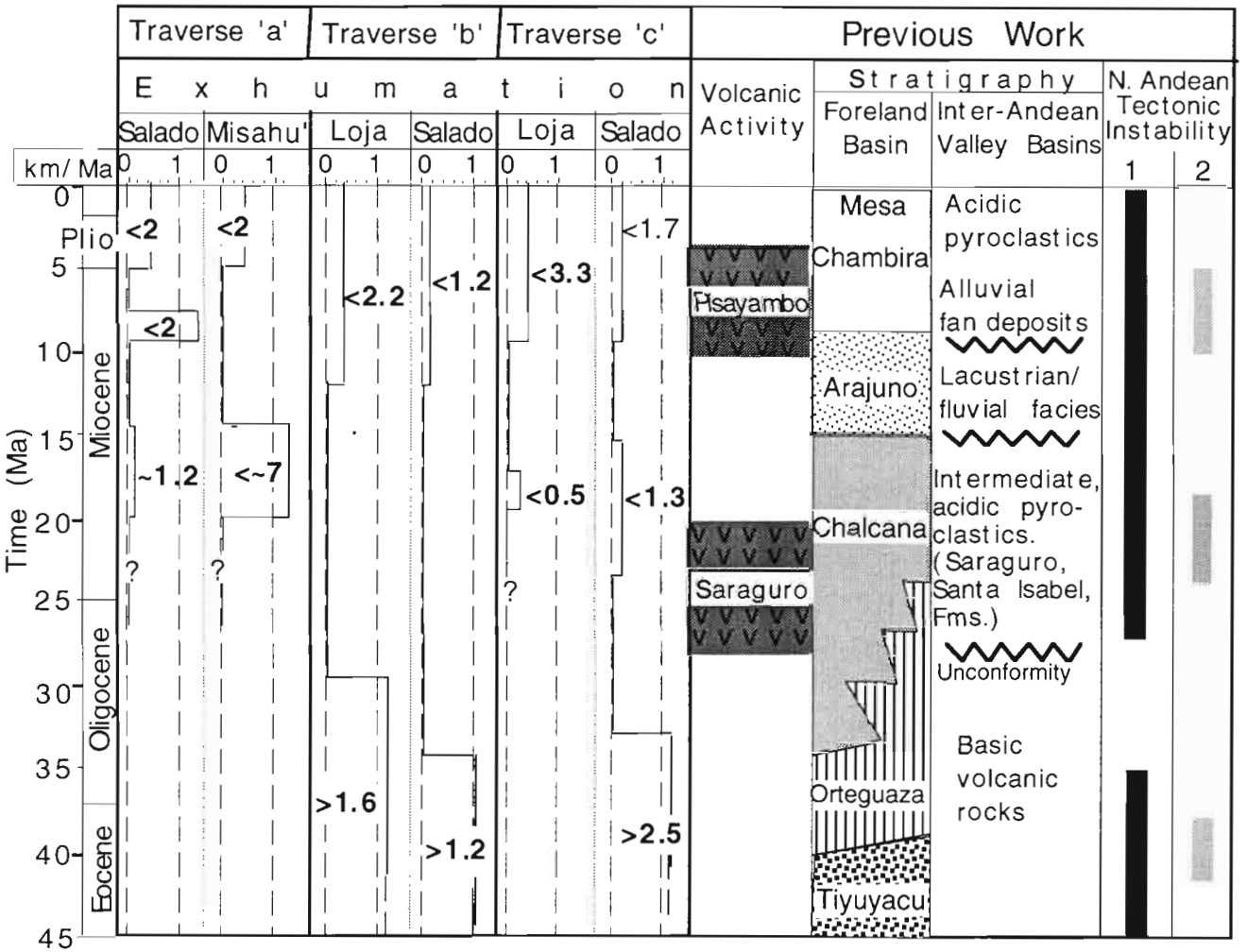

Fig. 3: Post Palaeocene exhumation rates and depths for each traverse and terrane sampled across the northern Cordillera Real. Periods of volcanic activity (Steinmann,1997 and Hungerbühler, 1997) within the Cordillera Real and simplified stratigraphic frameworks for the Foreland and Inter-Andean basins are shown. 1: Noblet et al., 1996, 2: Steinmann, 1929.

NEOTECTONICS AND LANDSLIDING IN NW ARGENTINA

M.R. STRECKER(1), R.N. ALONSO(2), R. HERMANNS(1), R.M. MARRETT(3) and M. TRAUTH(1)

(1) Universität Potsdam, Inst. f. Geowissenschaften, P.O. Box 601553, 14415 Potsdam, Germany
(2) Univerisad Nacíonal de Salta. Buenos Aires 177, 4400 Salta, Argentina
(3) Department of Geological Sciences, UT Austin, Austin, TX 78712-1101, U.S.A.

KEYWORDS: Neotectonics, kinematic change, landslides, climate change

INTRODUCTION

Many active plate boundaries record important changes in their kinematic history, which caused far-reaching effects on the overall structural, volcanic, and geomorphic development of these regions. In the central Andes of Argentina between 23 and 27•S, a regionally consistent change in the shortening direction has been (Marrett et al., 1994). An early thrust phase of deformation beginning by 17 Ma was characterized by WNW-ESE shortening and sub-vertical extension. New radiometric data from the Quebrada del Toro at about 24°S show that this kinematic regime was replaced by the neotectonic kinematics with ENE-WSW shortening and NNW-SSE extension at about 4.17 Ma (unpubl. data, M. Strecker), which had an important bearing on intraplate deformation and associated active surface processes that are influenced by tectonic style. The relation between tectonism and surface processes is manifested in the regional distribution of large landslide deposits, characterized by lobate morphology, inverse stratification, and volumes in excess of $10^6 m^3$. In the tectonically active Cordillera Oriental and adjacent structural provinces of the semi-arid NW Argentine Andes numerous large landslides occur along mountain fronts with pronounced relief contrast (Marcuzzi et al., 1994). The majority of these landslides are lithologically and structurally controlled and were generated in the steep hanging walls of thrust and reverse faults with recurrent Quaternary activity (Hermanns and Strecker, 1999). The close spatial association of landslides, tectonically active mountain fronts, and rock masses with favorably oriented planes of weakness suggests that seismic shaking triggered most of these landslides in rocks that were

already inherently predisposed to mountain-front collapse. Apart from structural, lithologic, and climatic variables commonly associated with preconditioning rock masses for landsliding, we present new evidence in this paper that an additional mechanism related to the kinematic evolution of mountain-bounding faults plays a significant role in preparing mountain fronts for failure. In particular, we show how the neotectonic change in the regional shortening direction of Andean deformation in northwestern Argentina resulted in a redistribution of localized uplift along fault systems; the changed relief conditions, contrasts in the erodibility of mountain fronts, and erosion of antecedent streams ultimately increased the risk of mountain-front collapse.

REGIONAL GEOLOGY AND LANDSLIDE DEPOSITS

The Cordillera Oriental contains major Neogene thrust faults that carry hanging-wall rocks of low metamorphic grade Proterozoic flysch and Paleozoic granitoids (e.g., Omarini, 1983), whereas the adjacent Santa Barbara province represents a Cretaceous-Tertiary rift that was inverted during the Neogene (Salfity and Marquillas, 1994). The early contraction on N- to NE-striking thrust faults (Marrett et al., 1994) was superseded by contraction and uplift on NW-striking thrust faults, as well as right slip along the previously generated thrust faults. Many valleys in the Cordillera Oriental and the Santa Barbara province are perpendicular to the late Cenozoic structures of the mountain fronts and contain evidence for repeated Quaternary faulting, deep incision, landsliding, and damming by landslides. Such a setting is well exemplified in the Quebrada de las Conchas (26°S, 66°W) and the Quebrada del Toro (25°S 66W). Both valleys are antecedent and were dammed by major landslides causing paleo-lakes at about 30 ka (Trauth and Strecker, 1999). For example, the paleo-lake in the Quebrada de las Conchas covered an area of 630 km^2. Unlike the majority of landslides along mountain fronts in the Cordillera Oriental, neither area is characterized by structurally or lithologically controlled anisotropies that dip directly toward the fault-bounded mountain front. Consequently, the typical conditions promoting landslide development are not applicable to either area, and other mechanisms must be called upon.

FAULTING GEOMETRY, KINEMATICS AND LANDSLIDES

The two landslide locations share a common Cenozoic kinematic history. In both areas, major drainages cross mountain-range bounding thrust faults at geometric irregularities, which are reactivated NW to WNW-striking lateral ramps linking en echelon thrust segments. The faults in both areas constituted major thrust systems during the main Neogene deformation phase and document a two-stage kinematic evolution

(Marrett et al., 1994). Dip-slip thrusting characterized movement on N to NNE-striking faults. Strike slip and oblique slip occurred on W to NW-striking lateral ramps. Most structural and topographic relief on the fault systems probably developed during this phase of deformation. However, relatively subdued relief would have been present where lateral ramps or soft-linked displacement transfer structures separated dip-slip fault segments. This may explain why both rivers cross the fault systems at obliquely striking segments. The younger phase of deformation in both regions involved neotectonic reactivation of older faults and the creation of new faults. Former thrust faults striking N to NNE were reactivated with oblique- to right-slip kinematics. Left stepovers along the dextral faults, such as the transfer structures at both study areas, were transformed into restraining bends characterized by predominantly dip-slip thrusting. If linking faults did not previously exist in displacement transfer zones, then new oblique fault segments bridged the throughgoing faults. Consequently, locally enhanced uplift developed at the restraining bends, where the Río Toro and the Río de las Conchas cross the fault systems.

CONCLUSIONS

The spatial coincidence of important localized landsliding activity and structurally complex areas recording changes in kinematic history emphasizes the role of tectonism in predisposing mountain fronts to landsliding. The regional kinematic change shifted the locus of uplift at the local scale in both areas. Uplift had been initially subdued at transfer structures during the thrust phase of deformation, localizing the river courses. During the neotectonic regime, however, uplift was locally enhanced at the transfer structures where the rivers cross the fault systems. Maintenance of river grade during Quaternary tectonic activity required progressively deeper incision into the ascending fault blocks, resulting in precipitous local topographic relief along the antecedent rivers. The ultimate trigger mechanism for these landslides is unknown. Considering that the landslides occur Quaternary faults, it is likely that seismic shaking played an important role. However, the juxtaposition of the downcutting rivers with thrusting of well-indurated rocks over highly erodible sediments, in addition to creating important relief energy, could equally have led to an increased landslide risk. Lateral erosion along the pronounced hanging wall-footwall lithologic contrast in both areas could have resulted in gravitational collapse of the undercut mountain fronts. It thus can be envisioned that this type of landslide dynamics was enhanced during colder and/or wetter periods, when lateral fluvial erosion was more efficient in removing material from the mountain fronts. This inference is supported by the ages of landslide-related lacustrine sediments at both locations, which coincide with a wet and cold period between 40,000 and 25,000 yr B.P. in subtropical South America (e.g., Wirrmann and Mourguiart, 1995; Trauth and Strecker, 1999).

REFERENCES

Hermanns, R. and Strecker, M.R. 1999. Structural and lithological controls on large Quaternary rock avalanches in arid northwest Argentina Geological Society of America Bulletin, in press.

Marcuzzi, J. J., Wayne, W. J., and Alonso, R. N. 1994. Geologic hazards of Salta Province, Argentina. *In* Proceedings, International Association of Engineering Geology, 7th, Lisbon: Balkema, Rotterdam, 2039-2048.

Marrett, R. A., Allmendinger, R. W., Alonso, R. N., and Drake, R. E.. 1994. Late Cenozoic tectonic evolution of the Puna Plateau and adjacent foreland, NW Argentine Andes. J. of South American Earth Sciences, 7, 179-207.

Omarini, R. H. 1983. Caracterización litológica, diferenciación y génesis de la Formación Puncoviscana entre el Valle de Lerma y la Faja Eruptiva de la Puna. [PhD thesis]. Provincia de Salta, Argentina, Universidad de Salta, 220 p.

Salfity, J. A., and Marquillas, R. A. 1994. Tectonic and sedimentary evolution of the Cretaceous-Eocene Salta Group Basin, Argentina. *In* Salfity, J. A., ed., Cretaceous tectonics of the Andes: Earth evolution sciences: Braunschweig-Wiesbaden, Friedrich Vieweg und Sohn, 266-315.

Strecker, M.R. and Marrett, R.M. 1999. Kinematic evolution of fault ramps and its role in development of landslides and lakes in the NW Argentine Andes. Geology, 27, 307-310.

Trauth, M. und Strecker, M.R. 1999. Formation of landslide-dammed lakes during a wet period between 40,000 - 25,000 yr B.P. in northwestern Argentina. Paleogeography, Paleoclimatology, Paleoecology, in press.

Wirrmann, D., and Mourguiart, P., 1995. Late Quaternary spatio-temporal limnological variations in the Altiplano of Bolivia and Peru. Quaternary Research, 43, 344-354.

BOLIVIA: LATE PROTEROZOIC – EARLY PALEOZOIC

Ramiro SUAREZ-SORUCO

Yacimientos Petrolíferos Fiscales Bolivianos. Casilla Postal 4324. Cochabamba-Bolivia – ramsu@bo.net

KEY WORDS: Gondwana. Bolivian Triple Juntion. Arequipa Microplate.

ABSTRACT

The geological history of Bolivia can be divided in two main events: the Pre-Andean and the Andean episodes. The separation between both is the result of the Gondwana breackup (ca. 200 Ma). In addition, the Pre-Andean episode can be separated in two stages: the first encompasses the Proterozoic cycles, until the formation of the "Bolivian Triple Juntion" at the end of the late Proterozoic, and the second stage, from the opening of the early Paleozoic rift, until the separation of the Gondwana. The Andean episode began in the early Jurassic and extends until our days.

Authors like Dalziel, consider that after the Pangea breackup, the new supercontinents Laurentia and Gondwana eventually displaced towards different latitudes (Dalziel, 1993, 1994, 1997). During the late Proterozoic and early Paleozoic, the oriental border of North America and the western border of the Gondwana underwent a parallel crossed displacement. Also, during this trip some terranes broke off, like the Argentinian Precordillera, that accreciones to the western border of Gondwana, and some rift basins was opened in the same border, like the Proterozoic-Paleozoic Bolivian Rift.

A preliminary reconstruction of this relative displacement of the two supercontinents, shows that the North American continent had lesser mobility than the South American and African. It remained almost permanently in an equatorial position, meanwhile the continent of Gondwana moved across the south pole, from the eastern hemisphere where the South America was located during the Proterozoic, to the western hemisphere into the position that it currently occupies. When South America was in the eastern hemisphere, its position was totally inverted to its current position. Illustrating this point with South American cities, in those days, Buenos Aires was to the north of Caracas. The south pole was located close to the north of Africa. Then, during the Upper Ordovician, due to the continous displacement towards high latitudes, the south pole placed itself in the north of Africa. Subsequently, in the Silurian and Devonian, its position changed, by means of a slight rotation and displacement, to Brazilian territory in South America. Finally, in the Upper Paleozoic, it was once again displaced and it rotated along the eastern Argentine border until the position which it occupies now.

During the Archeozoic and Proterozoic, the primitive Brazilian Shield that formed the western border of the Gondwana, experienced a series of consistent modifications in the accretion of new terranes, formation of some intracratonic basins, and development of important Proterozoic orogenic belts, like San Ignacio, Sunsás and Aguapei (Litherland *et al.*, 1986). Subsequently, and while the displacement of the supercontinents was taking place, at the end of the Proterozoic or the beginning of the Paleozoic, the "Bolivian Triple Juntion" also took place in the western border of the Gondwana, which gave origin to the "Arequipa's Microplate" and the Bolivian Rift (Suarez-Soruco, 1989). The center of this triple juntion, which developed almost entirely in Bolivian territory, was located approximately in the region of the Chapare (Cochabamba), and consisted of the following branches: first brach with W-E orientation in

the region of Chiquitos; a second with N-S orientation, from Chapare to Northern Argentine, and a third with SE-NW orientation from the Chapare towards Peruvian and possibly, Equatorian territory. The extensional development of the fractures (N-S and SE-NW), caused the fractures to become connected to one another, creating a great rift, and the formation of the Arequipa's Microplate.

Nevertheless, some authors consider the Arequipa's Microplate like an allochthonous terrane (Wasteneys et al., 1995), that originated in the continent of Laurentia during the Grenvillian orogeny.

In Bolivian territory, as well as in the Peruvian and Northwestern Argentine territories, the gradual separation of the mobile plate of Arequipa formed a Paleozoic intracratonic marine basin, the development of which will be object of further analysis.

REFERENCES

Dalziel I.W.D. 1991. Pacific margins of Laurentia and East Antarctica-Australia as a conjugate rift pair: evidence and implications for an Eocambrian supercontinent. Geology, 19, 598-601.

Dalziel I.W.D. 1993. Tectonic tracers and the origin of the Proto-Andean Margin. XII Congreso Geológico Argentino y II Congreso de Exploración de Hidrocarburos, Actas II, 367-374.

Dalziel I.W.D. 1997. Neoproterozoic-Paleozoic geography and tectonics: Review, hypothesis, environmental speculation. Geological Society of America, 109, 1, 16-42.

Litherland, M. & K. Bloomfield 1981. The Proterozoic history of Eastern Bolivia. Precambrian Research, 15, 157-179.

Litherland, M., B.A. Klinck, E.A. O'Connor & P.E.J. Pitfield 1985. Andean-trending mobile belts in the Brazilian Shield. Nature, 314, 345-348.

Martinez, C., C. Dorbath & A. Lavenu 1996. La cuenca subsidente cenozoica noraltiplánica y sus relaciones con una subducción transcurente continental. Memorias del XII Congreso Geológico de Bolivia, 1, 3-28.

Suarez-Soruco, R. 1989. Desarrollo tectosedimentario del Paleozoico inferior de Bolivia. Información Geológica UATF, II, 1-11, Potosí.

Wasteneys, H.A., A.H. Clarke, E. Farrar & R.J. Langride 1995. Grenvillian granulite – facies metamorphism in the Arequipa Massif, Perú: a Laurentia-Gondwana link. Earth and Planetary Sciece Letters, 132, 63-73.

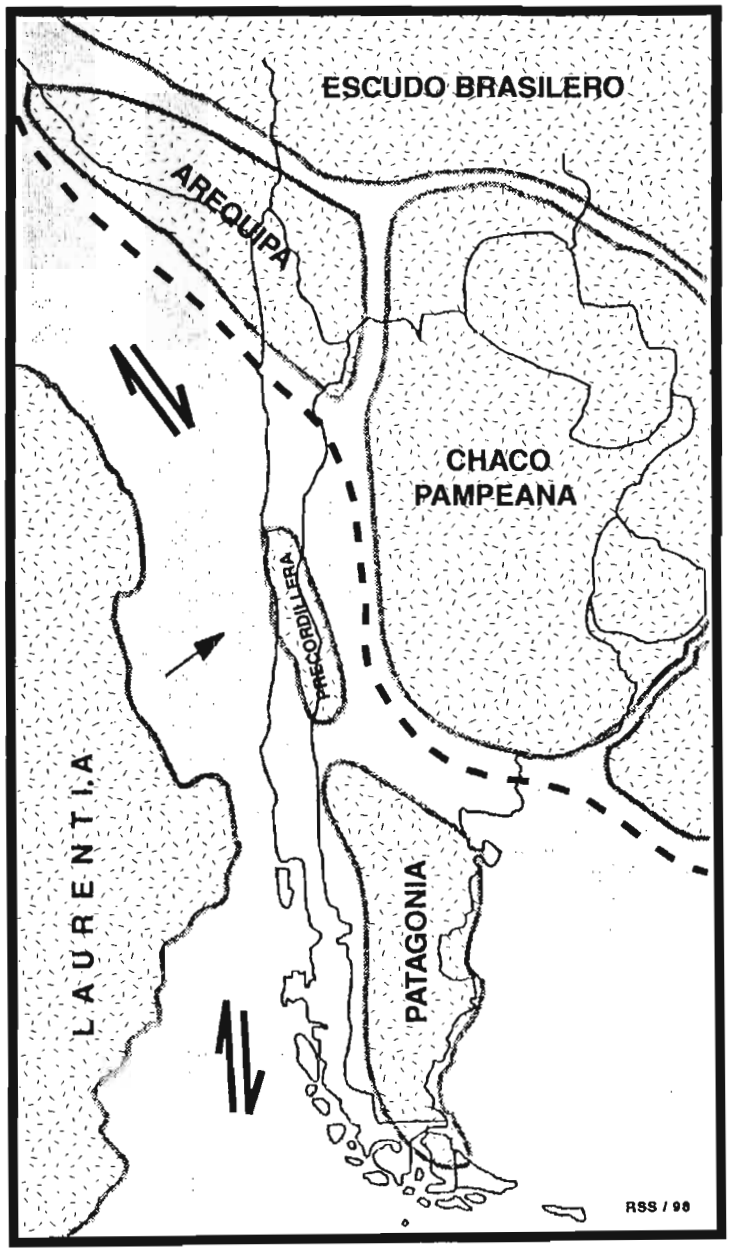
ESCUDO BRASILERO
AREQUIPA
CHACO
PAMPEANA
PRECORDILLERA
LAURENTIA
PATAGONIA
RSS / 98

GEODYNAMICS OF THE NORTHERN ANDES: INTRA-CONTINENTAL SUBDUCTION AND THE BUCARAMANGA SEISMICITY NEST (COLOMBIA).

A. TABOADA (1,2) , L.A. RIVERA (3), A. FUENZALIDA (4) , A. CISTERNAS (3), H. PHILIP(1), J.E. CASTRO (4) , C. RIVERA (4)

(1) Laboratoire de Géophysique, Tectonique et Sédimentologie, UMR CNRS-UMII 5573, Université Montpellier II, 34095 Montpellier Cedex 5, France.
(2) Universidad de Los Andes, Depto de Ingenieria Civil, Cra 1 No 18A-70, Bogota, Colombia.
(3) Institut de Physique du Globe. Université Louis Pasteur. 5 rue René Descartes. 67084 Strasbourg Cedex. France.
(4) INGEOMINAS, Diag. 53 No 34-53, Bogota, Colombia.

ABSTRACT

Intracontinental deformation in the Northern Andes results from the complex interaction between three lithospheric plates (Figure 1). The Nazca oceanic plate is converging eastwards at 6 cm/yr relative to North-Western South America (NWSA); the Caribbean plate is moving at 1-2 cm/yr to the E-SE relative to NWSA [Freymueller et al., 1993]. The Eastern Cordillera (EC) of Colombia is a N-NE trending intracontinental orogenic belt extending for 750 km from the Ecuadorian to the Venezuelan border.

In this contribution we examine the tectonic structure of the northern segment of the EC (which extends from Tunja to Bucaramanga), and its relationship with the Bucaramanga intermediate seismicity nest (Figure 1). Based on new seismological and tectonic data, we re-evaluate the seismotectonics of Colombia and we propose a new interpretation of the EC and the Bucaramanga nest in terms of intracontinental deformation.

The Colombian Andes displays three main ranges between latitudes 1°N and 8°N, the Western, Central and Eastern Cordilleras, which merge southwards into a single range. The Serranía del Baudo is a narrow moderate range located to the west of the Western Cordillera. It is an exotic piece of Central America, which was part of an island arc located along the western margin of the proto-Caribbean plate. Collision between the exotic "Choco Block" (CB) and NWSA occurred towards Middle Miocene (12 Ma) [Duque-Caro, 1990]. The CB is limited by active fault systems such as the N-NW trending Uramita fault zone to the east, and the N60°E Garrapatas right-lateral fault zone to the south (Figure 1). Accretion of the

CB is contemporary with the onset of the major tectonic deformation phase in the EC, which began at 10,5 Ma and continued during Plio-Quaternary Time [, Taboada et al., 1998].

The EC is characterized by basement rocks covered by a thick sequence of Mesozoic and Cenozoic sedimentary rocks, strongly deformed during Neogene by thrusting and folding. Jurassic and Cretaceous sedimentary rocks were deposited within large N-NE trending basins. The oblique accretion of the San Jacinto terrane and of oceanic crustal fragments of the Western Cordillera during early Cenozoic, created incipient transpressive deformation in the EC. The middle Eocene tectonic phase which created folding and thrusting along west-vergent faults located in the Magdalena Valley [Cooper et al. 1995], seems to be well correlated with active deformation and emergence of the San Jacinto Belt.

The EC widens progressively northwards showing different tectonic styles and a varying morphology. The southern segment corresponds to a narrow moderate range. Major right-lateral faults trending NE run across basement rocks (e.g. Algeciras - Altamira faults). The central segment encloses the "Sabana de Bogotá" high-plateau. Reverse faults dipping towards the range are observed in both foothills. Compressional deformation and thrusting along "en échelon" reverse faults located in the eastern foothill is mainly associated with collision and convergence of the Panama-Baudo island arc located westwards. These faults also absorb right-lateral slip along the Algeciras-Altamira faults in the southern segment. Evidences of active faulting are numerous and include thrusted Quaternary terraces.

The northern segment of the EC extends from Tunja to Bucaramanga. This segment is bounded northwards by the major continental Santa Marta-Bucaramanga left-lateral (SMB) fault. Movement along the SMB fault, estimated at 100 km [e.g. Tschanz et al. 1974], is absorbed southwards by west vergent reverse faults which overthrust the Magdalena Valley and the axial zone of the EC (Salinas, Boyaca and Soapaga faults). Left-lateral movement along the SMB fault may have initiated during the Eocene compressional event, and occurred mainly since Upper Miocene (Boinet et al. 1989), and is concomitant with thrusting and uplift in the EC.

Seismicity and Tectonics of the Eastern Cordillera (Colombia)

The National Seismological Network of Colombia (NSNC) is operating since June 1993, and consists of 15 short period stations monitoring the seismicity over the Colombian territory west of the Llanos Basin [Taboada et al., 1998].

The data base used in this work corresponds to the catalog of seismicity during the period going from June 1993 to December 1996. Crustal earthquakes concentrate along the foothills of the cordilleras, and aligned with the main faults observed at the surface. Intermediate seismicity shows a well defined cluster along the northwestern margin of the Eastern Cordillera. It corresponds to a neat slab running from 5.2° N to 7° N in latitude along 150 km, from the north of Bogota to the Bucaramanga nest. The activity continues down to 180 km in depth under the Eastern Cordillera, it is roughly oriented N30°E, and dips to the E-SE. This elongated cluster corresponds to a well defined subduction segment, not known before the installation of the NSNC. Intermediate seismicity is mostly observed beneath the western flank of the EC,

and extends northwards beneath the Santander Massif (SM). Seismicity associated to this subduction changes orientation north of the Bucaramanga nest, trending along a N340° direction. The seismic cluster located beneath the Bucaramanga area is known as the intermediate Bucaramanga seismicity nest (BSN). This study shows that the Bucaramanga nest is related to an inflection of the subducting surface, more precisely, it is placed at the end of the most active segment of this subduction.

Figure 2 shows a cross-section of seismicity which allow us to analyze the geometry and the nature of subduction beneath the EC (Fig. 1). Cross section A-A' is perpendicular to the mountain range and it includes seismicity within a band that covers entirely the subduction zone (the half-width of the band is 150 km, measured from A-A'). The section clearly shows a subducting slab that dips approximately 45°SE, extending between 60 and 200 km depth. Earthquakes from the BSN are located within the cluster around 150 km depth. Shallow seismicity, corresponding to active faulting, is concentrated near the foothills of the EC and along the Magdalena Valley. The scarce seismicity in the zone lying between the upper crust and the subducting slab (between 25-55 km depth), is interpreted as corresponding to the lower crust. We propose that the overall seismicity pattern in cross section A-A' results from shortening of continental lithosphere and subduction of infracontinental lithospheric mantle beneath the EC. The seismicity pattern results from continental subduction of relatively cool and brittle rocks beneath the EC. This hypothesis is supported by : a) Intermediate depth seismic activity which concentrates beneath the subduction fault zone and fades out towards the NW (Fig. 2); b) The existence of small plutons of K/Rb rich rhyolites eastwards of the Tunja area, which constitute the sole Tertiary volcanic rocks known in the EC [Martinez, 1989]. The chemical composition of these rocks suggests that they are linked to partial melting in the lower crustal root and not to oceanic subduction.

Two lithospheric scale tectonic cross sections perpendicular EC indicate that continental crust is dragged down to great depth by the subducting plate, as a consequence of shortening of the continental lithosphere. The cross section across the Tunja area allows to calculate shortening and kinematics of major faults :

The western margin of the EC is characterized by thrusting and folding with vergence towards the Magdalena Valley. These faults root at depth into the east-dipping continental subduction zone. The vergence of thrusting and folding in the axial zone, and in the eastern foothill, is towards the South American Craton. Main east vergent thrusts tend to join a low-angle ductile shear zone in the lower crust [Colletta et al., 1990]. The total amount of shortening which we obtained during the Andean phase is about 70 km - quite the same as proposed by Cooper et al., [1995].

The analysis of structural data from 43 different outcrops in the EC, by means of numerical and graphical methods allowed us to determine the principal stress directions and to establish a new neotectonic stress map at a regional scale. Stress results in the axial zone of the EC (north of Tunja) indicate a rather homogeneous E-SE compressive regime (N125°E). Regional stress results in the eastern foothill indicate again an E-SE compression direction (N120°E), consistent with thrusting along active faults. Further west, in the Magdalena Valley area, the orientation of $_1$ is close to N110°E. Two types of solutions were observed in the Bucaramanga sector where two major fault systems converge (SMB and

Suarez faults) : a) a late andean N80° uniaxial compression which is sub-orthogonal to the SMB fault and b) an early andean NW-SE compressional axis.

The intermediate seismicity beneath the EC is limited southwards, along a roughly E-W trending boundary located at around 5.2° N. This boundary aligns with the northern termination of intermediate seismicity beneath the Western and Central Cordilleras. This boundary may correspond to a major E-W transform shear-zone located in the infracontinental lithospheric mantle. The fault aligns with the southern termination of the Baudo range and its formation is probably linked with the accretion of the CB. This shear zone, along with the SMB fault and the continental subduction zone, are the boundaries of a deformable continental wedge (Figure 3). Progressive movement of the wedge towards the E-SE is absorbed northwards in the Maracaibo Block, along the Perija and Andes de Merida ranges. Intra-continental subduction beneath the Andes de Merida range (Colletta et al., 1997), results from indentation of the wedge, and should display a right-lateral component. Total shortening in the EC area during compressional Cenozoic events is approximately 80 km, which is coherent with the estimated 100 km displacement along the SMB fault during Cenozoic. The Bucaramanga seismicity nest is located at a depth of 150 km, on the apex of the wedge. The Maracaibo block is ejected northwards at a rate of about 2 mm/y with respect to South America. These results are compatible with E-W compression and N-S extension obtained from a microseismic experiment around the Bucaramanga nest [Rivera, 1989].

In conclusion, the accretion of the CB at 12 Ma blocked normal oceanic subduction of the Caribbean plate beneath NWSA. The convergence rate along the oceanic trench decreased and active deformation shifted eastwards towards weak zones of the continental lithosphere. Shortening localized along Mezosoic extensional basins creating tectonic inversion of old normal faults. The result of progressive shortenning was the formation of intra-continental mountain chains (the EC, Santander Massif and the Mérida and Perijá ranges). Shortening of the continental lithosphere induced large left-lateral displacements along the SMB fault and E-SE dipping intra-continental subductions beneath the EC and the Andes de Mérida range. The Andean tectonic phase in the EC, which began at 10.5 Ma, induced thickening of the continental crust and around 70 km shortening. The mean convergence rate absorbed in the EC during the Andean phase is around 7 mm/y.

The convergence between the Nazca plate and NWSA is partly absorbed along an active subduction zone which is clearly identified by intermediate seismicity southwards of the CB. North of latitude 5°N the subduction zone is not well defined by seismicity, and it ought to be located beneath the Baudo Range and the Western Cordillera. Notice that the subducting plate corresponds to the Northern termination of the Nazca plate, which also subducts beneath Western Panama.

REFERENCES

Boinet, Th., J. Bourgois, H. Mendoza and R. Vargas, La falla de Bucaramanga (Colombia) : su funcion durante la orogenia andina, Geol. Norandina, 11, 3-10, 1989.

Colletta, B., F. Roure, B. De Toni, D. Loureiro, H. Passalacqua and Y. Gou, Tectonic inheritance, crustal architecture, and contrasting structural styles in the Venezuela Andes, Tectonics, 16, 777-794, 1997.

Colletta, B., F. Hebrard, J. Letouzey, P. Werner and J. Rudkiewicz, Tectonic Style and Crustal Structure of the Eastern Cordillera (Colombia) from a balanced cross section, J. Letouzey ed. Petroleum and Tectonic in Mobile belts, Paris, 81-100, 1990.

Cooper, B., F. Addison, R. Alvarez, M. Coral, R. Graham, A. Hayward, S. Howe, J. Martinez, J. Naar, R. Peñas, A. Pulham, and A. Taborda, Basin development and tectonic history of the Eastern Cordillera and Llanos Basin, Colombia, AAPG Bull., 79, 1421-1443, 1995.

Duque-Caro, H., The Chocó Block in the northwestern corner of South America : structural, tectonostratigraphic, and paleogeographic implications, J. South Am. Earth Sci., 3, 71-84, 1990.

Freymueller, J., J. Kellogg, and V. Vega, Plate motions in the North Andean Region, J. Geophys. Res., 98, 21853-21863, 1993.

Martinez, A., Géologie de la région d'Iza, Boyacá. Cordillère Orientale de Colombie, Mem. Inst. de Minéralogie et Géol., Univ. de Lausanne, 34 pp, 1989.

Rivera, L. A., Inversion du tenseur de contraintes à partir des données de polarité pour une population de séismes: Aplication au Nid de Bucaramanga, Ph. D. thesis, 266 pp., IPGS, France, 1989.

Taboada, A., C. Dimaté, and A. Fuenzalida, Sismotectonica de Colombia: deformacion continental activa y subduccion, Fis. de la Tierra, Madrid, 10, 111-147, 1998.

Tschanz, C., R. Marvin, B. Cruz, H. Mehnert and C. Cebulla, Geologic evolution of the Sierra Nevada de Santa Marta, Northeastern Colombia, Geol. Soc. Am. Bull., 85, 273-284, 1974.

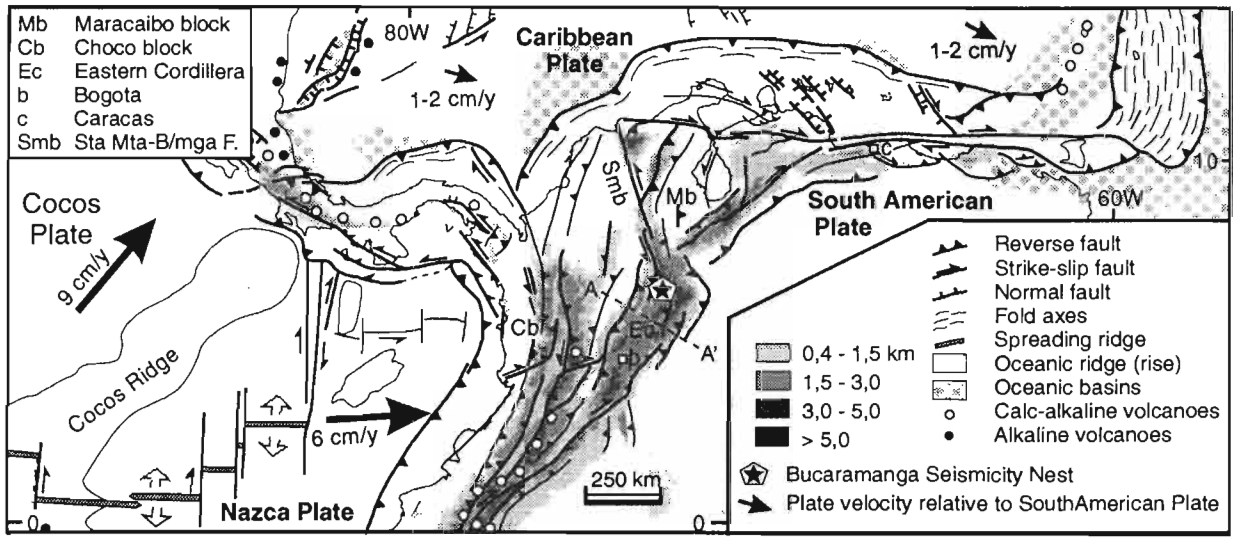

Figure 1: Neotectonic map of the Northern Andes and the Caribbean Region

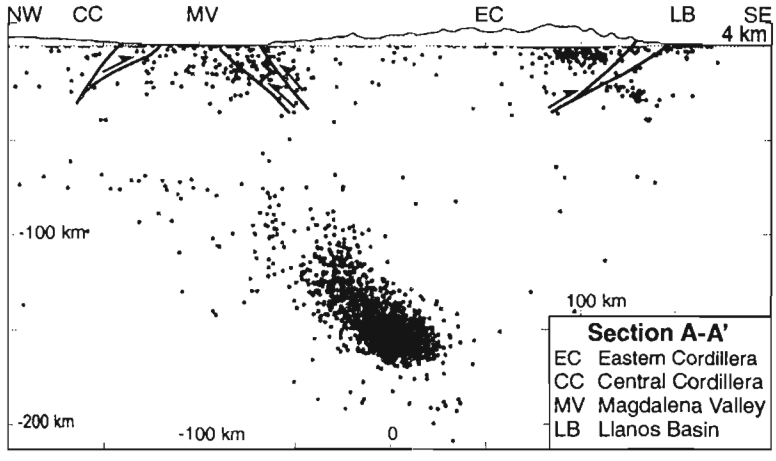

Figure 2 : Cross section A-A' orthogonal to the Eastern Cordillera (Figure 1), including seismicity within a band that covers the northern segment of the range (from Tunja to Bucaramanga). Intermediate seismicity is interpreted in terms of subduction of infracontinental lithospheric mantle beneath the EC. The vertical exagerated for topography = 3.

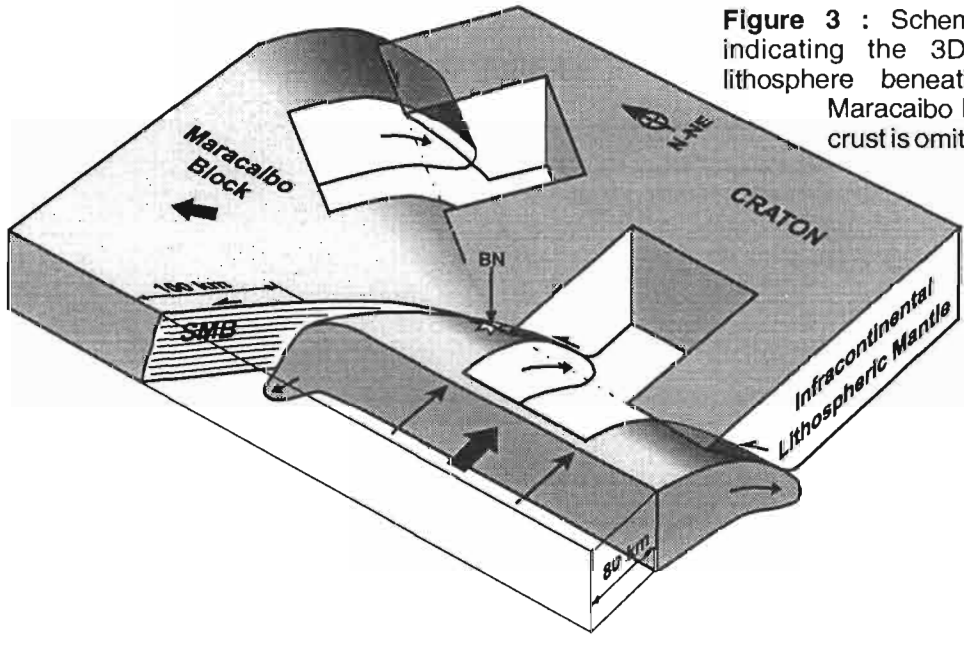

Figure 3 : Schematic block diagram indicating the 3D geometry of the lithosphere beneath the EC and the Maracaibo block (the continental crust is omitted). Intracontinental subductions are defined beneath the EC and the Mérida Andes. The Bucaramanga seismicity nest (BN) is located in the inflected zone where the EC subduction joins the SMB fault.

TWO-DIMENSIONAL FINITE-ELEMENT, THERMAL MODELLING OF THE ANDEAN CRUSTAL SECTION AT 21°S FROM 60 MA TO PRESENT; IMPLICATIONS FOR THERMAL EVOLUTION

David C. TANNER(1), Gerhard WÖRNER(2) and Andreas HENK(3)

(1) Geochemisches Institut, Universität Göttingen, Goldschmidtstraße 1, D-37077 Göttingen, Germany (dtanner@ugcvax.dnet.gwdg.de)
(2) Geochemisches Institut, Universität Göttingen, Goldschmidtstraße 1, D-37077 Göttingen, Germany (gwoerne@gwdg.de)
(3) Geologisches Institut, Universität Würzburg, Pleicherwall 1, D-97077 Würzburg, Germany (a.henk@mail.uni-wuerzburg.de)

KEYWORDS: Andes, finite-element modelling, thermal evolution, lower crust melting

INTRODUCTION

The Andean lithospheric section at 21°S, perpendicular to the eastward-directed subduction of the Nazca Plate, is unique for a number of reasons: The crust has been thickened to *ca.* 70 km (Beck et al. 1996), producing the 4 km elevated Altiplano plateau but without a continent-continent collision (Lamb & Hoke, 1997). The back-arc has been continually shortened by thrusting by at least 200 km (e.g. Sheffels 1990) and the asthenosphere is at present very close to the base of the crust for at least 250 km under the arc zone (Hoke et al. 1994).

We attempt to reconstruct the 2D thermal history of this Andean section for the last 60 Ma by finite-element forward modelling to answer these questions:

1. What is the present thermal structure within the Andean lithosphere.
2. How much crustal melting has taken place beneath the arc zone?
3. What is the effect of the interplay between advective heat input, crustal heat production and crustal thickening ?

METHOD

We produced 400 km-deep cross-sections of the Andean section from the Pacific Ocean to the Chaco Plains for the time period 60 Ma to present at 5 Ma increments. As well as the present geophysical structure of the Andes, the sections were based on a number of data sources. Crustal sections over time were constructed from data on rates and timing of uplift, morphological and sedimentological data, and shortening data (e.g. Sheffels 1990) (see Fig. 1).

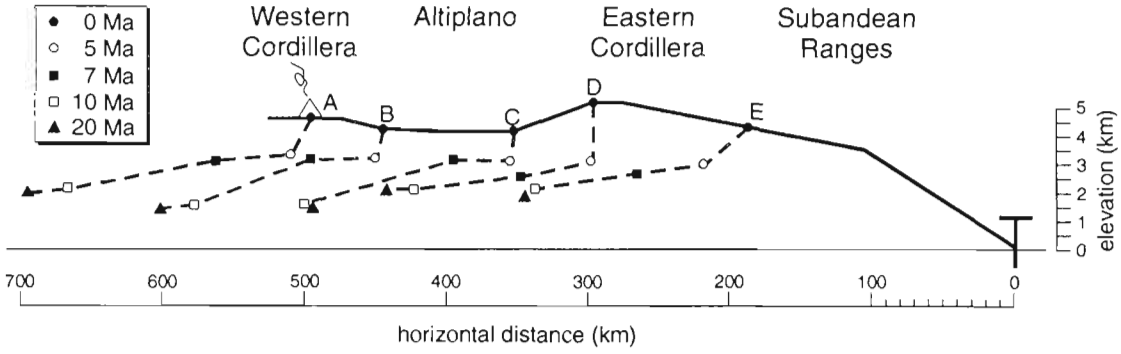

Figure 1: Displacement paths of various points (A-E) in the Central Andes from 20 Ma to present. Note the time intervals are not constant. The total finite shortening is 200 km, but this is heterogeneously distributed in space and time. All paths display mainly horizontal displacement from 20 to 5 Ma (velocities up to 30 mm a^{-1}; A, C) and then mainly vertical displacement (velocities up to 2 mm a^{-1}). A general west to east temporal shift of tectonic displacement is also apparent.

Airy isostatic equilibrium was assumed. Area balance in the two dimensional sections is only maintained if the Brazilian Shield is assumed to have been thrusted from east to west under the Andes by *ca.* 200 km (e.g. Watts et al. 1995) over the last 15 Ma ($1\sigma = 3\%$).

Fore-arc geometry was mainly determined by the subduction angle and rate of tectonic erosion (as seen by the easterly retreat of the arc). Flattening of the subduction angle was accommodated by temporary growth of the forearc, but with a maximum growth rate of 300 km^2 Ma^{-1} (Kopf 1995).

We envisage three sources of heat;

1. internal heat production in the crust,
2. basal heat input by conduction from the lower mantle and
3. advective primary melt movement as intrusions into the "arc zone", the width and location at a given time interval of which was taken from geochronological data.

To model the first two sources, realistic values were given to the model in finite-element space (respectively, 0.5-3 μW m^{-3}, depending on lithology and 15-30 mW m^{-2}). The latter was modelled by placing (randomly in the vertical axis and with a Gaussian distribution in the horizontal axis) a number of

5-50 km^2 squares (the total area of which equalled the primary magma input; Table 1) in the arc zone conduit every 5 Ma with basalt liquidus temperatures.

Table 1: Parameters used to construct the model.

time period (Ma)	subduction angle (°) [1]	eastward migration of the arc zone (km) [2]	width of arc zone (km) [2]	primary magma input (km^2 Ma^{-1}) [3]
0 - 5	30	0	120	16
5 - 10	20	0	95	16
10 - 15	15	10	105	16
15 - 20	20	20	115	16
20 - 25	15	10	130	16
25 - 30	12	15	25	frozen [4]
30 - 35	12	15	35	frozen [4]
35 - 40	65	0	30	20
40 - 45	35	5	30	20
45 - 50	35	0	35	20
50 - 55	60	40	30	20
55 - 60	60	0	20	20

[1] calculated from the plate convergence velocity (after Tovish & Schubert 1977).
[2] estimated from position of the harmonic mean and range of radiometric ages of plutonites, for each time period.
[3] own unpublished data, based on erupted magma volumes, estimates for fractionation, intrusion/extrusion rates and crustal recycling rates from isotope measurements.
[4] denotes the arc zone was closed to the passage of melt due to very flat subduction.

CONCLUSIONS

We generated a 2D finite-element model of the 21°S Andean section from uplift, sedimentological and geophysical data for the time period 60 Ma to the present. Three heat sources were considered: basal heat flow, radiogenic crustal heat production and advection of mantle magmas into the arc zone.

The model predicts the thermal evolution of the Andean crustal section and, in particular, timing and volume of lower crustal melting under the arc zone. This is important for a number of reasons. It can:

1. Quantify the amount of partial crustal melting through time to the present under the Andean arc (as suggested by geophysical evidence, e.g. Rietbrock & Haberland 1998),
2. Constrain models which allow coeval thickening of the crust and thinning of the mantle lithosphere in a subduction environment, as in the case of the Andes.
3. By providing evidence for the rheological structure of the lithosphere, improve structural models of the Andean evolution.

REFERENCES

Beck, S., Zandt, G., Myers, S. C., Wallace, T. C., Silver, P. G. & Drake, L. 1996. Crustal thickness variations in the Central Andes. Geology, **24**, 407-410.

Hoke, L., Hilton, D. R., Lamb, S. H., Hammerschmidt, K. & Friedrichsen, H. 1994. ^{3}He evidence for a wide zone of active mantle melting beneath the Central Andes. Earth and Planetary Science Letters, **128**, 341-355.

Kopf, A. 1995. Feststoffbilanzierung akkretierten und subduzierten Sediments und comptergestützte Rückwarts-modellierung deformierter Krustenquerschnitte am Kontinentalrand von Südchile. Giessener Geologische Schriften, **55**, 1-225.

Lamb, S. & Hoke, L. 1997. Origin of the high plateau in the Central Andes, Bolivia, South America. Tectonics, **16**(4), 623-649.

Rietbrock, A. & Haberland, C. 1998. ANCORP 96: das passive seismologische Experiment. Berichtsband 1996-1998 der Sonderforschungsbereich 267, "Deformationsprozesse in den Anden", 470-480.

Sheffels, B. M. 1990. Lower bound on the amount of shortening in the central Bolivian Andes. Geology, **18**, 812-815.

Tovish, A. & Schubert, G. 1977. Correlations between angle of subduction, arc curvature, and convergence velocity. Eos, Transactions, American Geophysical Union, **58**(12), 1232.

Watts, A. B., Lamb, S. H., Fairhead, J. D. & Dewey, J. F. 1995. Lithospheric flexure and bending of the Central Andes. Earth and Planetary Science Letters, **134**, 9-21.

MAGNETIC PROPERTIES OF LA NEGRA FORMATION (CHILEAN COASTAL CORDILLERA): COMPARATIVE ANALYSIS BETWEEN ZONES WITH AND WITHOUT COPPER MINERALIZATION

Andrés TASSARA (1), Pierrick ROPERCH (1) & Patricio SEPULVEDA (2)

(1) Laboratorio de Paleomagnetismo, IRD (ex ORSTOM) - Departamento de Geología, Universidad de Chile, atassara@cec.uchile.cl, properch@dgf.uchile.cl,
(2) Compañia Minera Carolina de Michilla, Antofagasta, psepulveda@michilla.cl

Key Words: Magnetic mineralogy and magnetic anomalies; Jurassic volcanism and metallogenesis.

INTRODUCTION

We present a characterization of the magnetic properties of La Negra Formation, the most important geological unit of the northern Chile Coastal cordillera. This formation corresponds to a nearly 7.000 m thick sequence of basalts to andesites that were deposited in an island arc to back arc position at Jurassic times. Contemporaneous intrusions (tonalite to granodiorite) cut the volcanics. Regionally distributed very low-grade metamorphism affects the lava flow sequence at different stages. La Negra Formation is the host unit of numerous Cu stratabound deposits [Boric et al., 1990], that provide the second source of Cu production in Chile. This metallogenic belt is the object of mineral exploration supported by high-resolution aeromagnetic data. However the interpretation and the modelization of magnetic anomalies usually do not rely on direct knowledge of the magnetic properties of the underlying rocks. The aim of the present study is to present an extensive characterization of La Negra Formation magnetic properties in areas with and without copper mineralization. The second objective is to use paleomagnetism in mineralized rocks to provide additional insights on mineralization processes, especially about the timing of mineralization events and the behavior of magnetic minerals upon increasing degrees of mineralization.

SAMPLING AND RESULTS

We have selected four areas along the Coastal cordillera between 22° and 25°S that allow us to obtain a regional characterization of the magnetic properties of different rock types from La Negra Formation. From north to south, these areas are (1) Tocopilla, (2) Carolina de Michilla mining district (3) Antofagasta and (4) Paposo (Figure 1). Areas 1, 3 and 4 correspond to non-mineralized sections of the

volcanic sequence. Sampling of rocks affected by hydrothermal alteration and copper mineralization was made in the stratabound deposits that characterize the Michilla district.

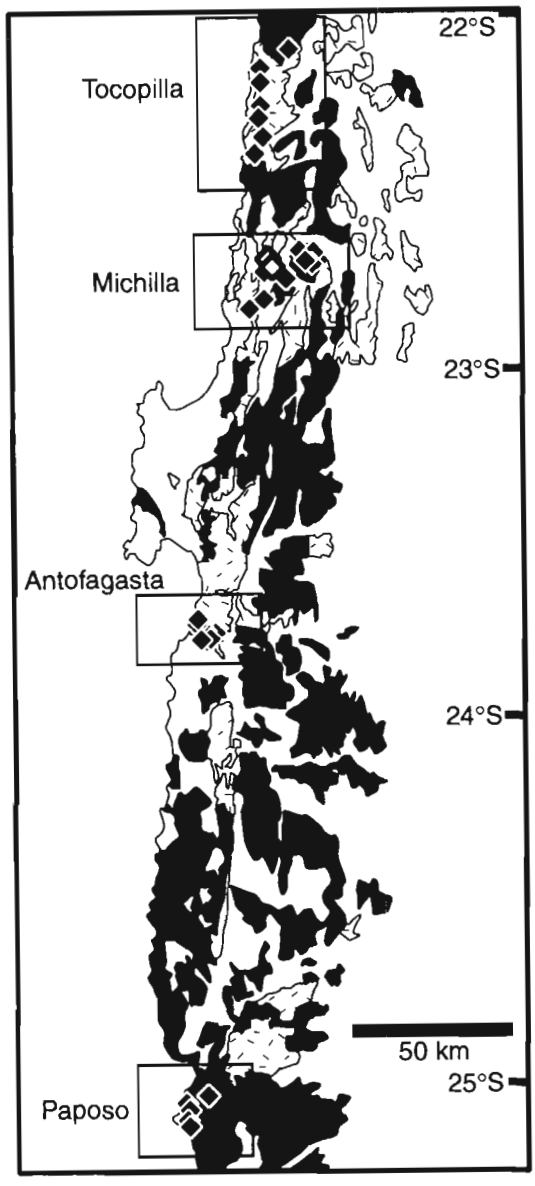

Figure 1: Paleomagnetic sampling in the coastal area of the Antofagasta region.

The paleomagnetic sampling corresponds to 13 sites in Tocopilla area, 9 at Paposo and 17 at Antofagasta, most of them in lava flows and a few in subvolcanic granodioritic to dioritic bodies. Near Antofagasta the paleomagnetic sampling was distributed along a 3000 meters thick profile in the type section of the Formation, "Quebrada La Negra". Evidence of low-grade metamorphism, characterized by the association epidote-clorite-calcite-chalcedonite-zeolites-prehnite-pumpellite is widespread, especially in the brecciated levels of the lava flows. This metamorphism appears more important near Antofagasta than near Tocopilla. In the Carolina de Michilla mining district region, we have taken 250 samples in 2 mining cores 250 and 350 meters long respectively. These cores cut orthogonal the lava flows and related intrusives affected by hydrothermal alteration and Cu-oxides mineralization. Ore bodies present vertical zonation from chalcopyrite-pyrite-magnetite at deeper zones to chalcosine-coveline-hematite to the surface with increasing quantities of Cu oxides.

MAGNETIC PROPERTIES

Magnetic susceptibility of the lava flows for all areas is usually high, ranging from 0.01 to 0.1 (S.I. units) (Figure 2). The highest values are found near Tocopilla, a feature that correlates with the minor amount of low-grade metamorphism. Intensities of magnetic remanence are distributed between 0.06 to 0.6 A/m, with rare values above 1 A/m.

Primary magnetization are found in most sites of the Tocopilla area, while secondary partial to total magnetic overprints characterized most samples collected in the Antofagasta and Paposo areas. As seen in figure 2, the distribution of the magnetic susceptibility versus intensity of remanent magnetization

for samples taken from the cores is roughly similar to the distribution found at other locations in rocks from La Negra Formation. Near Tocopilla, large crystals of magnetite are often seen and laboratory experiments indicate multidomain magnetites as the magnetic carrier.

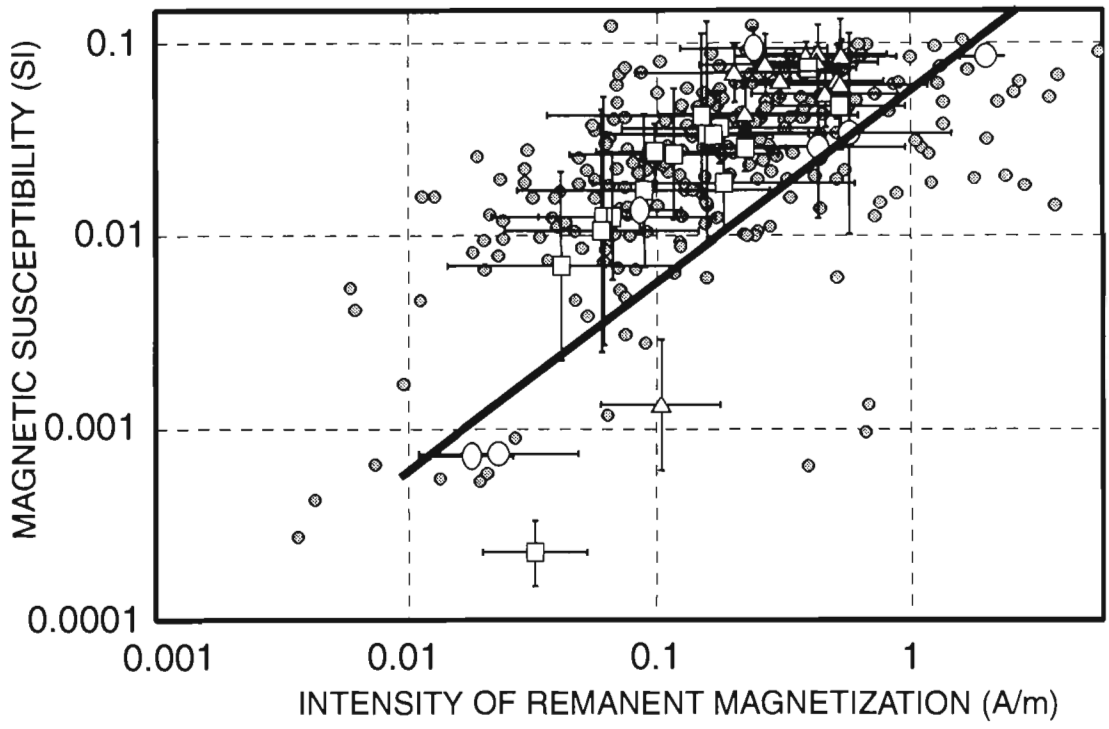

Figure 2: Log-Log plot of the magnetic susceptibility (K) versus intensity of remanent magnetization (J_{NRM}). The thick line corresponds to a Koenigsberger ratio (J_{NRM} /KH) of one. (H is the intensity of the Earth Magnetic Field in northern Chile (~21A/m)) . Data above this line correspond to rocks with an induced magnetization greater than the remanent magnetization. Filled circles are individual samples from the mining cores. White triangles, squares and circles with associated standard deviation are geometric mean site values from Tocopilla, Antofagasta and Paposo areas.

The low magnetic stability of multidomain grains explains why the intensity of natural remanent magnetizations is relatively low. The Koenigsberger ratio is significantly less than one and remanent magnetizations will not contribute much in producing strong magnetic anomalies (Figure 2). Magnetite and maghemite are the principal carrier of the magnetic susceptibility. The presence of maghemite was essentially deduced from the sharp drop in susceptibility during laboratory heating in the temperature range 300°-350°C. Maghemitization due to low-temperature oxidation of magnetite is widespread in these andesitic lavas, probably related to low grade metamorphism. The similar susceptibility of both minerals permits however to maintain a relatively high bulk susceptibility for these rocks. As seen in figure 3, samples with a high maghemite content have the same range of susceptibilty values than those containing magnetite. Maghemitization affects essentially the lavas and not the intrusive bodies.

Maghemization is however a significant factor in reducing the initial remanent magnetization acquired during the emplacement of the volcanic rocks.

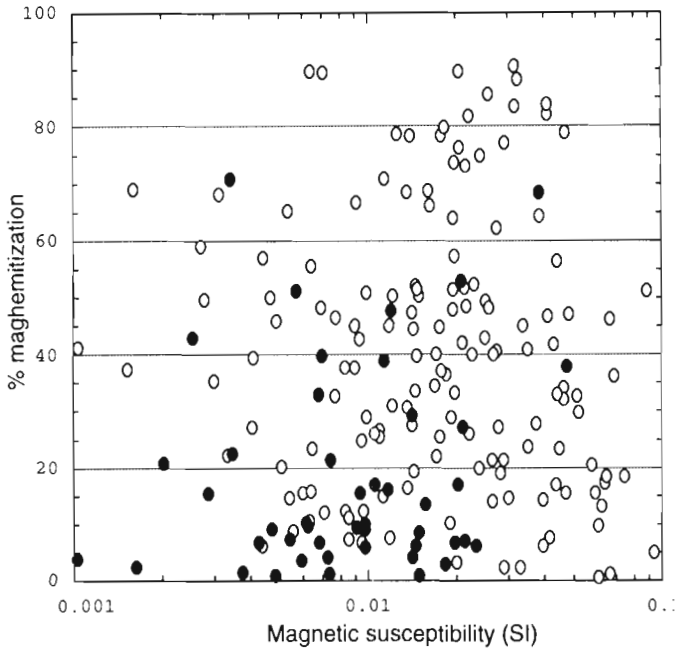

Figure 3: Importance of the maghemitization (defined by the decrease of magnetic susceptibility between 250°C and 350°C) with respect to initial magnetic susceptibility. Samples from the two mining cores.

There is no significant difference between the magnetic properties of non-mineralized areas and the two drill cores from Michilla district (Figure 2). At the regional scale of an aeromagnetic survey, Cu metalogenic processes do not generate relevant changes in magnetic properties of La Negra rocks that would be useful as prospective keys in magnetic surveys. There is however complete destruction of primary magnetic mineralogy only at metric scales where an important concentration of chalcosine and coveline is observed.

In this case, low magnetic susceptibility indicates that hematite is the dominant magnetic carrier. It is interesting to note that these mineralized rocks have stable univectorial remanent magnetizations. Further work is in progress to relate the paleomagnetic information contained in these rocks with the hydrothermal processes

CONCLUSIONS

Magnetic properties of La Negra Formation are characterized by high magnetic susceptibility and relatively low magnetic remanence, consequence of relict primary mineralogy and secondary effects related to very low grade metamorphism. These characteristics are not affected at district to regional scales by Cu stratabound metallogenic processes. At these scales there is no contrast in terms of magnetic susceptibility between mineralized and non-mineralized zones, that could generate a significative magnetic anomaly. Only at local (metric) scales would be seen in very high-resolution magnetic survey some anomalies related to small intrusive bodies with low total magnetization and mineralized bodies with very low susceptibility linked to chalcosine-coveline-hematite. Conclusions, drawn in this paper, are obviously related to the type of mineral deposits observed in the Michilla district and may not apply to other environments.

MESOZOIC MAGMATISM IN BOLIVIA AND ITS SIGNIFICANCE FOR THE EVOLUTION OF THE BOLIVIAN OROCLINE

TAWACKOLI(1), Reinhard RÖSSLING(1), Bernd LEHMANN(2), Frank SCHULTZ(2), Marcelo CLAURE ZAPATA(1) & Boriz BALDERRAMA(1)

(1) Servicio Nacional de Geología y Minería (SERGEOMIN), Casilla 2729, La Paz, Bolivia
(2) Institut für Mineralogie und Mineralische Rohstoffe, Technische Universitaet Clausthal, Adolph-Roemer-Strasse 2a, D-38678 Clausthal-Zellerfeld, Germany

KEY WORDS: Bolivia, Mesozoic, alkaline-tholeiitic magmatism, rifting, triple junction

INTRODUCTION

Mesozoic outcrops in Bolivia (Fig.1) occur in four distinct morphotectonic units. In the Bolivian Altiplano mostly fault bounded Cretaceous sedimentary rocks reach the surface at ca. 3700 m caused by the Andean deformation and the subsequent uplift of the plateau.

In the Eastern Cordillera (EC) the Mesozoic outcrops follow the bending of the Andean orocline with mainly isolated occurrences of continental to partly marine clastic deposits of Jurassic? - Cretaceous age. The stratigraphy of these redbeds, due to its poor fossil content, is based on a few age determinations of intercalated mafic volcanic rocks as lava flows and associated dikes, sills and stocks. The latter ones intruded also the Paleozoic sediments of the EC with locally notable amounts of extension. The present-day erosion level of the Paleozoic basement in the EC cuts only few intrusive bodies of Cretaceous age.

Other Mesozoic outcrops in Bolivia are lined up along the Subandean fault and thrust belt. Herein the Triassic?-Cretaceous continental sedimentation is accompanied by magmatic events of a wide time range. Further to the east the few Mesozoic outcrops rise up like inselbergs from the Chaco plain and the Precambrian shield. The Mesozoic rocks here are represented by fluvio-eolian Jurassic? - Cretaceous deposits as well as intrusive Cretaceous alkaline complexes found only in metamorphosed Precambrian host rock.

So far the available ages of single magmatic events support the assumption of several distinct Mesozoic magmatic phases in Bolivia (Soler & Sempere, 1993; Avila-Salinas, 1986). However, neither the rock compositions nor the rock ages can be regionally correlated in a satisfying manner. Most of these magmatic rocks have suffered profound thermal and chemical alteration (also due to the periodic cover by

sea water (Sempere, 1994)), so that geochemical data for classifications and age determinations only allow poorly reliable interpretations. Another aspect, which complicates the evaluation of magmatic events is the structural overprint of the corresponding rocks due to the Andean back-arc shortening (Kley et al., 1997).

This study resumes the available and some additional recent data about the alkaline magmatism in the Bolivian Andes with special regard to its importance for the evolution of the Bolivian orocline.

GEOLOGICAL FRAMEWORK

Mesozoic igneous rocks in Bolivia are strongly concentrated in the EC along a bended belt parallel to reactivated Eohercynian structures (Tawackoli, 1997). A few more outcrops are located in the Subandes and the Precambrian shield. In general intrusive rocks like dikes, sills and plutonic complexes are predominant over the known extrusive rocks, which can be used as stratigraphic markers. Major known Mesozoic magmatics are shown in Fig.1 and can be described as follows:

Figure 1: Mesozoic outcrops and the distribution of intrusive and effusive magmatism in Bolivia.

Mesozoic intrusives

a-Cerro Sapo

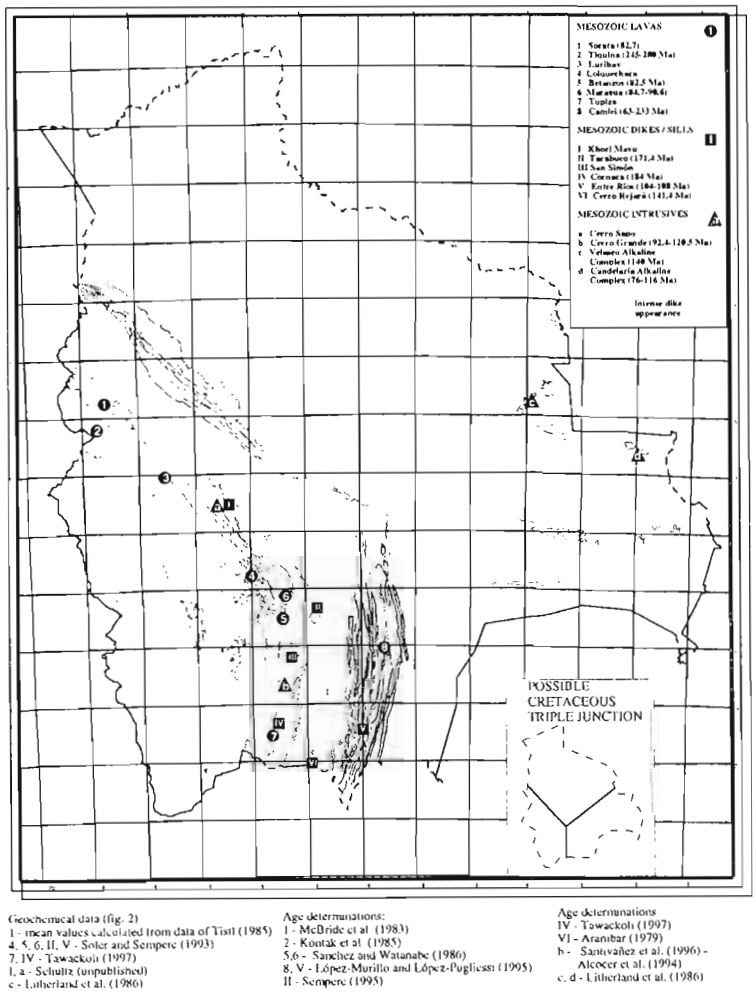

Cerro Sapo builds a NW/SE orientated nepheline-syenitic alkaline complex in the EC with local sodalite enrichment, which has been exploited since Incaic time. The intrusion is situated in marine Caradocian? shales. Carbonatitic dikes and stocks are present in the vicinity of the complex. A nearby breccia-pipe with kimberlitic clasts has been K-Ar dated by Kennan et al. (1995) with 97.7±2.8 Ma.

b-Cerro Grande

Cerro Grande is a poorly studied highly potassic gabbroic to syenitic intrusion situated in turbiditic Ordovician rocks in the southern EC. Santivañez et al. (1996) described the intrusion and the surrounding dikes as syenites and alkaline gabbros with an apparent age of 92.4 Ma. Rössling (in Alcocer et al., 1994) dated the stock with 120.0±0.5 Ma by K-Ar using two different biotite fractions.

c-Velasco Alkaline Complex (VAC)

This complex is composed of a suite of plutonic rocks intruded into the Precambrian gneiss and granulite basement. The rocks range from foyaites through pulaskites to nordmarkites, syenites and granites. Many silica-oversaturated dikes crosscut the complex and the surrounding basement. Rb-Sr and K-Ar dates gave a reliable age of ca. 140 Ma for the complex (Litherland et al. 1986). Another alkaline complex, the carbonatitic Manomó Complex occurs in the NE extension of the VAC-trend and is also believed to be of Mesozoic origin (Litherland et al. 1986).

d-Candelaria Alkaline Complex

This complex, located SE of the VAC, is buried for the most parts by the alluvium of the Pantano basin. K-Ar-ages vary from 116-76 Ma and the lithology is more restricted but similar to the one described for the VAC (Litherland et al. 1986). The complex is cut by dikes of different composition in NE/SW direction.

Mesozoic dikes/sills

I-Khori Mayu, III-San Simón, IV-Cornaca

Within the belt of alkaline magmatism in the EC, two regions are distinguished by intense occurrences of dikes and dike swarms following the regional structures (Fig.1). In the northern limb of the belt NW/SE orientated dikes can be observed between Cochabamba and Cerro Sapo and probably further towards NW up to Apolo along a distance of up to ca. 400 km. Dikes from the Rio Khori Mayu (near Cerro Sapo) have been classified by Schultz (unpublished) as lamprophyre (camptonite) and alkali-lamprophyre.

In the southern part of the limb, from the south to the north NNE/SSW to NE/SW trending dikes occur along a distance of ca. 120 km between Tupiza and Potosi. In the northern part, like in San Simón, the dikes point towards the Precambrian alkaline complex VAC. In the southern part near Cornaca a basanitic dike gave an apparent age of 184±4.9 Ma (Tawackoli, 1997). Ni-bearing ultramafic breccia pipes and pebble dikes are lined up N/S along a major fault zone.

II-Tarabuco, V-Entre Rios, VI-Cerro Rejará

In southern Bolivia, thick basaltic outcrops are preserved in two distinct synclines accompanied by Mesozoic sediments. The corresponding basalts (fig.1) of Tarabuco (171.4 Ma) and Entre Rios (104 and 108 Ma) are characterized by aphanitic, vesicular textures and have long been believed to be of extrusive origin. Recently, Sempere et al. (1998) described the basalts as parts of a giant sill of theoleiitic composition. Further south, at the Argentinean border, doleritic dikes cutting the Neoproterozoic? or Cambrian? alkaline granites of Rejará were dated with 141±10 Ma (Aranibar, 1979).

Mesozoic lavas

1-Sorata

A thick lava unit in Cretaceous redbeds is exposed near Sorata. McBride (1983) calculated an apparent K-Ar age of 82.7±2.0 Ma for these volcanics. The altered lavas are classified as trachyandesites to andesites of the calcalkaline (arc-related) series based on major oxides (Tistl, 1985) but need verification by immobile-element abundances.

2-Tiquina

The oldest Mesozoic lava flows have been dated near Lake Titicaca at Tiquina. Two distinct K-Ar ages of 245±5.8 and 280±7.6 Ma have been documented by Kontak et al. (1985). These basalts are intercalated with coastal sediments of upper Permian? to lower Triassic? age.

3-Luribay

Very little is known about the basalts of the syncline of Luribay. Due to the stratigraphic position above Cretaceous continental redbeds, Almendras-Alarcon (1993) assumed a Campanian-Maastrichian age for the basalts.

4-Colquechaca , 5-Betanzos , 6-Maragua

Layers of basalt are described near Colquechaca within late Jurassic? to early Cretaceous alluvial sediments (Soler & Sempere, 1993). Another deformed basalt outcrop can be observed in the syncline of Betanzos. An apparent age of 82.5 Ma is mentioned by Sanchez & Watanabe (1986) for these in general highly altered effusive rocks. Further north in the syncline of Maragua similar basalt flows are mapped by SERGEOMIN (1996). In the corresponding map two ages of 90.6±4.5 and 84.7±9.2 have been assigned to the basalts without references.

7-Tupiza

Highly altered, intercalated lavas in the syncline of Tupiza have been classified by trace-element geochemistry as alkaline basalts, basanites and nephelinites (Tawackoli, 1997). Near Tupiza, different lava horizons can be observed in redbeds overlapping fluvial quartzites, which form the base of the Cretaceous basin(s). The estimated age for these quartzites has been derived through regional correlation of similar lithologies. A recent reevaluation of these sediments in the EC suggest a Jurassic age (Sempere et al., 1998) for this rock group.

8-Camiri

In the Subandes the basalts of Camiri gave two widely spread ages of 63 and 233 Ma, documented by Lopez-Murillo & Lopez-Pugliessi (1995). These lavas overlie Permian-Triassic siliceous limestones and are characterized by intense alteration.

PETROLOGY AND TECTONIC IMPLICATION

In general the Mesozoic magmatic activity in Bolivia can be grouped into two partly overlapping intrusive phases. During the first phase from Middle Jurassic to Early Cretaceous (184-104 Ma) the emplacement of dikes and sills along a weakened zone in the EC is related to deep extensional structures. The main outcrops follow Paleozoic structures in the bend of the EC. Alkaline rift magmatism, as well as subalkaline, continental tholeiitic magmatism (Fig.2) is represented by lamprophyres, carbonatitic lamprophyres and minettes.

In the following Cretaceous phase (120.5-76 Ma) alkaline rocks like alkali-syenites, sodalite syenites, foyaites, alkali-gabbros, essexites and carbonatites intrude not only the formerly described weakened zone. Possibly, due to the establishment of a triple junction (Fig.1), with a center at the inflection point of the bend, the occurrence of Cretaceous intrusions in the stable Brazilian craton can genetically be related to those of the EC.

ROCK TYPE	MAIN-MINERALS	ACCESSORIES	ALTERATION MINERALS
intrusion (alkalisyenite, sodalite syenite, foyaite, alkali-gabbro, essexite, carbonatite)	alkaline feldspar (orthoclase, microcline, albite), nepheline, biotite, sodalite, ankerite, barite, clinopyroxene (augite-titanaugite, diopside), amphibole (hornblende, barkevikite), carbonate (ankerite)	apatite, sphene, zircon, pyrite, chalcopyrite, bornite, tourmaline, natrolite, magnetite, phlogopite, pyrochlore	carbonate, sericite, chlorite, serpentine
dikes/sills (lamprophyre, carbonate-lamprophyre, minette)	alkaline feldspar (orthoclase, microcline), plagioclase (bytownite, labradorite), Ti-biotite, amphibole (hornblende), clinopyroxene (augite-Ti-augite), orthopyroxene (hyper-sthene), olivine	apatite, perovskite, pyrite, sphene, hematite, chalcopyrite, magnetite	carbonate, sericite, chlorite, serpentine, antigorite, phlogopite, talc
lavas (alkali-basalt, basanite, nephelinite)	alkaline feldspar, plagioclase (labradorite), clinopyroxene (augite, diopside), biotite, analcim, nepheline, olivine, volcanic glass	apatite, hematite, magnetite	carbonate, sericite, chlorite, zeolite

Table 1: Major rock description and mineral content of the Mesozoic alkaline and tholeiitic magmatites of Bolivia.

The age range determined for the Mesozoic extrusive basalts in Bolivia spans the entire Mesozoic era. Most of the alkaline lava flows (Fig. 2) can be classified as alkali-basalts, basanites and nephelinites. Commonly the basalts are affected by thermal and/or chemical alteration (Tab. 1), so that one has to doubt the extreme K-Ar age range. There is a Late Cretaceous age maximum between 82.5-94.7 Ma. This is why the extrusive magmatism is considered to be coeval to the second igneous phase of plutonic emplacement in shallow crustal levels.

So far, the shape of the Bolivian orocline has been discussed as a result of different amounts of Andean crustal shortening (Isacks, 1988). However, the fault-related Mesozoic alkaline and tholeiitic magmatism in the EC frames the orocline and gives reason for the assumption, that the uplift of the Andean orogeny was influenced by the reactivation of Mesozoic and probably coaxial Paleozoic structures.

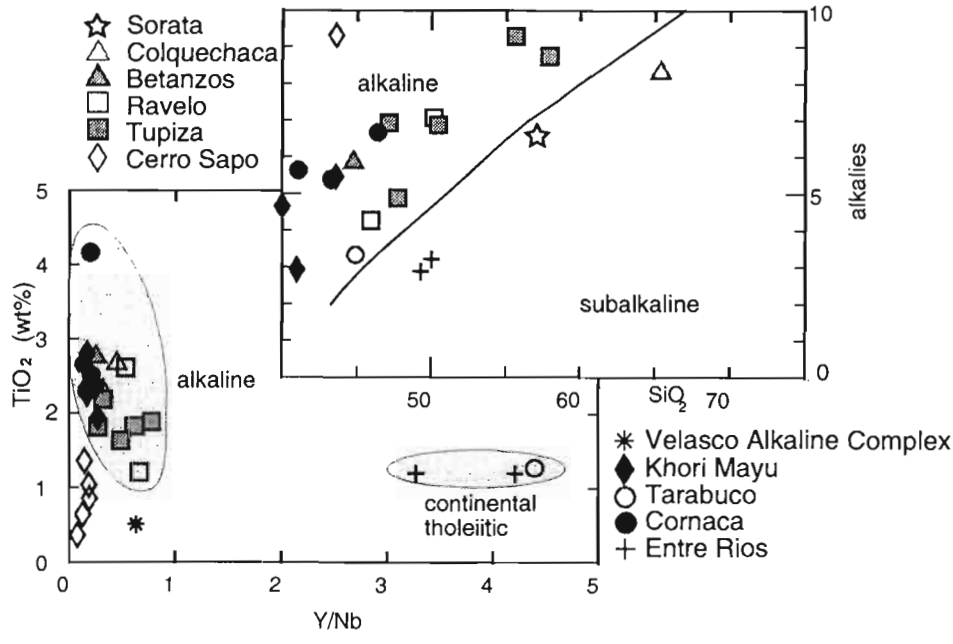

Figure 2: Classification of Bolivian Mesozoic alkaline, subalkaline and tholeiitic magmatism after Irvine & Baragar (1971) and Floyd & Winchester (1975). Source of data referenced in Fig. 1.

REFERENCES

Alcócer I., Amador J., Arequipa P., Argandoña J.L., Borja G., Grissemann Chr., Medina A., Mylius H.-G., Nuñez G., Palenque H., Riera C., Rössling R., Schneider A. & W. Schröder, 1993, Prospección y Exploración de Metales Basicos y Preciosos en el Departamento de Potosí / Bolivia: Informe Final inedito, proyecto Geobol-BGR.

Almendras-Alarcon, O., 1993, Estudio geológico regional Area Yaco-Caxata: Tesis U.M.S.A. La Paz – Bolivia. 52 p.

Aranibar, O., 1979, Geología regional de la parte sur de la hoja geológica Padcaya (n° 6628), Dpto. de Tarija: Informe interno GEOBOL, 27 p.

Avila-Salinas W., 1986, El Magmatismo Cretácico en Bolivia: Proccedings Simposium International Proy. 242 IGCP, p. 52-70, La Paz.

Floyd, P.A. & J.A. Winchester, 1975, Magma-type and tectonic setting discrimination using immobile elements: Earth. Planet. Sci. Lett. 27: 211-218.

Irvine T. N. & W.R.A. Baragar, 1971, A guide to chemical classification of the common volcanic rocks: Can. J. Earth Sci. 8: 523-548.

Isacks, B. L., 1988, Uplift of the Central Andean Plateau and bending of the Bolivian Orocline: J. Geophys. Res. 93: 3211-3231.

Kennan, L., Lamb, S. & C. Rundle, 1995, K-Ar dates from the Altiplano and Cordillera Oriental de Bolivia: Implications for Cenozoic stratigraphy and tectonics: J. South American Earth Sci. 8: 163-186.

Kley J., Müller J., Tawackoli S., Jacobshagen V. & E. Manutsoglu, 1997, Pre-Andean and Andean-age deformation in the eastern Cordillera of southern Bolivia: J. South American Earth Sci. 10: 1-19.

Kontak, D.J., Clark, A.H., Farrar, E. & D.F. Strong, 1985, The rift associated Permo–Triasic magmatism of the Eastern Cordillera: A precursor to the Andean orogeny, In: Magmatism at a plate edge: The Peruvian Andes, Pitcher, W.S., Atherton, M.P., Cobbing, J. & R.D. Beckinsale (eds.), p. 26-44, London.

Litherland, M., Anells, R.N., Apleton, J.D., Berrangé, J.P., Bloomfield, K., Fletcher, C.J.N., Hawkins, M.P., Klinck, B.A., Llanos, A., Mitchell, W.I., O'Connor, E.A., Pitfield, P.E.J., Power, G. & B.C. Webb, 1986, The Geoloy and mineral resources of the Bolivian Precambrian shield: British Geological Survey. Overseas Memoir 9: 1-153.

Lopez-Murillo, R.D. & J.M. Lopez-Pugliessi, 1995, Estratigrafia del Grupo Tacurú de las Sierras Subandinas: Rev. Técn. YPFB 16: 27-36.

McBride, S.L., Robertson, R.C.R., Clark, A.H., & E. Farrar, 1983, Magmatic and metallogenetic episodes in the Northern tin belt, Cordillera Real, Bolivia: Geol. Rdsch. 72: 685-713.

Sanchez, A. & M. Watanabe, 1986. Edades radiométricas de Bolivia: Convenio Instituto de Geología Económica U.M.S.A.-J.I.C.A. La Paz-Bolivia, v. 1, 53 p.

Santivañez, R., Motomura, Y. & A. Sanchez, 1996, Características petrológicas del magmatísmo de la zona de Vichacla-Cotagaita: Memorias del XII Congreso Geológico de Bolivia – Tarija. p. 869-878.

Sempere T., 1994, Kimmeridgian? to Paleocene Tectonic Evolution of Bolivia: In: Salfity J.A. (Ed.) Cretaceous Tectonics of the Andes, Vieweg, p. 168-212.

Sempere T., Carlier G., Carlotto, V. & J. Jacay, 1998, Rifting Pérmico Superior-Jurásico Medio en La Cordillera Oriental de Perú y Bolivia: 13. Congr. Geol. Boliviano, Memorias I, p. 31-38, Potosi, Bolivia.

Sempere, T., 1995, Phanerozoic evolution of Bolivia and adjacent regions: In: Petroleum Basins of South America, *A.J. Tankard, R. Suarez-Soruco & H.J. Welsink* (eds), AAPG Memoir 62, p.207-230.

SERGEOMIN, 1996, Thematic maps of mineral resources of Bolivia (1:250000), Sucre Quadrangle, SE 20-13: Sergeomin, La Paz, Bolivia.

Soler, P. & T. Sempere, 1993, Stratigraphie, géochimie et signification paleotectonique des roches volcaniques basiques mésozoïques des Andes boliviennes: Comptes Rendus de l'Academie des Sciences de Paris, Série II, 316: 777-784.

Tawackoli, S., 1997, Andine Entwicklung der Ostkordillere in der Region Tupiza (Südbolivien). PhD-thesis, Freie Universität Berlin, 116 p.

Tistl, M., 1985, Die Goldlagerstätten der nördlichen Cordillera Real/Bolivien und ihr geologischer Rahmen: Berliner Geowiss. Abh. A 65, 1-102.

A NEW TWIST TO THE SEARCH FOR MINERALISATION IN NORTHERN CHILE

Graeme K TAYLOR(1) and John GROCOTT(2)

(1) Department of Geological Sciences, University of Plymouth, Drake Circus, Plymouth, PL4 8AA, U.K. GTaylor@Plymouth.ac.uk
(2) School of Geological Sciences Kingston University, Kingston-upon-Thames, Surrey KT1 2EE, U.K. JGrocott@Kingston.ac.uk

KEY WORDS: Chile, Magnetic anomalies, Palaeomagnetism, Mineralisation, Rotation

INTRODUCTION

The Chilean Iron Belt is located in the eastern part of the Coastal Cordillera of Northern Chile between 25.5°S and 31.0° S. In its northern half, at least, intersections of major N-S to NNE-SSW structures, such as the Atacama Fault Zone, and NW-SE trending sinistral faults are common elements in the structural control of the location of Fe-Cu deposits (e.g. Bonson et al., 1997). These NW trending sinistral faults have also been linked to palaeomagnetically observed rotations in the same area (Randall et al., 1996; Taylor et al., 1998) which are thought to result from transpression during oblique subduction at the margin during and after the mid-Cretaceous. The deposits include the recently developed major Cu-Au deposit of Candelaria located some 20 km south of Copiapó. This paper will show that interpretation of the magnetic anomaly of Candelaria is readily linked to the known palaeomagnetic determined rotations in the area and that knowledge of the remanence vector may well be important in modelling magnetic anomalies associated with mineral deposits in northern Chile.

Palaeomagnetic studies in the region of 25 - 27°S in northern Chile (Forsythe et al., 1987; Riley et al., 1993; Randall et al., 1996; Taylor et al, 1996; and unpublished data) all consistently show large clockwise rotations of the crust in this part of northern Chile (Figure 1). These rotations are derived from measurements of the declination of the palaeomagnetic remanence. We have established that in at least one case, Mina Freesia (Figure 1 and 2) which is a magnetite-apatite deposit, that magnetite orebodies can carry a stable remanence whose declination is consistent with the observed remanence directions from volcanics, plutons, dykes and sediments measured throughout the area.

Exploration for economic mineral deposits frequently makes use of magnetic surveys to detect a

characteristic magnetic signature. Such anomalies arise from both an induced component, due to the present magnetic field interacting with the susceptibility of the deposit, and the remanent magnetic field due to the palaeomagnetism of the body. However only infrequently is the remanent field considered in the analysis of such anomalies because it is difficult to determine and most commonly is small in comparison to the induced field. However Roperch & Chauvin (1997) highlighted the fact that in northern Chile remanence may play an important part in the observed anomalies.

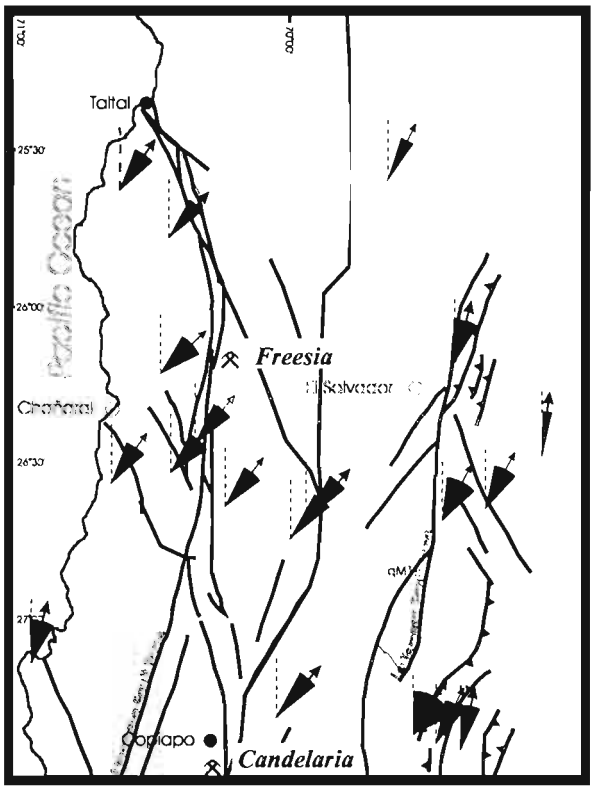

Figure 1 . Sketch map of northern Chile between 25 and 27°S showing major N-S and NW trending faults. Arrows represent the declination of the observed magnetic remanence directions and their 95% confidence cones.

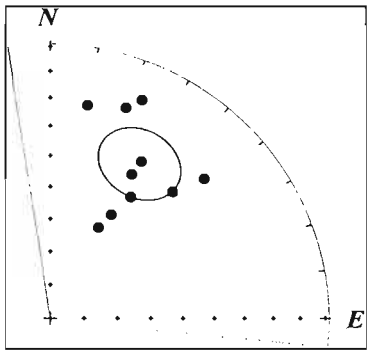

Figure 2. Palaeomagnetic results from the magnetite-apatite mine Mina Freesia showing a declination of about 30° consistent with the regional pattern of Figure 1.

CANDELARIA

Candelaria is the largest deposit in the Punta del Cobre belt and has mineable reserves of some 400 Mt at 1.0% Cu, 0.20 g/t Au and 4.5 g/t Ag at a cut-off grade of 0.4% Cu (Martin et al., 1997). Magnetite makes up 10-15% of the ore, occurs in a variety of forms and appears to be associated with both early and main phases of mineralisation (Ryan et al., 1995; Martin et al., 1997). The age of mineralisation in the Punta del Cobre district lies between 114 and 117 Ma (Marschik et al., 1997; Arévalo pers. comm., 1999), i.e.within the Cretaceous long Normal Polarity Interval.

Discovery and location of the deposit was essentially due to a single discovery borehole and IP geophysical exploration (Ryan et al., 1995). As part of the exploration effort a ground magnetic survey was carried out (Figure 3). Little interpretation was given for this map other than that

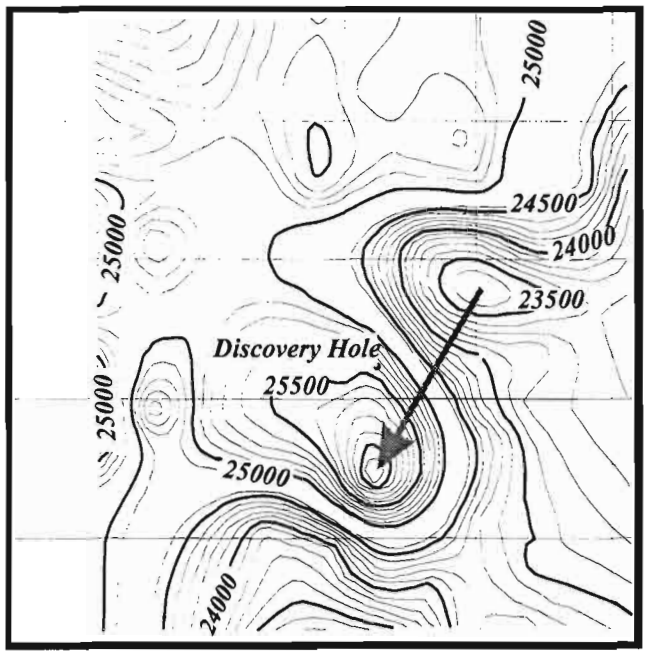

Figure 3. Ground magnetic anomaly map of the Candelaria area. The original discovery hole is located close to NE-SW trending axis of the anomaly (marked by the arrow). Note the low and high parts of the anomaly are located to the NE and SW respectively. Grid lines are every 500m and magnetic anomaly values are in nT(after Ryan et al., 1995).

the anomalies associated with the deposit lay in an area of high magnetic gradient between higher magnetic susceptibility rocks to the NW (the Coastal Cordillera batholith) and lower susceptibility rocks to the SE. It was also noted that regional aeromagnetic anomalies correlated well with the ground magnetic data and led to the discovery of the Alcaparrosa Deposit (Ryan et al., 1995).

The Candelaria magnetic anomaly (Figure 3) clearly shows a low to the NE and a high to the SE of the orebody. An anomaly arising from an induced component only would be expected to give rise to a high to the north and a low to the south of an orebody. Clearly the axis of this anomaly trends 030-210 and the polarity is reversed. Magnetic modelling results show that this is compatible with a strong remanent field (5-10 times the induced) with a declination of 215° and inclination of 40°, constraining the depths of the body using the published profiles (Ryan et al., 1995; Martin et al., 1997). This orientation is totally consistent with the observed palaeomagnetic declinations in the region (Figure 1) indicating the deposit has been rotated clockwise consistent with the regional observations. The polarity of the remanence is however reversed, implying either that it was acquired during a short reversal event in the Cretaceous Normal Polarity Superchron or that it was remagnetised post this period. If it is remagnetised this would be consistent with the remagnetisation event that affects the Cerillos formation rocks which lie to the east of the deposit (Riley et al., 1993; our unpublished data) and would probably have to post-date 83.5 Ma (the end of the Cretaceous Normal Polarity Superchron). A Palaeocene reheating event has previously been suggested on geochronological grounds (Marschik et al., 1997) which may have led to the remagnetisation. Such an age would imply that crustal rotation is considerably younger than the currently proposed mid-Cretaceous age for rotations in the Coastal Cordillera (Taylor et al., 1998).

CONCLUSIONS

The outcome of this study is that NE-SW orientated dipolar magnetic anomalies in much of northern Chile should be the norm for bodies whose magnetic signature is dominated by remanent rather than induced components of the magnetic field. A pre-rotation remagnetisation event, post 83.5 Ma, has affected the Candelaraia deposit. Magnetic anomalies with both normal and reversed polarities dominated by the remanence signle may be recognised from their rotated axes. An anomaly which requires a body some 10-20 times the size/magnetisation of the Candelaria deposit has already been identified in a structurally favourable location.

REFERENCES

Bonson, C. G., Grocott, J. & Rankin, A. H. 1997. Structural model for the development of Fe-Cu mineralisation in the Coastal Cordillera, Northern Chile (25°15'-27°15'S). VIII Congreso Geologico Chileno, Universidad de Catolica Norte, Antofagasta, Oct 1997, p 1608-1612.

Forsythe, R. D., Kent, D. V., Mpodozis, C. and Davidson, J., 1987. Paleomagnetism of Permian and Triassic rocks, central Chilean Andes. In: G.D. Mackenzie (Editor), Gondwana 6: Structure, tectonics and Geophysics. A.G.U. Monograph series, 40, pp. 241-252.

Martin, W., Díaz, R., Núñez, R., Olivares, R., Calderón, C. and Calderón, P., 1997. The updated Candelaria Geologica Mine Model. VIII Congreso Geologico Chileno, Universidad de Catolica Norte, Antofagasta, Oct 1997, p 1063-1067.

Marschik, R., Singer, B. S., Munizaga, F. Tassarini, C., Moritz, R. and Fontboté, L., 1997. Age of Cu (-Fe)-Au mineralization and thermal evolution of the Punta Del Cobre district, Chile.Mineralium Deposita, 32, 531-546.

Randall, D. E., Taylor, G. K. and Grocott, J., 1996. Major crustal rotations in the Andean Margin: Paleomagnetic results from the Coastal Cordillera of N. Chile. J. Geophys. Res., 101: 15783-15798.

Riley, P. D., Beck, M. E., and Burmester, R. F., Mpodozis, C. and Garcia, F., 1993. Palaeomagnetic evidence of vertical axis block rotations from the Mesozoic of Northern Chile. J. Geophys. Res., 98: 8321-8333.

Roperch, P., and Chauvin, A., 1997. Propiedades magneticas de las rocas volcanicas de Chile e interpretacion de las anomalias magneticas. VIII Congreso Geologico Chileno, Universidad de Catolica Norte, Antofagasta, Oct. 1997, p 790-794.

Ryan, R. J., Lawrence, A. L., Jenkins, R. A., Mattews , J. P., Zamora, J. C., Marino, W. E. and Urqeta, I. 1995. The Candelaria copper-gold deposit, Chile: In Pierce, F.W. and Bolm, J.G. (eds), Porphry Copper Deposits of the American Cordillera, Arizona Geological Society Digest, 20, 625-645.

Taylor, G. K., Randall, D.E., and Grocott, J., 1996. Palaeomagnetism strike-slip fault systems and crustal rotation in the region 25-27°S of northern Chile. Proceedings of the 3rd International Symposium on Andean Geodynamics, ISAG, Saint Malo, France, Sept. 1996, p 509-512.

Taylor, G. K., Grocott, J., Pope, A. and Randall, D. E., 1998. Mesozoic fault systems, deformation and fault block rotation in the Andean forearc: A crustal scale trike-slip duplex in the Coastal Cordillera of Northern Chile. Tectonophysics, 209, 93-109.

ORDOVICIAN COLLISION OF THE ARGENTINE PRECORDILLERA WITH GONDWANA, INDEPENDENT OF LAURENTIAN TACONIC OROGENY

William A. THOMAS(1) and Ricardo A. ASTINI(2)

(1) Department of Geological Sciences, University of Kentucky, Lexington, Kentucky 40506-0053 USA (geowat@pop.uky.edu)
(2) Cátedra de Estratigrafía y Geología Histórica, Universidad Nacional de Córdoba, Av. Vélez Sársfield 299, CC 395, 5000 Córdoba, Argentina (rastini@satlink.com)

KEY WORDS: Precordillera, Ocloyic, Taconic, Laurentia

INTRODUCTION

Substantial consensus holds that the Argentine Precordillera collided with Gondwana in mid-Ordovician time, and that the Precordillera was rifted from the Ouachita embayment of southern Laurentia. How the Precordillera arrived at the Gondwana margin, however, has continued to be interpreted in two different ways. In one interpretation, the Precordillera was rifted from Laruentia in Cambrian time; and, following independent drift in the Iapetus Ocean, the far-traveled Precordillera microcontinent collided with Gondwana (Astini et al., 1995; Thomas and Astini, 1996). In this microcontinent hypothesis, the collision of the Precordillera with Gondwana (the Ocloyic orogeny) was coincident in time with, but genetically unrelated to, the mid-Ordovician Taconic orogeny of southeastern Laurentia. In the other interpretation, a continent-continent collision of Laurentia with Gondwana in mid-Ordovician time was followed by rifting that left the Precordillera fragment of Laurentia attached to Gondwana (Dalla Salda et al., 1992). This continent-continent-collision hypothesis derived from the interpretation of a single continuous Taconic and Ocloyic orogenic belt which was severed by post-collisional rifting. Paleontological data, however, demonstrate that the Precordillera was isolated from Laurentia by Early Ordovician time (Astini et al., 1995; Benedetto, 1998). To attempt to accommodate the paleontologic data, the continent-continent-collision hypothesis has been modified by considering the Precordillera as a distal plateau on greatly stretched Laurentian crust prior to collision with Gondwana (Dalziel, 1997); however, the suggested modern analog, the Malvinas plateau, does not show faunal isolation from South America (Benedetto, 1998). The objective of this research is to consider

the possible relationships of the Taconic and Ocloyic orogenic belts through the use of direct evidence from synorogenic rocks.

OCLOYIC OROGENY

An upward transition from shallow-marine carbonate facies to black shales beginning in Arenig time and progressing diachronously southward indicates initial flexural subsidence of a foreland basin on the Precordillera in association with approach to a subduction zone beneath western Gondwana (Astini et al., 1995). Bentonites in mid-Arenig to Llanvirn strata document proximity to a volcanic arc (Huff et al., 1998). The black shales grade upward into a flysch-like synorogenic clastic wedge of mudstones, sandstones, and conglomerates, reflecting continued subsidence of the foreland basin and dispersal of sediment from an orogenic terrain on the east (Astini et al., 1995; Astini 1998). Local carbonate deposits, as well as a regionally diachronous unconformity, suggest migration of a peripheral bulge. The clastic wedge contains large blocks of the older passive-margin carbonate-shelf facies indicating block faulting within the subsiding foreland basin (Astini, 1998). The upper part of the clastic wedge includes glacial deposits, linking the Precordillera to Late Ordovician Hirnantian glaciation of Gondwana.

The synorogenic clastic wedge has a maximum thickness of ~1100 m in the northern Precordillera (Astini et al., 1995). The thickest part of the clastic wedge contains generally coarser components from the orogenic belt. The clastic wedge thins and fines southward along the Precordillera.

TACONIC OROGENY

In the Tennessee salient of the southern Appalachians, initial flexural subsidence of a foreland basin is indicated by an upward transition from shallow-marine carbonate facies to black shales beginning in early Middle Ordovician time (Drake et al., 1989). The black shales grade upward into a coarsening-upward synorogenic clastic-wedge turbidite succession of mudstones, sandstones, and conglomerates, reflecting continued subsidence of the foreland basin and sediment dispersal from an orogenic terrain on the east (Shanmugam and Lash, 1982). The detritus shows that the orogenic belt included the pre-Middle Ordovician passive-margin succession, older synrift sedimentary rocks and lavas, and Grenville basement (Drake et al., 1989). At the top, the clastic wedge grades upward into shallow-marine redbeds and sandstones. Bentonite beds extend cratonward beyond the clastic wedge.

The maximum thickness of the clastic wedge is ~2500 m in the central part of the Tennessee salient. The clastic wedge thins and fines southwestward (Thomas, 1977). Black shale with local sandstone interbeds thins southwestward to less than 200 m along the interior (proximal) structures of the thrust belt. In the foreland, shallow-marine redbeds and sandstones in the distal toe of the clastic wedge grade out westward into a carbonate facies.

COMPARISON OF THE RECORDS OF TACONIC AND OCLOYIC OROGENIES

The Taconic clastic wedge is thickest and coarsest in the Tennessee salient, and it thins and fines southwestward toward the Laurentian margin. The southern margin of eastern Laurentia is defined by the Alabama-Oklahoma transform fault (Thomas, 1991), which also marks the northern margin of the Precordillera (Thomas and Astini, 1996). At the northern margin of the Precordillera, the Ocloyic clastic wedge is thickest and coarsest, and it fines southward. In a reconstruction of a continuous Taconic-Ocloyic orogenic belt, the northern Precordillera is adjacent to the Alabama-Oklahoma transform margin of Laurentia, and the thin distal toe of the Taconic clastic wedge is adjacent to the thickest and coarsest part of the Ocloyic clastic wedge. The incompatible stratigraphic gradients argue strongly that these clastic wedges represent two distinct sediment dispersal centers and not the dismembered parts of a single clastic wedge. In addition to the stratigraphic gradients, other aspects of orogenic history provide equally strong evidence of two independent orogenic events. The bentonites of the Precordillera are older than those of the Taconic foreland (Huff et al., 1998). The upper part of the clastic wedge in the Precordillera contains characteristic Gondwanan glacial deposits, but the Taconic clastic wedge contains no glacial deposits. The Precordillera was strongly affected by normal faulting during subsidence of the foreland basin, in contrast to the Taconic foreland. Finally, a latest Ordovician, post-orogenic phase of extension strongly affected the Precordillera, but no manifestation of that extension has been recognized on southern Laurentia.

CONCLUSIONS

Differences in dispersal systems of clastic-wedge sediment, ages of bentonite beds, glacial deposits, and post-collision extension all argue strongly that the Taconic and Ocloyic orogenic belts represent two separate events and were not originally continuous. The two orogenic events occurred at approximately the same time on opposite sides of the Iapetus Ocean.

REFERENCES

Astini R.A. 1998. Stratigraphical evidence supporting the rifting, drifting and collision of the Laurentian Precordillera terrane of western Argentina. In Pankhurst R.J., Rapela C.W. (eds) The Proto-Andean Margin of Gondwana. Geological Society, London, Special Publications, 142, 11-33.

Astini R.A., Benedetto J.L., Vaccari N.E. 1995. The early Paleozoic evolution of the Argentine Precordillera as a Laurentian rifted, drifted, and collided terrane: A geodynamic model. Geological Society of America Bulletin, 107, 253-273.

Benedetto J.L. 1998. Early Palaeozoic brachiopods and associated shelly faunas from western Gondwana: their bearing on the geodynamic history of the pre-Andean margin. In Pankhurst R.J., Rapela C.W. (eds) The Proto-Andean Margin of Gondwana. Geological Society, London, Special Publications, 142, 57-83.

Dalla Salda L.H., Dalziel I.W.D., Cingolani C.A., Varela R. 1992. Did the Taconic Appalachians continue into southern South America? Geology, 20, 1059-1062.

Dalziel I.W.D. 1997. Neoproterozoic-Paleozoic geography and tectonics: Review, hypothesis, environmental speculation: Geological Society of America Bulletin, 109, 16-42.

Drake A.A.Jr., Sinha A.K., Laird J., Guy R.E. 1989. The Taconic orogen. In Hatcher R.D.Jr., Thomas W.A., Viele G.W. (eds) The Appalachian-Ouachita Orogen in the United States. Geological Society of America, Geology of North America, F-2, 101-177.

Huff W.D., Bergström S.M., Kolata D.R., Cingolani C.A., Astini R.A. 1998. Ordovician K-bentonites in the Argentine Precordillera: relations to Gondwana margin evolution. In Pankhurst R.J., Rapela C.W. (eds) The Proto-Andean Margin of Gondwana. Geological Society, London, Special Publications, 142, 107-126.

Shanmugam G., Lash G.G. 1982. Analogous tectonic evolution of the Ordovician foredeeps, southern and central Appalachians. Geology, 10, 562-566.

Thomas W.A. 1977. Evolution of Appalachian-Ouachita salients and recesses from reentrants and promontories in the continental margin. American Journal of Science, 277, 1233-1278.

Thomas W.A. 1991. The Appalachian-Ouachita rifted margin of southeastern North America: Geological Society of America Bulletin, 103, 415-431.

Thomas W.A., Astini, R.A. 1996. The Argentine Precordillera: A traveler from the Ouachita embayment of North American Laurentia. Science, 273, 752-757.

THE ASSOCIATION BETWEEN ISLAND ARCS, TONALITIC BATHOLITHS AND OCEANIC PLATEAUX IN THE NETHERLANDS ANTILLES: IMPLICATIONS FOR CONTINENTAL GROWTH

Patricia M. E. THOMPSON (1), Rosalind V. WHITE (2), John TARNEY (3), Pamela D. KEMPTON (4), Andrew C. KERR (5) and Andrew D. SAUNDERS (6)

(1) pmet1@le.ac.uk
(2) rvw1@le.ac.uk
(3) art@le.ac.uk
(4) pdk@wpo.nerc.ac.uk NERC Isotope Geoscience Laboratory, Keyworth, Nottingham, NG12 5GG
(5) ack2@le.ac.uk
(6) ads@le.ac.uk Department of Geology, University of Leicester, LE1 7RH, UK

KEYWORDS: island arc; oceanic plateau; tonalitic batholith; crustal generation; Bonaire; Caribbean

INTRODUCTION

Greenstone belts have been increasingly regarded as accreted fragments of Precambrian oceanic plateaux and/or island arcs, typically characterised by dominantly mafic rocks – both of plateau and island arc-type chemistry – enveloped by tonalitic batholiths. We examine the close association of fragments of accreted oceanic plateaux (including komatiites), island arc sequences and tonalitic batholiths on the northern margin of South America, as a possible modern analogue of a greenstone-granite belt, in order to investigate the importance of plateau and arc accretion for continental crust formation.

TECTONIC AND REGIONAL SETTING

The Cretaceous Caribbean oceanic plateau is situated in the region covered by the Caribbean Sea (Fig. 1) and is generally believed to have formed as part of the Farallon plate, possibly representing the initial burst of magmatism from the Galápagos mantle plume. Whilst the majority of the plateau is not exposed, a series of fragments have been uplifted and obducted onto the margins of the South (and North) American plate. The Netherlands Antilles, in particular Curaçao and Aruba, represent fragments of oceanic plateau that have been accreted to South America as the plateau was transported eastwards

relative to the Americas along the southern Caribbean strike-slip plate boundary zone. Accreted fragments are also found in N. Ecuador and Colombia, and the island of Gorgona, off the Pacific coast of Colombia, boasts the only known occurrence of Phanerozoic komatiites (Echeverria, 1980; Kerr *et al.*, 1997).

The island of Curaçao consists of a >5 km sequence of tholeiitic pillow basalts, with picrites concentrated near the base of the succession and hyaloclastites towards the top, overlain by cherts and tuffaceous sediments. The adjacent island of Aruba comprises a sequence of basaltic lavas, interbedded with volcaniclastics, and intruded by a large tonalitic batholith. Whilst the lavas and volcaniclastics are believed to comprise part of the plateau, the batholith shows some subduction-related characteristics, such as a negative Nb anomaly (White *et al.*, 1999). The subduction-related rocks are closely related temporally with the plateau, with dates of 88-91 Ma for the plateau (Sinton *et al.*, 1998) and 85-82 Ma for the batholith (White *et al.*, 1999). Bonaire also has an island arc affinity, with rhyodacitic lavas, reworked tuffs and shallow columnar-jointed sills, intruded by dolerites. The relationship between the island arc volcanic rocks on Bonaire and the plateau is poorly known, and the aim of this study is to elucidate the nature of the association.

Fig. 1

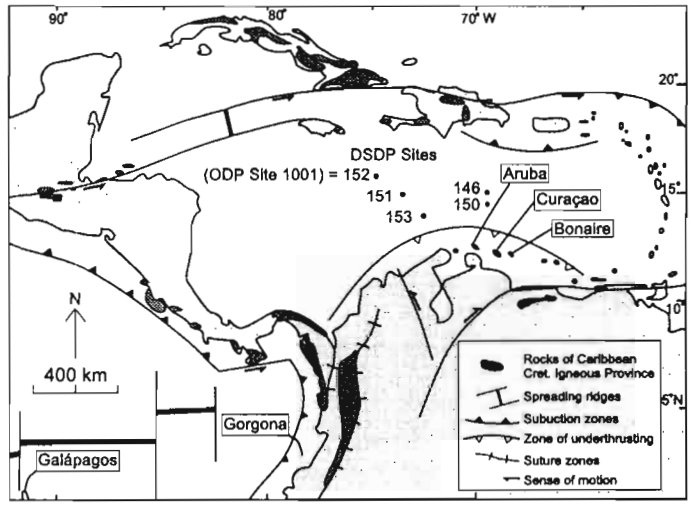

BONAIRE - FIELD OBSERVATIONS, GEOCHEMISTRY AND GEOCHRONOLOGY

Cretaceous rocks of island arc affinity (the Washikemba Formation) outcrop in two separate areas of Bonaire. The northern outcrop is better exposed and studied, and consists of a >5 km thick sequence of rhyodacitic lava flows with intercalations of turbiditic volcaniclastics, conglomeratic debris flows, cherts and cherty limestones. The middle of the sequence also comprises shallow-level, columnar-jointed rhyodacitic sills, and both the basal and the upper portions of the sequence are heavily intruded by dolerites. The presence of radiolarites within both the volcaniclastics and the cherts, along with thinly bedded limestones and basaltic pillow lavas confirm a submarine environment, albeit with temporary emergence resulting in boulder bed formation towards the top of the sequence.

The north-eastern outcrop of the Washikemba Formation is rather different in character; a series of rhyolite domes form the higher relief areas, and intrude into a poorly exposed series of alternating volcaniclastic distal turbidites and tuffs with subordinate intrusions of dolerite. A distinctive debris flow deposit, with predominantly rhyodacite clasts, is found in both outcrops of the Washikemba Formation.

Geochemically, the rocks are classified as island arc tholeiites, with the rhyodacites and volcaniclastics lying within the low-K, and the dolerites within the medium-K field. The rocks are altered, however, with plots of elements vs. Zr indicating a degree of mobility of many elements, in particular K and Ca. Chondrite-normalised multi-element diagrams (Fig. 2) show negative Nb anomalies, along with positive Ba and La. There are two main trends: the dolerites exhibit a flatter trend with high Sr, whereas the majority of the rhyodacites are characterised by a more spiky pattern and low Sr. A subset of the north-eastern rhyodacites, however, demonstrate higher elemental abundances, particularly for La, Ce, Nd and Zr.

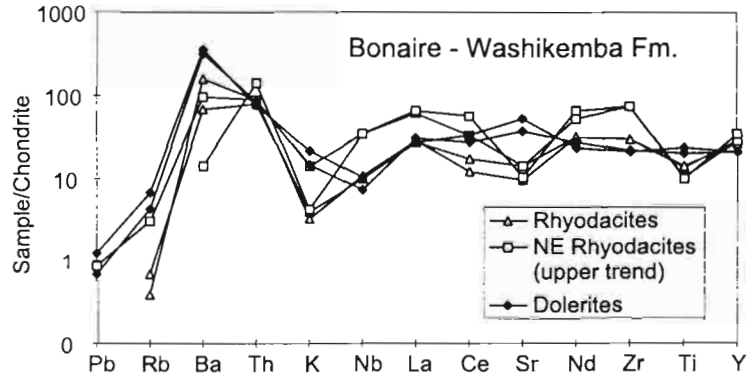

Fig. 2: Chondrite-normalised (Sun and McDonough, 1989) multi-element plot for selected Bonaire data.

The age of the Washikemba Formation is not well constrained. Poorly-preserved ammonites (which may be reworked) within the lower part of the Formation indicate Albian ages (112-97 Ma: Harland *et al.*, 1990), and inoceramids in the upper portion are Turonian-Coniacian (90.5-86.5 Ma: Harland *et al.*, 1990) in age (Beets *et al.*, 1977). K-Ar dating of hornblende yielded an age of 88 ± 2 Ma for near the top of the succession (Priem *et al.*, 1979); this is indistinguishable from the age of plateau formation. These age constraints, although poor, suggest that the sequence formed in more than 25 Ma. This large age range for a continuous magma series may question the validity of the data.

IMPLICATIONS FOR CONTINENTAL GROWTH

In order to make deductions about the mechanisms of continental growth, the origins of the island arc sequences and tonalitic batholiths found obducted around the margins of the plateau must be resolved. Possible processes are: (1) that the arcs are the manifestation of earlier subduction, and have been swept up in front of the accreting plateau; (2) that the arcs were formed on top of the plateau, as a result of subduction-flip or back-step; or (3) rocks with an apparent arc affinity were formed by the recycling of mafic components internal to the plume itself.

The tonalitic batholith that intrudes the plateau sequence on Aruba is thought to represent the earliest stages of subduction beneath the plateau (White *et al.*, 1999). The island arc sequence on Bonaire, however, is older than the Aruba batholith and appears to largely pre-date the plateau formation. It may therefore be the result of accretion of the product of an earlier phase of subduction to the margins of the plateau. Precise radiometric ages and geochemical data are needed before the origin of the island arc can be unequivocally distinguished. Nevertheless, the association of rocks with both oceanic plateau and island arc affinities in the Caribbean region demonstrates that Phanerozoic tectonic processes are capable of generating new areas of continental crust that have strong parallels with greenstone belts.

REFERENCES

Beets, D.J., MacGillavry, H.J. and Klaver, G.Th., 1977. Outline of the Cretaceous and early Tertiary of Bonaire. *Eighth Caribbean Geological Conference Guide to the Field Excursions on Curaçao, Bonaire and Aruba:* GUA Papers of Geology, 10, 18-28.

Echeverría, L. M., 1980. Tertiary or Mesozoic komatiites from Gorgona Island, Colombia: field relations and geochemistry. *Contrib. Mineral. Petrol.* **73**, 253-256.

Harland, W. B., Armstrong, R. L., Cox, A. V., Craig, L. E., Smith, A. G. & Smith, D. G., 1990. *A Geologic Time Scale 1989.* Cambridge University Press. Cambridge. 263 pp.

Kerr, A.C., Tarney, J., Marriner, G.F., Nivia, A. & Saunders, A.D., 1997. The Caribbean-Colombian Cretaceous Igneous Province: The internal anatomy of an oceanic plateau. In: *Mahoney, J. and Coffin, M. (eds.) Large Igneous Provinces: Continental, Oceanic and Planetary Flood Volcanism.* American Geophysical Union, *Geophysical Monograph* **100**, 123-144.

Priem, H.N.A., Andriessen, P.A.M., Beets, D.J., Boelrijk, N.A.I.M, Hebeda, E.H., Verdurment, E.A.Th. & Verschure, R.H., 1979. K-Ar and Rb-Sr dating in the Cretaceous island arc succession of Bonaire, Netherlands Antilles. *Geologie en Mijnbouw* **58**, 367-373.

Sinton, C. W., Duncan, R. A., Storey, M., Lewis, J. & Estrada, J. J., 1998. An oceanic flood basalt province within the Caribbean plate. *Earth Planet. Sci. Lett.* **155**, 221-235.

White, R.V., Tarney, J, Kerr, A.C., Saunders, A.D., Kempton, P.D., Pringle, M.S. & Klaver, G.Th., 1999. Modification of an oceanic plateau, Aruba, Dutch Caribbean: Implications for the generation of continental crust. *Lithos* **46**, 43-68.

FISSION-TRACK THERMOCHRONOLOGY OF THE SOUTHERN CHILEAN ANDES (42°S TO 48°S)

Stuart N. THOMSON(1), Francisco HERVÉ(2), Manfred R. BRIX(1) and Bernhard STÖCKHERT(1)

(1) Institut für Geologie, Ruhr-Universität Bochum, D-44780 Bochum, Germany
E-mail: stuart.thomson@ruhr-uni-bochum.de
(2) Departamento de Geologia, Universidad de Chile, Casilla 13518 Correo 21, Santiago, Chile

KEY WORDS: Chile Triple Junction, Liquiñe Ofqui Fault, geochronology, fission-track analysis, thermal history, denudation

INTRODUCTION

At the Chile Triple Junction (CTJ), situated at about 46°S on the Peru-Chile Trench, the Chile Rise, a mid-oceanic ridge, is being actively subducted beneath Andean-type continental lithosphere. In the overriding plate close to the CTJ the response to ridge subduction includes increased thermal activity and higher topography. Another important consequence of ridge subduction is the Liquiñe Ofqui Fault (LOF), a 1000km trench parallel dextral strike-slip fault that extends northward from Golfo de Penas (ca. 47°S). The passage of subducted ridge segments as lithospheric windows has been shown to correspond spatially with both an arc seismic gap and large areas of back-arc plateau lavas. Another apparent effect is a 'tectonic discontinuity' at the latitude of the Golfo de Penas. This is shown by a significant increase in the maximum elevation and an apparent deeper level of erosion of the Andes south of the CTJ, and the dying out of the back-arc fold and thrust belt of southernmost Patagonia north of the latitude of the CTJ. This study has applied fission-track (FT) analysis on both apatite and zircon to assess the low temperature cooling and hence the denudation history of the overriding plate in relation to the late Tertiary evolution of the CTJ. The majority of samples have been collected from areas affected by the southern part of the Liquiñe Ofqui Fault Zone and further south from rocks of the Patagonian Batholith and neighbouring basement east and south of the present day CTJ under which segments of the Chile Rise are part of the subducted slab.

RESULTS

26 apatite and 21 zircon FT ages and 32 mean apatite confined track length values are presented in this abstract from the Andes in the region of the CTJ and LOF. The location and values of these data are summarised on the map shown in Figure 1.

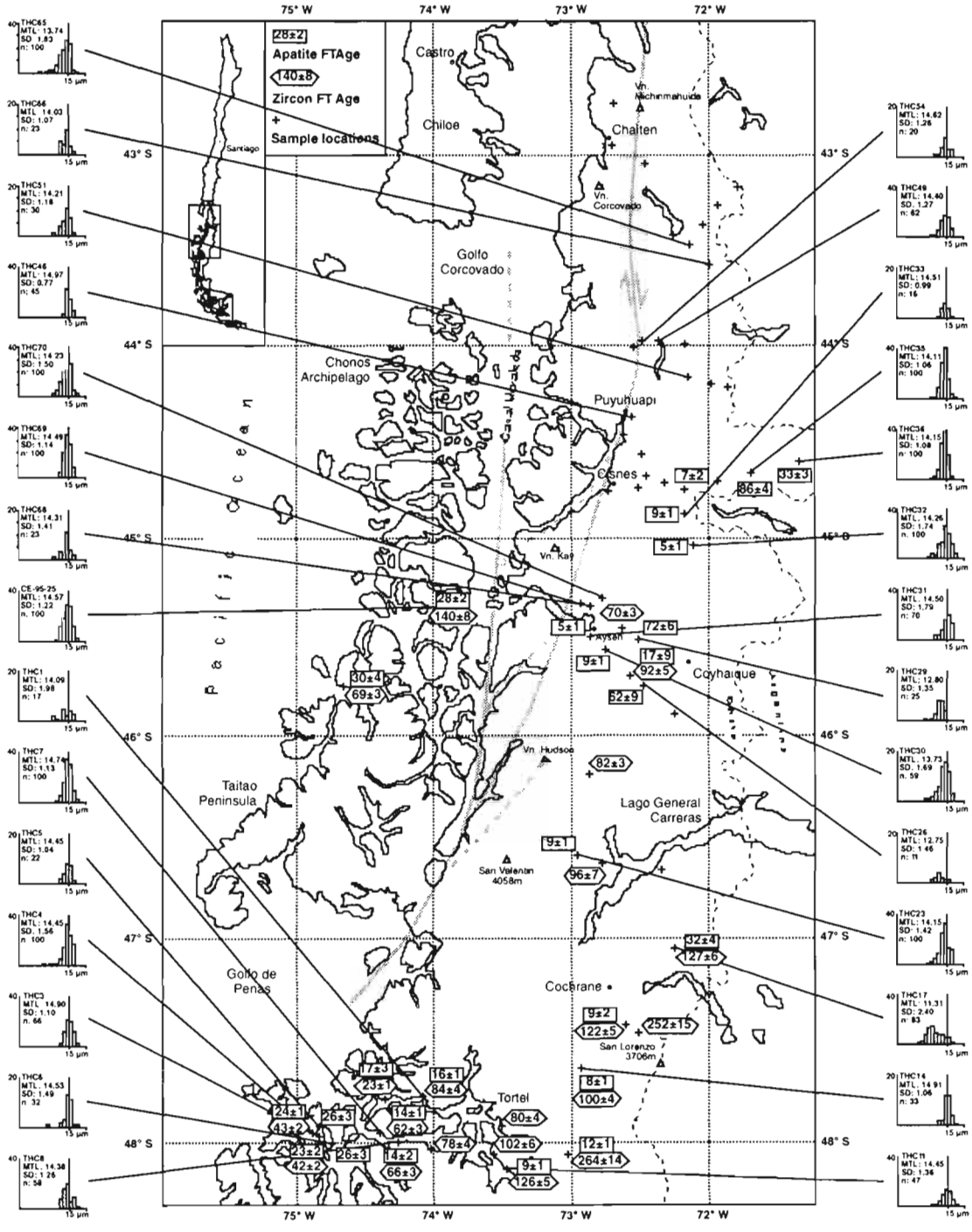

Figure 1

Zircon and apatite fission-track ages and apatite confined track length measurements from various rocks of the southern Andes between 42°S and 48°S

APATITE DATA

The apatite FT ages show a wide variation from 5±1 to 86±4 Ma. However, they do show a certain geographical pattern. The youngest ages (between 5 and 12 Ma) occur along the main N-S topographical high of the Andes in this region, with the youngest ages (<5 Ma) found closest to the LOF. In the Canal Baker area the apatite ages within the Patagonian Batholith increase westward to values of up to 26 Ma closest to the Pacific Margin. East of the main Andes chain older ages of up to 86 Ma are obtained from the eastern margin of the Patagonian Batholith. Two apatite ages from the Chonos Archipelago yield ages of 28 and 30 Ma. The corresponding apatite confined track length measurements from the whole region show largely high mean values >14μm and narrow standard deviations of <1.5μm. Such values are typical for samples that have cooled quickly through the apatite FT partial annealing zone (PAZ) from ca. 120°C to below ca. 60°C. The one significant exception is the low mean length of 11.3μm shown by the 32 Ma sample from the easternmost part of the Patagonian Batholith.

Initial interpretation of the apatite FT data indicates that the most recent significant rapid cooling through the apatite PAZ occurred along what is at present the highest N-S topographic expression of the Andes. It is possible that this is related to increased denudation and erosion at the point of highest topography and relief along this segment of the Andes. The influence of the subduction of the Chile Rise beneath the upper plate to subduction at around 6 to 8 Ma in the Canal Baker region does not appear to have caused significant resetting of the apatite FT ages. Although partial resetting cannot be totally ruled out, this is not supported by the confined track length data. The younger apatite FT ages closer to the LOF suggest more recent or greater denudation related to the fault zone, although more data are needed to confirm this. The older apatite ages (25 to 30 Ma) with long mean track lengths (>14μm) in the western part of the studied region imply a rapid cooling within these rocks at this time. This may be related to an increase in the convergence rate between the Nazca and South American plates identified between ca. 28 and 26 Ma (Somoza, 1998). Finally, the much older ages within the Patagonian batholith east of the main Andean divide, one with a short mean track length measurement of 11μm, indicate that the rocks in this region have been at temperatures of below 120°C (i.e. experienced no more than of 3-4km denudation) since 32 Ma, and in some samples since 80Ma.

ZIRCON DATA

The zircon FT ages show a very wide range from 23±1 to 264±14 Ma. The ages can be divided into several groups. The ages obtained from the Patagonian batholith vary from 23 Ma to 127 Ma. When compared to the probable ages of intrusion derived by Bruce et al. (1991) most of the zircon FT ages are around 20 Ma younger. Using a zircon FT closure temperature of 260±30°C implies that the granitoids of the Patagonian Batholith cooled at rates of ca. 20°C / My. following intrusion. This most likely represents cooling of the individual plutons within originally warm country rock. Cooling related

to denudation is considered unlikely, as this would require that denudation was restricted in time and locale to each individual pluton. An exception to the general pattern are zircon FT ages from batholithic rocks in the western part of Canal Baker. These ages (66 to 42 Ma) are up to 80 Ma younger than the intrusion ages from rocks in the same area (Bruce et al., 1991). This means that these rocks were either cooled much more slowly following intrusion, implying that they were intruded into country rocks of a higher temperature and hence at a greater depth, or that they were reset by reheating, possibly related to subduction of a mid-oceanic ridge separating the Farallon and Aluk plates at around 40 and 50 Ma (Ramos and Kay, 1992). The two old zircon FT ages of 252 and 264 Ma from the eastern part of the region were obtained from metamorphic basement (phyllites and quartzites) east of the main Patagonian Batholith. Such ages suggest either that metamorphism of these rocks was pre-Permian in age or that the conditions of metamorphism never reached temperatures >ca. 230°C meaning the zircon FT ages obtained relate to the provenance of these rocks. The 140±8 Ma zircon FT age from the Chonos Archipelago, from a low grade metamorphic sandstone of probable Triassic age, indicates that these rocks have experienced temperatures of >230°C since their deposition. Indeed, this age may represent the timing of metamorphism in these rocks prior to their intrusion by granitoids, dated as 135 Ma (Hervé et al., 1996) close to the dated sample.

ACKNOWLEDGEMENTS

Fieldwork in Chile was supported by Catedra Presidencial en Ciencias and Fondecyt Grant 1980741 to FH. SNT, MRB and BS were supported by DFG Grant Sto196/11-1 and SNT by DFG Stipendium Th 573/2-1.

REFERENCES

Bruce, R.M., Nelson, E.P., Weaver, S.G. & Lux, D.R. 1991. Temporal and spatial variations in the southern Patagonian batholith; Constraints on magmatic arc development. Geological Society of America Special Paper, 265, 1-12.

Hervé, F., Pankhurst, R.J., Demant, A. & Ramirez, E. 1996. Age and Al-in-hornblende geobarometry in the north Patagonian Batholith, Aysén, Chile. Third ISAG, St. Malo (France), abstracts, 579-582.

Somoza, R. 1998. Updated Nazca (Farallon) - South America relative motions during the last 40 My: implications for mountain building in the central Andean region. Journal of South American Earth Sciences, 11, 211-215.

Ramos, V.A. & Kay, S.M. 1992. Southern Patagonian plateau basalts and deformation: Back-arc testimony of ridge collisions. Tectonophysics, 205, 261-282.

LARGE-SCALE EXPLOSIVE ERUPTION AT HUAYNAPUTINA VOLCANO, 1600 AD, SOUTHERN PERU

Jean-Claude THOURET (1) and Jasmine DAVILA (2)

(1) IRD Institut de Recherche pour le Développement (UR 6) c/o
UMR6524-CNRS 'Magmas et Volcans', Université Blaise Pascal, Clermont-Ferrand, France.
(2) Instituto Geofísico del Perú, Calle Calatrava 216, Urb. Camino Real, La Molina, Lima 12, Perú
(jct@geo.igp.gob.pe)

KEY WORDS : Plinian eruption · Stratigraphy . Tephra · Ignimbrite · Huaynaputina Peru

INTRODUCTION

The largest explosive eruption in historical times (VEI 6) in the Andes took place in AD 1600 at Huaynaputina, a small, eroded stratovolcano in southern Peru (Central Andean Volcanic Zone). The eruption began on 19 February 1600 with a plinian phase following 4 days of intense seismic activity, and lasted at least until 6 March. Repeated tephra falls, pyroclastic flows, and surges devastated the landscape within an elliptic area about 90 · 60 km west of the volcano, claimed ~1500 lives, and affected indirectly all southern Peru. Earthquakes shook the town of Arequipa 75 km away and large-scale lahars (•0.18 km^3), likely fed by ignimbrites and triggered by lake outbursts, swept the 120-km-long valley of Rio Tambo and entered the Pacific Ocean during and after the eruption.

The erupted tephra (medium-K dacite), totalling 11.9-13.5 km bulk volume (DRE 7-9.5 km^3 ; Table 1), include eight deposits (Fig. 1) : (1) a widespread (~360,000 km^2, Fig. 2) and voluminous pumice-fall deposit (~8.1 km^3, DRE 4.6-4.9 km^3, Table 1) in one extensive lobe (), (2) several alternate ash layers, (3) ignimbrites 1.5-2 km^3 from pumice-rich flow deposits channeled •40 km in the Tambo canyon, with (4) ground-surge and ash-cloud surge deposits, (5) base-surge deposits, (6) crystal-rich flow/surge deposit

toward the west-northwest, (7) unconfined ash-flow deposits with proximal lag breccias and ground surge deposits, which travelled at least 60 km from the vent over •1000-m-high topographic barriers, and (8) late ash-fall and surge deposits.

By linking up the seven series of events inferred from chronicles to measured deposits, we distinguish seven eruptive phases: plinian, ash-bearing, ignimbritic, phreatomagmatic, and emplacement of crystal-rich flows/surges, ash flows, and late ash falls and surges.

A plinian eruption column 33-35 km high was sustained at least 13 hours and lasted likely as much as 19 hours from 19 February to 20 February 1600. The volumetric eruption rate was short of 10^5 m^3/s and the mass eruption rate ranged from 1.2 to 1.75 x 10^8 kg/s (Table 1). The plinian phase probably included the disruption of a hydrothermal system enclosed in the pre-AD 1600 amphitheater. Fallout dispersal has shifted through time, first from south to southwest, then to west and west-northwest, owing to three wind patterns over the vent area. Stratospheric winds in excess of 30 m/s carried aloft ash •600 km to west and west-northwest well into the Pacific Ocean. An area •100 000 km^2 was also covered by >1-cm-thick layer of co-plinian ash and co-ignimbrite ash (deposits 2 and 3).

The post-plinian ignimbritic phase and subsequent phreatomagmatic interactions promoted a catastrophic erosion, leading to the formation of four nested vents, and to the eruption of a crystal-rich magma toward the end of the event. Close association and sharp contact between two pairs of crystal-rich flow deposit and thin, overlying layers of vitric ash suggest that they result from segregation/elutriation during flow transport, owing to strong influence of the rugged topography on the emplacement of relatively small-volume, shallow pyroclastic density currents with internal stratification. At the end of the eruption, unconfined ash flows may have been strongly turbulent, pulsatory, subcritical flows (Ri >1, velocity 50-110 m/s), but so fluidized that they were able to surmount ridges •1000 m high as far as 60 km due west from source.

CONCLUSION

Such a voluminous explosive eruption (VEI 6, Table 1) occurred in this site because : (1) an hydrothermal system was disrupted during the plinian phase, (2) hydromagmatic interactions followed the ignimbritic phase, and (3) a crystal-rich magma was tapped, and ash flows and surges were delivered toward the end of the eruption. Although the total DRE 7-9.5 km^3 volume of erupted tephra did not involve caldera collapse, ring-fractures cut through the vents and the floor of the pre-1600 amphitheater, pointing to the onset of a funnel-type caldera collapse. The lack of caldera collapse may be due to the unusual depth and/or to the size and shape of feeding dykes through the weathered volcanic bedrock. The AD 1600 eruption was the largest historical event in southern Peru, but was neither the single nor the largest event in the Huaynaputina eruptive history. Four large-scale (>1 km^3) eruptions from Huaynaputina and adjacent stratovolcanoes over the past 2500 years suggest a rapid regeneration of silicic magma and potential for voluminous explosive eruptions in southern Peru.

Table 1. Volcanological data for the AD 1600 plinian and ignimbritic eruption

Extent of the plinian fallout (within 1-cm isopach)	~100 000 km^2
Extent of reported ash and dust fallout (from Fig. 1B)	~360 000 km^2
Volume of plinian ejecta (within 1-cm isopach and from Fig. 1B)	~6.9 and 8.1 km^3
Weight % ejecta < 1 mm (at 0.1T, thickness= 90 cm and 0.01 Tmax)	73.5 and 98.3%
Weight % ejecta < 63 microns (at 0.1 T and 0.01 Tmax)	57.6 and 93.4%
Minimum volume percent beyond 1 cm isopach	•17.5%
Minimum volume DRE (80% pumice, density 0.58-0.66 g/cm^3)	~4.6 - 4.9 km^3
Minimum volume of lithics (1-11% of fallout, density 2.4 g/cm^3)	~0.8 - 1.05km^3
Minimum volume of magma	~3.6 - 4.1 km^3
Duration of the plinian phase	13 to 19 h
Mass eruption rate (SCS, 13-19 h, DRE magma, density 2.4 g/cm^3)	~1.2-1.7 · 10^8 kg/s
Volumetric eruption rate (same characteristics as above)	~7.2 - 9.9 · 10^4 m^3/s
Peak mass eruption rate (SCS)	~1.75 - 2 · 10^8 kg/s
Peak mass eruption rate (WW)	~3 · 10^8 kg/s
Peak wind velocity (SCS)	~32 - 33 m/s
Column height Ht	~33 - 35 km (SCS) ; ~27 - 28 km (WW)
Column neutral buoyancy Hb	~23.5 – 25.4 km (SCS) ; 20.5 – 21.3 km (WW)
Column radius R	~8.5 – 9 km (SCS) ; 7 – 7.25 km (WW)
Half-thickness distance b_1 ; half-clast distance b_2	~8.25 km ; 7-7.5 km
Tropospheric injection	substantial
Stratospheric injection (inferred from ice cores and tree-ring chronology)	definite
Volume of ash layers (deposit 2)	0.2 – 0.25 km^3
Volume of channeled pyroclastic-flow deposits 3 (from Fig. 3B)	~1.5 - 2 km^3
Travel distance of channeled pyroclastic flows (Rio Tambo valley)	40 - 45 km
Volume of pyroclastic-surge deposits (deposits 4 and 5)	~0.05 - 0.06 km^3
Volume of crystal-rich deposit (deposit 6)	~0.5 - 0.6 km^3
Volume of ash-flow deposit and late ash layers (deposit 7 and 8)	~0.15 – 0.2 km^3
Minimum travel distance of ash flows over •1000-m-high topographic barriers	60 km
Volume of distal co-ignimbrite ash and/or co-plinian ash beyond 5-cm isopach	~1.2 - 2.4 km^3
Total bulk volume (plinian and post-plinian tephra)	~11.9 - 13.5 km^3
Total volume DRE (plinian and post-plinian tephra)	~7 - 9.5 km^3
Volcanic explosivity index	6
Volume of lahar deposits in Rio Tambo	average 0.12 km^3, maximum 0.18 km^3

SCS refers to the methods of Sparks (1986) and Carey and Sparks (1986) for a tropical atmosphere, using lithic and pumice isopleths fromThouret et al. (1999) and a magma temperature of 850 °C appropriate for dacite. WW refers to the method of Wilson and Walker (1987), assuming 1-3% magmatic water, 200-250 m vent radius, and 200 m/s muzzle velocity. MER is mass eruption rate of magma. VER is volumetric eruption rate, in terms of dense-rock equivalent (DRE) of a dacitic magma having a density of 2.4 g/cm^3

REFERENCES

Carey S and Sparks RSJ, 1986. Quantitative models of the fallout and dispersal of tephra from volcanic eruption columns. Bull Volcanol 48, 109-126.

Sparks RSJ, 1986. The dimensions and dynamics of volcanic eruption columns. Bull Volcanol 48, 3-15.

Thouret J-C, Davila J, Eissen J-P. 1999. Largest explosive eruption in historical times in the Andes at Huaynaputina, AD 1600, southern Peru. Geology GSA, 29 April issue.

Wilson L and Walker GPL. 1987. Explosive volcanic eruptions - VI. Ejecta dispersal in plinian eruptions: the control of eruption conditions and atmospheric properties. Geophys J Royal Astron Soc 89, 657-679.

CHRONOLOGY OF THE VOLCANIC ACTIVITY AND REGIONAL THERMAL EVENTS: A CONTRIBUTION FROM THE THEPROCHRONOLOGY IN THE NORTH OF THE CENTRAL CORDILLERA ,COLOMBIA

TORO, G.(1), POUPEAU, G.(2), HERMELIN, M.(3), SCHWABE, E. (4)

(1)gtoro@sigma.eafit.edu.co
(2)hermelin@sigma.eafit.edu.co
(3)poupeau@ujf-grenoble.fr
(4)schwabe@sigma.eafit.edu.co

KEY WORDS : theprochronology, geochronology, fission track, volcanism, superficial formations, stone line, Colombia, Northern Andes

INTRODUCTION

The study and dating of zircon crystals associated with the superficial volcano-sedimentary formations in the northern region of the Central Cordillera in Colombia allowed us, through the analysis of populations, to isolate within the limits of the fission track dating method, different thermal events. We will present a synthesis of the chronological data which reflects the thermal history of the region and part of the history of Colombia's volcanism. In this work, we employ the fission track dating and ^{14}C dating.

The zone of study is localized in the Antioquia Department, in the North of the Central Cordillera, Colombia. The two most important geomorfological features in this region are the erosion surface (Hermelin, 1992) and the tectonic depression of the Aburra Valley (Fig 1).

We studied different superficial formations starting from the basement, which is constituted in the region for metamorphic rocks and igneous intrusives. The biggest of the intrusions is the Antioqueño Batholith, a granodiorite of Cretaceous Age (Botero, 1963, Restrepo, 1983, Gonzales, 1993).

Research partially financed by COLCIENCIAS and Foundation for the promotion of science and technology, Banco de la República, Colombia

The superficial formations from where the dated material comes are : two terraces associated with the rivers Río Grande and Rionegro (Durango, 1975); an alluvial sequence related to the paleohydrographi without visible connection with the actual hydrographical net; four lacustrine deposits localized over the plateau; the concentrated material in the stone line, which is the stratigraphic level of reference in West Antioquia; the upper volcanic ash layers which cover the landscape uniformly, and two volcanic ash layers concentrated in paleosoils. These last layers separate slope deposits in the interior of the Aburra Valley (Figure 1).

RESULTS

The results we obtained over 55 dated samples and its posterior analyses of populations, according to the methodologies proposed by Brandon (1992, 1996), Galbraith and Grenn (1990) and Galbraith and Laslett (1993), permitted us to establish the presence of 22 populations of zircon with ages superior to 6,1 Myr which we interpret as the basement age, and 44 populations of fission track ages inferior to 6,1, which we interpret as contribution of tephra from the volcanic centers.

From 19 samples of the basement with ages between 75 y 35 Myr, 16 correspond to the Paleocene. These apparent ages indicate that the cooling of the basement below 300°C took place essentially during the Paleocene. An older dating we obtained of 185±5,5 Myr could indicate that the entire basement could not have been thermally affected above 300°C during all the thermal events in the Cretaceous.

The ages obtained from the volcanic zircons show that from over 44 populations in total, the ages of the thermal events are comprised between 0,35±0,05 Myr and 6,19±0,23 Myr. with an important peak between 1 and 4 Myr. There is a diminution in the tephra contribution in the region towards 20-30 kyr. This age was obtained by the ^{14}C method in several sectors in West Antioquia, for a volcano-sedimentary level situated between 30 and 50 cm deep. The last event of volcanic ash contribution in the area was therefore posterior to 20-30 kyr. The source of this piroclastic material could be the Volcanic Massive Ruíz-Tolima. The obtained chronology for this sector is concordant with the one established by Thouret, 1988.

CONCLUSION

Due to the fission track method permits the obtention of ages grain by grain, it constitutes an important tool in the study of superficial formations in the Department of Antioquia, Colombia. These volcano-sedimentary formations contributes with basic information in the knowledge of the thermal history of the region and the reconstruction of the Colombia's volcanism.

REFERENCES

Brandon, M.T. 1992. Decomposition of fission-track grain-age distribution. American Journal of Science, 292, 535-564.

Brandon, M.T. 1996. Probability density plot for fission-track samples. Radiation Measurements, 26, 793-837.

Botero, G. 1963. Contribución al conocimiento de la geología de la zona central de Antioquia. Anales Facultad de Minas, 57. 101 p.

Durango, J.R. 1975. Terrazas del valle del Rionegro y sus afluentes. Tesis Facultad de Minas, U. Nacional, 59 p.

Galbraith, R.F., & Grenn, P.F. 1990. Estimating the component ages in a Finite Mixture. Introduction Journal Radiation Application Instruments, Part D, 17, 207-214.

Galbraith, R.F. & Laslett, G.M. 1993. Statistical models for mixed fission tracks ages. Nuclear Tracks Radiation Measurements. 21, 459-470.

Gonzales, H.1993. Variaciones mineralógicas y químicas relacionadas con la zona de cizalladura de cristales, batolito antioqueño, Cordillera Central, Colombia. Revista INGEOMINAS, 2, 84-93.

Hermelin, M.1992. Los suelos del oriente antioqueño, un recurso no renovable. Bulletin Institut Française études andines, 21, 25-36.

Restrepo, J.J.1983. Compilación de edades radiométricas de Colombia, departamentos andinos hasta 1982. Boletin de Ciencias de la Tierra, 78, 201-246.

Thouret, J.C. 1988. Morphogenèse Plio-Quaternaire et dynamique actuelle et récente d' une cordillère volcanique englacée. Thése d'état Université Joseph-Fourier, Grenoble-I, 1040 p.

GALENA LEAD ISOTOPE CHARACTERIZATION FROM ORE DEPOSITS OF THE AYSÉN REGION, SOUTHERN CHILE : METALLOGENIC IMPLICATIONS

Brian K. Townley
Departamento de Geología, Universidad de Chile
P.O. Box 13518, Santiago, Chile
e-mail : btownley@cec.uchile.cl

Key Words : Lead isotopes, mineralization, metallogenesis, Aysén region, Patagonia.

Expanded Abstract

The Aysén region, in southern Chile (between latitude 44.46° and 47.25° south and longitude 71.35° and 72.46° west; fig. 1) consists of a Carboniferous to Upper Triassic metamorphic basement (1), discordantly overlain by an Upper Jurassic to Upper Cretaceous volcanic and sedimentary sequence (2). In turn this is overlain discordantly by Upper Cretaceous - Tertiary basalt, andesite and tuff associated with lesser marine and continental sedimentary rocks (4). The Paleozoic to Cretaceous rocks are intruded by stocks related to the mainly Upper Jurassic to Lower Cretaceous Patagonian batholith (3). Minor Quaternary and active volcanism occurs in the area.

Lead isotope analyses of galena from five ore deposits and six prospects in the Aysén region are reported. Most of the deposits are either epithermal gold-silver veins or skarn and manto deposits. The majority of the deposits sampled are either suspected to be or dated as Late Jurassic to mid-Cretaceous.

Galena lead isotope data for most of the deposits from southern Chile cluster near the 'orogene' within a 'plumbotectonic' model framework. Average values ($^{206}Pb/^{204}Pb$ = 18.53, $^{207}Pb/^{204}Pb$ = 15.63, and $^{208}Pb/^{204}Pb$ = 38.49) are near Jurassic to Cretaceous model ages on the 'orogene' curve of Doe and Zartman (1979) and the second stage curve of Stacey and Kramers (1975) on a $^{206}Pb/^{204}Pb$ versus $^{207}Pb/^{204}Pb$ plot. These model ages are compatible with absolute ages as currently known. Elongation trends in the general cluster indicate variable mixing of lead from mantle, upper crust and lower crust reservoirs—as expected within an orogene. Galena lead associated with one deposit is relatively radiogenic. This lead models as Jurassic on the 'upper crustal' curve of Zartman and Doe (1981), which is compatible with the Ar/Ar age of the deposit.

Three main groups of deposits may be discerned based on galena lead isotope clusters. These three groups, Groups 1 to 3, appear to be related to three mineralizing events based on K-Ar and Ar/Ar radiometric dates: one in the Late Jurassic (Group 3), and in the Early and mid-Cretaceous (Groups 1 and 2, respectively). The Late Jurassic event (Group 3) is related apparently to the initial development of arc - back arc evolution and exhibits evidence for mixing of orogene lead with more highly radiogenic lead. The Cretaceous deposits (Groups 1 and 2) are marked isotopically by orogene type lead that exhibits increasingly radiogenic lead with an increase in south latitude. A linear array of more radiogenic lead in Group 3 probably was formed by mixing of orogene lead with highly radiogenic lead extracted by selective leaching, with mineralizing hydrothermal solutions, of the metamorphic basement.

Each one of these groups are named after the main deposit contained, defining the El Toqui group (group 1), the Fachinal group (group 2) and the El Faldeo group (group 3).

Mineralization of the El Toqui group (44°30'-46°05' S; fig. 2) is of lower Cretaceous age, hosted by volcanic, intrusive and marine sedimentary rocks. The El Toqui group comprises Au-rich Zn-Pb skarns and associated polymetallic veins, as well as Au-Ag-rich epithermal mineralization. Lead isotope studies indicate a mixed source for lead, orogen, mantle and upper and lower crust.

Mineralization of the Fachinal group (46°05'-47°05' S; fig. 2) is of lower Cretaceous age, hosted by volcanic rocks or by rocks of the metamorphic basement. Except for Mina Silva and Manto Rosillo deposit, a Zn-Pb skarn, mineralization in this area is of the Au-Ag epithermal type. Lead isotope studies indicate an orogenic source of lead.

Mineralization of the El Faldeo group (south of 47°05' S; fig. 2) is the oldest recognized in the region (late Jurassic), hosted by volcanic and sedimentary rocks and/or by rocks of the metamorphic basement. The El Faldeo group presents Zn-Pb skarn and associated polymetallic massive sulphide veins locally overprinted by late Au-rich epithermal mineralization. Lead isotope studies indicate an orogenic source of lead with an important upper crust component.

Based on geological, geochronological and lead isotope data, three metallogenic provinces and two metallogenic epochs are proposed for the Aysén region: the El Faldeo metallogenic province of late Jurassic age; and the Fachinal and El Toqui provinces, of early Cretaceous age (fig. 2).

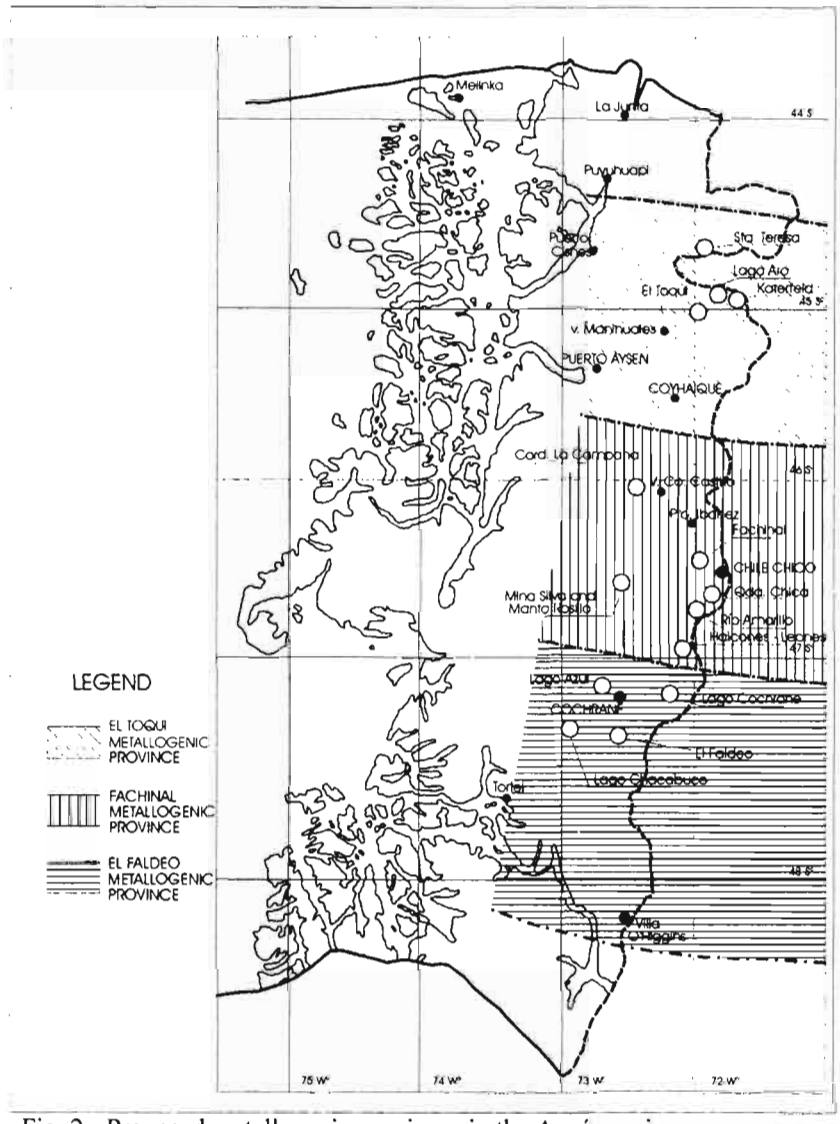

Fig. 2.- Proposed metallogenic provinces in the Aysén region.

References.

Stacey, J.S. and Kramers, J.D., 1975, Approximation of terrestrial lead isotope evolution by a two stage model: Earth and Planetary Science Letters, v. 26, p. 207-221.

Doe, B.R and Zartman, R.E., 1979, Plumbo-tectonics I, the Phanerozoic, *in* Barnes, H.L., ed., Geochemistry of hydrothermal ore deposits, 2nd edition: New York, Wiley Interscience, p. 22-70.

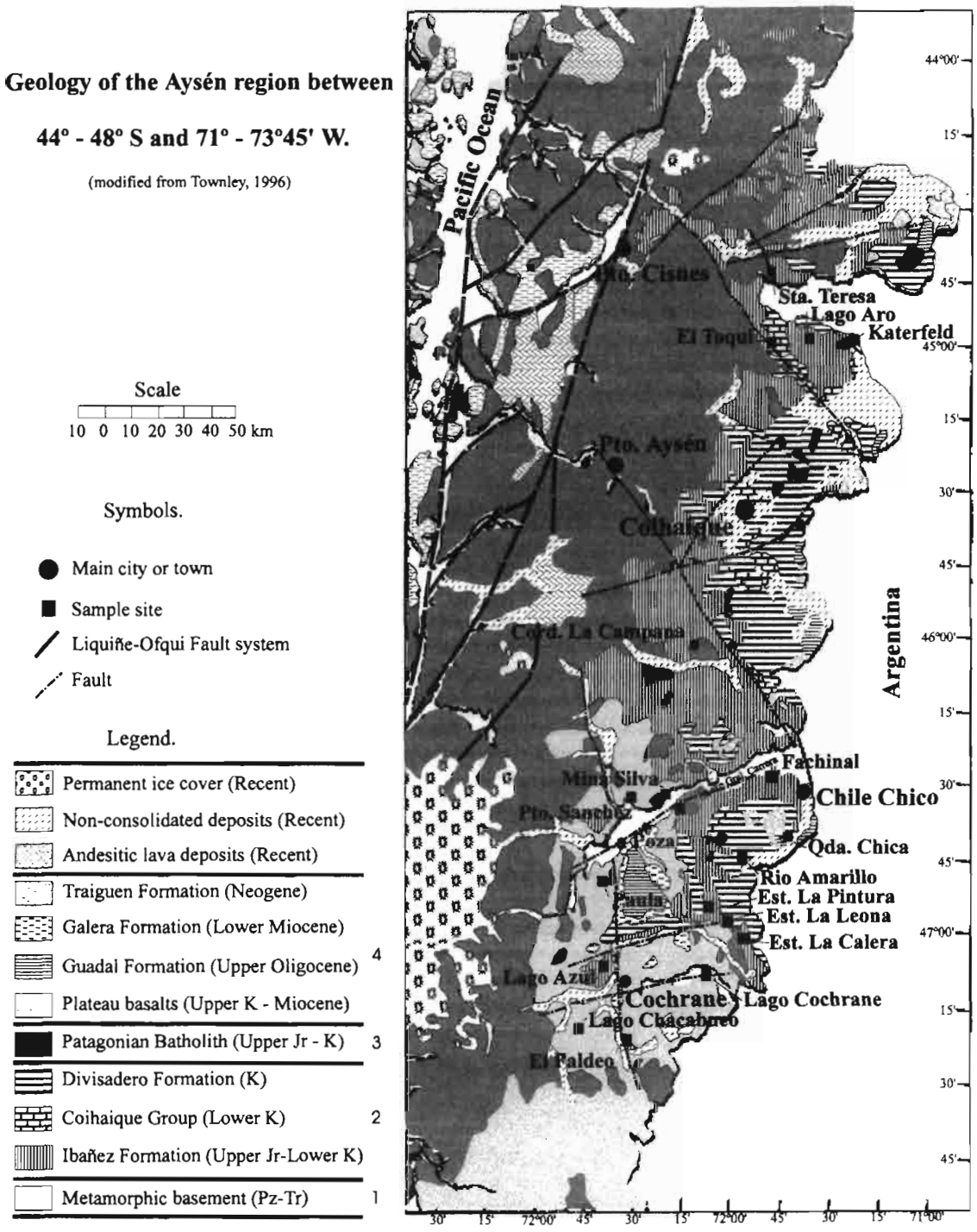

Fig. 1.- Location and geology of the Aysén region. Major map units (1-4) keyed in the text are indicated by their respective number in the legend.

TERTIARY GOLD MINERALIZATION IN SAN LUIS, ARGENTINA

Nilda E. URBINA (1) and Lidia MALVICINI (2)

(1) Universidad Nacional de San Luis, Av. Ejército de los Andes 950. (5700) San Luis. Argentina. email urbina@unsl.edu.ar
(2) CONICET. Universidad Nacional de San Luis, Av. Ejército de los Andes 950. (5700) San Luis. Argentina. email lmalvi@unsl.edu.ar

KEY WORDS: Mineralization, Metallogeny, Epithermal, Porphyry, Gold-Copper, Models.

INTRODUCTION

Tertiary gold-bearing volcanic belt in the Sierras Pampeanas of San Luis, Argentina, outcrop along an 80-Km NW-SE-trending belt from Tres Cerritos-La Carolina in the west to El Morro in the east (Fig.1). Volcanics are hosted in the Precambrian to earliest Paleozoic igneous-metamorphic basement that comprise metamorphic units, granitoids, and ultramafic rocks (Ortiz Suarez et al., 1992). Old-fault reactivation during Andean orogenic cycle gave the Sierras Pampeanas of San Luis a fault-block style of deformation. This structural pattern controlled the Tertiary magma emplacement and the related hydrothermal deposit formation. The magmatism belongs to normal to high-K calc-alkaline and shoshonitic magma types and display a K enrichment as function of time (Brogioni, 1987; Urbina et al., 1997).

The purpose of this paper is to offer speculative schematic cross-sections of the main mineralized districts.

STYLES OF MINERALIZATION

Several gold deposits (Fig. 1) are closely associated with the Tertiary volcanic rocks from the Sierras Pampeanas of San Luis. In La Carolina district, the most important mineralization is the La Carolina

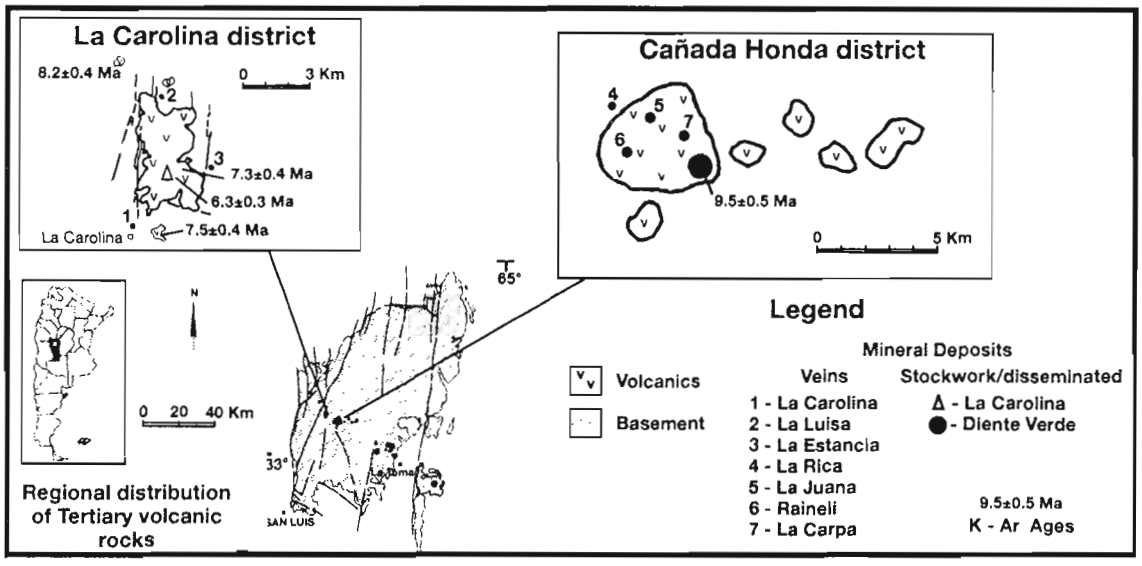

Fig.1 Location of the Tertiary volcanic belt and associated deposits in the Sierras Pampeanas of San Luis

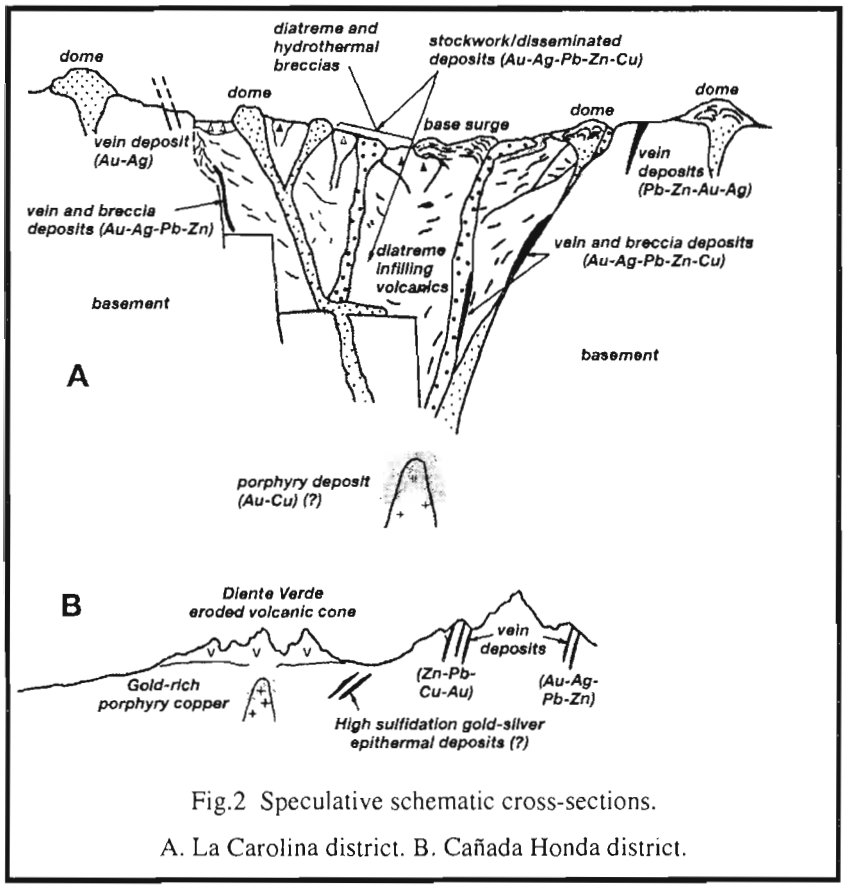

Fig.2 Speculative schematic cross-sections.
A. La Carolina district. B. Cañada Honda district.

volcanic-hosted, low sulfidation sulfide-rich base metals, gold and silver epithermal deposit related to a dome-diatreme complex. In this district there also are gold and base metals epithermal veins hosted by pre-existing fractures in the basement such as the La Carolina, La Estancia and La Luisa deposits. In the Cañada Honda district, the main mineralizations are the Diente Verde gold-rich porphyry copper deposit associated with an andesitic monogenetic cone and the La Rica low

Table 1 . Characteristics of main deposits in the Late Tertiary gold-bearing volcanic belt, Sierras Pampeanas of San Luis

	Host Rock	Form of Deposits	Ore Minerals	Gangue Minerals	Dominant Metals	Minor Metals	Classification of Deposits
La Carolina[1]	Igneous-metamorphic basement	Open space veins dominant	Gold-bearing pyrite, gold, sphalerite	Quartz, sericite	Au, Zn		Low Sulphidation Epithermal
La Estancia[2]	Igneous-metamorphic basement	Open space vein	Gold, pyrite,galena,sphalerite marcasite, pyrrhotite, arsenopyrite, chalcopyrite, greigite, electrum, silver, graphite,boulangerite, jamesonite, pyrargyrite, wolframite	Quartz, sericite, minor clay minerals, rare barite and chlorite	Pb, Zn, Au, Ag, As	Cu, Sb, W	Low Sulfidation Epithermal
La Carolina[3]	Late Miocene volcanic rocks	Stockwork/ disseminated	Pyrite, arsenic-rich pyrite, gold, galena, sphalerite, marcasite, magnetite, chalcopyrite, pyrrhotite, wurtzite, arsenopyrite, tennantite-tetrahedrite, pyrargyrite, hessite, sylvanite	Quartz, calcite, chalcedony, clay minerals, minor dolomite, sericite and chlorite, rare fluorite and adularia	Au, Ag, As, Pb, Zn, Mn	Cu, Sb, Te, Se, Co, Cd, Ti, Ge, Sn, Bi, Ni, Hg, Tl	Low Sulfidation Epithermal
La Rica[4]	Igneous-metamorphic basement	Open space vein	Pyrite, galena, sphalerite, electrum, chalcopyrite, tennantite-tetrahedrite, pyrrhotite	Quartz, sericite, rare alunite	Au, Ag, Pb, Zn	Cu, Sb	Low Sulfidation Epithermal
Diente Verde[5]	Late Miocene volcanic rocks	Stockwork/ disseminated	Chalcopyrite, pyrite, electrum, digenite, tennantite, bornite, covellite, pyrrhotite, magnetite, ilmenite, rutile, specularite	Quartz, biotite, albite, K-felspar, sericite, smectite, kaolinite, chlorite	Cu, Au, Ag	As, Fe, Ti	Gold-rich porphyry copper

Note: Based on (1) Bassi (1992); (2) Marquez Zabalia and Galliski (1994); (3) (5) Sruoga et.al. (1996), Urbina et.al. (1997,1998) and additional data from electron m icroprobe analyses; (4) Bassi (1992) and Malvicini and Urbina (1994).

sulfidation gold epithermal veins which are hosted by basement rocks. Other minor gold and base metals epithermal mineralizations hosted by both basement and coeval volcanics, are the Raineli, La Juana and La Carpa deposits. The characteristics of the main deposits are summarized in Table 1.

The genetic, spatial, and temporal relations between precious and base metal deposits and subvolcanic, intrusion-related deposits have been pointed out by Sillitoe and Bonham (1984) and Sillitoe (1993). The association between igneous activity and mineralization is clearly evident in the distribution in time and space of mineral deposits in the Tertiary volcanic belt in the Sierras Pampeanas of San Luis. The correlation between igneous rock composition, volcanic landforms and mineral deposit types is remarkably close. These relations can be observed mainly in the best-known deposits at La Carolina and Cañada Honda districts (Urbina et al.,1997). In the La Carolina district concealed mineralizations may be expected according to the idealized schematic cross-sections from Fig. 2A. In the Cañada Honda area, the spatial distribution of several deposits could be interpreted as an intrusion-centered district as shown in the schematic cross-sections of Fig.2B.

REFERENCES

Bassi H. G. 1992. The Sierra Alta de San Luis a case of regmagenic control of gold mineralization. Rickard, M. et al., eds. Basement Tectonics. 9. 211-222.

Brogioni N. 1987. Petrología del vulcanismo Mio-Plioceno de la Provincia de San Luis. Revista Museo de La Plata. Sección Geología. X (83). 71-100.

Malvicini L. and Urbina N. E. 1994. Mina La Rica, un depósito epitermal de tipo sericita-adularia asociado a rocas volcánicas terciarias de la Sierra de San Luis, Argentina. 7° Congreso Geológico Chileno. II. 853-854.

Márquez Zabalía M. F. and Galliski M. A. 1994. Mineralogía y paragénesis de "La Estancia", un depósito epitermal de la Sierra de San Luis. Revista de la Asociación Geológica Argentina. 49 (1-2). 39-47.

Ortiz Suárez A., Prozzi C. y Llambías J. E. 1992. Geología de la parte sur de la Sierra de San Luis y granitoides asociados, Argentina. Estudios Geológicos, España. 48(5-6). 209-381.

Sillitoe R. H. and Bonham F. L. 1984. Volcanic landforms and ore deposits. Econ. Geology. 79. 1286-1298.

Sillitoe R. H. 1993. Epithermal models: Genetic types, geometrical controls and shallow features. In Kirkham, Sinclair, Thorpe, and Duke, eds. Mineral Deposit Modeling: Geol. Assoc. of Canada. Spec.Paper 40. 403-417.

Sruoga P., Urbina N. and Malvicini L. 1996. El Volcanismo Terciario y los depósitos hidrotermales (Au, Cu) asociados en La Carolina y Diente Verde, San Luis,Argentina.XIII Congreso Geológico Argentino.3.89-100.

Urbina N. E., Sruoga P. and Malvicini L. 1997. Late Tertiary Gold-Bearing Volcanic Belt in the Sierras Pampeanas of San Luis, Argentina. International Geology Review. 39. 287-306.

Urbina N., Guerstein P. and Malvicini L. 1998. Hallazgo de telururos de Ag y Au-Ag en el yacimiento diseminado La Carolina, Provincia de San Luis,Argentina. IV Reun. de Mineralogía y Metalogenia. 275-279.

MEZOZOIC - CENOZOIC EVOLUTION OF THE NORTHERN SUBANDEAN ZONE, ECUADOR

Cristian VALLEJO(1)

(1) Departamento de Geología, Escuela Politécnica Nacional, Quito. email: cristianvallejo@hotmail.com

KEY WORDS: Subandean zone, Oriente basin, Foredeep, Napo Uplift

INTRODUCTION

The Oriente Basin of Ecuador occupies an area of approximately 100000 km^2, developping between the guyana shield to the east and the andean magmatic arch to the west.
Is classified as a retroarc type Basin (Dickinson, 1974). And has been filled with rocks of Paleozoic age to recent . The subandean zone is a region localized to the east from the ecuadorian Eastern Cordillera (Cordillera Real) and understood a transition zone between Oriente Basin and Eastern Cordillera, in this zone actually is concentrated the major deformation associated with the eastward migration of the orogenic wedge and the retroarc basin system according to the DeCelles and Giles (1996) model.

CONCLUSIONS

The evolution of the subandean zone and Oriente basin, could be separated in three cycles: Precretaceous, Cretaceous and postcretaceous.The Precretaceous depositional cycle was in a stable marine shelf, overlaying the guyana shield, with sea level rises . The accretion of the Alao terrane in the late jurassic, was the meaningful structural event in the development of the Eastern Cordillera and Subandean zone, and was defined by Litherland (1994) as an oceanic crust allochtonous fragment, acretted to the south

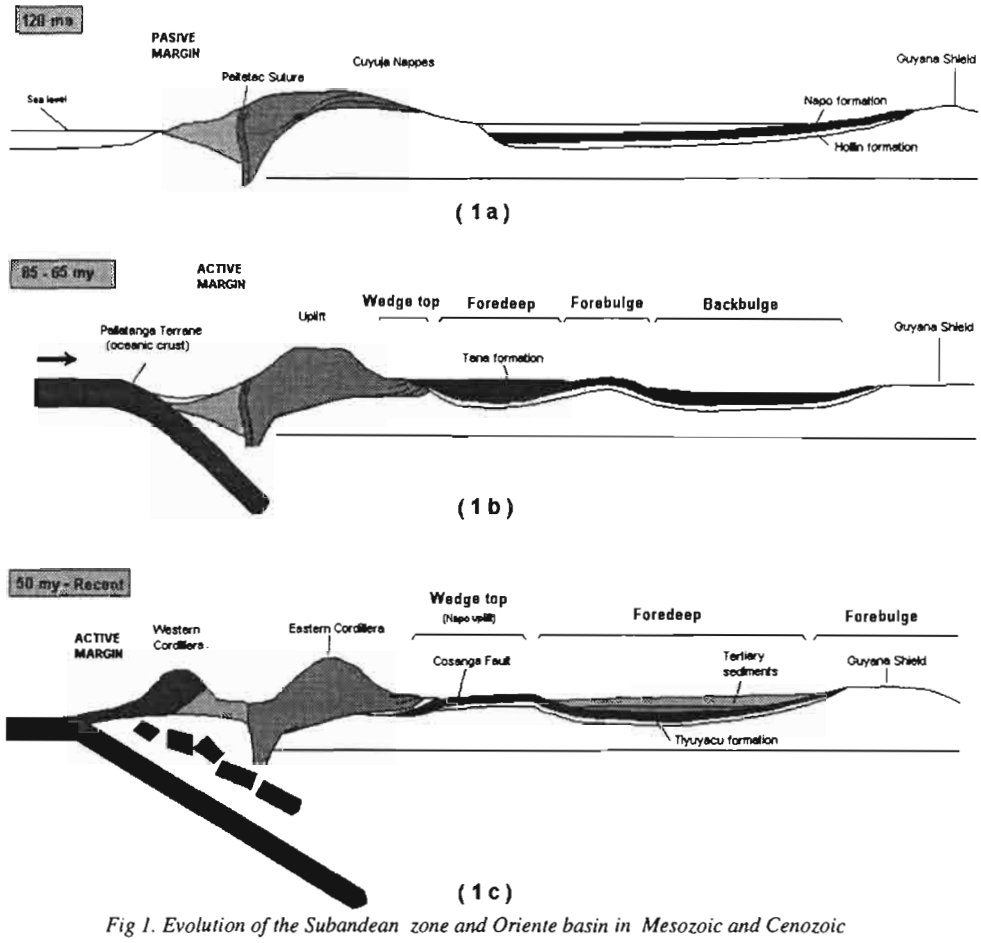

Fig 1. Evolution of the Subandean zone and Oriente basin in Mesozoic and Cenozoic

american craton. This acretion is marked by the ofiolitic suture of Peltetec. The collision was of transpresional type, with a thrusting component, giving place to the development of the Cuyuja nappes in the Eastern Cordillera (Litherland et al,1994) (Fig 1a)

The late cretaceous deposition occurs in an enviroment of stable marine plattform of pasive margin, separated from the influence of oceanic currents, by means of a uplifted zone (Fig 1a), This uplifted area probably corresponded to paleozoic rocks of actual Eastern Cordillera, that were uplifted in the acretion of Alao volcanic arch (Litherland et al, 1994), creating a structural relief that isolate the late cretaceous basin from the influence of marine currents. The tectonic stability of the late cretaceous, is evident by the very low subsidence, close to 3, 7- 10 meters / my, (Jaillard, 1997). This sedimentary cycle, includes the deposition of the marine Napo Formation .

In the Campanian the Pallatanga unit geochemically similar to Piñon Formation of oceanic floor, collided with west of South america, covering the intervale of 85- 65 my, beggining the andean deformation, evidencing in a readjustment of isotopics K/Ar systems in precretaceous rocks of the actual

Eastern Cordillera as Ecuador as Colombia, (Aspden & McCourt, 1998). In this period is produced the change from passive margin basin, to retroarc basin in an active margin (Fig 1b).

The compressional system established , produces a flexural uplift in response to the subducted slab beneath South America and the pressure generated by the collision of Pallatanga terrain, this zone is actually known as "Napo Uplift", and corresponded to the late Cretaceous- Paleoceno forebulge depozone, in agreement to the DeCelles & Giles (1996) model. The foredeep depocenter of the continental type sediments of Tena Formation was located to the west of the forebulge and covered the Napo Formation sediments sufficiently deep to initiate the maturation of the petroleum recovered to the east.

The Tena formation deposition, extend probablely to Paleoceno- Eoceno limit, and was followed by a tectonic pulse and the deposition of the clastic wedge Tiyuyacu Formation overlaying in angular unconformity the Tena sediments. The beggining of this deposition coincides with the eastward migration of the foredeep depocenter (Fig 1c), confirmed by Tiyuyacu Formation isopach maps (Dashwood & Abbots,1990) . During this period the cretaceous Hollín, Napo and Tena sediments were incorporated to the orogenic wedge, being affected by high pressure, low temperature metamorphism due to the compression generated by the eastward advance of the foreland basin system.

Actually In the most proximal part of the, sediments is being deposited above thrusting structures in the western border of Napo Uplift, this zone in agreement to the classification of DeCelles and Giles 1996, corresponds to the wedge top depozone. Deposits consist in immature aluvial sediments derived from the orogenic wedge, deposited in piggy back basins (Baeza-El Chaco, Cosanga) above imbrications and duplex structures affecting the cretaceous rocks. The thrust front is classified as buried type of slow stress relaxation (Morley, 1986). The main detachment horizon has not been abandoned, and is located above the Misahuallí Formation of jurassic age (Fig. 2) . The tip line is located beneath the cuaternary volcanic rocks that overlaying the cretaceous sediments in the Napo uplift. The zone of major deformation is located close to the orogenic wedge , where the calculate shortening is 55 %. Toward the eastern edge of the Napo uplift, exist a broad zone of low deformation, characterized by narrow anticlines (Payamino anticline), pop ups and triangular zones, evidencing the eastward slow stress relaxation. The Cosanga fault is the tectono-metamorphic boundary to the east of the orogenic wedge, evidenced by the absence of deformation in the Hollín, Napo, and Tena, sediments eastward of this structure. The foredeep depocenter has kept stable since Eoceno and has been filled with a potent sedimentary sequence of approximately 2000m, decreasing in thickness toward the Guyana shield, consisting in aluvial fans derived from the Eastern Cordillera.

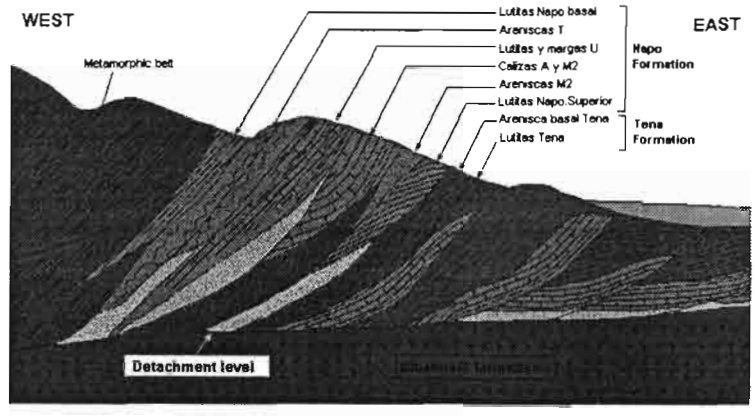

Fig 2 Section in the thrust front, and correlation with the cretaceous sediments

Three principal deformational events have been registered in the subandean zone and Eastern Cordillera since the Eoceno to present, producing deformation of the rocks in the subandean zone evidenced by S1, S2 and S3 foliations in the cretaceous sediments, and uplift in the Eastern Cordillera. These events has been dated in 40, 20 and 9 my. (AFTA, R. Spikings, personal com). The first of wich (40 ma), could be correlated to the oblique accretion of the Macuchi island arch (Aspden & McCourt, 1998) against the north of south america, the second to the rupture and reorganization of the Farallón plate, and the third due to the subducción of the Carnegie ridge beneath the ecuadorian trench.

REFERENCES

-Dashwood, M.F. and Abbotts, I.L. 1990. Aspects of the petroleum geology of the Oriente Basin, Ecuador; Classic Petroleum Provinces, Geological Society Special Publication No 50, pp 89-117.

-Dickinson. W. 1974. Plate tectonics and sedimentation. In: Tectonics and sedimentation, pp 1-27 , Tulsa.

-De Celles, P. And Giles, K. 1996. Foreland basin systems ; Blackwell Science Ltd. Basin Research (1996) 8, pp. 105 - 123. USA.

-Horton, B., De Celles P. 1997. The Modern foreland basin system adjacent to the Central Andes., Geology., v 25, No 10, pp. 895-894.

-Jaiillard, E. 1997. Síntesis Estratigrafica Y Sedimentológica del Cretácico y Paleógeno de la Cuenca Oriental del Ecuador; Informe final del convenio Orstom-Petroproducción. Pp.164.

- Litherland, M., Aspden, J.A., and Jemielita, R.A. 1994. The metamorphic belts of Ecuador. Overseas memoir of British Geological Survey. No.11.

-Morley, C.K. 1986. A clasification of thrust fronts. The American Association of Petroleum Geologist bulletin. Vol.70. No.1. Pp.12-25.

LATE CENOZOIC GEOMORPHOLOGIC EVOLUTION OF THE ANTOFAGASTA AREA, NORTHERN CHILE

Gabriel VARGAS (1, 2, 3), Luc ORTLIEB (3) & Nury GUZMÁN (3, 4)

(1) Depto. Geol., Univ. de Chile, Plaza Ercilla 803, Santiago, Chile (Gabriel.Vargas@bondy.ird.fr)
(2) DGO, UMR 5805, Univ. Bordeaux I, Av. des Facultés, F-33405 Talence Cedex, France
(3) IRD, 32 Avenue Henri Varagnat, F-93143 Bondy-Cédex, France (Luc.Ortlieb@bondy.ird.fr)
(4) FAREMAR, Univ. de Antofagasta. Casilla 170, Antofagasta, Chile (nuryguzman@yahoo.com)

KEY WORDS: Neotectonics, Paleoclimate, Coastal Scarp, Neogene, Quaternary, Chile

INTRODUCTION

Recent observations in the southeastern part of Antofagasta bay (23°S) shed some new light on base level and paleoclimatic aspects of late Cenozoic deposits related to the genesis of the major regional features. In the Coastal Cordillera and coastal plain of the Antofagasta area a sequence of continental sediments overlie a series of old marine terraces in staircased disposition, with the oldest depositional units systematically higher than the younger units. The relative morphologic position of these units with respect to the late Pliocene-early Pleistocene "Antofagasta Terrace" (Martínez y Niemeyer, 1982; Ortlieb *et al.*, 1997) leads to distinguish pre-Pleistocene units from Quaternary units.

THE NEOGENE SEQUENCE

The oldest Neogene unit is composed of well-sorted sediments of regular textural maturity, which indicate an alluvial origin and suggest a relatively long transport from the source. These sediments may also include some lenses of coastal reworked material (therefore suggesting that the coastline was near-by). The surface of these deposits (unit 6, Fig. 1b and 1c) lies at elevations comprised between +210 m (above present sea level) at Coloso to +450 m inland.

The second older unit is composed of alluvial fan remnants (units 4 and 5, Fig.1b), whose upper surface lies at elevations varying between +300 m to +450 m. It corresponds to continental and coastal eolian deposits which cover marine terraces that are located at +330 m to +380 m elevations. From the texture of the alluvial sediments, the high proportion of eolian sands at the base of the sequences, and the wide areal extent and large thickness of these deposits (probably related to important erosion rates in the

Coastal Cordillera), we infer that they were deposited under less arid climatic conditions (more frequent rains) than nowadays and that they may have been coeval with a stage of continental uplift.

The youngest Neogene unit corresponds to alluvial fans (units 2 and 3, Fig. 1b) which lie at elevations increasing from +110 m to +300 m. The large proportion of eolian sand in the matrix of these deposits, and the important topographic upset between the upper surfaces of the fan remnants (30 m to 40 m observed), suggest that their deposition was directly linked to a relatively fast continental uplift motion, coeval with relatively wet conditions. In the Roca Roja locality, immediately north of Coloso, the unit includes coastal marine sediments which overlie a 10 m-thick alluvial sequence of the unit 2 (Fig. 1b). The presence of the pecten *Chlamys vidali* within these sediments suggest a late-Pliocene age (Herm, 1969).

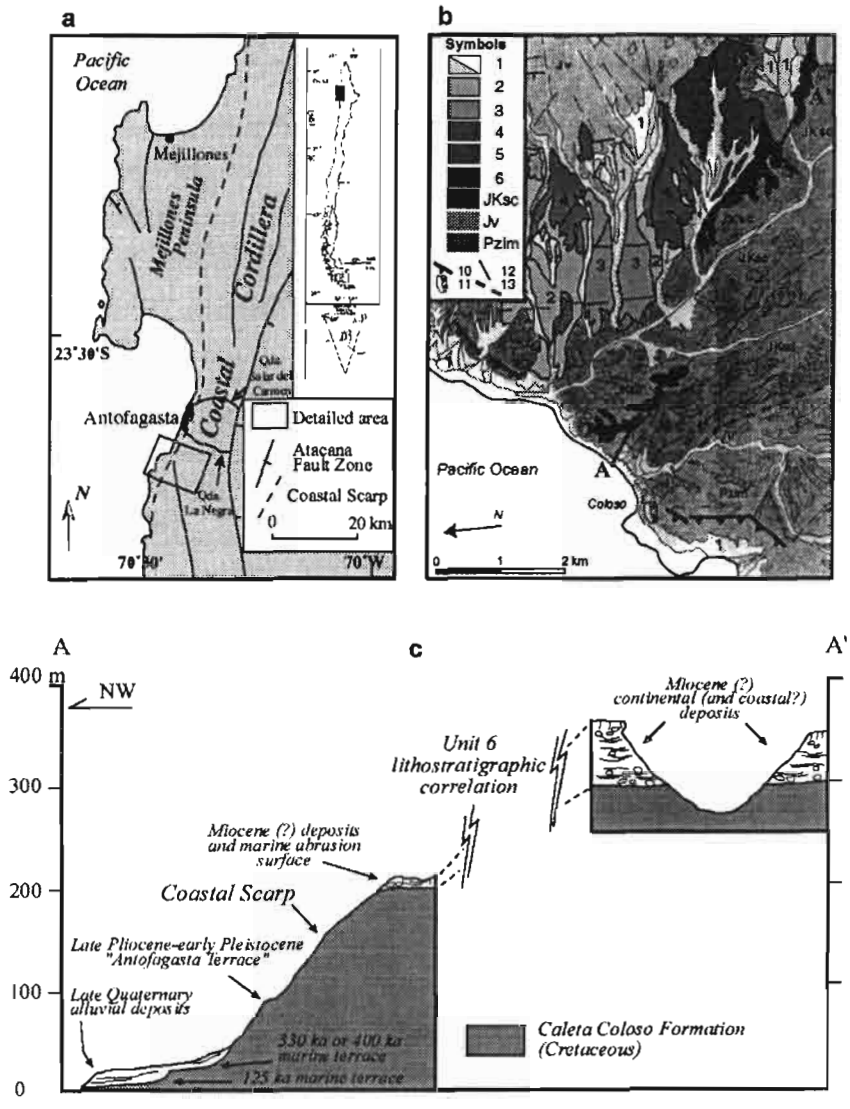

Figure 1. Major geomorphological features in the Antofagasta area

Fig1.: **a:** Localization map; **b:** Geomorphological sketchmap of the southeastern rim of Antofagasta bay; **c:** Schematic profile A-A' (see b) showing geometric relationships between the major sedimentary units and morphological features.

Symbols of sketchmap b : 1: Quaternary alluvial and eolian sediments. 2: Late Pliocene continental sediments. 3: Middle (?) Pliocene continental sediments. 4 and 5: Late Miocene to Early Pliocene (?) continental deposits. 6: Miocene (?) coastal and continental sediments. «JKsc»: Caleta Coloso Fm (Cretaceous). «Jv»: La Negra Fm (Jurassic). «Pzim»: Bolfin Fm (Paleozoic). 10: Coastal Scarp. 11: «Antofagasta Terrace». 12: Lineaments and/or fault scarps. 13 Caleta Coloso Fault.

THE QUATERNARY SEQUENCE

Three marine terraces, covered with Pleistocene-Holocene terrestrial deposits, are preserved in the narrow coastal plain that borders the small Coloso cove (Fig. 1). The highest-lying terrace, at +90 m, is the "Antofagasta Terrace" which has been assigned a Pliocene (Martínez y Niemeyer, 1982), or Plio-Pleistocene (Ortlieb *et al.*, 1995, 1997), age. The intermediate terrace, at +30 m, was interpreted as probably coeval with isotopic stages 9 (330 ka) or 11 (400 ka) high seastands (Radtke, 1989; Ortlieb *et al.*, 1995). The youngest marine terrace at Coloso which lies at a +6 m elevation (max. +11 m) was radiometrically dated as coeval with the isotopic stage 5e (125 ka) (Radtke, 1989; Ortlieb *et al.*, 1995).

Due to the uncertainty of the precise age of the Antofagasta Terrace, at Coloso, it is difficult to infer an uplift rate for Quaternary times. The total lack of diagnostic Pliocene fossils (*Chlamys vidali, Fusinus remondi, Herminespina mirabilis, Chorus* sp.) in the marine sediments that cover the narrow terrace at Coloso leads us to infer that it was formed during one (or several?) early Pleistocene high seastand(s), *i.e.* some time during the 1.8 to 0.8 Ma period. Accordingly, a range of mean uplift rate between 112 mm/ky and 50 mm/ky can be estimated for the last 1 or 2 Ma (Ortlieb *et al.*, 1996; Ortlieb *et al.*, 1997).

Regarding the 30-m terrace, a mean uplift rate of the order of 90 mm/ky, or 75 mm/ky can be calculated for the last 300 or 400 ky under the assumption that the sea level was in a similar position to its present datum at the maximum of the transgression during the isotopic stage 9, or 11 (Shackleton, 1987; Ortlieb *et al.*, 1996).

The position of the coastal sediments and erosive features of the youngest Pleistocene marine terrace strongly suggests that during the last 125 ky, the local uplift rate was much slower, and possibly nil (0 mm/ky) if one accepts the so-called eustatic model of a « global » sea level some 6 m above the present datum during the maximum of the last interglacial episode (isotopic substage 5e).

Beside the uncertainties regarding the respective age of the preserved terraces and the fact that the marine terrace record is limited to only three remnants in the area of Coloso, these data strongly suggest a

diminution of the uplift rate of the coastal region, throughout the Quaternary. It is not clear from the available data whether the variation in the uplift rate was progressive or sudden.

OTHER MORPHOSTRUCTURAL OBSERVATIONS IN THE AREA

A series of morphostructural observations in the Coastal Cordillera and in the coastal plain (Vargas, 1996) show that the Late Cenozoic deformation of the area is closely controlled by regional and local structural features which induce faulted block tectonics.

1. The altimetric position of altogether the youngest and oldest Pleistocene terraces in the northern reaches of the town of Antofagasta, indicate that the Antofagasta coastal plain was uplifted at a higher rate than the Coloso area, south of the town.
2. Quebrada Salar del Carmen separates two areas in terms of relationship between the dimensions of alluvial fans and the areal extent of their respective watershed.
3. There is a change in the general orientation of the coastline and the coastal scarp between Coloso and the southern sector of Antofagasta bay (grossly NE-SW) on one hand, and the centre and north of the Antofagasta coastal plain (N-S), on the other.
4. N-S, NW, NE and ENE lineations and fracture systems in the Coastal Cordillera are predominant in the watersheds, and show various changes across the quebradas Salar del Carmen and La Negra.
5. The geographical orientation of the Coastal Scarp and of some major lineations at a local scale are parallel.
6. There is also a parallelism between local scarps with associated grabens or semi-grabens in Pleistocene and pre-pleistocene alluvial sequences with some of the main lineation systems. One of these small scarps is oriented in the same direction that the Coastal Scarp.
7. Last but not least, there is a regional pattern of inflections in the vertical profiles of the quebradas that cut the Coastal Cordillera. The inflections, which are aligned in the different quebradas and follow some of the major structural lineations, determine a steeper gradient in the upper part of the coastal plain than within the Coastal Cordillera.

DISCUSSION

The geomorphologic evolution of the area was dominated by a net relative sea level fall, which may have begun in the Miocene, and was strongly controlled by structural features. This relative motion depicts an important regional uplift of the coastal region. Because of large uncertainties regarding the « eustatic » (worldwide), or regional, evolution of the sea level during the Miocene and the Pliocene, it is not possible to quantify the uplift motions during the Neogene within the considered area. Nevertheless,

several morphostratigraphic features and the general staircase disposition of the landforms point to a strong vertical deformation that seems to have been particularly active during the Neogene.

The oldest deposits (unit 6) that were laid before the formation of the Coastal Scarp suggest climatic conditions very different from the present ones. Units 5 and 4, which are tentatively assigned a late Miocene age, were possibly coeval with the large alluvial fan, described by Dörr *et al* (1995), which was also deposited under a wet climate and during a phase of strong uplift. From their mosphostratigraphic relations with the sediments containing *Chlamys vidali* fossils at Roca Roja and with the Antofagasta Terrace, units 3 and 2 are assigned a middle (?) Pliocene and late Pliocene age, respectively. At least during the deposition of unit 3 the uplift motions remained strong. During the episode of unit 2, it seems that the rate of uplift diminished, as suggested by the similar elevations of the Antofagasta Terrace and of the coastal sequence at Roca Roja. As previously observed on the north rim of Quebrada La Negra (Ortlieb *et al.*, 1995, 1997), the Coloso data indicate that during the early Pleistocene, the sea reoccupied a marine terrace previously formed during the late Pliocene. These observations suggest that the vertical motions of the coastal area were of limited amount between the late Pliocene and the early Pleistocene, and inclusively that they were slower than afterwards , during the middle Pleistocene. At the end of the Quaternary (late Pleistocene), these motions were drastically reduced.

At Antofagasta, as along the coastal plain north of Mejillones and Hornitos, the Coastal Scarp thus seems to have been formed essentially before the late Pliocene (*i.e.* middle Miocene to middle Pliocene), when strong uplift motions were registered. These regional vertical motions (of several hundred metres) co-occurred with the activation of a grossly N-S oriented major fracture system and produced the Coastal Scarp. During Quaternary times, the Antofagasta area, which was uplifted by about a hundred metres, was affected by tectonic deformations that are consistent with an E-W extensional stress regime (Delouis *et al.*, 1996).

REFERENCES

Delouis B., Philip H., Dorbath L. 1996. Extensional stress regime in the Antofagasta coastal area (Northern Chile). Third ISAG, St. Malo, France. 169-171.

Dörr M.J., Götze H.J., Ibbeken H., Kieffer E. 1995. The Arcas fan in northern Chile : andean deformation and sedimentary response. IGCP 324 and IAS meeting. Abstr. vol., A. Sáez ed., 7-8.

Herm D. 1969. Marines Pliozän und Pleistozän in Nord und Mittel-Chile unter besonderer Berücksichtigung der Enwicklung der Mollusken-Faunen. *Zitteliana* (München), 2, 1-159

Martínez E., Niemeyer H. 1982. Depósitos marinos aterrazados del Plioceno superior en la ciudad de Antofagasta, su relación con la falla Atacama. III Congreso Geológico Chileno,1, A176-A188.

Ortlieb L., Goy J.L., Zazo C., Hillaire-Marcel C., Vargas G. 1995. *Late Quaternary coastal changes in northern Chile.* Guidebook for a fieldtrip, II ann. meet. of IGCP Proj. 367, Antofagasta, Chile, 175 p.

Ortlieb L., Zazo C., Goy J .L., Hillaire-Marcel C., Ghaleb B., Cournoyer L. 1996. Coastal deformations and sea-level changes in the northern Chile subduction area (23°S) during the last 330 ky. *Quaternary Science Reviews*, 15, 819-831.

Ortlieb L., Guzmán N., Vargas G. 1997. A composite (Pliocene/Early Pleistocene) age for the « Antofagasta Terrace » of Northern Chile. VIII Congr. Geol. Chileno, 1, 200-204.

Radtke U. 1989. Marine Terrassen und Korallenriffe. Das Probleem der Quartären Meeresspiegelschwankungen erlänter an Fallstudien aus Chile, Argentinien und Barbados. *Düsseldorfer Geographische Schriften*, Heft 27, 245 p.

Shackleton N.J. 1987. Oxygen isotopes, ice volume and sea level. *Quatern. Sci. Rev.*, 6, 183-190.

Vargas G. 1996. Evidencias de cambios climáticos ocurridos durante el Cuaternario en la zona de Antofagasta, II Región. Tesis Magister en Ciencias, Depto. Geología Universidad de Chile, 174 p.

IDENTIFICATION OF VOLCANIC MATERIAL PRONE TO MASS REMOVAL EVENTS ASSOCIATED WITH SLOPE INSTABILITIES IN THE PRE-ANDEAN SECTOR ADJACENT TO THE CENTRAL VALLEY BETWEEN LATITUDES 33°S AND 34°S, CHILE

Nicole VATIN-PERIGNON(1), Sara ELGUETA(2), Sofía REBOLLEDO(2) and Guy KIEFFER(3)

(1) Laboratoire de Géologie et UPRES - A 5025 CNRS, Université Joseph Fourier de Grenoble, 15 rue Maurice Gignoux, 38031 Grenoble Cedex, France, e-mail : perignon@ ujf-grenoble.fr
(2) Departamento de Geología, Facultad de Ciencias Físicas y Matemáticas, Universidad de Chile. Plaza Ercilla 803, Santiago, Chile. e-mail : selgueta@cec.uchile.cl and srebolle@cec.uchile
(3) Département de Géographie et UPRES – A 6042 CNRS, Université Blaise Pascal, 29 Boulevard Gergovia, 63037 Clermont-Ferrand Cedex 1, France. e-mail : gkieffer@cicsun.univ-bpclermont.fr

KEY WORDS : wet surge deposits, pyroclastic flows, ash flow tuffs, lahars, Miocene, Central Chile

INTRODUCTION

Volcanic Abanico and Farellones Formations are prone to mass removal in the pre-Cordilleran zone of Santiago (Metropolitan Region) mainly because of the combined effects of high precipitation, uplands slope instabilities and narrow steep valleys. Since 1958, numerous debris flows, lahars and rockslide avalanches have periodically occurred in this region and some travelled down ríos Mapocho and Maipo to eastern and south-easten zones of Santiago which are the most hazardous and vulnerable areas (Hauser 1985, 1993). Extensive prehistoric debris avalanche, debris flow and other mass flow deposits are known in the Cerro Plomo - Farellones region and may have been generated by caldera collapse followed by gravitational collapse of flank sector of a Pleistocene volcano. Recent megaslides from slope failures

occurred in valleys of ríos Colorado and Yeso and became reworked in the major valley of río Maipo to form the upper terrace with predominanty volcaniclastic deposits.

The ECOS-CONICYT project* concerns slope instabilities and mass movements of Abanico and Farellones volcanic materials. Three pre-cordilleran characteristic sites have been chosen near Santiago : (1) Cajon del Maipo and the valley of río Volcán, (2) the Lagunillas site between valleys of río Colorado and río Yeso, tributaries of río Maipo to the east and (3) the Farellones - la Parva - Valle Nevado site, before the confluence of río San Francisco and río Molino to form the río Mapocho. Identification of volcanic products and events interpreted from them provides the basis for assessing potential hazards on the assumption that the same general aeras will most likely to be affected by future events of the same kinds and at about the same average frequency as in the past.

The purpose of this paper is to identify Miocene volcanic deposits of Abanico and Farellones Formations and to determine which ones should be prone to high magnitude mass removal events.

ABANICO AND FARELLONES FORMATIONS

Megaslides and mass movements of volcanic materials principally affect the Miocene products of Abanico and Farellones Formations which are the most important volcanic deposits in the Pre-Cordilleran sector. The long history of volcanism, the large number of major and minor eruptive events and the surimposition of successive structures make this region exceptionally complex. Numerous eruptions of tuffs and lavas occurred over a period of 10 Ma during the Miocene between about 26.7 Ma for the oldest phases (Rivano & Vergara 1996) and 17.3 Ma (Drake *et al.*, 1976) for the youngest.

The Abanico Formation has been previously described by Villarrolel and Vergara (1988) and corresponds to numerous volcanic centres for which the present-day color of their products has been obtained by diagenesis. The total thickness of continental volcanic and volcanoclastic deposits ranges to about 1900 m. Three principal units have been distinguished in these deposits. The earliest activity involved eruptions of pumice-rich pyroclastic flow deposits (ignimbrites) and other pyroclastic flows associated with reworked pyroclastic and epiclastic rocks. These formations were followed by basaltic andesite and andesite lava flows and lava blocks occurring in sheets and tephra fall beds cut by andesitic dykes. Overlying pyroclastic deposits are interbedded with thin lapilli-fall layers. The interpretative model of eruptive and depositional mechanisms requires a paroxismal explosive eruption at the top of a zoned reservoir to explain the volume of pumiceous pyroclastic deposits followed by a decline in the amount of silicic andesite erupted during effusive and Strombolian periods of activity. The last period of activity may be related to a final stage of a volcanic complex and represent a distinctive volcano-stratigraphic unit.

The Farellones Formation has been redefined at Cerro La Gloria (type locality) by Rivano *et al.* (1990) as a succession of rhyolitic welded and non-welded ignimbrites and air-fall deposits interbedded with lacustrine sediments (lower member of 300 m) and followed by andesite lavas intercalated with tuffs (upper member up to 1500 m). Systematic studies of lithofacies and previously unrecognized large-scale dynamical characteristics of these deposits have led Elgueta *et al.* (this issue) to recognize different regimes and to reconstruct the past eruptive history of the Farellones Formation. Establishing the stratigraphy of this formation is a difficult task, however, the author and co-workers discuss in detail the Farellones products in terms of different facies of a volcanic complex and present a stratigraphical reconstruction of its volcanic history. They identify three principal eruptive cycles in the Farellones Formation and relate to eruptive mechanisms and depositional environments. The first cycle (300 m thick) could be related to *emplacement of basal ash and lapilli tuffs, collapse of lava dome, opening of a large amphitheatre and composite cone-building phase*. The early phase of lapilli tuffs involves lateral transport and is interpreted as the product of deposition from dilute turbulent pyroclastic surge clouds. During this period, products due to magmatic (lapilli) and hydromagmatic (fine ash) fragmentation processes are present together. It was followed by pyroclastic flows which may be related to collapse of lava domes and may have led to creation of an amphitheatre-shaped hollow (?). The relatively high crystal concentration of fallout deposits erupted contemporaneously was produced by a strong vertical Plinian column. The morphology was modified by construction of a composite cone with lava flows associated with airfall material and interbedded thin lahars. For the following phases , 550 m and 450 m thick respectively, the authors recognise different stages in the development of the volcanic complex. The majority of the eruptions that built up the new *volcanic edifice* corresponds to Plinian eruptions. Reworking of material on these flanks led to widespread emplacement of lahars and alluvial fans. The last activity corresponds to *extrusion of several domes and coulées* related to specific centers and subsequent reworking of material (lahars).

VOLCANIC MATERIAL PRONE TO MASS REMOVAL

In the stratigraphical reconstruction of the eruptive history of the Farellones Formation by Elgueta *et al.* (this issue) in the Lagunillas and Farellones sites, it is noted the frequent presence of air fall ash deposits, pyroclastic flow deposits, surges and fluvial tuffs. In study aeras, these types of fragmental volcanic deposits have been transformed in past destructive mudflows and lahars which fill in numerous valleys as ríos Colorado, Yeso and Maipo that coud be again affected by comparable events. Volcanic sequences have been entrained into past avalanching mass causing debris laden flood (lahars), flowing mixtures of water and rock debris. Extensive prehistoric debris avalanches initiated by large-scale sector collapses or by similar mass-removal events in glacierized areas are known in the pre-Cordilleran region.

Most of these debris may have originated from a large amphitheatre--shaped basin excavated into the Cerro Plomo - Farellones region and now deposited in the relatively limited drainage aera of río Mapocho. These debris avalanches can also be aggraded with lacustrine and fluvial deposits, reworked volcaniclastics and tiggered debris flows down the valleys.

REFERENCES

Drake R.E., Curtis G. & Vergara M. 1976. Potassium-Argon dating of igneous activity in the Central Chilean Andes, latitude 33° S. *J. Volcanol. Geotherm. Res.* 1, 285-295.

Elgueta S., Charrier R., Aguirre R., Kieffer G. & Vatin-Perignon N. 1999. Volcanogenic sedimentation model for the Miocene Farellones Formation, Andean cordillera, Central Chile. *4th International Symposium on Andean Geodynamics*, (this issue)

Hauser A. 1985. Flujos de barro en la zona preandina de la region metropolitana : caracteristicas, causas, efectos, riesgos y medidas preventivas. *Revista Geológica de Chile*, 24, 75-92.

Hauser A. 1993. Remociones en masa en Chile. *Servicio Nacional de Geología y Minería*, 45, 75 p.

Rivano S., Godoy E., Vergara M. & Villarroel R. 1990. Redefinición de la Formación Farellones en la Cordillera de los Andes de Chile Central (32-34°S). *Revista Geológica de Chile*, 17, 205-214.

Rivano S. & Vergara M. 1996. La discordancia basal de Farellones : un ejemplo del relieve premioceno. *Servicio Nacional de Geología y Minería*, carta geológica de Chile.

Vergara M., Charrier R., Munizaga F., Rivano S., Sepulveda P., Thiele R. & Drake R. 1988. Miocene volcanism in the Central Chilean Andes. *J. South American Earth Sci.* 1, 199-209.

Villarroel R. & Vergara M. 1988. La formación Abanico en el area de los cerros Abanico y San Ramon, Cordillera de Santiago. *V Congreso Geol. chileno*, 1, 327-337.

* Contribution to *C97U02 ECOS-CONICYT project* : « Analysis and management of natural hazards associated with slope instabilities and identification of pyroclastic deposits implicated in the pre-Cordilleran sector adjacent to the central valley between 33° - 34° S, Chile ».

$^{40}Ar/^{39}Ar$ AGES, VERY LOW-GRADE METAMORPHIISM AND GEOCHEMISTRY OF THE VOLCANIC ROCKS FROM "CERRO EL ABANICO", SANTIAGO ANDEAN CORDILLERA (33°30´S-70°30´-70°25´W)

Mario VERGARA(1), Diego MORATA(1), Renato VILLARROEL(1), Jan NYSTRÖM(2) and Luis AGUIRRE(1)

(1) Departamento de Geología. Facultad de Ciencias Físicas y Matemáticas. Universidad de Chile. Casilla 13518, Correo 21, Santiago, Chile. E-mail: mariover@cec.uchile.cl
(2) Swedish Museum of Natural History, SE-10405 Stockolm, Sweden.

KEY WORDS: Geochronology, $^{40}Ar/^{39}Ar$, geochemistry, Tertiary, magmatism, Andes.

INTRODUCTION

The Abanico Formation, first described by Muñoz Cristi (*in* Hoffstetter *et al.*,1957), crops out in their type-locality at *Cerro El Abanico,* placed at the foothills of the Andean Cordillera, due east from Santiago. Here, the formation is made up of a 1900 m thick sequence of basic lavas, tuffs and intermediate pyroclastic flows, as well as volcanoclastic rocks with lenticular interbedded lacustrine sedimentary rocks. The rocks are folded in a north-south axed syncline, inversely faulted in the axial region. All these rocks present a secondary mineralogy related to very low-grade metamorphism characterized by a progressive change in the Al-Ca silicates from a yugawaralite (±laumontite) zone to a wairakite zone up to an epidote dominant zone at the bottom of the sequence. (Vergara *et al.*, 1993). The existence of yugawaralite evidences the presence of a paleogeothermal field in the area of *Cerro El Abanico*, since this mineral is only found in active and fossils geothermal systems elsewhere.

$^{40}Ar/^{39}Ar$ AGES

Three basic to intermediate volcanic rocks (Table 1) from the western limb of *Cerro El Abanico* were selected for the $^{40}Ar/^{39}Ar$ geochronological study.

Table I.- Analytical values of the $^{40}Ar/^{39}Ar$ radiometric ages (Berkeley Geochronological Centre) plagioclase phenocrysts (total laser fusion dating method).

Samples	$^{40}Ar/^{39}Ar$	$^{37}Ar/^{39}Ar$	$^{36}Ar/^{39}Ar$	$^{40}Ar^*/^{39}Ar$	% Ar_{rad}	$^{40}Ar_{atm}$	Age (Ma)
ABV-4	104.73	16.56	0.29	21.59	20.4	12.47	30.93 ± 1.90
R-15	61.05	1.28	0.15	17.86	29.2	29.31	25.62 ± 0.64
Ab-1	91.82	2.85	0.25	17.88	19.4	10.55	25.65 ± 1.09

The radiometric ages obtained (Early to Late Oligocene) are consistent with the stratigraphic position of the dated samples. Thus, sample ABV-4 (30.93 ± 1.90 Ma) belongs to a volcanic rock cropping out close to the bottom of the western syncline limb of *Cerro El Abanico*, near the Central Valley of Santiago, whereas samples R-15 and Ab-1 (25.62 ± 0.64 and 25.65 ± 1.09 Ma, respectively) belong to the upper levels of this section.

GEOCHEMISTRY

Geochemical data from Villarroel (1990) for the volcanic rocks of the Abanico Formation in their type-locality (Table 2) first allowed to define these rocks as belonging to the low-K tholeiitic series, with a high FeO/MgO ratio in the basaltic rocks and $(La/Yb)_n$ values between 3.14 to 3.22 and a negative Europium anomaly. All these geochemical features are compatible with the tholeiitic nature proposed for these rocks, which could have been generated in a geotectonic setting characterized by crustal thinning.

The first isotopic (Sr-Nd) data for the volcanic rocks of the Abanico Formation in their type-locality were obtained by Nyström *et al.* (1993). These authors point out a geochemical evolution towards a MORB-like signature for the Cretaceous - Oligocene magmatism in central Chile. In particular, for the volcanic rocks of the Abanico Formation in the Andean Cordillera of Santiago, these authors suggested a genesis involving a fast mantle upwelling episode related to crustal thinning.

DISCUSSION AND CONCLUSIONS

The age of the volcanic rocks of the Abanico Formation has been a continuous controversial topic among researchers working in the Tertiary sequence of central Chile. The presence of zeolites and other very low-grade metamorphic minerals is a strong limiting factor to the precision of the analytical methods used to determine the age of these rocks due to the difficulty in finding rocks free from

alteration. Paleontological and geochronological research by Charrier *et al.* (1996) allowed to assign a Tertiary age to the Abanico Formation. These authors found Tertiary mammals associated with volcanic rocks with K-Ar and Ar/Ar ages of 31 to 37 Ma belonging to the lower levels of the Coya-Machalí Formation (equivalent to the Abanico Formation) in the area of Termas del Flaco (35°S). Recently, Gana and Wall (1997) studied the volcanic rocks, sills and associated dykes from the Abanico Formation in the Andean pre-cordillera north of *Cerro El Abanico*, obtaining the first progressive-heating-speed Ar/Ar radiometric ages ranging between 34 to 19 Ma.

The Abanico Formation, in their type-locality of *Cerro El Abanico*, is composed of volcanic rocks with radiometric $^{40}Ar/^{39}Ar$ (total fusion) ages ranging between 30.93 Ma in the bottom to 25.62 Ma at the top (Oligocene). These ages are consistent with those obtained by other authors in other areas of the Chilean Andes in volcanic rocks which can be correlated with those of the Abanico Formation. The volcanic rocks of the Abanico Formation belong to the tholeiitic series, having a primitive isotopic signature which evidences a magmatism related to a geotectonic setting dominated by crustal thinning . The presence of very low-grade metamorphic minerals associated with paleogeothermal fields confirms the existence of a high paleothermal gradient during the deposition of this formation.

The geochemical, isotopic and secondary mineralogical characteristics of the volcanic rocks from the Abanico Formation are similar to those found in sequences of Late Eocene to Oligocene age exposed in the central Chilean Andes (33-36°s). These particular features are unique in the Meso-Cenozoic magmatism of the Andes. For this reason, it can be used to differentiate these rocks from those belonging to other volcanic sequences of different ages in areas in which the structural and stratigraphic relationships are not well established.

Table 2.- Chemical analyses of three representative samples of volcanic rocks from the Abanico Formation in their type-locality (major elements in % in weight and rare earth elements in ppm).Chemical analyses were carried out in an induced coupled plasma equipment (Centre de Recherches Pétrographiques et Géochimiques, Nancy, France).

Sample *Type*	**Rb-7** *Basalt*	**Rb-9-B** *Basalt*	**Rb-6-1** *Andesite*
SiO_2	48.84	49.82	58.54
Al_2O_3	16.60	16.07	15.53
TiO_2	1.37	1.53	0.73
Fe_2O_3	12.71	12.78	8.25
MnO	0.19	0.22	0.13
MgO	3.72	3.72	3.59
CaO	8.94	8.66	6.17
Na_2O	3.00	3.50	3.42
K_2O	0.59	0.53	2.04
P_2O_5	0.32	0.35	0.27
L.O.I.	3.47	2.82	1.84
Total	99.75	100.00	100.51
La	11.38	13.02	14.74

Ce	33.50	38.97	39.41
Nd	17.22	18.57	19.79
Sm	4.59	5.03	5.19
Eu	1.27	1.39	1.02
Gd	4.42	4.95	5.01
Dy	4.44	4.91	5.15
Er	2.56	2.84	3.16
Yb	2.38	2.70	3.14
Lu	0.45	0.58	0.54

ACKNOWLEDGMENTS

This work has been supported by the FONDECYT Project 1998050 and the Enlace-98Project of the Departamento de Investigación y Desarrollo de la Vicerrectoría de Asuntos Académicos y Estudiantiles, of the University of Chile. The authors thank Drs. Robert Drake and Francisco Munizaga for the $^{40}Ar/^{39}Ar$ radiometric analytical data.

REFERENCES

Charrier R., Wyss A., Flynn J., Swisher C.C., Spichiger S. and Zapatta F. 1996. New evidence for Late Mesozoic-Early Cenozoic evolution of the Chilean Andes in the upper Tinguiririca Valley (35°S), Central Chile. *Journal of South American Earth Sciences*, 9, 393-422.

Gana P. and Wall R. 1996. Geocronología de los eventos magmáticos del Cretácico-Terciario, en el borde occidental de la Cordillera Principal, al sur de la Cuesta de Chacabuco, Chile central (33°-33°30'S). Informe Registrado IR-96-7,SERNAGEOMIN,57 p. y un mapa 1:100.000.

Hoffstetter R., Fuenzalida H. and Cecioni G. 1957. Lexique Stratigraphique International, Amérique Latine, Chili-Chile. *Paris, Centre National de la Recherche Scientifique*, v. 7, 444 p.

Nyström J.A., Parada M.A. and Vergara M. 1993. Sr-Nd isotope compositions of Cretaceous to Miocene volcanic rocks in Central Chile: a trend towards a MORB signature and a reversal with time. *2nd International Symposium on Andean Geodynamics (ISAG)*, 411-414.

Vergara M., Levi B., Villarroel R. 1993. Geothermal-type alteration in a burial metamorphosed volcanic pile, central Chile. *Journal of Metamorphic Geology*, 11, 449-454.

Vergara M., Morata D., Hickey-Vargas R.M. and López-Escobar L. 1999 Volcanismo toleítico del Terciario del área de Colbún, Precordillera de Linares, Chile central (35°35' – 36°S). *Revista Geológica de Chile*, (in press).

Villarroel R. 1990, Geología del área del Cerro San Ramón, Cordillera Principal, Región Metropolitana. Proyecto III-Curso de Magister en Geología. (Inédito). *Departamento de Geología, Universidad de Chile*, 34 pp.

UPLIFT AND SURFACE MORPHOLOGY OF THE WESTERN ALTIPLANO: AN EFFECT OF BASAL ACCRETION AND TECTONIC SHORTENING?

Pia VICTOR & Onno ONCKEN (1)

(1) GeoForschungsZentrum Potsdam, Telegrafenberg, D-14473 Potsdam, Germany
(victor@gfz-potsdam.de)

KEY WORDS: Central Andes, structural geology, plateau uplift, crustal thickening

INTRODUCTION

The Altiplano-Puna Plateau of the Central Andes is the second largest plateau on earth next to Tibet. The high plateau is part of an active continental margin where terrane accretion is lacking and tectonic erosion removes material prior and even during plateau uplift. In this study we combine the interpretation of surface morphology, kinematic analysis and sedimentary processes to propose a model for the uplift of the western Altiplano. The study area is located in a region of extreme aridity, where morphological structures recording deformation are exceptionally well preserved. The time frame for the study spans the Neogene to recent, which is the period in which plateau uplift took place.

GEOMORPHOLOGICAL AND GEOLOGICAL SETTING

The study area is located in the forearc of northern Chile between 20°-21°S at the western border of the Altiplano plateau (fig.1). The topography rises from 1000m in the Longitudinal Valley to over 4000m in the Precordillera. To the east the Altiplano-Puna plateau rises to an average elevation of 4000m above a region where the crust has been thickened up to 70km. The plateau overlies a 30° east-dipping segment of

the subducting oceanic Nazca-plate. The direction of convergence is oblique with regard to the Chile trench.

Besides Pliocene to recent andesitic stratovolcanoes and ignimbrites the geology of the study area is dominated by the Miocene Altos de Pica Formation (APF) (Dingman & Galli 1965). This formation is composed of continental clastic members intercalated with two ignimbrite sheets. The APF covers most of the Precordillera down to the Longitudinal Valley.

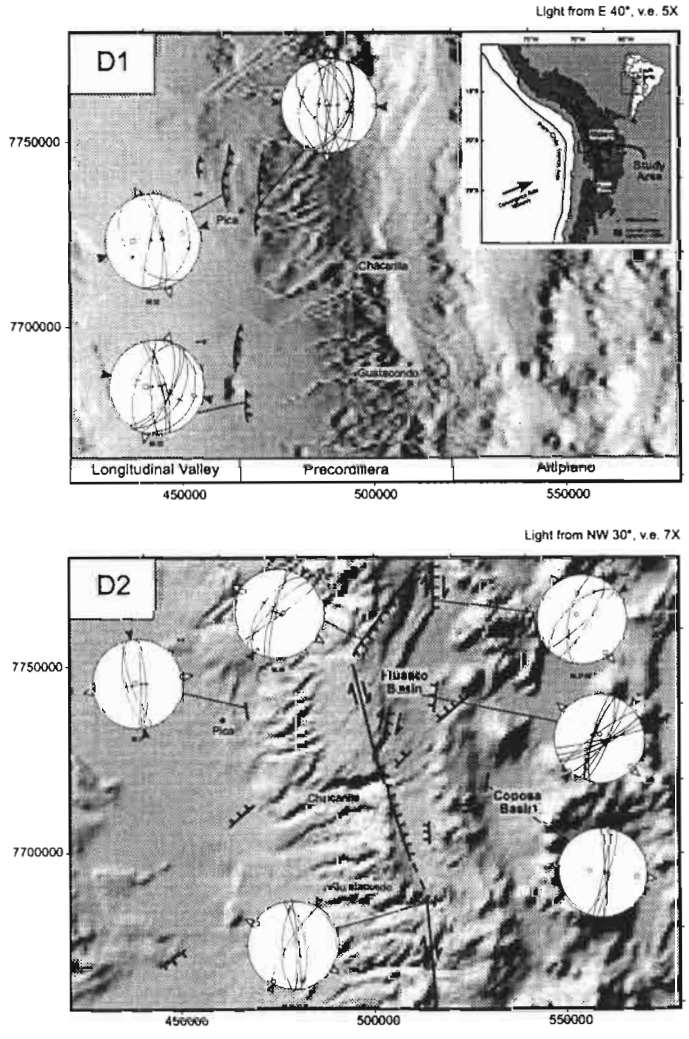

Fig.1: Two contrasting tectonic regimes can be distinguished in the study area. An E-W compressional regime D1 predates a NW-SE extensional regime D2. The inset shows the study area located at the western edge of the Altiplano Plateau.

KINEMATIC ANALYSIS

In the study area we observe two deformation events (fig.1). At the base of the Precordillera N-S striking compressive structures are related to thrusts that have been active syndepositional to the APF. The thrust front propagated from east to west (fig.2). The oldest thrust in the east cuts only lower members of the APF, whereas the westernmost thrust affects the whole formation. These faults are formed during a deformation event (D1) with dominant E-W compression. Knowing the ages of the ignimbrite sheets of the APF (24.0+/-0.4m.y.-20.3+/-0.3m.y. for the older and 17.8+/-0.3m.y.–16.3 +/- 0.3m.y. for the younger sheet; this study) we date the D1 event to 24-8 m.y. ago. The upper limit for D1 is given by quaternary deposits covering the thrusts. During D1 the main phase of ignimbrite eruptions in the area took place. A second tectonic regime (D2) is exposed at the western edge of the Altiplano. There dextral strike slip faults and normal faults led to subsidence of pull-apart basins which developed in a NW-SE extensional regime. Related faults cut the Pastillos ignimbrite that has been dated at 0.73-0.75m.y. (Baker 1977). In the Longitudinal Valley normal faults striking NE-SW offset quaternary alluvial strata (fig.1). This NW-SE extensional regime D2 postdates the W-E compressional regime D1 and might still be active today.

Since the upper Oligocene velocity and direction of plate convergence have not changed, still we observe two contrasting tectonic regimes. We conclude that strain partitioning and the kinematic evolution of the overriding plate are not controlled by oblique convergence alone.

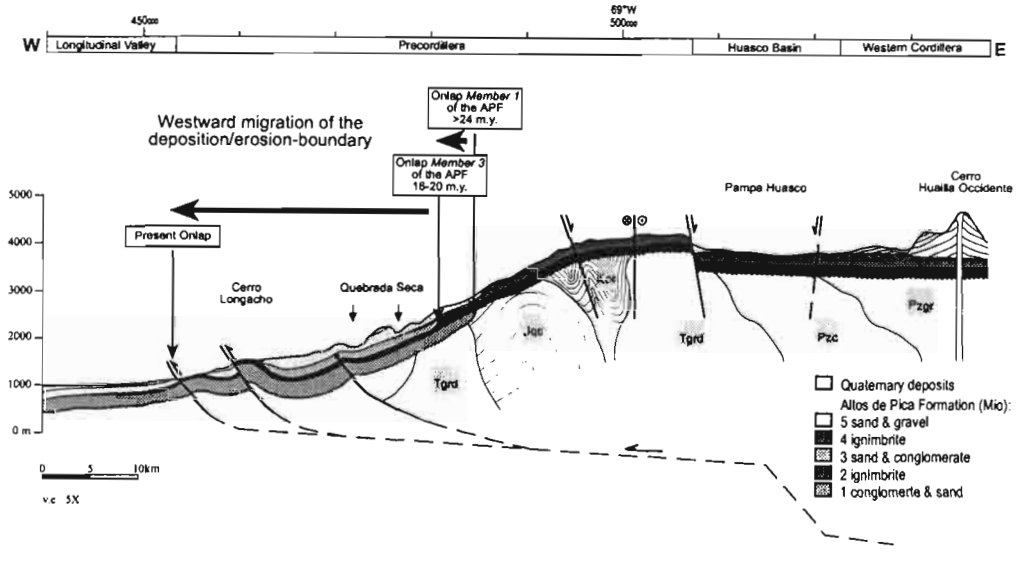

Fig.2: Schematic cross-section at 20°23´S showing the propagation of the D1 thrusts and the westward growth of the Altiplano.

RECONSTRUCTION OF UPLIFT

The age of deposition and the sedimentation rate of the clastic members of the APF are well constrained from the ages of the ignimbrites. The initial uplift is indicated by the deposition of coarse clastic sediments (member 1 of the APF, fig.2) that are derived from the uplifting Precordillera. These deposits discordantly overly Mesozoic and Paleozoic basement. A maximum age for the onset of uplift of 29 m.y. has been calculated by extrapolating a sedimentation rate of 61m/m.y., that we determined for a well suited member of the APF. The position of onlaps of the clastic members of the APF and the recent position of the erosion/deposition boundary indicate a westward migration of that boundary since uplift started (fig.2). This documents a growth of the Altiplano to the west during the Miocene until the Quaternary.

CONCLUSIONS

1) Uplift of the western Altiplano between 20° and 21°S started as early as 24-29 m.y. ago and is associated with the deposition of synuplift sediments of the APF in the Longitudinal Valley.
2) A compressive deformation event D1 affected the APF and was active between approximately 24-8 m.y.. Syndepositional to the APF the thrust front of D1 propagated to the west. The temporal correlation of uplift and thrusting as well as the westward migration of the deposition/erosion boundary suggest, that a major proportion of the topographic uplift is generated by thrust mechanisms during the Miocene.
3) During D1 we observe a main phase of ignimbrite eruptions.
4) An extensional tectonic regime evolved during the Quaternary, probably in response to the high topography and steep topographic gradient at the western flank of the plateau.
We propose the following model for the uplift of the western Altiplano:
Thermal weakening of the upper plate and the increase of the velocity of plate convergence initiated contractional uplift of the western Altiplano during the lower to middle Miocene. Synchronously to plateau formation the crust thickened by basal accretion of tectonically eroded material. The transtensional deformation in the Quaternary is a result of the gravitationally unstable crust and oblique convergence.

REFERENCES

Baker M.C.W. 1977. Geochronology of upper Tertiary volcanic activity in the Andes of north Chile. Geologische Rundschau, 66, 455-465.
Dingman R. and Galli C.O. 1965. Geology and groundwater ressources of the Pica area, Tarapaca province, Chile. Geological Survey Bulletin, 1189, 1-100.

SEISMIC ACTIVITY AT GUAGUA PICHINCHA VOLCANO, ECUADOR

Darwin VILLAGÓMEZ [1], Mario RUIZ [1], Hugo YEPES [1], Minard HALL [1], Bertrand GUILLIER[1, 2], Alex ALVARADO [1], Mónica SEGOVIA [1] and Alcinoe CALAHORRANO [1]

(1) geofisico@accessinter.net
(2) IRD, Apartado 17.72.857 Quito-Ecuador. bguillier@ednet.net

KEY WORDS: volcano, andes, seismic activity, phreatic activity, b-value

INTRODUCTION

Guagua Pichincha volcano, located in the Western Cordillera of the Ecuadorian Andes, is one of the most dangerous active volcanoes in the country. It is located 12 km to the west of Quito (population 1.5 million). Guagua Pichincha has shown a progressive reactivation since its onset in 1981 that consists mainly in phreatic explosions, shallow seismicity and morphological changes in the interior of the caldera. This volcano has been permanently monitored by the Instituto Geofísico since 1981.

Eleven years ago, from July to December 1988, a swarm of 785 volcano-tectonic (VT) events occurred 8 km SE from the cardera. This activity migrated toward the caldera as well as the depth location did from 10 km to 4-5 km (Bonilla et al., 1992). Between 1989 and 1997, the average seismic activity was 130 LP and VT events per year. Since June 1998, a swarm of about 4000 events has been registered in the north of Quito (16-km NE from the caldera, 10-20 km depth). It could be related with Guagua Pichincha present activity (Calahorrano et al., This volume).

On August 4,1998 a major subduction earthquake (Mw=7.1) (Segovia et al., This volume) hit the Ecuadorian coast near Bahía de Caráquez, 210 km west from the volcano. Three days later, on August 7, an abnormal phreatic activity began with a moderate explosion (Reduced displacement RD=0.63 cm^2). For the past 8 months, until present, this activity has continued. More than 140 explosions have been recorded. October 1998 and February 1999 have been the months with the greatest number of explosions (26 and 28 respectively), although the number of explosions has been moving up and down with time. It is remarkable that 8 of the 10 biggest explosions have occurred since December 23, 1998.

SEISMICITY

The total number of seismic events increased dramatically from 64 in August 1998 to 1840 in September 1998, then it decreased progressively until December (294 events) to increase again until February (2359 events).

Seismicity during this period has principally consisted of VT, LP, and MP (medium period or "moscas") events (Figure 1). MP are similar to those observed at Soufriere Hills Volcano from July 1995 to September 1996 (White et al., 1998). White proposed that these events were produced as the magma column degassed into adjacent cracks.

Events from January 1998 to March 1999 were relocated using a new velocity model and HYPOELLIPSE (Lahr, 1995). Map and cross-sections show that hypocenters are well constrained to a zone 0-4 km beneath the caldera (Figure 2).

TEMPORAL VARIATION OF B-VALUE

Temporal variation of the b-value obtained from the frequency-magnitude distribution was calculated using a least squares method over the period January 31, 1998 to February 24, 1999, for windows of 100 located events overlapped 25% (Figure 3). The b-value for Guagua Pichincha earthquakes ranges between 1.0 to 1.6 for this period.

The decrease in b-value from November to December 1998 can be correlated with a decrease in seismicity. Similarly, since late December, the b-value increased again as well as the number of seismic events did.

There are a number of possible explanations for the changes in b-values and seismicity observed in this period. Factors that can alter b-value include increased heterogeneity of the material (Mogi, 1962), and an increase in applied or effective stress (Wyss, 1973; Urbancic et al., 1992).

CONCLUSIONS

Guagua Pichincha volcano has been presenting abnormal high seismic and phreatic activity since August 1998. Although during November and December 1998, it shows an important decrease in the number of seismic events that can be correlated with lower b-values, which could be correlated to an increase in the stress field applied under the volcano.

On the other hand, the progressive increment in b-value since the end of December could be correlated with an increase in the energy of phreatic explosions. More frequent and energetic explosions could be more efficiently fracturing the material in the volcano conduit. Understanding these phenomena can be useful in predicting the future activity of Guagua Pichincha volcano.

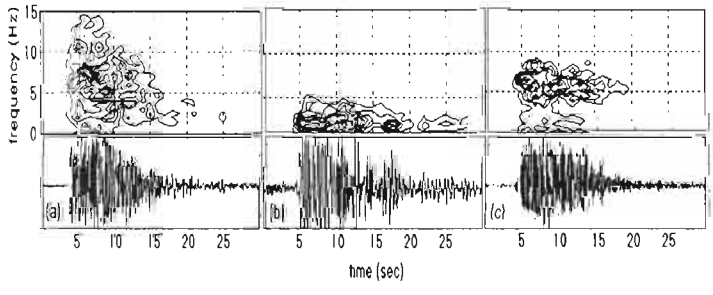

Fig. 1: spectrograms for (a) a VT, (b) a LP, and (c) a MP event, all registered at CGGP station (inside the caldera)

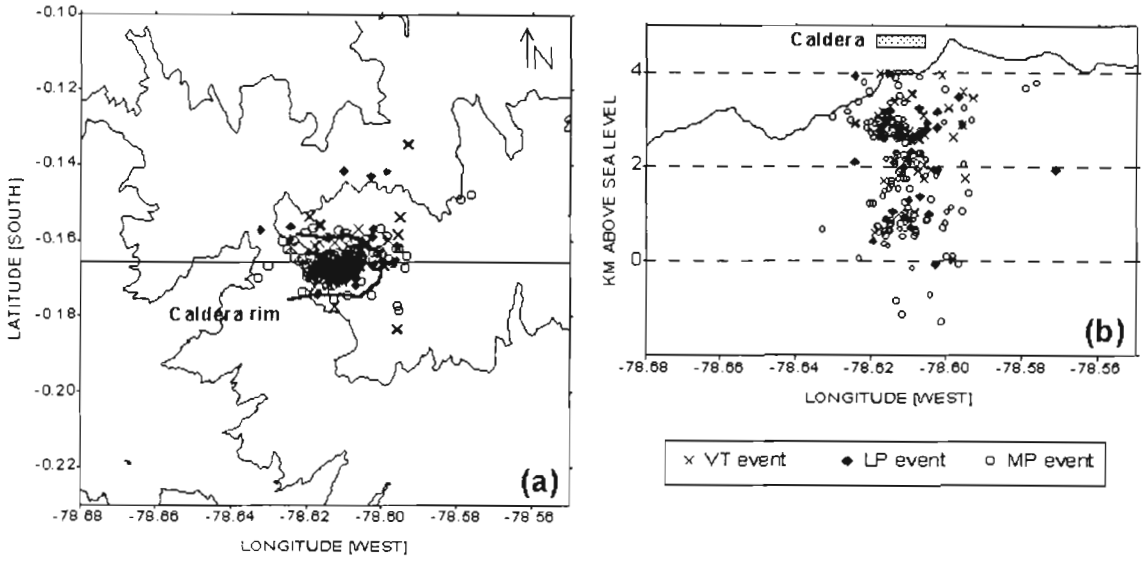

Fig.2: (a) Map and (b) west-east vertical section showing selected hypocenters (rms<0.1 seg, vertical and horizontal errors<1 km)

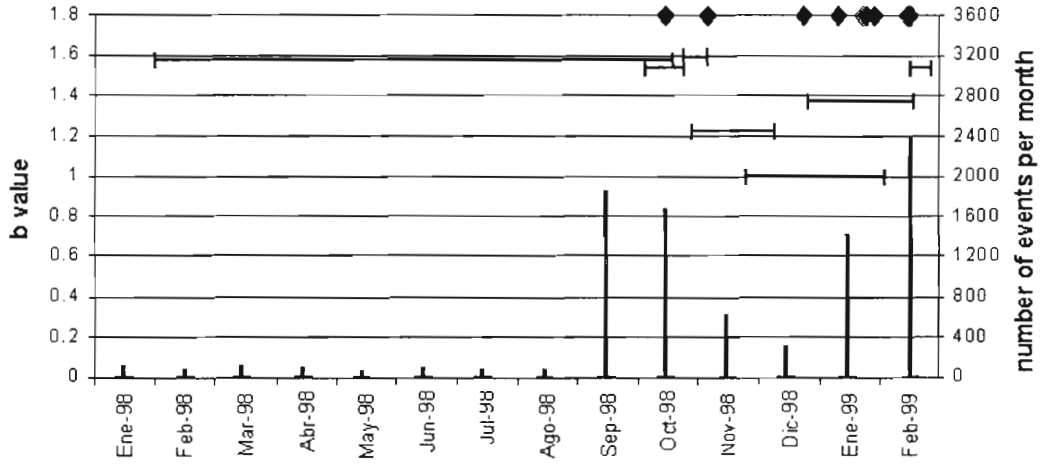

Fig.3: Relationship between monthly seismicity, b-value and phreatic explosions. Horizontal bars are temporal variation of b-value (see text), columns are total number of seismic events per month, and diamonds are the 10 biggest explosions as reference.

REFERENCES

Bonilla F.L., Pérez V.H., Sánchez A., Ruiz M., Yepes A., Chatelain J.L. 1992. Análisis preliminar de la microsismicidad de la zona de Quito-Ecuador Período: 1988-1992, Segundas Jornadas en Ciencias de la Tierra, Quito-Ecuador, 12-14

Calahorrano A., Yepes H., Guillier B., Segocia M., Villagómez D., Andrade D., 1999, Seismic Swarm in Quito(Ecuador): tectonic or volcanic origin?, This volume

Lahr J.C. 1995. HYPOELLIPSE/Version 3.0: A computer program for determining hypocenter, magnitude, and first motion pattern of local earthquake. U.S. Geol. Surv.,Open-File Rep. 95-xxx, 90p.

Mogi K. 1962. Magnitude-frequency relation for elastic shocks accompanying fractures of various materials and some related problemm in earthquakes. Bull. Earthq. Res. Inst., 40, 831-853.

Segovia M., Pacheco J., Shapiro N., Yepes H., Guillier B., Riuz M., Calahorrano A., Andrade D., Egred J., 1999, The August 4, Bahia Earthquake (Mw=7.1) Rupture Mechanism and comments on the potential seismic activity, This volume

Urbanicic T.I., Trifu C.I., Long J.M., and Toug R.P. 1992. Space-time correlations of b-value with stress release, PAGEOPH, 139, 449-462.

White R.A., Miller A.D.,Lynch L., Power J. 1998. Observations of hybrid seismic events at Soufriere Hills Volcano, Monserrat: July 1995 to September 1996, Geophys. Res. Let., 19, 3657-3660

Wyss M.K. 1973. Towards a physical understanding of the earthquake frequency distribution, Geophys. J.R. Astr. Soc. , 31, 341-359.

DIVERSITY IN THE CONVERGENT MARGIN STRUCTURE OFFSHORE SOUTH AMERICA

R. von HUENE and C.R. RANERO (1)

(1) Geomar Marine Research Institute, Wischhofstr 1-3, D-24148, Kiel, Germany
rhuene@geomar.de, cranero@geomar.de

KEY WORDS: Tectonics, South American convergent margin, marine seismic, multibeam bathymetry

INTRODUCTION

The Pacific margin of South America, from Carnegie Ridge in the north to Tierra del Fuego in the south, includes a full spectrum of convergent margin structural styles and tectonic processes. Structural end-members are the large young accretionary prism in the south and the extensive subduction erosion from central Chile northward. Margin structure can be divided into characteristic segments by extending 3 aseismic ridges and a spreading ridge in the Pacific basin from their current entry location at the trench across the continental slope (Figure 1). Although ocean plate boundaries migrate along the margin with time, the upper plate leading edge responds rapidly to the character of the subducting lower plate. Some of these segment boundaries correspond with changes in arc volcanism. Here we summarize structure in each segment and comment on material flux that affects the Andean orogen.

SEGMENTS AND STRUCTURE

In the southern most segment from Tierra del Fuego to the Chile Triple Junction, convergence with the Antarctic Plate is only 2 cm/yr and thus much slower than elsewhere along South America. From its zero age at the Chile triple junction, the ocean crust age increases to 22 Ma, and the trench

depth and width increases accordingly. Paralleling the increased sediment supply, the accretionary prism widens from <10 to 70 km and the subducted sediment layer thickens to 2 km.

The northern segment boundary is the Chile triple junction and as swathmapping shows, the subducting ridge structure as well as the slope are complex. ODP drilling sampled only Quaternary sedimentary rock from the associated accretionary wedge. From the Chile Triple Junction to Juan Fernandez Ridge, the trench again deepens as the age of the subducting ocean crust increases northward to 38 Ma. The trench fill deepens and widens, but the active accretionary prism is commonly 25 km wide or less. The prism abuts the eroded continental framework which contains the roots of the Mesozoic volcanic arcs. Here the rate of convergence increases to 9.5 cm/yr. As in the previous segment, relief from normal faulting on the ocean crust flexing into the trench is relatively low and the thickness of subducting sediment layer is 1 to 2 km. The east-west trending Juan Fernandez Ridge segment boundary deviates to the northeast just before entering the trench where it forms a major basement high that prevents trench sediment transport northward. Its subducted extension beneath the slope is followed to the shelf break with morphology in swathmaps.

In the next segment, between the Juan Fernandez and the Nazca Ridges, the age of the ocean crust entering the trench reaches a maximum as does the trench depth. Here the ocean crust flexes considerably more than in other segments and off Antofagasta where it is observed with swathmapping, its rugosity from normal faulting is extreme. Most sediment which occurs locally in small ponds is subducted. Subducted sediment thickness is poorly imaged and an ephemeral frontal prism has been inferred from bathymetric and seismic observations.. The intersection of Nazca Ridge has been mapped with a SeaMarc backscatter instrument but because of its complexity a much greater area should be mapped for a satisfactory interpretation. This segment boundary is broad and migrates rapidly southward. Local erosion destroys most of the accretionary prism

Between the flanks of Nazca and Carnegie Ridges trench sediment volume increases and the accretionary prism again reaches a ~25 km stable width. Subducting ocean crust decreases in age northward and carries with it underthrust sediment from less than 1 to 1.5 km thick. Convergence is about 8 cm/yr. Here, as along the whole South American margin, wherever the basement has been sampled or continued geophysically from shore, it consists of the Paleozoic and Mesozoic continental framework intruded by Jurassic and Cretaceous arc magmas.

CONCLUSIONS

The relation of structure to tectonic processes follows that documented along convergent margins globally. Where sedimentation rates are high, and convergence is slow, the subducting slab has a shallow dip, and a wide accretionary prism forms. Where the rate of convergence and the dip of

the slab increase, a modest prism forms. The sediment starved trenches with a steeply dipping rugged subducting seafloor morphology are erosional. They are not without a form of frontal prism but it is only large enough to facilitate the subduction of both ocean basin sediment and mass wasting debris from the slope. Prisms of modest width (25 km wide) are common along South America and apparently self-limiting. Where the Nazca Ridge subducts beneath Peru, the area of local erosion gives way to rapid growth of a frontal prism which achieves critical size in 4-6 Myr. Accretion and erosion have alternated in the past consistent with the lack of large residual accretionary prisms seaward of the truncated continental crust. Convergence was rapid during much of Andean mountain building, and considerable terrigeneous material was subducted.

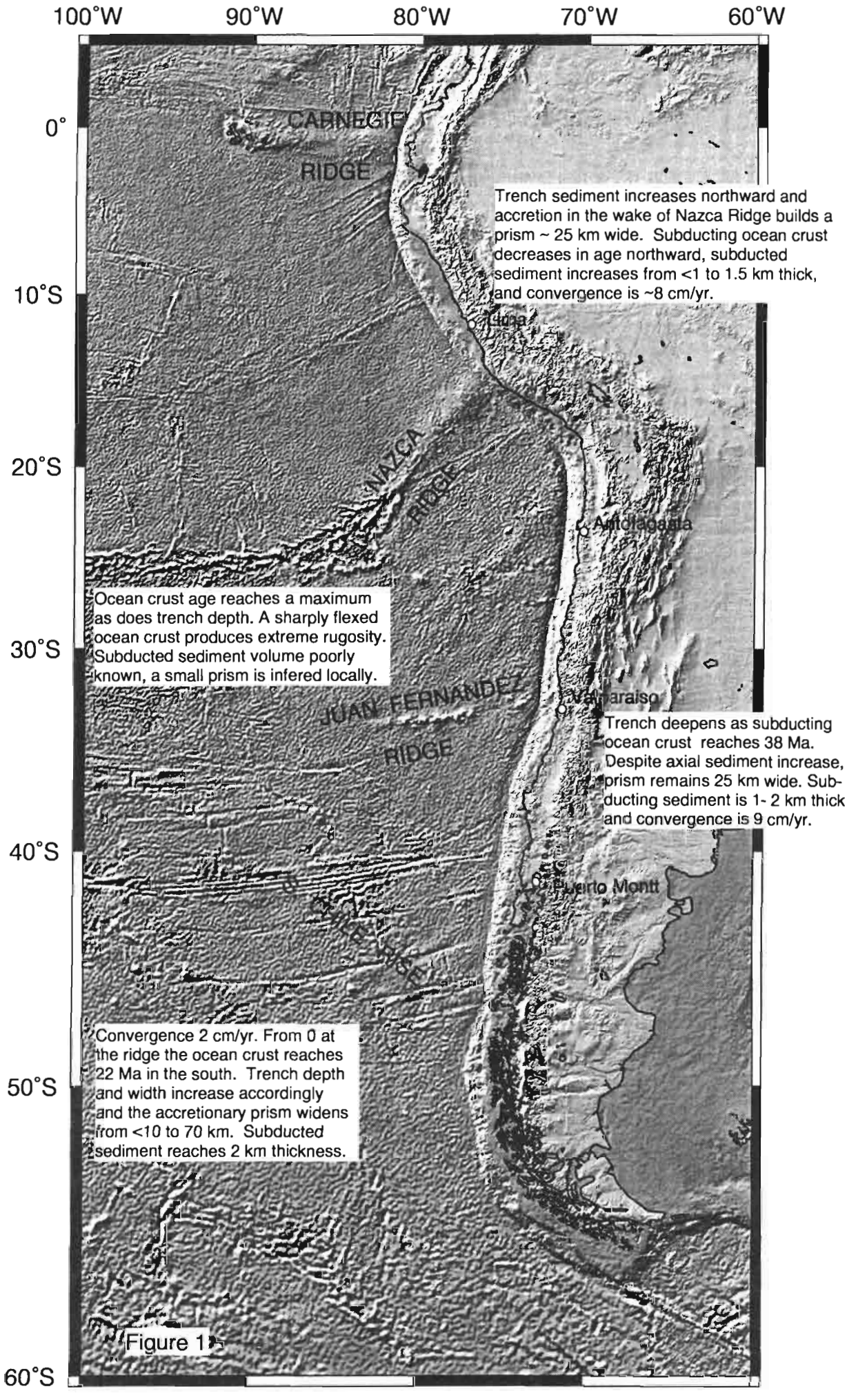
100°W
90°W
80°W
70°W
60°W
0°
10°S
20°S
30°S
40°S
50°S
60°S
CARNEGIE
RIDGE
NAZCA
RIDGE
JUAN FERNANDEZ
RIDGE
Lima
Antofagasta
Valparaiso
Puerto Montt
Trench sediment increases northward and accretion in the wake of Nazca Ridge builds a prism ~ 25 km wide. Subducting ocean crust decreases in age northward, subducted sediment increases from <1 to 1.5 km thick, and convergence is ~8 cm/yr.
Ocean crust age reaches a maximum as does trench depth. A sharply flexed ocean crust produces extreme rugosity. Subducted sediment volume poorly known, a small prism is infered locally.
Trench deepens as subducting ocean crust reaches 38 Ma. Despite axial sediment increase, prism remains 25 km wide. Subducting sediment is 1- 2 km thick and convergence is 9 cm/yr.
Convergence 2 cm/yr. From 0 at the ridge the ocean crust reaches 22 Ma in the south. Trench depth and width increase accordingly and the accretionary prism widens from <10 to 70 km. Subducted sediment reaches 2 km thickness.

Figure 1

A LOWER CRUSTAL AND UPPER MANTLE MODEL FOR SOUTHERN COLOMBIA, BASED ON XENOLITH EVIDENCE

Marion WEBER (1), Ray KENT(2) and John TARNEY(2)

(1) Facultad de Minas, Universidad Nacional de Colombia, Sede Medellín
(2) Department of Geology, University of Leicester, LE1 7RH, UK

KEY WORDS: Xenoliths, crustal model, Andean Northern Volcanic Zone, granulite-amphibolite facies transition, peridotite.

INTRODUCTION

The Northern Volcanic Zone (NVZ) of the Andes is characterised by the subduction of the Pacific plate underneath the South American Continent. Nevertheless, the nature and the processes of the NVZ, in particular in Colombia, are poorly understood, especially the source of the volcanism and the crustal make-up. Crustal growth in the Colombian Andes is characterised by lateral and vertical accretion, but the balance of these processes remains unknown. Lateral accretion in Colombia occurs through diverse subduction-obduction-accretion events of oceanic and continental lithosphere. Vertical accretion in Colombia remains controversial and may occur through emplacement of mantle- or lower crustal-derived magmas, or through basaltic underplating. The Mercaderes-Río Mayo crustal and mantle xenolith occurrence in the midst of the Northern Volcanic Zone (NVZ) provides a unique insight into the lower crust and upper mantle of the NVZ, and may help constrain the processes of crustal growth in the area.

The xenoliths are found within a Tuff (Granatífera Tuff) located in the western flank of the Colombian Central Cordillera. The Central Cordillera contains the surface boundary (Cauca-Almaguer fault system) of rocks between continental affinity to the east and oceanic affinity to the west.Based on their petrology and geochemistry the Mercaderes-Río Mayo xenoliths have been divided into three groups: mantle-derived, lower crustal and igneous xenoliths.

- The mantle-derived rocks range from garnet peridotite to garnet websterite and pyroxenite. The garnet peridotites are highly deformed and sheared lherzolites, whereas most of the websterites and pyroxenites have equigranular textures. Temperatures and pressures obtained for the garnet peridotites (maximum values ~1200°C and 29-41 kbar) indicate that the magma sampled material from ~90 km in depth and therefore the source must lie deeper within the mantle. Temperatures obtained for hornblende-bearing mantle-derived rocks range from 930 to 1101°C and pressures concentrate around 18 kbar, whereas clinopyroxenites yield temperatures between ~720 to 950°C. It is likely that most of the mantle rocks in the Mercaderes area are garnet peridotites. An absence of peridotite xenoliths derived from the pressure-range between 16 and 30 kbar suggests that the uppermost mantle in Mercaderes is made up of a "transition zone" of mafic rocks that most likely include garnet clinopyroxenites and websterites, in addition to hornblende-bearing rocks. The origin of these rocks may be the continuous intrusion of magmas derived from melting of the mantle wedge. Evidence such as spongy rims, "inclusion trails" and garnet breakdown of garnet at the rims, shown exclusively by the mantle-derived rocks, suggest introduction of fluids, possibly released from the subducting slab (Nazca plate).
- The lower crustal suite is made up of a variety of rocks that include pyribolites (c.f. Mehnert, 1978), hornblendites, granulites, pyroxenites and gneisses. Petrographical evidence places many of these rocks at the amphibolite facies - granulite facies transition. This involves dehydration and possible melting of hydrous phases (amphibole & mica) and the formation of clinopyroxene and additional garnet. The prograde metamorphic path is further indicated by *P-T* conditions calculated for these rocks. Amphibole and mica-free rocks generally show higher rim temperatures (~950 to 1050°C at 13 to 15 kbar) than amphibole and mica-bearing rocks (~730 to 830°C at 9 to 14 kbar). Furthermore, *P-T* calculations and zonation profiles of most of the rocks record prograde *P-T* conditions within the same rock. Only in rocks that have reached sufficiently high temperatures, has the record been obliterated (homogenisation). The amphibole - granulite transition in Mercaders probably involves the transformation of amphibole-bearing rocks to pyribolites, pyriclasites, pyroxenites and granulites. Given that the Mercaderes xenoliths exceed the temperature at which many rocks are likely to undergo fluid-absent melting reactions (>850°C) (Vielzeuf, 1988; Stevens and Clemens, 1993), a heat producing source must exist under Mercaderes. Such a source could be the underplating of intrusion/passage of hot magma. Therefore, dehydration-melting and magma intrusion/formation beneath Mercaderes are not independent processes, but intimately linked. The melting of lower crustal rocks are likely to produce melts that can have migrated upwards to produce felsic igneous rocks.
- Igneous xenoliths in Mercaderes are of two types:

1) Volcanic rock fragments and bombs, with dacitic and andesitic, and lamprophyric petrographical characteristics; and 2) Plutonic xenoliths of dioritic composition.

The volcanic rocks comprise two different populations that have been classified petrographically as andesites and lamprophyric rocks. The lamprophyric rocks are often seen surrounding mantle-derived samples and therefore are believed to have transported these rocks. This suggests that these magmas originated from a

source that lies within the mantle.

Geochemical evidence indicates that the Mercaderes-Río Mayo andesites show similarities to adakites, i.e. magmas believed to have formed by high-pressure partial melting of a basaltic source (cf. Defant and Drummond, 1990, Atherton and Petford, 1993). However, their chemical character lies between the lamprophyres and the dacite, indicating possible magma interaction (mixing?) between these "end-members" within the deep crust.

The plutonic rocks are diorites, which contain essential amphibole and feldspar. The diorites show increasing degrees of metamorphism, which is evidenced by the formation of garnet (therefore, strictly amphibolite). These rocks have a different chemical character when compared to the andesites, suggesting essential differences in their petrogenesis.

The overall picture that emerges from the studied xenolith population in the Mercaderes-Río Mayo area is that the evolution of the crust and mantle beneath Mercaderes may have been dominated by at least two processes:

- Intrusion of mantle-derived magmas into the upper mantle and lower crust;
- Possible melting of the lower crust (and upper mantle?), and formation of felsic melts (adakites?) leaving behind a refractory restite.

A suggested model for the Mercaderes-Río Mayo area is presented in figure 1, which illustrates the link between the different processes recognised for the Mercaderes-Río Mayo area (accretion (?) - melting - intrusion/underplating) and highlights the importance that vertical accretion may have in this area, and possibly in much of the NVZ. In addition, figure 1 clearly shows that there is a relatively good agreement between the seismically-defined Moho ($V_p \geq 8$ km/sec) in Mercaderes and the petrological Moho suggested by the xenolith evidence. The petrological Moho described here follows the definition of Griffin and O'Reilly (1987a, b): i.e., it represents the boundary between silicic and ultramafic rocks. Therefore, although rocks from the ~50 to 90 km depth range are believed to comprise predominantly websterites and pyroxenites (which result from frozen magma bodies that originated by melting in the mantle wedge), these are still strictly part of the upper mantle. The lower crust/upper mantle boundary beneath Mercaderes-Río Mayo is likely to be transitional, which is in agreement with the observations from other world-wide areas (Griffin and O'Reilly, 1987).

The model presented here suggests that the volcanism that characterises this part of the NVZ may be dominated by magma formation and their interaction (e. g., mixing). In Mercaderes the source of these magmas possibly lies within the mantle **and** the lower crust, leaving behind a refractory restite material. The main resulting rocks have characteristics similar to those of adakites. This source for adakitic volcanic rocks is different to the sources postulated for similar rocks from the CVZ and AVZ (e.g., Atherton and Petford, 1993, Stern and Kilian, 1996). The CVZ volcanic rocks are thought to have formed by partial melting of lower crust that was overthickened by underplated mafic magma (Atherton and Petford, 1993, 1996). In Mercaderes, the

crust is envisaged to melt *because* of underplated/intruded mantle-derived melts within the lower crust, i.e. due to magmatic heat input. The adakite volcanism in the AVZ is believed to be the result of melting within the subduction plate and subsequent interacting with the mantle, and limited interaction with the crust (Stern and Kilian, 1996). The evidence presented here suggests that in Mercaderes interaction with the crust plays an important role in the generation of magmas.

REFERENCES

Atherton, M. P. and Petford, N., 1993. Generation of sodium-rich magmas from newly underplated basaltic crust. Nature, 362, 144-146.

Defant, M. J. and Drummond, M. S., 1990. Derivation of some modern arc magmas by melting of young subducted lithosphere. Nature, 347, 662-665.

Griffin, W. L. and O'Reilly, S. Y., 1987. The composition of the lower crust and the nature of the continental Moho - Xenolith evidence. In: Mantle Xenoliths, Nixon, P. H. (Ed.), John Wiley & Sons, Chichester, 413-430.

Mehnert, K. R., 1972. Granulites - Results of a discussion II. Neues Jahrbuch f¸r Mineralogie. Monatshefte, 139-150.

Meissner, R. O., Flueh, E. R., Stibane, F. and Berg, E., 1976. Dynamics of the active plate boundary in southwest Colombia according to recent geophysical measurements. Tectonophysics, 35, 115-136.

Stern, C. R. and Kilian, R., 1996. Role of the subducted slab, mantle wedge and continental crust in the generation of adakites from the Andean Austral Volcanic Zone. Contributions to Mineralogy and Petrology, 123, 263-281.

Stevens, G. and Clemens, J. D., 1993. Fluid-absent melting and the role of fluids in the lithosphere: A slanted summary? Chemical Geology, 108, 1-17.

Vielzeuf, D., 1988. Granulites and their problems. Terra Cognita, 8, 237-239.

Figure 1. Suggested model for the Mercaderes-Río Mayo mantle and crust * indicates areas of possible magma production for Mercaderes-Río Mayo. The cross section area is inferred from velocity values given by Meissner *et al.* (1976) for a transect north of Mercaderes.

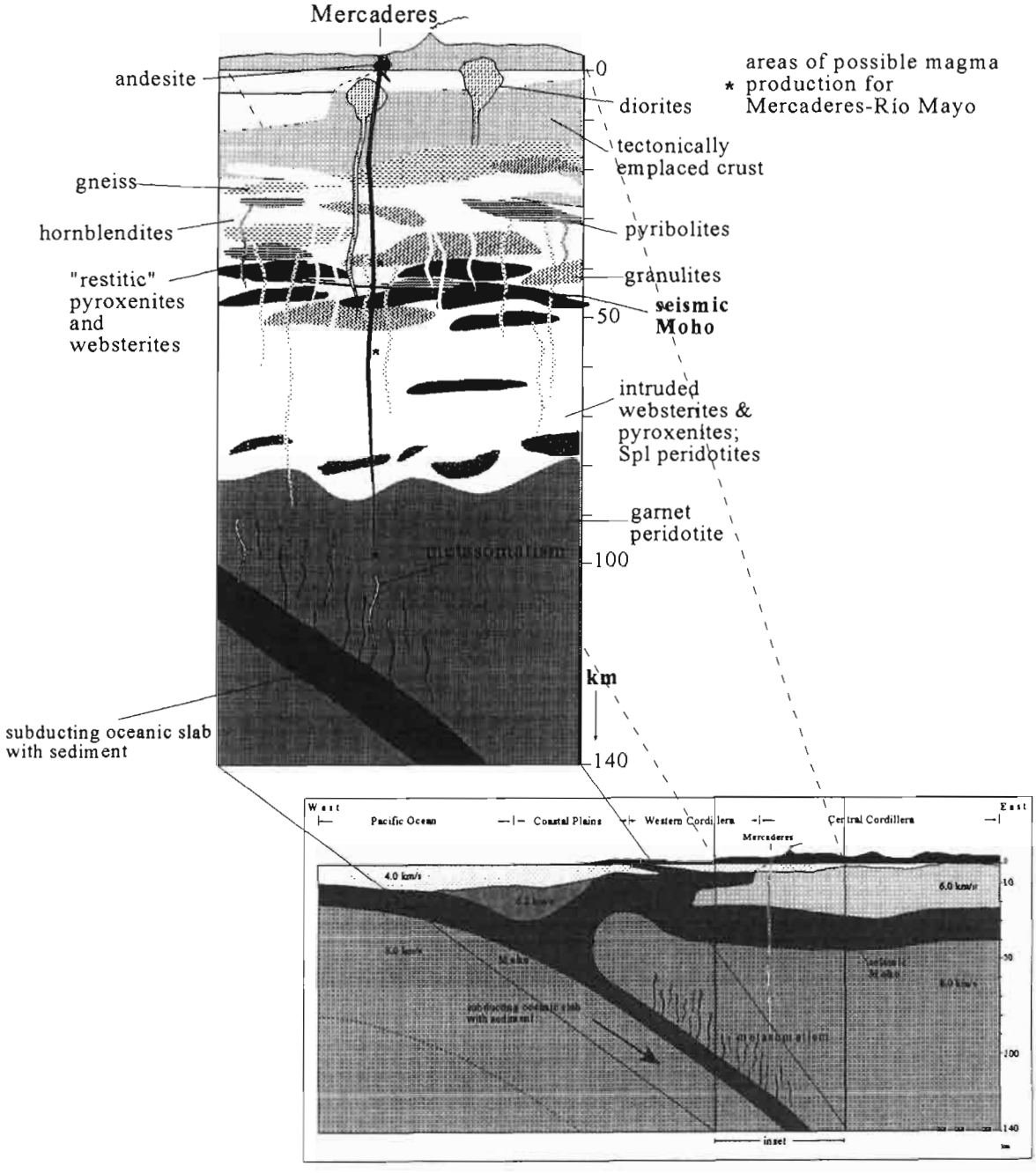
Mercaderes
andesite
gneiss
hornblendites
"restitic" pyroxenites and websterites
subducting oceanic slab with sediment
0
50
100
140
km
diorites
tectonically emplaced crust
pyribolites
granulites
seismic Moho
intruded websterites & pyroxenites; Spl peridotites
garnet peridotite
areas of possible magma production for Mercaderes-Río Mayo
West
Pacific Ocean
Coastal Plains
Western Cordillera
Central Cordillera
East
Mercaderes
4.0 km/s
6.0 km/s
inset

THE IMPACT OF TECTONICS AND TOPOGRAPHY ON THE EXTENT OF THE LAST GLACIATION OF THE SOUTHERN PATAGONIAN ICEFIELD (CHILE, ARGENTINA)

Gerd WENZENS(1)

(1)Geographisches Institut, Universitätsstrasse 1, 40225 Duesseldorf, wenzens@uni-duesseldorf.de

INTRODUCTION

The Southern or Patagonian Andes extending north-south from 39° to 52° latitude S, have a mean elevation of ca. 2,000 m. West of this ridge, stretching along the Pacific Coast, lies a mountainous archipelago which is frequently dissected by fiords south of lat. 44° S. To the east, the Andean Central Cordillera is flanked by the precordillera, a mountain zone, 5 - 20 km wide and up to 2,500 m high. In the east it merges into the Patagonian mesetas, declining from around 1,500 m to 500 m near the Atlantic Ocean. Between the lat. of 47° 20' and 48° 10' S the Andes chain is severed, over a 100 km stretch by diverse branchings of the Canal Baker flowing into the Golf de Penas. Despite the relatively low mean altitude of the Patagonian Andes, two icefields exist north and south of this gap. The North Patagonian Icefield (NPI) covers an area of ca. 4,200 km^2 and stretches between the lat. of 46° 30' and 47° 30' S. The Southern Patagonian Icefield (SPI) forms the largest ice cap in temperate latitudes of the world with an area of approximately 13,000 km^2. Its northern part has a maximum width of 90 km and sustains the largest outlet glaciers, namely, Pio XI Glacier (64 km length) in the west, Jorge Montt Glacier (42 km) in the north and O'Higgins Glacier (ca. 40 km), Viedma Glacier (50 km) and Upsala Glacier (56 km) in the east. The area of study (Fig. 1 and 2) includes these eastern outlets which terminate in the Lago O'Higgins (253 m a.s.l.), the Lago Viedma (250 m a.s.l.), and the Lago Argentino (151 m a.s.l.) and the adjacent precordillera as well. In accordance with its name of reference in Argentina, the Lago O'Higgins will be referred to as Lago San Martín. This large icefield exists because the regional climate is dominated by the topographic barrier of the Andes lying athwart the westerlies. The mean annual precipitation on the icefield is

estimated at about 6,000 - 8,000 mm, decreasing significantly to the east. The weather station of El Calafate, located only 55 km east of the SPI, has an annual mean precipitation of only 200 mm.

During the Pleistocene glaciations, a continuous ice sheet merged in the Andes south of the lat. 39° S that terminated in the piedmont zones east and west of the mountain divide. Caldenius (1932) has made the only attempt to distinguish moraine belts of different ages east of the Patagonian Andes. He mapped four advances, three of which (Dani-, Goti- and Finiglacial) he assigned to the last glaciation. It is generally acknowledged that the Gotiglacial ice limit corresponds to the Last Glacial Maximum (LGM). Schellmann (1998) and Wenzens and Wenzens (1998) classified three late-glacial advances at Lago Argentino and Lago Viedma respectively, the youngest of which corresponds to the Finiglacial ice limit at Lago Argentino as well as the limit south of Lago Viedma. It has not yet been proven whether this readvance occurred during the European Younger Dryas Stade (ca. 11,000 to 10,000 yr B.P.). Mercer's (1976) view that both icefields existed within present boundaries during this time is also controversial (Wenzens 1999). Subsequently, nearly all authors describing the fluctuations of the ice margin of the SPI during the last glaciation accepted the Gotiglacial ice limit as the LGM. This paper investigates whether the icefield margin during the LGM and the late Lateglacial really corresponds to the Goti- and the Finiglacial ice limits of Caldenius respectively. This study is based on the detailled mapping of terminal moraines of these advances in the east of the northeastern icefield between Lago Argentino in the south and Lago San Martín in the north.

Several north-south-inclining fault zones run parallel to the Andean east flank north of Lago Argentino, and thus determine the discharge of the Upsala Glacier to the south (Fig. 1). As a result, the tectonic weak zones were glacially eroded. Today, they form the branches extending north of Lago Argentino and their fluvial extensions. In the east this area is dwarfed by the almost vertical flank of the precordillera which starts north of Lago Argentino at an altitude of 2,000 m and rises to 2,500 m south of Lago Viedma. Moraines on the northwestern slope of Lago Argentino which could be assigned to the LGM, are found at an altitude of 800 m. If the altitude of the ice surface at this site is applied to the icefield, even an increase of ca. 1,000 m in ice thickness compared to today,would not have been sufficient to enable outlet glaciers to descend eastwards during the LGM. Today, east of the precordillera, there are small cirque glaciers which developed into valley glaciers during the last glaciation. As the precordillera is inclined to the east, almost all the glaciers flew in this direction and merged into the Guanaco- and Cóndor valley glaciers (Wenzens 1999). In contrast to Caldenius' (1932) view that the icefield advanced eastwards between Lago Argentino and Lago Viedma covering this part of the precordillera and the adjoining mesetas as a continuous ice cap during the last glaciation, the geomorphological evidence indicates that the icefield west of the precordillera could only discharge to the south. Simultaneously, east of the precordillera, valley glaciers extended towards the meseta of which the catchment areas were independent from the icefield.

North of Lago Viedma the precordillera expands and is characterized by N-S running ridges and valleys. The western chain rises up to 2,5000 m and constitutes the watershed between the icefield and various valley glaciers descending to the east. Where the catchment area of the Viedma Glacier discharging to the south adjoins that of the Chico Glacier discharging to the north at an altitude of only 1,350 m, the ridge of the precordillera is severed and creates a 5 km wide transition of the icefield to the east. This part of the precordillera is drained by the Río de las Vueltas flowing into Lago Viedma. During the LGM all the glaciers of this region converged into this valley and merged with the Viedma Lobe. The glacially deepened Río de las Vueltas valley, situated approximately 15 km east of the icefield, contrasts markedly with the V-shaped valleys in the east, where valley glaciers have never existed. According to Caldenius (1932) the Gotiglacial ice margin of the icefield between Lago San Martín and Lago Viedma was situated 40 km east of the recent watershed. The Finiglacial ice limit of Caldenius still lies about 10 km east of the Río de las Vueltas. In fact all the glaciers of the precordillera including the small outlet terminated west of the Río de las Vueltas valley during the late Lateglacial. At that time the Viedma Lobe invaded the lower reaches of the Río de las Vueltas, blocking the outflow of meltwater.

The morphogenesis of the glacial landscape in the Lago San Martín area differs considerably from that in the southern area of the study. In this region the icefield's development during the LGM has been largely influenced by the topography of the precordillera. The landscape east of the icefield consits of a network of interconnected fiords separated by mountains rising to heights of more than 1,500 m a.s.l (Fig. 2). As a result, the discharge of the extending icefield occurred in the form of long and narrow glaciers flowing to the north (Brazo Norte Occidental), and to the southeast. This outlet, referred to here as San Martín Lobe, merged with the glacier which advanced into the Brazo Norte Oriental from the north. The catchment area of this glacier consisted of several mountain groups in the vicinity and the highest peeks of the Peninsula Florida. The terminal moraines of the LGM surround the Lago Tar just as Caldenius (1932) mapped them. The reconstruction of the former icefield expansion in this area shows however, that the advance did not occur in form of a large, wide piedmont outlet glacier as Caldenius believed, but was restricted to single glaciers which advanced in deep valleys of a pre-existing drainage pattern. Between these long, narrow, steep-sided and glacially eroded basins, ridges of the precordillera formed high and almost continuous topographic barriers, some of which supported the cirque - and valley glaciers descending into the ice-accumulated fiords. For other parts of the Andes, Clapperton (1993) also emphasized the significance of the topography as a key role determing the past development of glacier expansion.

The general view that the South Andes developed a continuous mountain ice cap, extending at least 40 - 50 km from the recent margin during the Last Glacial Maximum, does not correspond with geomorphological evidence east of the Andes. Only single outlet glaciers which developed through the union of several glaciers, extended out of the mountains and eroded the large lake basins such as Lago Argentino and Lago Viedma. The expansion of the icefield between these large discharging piedmont outlet glaciers was

restricted to only a few kilometres. The terminal moraines of the LGM of these outlet glaciers correspond to the Gotiglacial ice limit and are situated between 100 and 120 km from the recent ice margin.

REFERENCES

Caldenius, C.C. (1932). Las glaciaciones cuaternarios en la Patagonia y Tierra del Fuego. Geografiska Annaler **14**. 1-164.

Clapperton, C. (1993). Quaternary Geology and Geomorphology of South America. Amsterdam.

Mercer, J.H. (1976). Glacial history of southernmost South America. Quaternary Research **6**. 125-166.

Schellmann, G. (1998). Jungkänozoische Landschaftsgeschichte Patagoniens (Argentinien). Essener Geographische Arbeiten **29**. 216.

Wenzens, G. and Wenzens, E. (1998). Late glacial and Holocene glacier advances in the area of Lago Viedma (Patagonia, Argentina). Zentralblatt Geologie und Paläontologie **I 1997, (3-6)**. 593-608.

Wenzens, G. (1999). Fluctuations of Outlet and Valley Glaciers in the Southern Andes (Argentina) during the last 13,000 Years. Quaternary Research (in press).

UPLIFT AND GRAVITATIONAL COLLAPSE OF THE WESTERN ANDEAN ESCARPMENT AT 18°S

G. WÖRNER (1) , H. SEYFRIED (2), D. UHLIG (2), I. KOHLER (2)

(1) Geochemisches Institut, Universität Göttingen, Goldschmidtstr. 1, 37077 Göttingen (Germany) Gwoerne@gwdg.de
(2) Institut für Geologie und Paläontologie, Universität Stuttgart, Herdweg 51, 74174 Stuttgart (Germany) hartmut.seyfried@geologie.uni-stuttgart.de

KEY WORDS: Stratigraphy, Miocen to recent, uplift, gravitational collapse, erosion, valley cutting

INTRODUCTION

Understanding the evolution of large mountain chains, their effect on climate and the role of climate in shaping mountain ranges is of prime interest in understanding our Earth system. The Central Andes are an excellent example for studying such interplay between tectonic stress and body forces and external effects of climate, erosion, and sedimentation. In addition, process and quantification of Andean uplift as well as balancing crustal thickening through compression, magmatic addition and other possible processes have been an issue of considerable debate. Most of the observations and arguments derive from studies on the Altiplano or from transects in the southern Central Andes. The western Andean Escarpment around 18°S near the so-called "Arica Bend", however, has received relatively little attention but provides considerable information on the process, timing and consequences of uplift in a hyperarid region (Salas et al., 1966; Muñoz and Charrier, 1996; Seyfried et al., 1994). This part of the western margin of South America is characterized by a difference in elevation from the trench at 7000 m depth to >5000 m height in the Western Cordillera over only 250 km. This difference represents the most extreme topographical gradient on Earth. At the same time the region is characterized by the driest desert, with an average rainfall at the coast of only 0,5 mm/year. As a result, erosion has been very slow over the past 20 Ma. This offers excellent conditions for the study of the evolution of the landscape and its control by tectonic, gravitational, volcanic, erosional, and sedimentary processes. In this study, we present an account of uplift, erosion, sedimentation, gravitational collapse, and volcanism on the Western Andean Escarpment (WARP, Figs. 1, 2) over the past 30 Ma. Our data and interpretations are based on field mapping, aerial photographs, and satellite imagery, sedimentological studies and Ar-Ar dating.

WARP evolution between 30 and 19 Ma: uplift, erosion and crustal melting

The lower WARP has been the depocentre of coarse-grained alluvial fan an braided river deposits which distally grade into fluvio-lacustrine and salar sediments. The clastic wedge has a volume of c. 10 km^3 per km N-S distance and accumulated from 25 to 20 Ma. Sediment type and ramp geometry suggests rapid uplift, a strong topographic gradient and sufficient water. Clast analysis identifies provenance from the present upper WARP. The average denudation oisf 285 m in 5 Ma. This episode of uplift and erosion ended with the deposition of four extensive ignimbrite sheets which total more than 900 m in thickness (Oxaya Ignimbrites, 22.72 ± 0.15 to 19.38 ± 0.02 Ma, Ar/Ar sanidine and biotite plateau ages). These rhyodacitic ignimbrites can be correltated over 130 km from the Western Cordillera to the Coastal Cordillera. N-S correlation of Oxaya Ignimbrites is possible for > 300 km from southern Peru to the Chilean Camarones Valley at ~20°S). Areal extent and measured thickness suggest a total volume of >3.000 km^3. The occurrence of these ignimbrites marks a major episode of crustal melting preceeded by crustal thickening, uplift, erosion, and sediment deposition.

Oxaya Ignimbrites today form the gently sloping ramp from the upper WARP to the Coastal Cordillera. It is dissected by a fossil drainage system, several deep active valleys and the giant tilted Oxaya Block. Within a narrow zone of minor reverse faulting (Western Andean Thrust Belt of Muñoz and Charrier, 1996), they are strongly folded and faulted. Further to the E they are again flat-lying and form some of the highest peaks of the Western Cordillera at altitudes between 4.300 and 5.200 m.

Alluvial ramps overlain by ignimbrites are also known from regions further south (20° to 21°S). If thick conglomeratic sediments coupled with overlying ignimbrites are taken as a general indicator of crustal thickening, uplift and crustal melting, then these processes have clearly not been synchronous along the strike of the Central Andes.

19 to 12 Ma ; andesite volcanism, block rotation and gravitational collapse

Oxaya ignimbrite volcanism (19.4 to 22.72 Ma) was accompanied and succeeded by large andesitic volcanoes giving Ar-Ar ages of 20.33±0.38, 20.02± 0.3, 18.70±0.80, 15.07±0.12, and 9.18±0.33 (Wörner et al., 1999). These andesite shields occur along a N-S oriented chain from 17°S to 20°, along the N-S extension of the Oxaya Ignimbrites. Simultaneously, a westward-oriented, parallel drainage system eroded into the gently sloping Oxaya surface). These andesite volcanoes provided characteristic detritus to the conglomeratic Diablo Formation on the lower WARP slope.

Continued uplift resulted in regional westward tilting and significant steepening of the Oxaya ramp producing the monoclinal structure known over several hundred km on the Western Andean margin (Allmendinger et al., 1997; Lamb et al., 1997). At 18°S, part of the steepened slope collapsed forming the Oxaya Block. This block is tilted antithetically and bounded in the W by the Ausipar reverse fault which has a displacement of about 1300 m. In the East, the bounding fault is obscured by younger sediments and volcanic rocks (see below), retreating erosion and younger reverse faulting. A total

vertical displacement of about 2000 m is given by the difference in elevation between Oxaya ignimbrites on the rotated block and the Western Cordillera. This maximum estimate needs to be corrected for later reverse faulting by about 200 m. The age of this block rotation must be older than the oldest sediments overlying it (>10.5 Ma). Its upper age limit is given by a lava flow, which is "flowing up slope" and was thus clearly rotated together with the Oxaya Block. The lava flow was dated by Muñoz and Charrier (1996) at 11.4±0.3 (K-Ar whole rock age). AnAr-Ar whole rock age from the nearby Copaquilla (15.07±0.12 Ma) is somewhat older. From these data we conclude that Oxaya block rotation occured after 12 (to 15 Ma) and before 10.5 Ma.
The age for the drainage system and valley incision on the Oxaya Block is clearly older than its rotation. For example, the Cardones Valley is tilted to the East although its morphology still indicates an E to W course. This valley was inactivated in its upper course by the Oxaya block rotation and thus must be older than at least c. 12 Ma !

The rotation of the Oxaya Block had several consequences : (1) the former E-W oriented drainage reversed and the upper course of the valleys became clogged with sediment, (2) extensive structures formed on the block (Fig. 1, 5), (3) a half-graben formed on its eastern side which became filled with alluvial, fluvial and lacustrine sediments (Huaylas Formation, see below). While the overall tectonic regime is compressive and regional tilting, steepening of the Western Altiplano Escarpment caused slope failure and extensional gravitational movements along normal faults. This conclusion contradicts that of Muñoz & Charrier (1996) who explained the tectonic style exclusively by compression and explain uplift by movements along reverse faults, which can be shown to be younger than Oxaya block rotation.

Another important consequence of the rotation and frontal uplift of the Oxaya Block along the Ausipar fault was the oversteepening of its western front. This resulted in a giant landslide. The "Lluta Collapse" is exposed on both sides of the Quebrada Lluta for 20 km to the E of Poconchile. It covers an area of about 600 km^2 and displaced a rock mass of 50 km^3. This mass is characterized by large tilted blocks up to 800 m thick and an irregular surface which in some places rises up to 200 m over the undisturbed ramp of the Oxaya Ignimbrite. The age of the Lluta collapse must be younger than the Oxaya Block rotation (12 Ma) and older than the Lluta Valley which dissects it. As a conservative estimate we can place the timing of the Lluta collapes at an age of 5 to 10 Ma.

12 and 2.7 Ma: continued uplift and increased aridity

Alluviall and fluvial braided stream sediments up > 200 m accumulated at elevations around 3000 m in the halfgraben between the Western Cordillera (upper WARP) and the tilted Oxaya block (Huayllas Formation). The age of this formation is constrained to range from about 10.5 to 2.7 by an intercalated ignimbrite (10.55 ± 0.05, Ar-Ar plateau and isochrone age on biotite), by mammalian fossils (8 to 9

Ma, Salinas et al., 1991) and by the Lauca-Peréz Ignimbrite (2.71±0.01 Ma, Ar-Ar sanidine plateau age) overlying the Huaylas sediments on a low-angle unconformity.

Compressive movements displaced the lower part of these sediments including an ignimbrite dated at 10.5 Ma. Oxaya Ignimbrites and Miocene andesites are thrusted onto Huaylas sediments (Garcia et al. 1996). Miocene sediments on the Chilean Altiplano (Kött et al., 1995) are not affected by tectonism. The westernmost Altiplano has therefore remained tectonically relatively inactive and has not experienced major climatic changes through uplift over the past 6 Ma.

At 2.7 Ma, the Western Andean Escarpment was characterized by a tectonically and morphologically differentiated stair-case topography with small N-S striking basins and ramps filled by fluvial and lacustrine sediments. This landscape was sealed by the 2.7 Ma Lauca-Perez-Ignimbrite. It is found as remnants filling the large valleys (Lluta, Cardones, and possibly Azapa). The Lauca-Pérez Ignimbrite probably entered the Pacific Ocean through the Lluta valley near Arica where it is found in the valley bottom at sea level.

2.7 Ma to Recent : valley incision and collapsing flanks

While the Cardones Valley has been largely inactive since it was filled by the Lauca Ignimbrite the two large Azapa and Lluta valleys gained on headward erosion. In the area of the Oxaya Block these valleys are deeply incised, reaching their maximum depth. In the middle course of Quebrada Lluta, the Lauca Ignimbrite is found some 800 m above their present valley shoulder. This gives a minimum value for incision since 2.7 Ma.

Where valley walls of the lower Lluta and Azapa Valleys are built of Miocene sediments and Oxaya ignimbrite, valley flanks are smooth and inclined at angles of 10° to 20 °. Satellite imagery and field observations show abundant gravitational slides with blocks up to 400 m in thickness and several km in length. Landslides of up to 1 km^3 dammed the rivers causing accumulation of up to several tens of metres of lacustrine sediments upstream (Seyfried et al., 1994).

Plate tectonic interpretation

The Western Escarpment of the Central Andes at 18°S is a good example of an oversteepend mountain range front. The overall tectonic regime is compressive and resulted in continued tectonic thickening, uplift, and erosion (Isacks, 1988). The modern Andean evolution is strongly influenced by (1) Collision of the East Pacific spreading centre with the North American Plate at 29 Ma resulted in Farallon Plate break-up, formation of the Nazca Plate, and increased subduction rates. (2) Opening of the Drake Passage at c. 23 Ma established the cold S-N Humboldt Current causing reduced precipitation inland. At the same time the slab flattened, shutting off arc magmatism and caused increased plate coupling and compressive crustal thickening. When the slab fell off and steepened again, widespread basaltic volcanism occured at 23 Ma in Bolivia (Tambillo basalts, Lamb et al., 1997) while uplift, erosion and enhanced sedimentation is observed at the Western Altiplano

Escarpment. After a period of thermal relaxation combined with mafic magmas intruding the base of the crust, crustal melting resulted in widespread ignimbrites at 22 to 19 Ma, immediately followed by mafic andesite volcanism. Increased aridifiaction from about 15 Ma onwards resulted in decreased erosion, morphological oversteepening and gravitational collapse at all scales: Oxaya Block, Lluta Collapse, valley-flank landslides, and local sagging. Reverse faulting of the Western Cordillera onto 11 to 3 Ma old sediments is limited to a few hundred metres at most. Therefore, further uplift since about 6 Ma would have to be by regional tilt of the Western Andean Escarpment and Oxaya ramp and en-block vertical movements of the Altiplano. Such movements can only be explained by simple shear shortening below the Altiplano and lower crustal flow from E to W (Allmendinger & Gubbels 1996).

REFERENCES

Allmendinger, R. W. & Gubbels, T., 1996, Pure and simple shear plateau uplift, Altiplano-Puna, Argentina and Bolivia. Tectonophysics, v. 259, p. 1-13

Allmendinger, R. W., Jordan, T. E., Kay, S. M., and Isacks, B. L., 1997, The Evolution of the Altiplano-Puna Plateau of the Central Andes: Annu. Rev. Earth Planet. Sci. v. 27, p. 139-174

Garica, M., Herail, G., Charrier, R., 1996, The Cenozoic forcarc evolution in Northern Chile: The western border of the Altiplano of Belén (Chile),- 3rd ISAG, Sept. 1996, St. Malo, Frankreich, Andean Geodynamics, ORSTOM Editions, Collection Colloques er Seminaires : p. 359-362.

Isacks, B.L., 1988, Uplift of the Central Andean Plateau and Bending of the Bolivian Orocline: Journal of Geophysical Research, v. 93, p. 3211-3231.

Kött, A., Gaupp, R., and Wörner, G., 1995, Miocene to Recent history of the Western Altiplano in northern Chile revealed by lacustrine sediments of the Lauca Basin (18°15° . 18°40'S/69°30'-69°05'W): Geol Rundsch, v. 84, p. 770-780

Lamb, S., Hoke, L., Kennan, L., Dewey J., 1997, Cenozoic evolution of the Central Andes in Bolivia and northern Chile. In: Orogeny through time, Burg, J.P., Ford, M. (eds.),

Muñoz, N., Charrier, R., 1996, Uplift of the western border of the Altiplano on a west-vergent thrust system, northern Chile: J South American Earth Sci, v. 9, p. 171-181

Salas, R., Kast, R.F., Montecinos, F. and Salas, I., 1966, Geologia y recursos minerales del departamento de Arica.: Inst. Investigac. Geol. Santiago, Bol., v. 21, p. 1-114.

Salinas, P., Villarroel, C., Marshall, L., Sepulveda P. and Muñoz, N., 1991, Typotheriopsis sp. (Notoungulata, Mesotheriidae), Mamifero del Mioceno superior en las Cercanias de Belen, Arica, norte de Chile: Congreso Geologico Chileno 1991. Resumenes Expandidos, Servicio Nacional de Geologia y Mineria Chile, v. p. 314-317.

Seyfried, H., Wörner, G., Uhlig, D. & Kohler, I., 1994, Eine kleine Landschaftsgeschichte der Anden in Nordchile. Wechselwirkungen (Jahrbuch der Universität Stuttgart für das Jahr 1994): 60-72.

Wörner et al. (1999) K-Ar and Ar-Ar ages of igneous rocks of northern Chile and the igneous and tectonic evolution of the Central Andes: Rev. Geol. Soc. Chile (in prep)

THE ROLE OF THE JUAN FERNANDEZ RIDGE IN THE LONG LIVED ANDEAN SEGMENTATION AT 33.5° S

Gonzalo YAÑEZ (1) and Cesar RANERO (2)

(1) Geodatos S.A.I.C., Roman Díaz 773, Santiago-Chile, gyanez@geodatos.cl
(2) GEOMAR, Christian-Albrechts-Universität zu Kiel, 24148 Kiel, Germany, cranero@geomar.de

KEYWORDS: tectonics, hot spot, seamount, magnetism, euler poles, flat slab

INTRODUCTION

The first order influence of subduction over continental geology and tectonism in the western margin of South America has been established from different lines of reasoning (i.e. Barazangi and Isacks, 1976; Jordan et al., 1983; Pardo-Casas & Molnar, 1987). Major features of the present Andean segmentation are associated with the angle of subduction. Active volcanism and broader topography are related with "dip" slab segments (~ 30°), whereas no volcanism and high deformation rates are associated with segments of "flat" slab (~10°). The origin of the flat slab geometry has been a matter of debate. The geographical correspondence between the Nazca and Juan Fernadez ridges with the flat slab segments of the Andes have been used by Pilger (1981), Nur & Bem-Avraham (1981), among others, to argue in favor of a causative relationship. According to their model, the buoyancy of the corresponding subducted ridges would cause the flat slab geometry. In contrast, Cahill & Isacks (1992) consider that the flat slab geometry is related to the curvature of the margin, and thus pointing to a continental plate rather than oceanic plate control.

Tectonic erosion and accretion of the margin have been documented by von Huene & Scholl (1991), establishing the role played by the subduction processes on each mechanism. The amount of sediments available at the trench seems to control the growth (fill trench) or destruction (empty trench) of the

margin. Evidences from tectonic erosion of the margin back in time have been documented to the north of 33.5° S (i.e. Mpodozis and Ramos, 1989, Stern and Mpodozis, 1991) with a consistent eastward magmatic arc migration since Meso-Cenozoic times. South of 33.5° S the margin has been preserved almost stationary, with a delicate balance between accretion and erosion (i.e. Mpodozis and Ramos, 1989). The common explanation for this bipolar behavior is attributed to climatic constraints, low rates of sediment supply in the (arid) northern flank in contrast to the pervasive erosion of the (humid) southern flank. However present climatic constraint cannot be extrapolated back in time to explain a rather continuous process that involves the entire Andean Cycle.

The origin of the flat slab geometry and the controlling mechanisms for the tectonic erosion of the margin are analyzed from the perspective of the Cenozoic indentation of the Juan Fernandez Ridge against the South American plate. We constrained the timing of the magmatism along the Juan Fernandez Ridge considering the magnetic data set acquired during the Condor Project (von Huene et al., 1997), in conjunction with an age of 8.5 +/- 0.4 Ma for the O'Higgins Guyot that belongs to the same chain (von Huene et al., 1997). In Figure 1 we present the age of the Nazca plate derived from 2-D and 3-D magnetic modeling (Yáñez et al., 1999). With this timing and the absolute plate motions during the Cenozoic (Gordon & Jurdy, 1986) we developed a precise path for the hot spot chain (for further details see in Yañez et al., 1999). In Figure 2 we show the theoretical path of the hot spot chain during the Upper Cenozoic, assuming a continuous magmatic activity. The most noticeable feature of the indentation against the continent is the rapid southward migration of the ridge-trench collision prior to 10 Ma. This oblique interaction is basically the result of the northeast absolute motion of the Nazca plate during the Eocene. In Figure 3 we superimposed the predicted path of the hot spot chain at present with the geometry of the subducting slab and the seismicity clusters. The figure shows the clear association between some of the most well defined intermediate and deep seismic clusters and the predicted location of the hot spot chain, further supporting the conception of a long lived magmatic activity over the Juan Fernandez Hot Spot.

DISCUSSION AND CONCLUSIONS

During the Lower Miocene a rapid southward migration of the indentation place have been taking place at a rate of ~200 km/Ma. If this configuration really took place, the effect on the margin was probably quite severe, in particular to the north of 33° S, where tectonic erosion has been permanent at least during the Cenozoic. The subduction of a nearly parallel aseismic ridge between 24 and 12 Ma roughly coincides in time with the geological evidences of a volcanism produced by an atenued athenospheric wedge in the northern flank (~26-28 ° S, Kay et al., 1991). Under this geometry, the entire subducting slab lithosphere probably underwent a thermal resetting, favoring a more buoyant behavior. The southward and eastward migration of the subducted ridge would further extend the flat slab segment, reaching a steady state

regime after 12-10 Ma. The contrasting shape of the flat slab segment (Figure 3), from a gentle bending in the northern flank (~27°-28° S) to a sharper flexure in the southern tip (~33.5°S), suggest a direct link with the southward migration of the buoyant force.

The tectonic boundary at 33.5° S is not just a present feature but rather a major tectonic boundary during the whole Andean Cycle (i.e. Mpodozis & Ramos, 1989). The long lived activity of the Juan Fernandez Hot Spot in connection with a minor north south displacement of the South American plate during the Meso-Cenozoic (i.e. Scotese & Sager, 1988), suggest a permanent modulation over this major tectonic boundary at 33.5° S.

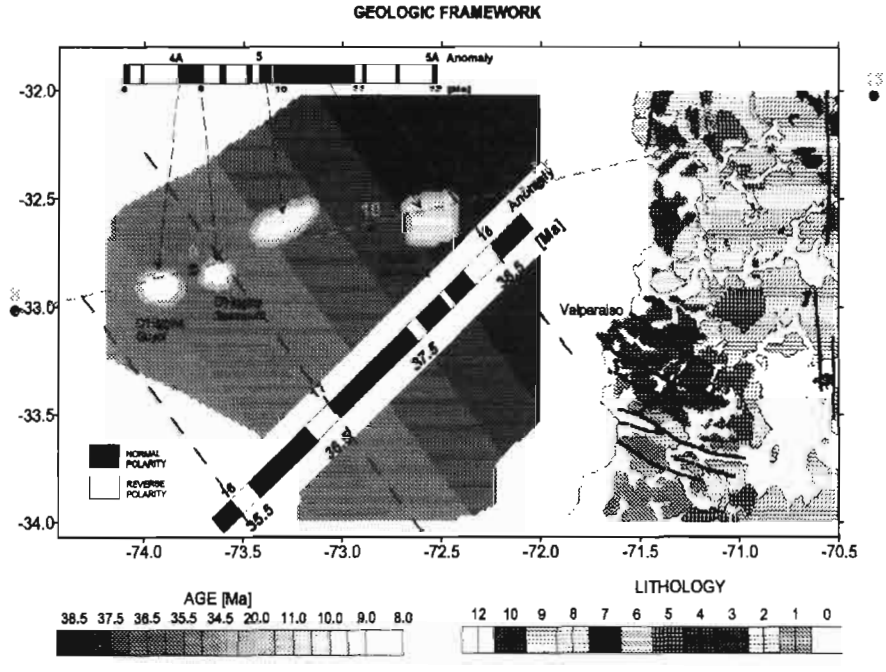

Figure 1: Geological, estructural, and geophysical compilation in the study area. In the ocean information is focoused in the magnetic results. In the continent the regional geology have been compiled from: Gana et al., 1994; Rivano and Sepulveda, 1991. Main geological units are: (1)Permo-Carboniferous granitoids; (2) Paleozoic-Jurassic orthogneisses and paragneisses;(3)Jurassic anfibolites and gneisses; (4)Jurassic granitoids; (5)Lower Cretaceous granitoids; (6)Upper Cretaceous-Miocene granitoids; (7)Triassic sedimentary deposits; (8)Jurassic volcanic sequence; (9)Neocomian volcano-sedimentary deposits; (10)Miocene volcanism; (11)Upper Tertiary sedimentary deposits; (12)Quaternary; (13)Magnetic Lineations; (14)Faults and structural lineations.

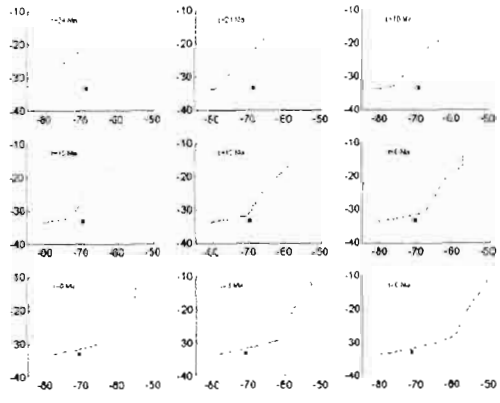

← Figure 2: Predicted path for the Juan Fernadez hotspot chain since Miocene times. The location of the hotspot is indicated by a fill triangle. The margin of South America (light continuous line) moves westward while the hotspot location remains stationary. Location of Valparaiso (filled square) is shown as a reference. Absolute plate motions from poles of rotations from Gordon & Jurdy (1986).

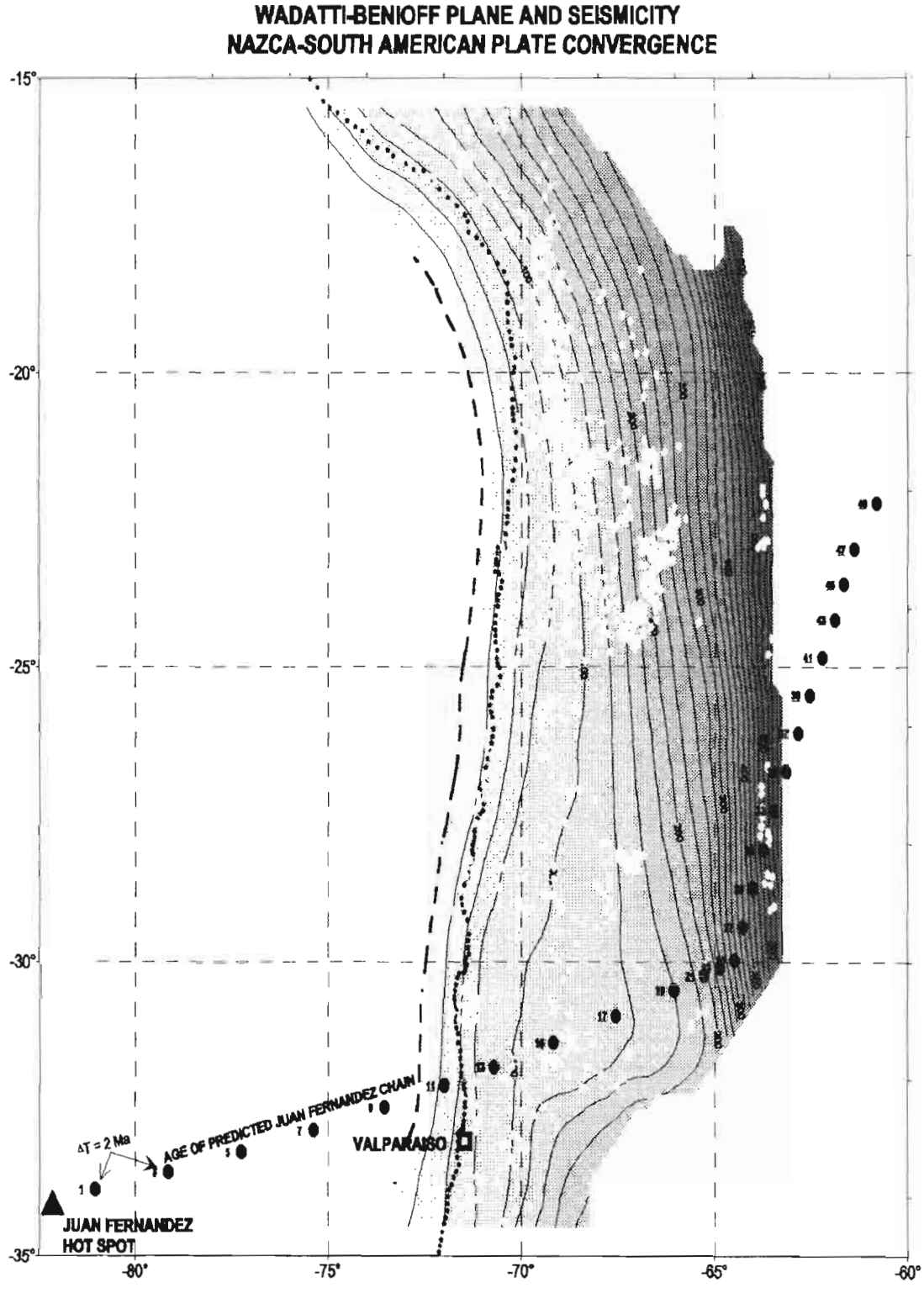

Figure 3: Predicted path of the Juan Fernadez hotspot chain at present. Numbers along the path represent the age of the predicted volcanic events [Ma]. White dots are the observed seismicity (from Kirby et al., 1998). The contour lines show the depth to the Wadatti-Benioff plane (from Cahill & Isacks (1992), and Kirby et al. (1998)).

ACKNOWLEDGMENTS

This paper has been partialy supported by a DAAD scholarsip granted to one of the authors (G.Y.).

REFERENCES

Barazagni M. and B.L. Isacks, 1976. Spatial distribution of earthquakes and subduction of the Nazca plate beneath South America: Geology, v. 4, 686-692.

Cahill T. and B.L. Isacks, 1992. Seismicity and shape of the subducted Nazca plate. *J. Geophys. Res.*, 97, B12, 17503-17529.

Gana P., Yañez G.A., Wall R.,1994. Evolución geotectónica de la Cordillera de la Costa del Chile Central (33-34 °S): Control Geológico y Geofísico. *Actas VII Congreso Geológico Chileno*, Concepción.

Gordon R.G. and D.M. Jurdy, 1986. Cenozoic global plate motions. *J. Geophys. Res.*, 91, 12389-12406.

Jordan, T.E., B. Isacks, R. Allmendinger, J. Brewer, V.A. Ramos, C. Ando. 1983. Andean tectonics related to the geometrye of subducted plates: *Geological Society of America Bulletin*, v. 94, p. 341-361.

Kay S.M., C. Mpodozis, V.A. Ramos, and F. Munizaga, 1991. Magma source variations for mid-late Tertiary magmatic rocks associated with a shallowing subduction zone and the thickening crust in the central Andes (28-33° S). Spec. Pap. Geol. Soc. Am., 265, 113-137.

Kirby S., E.R. S. Stein, E. A. Okal, D. C. Rubie, 1996. Metastable mantle phase transformations and deep earthquakes in subducting oceanic lithosphere, Reviews of Geophysics, 34, 2, 261-306.

Mpodozis, C. & Ramos, V., 1989. The Andes of Chile and Argentina, in *Geology of the Andes and its Relations to Hydrocarbon and Mineral Resources*. Ericksen G.E., Cañas Pinochet, M.T. and Reinemund J.A., Editors, Houston, Texas, Circum - Pacific Council for Energy and Mineral Resources Earth Science Series, Vol.11.

Nur A. and Z. Ben-Avraham, 1981. Volcanic gaps and the consumption of aseismic ridges in South America, Mem. Geol. Soc. Am., 154, 729-740.

Pardo-Casas F. and P. Molnar, 1987. Relative motion of the Nazca (Farallon) and South American plates since Late Cretaceous time, Tectonics, vol 6, N° 3, 233-248.

Pilger R.H., 1981, Plate reconstructions, aseismic ridges, and low angle subduction beneath the Andes, Bull. Geol. Soc. Am., 92, 448-456.

Rivano S. and P. Sepúlveda, 1991, Hoja Illapel, Region de Coquimbo, Carta Geológica de Chile, N° 69, 1:250,000, Servivio Nacional de Geología y Mineria.

Stern C.R. and C. Mpodozis, Geologic evidence for subduction erosion along the west coast of central and northern Chile, 1991. *Actas VI Congreso Geológico Chileno*, V. 1, 205-207.

Scotese, C.R., and W.W. Sager, 1988, Mesozoic and Cenozoic Plate Tectonic Reconstructions. Tectonophysics, 155: 27-48.

Von Huene R., J. Corvalan, E.R. Flueh, K. Hinz, J. Korstgard, C.R. Ranero, W. Weinrebe, and the Condor Scientists, 1997, Tectonic control of the Juan Fernandez Ridge on the Andean margin near Valparaiso, Chile, Tectonics, v. 16, N°3, 474-488.

Von Huene R., D.W. Scholl, 1991, Observations at convergent margins concerning sediment subduction, subduction erosion, and the growth of continental crust, 1991, Reviews of Geophysics, 29, 3, 279-316.

Yáñez G., C. Ranero, R. von Huene, J. Díaz, 1999, A tectonic interpretation of magnetic anomalies across a segment of the convergent margin of the Southern Central Andes (32°-34° S), (submitted JGR)

GUAGUA PICHINCHA: MANAGING THE CRISIS

Hugo A. YEPES(1)

(1) Instituto Geofisico, P.O.Box 17-01-2759, Quito, ECUADOR, geofisico@accessinter.net

KEY WORDS: volcanic unrest, crisis, preparation

INTRODUCTION

Guagua Pichincha volcano is located 12 km west of Quito, the capital of Ecuador. It is one of seven historically active volcanoes in Ecuador. The last eruption of Guagua Pichincha occurred in 1660, when it had an eruptive episode which lasted around one month. The plinean eruption deposited few centimeters of ash in Quito. Earlier eruptions occurred in 1560, 1575, and 1582. The geological record shows that the volcano has an recurrence period of approximately 500 years. The most significant eruption of the volcano during the last several thousand years was in 970 AD, when 20 cm of ash was deposited in the environs of the volcano.

No explosive activity has been reported during the last 330 years. In 1981, unrest period began with the formation of a phreatic explosion crater in the dome northern lobe inside the volcanic caldera. Since then there have been periodic explosions during the rainy seasons, caused by the intrusion of water into the phreatic system. A swarm of volcano-tectonic earthquakes occurred in 1988. This was the first clear symptom of anomalous earthquake activity since 1981, when the first seismic monitoring equipment was installed in the area. Just prior to the 1988 swarm, the Geophysical Institute began the installation of a seismic/deformation monitoring network.. In July/August of 1998 the commencement of seismic and explosive activity at levels superseding those seen since the installation of the monitoring network was detected, unrest that has continued for eight months. This increased activity by the Guagua Pichincha volcano precipitated the declaration of a yellow alert by the city of Quito on 1 October 1998. The following is a synopsis of efforts to prepare for a potential eruption.

TECHNICAL RESPONSE

The declaration of a yellow alert spurred several organizational and educational efforts by the Escuela Politecnica Nacional (EPN) and the city government to manage the crisis. Among the actions taken by the EPN's Geophysical Institute and Hydraulics Department were:

- Improvement of the monitoring capability around the volcano, in cooperation with the USGS, ORSTOM and the University of Montreal;
- Updating of the volcanic hazard map previously prepared in 1988;
- Preparation of detailed rain triggered mud flows hazard map showing at risk areas inside the city
- Development of theoretical and physical models to simulate triggering of mud flows by the rain;
- Institution of a 24 hour a day manning schedule;
- Issuance of daily bulletins of the volcano's activity;
- Development of a comprehensive web site;
- Establishment and refinement of the alert system
- Compilation of a call-down list to notify appropriate officials of significant events;
- Initiation of weekly meetings with local crisis management officials;
- Working with government agencies in preparatory efforts; i.e., determining likely affected areas, providing guidance to civil aviation.
- Conducting educational campaigns, including briefings to government entities, civic organizations, business groups, schools, etc.;
- Production of educational materials as one 14 minutes video, flyers, posters, etc.;
- Coordination of visits and cooperation with scientists from several other countries;
- Maintenance of an official record/log.

CITY'S RESPONSE

The initial step for the government in dealing with the crisis was the designation of the mayor of Quito as the overall response coordinator. The city's first efforts can be divided into three areas: preparation, contingency planning, and educational efforts.

Preparation

- Establishment of an operations/information center CES;
- Determine populated areas at risk;
- Identify public sectors likely to be affected and perform minor preventive work (i.e., water supply, power grid, telecommunications, aviation, transit, etc.);
- Clear debris from flow areas and potential evacuation routes.

Contingency planning

- Planning for evacuation drills and testing of call down lists
- Meeting frequently with representatives of the Geophysical Institute, Civil Defense, National Police, Ministry of Health, Defense, Agriculture, Red Cross, and others
- Solicitation of needed items from foreign governments and NGOs (ex. Heavy equipment, medical supplies, non-perishable food items, etc.)
- Develop plans to minimize impact to water supply, power grid, telecommunications, etc.
- Plan for ash removal, police deployment, evacuation of aircraft, ingress/egress of city, procurement of critical items such as food and fuel

Educational efforts

- Issuance of a daily bulletin similar to that issued by the Geophysical Institute;
- Holding press conference s upon declaration of a yellow alert and later;
- Conducting information sessions for various groups, including civil defense personnel, foreign embassies, business groups, inhabitants of potentially seriously affected areas, etc.
- Releasing information on dealing with a volcanic eruption to the media;
- Contracting NGOs to educate local neighborhoods locate at risk areas.

After the first few weeks of somehow isolated efforts, the city government focused its action on its own response capabilities by using the lifelines city companies such as the water, electricity, transportation, public works companies as well as the city government organization. During weekly meetings evolution of the volcano activity has been evaluated, actions programmed and follow ups done in order to accomplish a better institutional preparedness.

Any crisis has its difficulties. Some problems are unavoidable, while some could be mitigated by adequate communication or funding and others are preventable. Among the difficulties encountered during the current exercise were:

- Inability to control rumors
- Inability to separate political issues from scientific facts
- Inability to maintain adequate public concern over the long term
- Discrepancies in alert systems used by the Geophysical Institute and the city

Some problems were peculiar to the city:

- Initial release of information concerning the volcanic activity was not well managed

- Slow development of contingency/evacuation plans. Slowness in identifying potential safehavens
- No public explanation of alarm system to be used in the event of an orange or red alert
- Reluctance to release all available information on potentially affected areas. The city must necessarily weigh the public's right to know against the possibility of causing undo panic. Information released to the general public has been too general to be useful
- Ill-defined role of the operations center
- Inadequacies encountered in testing of the city's call-down list (several individuals were unreachable)
- Failure to adequately ensure that all government entities are making necessary preparations

The following inadequacies were specific to the technical area:

- Lack of sufficient and modern monitoring equipment
- Over-reliance on a non-redundant computer monitoring system
- Lack of on-site computer expertise and modern hardware
- No formal mechanism for coordinating press activities
- Burnout and inadequate compensation of limited staff
- No access to enough helicopter time, no access to satellite imagery
- No budget for long term operation and maintenance of the monitoring equipment

CONCLUSIONS

Both, the city government and population were not ready to receive a yellow alert declaration due to its close neighbor's unrest: Guagua Pichincha volcano. After the first few days of hectic reaction, when the alert level was misinterpreted as a sure eruption, part of the population related the issue with some political maneuver to distract people's attention from tough economic decisions taken to cope with Ecuador's most serious economic crisis in 50 years. It was clear that there was no preparedness at any level and awareness was very low among Quito's authorities and inhabitants. The permanent attention and work given by the EPN and the Municipality, as well as the interest shown by the media, permitted to increase awareness and to provoke official, institutional and private efforts to start preparing emergency plans. The city is better prepared now to respond to an eruption, but there is still a very long way to go. The newly created city's office for emergency management is the answer to that.

CHARACTERIZATION OF THE ALTIPLANO-PUNA MAGMA BODY CENTRAL ANDES, SOUTH AMERICA

George ZANDT(1), Josef CHMIELOWSKI(1), Christian HABERLAND(2), Xiaohui YUAN(3), Rainer KIND(3)

(1) Southern Arizona Seismic Observatory and Department of Geosciences
University of Arizona, Tucson AZ, 85721, USA, zandt@geo.arizona.edu
(2) Freie Universitaet Berlin, Fachrichtung Geophysik, Berlin, Germany
(3) GeoForschungsZentrum, Potsdam, Germany

KEY WORDS: Altiplano, Puna, magma body, receiver functions

INTRODUCTION

Since the late Miocene an ignimbrite "flare-up" has produced a major silicic volcanic province, the Altiplano-Puna Volcanic Complex (APVC) in the central Andes of South America. The APVC covers some 50,000 km^2 between 21° and 24°S and constitutes the largest ignimbrite concentration in the Central Volcanic Zone of the Andes, and one of the largest in the world [de Silva, 1989]. The APVC is located at the southward transition between the ~4 km high plateau of the Altiplano and the ~5 km high Puna, a change that may be associated with a rapid southward thinning of the South American lithosphere. Studies of the voluminous ignimbrites by de Silva [1989] and others suggest the flare-up is due primarily to crustal melting in response to tectonic crustal thickening associated with the building of the central Andes, with a lesser contribution from subduction related melts. The region has been the site of large-scale silicic magmatism since 10 Ma with several major caldera-forming eruptions [de Silva, 1989; Kay et al., 1998]. The youngest major ignimbrite in the APVC is a 1 Ma old eruption from the Purico center [de Silva, pers. comm., 1998]. Late Pleistocene to Recent volcanic activity in the form of large silicic lava flows and domes and two major geothermal fields indicate that the province remains magmatically active.

CONCLUSIONS

From October, 1996 to September, 1997 we operated 7 PASSCAL broadband seismic stations in the Bolivian portion of the APVC to record teleseismic earthquakes and local Benioff zone events in the underlying subducting Nazca plate. One station was located near Uyuni and reoccupies the southernmost site of the 1994-1995 BANJO/SEDA deployment to provide a tie-point with the previous data set. The remaining 6 stations were deployed over the APVC covering an area approximately 150 km by 75 km. We used the method of teleseismic receiver functions as described in Owens et al. (1985) to probe the crust for sub-horizontal magmatic structures. The receiver functions for all of the APVC stations display a large amplitude, negative polarity arrival at ~2 seconds after the direct P that we identify as a P-to-S conversion from the top of a pronounced low–velocity layer at ~19 km depth. A smaller amplitude, opposite polarity Ps is not as consistent but is observed on most of the receiver functions between 4-5s after the direct P and is interpreted as the conversion from the bottom of the low-velocity layer. The consistency of this Ps phase for all azimuths and all APVC stations (combined with its absence at stations outside the APVC) strongly support the interpretation of a regionally pervasive low–velocity layer associated with the APVC.

We tested numerous low-velocity models with varying layers, thickness, velocities, and depths, and found the Vs must be close to zero (Vs<0.5 km/s, independent of Vp) in the low-velocity layer to match the amplitude of the observed ~2s arrival for the Laguna Colorado station. The modeling indicates that the depth to the top of the low-velocity layer is ~19 km. The second ~5s positive polarity is a Ps from the bottom of the low–velocity layer and its timing constrains the thickness of the layer. If the low-velocity layer Vp is 3.0 km/s, then the thickness of the layer is ~810 m, while a Vp=5.0 km/s yields a 750 m thick layer. Because of the thinness of the layer we have confirmed the forward modeling with full reflectivity methods. Modeling further confirms that the smaller amplitude of the bottom Ps is due to S-to-P conversion at the top interface, and that the relative amplitudes of the two Ps phases are consistent with a simple one layer low-velocity zone. We interpreted the low-velocity layer as a regional sill-like magma body associated with the Altiplano-Puna Volcanic Complex and named it the Altiplano-Puna magma body (APMB) [Chmielowski et al., 1999].

The 1996-1997 APVC deployment was largely confined to the northeast portion of the Altiplano-Puna volcanic complex. We were able to greatly extend our analysis to include most of the APVC using data from the SFB-267 project (Deformazion in den Anden). This large-scale project consisted of numerous short period instruments deployed in three separate, overlapping experiments: the 1996-1997 ANCORP experiment covered the western portion of the APVC along the Chilean/Bolivian border; the 1994 PISCO experiment covered the area just southwest of the junction of Chile, Bolivia and Argentina; and the 1997 PUNA experiment covered the southeastern portion of the APVC in northwestern Argentina (Fig. 1).

The APMB was considered present beneath a station if the amplitude of the first negative Ps conversion in its receiver function was >50% of the amplitude of the direct P-wave and if this conversion arrived between 1.5 and 3.0 seconds after the P-wave. If the Ps conversion was between 30-50%, the presence of the APMB was considered ambiguous. Finally, if the amplitude of the Ps conversion was <30% of the direct

P-wave, or if its timing was not between 1.5 and 3.0 seconds, we considered the APMB absent beneath the station. The combined data clearly delineates the western and southern boundaries of the regional low-velocity layer from 20°S to 24°S (Fig. 1). Despite some complexities in the lateral boundaries and some inconsistencies in results from different teleseismic events and deployments, general trends in the APMB boundaries are readily apparent. To first order, the APMB appears to correlation with the 10-3 Ma ignimbrite volcanic centers [Kay et al., 1998] and not with the Quaternary arc volcanoes. The depth to the top of the APMB is consistent with a rheological control on the emplacement of this sill-like body that separates a brittle upper crust and a more ductile lower crust. Based on its approximate areal extent and thickness, the regional low-velocity layer has a minimum volume of ~60,000 km^3. The strong nonlinearity of the relationship between seismic velocity and the percentage of melt in a rock makes it difficult to estimate the amount of melt. Using existing experimental and theoretical relationships [e.g., Makovsky and Klemperer, 1999], our extremely low Vs estimates requires more than 15% melt. Even such a minimum percentage leads to an estimate of 9000 km^3 of melt, although it could be substantially greater. We speculate that this magma body is a storage/accumulation level for silicic melt between a lower crustal/upper mantle magma generation zone and shallower caldera-forming plutons.

REFERENCES

Chmielowski, J., G. Zandt, and C. Haberland, The Central Andean Altiplano-Puna magma body, *Geophys. Res. Lett.*, *26*, 783-786, 1999.

de Silva, S. L., Atliplano-Puna volcanic complex of the central Andes, *Geology*, 17, 1102-1106, 1989.

Kay, S. M., C. Mpodozis, and B. Coira, Neogene magmatism, tectonism, and mineral deposits of the central Andes (22°S to 33°S), in Geology and Mineral Deposits of the Central Andes (B. Skinner, Ed.), Soc. Econ. Geol. Spec. Pub. 7, in press, 1998.

Makovsky, Y., and S. L. Klemperer, Measuring the seismic properties of Tibetan bright spots: evidence for free aqueous fluids in the Tibetan middle crust, *J. Geophys. Res.*, in press, 1999.

Owens, T. J., Zandt, G., and S. R. Taylor, Seismic evidence for an ancient rift beneath the Cumberland Plateau, Tennessee: A detailed analysis of broadband teleseismic P waveforms, *J. Geophys. Res.*, 89, 7783-7795, 1984.

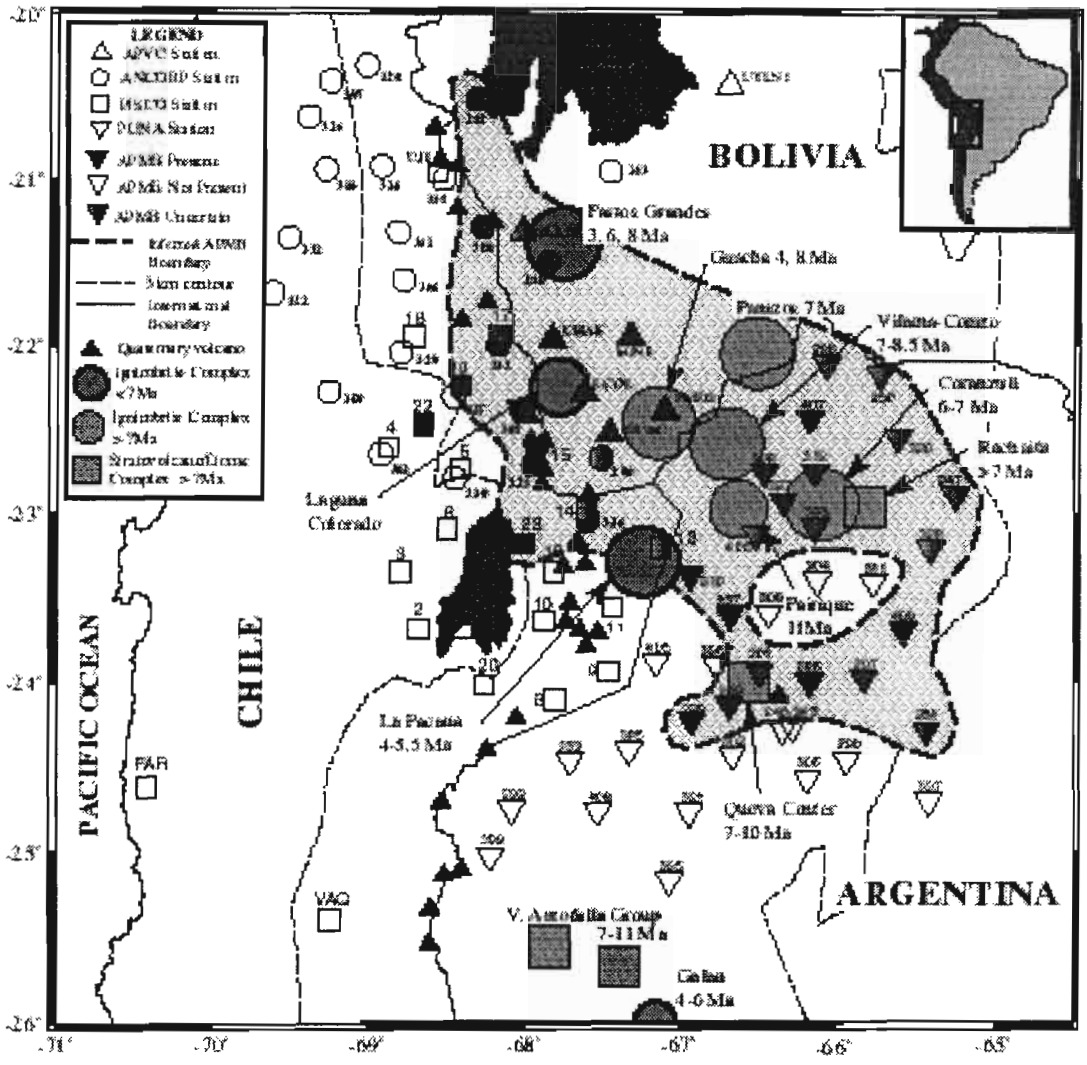

Figure 1: Map of the Central Andean Altiplano-Puna magma body (APMB). APVC results are based on 14 teleseismic events. The SFB-267 results are based on specific high quality events: ANCORP results are based on the 01/11/97, 12/10/96 and 12/09/96 events; PISCO results are from the 02/12/97 and 03/14/97 events; and PUNA results are from the 09/02/97 and 11/09/97 events. Note the close correlation of the magma body with 12-3 Ma magmatic centers [Kay et al., 1998].

LOWER ORDOVICIAN GRAPTOLITES PROPOSE A NEW STRATIGRAPHIC SUBDIVISION FOR THE SOUTHERN PUNA (NW ARGENTINA): FIRST FINDS OF *ARNEOGRAPTUS MURRAYI* AND *CLONOGRAPTUS SP.* IN THE PUNA

U. ZIMMERMANN (1), M.C. MOYA (2) & H. BAHLBURG (3)

(1)Geol.-Pal.-Institut, INF 234, D-69120 Heidelberg, Alemania
(2)UNSA-CONICET-Fac. de Cienc. Nat.-Buenos Aires 177-4400 Salta, Argentina
(3) Geol.-Pal.-Institut, Correnssstr.24, D-48149 Münster, Alemania

INTRODUCTION

New finds of graptolites, brachiopods and phyllocariids in Ordovician deposits in the Southern Puna (NW Argentina) give new stratigraphic evidence for the subdivision of the lower Ordovician sedimentary successions. Sampled outcrops are in the south (outcrop 1) and in the SE of the Salar de Pocitos (outcrop 2) as well as in the central part of the Sierra Calalaste (outcrop 3). Previous studies referring to the paleontological record of the Ordovician strata in the Southern Puna by Aceñolaza & Toselli (1971) and Aceñolaza et al. (1975 & 1976) suggested a stratigraphic age of the sampled graptolites ranging from the upper Arenig to the (?)Caradoc. Farther in the north, near Salar de Rincón, trilobites found by Moya et al. (1993) indicate a Lower Tremadoc age of these rocks. Near Catua Aceñolaza & Durand (1975) described graptolites of Arenigian to Llanvirnian age. In the investigated localities of the Southern Puna the Lower Ordovician clastic sedimentary rocks represent a transition from a stable siliciclastic platform to an active continental margin and a continental arc signature and were deposited in a back-arc basin on stretched continental crust behind a westerly volcanic arc associated with intrusive and volcanic rocks.

In outcrop 1 and close to a discordant contact to a large mafic to ultamafic body we found a volcanoclastic formation overlying quartz arenites which yielded *Araneograptus murrayi*, *Clonograptus* sp. and *Caryocaris* sp. Because of significant deformation the latter two could not be determined more exactly. However, *Araneograptus murrayi* dates the volcanoclatic succession close to the Tremadoc-Arenig boundary. Associations of *Caryocaris* sp. with graptolites are very common. Outcrop 2 contains deformed specimens of *Phyllograptus* sp. However, the fossils place the siliciclastic turbidites of outcrop

2 in the Arenig. In outcrop 3 we sampled *Phyllograptus* sp. and still undetermined orthides. The latter are poorly preserved and were collected from deformed volcanoclastic conglomerates. This graptolite fauna assigns the volcanoclastic rocks and the siliciclastic turbidites to the same time interval recorded in outcrop 2.

Based upon this first find of Lower Ordovician graptolites in the Southern Puna a new stratigraphic subdivision may be proposed. The first member of the sedimentary succession south of the Salar de Pocitos (outcrop 1) is represented by a quarz arenite formation of Tremadoc age, its basis is not defined. This unit is overlain by volcanoclastic sedimentary rocks near the Tremadoc-Arenig boundary, a peak of volcanic activity in the Arenig may be recorded in the Sierra de Calalaste. The occurrence of *Phyllograptus* sp. both in the siliciclastic turbidites at Salar de Pocitos and in the volcaniclastic rocks at Sierra de Calaste make two interpretations possible: the sedimentary rocks of Salar de Pocitos outcrop 2 are slightly younger (probably of Upper Arenigian time) than the volcanoclastic formation of outcrop 3. This may be inferred from a decrease in recorded volcanism in the Upper Arenigian, which is stated for the northern Puna (Monteros et al. 1996), as the provenance of these turbidites changed to more siliciclastic compositions. Alternatively, the siliciclastic turbidites now located east of the volcanic zone have a distinct provenance and were probably derived from metamorphic sources now exposed in the Cordillera Oriental.

REFERENCES

Aceñolaza, F.G. & Toselli, A.J. (1971): Hallazgo de graptolites Ordovicicos en el supuesto Precambrico de la Puna de Catamarca y de Salta, Republica Argentina; Revista Asociación Geológica Argentina, XXVI (1-3), p 274

Aceñolaza, F.G. & Durand, F.R. (1975): Contribución al conocimiento bioestratigrafico del Ordovicico Puneño; Actas I Congreso Paleontología y Bioestratratigrafía, Vol. I: 77-89

Aceñolaza, F.G., Toselli, A.J. & Durand, F.R. (1975): Estratigrafía y paleontología de la región de Hombre Muerto, Provincia de Catamarca, Argentina; Actas I Congreso Paleontología y Bioestratratigrafía, Vol. I: 109-123

Aceñolaza, F.G., Toselli, A.J. & Gonzalez, O. (1976): Geología de la región comprendida entre el Salar del Hombre Muerto y Antofagasta de la Sierra, Provincia de Catamarca; Revista Asociación Geológica Argentina; XXXI (2): 127-136

Moya, M.C., Malanca, S., Hongn, F.D. & Bahlburg, H. (1993): El Tremadoc temprano en la Puna Occidental Argentina; XII Congr. Geol. Arg. y II Congr. de Expl. de Hidrocarb., Actas I, II: 20-30

Monteros, J.A., Moya, M.C., Monaldi, C.R. (1996): Graptofaunas arenigianas en el borde occidental de la Puna Argentina. Implicaciones paleográficas; XII Congreso Geologia de Bolivia, Actas II: 733.746

THE EVOLUTION OF THE ORDOVICIAN SOUTHERN PUNA RETRO-ARC BASIN (NW ARGENTINA): PROVENANCE ANALYSIS AND PALEOTECTONIC SETTING

U. ZIMMERMANN(1) & H. BAHLBURG(2)

(1)Geologisch-Palaeontologisches Institut, INF 234, 69221 Heidelberg, Germany;
uzimmerm@ix.urz.uni-heidelberg.de
(2)Geologisch-Palaeontologisches Institut, Corrensstr. 24, 48149 Münster, Germany;
bahlbur@uni-muenster.de

INTRODUCTION

Data concerning provenance and depositional area of Lower Ordovician sedimentary rocks in the Southern Puna was obtained by sediment petrographical and geochemical analyses. These rocks are associated with mafic and ultra-mafic magmatic rocks and intermediate lava flows. This association have been interpreted as an ophiolite sequence which formed during the amalgamation of the Puna Terrane and Gondwana iniciated by the collision of the exotic Arequipa-Antofalla Terrane in Upper Ordovician times. In the Southern Puna crop out Tremadocian quartz-rich turbidites (Tolar Chico Formation), overlain by volcaniclastic rocks of Tremadoc-Arenig age (Tolillar Formation) as indicated by Araneograptus murrayi. These rocks are tectonically associated with mafic to ultramafic bodies. The overlying volcaniclastic rocks are characterised by a higher amount of volcanic components (Diablo Formation) and are intercalated with synsedimentary lava flows. All units were deformed in the Oclóyic Orogeny (Upper Ordovician), with isoclinal folding verging dominantly to the west.

According to component relations, the quartz arenites are classed as having a "continental block" provenance while the overlying volcaniclastic rocks show an increase in volcanigenic debris and have a "dissected arc" to "transitional arc" signature. Data on illite crystallinity show that the studied rocks experienced very low grade metamorphism (anchimetamorphic zone) which can be correlated to pumpellyite-prehnite mineral facies conditions. The average CIA value of the sedimentary rocks is 65. Trace element and REE ratios show that the quartz arenites have a "rifted margin" signature, which is

interpreted as a result of reworking. From base to top, the geochemical features of the volcaniclastic rocks indicate a change of the provenance from active continental margin to continental arc sources. The REE patterns of the samples show affinities to the PAAS standard and their characteristics are correlatable to felsic and intermediate source rock compositions. Ratios of REE and HFSE show average values of the upper continental crust. The $_{Nd}$ and the T_{DM} values point to variable provenances for the different units. The Tolar Chico Formation has T_{DM} of 1.9 Ga and $_{Nd(t)}$ of -9 and imply a mesoproterozoic basement source. The Tolillar Formation has T_{DM} of 1.5 to 1.6 Ga and $_{Nd(t)}$ of -5 which are similar to the basement values of the Late Proterozoic Sierras Pampeanas Terrane. The Diablo Formation contains the youngest T_{DM} of 1.2 to 1.3 Ga and $_{Nd(t)}$ of -1.9. We interprete the whole sedimentary succession as recycled from older continental crust with ` a slightly primitive input from a Lower Ordovician volcanic arc (Puna-Famatina volcanic arc) which evolved on continental crust.

Petrology and geochemistry of Mg-rich basalts from Western Ecuador : remnants of the Late Cretaceous Caribbean plateau ?

Marc Mamberti [1,3], Delphine Bosch [2], Henriette Lapierre [1], Jean Hernandez [3], Etienne Jaillard [1,4] and Mireille Polvé [5].

(1) UPRESA 5025-CNRS, UJF, 15 rue Maurice Gignoux, 38031 Grenoble Cedex, France. Mamberti@ujf-grenoble.fr
(2) UMR 5567-CNRS, Université Montpellier II, Place Eugène Bataillon, 39095 Montpellier, France
(3) Université de Lausanne, Institut de Minéralogie et de Pétrographie, 1015 Lausanne, Switzerland
(4) IRD, Dept. RED, 209-213 rue Lafayette, 75840 Paris cedex 10, France
(5) UMR 5563-CNRS, Université Paul Sabatier, 38 rue des 36-Ponts, 31400 Toulouse, France.

KEY-WORDS : Late Cretaceous, oceanic plateau, isotope geochemistry, mineral chemistry, Ecuador.

Introduction

Western Ecuador partly consists of Cretaceous oceanic terranes accreted to the Andean continental margin between the late Cretaceous and the late Eocene (Goossens & Rose 1973; Feninger & Bristow 1980; Cosma et al., 1998). Igneous rocks of mafic and ultramafic compositions caught along the Cretaceous and Paleocene sutures are interpreted as remnants of an Early Cretaceous oceanic plateau (Lapierre et al., 1999; Mamberti et al., 1999). However, exposures of picrites and clinopyroxene-rich basalts were recently discovered and studied. New geochemical data show that these mafic lavas are different from the Early Cretaceous rocks but similar to the ≈ 90 Ma basalts from the Caribbean Colombian Oceanic Plateau (CCOP). The aim of this paper is to present the petrology and geochemistry of these picrites and Mg-rich basalts from Ecuador and to compare these rocks with the well studied Cretaceous CCOP crust fragments that outcrop in the Caribbean.

Geological setting

Ecuador is divided into three main geological domains (Fig. 1). The "Oriente" represents the foreland basin of the Andean orogeny. The second domain comprises two cordilleras separated by the inter-Andean valley. The Eastern Cordillera consists of metamorphic material (Litherland et al., 1994) whereas the Western Cordillera is made of oceanic terranes accreted to the Andean margin during the Campanian (85-80 Ma) and the late Paleocene (59-56 Ma; Cosma et al, 1998). The third domain is represented by the coastal zone which consists of Cretaceous basalts and dolerites of oceanic plateau affinity (Piñon Formation; Goossens & Rose, 1973 ; Reynaud et al., 1999) overlain by Late Cretaceous island arc-rocks.
The Western Cordillera includes two distinct assemblages. The Eastern assemblage is composed of (1) 123 Ma ultramafic-mafic cumulates (San Juan cumulates, Fig. 1), (2) pillow basalts, dolerites and shallow gabbroic stocks (Merced-Multitud sequence; Fig. 1). The San Juan cumulates likely represent the basalts and dolerites plumbing system. Those rocks are assumed to be likely coeval with the Piñon Formation. The western assemblage is composed of olivine and clinopyroxene (cpx)-rich basalts, which form massive flows interbedded with lapilli and crystal tuffs. These flows show evidence for accumulation of olivine and clinopyroxene (cpx) crystals at their base, while their tops are highly vesicular.
Along the San Juan and Merced-Multitud sections, the eastern and western assemblages are separated by major NNE-trending faults. East of Guaranda (Fig. 1), the cpx-rich basalts are in fault contact with Tertiary rocks. West of Otavalo (Selva Alegre section, Fig. 1), the eastern assemblage is not exposed and the field relations of the cpx-rich basalts with the surrounding units are unclear.

Petrology and geochemistry

The cpx-rich basalts are locally associated with rare picrites. Both lavas are formed by cpx microphenocrysts asssociated or not with olivine pseudomorphs. Cpx has a diopside composition (Wo 44-47, En 47-50) and shows FeO-enriched rims in the Selva Alegre basalts.
Basalts and picrites have high MgO contents (11% to 25%). Picrites are slightly depleted in light rare-earth elements (LREE) relative to heavy (H) REE [0.70 < (La/Yb)n < 0.97] and their REE concentrations do not exceed 3 times chondritic abundances (Fig. 2). The Mg-rich basalts are LREE-enriched [(La/Yb)n = 1.79] and, compared to the picrites, have higher REE abundances (20 times chondrites). Cpx separated from the Guaranda basalts (Fig. 3) are depleted in LREE relative to HREE [0.18 < (La/Yb)n < 0.42] while those isolated from Selva Alegre basalt differ by higher REE abundances and an enrichment in LREE relative to HREE [(La/Yb)n = 1.94]. However, these Selva Alegre cpx show a small depletion in La and Ce relative to Sm and Nd [(La/Sm)n = 0.63].
REE compositions of melts in equilibrium with the cpx were calculated using the partition coefficientsof Hart and Dunn [1993]. The REE patterns of these calculated melts, based on cpx compositions (Fig. 4), are depleted in LREE relative to HREE [0.25 < (La/Yb)n < 0.56]. Since they differ significantly from those of their host rocks, the cpx are not in equilibrium with their host rocks.
Relative to primitive mantle, picrite and Mg-rich basalts display rather flat patterns with Ba and Rb enrichments and a marked depletion in Th (Fig. 5). Both types of lavas display a range of initial 87Sr/86Sr ratios (0.70297 < (87Sr/86Sr)i < 0.70306) while their _Nd(T= 90 Ma) and 206Pb/204Pb ratios are homogeneous. Picrites and Mg-rich basalts from Guaranda have the highest _Nd(T= 90 Ma) (+10.24 < _Nd < + 8.20; Fig. 6) while those from Selva Alegre have significantly lower values (+5.3). All these _Nd fall in the range of Oceanic Island Basalts (OIB). Picrites and basalts have high (206Pb/204Pb)i ratios [19.01 < (206Pb/204Pb)i < 19.59] (Fig. 7).

Comparison of the Mg-rich basalts with the lower Cretaceous Piñón Formation and the 90 Ma Caribbean basalts

Mg-rich basalts and picrites differ significantly from Lower Cretaceous dolerites and basalts from the Piñón Formation for the following reasons : (1) higher MgO contents, (2) larger LREE enrichments, (3) lack of Nb and Ta positive anomalies and (4) significantly lower (206Pb/204Pb)i ratios (17.89 < (206Pb/204Pb)i < 18.58).
Compared to Duarte Mg-rich basalts (Dominican Republic), the Ecuadorian mafic lavas are less LREE enriched and have lower Nb, Ta, Th and TiO2 abundances. However, Mg-rich lavas from Ecuador and Dominican Republic display some characteristics common to the oceanic plateau basalts of the Nicoya complex (Costa Rica), and to picrites and basalts from the Dumisseau Formation (Haiti; Sen et al,, 1988). They all have Pb isotopic compositions suggesting that they derive from an enriched source, whose composition includes the HIMU component characteristic of the Galápagos hotspot.

Conclusions

Using petrography, major, trace element and isotopic chemistry, we show that the Ecuadorian picrites and Mg-rich basalts display striking similarities with the Upper Cretaceous plateau basalts. The geochemical differences (i.e., lower LREE, Ti, Nb, Ta levels) are probably related to a higher degree of partial melting. The rather large range of _Nd values reflects heterogeneities in the enriched plume source. The Ecuadorian Mg-rich basalts could represent remnants of the Caribbean plateau accreted on the Andean margin sometimes between the end of the Cretaceous and the Paleogene.

References

Cosma (L.), Lapierre (H.), Jaillard (E.), Laubacher (G.), Bosch (D.), Desmet (A.), Mamberti (M.), Gabriele (P.), 1998 - Pétrographie et géochimie des unités magmatiques de la cordillère occidentaled'Equateur (0°30'S) : implications tectoniques. Bull. Soc. Géol. Fr., 169 : 739-751.

Fenninger (T.) Bristow (C.R.), 1980 - Cretaceous and Paleogene history of coastal Ecuador. Geol. Rundsch., 69 : 849-874.

Goossens (P.J.), Rose (W.I.), 1973 - Chemical composition and age determination of tholeitic rocks in the basic Cretaceous Complex, Ecuador. Geol. Soc. Am. Bull., 84 : 1043-1052.

Hart (S.T.), Dunn (T.), 1993 - Experimental cpx/melt partitioning of 24 trace elements. Contrib. Mineral. Petrol., 113 : 1-8.

Juteau (J.), Mégard (F.), Raharison (L.), Whitechurch (H.), 1977 - Les assemblages ophiolitiques de l'Occident équatorien : nature pétrographique et position structurale. Bull. Soc. géol. Fr., 19 : 1127-1132.

Lapierre (H.), Bosch (D.), Dupuis (V.), Polvé (M.), Maury (R.C.), Hernandez (J.), Monié (P.), Yeghicheyan (D.), Jaillard (E.), Mercier de Lépinay (B.), Mamberti (M.), Desmet (A.), Keller (F.), Sénebier (F.), 1999 - Multiple plume events in the genesis of the peri Caribbean Cretaceous oceanic plateau province. J. Geophys. Research, in press.

Lebrat (M.), Mégard (F.), Dupuy (C.), Dostal (J.), 1987 - Geochemistry and tectonic setting of pre-collision Cretaceous and Paleogene volcanic rocks of Ecuador. Geol. Soc. Am. Bull., 99 : 569-578.

Litherland (M.), Aspden (J.A.), Jemielita (R.A.), 1994 - The metamorphic belts of Ecuador. British Geological Survey, Oversas Memoir, 11, 147 pp., 2 cartes h.t.

Mamberti (M.), Hernandez (J.), Lapierre (H.), Bosch (D.), Jaillard (E.), Polvé (M.), 1999 - Are there two distinct Cretaceous oceanic plateaus in Ecuador ? E.U.G., abstract, 380.

Reynaud (C.), Jaillard (E.), Lapierre (H.), Mamberti (M.), Mascle (G.), 1998 - Oceanic plateaus and island arcs of southwestern Ecuador : their place in the geodynamic evolution of northwestern South America. Tectonophysics, in press.

Sen (G.R.), Hickey-Vargas (R.), Waggoner (D.G.), Maurasse (F.), 1988 - Geochemistry of basalts from the Dumisseau Formation, Southern Haiti : implications for the origin of the Caribbean Sea Crust. Earth Planet. Sci. Letters, 87 : 423-437.

Sinton (C.W.), Duncan (R.A.), Denyer (P.), 1997 - Nicoya Peninsula, Costa Rica : A single suite of Caribbean oceanic plateau magmas. J. Geophys. Research, 102 : 1507-15520.

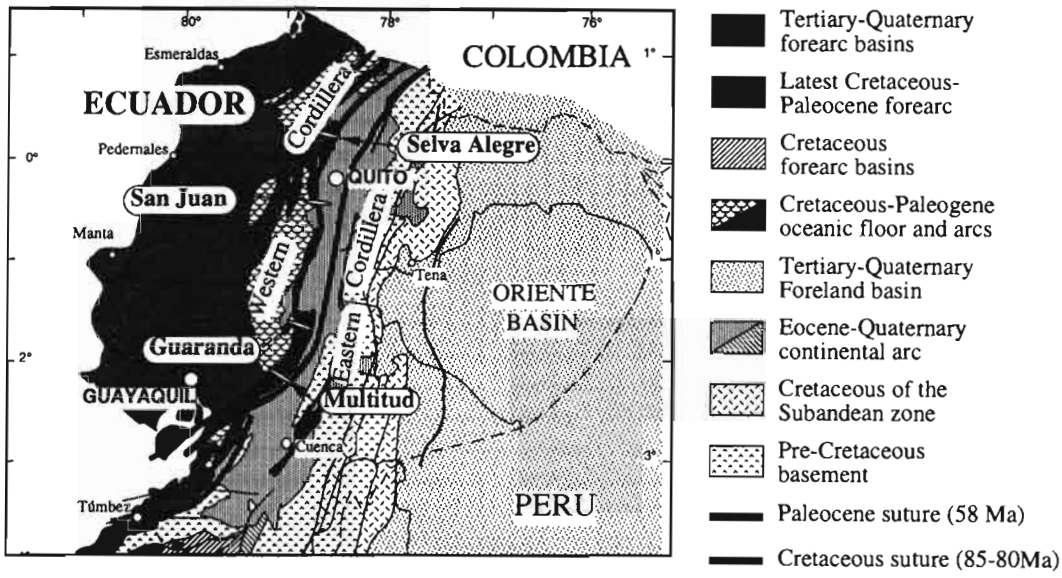

Figure 1: Simplified geological map of Ecuador.

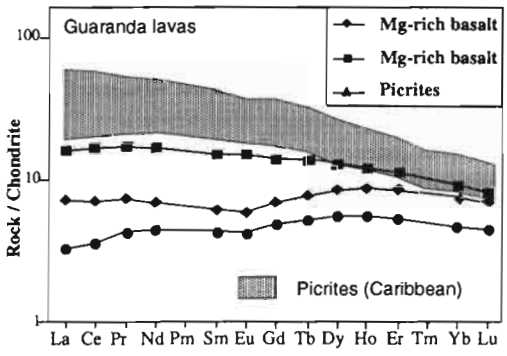

Fig 2 : Chondrite-Normalized rare earth elements patterns of picrites and Mg-rich basalt (chondrite values from Sun & Mac Donough, 1989).

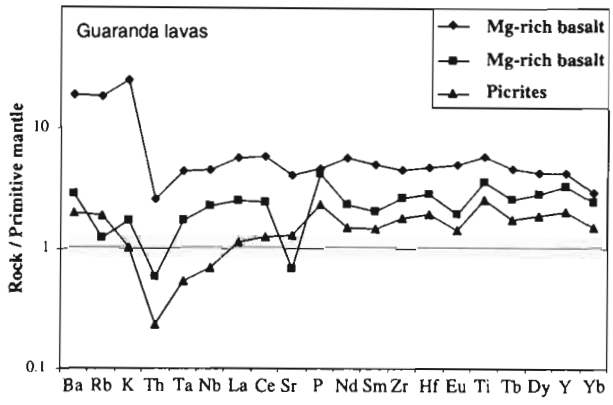

Fig 5 : Primitive mantle-normalized (N) trace element patterns of picrites (primitive mantle values from Sun & Mac Donough, 1989).

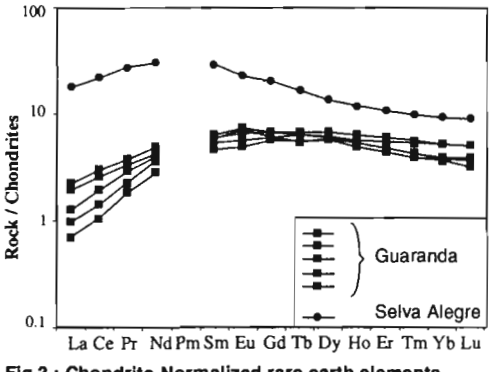

Fig 3 : Chondrite-Normalized rare earth elements patterns of cpx (chondrite values from Sun & Mac Donough, 1989).

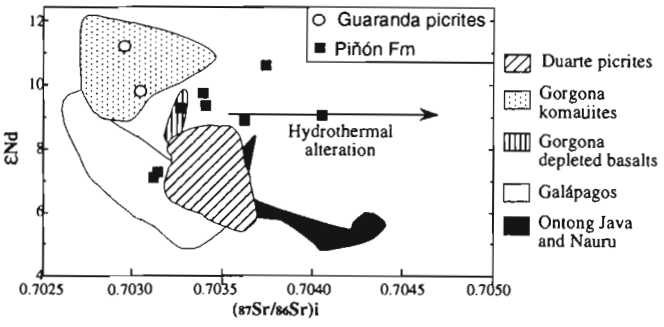

Fig. 6 : εNd-($^{87}Sr/^{86}Sr$)$_i$ plots for the minerals and host rock from Ecuador.

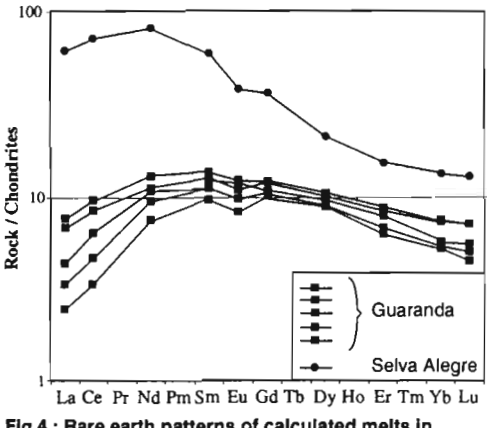

Fig 4 : Rare earth patterns of calculated melts in equilibrium with the clinopyroxenes (chondrite values from Sun & Mac Donough, 1989).

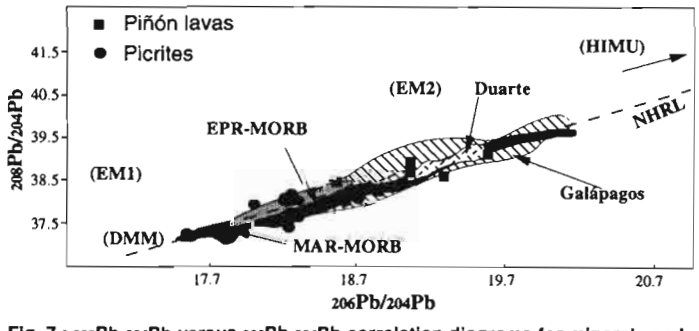

Fig. 7 : $^{208}Pb/^{204}Pb$ versus $^{206}Pb/^{204}Pb$ correlation diagrams for minerals and host rocks.

GEODYNAMIQUE ANDINE

ISAG 99

Résumés

Sur la signification de la tectonique décrochante transverse pour la structuration du Sud des Andes Centrales
A. Abels

La fabrique structurale actuelle du Sud des Andes centrales suggère une influence régionale de décrochements transverses liés aux structurations pré-andines obliques sur les directions andines. Trois exemples potentiels sont discutés, qui illustrent la complexité d'une telle déformation. De la côte à la Puna orientale, la déformation est principalement associée à des déplacements sénestres le long de structures d'orientation ≈ NW-SE, tandis que le front oriental de déformation andin est caractérisé par une transpression dextre affectant des domaines orientés ≈ NE-SW.

Évolution des terrains Protérozoïque-Paléozoïque inférieur dans l'Ouest de l'Amérique du Sud
F.G. Acenolaza, H. Miller et A.J. Toselli.

La Précordillère argentine est un terrain exotique situé au front occidental des Sierras Pampeanas de l'Ouest de l'Argentine. Elle est principalement interprétée comme une partie de la Laurentia accrétée au Gondwana au Paléozoïque inférieur. Nous montrons que des mouvements décrochants en bordure du Gondwana permettent également d'expliquer l'allochtonie des faciès de la Précordillère.

Utilisation de données AMS pour la localisation de chambre magmatiques sous les dykes doléritiques de l'île Magdalena, Sud Chili.
T. Aïfa, J.-P. Lefort et F. Hervé.

Pour localiser les chambres magmatiques à l'origine des nombreux filons de dolérites d'âge supposé Miocène inférieur qui affleurent sur l'île Magdalena et ses alentours (Los Chonos, Chili), une étude d'ASM sur 260 carottes orientées a permis de montrer que : (1) les trajets du flux magmatique associé au stress du point triple les localisent probablement sous les volcans holocènes, (2) les chambres magmatiques ont été actives au moins jusqu'au Miocène supérieur, ou bien les filons étudiés sont holocènes.

Complications transtensives de la tectonique du bord occidental des Andes équatoriennes : le cas de Mindo.
A. Alvarado, S. Bes de Berc, J.-F. Dumont, M. Sébrier et O. Bellier

À partir d'études de photographies aériennes, de MNT et de données cinématiques, on a réalisé une étude de l'état de déformation du bassin de Mindo, situé entre la cordillère occidentale et les bassins tertiaires de la côte équatorienne. Deux directions structurales principales ont été trouvées : NNE-SSW et NW-SE, respectivement dextre et sénestre. Il a été développé un modèle d'évolution cinématique basé sur une transpression qui a initialement généré le bassin et qui ensuite a évolué, probablement en fonction de la géométrie des structures héritées.

Le séisme du 9 juillet 1997 au Vénézuela : Arguments pour l'activité de la faille El Pilar.
P. Alvarado, A. Belmonte, E. Gajardo et M. Schmitz

Le 9 juillet 1997 un fort séisme (Mw=6.9) affecta le Nord-Est du Venezuela, endommageant les villes de Cariaco et Casanay. Le séisme détruisit toutes les constructions dans la zone épicentrale et causa l'effondrement d'immeubles, malheureusement occupés, à Cumaná, 75 km à l'Ouest de l'épicentre. On dénombra 73 morts. Malgré une rapide destruction des évidences de déplacements de surface par l'altération et l'érosion, le séisme principal était associé à une rupture de surface le long de la faille El Pilar.
Les résultats présentés ont été déterminés au moyen de l'enregistrement par l'Université du Chili de l'activité sismique pendant les 2 semaines qui suivirent le séisme. Six stations sismologiques (appareils EDA de courte période) correspondant à un réseau temporaire de 43 stations sismologiques (groupe RESICA) ont surveillé les répliques, impliquant le FUNVISIS, l'Université de l'Oriente et l'UDO (Venezuela), la Northwestern University (Illinois, USA), le German Task Force for Earthquake, le GFZ de Potsdam et l'Université Bauhaus de Weimar (Allemagne), et l'Université du Chili (Santiago).
Environ 250 répliques ont été enregistrées avec ce réseau local. La localisation de l'hypocentre (rapport FUNVISIS) et les répliques sont associées à un plan qui peut être relié à un segment de la faille El Pilar. Ainsi, les épicentres étaient concentrés le long d'un segment linéaire septentrional, presque Est-Ouest, de 60 km de large. De plus, les événements s'étendent sur environ 15 km de large et définissent un plan à pendage de 60° vers le Nord, qui inclut également l'hypocentre. Les résultats obtenus sont en accord avec des déterminations préliminaires effectuées par le FUNVISIS et l'UDO. Le traitement en cours des informations, en collaboration avec d'autres groupes, devrait préciser les caractéristiques de ce séisme et répondre à d'autres questions importantes.

Évolution de la Cordillère de Domeyko, Nord du Chili
A. Amilibia, F. Sàbat, G. Chong, J. A. Muñoz, E. Roca et A. Rodríguez-Perea

La Cordillère de Domeyko, formée pendant un régime de convergence oblique, résulte de l'inversion au Cénozoïque du bassin en extension triasico-jurassique. La majorité des structures observées ont une direction N-S et sont le résultat du raccourcissement E-W. On peut aussi observer quelques failles distensives et décrochantes, mais cela ne signifie pas nécessairement que la Cordillère de Domeyko soit le résultat d'un décrochement.

Les gisements épithermaux à Au-Ag du district de Shila (Sud Pérou) : données de la microfissuration et des inclusions fluides.
A.-S. André, J. Leroy, participants à la mission GdR métallogénie Pérou 97-98

Six gisements épithermaux (Au-Ag) du district minier de Shila (Sud Pérou) ont été étudiés d'un point de vue microstructural et fluides. L'analyse des plans d'inclusions fluides dans les quartz montre deux orientations structurales (N20-40°E et N100-120°E) identiques à celles contemporaines à la fois de la fracturation et de la minéralisation épithermale. L'étude des fluides met en évidence un phénomène d'ébullition à l'origine de la minéralisation souvent associée à de la bladed calcite.

La Zone de Faille Liquiñe-Ofqui : Un exemple de partition de la déformation en limite de plaque en transpression soumise à convergence oblique (Andes du Sud)
G. Arancibia, G. López et J. Cembrano

Des zones de milonites d'âge Miocène supérieur-Pliocène sont developpées dans l'extrême Sud de la Zone de Faille Liquiñe-Ofqui (Andes sud-chiliennes). La présence d'indicateurs

cinématiques dextres, les foliations subverticales et des linéations d'étirement et minérales horizontales, verticales et obliques, suggérent un rôle important joué par la partition de la déformation dans ce régime global transpressif dextre, et une composante triaxiale de la déformation.

Structure lithosphérique des Andes Centrales méridionales, résultats préliminaires (38°- 42°S)
V.M. Araneda

Des résultats préliminaires sur la gravité, le magnétisme et la sismique sont présentés pour la région des Andes du Chili et d'Argentine située entre 38° et 42°S. L'anomalie de Bouguer, l'équilibre isostatique et les isogrammes sont sous forme de carte. L'analyse sismique correspond à la réinterprétation de données de sismique réflection de prospection pétrolière. L'objectif de cette recherche est d'examiner l'orogène lié à la subduction des Andes Centrales méridionales et de le comparer avec la région plus au Nord (22°-28°S).

La sismicité superficielle dans le Nord-Ouest de l'Argentine et ses relations avec la tectonique
M. Araujo, G. Tello, A. Pérez, I. Pérez et C. Puigdomenech

La région étudiée correspond à la Puna et aux chaînes subandines du Nord-Ouest de l'Argentine. On y a étudié les relations entre sismicité superficielle, structures régionales et failles récentes. On observe qu'à l'Est de la courbe de niveau 3000 m, qui limite les deux régions, il existe une importante sismicité, liée aux régions en compression. La sismicité diminue de façon remarquable à l'Ouest, le volcanisme y devient important, et on observe des structures en extension.

Activité sismique induite par un glacier en zone volcanique : Application au versant nord du volcan Cotopaxi, Équateur.
S. Araujo et J.-Ph. Métaxian

Plusieurs volcans actifs d'Equateur présentent la particularité d'être couvert par une calotte glaciaire. Ces volcans se caractérisent aussi par une activité sismique relativement importante alors qu'ils sont manifestement dans un état de repos. Nous avons pu mettre en évidence qu'une proportion importante de l'activité sismique enregistrée sur le volcan Cotopaxi est due à la présence du glacier. Pour parvenir à ce résultat, nous avons comparé les signaux sismiques enregistrés en deux sites proches, l'un sur le glacier et l'autre sur la roche. Nous présentons dans ce résumé les caractéristiques des signaux de glace enregistrés sur le Cotopaxi. Ces signaux ressemblent beaucoup aux signaux basse fréquence d'origine volcanique lorsqu'on compare les enregistrements réalisés sur la roche, en revanche on constate que les enregistrements effectués dans la glace présentent des différences notables, ce qui permet de différencier les deux types d'activité.

Rotation de blocs le long de la bordure orientale de la Cordillère de Domeyko entre 22°45' et 23°30'S
C. Arriagada, P. Roperch et C. Mpodozis

Les résultats paléomagnétiques dans les couches rouges et roches volcaniques du Groupe Purilactis apportent de nouveaux arguments en faveur de rotations horaires associées à la déformation de la Cordillère de Domeyko à l'est du Salar d'Atacama. Ces nouvelles données confirment que les rotations horaires sont une caractéristique essentielle de l'évolution structurale des Andes du Nord Chili. Cependant, la variation spatiale dans la magnitude des

rotations de 10 à 50°, indiquent qu'elles sont fortement liées à la déformation locale de blocs, probablement au cours de la déformation compressive de l'Eocène.

Forme et style des intrusions du Batholithe Côtier, Pérou
M. Atherton et M. Haederle

Le Batholithe côtier du Pérou est un batholithe polyphasé de plus de 1600 km de long, composé d'environ 1000 plutons, dont la mise en place est contrôlée par un linéament. Sa géométrie est celle d'une tranche plate (rapport longueur/largeur ≈ 17,5 à 21,5). À l'Ouest, une profonde racine est considérée comme le conduit principal transportant le magma depuis la source. L'espace est créé dans la croûte supérieure par la montée du magma et le collapse de la roche hôte.

Structure des Andes de Mérida, Vénézuéla: faits et models.
F.E. Audemard et F.A. Audemard

Les Andes vénézuéliennes prolongent la Cordillère orientale colombienne vers le NE, mais ne gardent aucune relation génétique avec celle-ci. Plusieurs modèles ont été proposés pour expliquer la structure profonde de cette chaîne. Initialement, la chaîne a été interprétée comme une méga-fleur positive, limitée sur ses flancs par des chevauchements de vergence opposée et coupée longitudinalement par un grand décrochement dextre (faille de Boconó). Néanmoins, cette structuration ne tenait pas compte de l'asymétrie de la chaîne mise en evidence par la gravimétrie. En conséquence, de nombreux modèles recents présentent la chaîne comme un prisme continental à vergence NW, lié à une subduction continentale, de polarité variable (SE ou NW) selon les modèles considérés. En dehors de la gravimétrie, l'information sismique disponible se limite aux piémonts de la chaîne et manque de données de sismique de reflection profonde.

Style et chronologie de la déformation dans le bassin Oriente d'Équateur
P. Baby, M. Rivadeneira, F. Christophoul et R. Barragán

Le Bassin Oriente d'Équateur est un bassin d'avant-pays qui s'est développé depuis le Crétacé supérieur. Il a été déformé par 3 événements tectoniques (Turonien-Maastrichtien; Éocène; Pliocène-Quaternaire) qui se sont traduits par le fonctionnement transpressif dextre de 3 zones de décrochements NNE-SSW, qui d'Est en Ouest sont : 1) le Système Subandin toujours très actif; 2) le Couloir Sacha-Shushufindi qui correspond à l'inversion d'un rift jurassique; 3) le Système Inversé de Capirón-Tiputini hérité d'un bassin extensif permo-triasique.

Processus d'évolution magmatique dans le Complexe Tatara-San Pedro, 36°S, Zone Volcanique Sud (SVZ), Andes du Chili
J. Barclay, A. Marzoli et M. Dungan

Le Volcan Tatara-San Pedro présente une gamme très étendue des tendances de différentiation en plus de la gamme des compositions chimiques des basaltes de ce centre volcanique. La diversité chimique, minéralogique et texturale des roches andésitiques est largement due à l'évolution magmatique selon divers processus de différentiation de type "système-ouvert". Cet abstract se focalise sur une comparaison de onze roches intermédiaires caractérisées par 55,8 ± 0,8 % poids SiO_2 qui ont néanmoins d'autres indices de différentiation très variables (5,4-2,3 % poids MgO), et qui ont été produites par des processus allant du mélange de magma à la cristallisation fractionnée. La majorité de ces échantillons reflète une évolution mixte en plusieurs étapes (polybarique, composants multiples). En octobre nous présenterons un grand nombre d'analyses chimiques de phénocristaux qui nous aideront à discuter du fonctionnement de ces divers processus et leurs

implications plus larges par rapport à l'évolution magmatique liée au volcanisme d'arc des marges convergentes continentales.

Un point chaud crétacé dans le Bassin Oriente d'Équateur : indicateurs géochimiques, géochronologiques et tectoniques.
R. Barragán et P. Baby

Un paléo-point chaud intra-continental a été identifié dans le bassin "Oriente" d'Équateur. Des corps magmatiques ont été rencontrés au sein des sédiments crétacés des formations Napo et Hollín. Les datations radiométriques montrent que leur mise en place a eu lieu entre l'Albien inférieur et le Campanien. Géochimiquement, ils sont caractérisés par une variation de composition réduite, des ratios d'éléments LIL/HFS et des éléments en trace comparables à ceux observés dans les contextes océaniques intra-plaques et dans plusieurs provinces à coulées basaltiques. Les données de sismique réflexion montrent que la plupart des sites éruptifs sont contrôlés par des structures extensives préexistantes, inversées par une tectonique transpressive durant le Turonien-Maastrichtien.

Vitesse des ondes S dans la lithosphère à travers les Andes Centrales
D. Baumont, A. Paul, H. Pedersen, G. Zandt et S. Beck

Nous présentons les résultats de la détermination des vitesses d'ondes S dans la lithosphère par analyse des courbes de dispersion des ondes de surface. De très fortes variations latérales de la vitesse de phase sont mises en évidence. La régionalisation qui a été effectuée montre que ces changements sont corrélées spatialement avec les différentes unités morpho-tectoniques.

Évolution tectonique Mésozoïque et Cénozoïque du Bassin Austral d'Amérique du Sud
C.M. Bell, M. Suárez et R. de la Cruz

Le bassin Austral Méso-cénozoïque du Sud de l'Argentine et du Chili s'est développé sur une croûte continentale en contexte d'rrière-arc. Son ouverture résulte de la subduction de la plaque pacifique sous la marge continentale sud-américaine. L'extension crustale et le volcanisme acide jurassique supérieur donnèrent lieu à une subsidence régionale au Crétacé. Celle-ci fut suivie jusqu'au Crétacé moyen à supérieur et au Tertiaire par le développement de failles transformantes et le développement subséquent du bassin d'avant-pays d'âge Crétacé terminal à Tertiaire.

Une classification granulométrique des minéraux ignés et métamorphiques au microscope pétrologique standard T.L. : Pourquoi le faire ?
L. Biermanns

Les études des roches plutoniques, volcaniques et métamorphiques incluent souvent aussi des recherches sur la granulométrie. Pourtant, on n'a pas fait jusqu'à présent de classement sur la taille des grains pour des analyses microscopiques. La classification d'un diamètre de 3 200 µm à 12,5 µm, la dénomination de classes granulométriques allant jusqu'à des minéraux à grain extrêmement fins, qui de plus, montrent typiquement des formes allongées ou irrégulières, seront commentés plus en détail.

Composition isotopiques en Nd et Pb de roches Paléozoïques du Nord-Ouest de l'Argentine et du Nord du Chili : Accrétion crustale et dynamique des Andes de l'Ordovicien au Permien
B. Bock, H. Bahlburg, G. Wörner et U. Zimmermann

Les isotopes du Nd et Pb ont été mesurés sur des roches permiennes à ordoviciennes des Andes Centrales méridionales pour reconstituer l'évolution de la marge occidentale du Gondwana au paléozoïque. Avant tout, le Nd indique une zone source homogène pour les roches sédimentaires de la marge gondwanienne. Le temps moyen de résidence dans la croûte est de 1,6 à 1,7 Ga, avec intervention temporaire d'une zone-source jeune à l'Arenig. Les compositions isotopiques du Pb sont nettement distinctes de celles du Massif d'Arequipa du Nord du Chili et Sud du Pérou, et sont comparables de celles de l'Altiplano Sud définies par Aitcheson et al. (1995).

Anomalies du champ de variations géomagnétiques dans les Andes (30°S - 34°S) et sa signification tectonophysique
E. Borzotta, I.I. Rokityansky, M. Muñoz, H. Fournier et M. Mamaní

On a réétudié les magnétogrammes de 15 stations situées entre les bassins de Río Bermejo et Beazley (Argentine) et l'Océan Pacifique. L'analyse géomagnétique indique un changement important de la résistivité sur la ligne N-S des vallées de Iglesia-Calingasta-Uspallata (Argentine), la conductivité à l'Ouest de cette ligne étant moindre. On détermine des anomalies de conductivité dans la Précordillère, la Cordillère Principale, la zone de Río Bermejo et la région de la côte chilienne près de Valparaiso. On discute enfin de l'emplacement en profondeur de ces anomalies et de leurs relations avec l'évolution tectonique de la région.

Déformation andine en régime transpressif, bord Est de la cordillère Orientale, Colombie
Y. Branquet, A. Cheilletz, P. Cobbold, P. Baby, B. Laumonier et G. Giuliani

Des études de terrain appuyées par líinterprétation de profiles simiques nous ont permis de réaliser une coupe du bord Est de la Cordillère Orientale de Colombie intégrant le massif de Quetame et la zone subandine des foothills du Guavio. Cette étude met en évidence l'importance du régime transpressif lors des phases orogéniques Andines responsables du soulèvement de la Cordillère Orientale.

Modèle tectonique de la zone subandine nord, Équateur
A.G. Buitron

La Zone subandine d'Équateur est analysée dans une perspective tectono-sédimentaire. On établit, de plus un modèle d'évolution pour cette zone, qui montre certaines relations avec les événements régionaux. Chaque élément considéré du système d'avant-pays : prisme tectonique, sommet du prisme, bassin en flexion et voussure en "rebond" est pris en compte avec ses variations de position et ses implications tectoniques.

Gestion de l'information en géosciences : le site Web du SFB267 : http://www.fu-berlin.de/sfb267
H. Burger, M. Alten et S. Mohr

Le "Collaborative Research Center 267" (SFB 267) intitulé "Processus de déformation dans les Andes" est un projet de recherche interdisciplinaire qui comprend plus de 100 scientifiques de plusieurs institutions de Berlin et Potsdam en Allemagne, et la coopération d'environ 10 institutions partenaires (universités, services géologiques) en Amérique du Sud.

Il est vite apparu que la communication dans et entre tous les groupes de travail joue un rôle important dans une environnement scientifique aussi dispersé. Le site Web SFB267 a été conçu pour fournir une information à deux niveaux: un module intranet pour l'usage interne (administration, échange de données et d'idées, groupes de discussion, annonces de colloques/séminaires) et un module internet qui sert de source d'information pour la communité scientifique globale, présentant les activités de recherche en cours, les résultats récents, les données et cartes disponibles, les adresses des membres du SFB etc. Ce travail décrit le principe de notre système d'information, la programmation et tire quelques leçons de notre expérience et expose certains problèmes rencontrés.

Extension dans les Andes méridionales, mise en évidence par un bassin intra-arc d'âge Oligo-miocène.
W.M. Burns et T.E. Jordan

Le bassin Cura-Mallín et un bassin intra-arc oligo-miocène s'étendant entre 36 et 38°S dans les Andes méridionales et la Vallée centrale du Chili. Le remplissage du bassin consiste en une succession de roches pyroclastiques et sédimentaires atteignant 2800 m d'épaisseur. La subsidence était liée au jeu de failles normales. En contradiction avec les modèles géodynamiques, cette extension coincidait avec une nette augmentation de la vitesse de convergence et une diminution de l'obliquité de convergence des plaques Nazca et Amérique duSud.

Essaim sismique de Quito (Équateur) : origine tectonique ou volcanique ?
A. Calahorrano, H. Yepes, B. Guillier, M. Ruiz, M. Segovia, D. Villagómez et D. Andrade

La ville de Quito est située sur une zone de forte activité sismique et volcanique, limitée à l'Est par un système de plis et failles, alors qu'à l'Ouest, la ville est bordée par le volcan Guagua Pichincha. Durant le deuxième semestre de 1998, un intense essaim sismique est apparu au Nord de la ville de Quito, enregistrant plus de 4000 événements. Initialement, cet essaim a été considéré comme ayant une origine tectonique, cependant la brusque reprise d'activité du Guagua Pichincha pourrait indiquer une origine volcanique.

Étude des inclusions fluides dans le Porphyry Gold de la mine de Marte, Copiapó, Chili
E. Campos

Des analyses d'inclusions fluides contenant des veines de quartz, provenant d'échantillons de la mine de Marte, révèlent une complexe évolution hydrothermale. En effet, lors de la formation du stockwerk, de fortes variations en salinité ainsi que des variations plus faibles concernant la température d'homogénisation ont été mises en évidence. Ce processus implique à la fois mélange et dilution de différents fluides, ceux ascendants de haute salinité caractéristiques d'environnements hydrothermaux magmatiques profonds tels que les dépôts porphyriques, et ceux d'environnements moins profonds ayant une salinité plus faible.

Caractérisation des inclusions fluides du Porphyry Copper de Zaldivar, Chili
E. Campos et J.R.L. Touret

Le porphyre cuprifère de Zaldivar (Chili) a été étudié, notamment pour les inclusions fluides et vitreuses. La roche est profondément altérée, mais les phénocristaux de quartz ont préservé des assemblages fluides précoces, que des restes d'inclusions vitreuses. Trois types de fluides ont été observés : des saumures très salées, associées à des inclusions gazeuses. L'égalité des températures d'homogénéisation indique des épisodes discrets d'ébullition (vers 500°C) d'un fluide d'origine magmatique. Deux autres fluides aqueux ont été identifiés, l'un

contemporain de l'ébullition, l'autre ayant envahi la roche à une température plus basse (environ 300°C). L'origine de ces fluides est plus discutable, probablement externe en ce qui concerne le second. Il n'a pas été possible pour le moment de relier l'un quelconque de ces fluides avec la minéralisation cuprifère.

Évolution stratigraphique et tectonique au Miocène supérieur-Quaternaire de l'Est du bassin d'avant-pays de Madre de Dios (SE du Pérou)
J. Cárdenas, V. Carlotto, D. Romero, W. Valdivia, W. Hermoza, L. Cerpa, O. Latorre et M. Mamaní

Des études stratigraphiques et tectoniques de surface effectuées dans la partie Est du bassin d'avant pays de Madre Dios (SE du Pérou) montrent une série Mio-Pliocène faiblement plissée et affectée par des failles inverses et des décrochements. L'origine de ces structures est attribuée à la tectonique mio-pliocène. Par ailleurs, le système de failles en échelon sénestres du Rio de la Piedras sépare deux domaines morpho-structuraux et contrôle l'évolution et le remplissage quaternaires.

Évolution sédimentaire et structurale du bassin Éocène-Oligocène des Couches Rouges : Arguments pour une délamination lithosphérique à l'Éocène supérieur dans l'Altiplano sud-péruvien
V. Carlotto, G. Carlier, É. Jaillard, Th. Sempéré et G.H. Mascle

L'évolution sédimentaire et structurale du bassin des Couches Rouges éocène-oligocènes à l'extrémité NO de l'Altiplano suggère qu'un processus de délamination lithosphérique s'est produit dans cette région à l'Eocène. La nature du magmatisme associé à ces dépôts appuie cette hypothèse.

L'enregistrement sédimentaire du Salar d'Atacama: implications paléohydrologiques
V. Carmona, J.J. Pueyo, C. Taberner, C. Ayora, R. Aravena et G. Chong

L'objet de cette étude est l'interprétation de l'évolution hydrologique du Salar d'Atacama. Des échantillons choisis de 7 sondages pour la prospection de lithium ont été étudiés. Sur ce matériel on a utilisé DRX, la microscopie optique, la microanalyse des inclusions fluides dans le sel avec cryo-SEM-EDS, et l'analyse isotopique (^{34}S, ^{18}O) dans les sulfates accessoires. On montre l'existence de variations tant verticales que latérales dans la composition chimique des saumures et la composition isotopique des sulfates, ce qui suggère la présence de deux sources principales d'eau qui changent relativement au cours du temps.

GIS ANDES: Un SIG métallogénique de la Cordillère des Andes
D. Cassard

GIS Andes est un système d'information homogène de l'ensemble de la Cordillère des Andes, qui couvre une surface de 3,83 10^3 km² et s'étend sur 8500 km de la Péninsule de Guajira (Nord du Vénézuela) au Cap Horn (Terre de Feu). Conçu comme un outil tant pour le secteur minier pour aider à l'exploration et au développement de gisements, que pour le secteur académique pour contribuer à développer de nouveaux modèles métallogéniques, GIS Andes est basé sur des synthèses et compilations originales.

Structure en "pop-up" d'échelle régionale dans la zone de bordure de plaque dans les Andes méridionales: une réponse cinématique à la transpression pliocène.
J. Cembrano, A. Lavenu, G. Arancibia, G. Lopez et A. Sanhueza

La déformation en transpression d'âge pliocène de la zone de bordure de la plaque continentale dans les Andes méridionales a été accomodée essentiellement par du cisaillement oblique dextre et du raccourcissement, suivant un sytème de failles régionales qui délimitent le Batholite Nord-Patagonique. De nouvelles datations 40Ar-39Ar suggèrent que la déformation ductile des zones de cisaillement s'est produite entre 6 et 4 Ma, en même temps que la collision des différents segments de la dorsale du Chili avec la plaque continentale.

Développement de chevauchements à vergence opposée dans la Précordillère et la Cordillère Occidentale du Nord du Chili et leur rôle dans l'évolution paléo-environnemental cénozoïque.
R. Charrier, G. Hérail, J. Flynn, R. Riquelme, M. García, D. Croft et A. Wyss.

L'évolution tectonique de la Précordillère et de la Cordillère Occidentale du Nord du Chili est caractérisée, à partir de 18 Ma, par le développement de structures chevauchantes à vergence opposée. Cette évolution créa une ligne de reliefs séparant, à l'est et à l'ouest, deux environnements très différents comme l'indiquent les sédiments contemporains de cette évolution et leur contenu paléontologique.

Processus de formation des veines du gisement Au-Ag épithermal de Shila-Paula (Pérou sud)
A. Chauvet, D. Cassard et L. Bailly

Les minéralisations épithermales à Au-Ag de la mine Shila-Paula sont caractérisées par un système de veines montrant l'association entre une veine principale sub-E-W et des fractures satellites N120 à N135°E. Les décrochements contrôlant les veines indiquent une direction de raccourcissement initiale NE-SW à ENE-WSW compatible avec celle généralement admise pour cette période. Dans un deuxième stade, ces structures sont ré-ouvertes pour servir de réceptacle aux fluides minéralisateurs.

Compositions isotopiques du Plomb dans les minéralisations et roches témoins d'événements géodynamiques dans les Andes équatoriennes
M. Chiaradia et L. Fontboté

Les résultats préliminaires d'isotopes du Pb dans des roches et minéralisations d'Équateur reflètent la situation géotectonique complexe des Andes du Nord caractérisées par l'accrétion de plusieurs terrains et par un style de subduction qui a changé dans le temps. Des contributions élevées de Pb provenant de sédiments pélagiques ont étés reconnues dans des roches magmatiques et des minéralisations d'arc insulaire. Les roches et minéralisations ont des compositions isotopiques qui dépendent strictement de la nature continentale, océanique ou transitionnelle des terrains sur lesquelles elles sont situées.

Différenciation des influences eustatiques et tectoniques dans le Bassin Oriente (Equateur), de l'Aptien à l'Oligocène
F. Christophoul, P. Baby et C. Dávila

Dans le Bassin Oriente équatorien, les cycles sédimentaires de l'Aptien au Turonien montrent une influence eustatique. A partir du début du Maastrichtien, le bassin s'inverse et la dynamique est directement liée à l'évolution d'un bassin d'avant-pays. Durant l'Eocène supérieur et l'Oligocène, les formations sédimentaires sont apparemment post-tectoniques, mais on montre qu'elles sont tout de même sous l'influence des Andes en surrection.

Analyse multifractale du séisme de 1995 d'Antofagasta, nord Chili
A. Cisternas, D. Comte, L. Dorbath, J. Campos et J.-P. Ampuero

Nous avons étudié le comportement multifractal de la séquence sismique associée au tremblement de terre d'Antofagasta du 30/07/95 (Mw=8.0) à partir de l'analyse de la distribution spatio-temporelle de la sismicité. Avant l'occurrence du choc principal et des répliques majeures, la dimension fractale calculée diminue systématiquement.

Une double zone sismique à Arica, nord Chili
D. Comte, L. Dorbath, M. Pardo, T. Monfret, H. Haessler, L. Rivera, M. Frogneux, B. Glass et C. Meneses

A partir de la sismicité enregistrée localement dans la partie septentrionale de la lacune sismique du nord Chili, nous avons mis en évidence l'existence d'une double zone sismique où les séismes sont localisés à 100 et 120-25 km de profondeur respectivement. La genèse du matériel lithosphérique au niveau de la ride océanique constituant la plaque Nazca pourrait en être la cause.

La zone de Wadati-Benioff autour de Copiapó, nord Chili, à partir de données enregistrées localement : résultats préliminaires.
D. Comte, L. Dorbath, B. Pontoise, M. Pardo, T. Monfret, H. Haessler, Y. Hello, E. Lorca et A. Lavenu

De septembre à novembre 1998, un réseau de 28 stations terrestres et 10 stations fond de mer (OBS) a été déployée entre les latitudes 26,5°S et 28,5°S pour enregistrer la sismicité locale. Nous présentons la géométrie de la zone de subduction obtenue à partir des 500 séismes localisés dans les 15 premiers jours de fonctionnement du réseau.

La structure crustale de la région du séisme de Cariaco, 1997, Vénézuela oriental, basée sur des données de sismique réfraction et de gravimétrie
R. Contreras, M. Schmitz, L. Alvarado, J. Castillo et S. Lüth

On a étudié la structure corticale en mettant à profit le tremblement de terre de Cariaco (Vénézuela nord-oriental). A telles fins, on a utilisé les répliques de ce tremblement de terre provenant de 43 stations d'enregistrement temporaires. La géométrie des sédiments du bassin de Cariaco est étudiée au moyen de 5 profils sismiques de 10 à 20 km de long, ainsi que par voie de gravimétrie. Dans la partie centrale du bassin, les vitesses sismiques augmentent de 1,5 km/s depuis la surface jusqu'à 4 km/s à 1,5 km en profondeur.

Déformations quaternaires et risque sismique dans le front orogénique andin (31°-33°S, Argentine) : une perspective paléosismologique
C. Costa, T.K. Rockwell, J. Paredes et C. Gardini

L'analyse des principales structures Quaternaires dans une région charactérisée par des charriages et plis actifs, met en évidence les implications paléosismologiques de ces derniers et l'incidence dans le risque sismique dans cette région.

Déformation cénozoïque et style tectonique du haut plateau de la Puna (Nord-Ouest argentin, Andes Centrales)
I. Coutand, P. Cobbold, A. Chauvin, E. Rossello et O. López-Gamundi

Le haut plateau de la Puna correspond à la terminaison sud de l'Altiplano bolivien. Il est constitué par l'alternance de chaînons de socle Protéro-Paléozoiques et de bassins intramontagneux cénozoïques. L'analyse cinématique de populations de failles couplée à des observations de terrain montrent que la déformation y est majoritairement compressive. En outre, la géométrie des remplissages sédimentaires des bassins indiquent que le raccourcissement et l'épaississement de la Puna se sont initiés à partir de l'Eocène moyen à supérieur.

Âge et pétrologie du complexe plutonique de Tusaquillas (Andes Centrales) : conséquences sur l'évolution d'un rift crétacé dans le Nord-Ouest de l'Argentine
C. Cristiani, A. Del Moro, M. Matteini, R. Mazzuoli et R. Omarini

Dans ce travail, nous présentons de nouvelles données géochimiques et chronologiques sur le complexe plutonique de Tusaquillas (23°S-66°W, Andes Centrales), considéré comme le plus important corps intrusif appartenant au magmatisme associé au rifting Jurassique supérieur-Crétacé inférieur dans le Nord-Ouest de l'Argentine. Ces données contribuent à la connaissance du magmatisme mésozoïque des Andes Centrales qui est de première importance pour comprendre l'évolution géotectonique de cette région de l'Amérique du Sud.

Évolution néogène des principaux bassins sédimentaires de l'avant-arc équatorien et apport des bilans de masse sédimentaire
Y. Deniaud, P. Baby, C. Basile, M. Ordoñez, G. Mascle et G. Montenegro

L'analyse de données stratigraphiques et sismiques dans les principaux bassins de l'avant-arc équatorien (Golfe de Guayaquil, Progreso, Manabí et Borbón) et des calculs de bilans de masse sédimentaire réalisés dans le cadre de la convention de coopération entre PETROPRODUCCIÓN et l'IRD permettent de proposer une évolution en trois étapes de l'avant-arc équatorien au Néogène.
Du Miocène inférieur au Miocène moyen la sédimentation est essentiellement argileuse et marine et se développe dans un contexte général extensif Nord-Sud. Du Miocène moyen au Miocène supérieur, l'enregistrement sédimentaire se caractérise par l'arrivée de matériel gréseux détritique. Les extrêmes Sud et Nord de la province côtière équatorienne enregistrent un contexte transgressif (bassins du Golfe de Guayaquil et de Borbon), alors que la partie centrale enregistre un contexte régressif (bassins de Manabi et de Progreso). Du Pliocène à l'Actuel, les bassins de Progreso et Manabi émergent tandis qu'une forte subsidence affecte les bassins de Borbon Est et du Golfe de Guayaquil où s'observe le piégeage sédimentaire le plus important du Néogène dans l'avant-arc.

Les volcans nevados de Chillán et Antuco (Andes méridionales) revisités: la remarquable illustration d'une différenciation par cristallisation fractionnée en système clos.
B. Déruelle et L. López-Escobar

Les volcans Nevados de Chillán et Antuco (36°-37°S) ont émis des basaltes alumineux, andésites, dacites et rhyolites. Fait exceptionnel dans les Andes Méridionales, la

différenciation de la série de laves, pour laquelle la contamination par la croûte continentale est exclue, s'explique parfaitement par la cristallisation fractionnée en système clos des phases minérales présentes en phénocristaux (plagioclase, olivine, clinopyroxène, magnétite, apatite).

Éruptions pliniennes Holocène inférieur du volcan Cotopaxi, Équateur
F. Desmulier, C. Robin et P. Mothes

L'Holocène inférieur (9000 - 4500 BP) du Cotopaxi est caractérisé par une activité fortement explosive dont les produits sont des ponces et des cendres rhyolitiques. Quatre retombées pliniennes accompagnées d'écoulements pyroclastiques et d'importants dépôts de cendres ont eu lieu vers 6000 BP, marquant la phase paroxysmale de cette activité. Une étude détaillée des dépôts permet de caractériser les divers événements.

Arguments pour l'extension de la glaciation Ordovicien terminal-Silurien inférieur à l'Altiplano péruvien : implications tectoniques
E. Díaz-Martínez, H. Acosta, R. Rodríguez, V. Carlotto et J. Cárdenas

La séquence stratigraphique paléozoïque inférieur qui affleure immédiatement au Nord d'Ayaviri (Altiplano péruvien) appartient au domaine tectono-stratigraphique de la Cordillère Orientale, et comprend les formations Sandía, San Gabán et Ananea. Les galets striés et façonnés trouvés dans les diamictites de la Formation San Gabán sont les premiers indices de dépôts glaciaires d'âge Ashgillien supérieur-Llandoverien sur l'Altiplano péruvien, où l'on pensait que cette époque était marquée par un hiatus. La nette différence entre les séquences paléozoïque inférieur des domaines tectono-stratigraphiques de l'Altiplano et la Cordillère Orientale suggère un raccourcissement tectonique important le long de la zone de failles qui les sépare.

Géochronologie $^{207}Pb/^{206}Pb$ et $^{39}Ar/^{40}Ar$ de la chaîne métamorphique côtière entre 41°et 42°S, Chili central-sud.
P. Duhart, J. Muñoz, M. McDonough, M. Martin et M. Villeneuve

Les âges $^{207}Pb/^{206}Pb$ et $^{39}Ar/^{40}Ar$ obtenus sur des mono-grains de zircon détritique et de muscovites métamorphiques dans des schistes pélitiques et semi-pélitiques provenant de la chaîne métamorphique côtière mettent en évidence respectivement un épisode sédimentaire post-Dévonien, et des événements de déformation et métamorphisme au Carbonifère-Trias. Les données géochronologiques disponibles permettent de distinguer des accrétions dévoniennes à triasiques pour ce segment, et plus d'un protolithe sédimentaire.

The Tatara-San Pedro volcanic complex (36°S, Chile): implications sur la genèse et l'évolution des magmas d'arc de la Zone Volcanique Sud des Andes
M. Dungan

Selon plusieurs études (Hickey et al., 1986; Hildreth et Moorbath, 1988; Tormey et al., 1991), le centre volcanique de Tatara-San Pedro (36°S, Andes chiliennes) se trouve dans une région "transitionelle" entre les volcans du sud (37-40.5°S) où les laves sont faiblement contaminées et celles de la partie nord (35-33°S) de la Zone Volcanique Sud (ZVS) qui sont fortement modifiées en fonction de leurs interactions assimilatives avec la croûte qui s'épaissit graduellement vers le Nord. Le centre de Tatara-San Pedro montre une gamme extraordinaire des tendances de différentiation, particulièrement par rapport aux éléments traces incompatibles et leurs rapports qui reflètent divers degrés d'assimilation, divers processus de différentiation de type "système-ouvert" et diverses compositions chimiques de magma parent et de la croûte. Cette complexité se distingue, apparemment de façon

importante, des centres volcaniques au sud et il semble de plus que le Tatara-San Pedro présente un décalage abrupt au comportement ouvert bien qu'il n'y ait pas d'indication que l'épaisseur de la croûte augmente brusquement. Si cette observation pouvait être vérifiée par des études géochimiques détaillées des volcans situés entre 36-37°S, il faudrait probablement modifier l'hypothèse d'Hildreth et Moorbath (1988) concernant une relation directe entre l'épaisseur de la croûte et l'importance de l'assimilation. Au minimum il faut considérer comme valable la proposition de Wood et Nelson (1988) concernant la segmentation de l'arc.

Modèle de sédimentation volcanogénique de la formation Farellones d'âge Miocene, cordillère des Andes, Chili Central (entre 33°20' et 34° de latitude sud)
S. Elgueta, R. Charrier, R. Aguirre, G. Kieffer et N. Vatin-Pérignon

Un modèle de sédimentation volcanogénique de la Formation Farellones est élaboré à partir de l'analyse séquentielle des associations de faciès et de leurs relations spatiales et génétiques. Ce modèle montre que la phase initiale de la sédimentation est liée à d'intenses éruptions phréato-magmatiques et qu'elle s'est poursuivie par le dépot de laves principalement andésitiques. Les faciès ont évolué d'une position intermédiaire à une position franchement proximale dans un complexe volcanique majeur.

Surveillance des paramètres géophysique et géochimiques du volcan Galeras, Colombie
E. Faber, S. Greinwald, D. Panten, G. Valencia, D. Gómez, R. Torres, C. Moran et A. Estupiñan

Pour une meilleure compréhension de l'activité et de la physique des volcans actifs, le Federal Institute for Geosciences and Natural Resources (BGR) et l'Instituto de Investigation en Geosciencias, Mineria y Quimica (INGEOMINAS) ont commencé une nouvelle approche pour mettre au point une station de surveillance multi-paramètres sur le volcan Geleras, situé dans les Andes méridionales de Colombie à l'altitude de 4270 m. Les données sont enregistrées en continu près ou dans la caldera et sont transmises par radio pour une analyse en temps réel. Ce travail décrira à les équipements électromagnétique et géochimique et des résultats préliminaires.

Architecture transpressive Néogene de la Péninsule de Santa Elena (Équateur) : nouvelles données à partir de données sismiques.
F. Fantin, P. Malone, E. Rossello et M. Miller

Les bassins pétroliers paléogènes de Ancón et Pacoa (Péninsule de Santa Elena, SW de l'Équateur) sont séparées par le seuil structurale de Japonesa-San Vicente-Baños qui se traduit par un alignement d'affleurements du substratum sédimentaire crétacé qui dessine une "arche" proche d'E-W sur environ 30 km. On l'interprète comme une structure transpressive dextre typique (en partie contemporaine du Groupe Ancón) de 5 km de large, caractérisée par des plis et des failles inverses raides (certaines étaient normales à l'origine). Ces structures provoquent la surrection de blocs du substratum sédimentaire crétacé présentant en section des structures positives en fleur asymétriques à vergence Sud.

Origine des grumeaux de cristaux et de leurs symplectites (Opx - Mag) dans les laves du volcan Licancabur.
O. Figueroa et B. Déruelle

Les laves du Licancabur ont une texture gloméro-porphyrique. Elles contiennent des grumeaux de cristaux (Pl + Cpx + Opx + Mat) où parfois des symplectites à Opx et Mag

sont présentes. Certains grumeaux proviennent de synneusis à des stades successifs de cristallisation. D'autres de la destabilisation des Hbl de HP. Les phénocristaux isolés peuvent provenir de la désagrégation des grumeaux.

Évaluation des menaces volcaniques dans la région d'Arequipa (700.000 habitants) à moins de 20 km de distance du volcan el Misti, Sud du Pérou
A. Finizola, J.-C. Thouret, J. Suni et M. Fornari

Le volcan El Misti résulte de l'édification d'un strato-cône du Pléistocène supérieur sur et contre un stratovolcan du Pléistocène inférieur à moyen. Le strato-cône a connu au moins sept périodes éruptives (dynamismes variés : subplinien, vulcanien, ignimbritique, péléen et phréato-magmatique) depuis environ 100 000 ans. Trois scénarios éruptifs sont fondés sur l'analyse d'événements récents reconnus dans l'histoire du Misti : un scénario probable, vulcanien, semblable à l'éruption cendreuse de 1440-1470, un scénario de type subplinien similaire à l'épisode explosif de 400 BC-340 AD et un scénario de grande magnitude, fondé sur des éruptions pliniennes et ignimbritiques pré-holocènes, à récurrence faible.

Décompression à température décroissante dans des métapélites à faciès éclogite (Complexe métamorphique El Oro, SW de l'Équateur) : enregistrement d'une exhumation rapide
P. Gabriele, M. Ballèvre, E. Jaillard et J. Hernandez

Le Complexe métamorphique El Oro comprend des métabasites et métapélites à faciès éclogites (Complexe Raspas), interprétés comme un paléo-prisme d'accrétion exhumé au Jurassique terminal-Crétacé basal. D'après l'étude minéralogique et thermo-barométrique de l'assemblage grenat-chloritoid-quartz-disthène des métapélites, ces roches ont atteint des conditions P-T proches de 560-600° et 12 à 20 Kb, et la décompression s'est accompagnée d'une baisse de la température. L'exhumation a donc eu lieu peu après le pic de pression, rapidement, et en contexte de faible gradient thermique.

Le volcanisme ignimbritique Oligo-Miocène du Nord du Chili (Région d'Arica): stratigraphie et géochronologie
M. García , G. Hérail et M. Gardeweg

Dans la région étudiée, le très volumineux volcanisme ignimbritique Oligocène supérieur-Miocène inférieur, est daté entre 25 et 19 Ma. A l'ouest (Formation Oxaya) les ignimbrites sont distales et peu déformées. A l'est (Formation Lupica) elles sont interstratifiées avec des laves et des sédiments alluviaux et lacustres, et sont fortement déformées. Les grandes différences dans la stratigraphie et le degré de déformation de ces séries contemporaines reflètent une différence dans l'environnement de dépôt et dans la contrainte tectonique postérieurement au dépôt. La forte affinité shoshonitique, en plus de l'abundance de la sanidine, suggèrent une origine d'arrière-arc pour les ignimbrites.

Âge et structure de l'Anticlinal d'Oxaya : un élément majeur des structures compressives miocènes du Nord du Chili
M. García, G. Hérail et R.Charrier

L'Anticlinal d'Oxaya est un pli ouvert et asymétrique (vergence ouest) qui représente la structure la plus occidentale de la frange de plis et chevauchements miocènes de la Cordillère Occidentale du Nord du Chili (région d'Arica). L'Anticlinal d'Oxaya s'est développé au Miocène supérieur (≈ 9 - 7,7 Ma). Le pli a été formé par la propagation et réactivation d'un chevauchement plus ancien, la faille Ausipar.

Dans quelle mesure l'ardisation post-15 Ma de l'Amérique du Sud a-t-elle modifié l'évolution de la dynamique crustale des Andes boliviennes ? - Grands traits d'un programme de recherche
R. Gaupp, F. Schlunegger et Th. Jahr

Des modèles couplés thermo-mécaniques et érosion à l'échelle crustale, calibrés avec des données sur les flux de masses érodées, l'épaisseur actuelle de croûte, la vitesse de convergence, le flux de chaleur et les anomalies gravimétriques permettent une évaluation critique des paramètres contrôlant l'érosion de surface sur l'évolution à long terme d'une chaîne de montagne. Nous proposons de contruire un tel modèle théorique avec ABAQUS sur les Andes boliviennes pour l'intervalle Miocene - Actuel. De plus, nous essaierons collecter les données nécessaires au calcul des flux de sédiments érodés. En utilisant le modèle théorique calibré avec les données géologiques mentionnées, nous nous proposons d'évaluer l'importance du contrôle de l'aridisation post-15 Ma sur l'initiation d'une accélération de l'accrétion crustale (déformation de la zone plissée et écaillée subandine).

Métallogenèse de la Cordillère côtière entre 26 et 27°S (Nord du Chili)
S. Gelcich

Les roches plutoniques et volcaniques de la Cordillère côtière, Nord Chili, contiennent de nombreuses minéralisations à Fe et Cu-Fe ± Au. Ces dépôts sont temporellement et spatialement liés, et définissent différents épisodes de minéralisation s'échelonnant entre le Jurassique supérieur et le Crétacé inférieur.

Étude pétrogénétique des laves émises au cours de l'éruption persitente (1990-1998) du volcan Nevado Sabancaya, Pérou
M.-C. Gerbe et J.-C. Thouret

Depuis 1990, le Nevado Sabancaya présente une activité volcanique explosive hydromagmatique à vulcanienne. Pendant les deux premières années, l'activité a été marquée par une augmentation de l'explosivité. A partir de 1995, la fréquence des explosions et leur intensité a fortement décru. Depuis 1997, seule une activité phréatique a persisté. Les laves émises au cours de cette éruption constituent une série magmatique andésitique à dacitique, dont l'évolution géochimique globale est compatible avec un processus de différenciation magmatique par cristallisation fractionnée. Néanmoins, des critères minéralogiques mettent en évidence des mélanges magmatiques andésite/dacite intervenus dans le réservoir magmatique bien avant l'éruption actuelle.

Le Bassin d'avant-pays néogène de Alto Tunuyán, Mendoza, Argentine
L. Giambiagi

Le bassin Alto Tunuyán, situé entre les cordillères Principale et Frontale (33°30'-34°S), Argentine, est un bassin d'avant-pays Néogène créé en réponse au chevauchement et à la surrection de la ceinture plissée et écaillée de l'Aconcagua. La migration vers l'Est de la déformation a provoqué la surrection du substratum cristallin de la Cordillère Frontale, générant un bassin d'avant-pays brisé. Ces hauteurs empêchant la propagation des chevauchements vers l'avant-pays, le bassin a été cannibalisé.

Évolution structurale longitudinale Nord-Sud de la Zone Subandine péruvienne
W. Gil, P. Baby, R. Marocco et J.-F. Ballard

La zone subandine péruvienne se caractérise par un changement géométrique Nord-Sud très complexe, dû au passage progressif d'une tectonique de socle à une tectonique de couverture. Cette variation latérale de la déformation est contrôlée par l'héritage tectonique triasique et

jurassique, qui a laissé des systèmes de rift obliques à la chaîne et une érosion plus ou moins forte des séries sédimentaires paléozoïques. Cette évolution Nord-Sud a pu être mise en évidence grâce à la construction de coupes équilibrées.

Géologie structurale du Sud de la ceinture chevauchante subandine, Bolive : un nouveau modèle de déformations.
R. Giraudo, R. Limachi, E. Requena et H. Guerra

Un nouveau modèle structural a été développé pour la partie sud de la ceinture plissée et écaillée subandine de Bolivie. Ses principales idées sont que le raccourcissement, qui résulte de la surrection de la Cordillère orientale à l'Oligocène, n'est transmis à l'avant-pays qu'au niveau des argiles basales de la Formation Kirusillas silurienne, étant partiellement accomodé dans les structures subandines ; que des chevauchements aveugles accomodent partiellement le raccourcissement ; et en conséquence, que des piles de duplex se développent dans les argiles dévoniennes de Los Monos.

Déformation diachrone des cordillères Centrale et Orientale de Colombie et sédimentation syn-tectonique dans le bassin de la vallée moyenne du Magdalena.
E. Gómez, T. Jordan, K. Hegarty et S. Kelley

Le bassin de la vallée moyenne du Magdalena de Colombie, d'âge Crétacé supérieur-Tertiaire moyen, est rempli de sédiments syntectoniques. L'analyse structurale et stratigraphique montre que la Cordillère Centrale, à l'Ouest, fut la principale source de sédiments est constitua le contrôle de premier ordre du remplissage. À l'Est, la déformation de la Cordillère Orientale est à l'origine des variations à plus court terme dans l'accomodation et des discontinuités qui définissent l'organisation des dépôts. La déformation de ces chaînes est longitudinalement diachrone.

L'histoire polyphasée Méso-cénozoïque du système de failles décrochantes d'Atacama, Cordillère côtière (21°-24°S), Nord du Chili
G. González, J. Cortés, D. Díaz, C. Baeza et H. Schneider

Le segment septentrional (21-24°S) du système de failles d'Atacama (SFA) présente une histoire cinématique polyphasée. Une première phase est caractérisée par des mouvements sénestres au Crétacé inférieur. Au Crétacé moyen, le SFA est dominé par des mouvements dextres qui sont associés à des fluides hydrothermaux de basse température circulant dans la zone affectée par la faille. À l'Oligo-Miocène, des déplacements verticaux en extension le long de certaines failles N-S provoquent une forte segmentation morphologique de la Cordillère côtière. Après cette phase d'extension, des coulissements dextres se produisent au Pliocène supérieur le long du bord ouest du bassin du Salar el Carmen. Les structures les plus jeunes du SFA sont des fractures en distension, liées à la déformation post-sismique associées au séisme d'Antofagasta de 1996.

Le champ de gravité, l'isostasie et la rigidité des Andes Centrales
H.-J. Götze, S. Schmidt, M. Araneda, G. Chong D., M. Kösters, R. Omarini et J. Viramonte

Le champ de gravité des Andes Centrales méridionales et de leur avant-pays oriental entre 20° et 30°S a été étudié en relation avec l'état isostatique, la structure de la densité crustale de l'orogène et la rigidité de la lithosphère andine. La plupart des unités morphologiques andines sont proches de l'équilibre isostatique. Une nouvelle méthodologie pour la modélisation 2D de la rigidité de la lithosphère, qui tienne compte de la surcharge de surface et subsurface, a été appliquée à la topographie et au champ de gravité. Elle donna des valeurs faibles (10^{-22} à 10^{-23} Nm) pour la zone des bassins intramontagneux internes, et 10^{-23} à

$5x10^{-23}$ Nm pour les régions arrière-arc, ce qui correspond à une épaisseur élastique effective de 35 à 45 km.

Partition de la déformation dans la plaque supérieure au niveau d'une zone de subduction : un exemple andin
J. Grocott, K. Taylor et E. Arevalo

La déformation crétacé supérieur de la Cordillère côtière du Nord du Chili (26°S-30°S) a été répartie en composantes parallèle et normale à la marge. Des déplacements parallèles à la marge eurent lieu le long du Système de Faille d'Atacama et d'un deuxième système de failles en bordure est de la Cordillère côtière. La composante normale à la marge a été absorbée par déplacements le long de failles de direction NW, accompagnés de la rotation des blocs entre les failles. La partition se produisit en réponse à une convergence oblique et à une période de transition, au début du cycle l'orogénique andin, entre une situation de retrait de la fosse (retreating) et une avancée (advancing) de celle-ci.

Activité continue de type LP sur le Volcan Cayambe, Equateur. Localisation, analyse spectrale et conséquences
B. Guillier, P. Samaniego, M. Ruiz, J.-L. Chatelain, M. Monzier, H. Yepes, C. Robin et F.Bondoux

Un réseau sismique a été installé durant 5 mois sur le Volcan Cayambe dans le but d'observer l'activité sismique de type longue-période (séisme LP). Ces séismes LP sont caractérisés par un rapport Vp/Vs très bas (1.210) ainsi qu'une vitesse d'onde « P » très basse aussi (800 m/s). D'autre part, ces séismes LP ont un contenu spectral très étendu (0.8 à 6.5 Hz) qui les classe dans des événements de type hybride, chaque séisme étant un mélange d'un LP vrai avec un séisme de plus haute fréquence.

Géomorphologie tectonique du Bloc Ambato (Nord-Ouest des Sierras Pampeanas, Argentine)
A. Gutiérrez

A partir de l'analyse méga-géomorphologique des images satellites, complétée avec des données de terrain, on interprète l'évolution tectonique d'un ensemble de reliefs situé au Sud du linéament de Tucumán, dans les Sierras Pampeanas nord-occidentales d'Argentine. Cet ensemble correspond à un bloc unique (Bloc Ambato), dont la morphologie et les caractéristiques actuelles ont commencé à se développer depuis la fin du Cénozoïque.

Segments à subduction plane sous les Andes : arguments en faveur de Plateaux océaniques subduits
M.-A. Gütscher, W. Spakman et H. Bijwaard

Le long de 10 % de toutes les marges convergentes modernes, une subduction "horizontale" a lieu, où deux lithosphères restent en contact sur plusieurs centaines de km. Dans presque tous les cas elle est liée à la subduction de plateaux océaniques. La flottabilité de ces plateaux et de la lithosphère, plutôt que l'âge de la croûte, semblent contrôler ce phénomène. Elle engendre des changements thermiques et rhéologiques importants dans la plaque supérieure, où la déformation se déplace vers l'arrière-arc.

Métallogénie et sismotectonique dans la partie centrale de l'Amérique du Sud andine
V. Hanus, J. Vanek et A. Spicak

Les zones sismiquement actives ont été délimitées dans la région des Andes centrales et leur corrélation avec les gisements métallifères a été effectuée. On constate que les grandes accumulations de métaux se trouvent dans les zones actives. Les époques de la minéralisation générée par le processus de subduction montrent une bonne corrélation avec les cycles de la subduction andine.

Caractères géochimiques indiquant une relation avec la subduction pour le volcanisme Crétacé inférieur du Nord de La Serena, Chili
L. Hernández, O. Rabbia et A. Demichelis

Les roches volcaniques du Crétacé inférieur du Chili Central (27°-34°S) ont été interprétées comme résultant de processus d'accrétion et subsidence avec développement d'un bassin marginal avorté. Nous présentons de nouvelles données géochimiques sur les roches volcaniques du Nord de La Serena (29°15'-29°25'S). Les valeurs normalisées au MORB en LILE, Ce, Sm, Ta, Nb, (Zr) et Ti, en plus des rapports Th/Yb, Ta/Y et Zr/Y, indiquent que les roches étudiées sont liées à la subduction.

Des âges U-Pb Permien supérieur sur monograins de zircon détritique contraignent l'âge de l'accrétion des basaltes océaniques à la marge du Gondwana sur l'Archipel Madre de Dios, Sud Chili
F. Hervé, M. Fanning, J. Bradshaw, M. Bradshaw et J. Lacassie

La présence de zircons détritiques du Permien supérieur dans le Complexe Duque de York indique que l'accrétion des basaltes océanique de type E-MORB du Complex Deanro, ainsi que les Calcaires Tarlton qui sont recouverts en discordance d'érosion par le Complex Duque de York, a eu lieu au Paléozoïque supérieur.

Chevauchements obliques, décrochements et partition des contraintes dans les collines de la zone du Boomerang, zone subandine de Bolivie
R. Hinsch, Ch. Gaedicke, C. Krawczyk, G. Rebay, R. Giraudo et D. Demuro

Dans les collines du Boomerang, zone subandine de Bolivie, le front de déformation actuel est controlé par des structures compressives à l'Est, et à l'Ouest par des décrochements interprétés comme un système conjugué de failles de Riedel. Les deux domaines structuraux sont liés à un niveau de décollement situé sous une séquence argileuse paléozoïque. Puisque les failles décrochantes peuvent s'enraciner dans des zones de faiblesse du socle, cette zone pourrait représenter la transition entre tectonique andine de socle et tectonique andine de couverture.

Contrôle de l'érosion sur le développement des ceintures chevauchantes dans les Andes boliviennes
B. Horton

Les taux d'érosion dans les Andes Centrales pourraient avoir eu des effets importants sur l'évolution de la ceinture chevauchante depuis le Miocène moyen-supérieur jusqu'à l'Actuel. Au nord de 17.5°S, une forte érosion pourrait avoir favorisé l'extension de la ceinture orogénique vers l'avant-pays, alors qu'au sud de 17.5°S, une faible érosion pourrait l'avoir inhibée.

Accrétions crétacée et tertiaire de terrains dans la Cordillère Occidentale des Andes d'Équateur
R. Hughes et L. Pilatasig

Les Andes d'Équateur comprennent deux chaînes parallèles, les cordillères Occidentale et Royale (orientale). La Cordillère Royale consiste en unités allongées de roches métamorphiques d'âge paléozoïque à crétacé, accrétées principalement au Jurassique supérieur-Crétacé inférieur, et intrudées au Mésozoïque inférieur par des granitoïdes de type S et I. La cartographie récente par le British Geological Survey-CODIGEM a identifié deux terrains dans la Cordillère Occidentale. Des basaltes de Ride Médio-Océanique et des péridotites d'âge Crétacé inférieur à moyen et des turbidites du Crétacé supérieur forment le terrain le plus ancien. Le terrain le plus jeune est une séquence andésitique-basaltique d'arc insulaire d'âge éocène inférieur à moyen.
Les âges K/Ar réajustés à 85-65 Ma dans la Cordillère Royale, ainsi que les grandes différences de faciès du Maastrichtien de part et d'autre de la Cordillère Royale indiquent un âge Campanien-Maastrichtien pour l'accrétion du terrain le plus ancien. La structuration, l'existence de plutons de granitoïdes de type I et les données stratigraphiques suggèrent que le terrain le plus jeune s'est accrété à l'Éocène moyen, probablement par cisaillement dextre.

Le bras de mer de Guayaquil - un passage entre l'océan Pacifique et l'Oriente d'Équateur au Miocène moyen
D. Hungerbühler, W. Winkler, D. Peterson, M.Steinmann et D. Seward

Le développement de la série de bassins miocènes d'Équateur s'est effectuée en deux stades : (1) un *Stade côtier pacifique*, entre 15 et 9,5 Ma, pendant lequel les bassins étaient au niveau de la mer et incluaient les golfes de Cuenca et Loja, et (2) un *Stade Intramontagneux* entre 9 et 6 Ma. Au Miocène moyen, le bras de mer de Guayaquil mettait en connection l'Océan Pacifique et l'Oriente d'Équateur et du Pérou, via le golfe de Loja. Un soulèvement régional se produisit à 9 Ma, entre les deux stades, et ferma le bras de mer.

Contrôles sur la thermicité dans les zones compressives. Un exemple du Subandin Bolivien.
L. Husson et I. Moretti

La thermicité des chaînes de montagnes est contrôlée par la combinaison de phénomènes de longueur d'onde et d'amplitude variables : profonds -crustaux et mantelliques- et superficiels -érosion, sédimentation, circulation de fluides, relief, climat. L'influence sur le flux de chaleur des effets de surfaces est modélisée dans le cas du Subandin bolivien afin de mettre en évidence d'éventuelles anomalies profondes.

Étude de la croûte sur un profil des Andes péruviennes à partir de données gravimétriques et d'ondulations du géoïde.
A. Introcaso et R. Cabassi

De l'étude d'une section des Andes péruviennes au niveau de la ville de Nazca, nous obtenons : (1) des anomalies métriques entre les ondulations du géoïde mesurées par satellite basées sur le modèle OSU1991 et les ondulations isostatiques du géoïde ; (2) des anomalies isostatiques par rapport au système de Airy ; (3) un modèle crustal par inversions des anomalies de Bouguer ; et (4) un modèle crustal par inversion des ondulations du géoïde. Nous avons trouvé un excellent accord morphologique entre (1) et (2), et entre (3) et (4). Chacune de ces techniques indique une sous-compensation isostatique de la Cordillère Orientale. Nous concluons que les ondulations du géoïde permettent d'analyser et définire les structures d'échelle andine.

Andes Centrales: le signal gravimétrique de la plaque subductante
C. Izarra, N. Kusznir et H. Davies

Les études sismiques de l'épaisseur de la croûte dans les Andes centrales indiquent que cette zone est en équilibre isostatique bien compensé (Beck et al. 1996) et les études gravimétriques montrent une anomalie isostatique résiduelle inférieure à 70 mgal (Götze et al. 1996). Cependant, les modèles thermiques de la plaque subduite sous les Andes centrales prouvent que l'effet de pesanteur de la plaque excède 160 mgal. Cette anomalie suggère que les mécanismes compensateurs dynamiques agissent d'annuler une partie de l'anomalie de pesanteur liée à la plaque subduite.

Plutonisme Paléozoïque supérieur-Mésozoïque inférieur et rifting associé dans la Cordillère Orientale du Pérou.
J. Jacay, Th. Sempere, G. Carlier et V. Carlotto

La Cordillère Orientale du Pérou a été le siège d'un abondant plutonisme au Mississipien, puis au Permien supérieur-Trias. Cette dernière phase correspond à la mise en place d'intrusions dans les racines d'un système de rift. Le rifting a débuté dès le Permien supérieur et s'est propagé dans le Sud du pays jusqu'au Jurassique moyen.

Déformation et métamorphisme hercyniens dans la Cordillère Orientale du Sud de la Bolivie
V. Jacobshagen, J. Müller, H. Ahrendt et K. Wemmer

Les déformations du socle Cambro-ordovicien de la Cordillère Orientale du Sud de la Bolivie ont été attribuées à divers orogénes paléozoïques. Or, les âges K/Ar sur les grains de phyllosilicates les plus fins des schistes ordoviciens vont de 310 à 280 Ma. En tenant compte des données géologiques sur les régions avoisinantes des Andes Centrales, nous envisageons qu'une orogenèse éohercynienne (Chanique) ait été effacée par des processus géothermiques orogéniques au Paléozoïque supérieur.

Le Trias continental d'Argentina : une réponse à l'activité tectonique
U. Jenchen et U. Rosenfeld

En Argentine le Trias continental repose sur un socle complexe, composé de divers terrains. Les sédiments sont déposés en grandes séquences qui reflètent des phases de surrection du socle. Ces phases de surrection se produisent pour la plupart de façon séparée dans les différents terrains. Elles controlent l'évolution des divers bassins Triasiques.

Styles structuraux du segment plissé de Bogotá, Cordillère orientale de Colombie
A. Kammer

Le plissement de la Cordillère Orientale de Colombie est étroitement lié à une déformation ductile du socle métamorphique. La couverture, par contre, se déforme de manière moins homogène, à mesure que le raccourcissement est absorbé par plissement vers les niveaux structuraux supérieurs. Ce plissement s'accompagne, de plus, d'un glissement gravitaire vers les dépressions structurales.

Changement de pendage de subduction et évolution magmatique et tectonique néogène de l'arc des Andes Centrales.
S. Kay

L'évolution magmatique et tectonique des Andes Centrales d'Argentine et Chili reflète des changements dans la géométrie de la plaque plongeante et le caractère de la croûte et du manteau continentaux. Au Néogène, les changements dans la géométrie du slab comprennent une diminution de l'angle de subduction sous la zone actuelle du Chili à subduction plane (≈ 33°-28°S), une augmentation du pendage de subduction sous le Nord de la Puna et le Sud de l'Altiplano (≈ 22°-25°S), et la persitance d'un pendage intermédiaire dans la zone de transition sous la Puna méridionale (≈ 25°-28°S).

Processus de métasomatose du manteau sous les Andes méridionales
R. Kilian, Franzen, M. Koch et R. Altherr

Les xénolithes du manteau remontés à la fin du Cénozoïque dans la chaîne orientale des Andes du Sud ont été métasomatisés de façon complexe. Lors d'une phase de métasomatose précoce, probablement liée à la subduction de la plaque de Nazca, le manteau harzburgitique a été enrichi en H_2O, CO_2, U, La, Pb et Sr. Ultérieurement, probablement durant la formation du "slab window" miocène, le manteau a été contaminé par un basalte de type "MORB-enrichi" (faible rapport La/Nb et anomalies négatives en Pb et Sr). La contamination la plus récente du manteau est locale, due à des liquides basaltiques liés à la subduction, et se manifeste par des rapports Sr/Y, La/Yb et U/Nb élevés et des rapports U/Th plutôt bas.

Pétrogenèse d'un complexe plutonique basique à acide (Complexe igné de Pocitos) et de ces roches encaissantes dans la Puna méridionale du Nord-Ouest de l'Argentine
T. Kleine, U Zimmermann, K. Mezger, H. Bahlburg et B. Bock

Le Complexe igné de Pocitos qui affleure dans la Puna méridionale du Nord-Ouest de l'Argentine consiste en roches plutoniques basiques à acides. L'assemblage de minéraux primaires (les phases dominantes sont la hornblende, le feldspath alcalin et le plagioclase) est typique de roches magmatiques produites en contexte d'arc insulaire. Cette interprétation est compatible avec les signatures en élément trace qui montrent des anomalies négatives prononcées en Nb-Ta et Ti. Pour mieux contraindre les sources de cette suite magmatique, les isotopes de Sr, Nd et Pb seront analysés. Des âges U-Pb sur titanite seront utilisés pour dater les corps intrusifs.

Évolution tectonique de la Cordillère Orientale entre 23 et 24°S, Argentine du Nord-Ouest, du Carbonifère à l'Actuel
J. Kley, H. Kocks, P. Silva et C.R. Monaldi

Le segment des Andes orientales compris entre 23 et 24°S ne présente pas de ceinture plissée et écaillée subandine. Tout le raccourcissement Néogène à Actuel est accomodé dans la Cordillère Orientale, comme l'indique sa déformation très récente. Au Nord de 23°S, le déplacement est transféré de la zone subandine à la Cordillère orientale, sur des failles normales d'âge Carbonifère à Crétacé et de direction ENE.

L'occurence de BSR dans le Bassin de Lima au large du Pérou central est-elle un indicateur de production de méthane sous la zone de stabilité du "gas hydrate" ?
N. Kukowski et I.A. Pecher

La subsidence tectonique du Bassin de Lima a entraîné une baisse de la base de la zone de stabilité du "gas hydrate" (BGHSZ). Du coup, le gaz libre de la BGHSZ est transformé en "gas hydrate" est ne peut donc plus former une zone à faible vitesse. Cependant, des BSRs ont été trouvés dans une partie au moins du Bassin de Lima, où des érosions ont lieu. Ceci implique que des quantités suffisantes de gaz sont fournies en continu à la BGHSZ, ce qui pourrait indiquer une production considérable de méthane bactérien sous la zone de stabilité du "gas hydrate".

Transferts de masse par érosion dasn les marges convergentes : contraintes apportées par les modèles analogiques et l'application du concept du Prisme de Coulomb
N. Kukowski, J. Adam et J. Lohrmann

Nous associons des modèles de prisme et des modèles analogiques en sable pour analyser les modes de transfert de masse, les mécanismes et les facteurs contrôlant l'érosion tetonique à long terme. Les résultats préliminaires suggèrent que l'érosion tectonique induit des schémas complexes de transfert de matière, due à la simultanéité de l'érosion tectonique, de la subduction et du sous-placage. Le transfert de masse est contrôlé par les variations mécaniques à la base du système avant-arc - prisme, et est reflété par la géométrie actuelle du prisme et la déformation active.

Nouvelles contraintes sur l'âge de la déformation compressive crétacée dans les Andes du Nord du Chili (Sierra de Moreno, 21°-22°10'S)
M. Ladino, A. Tomlinson et N. Blanco

Dans la Pré-Cordillère du Nord du Chili (Sierra de Moreno, 21°-22°10'S), de nouveaux âges radiométriques et les relations géologiques, comme l'emplacement de plutons syntectoniques, indiquent que raccourcissement et surrection eurent lieu entre le Crétacé inférieur tardif et le milieu du Crétacé supérieur. La surrection de la Sierra de Moreno perturba la paléogéographie et la sédimentation continentale et créa de part et d'autre du relief, deux bassins alluviaux Crétacé supérieur contemporains, les bassins Tambillo et Tolar.

Passage d'un régime compressif à un régime extensif au front des Andes de Patagonie (46°S-47°S) : conséquence de la subduction de la ride active du Chili ?
Y. Lagabrielle, J. Bourgois, M. Suarez, R. De La Cruz, E. Garel, O. Dauteuil et M.-A. Gutscher

Nous présentons les résultats de recherches de terrain menées dans la région du Lac Général Carrera dans les Andes de Patagonie. Dans cette région, la croûte continentale pourrait être soumise aux contraintes imposées par le fonctionnement, en profondeur de segments de dorsale et de zones de fracture, passés en subduction depuis 6 Ma. Au sud de la ville de Chile Chico on observe des marques claires de la compression d'âge miocène supérieur, ce qui indique que le front de la chaîne des Andes Patagoniennes peut être suivi jusqu'au Lac G. Carrera au moins. Nous montrons que la tectonique compressive est prise en relai par une tectonique distensive se manifestant par des failles normales bien visibles dans le Tertiaire et dans les terrains quaternaires glaciaires et post-glaciaires (moraines et roches moutonnées décalées, varves basculées, réseau hydrographique perturbé). Le passage de la compression à l'extension a eu lieu au plus tôt avant 8 Ma, selon les corrélations établies pour les séries

concernées. Dès lors, nous pensons que l'arrivée et la progression vers l'est d'un segment de la dorsale a pu contrôler, en partie au moins, ce changement de régime tectonique.

Volcanisme et tectonique dans l'arc volcanique Pléistocène-Holocène des Andes du Sud (40.5°-41.5°S)
L. Lara, H. Moreno et A. Lavenu

La relation entre volcanisme et structures crustales est particulièrement intéressante dans ce segment des Andes méridionales, où coexistent des strato-volcans, des cônes principaux ou adventifs, de compositions diverses, organisés en bandes transversales d'orientation NE-SW et NW-SE, liées à une faille majeure régionale d'orientation Nord-Sud. Les fractures anciennes du substratum favorisent le déplacement le long des structures orientées NE soumises à un régime transpressif dextre actif depuis le Miocène.

Contexte structural et âge des gisements d'émeraude colombiens : conséquences sur l'évolution tectonique de la cordillère orientale
B. Laumonier, Y. Branquet, A. Cheilletz et G. Giuliani

A l'est de la cordillère, les gisements se sont formés en contexte extensif, à la limite Crétacé-Tertiaire, bien avant les compressions andines néogènes à l'origine de la chaîne plissée et chevauchante vers l'est. A l'ouest de la cordillère, les gisements et la chaîne plissée chevauchante vers l'ouest se sont formés simultanément, en régime compressif, à l'Eocène supérieur ou au début de l'Oligocène, indépendamment des phases andines néogènes.

Déformation en extension quaternaire et déplacement vertical récent le long de la côte chilienne (entre 23°S et 46°S)
A. Lavenu, C. Marquardt, D. Comte, M. Pardo, L. Ortlieb et T. Monfret

La côte pacifique du Chili est le siège de nombreuses terrasses marines quaternaires soulevées. Ces terrasses marines sont affectées par des failles normales dues à une déformation en extension de direction E-W. Ce soulèvement et cette déformation en extension sont la conséquence de l'accomodation co- et/ou post-sismique à de grands séismes le long du plan de Benioff, alors que plus à l'intérieur de l'avant-arc, la déformation quaternaire est en compression de direction N-S.

Compétition entre les contraintes associées au flux magmatique et à la subduction dans un complexe doléritique situé près de la subduction de la dorsale du Chili (Patagonie). Une étude structurale et d'anisotropie de susceptibilité magnétique
J.-P. Lefort, T. Aïfa et F. Hervé

Une étude structurale et d'anisotropie de la susceptibilité magnétique a été menée sur un complexe doléritique situé au nord du point triple déterminé par la subduction de la ride océanique du Chili et la plaque sud américaine. On peut y observer qu'il y a eu compétition entre les contraintes liées à cette subduction et celles associées à la montée du magma vers la surface.

Conductivité électrique sous le volcan Tuzgle et les centres volcaniques voisins, Nord-Ouest de l'Argentine
P. Lezaeta et H. Brasse

Un modèle électrique 2-D d'un profil NE-SW le long du linéament El Toro montre des zones de fortes conductivité (HCZ) au niveau de la croûte et du manteau supérieur, qui sont associés au volcanisme récent de la Puna où est situé le volcan Tuzgle. Alors que les HCZ de

la croûte supérieure révèleraient des fluides salés remontant le long de failles, les HCZ de la croûte moyenne ou inférieure pourrait être liées à la fusion partielle. Les HCZ dans le manteau supérieur renfocent l'hypothèse de l'existence d'une "lithosphère affaibli" à cette latitude (24°S).

Le volcan Antuco : un des strato-volcans isotopiquement les plus primitifs des Andes du Sud (37°25'S)

S. Lohmar, L. López-Escobar, H. Moreno et B. Déruelle

Le volcan Antuco est un strato-volcan composite situé dans la Zone Volcanique Sud (SVZ) des Andes chiliennes. On y distingue 2 unités principales : (1) un premier édifice (Antico 1) dont l'évolution culmine avec la formation d'une caldera provoquée par une éruption phréato-magmatique de type Bandai, suivie par une volumineuse avalanche volcanique et des vagues pyroclastiques à base humide; et (2) un cône plus récent (Antuco 2) logé dans la caldera. Le volcan Antuco a été décrit jusqu'ici comme une strato-volcan de composition basaltique à andésitico-basaltique. Ceci paraît n'être valable que pour l'Antuco 2 puisque, d'après nos études, l'Antuco 1 serait constitué de laves basaltiques à andésitiques acides et éventuellement, dacitiques.

Les roches basaltiques de l'Antuco présentent un des rapports isotopiques $^{87}Sr/^{86}Sr$ les plus bas des Andes du Sud (0,70369). Ces valeurs sont semblables à celles des îles océaniques de la plaque Nazca. Les faibles teneurs générales en Mg, Ni et Cr des roches basaltiques du volcan Antuco indiqueraient qu'elles ne dérivent pas de magmas primaires, mais qu'elles ont subi un fractionnement, des olivines et des pyroxènes au moins, avant leur emplacement. Les teneurs relativement élevées en Sr suggèrent que le fractionnement des pyroxènes a prévalu sur celui des plagioclases, ce qui indiquerait que les magmas basaltiques ont évolué principalement sous haute pression.

Les roches plus siliceuses seraient liées aux plus basiques par un fractionnement dominé par l'olivine et le pyroxène dans la transition basalte-andésite basaltique, et par le plagioclase dans la transition andésite basaltique-andésite. Les roches siliceuses ont des rapports isotopiques en Sr similaires à ceux des basaltes, ce qui exclut un contamination crustale significative dans l'évolution des magmas de ce volcan.

Volcanisme basique à intermédiaire jurassique moyen dans le Massif Nord-patagonien: le réseau de dykes de la Sierra de Mamil Choique

M. López de Luchi et A. Rapalini

Un complément pour l'analyse des termes les moins évolués du volcanisme jurassique en Patagonie (Argentine), est constitué par le réseau de dykes basiques à intermédiaires (47-61% SiO_2) qui recoupent le socle paléozoïque du bord sud-occidental du Massif nord-patagonien. Là coexistent des basaltes et andésites basiques calco-alcalines faiblement potassiques, et des trachy-andésites et trachy-basaltes alcalins hautement potassiques. Les âges K/Ar indiqueraient que le magmatisme alcalin précède légèrement le calco-alcalin, l'emplacement des dykes étant fortement contrôlé par des fractures en extension de direction variant entre N80 et N120°. Les pôles les plus basiques de chaque type peuvent être liés par des taux différents de fusion d'une même source. (La/Lu)N varie de 8 pour les trachytes à 6 pour les basaltes et andésites basiques calco-alcalines. Les processus de critallisation fractionnée sont dominés par clinoamphibole ± magnétite, et le plagioclase fractionne dans les termes les plus évolués, dans un milieu à haute figacité d'Oxygène. Les rapports Zr/Y de 6-11 sont typiques de basaltes intra-plaques. Cette succession de termes liés à une source unique avec des taux différents de fusion est typique des contextes intra-continentaux.

Un Plomb chaotique dans le socle des Andes Centrales (18°-27°) ?
F. Lucassen, R. Becchio, R. Harmon et G. Franz

Les rapports isotopiques du Plomb des feldspaths du substratum magmatique paléozoïque et du socle métamorphique indiquent une large gamme de composition en Plomb pour les roches d'âge supérieur à 500 Ma, et des compositions beaucoup plus homogènes pour les roches plus jeunes. Les rapports isotopiques du Neodyme de toutes les roches feldspathiques du socle paléozoïque sont similaires et indiquent une source crustale pour les roches magmatiques et métamorphiques étudiées. Nous proposons qu'une croûte Protérozoïque à signature isotopique en Plomb hétérogène a été largement homogénéisée lors d'un événement métamorphique de haut grade vers 500 Ma.

Composition isotopique de roches mafiques mésozoïques des Andes (23°-32°S) : À quel point la source mantellique est-elle hétérogène ?
F. Lucassen, M. Escayola, R. Romer, J. Viramonte et G. Franz

Les roches magmatiques basiques de l'arc jurassique de la chaîne côtière chilienne et du système de rift crétacé supérieur du Nord-Ouest de l'Argentine indiquent différentes sources mantelliques et l'influence de la contamination crustale. Les isotopes du Sr, Nd et Pb indiquent une source mantellique appauvrie pour les magmas jurassiques de la chaîne côtière, une source HIMU avec possible mélange d'une source appauvrie et une contamination crustale pour les basanites de la région de Salta (Argentine) et une source mantellique enrichie pour les roches magmatiques basiques de la région de Córdoba (Argentine). La source mantellique enrichie est similaire au manteau lithosphérique connu pour la province magmatique mésozoïque du Paraná.

Apport des mesures de Potentiel Spontané (PS) et de Température (T) au sol dans l'investigation des limites structurales et du système hydrothermal du volcan Ubinas (Pérou)
O. Macedo, A. Finizola, K. Gonzales et D. Ramos

Les mesures de PS effectuées à l'échelle du volcan Ubinas, montrent la présence d'une anomalie négative circulaire d'environ 6 km de diamêtre qui délimite le systême hydrothermal actuel. Toutefois l'absence d'anomalie PS et T dans la partie interne de la caldeira montre que le systême hydrothermal superficiel se limite exclusivement à la zone fumerolienne au fond du cratère actif.

Le Complexe métamorphique de Raspas (Sud de l'Équateur) : restes d'un prisme d'accrétion Jurassique supérieur-Crétacé inférieur - Contraintes géochimiques et isotopiques.
J.-L. Malfere, D. Bosch, H. Lapierre, E. Jaillard, R. Arculus et P. Monié

Le complexe métamorphique de Raspas appartient au bloc éxotique des Amotape, et contient des roches magmatiques et sédimentaires métamorphisées en faciès éclogite à schiste vert. Leurs compositions en éléments majeurs, traces et isotopes (Nd, Sr, Pb) révèlent 3 groupes. Les métabasaltes, un gabbro et une harzburgite proviennent d'une source appauvrie de type N-MORB. L'éclogite, un basalte et une amphibolite à grenat, bien qu'altérés, sont issus d'une source enrichie de type OIB ou E-MORB. Les métapélites dérivent d'une croûte continentale d'âge Protérozoïque ou Archéen.Ces origines distinctes sont compatibles avec l'interprétation d'un prisme d'accrétion.

Caractérisation stratigraphique du Groupe Ancón à partir de données sismiques (Péninsule de Santa Elena, Équateur)
P. Malone, F. Fantin, E. Rossello et M. Miller

Le Bassin Ancón se situe sur le seuil de Santa Elena, sur la côte sud-occidentale de l'Equateur et comprend des dépôts marins turbiditiques crétacés à paléogènes. Des levés sismiques récents montrent que le Groupe Ancón (Éocène) est constitué de 2 séquences, qui peuvent être à leur tour subdivisées. La séquence A (unités Clay Pebble Beds, Grès Santo Tomás et Passage Beds) est constituée de dépôts chaotiques et de coulées turbiditiques contrôlés par des structures synsédimentaires ; et la séquence B (Fms Socorro, Seca et Punta Ancón) indique une diminution progressive de la profondeur de dépôt et une progradation sur les unités antérieures.

Pétrographie et géochimie des basaltes magnésiens de l'Ouest de l'Équateur : fragments du Plateau Caraïbe du Crétacé supérieur ?
M. Mamberti, D. Bosch, H. Lapierre, J. Hernandez, E. Jaillard et M. Polvé.

Des plateaux océaniques se sont accrétés à différentes périodes à la marge équatorienne. La suture d'âge crétacé supérieur contient des roches cumulatives mafiques et ultramafiques datées à 123 Ma (San Juan). Plus à l'ouest, la suture paléocène contient des picrites et basaltes riches en Mg qui diffèrent des précédentes. Elles ont en particulier des _Nd plus élevés et sont beaucoup plus radiogéniques en Pb que celles de San Juan. Elles présentent de fortes similitudes avec les roches crétacé supérieur du Plateau Caraïbe et pourraient représenter des fragments de ce dernier, accrétés en Equateur vers 55 Ma.

Pétrographie et géochimie du Complexe Volcanique de Doña Juana, Sud)Ouest de la Colombie.
M. Marín, M. Molina, O. Ordoñez et M. Weber.

On présente de nouvelles données pétrographiques et géochimiques (majeurs, traces et isotopes) sur le volcan actif de Doña Juana de Colombie. Ce volcan, situé au Sud des Andes colombiennes (NVZ), est représentatif du volcanisme calco-alcalin trachy-andésitique récent connu dans cette région. Les données préliminaires sur les isotopes du Nd indiquent pour ces magmas une source mantellique dominante, bien que l'assimilation et la contamination de roches crustales soient suggérées par les valeurs préliminaires de "T-DM model ages".

Déformation fragile quaternaire dans la région de Caldera, Nord du Chili (27°S)
C. Marquardt et A. Lavenu

Près de Caldera (27°-28°S) des terrasses quaternaires sont affectées par une déformation cassante mise en évidence par des failles normales à fort pendage, de direction préférentielles NW-SE et NE-SW. Ces failles déplacent, avec des rejets pouvant atteindre 4 m, des niveaux sédimentaires d'âge pléistocène supérieur à holocène. Nous proposons que la déformation cassante en extension, dont la direction varie de WNW-ESE à NNW-SSE, est associée à une réactivation cosismique des structures pré-existantes. Le mouvement des blocs, le long des failles principales, génère un réajustement syntectonique qui provoque des rotations associées à de petites failles normales et inverses.

Mouvements verticaux récents et terrasses marines quaternaires dans la région de Caldera, Nord du Chili (27°S)
C. Marquardt, L. Ortlieb, A. Lavenu et N. Guzman

Dans la région de Caldera (Nord Chili), entre 27° et 28°S, l'altitude des terrasses marines quaternaires indique que le soulèvement durant les derniers 430 ka, n'a pas été uniforme le

long des 120 km de côte étudiés. En effet pour l'ensemble des terrasses marines quaternaires un taux de soulèvement, relativement rapide, est estimé entre 0,39 et 0,2 m/ka selon les latitudes considérées.

La Province basaltique continentale de l'Atlantique Central, et ses possibles relations avec le magmatisme du Trias-Jurassique dans les Andes
A. Marzoli, P. Renne, E. Piccirillo et M. Ernesto

La Province Magmatique de l'Atlantique Central est définie par des basaltes tholéitiques, présents en Amérique du Nord et du Sud, en Europe et en Afrique. De nouvelles datations $^{40}A/r^{39}Ar$ indiquent, sur ces continents, que le magmatisme s'est mis en place rapidement aux alentours de 200 Ma, sur une surface de plus de 6 millions de km^2, produisant environ 2 à 3 millions de km^3 de coulées basaltiques. Cet important magmatisme de plume de la partie Nord-Est de l'Amérique du Sud et l'extension continentale qui lui est associée, a apparemment accéléré la subduction de la plaque océanique Pacifique sous la marge ouest de l'Amérique du Sud. Ceci est peut-être à l'origine du magmatisme Trias-Jurassique le long de la marge convergente d'Amérique du Sud.

Nouveaux aperçus sur la structure du complexe d'accrétion paléozoïque supérieur-mésozoïque de la Cordillère côtière du Chili central et Sud
New insights into the structure of the Upper Palaeozoic / Mesozoic accretionary wedge complex of the Coastal Cordillera of Central and Southern Chile
H.-J. Massonne, L. Hufmann, P. Duhart, F. Hervé et A.P. Willner

L'étude pétrologique récente des roches métamorphiques paléozoïque supérieur-mésozoïques dans plusieurs régions de la Cordillère côtière chilienne indique des conditions métamorphiques similaires tout au long de la chaîne. Des conditions HP-BT ont prévalu au début de l'évolution métamorphique. Dans ces circonstances, l'idée que l'épaisse séquence clastique soit une partie d'un prisme d'accrétion est largement prouvée. Les résultats sur la tectonique qui a affecté les méta-psammopélites de bas grade ont été principalement obtenues le long d'une coupe E-W le long de la côte Sud de Chiloé et sont compatible avec cette interprétation.

Exploration de la partie nord du Batholithe Sud-patagonien, Sud Chili, associant données satellitaires spectrales et hyperspectrales et vérifications de terrain
H.-J. Massonne, J.-U. Mohnen, H.-G. Klaedtke, A. Kleusberg et F. Hervé

De récents travaux de terrain sur la partie nord du Batholithe Sud-patagonien vont être combinées avec l'étude des données Landsat 5-TM, des données satellitaires optiques, des données satellitaire hyperspectrales de haute résolution, ainsi que d'images radar. À ce jour, nous avons cartographié la région en zones englacées, eau, zones de forêt primaire et zones découvertes. Nous tentons de subdiviser ces dernières régions en classes lithologiques. Cependant, notre projet a pour but d'étendre la collecte d'information géologique à toute la zone. Nous pensons que ce traitement pourrait guider vers des gisements minéraux intéressants.

Étude géophysique du volcan Cotopaxi, Équateur : sismicité, structure et déformation de surface.
J.-Ph. Métaxian, M. Ruiz, A. Nercessian, S. Bonvalot, P. Mothes, G. Gabalda, F. Bondoux, P. Briole, J.-L. Froger et D. Rémy

Une étude géophysique du volcan Cotopaxi est menée depuis 1996 par l'IRD et l'Instituto Geofisico de la Escuela Politécnica National de Quito, Ecuador (IG-EPN). Nous avons réalisé

une campagne de sismologie en 1996-1997 afin de caractériser et d'analyser la sismicité associée au volcan et afin de déterminer un modèle préliminaire de la structure interne. Dans le cadre de ce programme, nous avons également installé un réseau de répétition GPS et microgravimétrique destiné à compléter les observations géodésiques de surveillance réalisées par l'IG-EPN et à servir de référence pour l'étude des déformations et des variations temporelles de pesanteur dans le cas d'une reprise d'activité volcanique. Nous présentons ici les résultats préliminaires de l'étude sismologique ainsi que des données géodésiques.

Géomorphologie, reconnaissance de textures, analyse de linéations tectoniques et classification de matériaux à l'aide d'images satellitaires dans le Batholithe Sud-Patagonien, Sud Chili
J.-U. Mohnen, H.-G. Klaedtke et H.-J. Massonne

Nous élaborons une banque de données d'images optiques à partir de données satellitaires variées pour une région du Batholithe Sud-Patagonien du Sud du Chili. Nous avons effectué des corrections de système et de terrain sur une banque de données de Landsat 5-TM. Nous présentons d'abord une classification des matériaux dominants. Nuages, glace, eau, roches dénudée et végétation seront évalués et quantifiés statistiquement. De plus, des linéations tectoniques peuvent être identifiées en utilisant un logiciel ER-mapper. Ces résultats sont présentés sous forme de diagramme en rose.

Les étapes de l'évolution de la Cordillère Orientale colombienne
J. Mojica

L'évolution géologique de la Colombie est due à la consolidation de deux provinces bien différentes : la première à socle sialique protérozoïque qui comprend la zone péricratonique du Bouclier Guyannais et la région andine jusqu'au système de failles de Romeral; la seconde, à l'Ouest de ce système de failles, est constituée d'une croûte océanique dont l'histoire remonte à peine au Jurassique?-Crétacé. L'examen de 23 cartes présentées montre qu'au Phanérozoïque, les processus tectoniques se sont concentrés dans une frange mobile, large et plus active au Nord, comprise entre les Failles de Romeral et celles du rebord amazonien. Ce dernier se dessine comme une limite bien marquée depuis le Dévonien.

Failles normales et grand glissements de roches dans le Nord des Sierras Pampeanas d'Argentine
R. Mon

Les Sierras Pampeanas de l'Argentine Centrale représentent un ensemble de blocs de roches métamorphiques appartenant au socle précambrien, remontés à la surface et basculés par de grandes failles inverses d'âge pliocène. Le but de cette communication est de présenter des données structurales qui mettent en évidence l'existence d'une phase d'extension beaucoup plus jeune (Pléistocène) reponsable des failles normales qui recoupent les structures antérieures.

Géochimie et tectonique de la terminaison sud de la Northern Volcanic Zone (volcans de la région de Riobamba, Équateur); résultats préliminaires
M. Monzier, C. Robin, M.L. Hall, J. Cotten et P. Samaniego

En Équateur, les volcans de Riobamba (Chimborazo, Tungurahua, Sangay, ...) forment la terminaison sud de la zone volcanique nord-andine. Ils se trouvent au-dessus d'une lithosphère océanique subductée plus ancienne et donc plus froide que celle située sous les autres volcans d'Equateur. La comparaison de leurs caractéristiques pétro-géochimiques avec

celles des autres volcans présente donc un intérêt particulier pour la compréhension des processus magmatiques actifs dans la région.

Géochimie des roches volcaniques triasiques de la chaîne côtière, Chili central
D. Morata, L. Aguirre, M. Oyarzún et M. Vergara

Les traits chimiques de roches volcaniques du Trias de la Cordillère côtière du Chili central sont discutés. Les résultats des analyses des éléments majeurs, traces et terres rares confirment la bimodalité et l'affinité tholeiitique de ces roches. En même temps, les relations isotopiques (Nd *vs* $^{87}Sr/^{86}Sr$ suggèrent de la contamination crustal qui aurait eu lieu en relation avec une période distensive pendant le Trias.

Géologie du bassin du Salar d'Atacama, Nord Chili : une réévaluation de la stratigraphie du Groupe Purilactis (Crétacé-Paléogène)
C. Mpodozis, C. Arriagada et P. Roperch

De nouvelles données stratigraphiques, géochronologiques, structurales et paléomagnétiques acquises lors de l'étude de la bordure orientale de la Cordillère de Domeyko à la latitude du Salar d'Atacama nous permettent de préciser la stratigraphie du Groupe Purilactis. Celui-ci comprend une succession de 7 séquences sédimentaires et volcaniques. L'observation de la polarité normale dans les unités inférieures du Groupe Purilactis suggère un age Crétacé moyen pour ces unités. Les nouveaux âges radiométriques K-Ar obtenus dans les unités volcaniques sus-jacentes montrent une activité volcanique d'âge Crétacé supérieur - Paléocène. Cette révision de la stratigraphie du Groupe Purilactis donne un nouveau cadre pour l'interprétation de la paléogéographie et des corrélations régionales pour le Crétacé-Paléogène des Andes Centrales.

La ceinture magmatique côtière Oligocène-Miocène inférieur dans les Andes du Chili sud-central (37°-44°S)
J. Muñoz, R. Troncoso P. Duhart, P. Crignola, L. Farmer et C. Stern

La ceinture magmatique côtière et la sédimentation associée se sont développées durant une période d'extension et d'amincissement crustaux, et de remontée mantellique, liée à une réorganisation majeure de la cinématique des plaques dans le Sud-Ouest Pacifique. La chaîne volcanique côtière représente un front volcanique anormal et les données géochimiques et isotopiques reflètent des sources magmatiques variées, incluant du manteau asthénosphérique océanique non modifié et de l'asthénosphère contaminée de façon variable par les processus de subduction et par l'assimilation continentale.

Flux de chaleur, température et bathymétrie des lacs Général Carrera et Cochrane, Sud du Chili
R. Murdie, D. Pugh, P. Styles et M. Muñoz

Nous avons entrepris des mesures de flux de chaleur dans les sédiments de 2 lacs du Sud du Chili, au niveau du Point Triple chilien où la subduction de la ride chilienne a lieu depuis 14 Ma. Ces mesures avaient pour but de voir, par les flux de chaleur, si la subduction de la ride chilienne a laissé une empreinte thermique au travers de la marge continentale sud-américaine. Les flux de chaleur mesurés sont élevés et les lacs se sont révélés les plus profonds mesurés à ce jour en Amérique du Sud.

Nouvelles contraintes sur la déformation crétacé-tertiaire de la Sierra de Moreno, Précordillère de la deuxième région d'Antofagasta, Nord du Chili
Cl. Nicolas, H.-G. Wilke, H. Schneider et F. Lucassen

On donne des contraintes d'âge et des données géométriques structurales pour deux phases de déformation (Albien-Santonien et Éocène), séparées par une période de quiescence tectonique, marquée par l'intrusion d'un granite d'origine mantellique, non déformé tectoniquement.

Evolution géochimique du volcanisme néocomien au Sud de Vallenar, Chili
A. Nova et M.E. Cisternas

Les études géochimiques de laves néocomiennes de la région de Las Cañas (sud de Vallenar), confirment l'existence d'un arc volcanique continental qui, comme son équivalent à Copiapó, montre une affinité tholéitique à calco-alcaline, avec un champ compositionnel allant des basaltes aux andésites.

ANCORP'96 : Imager la limite de plaques et la plaque supérieure dans les Andes Centrales
O. Oncken, S. Sobole, M. Stiller et P. Giese

La limite océan-continent en domaine convergent est traditionnellement définie par les hypocentres des séismes. Un profil de sismique réflexion profonde, long de 400 km, et l'enregistrement de séismes à travers les Andes Centrales montrent de façon inattendue que les hypocentres des séismes sont décalés de la limite de plaques imagée dans le manteau océanique. Cette image claire jusqu'à 80 km de profondeur et une zone intra-crustale claire à l'Ouest de l'arc volcanique, ainsi qu'une forte réflectivité intra-crustale sous l'Altiplano sont probablement dus à des processus pétrologiques contrôlés par la subduction et liés aux fluides et produits de fusion.

Nouveaux âges U-Pb et données Sr-Nd sur le batholithe composite de la Cordillère Frontale, Mendoza : implications sur la source et l'évolution magmatiques
H.M. Orme et M.P. Atherton

Des âges U-Pb sur trois stocks et des données Sr-Nd sur sept stocks du Batholithe composite de la Cordillère Frontale, Mendoza, donnent 276 Ma (stock de Punta Blanca), 263 Ma (stock de Cerro Médanos) et 262 Ma (stock de Cerro Bayo). Ces âges sont tous Permien inférieur et diffèrent de ceux de la littérature, qui ont été affectés par la déformation et l'altération visible dans ces stocks. _Ndt et $^{87}Sr/^{86}Sri$ suggèrent des variations isotopiques liées à la source plutôt qu'à des processus poussés d'assimilation et/ou de cristallisation fractionnée.

Volcanisme siliceux épisodique en Patagonie et dans la Péninsule antarctique : l'influence des panaches et de la subduction, associés à la fragmentation du Gondwana
R.J. Pankhurst, T.R. Riley, C.M. Fanning et S.P. Kelley

De nouvelles données géochronologiques sur la province volcanique acide jurassique de Patagonie et de la Péninsule Antarctique révèlent trois épisodes d'éruption : 184 ± 2 Ma, 168 ± 3 Ma et 153 ± 2 Ma, interprétés comme représentant trois épisodes de tectonique distensive liés à la fragmentation du Gondwana. Les périodes intercalaires sont caractérisées

par du magmatisme granitique, mais apparemment, les principaux batholithes andins ne se sont formés qu'après la fin du volcanisme.

Thermochronologie du pluton Crétacé inférieur de Caleu dans la chaîne côtière du Chili : implications tectono-stratigraphiques
M.A. Parada et P. Larrondo

Les âges ^{40}Ar-^{39}Ar sur hornblende et biotite du pluton de Caleu varient entre 117 et 94 Ma. En revanche, les âges de traces de fission sur apatites indiquent l'intervalle 96-82 Ma. Le pluton Caleu recoupe la Formation Veta Negra dont l'âge est compris entre l'Hauterivien (âge de la formation sous-jacente) et 117 Ma. La Formation Veta Negra est une accumulation volcanique déposée dans des bassins dont la subsidence était d'environ 1,4 mm/an. La vitesse de surrection-érosion la plus rapide du pluton Caleu (1,0 mm/an) a eu lieu entre 100 et 93 Ma et est associée au début de l'orogenèse et du dépôt molassique subséquent (Formation Las Chilcas).

Le tremblement de terre de Punitaqui du 14 octobre 1997 (Ms=6,8): un événement intraplaque destructeur au Chili Central.
M. Pardo, D. Comte et T. Monfret

Les séismes du 14 octobre 1997 et 3 novembre 1997, bien que de magnitude modérée, ont occasionné d'importants dégâts dans la région de Punitaqui-Ovalle, au Chili Central. Nous proposons de relocaliser ces événements afin de mieux étudier leurs mécanismes et leurs liens avec des essaims de séismes qui les ont précédés.

Des témoins d'un terrain océanique accrété dans l'Éocène inférieur du nord du Pérou : implications tectoniques
L. Pecora, E. Jaillard et H. Lapierre

L'Ouest de l'Équateur est formé de terrains allochtones d'origine océanique accrétés entre le Crétacé supérieur et le Paléocène supérieur. La présence dans la région de Paita de galets de microdiorites issues d'un arc insulaire resédimentés vers la limite Paléocène-Éocène prouve que des terrains océaniques étaient à l'érosion vers 55 Ma dans le Nord-Ouest du Pérou. Les terrains océaniques les plus proches étant situés actuellement en Équateur, 250 km plus au Nord, ils ont nécessairement dérivé le long de décrochements dextres à une vitesse minimale de 4,5 mm/an.

Mécanisme et conséquences de l'érosion tectonique dans l'avant-arc du Nord du Chili (20-22°S)
K. Pelz et O. Oncken

La tectonique de l'avant-arc du Nord du Chili depuis le Néogène est caractérisée par un mécanisme d'érosion tectonique basale. Les observations de terrain et les données sismiques amènent à un modèle intégrant le mécanisme et la géométrie de ce processus. Les mouvements verticaux de certains domaines donnent des données indirects pour déduire la géométrie des structures érodées.

Évolution géomorphologique du secteur Salinas Grandes/Quebrada Huamahuaca en relation avec la tectonique et le climat du Nord-Ouest de l'Argentine
F.X. Pereyra et P. Tchilinguirian

Le but de cette contribution est de caractériser les structures géomorphologiques du secteur de transition entre Puna - Cordillère orientale - Collines subandines du Nord-Ouest de

l'Argentine, en relation avec le contexte structural, les phases orogéniques andines depuis le Miocène supérieur, et les changements climatiques néogènes.

La série volcanique de la Cordillère Las Yaretas, Cordillère Frontale (34°S), Mendoza, Argentine
D. Pérez et L. Korzeniewski

La série volcanique éocène de la Cordillère de las Yaretas et ses relations avec l'évolution de la région sont étudiées. Les nouvelles données radiométriques et géochimiques exposées sur le Complexe volcanique Yaretas apportent des contraintes importantes sur l'évolution de la région de Las Yaretas. Les séquences volcaniques sont d'excellents outils pour dater l'évolution de la Cordillère.

Sédiments volcaniques du dernier interglaciaire sur la côte de Valdivia, Sud du Chili
M. Pino Q.

On décrit un type particulier de sable volcanique hyperconcentré (≈ 38°30'-40°S). L'âge le plus probable correspond à l'interglaciaire Riss-Würm. Ce faciès volcanique allochtone présente des intercalations de faciès biogéniques et terrigènes autochtones. On n'a pu attribuer ces dépôts volcaniques à un événement déterminé, les roche volcaniques pré-glaciaires ayant été recouvertes ou détruites par les dépôts de la dernière glaciation.

Enregistrement sédimentaire de la déformation cénozoïque de la bordure occidentale de l'Altiplano du Nord du Chili (Région de Tarapaca, 19°-19°30'S).
L. Pinto, G. Hérail et R. Charrier

La déformation tectonique de la bordure ouest de l'Altiplano dans la région de Moquella est caractérisée par la présence d'une flexure régionale de vergence ouest de 300 m de rejet. Elle s'est développée au cours du Miocène, entre 19 Ma et 9 Ma.

Soulèvement tectonique rapide révélé par les changements pédologiques : le massif d'Oña, Sud de l'Équateur central
J. Poulenard, Th. Toulkeridis et P. Podwojewski

Les sols du massif d'Oña au sud de l'Équateur, à 3000 m d'altitude, formés sur des dacites du Miocène présentent des caractéristiques ferrallitiques à leur base et andiques près de la surface. Les analyses géochimiques et minéralogiques montrent que le sol n'est pas polyphasé et qu'il s'est d'abord développé sous climat chaud à faible altitude, puis sous climat froid, en accord avec une vitesse de surrection d'environ 0,6mm/an.

Relations entre séismes et péninsules dans la région Biobio, Sud du Chili central
J. Quezada F.

La plupart des séismes de la région Biobio du Chili est localisée sur la côte, près des péninsules de Arauco et Tumbes. Ces péninsules et les îles côtières sont caractéristiques de cette région et la ligne de côte est déviée vers l'Ouest, en direction de la fosse. Cette étroite relation entre séismes et présence de péninsules s'expliquerait par un effet de barrière de ces péninsules vis-à-vis du mouvement de la plaque Nazca qui provoquerait une augmentation de l'énergie et des points de nucléation pour les séismes le long de la zone Wadatti-Benioff.

Mammifères fossiles de la région de Cuzco
J.A. Ramirez P.

La région de Cuzco, particulièrement des vallées de Cuzco et Ayusbamba, recèle des fossiles de mammifères. G.F. Eaton les ayant décrit d'abord en 1912, j'ai poursuivi l'étude de ces fossiles à partir des années 50, découvrant de nouveaux sites et de nouvelles éspèces. Ces fossiles, qui se trouvent dans des dépôts continentaux pléistocènes, ont été datés de 1,1 Ma par l'équipe du Dr. R. Bouchez (Grenoble), par spectrométrie RPE sur l'émail des défenses de mastodontes d'Ayusbamba. Les mammifères les plus importants sont : *Megatherium americanum*, *Gliptodon clavipes*, *Scilodotheriom* sp., *Macrauchenia patachonica*, *Cuvieronius hydon*, *Equus andinum*, *Parahiparion* sp. et *Mazama (Protozama) andina*.
La présence de mammifères dans les Andes de la région de Cuzco entre 3000 et 4000 m d'altitude pose le problème de la cause de la migration massive de nombreuses éspèces de mammifères depuis les parties basses du continent vers les zones hautes au Pléistocène inférieur à moyen.

Les Andes de Neuquén (36°-38°S) : Arguments en faveur d'un régime transtensif cénozoïque le long de l'arc
V. Ramos et A. Folguera.

Entre 36 et 38°S, les Andes sont contrôlées par un régime transtensif le long de structures orientées Nord-ouest. Ces structures partitionnent la contrainte produite par la convergence, en systèmes de décrochements lévogyres et donnent naissance à leur tour à des systèmes principalement transtensifs, responsables du développement de calderas rhomboédriques, comme la caldera del Agrio. Ces structures coexistent avec des systèmes de plis localisés au front tectonique actuel à ces latitudes.

Données paléomagnétiques préliminaires en faveur d'une rotation anti-horaire très importante de l'Archipel Madre de Dios, Sud du Chili
A. Rapalini, F. Hervé et V. Ramos

Une étude paléomagnétique a été menée sur les unités paléozoïque supérieur affleurant dans l'archipel Madre de Dios du Sud du Chili. Les résultats préliminaires indiquent la présence d'une magnétisation post-tectonique (post-jurassique) qui suggère qu'une large portion de l'archipel a subi une rotation anti-horaire très importante (> 90°) et un déplacement vers le Nord faible voire négligeable.L'âge post-jurassique de la rotation ne peut être précisé.

Modèles d'érosion tectonique au large du Nord du Chili
Ch. Reichert, pour le Groupe de Travail CINCA

L'hypothèse de l'érosion tectonique par subduction de la marge continentale du Nord du Chili a été émise depuis longtemps. Les dernières études multi-disciplinaires et l'établissement de bilans approximatifs montrent que la majeure partie de l'érosion a lieu à la base de la plaque continentale, qui est abaissée le long de nombreuses failles normales. La morphologie sous-marine de la marge impose des contraintes importantes sur les mécanismes et la friction à la limite inter-plaque.

Mécanismes de la déformation andine dans la Puna orientale, Nord-Ouest de l'Argentine
U. Riller, M. Strecker et O. Oncken

Les relations entre orientation des plis de premier ordre dans les sédiments tertiaires et direction des failles inverses limitant les vallées, ainsi que la courbure des pendages dans la

vallée du Río Calchaquies indiquent une transpression sénestre sur des accidents N-S, parallèles à la chaîne, pendant la tectonique andine.

Le bassin Oriente d'Équateur : un environnement tectono-sédimentaire optimum pour la génération et l'accumulation d'huile
M. Rivadeneira et P. Baby

Le Bassin Oriente d'Équateur a eu une évolution tectono-sédimentaire très favorable à la génération et l'accumulation de pétrole. Une alternance de cycles sédimentaires crétacés a permis l'interstratification de roche-mères et de réservoirs. Les événements tectoniques du Crétacé terminal et du début de l'Éocène sont à l'origine de pièges structuraux. Ces pièges se sont remplis de pétrole à la suite d'une expulsion et dune maturation accélérées des roche-mères ayant subi les effets d'une anomalie thermique due à un point chaud crétacé.

La mégafracture bajo de Velis-San Felipe-Yulto (San Luis, Argentina): un exemple de réactivation andine d'une discontinuité crustale récurrente
E. Rossello, M. López De Luchi, A. Massabié et C. Le Corre

La mégafracture Bajo de Velis-San Felipe s'étend sur 200 km le long du flanc oriental des Sierras de San Luis, dans l'avant-pays andin typique que sont les Sierras Pampeanas. Cette mégastructure est une structure andine majeure qui, tout au long de l'histoire géologique du substratum cristallin, se comporte comme une discontinuité pérenne et récurrente, avec quatre types différents d'activité tectonique, (1) au Ordovicien-Silurien, (2) au Dévonien-Carbonifère inférieur, (3) au Carbonifère supérieur-Permien, et (4) au Néogène.

Analyse par Traces de Fission sur apatite et zircons de la zone subandine d'Équateur (Napo) : un enregistrement de la géodynamique de l'Oriente depuis le Jurassique inférieur
G. Ruiz, R. Spikings, W. Winkler et D. Seward

A l'aide d'analyses de traces de fission (apatites et zircons) une extrusion d'âge minimum Toarcien a été trouvée pour l'unité volcanique Misahuallí affleurant dans la zone sub-andine nord. Une modélisation thermique (apatites) sur cette même unité a été réalisée. Elle suggère une exhumation (≈ 145-120 Ma) puis un enfouissement (≈ 105-90 Ma). Ces enregistrements peuvent être corrélés à la phase Peltetec et au dépôt des formations sédimentaires Hollín et Napo respectivement.

L'activité sismique du volcan Tungurahua (Équateur) : corrélation entre "tremors" et taux de précipitation
M. Ruiz, M. Hall, P. Samaniego, A. Ruiz et D. Villagómez

Le volcan Tungurahua est un grand volcan actif d'Équateur. Son activité sismique est caractérisée par des essaims sismiques, par des changements brutaux du facteur b ainsi que par la présence d'épisodes de trémors de longues durées. L'énergie libérée par les trémors est directement corrélable au taux de précipitation sur la zone. Ainsi, pour le suivi en continu du volcan et les pronostiques d'éruption, le taux de précipitation est un élément clé, surtout pour un tel système hydrothermal ouvert.

Géochimie des complexes volcaniques du Cayambé et de Mojanda-Fuya Fuya : arguments en faveur d'une interaction entre magma issu de la fusion du slab et coin mantellique ?
P. Samaniego, H. Martin, C. Robin, M. Monzier, J-Ph. Eissen et M.L. Hall

La caractérisation géochimique des roches des complexes volcaniques du Cayambe et du Mojanda-Fuya Fuya a mis en évidence l'existence de deux séries magmatiques distinctes : une série calco-alcaline classique et une série de tendances adaquitiques. La pétrogenèse de l'ensemble des roches s'explique par un faible taux de fusion partielle de la plaque plongeante et une intense interaction avec le coin de manteau. Cette fusion de la plaque plongeante peut être liée à la subduction de la Ride de Carnegie sous l'arc volcanique équatorien.

Fluctuations des efforts tectoniques et gravitaires et séismes dans le Nord du Chili
K.H. Schäfer

Depuis 1988, cinq "strainmeters" mesurent l'effort horizontal dans trois directions (N-S, NE-SW, E-W) dans le Nord du Chili. A Iquique, l'effort horizontal maximum dans tous les sites de mesure s'est révélé compressif dans toutes les directions : 49µm/m en E-W, 24,3 µm/m en NE-SW, et 2,4 µm/m en N-S. Les tiltmètres situés à des centaines de km de distance ont enregistré des efforts compressifs qui diminuent et augmentent, respectivement selon les directions E-W et NE-SW, provoquant dans le même temps des séismes (M 3,8 à M 5,2).

Basculement crustal récent entre le Salar d'Atacama et le volcan Lascar dans le Nord du Chili
K.H. Schäfer

Des mesures de basculement sont effectuées 2 fois par an entre le Salar d'Atacama (2310 m) et le volcan Lascar (5641 m). Entre 1993 et 1999, elles révèlent un subsidence du Lascar et de ses abords, alors qu'entre Talabre et le bord est du Salar d'Atacama, les tiltmètres de forage enregistrent une subsidence prononcée de la dépression du Salar d'Atacama. Deux tiltmètres situés sur le flanc NW du Lascar (4350 m) ont enregistré des variations correspondant à des éruptions mineures.

Modèle 3D de densité, équilibre isostatique et rigidité des Andes Centrales
S. Schmidt, H.-J. Götze, A. Kirchner et M. Kösters

Utilisant quelques 15.000 observations gravimétriques re-traitées sur les Andes Centrales, nous avons établi un modèle de densité 3D, contraint par d'autres types de données géphysiques sur la région. Des minima locaux le long de l'arc volcanique récent indiquent des zones de fusion partielle (10 à 15% de fusion) à des profondeurs de 10 - 15 km, et du matériel volcanique léger proche de la surface. La géologie régionale et la signature gravimétrique sont dominés par des alignements NNE-SSW de granites et roches volcaniques liées à l'accrétion de ceintures et terrains volcaniques linéaires. Leur juxtaposition avec des noyaux paleo- protérozoïques indiquent une mobilité crustale significative.

Evaluation de la profondeur pour la génération de produit de fusion intracrustale et pour les zones de stockage de magma dans les Andes Centrales. Aperçu à partir de la pétrologie et géochimie des ignimbrites
A. Schmitt, R. Trumbull, J. Lindsay et R. Emmermann

Les ignimbrites acides du Complexe Volcanique de l'Altiplano-Puna ont des caractéristiques isotopiques et géochimiques qui suggèrent des sources magmatiques mixtes comprenant 50 à 70 % de produit de fusion crustale. Les estimations directes P-T (780-820°C et 100-200 MPa) reflètent un stockage des magmas dans des chambres superficielles. L'estimation à 20-30 km de la profondeur des sources, basée sur les coefficients de partage entre produits de fusion et assemblages minéraux sensibles à la pression (Cpx/Pl et Gr/Opx), est en accord avec les arguments géophysiques en faveur d'une zone de fusion partielle sous la CVZ actuelle.

Structure crustale et équilibre isostatique du Bouclier guyanais, Vénézuela
M. Schmitz, D. Chalbaud, J. Castillo, C. Izarra et S. Lüeth

On présente les premiers résultats d'études de sismique-réfraction, et de recherches gravimétriques et magnétiques du bouclier Guyanais vénézuélien. L'épaisseur de la croûte varie entre 45 et 48 km du côté ouest et la vitesse moyenne y atteint 6,6 km/s, conformément aux valeurs moyennes connues dans les zones de boucliers. Néanmoins, le profil analysé concerne une zone de transition de la croûte Archéenne (à l'est) et Protérozoïque (à l'ouest), de telle manière que le Moho pourrait être incliné vers l'ouest.

Anomalies de conductivité électrique autour du profil ANCORP : un aperçu des résultats nouveaux
K. Schwalenberg, P. Lezaeta, W. Soyer et H. Brasse

Des mesures magnétotelluriques (MT) ont été effectuées dans le Nord du Chili et le Sud de la Bolivie. Les modèles issus de l'inversion 2D montrent que, contrairement aux régions plus au Sud, l'arc magmatique récent sous la Cordillère occidental n'est pas connecté à un bon conduit magmatique. Sur un profil a 20°S, une nette zone de conduit est modélisée sous la Faille occidentale. La modélisation de la partie Altiplano du profil ANCORP révèle un large conduit dans la croûte moyenne et inférieure, probablement causée par la fusion partielle.

Le séisme de Bahía, 4 août 1998 (Mw=7.1) : mécanisme de rupture et analyses du potentiel de risque sismique
M. Segovia, J. Pacheco, N. Shapiro, H. Yepes, B. Guillier, M. Ruiz, A. Calahorrano, D. Andrade et J. Egred

L'analyse des ondes P et SH de données télésismiques de large bande a permis de déterminer le mécanisme focal (proche de celui calculé par Harvard) et la durée de la rupture du séisme de Bahía de 1998 évaluée à 10 secondes. La localisation des répliques à partir d'enregistrements locaux et régionaux a permis de définir la zone de rupture, qui correspond au sud de la rupture du séisme de 1942 (Mw=7.9). Il en découle que la partie N de la rupture du séisme de 1942 n'a pas été rompue ce qui laisse présager un séisme de moyenne à forte intensité dans un futur proche.

Les stocks subvolcaniques miocène inférieur du piémont andin du Chili Central : un cas de fusion de la plaque océanique ?
D. Sellés M. et E. Godoy

Les stocks andésitiques à dacitiques qui intrudèrent les affleurements volcaniques occidentaux de la Formation Abanico (33-34°S) immédiatement après la fin du volcanisme, présentent un signature géochimique qui exclut une région-source similaire au magmatisme antérieur et postérieur. Les sources possibles pour ces stocks sont la fusion d'un slab chauffé par conduction et celle d'un matériel terrigène entraîné en profondeur. Des analyses

supplémentaires, comme celle des isotopes radiogéniques, sont nécessaires pour explorer plus avant ces hypothèses.

Les rifts Permien supérieur-Mésozoïque inférieur eau Pérou et en Bolivie et leur rapport avec la tectonique andine
Th. Sempéré, G. Carlier, V. Carlotto, J. Jacay, N. Jiménez, S. Rosas, P. Soler, J. Cárdenas et N. Boudesseul

Des processus de rifting ont affecté le Pérou central dès le Permien supérieur et se sont propagés jusqu'au Jurassique moyen en Bolivie et dans la zone côtière du Sud du Pérou. Les hétérogénéités lithosphériques produites alors ont fortement influencé la localisation et les modalités des déformations d'âges jurassique terminal-crétacé basal, crétacé supérieur et cénozoïque. L'Altiplano correspond à un domaine encadré par deux branches de ce système de rifts. L'inversion de la branche orientale au Néogène est à l'origine de la Cordillère Orientale.

Le magmatisme acide néogene des Andes sud à centrales : nouveaux aspects sur la formation des ignimbrites
W. Siebel, W. Schnurr, K. Hahne, B. Kraemer et R. Trumbull

Cette étude compare la composition chimique et isotopique d'ignimbrites rhyolitiques riches en Silice de l'arc volcanique (Salar de la Isla, Chili) et de la zone adjacente d'arrière-arc (Salar de Antofalla, Argentine) dans le Sud de la Central Volcanic Zone. Les compositions isotopiques des ignimbrites recouvrent celles des andésites d'arc, et la modélisation géochimique appuie l'interprétation selon laquelle les ignimbrites se sont formées par la cristallisation fractionnée de magmas andésitiques précurseurs.

Domaines à contrainte uniforme dans la zone de Wadati-Benioff de l'Amérique du Sud andine
A. Slancova, A. Spicak, J. Vanek et V. Hanus

Des variations détaillées de la contrainte ont été déterminées pour la zone de Wadati-Benioff sous les Andes. La distribution de l'activité sismique (ISC) et l'orientation des axes P et T des mécanismes focaux (HCMT) ont été pris pour tracer les 30 domaines qui représentent des régions à contrainte uniforme. On montre que la contrainte change plus systématiquement avec la profondeur que latéralement le long de la zone de Wadati-Benioff, et qu'elle s'adapte au changement de la forme de la zone de Wadati-Benioff.

Nouvelles données paléomagnétiques dans le Nord du Chili : contraintes spatio-temporelles supplémentaires sur les rotations tectoniques de la région
R. Somoza et A. Tomlinson

La déformation andine dans le Nord du Chili est caractérisée par de nombreuses rotations horaires à axe vertical. De nouvelles données paléomagnétiques sur la région indiquent que les rotations tectoniques se produisent à différentes époques et en différents lieux. Dans la région de Pica (20°30'S), nous avons detecté une rotation néogène affectant à la fois les roches crétacées et miocène inférieur. En revanche, les roches crétacées de la région de Calama (22°S) montrent une rotation horaire alors que les roches miocène inférieur ne montrent aucun indice de rotation. Nos données paléomagnétiques situent la limite entre rotations horaires et anti-horaires dans l'avant-arc des Andes Centrales à une région étroite de 1,5° de latitude.

Salar de Antofalla: un régime transpressif dans la Puna argentine
J.A. Sosa Gómez

Le Salar de Alnofalla représente un bassin de morphologie particulière de la Puna argentine.Son aspect en "Z" étiré, la polarisation des appareils volcaniques ainsi que la géométrie structurale, font attribuer l'origine du Salar de Antofalla à un régime transpressif.

Morphologie de la zone Wadati-Benioff et structure sismotectonique de la lithosphère andine dans la région du coude d'Arica
A. Spicak, V. Hanus, J. Vanek et A. Slancova

L'analyse géométrique de la distribution des tremblements de terre a permis d'établir la limite digitiforme de la partie inférieure de la zone de Wadati-Benioff sous le domaine asismique, et de délimiter les zones de fracture sismiquement actives dans le coin continental andin de la région du coude d'Arica.

Thermochronologie de Basse Température du Nord de la Cordillère Royale, Équateur : aperçu sur la tectonique tertiaire
R. Spikings, D. Seward et W. Winkler

Des mesures de trace de fission (zircons et apatites) ont été réalisées à partir de 3 transects à travers le nord de la Cordillère Real. Ces 40 âges définissent les grandes lignes de l'évolution tectonique et thermique post-paléocène de l'orogène. Ils montrent entre 4 et 8 kms d'exhumation de la Cordillère Real lors des 40 derniers millions d'années avec des taux supérieurs à 1.2 km/Ma lors de périodes distinctes.

Néotectonique et glissements de terrain dans le Nord-Ouest de l'Argentine
M.R. Strecker, R.N. Alonso, R. Hermanns, R.M. Marrett et M. Trauth

Les vallées intramontagneuses du Nord-Ouest argentin sont le siège d'une importante activité tectonique, de glissements de terrain répétés. En outre, elles endiguent les principaux systèmes de drainage. Les glissements de terrain se produisent principalement au niveau d'une ancienne zone de transfert décrochante, réactivée en faille inverse dans des zones courbes restreintes. Cette réactivation résulte d'une réorganisation cinématique du raccourcissement depuis une direction initiale NO-SE vers une direction néotectonique NE-SO.

Bolivie : Le Protérozoïque supérieur-Paléozoïque inférieur
R. Suárez-Soruco

Durant l'Archéen et le Protérozoïque, le Bouclier brésilien qui formait la bordure Ouest du Gondwana subit une série de modifications significatives lors de l'accrétion de nouveaux terrains, la formation de bassins intracratoniques et le développement d'importantes chaînes de montagne protérozoïques. À la fin du Protérozoïque ou au début du Paléozoïque, un "Point triple bolivien" sur la bordure ouest du Gondwana donna lieu au "Bloc d'Arequipa" et au Rift bolivien.

Section crustale à 21°S, de 60 Ma à aujourdhui : implications sur l'évolution thermique
D. Tanner, G. Wörner et A. Henk

Nous avons tenté la modélisation thermique d'une section de la lithosphère supérieure des Andes à 21°S pour la période 60-0 Ma, en utilisant la technique des éléments finis. Des sections ont été construites tous les 5 Ma, en utilisant les valeurs de surrection, et les

données géologiques et structurales. On considère trois sources de chaleur : la chaleur radiogénique interne, le transport de magmas sous l'arc et la chaleur fournie par conduction par le manteau. Le modèle donne un aperçu sur la fusion de la croûte inférieure sous les Andes, et sur les mécanismes contemporains d'épaississement crustal des Andes et d'amincissement du manteau lithosphérique.

Propriétés magnétiques de la Formation La Negra (Cordillère de la Côte du Chili): Analyse comparative entre zones avec et sans minéralisations cuprifères
A. Tassara, P. Roperch et P. Sepúlveda

Les propriétés magnétiques de la Formation La Negra, séquence de basaltes et andésites d'âge jurassique, affleurant dans la Cordillère de la Côte du Nord Chili, sont caractérisées par une forte susceptibilité magnétique (0.02-0.06 SI) et une aimantation rémanente inférieure à 1 A/m. La maghémitisation, probablement associée au métamorphisme de bas degré, est importante, mais ne tend à réduire la susceptibilité que faiblement. À l'échelle régionale, il n'y a pas de différence significative entre les zones minéralisées et non minéralisées. Localement, les zones minéralisées à chalcosine-coveline-hématite présentent cependant une destruction complète de la magnétite et de la maghémite.

Le magmatisme mésozoïque de Bolivie et sa signification dans l'évolution de l'orocline bolivien
S. Tawackoli, R. Rössling, B. Lehmann, F. Schultz, M. Claure et B. Balderrama

L'activité mésozoïque en Bolivie est marquée par deux phases d'intrusions qui se recouvrent en partie. Lors de la première phase du Jurassique moyen au Crétacé inférieur (184-104 Ma); la mise en place de dykes et sills tholéitiques le long d'une zone amincie de la Cordillère Orientale est liée à des structures profondes en extension. Pendant la phase suivante d'âge Crétacé (120,5-76 Ma), des intrusions et des roches effusives, principalement alcalines, se mettent en place dans la même zone mais aussi le long d'une zone amincie du substratum pré-cambrien constituant une ramification de la précédente. Le magmatisme mésozoïque et les structures extensives associées structurent l'orocline bolivien. La ré-activation andine de ces structures pourrait avoir influencé l'évolution et la structure courbe actuelle de l'orocline.

Un nouveau tournant dans la recherche de minéralisations dans le Nord du Chili
G.K. Taylor et J. Grocott

On démontre que l'anomalie magnétique associée au gisement majeur de Cu-Au-Fe de Candelaria dans le Nord du Chili est dominée par une composante rémanante de magnétisation inversée et tournée. La rotation est en accord avec la tectonique régionale, mais la direction inversée suggère une remagnétisation postérieure à la minéralisation. La reconnaissance de l'importance de la rémanence dans les anomalies magnétiques peut amener à la découverte de nouveaux gisements ailleurs dans la région.

La collision ordovicienne de la Pré-Cordillère d'Argentine avec le Gondwana, indépendante de l'orogène taconique-laurentien
W. Thomas et R. Astini

La répartition des prismes sédimentaires synorogéniques démontre que l'orogène ocloïque (collision de la Pré-Cordillère argentine avec le Gondwana) et l'orogène taconique (Sud Laurentia) se sont produits à peu près au même moment mais à des endroits différents, et sur des bords opposés de l'Océan Iapetus. Cette conclusion appuie l'hypothèse selon laquelle la Pré-Cordillère s'est séparée par rifting de la Laurentia au Cambrien, a dérivé comme un microcontinent séparé, et est entré en collision avec le Gondwana à l'Ordovicien.

L'association entre arcs insulaires, batholithes tonalitiques et Plateaux océaniques dans les Antilles hollandaises : implications sur l'accrétion continentale

P. Thompson, R. White, J. Tarney, P. Kempton, A. Kerr et A. Saunders

Les Antilles néerlandaises, situées sur la marge nord de l'Amérique du Sud, sont un endroit idéal pour étudier la formation de la croûte continentale dûe à l'accrétion de plateaus et d'arcs. Des fragments du Plateau Caraïbe daté à 91-88 Ma ont été soulevés et obductés sur les îles d'Aruba et Curaçao. L'île de Bonaire, cependant, consiste en une séquence d'arc insulaire d'âge similaire, et la séquence de plateau d'Aruba a été intrudée par un batholithe tonalitique daté à 85-82 Ma. Les relations entre Plateau, arc insulaire et batholithe sont énigmatiques et ont d'importantes implications sur l'accrétion continentale.

Thermo-chronologie par Traces de Fission des Andes sud-chiliennes (42° à 48°S)

S.N. Thomson , F. Hervé, M.R. Brix et B. Stöckhert

Des données thermochronologiques par Traces de Fission (FT) ont été obtenues sur de nombreux échantillons des Andes méridionales (entre 42°S et 48°S) proches du Point Triple Chilien et de la Faille Liquiñe-Ofqui (LOF). La plupart des âges FT sur zircons indique un refroidissement post-intrusion relativement rapide pour des plutons d'âges variés du Batholithe de Patagonie, et précisent également l'histoire du refroidissement du socle de la région. Les FT sur apatite ont révélé des refroidissements différentiels au travers des Andes à ces latitudes. Ces données impliquent une dénudation plus importante et plus récente d'Est en Ouest, en particulier le long de la principale chaîne topographique des Andes et spécialement près de la LOF.

Eruption explosive de magnitude 6 au volcan Huaynaputina, février-mars 1600, Pérou méridional

J.-C. Thouret et J. Dávila

L'éruption explosive la plus volumineuse de l'histoire dans les Andes (12-13.5 km^3) est survenue en 1600 au volcan Huaynaputina, un petit centre volcanique du Perou méridional. L'éruption débuta le 19 février 1600 par une phase plinienne, suivie par au moins six phases éruptives distinctes jusqu'au 6 ou 15 mars 1600.Les retombées, coulées et déferlantes pyroclastiques ont dévasté une région de 90 x 60 km autour du volcan et ont affecté indirectement l'ensemble du Pérou méridional. De volumineux lahars ont dévasté la vallée du Rio Tambo jusqu'à l'Océan Pacifique à 120 km de distance. Une éruption plinienne et ignimbritique de cette magnitude n'est pas unique, ni au Huaynaputina, ni au sud du Pérou.

Âges des événements volcaniques et érosifs dans le département d'Antioquia (Colombie) : une contribution de la téphrochronologie

G. Toro, G. Poupeau, M. Hermelin et E. Schwabe

Nous avons daté par traces de fission (TF) et ^{14}C des formations superficielles de l'Altiplano et de la valle d'Aburrá, les deux surfaces géomorphologiques principales du département d'Antioquia. Les résultats montrent que les formations superficielles se sont déposées au cours des six derniers Ma et retravaillent des tephras qui proviennent du massif volcanique du Ruíz-Tolima. Les datations par TF obtenues sur des zircons volcaniques ou provenant du socle cristallin permettent une reconstitution de l'histoire thermique, volcanique et tectonique récente de la région.

Caractérisation par isotopes du Plomb de galène de gisements de la région de Aysén, Chili du Sud : implications métallogéniques.
B. Townley

L'analyse isotopique du plomb de la galène de cinq gisements et six prospects de la région d'Aysén (Sud du Chili), associées aux données existantes des isotopes du plomb, indiquent des variations Nord-Sud. La localisation géographique, le contexte géologique et tectonique, ajoutés aux données isotopiques du plomb, suggèrent l'existence de trois groupes principaux de gisements qui sont du Nord au Sud, les groupes El Toqui, Fachinal et El Faldeo. Sur la base de données géologiques, géochronologiques et isotopiques du plomb, on propose l'existence de trois provinces et deux périodes métallogéniques : les provinces El Toqui et Fachinal d'âge Crétacé inférieur, et la province El Faldeo d'âge Jurassique supérieur. Ces provinces sont spatialement et temporellement liées à l'évolution au Jurassique supérieur et Crétacé de l'arc et l'arrière-arc, qui surmontent le socle métamorphique paléozoïque.

Minéralisations d'or tertiaires à San Luis, Argentine
N. Urbina et L. Malvicini

La ceinture volcanique tertiaire aurifère des Sierras Pampeanas de San Luis, Argentine, présente des dépôts épithermaux de métaux précieux et des "Porphyry gold-copper". Les caractéristiques morphologiques, minéralogiques, géochimiques et génétiques de ces dépôts sont exposées, et des sections interprétatives schématiques des principaux districts minéralisés sont présentées.

Évolution méso-cénozoïque du Nord de la Zone Subandine, Équateur
C. Vallejo

La zone subandine, située à l'Est de la Cordillère des Andes, constitue une zone de transition entre le Bassin Oriental et la Cordillère Orientale d'Equateur. Dans cette zone se concentre le gros de la déformation associée à la migration vers l'Est du prisme orogénique et de tout le système de bassins d'arrière-arc, en accord avec le modèle de De Celles, Giles et al. (1996). Les sédiments crétacés exposés dans cette zone ont été en partie incorporés au prisme orogénique et sont affectés par des structures chevauchantes et par un métamorphisme de bas degré.

Évolution géomorphologique au Cénozoique supérieur de la région d'Antofagasta, Nord Chili
G. Vargas, L. Ortlieb et N. Guzmán

Les relations morphostratigraphiques entre des séquences de sédiments continentaux et des superficies d'abrasion marine d'âge Pliocène et Quaternaire, au sud de la ville d'Antofagasta, ainsi que diverses observations morphostructurales dans la Cordillère de la Côte et sur la frange côtière permettent de préciser certains grands traits de l'évolution géomorphologique de la bordure continentale de la région d'Antofagasta. Une forte surrection qui s'est produite entre le Miocène et le Pliocène (moyen ?) a joué un rôle important dans la formation de l'Escarpement Côtier.

Identification du matériel volcanique susceptible de glissement en masse associé aux instabilités de versant dans le secteur pré-andin adjacent à la vallée centrale entre 33° et 34°S (Chili).
N. Vatin-Pérignon, S. Elgueta, S. Rebolled et G. Kieffer

L'analyse des séquences éruptives relatives aux dépôts volcanoclastiques oligo-miocènes des formations Abanico et Farellones dans les secteurs de Cajon del Maipo, Lagunillas et Farellones-la Parva-Valle Nevado met en évidence l'importance du phréatomagmatisme et des violentes explosions (déferlantes basales) au cours des premiers stades de développement de ces complexes volcaniques, suivis par des écoulements pyroclastiques denses (ignimbrites) lors de la formation des calderas et par la montées de dômes et coulées. Le remaniement des matériaux volcanoclastiques (lahars) intervient lors de la construction des stratovolcans.

Âges $^{40}Ar/^{39}Ar$, métamorphisme de très bas degré et géochimie des roches volcaniques du "Cerro El Abanico", Cordillère des Andes de Santiago (33°30'S-70°30'-70°25'W).

M. Vergara, D. Morata, R. Villarroel, J. Nyström et L. Aguirre

La Formation Abanico, dans sa localité-type du Cerro El Abanico, est composée de roches volcaniques avec des âges radiométriques $^{40}Ar/^{39}Ar$ (fusion totale) oligocènes compris entre 30.93 Ma à la base et 25.62 au toit de la séquence. Ces roches ont les caractéristiques chimiques typiques des séries tholéitiques avec une signature isotopique primitive. Le contexte géodynamique de leur genèse est celui d'une croûte continentale amincie. La présence de minéraux métamorphiques de trés bas degré associés aux champs paléogéothermaux confirme l'existence d'un fort gradient thermique lors du depôt de cette formation.

Surrection et morphologie de la surface de l'Altiplano occidental : un effet de l'accrétion basale et du raccourcissement tectonique ?

P. Victor et O. Oncken

L'avant-arc continental des Andes Centrales est caractérisé par une croûte anormalement épaisse et un fort gradient topographique en bordure ouest de l'Altiplano. En interprétant la morphologie de surface, l'évolution tectonique et les processus sédimentaires, nous proposons le modèle suivant d'évolution de l'Altiplano occidental. L'affaiblissement thermique de la plaque supérieure initia la surrection en compression de l'Altiplano. Dans le même temps, la croûte s'épaissit par accrétion basale. La déformation en extension observée actuellement résulte de l'instabilité gravitaire de la croûte supérieure et du fort gradient topographique.

Activité sismique du volcan Guagua Pichincha, Équateur

D. Villagómez, M. Ruiz, H. Yepes, M. Hall, B. Guillier, A. Alvarado, M. Segovia et A. Calahorrano.

Depuis août 1998, le volcan Guagua Pichincha, situé dans la cordillère occidentale des Andes équatoriennes, montre une forte activité sismique et magmato-phréatique. Cependant, cette activité est instable dans le temps comme le montre les variations du facteur b. Ce comportement pourrait être en relation avec des changements du champs de contrainte observé autour du volcan. Une bonne compréhension de ces phénomènes est essentielle pour la surveillance et la prévision de l,activité de ce volcan.

Un modèle de croûte inférieur et de manteau supérieur pour le Sud de la Colombie, basé sur l'étude de xénolithes.

M. Weber, R. Kent et J. Tarney

Les xénolithes de Mercaderes-Río Mayo représentent un aperçu unique sur la croûte inférieure de la NVZ. Les caractèristiques des xénolithes indiquent que l'accrétion verticale par intrusion magmatique est un processus essentiel de formation de croûte dans la région.

Au moins deux sources magmatiques peuvent être distinguées : fusion d'un manteau préalablement somatisé, et fusion (dehydratation melting) de magmas déjà solidifiés dans la croûte inférieure, laissant du matériel restitique réfractaire.

Impact de la tectonique et de la topographie sur l'importance de la dernière glaciation sur la calotte glaciaire du Sud de la Patagonie (Chili, Argentine)
G. Wenzens

L'opinion courante selon laquelle une calotte glaciaire cohérente se forma dans les Andes du Sud pendant la dernière période glaciaire ne correspond pas aux faits géomorphologiques relevés dans l'Est des Andes. Seuls quelques grands glaciers s'étendirent et s'avancèrent considérablement vers l'Est, la largeur de la calotte glaciaire intermédiaire étant limitée à quelques kilomètres.

Le rôle de la Ride Juan Fernández dans la segmentation persistante des Andes à 33,5°S
G. Yañez et C. Ranero

Le poinçonnement cénozoïque de la Ride Juan Fernandez contre la marge active sud-américaine indique une migration rapide vers le Sud d'Arica vers Valparaiso dentre 20 et 10 Ma. La forme contrastée du segment à subduction plane, son infléchissement progressif vers le Nord (≈ 27-28°S) et sa flexure plus raide au Sud (≈ 33,5°S), suggère qu'elle est directement influencée par la flottabilité de la Ride Juan Fernandez en cours de collision. Cette relation est confortée par les données géologiques qui montrent un diminution vers le Sud du pendage de la subduction pendant la même période.

Caractérisation du corps magmatique de l'Altiplano-Puna, Andes Centrales, Amérique du Sud.
G. Zandt, J. Chmielowski, Ch. Haberland, X. Yuan et R. Kind

Depuis le Miocène supérieur, une "flambée" d'ignimbrite a produit une province majeure de volcanisme acide dans les Andes Centrales d'Amérique du Sud, le Complexe Vocanique Altiplano-Puna. Entre Octobre 1996 et Septembre 1997, nous avons installé 7 stations sismique large bande PASSCAL dans la partie bolivienne de la province volcanique, pour enregistrer les télé-séismes et les événements locaux sur le plan de Benioff de la plaque Nazca sous-jacente. En utilisant la méthode des "receiver functions" pour visualiser les structures magmatiques subhorizontales, nous avons identifié une couche régionale à faible vitesse que nous interprétons comme un corps magmatique en forme de sill associé au Complexe Volcanique Altiplano-Puna. Nous supposons que ce corps magmatique représente un niveau de stockage/accumulation des produits siliceux entre une zone de génération de magma au niveau du manteau supérieur/croûte inférieur, et des plutons plus superficiels formant des calderas.

L'évolution du bassin arrière-arc ordovicien de la Puna méridionale (Nord-Ouest de l'Argentine) : analyse des sources détritiques et contexte paléotectonique
U. Zimmermann et H. Bahlburg

Les séries clastiques de l'Ordovicien inférieur de la Puna méridionale (Formations Tolar Chico, Tolillar et Diablo, Nord-Ouest de l'Argentine) sont interprétées comme recyclées d'une croûte continentale ancienne (TDM 1,6 à 2,0 Ga), avec un léger apport de matériel un peu plus jeune (TDM 1,3 Ga) dans l'Arenig (Formation Diablo) d'un arc volcanique ordovicien inférieur (arc Puna-Famatinien) développé sur croûte continentale.

Nouvelle subdivision stratigraphique pour la Puna méridionale (NW Argentine) sur la base de graptolites Ordovicien inférieur : premières découvertes de *Araneograptus murrayi* et *Phyllograptus* sp. dans la Puna

U. Zimmermann, M.C. Moya et H. Bahlburg

De nouvelles découvertes de graptolites, brachiopodes et phyllocariidés dans les dépôts ordoviciens de la Puna méridionale (NW Argentine) permettent une nouvelle subdivision de l'Ordovicien inférieur de cette région. *Araneograptus murrayi* indique la limite Tremadoc-Arenig pour la Formation Tolillar et *Phyllograptus* sp. un âge Arenig à Llanvirn inférieur pour les formations Diablo et Coquena.

AUTHOR INDEX

Achevé d'imprimer sur rotative
par l'Imprimerie Darantiere à Dijon-Quetigny
en septembre 1999

Dépôt légal : 3e trimestre 1999
N° d'impression : 99-0923